

AFML-TR-73-126

# CONFERENCE ON TRANSPARENT AIRCRAFT ENCLOSURES

*FEBRUARY 5-8 1973  
LAS VEGAS, NEVADA*

*COMPILED BY  
ROBERT E. WITTMAN*

TECHNICAL REPORT AFML-TR-73-126

JUNE 1973

Reproduced From  
Best Available Copy

Approved for public release; distribution unlimited.

AIR FORCE MATERIALS LABORATORY  
AIR FORCE SYSTEMS COMMAND  
WRIGHT-PATTERSON AIR FORCE BASE, OHIO

20011009 132

## NOTICE

When Government drawings, specifications, or other data are used for any purpose other than in connection with a definitely related Government procurement operation, the United States Government thereby incurs no responsibility nor any obligation whatsoever; and the fact that the government may have formulated, furnished, or in any way supplied the said drawings, specifications, or other data, is not to be regarded by implication or otherwise as in any manner licensing the holder or any other person or corporation, or conveying any rights or permission to manufacture, use, or sell any patented invention that may in any way be related thereto.

Copies of this report should not be returned unless return is required by security considerations, contractual obligations, or notice on a specific document.



# **CONFERENCE ON TRANSPARENT AIRCRAFT ENCLOSURES**

*COMPILED BY  
ROBERT E. WITTMAN*

Approved for public release; distribution unlimited.

## FOREWORD

This report was prepared by the Materials Engineering Branch and was initiated under Project 7381 "Materials Application," Task No. 738106, "Materials Engineering and Design Data for Air Force Weapons Systems." It was administered under the direction of the Air Force Materials Laboratory, Air Force Systems Command. Mr Robert E Wittman (MXE) served as Project Engineer.

The technical papers contained in this report were presented at the Air Force Materials Laboratory/Air Force Flight Dynamics Laboratory Conference on "Transparent Aircraft Enclosures," which was held at the Hotel Sahara, Las Vegas, Nevada, on 5-8 February 1973.

This report was submitted by the author on 10 May 1973.

Publication of this report does not constitute Air Force approval of the reports, findings, or conclusions. It is published only for the exchange and stimulation of ideas.

## ABSTRACT

The purpose of this report is to make available the technical papers presented at the recent Tenth Conference on "Transparent Aircraft Enclosures." This Conference was held for the exchange of knowledge on new developments and design concepts concerned with vision areas of crew enclosures. Also to make known the state-of-the-art with respect to transparent plastics, interlayer materials, and glass, of the type suitable for these applications.

The papers contained herein have been reproduced directly from the original manuscripts.

## TABLE OF CONTENTS

|  | <u>Page</u> |
|--|-------------|
| <u>SESSION 1 - OPTICAL CONSIDERATION DESIGN CONCEPTS</u>   |             |
| Windshield Design Concepts   |             |
| P.N. Beaumont and S. Parker, Boeing-----   | 3           |
| Transparencies For European Aerospace - The Problems<br>And Future Trends                        |             |
| P.J. Sharp, Lucas Aerospace-----   | 15          |
| A User-Oriented Design Criteria For Helicopter Glazings  |             |
| H.C. James, Goodyear Aerospace-----  | 37          |
| Optical Requirements For Aircraft Transparencies   |             |
| N.S. Corney, Ministry of Defense-----  | 47          |
| Correction Of Optical Deviation In Curved Windshields  |             |
| R.W. Fisher, McDonnell Aircraft-----   | 69          |
| Alternatives To Windshields  |             |
| P.N. Beaumont, Boeing-----   | 83          |
| <u>SESSION 2 - MATERIALS AND PROCESSES (Part I)</u>  |             |
| A Status Report - New Transparent Plastic Materials  |             |
| E.A. Arvay, Air Force Materials Laboratory-----  | 99          |
| Polyarylsulfone - A New Dimension In High Performance<br>Aircraft Transparencies                 |             |
| R.L. Burns, H.A. Vogel, and A.T. Worm, 3M and<br>E.A. Arvay, Air Force Materials Laboratory----- | 125         |
| Production Process For Transparent Spinel (MgAl <sub>2</sub> O <sub>4</sub> )                    |             |
| D.W. Roy, D.R. Johnson, and D.L. Mann, Coors Porcelain--   | 138         |

## TABLE OF CONTENTS (CONT'D)

Page

|   |     |
|---|-----|
| Environmental Data and Machining Techniques of Polycarbonates<br>G.E. Husman, Air Force Materials Laboratory and<br>R.J. Kuhbander, University of Dayton----- | 147 |
| Material Evaluation, B-1 Crew Module Windshield<br>J.E. Mahaffey, North American Rockwell-----  | 173 |
| The Development of Transparent Composites and Their Thermal Responses<br>J.A. Parker, G.M. Fohlen, and P.M. Sawko, NASA/Ames-----                             | 197 |

### SESSION 3 - MATERIALS AND PROCESSES (Part II)

|   |     |
|---|-----|
| Plate Versus Float Glass In Aircraft Transparencies<br>R.E. Maltby, Jr., Libbey-Owens-Ford-----   | 233 |
| Effect of Adhesive on the Impact Resistance of Laminated Plastics for Windshield Applications<br>J.L. Illinger and R.W. Lewis, Army Materials and<br>Mechanics Research Center----- | 243 |
| Plexiglas 70 - A New High Impact Plastic<br>W.E. Feely, Rohm and Haas-----  | 267 |
| Interlayer Needs For Subsonic Windshields<br>G.E. Bickford, Boeing-----   | 271 |
| Engineering Data on Ethylene Terpolymer as an Adhesive for Polycarbonate Composite Aircraft Transparencies<br>G.L. Ball and I.O. Salyer, Monsanto Research-----                     | 289 |
| Interlayer Design for Aircraft Transparencies<br>N.G. Nixon, Swedlow-----   | 293 |

### SESSION 4 - BIRD AIRCRAFT STRIKE HAZARD (Part I)

|   |     |
|---|-----|
| Flight Safety Aspects of Precision Radar Near Air Bases<br>W.L. Flock, University of Colorado and<br>B.B. Balsley and J.L. Green, National Oceanic and<br>Atmospheric Administration----- | 307 |
| Composite Bird-Resistant Aircraft Transparencies<br>H.E. Littell, Jr., PPG-----   | 321 |

| TABLE OF CONTENTS (CONT'D)   | Page              |
|--|-------------------|
| Altitude and Predictability Studies of Whistling Swan<br>Migrations<br>W.J.L. Sladen and J.G. Reese, John Hopkins University and<br>W.W. Cochran, Illinois Natural History Survey----- | 343               |
| Experimental Investigation Into The Bird Impact Resistance<br>Of Flat Windscreen Panels With Clamped Edges<br>M.J. Mott, Hawker Siddeley Aviation-----                                 | 347               |
| Physical Techniques For Controlling Birds To Reduce Aircraft<br>Strike Hazards<br>S.I. Lustick, The Ohio State University-----   | 373               |
| <u>SESSION 5 - BIRD AIRCRAFT STRIKE HAZARD (Part II)</u>   |                   |
| The Bird Aircraft Strike Hazards In The USAF<br>Capt. J.P. Nemergut, Air Force Weapons Laboratory-----   | 423               |
| Ecological Aspects Of The Gull Aircraft Hazards<br>W.H. Drury, Massachusetts Audubon Society-----  | 449               |
| Hail Impact On Aircraft Transparencies<br>I.I. McNaughtan, Ministry of Defense-----  | 457               |
| Short Status Reports<br>J.H. Lawrence, McDonnell Douglas-----<br>G.E. Wintermute, Goodyear Aerospace-----<br>E.J. Sanders, Arnold Engineering Development Center-----                  | 481<br>489<br>491 |
| Quantification Of Bird Echoes On Airport Surveillance Radars<br>S.A. Gauthreaux, Jr. Clemson University-----   | 515               |
| The Design Development Of A Bird-Proof Windshield For The<br>B-1 Strategic Bomber<br>F.T. McQuilkin, North American Rockwell-----  | 531               |
| <u>SESSION 6 - DESIGN AND PERFORMANCE</u>  |                   |
| Transparency Development In Civil Airline Operation<br>B.D. Gibbs, British European Airways-----   | 559               |
| Performance Of Glass/Plastic Windshields In Airline Service<br>J.B. Olson, Sierracin-----  | 577               |
| Study of Failed TA-4 Aircraft Canopies<br>I. Wolock, D.R. Mulville, and R.J. Thomas,<br>Naval Research Laboratory-----   | 617               |

| TABLE OF CONTENTS (CONT'D)  | Page |
|---|------|
| Static Fatigue - Its Implication To Reliability In Window Design<br>A.F. Shoemaker, Corning-----  | 641  |
| Helicopter And Other VTOL Transparencies - An Updating<br>G.E. Freeman and J.B. Perkins, PPG-----   | 653  |
| Crack Initiation in F-4 Canopies<br>D.R. Mulville, I. Wolock, and R.J. Thomas, Naval<br>Naval Research Laboratory-----  | 667  |
| The Design, Development, And Testing Of Flat And Curved All Glass Windshields For Wide Bodied Aircraft Using The Latest Developments In High Strength Glass And Electro-Conductive Coatings<br>W.G. Roberts, Triplex----- | 683  |

#### SESSION 7 - COATINGS FOR ENCLOSURES

|  |     |
|--|-----|
| Development Of Scratch And Spall Resistant Windshields<br>Capt. J.R. Plumer, Army Materials and Mechanics<br>Research Center-----  | 713 |
| Vacuum Deposited Electrically Conductive Coating Design<br>N.G. Nixon, Swedlow-----  | 745 |
| Ocular Hazard From Viewing The Sun Unprotected And Through Various Windows and Filters<br>W.T. Ham, Jr., H.A. Mueller, and R.C. Williams,<br>Virginia Commonwealth University----- | 753 |
| A Coating For Helicopter Canopies<br>G.A. Lundgren, Optical Coating Laboratory-----  | 779 |
| Protective Coating<br>D.L. Voss, Sierracin-----  | 801 |
| An Analytical Investigation Of Aircraft Windshield Anti-Icing Systems<br>G.C. Letton, Jr., Aeronautical Systems Division-----  | 831 |
| Salt Blast Erosion Test For Aircraft Plastic Windshield<br>M.S. Tarnopol, PPG-----   | 903 |

SESSION 1

OPTICAL CONSIDERATION DESIGN CONCEPTS



## **WINDSHIELD DESIGN CONCEPTS**

**Peter N. Beaumont and Stone Parker  
The Boeing Commercial Airplane Company  
Seattle, Washington**

## **WINDSHIELD DESIGN CONCEPTS**

**Peter N. Beaumont**

**Stone Parker**

**The Boeing Commercial Airplane Company  
Seattle, Washington**

### **ABSTRACT**

The amount of time and money spent on windshield design and development on both commercial transport and military airplanes is testimony to there being a substantial problem with, as yet, no solution. This paper deals principally with commercial transport airplane windshields but many of the comments and proposed solutions are also applicable to military vehicles.

A qualitative summary of the basic windshield requirements is presented and the influence each has on the design is described. Additional constraints imposed by configurators such as noise, drag, shape, etc., are also examined.

No specific windshields in current use are analyzed but the effect of design constraints and requirements and their influence on windshield performance with materials currently in use is discussed. Conclusions reached from the above are being used in a design development program by Boeing to examine new windshield concepts, in an attempt to significantly increase windshield life without prejudicing the level of safety currently being achieved.

These new concepts utilize various combinations of materials, including some that were not available when the current generation of windshields were being designed. The use of polycarbonate in conjunction with other structural materials is discussed, and the use of different interlayer materials such as silicone and polyurethane is described.

Specific windshield assembly concepts are presented and their characteristics summarized.

## INTRODUCTION

The Structures Design Development group at Boeing is presently conducting a development program with the objective of substantially increasing windshield service life by eliminating the failure modes being experienced in current commercial transport airplane windshields. The purpose of this paper is to identify and discuss various new design concepts which attempt to meet the stated objective without adversely affecting the high degree of structural reliability currently being achieved.

## DESIGN REQUIREMENTS FOR CURRENT WINDSHIELDS

Before discussing windshield durability, a summary of the basic requirements which led to the design of present day windshields and how they may affect tomorrow's windshields is needed. The applicable Federal Aviation Regulations comprise four broad categories. First, the field of view considered necessary for safe operation of the airplane has to be provided, and the desire for increased operational flexibility in bad weather conditions plus the trend toward wider flight decks is tending to increase the size of the opening the windshield is going to have to fill (see Figure 1). Secondly, a minimum level of structural integrity and redundancy is required with

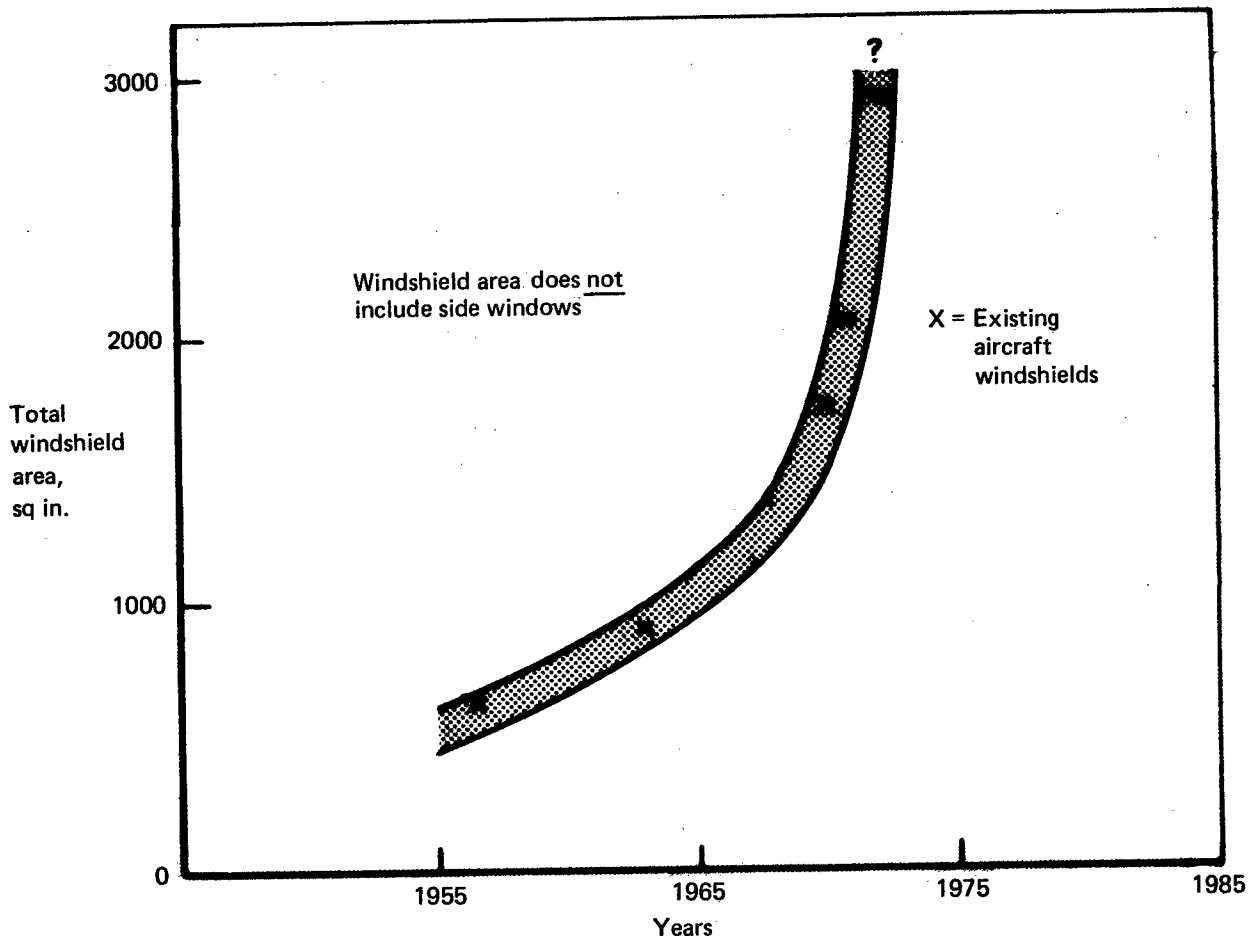


FIGURE 1.—WINDSHIELD GROWTH

appropriate margins of safety applied to each part. Thirdly, a clear view has to be provided under rain, icing, and fogging conditions while fourthly, the windshield must be able to contain or resist the impact of a 4-pound bird without penetration at 375 knots.

In addition, the airframe manufacturer has his own requirements relating to such things as the windshield/airframe interface, load transfer methods, effects of airplane configuration on windshield shape, and the influence of aerodynamic drag and noise.

### CURRENT WINDSHIELD DESIGNS

Until recent years, windshields in commercial jet transport airplanes were flat and utilized chill-tempered soda lime glass for the primary structural plies, with a substantial amount of polyvinyl butyral (PVB) bonded to the glass. The PVB served the purpose of a fail-safe diaphragm as well as being the ultimate bird-stopping agent (see Figure 2). In all cases a relatively thin outer

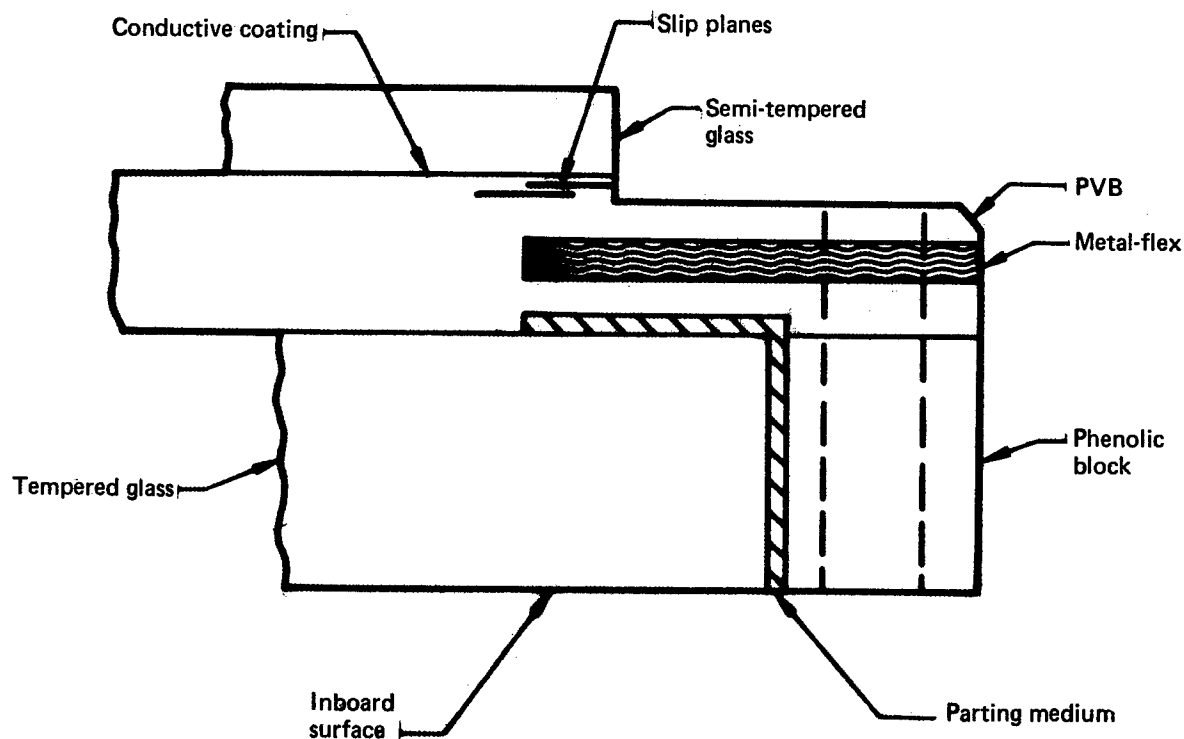
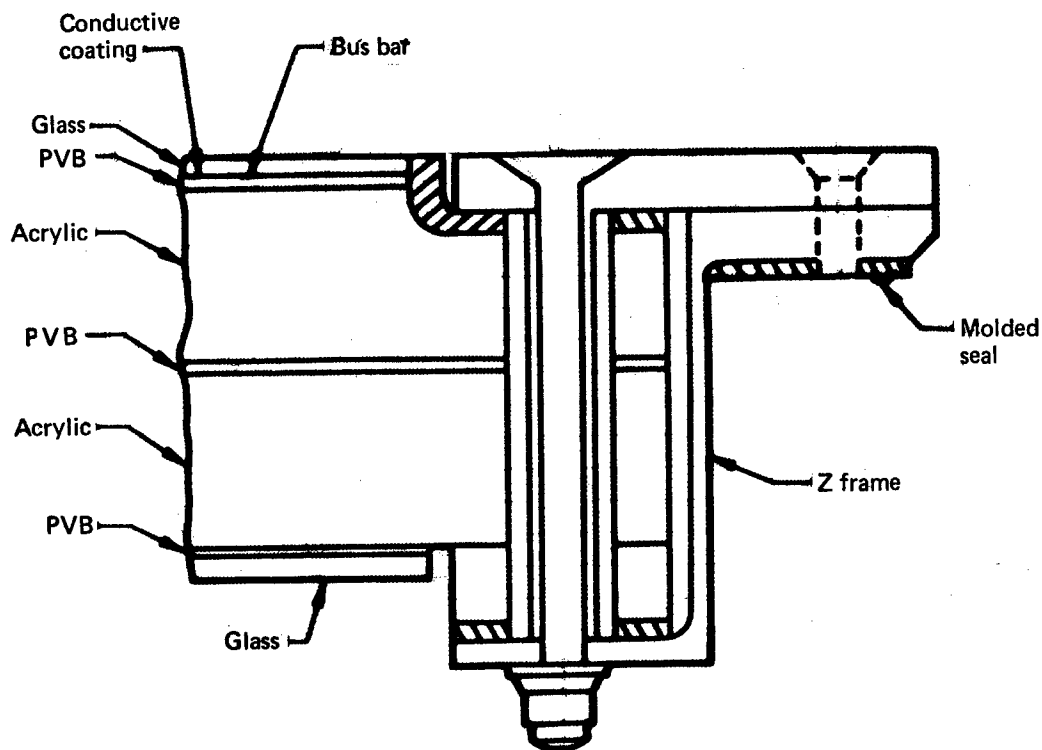


FIGURE 2.—CURRENT GLASS-PVB FLAT WINDSHIELD

glass ply was bonded to the PVB and this served two purposes, one being to protect the surface of the PVB and the other to carry the electrically conductive de-icing coating, which is also used to keep the PVB warm. These are predominantly "bag the bird" windshields and, consequently, airplanes with this feature have a very limited "cold dispatch" certification. "Cold dispatch" is defined as the ability to dispatch an aircraft without powering the electrically conductive coating.

Curved, stretched acrylic composite windshields were introduced into commercial aircraft on the Boeing 747, followed closely by the Lockheed L-1011 and Dassault Mercure (see Figure 3). These windshields again use glass faceplies to protect the stretched acrylic structural plies from abrasion as well as providing the EC coating substrate. PVB is once again used on the 747 and L-1011 as the interlayer, although reliance is placed on the stretched acrylic to provide the bird impact resistance. These windows are essentially "bounce the bird" windows.



**FIGURE 3.—CURRENT CURVED ACRYLIC WINDSHIELD**

### **SERVICE PROBLEMS AND FAILURE MODES OF CURRENT DESIGNS**

Although the two windshield types are basically different, experience to date has indicated little noticeable improvement in durability of the curved, acrylic windshields over that of flat, glass windshields. Although the modes of failure are somewhat different, the locations of the failures are the same, namely, at the outer glass ply and adjacent to the interlayer.

Before a windshield design improvement can be investigated, a thorough knowledge of service problems and failure modes is necessary. First, the structural integrity of commercial transport airplane windshields has been adequately demonstrated; consequently, the basic rules established by experience can be used for defining material thicknesses and fail-safe requirements on future windshields. Optical quality in most cases can be economically achieved to the extent that it is considered adequate for safe airplane operation. The primary cause of concern is the deterioration of optical quality in service due to delamination, coating burnouts, and breaking or abrading of nonstructural members due to hail impact and flying debris. In every large

pressurized commercial transport airplane with a windshield durability problem there is a relatively thin piece of glass (0.050-0.200 inch thick) on the outside carrying a de-icing coating. It is the failure of this member or the interface between it and the main body of the windshield that is the cause for premature removal. Examination of a number of different operators' experience with the same airplane model shows some differences in MTBR's, probably due to different operating procedures for applying heat, the type of flight leg flown, and differences of opinion as to what are tolerable deficiencies.

Taking each of these factors separately and examining its effect on the windshield assembly provides a number of clues to what should be considered in the next generation of windshields.

1. *High-temperature gradients with cold edges.* (See Figure 4.) The temperature at the edge of a windshield outer ply and of the adjacent PVB, on a normally heated windshield, is about  $-4^{\circ}\text{F}$  at cruise altitude. The elastic modulus of PVB at this low temperature is sufficiently high (about 250,000 psi), and its shrinkage relative to the glass is of sufficient magnitude, to create high interlaminar shear loads. The inevitable result is delamination, pulling of chips from the glass, or cracking of the vinyl. Furthermore, local thickness shrinkage of the vinyl contributed flatwise tensile loads which had to be offset by further design changes (such as slip planes), which tended to increase design risk. A further damaging element encouraging

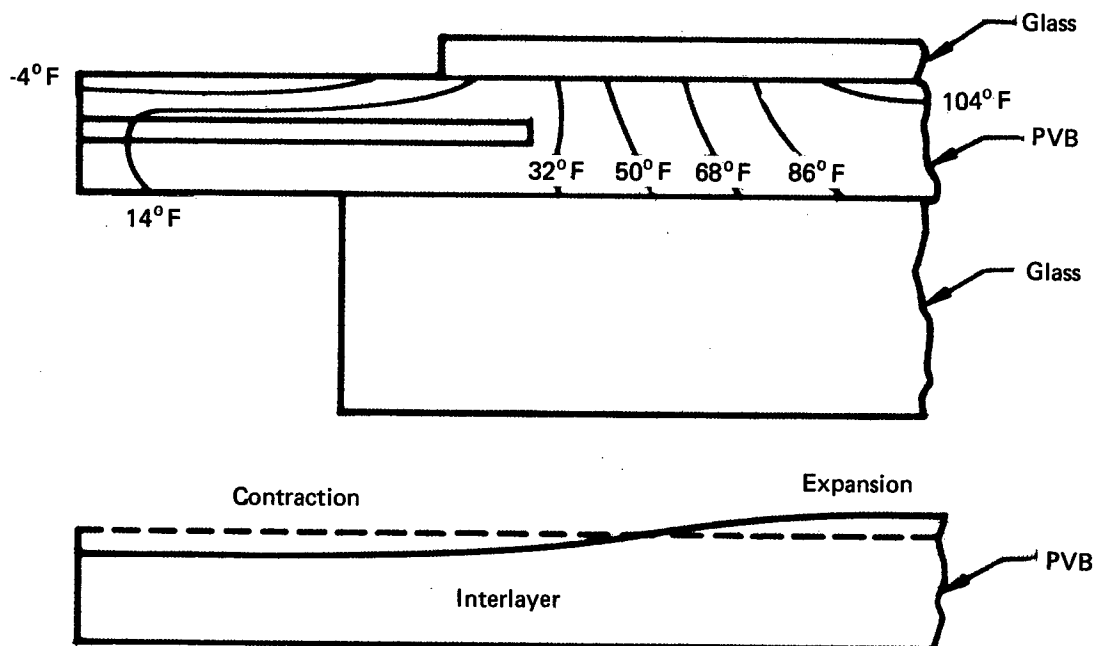


FIGURE 4.—EFFECT OF TEMPERATURE GRADIENT IN WINDSHIELDS

delamination is the cold-soak condition on the ground with the vinyl trying to shrink across the whole windshield width.

2. *Moisture.* All windshields utilizing thin glass and PVB contravene the basic rules of weather sealing, inasmuch as the moisture path is short and the seal has an opportunity to open when the airframe is subjected to pressure differential and temperature. This contributes to EC coating failures.
3. *Deflections.* While total deflections of windshields in general are small, the rate of change of deflection at the edge of a uniformly loaded, simply supported plate is substantially greater than in the center (see Figure 5). Since none of the windshield assemblies under discussion have a retainer cap over the outer ply, flatwise tensile loads at the very edge of the glass can be high because of the high modulus of the glass in comparison to that of PVB.

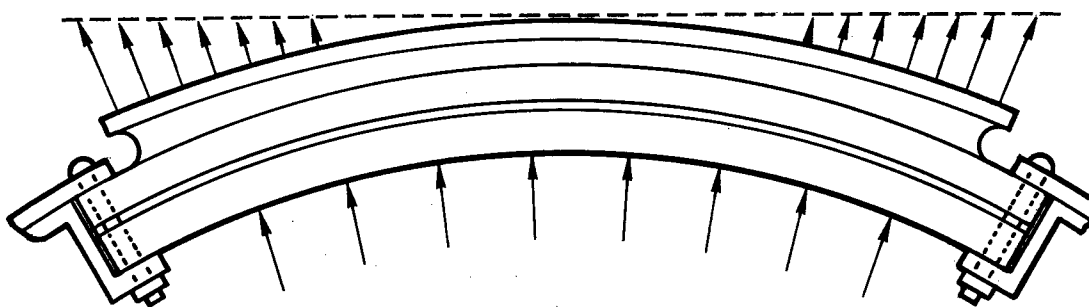


FIGURE 5.—EFFECT OF WINDSHIELD DEFLECTION

The combination of all these damaging features makes initial windshield design difficult. As a result, dependence is placed on the windshield manufacturer and on subsequent development programs to produce a durable windshield. Until very recently the only interlayer material with any chance of meeting structural and optical requirements has been PVB. It is regrettable that it has taken so long to develop an interlayer superior to PVB. Furthermore, the chance of designing a new windshield using the best combination of available materials and techniques is not improved much unless these materials can all be brought together. For example, the glass, interlayer, and EC system materials may have to be procured from three separate manufacturers. In many cases, items used are proprietary, and unless cooperation between these separate manufacturers is firmly established, optimum windshield design is prejudiced.

## NEW DESIGN CONCEPTS

Assuming that the optimum choice of materials is available, a number of different windshield configurations can be proposed to meet the basic requirements mentioned earlier. There are two basic types of windshield construction: those which use glass and those which use plastic as structural plies. Since the outer ply of glass and its interlayer represent the principal problem area on today's windshields, we can either eliminate those parts or find a better way of applying them.

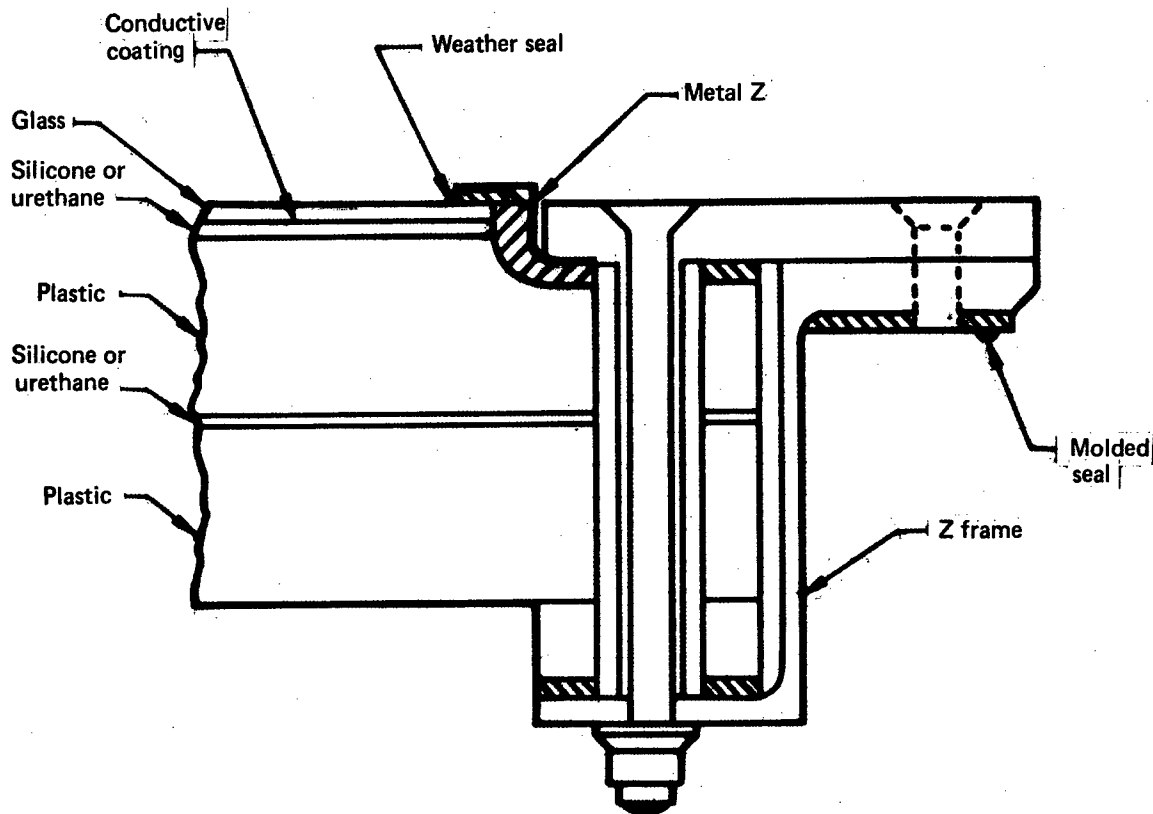
### Plastic

In the case of the plastic windshield, the designer is immediately confronted with the need to protect the surface from windshield wiper damage, scratches, and other abrasion. Hard coatings have been developed which provide a degree of protection but, as of the present, not enough. An alternate way of putting a hard face on plastic would be to eliminate the interlayer completely and bond ultra-thin annealed glass (about 0.006 to 0.009 inches thick) onto the outer face of the plastic. The glass could be wrapped onto the surface of the plastic without incurring high flexural stresses, and if the adhesive is cured with the whole assembly at, say, 180°F, a compression stress could be induced in the glass on cooling. The glass would then have the mechanical characteristic of tempered glass, providing considerable resistance to damage. This concept is being investigated by Boeing, and a search for the best adhesive for the job is proceeding.

Reluctantly conceding that at present glass is the only material which has the properties needed for the outer ply, one area where improvement over existing plastic windshields can be obtained is in the interlayer. Since this is inevitably plastic, the designer must accept coefficients of thermal expansion of the order of ten times that of glass. However, if the interlayer will remain elastic with low modulus at low temperatures, a significant improvement over PVB will be realized. An alternate method of eliminating problems caused by temperature gradients is to thermally insulate the edges of the windshield. A substantial amount of development work has been done in recent years on transparent silicones and urethane compounds as replacements for PVB. Both have been developed as cast-in-place interlayers rather than as laid-up sheet, the method used to form PVB. Both have very low values for elastic modulus (E) at room temperature (of the order of 500 psi) and retain relatively low E's at -65 F. The silicone in particular shows a reduction in E at the lower temperatures. Consequently, if a good bond line can be promoted on both glass and plastic, one of the main damaging features of today's windshields will be minimized. The development of a room temperature cure for these materials will assist in eliminating residual thermal stresses that are inherent in PVB. It seems reasonable, therefore, to pursue the current plastic windshield concepts using these interlayers.

Extrapolating from the current plastic windshields, one with improved durability would probably look like that shown in Figure 6. The basic stretched acrylic plies would be sized using a maximum allowable flexural strength consistent with a craze-free life in the windshield assembly of, say, 20,000 hours. An interlayer of either silicone or urethane (cast-in-place) on the outside of the outer acrylic ply would carry a piece of glass. The thickness of the interlayer would be of the order of 0.20 to 0.25 inch. The coating would be of the EC low resistance





**FIGURE 6.—NEW PLASTIC WINDSHIELD DESIGN EXAMPLE**

type (7-10 ohms per square) applied to the glass inner face. Coating temperatures would be about 85°F for de-icing in the most adverse conditions. To meet the self-imposed requirements, the airplane must be certified for takeoff at all times without heat except when icing conditions prevail. This type of windshield cross section is better suited to curved parts because of the membrane stresses introduced which offsets the low elastic modulus of the stretched acrylic. Deflections start to get large in flat windows where membrane stresses are small initially. In the next generation of windshields, we are probably going to come close to the maximum size this type of assembly can tolerate unless we can develop an ability to manufacture thicker parts of stretched acrylic that will still provide the degree of crack propagation resistance that makes stretched acrylic a good bird-stopping material. A modification of this concept, recognizing that some hoop tension loads will be present, would be to design the windshield as an integral part of the airframe, thus distributing the loads more homogeneously throughout the window to control deflections. To do this efficiently, the basic configuration of the windshield, cab, and side windows must have concurrent and equal consideration during the cabin structural design.

#### **Glass**

The alternative to the plastic windshield is one containing glass structural plies. As stated earlier, conventional glass windshields are already in use in substantial numbers and do not, in the main, come close to the service life represented by current objectives, nor are they regarded as a standard cold-dispatch windshield. If improvements are to be made, more efficient use of the glass has to be made. Replacement of the outer thin ply of glass with a thicker piece sized to act

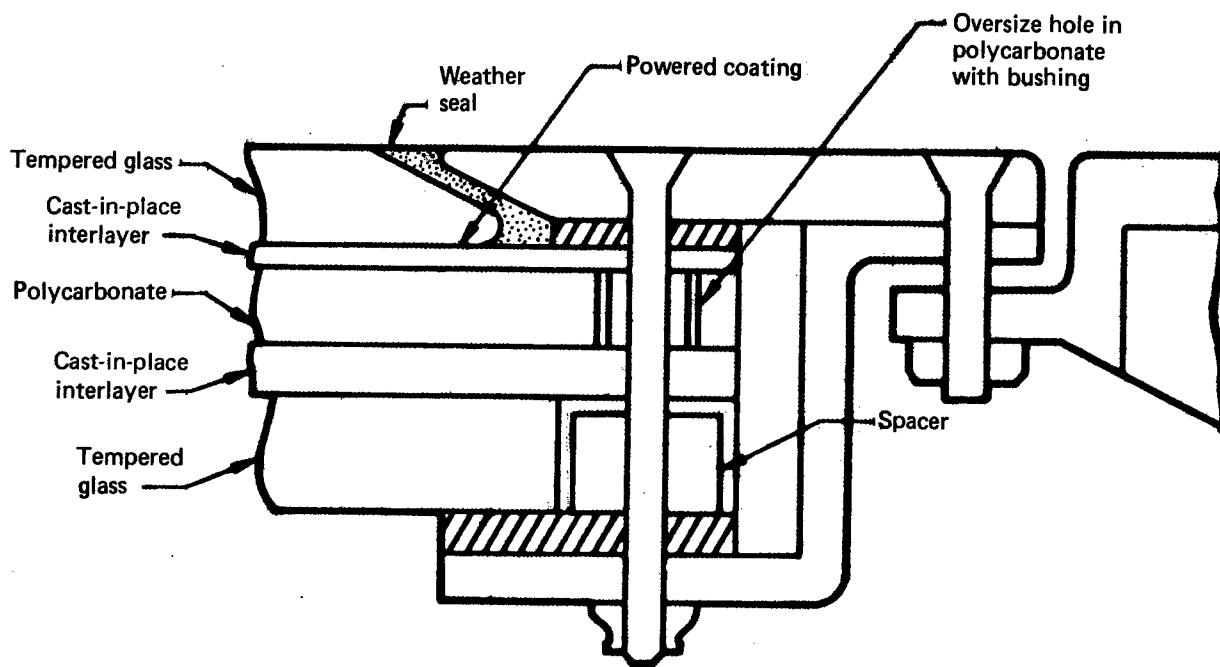
as a structural member would require higher coating temperatures than are being used in today's windshields. Temperatures may have to be as high as 180°F to maintain outer surface temperatures at 35°F in the worst icing conditions.

The conventional use of PVB either as a bird stopper or a fail-safe membrane is unattractive because of PVB's properties at these temperatures. However, the physical properties of selected urethane and silicone interlayers are not substantially altered by this type of environment; and in the right thicknesses may, in fact, be made to work as a fail-safe membrane. This type of concept, however, encourages the use of polycarbonate as a fail-safe membrane and an ultimate bird stopper in conditions beyond those required for certification where the structural plies may fail. Bird impact tests conducted on polycarbonate panels have revealed some interesting phenomena. Panels of various thicknesses from 1/4 to 5/8 inch measuring about 34 by 34 inches were mounted in a rigid test fixture and subjected to center and edge impacts. Two significant observations were made: one is that monolithic panels exhibited brittle fracture when impacted at a speed in excess of what the panel could react to by deflecting, whereas laminated panels did not shatter and bolt holes were torn out as a mode of failure; secondly, the ability of a polycarbonate panel to absorb an edge shot appears to be substantially higher than what the panel will take in the center.

Even though polycarbonate is an excellent impact-resistant material, it does have several properties which present problems: its adverse reaction to ultraviolet radiation, its reaction to solvents, its ability to store energy, and its adverse reaction to high processing temperatures. Anticipating R&D programs to establish the true parameters of polycarbonate, it would be wrong to preclude its consideration for windshield design.

Because of its high elastic modulus, glass is an attractive windshield material provided that a relatively high strength can be imparted to it with a high degree of reliability. Exceptionally high strength (up to 85,000 psi) can be achieved using chemical tempering, but technical problems in obtaining quality parts in thicknesses much in excess of one-quarter inch, plus its high cost, discourage its use as a structural member. Thermally tempered soda lime glass with a flexural modulus of rupture up to about 26,000 psi is readily available in thicknesses up to 1 inch. In recent times the development of methods for better controlling the temperature gradients during the tempering process have made it possible to obtain flexural strength moduli up to 45,000 psi in thicknesses up to about 0.5 inch.

A typical windshield assembly using glass might be similar to what is shown in Figure 7. A thick outer ply is used which has a chamfered edge with a retainer designed to discourage moisture ingestion in the weather seal. An inner ply of thick glass provides a second load path, both panes being sized for the appropriate load conditions. Sandwiched between the two glass plies is a core which might be a thick cast-in-place interlayer, or, if material properties permit, polycarbonate. Preliminary tests indicate that in this type of construction the interlayer material must have a high enough section modulus to prevent localized deflections in the glass upon bird impact. Exact interlayer thickness determinations have yet to be made. The bus bars and coating extend behind the retainer, and the inner core has a conventional insert if the material is silicone or polyurethane and, if the core is polycarbonate, simple bolts through oversized bushings are used. Thus, the polycarbonate can move freely within the body of the windshield without picking up load from the bolts. The windshield has a very considerable potential for gaining certification for dispatch without heat as standard procedure. The interlayer materials are thick enough to create a sufficiently large temperature gradient to maintain the windshield inner surface at an acceptable temperature for crew comfort when power is applied to the EC coating.



*FIGURE 7.—NEW GLASS WINDSHIELD DESIGN EXAMPLE*

**TRANSPARENCIES FOR EUROPEAN AEROSPACE  
THE PROBLEMS AND FUTURE TRENDS**

**P. J. Sharp  
Lucas Aerospace Ltd.  
Luton, Bedfordshire, England**

TRANSPARENCIES FOR EUROPEAN AEROSPACE  
THE PROBLEMS AND FUTURE TRENDS

by  
P.J. SHARP  
of  
LUCAS AEROSPACE LTD.

ABSTRACT

The subsequent European expansion of the aircraft industry after the Second World War in both civil and military fields, resulted in a need for transparency materials and fabrication techniques throughout the continent. Therefore, today, a multitude of specifications and requirements which may be considered during the design phase results in a waste of time and effort. The trend towards multi-National projects has highlighted the need for common standards and the Association Internationale Des Constructeurs De Materiel Aerospatial is the organisation through which standardisation within the European industry will come about. The problems of formulating acceptable standards are considered and this paper takes thickness tolerances of acrylic sheet as an example.

The current types of aircraft transparencies are considered in greater detail with reference to some particular problems experienced in Europe. In particular, the use of laminated all plastic forward facing windscreens for sophisticated jet aircraft.

The tendency towards windscreen heating on all types of aircraft has led towards an acceptance of compromises when only a 28 volt system is available, although there is interest in high voltage generation equipment for quite small aeroplanes. The new dual output generator which supplies both 28 volts D.C. and 200 volts 3 phase a.c. suitable for fitting to engines in the 600 S.H.P. class is reviewed. This enables the lighter aeroplane to make use of electrically heated windshields without the disadvantages associated with the 28 volt D.C. system.

The future of European aircraft transparencies is reviewed, not only technically but taking into consideration the advantages - and problems - of operating within a common European aircraft industry.

# TRANSPARENCIES FOR EUROPEAN AEROSPACE

## THE PROBLEMS AND FUTURE TRENDS

by

P.J. SHARP

of

LUCAS AEROSPACE LTD.

### 1. INTRODUCTION

The problems of developing and certifying a new type of complex aeroplane make co-operation - rather than competition - very attractive. Within Europe, this means co-operation of companies situated in different countries and possibly speaking different languages. But the idea is still attractive.

In re-establishing their aircraft industries after World War II, each European country attempted to integrate the latest knowledge available from the major powers, with familiar tried and proven practices. Therefore a multi-National co-operative design is complicated by the existence of a large number of differing specifications for the same item of equipment. Yet co-operation does succeed, and succeed very well.

The Concorde, the Transal C-160, the A.300 Airbus are examples. Another is the S.E.P.E.C.A.T. Jaguar shown in Figure 1. This advanced trainer/tactical support aircraft is now being produced by Dassault Breguet of France and the British Aircraft Corporation for the Royal Air Force and the French Services. The centre glass windshield and plastic canopy are manufactured in France; the stretched acrylic windshield side panels in England by Lucas Aerospace.

### 2. STANDARDISATION

On projects of this sort, the large number of equipment and material specifications which may be considered during the design phase presents a formidable task, resulting in a waste of time and effort. But firm progress towards common specifications is being made by the Association Internationale des Constructeurs de Materiel Aerospacial (A.I.C.M.A.), through which standardisation within the European industry will come about. Set up in the early 1960's as a forum through which leading members of the European aircraft industry could meet and

discuss their mutual problems, A.I.C.M.A. is developing as a powerful (consultative) organisation covering the whole of Western Europe.

Working for Lucas Aerospace Limited, I am a member of the Society of British Aerospace Companies' delegation to the A.I.C.M.A. Transparent Materials Committee, and it is of interest to consider the problems facing this organisation as they affect the transparency designer.

To arrive at any measure of agreement, there has to be give and take, and a National specification which has served that particular country's industry well for many years, has to be reconsidered in the multi-National concept. Differences are often small, and decisions can be made by delegates at the meeting. However, there are cases where it may be necessary for a test method or physical property to be referred back by the delegates to their particular experts for further consideration. An example is the question of thickness tolerances. Figure 2 shows the various tolerances stated in the relevant European Specifications and the American MIL Specifications MIL-P-8184 and MIL-P-25690 against a horizontal scale of thickness. The MIL Specifications are included as a large proportion of acrylic used in Europe is of American manufacture. Also, the Committee is aware that European aircraft sold in the United States should include transparency material which is acceptable to the U.S.A.

To replace the jungle of lines with a single curve is not a practical solution. Some material manufacturers will claim that in being forced into tighter tolerances, their product will become too expensive.

Aircraft constructors will argue that, with wide tolerances, they cannot design their structures efficiently, nor produce transparencies to their required optical standards. Yet we are all aware that in their respective countries these specifications have been used to design aircraft meeting that countries particular requirements. At this time, the problem is still under consideration and has not been finally resolved.

### 3. ENVIRONMENTAL AND OTHER PROBLEMS

In general, the problems created by the environment in Europe are not unique, but the mountains of the Alps, extending into Switzerland, Italy, France and Austria, influence a major proportion of international flights and violent weather activity may be experienced at the highest operating altitudes.

Rather more a self inflicted problem, is the desire for the industry of each country to create its own brand of individuality. The nose and windshield areas of an aircraft are suitable for such treatment. Whether the expensive Italian car is liked or not, one cannot deny the eye catching profile. But where as a complex shaped automobile windshield will add little to the production cost, the same does not apply to the laminated and heated aircraft equivalent, besides complicating the technical problems to a point where performance is affected. The twin jet shown in Figure 3 however, the Piaggio PD.808, combines an impressive appearance, with simplicity, in the form of cylindrically shaped windshields.

Consider one or two problems in greater detail. Figure 4 is a photograph of the Hansa Jet, designed by the Hamburger Flugzeugbau of Germany, now Messerschmitt-Bölkow-Blohm. The forward windshields are slightly double curved, the side panels more so. These large components are electrically heated over their entire area, each forward half windshield consuming 3.55 K.W. of electrical power. The total transparency consumption of 7.6 K.W. represents a major load on the alternators. Therefore a 3 phase balanced load is essential, which complicates the design and complexity of the control system.

The construction of the forward windshields (Figure 5) is essentially a split main structural member, consisting of two plies of stretched acrylic, laminated together with an interlayer of polyvinyl butyral, and a thin outer facing ply, again using polyvinyl butyral as the laminating medium in which the electrical features are encapsulated. The original face ply was allyl diglycol carbonate, a relatively abrasion resistant material, thought to be necessary for an aircraft of high sub-sonic performance, and utilising rain clearance by wipers. All ground tests were passed with little modification, but once flight testing was well advanced, troubles began to get serious. At that time, windshield static electrification was known in Europe only as a nuisance, but has since been established to be a serious problem on many types of aircraft. In the Hansa jet it became a hazard of the highest order. This phenomenon has been investigated by Messerschmitt-Bölkow-Blohm and Lucas Aerospace, and reported at previous conferences, but if there is still doubt as to the power of this elusive force, it is now possible to demonstrate its effects under controlled laboratory conditions.

Ice crystals are known to be a major cause of aircraft electro-static problems. Lucas Aerospace operate a small wind tunnel, built into a refrigerated building, enabling the full range of aircraft icing conditions to be investigated, including ice crystals. A small flat glass windshield incorporating an electrically conducting heating element was manufactured, and positioned within the tunnel so as to be



struck by an ice crystal laden airstream as shown in Figure 6. A camera was mounted so as to view the windshield. By running the facility in complete darkness with the camera lens open, visible electrical discharges were recorded.

Figure 7 shows an edge discharge of the kind experienced on the Hansa. Laboratory tests using high voltage ground equipment showed such discharges to be capable of causing rupture of electrical windshield heating films.

Figure 8 shows two discharges which occurred within a few minutes of each other, and in both cases, the thin glass outer ply was penetrated. This second type of failure did not occur on the Hansa due to the outer ply being plastic. Plastic has a higher dielectric strength than glass.

One method of minimising the effect was to install devices within the electrical heating element supply. Another was to treat chemically the allyl diglycol carbonate to make the outer surface partially conductive. Although the treatment had the desired effect electrically, it gave rise to secondary problems. The advantage of allyl diglycol carbonate relative to acrylic, was that it had an abrasion resistant surface, but it was also somewhat notch sensitive. The chemical treatment increased the notch sensitivity in certain circumstances and cracking of face plies became prevalent. Also, the optical deterioration resulting from the treatment tended to increase with time. Many alternative solutions were tried without success, and face ply failures were becoming so frequent that they restricted the use of the aircraft. A change was therefore made to stretched acrylic, a material of low notch sensitivity. The thickness was also slightly increased, as good optical quality material was not obtainable in the identical thickness. Stretched acrylic cannot be treated to reduce its surface resistance in the same way as allyl diglycol carbonate and a return of the static hazard was anticipated. Also, it has less abrasion resistance. The aircraft manufacturers therefore instructed operators to restrict the use of the windscreen wipers, and to clean and polish the windshields at regular intervals with polish containing anti-static additives. A rain repellent system is a standard fitment.

This solution has proved to be more than satisfactory. Static is no longer any problem, cracking of face plies no longer occurs, and surface scratching is far less than anticipated.

At one stage in the programme, the windshield was changed from slight double curvature, as originally designed and manufactured, to single curvature. This move was made to enable a larger range of materials to be considered for an outer

ply, such as thin glass. The double curvature was lost entirely by sculpture machining of the edge rebate, and no change to the aircraft structure was made. In principle, we have learned to avoid double curvature for complex forward facing de-iced windshields whenever possible.

A trend in all types of aircraft in Europe, including the light twins, is to consider electrical windshield de-icing as standard. If a commercial aeroplane is to be of use in Europe airframe ice protection has long been accepted, but opening the side window was the usual answer to an iced-up windshield. Now, the windshield is considered along with the airframe; one example being the German Dornier DO 28 D2 Skyservant. This unpressurised piston engined aircraft is fitted with 2 laminated stretched acrylic windshields (Figure 9) each one incorporating an electrically heated patch of 11 inches wide by  $7\frac{1}{2}$  inches high. The heating film is vacuum deposited Sierracote 3 running at 115 volts a.c., and the small size is due to the limited power available, but it is entirely adequate for its purpose.

Nearly all heating films have the limitation of excessive light loss at very low resistances, and this restricts busbar spacing, especially when only 28 volts is available. There is no such limitation if the element consists of a matrix of fine wires as used in the windshield of the Spanish C.A.S.A. 212 light transport shown in Figure 10. The busbars are located at each side of the panel and fed with 34 amps at 28 volts.

Even busbars within the vision area are no disadvantage if they are relatively narrow. The configuration of windshield shown in Figure 11 is flying on the Westland Wessex helicopter has been found to be entirely adequate, the central busbar being affectively unseen by the pilot. The Sierracote 3 electrical heating film in this case has a total power consumption of 580 watts at 28 volts.

There are certain advantages in using high voltage a.c. rather than low voltage d.c. The magnetic compass, for instance, has a habit of always directing you to the windshields in a d.c. installation, and the currents can get embarrassingly high. Lucas Aerospace Limited, which is the largest supplier of aircraft equipment in Europe, has solved this problem and is now marketing a dual output generator for the smaller aeroplane. This unit, which is shown in Figure 12, was designed basically for the United Aircraft of Canada P.T.6. engine and in addition to electrical engine starting, provides 28 volt d.c. and 200 volt 3 phase a.c. outputs all in a single unit. The 3 phase is supplied from additional windings in the d.c. starter generator and provides up to 1.5 K. watts frequency wild a.c. suitable for windshield heating or similar resistive loads. An aircraft such as a Beech 99, can be supplied with high voltage a.c. to heat its windshields without any of the

limitations likely to be encountered using d.c., with relatively little modification to the aircraft electrical system,

#### 4. CONCLUSIONS

So, where is Europe going ? As multi-National complex aircraft projects become the norm, there will be greater stability and a determination to rationalise standards. May be this will result in a little less individuality in aircraft design, but the developments in windscreen construction, the ability to heat windshields of smaller aeroplanes and provide adequate generation; and a greater understanding of wind-shield problems will lead to advanced designs which give better value for money.

#### 5. ACKNOWLEDGEMENTS

I wish to thank the United States Air Force Materials and Flight Dynamics Laboratories for being asked to present this paper, and Messrs. Dornier A.G., Messerschmitt-Bölkow-Blohm G.m.b.H. the Association Internationale des Constructeurs de Materiel Aerospacial, the Royal Navy, the British Aircraft Corporation, Westland Helicopters Limited and my own company, Lucas Aerospace Limited for their kind assistance and permission to use their material.



Figure 1.  
Windshields and Canopy of the S.E.P.E.C.A.T.  
Jaguar.

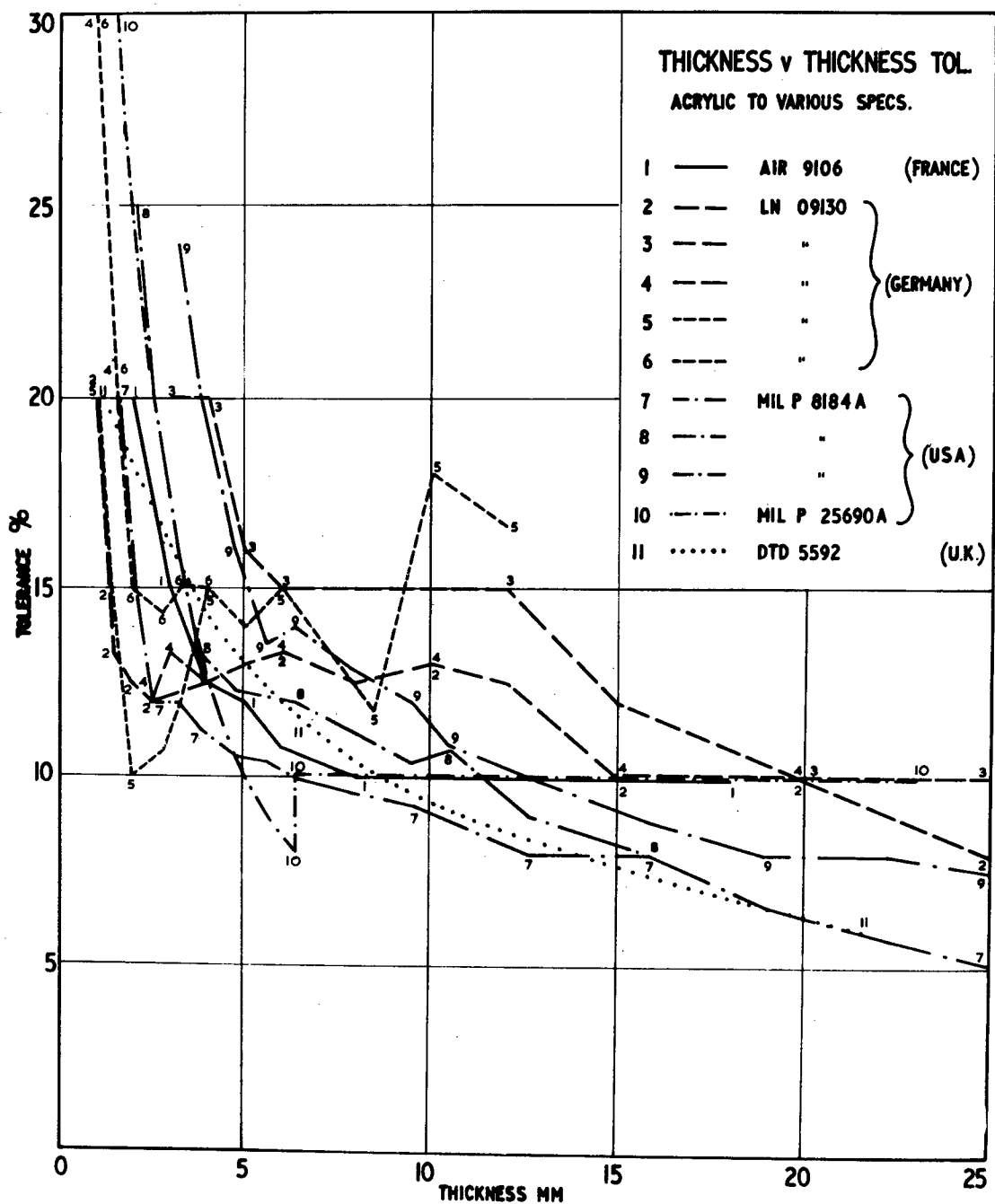


Figure 2

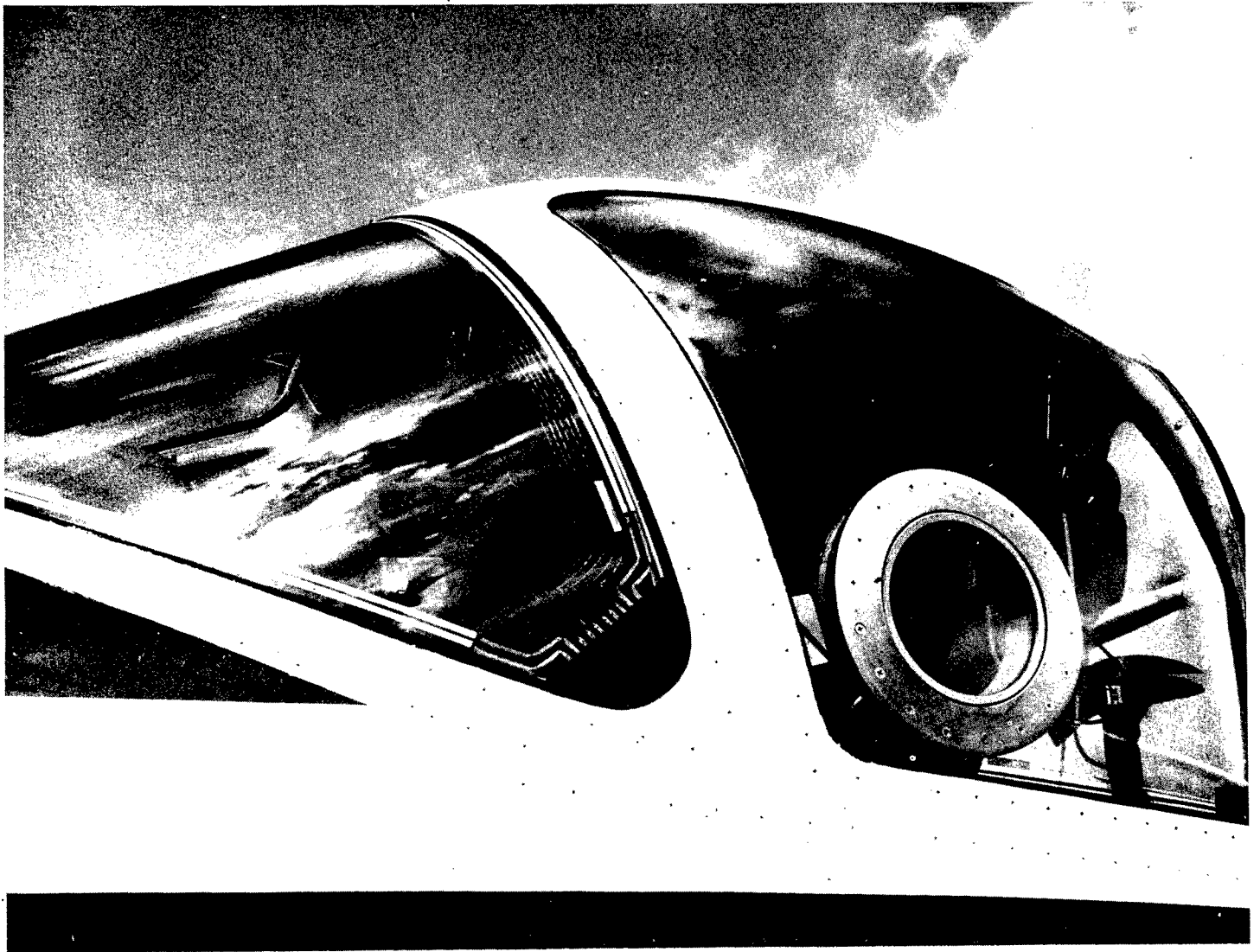


Figure 3  
Front and Side Windshields of Piaggio P.D. 808

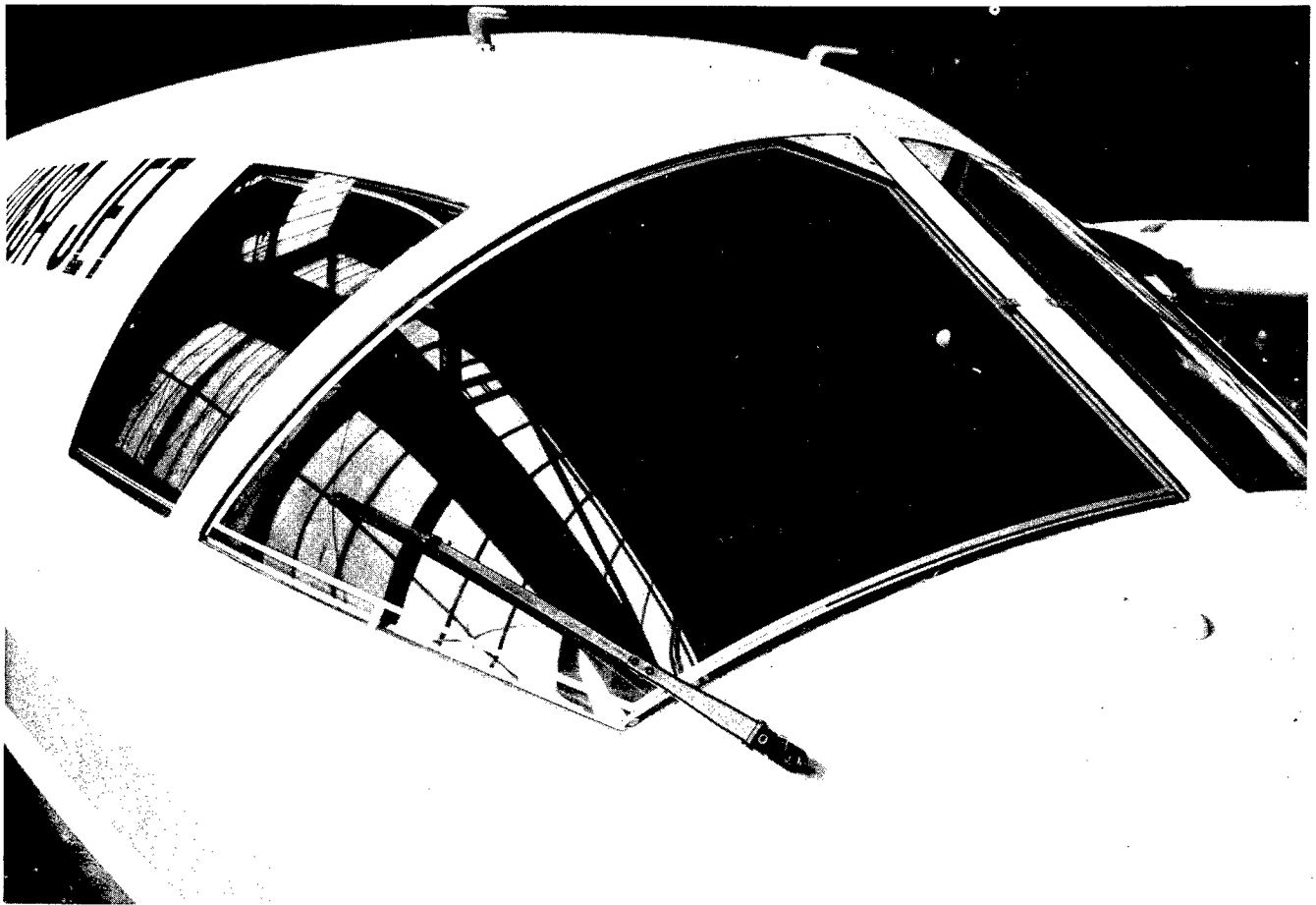


Figure 4  
Windshield area of M.B.B. H.F.B. 320 Hansa  
Twin Jet.

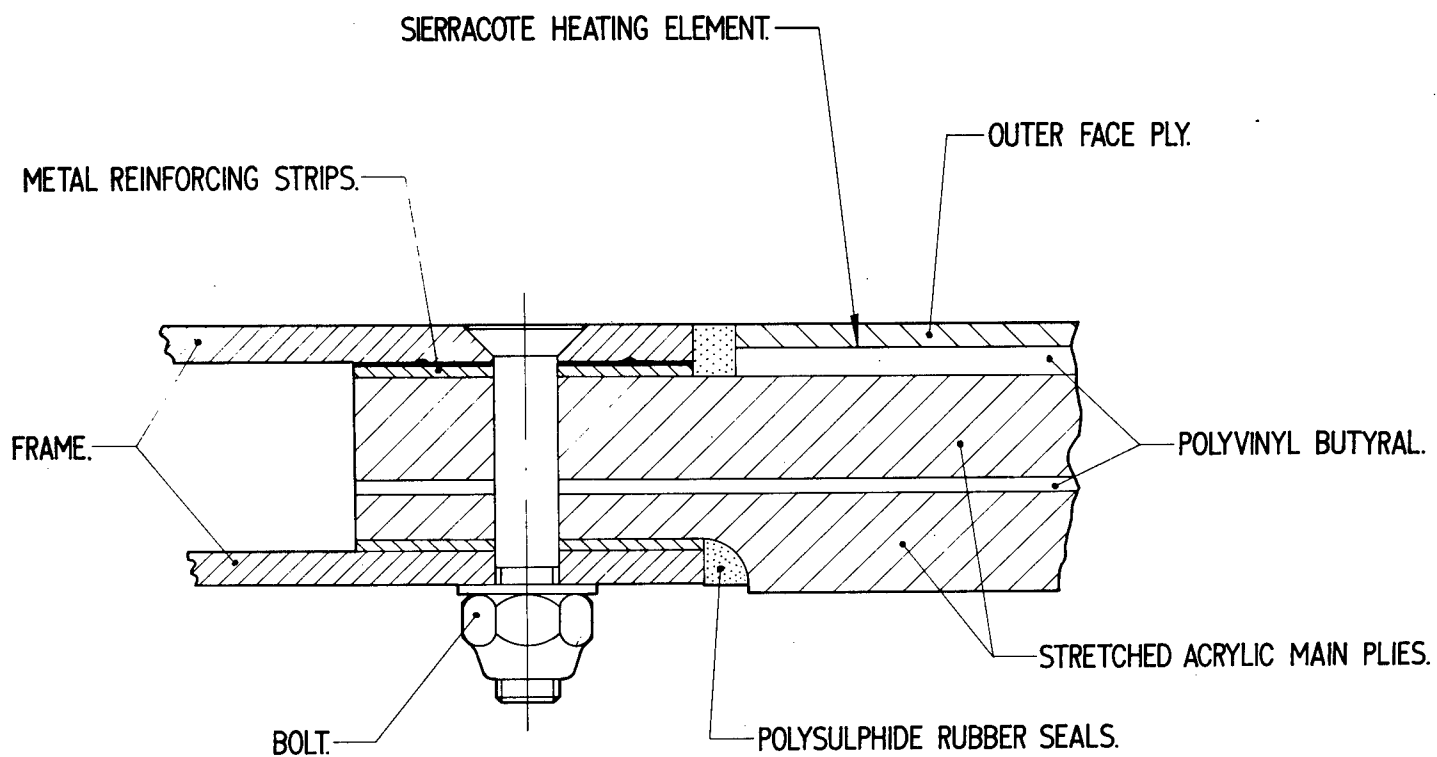
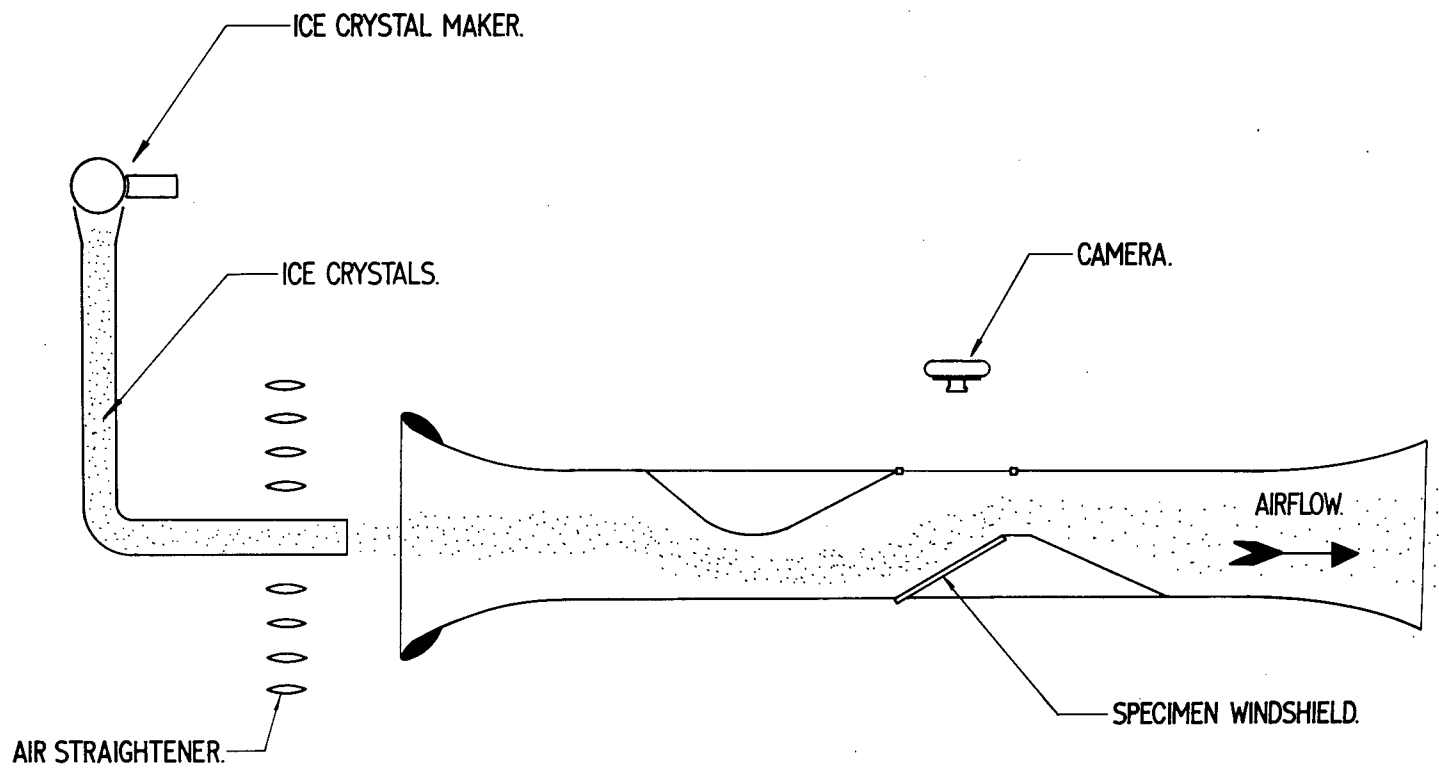


Figure 5  
Cross Section of Hansa Front  
Windshield





WIND TUNNEL ARRANGEMENT FOR WINDSHIELD ELECTRO STATIC TESTS.

Figure 6



Figure 7

Electro-static discharge from centre to edge of  
transparency specimen.

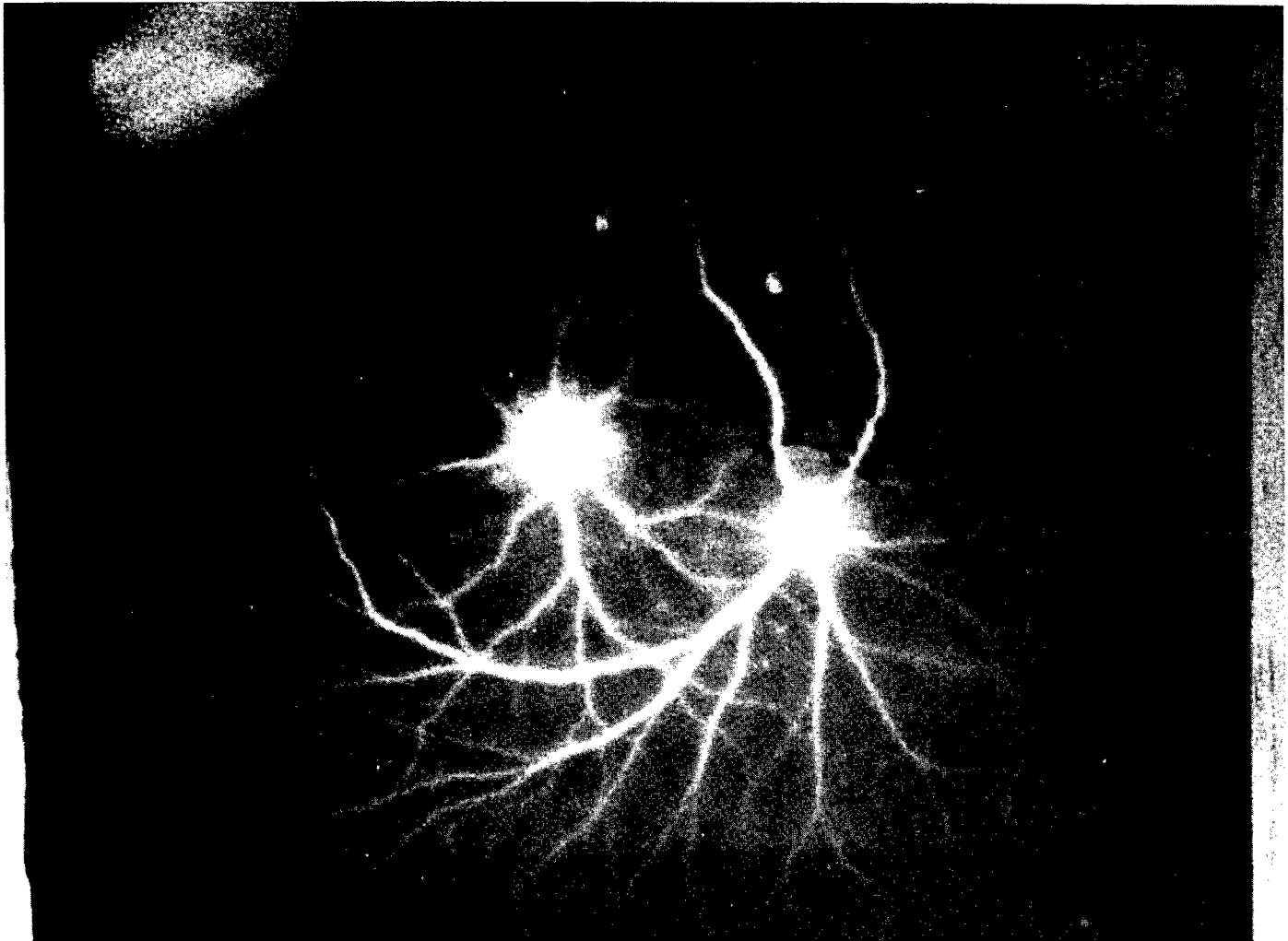


Figure 8

Electro-static discharges resulting in rupture of outer glass ply.



Figure 9

Dornier DO 28 D2 Sky Servant showing  
Windshield Heated Areas.

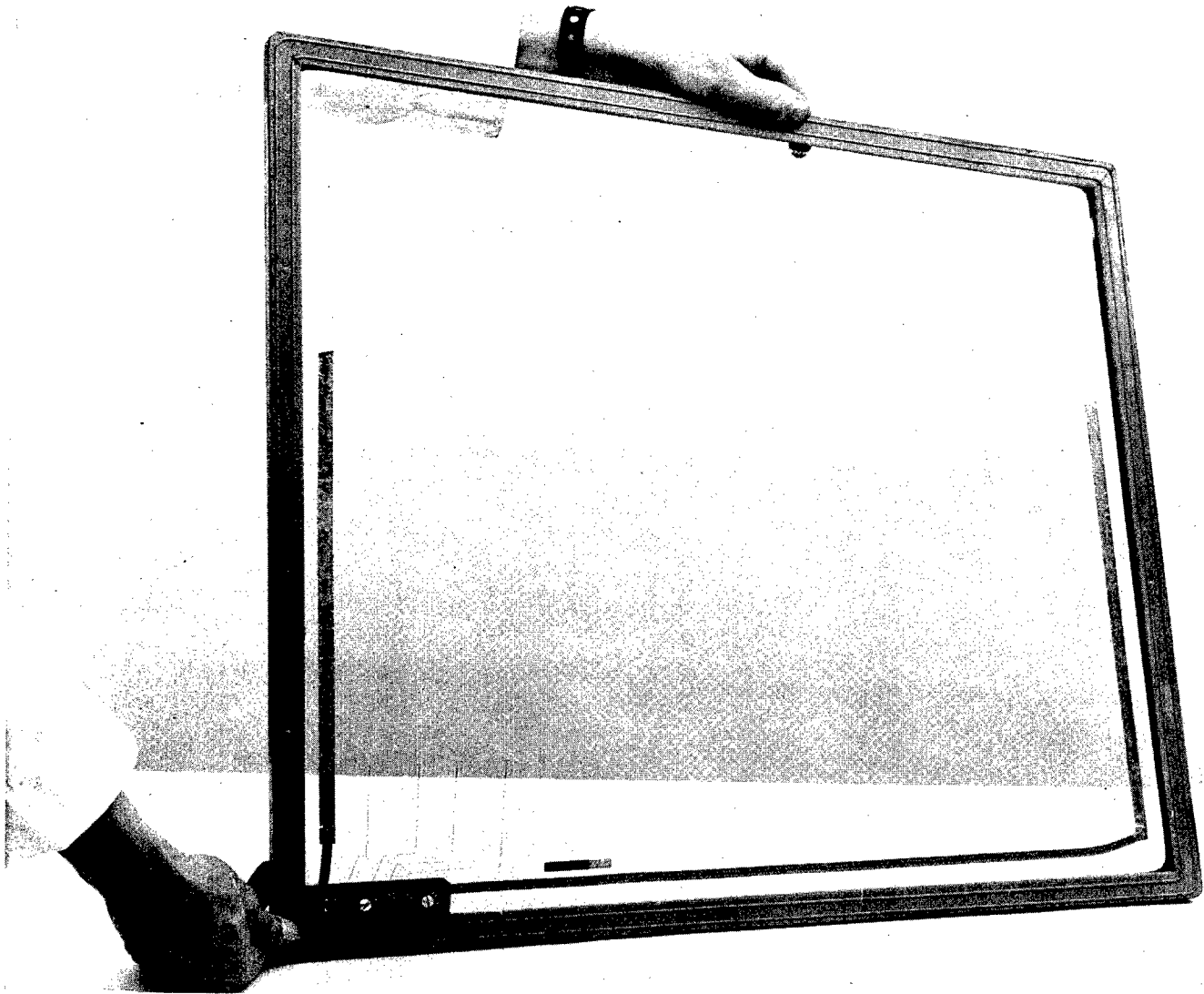


Figure 10  
Wire heated windshield fitted to Spanish  
C.A.S.A. 212

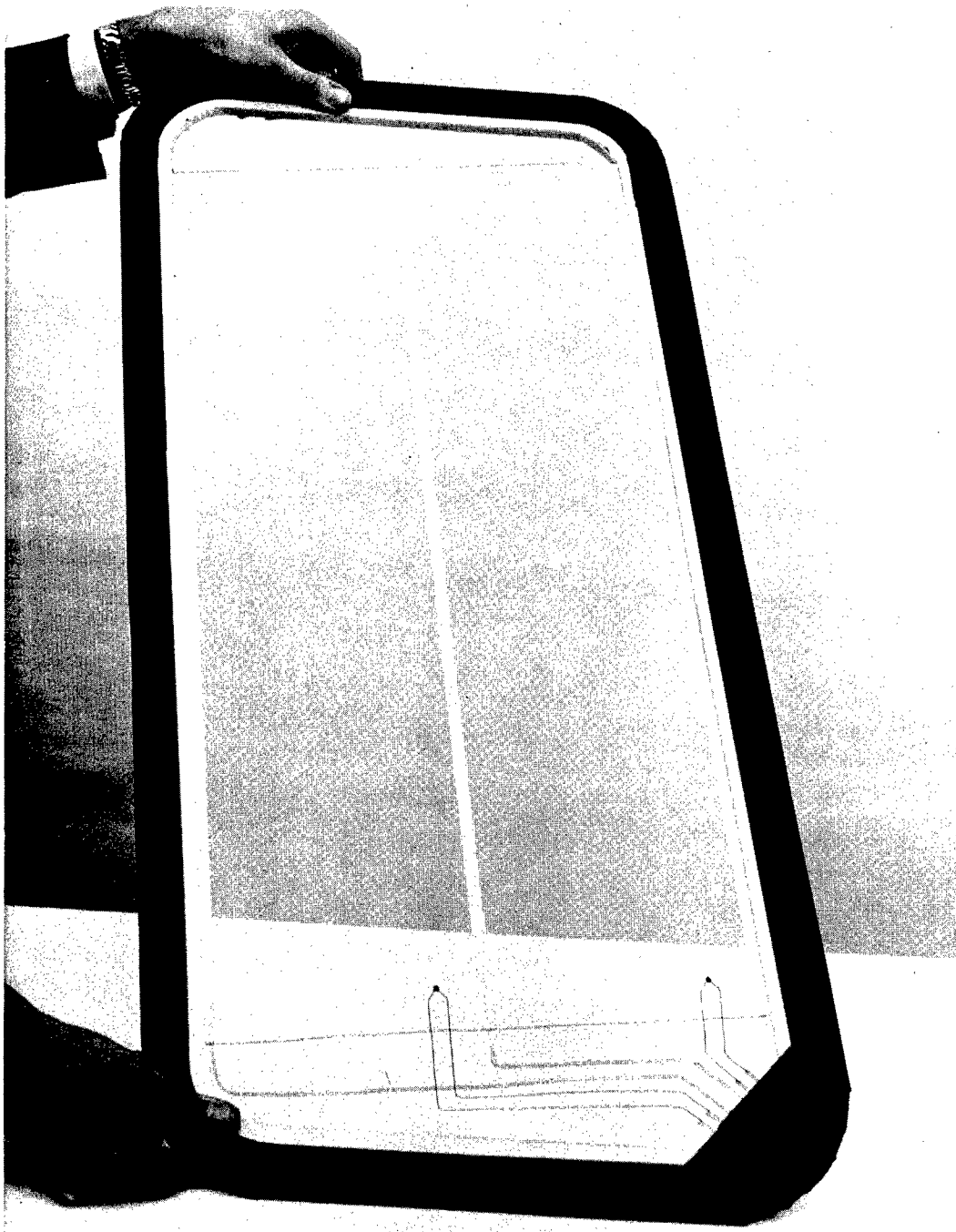


Figure 11

28 volt film heated windshield with multi busbars as flown  
on the Westland Wessex Helicopter.

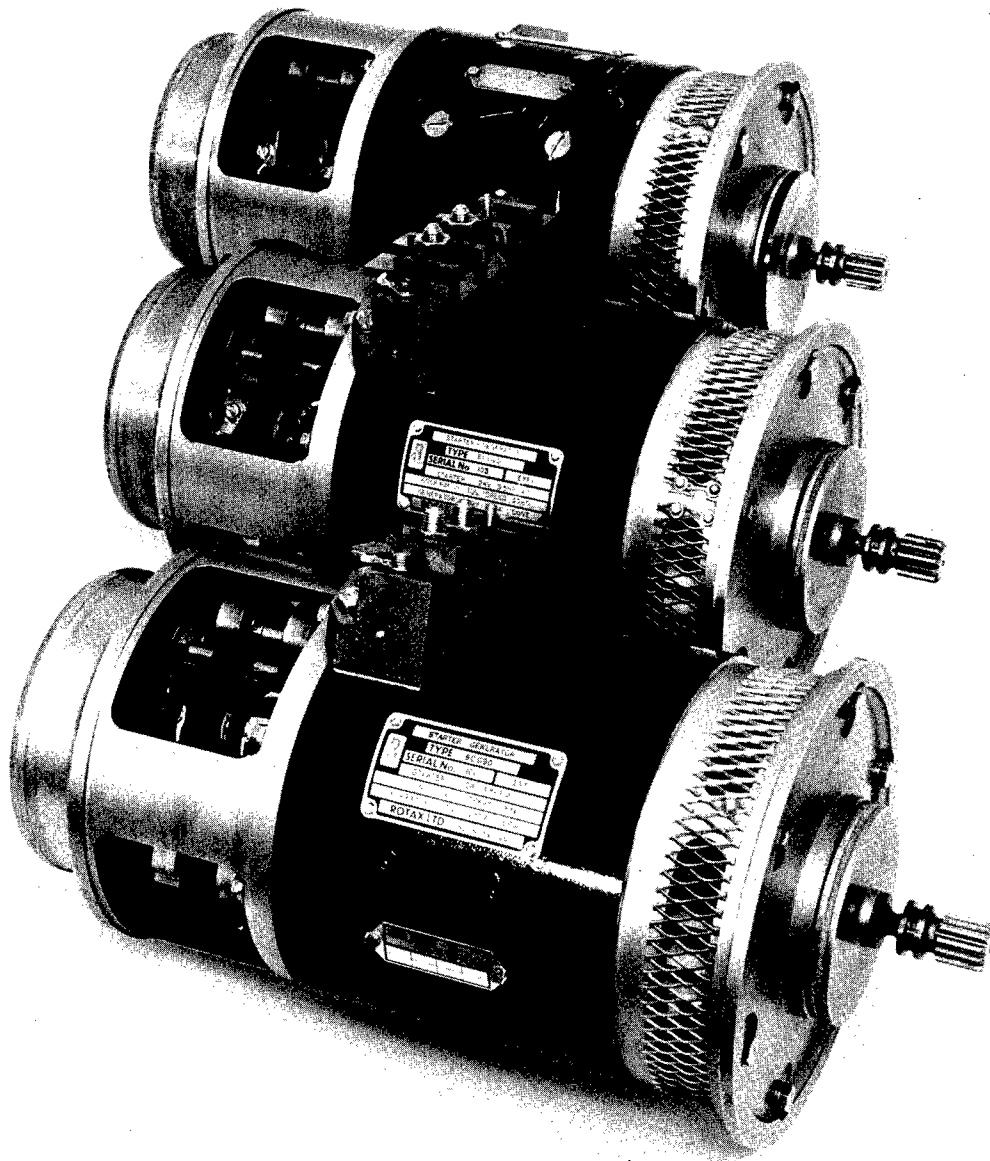


Figure 12

Lucas dual output starter/generator. This unit provides both 28 volts d.c. and 200 volts 3 phase a.c. outputs.

**A USER-ORIENTED DESIGN CRITERIA FOR  
HELICOPTER GLAZINGS**

**H. C. James  
Goodyear Aerospace  
Litchfield Park, Arizona**



# A USER-ORIENTED DESIGN CRITERIA FOR HELICOPTER GLAZINGS

H C JAMES

GOODYEAR AEROSPACE

A recent study by the Army disclosed that the average life of a UH-1 Helicopter windshield was approximately 300 flying hours.

This 300 hour life expectancy figure is obviously only a small percentage of the 2200 flight hour cyclic overhaul criteria for the UH-1 helicopter. This extremely short life expectancy drew considerable attention by the Army. As a result of this attention, the Army issued a contract for the Design, Test and Acceptance Criteria for Army Helicopter transparent structures.

The implementation of the design criteria study program was made in two major phases. The first phase was the accumulation of existing data regarding helicopter transparencies. The typical data collected consisted of drawings, performance requirements, specification control drawings and Qualification Test Procedures. In addition to this engineering data, considerable computer data was procured that listed maintenance actions regarding transparencies on several different types of helicopters.

The major source of computer data was procured from the Army's Aviation System Command Data Bank in St. Louis, but significant data was also procured from several prime helicopter manufacturers.

Another significant type of data collected was the subjective interview with the users of helicopters. These users consisted of pilots, maintenance personnel, and various levels of management personnel. The information obtained from these using personnel, although of a subjective nature, is very significant.

In order to obtain this subjective data we first made an effort to establish a good communication with the pilots and maintenance personnel. Then once this rapport was established we requested permission to document the interview with a small portable tape recorder. We were pleasantly surprised at the ease with which the majority of the personnel accepted the tape recorder. These taped interviews were then brought back to our facility and the data was then manually documented and tabulated for analysis.

This tabulated data, both objective and subjective types, then became the guidelines for the helicopter transparency design considerations.

The design considerations were then broken down into three major design groups.

These three design consideration groups were: 1 - Primary Design Considerations; 2 - Inherent material properties, and 3 - Management design considerations. The first group, the primary design considerations, are the properties that will be established through the basic mechanical design effort. These properties or charac-

teristics are established by the mission and performance planned for the helicopter as well as design arrangement, and can be changed over a given range by the designer. These considerations or characteristics include the following:

1. Optical performance
2. Abrasion resistance
3. Ease of maintenance
4. Installation and removal technique
5. Fail safe construction
6. Crashworthiness/safety
7. Reliability
8. Life cycle cost
9. Total weight
10. Structural integrity

The second group, the inherent material properties are the design characteristics of a material. These properties have established values for specific materials under fixed conditions and include:

1. Mechanical physical properties
2. Abrasion resistance
3. Fracture resistance
4. Chemical resistance
5. Ballistic spall
6. Resistance to thermal shock
7. Heat transfer
8. Fire resistance
9. Specific weight
10. Static discharge
11. Coefficient of thermal expansion
12. Optical properties including index of refraction luminous transmittance and haze

The third group, the management design considerations, are involved with attributes that are of an add-on classification. Their addition or omission is dictated essentially by the mission of the helicopter and the corresponding increased cost to implement the considerations. These considerations are:

1. Radar reflective coating
2. Birdproofing
3. Anti-reflective coating
4. Rain removal techniques
5. Defogging/de-icing techniques
6. Abrasion resistance improvement
7. Polarization

## PILOT & MAINTENANCE PERSONNEL PROBLEMS

Since this report is entitled a "User-Oriented Design Criteria for Helicopter Glazings", I would like to mention the problem areas regarding transparencies as reported by the using personnel. Then perhaps I can mention a few approaches toward the solution of these problems.

### 1. SCRATCHES & ABRASIONS

The foremost problem encountered regarding helicopter glazings in the field was the frequency and magnitude of scratches and abrasions on plastic transparencies.

These scratches and abrasions are caused primarily by windshield wipers, hand wiping dry, wiping with improper materials, opening and shutting sliding windows with an accumulation of dust or grit on rubbing strips and the use of sliding window friction locks. This type of window lock results in an abraded area which is equal in width to the diameter of the friction lock and as long as the travel of the window. This heavily abraded area is more distracting to the pilot than a designed opaque area.

The use of windshield wipers on the surface of any currently existing transparent material other than inorganic glass will cause wear to the surface which should receive greater attention in design than it has received in the past. The investigation suggests the possibility of at least three different approaches to solution:

- a. Replace the windows with glass or laminate glass to the surfaces. Penalties will be paid in weight, initial and replacement cost, shatter resistance, and formability.
- b. Re-evaluate the need for windshield wipers. There were many instances in which the wipers were made inoperative without apparent compromise to the vehicle's utility. To illustrate this point, more than one unit commander in the field has ordered the windshield wipers made inoperative.
- c. Establish a design with the plastic material, with or without abrasion resistant coating, which MTBF and cost trade off studies determine to be most advantageous, design for convenient transparency replacement, and establish set intervals at which the transparencies are to be replaced.

### 2. CRAZING OF PLASTICS

Crazing of acrylic is another problem area that using personnel complain about frequently. Crazing may be defined as very fine cracks which may extend in a network over or under the surface or through a plastic. These cracks gradually enlarge with continued application of load. Crazing is frequently quite difficult to discern except when viewed at varying angles to the incident light. It is most prevalent with construction, using as-cast acrylic and especially that which doesn't have some cross linking to meet MIL-P-8184. Extended exposure to service environment combined with a constant stress condition which may be a residual from the forming operation or a function of the design and/or installation are primary causes of crazing.

It should be noted that crazing is an irreversible property. One might note that the visible evidence, i.e., the detection of the minute "fissures" by reflection, may disappear. However, the crazing is still existent even though the visible evidence is not discernible.

### 3. FRACTURE RESISTANCE OF MATERIAL

The third most frequently mentioned area of concern to using personnel was that of fracturing of the transparencies.

An analysis of the computer data obtained from the several sources previously mentioned shows that a high incidence of repair and replacement actions documented for helicopter glazings were identified in the chipped, cracked, and broken classifications. It is felt that these service failures are as sensitive to design control as to material specification control. The fracture resistance of presently used glazing materials is not likely to increase in the near future. Design attention to improvements in edge attachments, glazing material and thickness selection, processing for minimized internal stress, and field installation methods offer promise of reducing the incidence of fracture related failures. Accidental damage incurred during field service will likely maintain a high level of chipped, cracked, and broken classification actions. Improper installation techniques, tools dropped through glazings, flying debris, inadvertent impacts while loading cargo, or from troops wearing back packs will continue to result in such damage. There are significant differences in the fracture resistance of the various materials used for transparencies. Glass is particularly subject to breakage. A significant improvement over glass is achieved with acrylic and particularly when the acrylic is stretched in accordance with MIL-P-25690, it significantly increases fracture resistance. Polycarbonate has the greatest resistance to fracture of all common helicopter glazing materials.

### 4. HEATED TRANSPARENCIES

The next problem area I would like to mention is the problems relative to heated windshields. Current helicopter windshields are heated utilizing two different basic techniques.

The first technique is the use of a hot air blast, utilizing turbine bleed air as the source. This technique is utilized on the AH-1 Cobra.

Either through a malfunction of bleed air valves or pilot error in operation of the controls, severe distortion and warpage of the center windshield takes place through the overheating of the acrylic windshield. It might be well to note that at least two military helicopter bases, it was common practice by the maintenance personnel to add a heat resistant plate immediately adjacent to the outlet of the heat duct. This heat barrier does help prevent the warpage of the center windshield.

The second technique of heating transparencies is the electrical heating procedure whereby a conductive film is made a part of the laminated assembly.

Heated transparencies of laminated construction have a notoriously short life span. The computer failure mode data for one specific helicopter showed that in excess

of one-third of all failures requiring replacement, were attributable to delamination. The mean time between failures for these windshields was computed at 259.5 hours. The reliability analysis by the prime contractor stated that due to the poor reliability and high cost of the windshield assemblies, aircraft are flying with window assemblies in a degraded state that should be replaced. There has been no attempt to adjust the MTBF of 259.5 hours to reflect this condition. During the data collection period of the study program, it was observed on several occasions that delaminated windshields were in aircraft that were still on a flying status.

The problems that frequently arise from this type of construction is a bubbling of the interlayer and or a delamination of the assembly. This delamination of the assembly manifests itself as a milky translucent area that frequently begins in the area of the electrical bus bar connections.

The delaminated areas gradually grow in area until replacement is mandatory due to the reduced optically clear area.

Repairs of these delaminated areas are not practical. Therefore it becomes necessary for a complete replacement program to be initiated.

An interlayer retaining good flexibility and bonding properties is desired to laminate such dissimilar materials. Interlayers in sheet and cast-in-place systems have been used for such purposes. A variety of materials, including PVB, polyesters, epoxies, silicones, and polyurethanes have physical properties which may be able to maintain laminate integrity when subjected to thermally induced stress. There are a considerable number of interlayers, most of which are considered company proprietary, used for laminating heated and nonheated windshield composites. Intensive interlayer development efforts have been undertaken by a number of companies. Significant improvements in interlayer technology has already resulted from these programs. Cast-in-place silicone and polyurethane systems are currently favored for most applications. Improvements in physical properties, adhesion to substrates and processing techniques have combined with advancing windshield design technology to produce better performing, longer-life products.

## 5. REFLECTIONS

The fifth area of concern is one of reflections. Reflections are also divided into two basic problem areas. The first problem area I would like to mention is the visual acquisition of a helicopter from the glint or glare as reflected by sunlight from the transparency toward personnel outside of the helicopter. Reduction of this glint or glare is an important survivability factor for helicopters in a combat area. Visible flash can reveal the approach of an aircraft long in advance of engine/rotor noise or, in case of low flying helicopters, radar. This problem is obviously most significant to combat vehicles and is not a consideration for a wide variety of designs.

The other problem area regarding reflections is the one of internal reflections which are distracting to the pilot. And a serious consideration in all designs. The source of these reflections are the instrument light, map lights and any other light source in the cockpit area.

One particularly disturbing reflection phenomena that was encountered in the study program and was reported by several pilots was the reflection directly into the pilots eyes of a light source on the ground. This phenomena occurred when the helicopter was in level flight at night and in passing directly over a light source the light was transmitted through the chin bubble and then reflected off the windshield. This gave the pilot the illusion of a light source directly ahead in his line of flight.

The use of laminated windshields add to the reflection problem. The gold conductive films used in heated windshields were a source of many comments by pilots regarding the impairment of night vision.

Anti-reflective coatings have been used for many years on camera lenses, optical windows, instrument faces, etc. Difficulties exist in applying the technology developed for coating these relatively small glass surfaces to larger contoured substrates. The deposition of magnesium fluoride and related materials requires higher processing temperatures than most plastics can accommodate.

The most promise appears to lie with several new coatings which have resulted from recent development efforts. At least one such coating has been applied to UH-1 windshields and AH-1G cockpit coated transparencies are being tested at Fort Hood, Texas.

The results of these evaluations will establish the relative merit of such coatings. The test articles are coated on both internal and external surfaces. The external aircraft environment is quite different from and much more severe than the internal environment. Coating durability has traditionally been a problem with anti-reflective coatings subjected to the rigorous aircraft environment.

Results to date indicate there is a long way to go in developing the coatings. They must be significantly more effective and be more durable before they are really effective.

## 6. INSTALLATION & REMOVAL TECHNIQUES

I have briefly mentioned the need for consideration of ease of replacement of transparency assemblies. This item was a constant source of complaint and adds significantly to the "cost of ownership" of transparencies.

The replacement of windshields and bubble canopies requires specialized skills and techniques. Data analyzed for the number of maintenance manhours required to replace a UH-1D windshield helps demonstrate this fact. A windshield replacement at a repair facility which performed this function one time required a total of 40 manhours. The same replacement required only 5 manhours at a more experienced repair facility which had performed 28 such actions.

The present trim and drill to fit requirements are dictated by deformation occurring in the framing structural members due to flight loadings as well as the ship-to-ship variations found in new aircraft.

A more efficient installation and removal technique will rely primarily on the innovative design of a more universal glazing to frame fit and attachment concepts.

## SUMMARY

To briefly summarize, I have touched on the following design considerations:

1. Abrasion and associated protective coatings
2. Crazing
3. Fracture resistance properties
4. Heating techniques
5. Internal and external reflections
6. The dire need for much greater emphasis on ease of replacement by the designer.

You will probably notice I have left out any direct reference to probably the most important characteristics that would apply to a helicopter windshield. That characteristic is the optical properties.

During the study program, the absence of complaints from the pilots of optical problems relating to new transparencies indicates that even the lowest current acceptance level for optical quality fulfills the functional requirements. This absence of complaint was maintained in the face of direct questioning and pointing out of examples for comment. It is therefore concluded that the most liberal optical standard being currently used is adequate for helicopter glazings.

To wind this review up, I believe all of you people are familiar with the present trends in advertising and public relations as exhibited on television. I have particular reference to the Ford Motor Company's slogan of "We Listen Better." I sincerely believe that we in the aircraft transparency business should do a little "listening better" to the transparency user.

OPTICAL REQUIREMENTS FOR AIRCRAFT  
TRANSPARENCIES

N. S. Corney  
Ministry of Defence  
London, England



OPTICAL REQUIREMENTS FOR AIRCRAFT  
TRANSPARENCIES

N.S. CORNEY B.Sc, Ph.D, F.R.I.C.

PROCUREMENT EXECUTIVE, MINISTRY OF DEFENCE  
UNITED KINGDOM

ABSTRACT

A paper given at the SBAC Symposium in London June 1971 outlined the principles governing satisfactory vision through aircraft transparencies and summarised the methods in general use for evaluating the parameters associated with vision. The present paper reports progress in this field and invites comment on the work in hand.

The parameters which have been established are optical resolution, optical transmission, distortion, double imaging, minor scratches and inclusions etc. These parameters must be assessed with the transparency mounted at the installed position relative to the users eye position, and there should be no deterioration in quality when de-icing or de-misting equipment is in use.

For the guidance of designers, aircraft transparencies are allocated to broad categories according to the optical function of each. For example one category includes forward facing panels or areas thereof requiring very high precision, and another category includes side panels with less stringent requirements; in drawing up these categories no distinction has been made according to the materials of construction.

Current work in progress includes the allocation of limiting values of the parameters for satisfactory performance of transparencies of each of these categories. A number of methods for determining these parameters are being assessed prior to recommendation.

Problem areas associated with this work are highlighted e.g. that of quantifying the experience of pilots and observers, and that of determining the acceptable limits of the parameters consistent with the requirements of good performance and economy in fabrication and inspection.

## 1. INTRODUCTION

In an earlier paper<sup>(1)</sup> the need for a rationalisation of the optical requirements for aircraft transparencies was stated, and a review was made of the methods available for assessing the parameters associated with the visual performance of such transparencies. Progress in this work can now be reported together with an attempt to assess standards of optical quality of aircraft transparencies related to the tasks for which they are used.

It is inevitable that the structural requirements for transparencies should receive prior consideration in aircraft design in view of their role in determining the safety of the aircraft. Nevertheless transparencies while satisfying structural requirements must also meet certain optical requirements in order that the mission of the aircraft, whatever it may be, is successfully accomplished. In spite of modern electronic aids, there is still a demand even in military aircraft, for increased vision area and improved quality of vision. This demand is producing new transparent materials of higher strength, lower density and improved quality of transparency, and it is the belief that alongside the developments of improved materials and progress in design philosophy must be an improved understanding of the factors associated with good vision and progress in the means of achieving improved performance of optical transparencies.

While it is not difficult to define the parameters which are associated with good vision, it has proved exceedingly difficult to allocate numerical values to these parameters which although ensuring high quality of vision, exceed the bounds of cost effectiveness. The balance of superlative quality against cost of fabrication and inspection must always be considered. With economy of effort in mind our aim has been to establish suitable methods for measuring these parameters and then to determine numerical values of each which will ensure satisfactory performance of a transparency in a number of roles associated with military aircraft. It is believed that many of the demands of civil aircraft may also be satisfied by this analysis.

## 2. OPTICAL PARAMETERS ASSOCIATED WITH AIRCRAFT TRANSPARENCIES

The parameters which influence vision through a transparency are listed in Table 1 and are grouped according to their effect on acuity, accuracy and efficiency of vision. Also in the table are shown the effects of neglecting each of these factors. In the following sections, each parameter is discussed in detail and the currently recommended method of measurement is outlined.

### 2.1 Optical Resolution

This may be defined as the ability to distinguish clearly between two objects which subtend some small angle at the eye. A transparency used by a pilot or observer engaged in reconnaissance duties for example should not

cause a degradation of the resolution. In the past this parameter does not appear to have been generally specified, however recent experience, particularly with some stretched acrylics would seem to indicate that some control is required. The generally accepted practical limit of resolution of the eye is 1 minute of arc under conditions of good illumination. Such experience as we have been able to accumulate indicates that this limit is quite easily attained with windscreen and side screen components of glass fabricated by the normal procedures. In common with most other factors reviewed in this paper, optical resolution is considered at the pilot's or user's normal viewing angle.

Originally we surveyed the possible methods of determining optical resolution on the basis of techniques used for lenses. Further experience has shown that the use of Cobb charts or the photoelectric method proposed earlier is not entirely practical and instead a slight modification of the telescope and collimator method used for absolute deviation is now proposed; the procedure can be used in conjunction with the scanning method used for absolute deviation so that only a little additional effort is involved in the inspection of a transparency for optical resolution. In this method (Figure 1) the collimator has a graticule with a double cross, the lines of the cross subtend an angle of 2 minutes of arc centre to centre, the lines are each 1 minute thick and therefore are separated by a space of 1 minute. The transparency under investigation is introduced between collimator and telescope and is scanned by movement of the panel. Any deterioration or fading of the double cross represents some deterioration in resolution from the 1 minute of arc level. If the limit is taken as the point where the lines of the cross cease to be recognisable as double lines then the interpretation becomes easy. It should be emphasised here that inspection of a transparency for resolution should be carried out from the user's normal eye position.

## 2.2 Optical Transmission

This is defined as the intensity of light emerging from the transparency for reception at the eye of the observer compared with the intensity of light incident upon it. Losses are due to absorption within the materials involved and reflections at the various interfaces where there are changes of refractive index. High light transmission is of particular importance when flying under conditions of low light level, or when observing objects under conditions of low contrast. For this reason it is now considered essential that measurements of optical transmission shall be made with transparencies mounted at the viewing angle, and not at normal incidence as has been the practice in the past.

The matter of colouration of transparencies arising from the use of electrically-conducting heating layers or even of deliberate "tinting" of the material to reduce the glare from strong sunshine, is an interesting topic which has been discussed in great detail by Clark<sup>(2)</sup>. He concludes that the effects of "tinting" can produce hazardous losses in visual

performance under conditions of twilight or night flying. The colouration which results from the use of some electrically conducting layers is also considered to be too dark for optimum visual performance in dim light, although quite clearly a balance has to be struck between this and the greater hazard which arises from misting or frosting of forward facing transparencies. There is obviously a considerable incentive towards the use of colourless heating films to improve visual performance under all conditions.

The allocation of minimum acceptable values of transmission for transparencies has proved to be a difficult task. Clark<sup>(2)</sup> recommends that all windows used by a flight crew should have a luminous transmittance as high as possible namely for CIE Illuminant A not less than 85%. Alternatively he suggests that for suitable signal visibility, the transmittance at any wavelength between 450nm and 680nm should be not less than 80%. Even accepting that these values are quoted as being measured normal to the transparency it seems unlikely using materials currently available whether these aims could be met for any transparency having bird impact resistance capability and de-icing film. Under our requirements where transmission is to be measured at the viewing angle we believe that a value of 55% transmission is the minimum acceptable consistent with the properties of materials available and the demands imposed by aerodynamic considerations with respect to forward facing transparencies.

The method (Figure 2) for light transmission measurements being recommended is fairly standard. A tungsten filament lamp operated by a stabilised power supply to meet the conditions of CIE Illuminant A is used with a photometer having a spectral response corrected to approximate to that of the human eye. The measurement is an integration of the light transmission over an area of at least 1cm<sup>2</sup>, the photocell having a comparable sensitive area. The percentage transmission is determined by measuring the decrease in the photocell response when the transparency is inserted in the light beam; prior calibration of the photocell response is required for this method. Alternatively the source-photocell distances may be compared before and after inserting the transparency in the beams and adjusting these distances to give the same photocell response in both cases.

### 2.3 Haze or halation

An obscuration of view or the spreading of an image beyond its proper limits can be caused by the scattering of light from tiny particles within the material or defects on the surface of the material. This has been known to occur from the deterioration of interlayer materials or from lack of surface polish. The presence of haze may affect resolution; alternatively the phenomenon may merge with that of minor defects and scratches discussed later.

The ASTM D 1003-52 method for the measurement of haze is well known. An alternative, rather simpler method has been found to be satisfactory; a measurement of the total transmission (a) is made with the transparency in

contact with the aperture of the integrating sphere. A second measurement (b) is made with the transparency moved away from the aperture a distance equal to the diameter of the sphere; the scattered light in this instance will fall outside the sphere aperture and will not be measured. The percentage haze is given by  $\frac{a-b}{a} \times 100$ . In this measurement the plane of the transparency is normal to the incident light, a situation which is almost unavoidable in view of the difficulty of measurement. Figure 3 illustrates both methods.

#### 2.4 Optical Deviation

On passage through a transparent panel, a ray of light can suffer a linear displacement within the material (which can be considerable if the panel is thick) and an angular deviation on leaving it, due to departure from parallelism between the two surfaces ("wedge"). This angle (designated "optical" or "absolute" deviation) between the true and the apparent direction of an object viewed through the panel is a function of the angle of incidence, the thickness of the panel and, if a curved panel is considered, the radius of curvature at the point of incidence.

Quite clearly the value of the optical deviation is important to a pilot as it might lead to misjudgement of the position of the aircraft relative to the ground or some object. In weapon aiming also the value of the deviation must be known if accuracy of aiming is to be achieved. For high quality transparencies, variation of the optical deviation over the whole area of a panel must be rigorously controlled in order to avoid distortion of the image received and to prevent binocular deviation both of which are discussed below. For a flat panel perfect parallelism of the surfaces would eliminate optical deviation and distortion; these cannot be completely eliminated for a curved panel although increasing the radius of curvature diminishes the effect.

In British specifications there has always been a requirement that optical deviation should be determined with respect to the designed eye position because of the variations which can occur with angle of incidence etc. The collimator/telescope method is recommended for measurement in view of the precision and amount of information which can be obtained by this method; furthermore it appears to be the only method which enables the optical deviation to be measured with respect to the pilot's eye position. Once the equipment is set up, the method of assessment is relatively simple and less time consuming than many of the other methods which are available especially those which require interpretation of results from photographs of grid-boards.

In the method adopted (Figure 4), collimator and telescope are aligned, the collimator having in its focal plane a black cross on a transparent ground (or a double cross as above if a simultaneous check on resolution is to be carried out). The telescope is arranged to have a magnification of about 15 and in its focal plane is a black cross with concentric circle or circles with diameters corresponding to the limits of deviation to be measured. When viewing through the telescope the illuminated graticule in

the collimator can be seen in the centre of the telescope graticule. When the panel under investigation is placed between collimator and telescope optical deviation will result in movement of the collimator cross as seen in the telescope. The magnitude of the deviation can be estimated by the movement in relation to the concentric circles. As the image is viewed at infinity distance, the method gives the absolute optical deviation. The supports for the panel are arranged to rotate about vertical and horizontal axes, both axes passing through the point which is the designed eye position. The area of the panel may be scanned by a series of horizontal and vertical traverses the angle of separation between each traverse being not greater than three degrees.

## 2.5 Optical Distortion

Variations in the "wedge" over the area of a plane panel, or in radius of curvature of a curved panel will bring about a lack of truth in the apparent shape, size or position of objects viewed through the panel, i.e. the occurrence of optical distortion. The effect which distortion can have on the misshaping of an image is psychological and therefore difficult to specify. The image of a grid board may appear very distorted but the average open scene viewed through the same transparency may hardly appear to be distorted because of a lack of known straight lines to form a basis of judgement. If the only consideration is visual effect, quite a high degree of distortion can be tolerated; however sharp changes in deviation can be disturbing as an image appears to jump as it traverses the panel.

Ideally, optical distortion of a panel could be precisely estimated by measuring the optical deviation over a lattice formed by very closely spaced traverses of the panel although this would be very time consuming. A widely used method of displaying the distortion of a panel consists of photographing through the panel a grid board about 5m distant from the panel, the camera being at the designated eye position. By making a double exposure with and without the panel in position and then preparing an enlarged print from this photograph a numerical estimate of the distortion can be made from the slopes of the lines of the image formed when the screen is in position.

It has been found that this method and variants upon it can become extremely time consuming if the inspector has to measure the slopes of hundreds of lines in order to assess the quality of the panel. In many cases qualitative assessment of a photograph may be sufficient to satisfy the requirements as to quality of distortion. For more stringent requirements we are hoping to provide a simple method of examining a suitable photographic method.

## 2.6 Binocular Deviation

This is defined as the difference in deviation of two parallel incident rays which for this application are considered to be 6.4cm apart in a horizontal plane, this being an average spacing of the human eyes. The concept was introduced in the past as a particular aspect of distortion, to ensure that vision through a panel did not result in eye fatigue. It is

known that the human eyes are capable of convergence, divergence and 'supervergence' (movement in a vertical plane) to a certain extent to counteract double vision. The least tolerance is available in the vertical plane and upon this is based the limit in British military specifications that binocular deviation must not exceed 10 minutes of arc. As noted above very stringent control of parallelism of a flat panel could prevent the occurrence of binocular deviation, and measurement of optical deviation on a sufficiently fine lattice would offer an inspection method. In fact the only method (Figure 5) recommended for measurement of binocular deviation is a modification of the collimator/telescope procedure already described. A suitable collimator system with graticule consisting of an opaque disc of angular dimension 10 minutes of arc at the centre of a cross, is arranged to provide two parallel beams 6.4cms apart; a large collimator with mask, twin collimators or single collimator with beam splitter will be suitable. In the absence of a panel these parallel beams enter a telescope system and appear superimposed in the focal plane of the telescope. The telescope is of sufficiently large diameter to accommodate a mask with apertures 6.4cms apart or is provided with a beam splitter to merge the incident beams. When the panel under investigation is placed in the light beams, a difference in deviation will cause the images to overlap until the binocular deviation exceeds 10 minutes of arc in which case they will separate. As before the support arrangements are such as to allow rotation of the panel about vertical and horizontal axes, both axes passing through the point which is the designed eye position of the panel. A scan of the whole vision area of the panel may be carried out as before.

## 2.7 Double Imaging

At an angle of incidence other than normal, internal reflections within even a simple panel will cause a secondary image to emerge from a different point on the panel to that of the primary image. With a multi-laminate panel multiple images may be formed although these images may not be separable unless one or more of the following conditions prevail:- the objects viewed are very bright, the panel is thick, and the angle of incidence is high. A particularly disturbing manifestation of this phenomenon is the appearance of multiple images of landing lights; the separation of images is magnified at higher values of the optical deviation. As far as is known, special provision for the prevention of multiple images has not been called up for aircraft panels except for the Concorde where stringent control of optical deviation has been applied in order to reduce the effect. It is interesting that a method for measuring double imaging has been provided in an official British Specification<sup>(3)</sup> for land transport, and alternative methods have been published more recently<sup>(4)</sup> involving more complicated equipment. In the present application a variant of the collimator/telescope method has been proposed but not yet tried out in detail.

## 2.8 Minor Optical Defects such as Scratches and Inclusions

Most materials of construction of transparencies contain a number of imperfections such as bubbles, and moreover foreign matter can be included

in lamination and fabrication processes. The detection of such defects relies very much on the method of illumination of the panel and the eye of the observer. During service, scratches certainly appear on the surface of aircraft panels, and the level at which these become acceptable appears to rest on the personal judgement of the pilot concerned or user of the panel. In setting up standards for acceptance it is important to bear in mind the task which the user must fulfil, and the noticeability of the defect i.e. its likelihood of causing distraction, close focussing or its ability to cause reflections.

A lower limit on the size of defect is clearly provided by that below which the eye cannot resolve at normal transparency-eye distance. One minute of arc corresponds to 0.1mm at 35cm so if one places the limit in size at 0.1mm, any defect less than this will be difficult to resolve and therefore would be unlikely to cause distraction. Groups of such small defects might be objectionable but would be expected to be detected as haze. Defects larger than 0.1mm are rather arbitrarily grouped as follows:-

(a) minor optical defects such as small bubbles, cavities, dirt, dust etc. 0.1mm to 0.5mm diameter, (or equivalent area) with fibres and hair scores up to 10mm long and less than 0.1mm wide.

(b) major optical defects such as bubbles, cavities, particles etc. 0.5 to 1.0mm diameter (or equivalent area), fibres and hair-like scratches 10-20mm long and 0.1-0.2mm wide.

A specification now under discussion would allow only one major defect in an area enclosed by a circle of 150mm radius centre at that defect, and four minor defects not less than 50mm apart in the same circle. In the absence of a major defect the circle of 150mm radius shall contain no more than 8 minor defects not less than 50mm apart. The inspection of a panel for optical defects may be conveniently carried out by viewing an evenly illuminated white screen through the panel and then by viewing a matt black screen with the panel being obliquely illuminated. Particular care must be taken to shield the source from direct vision and to present any direct reflections therefrom. The defects may be measured by a microscope with 10 times magnification provided with a graticule graduated in 0.1mm.

There appears to be little recorded experience on the distracting effect of minor inclusions and imperfections so that the standards tend to be determined by the quality of materials available and standards of fabrication.

### 3. FUNCTIONAL CLASSIFICATION OF AIRCRAFT TRANSPARENCIES

#### 3.1 General Considerations

A review of aircraft transparencies has led to a classification into four broad categories according to the quality of visual performance judged to be necessary. In each category limiting values of the parameters have been allocated in order to ensure satisfactory performance. These values are shown in Table 2 together with examples of transparencies which might appear in each of the categories. Certain general points should be



emphasised; for every parameter except haze, measurements must be made from the user's normal eye position to ensure satisfactory quality. It must be demonstrated also that the operation of heating films or elements associated with de-misting or de-icing does not cause a deterioration in visual performance. An area around the edges of transparencies is commonly allowed for the inclusion of electrical busbars, leads and sensor elements and is not subject to stringent optical requirements.

It is considered that the aircraft designer together with the potential user will be best qualified to identify the category into which any particular transparency will fall; the examples given at the foot of Table 2 can be taken only as a guide based on past experience. It has always been common practice to identify certain areas of transparencies as requiring specific properties and this is justifiable; a head-up display for example may require an area which is very critically controlled, while the remainder of the transparency could be satisfied by a relaxed specification. It should be noted that windows for survey and reconnaissance cameras have not been included in the classification as these are considered as essentially optical components with very special requirements. Helicopter windows have as yet not been given serious consideration; these generally need only be quite thin to satisfy bird impact and aerodynamic requirements and so do not present such difficult optical problems as thick windows. On the other hand they are rarely flat so distortion problems are not uncommon.

### 3.2 Qualities Associated with Acuity

As noted earlier it is considered that high quality transparencies should not cause a deterioration in the natural resolution of the eye, hence the upper limit for categories I and II is placed at 1 minute of arc. A relaxation is allowed for category III and no limit should be necessary for cabin windows. With respect to haze, it has been found that 2.5% is an acceptable limit which can be met in fabrication. For light transmission the limit of 55% is considered to be the minimum acceptable for high quality screens in order to admit the use of heating films. There is no doubt that a higher value would be desirable and this should be possible with the introduction of colourless heating films. There appears to be no need to specify this more closely with regard to spectral distribution especially as in measurement the photocell is corrected in response to the human eye. However occasionally in the past attention has been drawn to the effects of transmission in the ultra-violet or infra-red. It is believed that the materials commonly used do not transmit sufficiently in these regions to cause concern, however the behaviour of new materials in this respect should be checked and if necessary suitable precautions should be taken.

A general comment in connection with the parameters associated with acuity concerns the use of vizors by pilots. Unless the material used in such is shown to be of high optical quality with respect to resolution, transmission and haze, this practice could lead to serious overall degradation in visual performance under conditions of low light and poor contrast. It is believed that precautions should be taken to avoid this and pilots should be warned accordingly.

### 3.3 Accuracy of Vision

An optical deviation of 1 minute of arc corresponds to a displacement of 29cms over a distance of one kilometre. The effect of optical deviation will clearly be most important in weapon aiming and the value demanded over the critical area of a transparency will be a function of the system concerned. The value given in Table 2 for category I is believed to represent a working limit which can be achieved in fabrication. The values given for categories II and III are typical of the quality of transparencies acceptable for normal flying conditions.

### 3.4 Efficiency of Vision

Optical distortion and binocular deviation both arise from variations of optical deviation over the area of the transparency and if such variations are sufficiently large disturbing psychological effects can occur and bring about poor performance and fatigue of the user. How important these effects are is clearly dependent upon the user and therefore very difficult to assess. The values given for distortion in categories II, III and IV have been allocated in a rather arbitrary fashion until more information is obtained. It is not necessary to quote a value for category I as the control placed on optical deviation should prevent distortion. With respect to cabin windows, it is believed necessary to specify some value here (1 in 5 may not be sufficiently critical) in order to avoid passengers suffering discomfort being misled into reporting the presence of UFOs. The value quoted for binocular deviation has already been discussed.

Some further study is required with respect to the extent of inspection required to control variation of optical deviation. If, for example a sufficiently detailed inspection for optical deviation over the whole area of a transparency could provide, by calculation, the required information for distortion and binocular deviation then this detailed inspection might be economic; this procedure is visualised for category I transparencies. For category II and III transparencies it may be sufficient to scan the panels in order to confirm that required limits for optical deviation and binocular deviation have not been exceeded and to provide a photograph of a grid board in order to check the distortion. It is difficult to generalise on the matter of inspection for these parameters in view of the possible range of qualities, thickness etc.

Insufficient experience is available at present on secondary images to indicate tolerable levels. The specification for the Concorde windscreen requires that the optical deviation shall not exceed 3 minutes of arc for a panel 36mm thick in order to overcome double images. This is believed to be unnecessarily critical. The automobile specification<sup>(3)</sup> mentioned demands maximum deviation of 15 minutes for a panel perhaps 6mm thick.

Again with respect to minor optical defects, more details of human reactions to existing standards are required to judge the proposal made in Section 2.8.

#### 4. CONCLUSIONS

One obvious conclusion from the work reported is that there is a lack of quantifiable evidence on the human reaction to deterioration of the various parameters which have been defined. For this reason most of the limits which have been proposed are derived from limitations imposed by materials properties, fabrication problems or the needs of economy. Human engineering studies are clearly required, however if these involve detailed flying programmes they are prohibitively expensive. One possible suggestion which has not been taken up, as far as is known, would involve fitting defective forward transparencies into simulator training units and to record the reactions of the students involved. Information on the effects of distortion, binocular deviation, secondary images and presences of inclusions etc might be obtainable by this means.

Current work involves the development of a simple method for double images and studies of simplification of inspection programmes to cover effectively and economically the parameters for the four categories which have been described.

#### 5. ACKNOWLEDGEMENTS

The assistance of Mr W Shaw of Aeronautical Quality Assurance Directorate, Harefield, for advice and for much of the experimental work associated with this paper is gratefully acknowledged. Many colleagues in M.O.D.(PE) and in the British Aircraft industry have contributed during the course of this work.

British Crown copyright; reproduced by permission of the Controller of Her Britannic Majesty's Stationery Office.

#### REFERENCES

- (1) N.S. Corney & W. Shaw  
S.B.A.C. Symposium on Aircraft Transparencies London  
June 1970.
- (2) B.A.J. Clark  
Consequences of Tinting in Aircraft Windshields  
Australian Department of Civil Aviation,  
Aviation Medicine Memorandum No 26, February 1970
- (3) British Standards Institution  
BS 857 : 1967 Safety Glass for Land Transport.
- (4) J.P. Acloque  
Double Images as Disturbing Optical Defects of Windscreens  
Glastechnische Berichte 43 (1970) 193-198.

# Optical parameters associated with aircraft transparencies

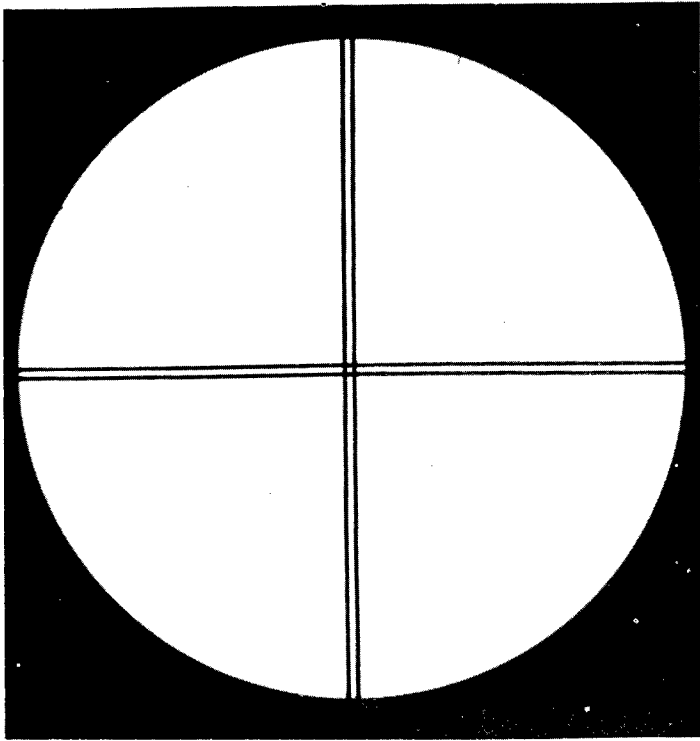
| <u>Parameters</u>           | <u>associated</u>  | <u>with</u> | <u>acuity</u>     |
|-----------------------------|--|-------------|-------------------|
| Optical resolution -        | inability to distinguish objects in close proximity                      |             |                   |
| Light transmission -        | inability to receive illumination of object to fullest extent            |             |                   |
| Haze or halation -          | obscuration by scattering of light                                       |             |                   |
| <u>Parameter</u>            | <u>associated</u>  | <u>with</u> | <u>accuracy</u>   |
| Optical deviation -         | angular displacement of image  |             |                   |
| <u>Parameters</u>           | <u>associated</u>  | <u>with</u> | <u>efficiency</u> |
| Optical distortion -        | image appears misshapen  |             |                   |
| Binocular deviation -       | each eye suffers different deviation                                     |             |                   |
| Double images -             | multiple images of lights appear   |             |                   |
| Scratches, inclusions etc - | eyes tend to focus on distracting defects rather than on distant objects |             |                   |

Table 1

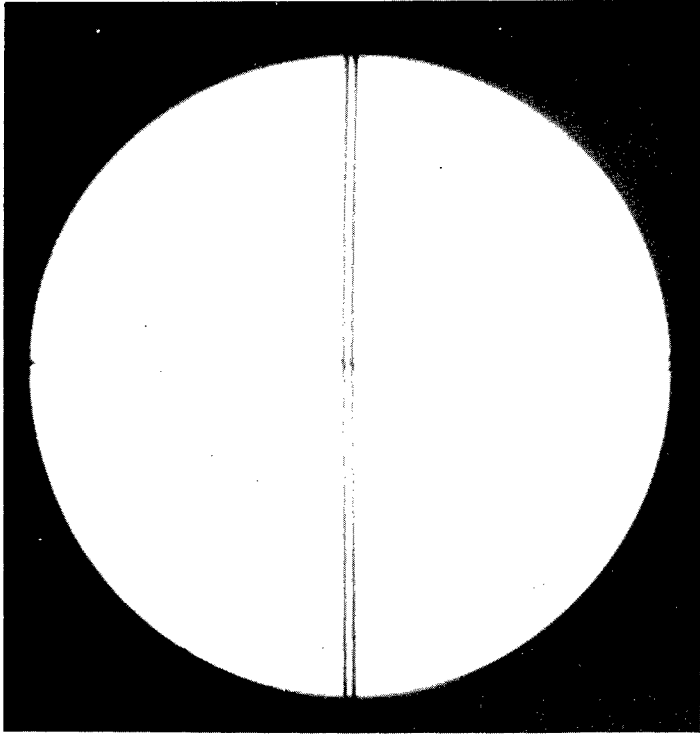
ACCEPTABLE VALUES OF THE PARAMETERS ASSOCIATED WITH VISION THROUGH OPTICAL TRANSPARENCIES

| Parameter   | Category I  | Category II  | Category III   | Category IV                                   |
|---|---|--|--|---|
| <u>Optical Resolution</u><br>value not to exceed      | 1 minute  | 1 minute   | 2 minutes  | -   |
| <u>Haze</u><br>value not to exceed                    | 2.5%  | 2.5%   | 2.5%   | -   |
| <u>Optical Transmission</u><br>not less than          | 55%   | 55%  | 55%  | 50%   |
| <u>Optical Deviation</u>                              | <5 minutes<br>tolerance from<br>and agreed value  | <15 minutes  | <20 minutes  | -   |
| <u>Distortion</u>                                     |   | Change in slope<br>not greater than<br>1 in 20   | Change in slope<br>not greater than<br>1 in 20       | Change in slope<br>not greater than<br>1 in 5 |
| <u>Binocular<br/>deviation</u><br>value not to exceed | 10 minutes  | 10 minutes   | 10 minutes   | -   |
| <u>Double<br/>Imaging</u>                             | ← Standards   | to be decided  | →  |   |
| <u>Scratches and<br/>Inclusions</u> etc               | ← Provisional   | Standards under  | discussion   |   |
| Type of transparency<br>(or area thereof)             | Forward facing<br>windscreen of the<br>highest quality -<br>suitable for weapon<br>aiming | Forward facing and side<br>panels for reconnaissance<br>and search: forward<br>panels for non-combat<br>aircraft | Side panels for<br>non-combat aircraft<br>- canopies | Cabin windows                                 |

Table 2



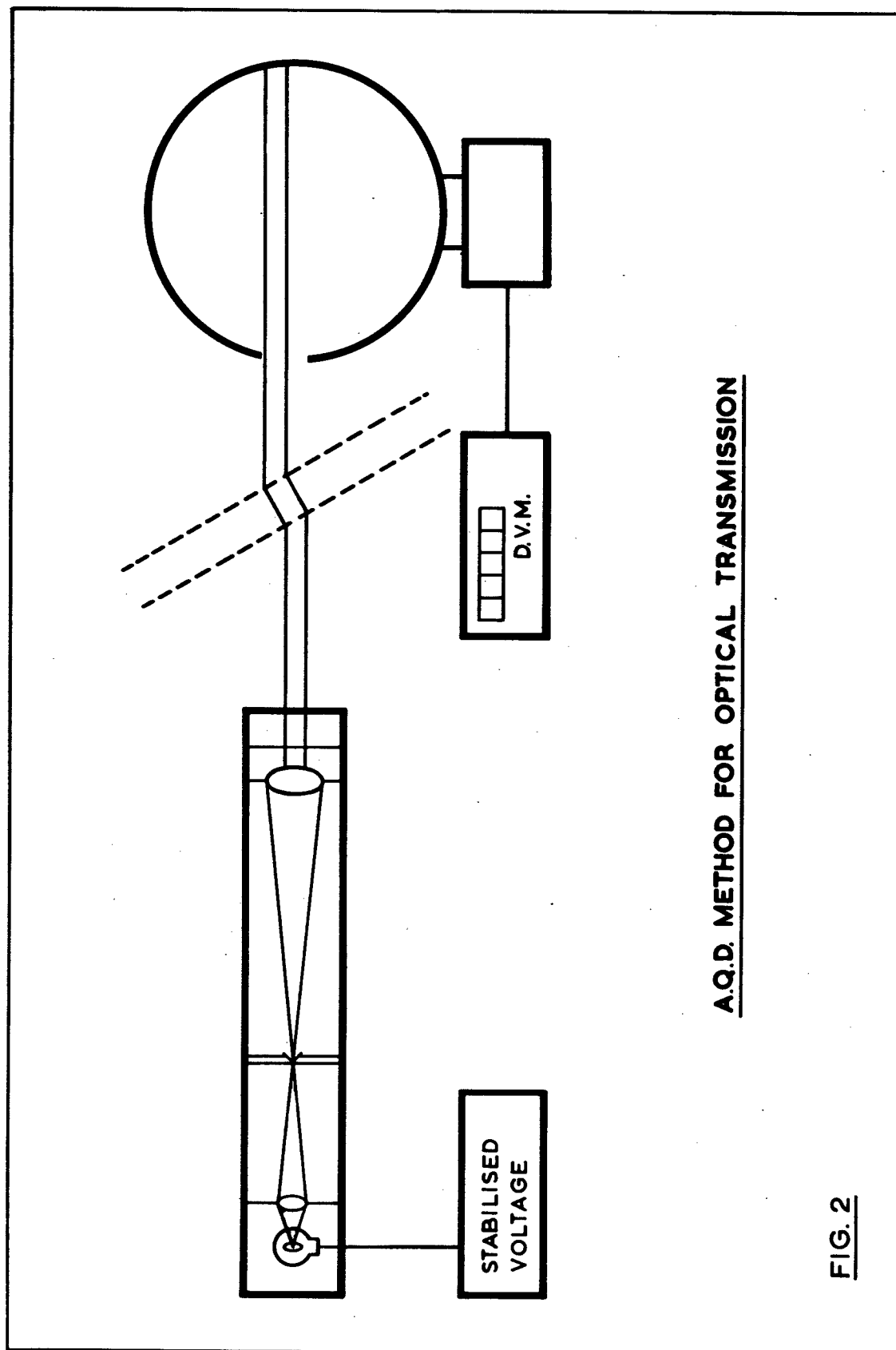
a) Satisfactory



b) Unsatisfactory

Optical resolution test; lines are 1 minute wide,  
separation of lines 2 minutes centre to centre

Figure 1

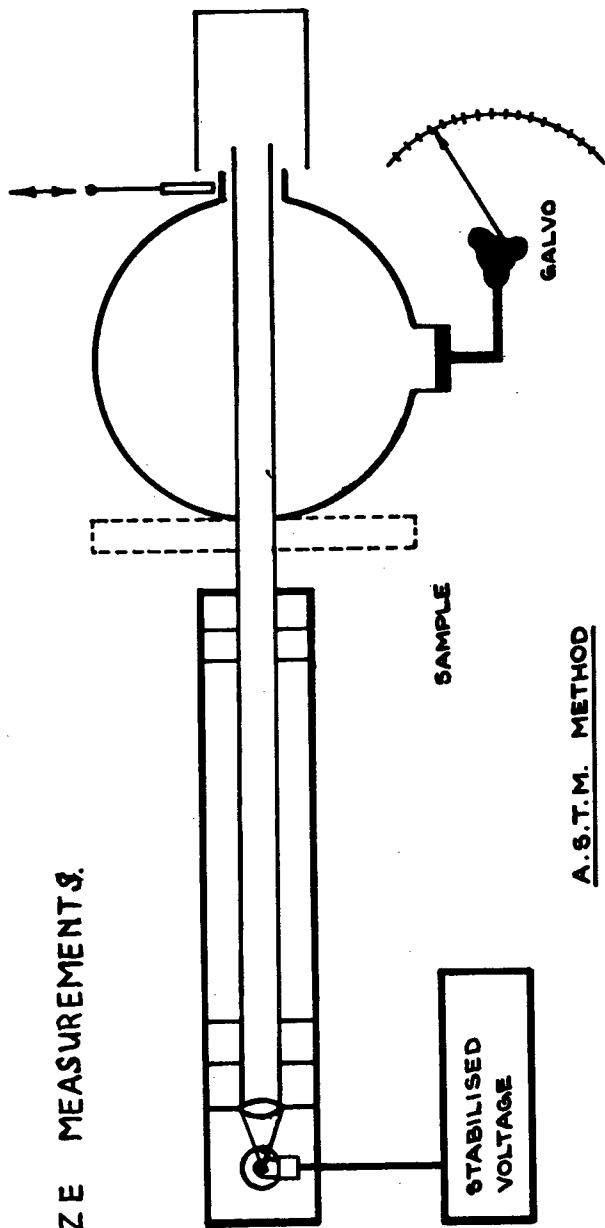


A.Q.D. METHOD FOR OPTICAL TRANSMISSION

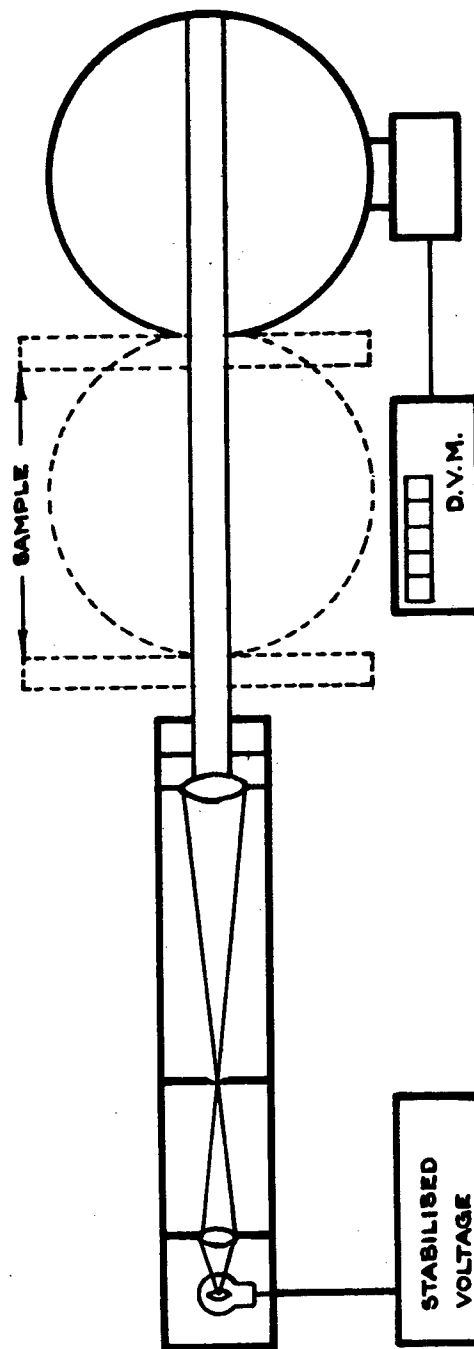
FIG. 2



FIG. 3 HAZE MEASUREMENTS.



A.S.T.M. METHOD



A.Q.D. METHOD

OPTICAL DEVIATION

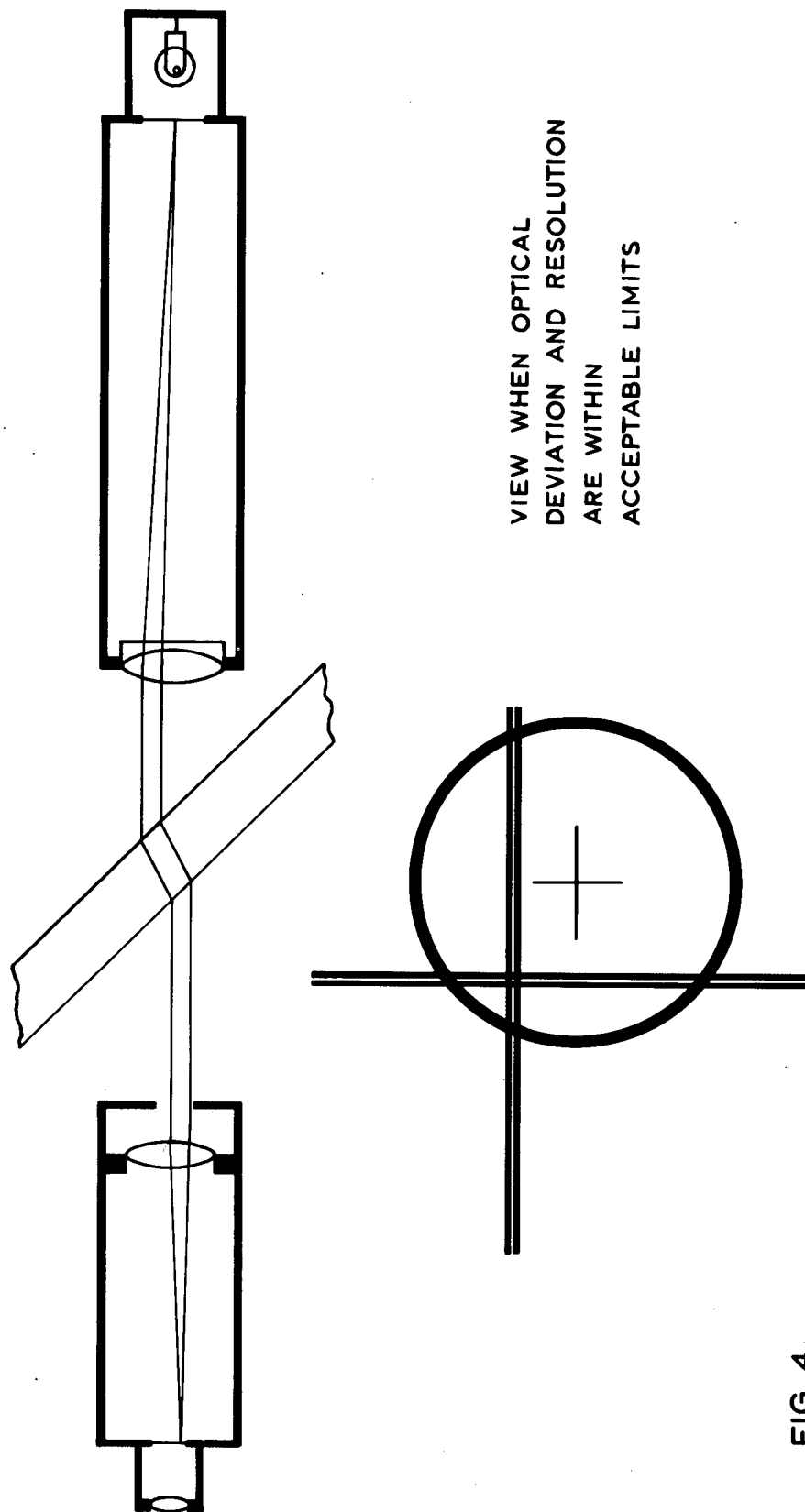
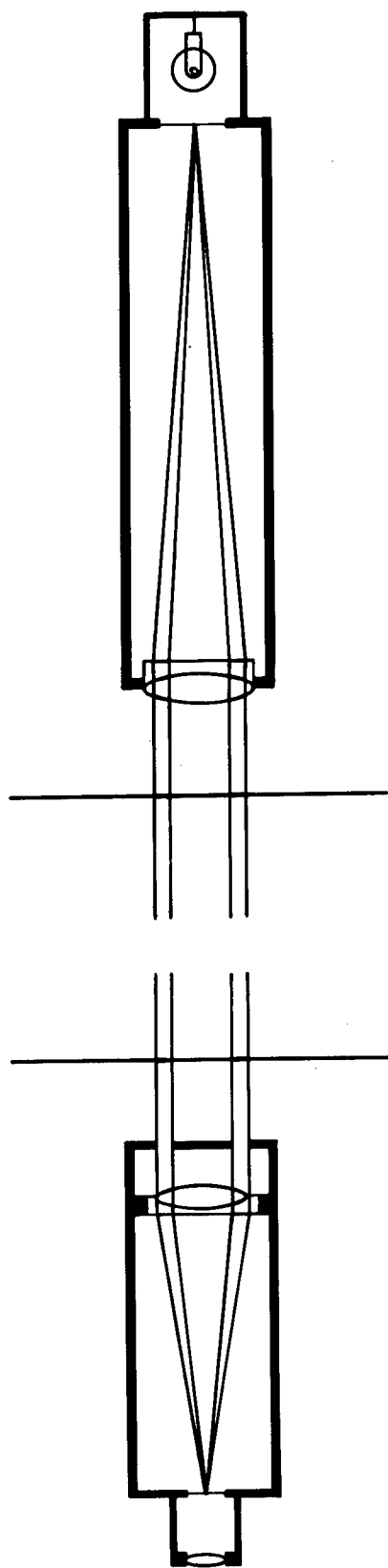


FIG. 4

BINOCULAR DEVIATION



VIEW WHEN BINOCULAR  
DEVIATION IS JUST WITHIN  
ACCEPTABLE LIMIT

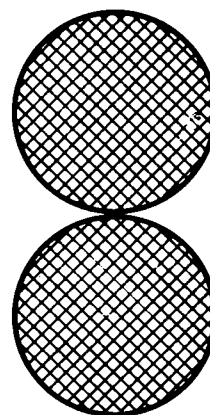


FIG. 5

**CORRECTION OF OPTICAL DEVIATION  
IN CURVED WINDSHIELDS**

**R. W. Fisher  
McDonnell Aircraft Company  
St. Louis, Missouri**

## "CORRECTION OF OPTICAL DEVIATION IN CURVED WINDSHIELDS"

R. W. Fisher, Branch Manager, Avionics Engineering Division,  
McDonnell Aircraft Company, St. Louis, Missouri

### ABSTRACT

The desire to attain maximum aerodynamic qualities and low cockpit noise in two place fighter aircraft has necessitated development of thick conical windshields with short radii of curvature. This combination of thickness and curvature leads to optical deviation in the pilot's sight line even if the windshield is of perfect optical quality. This deviation can be as high as 10 milliradians, and obviously can not be tolerated in future weapon systems that require visual target acquisition with accuracies of 1 milliradian or less. Another cause for concern is the fact that sight lines from each eye are deviated differently. While the eyes easily compensate for this with no loss in visual acuity, eye fatigue and false illusions of target motions may result.

This paper describes how optical deviations are theoretically charted using computer-graphic techniques and experimentally measured using a unique laser test apparatus. Theoretical results are compared to experimental measurements to show manufacturing errors in representative curved windshield assemblies. Various corrective techniques are studied including optical correction applied to either windshield or gunsight, electronic correction to gunsight, and geometric correction which establishes the optimum relationships between windshield radii, axis of curvature, and the pilot's nominal head-position. The corrective techniques are compared with respect to accuracy, limitations, and cost.

## Introduction

The desire to attain maximum aerodynamic qualities and low cockpit noise in two place fighter aircraft has necessitated development of thick conical windshields having short radii of curvature. This combination of thickness and curvature leads to optical deviation of the pilot's sight line even if the windshield is of perfect optical quality. Another cause for concern is the fact that sight lines from each eye are deviated differently. While the eyes easily compensate for this with no loss in visual acuity, eye fatigue and false illusions of target motions may result. This differential deviation also causes a visual disparity when an aiming reticle is introduced into the visual system through the Head Up Display (HUD). The following paragraphs describe how these effects can be quantified, measured, and corrected to yield a satisfactory windshield optical system.

### The Problem

A simplified explanation of optical sightline deviation caused by windshield curvature is illustrated in Figure 1. In this figure, parallel sightlines from three different eye positions are projected through a curved windshield. (The windshield geometry is reduced to two dimensions for simplicity.) The conditions causing optical deviations are amplified to the right in this example.

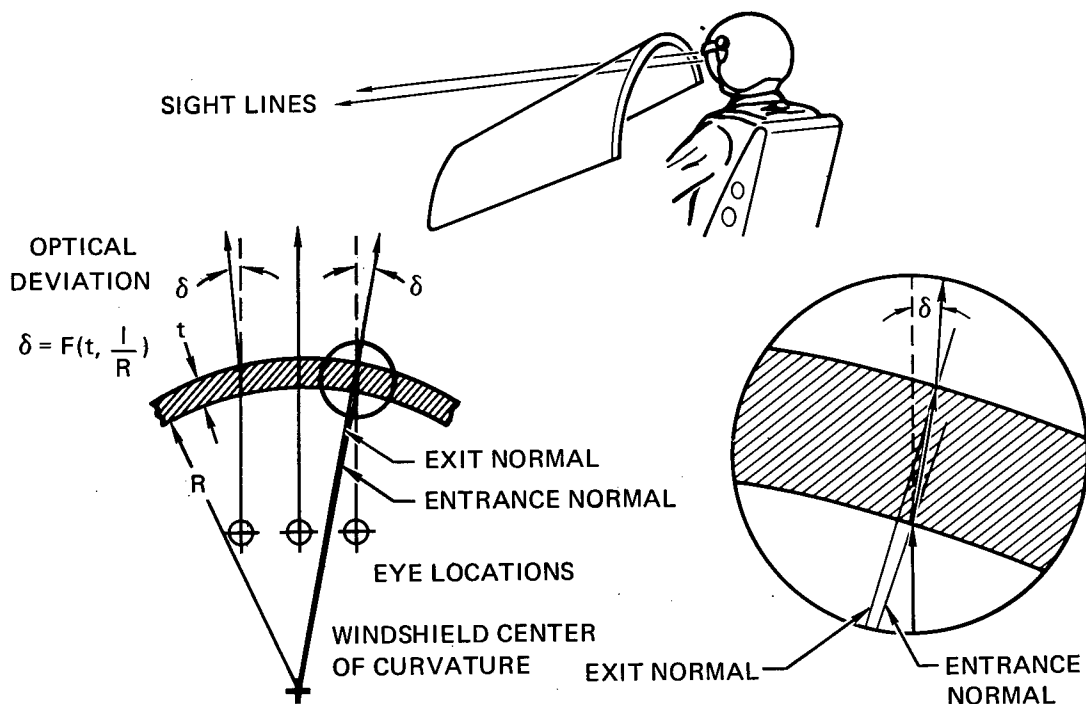


FIGURE 1  
THE CURVED WINDSHIELD PROBLEM - ANGULAR DEVIATION

GP73-0056-1

As the sightline passes through the windshield it translates in the tangential direction causing it to exit from a plane that is not parallel to the plane of entrance. The result is a prism action which causes the sightline to experience an angular deviation. This prism effect exists for all sightlines except those contained in the radius plane (center eye position on Figure 1) (1).

Note how the deviation will increase with either increases in windshield thickness or reductions in radius of curvature. Increased thickness causes the sightline to experience greater tangential translation between entrance and exit points. This creates a larger angle between entrance and exit planes and a corresponding increase in deviation. A shorter radius of curvature causes more deviation by directly increasing the angle between entrance and exit planes.

The deviation increases with the distance of the sightline from the radius plane and a sign change in deviation occurs as the sightline shifts through the radius plane. This rate of change of deviation (distortion) causes another undesirable effect; that of binocular parallax. The visual effects of this are shown on Figure 2. Note on the left side of this figure that the eyes must misalign their optical axes in order to view an outside object normally. For small magnitude of misalignment or parallax (1-5 mr) the pilot readily adapts to this situation and observes a high acuity target image. The unacceptable situation arises when an aiming reticle is introduced. This reticle is normally collimated so it appears to be at an infinite distance. With this kind of collimation all rays

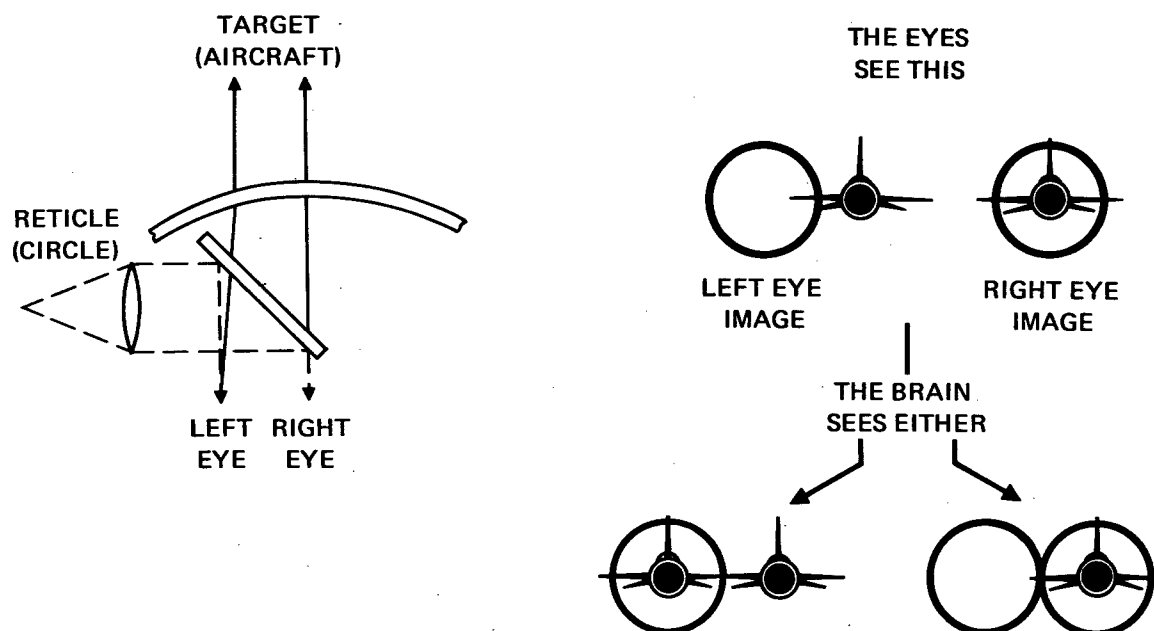


FIGURE 2  
THE DISPLAY PROBLEM - VISIBLE PARALLAX

GP73-0056-2

(1) The radius plane is any plane containing the cone axis.

originating from any point on the reticle are parallel and will enter each eye from the same direction (dashed lines on Figure 2).

If one looks at the combined reticle/target image on the retina of each eye, the situation shown to the right of Figure 2 is observed. The right eye sees the target properly centered within the reticle while the left eye sees the reticle well to the left of the target. The brain will interpret this situation in either of two ways. It will either adjust the eyes to bring the reticles in coincidence and see two targets, or it will do the converse causing one target to be seen with two reticles. These two possible conditions are shown to the lower right of Figure 2.

Experimentation at MCAIR has shown that the brain will normally cause the image with the most spatial detail to be brought into registration; i.e., one target and two reticles. When the reticle appears by itself, such as against the sky, it is brought into registration but the moment anything with more spatial detail appears, the eyes will shift to favor the target. It is this shifting of eye alignment that is most distracting to the pilot.

Of equal importance to the target acquisition problem is the difficulty of positioning multiple reticles and the basic error in target location caused by optical deviation. In order to quantify these problems and study possible solutions optical deviations were computed for a 1-inch thick F-5 windshield.

#### Theoretical Analysis

Optical sightline deviations can be easily calculated by applying the basic optical refraction equations (Snell's law) to both windshield surfaces. However, the complexity of the nearly conical windshield and three dimensional application of Snell's law necessitate the use of a computer. The IBM 360 computer was used with a graphic interface as shown in Figure 3. This interface allowed parametric studies involving head position or windshield geometry shifts to be conducted at ease and in near real time. The best form of data display was found to be error contour plots for each eye as shown on Figure 4. This shows optical deviations experienced by an eye located on the windshield axis butt line (Figure 4a), shifted 2 inches to the right (Figure 4b), and shifted 4 inches to the right of the axis butt line (Figure 4c). Each of the plots shows the optical deviation as a function of sightline azimuth and elevation. For the eye located on BL 0 no deviation is seen in the elevation plane at zero azimuth. This is as expected because all sightlines at zero azimuth lie in the radius plane of the windshield cone. Within the normal azimuth range of target acquisition ( $\pm 10^\circ$ ) optical deviation is within about  $\pm 2.5$ mr. For the BL 2 eye, worst-case deviations are seen to increase to about 4mr. These errors further increase to about 6mr when the eye is offset 4 inches. The plots clearly show that observed optical deviation is very significant, and that it is a function of both eye location relative to the windshield and angular direction of viewing.





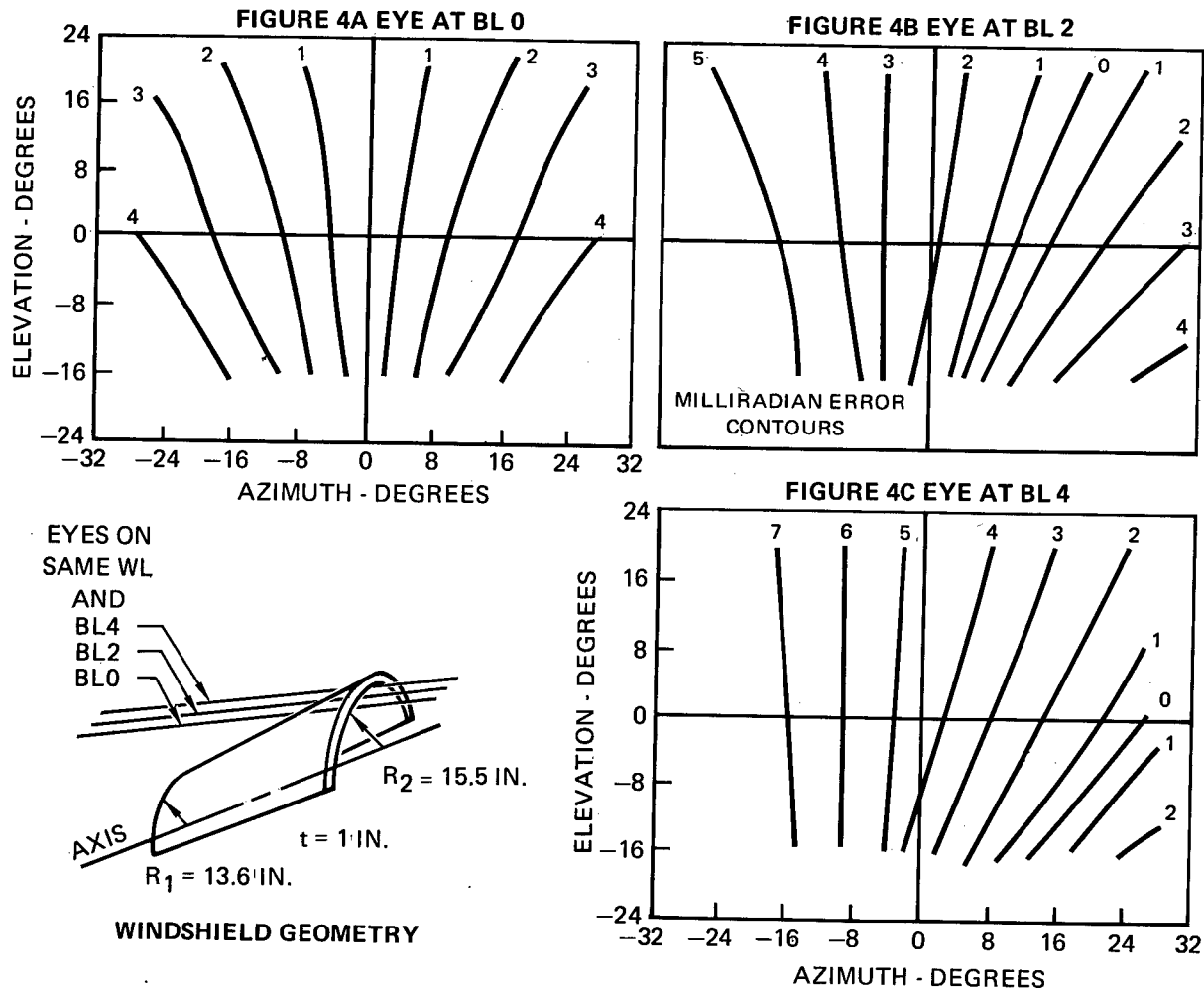
**FIGURE 3**  
**COMPUTER GRAPHIC TERMINAL**

GP73-0056-3

Binocular parallax can also be deduced from Figure 4 because adjacent plots very nearly represent the human interocular separation. Therefore, Figures 4a and 4b represent the situation viewed by the head offset 1 inch to the right of center. Correspondingly, Figures 4b and 4c show deviations for each eye when the head is shifted 3 inches to the right of center. A close look at these pairs of plots shows that differential deviation between the eyes remains fairly constant at about 2mr.

#### Corrective Techniques

The four corrective techniques that have been studied at MCAIR are summarized in Figure 5. The first, the electronic technique, consists of electronically biasing the reticle to minimize aiming error. This can obviously be done correctly for only one eye location. If this were done for the BL 0 position, this error plot could be subtracted from errors existing at other eye positions. The results show that the inherent 6mr error discussed above could be reduced to about 3mr. If a head position sensor were incorporated, this error could be reduced down to an acceptable level (about 1mr). However, this would require a complex and costly electronic system. Even more significant, it would still not compensate for parallax which is probably the most important effect for reasons previously stated.


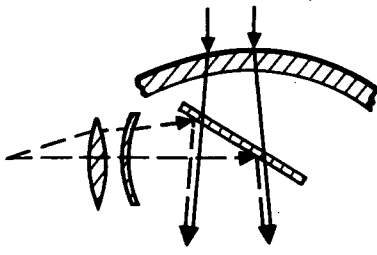
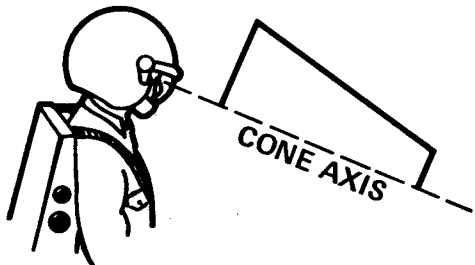


**FIGURE 4**  
**WINDSHIELD ERROR MAPS**

GP73-0056-4

The second corrective technique shown on Figure 5 involves correcting for windshield curvature by interposing corrective optical elements between the windshield and pilot. Preliminary studies indicate the need for several such optical elements. Besides being costly and heavy, these elements would block vision or cause a deviation discontinuity as large as 6mr at their effective field edges. Experiments conducted at MCAIR show step changes in parallax to be very disconcerting. This approach is therefore unacceptable.

The third corrective technique uses a corrector on the reticle projection system to decollimate the display in the same manner that the windshield decollimates the outside world. While it was first thought to be unworkable, theoretical and experimental evaluations have shown this technique to be both effective and simple to implement. The corrections can be confined entirely to the display projection system either as a refractive element at the objective lens or as a reflective element at the combining glass. This technique is relatively inexpensive if employed early in vehicle avionic equipment definition.

| <u>TECHNIQUE</u>   | <u>DESCRIPTION</u>                            | <u>COMMENTS</u>  |
|--|---|--|
| ELECTRONIC   | ELECTRONIC BIAS OF HUD<br>RETICLE             | LOW ACCURACY - 3 MR<br><br>NO PARALLAX CORRECTION              |
| OPTICAL CORRECTOR  | OPTICAL ELEMENTS BEHIND<br>WINDSHIELD         | LARGE HEAVY ELEMENTS REQUIRED<br><br>DISCONTINUITY AT BOUNDARY |
|     |   |  |
| HUD OPTICAL<br>CORRECTOR   | DECOLLIMATE HUD TO MATCH<br>WINDSHIELD EFFECT | CORRECTION CONFINED TO HUD                                     |
|    |   |  |
| GEOMETRIC  | LOCATE NOMINAL EYE POSITION<br>ON CONE AXIS   | MODERATE ACCURACY - 2 MR<br><br>NO PARALLAX CORRECTION         |
|  |   |  |

**FIGURE 5**  
**COMPENSATION TECHNIQUES**

GP73-0056-5

The last corrective technique shown on Figure 5 is very interesting because it can be easily accomplished at no cost if it is selected early in the aircraft design cycle. This technique is accomplished by designing the nominal head position at an eye waterline coincident with the windshield axis. Since an eye on the windshield axis experiences no deviation (all sightlines lie in radius planes) eye displacements from this position should show minimum deviation. This was studied by shifting the windshield of Figure 4 so the eye at BL 0 lies on the cone axis. The resulting error

contours are shown in Figure 6. The BL 0 eye, Figure 6a demonstrated zero deviation as expected while the BL 2 eye demonstrated maximum errors of about 2mr. This is a significant improvement over the 4mr observed on Figure 4 for the same eye offset. The main difficulty with this approach is that parallax is not corrected - it remains about 2mr as before. In spite of this, the geometric technique provides minimum error at essentially no cost and should therefore be considered as a starting point for other corrective techniques. The use of this geometry will minimize the complexity, tolerances, and cost of whatever correction technique is utilized.

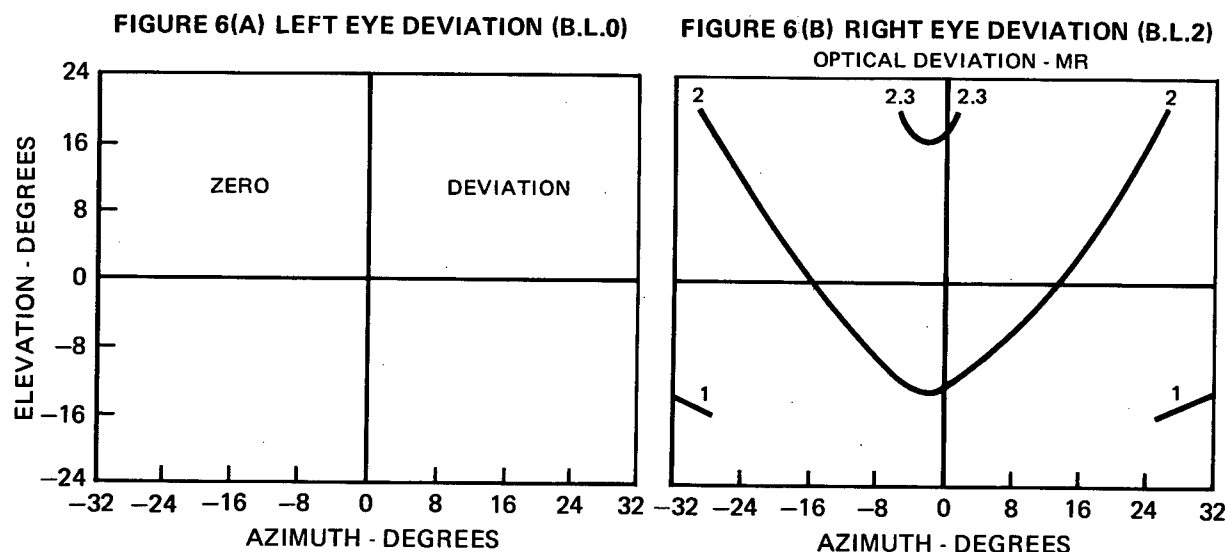
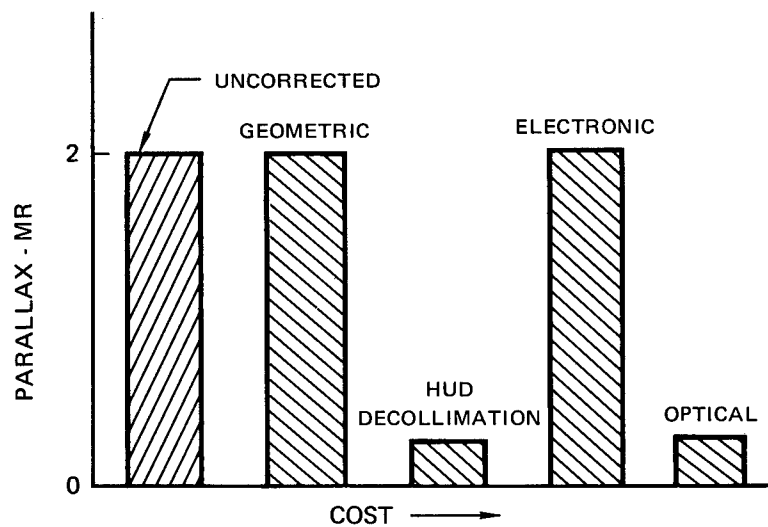
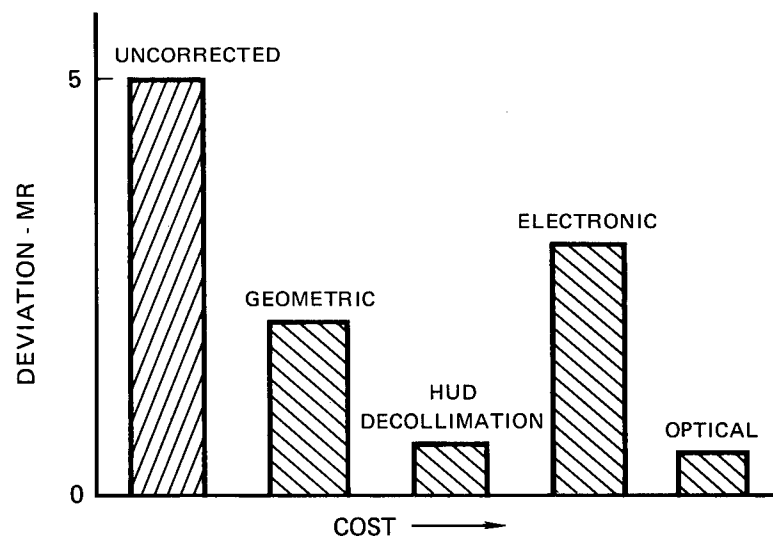


FIGURE 6  
GEOMETRIC CORRECTION EFFECTIVENESS

GP73-0056-6

In Figure 7, the four corrective techniques are compared with respect to cost and their effectiveness in correcting both optical sightline deviation and parallax. From these approximate plots it is clear that the HUD decollimation corrective technique is the best approach. Again it should be pointed out that application of the geometric technique will lower requirements and cost of other corrective techniques and should be employed, if possible, on any new vehicle design.

At this point in the discussion we must return to reality and recognize that the effectiveness of the above corrective techniques are based on an "optically perfect" windshield. It is conceivable that optical imperfections occurring in the windshield manufacturing process could make the correction ineffective. For this reason MCAIR evaluated several curved windshields to determine how closely they matched theoretical predictions.

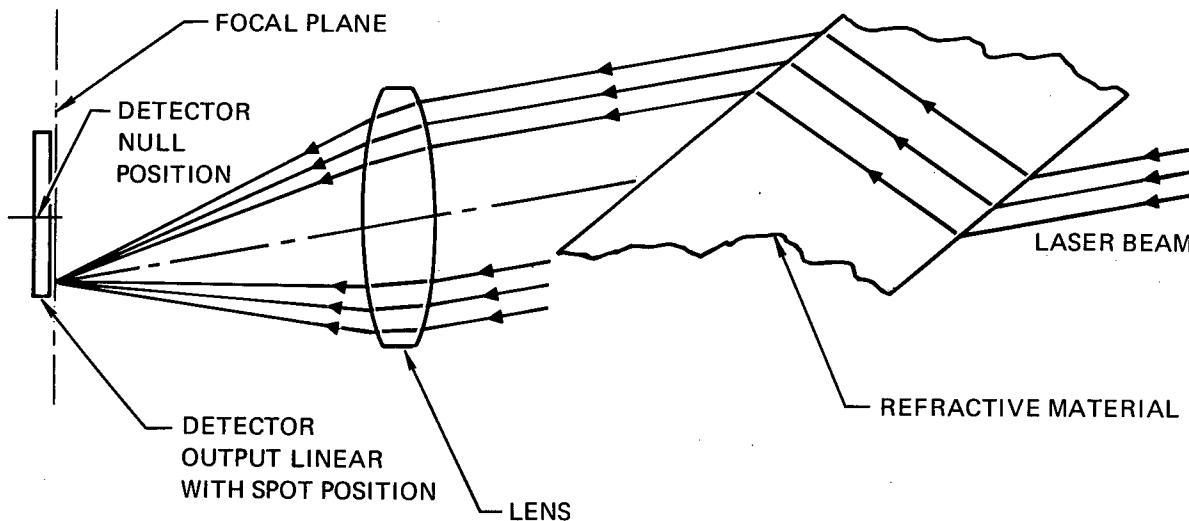


**FIGURE 7**  
**EFFECTIVENESS AND COST OF CORRECTIVE TECHNIQUES**

GP73-0056-7

## Experimental Results

It became apparent early in planning for optical deviation tests that present test apparatus and techniques were not applicable to thick curved windshields. The primary problem occurs in separating optical offset or refraction from optical deviations. In flat panels this is accomplished by orienting the panel normal to the line-of-sight. In the curved windshield this is obviously impossible. Thus an entirely new technique had to be developed. The concept (Figure 8) uses a collimated small diameter (5mm) laser beam to trace sightlines from any desired eye position. The key to this device is the receiver's ability to recognize only angular deviation as is illustrated in Figure 8. The receiver shown to the left of the figure consists of an optical detector which produces an electrical output proportional to the location of light energy along its length, and a lens located so that detector is at its focal plane. Energy entering the lens anywhere from the same angle falls on the same location on the detector. Only angular changes in the input beam will cause a change in detector response. By employing a two axis detector both the magnitude and direction of beam angular motion can be accurately measured.

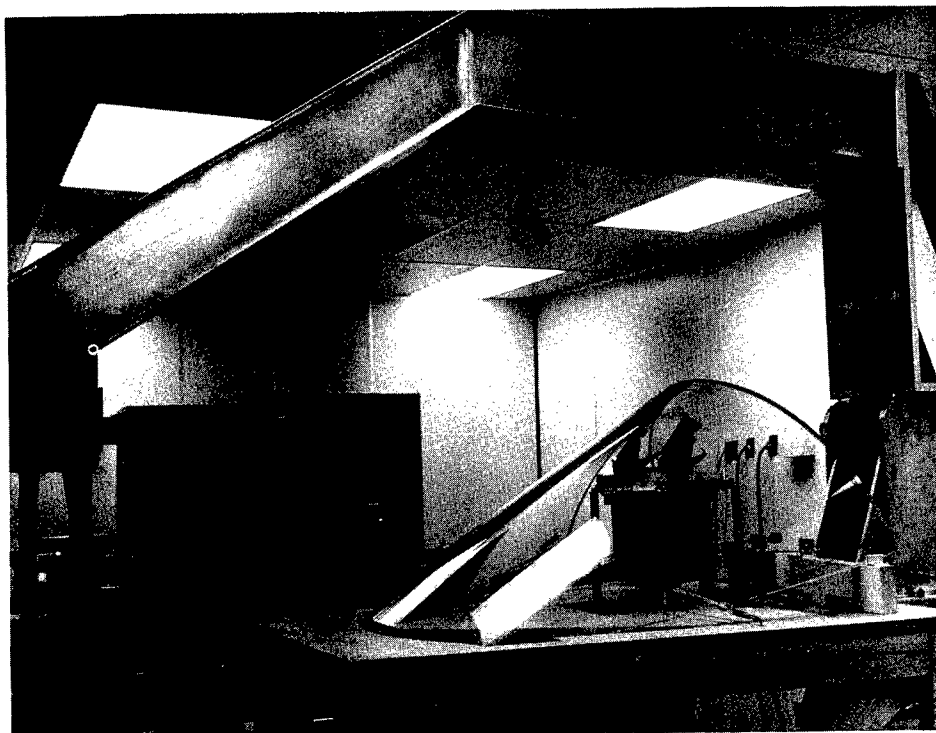


NOTE: CELL OUTPUT UNAFFECTED BY LATERAL  
TRANSLATION OF INCIDENT LIGHT BEAM

**FIGURE 8**  
**LASER ANGULAR ALIGNMENT CONCEPT**

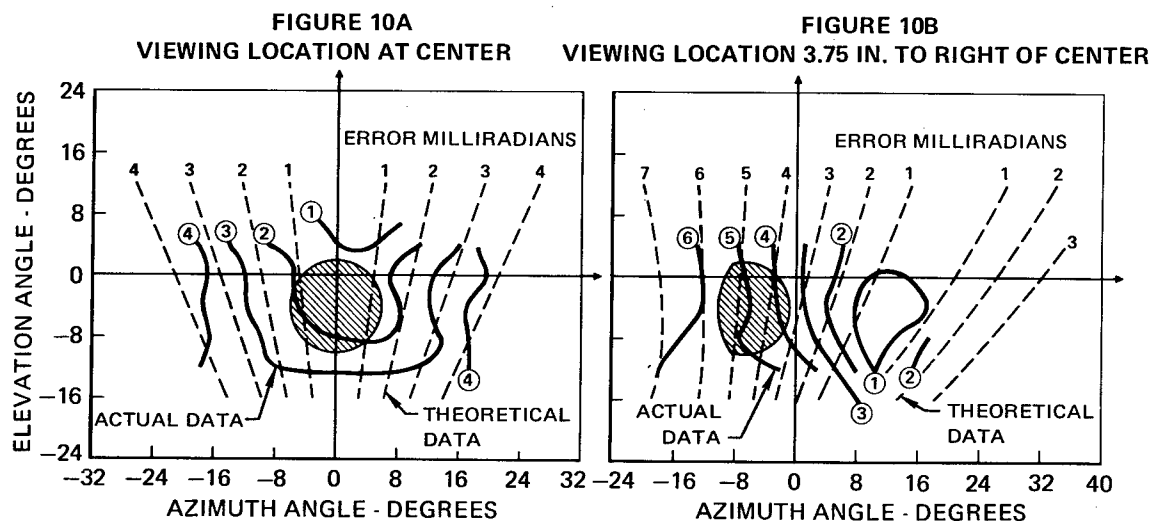
GP73-0056-8

The entire test apparatus is shown in Figure 9. Practical considerations dictated locating the receiver at the test eye position and the laser at the outer end of the beam. Gimbals are arranged so that the laser source pivots about the receiver aperture to cause azimuth and elevation motions around the desired eye position. To evaluate new eye positions the windshield is simply translated so that the detector is in the new desired position relative to the windshield. Through gimbal angle electronic readouts and electronic processing of detector outputs it is possible to provide error contour plots directly in the form shown on Figure 4. Typical of data obtained on a windshield of slightly different geometry than that of Figure 4 are shown on Figure 10. Also shown in dashed lines on this figure are theoretical predictions for the same geometry. Data are shown for a BL 0 eye position and one that is 3.75 inches offset to the right. The shaded areas represent typical HUD reticle positions observable from these two eye positions. These are the areas where deviation compensation must be effective. Note that the error contours agree within about 1mr in the azimuth direction but that elevation errors are indicated by the horizontal fold-over of error contours. It is of particular interest to note how well the large eye offset and large error regions agree. For example theoretical corrections made per the dashed lines on Figure 10b would reduce the worst-case aiming error from 5.5mr to about .5mr. For the centered eye, accuracy would be slightly less - about 1mr residual error in this case.



**FIGURE 9**  
**TEST APPARATUS**

GP73-0056-9



**FIGURE 10**  
**TYPICAL WINDSHIELD MEASUREMENTS**  
**THEORETICAL AND ACTUAL OPTICAL DEVIATION COMPARISON**

GP73-0056-10

Application of the HUD decollimation correction technique to this windshield and several others demonstrated essentially no visible binocular parallax and no more than 1mr reticle motion with head motion. Without the correction, parallax and reticle movement with head motion were clearly visible and unacceptable.

All data accumulated by MCAIR to date indicates that optical deviation introduced by curved windshields of the geometry tested can be compensated within 1 to 2 mr by the HUD decollimation technique. In addition, it appears that visible binocular parallax can be essentially eliminated by this same technique.



## ALTERNATIVES TO WINDSHIELDS

Peter Beaumont  
The Boeing Commercial Airplane Company  
Seattle, Washington

## INTRODUCTION

A view of the outside world from the pilot's station has traditionally been the requirement on any type of airplane, and as equipment becomes more and more sophisticated, enabling the airplane to operate in poorer and poorer weather, so the demand for a matching improvement in visibility has prevailed. Windshields have grown in size (see fig. 1), particularly to accommodate increased downward vision for a better view of the ground during landing approaches in poor visibility. Up to the time when automatic landing systems were developed and incorporated on airplanes, the pilot's vision was a prime factor during the landing phase, and so long as he had the visual range, the downward vision was required to match it. However, the inclusion of automatic landing systems has made it possible to land airplanes in visibility conditions where the naked eye will no longer perform, regardless of the downward vision available to the pilot.

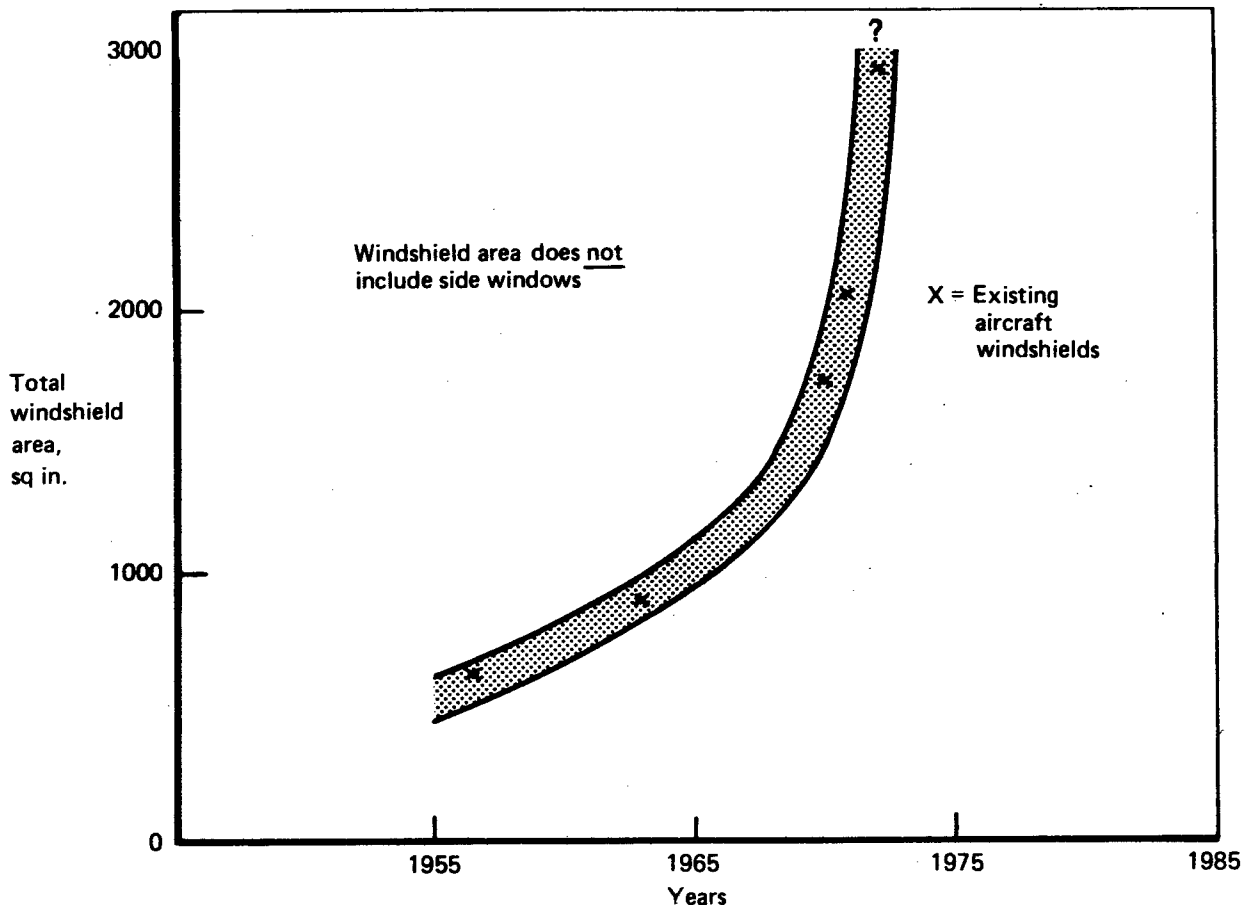


FIGURE 1.—WINDSHIELD GROWTH

The question may legitimately be raised as to what role a windshield should be required to fill in future airplanes that are certified for total, blind landing capabilities and a still further question as to whether there is an alternative which will do the job more efficiently than windshields. It is not the intent here to speculate on the administrative problems of introducing a system alternative to a windshield, since this may confuse the issue at hand, which is to explore potential.

## DISCUSSION

It is the purpose of this paper to examine the requirements that a commercial transport airplane's windshield attempts to meet and what alternative methods, within the current state of the art, could be employed that would achieve the real objectives. These objectives can be stated broadly at this point as (1) to provide the pilot with an adequate view of the outside world so as to enhance the safe operation of the airplane, (2) to do this with the minimum adverse effect on the airplane optimum configuration, and (3) to do this with as high a degree of reliability as possible. Before discussing these objectives in more detail, the alternative methods of complying with them that are available today should be identified.

Since the windshield is a simple optical system permitting an adequate amount of light to be transmitted through an aperture in the structure, it is reasonable to assume that any sensor which can react to this or similar reflected radiation and transform it into imagery recognizable to the pilot, is a contender. Families of sensors such as television, radar, lasers, and infrared are all either capable of, or have the potential for producing recognizable imagery as do pure optical systems, which are in essence an extension of the windshield optical system itself.

Returning to the broad objectives discussed earlier, we can very quickly assess the relative potentials of the various groups of candidates. Taking the first objective, which is to provide an adequate field of view to safely operate the airplane, the author believes that life-size imagery is essential if the pilot is to be given the maximum opportunity to operate the airplane safely, particularly in an emergency where instinctive reactions are important. Consequently, the view provided the pilot must reproduce real angles in relationship to an object's actual direction from the observer. This requirement alone narrows the search for a windshield alternative, eliminating television and infrared sensors because they are very definitely systems with a two dimensional presentation of a three dimensional situation. The windshield alternates remaining are radar, perhaps lasers, and optical relay systems.

The second objective, that is, to minimize adverse effects on the airplane optimum configuration, is readily achievable since all the systems considered are capable of transporting imagery from any one selected point to another, thus permitting the choice of viewing port location for minimum effect on the airplane configuration.

The third objective, to maintain the maximum degree of reliability, damages the cause of those systems that rely on independently generated sources of power in order to provide prime imagery. Neither television, radar, infrared, or lasers can provide relayed imagery without some kind of electrical power and consequently cannot be considered as passive systems by comparison with a windshield. The only alternative to a windshield which has succeeded in meeting these three basic, important requirements is the family of optical systems requiring no power in order to provide imagery. Optical viewing systems such as the periscope or telescope are capable of doing this and have been in existence for several hundred years. Furthermore, optical relay systems have been used in airplanes from time to time when they were required for a specific job. Charles Lindberg was probably the first to use one in the "Spirit of St. Louis." Unfortunately, the types of optical system which will relay imagery and present it as the real world appears are basically constrained to relatively narrow fields of view if the magnification factor is to be unity and the imagery is to be of the same quality or better than that seen through a windshield.

One of the principal manifestations of poor image quality in wide field of view systems is field curvature brought about by the large diameter, short focal length elements necessary in such a system. This kind of aberration is called the Petzval effect and is the biggest single obstacle facing the designer of wide angle optical systems. The camera lens designer overcomes this difficulty by combining materials in the lens assembly which have different refractive indices such that he can create short focal length lenses with wide fields of view and with field curvature controlled so that the image is focused on the entire film area. In recent years, the lens which was once an extremely expensive item in a camera has now become relatively cheap and the reason for this is the development of computer programs capable of solving iteratively in a matter of hours equations which, when done manually, may take several years.

Similar computer program development has taken place with the more exotic optical systems we are talking about with relation to airplane systems. However, on the face of it we are still constrained to relatively narrow fields of view from a single system if unity magnification is to be provided and if the size of the elements in the system is not to become prohibitive in weight and cost. Since a practical, undistorted field of view achievable in a pure refractive or reflective system is about  $25^\circ$  and we are looking for fields of view wider than, say,  $60^\circ$  laterally and  $35^\circ$  vertically if we are to match a windshield, then the optical system designer has to be somewhat more innovative than just a computer programmer.

Two attractive ways of beating the constraint were proposed for the Boeing SST and from them one was selected for development for the production airplane as being more compatible with the flight deck arrangement of that airplane.

Before describing these systems it would be opportune to mention the problems peculiar to the Boeing SST which motivated the search for alternatives to windshields. First of all, the supersonic configuration required a high-fineness-ratio nose profile ahead of the flight deck for minimum supersonic drag and noise. Vision in supersonic flight was provided by windows in the fairing (see fig. 2) which gave a minimum acceptable field of view and used a lot of glass. Vision in subsonic flight was provided by rotating the nose fairing (or forebody) downwards from in front of the forward facing windshields (see fig. 3). The structural weight of the forebody and actuating mechanism, while not intolerably heavy, still presented undesirable weight penalties. Noise levels in subsonic cruise with the nose drooped were also suspected to be high. All of the above was done purely to provide forward vision but this difficulty was compounded by the inadequacies of transparent materials then available to endure the SST environment for any substantial time. The development potential of new materials presented a risk. It should be emphasized too, that the main requirement for vision was in the subsonic flight modes. The search was started for an alternative to windshields in the generally accepted sense and an RFP was published for a passive optical system design.

One design, proposed by Singer Librascope, was to combine five  $25^\circ$  systems into one eyepiece with the field of view of the individual systems overlapping to the extent necessary for complete and uninterrupted viewing up to  $65^\circ$  laterally and  $45^\circ$  vertically. Each of these systems was basically a refractive, unity magnification telescope with an ambinoocular eyepiece, which when observed from the pilot's seat looked like a windshield insofar as it presented the same type of imagery. However, this system concept was considered to be less compatible with the SST flight deck than was a system conceived by and is proprietary to the Farrand Optical Company.

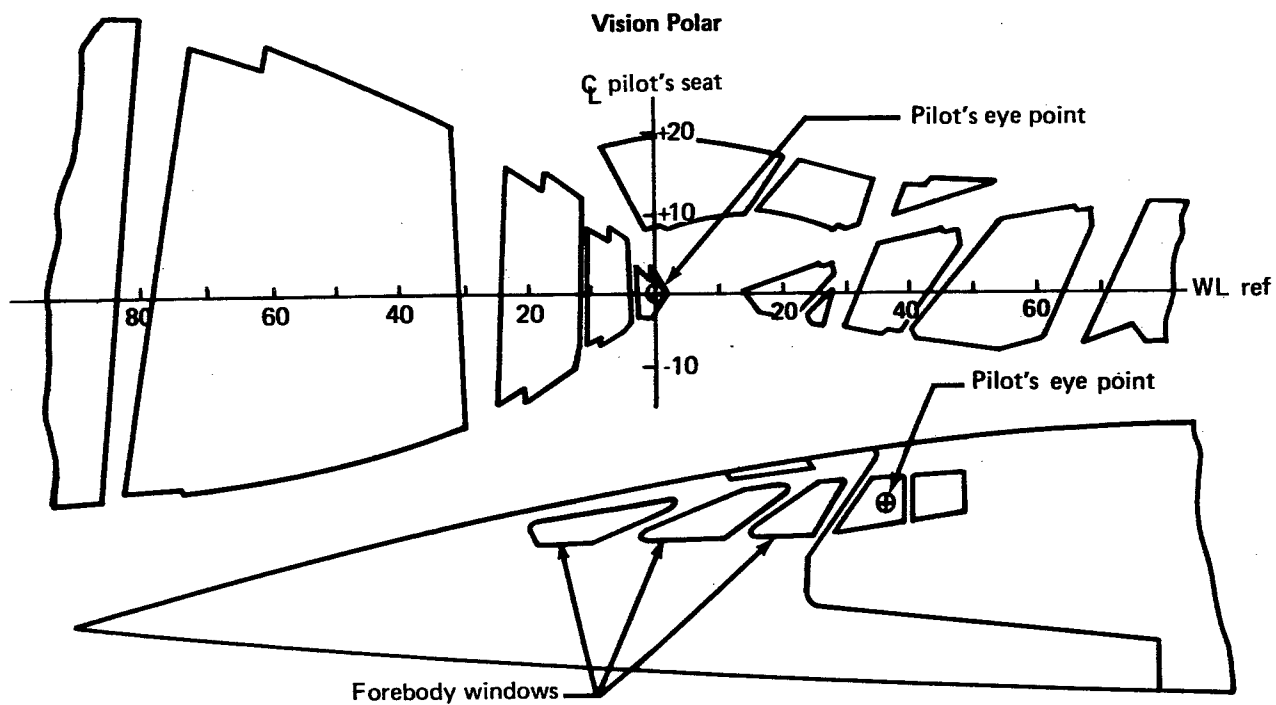


FIGURE 2.—SST NOSE CONFIGURATION FOR SUPERSONIC FLIGHT

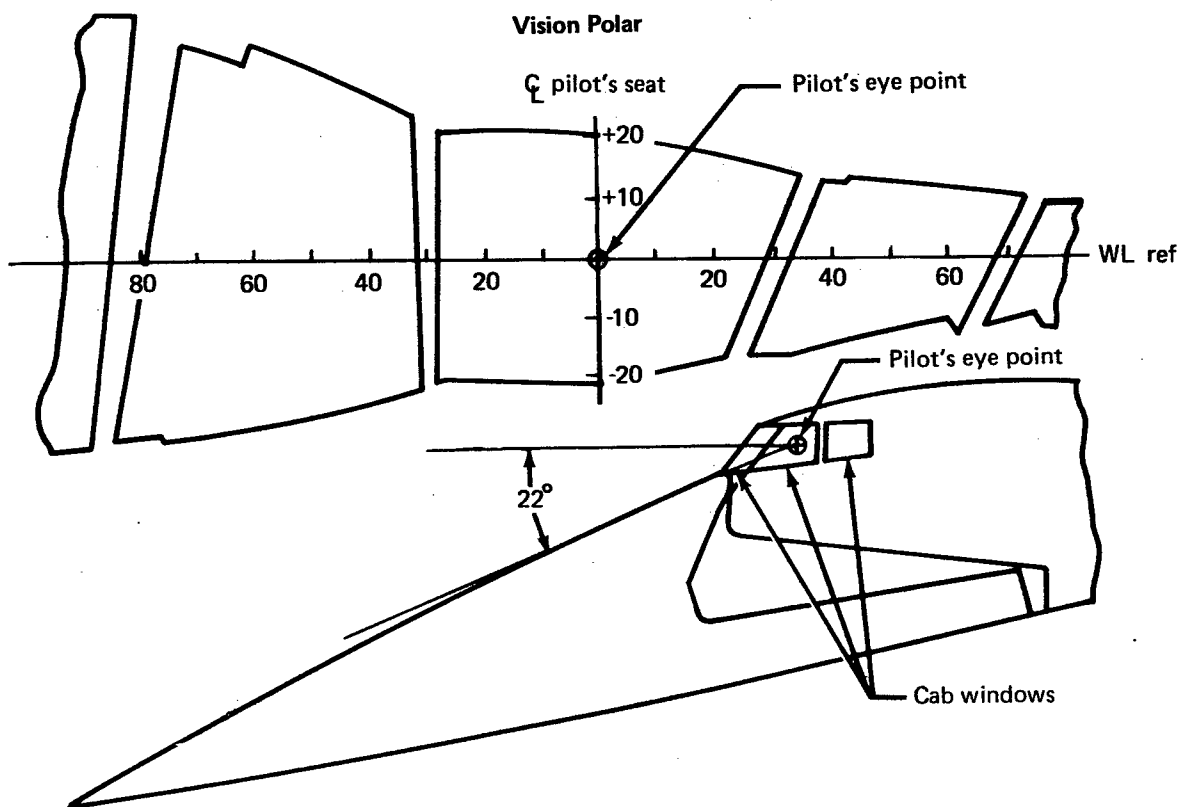


FIGURE 3.—SST NOSE CONFIGURATION FOR SUBSONIC FLIGHT

Farrand proposed a wide field of view system comprising short focal length concave mirrors and positive lenses whose field curvature was excessive within the system but was eliminated at the eyepiece because the mirror field curvature was cancelled by the equal and opposite field curvature of the short focal length lenses (see fig. 4). The result was a relatively compact system whose entrance port was at the skin of the airplane in the form of a small blister, 4 inches high, which provided a field of view for pilot and copilot of  $65^\circ$  laterally and  $30^\circ$  vertically.

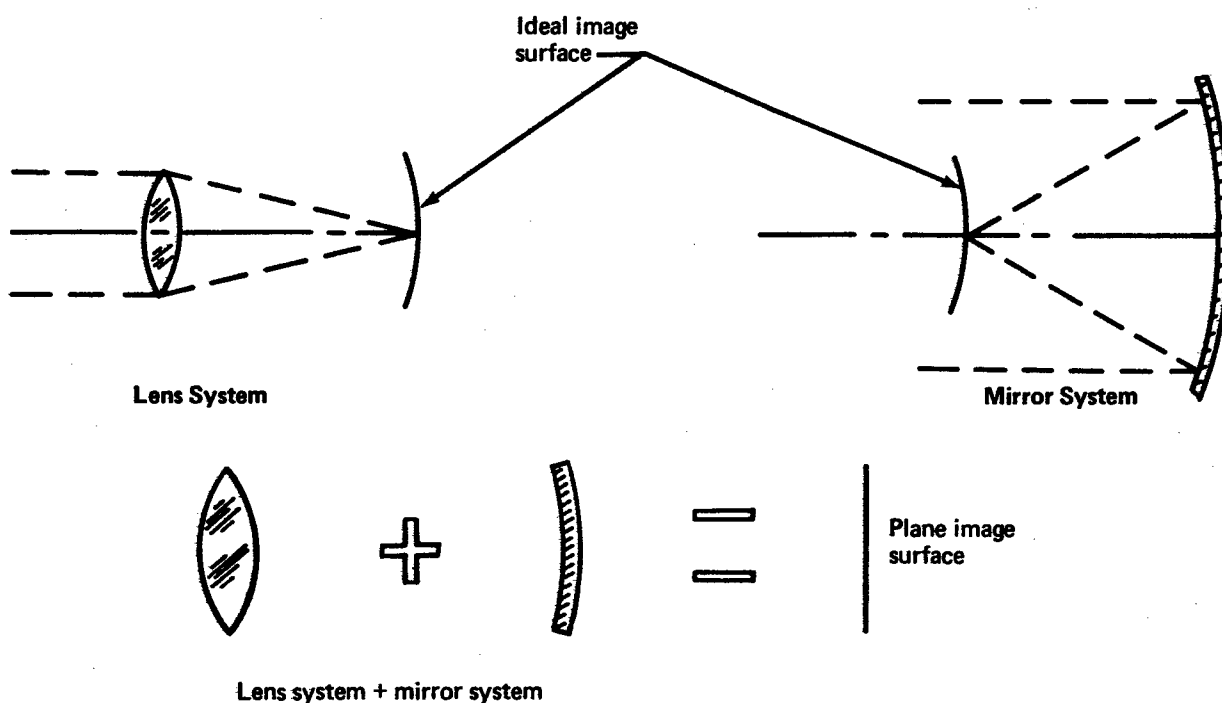


FIGURE 4.—OPTICAL VIEWING SYSTEM PRINCIPLE

This field of view was available to the pilot at all times but was not sufficient to meet the downward vision requirements for landing because the forebody obscured the view below. A second, retractable, entrance port was situated in the lower lobe of the now-fixed forebody and thus, when extended, provided the necessary additional downward vision for landing. The two images were combined at the eyepiece and gave a total field of view vertically of about  $50^\circ$ . In essence, an optical hole had been created in front of the pilot (and copilot) the size of the eyepiece 18 inches ahead of the crew.

Incorporating this system permitted deletion of the translating nose, replacing it with a fixed forebody, and the deletion of all forward looking windows. The system had a potential life of 50,000 hours in the SST environment and a light transmission approaching 85 percent. In an optical system of this kind, there are certain constraints on the location of the pilot's head if the full field of view is to be sustained. Movement of the eye outside this area, or exit pupil as it is called, causes a stopping down of the field of view (or vignetting) in a certain direction similar to the effect of trying to look around a window post. The size of the exit pupil needed to accommodate what is considered to be reasonable head movement without vignetting was determined to be about 5 inches laterally and 3 inches vertically. However, the precise size of exit

pupil that would satisfy pilots from the standpoint of ultimate ease of operation has yet to be determined in practical terms. The size of the exit pupil has a significant effect on the size of some of the optical components in the system. Fore and aft head movement was limited to about  $\pm 6$  inches from the optimum eye position and was considered more than adequate. The cab side windows were retained for image continuity and to provide the pilot with peripheral vision considered necessary for proper judgement of distances and speed.

Figure 5 shows the installation of such a system in the SST flight deck, along with the comparative vision polars provided by windshields and optical system combined with the cab side windows. A comparison of the vision and windshield requirements and an assessment of how well an optical system would perform provides, the obvious conclusion that, on this particular airplane, an optical system was very definitely superior to windows.

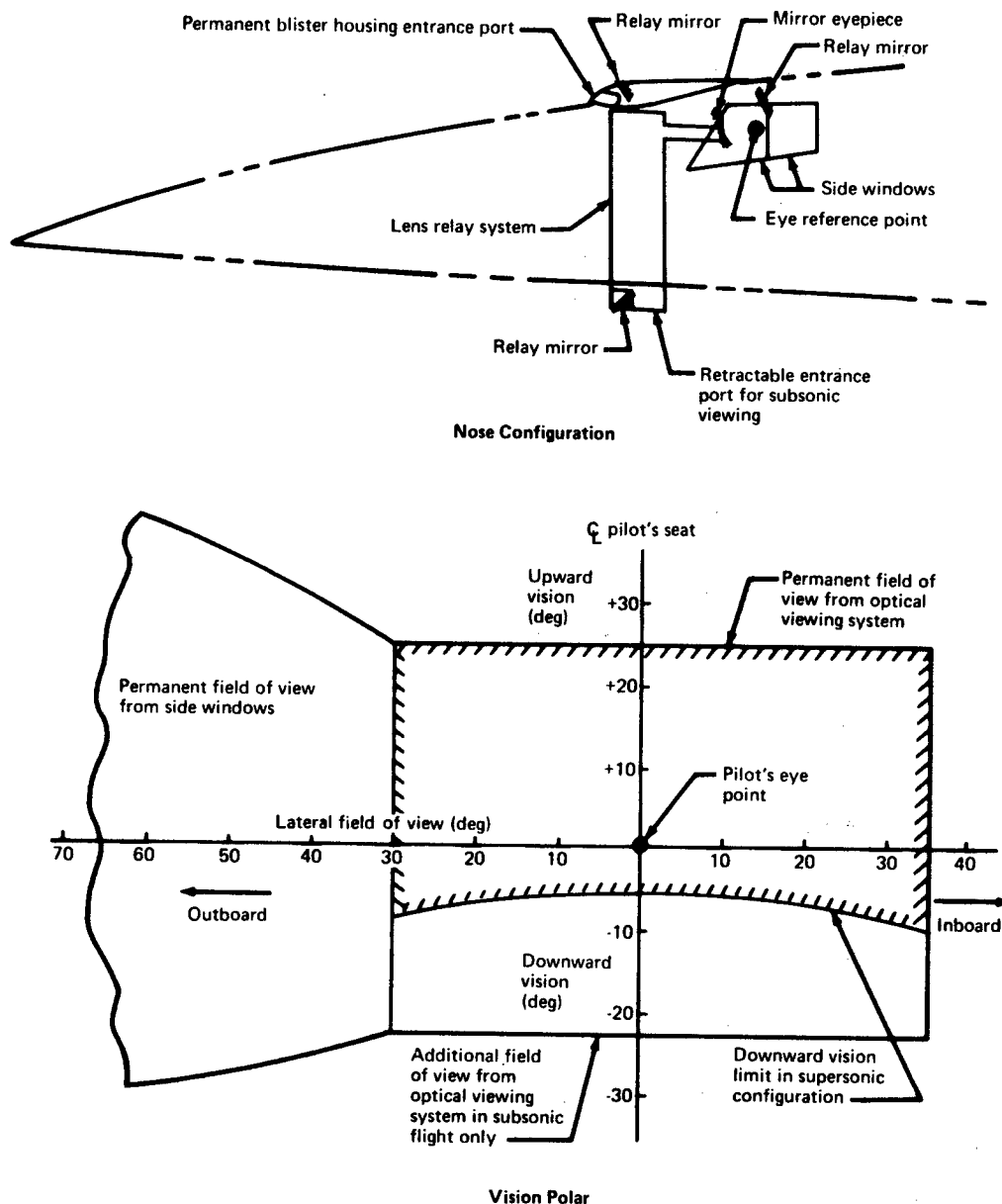


FIGURE 5.—SST OPTICAL VIEWING SYSTEM ARRANGEMENT

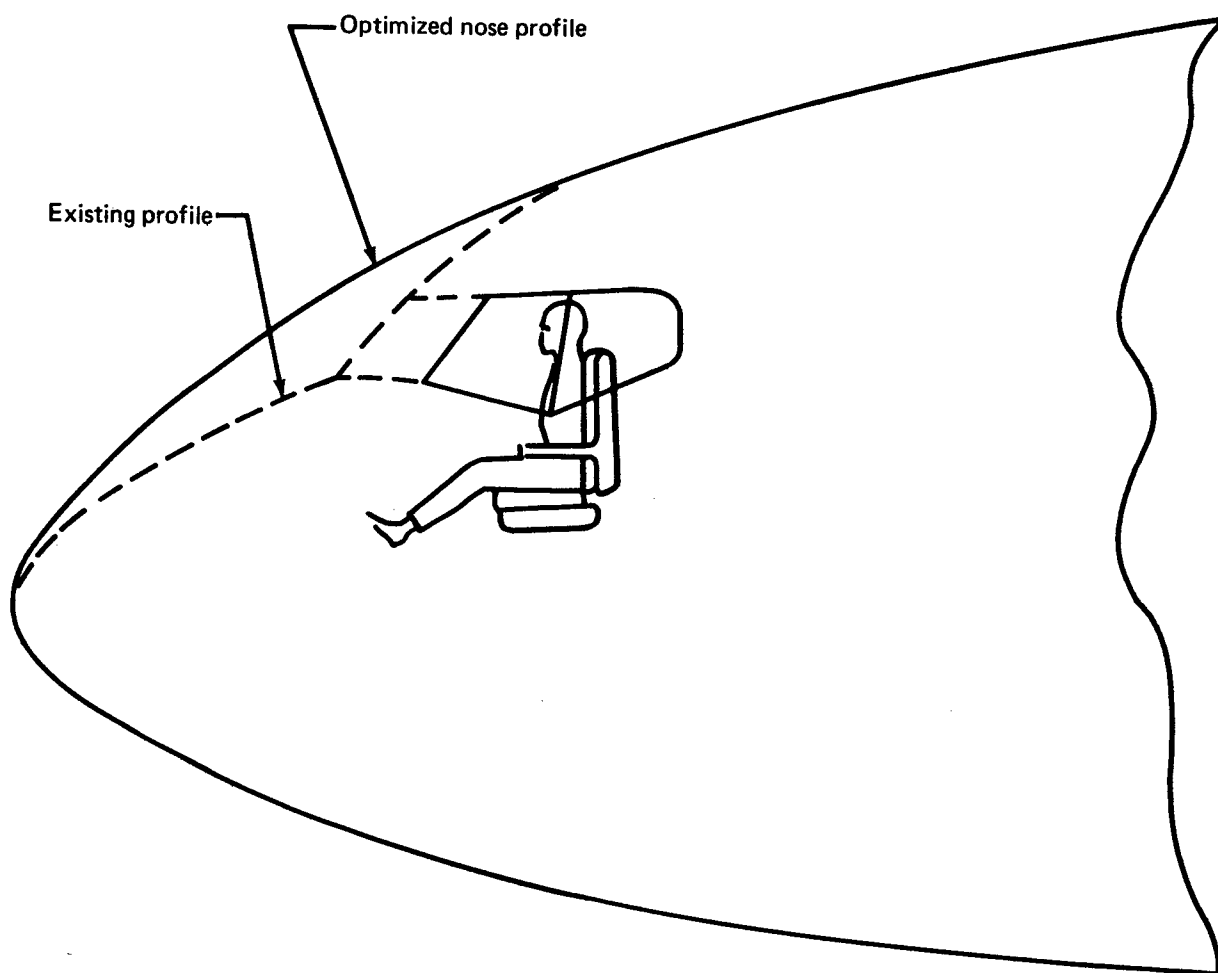
Taking the SST optical viewing system concept a stage further and looking at its application to subsonic transport airplanes in general shows it to be even more attractive than on the SST, but for somewhat different reasons. Federal Aviation Regulations do not define field of view required or what quality of imagery should be provided. Structural adequacy is also vaguely defined, although attempts are being made to make these requirements more definitive. This does not significantly alter the windshield designer's task, since it makes mandatory those rules he has been working with in recent years anyway. Assuming, then, that today's windshields will meet all that the book says they should, a comparison of windshield characteristics and, say, the SST optical system would show us where we stand if a change to optical viewing systems were made (table 1).

**TABLE 1.—CHARACTERISTICS COMPARED FOR WINDSHIELD AND SST OPTICAL SYSTEM**

| Parameter   | Windshield  | Optical viewing system  |
|---|---|---|
| Forward field of view                             | 20° up, 22° down<br>25° outbd, 35° inbd<br>(typical)                                | 50° vertical, oriented in<br>any direction<br>65° lateral, oriented<br>in any direction |
| Light transmission                                | 70% normal to window<br>35% over lower sill   | 85% over total field of view  |
| Optical quality                                   | Gunsight optics in limited<br>critical viewing area only<br>Lower quality elsewhere | Better than gunsight<br>optics throughout   |
| Crew protection (bird<br>impact, fail safe, etc.) | Critical design item  | Not critical  |
| Durability  | Limited   | Life of airplane  |
| Passive system                                    | Requires supplementary<br>power for deicing, etc.                                   | Requires less power than<br>windshield for deicing, etc.                                |
| Drag and noise                                    | Pronounced effect   | Minimal effect  |
| Flight deck geometry                              | Strong influence  | Moderate influence  |
| Development risk and cost                         | High  | Low following initial develop-<br>ment  |
| Constraints on viewing<br>station                 | None  | Limited to pilot and copilot<br>station   |
| Support structure                                 | Critical and heavy  | Minimum required  |
| Post geometry                                     | Critical design item  | Side window forward post<br>hidden behind eyepiece                                      |

The typical nose profile optimized for subsonic cruise on a transport airplane would look something like that shown in figure 6, which represents the Boeing 707 nose. The broken line shows where the existing profile lies and how it is influenced by the windshield geometry. Figure 7 shows the optimized shape but with an optical viewing system providing vision and shows how much simpler a system can be than that proposed for the SST, because one viewing port can provide the full field of view needed.





*FIGURE 6.-707 OPTIMIZED NOSE*

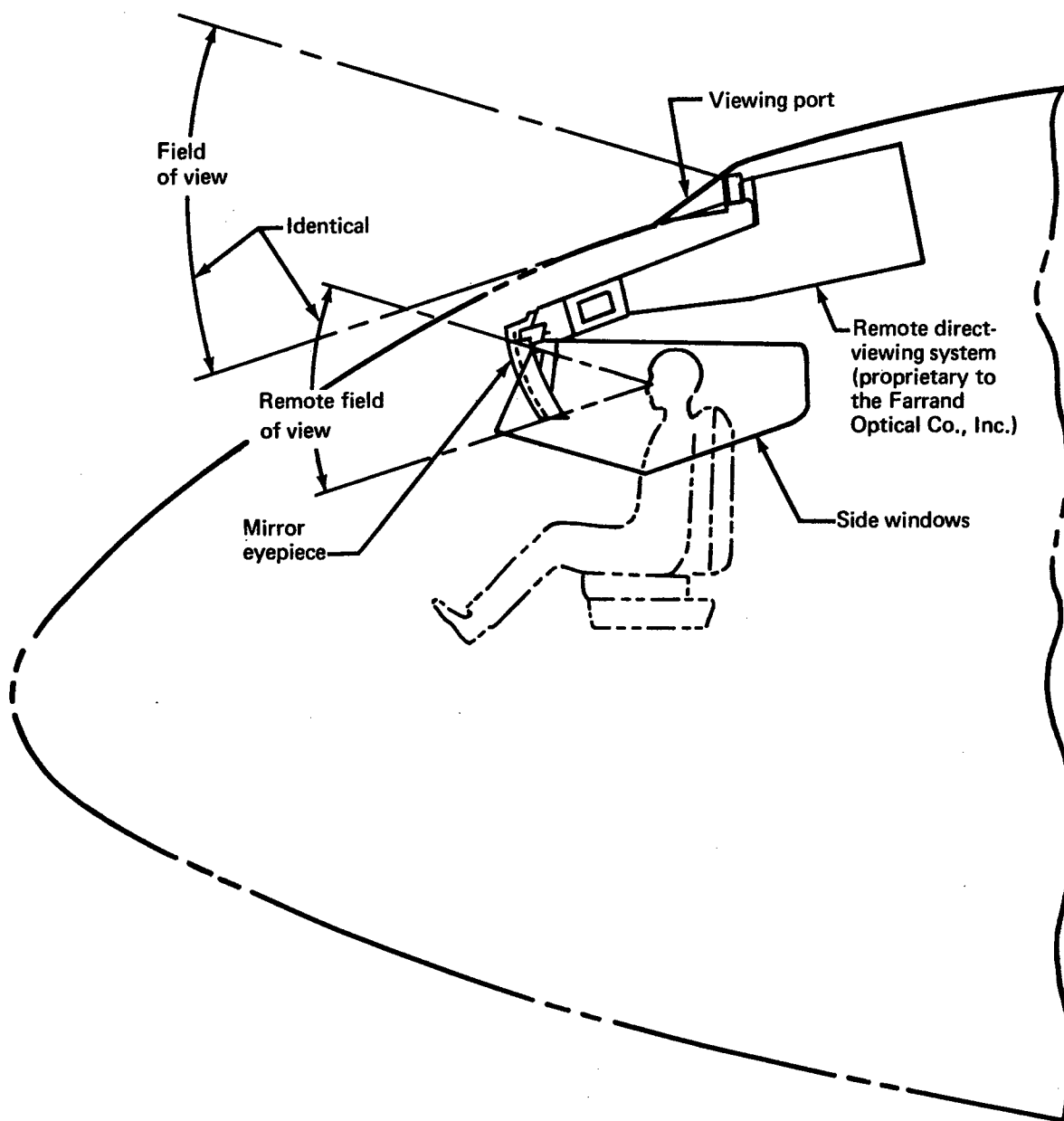


FIGURE 7.—707 OPTIMIZED NOSE WITH OPTICAL VIEWING SYSTEM

The system assembly comprises an entrance port on the top of the cab section with a relay mirror set above and behind the pilot's head. Between that mirror and the mirror eyepiece is a relay lens assembly which compensates for field curvature, puts the image in correct perspective, that is, puts it the right way up and the right way round, and is a convenient means of transporting the imagery. Adequate head clearance is provided and the whole system is coupled together with sufficient stiffness to prevent relative movement of optical elements from vibrations that might affect imagery. It should be pointed out that the system as a whole can vibrate substantially in any mode without any image displacement taking place relative to the eye.

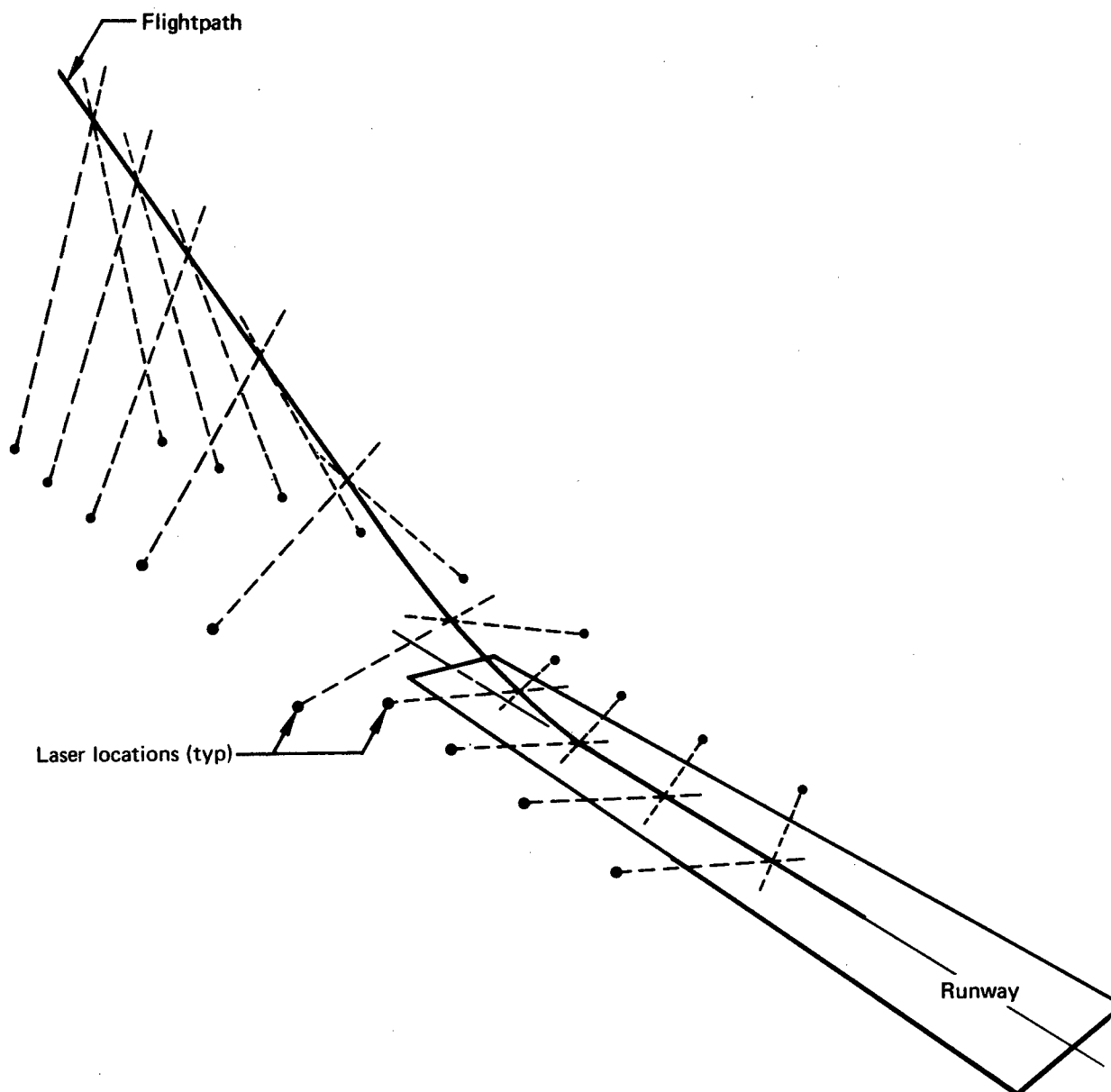
The side windows are retained for full field of view continuity, thus eliminating the tunnel vision effect which in some cases makes an object appear smaller. The system has an exit pupil 7 inches wide by 3 inches high at the pilot's station and the field of view is 60° vertically and 70° laterally. Its production cost would be about that of a large commercial transport windshield and its guaranteed life matches that of the airplane.

However, in the author's opinion, the improvements so far demonstrated are merely the tip of the iceberg. One other major constraint on flight deck geometry is the instrument panel and the equipment it has to house. Removal of the major portion of the flight instruments could result in a complete reorientation of flight deck layout. Without wishing to become involved in any controversy over head-up displays, the author believes the optical viewing system presents this possibility since insertion of data into the system is readily accomplished with an optical beam splitter and a cathode ray tube. The imagery on the cathode ray tube, which can represent any collection of instruments, is presented to the pilot as an infinity display superimposed on his view of the outside world. This way, the pilot does not have to refocus his eyes to read instruments whose information can be presented to him in any convenient form. The instrument panel would then probably contain only miniaturized backup instruments for use in the event that his head-up display system failed for any reason. It should be emphasized that at no time does the pilot lose his view of the outside world.

Since we now have a passive system for external viewing, vision augmentation by further data insertion might come from TV cameras for viewing the outside world in visibility conditions where the naked eye is hampered by low image contrast, or image intensifiers might be used for creating near-daylight conditions at night. The permutations and combinations of systems capable of being displayed are endless and it is not the intent of this paper to redesign and optimize a flight deck. However, since part of the function of windshields is to provide the pilot with a view for landing and since visual monitoring of automatic landing systems would still seem to be desirable down to the minimum visibility conditions for which a particular airplane is certified, an examination of how an optical viewing system can better provide this capability is justified.

Analysis by Boeing of landings carried out in various visibility conditions has shown that, as visible attenuation reaches the lower limits of Category II, the pilot's ability to see sufficiently well to be confident that his approach path is adequate prior to reaching his minimum decision height is seriously impaired, particularly in daylight. The conclusion is drawn that, unaided, the human eye is incapable of doing the job it is being asked to do if the visibility falls below that of Category II minimum (i.e., less than 1200 feet, runway visual range condition). The problem can be stated simply: what do you have to provide the pilot with so he can visually monitor the performance of his autoland system in visibility conditions down to the very minimum that nature can impose? A most attractive method of doing this has been demonstrated in the laboratories at Boeing with a system of crossed lasers.

Figure 8 shows a number of laser pairs set at discreet positions on the approach path and along the runway. Each pair crosses at a point on the approach path or down the runway centerline. In clear weather, the lasers are invisible, but as the moisture content or contaminate in the atmosphere increases, so the lasers become more visible and the point at which each pair crosses becomes brighter. Theoretically, then, the poorer the visibility the better the pilot can see his approach and rollout path.



**FIGURE 8.—INTERSECTING LASER BEAM LANDING PATTERN**

However, one set of conditions prevails where this concept breaks down and that is in severely attenuated visibility in broad daylight. In this case, the lasers have insufficient contrast by comparison with the ambient light conditions for the human eye to identify them. Nevertheless, the inclusion of a television camera with a narrow band pass filter on board the

airplane, set to look down the approach path and projecting the picture into the optical viewing system in the right perspective, will restore the pilot's ability to see in even these most severe conditions. Consequently, a complete visual monitoring of the autoland system can be made available at the cost of a few lasers whose total power requirement is no more than that of one approach light.

One final condition remains unanswered in reference to the tabular comparison of windshield versus optical viewing system and that is the inability of anyone to see through the eyepieces effectively from anywhere but the pilot and copilot stations, except through the side windows of course. A third crew member station is provided on many commercial transport airplanes. This crew member's services as an observer could be utilized to the full by providing a third optical viewing system at this station equipped with a rotatable, retractable, entrance port that would give him the ability to see in any direction with a real view of the outside world. A 360 global view can be provided with a wide field or zoom capability if a television camera is inserted in the system. This would add the capability of seeing any part of the airplane from a most advantageous position, namely from outside the airplane. The entrance port is made retractable, since it would be required very little during cruise.

In conclusion, it is the author's belief that an alternative system will replace windshields sooner or later, and that right now there is a system concept available that is capable of doing just that without in anyway reducing the pilot's ability to see and in many ways improving safety, which after all is what this is all about. However, no specific system of the kind discussed here has been built, let alone flown. But systems with similar optical requirements have been flown and have performed well. The incentive is there to build and fly a system to see whether the paper exercise is borne out in practice.

**SESSION 2**

**MATERIALS AND PROCESSES (Part I)**

A STATUS REPORT - NEW TRANSPARENT  
PLASTIC MATERIALS

Edward A. Arvay  
Air Force Materials Laboratory  
Wright-Patterson Air Force Base, Ohio

## A Status Report -

### New Transparent Plastic Materials

Edward A. Arvay  
Air Force Materials Laboratory

#### ABSTRACT

Research and development efforts on new and improved transparent plastics for aircraft enclosures have been nominal for almost two decades. This lack of emphasis is evident in the shortage of candidate materials for use in advanced aircraft. The scarcity of available options in the choice of materials is heightened by ever increasing requirements for thermal stability, impact resistance and retention of properties on processing and aging. R&D efforts for more thermally stable, tougher plastics for composites and molding compounds have resulted in new materials; however, these are generally highly colored, opaque materials. If these and other polymeric systems can be modified or purified to eliminate color and enhance transparency, a new generation of transparent plastics may be in the offing. A number of polymeric systems will be discussed emphasizing those characteristics which are desirable in enclosure materials. Many of these systems are experimental, not originally intended for aircraft use and most are not fully evaluated. Additional research and evaluation of these materials will be necessary. However, unless enclosure fabricators and chemists can be brought together and mutual interest generated, R&D directions cannot be defined. New transparent plastic materials availability for future aircraft will depend on today's research.



## I Introduction

It is well established that flight crews perform better and have a mental attitude when they have the direct viewing capability through a transparent enclosure rather than an indirect viewing system such as a periscope or closed circuit television. The material which affords them the unobstructed, undistorted, color true view of their path could be either a glass or a plastic or a combination of these. Ground crews could be expected to prefer glass because of its in service stability. However, designers and fabricators prefer plastics for the weight savings, impact resistance and fabricability.

Transparent plastics have been used on aircraft as windscreens, windshields, canopies or windows for many years. It is important to occasionally recall past materials to illustrate and dramatize the changes in plastics as aircraft have changed; and based on this experience to anticipate future changes. Plastics used or evaluated in the past have been many and varied.

Cellulose acetate and cellulose nitrate were among the first transparent plastics used on aircraft sometime around the mid 1930's. These two were replaced by cast acrylic of the original polymethacrylate type in the early 1940's, and found use up to the 1950's. The introduction of jet propelled aircraft spurred the research and development of materials which resulted in the introduction of many new and improved materials. Rigid vinyls, newer acrylics by Rohm and Haas and duPont, polyesters by Sierracin and PPG, allyl carbonate, chlorinated and fluorinated acrylics by General Aniline, epoxies, silicones and others appeared from various supplies. Names like Plexiglas II, Polymer K, Selection 44, 5106XP, Lucite 212, Sierracin 611, CR-39, PMACA and Gafite all represented advances in the state of the art. Then in about 1950 the properties of stretched acrylics became known and the flow of new materials virtually ceased. During this period the temperature requirements for transparent plastics climbed from ambient to about 200°F. Evaluations; however, were conducted up to 350°F in the laboratories. The important thing is that materials with improved properties were available to meet the requirements of improved performance aircraft.

## II Current Materials and Future Requirements

Materials generally considered as available for use are limited to essentially "three" types - acrylic (either as cast or stretched), acrylic clad polycarbonate and polycarbonate. The acrylics are similar to those

used for many years as either monolithic material or in a laminated composite with glass and various interlayers. The polycarbonates emerged as a transparent in about 1967 although the basic resin system was introduced almost ten years before. This material possess a combination of impact resistance and thermal stability never before available in a single plastic. The "growing pains" now being experienced by this material is probably typical of all other materials used in the past. Modifications of the material or the use of coatings may be necessary to make this material perform as anticipated. The clad materials looked very promising as a solution to short comings of the polycarbonate -abrasion and solvent resistance and optics. However, the addition of the acrylic layer decreased the impact strength of the polycarbonate and interest waned. The current materials appear to be satisfactory for aircraft systems in production and those nearing the production phase.

Judging from the past and current requirements - those of the future will probably be more demanding in every respect. We can expect most aircraft to go faster, fly higher and fly lower which will increase the materials requirements for thermal resistance, optical clarity and increased retention of properties under other adverse conditions. Thermal resistance will also be extended to low temperatures and thermal shock resistance may again be critical. Overall reliability of the transparency could become the prime effort.

Table 1 shows some property values which could be typical future materials requirements.

Table 1  
Future Requirements

|                             |                               |                  |
|-----------------------------|-------------------------------|------------------|
| Maximum Temperature         | 450-500°F                     |                  |
| Thermal Gradient            | 380-390°F                     |                  |
| Thermal Shock               | -40 to 500°F                  |                  |
| Heat Distortion Temperature | 400-600°F                     |                  |
| Coef. of Thermal Expansion  | $<80 \times 10^{-6}$          |                  |
|                             | <u>Short Time</u>             | <u>Long Time</u> |
| Tensile Strength ambient    | 12-18,000 psi                 | -                |
| Tensile Strength 250°F      | 8-10,000 psi                  | 6-8,000 psi      |
| Tensile Strength 500°F      | 5-8,000 psi                   | 3-6,000 psi      |
| Tensile Elongation ambient  | 10-75%                        |                  |
| Tensile Elongation 250°F    | >100%                         |                  |
| Tensile Elongation 500°F    | >200%                         |                  |
| Impact Strength 1 zod       | $3-10^4$ ft.lb./in of notch   |                  |
| Impact Strength Dart        | 8-12 feet                     |                  |
| Fracture Toughness          | $3-6 \times 10^3$ lb/in $3/2$ |                  |

Table 1 (continued)

|                     |             |
|---------------------|-------------|
| Transmittance       | >90%        |
| Haze                | < 1%        |
| Color               | Water white |
| Index of Refraction | 1.3 - 1.7   |
| Specific Gravity    | 0.9 - 1.4   |

The maximum temperature range is probably a reasonable estimate of the outboard surface temperature of windshields with slightly reduced temperatures on canopies.

The next two listed properties are considered to be possible new test requirements - tensile and flexural strengths with an imposed thermal gradient of some 380°F, and also strengths after cyclic thermal shock between the listed temperatures.

The heat distortion temperature of materials to meet the above requirements will need to be in the 400-600°F range.

The coefficient of linear thermal expansion should be as low as possible to permit bonding of materials which will not cause excessive stress by differential expansion.

The next item considers tensile strength and tensile elongation of materials at various temperatures and after various periods of continued or accumulated exposure at the temperatures. These tests would establish the reliability of materials in operational use.

The impact strengths are the usual tests for this property to determine the degree of bird impact resistance, it is anticipated that such tests at elevated temperatures or depressed temperatures could also be required.

Fracture toughness of materials may become an important criteria especially for load bearing structures. The requirement is a compromise value between stretched acrylic and polycarbonate.

The optical requirements are not overwhelming in light of the difficulties encountered in preparing optically clear materials. Anticipating greater viewing angles in advanced aircraft - transmittance should be maximized and haze minimized. Color requirements may be of necessity reduced to very pale color (yellow). The index of refraction is listed only as a possible clue to new materials. Specific gravity requirements are given to encourage the search for even lighter materials.

Some of the properties listed are those that are very often run on new polymers which could recommend the material for use as a transparent. These are Heat Distortion Temperature, Coefficient of Thermal Expansion, Tensile strength and elongation, Clarity, Index of Refraction and Specific gravity.

This list gives only desirable properties and property values which would recommend a material of possible use in aircraft. The new tests would hopefully disclose material weaknesses before the evaluations progressed too far.

Not included in the list are requirements for property retention after natural weathering or accelerated weathering of the material. This exposure and ultraviolet radiation in particular has been found to be critical in the degradation of physical properties as well as causing discoloration. Ultraviolet discoloration and loss of optical clarity are standard tests, but strength reduction are usually not determined. Solvent and environmental crazing in stressed and unstressed conditions are also critical characteristics which should be determined. At the anticipated increased speeds of future aircraft abrasion resistance and rain erosion resistance will become even more of concern.

#### IV Candidates for Near Future Use

Materials considered to be candidates as structural materials (not interlayers) for near future use include some new materials and some which have undergone at least preliminary evaluations. Because of either their newness or disclosed shortcomings all will require additional research and development.

The following tables will show on the right conservative values for the properties of stretched acrylic and polycarbonate plastics as reference values. Under the candidate tag will be given those materials which could find use. The candidate is given by class of polymer with a footnote identifying the material and supplier. Table 2 shows a limited number of values for the Polyarylsulfone, Polymer A. This and other similar materials will be discussed in later papers. Note the much higher heat distortion temperature of Polymer A which indicates increased strengths at elevated temperatures. The opticals are good and represent a great improvement over the original materials. This material is affected by UV exposure which causes discoloration (deepening of the slight yellow color). Current efforts are directed toward developing either internal or external (coating type) UV absorbers to eliminate this problem. The UV problem and the temperatures necessary to form this material are considered the major drawbacks. Currently 1/4" x 12" x 12" panels have been compression molded with some work being done on extrusion. These

sheets will be made available for evaluation of physical properties and secondary processing - i.e., forming, handling, etc.

Table 3 shows the comparison of the reference materials and another polyarylsulfone designated Polymer C. This is more thermally stable than even Polymer A as indicated by the HDT. R&D efforts on Polymer C were begun after those on Polymer A on an Air Force contract to the AFML.

The high temperature polycarbonate shown in Table 4 will also be discussed later in this program. The material developed by Dow Chemical under a NASA contract has a HDT of over 500°F, has good color and good opticals. The values given are from our measurements on an unpolished sample with the indicated thickness. Both this material and the previous one Polymer C will require high temperatures for forming. And both are available in only limited quantities.

Table 5 compares a polyphenylene oxide with the standards. Again the HDT is much higher with the strength properties being comparable except for the impact strength. We had no data on the opticals at the time of writing. Notice the lower specific gravity of this material. Provided the opticals are within range this material is a promising candidate for use in aircraft transparencies.

Table 6 shows data on a polysulfone material, transparent versions of which have been reported; however, these do not represent the ultimate in optical clarity. Our measurements on an injection molded samples are given. There is a yellow color -but not deep yellow to the samples. The HDT is again higher than the reference materials and physicals are comparable. Discoloration by UV radiation is also a problem with this material.

Table 7 gives data on a polymethyl pentene polymer which has a serious UV radiation exposure problem leading to degradation of the material. The thermal stability is less than the previous materials and the two references. However, the reported transmittance and haze and the specific gravity do recommend this material.

From these materials and future materials to be introduced by the suppliers of current polycarbonates will come the transparent materials with a greater margin of safety - especially in thermal resistance. With most of these materials a complimenting coating for abrasion resistance and improved UV resistance are necessary and the availability of material will have to be increased even for an evaluation program.

## V Materials with Potential

Many of the materials to be called out in this section have not to our knowledge been considered by the suppliers as candidates for use as transparents. Some are commercially available and others are strictly experimental; however, they all have one or more properties which make them candidates.

The polybutadienes shown in Table 8 are family of resins with variable end cappings and molecular weights which provide materials varying from rubbery to hard. The materials are low in color and require only short elevated temperature cures at less than 400°F. Shown on the slide are properties of Hystl formulation 110. Notice the HDT and the specific gravity of this material as compared to the references. The present materials tend to be brittle with low elongation and low impact strength. Inherent color in these materials is reportedly low. Tensile strength is also less than the references. Polybutadienes have a low cost factor of about \$1.00/lb.

Table 9 gives data on a modified polybutadiene closely related to the previous one except that a different hardner was used to increase the compressive strength. This detrimentally affects the tensile and impact strengths. Transmittance is good as indicated and the specific gravity is low. The HDT by the standard test is 327°F; however, a more effective distortion temperature (by thermoanalyzer) is closer to 525°F. This too is a low cost material with some attractive potential.

A Polyimide candidate is shown in Table 10. Materials of this type which we have seen retain a considerable amount of color and evidence of included contaminants. The figure shows the available data on Sablon which was not intended to be a transparent and therefore was not cleaned or purified but rather was a sample which showed transparency. The HDT of this class of material is high as expected; however, curing to shape temperatures would be much lower. Our measurements of transmittance and haze on two available samples are

|              |                     |
|--------------|---------------------|
| Sablon       | 10% (0.088" thick)  |
| XPI-182-97-1 | 51%T 35% H (0.129") |

The latter is by American Cyanamid. At least two others are known to be in development stages by IITRI and duPont.

The polyamide shown in Table 11 is an interesting material (which we understand is being evaluated as a canopy material) with some excellent properties. Although the HDT is only slightly higher than the polycarbonate, its tensile strength and impact strengths are comparable.

Elongation is slightly low and the specific gravity is only moderately low. Transmittance and haze values are certainly acceptable for the material at this stage. Polyamide color is essentially water white and the material lends itself to injection molding.

Table 12 gives the available data on one of several polypeptide materials. As with so many of the other materials these were developed for biomedical applications rather than aircraft transparencies. This indicated thermal stability comes from the midpoint of their TGA curves in air. Property values were obtained on thin films. It was indicated that thicker samples would also be water white; however, no samples are available. Polypeptides represent a family of materials which can be tailored for a particular end use.

Transparent ABS plastics are low temperature materials as seen in Table 13. A heat distortion temperature of 181°F would limit this material to low performance aircraft. However, the material shown here has an impact resistance in this range of 10-16 which may open up possibilities. Strength values are not impressive and we have no good haze and transmittance values except those reported. To the table we could add Marbons CIT ABS material.

The next candidate shown in Table 14 comes from a paper reporting the preparation of these materials. Information only covered those properties given - a high melting point and that the material was clear and flexible.

The last material to be mentioned is shown in Table 15, a 85% crystalline polyethylene with a melting point of 266°F. This material was only available as a fiber which showed a 5 fold increase in modulus over conventional high density polyethylene. Whether this material could be made available in thick sheet is not known.

We know that the above materials list is not complete and that other materials with equal or better properties are in existence. But these are the ones on which some data was available.

## VI Summary

The materials mentioned as near future candidates all require additional work to alleviate known problems and to provide increased

quantities in sheet form for evaluation. Several of these are being actively pursued to make quantities and data available.

The materials given as having potential will require an even greater effort to provide preliminary data, to produce sufficient quantities for a more comprehensive evaluation.

New materials, in the tradition of the old ones, are being developed; however, their availability will depend upon the interest shown by the industry and government agencies.



Table 2

## Selected Properties Of Plastics

| PROPERTY                 | CANDIDATE        |  | AVAILABLE            |                    |
|--------------------------|------------------|--|----------------------|--------------------|
|                          | POLYARYLSULFONE* |  | STRETCHED<br>ACRYLIC | POLY-<br>CARBONATE |
| Heat Distortion Temp. °F | 420°F            |  | 212                  | 270                |
| Tensile Strength psi     |                  |  | 13,200               | 10,000             |
| Transmittance %          | >80              |  | 91                   | 75-85              |
| Haze %                   | <5               |  | 1                    | 1-2                |
| Color                    | Pale Yellow      |  | Water White          | Water White        |
| Specific Gravity         | 1.36             |  | 1.19                 | 1.20               |

\*Polymer A, 3M Company

Table 3

## Selected Properties Of Plastics

| PROPERTY                | CANDIDATE        |                      | AVAILABLE          |  |
|-------------------------|------------------|----------------------|--------------------|--|
|                         | POLYARYLSULFONE* | STRETCHED<br>ACRYLIC | POLY-<br>CARBONATE |  |
| Heat Distortion Temp °F | 520°F            | 212                  | 270                |  |
| Tensile Strength psi    |                  | 13,200               | 10,000             |  |
| Transmittance %         | >40              | 91                   | 75-85              |  |
| Haze %                  | <10              | 1                    | 1-2                |  |
| Color                   | Pale Yellow      | Water White          | Water White        |  |
| Specific Gravity        | 1.36             | 1.19                 | 1.20               |  |

\*Polymer C, 3M Company

Table 4  
Selected Properties Of Plastics

| PROPERTY                | CANDIDATE      |                   | AVAILABLE        |  |
|-------------------------|----------------|-------------------|------------------|--|
|                         | POLYCARBONATE* | STRETCHED ACRYLIC | POLY - CARBONATE |  |
| Heat Distortion Temp °F | >500           | 212               | 270              |  |
| Tensile Strength psi    |                | 13,200            | 10,000           |  |
| Transmittance %         | >81 (0.248")   | 91                | 75-85            |  |
| Haze %                  | <9             | 1                 | 1-2              |  |
| Color                   | Water White    | Water White       | Water White      |  |
| Specific Gravity        |                | 1.19              | 1.20             |  |

\* NASA/Dow Chemical

Table 5

## Selected Properties Of Plastics

| PROPERTY                                | CANDIDATE               |                      | AVAILABLE          |  |
|---|-------------------------|----------------------|--------------------|--|
|   | POLYPHENYLENE<br>OXIDE* | STRETCHED<br>ACRYLIC | POLY-<br>CARBONATE |  |
| Heat Distortion Temp °F                 | 375                     | 212                  | 270                |  |
| Tensile Strength psi                    | 10,500                  | 13,200               | 10,000             |  |
| Elongation %                            | 50-100                  |                      | 110                |  |
| Flexural Strength psi                   | 13,500                  | 17,000               | 13,500             |  |
| Flexural Modulus psi                    | 370,000                 | 430,000              | 340,000            |  |
| Impact Strength 120D FtLb/<br>in. notch | 2.6                     | 11                   | 14                 |  |
| Transmittance %                         |                         | 91                   | 75-85              |  |
| Haze %                                  |                         | 1                    | 1-2                |  |
| Color                                   |                         | Water White          | Water White        |  |
| Specific Gravity                        | 1.06                    | 1.19                 | 1.20               |  |

\*PPO C-1001, General Electric Company

Table 6

## Selected Properties Of Plastics

| PROPERTY                                | CANDIDATE    |                      | AVAILABLE          |  |
|---|--------------|----------------------|--------------------|--|
|   | POLY SULFONE | STRETCHED<br>ACRYLIC | POLY-<br>CARBONATE |  |
| Heat Distortion Temp °F                 | 345          | 212                  | 270                |  |
| Tensile Strength psi                    | 10,200       | 13,200               | 10,000             |  |
| Elongation %                            | 50-100       |                      | 110                |  |
| Flexural Strength psi                   | 15,400       | 17,000               | 13,500             |  |
| Flexural Modulus psi                    | 390,000      | 430,000              | 340,000            |  |
| Impact Strength 120D FtLb/<br>in. Notch | 1.3          | 11                   | 14                 |  |
| Transmittance %                         | 67 (0.136")  | 91                   | 75-85              |  |
| Haze %                                  | 8            | 1                    | 1-2                |  |
| Color                                   | Amber        | Water White          | Water White        |  |
| Specific Gravity                        | 1.24         | 1.19                 | 1.20               |  |

\*P-1700, Union Carbide

Table 7

## Selected Properties Of Plastics

| PROPERTY                | "CANDIDATE"        |  | AVAILABLE            |                    |
|-------------------------|--------------------|--|----------------------|--------------------|
|                         | POLYMETHYL PENTENE |  | STRETCHED<br>ACRYLIC | POLY-<br>CARBONATE |
| Heat Distortion Temp °F |                    |  | 212                  | 270                |
| "Thermal Resistance"    | 250-320°F          |  |                      |                    |
| Tensile Strength psi    | 3500 - 4000        |  | 13,200               | 10,000             |
| Elongation %            | 13-22              |  |                      | 110                |
| Transmittance %         | >90                |  | 91                   | 75-85              |
| Haze %                  | <5                 |  | 1                    | 1-2                |
| Color                   |                    |  | Water White          | Water White        |
| Specific Gravity        | 0.83               |  | 1.19                 | 1.20               |

\*TPX, Imperial Chemicals

Table 8

## Selected Properties Of Plastics

| PROPERTY                                | CANDIDATE       |                      | AVAILABLE           |  |
|---|-----------------|----------------------|---------------------|--|
|   | POLY BUTADIENE* | STRETCHED<br>ACRYLIC | POLY -<br>CARBONATE |  |
| Heat Distortion Temp °F                 | 490             | 212                  | 270                 |  |
| "Thermal Resistance"                    |                 |                      |                     |  |
| Tensile Strength psi                    | 8200            | 13,200               | 10,000              |  |
| Elongation %                            | 4               |                      | 110                 |  |
| Impact Strength 120D FtLb/<br>in. Notch | .66             | 11                   | 14                  |  |
| Transmittance %                         |                 | 91                   | 75-85               |  |
| Haze %                                  |                 | 1                    | 1-2                 |  |
| Color                                   | Low             | Water White          | Water White         |  |
| Specific Gravity                        | 1.00            | 1.19                 | 1.20                |  |

\* HYSTL 110, HYSTL Development Co.

Table 9

## Selected Properties Of Plastics

| PROPERTY                                | CANDIDATE                 |                      | AVAILABLE          |  |
|---|---------------------------|----------------------|--------------------|--|
|   | MODIFIED<br>POLYBUTADIENE | STRETCHED<br>ACRYLIC | POLY-<br>CARBONATE |  |
| Heat Distortion Temp °F                 | 327 <sup>+</sup>          | 212                  | 270                |  |
| "Thermal Resistance"                    | 527 (Thermoanalyzer)      |                      |                    |  |
| Tensile Strength psi                    | 2,500                     | 13,200               | 10,000             |  |
| Elongation %                            | 1.4                       |                      | 110                |  |
| Flexural Strength psi                   | 8,200                     | 17,000               | 13,500             |  |
| Flexural Modulus psi                    | 310,000                   | 430,000              | 340,000            |  |
| Impact Strength 120D FtLb/<br>In. Notch | .21                       | 11                   | 14                 |  |
| Transmittance %                         | 84 (0.328")               | 91                   | 75-85              |  |
| Haze %                                  | 4                         | 1                    | 1-2                |  |
| Color                                   | Water White               | Water White          | Water White        |  |
| Specific Gravity                        | 0.98                      | 1.19                 | 1.20               |  |

Whittaker Corp.



Table 10

## Selected Properties Of Plastics

| PROPERTY                                |     | AVAILABLE   |                      |                    |
|---|-----|-------------|----------------------|--------------------|
|   |     | "CANDIDATE" | STRETCHED<br>ACRYLIC | POLY-<br>CARBONATE |
| Heat Distortion Temp                    | °F  | 608         | 212                  | 270                |
| Tensile Strength                        | psi | 18,700      | 13,200               | 10,000             |
| Elongation                              | %   | 4           |                      | 110                |
| Flexural Strength                       | psi | 23,000      | 17,000               | 13,500             |
| Flexural Modulus                        | psi | 600,000     | 430,000              | 340,000            |
| Impact Strength 120D FtLb/<br>In. Notch |     | 1.5         | 11                   | 14                 |
| Transmittance                           | %   | 10 (0.088") | 91                   | 75-85              |
| Haze                                    | %   |             | 1                    | 1-2                |
| Color                                   |     | Dark Amber  | Water White          | Water White        |
| Specific Gravity                        |     | 1.40        | 1.19                 | 1.20               |

\* SABLON, SOLAR  
XPI-182, American Cyanamid  
NR-130, duPont

Table 11

## Selected Properties Of Plastics

| PROPERTY                                | "CANDIDATE" |                      | AVAILABLE          |  |
|---|-------------|----------------------|--------------------|--|
|   | POLY AMIDE* | STRETCHED<br>ACRYLIC | POLY-<br>CARBONATE |  |
| Heat Distortion Temp °F                 | 293         | 212                  | 270                |  |
| Tensile Strength psi                    | 12,000      | 13,200               | 10,000             |  |
| Elongation %                            | 9.5         |                      | 110                |  |
| Flexural Strength psi                   | 17,800      | 17,000               | 13,500             |  |
| Flexural Modulus psi                    | 380,000     | 430,000              | 340,000            |  |
| Impact Strength 120D FtLb/<br>In. Notch | 10-15       | 11                   | 14                 |  |
| Transmittance %                         | 84 (0.262") | 91                   | 75-85              |  |
| Haze %                                  | 4           | 1                    | 1-2                |  |
| Color                                   | Water White | Water White          | Water White        |  |
| Specific Gravity                        | 1.12        | 1.19                 | 1.20               |  |

\*Trogamid T, Dyanamid-Nobel

Table 12

## Selected Properties Of Plastics

| PROPERTY   |     | AVAILABLE    |                      |                    |
|--|-----|--------------|----------------------|--------------------|
|  |     | "CAN DIDATE" | STRETCHED<br>ACRYLIC | POLY-<br>CARBONATE |
| Heat Distortion Temp                                     | °F  |              | 212                  | 270                |
| Coef. of Thermal Expansion<br>In/In/°F x 10 <sup>5</sup> |     | --           | 42                   | 38                 |
| Tensile Strength   | psi | 7,000        | 13,200               | 10,000             |
| Elongation   | %   | 111          |                      | 110                |
| Transmittance  | %   |              | 91                   | 75-85              |
| Haze   | %   |              | 1                    | 1-2                |
| Color  |     |              | Water White          | Water White        |
| Specific Gravity   |     |              | 1.19                 | 1.20               |

\*Gulf South Research

Table 13

## Selected Properties Of Plastics

| PROPERTY                                | "CANDIDATE" |                      | AVAILABLE          |  |
|---|-------------|----------------------|--------------------|--|
|   | ABS*        | STRETCHED<br>ACRYLIC | POLY-<br>CARBONATE |  |
| Heat Distortion Temp °F                 | 181         | 212                  | 270                |  |
| Tensile Strength psi                    | 5,000       | 13,200               | 10,000             |  |
| Elongation %                            | 60          |                      | 110                |  |
| Flexural Strength psi                   | 7,800       | 17,000               | 13,500             |  |
| Flexural Modulus psi                    | 280,000     | 430,000              | 340,000            |  |
| Impact Strength 120D FtLb/<br>In. Notch | 10-16       | 11                   | 14                 |  |
| Transmittance %                         | 70-90       | 91                   | 75-85              |  |
| Haze %                                  |             | 1                    | 1-2                |  |
| Color                                   | Water White | Water White          | Water White        |  |
| Specific Gravity                        | 1.08        | 1.19                 | 1.20               |  |

\*Toyolac 900 Series, Toyo Rayon, Japan

Table 14

## Selected Properties Of Plastics

| PROPERTY                | "CANDIDATE"   | DIAMIDE-CARBONATES* | STRETCHED ACRYLIC | POLY-CARBONATE |
|-------------------------|---------------|---------------------|-------------------|----------------|
| Heat Distortion Temp °F |               |                     | 212               | 270            |
| "Thermal Resistance"    | 527°F mp(DTA) |                     |                   |                |
| Tensile Strength psi    |               |                     | 13,200            | 10,000         |
| Elongation %            |               | Flexible            |                   | 110            |
| Transmittance %         |               |                     | 91                | 75-85          |
| Haze %                  |               |                     | 1                 | 1-2            |
| Color                   |               | Clear               | Water White       | Water White    |
| Specific Gravity        |               |                     | 1.19              | 1.20           |

\*11TR1

Table 15

## Selected Properties Of Plastics

| PROPERTY                | "CANDIDATE"                     |                      | AVAILABLE          |  |
|-------------------------|---------------------------------|----------------------|--------------------|--|
|                         | 85% CRYSTALLINE<br>POLYETHYLENE | STRETCHED<br>ACRYLIC | POLY-<br>CARBONATE |  |
| Heat Distortion Temp °F |                                 | 212                  | 270                |  |
| "Thermal Resistance"    | 266 °F mp                       |                      |                    |  |
| Tensile Strength psi    |                                 | 13,200               | 10,000             |  |
| Transmittance %         |                                 | 91                   | 75-85              |  |
| Haze %                  |                                 | 1                    | 1-2                |  |
| Color                   | Water White                     | Water White          | Water White        |  |
| Specific Gravity        |                                 | 1.19                 | 1.20               |  |

\*University of Massachusetts

POLYARYLSULFONE - A NEW DIMENSION  
IN HIGH PERFORMANCE AIRCRAFT  
TRANSPARENCIES

R. L. Burns, H. A. Vogel, and A. T. Worm  
3M Company  
St. Paul, Minnesota  
and  
E. A. Arvay  
Air Force Materials Laboratory  
Wright-Patterson Air Force Base, Ohio

POLYARYLSULFONE - A NEW DIMENSION IN HIGH  
PERFORMANCE AIRCRAFT TRANSPARENCIES

by

R. L. Burns, H. A. Vogel, A. T. Worm, 3M

and

E. A. Arvay, Air Force Materials Laboratory

ABSTRACT

Three polymer structures, Polymers A, C and D, of the family of plastics known as polyarylsulfones have been evaluated as candidates for high temperature aircraft transparencies. The effects of modifications and improvements in polymer preparation and fabrication procedures on luminous transmittance and haze have been studied. Substantial improvements in light transmission and haze values have been made with all three polymer structures. Polymer A has exhibited the best optical properties of 84 percent transmittance and 3 percent haze. Other properties measured included mechanical properties at both room temperature and elevated temperatures, surface abrasion, water absorption and heat distortion. These data show the candidate polyarylsulfone polymers to possess outstanding strength and thermal stability in the 400° to 500°F range. The ultraviolet radiation stability of the polyarylsulfones was shown to be poor by ten day Fadeometer tests. An evaluation of commercially available high temperature, ultraviolet stabilizers has not produced satisfactory improvements as yet, due to the poor compatibility with the polymers and the high molding temperatures required to process polyarylsulfone resins. Solvent stress cracking tests have shown the polyarylsulfones to possess excellent solvent resistance. Solvent resistance was found to increase with increasing heat distortion temperature among polymers A, C and D. Ten day thermal cycling between -100°F and 350°F had no effect on the appearance, luminous transmittance or haze of all three polymer candidates evaluated.



## INTRODUCTION

The replacement of glass by plastics in aircraft transparencies is finding increasing acceptance. Aside from comparable optical properties, plastics offer significant weight savings, excellent structural properties, greater design latitude and easier sealing. However, there are a number of other requirements placed upon windshields, canopies and windows, where plastics show deficiencies, especially in the area of thermal stability and abrasion and solvent resistance.

Thermal properties become a critical factor in advanced aircraft which may attain skin temperatures of 450°F at supersonic speeds. The plastics in principal use at the present time are acrylics and polycarbonates, their upper use temperature is about 200° to 250°F. In recent years other engineering thermoplastics with improved thermal capabilities have become commercially available. Among these the polyarylsulfone resins possess a unique combination of physical properties and appear to offer a solution to the requirements of the next generation high performance aircraft transparencies. The work reported in this paper has been performed under USAF Contract F33615-71-C-1154. The program was administered by the Air Force Materials Laboratory, Wright Patterson Air Force Base, Ohio. (1)

## TECHNICAL DISCUSSION

### A. Polymer Structures Evaluated

The particular class of polyarylsulfones evaluated under this program consist of phenyl and biphenyl groups linked by ether and sulfone groups. Specifically these polymers are characterized by having the units  $\text{-(}\phi\text{-}\phi\text{-SO}_2\text{)}_x\text{-(}\phi\text{-O-}\phi\text{-SO}_2\text{)}_y$ , where  $\phi$  is phenyl, with no aliphatic bonds present in the polymer chain backbone. They are amorphous rather than crystalline materials. They are basically colorless, since no chromophoric groups are present in the polymer repeat unit. The polyarylsulfones also have outstanding thermal and thermo-oxidative stability and excellent chemical resistance.

The main objective of the program was to obtain a polyarylsulfone with a use temperature of 500°F, 85% luminous transmittance and 3% haze. Three candidate polyarylsulfones were selected for evaluation as described below:

1. Polymer A - The polymer with the lowest glass transition temperature (T<sub>g</sub>) of the polyarylsulfones evaluated.
2. Polymer B (D) - Polymers with a glass transition temperature between Polymers A and C. During the preliminary testing Polymer B was found to be too brittle for further development and was subsequently replaced by the more flexible Polymer D.
3. Polymer C - The polymer with the highest glass transition temperature. This polymer is structurally very similar to the commercially available "ASTREL" Brand 360 Plastic.\*

The three candidate polymers allowed a wide range of polymer preparation and fabrication conditions. Since the very high temperatures required in the manufacture of sheets were expected to cause some lowering of the optical properties, it was believed that a certain sacrifice in T<sub>g</sub> would be a worthwhile compromise towards less severe processing conditions.

#### B. Preliminary Evaluation

Exploratory work and preliminary testing of the polymers to determine the transmittance and haze were performed on 100g samples. Materials needed to establish fabrication parameters and complete baseline data were prepared in three pound quantities.

The first series of the candidate polymers was made by the best known current techniques used for the production of the commercial "ASTREL" 360. The optical properties of these materials were found to be quite poor, with luminous transmittance on 1/4 inch thick specimens ranging from about 20% to 30%.

\* ASTREL<sup>®</sup> Brand 360 Plastic is an injection moldable polyarylsulfone produced by the 3M Company.

A significant improvement in the transmittance and haze values was achieved with the second series of the candidate polymers. These materials were also used to establish suitable molding conditions for each polymer candidate. The data obtained from these preliminary investigations are summarized in Table 1.

Table 1.

Preliminary Properties Evaluation

(1/4 inch Test Specimens)

| Polymer Designation | Tg, °F | Compression Molding Temp., °F | Trans., % | Haze, % |
|---------------------|--------|-------------------------------|-----------|---------|
| Polymer A           | 440    | 500-575                       | 60        | 25      |
| Polymer B (D)       | 500    | 600-675                       | 50        | 15      |
| Polymer C           | 550    | 700-750                       | 50        | 45      |
| "ASTREL" 360        | 550    | 700-750                       | 10        | 50      |

Property data of the commercially available "ASTREL" 360 have been included for comparison.

C. Comprehensive Evaluation

1. Optical Properties

Polymer A, because of its easier fabrication characteristics, showed the most promise of reaching the target properties in luminous transmittance and haze. Therefore, the main development effort toward further improving color and clarity was concentrated on Polymer A. Subsequently, the improved techniques developed for Polymer A were also applied to Polymers D and C with beneficial results. The best optical properties achieved for each of the polymers at the conclusion of the program are listed in Table 2.

Table 2.

Final Optical Properties  
(1/4 inch Test Specimens)

|           | <u>Transmittance</u><br>% | <u>Haze</u><br>% |
|-----------|---------------------------|------------------|
| Polymer A | 84                        | 3                |
| Polymer D | 60                        | 4                |
| Polymer C | 70                        | 4-10             |

2. Physical And Mechanical Properties

Sufficient progress in the level of optical properties of each of the three candidate polymers had been demonstrated to warrant proceeding with a comprehensive physical properties evaluation. Future changes and improvements in polymer processing were not expected to significantly affect the polymers general physical properties. Table 3 lists various physical and thermal property data of the candidate polymers.

Table 3.

General Physical Properties

| <u>Property</u>                              | <u>Polymer A</u> | <u>Polymer D</u> | <u>Polymer C</u> | <u>"ASTREL" 360</u>  |
|--|------------------|------------------|------------------|----------------------|
| Specific gravity                             | 1.35             | 1.36             | 1.36             | 1.36                 |
| Heat Distortion, °F                          | 415              | 485              | 520              | 525                  |
| Moisture Absorption<br>%, 24 hr. immersion   | 0.7              | 1.0              | 1.3              | 1.1                  |
| Taber Abr., mg., CS17<br>whl., 1kg, 1000 cl. | 23               | 31               | 21               | 18                   |
| Flammability                                 | Self Ext.        | Self Ext.        | Self Ext.        | Self Ext.            |
| Refractive Index                             | -                | -                | -                | 1.67                 |
| Coeff. Linear Exp.<br>in./in., °F            | -                | -                | -                | $2.6 \times 10^{-5}$ |
| Impact Strength,<br>Notched Izod             | -                | -                | -                | 1.5 ft. lbs/in.      |
| Rockwell Hardness                            | -                | -                | -                | M110                 |

The polyarylsulfones show a lower moisture absorption than nylons, but the values are higher compared with most other plastics. The values for abrasion resistance are comparable to other plastics, such as acetals, polypropylene and polysulfone. Compared with polycarbonate the polyarylsulfones show a higher loss in the Taber Abrasion test.

Mechanical properties of the candidate polymers tested at room temperature and elevated temperatures are reported in Table 4.

Table 4.

| <u>Property</u>        | <u>Mechanical Properties</u> |                  |                  | <u>"ASTREL"</u> |
|------------------------|------------------------------|------------------|------------------|-----------------|
|                        | <u>Polymer A</u>             | <u>Polymer D</u> | <u>Polymer C</u> | <u>360</u>      |
| Tensile Strength, psi  |                              |                  |                  |                 |
| 73°F                   | 10,900                       | 13,100           | 13,100           | 13,100          |
| 300°F                  | 5,100                        | 7,000            | 8,900            | -               |
| 400°F                  | 2,100                        | -                | -                | -               |
| 435°F                  | -                            | 3,100            | -                | -               |
| 500°F                  | -                            | -                | 4,100            | 4,100           |
| Tensile Modulus, psi   |                              |                  |                  |                 |
| 73°F                   | 370,000                      | 370,000          | 360,000          | 370,000         |
| 400°F                  | 330,000                      | -                | 310,000          | 300,000         |
| Elongation at Brk., %  |                              |                  |                  |                 |
| 73°F                   | 6                            | 17               | 20               | 18              |
| 300°F                  | 4                            | 8                | 11               | -               |
| 400°F                  | 3                            | 4                | -                | -               |
| 500°F                  | -                            | -                | 15               | 15              |
| Flexural Strength, psi |                              |                  |                  |                 |
| 73°F                   | 15,500                       | 17,500           | 17,700           | 17,200          |
| 300°F                  | 7,800                        | 7,700            | 13,400           | -               |
| 400°F                  | 2,500                        | -                | -                | -               |
| 435°F                  | -                            | 4,200            | -                | -               |
| 500°F                  | -                            | -                | 6,000            | 6,500           |
| Flexural Modulus, psi  |                              |                  |                  |                 |
| 73°F                   | 360,000                      | 370,000          | 380,000          | 395,000         |
| 400°F                  | 220,000                      | -                | -                | -               |
| 435°F                  | -                            | 280,000          | -                | -               |
| 500°F                  | -                            | -                | 260,000          | 250,000         |

Tensile and flexural strengths of all three polymers are high for unreinforced plastics. Acceptable structural properties are retained up to 400°F for Polymer A, 435°F for Polymer D and 500°F for Polymer C.

### 3. Solvent Resistance

The polyarylsulfones generally have excellent chemical resistance; they are stable to hydrolysis, even in contact with strong acids and bases. The solvent resistance of the candidate polymers was first tested on compression molded specimens under unstressed conditions. The unstressed polymers showed no effect from immersion in typical solvents and cleaning agents used around aircraft, except Polymer A was softened by acetone. Using highly stressed 1/8 inch test specimens the polymers showed decreasing susceptibility to solvent attack with increasing heat distortion temperature. Polymer C, the most thermally stable material, was also the most solvent resistant as shown in Table 5.

Table 5.

#### Solvent Stress Cracking Resistance

(Stressed at 150° included Angle, 10 Day Immersion)

| <u>Agent</u>               | <u>Polymer A</u>         | <u>Polymer D</u>            | <u>Polymer C</u>            |
|----------------------------|--------------------------|-----------------------------|-----------------------------|
| Ethyl Alcohol              | Stress Cracks in 10 days | No Effect                   | No Effect                   |
| Acetone                    | Breaks in 5 seconds      | Stress Cracks in 15 minutes | Stress Cracks in 2 1/2 hrs. |
| Toluene                    | Breaks in 30 seconds     | Stress Cracks in 30 seconds | Stress Cracks in 30 seconds |
| Freon 113                  | No Effect                | No Effect                   | No Effect                   |
| Trichloroethylene          | Breaks in 1 day          | Stress Cracks in 10 days    | No Effect                   |
| Hydraulic Fluid Skydrol LD | Breaks in 10 seconds     | Breaks in 20 seconds        | Breaks in 2 minutes         |
| 10% Soap Solution          | No Effect                | No Effect                   | No Effect                   |

#### 4. Ultraviolet Radiation Stability

The effect of UV light on the candidate polymers was determined by evaluating the optical properties before and after a ten day exposure to a carbon arc UV source with an output of about 7.5 times sunlight. Significant surface degradation resulted on the test samples as evidenced by substantial coloration, haze formation and chalking. The UV data are shown in Table 6.

Table 6.

##### Ultraviolet Stability

(Atlas FDA-RC Fadeometer)

| Exposure<br>Time | Polymer A  |        | Polymer D  |        | Polymer C  |        |
|------------------|------------|--------|------------|--------|------------|--------|
|                  | % Transm., | % Haze | % Transm., | % Haze | % Transm., | % Haze |
| Initial          | 83.7       | 3.9    | 53.5       | 5.3    | 72.7       | 30.0   |
| 4 days           | 77.9       | 5.1    | 29.0       | 4.5    | 68.4       | 32.0   |
| 10 days          | 66.8       | 24.7   | 22.1       | 29.4   | 54.3       | 37.2   |

Screening tests of commercially available UV stabilizers recommended for use at elevated temperatures revealed that none had sufficient thermal stability to withstand the polymer processing temperatures, or they were not completely compatible with the polymers. The study of UV stabilization was then shifted from the solid additive approach to surface protection by solution coated stabilizers. Initial results of this approach looked promising. Stabilizer coated specimens showed substantially better haze values after the ten day UV exposure, but the rate of decrease in transmittance was not significantly different from uncoated samples. The effect of UV exposure on Polymer A coated with an experimental stabilizer is shown in Table 7.

Table 7.

##### Effect of UV Exposure on Stabilized Polymer A

| Time    | Uncoated   |      | Light Coating |      | Heavy Coating |      |
|---------|------------|------|---------------|------|---------------|------|
|         | % Transm., | Haze | % Transm.,    | Haze | % Transm.,    | Haze |
| Initial | 83.7       | 3.9  | 77.0          | 3.6  | 76.7          | 3.2  |
| 4 days  | 77.9       | 5.1  | 68.6          | 4.4  | 71.4          | 3.6  |
| 10 days | 66.8       | 24.7 | 57.3          | 6.3  | 68.8          | 3.8  |

## 5. Polishing

Normal compression molding produced slight surface imperfections in the test specimens which reduced the transmittance and increased the haze. In an attempt to correct this problem Polymer A samples were submitted to Goodyear Aerospace Corporation to evaluate the feasibility of grinding, polishing and press polishing polyarylsulfones. Their standard polishing techniques noticeably cleaned the surface by improving values from an initial 79.0% transmittance and 5.7% haze to 80.0% transmittance and 2.3% haze. Attempts to press polish Polymer A have not been successful so far due to improper drying and choice of temperature conditions.

## 6. Thermal Cycling

Thermal cycling of the candidate polymers between -100°F and 350°F for ten days produced no change in luminous transmittance or haze. Surfaces were unaffected by direct contact with dry ice or the thermal shock of 450°F temperature changes.

Continuous exposure of Polymer C specimens to 500°F for seven days only lowered the transmittance from an initial 70.1% to 63.6% and increased the haze from 7.0% to 8.7%. These results confirm the high thermal and thermo-oxidative stability common to the family of polyarylsulfone resins.

## SUMMARY AND CONCLUSIONS

An evaluation of three polyarylsulfone plastics has been conducted in an effort to determine their potential to meet the optical and general physical property requirements of high performance aircraft transparencies.

Significant improvements in the luminous transmittance and haze of all three candidate polymers were achieved. Polymer A, the polymer with the lowest Tg of 440°F, was improved the most with best values of 84% luminous transmittance and 3% haze on 1/4 inch thick compression molded panels. Polymer D, with an intermediate Tg of 500°F, showed 60% transmittance and 4% haze. Polymer C, offering the highest use temperature with a Tg of 550°F, was improved to a luminous transmittance of 70% and a haze of 4-10%.

Prolonged exposure to isothermal aging at temperatures of 500°F, as well as thermal cycling did not significantly affect the physical or optical properties. The polymers showed high mechanical strength at room temperature and in the 400° to 500° range. Solvent resistance increased with increasing heat distortion temperature from Polymer A to



Polymer C. Polymer C was attacked by hydraulic fluid, but only under highly stressed conditions.

Ultraviolet radiation caused a surface degradation on all three polymers. No commercially available stabilizer has been found which has sufficient thermal stability to be used as a solid additive. The solution coated stabilizer approach is showing promise.

The investigation of new heat resistant stabilizers and coatings to improve the ultraviolet light stability as well as the abrasion resistance should be continued.

#### REFERENCES

1. R. L. Burns, H. A. Vogel, A. T. Worm, 3M Company, Technical Report AFML-TR-72-110, December 1972, Nonmetallic Materials Division, AFML/MBC, Plastics and Composites Branch, Wright Patterson Air Force Base, Ohio 45433
2. B. A. Benson, R. P. Bringer, H. A. Vogel and N. L. Watkins, SPE Journal, 23 No. 7, 33 (1967)
3. H. A. Vogel and W. D. Womer, J. Paint Technol., 40 80 (1968)
4. G. A. Morneau, Modern Plastics, 47, 150 (Jan. 1970)
5. H. A. Vogel, J. Poly. Sci., Part A-1, 8 2035-2047 (1970)

PRODUCTION PROCESS FOR TRANSPARENT  
SPINEL,  $\text{MgAl}_2\text{O}_4$

D. W. Roy, D. R. Johnson, and D. L. Mann  
Coors Porcelain Company  
Golden, Colorado

## Production Process for Transparent Spinel, $\text{MgAl}_2\text{O}_4$

by: D. W. Roy, D. R. Johnson, and D. L. Mann  
Coors Porcelain Company  
Golden, Colorado 80401

### ABSTRACT

The fabrication and physical and mechanical properties of transparent polycrystalline spinel are described. Spinel optics are fabricated by conventional ceramic processes: sintering - for complex but thin-walled shapes, and hot-pressing - for flat shapes in greater wall thicknesses. Transparent spinel ceramics are now commercially available in limited quantities. Fully dense spinel is transparent in the visible and infrared to  $6.5 \mu\text{m}$ . The optical properties of spinel are discussed. Spinel has a low dielectric constant, 8.2, and dissipation factor,  $2 \times 10^{-5}$ , and thus an exceptionally low dielectric loss index,  $2 \times 10^{-4}$ . Spinel exhibits high strength, 20-34 ksi, in bending, and hardness,  $1300 \text{ kg/mm}^2$  Knoop, resulting in good rain erosion and ballistic properties.

### INTRODUCTION

Polycrystalline spinel ceramics are now commercially available in transparent shapes. The present paper describes the fabrication and properties of spinel optics.

Magnesium aluminate,  $\text{MgAl}_2\text{O}_4$ , occurs in nature and has some commercial value as a gemstone. A large class of natural and synthetic materials--for example, the soft ferrites--have the same atomic crystal structure; all of these materials are called "spinel". The material described in the present work is stoichiometric, synthetically produced polycrystalline magnesium aluminate.

Spinel is optically isotropic; when fabricated in high purity polycrystalline shapes free of porosity and second phases it is transparent in the visible and infrared to  $6.5 \mu\text{m}$ . The commercial production of transparent spinel is a relatively recent development.

Spinel is exceptionally strong, hard, and refractory for an optical material. The physical and mechanical properties are summarized in Table 1.

The exceptional strength, hardness, and thermal and chemical stability of spinel make it potentially useful for aircraft enclosures subject to severe environments. Possible applications include transparent ballistic armor, laser windows, radomes, bomb sights, and windows subjected to supersonic erosion and abrasion or impact by foreign objects such as birds.

---

Supported in part by the Air Force Materials Laboratory, Manufacturing Technology Division, Wright-Patterson Air Force Base, Ohio, under Contract No. F33615-72-C-1133; L. Kopell (AFML/LTP), Project Engineer.

Table 1. Physical and Mechanical Properties of  $\text{MgAl}_2\text{O}_4$

|   |  |
|---|--|
| Lattice Parameter (1)                               | 8.0833 Å   |
| Density (1)   | 3.584 g/cc                                       |
| Melting Point (1)                                   | 2135°C   |
| Coefficient of Linear Thermal Expansion             |  |
| 25-200°C  | $5.6 \times 10^{-6}/^\circ\text{C}$              |
| 25-500°C  | $7.3 \times 10^{-6}/^\circ\text{C}$              |
| 25-1000°C   | $7.9 \times 10^{-6}/^\circ\text{C}$              |
| Thermal Conductivity (1)                            |  |
| 100°C   | 0.0357 cal/(sec)(cm)(°C)                         |
| 1200°C  | 0.0130 cal/(sec)(cm)(°C)                         |
| Specific Heat (1)                                   |  |
| 20°C  | 0.200 cal/g °C                                   |
| 1040°C  | 0.214 cal/g °C                                   |
| Index of Refraction                                 | 1.716  |
| Dielectric Constant                                 |  |
| $10^3$ Hz   | 8.2  |
| $10^6$ Hz   | 8.2  |
| $9.3 \times 10^9$ Hz                                | 8.3  |
| Dissipation Factor                                  |  |
| $10^3$ Hz   | $3.0 \times 10^{-5}$                             |
| $10^6$ Hz   | $2.0 \times 10^{-5}$                             |
| $9.3 \times 10^9$ Hz                                | $1.3 \times 10^{-5}$                             |
| Loss Index  |  |
| $10^3$ Hz   | $2.5 \times 10^{-4}$                             |
| $10^6$ Hz   | $2.0 \times 10^{-4}$                             |
| $9.3 \times 10^9$ Hz                                | $1.0 \times 10^{-4}$                             |
| Strength (1)  |  |
| Ultimate Strength in Four-Point Bending             |  |
| 25°C (2)  |  |
| Sintered  | 33,400 psi                                       |
| Hot-Pressed   | 25,000 psi                                       |
| 1260°C  | 33,000 psi                                       |
| Yield Stress in Four-Point Bending at 0.005 in/min. |  |
| 25°C  | --   |
| 1250°C  | 11,470 psi                                       |
| Ultimate Compressive Strength                       |  |
| 25°C  | 390,000 psi                                      |
| 1550°C  | 6,220 psi at $5 \times 10^{-4} \text{ min}^{-1}$ |
| Hardness-Knoop                                      | 1300 Kg/mm <sup>2</sup> (200 g load)             |
| Modulus of Elasticity (1)                           |  |
| $35 \times 10^6$ psi Static                         |  |
| $39.9 \times 10^6$ psi Dynamic                      |  |
| Shear Modulus (1)                                   | $15.89 \times 10^6$ psi Dynamic                  |
| Bulk Modulus (1)                                    | $27.93 \times 10^6$ psi Dynamic                  |
| Poisson's Ratio (1)                                 | 0.2608   |

## OPTICAL PROPERTIES

Polycrystalline spinel in reasonably thin shapes exhibits excellent transparency in the visible and IR to  $6\mu\text{m}$ . Figure 1 shows typical transmission data for sintered and hot-pressed parts. Note the absence of any discrete absorption peaks in the visible and near infrared.

Figure 2 is a plot of the loss coefficient (sum of scattering and absorption coefficients) as a function of wavelength for hot-pressed and sintered spinel. The losses are primarily due to scattering of light by residual porosity. A small fraction of a percent of porosity is sufficient to cause transmission losses by scattering of light. Residual porosity is due to incomplete densification during fabrication and can, in principle, be eliminated by making appropriate adjustments in the fabrication parameters. However, in practice the removal of the last vestiges of porosity is extremely difficult. Research is continually in progress to reduce optical scattering in polycrystalline spinel. These improvements come in small, hard fought increments.

The extreme hardness and chemical stability of spinel result in excellent resistance to surface degradation in service; i.e., light transmission is not easily degraded by weathering, pitting, scratching, etc.

The properties of spinel are, in general, very stable at elevated temperatures. Table 2 lists the available transmission data at elevated temperatures. These data indicate that the transmittance at  $2.5$  and  $4.5\mu\text{m}$  and at temperatures up to  $400^\circ\text{C}$  is nearly invariant with temperature.

The refractive index of spinel for wavelengths from  $0.4 - 6.0\mu\text{m}$  is listed in Table 3. These values correspond to reflection losses from two uncoated surfaces during transmission of 13%. Spinel can, of course, be coated with nonreflecting or bandgap coatings. Dispersion of light by spinel is moderately low. The Nu value, calculated from the refractive indices at the hydrogen F line,  $n_f$ , hydrogen C line,  $n_c$ , and sodium D line,  $n_d$ , is given by:

$$\text{Nu} = \frac{n_d - 1}{n_f - n_c} = 53$$

The refractive index at the sodium D line is 1.716.

## THERMAL AND MECHANICAL PROPERTIES

The mechanical properties of polycrystalline ceramics are sensitive to microstructure, which is in turn determined by fabrication conditions. Thus, the strength of transparent spinel may be varied from 20-34 ksi, depending upon the fabrication conditions. The hardness and elastic modulus of fully dense, pure spinel are relatively invariant. Spinel is mechanically stable at temperatures up to  $1250^\circ\text{C}$ ; the data in Table 1 indicate that spinel undergoes virtually no loss in strength up to  $1250^\circ\text{C}$ . The polycrystalline structure results in blunting and redirecting of cracks at grain boundaries; thus

offering greater toughness than spinel single crystals.

Rain erosion resistance is very important for exposed windows on supersonic missiles and aircraft. The limited data available indicate that spinel has extremely good resistance to rain erosion. In June, 1972 a rain erosion test was conducted at the Naval Weapons Center, China Lake, California. A number of materials were simultaneously tested: spinel; single crystal sapphire and YAG; calcium and magnesium fluoride, with and without sapphire coatings; magnesium oxide; and two infrared transmitting glasses. In each run samples of the various materials were mounted in a special fixture on a rocket sled and run through a rain field at Mach 1.4. In this accelerated test all the specimens except the spinel failed mechanically. The spinel showed virtually no damage. The sapphire and YAG failed via a single line fracture, the others shattered into many pieces. While a less severe test that would show the relative amount of pitting on each sample would be more satisfying experimentally, supersonic rain erosion failures in service are frequently catastrophic.<sup>(3)</sup>

The high hardness, 1300 kg/mm<sup>2</sup>, and moderate density, 3.58 g/cc, of spinel make it a suitable material for transparent ballistic armor. The ballistic limit for spinel is comparable to that of sapphire.<sup>(4)</sup>

#### DIELECTRIC PROPERTIES

The dielectric properties of spinel are listed in Table 1. Spinel has an unusually low dielectric loss index, comparable to that of fused silica glass.

#### PRODUCTION

A highly pure, finely divided spinel powder is required for fabrication of spinel optics. Reactive, high purity powders can be formed by a number of methods. Spinel powders may be synthesized by the chemical coprecipitation and subsequent thermal decomposition of aluminum and magnesium salts. An alternate method is the direct union of magnesium and aluminum oxides at elevated temperatures.

In order to form transparent polycrystalline spinel ceramics, the spinel powder must be consolidated into fully dense, virtually pore free shapes. The consolidation requires a significant amount of atomic mobility and, thus, must occur at a high temperature. The successful elimination of porosity (which began as the voids between the compacted spinel particles) depends to a large extent upon the purity of the powder and particulate properties, such as particle size and shape, particle size distribution, surface area, and the quantity and type of adsorbed anions.

Polycrystalline spinel optics are formed by either sintering or hot-pressing. Sintering is accomplished by pressing spinel powder to a green density of ~ 65% of theoretical density and then heating to ~ 1800°C to affect consolidation and removal of porosity. In hot-pressing, a uniaxial pressure of ~ 7.5 ksi is applied to the powder, constrained in a punch-and-die set, while it is being heated. Fully dense, transparent parts can be formed at

a lower temperature than with sintering: 1550°C. Typical microstructures for sintered and hot-pressed parts are shown in Figure 3 and 4.

Circular discs 6" diameter x  $\frac{1}{2}$ " thick are presently being fabricated by hot-pressing. The hot-pressed part size is being scaled up to 10" x 10" x  $\frac{1}{2}$ " thick windows under contract to the Air Force. \* The state-of-the-art is currently limited to flat shapes.

Sintered parts having good transmission in the visible and infrared are presently limited to 0.080" wall thickness. As improved synthesis and fabrication methods are developed, optically clear shapes with thicker walls will become available. Sintering does not have the shape limitations of hot-pressing. Domes, tubes, rods, and other complex shapes may be formed by sintering. Because of economy, versatility, and large production capability, sintering is the preferred method for fabricating thin-walled shapes.

Table 2. Transmittance Versus Temperature<sup>(5)</sup>

| Temperature (°C) | % Transmission at |                   |
|------------------|-------------------|-------------------|
|                  | 4.5 $\mu\text{m}$ | 2.5 $\mu\text{m}$ |
| 23               | 73                | 69                |
| 106              | 73                | 69                |
| 172              | 73                | 69                |
| 220              | 72                | 69                |
| 265              | 73                | 70                |
| 338              | 72                | 69                |
| 402              | 70                | 69                |

Table 3. Index of Refraction Versus Wavelength<sup>(5)</sup>

| $\lambda$ , $\mu\text{m}$ | n     |
|---------------------------|-------|
| 0.4047                    | 1.736 |
| 0.5461                    | 1.719 |
| 1.0140                    | 1.703 |
| 1.0000                    | 1.704 |
| 2.0000                    | 1.702 |
| 3.0000                    | 1.698 |
| 4.0000                    | 1.685 |
| 5.0000                    | 1.659 |
| 6.0000                    | 1.558 |

\* Contract No. F33615-72-C-1133

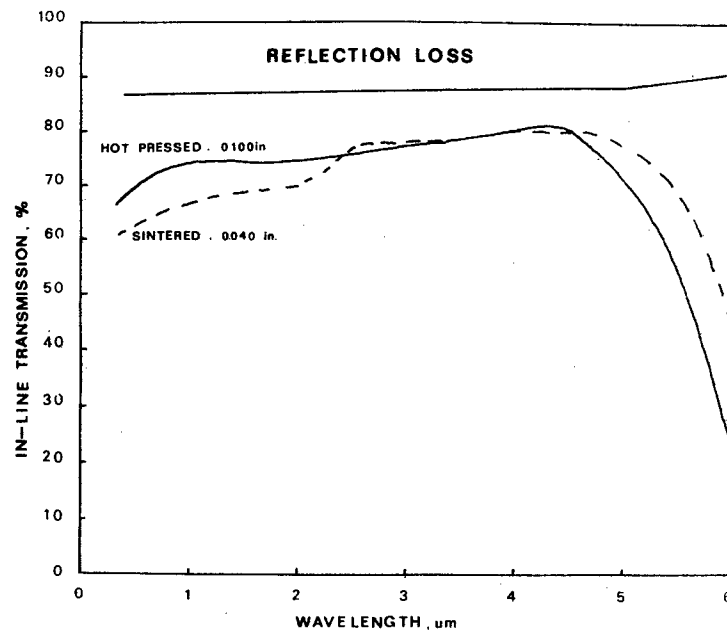


Figure 1. In-Line Transmission versus Wavelength For Sintered and Hot-Pressed Spinel

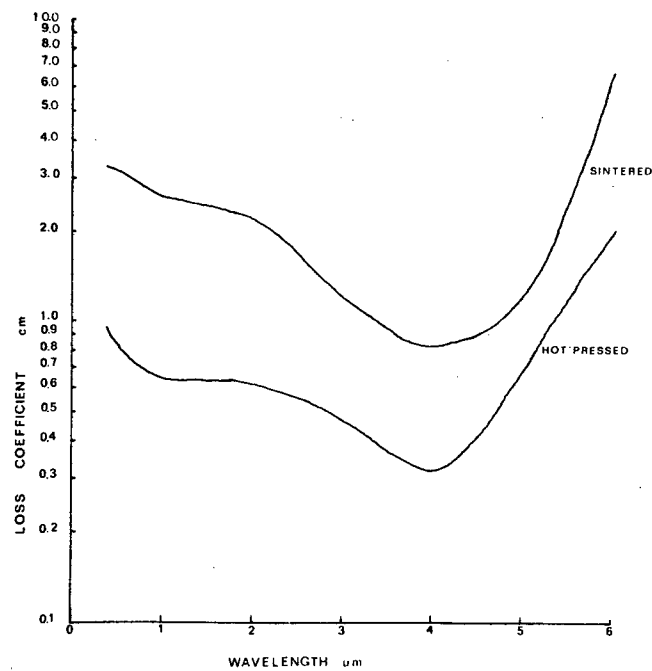
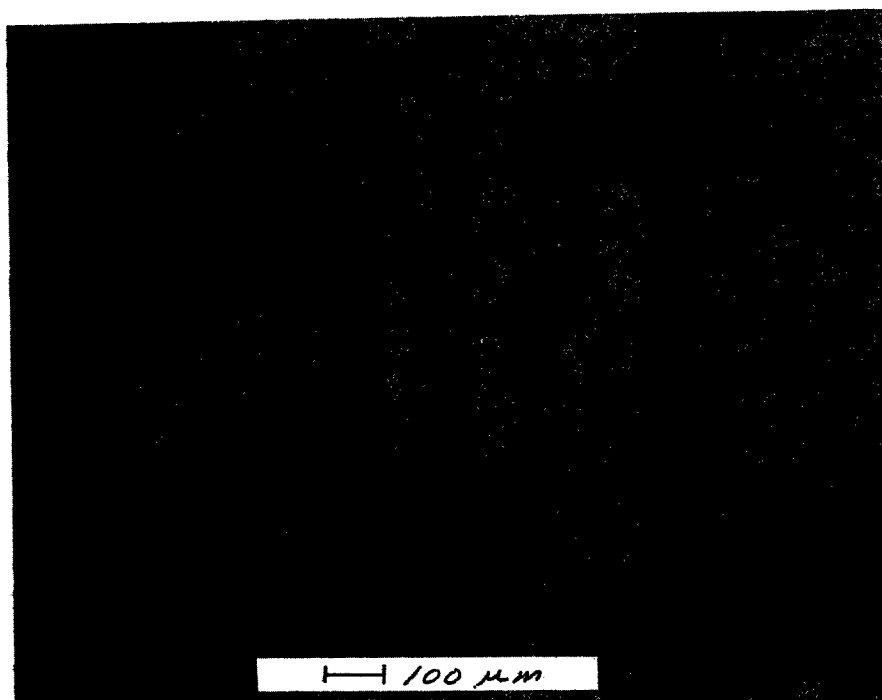
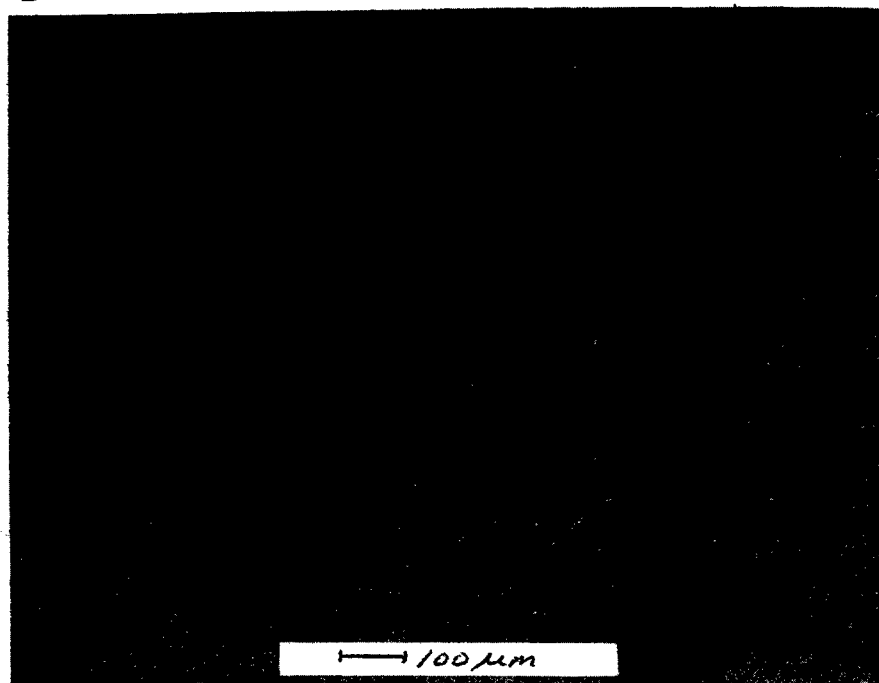


Figure 2. Optical Loss Coefficient versus Wavelength For Sintered and Hot-Pressed Spinel





**Figure 3. Microstructure of Sintered Spinel**



**Figure 4. Microstructure of Hot-Pressed Spinel**

#### REFERENCES

1. Hayne Palmour III, "Flow and Fracture in Spinel Structured Ceramics", Contract DA31-124-ARD-D-207, Department of the Army Project No. 2001050113700, Army Research Office, Durham N.C., 4932-MC Jan 1970.
2. Coors Porcelain Company, Golden, Colorado.
3. George F. Schmitt, Jr., Air Force Materials Laboratory, Wright-Patterson Air Force Base, Ohio - Private communication.
4. Gordon R. Parsons, Army Materials and Mechanics Research Center, Watertwon, Massachusetts - private communication.
5. A. R. Hilton, Texas Instruments, Inc., Dallas, Texas - private communication.

ENVIRONMENTAL DATA AND MACHINING  
TECHNIQUES OF POLYCARBONATES

George E. Husman  
Air Force Materials Laboratory  
Wright-Patterson Air Force Base, Ohio  
and  
Ronald J. Kuhbander  
University of Dayton  
Dayton, Ohio

# ENVIRONMENTAL DATA AND MACHINING TECHNIQUES OF POLYCARBONATES

by

George E. Husman  
Air Force Materials Laboratory  
Wright-Patterson Air Force Base, Ohio

and

Ronald J. Kuhbander  
University of Dayton  
Research Institute

## ABSTRACT

The use of polycarbonates for bird-impact resistant windscreens offers a great potential to Air Force systems. The excellent toughness and impact strength of polycarbonates far exceed that of acrylic plastics used for windscreen applications. There is, however, little production experience or service experience available on polycarbonates for this type of application. A study was conducted by the Air Force Materials Laboratory and the University of Dayton Research Institute to evaluate possible problems that could occur in production and service. Problem areas were identified and methods of alleviating these problems were evaluated. The most glaring deficiency of the material was found to be its susceptibility to stress-cracking or crazing. The material tends to stress-crack readily upon exposure to a wide range of solvents and exposure to heat and humidity. This problem appears greatly accelerated at machined surfaces. These cracks or crazes greatly reduce the total elongation of the material even when they are microscopic in size and larger ones can cause brittle failure.

Data developed in this study are presented and test procedures are fully described. In addition, an evaluation of the future of polycarbonates for aircraft windscreen applications is presented.

## 1. INTRODUCTION

The need for new and improved materials and designs for bird-impact resistant aircraft windscreens has been an area of increasing concern to the Air Force for several years. Emphasis has been placed on developing total reliability in aircraft systems, i. e., a system that will survive all service conditions and environmental hazards that could be encountered in the aircraft lifetime. The advent of terrain following radar and the increased performance requirements of aircraft systems have greatly increased the requirements of windscreens to be lightweight, withstand high velocity impacts, as well as maintaining high optical properties. Polycarbonate plastic materials offer a great potential in these applications and are being considered for use on several present and future aircraft systems.

## 2. DISCUSSION

Polycarbonate materials offer a unique combination of properties that make them extremely advantageous for windscreen applications. Probably the most outstanding property of polycarbonate is its impact strength. Izod impact strength on 1/8 inch ASTM standard bars is 12 to 16 foot-pounds per inch of notch, and unnotched bars show impact resistance greater than 60 foot-pounds per inch <sup>(1)</sup>. Another outstanding characteristic of polycarbonate is its high temperature resistance. Its heat deflection temperature of 270°F at 264 psi fiber stress is higher than most thermoplastics <sup>(2)</sup>. In addition, the material has excellent optical clarity and good mechanical properties as shown in Table 1.

Table 1. Mechanical Properties of Polycarbonate <sup>(2)</sup>

| Tensile Strength<br>(psi) | Tensile Elongation<br>(%) | Tensile Modulus<br>(x 10 <sup>5</sup> psi) |
|---------------------------|---------------------------|--|
| 8000-9500                 | 100-130                   | 3.5  |

Although polycarbonate has these excellent properties, it is not an entirely problem free material. Machined surfaces, such as holes and edges, are extremely susceptible to environmental stress-cracking and crazing, i. e., under tensile stress and exposure to a wide variety of chemicals, solvents, and even high humidity at elevated temperature the material will craze or form stress-cracks. This type of material degradation will generally result in a loss of elongation and impact strength. In addition,

the material undergoes a ductile to brittle transition at a thickness between 0.140 to 0.180 inch, which would make the presence of cracks extremely critical in thick parts. Polycarbonate is also susceptible to degradation from exposure to ultraviolet radiation, however, additives are available that will reduce these effects. Finally, the material does not have good abrasion resistance and must be protected to maintain its optical clarity.

Being a relatively new material, there is little production experience or service experience available on polycarbonate for aircraft applications. The purpose of this study was to evaluate possible problems that could occur in production and service and evaluate methods of alleviating these problems.

### 3. EXPERIMENTAL

Environmental stress-cracking is probably the most glaring deficiency of polycarbonate materials and is expected to be the greatest problem encountered when using polycarbonates for aircraft windscreens. In order for stress-cracks to form, three conditions are necessary; a tensile stress, a contaminating environment, and time. The magnitude of the tensile stress and the length of time required to form stress-cracks are interdependent and both depend on the contaminating environment present. The contaminant can vary widely from a large number of chemicals and solvents to a high humidity at elevated temperature environments. The environments encountered by a windscreen during its lifetime can vary widely and would be nearly impossible to completely control. Coatings can offer some protection against environmental exposures, but even the best coatings cannot completely protect against all environmental conditions. Therefore, it is necessary that the polycarbonate be subjected to minimum tensile stresses, especially for long durations. Minimum structural stresses can be achieved by proper design and these stresses generally do not occur for long durations. However, residual stresses in the material due to processing and machining can be a problem. This problem was studied under this investigation and was found to be quite significant.

A study of varying drilling procedures on 1/2-inch thick polycarbonate sheet indicated that extreme care must be exercised to prevent the introduction of residual stresses. Photoelastic pictures of two extremes are shown in Figure 1. The poorly drilled hole was made with a dull bit, no coolant, and no control of feed rate, while the well drilled hole was made with a sharp bit, a parafin oil coolant, and a slow feed rate. Although the holes appeared nearly the same visually, photoelastic examination of the holes shows a large residual stress pattern around the poorly drilled hole. Photoelastic analysis of holes estimated a residual stress of approximately 1080 psi around the poorly drilled hole. Because of the high creep resistance of polycarbonate, these machining stresses cannot be relieved by creep

mechanisms, and although annealing could help, it cannot completely relieve the stresses. The presence of such stresses in a windscreen would most probably lead to the formation of stress-cracks at sometime in the structure's lifetime.

To demonstrate the severity of stress-cracks, a specimen was designed to represent an edge attachment hole on the periphery of a windscreen (see Figure 2). Stress-cracks approximately 1/8-inch long were introduced by applying a slight tensile load on the specimen and then lightly dabbing acetone on the edge of the hole. The specimen configuration closely resembles the compact tension specimen used in fracture toughness tests for metals and was in fact designed to demonstrate the Mode I fracture resistance of the material. The specimens were tested on an MTS 810-Materials Test System at a ram displacement rate of 43 inches/second in an attempt to more closely represent impact loading. The results of the tests are presented in Table 2. An examination of the failed specimens (Figure 3) and the load-deflection curves (Figure 4) clearly indicate that the presence of the stress-crack caused a brittle fracture of the specimen and a greatly reduced load and deflection. In addition to these tests, cracked specimens were reamed to remove the cracks and then tested to verify that removal of the crack would restore the specimen toughness.

Table 2. Load to Failure for Edge Attachment Specimens

| Testing Speed, 43 in/sec.      | Load, lbs. |
|--------------------------------|------------|
| Visible Stress-Cracks          | 1225       |
| No Stress-Cracks               | 3260       |
| Reamed to Remove Stress-Cracks | 3000       |

The problem of residual stresses and stress-cracking does not only exist around drilled holes but also along machined edges. Figure 5 shows the two extremes of a poorly machined edge and a carefully machined edge. The requirements for stress free machined surfaces are the same for holes and edges. The first requirement is to keep the part cool. This is accomplished by using slow to medium cutting speeds and feed rates, and the use of a coolant. Water is an excellent coolant and any other must be checked for its compatibility with polycarbonate. The second requirement is to maintain sharp cutting edges at all times. For best results, holes should be drilled undersize and reamed by use of precision reamers or end mills, in steps not exceeding 1/64 inch, to the desired size. The best machined edges were those which were milled using the recommended coolant.

A photoelastic analysis of machined edges indicate stresses on the order of 360 psi exist along a poorly machined edge. Although no measurable stresses were found along a carefully machined surface by photoelastic analysis, it is believed that significant stress does exist locally along the machined surface. To demonstrate the significance of these machining stresses, a series of tests were performed. A series of standard dogbone tensile specimens with carefully machined edges were aged in a 95% relative humidity at 125°F environment for 2, 4, and 6 days and then tested at room temperature. The tests conducted were similar to those suggested in ASTM-D-638. A dogbone specimen having a 0.5-inch wide by 2-inches long gage section was used for all tests. The testing speed was 20 inches/minute. The resulting load-deflection curves (Figure 6) show a decrease in elongation with increased aging time. It was noted during the testing of the aged specimens numerous cracks formed all along the machined edges and grew until one reached critical length causing failure. This cracking did not occur on unaged specimens until just prior to failure and only at the failure location. Photomicrographs of this phenomenon are shown in Figure 7 and a more clear demonstration of this is shown in the photoelastic pictures in Figure 8. The data indicates that microcracks are forming along the machined edge during aging causing the reduction in elongation. In order to validate that these results were due to the stress-cracking at the machined surfaces, two additional tests were performed. First, specimens that had been aged for six days were oven dried before testing to remove the possibility of surface moisture causing cracks to form during the test. The results were the same as the six day aging specimens without drying as expected. Second, panels of the polycarbonate material were aged for six days and then the tensile specimens were cut from the panels and tested. The results were the same as unaged specimens indicating that previous failures were indeed due to edge effects and not to material degradation.

This data indicates that even the carefully machined edges had high enough stresses along the surface to cause the formation of stress-cracks in an environment that could very possibly be encountered by an aircraft. Attempts were made to solvent polish the machined edge with Dichloro-Methane to see if that offered any improvement in resistance to stress-cracking. Although the solvent polishing resulted in a smooth glassy surface, no noticeable improvement in resistance to stress-cracking was experienced. Additional studies need to be performed to determine optimum machining and finishing techniques to help prevent this problem.

A series of tests to evaluate the effectiveness of coating the machined surfaces were performed under the same conditions as above. Two silicone coatings known to be compatible with polycarbonate were evaluated. Tensile specimens with coated edges were aged for 2, 4, and 6 days in the high humidity temperature environment. The results are summarized along with the uncoated data in Table 3 and Figure 9. The results indicate that the



coating can afford some protection to machined surfaces, at least against a high humidity atmosphere. Additional studies should be performed to find other coatings and to evaluate other chemical and environmental conditions.

Table 3. Tensile Properties After Six Days at 125°F and 95% Relative Humidity

| Yield Strength, psi | Percent Elongation | Specimen Condition   |
|---------------------|--------------------|----------------------|
| 10,740              | 101                | Control              |
| 10,780              | 29                 | Dried                |
| 10,560              | 34                 | As Machined          |
| 10,820              | 54                 | D. C. 236 Coating    |
| 10,840              | 82                 | D. C. 92-009 Coating |

All data reported thus far has been on 1/2-inch thick material. Previous data by Mobay Chemical Company reported in a paper by Thor Smith of IBM Research Laboratory (3) verified the existence of a ductile to brittle transition in polycarbonate at a thickness around 0.180 inch. This data (shown in Figure 10) shows notched Izod impact strength versus material thickness and the sharp transition is readily apparent. This data indicates that the material loses its notch sensitivity at thicknesses below 0.180 inch at least for notch geometries used in Izod test specimens. To verify this thickness effect, a series of double edge-notched tensile specimens were tested using different thicknesses of polycarbonate material. The exact procedure used is ASTM-E-338. As stated in the ASTM standard, the significance of this test is to provide a comparative measure of the resistance of sheet materials to fracture originating from the presence of cracks and crack-like stress concentrators. The sharp edge-notch specimen was selected because of its relative ease of fabrication. The testing speed was 0.05 inch/minute. The results (shown in Table 4 and Figure 11) verify that there is a ductile to brittle transition between 1/8-and 1/4-inch. The difference in failure mode between the 1/8-inch and the thicker material is shown in Figure 12. It can be seen that even in the presence of a sharp notch, the 1/8-inch thick material fails in a ductile manner while the thicker material fails in a brittle manner. The stress intensity factors calculated correspond to surface energies of  $1.245 \times 10^7$  erg/cm<sup>2</sup> for the 1/8-inch material and  $2.77 \times 10^6$  erg/cm<sup>2</sup> for the thickness of 1/4-inch and above. Even these values for the thicker material are an order of magnitude better than PMMA which has a reported surface energy of  $1.25 \times 10^5$  erg/cm<sup>2</sup>. (4)

Table 4. Sharp Edge-Notch Properties

| Specimen Thickness (in) | Sharp Notch Strength (psi) | Stress Intensity Factor KSI-in <sup>1/2</sup> | <u>Sharp Notch Strength</u><br>Yield Strength |
|-------------------------|----------------------------|---|---|
| 1/8                     | 7380                       | 7.0   | 0.76  |
| 1/4                     | 3480                       | 3.3   | 0.34  |
| 3/8                     | 3350                       | 3.2   | 0.31  |

Although the material apparently loses its notch sensitivity at these thin thicknesses, it is still not free from the problem of stress-cracking. This problem was evaluated in the final series of tests performed under this investigation. A series of 1/8, 1/4, and 3/8-inch tensile specimens with carefully machined edges were aged in the high humidity at elevated temperature environment for six days and then tested at room temperature. The results shown in Figure 13 indicate that stress-cracks were developed along the machined edge of all of the specimens resulting in reduced elongation to failure.

The reduced elongation of the 1/8-inch material was greater than anticipated. This is probably due to constraints put on the material due to the specimen size and the interaction of stress fields at the numerous crack tips along the edge which prohibits normal deformation at the crack tips. In any case, it must be remembered that these tests were designed to demonstrate environmental stress-cracking and not fracture toughness. The results do indicate that residual machining stresses and environmental stress-cracking does occur regardless of material thickness. Although the presence of stress-cracks is not as critical in the thin material as it is in the thicker material, the presence of stress-cracks will always cause a reduction in properties and must be considered when using this material.

#### 4. CONCLUSIONS

Polycarbonate materials offer a great potential to aircraft systems as materials for bird-impact resistant windscreens. However, the problem of environmental stress-cracking must be carefully considered in the design, fabrication, and use of polycarbonate windscreens. Extreme care must be taken to minimize the presence of tensile stresses in the material. Stress risers such as holes and sharp corners should be kept at a minimum and eliminated if possible, especially if material thicknesses are equal to or greater than the ductile to brittle transition thickness.

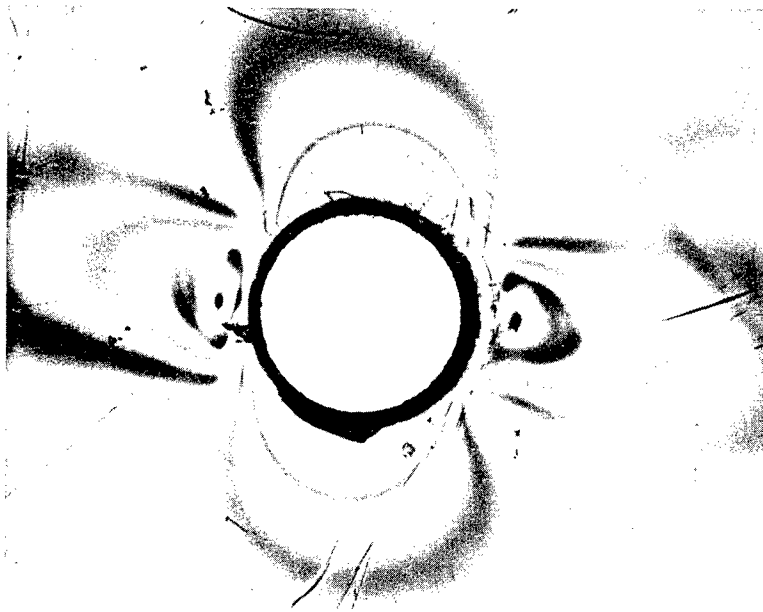
Although this program developed machining and drilling trends, it has by no means attempted to optimize the techniques. Additional studies should be performed to develop optimum drilling and machining techniques. In addition, studies of finishing techniques should be performed to evaluate their effectiveness in removing skin stresses on machined surfaces. Techniques developed for metals, such as coining, stamping, etc., should be evaluated for polycarbonates. It is very possible that pulling an oversized mandrel through a drilled hole and putting the material around the hole in residual compression could completely eliminate the stress-cracking problem.

In addition to reduction of tensile stresses in the material, all machined surfaces should be coated to provide environmental protection. The coatings evaluated under this program did show considerable promise, however, only two coatings and one environment were evaluated. Additional coatings and chemical and environmental conditions need to be evaluated to determine the best coatings for windscreen applications. Even with these precautions, highly reactive stress-cracking agents such as acetone and carbon tetrachloride must be kept away from the material.

The optimum use of polycarbonate materials will be in laminated windscreens, (Figure 14) keeping the individual polycarbonate ply thickness below 0.140 inch and eliminating as much as possible machined edges and attachment holes. Because of the structural redundancy of this type of design, highly reliable bird-impact resistant windscreens should result. Development programs are being pursued in this area with some success. It is envisioned that by taking the proper precautions, the problem of stress-cracking can be greatly alleviated and possibly eliminated, and in the near future, polycarbonate materials will be utilized and developed into highly reliable, bird-impact resistant aircraft windscreens.

## REFERENCES

1. General Electric Company, Lexan Product Manual
2. Smith, Thor L., "Fracture of Polymers in Biaxial and Triaxial Tension," Polymer Science Symposium No. 32, 1971.
3. Modern Plastics Encyclopedia, Vol. 46: No. 10A, October 1969.
4. Broutman, L. J. and McGarry, J. J., "Fracture Surface Work Measurements on Glassy Polymers by a Cleavage Technique," I. "Effects of Temperature," J. Appl. Polymers Sci. 9, 589-608, 1965.



POOR MACHINED HOLE



GOOD MACHINED HOLE

Figure 1. Photoelastic Pictures of Poorly Machined Hole versus Carefully Machined Hole

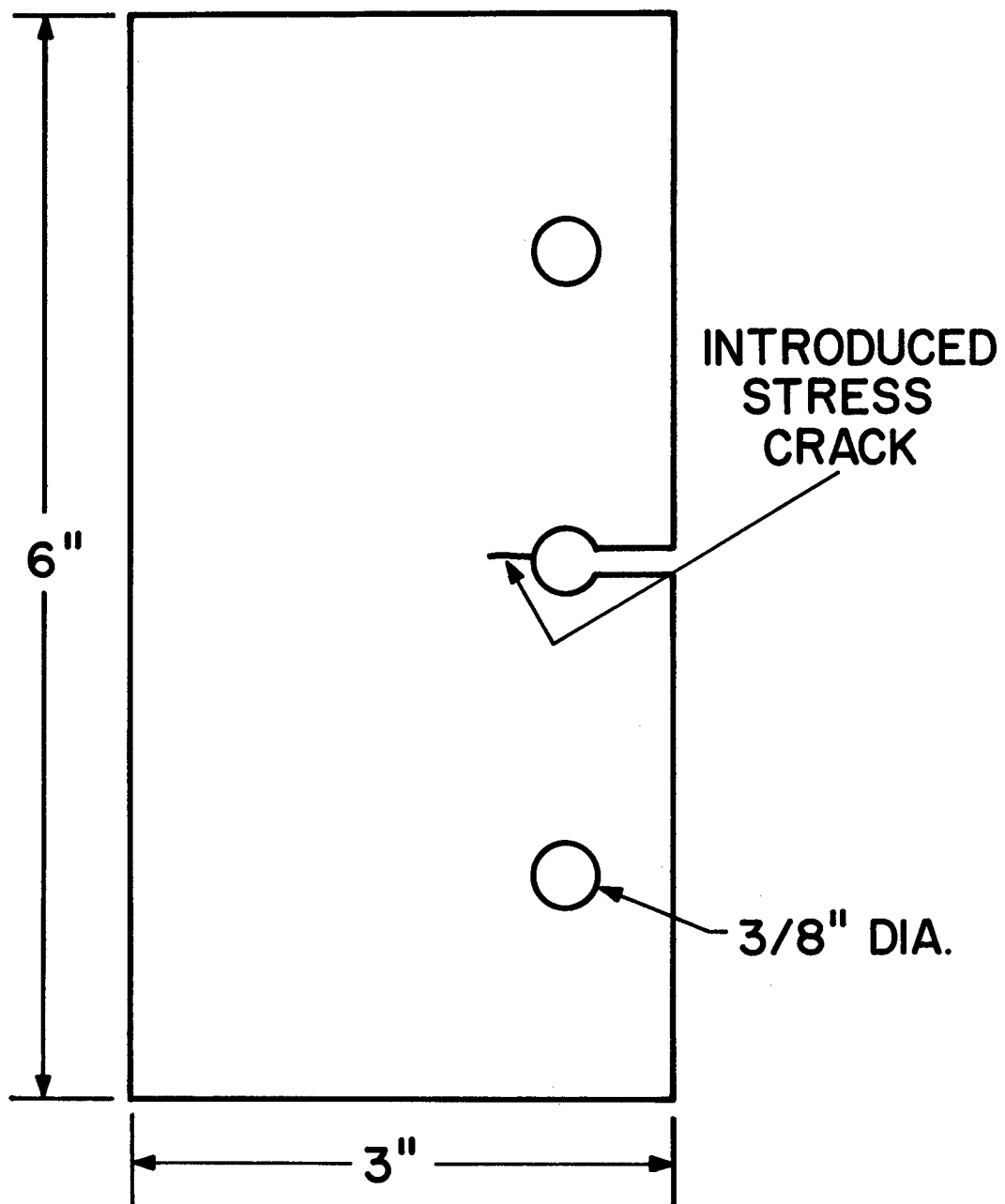


Figure 2. Drawing of Edge Attachment Specimen

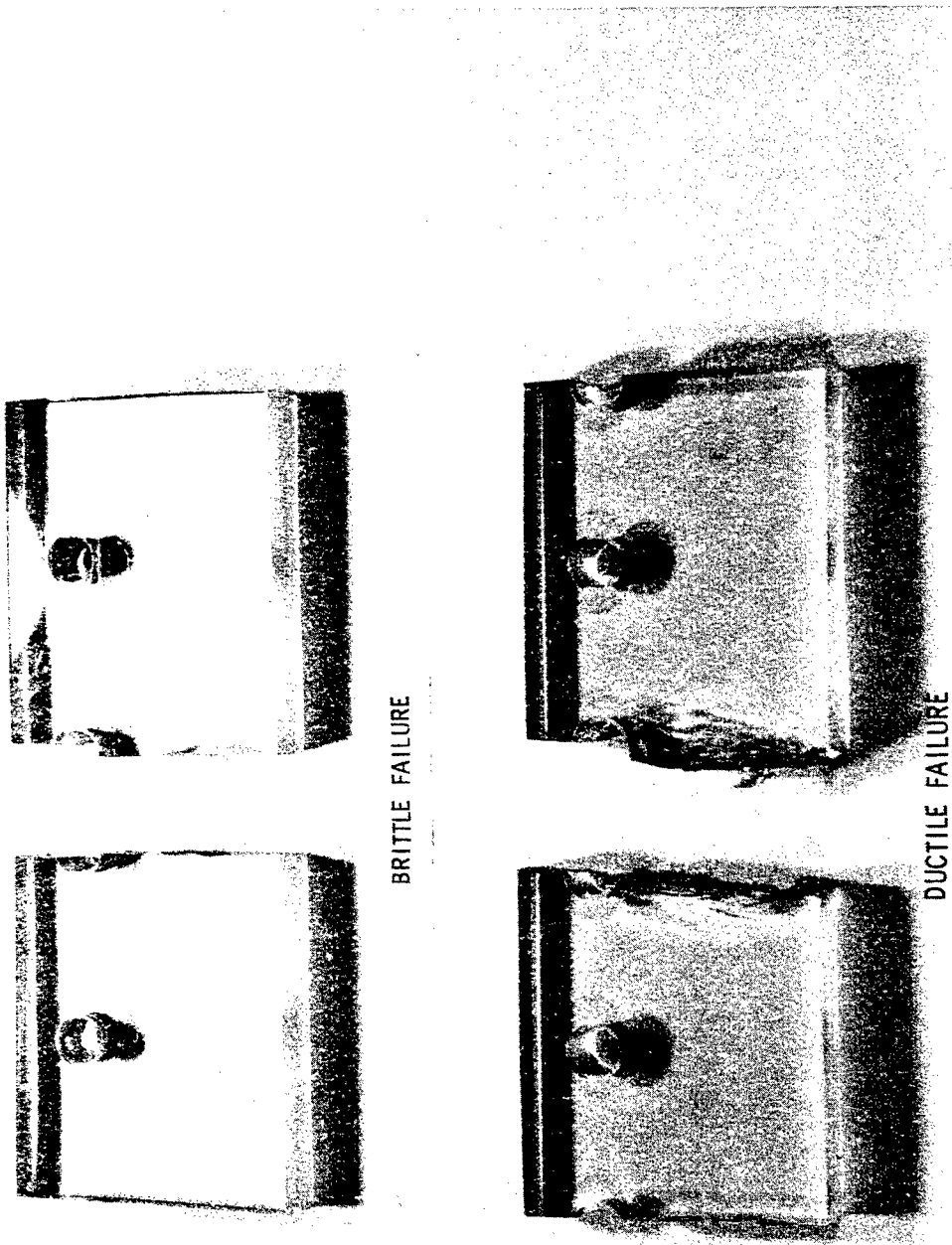


Figure 3. Photograph of Failed Edge Attachment Specimens,  
Brittle versus Ductile Failure

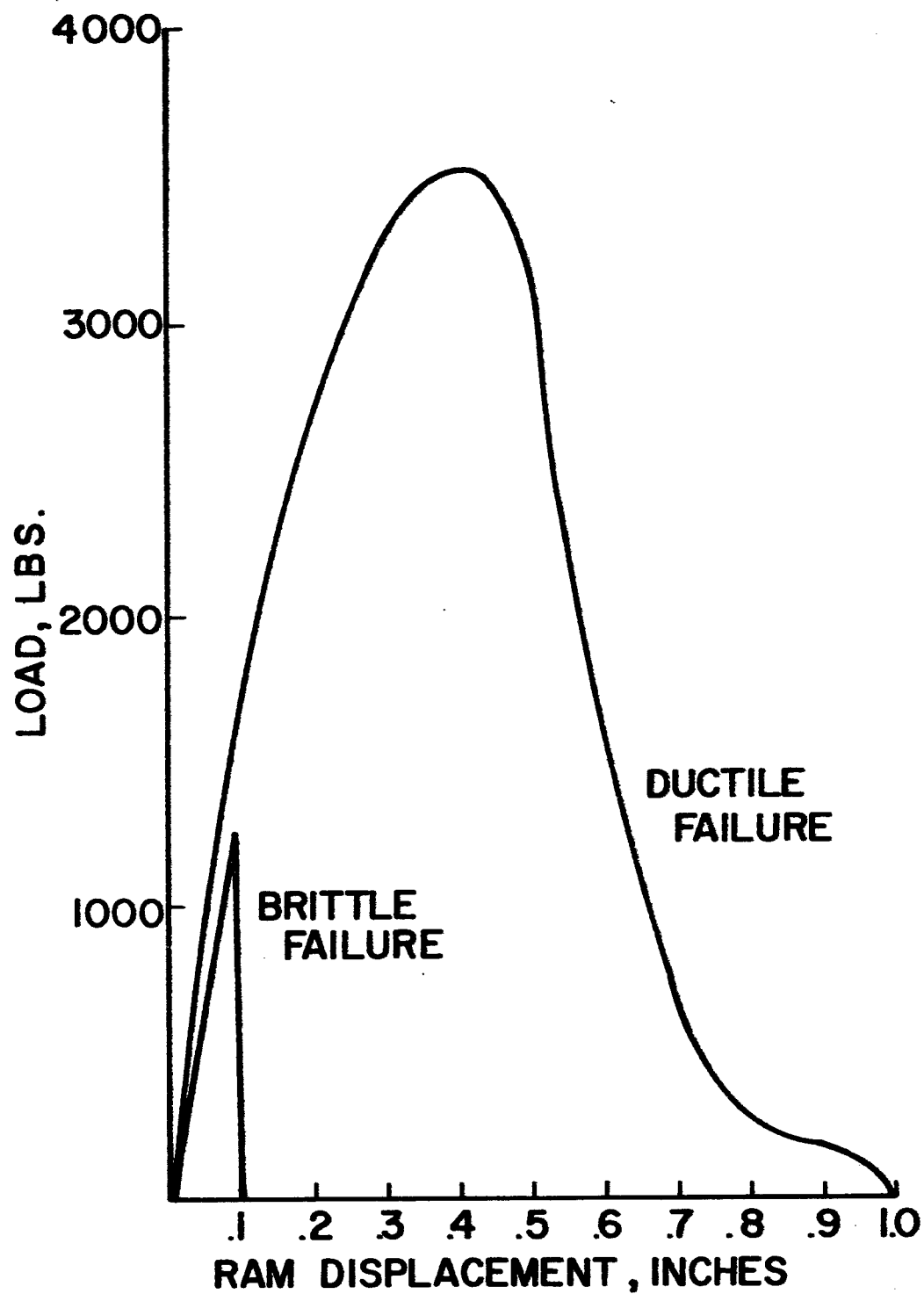
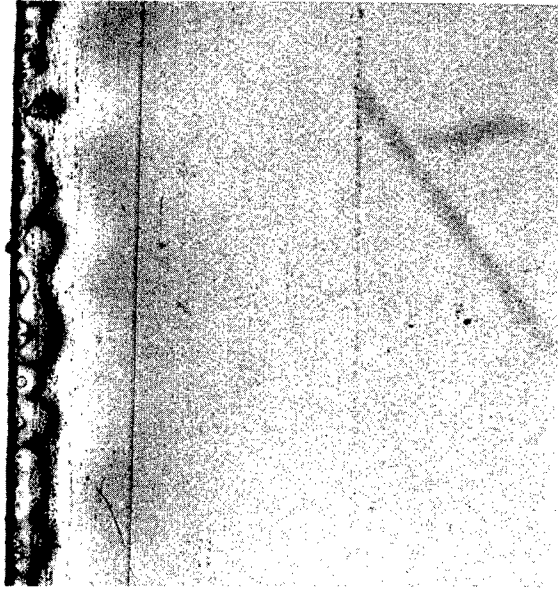
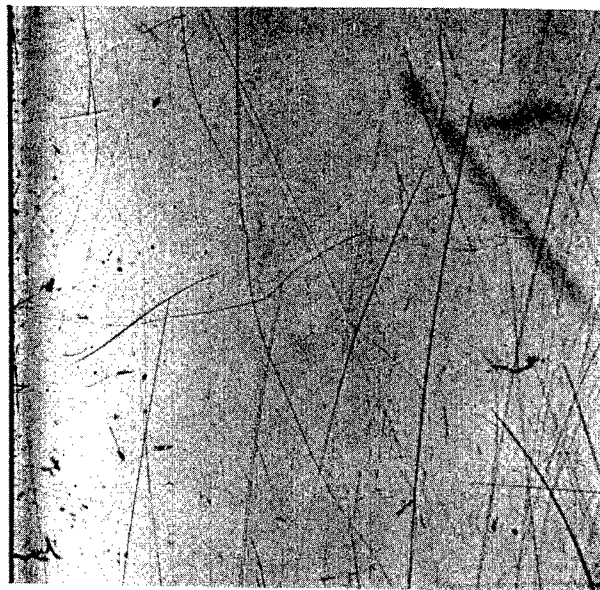


Figure 4. Load-Deflection Curves for Edge Attachment Specimens





**POOR MACHINED EDGE**



**GOOD MACHINED EDGE**

**Figure 5. Photoelastic Pictures of Poorly Machined Edge versus Carefully Machined Edge**

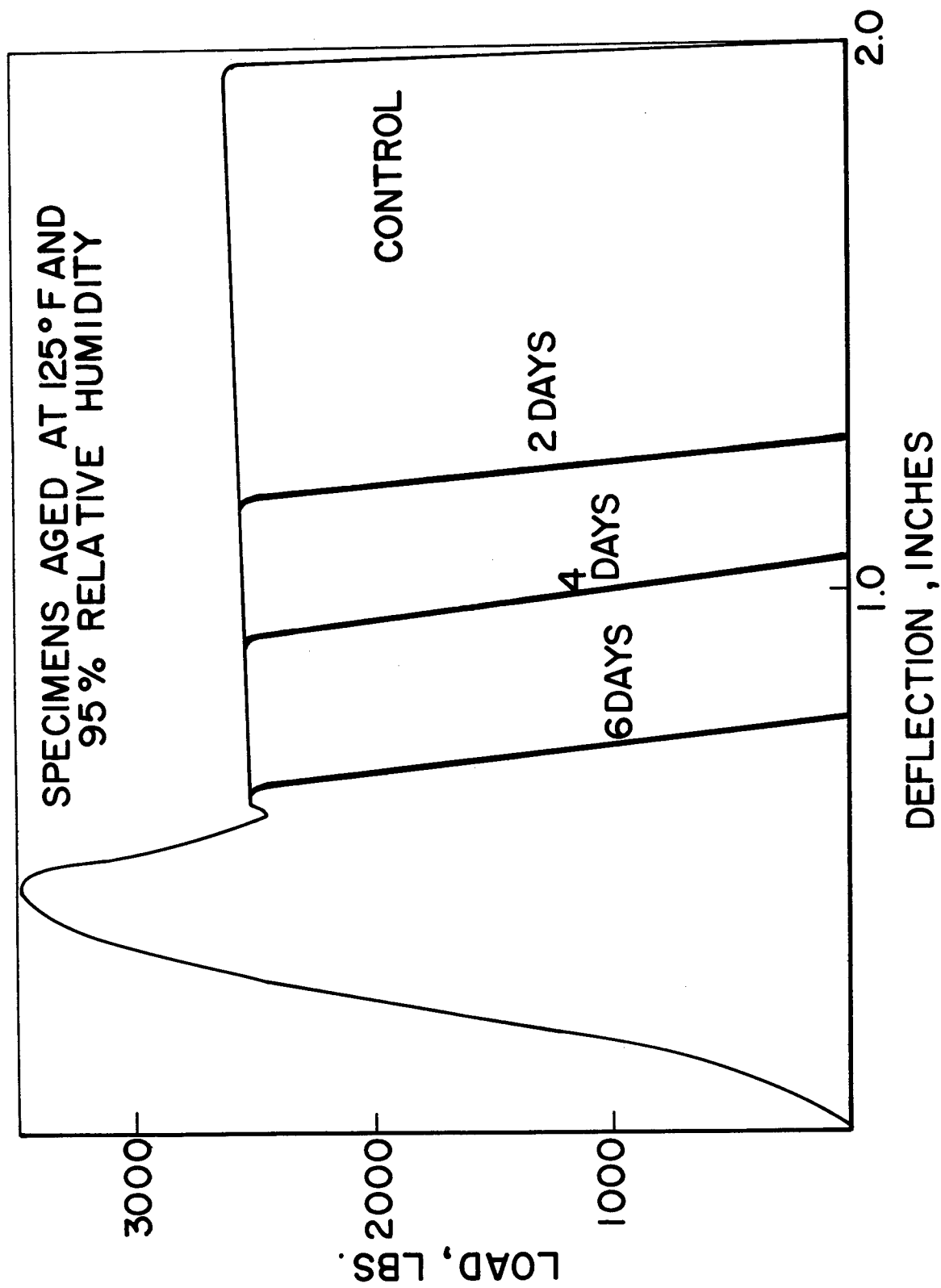
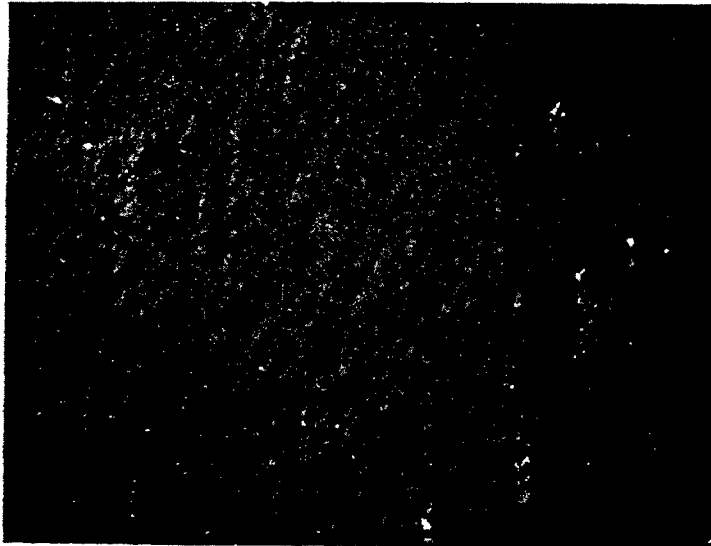
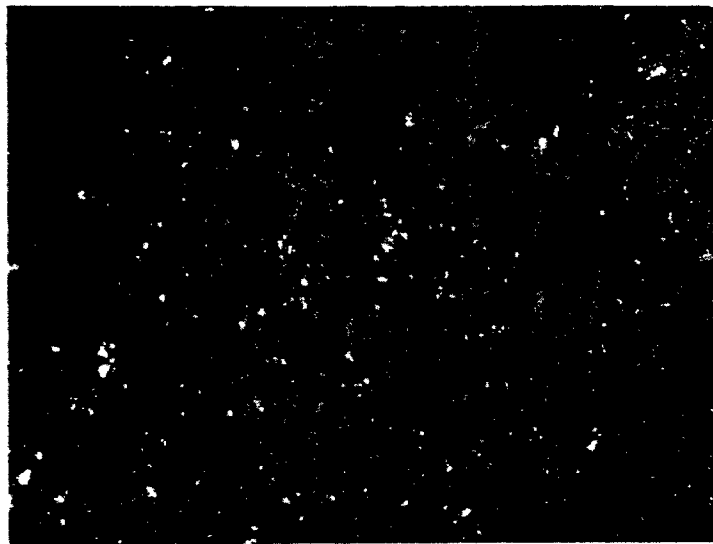


Figure 6. Load-Deflection Curves of Tensile Specimens After Humidity Aging

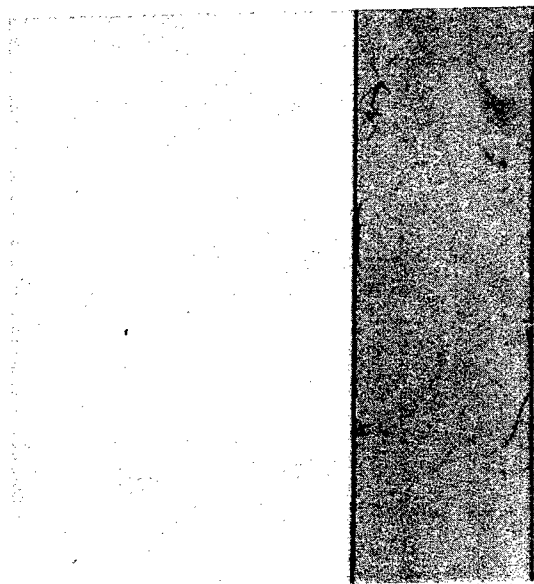


CONTROL



AGED SIXDAYS AT 125°F  
AND 95% RELATIVE HUMIDITY

**Figure 7. Photomicrographs of Machined Surfaces of Tensile Specimens after Testing, Control versus Six Day Humidity Aged Specimens, 50X**



**CONTROL**



**AFTER SIX DAYS AT 125°F  
AND 95% RELATIVE HUMIDITY**

**Figure 8. Photoelastic Pictures of Tensile Specimens after Testing,  
Control versus Six Day Humidity Aged Specimen**

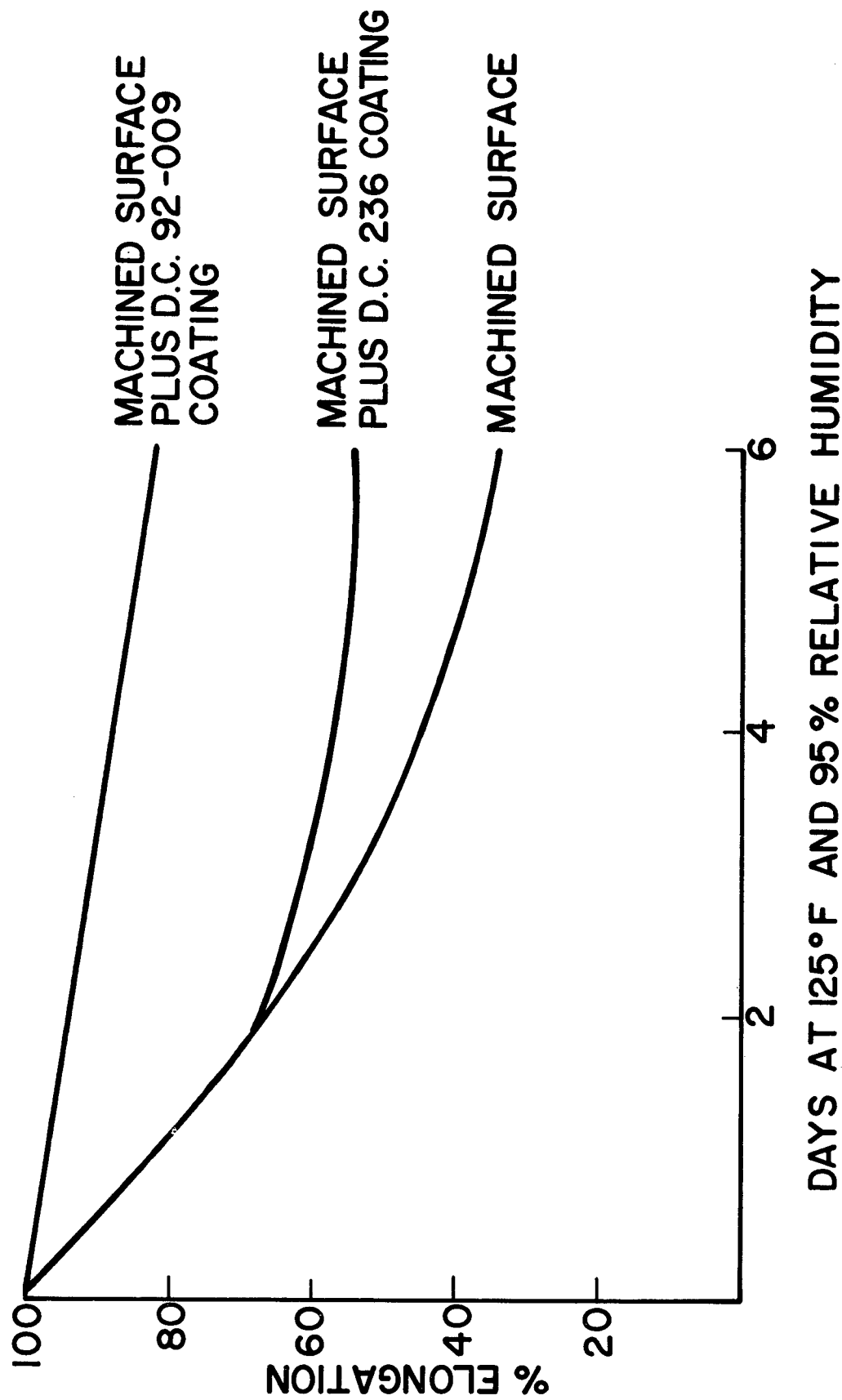


Figure 9. Effect of Humidity Aging on Tensile Elongation

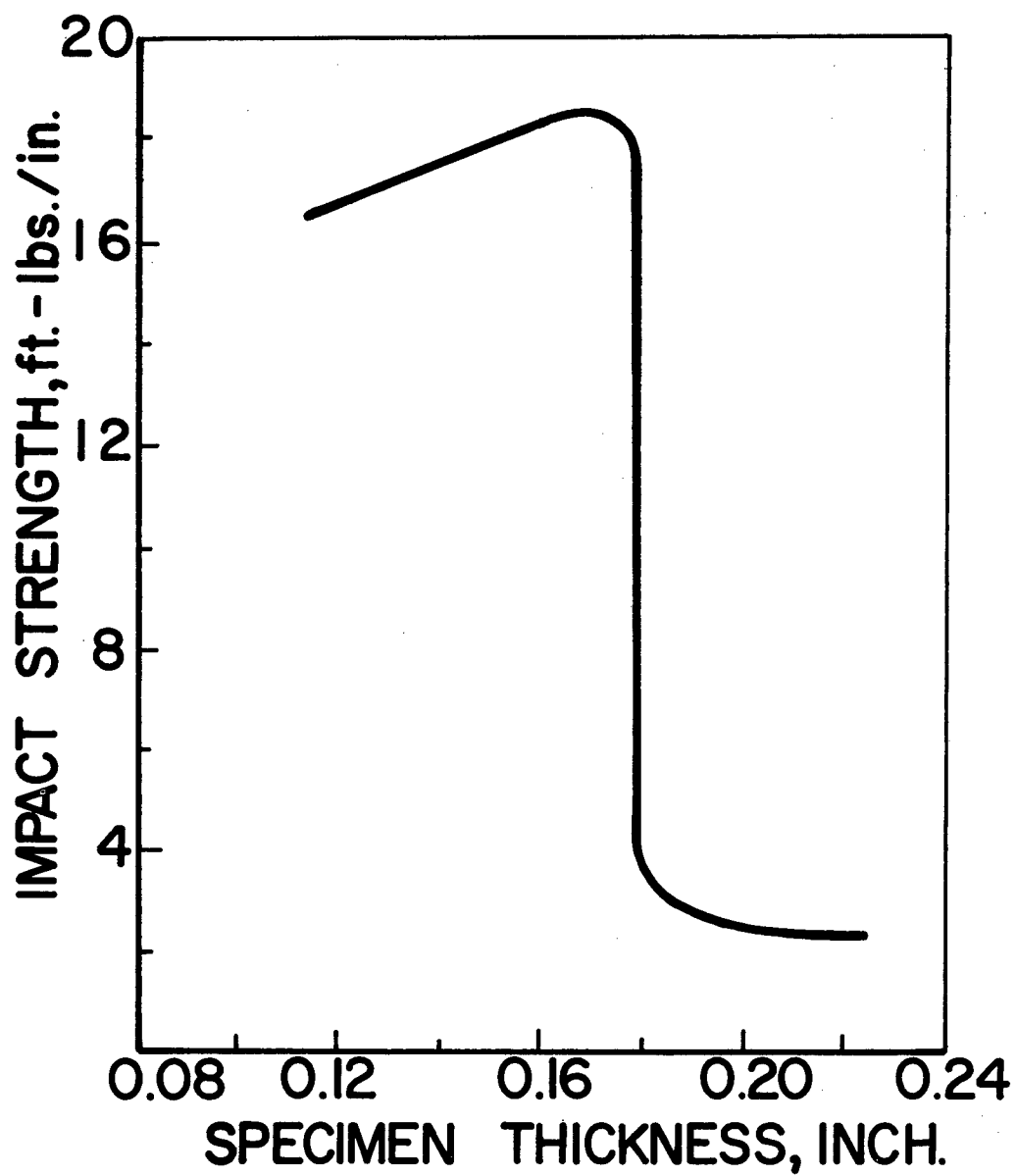


Figure 10. Notched Izod Impact Strength versus Material Thickness

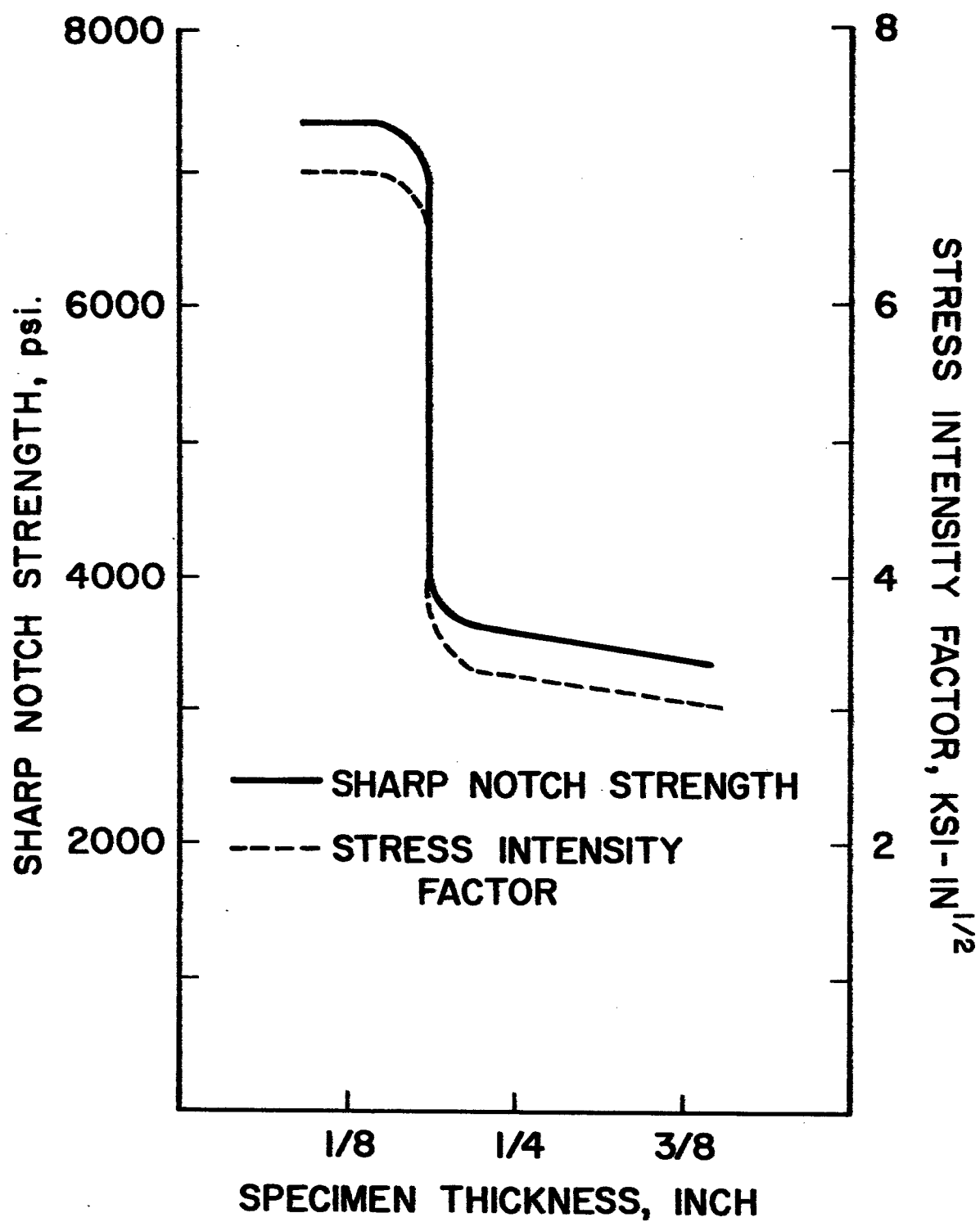
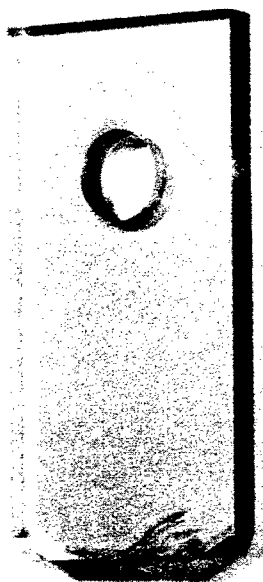
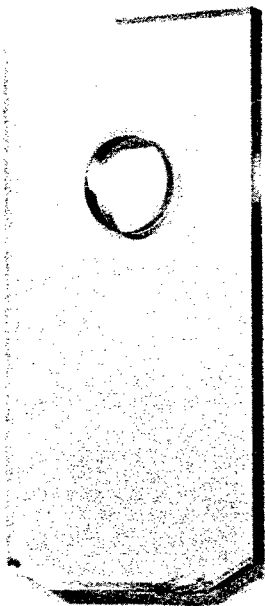


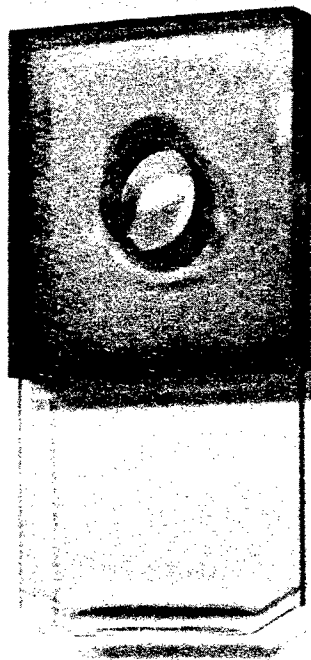
Figure 11. Effect of Sharp Edge-Notch Properties versus Material Thickness



3/8 INCH POLYCARBONATE



1/4 INCH POLYCARBONATE



1/8 INCH POLYCARBONATE

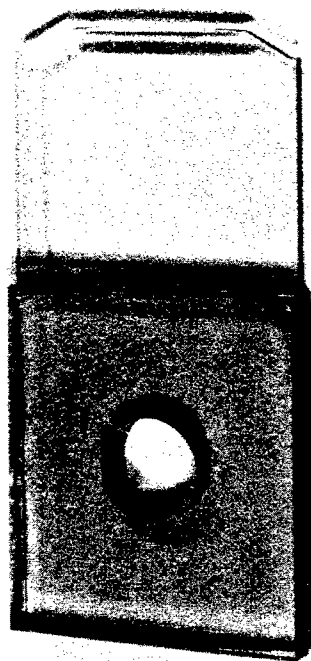


Figure 12. Photograph of Failed Sharp Edge-Notch Specimens



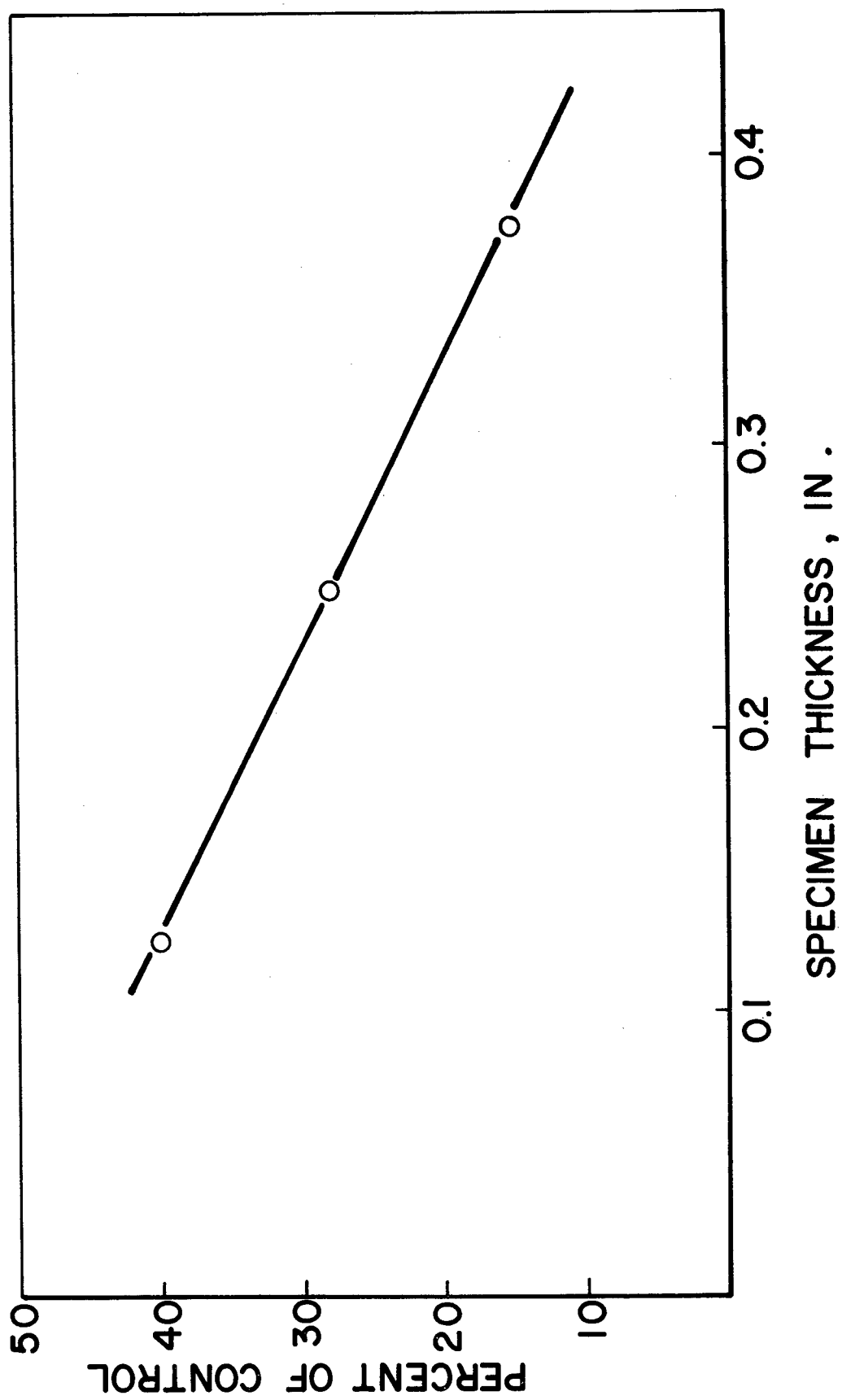


Figure 13. Effect of Thickness on Tensile Elongation after Six Days  
at 125°F and 95% Relative Humidity

# LAMINATED WINDOW

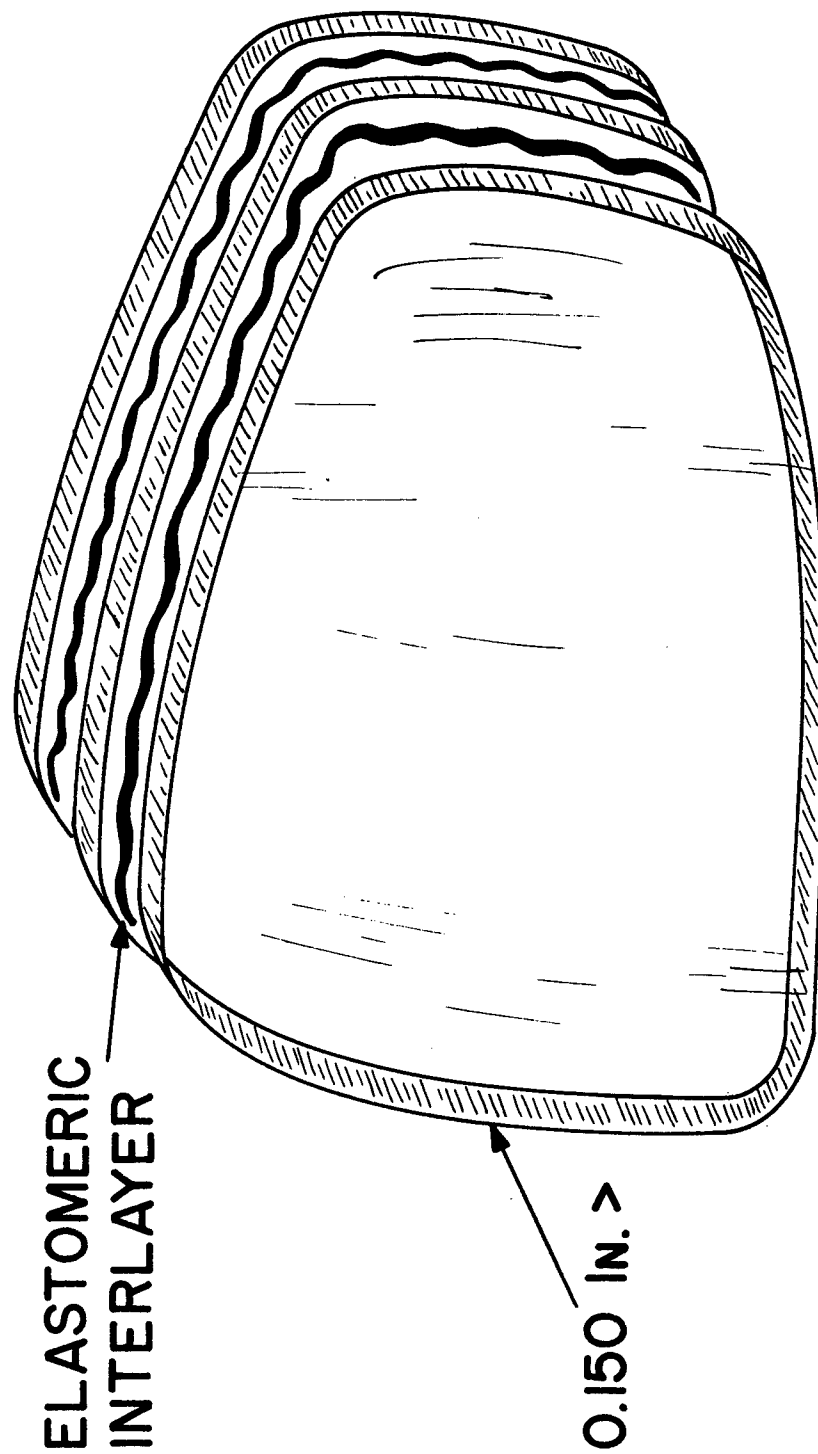


Figure 14. Optimum Polycarbonate Windscreens

**MATERIAL EVALUATION B-1 CREW  
MODULE WINDSHIELD AND WINDOWS**

**J. E. Mahaffey  
North American Rockwell Corporation  
Los Angeles, California**

NA-73-35

**MATERIAL EVALUATION**  
**B-1 CREW MODULE WINDSHIELD AND WINDOWS**



**B-1 Division**  
North American Rockwell

## INTRODUCTION

Materials selection for the B-1 crew module windshield and windows was extremely important to insure an optimum design concept, considering the relatively severe windshield functional requirements, weight, and cost. A comprehensive windshield trade study was initiated, early in the B-1 program, which included a materials trade study as a basic part of the overall trade study. Specific materials were selected in the trade study as candidate materials for the B-1 windshield and windows. Figure 1 shows the configuration of the B-1 crew module windshield and windows.

Comprehensive materials evaluation was not performed in an effort to reduce development costs in the B-1 program. A significant amount of data were available for most of the candidate materials, and a concerted effort was made to utilize these data where possible. Material property tests were performed only where required data were not available or where existing data could not be directly correlated to the B-1 requirements. Most of the physical testing was concerned with polycarbonate and proprietary interlayer materials. This paper summarizes the materials testing performed in direct support of the B-1 windshield design development program. Additional background data and information pertaining to the B-1 windshield and windows will be presented in a subsequent paper.

## DISCUSSION

A total of 10 transparent structural materials and four elastomeric interlayer materials were considered in the materials trade study. The criteria used to select candidate materials were mechanical properties, heat resistance, density, optical quality, availability, technical risk, past experience, and cost considering the B-1 windshield functional requirements. Mechanical properties considered included tensile strength, modulus of elasticity, creep, and impact strength. Data and information for the trade study were obtained from available literature, material suppliers, and subcontractors. Physical testing was not performed in this phase of the program. Based on the trade study, the following materials were selected as candidate glazing materials for the B-1 windshield and windows:

### Structural Materials

### Interlayers

Acrylic

MIL-P-8184

Stretched acrylic

MIL-P-25690

Silicone

Polycarbonate

MIL-P-83310

Polyurethane

Glass

MIL-P-25667

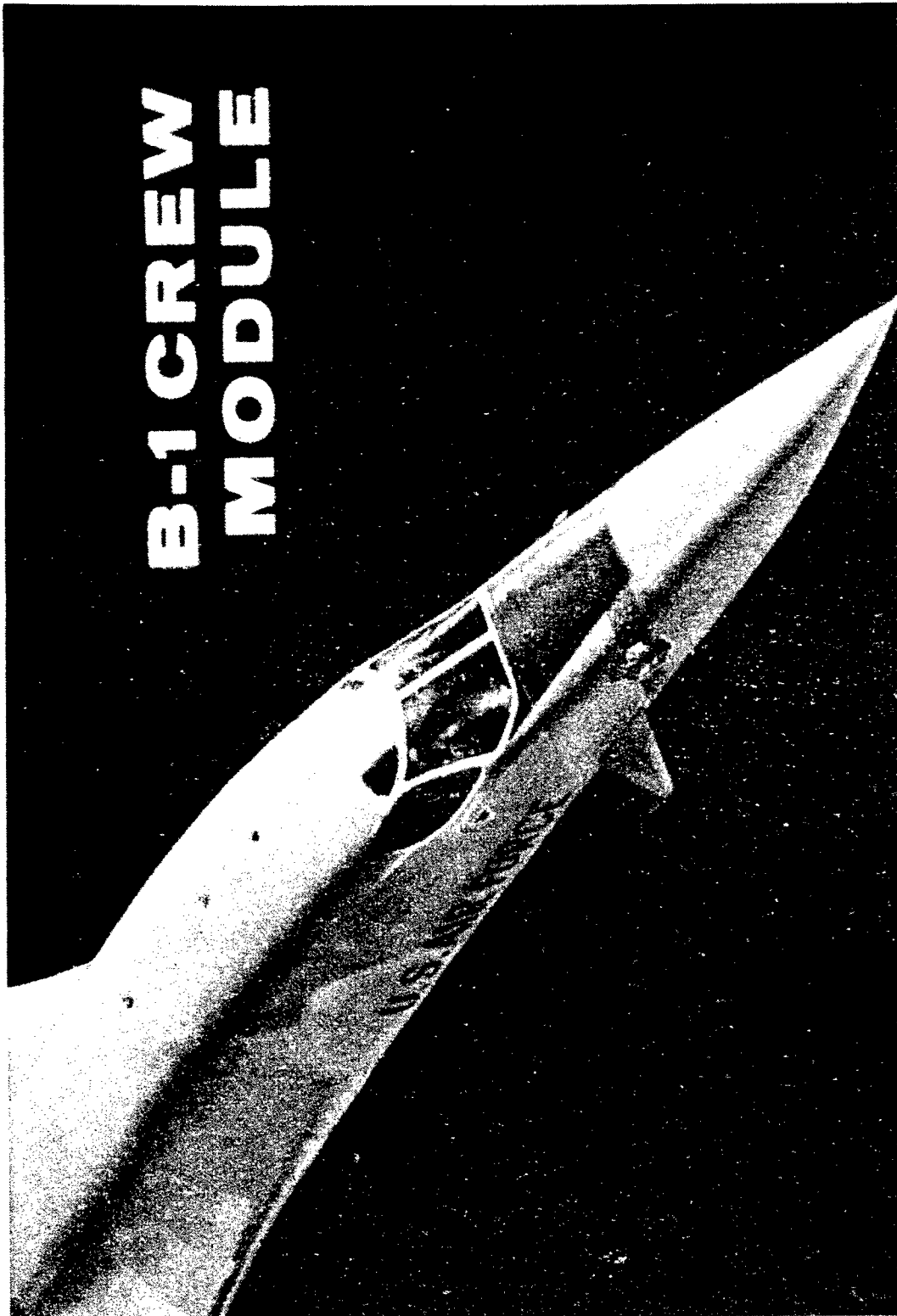


Figure 1. B-1 Crew Module - Window and Windshield Area

## CYCLIC CREEP TESTS

Published creep data for stretched acrylic and polycarbonate are concerned with constant temperature and loads over long time periods. It was believed that creep under cyclic loading conditions involving temperature changes may be significantly less than published creep data. In addition, it was desired to compare the creep properties of acrylic and polycarbonate directly. Cyclic tensile creep tests were performed on stretch acrylic and polycarbonate where the test conditions were based on typical B-1 mission profiles. The specimen configuration for these tests is illustrated in figure 2. The tests were performed on an Instron test machine with an environmental chamber. An extensometer was used to measure strain during the test cycle. Gage marks were placed in the test section of the specimen approximately 2 inches apart. Permanent tensile creep was measured with a creep telescope at the completion of each test cycle, using the gage marks.

A test cycle consisted of application of load and increasing temperature simultaneously to a tensile stress level of 2,600 psi and the specified test temperature. The load and temperature were maintained for 18 minutes, at which time the load was removed and the specimen cooled to room temperature. Strain was recorded during the test cycle, and permanent deformation was measured with the creep telescope at ambient temperature prior to initiating the next cycle. The cyclic creep tests were conducted at temperatures of 160° and 180° F for stretched acrylic; 180°, 200°, and 220° F for polycarbonate; 10 test cycles per specimen. It was originally planned to continue the tests for considerably more cycles, but since a definite trend in creep properties was established after 10 cycles, the tests were terminated at this point.

At the conclusion of the tests, very fine stress crazing was noted in the test section of the polycarbonate specimens. It was believed that contamination incurred from handling the specimens during the tests caused the stress crazing. Additional tests were conducted where the specimens were carefully cleaned and handled with clean cotton gloves. Stress crazing did not occur in these tests, which demonstrated that exposed surfaces of polycarbonate must be protected from contamination to prevent stress crazing when the material is subjected to tensile stresses.

A summary of the cyclic creep tests is presented in figure 3. It is apparent that the creep properties of polycarbonate in this temperature range are significantly better than stretched acrylic. Both total strain under load and permanent deformation are less in polycarbonate at 200° F than stretched acrylic at 160° F. The results of these tests were important in the selection of polycarbonate as the structural material for the B-1 windshield and windows. Other design development tests which led to the selection of polycarbonate are discussed in a subsequent paper.

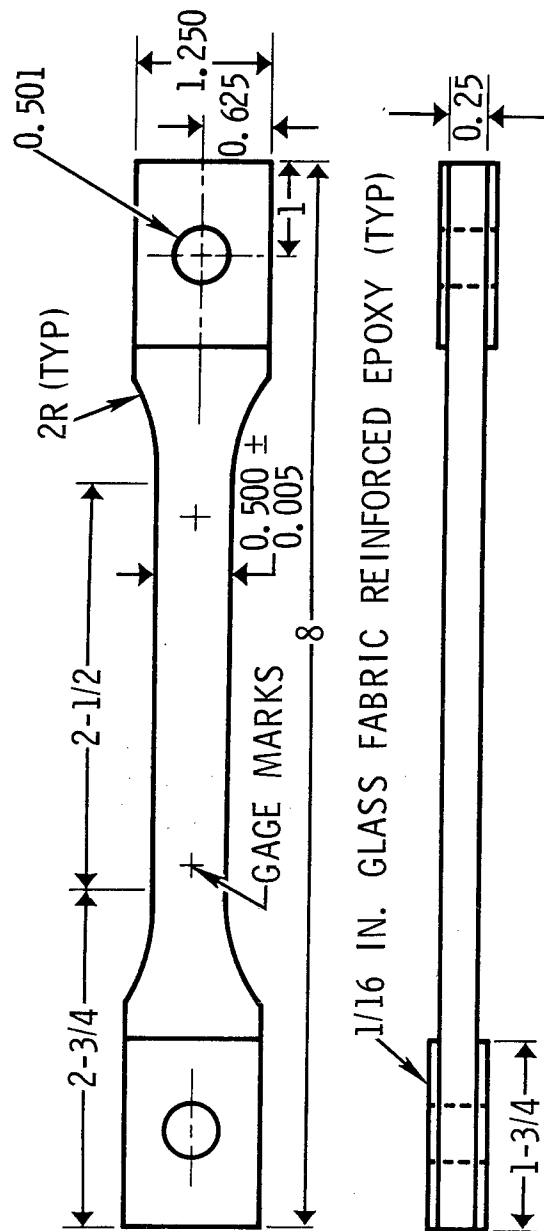


Figure 2. Tensile Creep Test Specimen



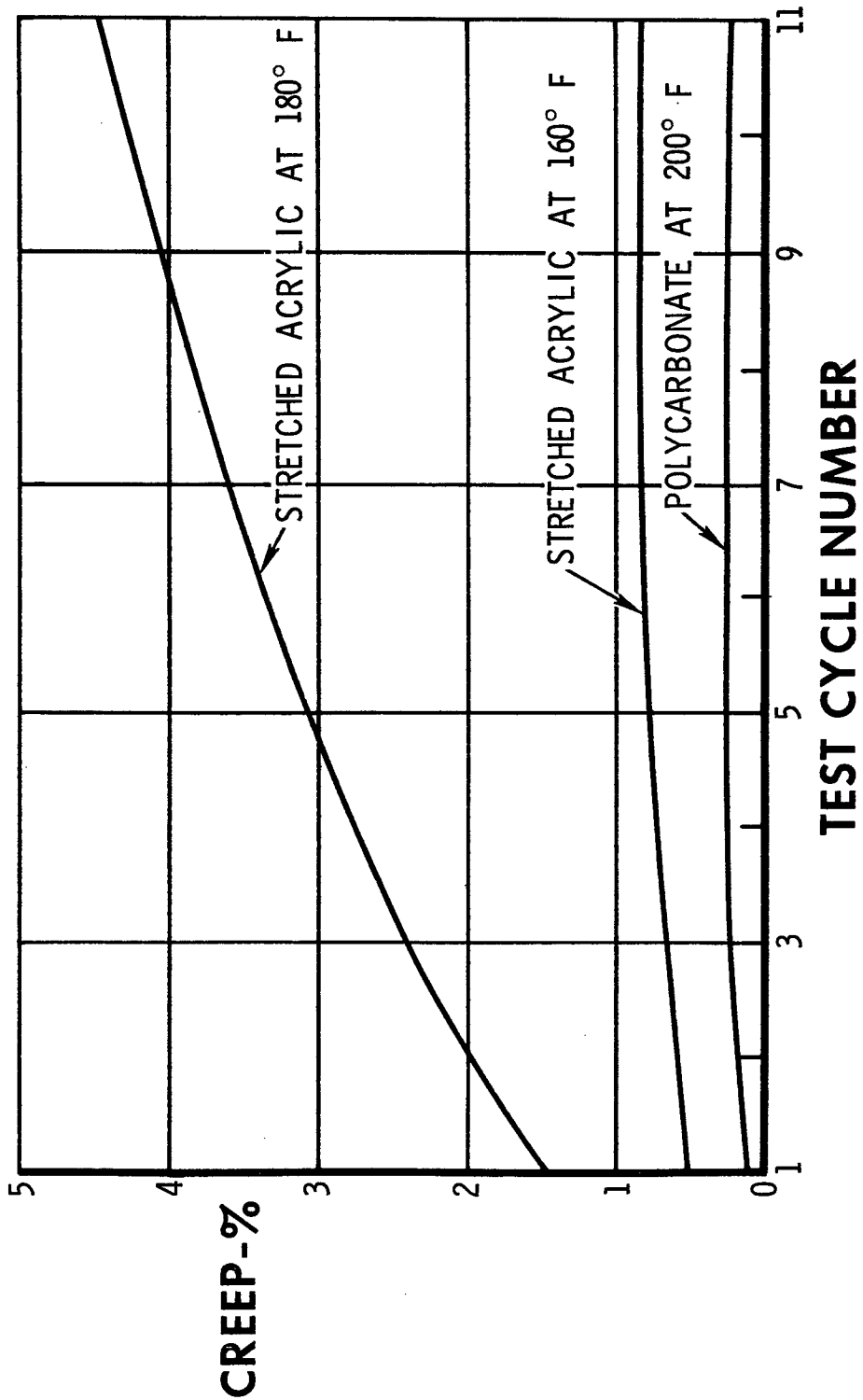


Figure 3. Stretched Acrylic and Polycarbonate Creep Properties

## INTERLAYER EVALUATIONS

The interlayer material adjacent to the outer ply of the B-1 front windshield is subjected to temperatures of  $-65^{\circ}$  to  $250^{\circ}$  F for extended time periods. The interlayer must accommodate the relative movement between the structural components of the windshield composite under these relatively severe environmental conditions and aircraft loads without delamination or failure in shear. The materials trade study indicated that currently available interlayers which will perform satisfactorily in this temperature range are limited. With the exception of polyvinyl butyral, most of the interlayers are the cast-in-place type and have been developed by subcontractors as proprietary materials.

A polyurethane and two silicone interlayers were selected for evaluation to the B-1 windshield requirements, based on available data and subcontractor recommendations. Ethylene terpolymer was considered for evaluation but development of this material had not progressed sufficiently at the time. The mechanical and physical property tests conducted on these materials are listed as follows:

1. Tensile strength and elongation as a function of temperature
2. Environmental resistance (heat aging and ultraviolet light)
3. Thermal conductivity and specific heat
4. Shear strength as a function of temperature (glass, acrylic, and polycarbonate substrates)

Tensile strength and elongation tests were conducted in accordance with ASTM test method D-412 at 20 inches per minute crosshead travel. These tests were conducted in the temperature range of  $-65^{\circ}$  to  $270^{\circ}$  F. Ultraviolet environmental tests consisted of 300 hours exposure in a carbon arc weatherometer; heat aging consisted of 390 hours exposure at  $270^{\circ}$  F. Thermal conductivity was performed in accordance with ASTM method C-177.

Shear strength tests were conducted on the silicone interlayers as a function of temperature in the range of  $-65^{\circ}$  to  $250^{\circ}$  F, using glass, stretched acrylic, and polycarbonate substrates. The specimen configuration was 2 by 2 inches square, consisting of two 1/4-inch-thick face sheets of the substrate and 1/8-inch interlayer. Since these specimens were originally intended for flatwise tensile tests, a special test fixture was designed to test the specimens in shear. The tests were conducted on an Instron test machine at 0.05-inch-per-minute crosshead travel where stress-strain curves were recorded on each test.

The results of the tensile and shear tests on the interlayer materials are presented in figures 4 and 5. Figure 4 compares the tensile strength and elongation of a typical silicone and polyurethane interlayer. These values will vary slightly, depending upon the supplier. These data show that the elongation of polyurethane is relatively low at  $-65^{\circ}$  and  $270^{\circ}$  F, while the silicone maintains good elongation characteristics over the entire temperature range. The tensile strength of the polyurethane is very good at low temperatures, but drops rapidly at elevated temperature. The tensile strength of the silicone is low by comparison at lower temperatures, but maintains strength over a wide temperature range. Figure 5 illustrates that the stress-strain relationship of the silicone interlayer remains relatively constant between  $-65^{\circ}$  and  $250^{\circ}$  F.

Based on the results of the interlayer tests, the silicone interlayer was considered the best available interlayer for use adjacent to the outer ply of the front windshield. This is based primarily on the superior mechanical properties at elevated temperature of the silicones and the fact that they remain flexible at low temperature. Other interlayer materials were considered satisfactory for that portion of the laminated composite not subjected to elevated temperature or large temperature gradients.

#### EDGE ATTACHMENT DESIGN DEVELOPMENT

The design approach for the edge attachment of the B-1 windshield and windows consists of mechanical fasteners through drilled holes in the structural plastic plies of the laminated composite. Bearing strength tests were conducted on polycarbonate in accordance with FIMS 406, method 1051, in the temperature range of  $75^{\circ}$  to  $250^{\circ}$  F. The results of these tests are presented in figure 6. The bearing properties reported are bearing strength based on 4-percent hole deformation and bearing ultimate for two edge distance ratios.

The structural loads and temperature environment associated with the B-1 windshield dictated that edge attachment reinforcement was necessary to react bearing loads. A nylon fabric-epoxy resin laminate was selected as the reinforcing material. This selection was based on the fact that the linear coefficient of thermal expansion of this material is very similar to that of polycarbonate.

Several adhesive systems were evaluated for bonding the epoxy laminates to polycarbonate. These included modified epoxies, polyurethanes, silicones, and modified acrylic. Most of these systems provide satisfactory bonds to polycarbonate at ambient temperature, but difficulty was experienced in obtaining good adhesion to polycarbonate at elevated temperature, specifically  $220^{\circ}$  F. An evaluation of several primer systems for polycarbonate

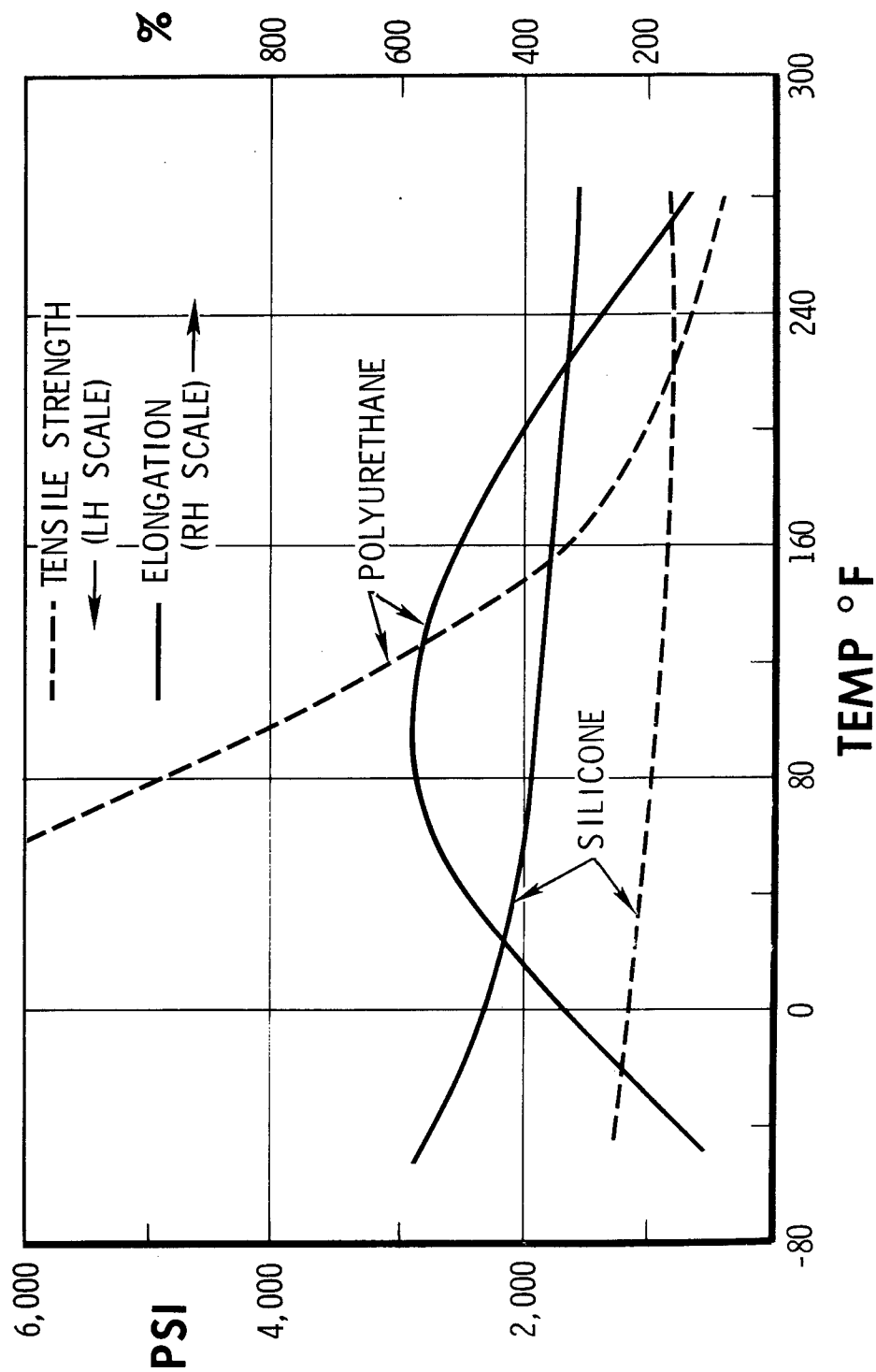


Figure 4. Tensile Strength and Elongation - Interlayer Materials

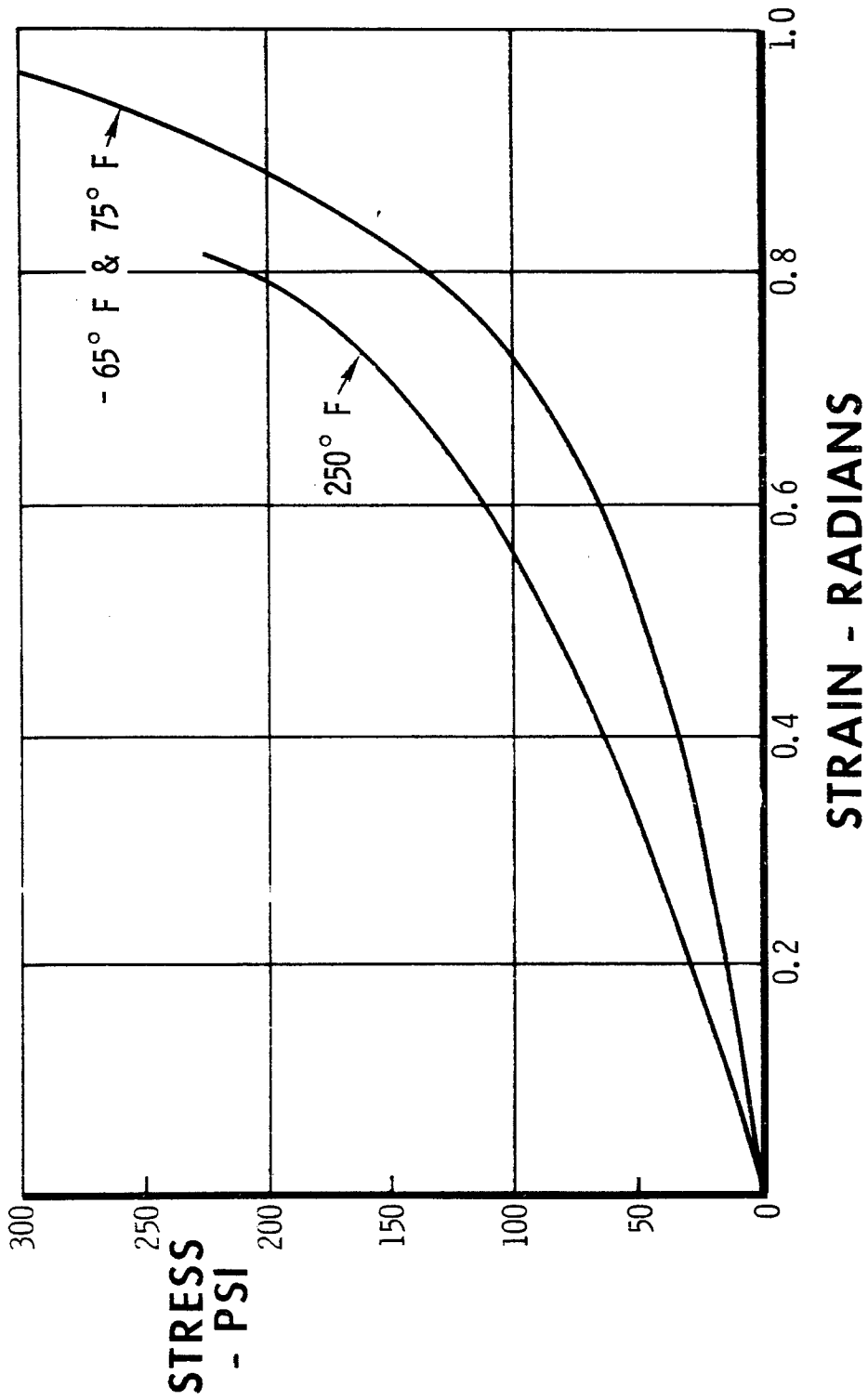


Figure 5. Shear Properties Silicone Interlayer

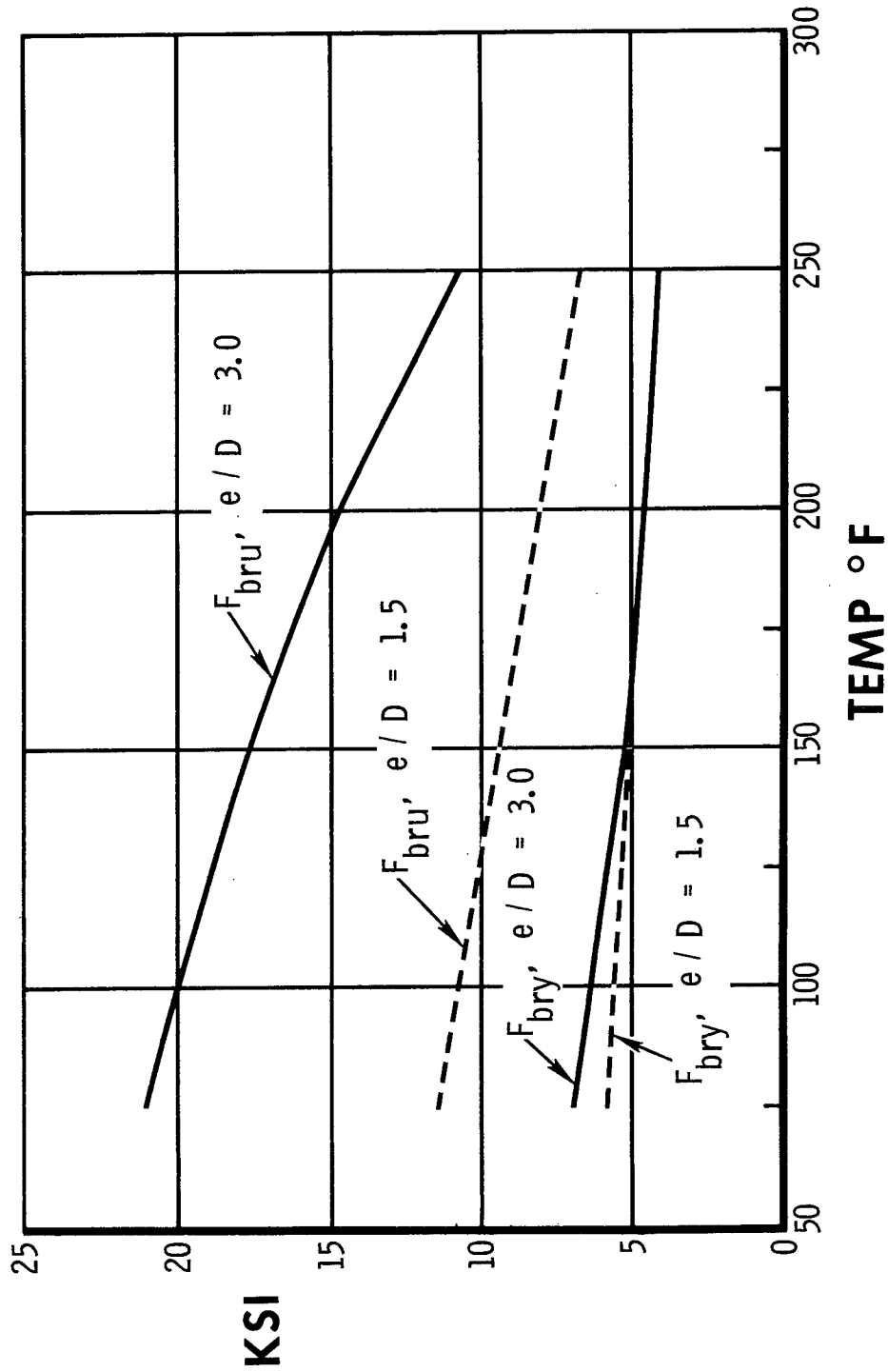


Figure 6. Polycarbonate Bearing Strength

was conducted to improve adhesion at elevated temperature, but resulted in insignificant improvement.

Based on the results of the adhesive investigation, a two-part silicone adhesive was selected for the B-1 windshield edge attachment. The material is identified as RTV-630 and SS 4120 primer manufactured by the General Electric Company. Initially, SS 4155 primer was specified, since slightly higher lap shear values were obtained with this primer system. The subcontractors for the windshield and windows subsequently experienced difficulty in obtaining consistently good adhesion to polycarbonate with this primer. An investigation of this problem indicated the SS 4155 primer was particularly sensitive to humidity conditions for optimum cure, and that the shelf life was apparently more critical than most primers. As a result of this investigation, SS 4120 primer was substituted for the SS 4155, and this primer system has proved satisfactory to date.

The lap shear strength of this adhesive system is presented in figure 7. These values are based on double-lap shear strength tests of the nylon fabric-epoxy resin laminates bonded to 1/4-inch polycarbonate with 1-inch overlap.

#### EDGE ATTACHMENT DESIGN VERIFICATION

The edge attachment design for the B-1 front windshield is illustrated in figure 8. The loads are reacted in double shear with titanium fasteners through drilled holes in the polycarbonate and reinforcing laminates. Glass fabric-epoxy resin bushings provide thermal insulation for the polycarbonate and serve as spacers for the outer retainer. The bearing strain under load and the creep properties of this design configuration were very important because the crew module loads are transferred directly through the windshield and windows. Creep and fatigue tests were performed on this edge attachment design concept, using bearing stresses and the temperature environments associated with crew module windshield and windows to verify the edge design.

The specimen configuration for these tests is illustrated in figure 9. The tests were performed on an Instron test machine, using an extensometer to measure bearing strain. Tests were conducted at soak temperatures of up to 220° F and bearing stresses of up to 5,500 psi. Specific temperatures, stress levels, and time periods were based on typical B-1 mission profiles. Cyclic creep tests were conducted based on one life cycle of the windshield and fatigue tests for four life cycles.

This test program revealed some problem areas concerning bearing holes in polycarbonate. The initial tests were performed on specimens fabricated and drilled at NR. No special procedures were developed or employed for

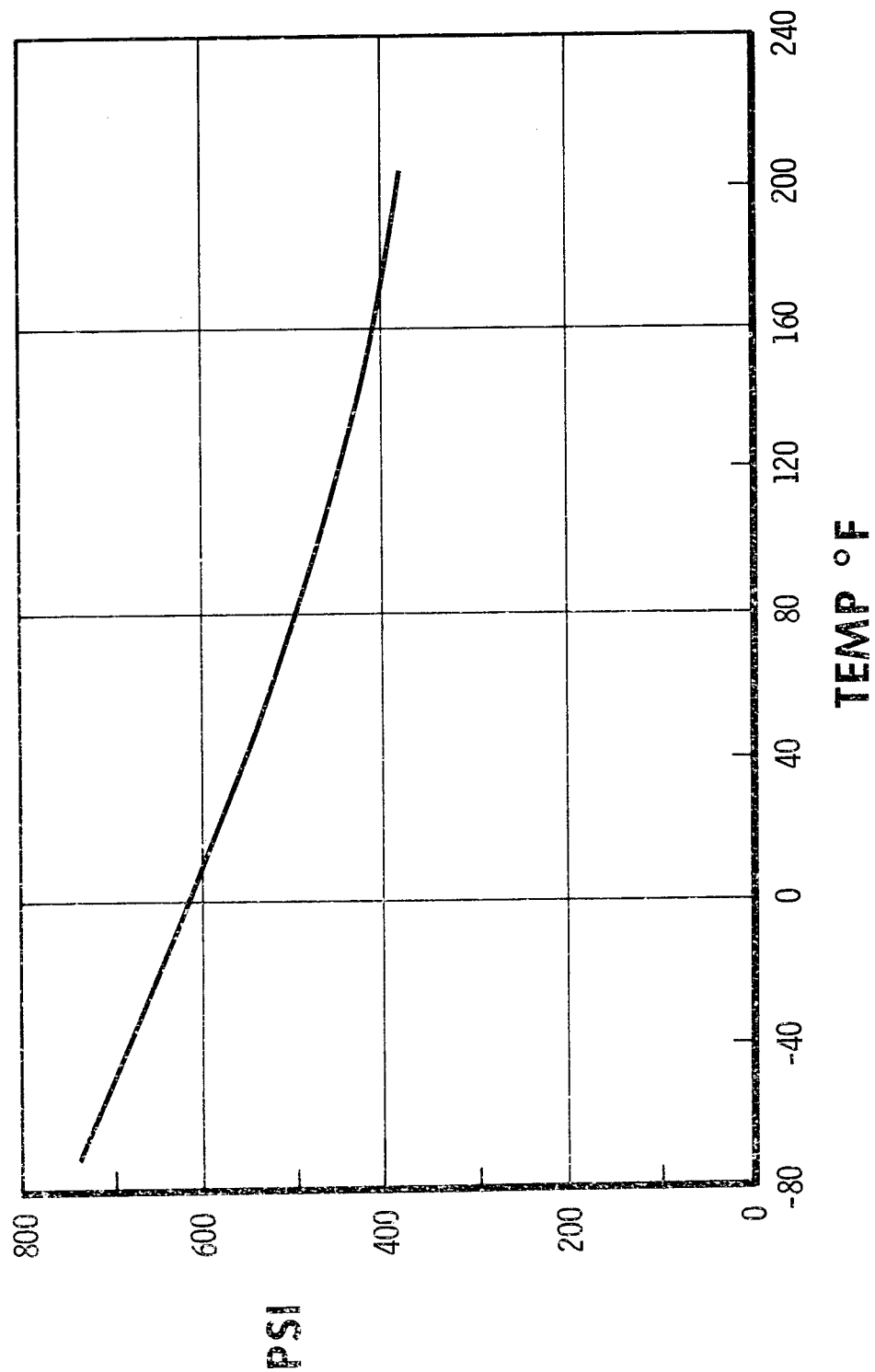


Figure 7. Lap Shear Strength



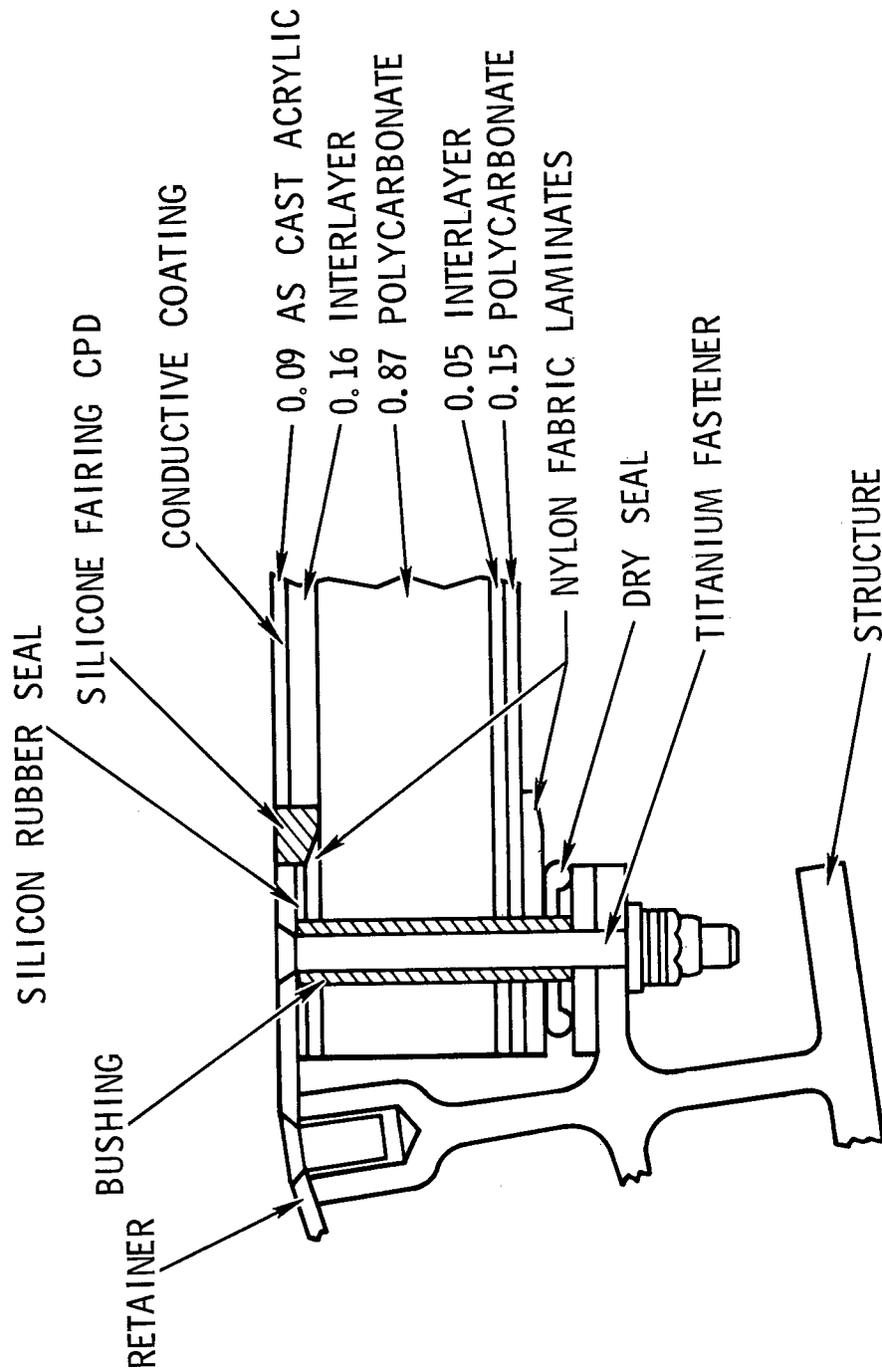


Figure 8. Typical Edge Attachment - B-1 Windshield

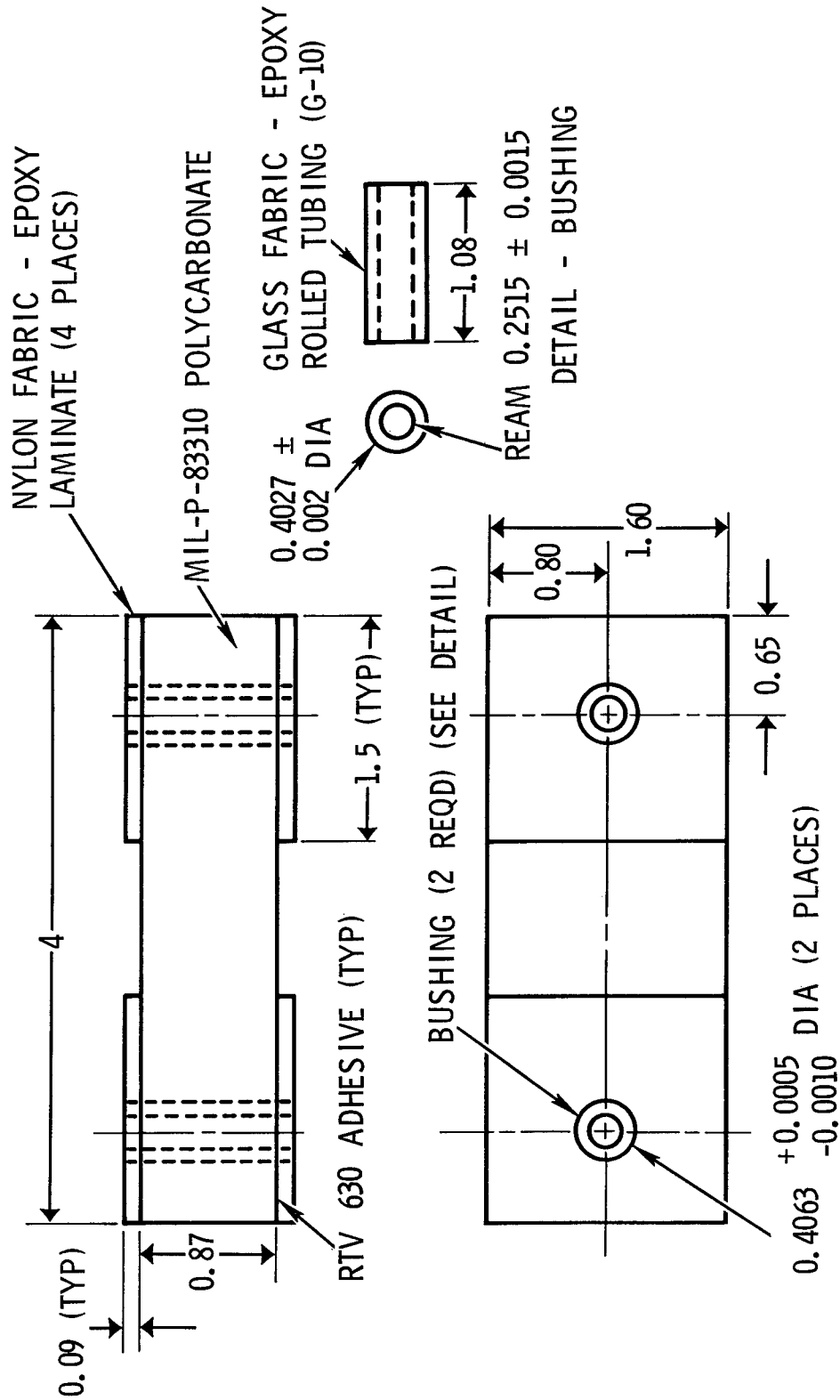


Figure 9. Edge Attachment Bearing Specimen

drilling holes in polycarbonate. The surface finish in the bearing hole was approximately 125 rms, and there was no attempt to clean the bearing hole or to stress relieve prior to test. After very short exposures to 3,000 psi, bearing stress, and 220° F temperature, stress crazing was incurred in the polycarbonate bearing hole.

An investigation of the cause of crazing was initiated. Examination of the specimens with polarized light indicated there were high stress concentrations around the drilled holes in the polycarbonate. It was also theorized that contamination of the polycarbonate, possible from several sources, may have been a contributing factor. Contacts with General Electric revealed that the surface finish of the drilled hole is also important. Additional specimens were tested where the specimens were annealed per the material suppliers' recommendations, and where the drilled holes were cleaned with isopropyl alcohol prior to test. Stress crazing was again encountered, but was significantly reduced, compared to the original tests.

Since the subcontractors for the windshield and windows will be drilling the edge attachment holes, specimens were procured from the subcontractors with the edge attachment holes drilled by the subcontractors. These specimens were procured with polycarbonate hole finish in the range of 20 to 65 rms. Special drilling techniques developed by the subcontractors were used to maintain hole tolerances, surface finish, and to minimize stress concentrations around the hole. The initial tests of the new specimens again resulted in slight stress crazing after a very short time at stress and temperature, and was noted in specimens with very good surface finish.

Cleaning of the drilled hole up to this point had been accomplished with a soft cloth saturated with isopropyl alcohol. A more sophisticated cleaning procedure was developed in an attempt to eliminate stress crazing. The specimens were cleaned first with aliphatic naphtha, using a pipette brush to scrub the hole thoroughly, followed by cleaning with isopropyl alcohol in the same manner. The bushings and test fixturing in the attachment area were also cleaned with both naphtha and isopropyl alcohol. Tests conducted after instituting this cleaning procedure resulted in no stress crazing at 200° F and bearing stress levels up to 5,500 psi. The same results were obtained with specimens with 20 and 65 rms hole finish. The cyclic creep and fatigue tests were continued without a stress-crazing problem. Design verification tests are currently in progress, using larger specimens and more sophisticated test parameters. To date, stress crazing has not been encountered in these tests.

The maximum strain under load in the 0.406-inch-diameter hole during the cyclic tests was 0.022 inch at a bearing stress of 3,000 psi and 200° F temperature. The permanent deformation or elongation in the 0.406-inch hole

after cyclic fatigue tests of four simulated windshield life cycles was only 1-1/2 mils.

The results of these tests and the cyclic tensile creep tests discussed previously demonstrate the sensitivity of polycarbonate to contamination of many types. It is considered mandatory to protect the material from hostile environments to prevent crazing when the material is subjected to tensile stresses. A procedure has been established to preclude contamination in the edge attachment holes for the B-1 windshield. This procedure consists of thoroughly cleaning the bearing hole and bushing with aliphatic naphtha and isopropyl alcohol, followed immediately by bonding the bushing in place with silicone sealant to preclude contamination of the polycarbonate prior to installation. After installation, the edge attachment area is considered adequately sealed.

#### OPTICAL TESTS

Optical quality requirements for the B-1 windshield will be difficult to obtain due to the high angle of incidence (65 degrees), the curved configuration, and multiple construction. The optical properties of polycarbonate, particularly light transmission and haze, are inferior to other transparent materials, although optical quality of polycarbonate has improved in recent months. To compound the problem, the B-1 windshield utilizes a conductive coating for anti-icing, which further reduces light transmission. It was considered necessary, early in the program, to obtain a segment representative of the cross section of the windshield for optical evaluation.

An optical test specimen was procured from Swedlow, Inc, the subcontractor for the front windshield. The specimen was flat, 10 by 10 inches square, and identical to the cross section of the B-1 windshield, as illustrated in figure 8. A conductive coating was applied to the inboard surface of the acrylic, in which the resistivity of the coating was uniformly graded between 5 and 30 ohms per square, from one side of the specimen to the other. The following optical tests were performed on the specimen.

1. Light transmission and haze as a function of angle of incidence and resistivity of the conductive coating.
2. Angular deviation in minutes of arc normal to the surface.
3. Optical distortion at 65-degree angle of incidence.
4. Multiple images of lights.

The light transmission of the optical specimen as a function of angle of incidence is presented in figure 10. Two light transmission values are given - one for the lower resistivity range of the conductive coating, and one for the higher resistivity range. The percent haze in the specimen was 3-percent maximum. These values are considered satisfactory for the B-1 windshield.

The angular deviation in the center portion of the specimen varied between 0.5 and 4 minutes of arc. Optical distortion in the same area did not exceed 1:12 slope of a deviated line of an optical grid board. Both of these values are considered satisfactory. The angular deviation and distortion around the periphery of the specimen were unsatisfactory. This was attributed to the fact that the specimen was fabricated only 1 inch oversize, whereas an actual windshield is fabricated 4 to 5 inches oversize and subsequently trimmed to the required dimensions. In this manner, inferior optical quality incurred around the periphery during processing is eliminated.

Multiple images of runway lights during night operations have been a problem in some aircraft. While there is no current requirement pertaining to multiple images for the B-1, a cursory evaluation of multiple images was made. Reflected images of a small-diameter light source viewed through the specimen were apparent, but the intensity of the reflected images were significantly less than the real image. Equipment required to measure the relative intensity of the reflected images to the real image was not available. An approximation of the relative intensity was made using photographic plates which indicated the relative intensity is in the order of 500 to 1. This investigation demonstrated that multiple images of runway lights viewed through the B-1 windshield may be apparent, but the magnitude of the problem is reduced by the large difference in intensity of the real and reflected images.

It is realized that the optical quality of a 10- by 10-inch flat specimen is not necessarily representative of the optical quality of a full-size curved windshield. This investigation demonstrated, however, that optical quality requirements are obtainable, and it provided basic optical quality data for evaluation. Since this evaluation, a change in the conductive coating has been made which will reduce the light transmission of the composite. At this writing, the magnitude of the reduction in transmission is not known and, therefore, an assessment of the impact of this change on the B-1 windshield optical quality cannot be made.

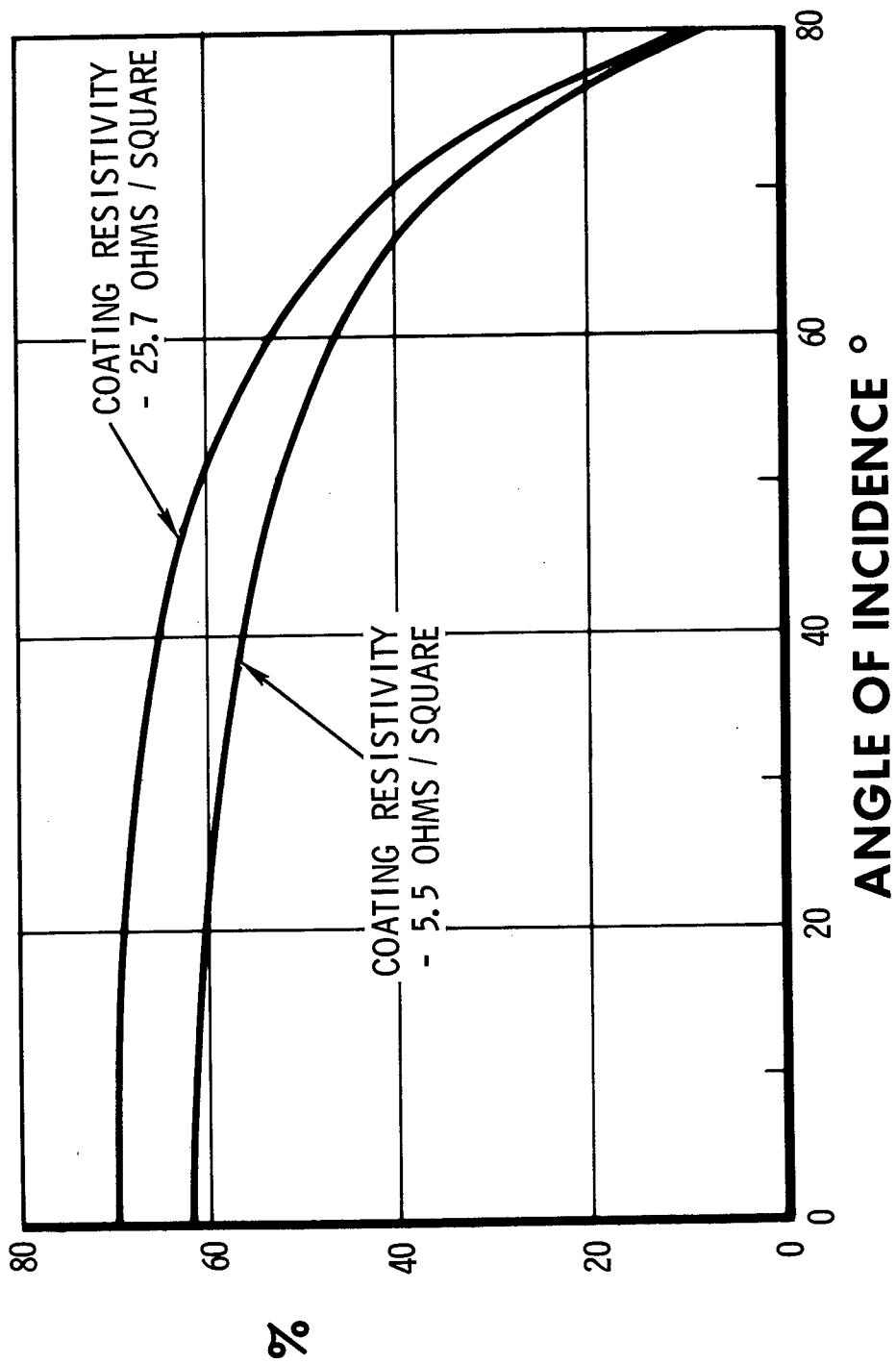


Figure 10. B-1 Windshield Luminous Transmittance

## CURRENT TESTING

### Antistatic Coating

Antistatic coatings are specified for all nonmetallic exterior surfaces of the B-1. The outer surfaces of the B-1 windshield and windows are plastic (acrylic or polycarbonate), and at present, there is no known permanent antistatic coating for transparent plastic materials. It will be necessary to develop a permanent antistatic coating for acrylic and polycarbonate for production B-1 aircraft if these surfaces remain as currently designed. In the meantime, it is necessary to provide antistatic protection for the RDT&E aircraft.

An evaluation of temporary "wipe on" type antistatic coatings is currently in progress for use on the three RDT&E B-1 aircraft. A total of six candidate antistatic coating materials have been procured for screening tests. These materials are commercially available antistatic liquid concentrates, soluble in water or isopropyl alcohol. Acrylic test panels with these coatings applied have been prepared and forwarded to the Lightning and Transit Research Institute for electrical tests. Those coatings, which possess the required resistivity (less than  $10^8$  ohms per square), will be evaluated for permanence of properties. The goal of this program is to find an antistatic coating which will perform satisfactorily for at least one flight, particularly one involving flight through rain.

### Polycarbonate Protective Coatings

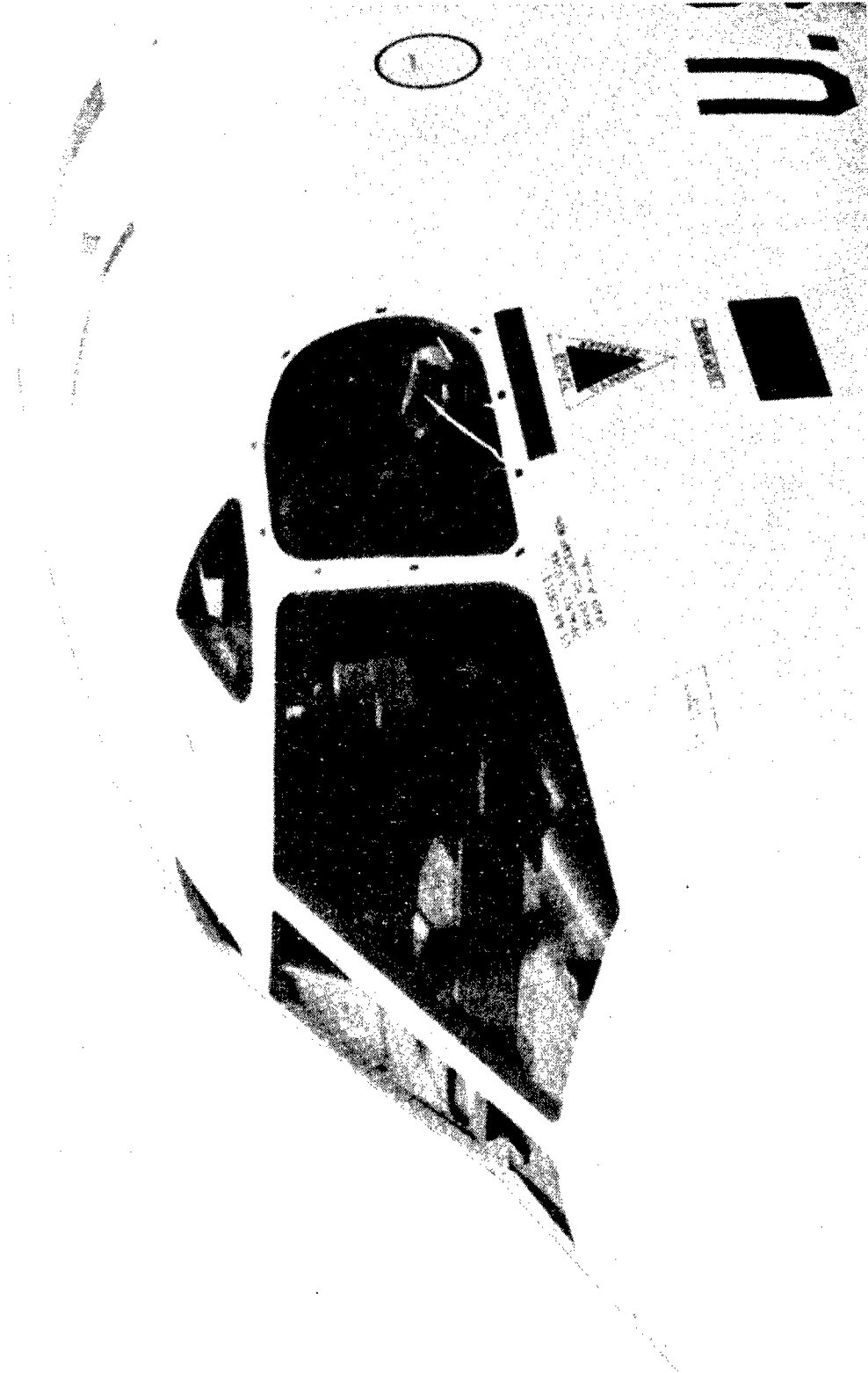
It has been demonstrated in this program and by other recent experience that exposed surfaces of polycarbonate aircraft glazings must be protected from hostile chemical environments, ultraviolet radiation, and abrasion. Accordingly, NR has specified protective coatings for all exposed surfaces of polycarbonate on the B-1 windshield and windows. Of particular concern, are the side and upper windows, where the exterior surfaces are polycarbonate. The protective coatings for polycarbonate glazings, available at this time, are proprietary materials formulation by subcontractors or the material supplier. Most of these are modifications of existing materials which have been used on acrylic with varying degrees of success. Since there is very little service history for these coatings, it was considered necessary to evaluate the specific coatings which will be used on the B-1.

Polycarbonate sheet coated with the protective coating which will be used on the side and upper windows has been procured from the subcontractor. Specimens will be exposed to various environments such as ultraviolet light, humidity, thermal cycling, and cyclic stress. After exposure, the specimens

will be evaluated for adhesion, optical properties, chemical resistance, and abrasion resistance. Unexposed specimens will be tested as control specimens. The investigation will include the effect of these environments on the coating after the coating has incurred damage such as cuts and scratches.



# B-1 CREW MODULE WINDSHIELD AND WINDOWS



NA-73-35

TSP73-00771A

DEVELOPMENT OF TRANSPARENT COMPOSITES  
AND THEIR THERMAL RESPONSES

J. A. Parker, G. M. Fohlen, and P. M. Sawko  
National Aeronautics and Space Administration  
Ames Research Center  
Moffett Field, California

## DEVELOPMENT OF TRANSPARENT COMPOSITES AND THEIR THERMAL RESPONSES

J. A. Parker, G. M. Fohlen and P. M. Sawko  
Ames Research Center, NASA, Moffett Field, Calif. 94035

### Abstract

This paper describes the development of two transparent, high-temperature-resistant polymers, and a composite derived therefrom which is potentially useful in meeting the thermal and impact requirements for transparent enclosures in military aircraft. The combination of polymer properties needed to obtain high-temperature mechanical strength, impact, fire, and high-energy thermal radiation resistance are defined in terms of the microstructural features of these two aromatic polymer systems.

Transparent panels, useful as windows for aircraft, which have heat distortion temperatures of 110°C and about six times the resistance to fuel-fire burn-through than conventional acrylate windows, can be obtained directly by casting 2,2-bis[p-(2,3 epoxypropoxy)phenyl]-propane, catalyzed by trimethoxyboroxine. This cross-linked transparent aromatic polymer system is thermochemically stable to 400°C, gives a thermogravimetric char yield of about 35%, and has a tensile strength of 92 MN/m<sup>2</sup> at 24°C. Replicas of conventional aircraft windows have been tested and results for fuel-fire tests are presented. Preliminary results show that epoxy-boroxine is more resistant to laser penetration than conventional acrylates.

The synthesis of thermally cross-linkable linear polycarbonates obtained from interfacial polymerization of phenolphthalein is described. These materials have glass transition temperatures of 280°C, a thermogravimetric char yield of about 54%, and about four times the fuel-fire burn-through resistance of the conventional acrylate window. Moldings of the neat polycarbonate have initial tensile strengths at room temperature of about 110 to 138 MN/m<sup>2</sup> and retain as much as 41.4 MN/m<sup>2</sup> at 200°C. As expected for this linear aromatic polycarbonate, the impact strength is about six times that of epoxy boroxine. To obtain the optimum thermal and impact properties for an aircraft enclosure, it is necessary to utilize these two polymers in the form of a laminate. This system may provide operational capability to 260°C, fuel-fire resistance, high-speed bird impact resistance, and be effective against high-energy thermal radiation.

### Introduction

The need for significant improvements in the thermal and mechanical properties of polymers intended for application as aircraft windows has been described by Arvay (ref. 1). These requirements are critical for advanced military aircraft, where cost, performance, and vulnerability are coupled (ref. 2). Within NASA's objectives, answers to these questions will provide the technological base for new transparent enclosures for advanced supersonic transports of the future operating in the speed range of Mach 3. Analysis (ref. 3) has shown that the cost and weight savings of

lightweight transparent plastic canopies must be supported by adequate thermal stability for intermittent service to 260°C. In addition, improvements may be made which will provide increased flight safety, crash-fire survivability, and reduced weapons vulnerability. Personnel losses from crash-fire episodes in military helicopters with large window areas have been considerable. Bird impacts on windows of high performance aircraft have taken their toll. The effects of high-energy coherent radiation sources on transparent enclosures may be an important consideration on vulnerability in the future. It now seems doubtful that any of the state-of-the-art transparent plastics or laminate combinations can provide the unique combination of optical, thermal, and mechanical properties needed to meet these diverse requirements.

It is the purpose of this paper to outline the polymer methodology by which it is possible to systematically modify the molecular microstructure of aromatic polymers to obtain the desired combination of thermal and mechanical properties. To demonstrate this approach, this paper describes in detail two structurally different high temperature resistant transparent polymers being developed at Ames Research Center (NASA). The first is an aromatic polycarbonate based on phenolphthalein. The second is a trimethoxyboroxine catalyzed epoxide. Both of these polymers are potentially useful either individually or in laminate combinations where high temperature performance is required. The paper first proposes a combination of desirable performance properties, and then redefines these requirements in terms of bulk polymer properties and compares them with the state-of-the-art transparent polymers in use today. Second, the paper offers a rationale for selecting aromatic polymers for development as candidate windows. The synthesis, processing, and characterization of molecular and thermal and physical properties of these two candidate polymers are described and compared with state-of-the-art materials. Finally, this paper reports the results obtained in evaluating both the polymers and laminates derived therefrom in several representative thermal environments.

### Discussion

Figure 1 outlines what is believed to be the desired performance characteristics for advanced aircraft canopies. First, for high-speed aircraft (Mach 3), it has been established that a canopy will encounter surface temperatures of about 260°C. The melt temperature ( $T_m$ ) and the decomposition temperature ( $T_d$ ) of any candidate polymer must therefore be greater than 260°C. High skin temperatures are experienced only for short intervals and influence only a limited thickness at the wall. With internal cooling, such canopy structures experience steep thermal gradients. The polymer need not retain all the same mechanical properties at 260°C that it has at 25°C, but the effect of temperature on strength should be reversible in that temperature range. The glass transition temperature ( $T_g$ ) may be used as a guide to estimate the retention of mechanical strength at elevated temperatures. For aircraft canopies, polymers that have glass transition temperatures above 260°C may be suitable for this aerodynamic heating environment. In general, the higher the glass transition temperature the greater the tensile strength one can expect at the service temperatures. Only the bisphenol-A polycarbonate type among state-of-the-art polymers is known to approach the impact resistance required to withstand a 308-m/sec bird strike. With the structure-property relationship of bisphenol-A polycarbonate as a model, a high molecular weight, linear aromatic polycarbonate must be obtained and microstructural modifications of the polycarbonate must be restricted to the pivotal carbon atom to obtain this impact resistance. With this concept as a guide, the polycarbonates described in this study were prepared.

None of the state-of-the-art transparent polymers are noted for their resistance to the heat penetration of burning jet fuel or thermal radiation penetration. Fish and Parker (ref. 4) have shown that the resistance of a polymer to the intrusion of thermal radiation, as in the case of a JP-4 fuel fire, is critically controlled by the number of multiply bonded aromatic rings present in the initial polymer or in its primary pyrolysis residues. It has been shown that 800°C anaerobic char yield values of about 40% are necessary with aromatic polymers to optimize their thermal protection effectiveness in a JP-4 fuel-fire environment. Parker and Winkler (ref. 5) have shown that this thermogravimetric property is directly related to the cross-link density of the aromatic polymers. It is known that the more highly cross-linked an aromatic polymer system becomes, the more rapidly it loses its toughness and may not meet the impact strength requirements even though it has considerable tensile strength at elevated temperatures. Also, the need for a cross-linked aromatic polymer to effect the desired thermal protection is not compatible with the thermal cycling requirements shown in Figure 1. Highly cross-linked aromatic polymers might be expected to be brittle near -50°C. The desired combination of properties, however, is possible in linear aromatic, transparent polymers that have been designed with functional groups available to provide cross-linking sites by thermochemical reaction at the decomposition temperatures.

Estimates have been made for minimum values of key bulk polymer properties required to secure the proposed combination of performance characteristics discussed above. These values (Figure 2) are compared with those properties available from the two state-of-the-art transparent polymers, polymethylmethacrylate and bisphenol-A polycarbonate. Also included in Figure 2 are some available data for a new polymer, polyarylsulfone, currently being developed by the USAF/AFML.

Even though the yield stress of polymethylmethacrylate and bisphenol-A polycarbonate is adequate for normal subsonic aircraft canopies, these values become zero at operating temperatures near 260°C. The polycarbonate, with a glass temperature of 150°C, is better than the polymethylmethacrylate, but it is unsatisfactory as a canopy material for aircraft operating at speeds up to Mach 3. On the other hand, the values reported for polyarylsulfone (ref. 6), with a glass temperature of 288°C, exceed this tensile yield stress requirement by a factor of 4. For this reason, polyarylsulfones as a class are potential candidates for advanced aircraft canopy applications. The transparency processing costs and weatherability of the polyarylsulfone shown in the figure may present difficulties for future development. The anaerobic char yield of this developmental sulfone is estimated to be between 30 and 40% and should exhibit good resistance to fire and radiation since this polymer is self-extinguishing and gives a limiting oxygen index of 35%. Laboratory-measured notched Izod impact strengths of polyarylsulfone and polycarbonate are comparable. This suggests that the polyarylsulfone may be sufficiently resistant to defeat a 308-m/sec impact. Polyarylsulfone has a tensile strength of 91.7 MN/m<sup>2</sup> at 25°C even though the value drops to about 28 MN/m<sup>2</sup> at 260°C without significant polymer degradation. If the values for polyarylsulfone are considered as a model for designing a linear aromatic polycarbonate, a candidate polymer must possess, in addition to the aforementioned thermochemical properties, a glass temperature ( $T_g$ ) of at least 250°C, a melt temperature ( $T_m$ ) of 260°C, and a decomposition temperature ( $T_d$ ) greater than 260°C. A temperature difference between  $T_m$  and  $T_d$  greater than about 100°C may be required to make processing practical. The two state-of-the-art polymers considered in Figure 2 are unsuitable for advanced window materials for the objectives defined in Figure 1. It is also clear from these comparisons that the properties and structures of linear aromatic polymers should be examined as a class to meet future requirements. Two classes of essentially linear aromatic polycarbonates and an aromatic polyether have been screened by means

of the thermochemical criteria described in Reference 5. The structure of the polymer was modified to optimize the properties of these aromatic polymers to obtain the desired bulk properties given in Figure 2.

Figure 3 shows the effect of aromatic structure on the thermochemical char yield of transparent polymers as well as some other aromatic polymers. Here, the char yield at 700°C versus the number of moles of multiply bonded aromatic rings per gram of polymer is plotted. The linearity established earlier (ref. 5) includes the epoxy-novolac, polyphenylene, and the phenolic-novolac types of polymer. These polymers are not useful for window applications because of their lack of transparency or deficiencies in mechanical properties. Two polymers reported here, epoxy-boroxine (ref. 7) and phenolphthalein polycarbonate (ref. 8), are plotted with the bisphenol-A polycarbonate for reference. The optimum fire resistance or thermal protection char yield for aromatic polymer systems as indicated by the studies of Fish and Parker (ref. 5) is shown to be about 40%. Epoxy boroxine approaches this value whereas phenolphthalein polycarbonate exceeds this char yield by about 15%. In general, the decomposition temperature, the glass transition temperature, and the melt temperature of these polymers tend to follow a similar curve as the concentration of aromatic rings increases. This relationship can provide a convenient means of characterizing polymers in terms of microstructure for selection as transparent composite components.

Bisphenols provide a means of increasing the concentration of bonded aromatic ring structures without perturbing the essential linearity of the aromatic polycarbonate. Initially, three bisphenol monomers were selected for polymerization (Figure 4) in which the central carbon atom was substituted with first one, then two phenyl rings to give the triphenyl and tetraphenyl monomers, respectively. To provide both an aromatic substitution and a thermochemical cross-linking site, phenolphthalein was chosen as another monomer. This choice was based on the observations of Butterworth and Parker (ref. 9) that it is possible to cross-link aliphatic ester side chains by ester-interchange reactions with aromatic polycarbonates.

The polymers were prepared by an interfacial reaction of an alkaline solution of these bisphenols with phosgene in the presence of a low concentration of a tertiary amine catalyst (Figure 5). Methylene chloride, present in the mixture as an immiscible organic phase, dissolved the polymer as it formed. The polymers were isolated by washing this organic phase and precipitating the polymer with methanol and/or acetone and dried. Polymers with average molecular weights from 40,000 to 100,000 were obtained. These powders were used for thermomechanical and thermogravimetric analysis. Complete details of these polymerization and isolation methods are given in Reference 8.

The effect of variations in the aromatic content on the thermal behavior of polycarbonates is shown in Figure 6. The glass transition temperature ( $T_g$ ), the melt temperature ( $T_m$ ), the decomposition temperature ( $T_d$ ), and the anaerobic char yield ( $Y_c$ ) at 800°C are presented. The values for all these properties tend to increase with an increase in aromatic substitution. The very high glass transition temperature of 278°C for phenolphthalein polycarbonate was an unexpected result. One would anticipate the asymmetry of this molecule to give even a lower glass transition temperature than the triphenyl derivative. The fact that the polymer does not melt or flow but softens seems to indicate that the polymer, before decomposition, undergoes some branching due to ester interchange with the lactone ring of phenolphthalein. The char yield of 54% for phenolphthalein polycarbonate can only be accounted for by assuming that the phenolphthalein reacts to

form the required degree of multiple bondedness, giving the necessary behavior for thermal protection. This cross-linking process is probably responsible for the high decomposition temperature of the phenolphthalein polymer. For these reasons, the phenolphthalein polycarbonate was selected for further development.

Characterization of the polymers included the determination of the glass transition temperature, the polymer melt temperature, a thermogravimetric analysis, infrared analysis, inherent viscosity, and solubility. A mass spectroscopic investigation of the volatile products from heating the phenolphthalein polycarbonate polymer in a high vacuum showed the main constituents to be water and carbon dioxide, with phenol, benzoic acid, carbon monoxide, and carbonate ion appearing in minor concentrations. An X-ray examination of this polymer failed to show any crystallinity. Examination of films under polarized light verified the amorphous character of this polymer. Figure 7 shows solubility characteristics of the polymer in a variety of solvents. The molecular weight was determined by gel permeation chromatography and correlated with the inherent viscosity. Studies of the thermal and mechanical properties of transparent moldings of this polymer for different molecular weights show that the maximum fire resistance and impact resistance are not obtained until a molecular weight of about 100,000 is attained for the phenolphthalein polymer.

The thermogravimetric analyses of all the polycyclic aromatic polycarbonates synthesized in this study are shown in Figure 8. The weight remaining is plotted as a function of temperature at a programmed heating rate of  $3^{\circ}\text{C}/\text{min}$  in a nitrogen atmosphere. The thermogravimetric char yield was determined by measuring the stabilized char residue at temperatures between  $600^{\circ}$  to  $800^{\circ}\text{C}$ . The phenolphthalein polymer has the highest decomposition temperature, the slowest average rate of decomposition, and a char yield that exceeds by almost a factor of 3 that of the bisphenol-A polycarbonate. The addition of a second phenyl group in the case of the tetraphenyl polymer has no effect on the char yield over the triphenyl polymer. This gives further credence to the fact that the high char yield of the phenolphthalein is due to the cross-linking arising from the ester interchange of the lactone ring.

In processing phenolphthalein polycarbonate, the relative closeness of the decomposition and melt temperatures required the application of a fugitive plasticizer for ease in processing. The processing method is outlined in Figure 9. The polymer, as isolated from the interfacial polymerization reaction, is first swollen by the addition of acetone. The acetone reduces the glass transition temperature. When the volatile content is about 40% by weight, it is molded at  $230^{\circ}\text{C}$  and  $7\text{ MN}/\text{m}^2$ . To achieve optimum properties, another solvent such as methylene chloride was added and the sample remolded at  $200^{\circ}\text{C}$  and  $7\text{ MN}/\text{m}^2$ . The transparent panels are then vacuum dried at  $150^{\circ}\text{C}$  until the volatile content is as low as 2% by weight at  $300^{\circ}\text{C}$  as shown by thermogravimetric analysis. Samples prepared in this manner show no tendency to undergo solvent crazing. The thermal properties of this system are little affected by this trace amount of entrapped solvent. Currently, studies are under way to form windows from this polymer using a high-speed impact press, and some success has been demonstrated in preparing specimens about 3.2 to 6.6 mm thick by this method.

The effects of temperature on the tensile strength of phenolphthalein and bisphenol-A polycarbonates are compared in Figure 10. Not only does phenolphthalein polycarbonate have a higher initial tensile strength than bisphenol-A polycarbonate by about  $21\text{ MN}/\text{m}^2$ , but the bisphenol-A material also has lost any mechanical strength at about  $150^{\circ}\text{C}$ . The phenolphthalein polycarbonate

retains almost  $28 \text{ MN/m}^2$  at  $250^\circ\text{C}$ , making it a useful candidate for the aerodynamic environment encountered during Mach 3 performance.

The bulk properties of these two polymers are compared further in Figure 11. The specific gravity of the phenolphthalein polycarbonate is slightly higher than that of the bisphenol-A polycarbonate. This would be expected from the higher degree of packing associated with the phenolphthalein polycarbonate, and suggests that the processed phenolphthalein polycarbonate sheet has some branching and/or cross-linking present. The Rockwell Hardness values of the two polymers are essentially equivalent. The Taber abrasion measurements of both polymers are comparable. The impact strength by means of the notched Izod was difficult to reproduce and served only as a guide to the relative impact strength of these materials. A control, bisphenol-A polycarbonate, gave values of  $69 \text{ N}\cdot\text{m/m}$  of notch. Impact measurements on phenolphthalein polycarbonate seemed sensitive to the molecular weight of the polymer specimen. One, at an average molecular weight of about 45,000, and another at about 100,000 were measured and the impact values for both of these are comparable to bisphenol-A polycarbonate. These values indicate that phenolphthalein polycarbonate can reduce the danger of high-speed bird impact observed with the state-of-the-art bisphenol-A polycarbonate.

The value for the refractive index of phenolphthalein polycarbonate is somewhat higher than that of bisphenol-A polycarbonate because of the contribution of the aromatic lactone ring. The tensile strength data for the two polymers as a function of temperature are also given in Figure 11. The retention of strength amounting to as much as  $57 \text{ MN/m}^2$  at  $175^\circ\text{C}$  of phenolphthalein polycarbonate contrasts markedly with the loss in strength of bisphenol-A polycarbonate. This retention of tensile strength at high temperatures coupled with the impact strength and the high-temperature thermochemical properties makes phenolphthalein polycarbonate an outstanding choice over state-of-the-art bisphenol-A polycarbonate. The values obtained for both phenolphthalein polycarbonate and bisphenol-A polycarbonate for abrasion resistance by means of the Taber abrader are comparable. Windows and canopies prepared from bisphenol-A polycarbonate become hazy after 500 to 1000 hours of flight time. On the basis of Taber abrasion values, phenolphthalein polycarbonate is expected to behave in a similar manner. The problem with the state-of-the-art bisphenol-A polycarbonate has been overcome by coating a thin layer of abrasion-resistant polymer as an outer layer. A similar technique could be used with laminates using phenolphthalein polycarbonate.

In addition to the above polycarbonate, the properties of an aromatic ether derived from the polymerization of a distilled version of diglycidyl ether of bisphenol-A catalyzed with trimethoxyboroxine (TMB) were examined (Figure 12). Polymerization with the TMB catalyst cures to a water-white cast plastic in contrast to the yellow materials obtained with amine catalysts. It is proposed that the polymerization of bisphenol-A diglycidyl ether by TMB proceeds by a Lewis acid type mechanism (ref. 7) through the glycidyl ether groups to give an aromatic polyether. During pyrolysis of this polymer, water is evolved, accompanied by intumescence and charring. This suggests that the polymer has a high concentration of secondary hydroxyl groups distributed along the chain. Further work must be done to characterize the molecular structure of the resulting polymer.

The catalyst, trimethoxyboroxine, used for this polymerization, together with its properties are shown in Figure 13.



The polymerization process and method of casting and forming of the EX-112 windows are given in Figure 14. A study has been made of the mechanical properties of the system as a function of the catalyst concentration and the optimum catalyst range is between 5 and 6.5 parts per hundred of the diglycidyl ether (ref. 7). After the diglycidyl ether and the catalyst are mixed and degassed, it can be poured into prewarmed metal molds, and cured between 80° and 180°C for 8-1/2 hours. Elemental analysis of the resultant polymer, however, shows very little of the TMB remaining after the cure is completed. Curved sheets can be obtained by warming the casting above its heat distortion temperature at 150°C. Replicas of aircraft windows were prepared by this method at a moderate cost.

Since applications of the EX-112 system are intended to replace the polymethylmethacrylate, comparisons of the thermochemical and thermophysical properties of these two materials have been made. In Figure 15, the thermogravimetric analysis made at 3°C/min in a nitrogen atmosphere is shown. The weight remaining is plotted as a function of temperature. The EX-112 begins to decompose at 420°C as compared to 265°C for the oriented polymethylmethacrylate sample. The polymethylmethacrylate decomposes by molecular unzipping (depolymerization) to give primarily the methacrylate monomer and has essentially zero char yield at 600°C. By contrast, the EX-112 leaves a residue of 32% at 600°C. This is expected for a multiply bonded aromatic system and approaches the required pyrolysis behavior for optimal fire resistance.

The physical and mechanical properties of these two polymer systems are compared in Figure 16. There is little difference in the specific gravities and the refractive indices of the two polymers. The ultimate tensile strength of EX-112 is 27.4 MN/m<sup>2</sup> higher at 25°C, and both polymers have substantially the same elongation. This stress-strain behavior of the EX-112 indicates that the EX-112 is a cured aromatic polyether with considerable linearity. Whereas the polymethylmethacrylate has lost its tensile strength at 120°C, the EX-112 has been reduced by about 1/2 to 34.5 MN/m<sup>2</sup> and would meet the requirements for Mach 3 application better than the polymethylmethacrylate. Similar behavior is seen in the measured flexural strength. The abrasion resistance of these two polymer castings is seen in the Taber values. The EX-112 is better than the polymethylmethacrylate by a factor of 2, but is poorer than the polycarbonates by a factor of 3. It is expected that a surface treatment would be required to improve the abrasion resistance of EX-112 to aerodynamic erosion. As expected for a cross-linked aromatic polymer system, the EX-112 exhibits a slight decrease in the measured Izod notched impact strength as compared to polymethylmethacrylate. However, such polymers alone do not have the impact resistance necessary to reduce the effect of high-speed bird collision. For this reason, it was necessary to examine composites derived from EX-112 and phenolphthalein polycarbonate interfacially bonded by an ethylene-propylene-vinylacetate terpolymer to provide the additional impact resistance.

Some of the key thermal properties of these candidate materials are compared with state-of-the-art polymethylmethacrylate and bisphenol-A polycarbonate in Figure 17. The ASTM D648 Heat Distortion Temperature (HDT) of phenolphthalein polycarbonate is 135°C higher than its nearest competitor, bisphenol-A polycarbonate, whereas polymethylmethacrylate and EX-112 exhibit HDT values of 106° and 112°C, respectively. For sustained performance in the 250°C range, a supporting backup sheet of phenolphthalein polycarbonate probably will provide greater reliability than bisphenol-A polycarbonate. Since even EX-112 would require this kind of high-temperature support, EX-112 probably can never be used alone in the high-speed environment.

With low limiting oxygen values, 18 and 21%, for polymethylmethacrylate and EX-112, respectively, these materials must be considered flammable in air and to have significant burning rates and flame spreads. Both bisphenol-A and phenolphthalein polycarbonate require higher oxygen concentrations than is available in the air to sustain combustion, namely, 23 and 47%, because the primary decomposition product for these polymers is carbon dioxide from the decarbonylation of the linear chains and correlates with the anerobic char yield. In addition to producing  $\text{CO}_2$ , phenolphthalein polycarbonate, because of its higher char yield, has a lower rate of production of flammable hydrocarbon species. The value of 47% oxygen required to support combustion makes it an extremely useful polymer for applications other than window materials, where high fire resistance, good ductility, and high-temperature performance are critical. This thermochemical behavior is reflected also in the burning rates that parallel the limiting oxygen values — polymethylmethacrylate having the highest value, EX-112 about half. Although bisphenol-A polycarbonate is self-extinguishing, it tends to melt and drip and the high surface area of the molten droplets tends to enhance the burning rate. This is particularly significant for aircraft canopies since the melting and formation of burning droplets can easily ignite the aircraft interior. On the other hand, the phenolphthalein polycarbonate shows no tendency to melt or burn.

Comparable values of the thermal conductivity and linear coefficient of expansion for two state-of-the-art materials are given. A somewhat higher value obtained for EX-112 would tend to reduce the effect of thermal shock. Little can be done in terms of the microstructural changes of the polymers to affect changes in the coefficients of thermal expansions, but laminates made from these polymers should not cause any difficulty because of differences in expansion. Clearly, the properties of the candidate EX-112 and phenolphthalein polycarbonate polymers offer substantial advantages over state-of-the-art materials.

Radiation is the principal mode of heat transfer to the surface of an object immersed in a large jet fuel-fire environment. It was of interest to compare these candidate polymers with state-of-the-art materials to determine their response in a pure thermal radiation environment. In Figure 18, the results of exposing polymethylmethacrylate, EX-112, and phenolphthalein polycarbonate to the radiation effects of a 260-W  $\text{CO}_2$  laser at  $10.6\mu$  are presented. About 50 mmX50 mm specimens were exposed to the 8-mm-diam laser beam for exposure times up to 1 minute. The polymethylmethacrylate and EX-112 samples exposed were about 13.2 mm thick whereas the phenolphthalein polycarbonate was available only in 3.2 mm thick pieces. Tests were run both in still air and at Mach 1 air velocity. It was found that polymethylmethacrylate burned through, leaving a clear hole with no char formation in about 6.5 seconds in still air, whereas in a Mach 1 airflow it burned through in only 2.9 seconds. For EX-112, at an exposure time of 60 seconds, there was a penetration of approximately 3.2 mm in the still air and 6.5 mm in the Mach 1 airflow; a hard, tough, black, nodular char formed in the area of impact. Phenolphthalein polycarbonate was evaluated only in still air in a thickness only about 1/4 of the reference pieces and was not burned through after about 29 seconds. It had about five times the resistance to laser penetration as the acrylate, but, as expected from the thermal protection correlation, it was not as good as the EX-112. It formed a fragile char with a penetration of about 1 mm backed by the formation of an ivory-like white zone within the structure itself. None of the samples showed any tendency to crack or undergo thermal shock. The white opacity, which serves to block partially the radiation in the case of phenolphthalein polycarbonate, is due to the decarbonylation and trapping of  $\text{CO}_2$  within the polymer sample. These show that the epoxy and polycarbonate are superior to the polymethylmethacrylate in preventing radiation penetration of a  $\text{CO}_2$  laser. It suggests that the same char-forming and ablation mechanisms that are useful in rejecting the

heating environment of a large jet fuel fire and of reentry into the earth's atmosphere are also applicable in rejecting the energy deposited by a  $\text{CO}_2$  laser.

A well-known technique in armoring technology is to provide a ductile, backup sheet for a hard, frangible, surface sheet to serve as a spall catcher. To take advantage of the high impact strengths available with phenolphthalein polycarbonate and bisphenol-A polycarbonate, structural laminates with the EX-112 material were made using an ethylene-propylene-vinyl acetate terpolymer adhesive provided by the USAF Materials Laboratory (ref. 10). Transparent laminates, free of defects, can be prepared by the procedure given. This adhesive interlayer is available in several thicknesses and in both low-temperature and high-temperature versions. A 0.8-mm layer of the low temperature type was supplied by the AFML for this investigation. These laminates were used to evaluate the effects of the JP-4 fuel fire and the falling weight of the Gardner Impact Tester. A laboratory simulation of a jet fuel fire was evaluated by the Ames-T-3 Thermal Test (ref. 4). The results obtained by exposing state-of-the-art polymers, stretched polymethylmethacrylate, and bisphenol-A polycarbonate, as well as phenolphthalein polycarbonate and EX-112, epoxy-boroxine experimental systems are shown in Figure 19. These exposures were carried out at two thicknesses and the time required to burn through was observed. The heating rate to the surface measured by a calorimeter during these tests was  $11.3 \times 10^4 \text{ W/m}^2$ . Burn-through was obtained for stretched polymethylmethacrylate on the 6.6-mm specimen in about 60 seconds and on the 13.2 mm specimen in about 100 seconds; it seems to be a linear function of thickness with a rate of 1.3 mm/sec. The epoxy-boroxine polymer in these laboratory specimens lasted 10 times longer than the stretched polymethylmethacrylate. It was near the end of the burn-through tests before any cracks or fissures appeared in the epoxy-boroxine polymer. The phenolphthalein polycarbonate is about five times more resistant to burn-through than the stretched acrylate and about three times more resistant than bisphenol-A polycarbonate. These results of the T-3 thermal tests closely parallel the observations of the thermal behavior of these polymers from thermogravimetric analysis.

The laminates were evaluated with both polycarbonate and epoxy-boroxine (EX-112) layers facing the fire source in successive tests. In every case, these equivalent laminates have improved the resistance to burn-through over that of either of the state-of-the-art materials. It is advantageous to have the intumescent EX-112 layer exposed to the fire environment. The laminate made with bisphenol-A polycarbonate had nearly twice the resistance to burn-through when the EX-112 side was exposed to the fire than when reversed. This difference disappears for the phenolphthalein polycarbonate laminate. The principal failure mode of these prototype materials during these fire tests has been the delamination and burning of the hydrocarbon adhesive inner layer. Improvements might be possible with another type of high-temperature adhesive. It is doubtful that the burn-through rate is adversely affected. Phenolphthalein polycarbonate serves as a ductile, impact resistant, and high-temperature supporting layer for the fire- and radiation-resistant layer of EX-112. The effect of qualitatively examining the radiation environment on the stretched polymethylmethacrylate at the point of burn-through is of interest. With this material, thermal failure is always manifested by the formation of deep fissuring that accompanies the anisotropic depolymerization of the polymer, resulting in cracks when burn-through occurs. The highly oriented regions of polymer melt at a slower rate than the more amorphous parts.

The formation of a tough, insulative, intumescent layer occurs on the surface of the EX-112 exposed to the fire, with the virgin polymer beneath maintaining its mechanical integrity. The sensitivity of the tensile modulus of the bisphenol-A polycarbonate and its failure to form a dense,

high yield of a carbonaceous residue are the reasons for failure. Sagging and melting of the bisphenol-A polycarbonate occur long before complete burn-through is achieved with the formation of a weak, fluffy char at the surface. This is consistent with the behavior expected based on the thermochemical char yield.

Full-scale 737 windows of EX-112 were prepared by the method described earlier. These windows were evaluated using a stretched polymethylmethacrylate 737 window as a control. An oil burner that provided a heat flux of  $11.3 \times 10^4 \text{ W/m}^2$  was used to simulate a JP-4 fuel fire. The acrylate window exposed to this environment exhibited the typical melting and reticulation with combustion; burn-through occurred in about 1 minute. The EX-112 prototype exposed to the same environment formed a hard, tough, surface char, which maintained internal protection for this window for about 6 minutes or about six times that of the standard window. Burn-through occurred from thermomechanical failure due to a small amount of stress. Laminates with improved impact resistance are contemplated for this test facility. Neel, Parker, and Fish (ref. 11) found that it is possible to apply foams and coatings to a fuselage to provide as much as 12 minutes of protection before burn-through. The need to improve the windows is a necessary complement to the crash-fire worthiness of aircraft protected by these advanced composites and coatings.

To compare the impact resistance of these new candidate polymers and their laminates with the state-of-the-art materials, the simple Gardner falling weight method was used. In this test, a 908-gm weight with a 13.2-mm ball on the end is dropped a distance of 35.6 cm. As shown in Figure 20, at 6.6 mm and 13.2 mm thicknesses, the stretched acrylic and the bisphenol-A polycarbonate are well able to resist repeated impacts of  $3.18 \text{ N}\cdot\text{m}$ . The epoxy-boroxine (EX-112), 6.6 mm thick, is less effective and breaks at  $1.82 \text{ N}\cdot\text{m}$ . Thirteen-millimeter sections of EX-112 were able to withstand repeated impact at  $3.18 \text{ N}\cdot\text{m}$ . This is a surprising result for a cross-linked aromatic resin system of the ether type.

The sensitivity of the impact strengths of phenolphthalein polycarbonate to molecular weight is also shown in Figure 20. Two thicknesses at two molecular weights were examined by means of the falling weight impact test. A polymer with an average molecular weight of about 45,000, indicated by an intrinsic viscosity of 0.42, broke at  $0.91 \text{ N}\cdot\text{m}$  of impact, while the polymer having a molecular weight of about 100,000 with an intrinsic viscosity of 0.98 resisted repeated impacts at  $3.18 \text{ N}\cdot\text{m}$ . A 13.2 mm laminate comprised of two 6.6 mm sections of EX-112 and bisphenol-A polycarbonate bonded with the ethylene terpolymer adhesive withstood repeated impacts of  $3.28 \text{ N}\cdot\text{m}$ . The EX-112 face of the laminate cracked after the fifth impact but remained intact. Similar results were obtained from the EX-112/phenolphthalein polycarbonate laminate even though the thickness of the phenolphthalein polycarbonate underlayer was about 1/2 the thickness of the bisphenol-A polycarbonate. The results show that the use of the adhesive inner layer with the polycarbonate backup sheet can provide improved impact strength in the laminated structure, taking advantage of the thermal resistance of EX-112. These impact results are preliminary and can be considered as a guide in selecting combinations of materials for further development. Further work to optimize the thicknesses of the individual components and selection of the adhesive inner layer for these laminates are required. Finally, more severe impacting conditions on larger specimens will be studied to optimize a laminate.

## Conclusions

It is possible to use thermogravimetric analysis as a means of classifying transparent polymeric materials for use as canopy materials, providing resistance to fuel fire burn-through, laser resistance, and exposure to high-temperature operating environments. This rationale has been applied to the design of two new transparent polymers. A high-temperature-resistant epoxy system with reasonable impact properties, and a phenolphthalein polycarbonate having a high glass transition temperature and impact resistance were evolved from this investigation. The results of this study, involving both thermal and mechanical properties of the individual polymer and prototype laminates, suggest that the best compromise of properties can be obtained from a laminate of the epoxy-boroxine polymer sheet with the high-temperature-resistant phenolphthalein polycarbonate. More work is needed to characterize the structure and mechanical properties of these transparent composites. Additional efforts must be expended to develop other processing techniques for phenolphthalein polycarbonate to make it more available for general canopy prototype development.

## References

1. E. A. Arvay, A Status Report — New Transparent Plastic Materials. Conference on Transparent Aircraft Enclosures, AFML/AFFD, Feb. 5, 1973.
2. Detailed Master Plan for 1973-5, Vol. II, Section 5.3.2.1, Dept. of Defense, Joint Technical Coordinating Group for Aircraft Survivability (JTCGAS).
3. Goodyear: Engineering Report, Evaluation of High Temperature Cast In Place Transparent Plastic Laminates Suitable for Canopies on Supersonic Fighter Aircraft, BNW, 59-61FSC, May 1962.
4. R. H. Fish and J. A. Parker, Relationship of Molecular Structure and Thermochemical Char Yield on Thermal Properties of Foamed Polymers, SAMPE, Los Angeles, Calif., April 1972.
5. J. A. Parker and E. L. Winkler, The Effects of Molecular Structures, NASA TR R-276, Nov. 1967.
6. College of Engineering Research Division and Technical Extension Service, Washington State Univ., New Polymeric Materials, Structure, Property, Applications, Aug. 19-21, 31, 1970.
7. Midwest Research Institute, Development and Evaluation of High Temperature Resistant Composite Plastic Plate, NBW, Feb. 1961.
8. C. E. Pannell, Synthesis of Optically Clear Polymeric Materials for High Temperature Windows, NAS2-6388, April 1972.
9. R. Butterworth and J. A. Parker, U. S. Patent 3,132,118, issued May 5, 1964.
10. G. L. Ball, I. O. Salyer, C. J. Nath and P. H. Wilken, Engineering Data on Ethylene Terpolymer as an Adhesive for Polycarbonate, AFML-TR-72-109, July 1972.
11. C. B. Neel, J. A. Parker and R. H. Fish, Heat Shields for Aircraft: A New Concept to Save Lives in Crash Fires. Astronautics and Aeronautics, Nov. 1971.

(a) RETENTION OF FUNCTIONAL PROPERTIES (MECHANICAL  
STRENGTH AND TRANSPARENCY) WITH INTERMITTENT  
SERVICE FROM  $\sim -50^{\circ}\text{C}$  TO  $+260^{\circ}\text{C}$

(b) CRASHWORTHY TO 308 METER PER SECOND\* IMPACT

(c) RESISTANT TO THE HEAT PENETRATION OF BURNING JET FUEL

(d) PROVIDES THERMAL PROTECTION FROM HIGH ENERGY  
COHERENT RADIATION

\* 600 knots

Figure 1. Desired combinations of properties for advanced transparent enclosures.

| PROPERTY   | POLYMER    |                           |                   |                        |
|--|------------|---------------------------|-------------------|------------------------|
|  | PMMA       | BISA-PC                   | POLYARYLSULFONE   | DESIREABLE REQUIREMENT |
| TENSILE STR., MN/m <sup>2</sup> (YIELD) 23°C           | 69         | 63                        | 89                | 62                     |
| 260° OR OTHER TEMPERATURE                              | 0 AT 120°C | 13.8 AT 150°<br>0 AT 175° | 28.3              | ~6.9 AT 260°           |
| T <sub>g</sub> , °C                                    | 103        | 150                       | 288               | 250                    |
| T <sub>m</sub> , °C                                    | 160-200°   | 263                       | —                 | 260                    |
| T <sub>d</sub> , °C                                    | 265        | 460                       | —                 | 260+                   |
| CHAR YIELD, N <sub>2</sub> , 700°C, %                  | 0          | 20                        | —                 | ~40                    |
| IMPACT STR. IZOD, 12.7 mm BAR                          | 16-21      | 70                        | 160               | —                      |
| N·m/m OF NOTCH   |            |                           |                   |                        |
| FLAMMABILITY, BURNING RATE, mm/min.                    | 25.4 SLOW  | DRIPS, S.E.               | S.E.              | S.E.                   |
| LIMITING OXYGEN INDEX, % O <sub>2</sub>                | 17.3       | 27                        | 35                | 725                    |
| BRITTLINESS TEMPERATURE, °C                            |            | -136                      | —                 | -100                   |
| CONTINUOUS USE TEMPERATURE, °C                         | 94°        | 130                       | 260               | ~260                   |
| HEAT DISTORTION TEMP., 1750 kN/m <sup>2</sup> LOAD, °C | 105°       | 132                       | 275               | ~260                   |
| HARDNESS, ROCKWELL                                     | M80-M100   | M73-78                    | M110              | M110                   |
| LINEAR COEFFICIENT OF EXPANSION                        |            |                           |                   |                        |
| m/m/°C×10 <sup>5</sup>                                 | 5.0-6.7    | 5.2                       | 4.7               | —                      |
| REFRACTIVE INDEX, n <sub>D</sub> <sup>20</sup>         | 1.50       | 1.58                      | —                 | —                      |
| TRANSMITTANCE, % VIS.                                  | 92         | 90                        | LIGHT AMBER COLOR | 90                     |

Figure 2. Comparison of some key properties of state of the art transparent polymers.

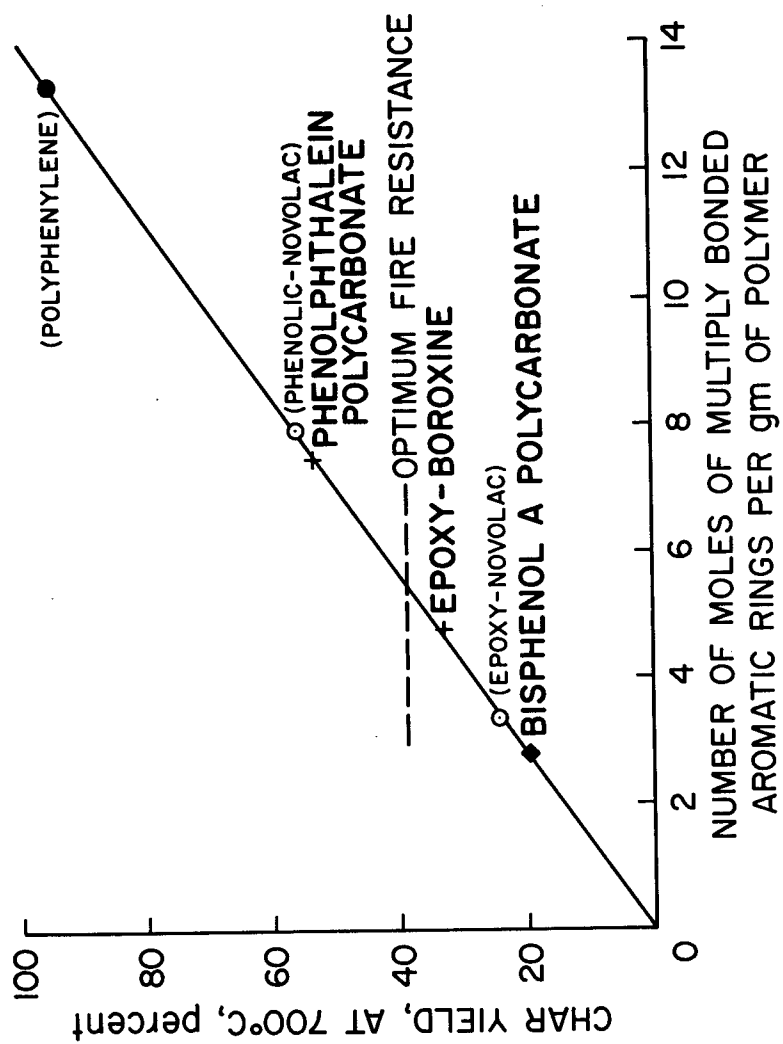


Figure 3. Effect of aromatic structure on thermochemical char yield of transparent polymers.



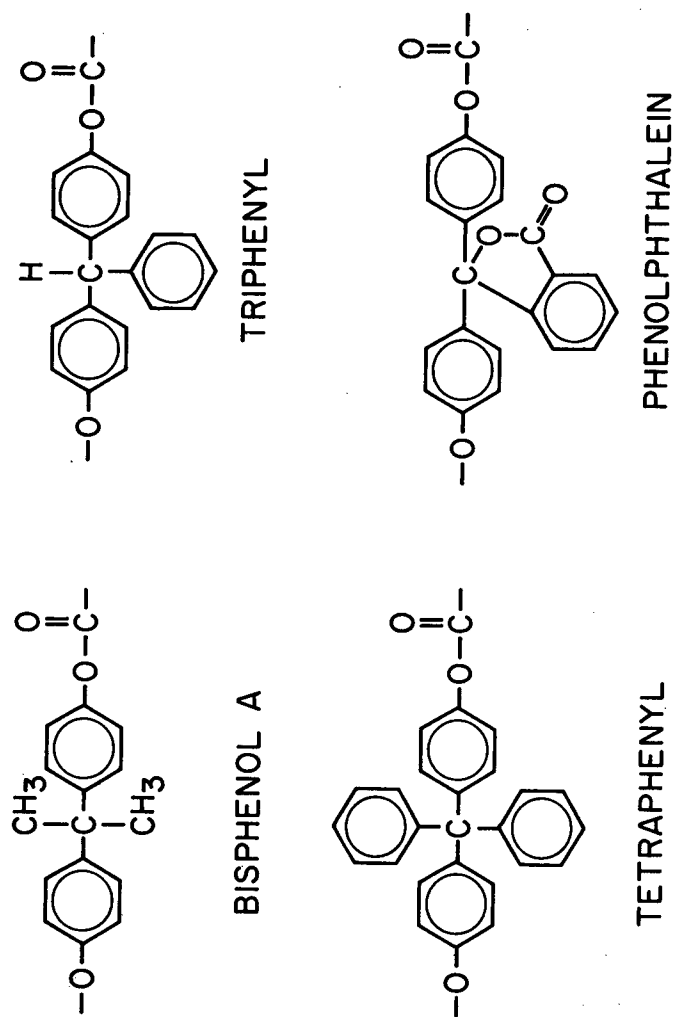


Figure 4. A comparison of the microstructural features of various aromatic polycarbonates.

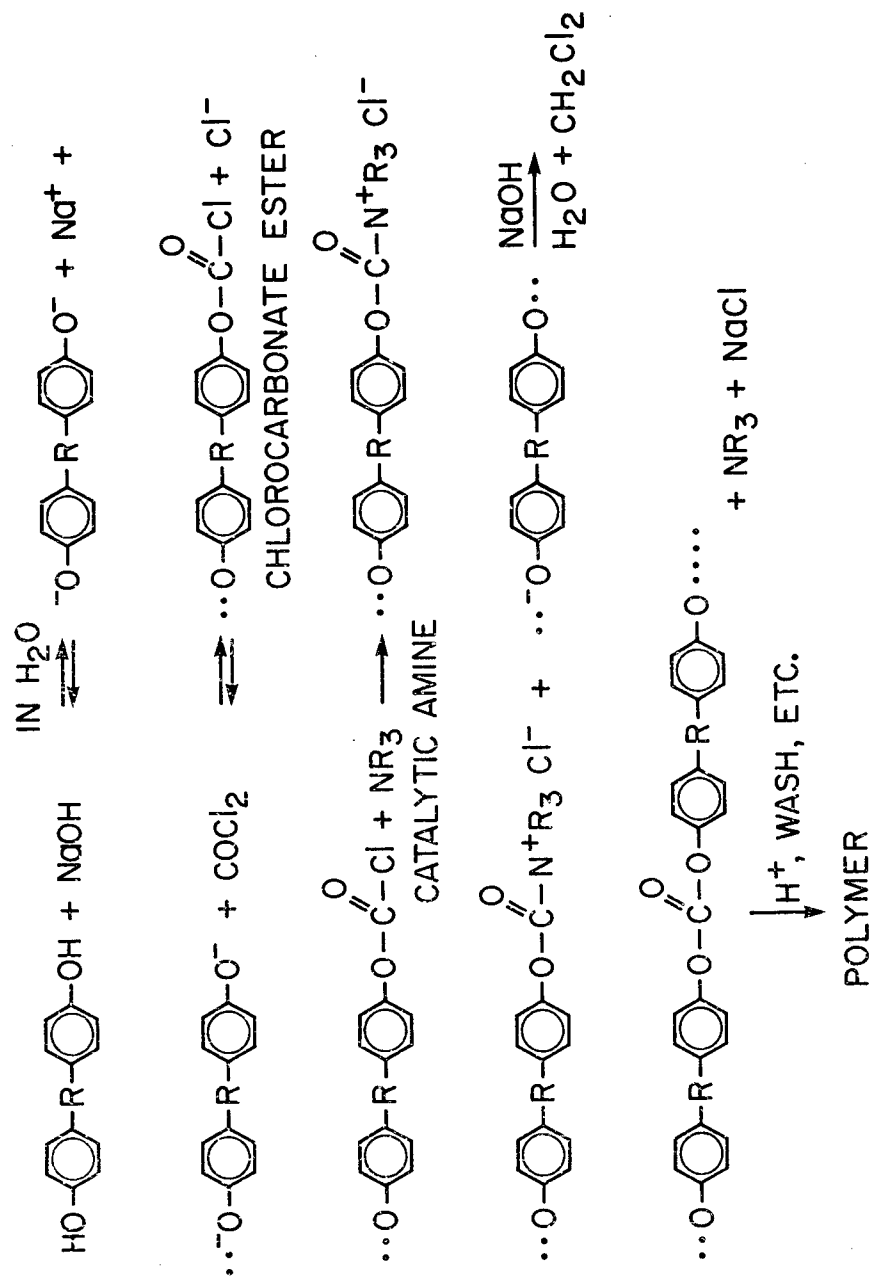


Figure 5. Interfacial polymerization mechanism for synthesis of bisphenol polycarbonates.

(DETERMINED IN N<sub>2</sub>)

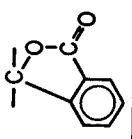
| POLYCARBONATE TYPE, -R-  | T <sub>g</sub> , °C | T <sub>m</sub> , °C | T <sub>d</sub> , °C | Y <sub>C</sub> <sup>800°</sup> , % |
|--|---------------------|---------------------|---------------------|------------------------------------|
| BISPHENOL A<br>$\begin{array}{c} \text{CH}_3 \\   \\ -\text{C}- \\   \\ \text{CH}_3 \end{array}$                   | 150                 | 190                 | 400                 | 20                                 |
| TRIPHENYL<br>$\begin{array}{c} \text{H} \\   \\ -\text{C}- \\   \\ \text{C}_6\text{H}_5 \end{array}$               | 180                 | 220                 | 325                 | 40                                 |
| TETRAPHENYL<br>$\begin{array}{c} \text{C}_6\text{H}_5 \\   \\ -\text{C}- \\   \\ \text{C}_6\text{H}_5 \end{array}$ | 220                 | 260                 | 397                 | 40                                 |
| PHENOLPHTHALEIN<br>            | 278                 | 295*<br>* SOFTENS   | 425                 | 54                                 |

Figure 6. Effect of monomer structure on the thermal properties of aromatic polycarbonates.

| SOLUBLE IN:   |                     |  |
|---|---------------------|--|
| DICHLOROMETHANE                                     | DIOXANE             |  |
| CHLOROFORM  | CYCLOHEXANONE       |  |
| DIMETHYLFORMAMIDE                                   | 1,2-DICHLOROETHANE  |  |
| PYRIDINE  | N-METHYLPYRROLIDONE |  |
| SYM-TETRACHLOROETHANE                               | M-CRESOL            |  |
| MOLECULAR WEIGHT (BY GEL PERMEATION CHROMATOGRAPHY) |                     |  |
| $\eta_{inh}$  | M.W.                |  |
| 0.64  | 43,000              |  |
| 0.93  | 145,000             |  |
| 1.14  | 155,000             |  |

Figure 7. Characterization of the solubility and molecular weight of phenolphthalein polycarbonate.

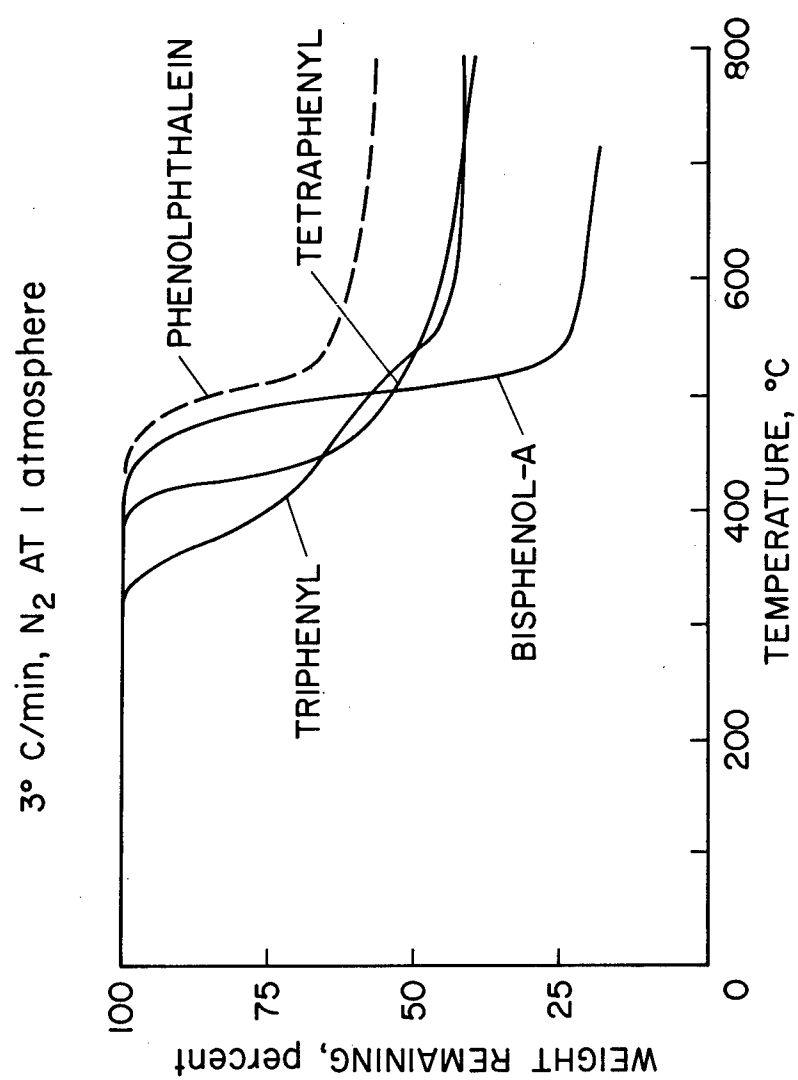


Figure 8. Thermogravimetric analyses of polycyclic aromatic polycarbonates.

- POLYMER POWDER IS SWOLLEN WITH ACETONE
- WHEN VOLATILES ARE ~40% BY WEIGHT  
MOLD AT 230°C  
AND 7 MN/m<sup>2</sup>
- REPLASTICIZE SPECIMEN BY IMMERSION IN DICHLOROMETHANE
- REMOLD AT 200°C AND 7 MN/m<sup>2</sup>
- HOLD IN VACUUM OVEN (150°C) UNTIL VOLATILE CONTENT IS  
SUFFICIENTLY LOW (2% AT 300°C)

Figure 9. Processing method for molding phenolphthalein polycarbonate.

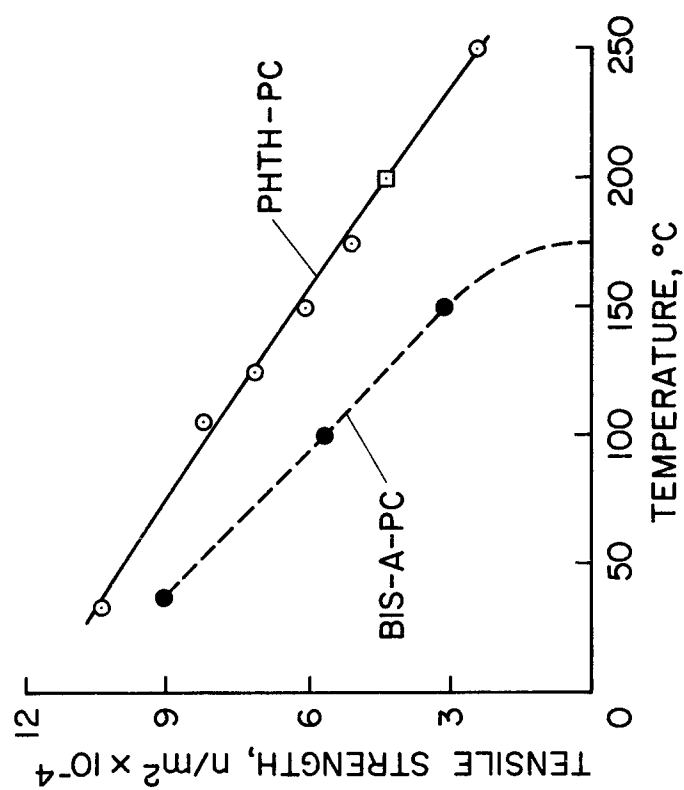


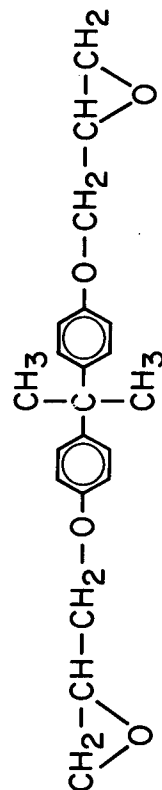
Figure 10. Effect of temperature on the tensile strength of phenolphthalein and bisphenol-A polycarbonates.

|  | BISPHENOL-A PC | PHENOLPHTHALEIN PC |
|--|----------------|--------------------|
| SPECIFIC GRAVITY                                   | 1.20           | 1.270              |
| HARDNESS, ROCKWELL                                 | R 115          | —                  |
| IMPACT STRENGTH                                    |                |                    |
| IZOD, N·m/m OF NOTCH                               | 69.2           | 80                 |
| REFRACTIVE INDEX $n_D^{20}$                        | 1.585          | 1.613              |
| TENSILE STRENGTH, MN/m <sup>2</sup>                |                |                    |
| 23°  | 82.7           | 91.7               |
| 93°  | 57.0           | 77.9               |
| 149°   | 31.9           | 60.0               |
| 177°   | 0              | 57.9               |
| TABER ABRASION, 500 gm LOAD<br>mg LOSS/1000 CYCLES | 7.6            | 6.7                |

Figure 11. Comparison of the physical and mechanical properties of bisphenol-A and phenolphthalein polycarbonates.



STRUCTURE:



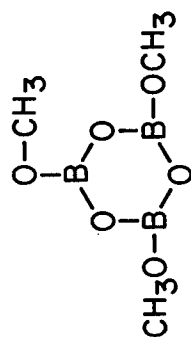
2, 2-BIS [p-(2, 3 EPOXYPROPOXY) PHENYL] PROpane  
OR "DIGLYCIDYL ETHER OF BISPHENOL A" OR DGEBA

PROPERTIES AND SPECIFICATIONS:

- EMPIRICAL FORMULA:  $C_{21}H_{24}O_4$
- DENSITY AT 20°C: 1.168 gm/cc
- MOLECULAR WEIGHT: 340 (calc)
- COLOR; ASTM D1544: 1 MAX
- EPOXIDE EQUIVALENT: 170 (calc)
- MELTING POINT PURE MTL. ~ 46°C
- FOUND: 172-178
- REFRACTIVE INDEX,  $n_D^{25}$  = 1.5690-1.571
- VISCOSITY, 25°C 4000-6000  $\mu m^2/s$
- HYDROLYZABLE CHLORIDE: ~ 0.05%
- DISTILLS AT 175°C AND 5  $\mu$  Hg PRESSURE

Figure 12. The properties of bisphenol-A diglycidylether monomer for transparent epoxy window.

STRUCTURE:



PROPERTIES AND SPECIFICATIONS:

- EMPIRICAL FORMULA:  $C_3H_9O_6B_3$
- MOLECULAR WEIGHT: 173.6
- COLOR AND FORM: COLORLESS LIQUID
- VISCOSITY, 25°C: 13-16  $\mu m^2/s$
- BORON CONTENT: CALCULATED 18.70%
- TYPICAL ASSAY: 18.3-18.64%
- BOILING POINT: DECOMPOSES ABOUT 130°C
- DENSITY, gm/ml, 25°C: 1.216
- REFRACTIVE INDEX,  $n_D^{25}$  - 1.3993
- FLASH POINT, C.O.C.: 28-60°C
- SOLUBLE IN ACETONE, BENZENE, CHLOROFORM
- INSOLUBLE IN PETROLEUM ETHER
- HYDROLYZES READILY ON CONTACT WITH WATER

Figure 13. The properties of the trimethoxyboroxine curing agent for EX-112.

## POLYMERIZATION REACTION

- THE POLYMERIZATION PROCEEDS VIA A LEWIS ACID TYPE CATALYZED ETHERIFICATION OF THE OXIRANE (EPOXIDE) GROUPS OF THE DGEBA BY THE TMB
- THE CATALYST (TMB) CONCENTRATION RANGE FOR OPTIMUM PHYSICAL PROPERTIES IS ABOUT 5.0-6.5 PARTS PER HUNDRED OF DGEBA

## PROCEDURE FOR CASTING POLYMER

- WARM DGEBA TO 40-45°C
- ADD 5 PARTS TMB TO 100 OF DGEBA, MIX THOROUGHLY ...
- DEGAS IN VACUUM CHAMBER GRADUALLY TO 6.8 KILOPASCALS
- POUR INTO PREWARMED METAL MOLDS
  - CURE AT 80°C FOR 3 HOURS
  - THEN 135° FOR 3 HOURS
  - AND 180° FOR 2 1/2-3 HOURS
- COOL SLOWLY BEFORE UNMOLDING
- FLAT MOLDS MAY BE USED - AND THE FLAT CASTINGS MAY BE CURVED TO SHAPE BY SAGGING AT 150°C

RAW MATERIAL COST FOR A 737 WINDOW LESS THAN \$ 2.00 !

Figure 14. Process for polymerization, casting, and forming of EX-112 windows.

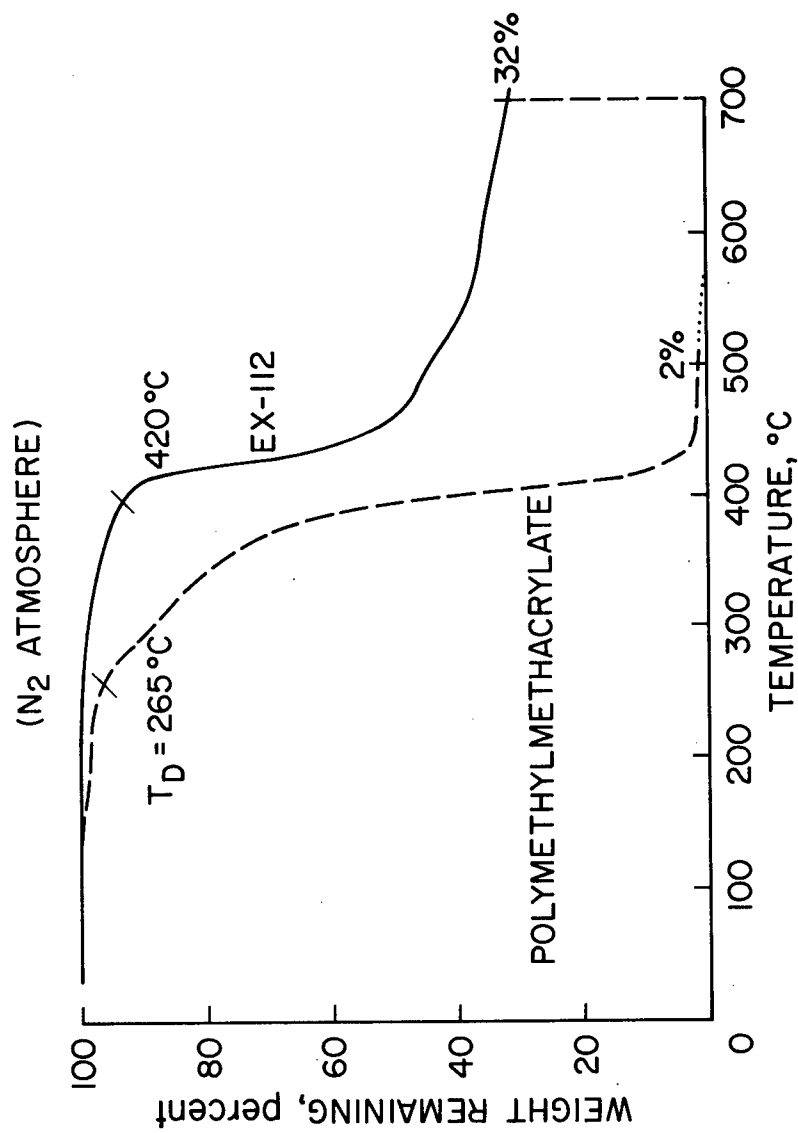


Figure 15. Thermogravimetric analysis of EX-112. Compared with polymethylmethacrylate.

|  | PMM             | EX-112               |
|--|-----------------|----------------------|
| SPECIFIC GRAVITY, 25°C   | 1.19            | 1.195*               |
| REFRACTIVE INDEX, $n_D^{20}$                                   | 1.50            | 1.60                 |
| ULT. TENSILE STRENGTH, MN/m <sup>2</sup><br>25°C<br>120°C      | 62.0<br>0       | 90.2<br>34.5         |
| ELONGATION, percent, 25°C                                      | 3-5             | 2.0                  |
| ULT. FLEXURAL STR, MN/m <sup>2</sup><br>25°C<br>120°C<br>150°C | 110.3<br>0<br>— | 143.4<br>37.9<br>4.6 |
| ABRASION, TABER,<br>500 gm LOAD, mg LOSS/1000 cy               | 46.5            | 21.4                 |
| IMPACT, IZOD, N·m/m OF NOTCH                                   | 19.7            | 13.9                 |

\*GLASS = 2.6

Figure 16. Comparison of the physical and mechanical properties of EX-112 and polymethylmethacrylate.

|  | MATERIAL    |          |        |        |
|--|-------------|----------|--------|--------|
|  | ST. ACRYLIC | BIS-A PC | PTH-PC | EX-II2 |
| HEAT DISTORTION TEMP<br>1750 kN/m <sup>2</sup> , °C                            | 106°        | 140      | 250    | 112°   |
| LIMITING OXYGEN<br>VALUE, % O <sub>2</sub>                                     | 18          | 23       | 47     | 21     |
| BURNING RATE ASTM,<br>mm/min   | 2.14        | S.E.     | N.B.   | 15.0   |
| THERMAL CONDUCTIVITY<br>W·cm/cm <sup>2</sup> ·°C, ×10 <sup>3</sup>             | 2.32        | 1.95     | —      | 3.50   |
| LOW TEMPERATURE<br>COEFF. OF THERMAL<br>EXPANSION, PER<br>°C × 10 <sup>6</sup> | 50-67       | 52       | —      | 42     |

Figure 17. Comparison of some key thermal properties of candidate transparent materials.

**BEAM DIAMETER: 8mm**

| MATERIAL                   | POLYMETHACRYLATE                   |           | EPOXY - 1112               |        | PHTH POLYCARBONATE                               |
|----------------------------|------------------------------------|-----------|----------------------------|--------|--|
| SAMPLE THICKNESS,<br>mm    | 12                                 | 12        | 12                         | 12     | 3.5  |
| CONDITION,<br>air velocity | STILL                              | MACH 1    | STILL                      | MACH 1 | STILL  |
| TIME OF TEST,<br>sec       | 6.5                                | 2.9       | > 60                       | > 60   | 29 sec   |
| PENETRATION,<br>mm         | BURN THRU                          | BURN THRU | 3.2                        | 6.0    | 2  |
| APPEARANCE                 | NO CHAR FORMATION -<br>-CLEAN HOLE |           | HARD BLACK<br>NODULAR CHAR |        | FRAGILE FRONT CHAR<br>WITH WIDE WHITE<br>OPACITY |

Figure 18. Effect of 260-Watt CO<sub>2</sub> laser (10.6  $\mu$ ) on candidate window materials.

| MATERIAL                                   | THICKNESS,<br>cm | TIME TO<br>BURN THROUGH,<br>sec | REMARKS   |
|--|------------------|---------------------------------|---|
| STRETCHED<br>POLYMETHYL-<br>METHACRYLATE } | 0.66             | 60                              | SHRUNKEN, RETICULATED APPEARANCE,<br>NO CHAR  |
|  | 1.37             | 100                             |   |
| BISPHENOL-A<br>POLYCARBONATE               | 0.66             | 360                             | FLAKY, BRITTLE CHAR   |
|  | 1.35             | 460                             |   |
| PHENOLPHTHALEIN<br>POLYCARBONATE           | 0.42             | 185                             | $\eta_{inh} = 0.42$ , INTUMESCENCE, ABLATION -<br>EROSION IN FLAME<br>$\eta_{inh} = 0.98$ , WHITE OPACITY ON BACKFACE |
|  | 0.51             | 540                             |   |
| EPOXY-BOROXINE<br>EX-112                   | 0.64             | 430                             | INTUMESCENCE, STRONG BLACK POROUS<br>CHAR FORMED<br>TEST TERMINATED BEFORE BURN-THROUGH                               |
|  | 1.22             | >1080                           |   |

LAMINATES — MADE USING ETP ADHESIVE

|                         |                        |     |  |
|-------------------------|------------------------|-----|--|
| EX-112 AND<br>BPA-PC    | 0.64 } 1.40<br>0.66 }  | 680 | DELAMINATION AND ADHESIVE BURNING<br>" |
|                         | 0.64 } 1.42*<br>0.66 } | 400 |  |
| EX-112 AND<br>PHENOL-PC | 0.64 } 1.18<br>0.51 }  | 610 | "                                      |
|                         | 0.64 } 1.21*<br>0.57 } | 640 |  |

\* POLYCARBONATE SIDE TOWARDS HEAT

ALL SAMPLES SIZE 5.1 x 6.3 cm, RESULTS ARE AVERAGES OF TWO RUNS

Figure 19. Results of T-3 thermal tests of candidate transparent materials.



| MATERIAL                            | THICKNESS, cm         | IMPACT FORCE, * N · m |  |
|-------------------------------------|-----------------------|-----------------------|--|
| STRETCHED<br>ACRYLIC                | 0.64<br>1.27          | > 3.18<br>> 3.18      |  |
| BISPHENOL A<br>POLYCARBONATE        | 0.64<br>1.27          | > 3.18<br>> 3.18      |  |
| PHENOLPHTHALEIN<br>POLYCARBONATE    | 0.42<br>0.51          | 0.91<br>> 3.18        | $\eta_{inh} = 0.42$<br>$\eta_{inh} = 0.98$ |
| EPOXY-BOROXINE<br>(EX-112)          | 0.64<br>1.27          | 1.82<br>> 3.18        |  |
| LAMINATES — IMPACTED ON EX-112 SIDE |                       |                       |  |
| EX-112 /<br>BIS-A-PC                | 0.63 } 1.30<br>0.63 } | > 3.18                |  |
| EX-112 /<br>PTH-PC                  | 0.63 } 1.12<br>0.42 } | > 3.18                |  |

\*GARDNER IMPACT TESTER

Figure 20. Comparison of impact resistance of candidate materials and laminates.

SESSION 3

**MATERIALS AND PROCESSES (Part II)**

PLATE VERSUS FLOAT GLASS IN AIRCRAFT  
TRANSPARENCIES

Robert E. Maltby, Jr.  
Libbey-Owens-Ford Company  
Toledo, Ohio

## Plate vs. Float Glass in Aircraft Transparencies

Robert E. Maltby, Jr.  
Libbey-Owens-Ford Company  
Toledo, Ohio

### Abstract

The flat glass industry has in the last ten years converted from grinding and polishing (i.e. the plate glass process) to the float process for producing high quality glass. Both plate and float are approved products for aircraft transparencies, but they are not identical products. The purpose of this paper is to compare the characteristics of these two products with reference to aircraft applications.

To facilitate understanding the products, a schematic description of the processes will be shown comparing the glass forming technologies. Some of the manufacturing boundary conditions which, in effect, control the glass characteristics for both processes will be discussed.

A more detailed discussion will be presented of the specific optical and mechanical properties of the surfaces of the two types of glass. The smoothness, flatness, and parallelism of the glass surfaces, and the differences between top and bottom surfaces of float glass are some of the properties that will be covered. Also, certain inspection methods and procedures will be covered that are relevant for evaluating magnitudes of specific properties.

## Introduction

World wide, plate glass manufacturing processes have almost all been replaced by float glass operations. These high quality products, plate and float glass, are so similar that in most applications both are satisfactory. Both of these products meet MIL specs for aircraft (MIL-G-25871 and MIL-G-25667) and are approved for use as aircraft transparencies, but they are not identical materials. This paper will examine the characteristics of these two equivalent but not identical products. In doing so, the two processes used to form these products will be discussed for two reasons. First, understanding the processes is helpful in understanding the products and second, I think that you will find, as I have, that these are interesting processes.

## History

The history of glass manufacturing goes back to the Egyptians of about 3000 years ago. The manufacture of commercial quantities of flat glass for windows of high quality goes back only to about the late 1700's. Until then, most flat glass was made either from blown cylinders which were split and flattened or by the crown method of hand spinning a hot gob of glass. The first high quality glass was obtained by grinding flat the surfaces of glass that was cast on tables and rolled into "plates" and then polishing them.

The basics of the plate process were (and are) to use a slurry of water and coarse sand as the abrasive to grind one surface of the glass flat and then to use finer and finer grinding sands followed by the use of a polishing agent such as rouge to obtain a smooth, polished surface. Then the glass was turned over and the process repeated on the opposite surface. In this century, forming and processing a continuous ribbon of glass was developed and eventually (by the mid 1900's) a twin grinding process evolved. This twin grinding, which substantially improved both quality and productivity, permitted both surfaces of the glass to be ground simultaneously. Twin polishing processes were just being developed, but were not in extensive use, when the float process was announced in 1959 by Pilkington Brothers of England. Since then, the float process has been installed world wide and has almost completely replaced the plate process for producing high quality flat glass.

In the early 1900's, making a continuous ribbon of flat glass by the sheet process was also accomplished. Although substantial improvements in optical and mechanical tolerances have been made, sheet glass has not been consistently produced at a quality level comparable with plate or float glass.

## The Plate Process

As in all flat glass manufacturing, the first step in plate glass manufacture is melting the raw materials and obtaining a thermally and chemically homogenous material output. Schematically, the melting tank of the plate glass operation is shown in Figure 1 as a box. It is a big box. Typically, a thousand tons or more of melt is in the "tank" at all times. Raw materials are continuously fed in, and glass in the form of a ribbon is continually taken away. (Note this is true whether the process is plate, float, or sheet.) The viscous glass exiting the melting tank is formed into a sized ribbon on the plate glass process by a pair of cylindrical rolls. These rolls are water-cooled and, as the hot glass is formed to a ribbon, it is also cooled by the rolls. In degrees Fahrenheit, the glass is about 1800° entering the rolls and 1200° or 1300° leaving them. In order to prevent the glass from sticking to the rolls and to obtain traction at this temperature range, the rolls are roughened by having a knurled pattern machined on both of the rolls. The ribbon then passes through the lehr where it is annealed and cooled to room temperature.

As the cooled glass surfaces have a knurl pattern imprinted on them, it must be removed. This is done by grinding first with a slurry of water and coarse sand and then with finer and finer grains to smooth the surfaces. Twin grinding, as shown schematically in Figure 1, is a process in which both surfaces of the ribbon are ground simultaneously. When it is noted that this ribbon is generally only 1/4" thick (or less), is ten feet wide, and is a brittle material, it becomes obvious that twin grinding is a precision alignment process. When the parallelism and flatness of plate glass is also noted, it is even more obvious that twin grinding is a high quality glass forming process. To finish the glass (that is remove the grinding pits) for final use, it must still be polished. This is usually done by cutting the ribbon into large rectangles, which we call "blanks," laying the blanks in a plaster bed on very flat tables, and traversing the tables and glass beneath polishing heads, first for one side of the glass and later for the second surface. As previously stated, a commercial grade polishing rouge slurry is used as a polishing compound. Note that in Figure 1, while both the sheet and float processes yield a finished product at cutting, the plate process requires the very substantial polishing operation after cutting to obtain a finished product.

The advantages and disadvantages of this process and the characteristics of the plate glass product are perhaps more meaningful when compared to those of the float process. Therefore, the evaluation of the merits of plate glass will be postponed until the float process has been described.

## The Float Process

The forming of high quality float glass is dependent on supplying a homogenous glass at about 1800°F to the float bath. Thus, the melting tank design requirements and mode of operation for float are very similar to the plate melting tank. The float bath is a very large "black box" into which the glass is fed at about 1800°F and out of which comes a formed ribbon of "fire-polished" glass at about 1200°F. The ribbon is formed while it "floats" on the bath. The bath contains molten tin which, as it is more dense than the glass, enables the glass to float upon it. Because the tin is a liquid, its surface is very flat and thus the glass surface in contact with the tin also becomes very flat. The glass poured into the bath and onto the tin spreads into a thinner and thinner layer at a rate controlled by the viscosity of the glass. As the glass spreads out on the tin, there are only a few forces acting on it. One, the force of gravity, is trying to make the glass surfaces parallel. Another force is the surface tension of the glass interfaces with the tin below and the atmosphere above. This surface tension force comes to equilibrium with the gravity force and stops the spread of the glass when the thickness of the glass is about one-quarter inch. This thickness is one used for many flat glass applications, and it is the "equilibrium" thickness of the float operation. This combination (the process's equilibrium thickness and the fact that it is a desirable thickness) is in part responsible for the float operation's great success in making a high quality product. Note that to obtain this equilibrium thickness no stretching is required, and the operation consists of carrying the ribbon out of the bath at precisely the rate material is fed in. Thus, in theory at least, the flatness is limited by the curvature of the earth and the parallelism only by "edge" effects of the surface tension force.

The formed ribbon at 1200°F is lifted from the float bath and conveyed down the lehr which anneals and cools the glass. At the end of the lehr is a fire-polished, finished glass ready for cutting and requiring no further processing of its surfaces.

## Comparison of Plate and Float Glass

The two processes, plate and float, each produce an annealed flat glass product that is of high quality. Both of these excellent optical quality products are, in fact, judged equivalent as to their acceptability for aircraft applications. From the process descriptions, however, it becomes clear that though the glasses are equivalent from an application point of view, they are not identical in all of their properties. Properties in which the two products are essentially identical include those which are a function of the raw materials and the melting and refining of those materials.

As both plate and float use essentially identical materials and melting procedures, some essentially identical properties include density, homogeneity, and index of refraction.

The differences between these two annealed glass products are primarily differences in properties associated with the surfaces. Due to the entirely different methods used to obtain "good" surfaces, it is not at all surprising that the surfaces exhibit different characteristics when examined very critically. The most obvious difference is that the float surfaces are "fire-polished," whereas the plate surfaces are mechanically polished. Grinding of plate glass, of course, essentially chips away and cracks the surface, and polishing removes the "tops" of the resulting peaks. Thus, residual cracks and pits are in plate glass even after appreciable polishing. It should be noted that these defects are very small but still large enough to scatter light. Pits typically have been about 200 microinches diameter or less in polished plate glass. Due to their small size and because, in high quality plate glass, almost all pits have been polished away, light scattering from this defect is negligible in most applications and usually is only seen by using dark field illumination. Float glass, while having no grinding pits, does have a "tin" bottom surface and an "atmosphere" top surface. In the bath above the molten tin, a non-oxidizing (inert) atmosphere is very carefully maintained to prevent contamination of the liquid tin and the hot glass. No obvious differences are noted between the two surfaces of float glass, but the tin (bottom) surface can be determined by noting the fluorescence that occurs when exposed to ultra-violet energy. Note some plate glass fluoresces on both surfaces when exposed to ultra-violet radiations due to residual rare earth polishing compounds in its grinding pits. Typically, on the float glass "tin" surface, the fluorescence is detectable only in a very dark room.

The microscopic surface cracks in plate glass are the cause of plate glass typically being weaker than float glass which has fire-polished, essentially crack-free surfaces. This strength property is, of course, assuming all other variables such as glass thickness, etc. are the same for both the float and plate glass. These strength differences become minimized after the glass has received the normal service damage.

Available thicknesses of float and plate glass range in steps from less than 0.1" to greater than 1.0 inch. The rate of change of thickness (that is, wedge in the glass) is also similar for both plate and float. The parallelism of both of these products is almost unbelievably good, particularly when considering that both of these glasses are formed at rates of thousands of square feet per hour. In both plate and float glass, the variation in thickness as measured with the direction of ribbon draw is negligible. Measured across the draw it is minimal but can be selected to be



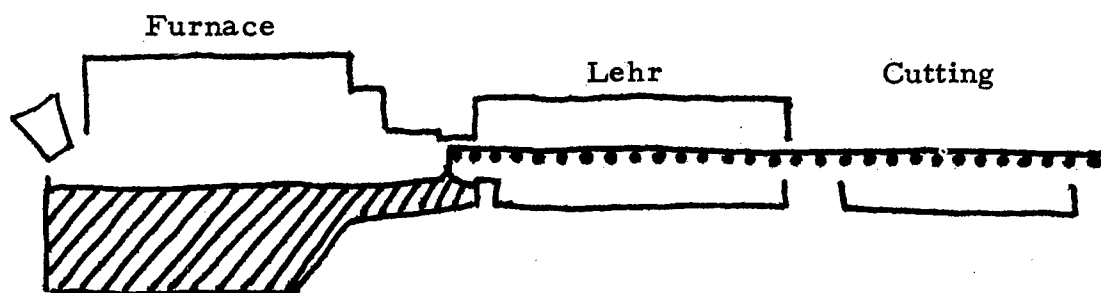
almost nil in particular areas. Because both processes have what might be called a "process inertia," once they are set up for a "good" operation they tend to stay that way. Thickness, thickness change, parallelism - call these properties what you will - are properties that are very similar and almost unchanging in both these processes, and they exemplify "process inertia."

Glass smoothness, or flatness, is not of identical character in plate and float glass. Both processes do, however, have the "process inertia" or consistency of character with respect to flatness and smoothness. A plate glass surface is, on a microscopic basis, "rough" in that it contains the residual of the grinding pits and cracks. Also, the plate glass surfaces have a "pebbly" characteristic resembling the surface of an orange peel but, of course, of substantially reduced magnitude. (The peaks and valleys are typically only a few microinches different in elevation.) Float glass exhibits neither of these characteristics but does have very elongated, narrow hills and valleys spaced typically one-half to one inch apart that are usually less than five microinches different in elevation. These are often parallel from one surface to the other, and thus the glass can exhibit better parallelism than flatness. The parallelism is of particular importance to the optics when viewing through the glass; whereas flatness is of more significance in reflected optics. Thus, parallelism is usually more significant for an aircraft transparency.

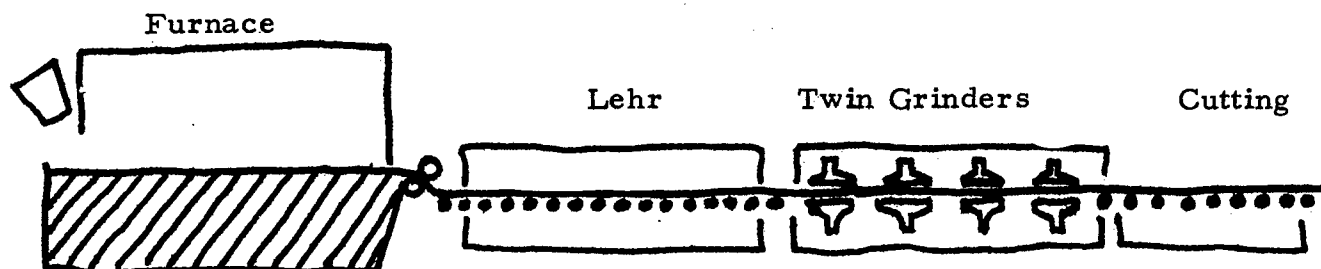
Measurement of the optical characteristics related to the mechanical properties of flatness, smoothness, and parallelism can be done a number of ways. One of the more interesting techniques employs a laser. Using only the property of the laser that it generates an extremely well collimated, narrow beam of light, it is quite simple to measure deviation of the light which is directly related to the parallelism of the glass. If, as the glass is scanned, an analog record of rate of change of deviation can be made, this becomes a measure of so-called "optical distortion." Similarly, reflected systems provide information about flatness and smoothness. Automated "distortion" meters of various degrees of sophistication and sensitivity are used in many laboratories which may eventually result in new ways to specify and inspect glass for various applications.

In my studies of plate and float glass, I have found that both products are of amazingly high quality, and, though definitely not identical products, they are equivalent products for virtually all applications including aircraft transparencies.

### SHEET GLASS PROCESS



### PLATE GLASS PROCESS



### FLOAT GLASS PROCESS

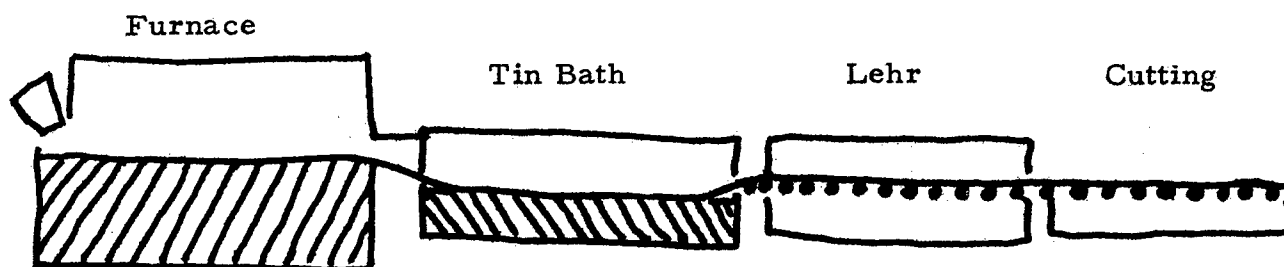


FIGURE 1

EFFECT OF ADHESIVE ON THE IMPACT  
RESISTANCE OF LAMINATED PLASTICS  
FOR WINDSHIELD APPLICATIONS

J. L. Illinger and R. W. Lewis  
Army Materials and Mechanics Research Center  
Watertown, Massachusetts

"EFFECT OF ADHESIVE ON THE IMPACT RESISTANCE OF  
LAMINATED PLASTICS FOR WINDSHIELD APPLICATIONS"

J. L. ILLINGER & R. W. LEWIS

Army Materials & Mechanics Research Center, Watertown, Mass.

Clamped acrylic-polycarbonate laminates (polycarbonate as back up) show improved resistance to penetration over that shown by either material alone. This resistance is dependent upon relative amounts of each material. Use of thermal bonding techniques to form a laminate resulted in a significant decrease in the ballistic resistance of these laminates. Use of a brittle epoxy adhesive to bond the materials gave similar results. The brittle adhesive induces spallation of the polycarbonate causing significantly lower impact resistance and changing the mode of failure from ductile to brittle.

Several flexible transparent segmented polyurethane adhesives were synthesized with systematic variation in proportions of monomer (diisocyanate and chain extender) and structure of the soft segments. Glass transition temperatures showed small differences with compositions. Ballistic resistance of laminates formed using these adhesives was improved by approximately forty percent over that of the clamped laminate. The change in relative amount of the hard segment (diisocyanate and chain extender) had no statistically significant effect upon the impact behavior. At constant molecular weight of the soft segment, variation of the structure also showed no effect.

Several proprietary flexible film adhesives were also tested. Strength of adhesive bonding was varied by a factor of two through changes in laminating temperature. However, no correlation between bond strength and ballistic performance was found. These film adhesives formed laminates slightly better than those using polyurethane adhesives. Thus, laminates using transparent flexible adhesives with sufficient bond strength to prevent delamination upon impact show ballistic resistance up to fifty percent better than Lexan polycarbonate which is currently considered the best commercially available transparent impact resistant polymeric material.

## INTRODUCTION

Currently Plexiglas is the transparent polymeric impact resistant material in widespread use for aircraft applications. Lexan polycarbonate with slightly higher impact resistance and a ductile mode of failure is replacing Plexiglas in some applications. However, there are some problems due to poor abrasion and poor solvent resistance. It is desirable to further increase the impact behavior of this type of material. This can be accomplished through three principle techniques: (1) toughening polymers by the inclusion of a rubbery material forming a copolymer (graft, block, random), (2) by the introduction of preferred orientation, and (3) by lamination of dissimilar materials.<sup>(1)</sup>

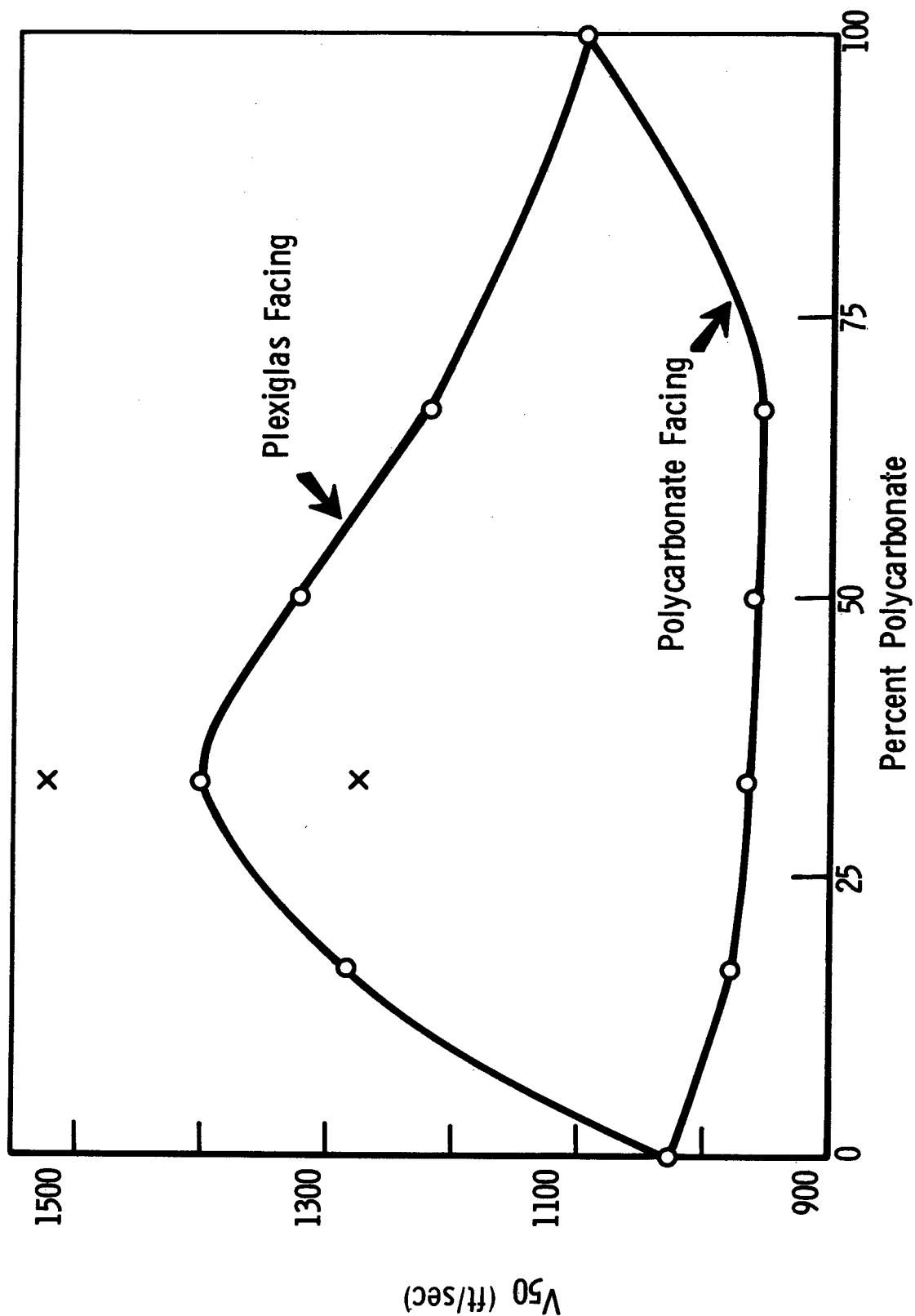
The synergism in ballistic performance due to lamination of dissimilar material has been shown for several systems including glass/plastic and plastic/plastic laminates.<sup>(2)</sup> Since Lexan and Plexiglas are very different polymeric materials it was not unreasonable to assume that laminates of these two materials would show enhanced ballistic resistance. As preliminary studies bore this out, an extensive investigation of the PMMA/PC with-out and with an adhesive interlayer was carried out.

## RESULTS & DISCUSSION

### NO BONDING, NO INTERLAYER

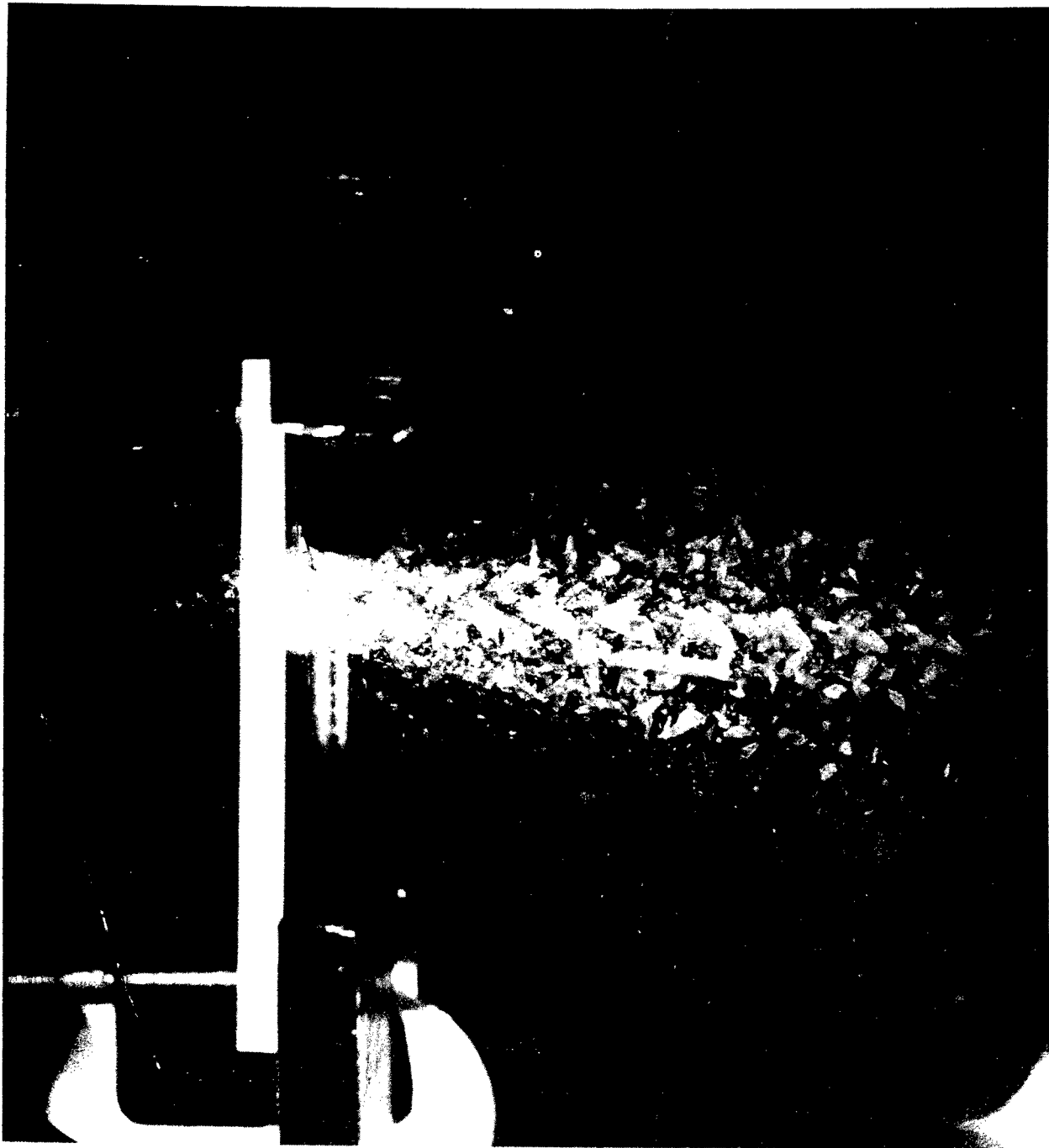
The ballistic performance of clamped Plexiglas/Lexan laminates was investigated over a range of relative compositions with results shown in Figure 1. At the extreme left is the ballistic resistance of 100% PMMA with a  $V_{50}$  of 1040 ft/sec. At the extreme right is 100% polycarbonate with a  $V_{50}$  of 1100 ft/sec. With PMMA facing the impact (upper curve), the optimum ballistic resistance of the combinations tested occurred at a 2:1 weight ratio of PMMA to PC ( $V_{50} = 1400$  ft/sec) in good agreement with the optimum ratios for glass to plastic. With the ductile PC facing the impact, however, (lower curve) there was a reduction in ballistic resistance compared to that of the homogeneous materials over the range of compositions investigated.

Under ballistic impact, with the 22 caliber 17 grain fragment simulating projectile (FSP), PMMA by itself behaves in a brittle fashion and undergoes cracking and spallation (Figure 2). Polycarbonate, on the other hand, is ductile, does not spall, and fails in shear (Figure 3). Both materials, however, have essentially the same  $V_{50}$  (PMMA  $V_{50} \sim 1040$ , PC  $V_{50} \sim 1100$  ft/sec Figure 1). In the laminated system, though, the brittle PMMA, when it is facing the impact, spreads out the impact over a wider area than a ductile material, while the ductile PC then serves both to absorb the impact and to prevent the brittle material from spalling (Figure 4) thereby allowing more extensive damage and raising the PMMA's resistance to penetration. With the ductile layer facing, however, the load is not spread out as efficiently, and there is nothing to prevent the brittle material from spalling (Figure 5); hence, less energy is absorbed during the penetration process. Consequently, the more efficient combination ballistically is for the more brittle PMMA to face the impact.



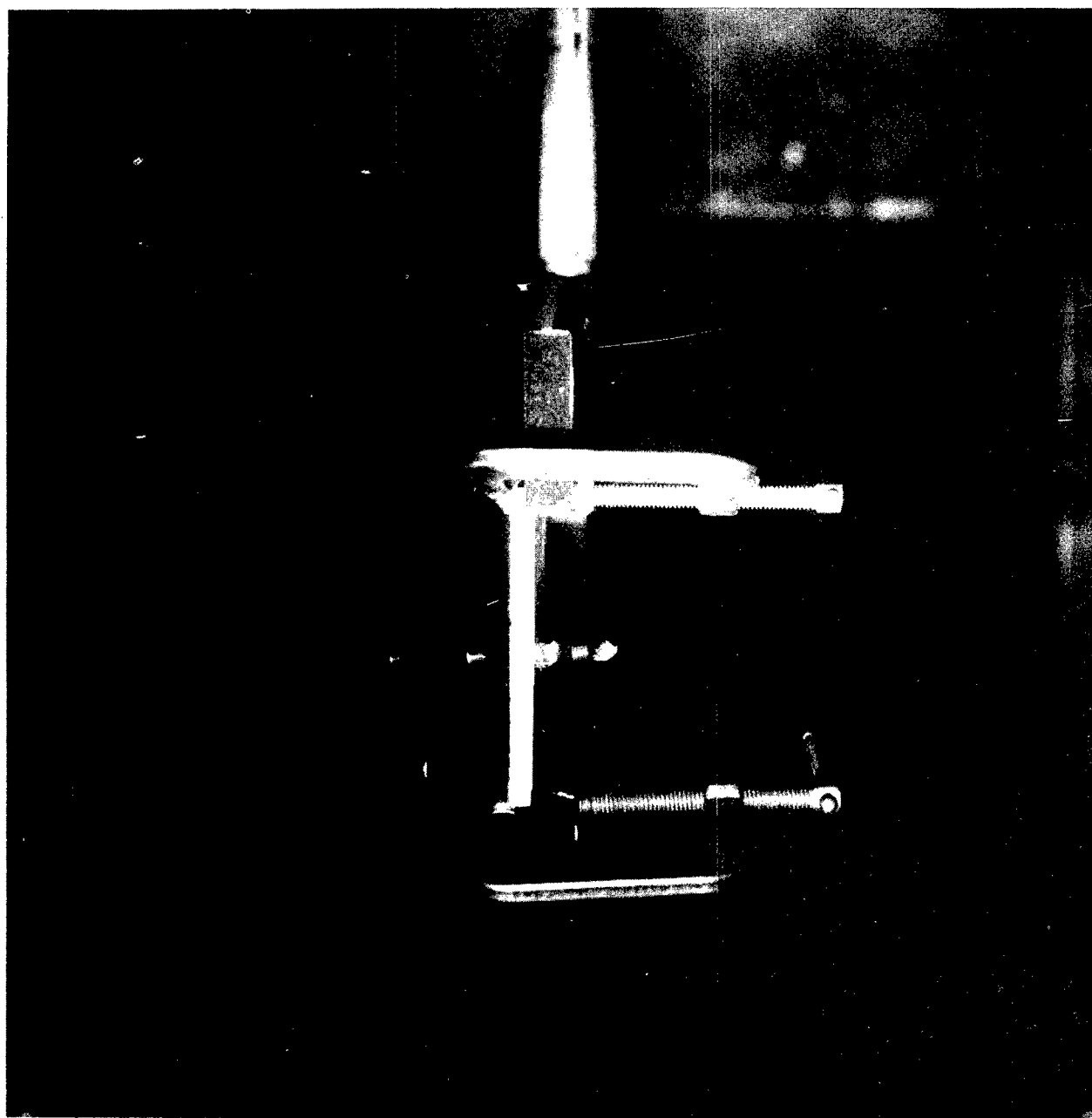
BALLISTIC BEHAVIOR OF PLEXIGLAS - POLYCARBONATE LAMINATES  
(17-Grain Fragment Simulators, 38 oz/sq ft)

ARMY MATERIALS AND MECHANICS RESEARCH CENTER  
19-066-1679/AMC-71



Multiflash photograph of 1/4" Plexiglas under ballistic impact. Edge of sample is shown, missile is moving from left to right.  
ARMY MATERIALS AND MECHANICS RESEARCH CENTER

19-066-156/AMC-72

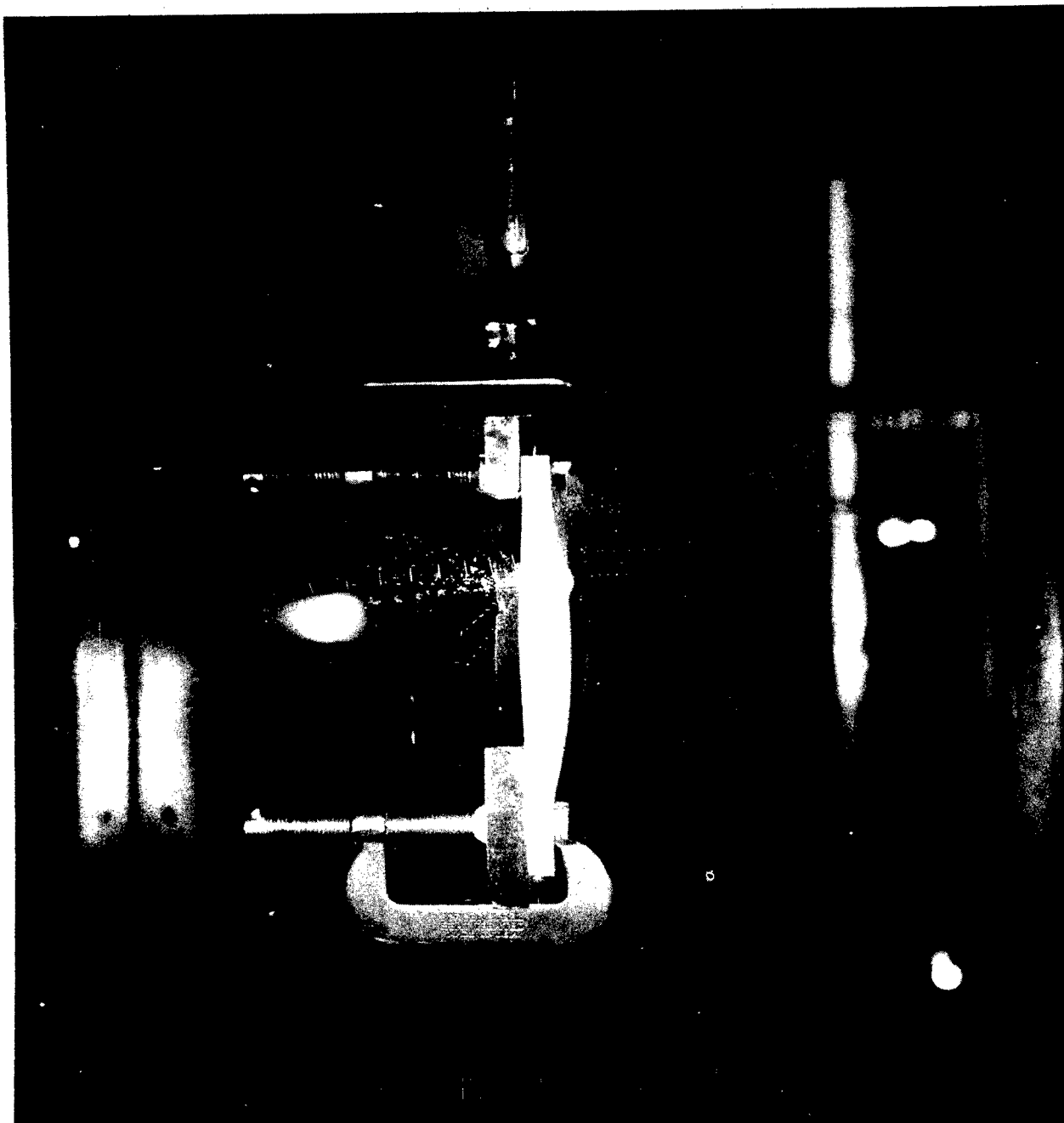


Multiflash photograph of 1/4" Lexan under ballistic impact.  
Edge of sample is shown, missile is moving from left to right.

ARMY MATERIALS AND MECHANICS RESEARCH CENTER

19-066-157/AMC-72

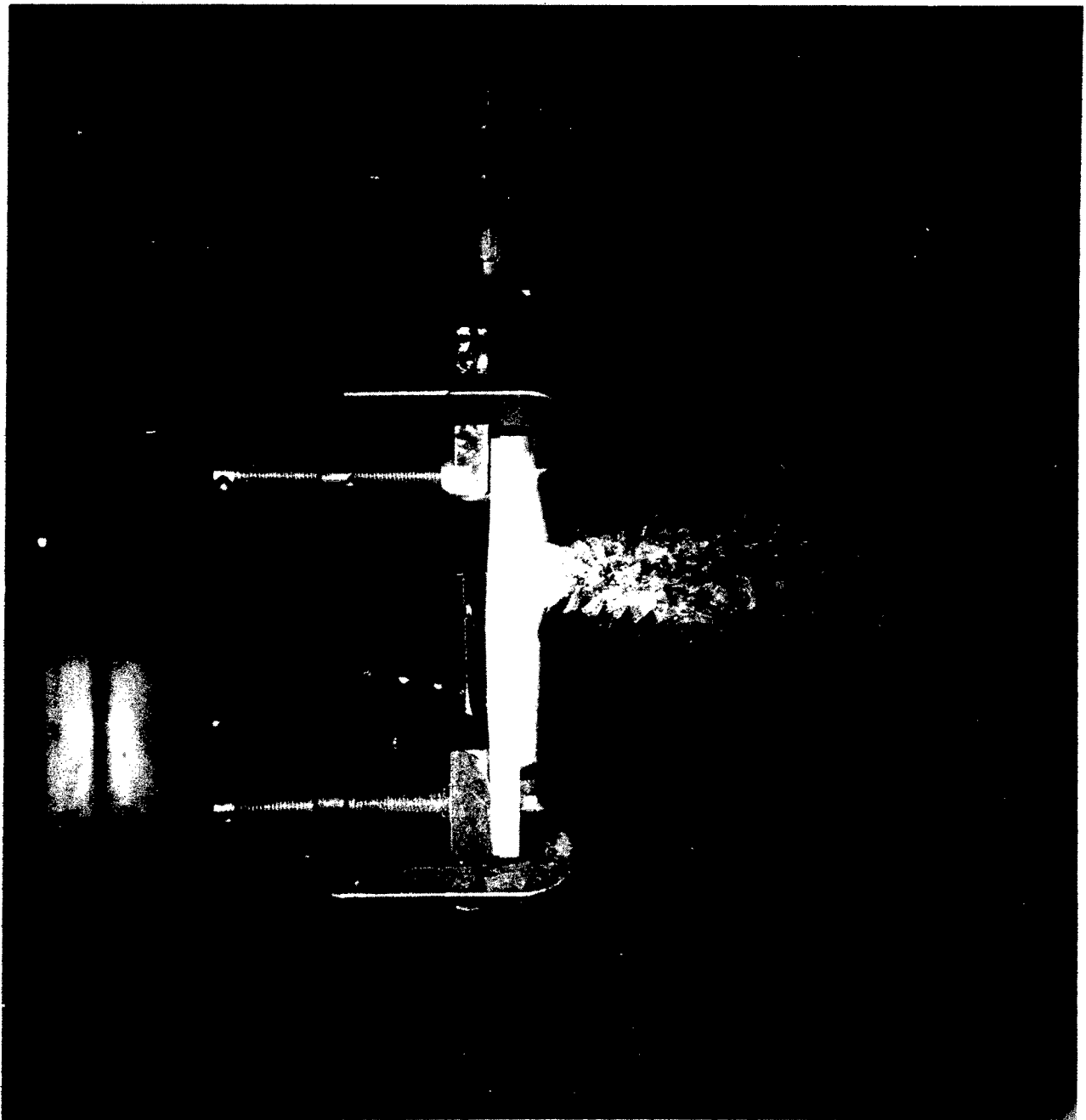




Multiflash photograph of Plex/Lex laminate under ballistic impact. Edge of sample is shown, Plexiglas is facing impact, missile is moving from left to right. Note front spall from Plexiglas but no rear spall from Lexan.

ARMY MATERIALS AND MECHANICS RESEARCH CENTER

19-066-158/AMC-72



Multiflash photograph of Plex/Lex laminate under ballistic impact. Edge of sample is shown, Lexan is facing impact, missile is moving from left to right. Note rear spall from Plexiglas.

ARMY MATERIALS AND MECHANICS RESEARCH CENTER

19-066-159/AMC-72

## THERMAL BONDING, NO INTERLAYER

In order for this laminated system to be useful for aircraft applications it would be necessary to bond the materials together, either thermally or by the incorporation of an adhesive interlayer. A thermally bonded sample would have the advantage of maintaining optical clarity without the problems associated with applying transparent adhesives to polycarbonate. Accordingly, a piece of 1/4" PMMA (lucite molding powder) and 1/8" Lexan were placed in a 6" x 6" mold. The mold was put into an 18" x 18" press and heated under an 18 ton load to 150°C. The press was held at a temperature in the vicinity of 150°C for thirty minutes and then cooled to room temperature.

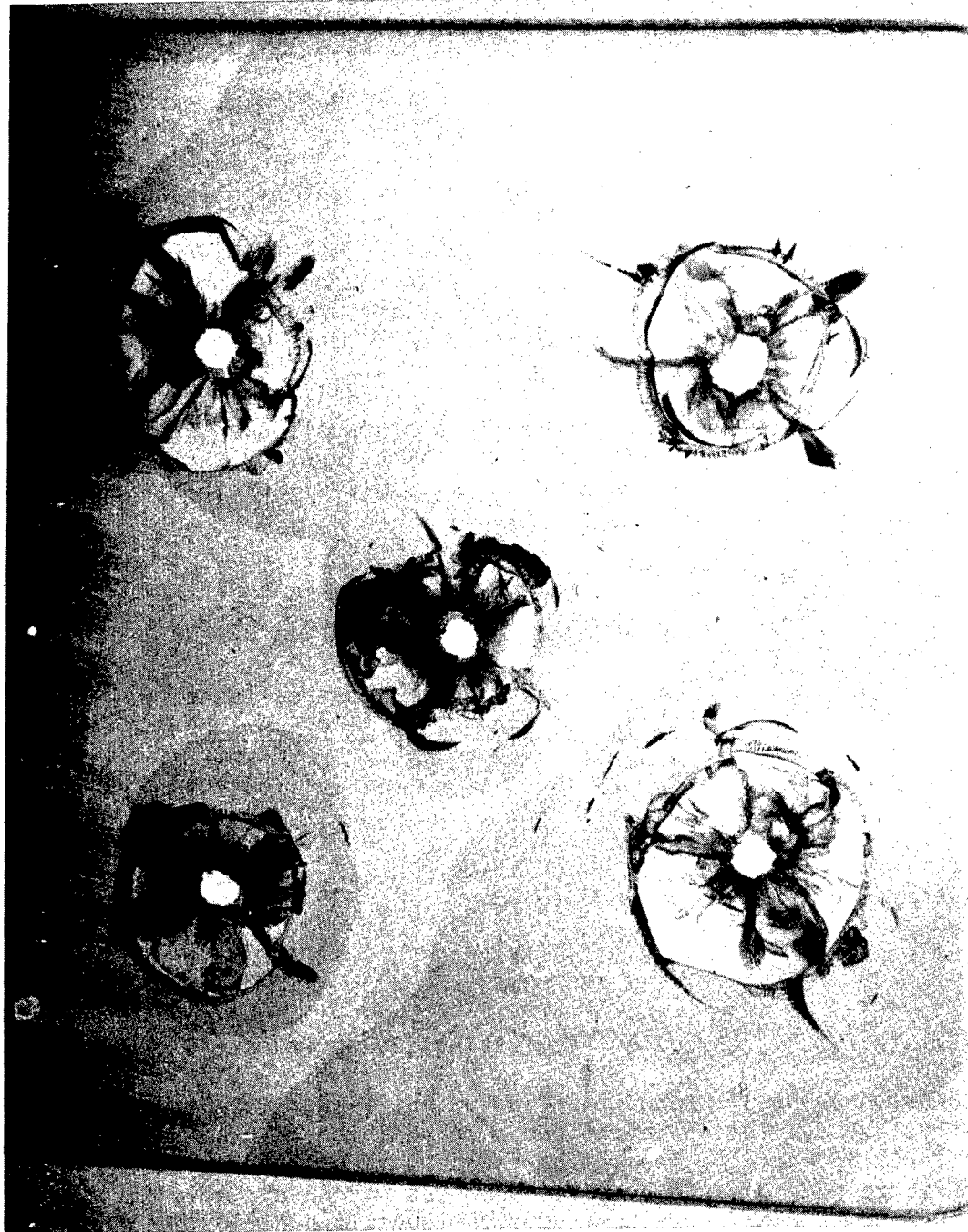
The resultant sample was ballistically evaluated and found to be substantially inferior to the nonbonded sample ( $V_{50} = 1110$  ft/sec at 36.9 oz/sq ft vs.  $V_{50} = 1400$  ft/sec for the nonbonded sample from Figure 1). It is interesting to note that unlike the situation when the samples are clamped together (Figure 4), here the polycarbonate is failing in a brittle fashion and spalling under ballistic impact (Figure 6). It is this spallation that results in the poorer ballistic resistance of the thermally bonded samples.

To verify that this degradation was not due to the thermal treatment per se, however, Lucite and Lexan were individually subjected to the same thermal treatment as the laminate and ballistically evaluated. The results are given in Table I.

TABLE I  
BALLISTIC BEHAVIOR OF PMMA AND LEXAN\*

| <u>Material<br/>Description</u> | <u>Areal<br/>Density<br/>(oz/sq ft)</u> | <u><math>V_{50}</math><br/>(ft/sec)</u> | <u>High<br/>Partial<br/>(ft/sec)</u> | <u>Low<br/>Complete<br/>(ft/sec)</u> |
|---------------------------------|---|---|--------------------------------------|--------------------------------------|
| Lucite PMMA<br>Mounting Powder  | 36.2                                    | 1096<br>(4 shot)                        | 1071                                 | 1122                                 |
| Plex 55 PMMA<br>(control)       | 37.4                                    | 1040<br>(8 shot)                        | 1015                                 | 1072                                 |
| Lexan<br>Press Molded           | 24.5                                    | 900<br>(6 shot)                         | 915                                  | 900                                  |
| Lexan<br>(control)              | 25.4                                    | 905<br>(6 shot)                         | 908                                  | 899                                  |

\*17 grain F.S.P., 0° obliquity



Thermally bonded Plex/Lex laminate, rear view. Note Lexan back-up has spalled under impact.

ARMY MATERIALS AND MECHANICS RESEARCH CENTER

19-066-155/AMC-72

It is evident from these data that the thermal treatment was not responsible for the degradation in ballistic resistance. Rather, it is apparently due to the absence of an interlayer. The interlayer, which may be either an adhesive or an air gap (as in the case of the clamped samples), prevents the polycarbonate from spalling.

The next step, then, was to investigate the effects of various adhesive interlayers.

#### ADHESIVE BONDING, BRITTLE INTERLAYER

Several brittle interlayers were evaluated. Typical of these was a commercially available epoxy adhesive, EPON 828 cured with 13 pph DEH24. A 12" x 12" laminate (2 PMMA: 1 PC) was fabricated using this adhesive system and tested ballistically. A complete penetration was obtained at 1291 ft/sec with a 6" diameter area of delamination. Damage to the facing Plexiglas was minimal, but the polycarbonate cracked and also spalled, unlike its normal ductile performance.

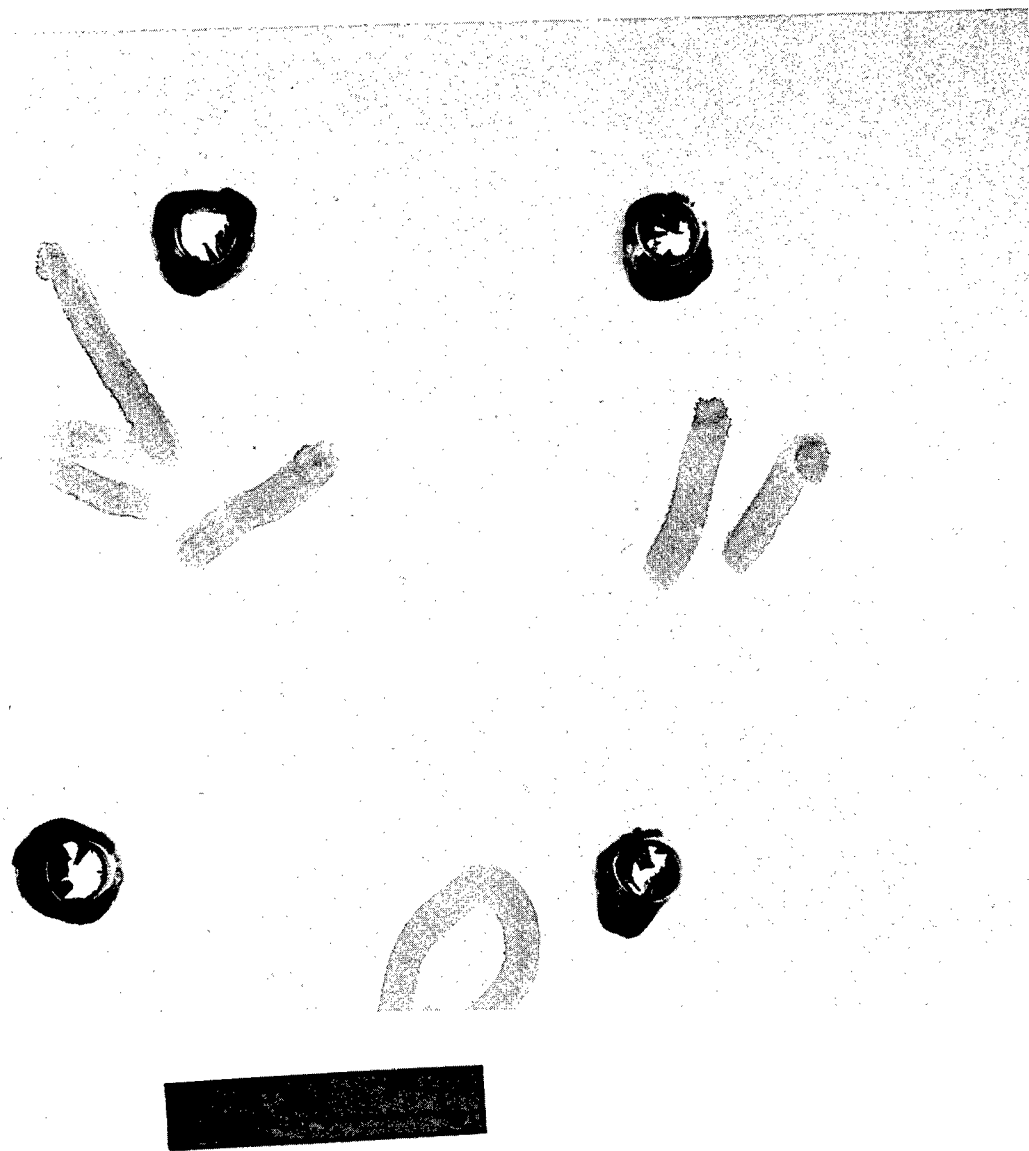
In an effort to explain the reason for this degradation a 12" x 12" sample of 1/8" Lexan was coated with a 15 mil thick layer of the EPON 828 adhesive. The ballistic resistance is given in Table II together with that of a control piece of Lexan.

TABLE II  
BALLISTIC BEHAVIOR OF LEXAN\*

|                          | <u>Lexan with<br/>EPON 828 Coating</u> | <u>Control Lexan<br/>(No Coating)</u> |
|--------------------------|--|---------------------------------------|
| V <sub>50</sub> (ft/sec) | 682 (10 shot)                          | 767 (8 shot)                          |
| High Partial             | 714                                    | 771                                   |
| Low Complete             | 639                                    | 753                                   |
| Areal Density            | 14.2 (12.8 Lexan<br>+ 1.4 EPON 828)    | 12.8                                  |

\*17 grain F.S.P., 0° obliquity, coating facing impact

There occurred about a 10% decrease in V<sub>50</sub> but a much larger overlay between partial and complete penetrations. In addition, the adhesive-coated Lexan spalled badly, quite unlike the normal ductile impact behavior (see Figures 7 & 8). Some of the adhesive was then removed from the Lexan, and the sample was reimpacted. The ductile behavior returned indicating that the adhesive had not chemically affected the polycarbonate. Apparently then, even a thin layer of brittle material is sufficient to affect the ductility and thus to lower the ballistic resistance of polycarbonate itself and of a laminate containing polycarbonate.



**UNCOATED LEXAN SUBJECTED TO BALLISTIC IMPACT**  
ARMY MATERIALS AND MECHANICS RESEARCH CENTER

19-066-56/AMC-73



EPON 828 COATED LEXAN SUBJECTED TO BALLISTIC IMPACT  
ARMY MATERIALS AND MECHANICS RESEARCH CENTER  
19-066-55/AMC-73

The poor ballistic behavior obtained with the brittle epoxies made it obvious that a more flexible adhesive was required.

#### ADHESIVE BONDING, FLEXIBLE INTERLAYER

##### a. Survey

Several commercially available adhesives were evaluated. The results are given in Table III.

TABLE III  
BALLISTIC BEHAVIOR OF PLEX/LEX LAMINATES  
WITH COMMERCIAL ADHESIVES\*

| <u>Adhesive</u>  | <u>Areal<br/>Density<br/>(oz/sq ft)</u> | <u>V<sub>50</sub><br/>(ft/sec)</u> | <u>High<br/>Partial<br/>(ft/sec)</u>          | <u>Low<br/>Complete<br/>(ft/sec)</u> |
|--|---|------------------------------------|---|--------------------------------------|
| Silastic - Si Rubber<br>(milky white)                  | 39.5                                    | 1496<br>(4 shot)                   | 1487  | 1493                                 |
| Silastic - Si Rubber**<br>(milky white)                | 38.0                                    |                                    | 1255  | 1427                                 |
| Silastic - Si Rubber<br>(experimental clear)           | 39.8                                    |                                    | 1340<br>(samples delaminated<br>after 1 shot) |                                      |
| Silastic - Si Rubber<br>(white opaque)                 | 40.3                                    |                                    | 1538  |                                      |
| Uralane 5716<br>Polyurethane<br>(Brownish-Transparent) | 39.7                                    |                                    | 1431<br>(samples delaminated<br>after 1 shot) | 1504                                 |
| Desmocoll 400<br>Polyurethane<br>(white)               | 39.8                                    | 1429<br>(4 shot)                   | 1437  | 1437                                 |

\*17 grain F.S.P., 0° obliquity, 1/4" Plexiglas laminated to 1/8" Lexan

\*\*Double laminate - 1/8" Plex/1/16" Lexan/1/8" Plex/1/16" Lexan

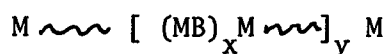
It is apparent that these flexible adhesives are substantially better ballistically than the epoxies and are all superior to the samples with no adhesive interlayer in Figure 1. However, each adhesive has a serious drawback. The Silastics are generally white or milky white and not optically acceptable, and the experimental clear Silastic delaminated after one shot. The Uralane 5716 cast in place polyurethane does not give very



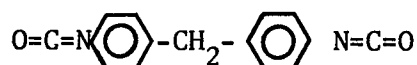
good adhesion, and total delamination occurs with one impact. The Desmocoll 400, a linear aliphatic polyurethane, is theoretically transparent but actually turned out to be white and optically unacceptable. Since the polyurethanes appeared to give good ballistic results a program was initiated to prepare systematically varied materials.

#### b. Synthesis and Composition

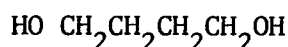
A standard two step synthesis was used to prepare three series of adhesive polymers. The general structure may be represented as



where M is MDI



B is 1,4 Butanediol



$\sim$  is a polymeric glycol

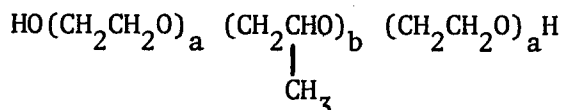


Table IV shows the variation in composition and structure of the available polymeric glycols.

TABLE IV  
GLYCOL COMPOSITION AND STRUCTURE

| <u>Glycol</u> | <u>Composition</u> | <u>a</u> | <u>b</u> |
|---------------|--------------------|----------|----------|
| C1540         | 100% PEG           | 0        | 35       |
| L35           | 50/50 PPG/PEG      | 11       | 17       |
| L44           | 60/40 PPG/PEG      | 10       | 23       |
| L43           | 70/30 PPG/PEG      | 6        | 23       |
| L42           | 80/20 PPG/PEG      | 3        | 22       |
| L61           | 90/10 PPG/PEG      | 2        | 33       |
| P2010         | 100% PPG           | 34       | 0        |

All three series had y held constant. Series I was made using L35 as the glycol and varying x from 0 to 1.0 at intervals of 0.2. Series II was made holding x constant at 0.4 and making polymers using each of the seven polymeric glycols for the soft segment. Series III was similar to series II except that x = 0.5.

Two additional polymers were evaluated both of composition 3.2 MDI; 2 Butanediol; 1 Glycol. One had a soft segment of molecular weight 1000 ( $a = 1$ ,  $b = 17$ ) and the other a soft segment of molecular weight 2000 ( $a = 11$ ,  $b = 17$ ).

c. Description and Characterization

The first series of polymers ranged from extremely sticky with very little elastomeric behavior to slightly tacky with very little permanent set, Table V.

TABLE V

VARIATION OF HARD SEGMENT

| MDI   | Butanediol | Glycol | Description   | $\bar{M}_n$ |
|-------|------------|--------|---|-------------|
| 1.05  | 0          | 1      | sticky, gradual flow, set, transparent                  | 30,000      |
| 1.261 | 0.2        | 1      | sticky, set, slightly elastomeric, transparent          | 39,000      |
| 1.471 | 0.4        | 1      | tacky, less set, elastomeric, transparent               | 40,000      |
| 1.576 | 0.5        | 1      | less tacky, still some set, elastomeric, transparent    | 40,000      |
| 1.681 | 0.6        | 1      | slightly tacky, very little set, elastomer, transparent | 41,000      |
| 1.891 | 0.8        | 1      | little tack, very little set, elastomer, translucent    | 42,000      |
| 2.1   | 1          | 1      | non tacky, no rapid set, elastomer, translucent         | 45,000      |

From  $x = 0.0$  to  $x = 0.6$  the polymers were transparent becoming translucent at  $x = 0.8$  and  $1.0$ . The molecular weights of all but  $x = 0$  are  $\sim 40,000$  so that the gradual change in tackiness, elastomeric properties and transparency must be due to change in structure due to increasing butanediol content. Differential scanning calorimetry was performed to determine  $T_g$  to see if there was any change with structure which might be related to ballistic performance.  $T_g$  shows a monotonic increase with increasing butanediol content (Figure 9) over a  $15^\circ\text{C}$  temperature range. Leveling off of  $T_g$  occurs above the butanediol content which remains transparent.

Table VI summarizes the properties of series II and III.

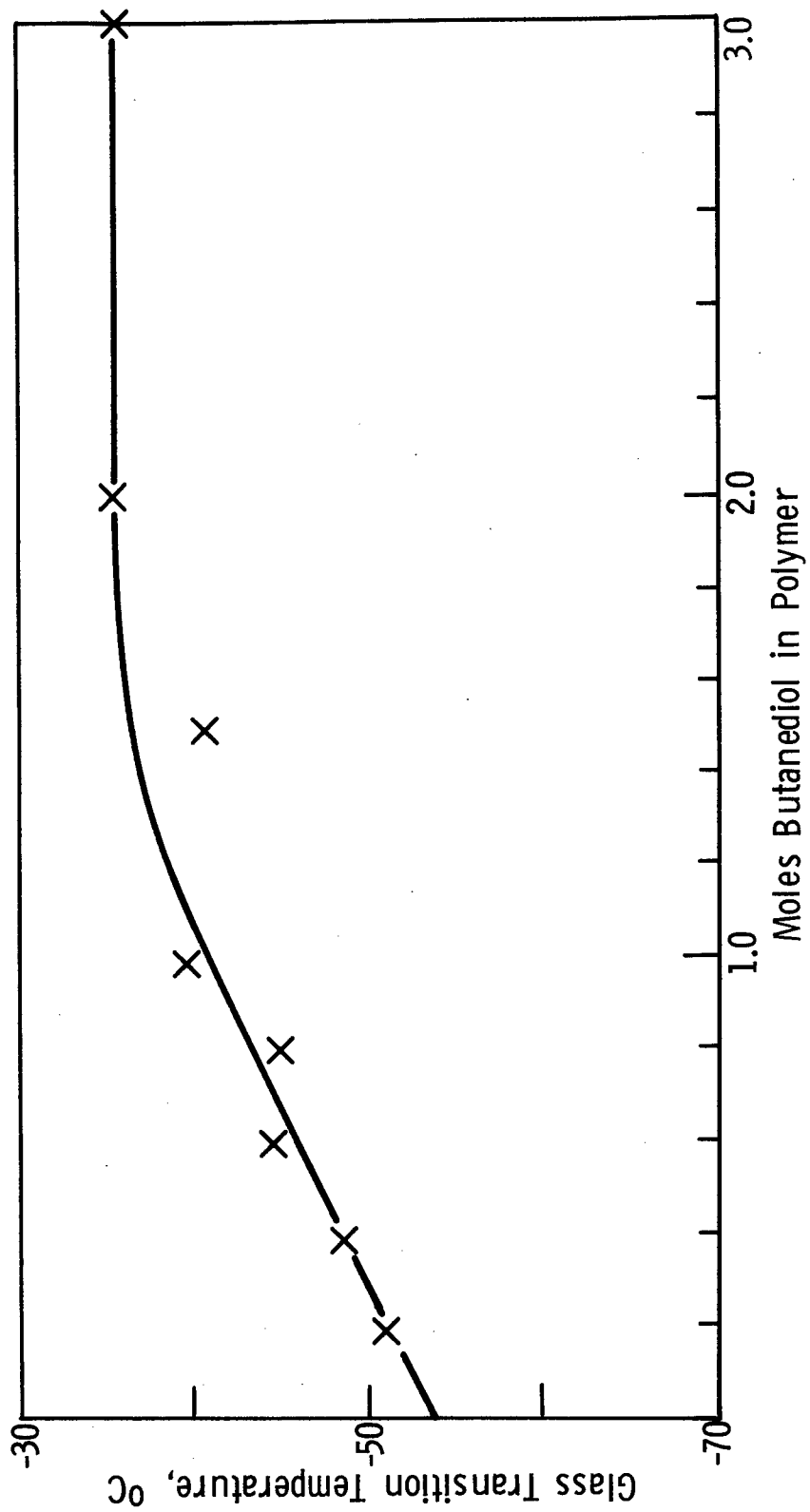


TABLE VI  
PROPERTIES OF SERIES II AND III

| <u>Glycol</u> | Series II  | Series III   |
|---------------|--|--|
|               | <u>1.471 MDI: 0.4 B'd: 1 glycol</u>                | <u>1.576 MDI: 0.4 B'd: 1 glycol</u>                |
| 100% PEG      | tacky, opaque in bulk<br>(transparent in laminate) | tacky, opaque in bulk<br>(transparent in laminate) |
| 50/50 PPG/PEG | tacky, transparent                                 | tacky, transparent                                 |
| 60/40 PPG/PEG | tacky, transparent                                 | tacky, translucent                                 |
| 70/30 PPG/PEG | sticky to tacky, transparent                       | tacky, transparent                                 |
| 80/20 PPG/PEG | sticky, transparent                                | sticky to tacky, transparent                       |
| 90/10 PPG/PEG | sticky, translucent                                | sticky, translucent                                |
| 100% PPG      | very sticky, translucent                           | sticky, translucent                                |

It appears that increasing amounts of polypropylene glycol in soft segments of around 2000 molecular weight leads to translucency at lower butanediol content.

T<sub>g</sub> behavior of these series showed no meaningful change.

Both samples with high MDI content were opaque. The polymer with the lower molecular weight soft segment showed some embrittlement as compared to the other.

d. Ballistic Resistance of Laminates

Laminates from 1/4" Plexiglas 55, 10 mil adhesive, 1/8" Lexan were fabricated at press conditions of 4000 lb. ram force over a 4" diameter ram at 95°C for 40 minutes residence time. The results of ballistic evaluation are shown in Table VII.

TABLE VII  
EFFECT OF BUTANEDIOL CONTENT ON BALLISTIC PERFORMANCE

| <u>Polymer Series I</u><br><u>Butanediol Content</u> | <u>V<sub>50</sub></u> | <u>Optical</u><br><u>Properties</u> |
|--|-----------------------|-------------------------------------|
| 0.0  | 1560                  | clear                               |
| 0.2  | 1570, 1600**          | clear                               |
| 0.4  | 1510                  | clear                               |
| 0.5  | 1550, 1580**          | clear                               |
| 0.6  | 1560                  | clear                               |
| 1.0  | 1410                  | translucent                         |

\*17 grain F.S.P., 0° obliquity, Plexiglas facing, 8 shot V<sub>50</sub>

\*\*Determination of V<sub>50</sub> for duplicate polymers

As long as the materials remain transparent the  $V_{50}$ 's of the laminates are essentially the same for this polymeric glycol. At sufficiently high butanediol content to give loss of transparency the  $V_{50}$  drops. The 1,0 butanediol content polymer was non-tacky, indicating some embrittlement. The lowered ballistic performance is in agreement qualitatively with earlier observations on the effect of brittle adhesives. Very small areas of delamination were observed with the synthesized transparent polymers in contrast to those commercially available. These adhesives showed definite improvement ballistically over the earlier survey.

As seen in Table VIII the structure of the polymeric glycol (molecular weight  $\sim 2000$ ) at constant MDI and butanediol composition had no significant effect on the ballistic performance of the laminates. These polymers were all transparent at the 10 mil thickness of the adhesive layer used for laminate evaluation.

TABLE VIII

EFFECT OF VARIATION OF POLYMERIC GLYCOL SERIES II & III

| <u>Glycol</u> | <u><math>V_{50}</math> (ft/sec)</u>          |   |
|---------------|--|---|
|               | <u>Series II</u><br>1.47 MDI:0.4Bd: 1 glycol | <u>Series III</u><br>1.576 MDI:0.5 Bd: 1 glycol |
| 100% PEG      | 1580   | 1584  |
| 50/50 PPG/PEG | 1510   | 1550, 1580**                                    |
| 60/40 PPG/PEG | ----   | 1585  |
| 70/30 PPG/PEG | 1586   | 1584  |
| 80/20 PPG/PEG | 1626   | 1581  |
| 90/10 PPG/PEG | 1592   | 1602  |
| 100% PPG      | ----   | 1580  |

\*17 grain F.S.P., 0° obliquity, Plexiglas facing

\*\*Determination of  $V_{50}$  for duplicate polymers

At another composition, i.e., 3.2 MDI: 2 Butanediol: 1 Polymeric Glycol a  $V_{50}$  of 1300 ft/sec was determined for a polymer with glycol 90/10 PPG/PEG 1000 molecular weight vs a  $V_{50}$  of 1550 ft/sec for a polymer with glycol 50/50 PPG/PEG 2000 molecular weight. Since changing the ratio of PPG showed no effect on ballistic behavior we conclude that halving the length of the glycol has drastically affected the performance of the laminate.

#### e. Effect of Adhesive Bond Strength

An industrial proprietary adhesive to bond polycarbonate to glass and other plastics was evaluated in the Plexiglas/Lexan system. Two configurations were investigated referred to here as Type A and Type B to

determine the effect of bond strength upon ballistic performance. The strength of the adhesive bond was markedly dependent upon laminating temperature. Samples were fabricated using 10 mil Type B and 5 mil Type A adhesive at 4 different temperatures. These samples were evaluated ballistically and by the cross-lap tensile adhesion test ASTM D1344. This test uses a 1 square inch cross section of adhesive between crossed adherends. The value of the peak load is a measure of the strength of the adhesive bond. The results of the adhesion test are shown in Figure 10.

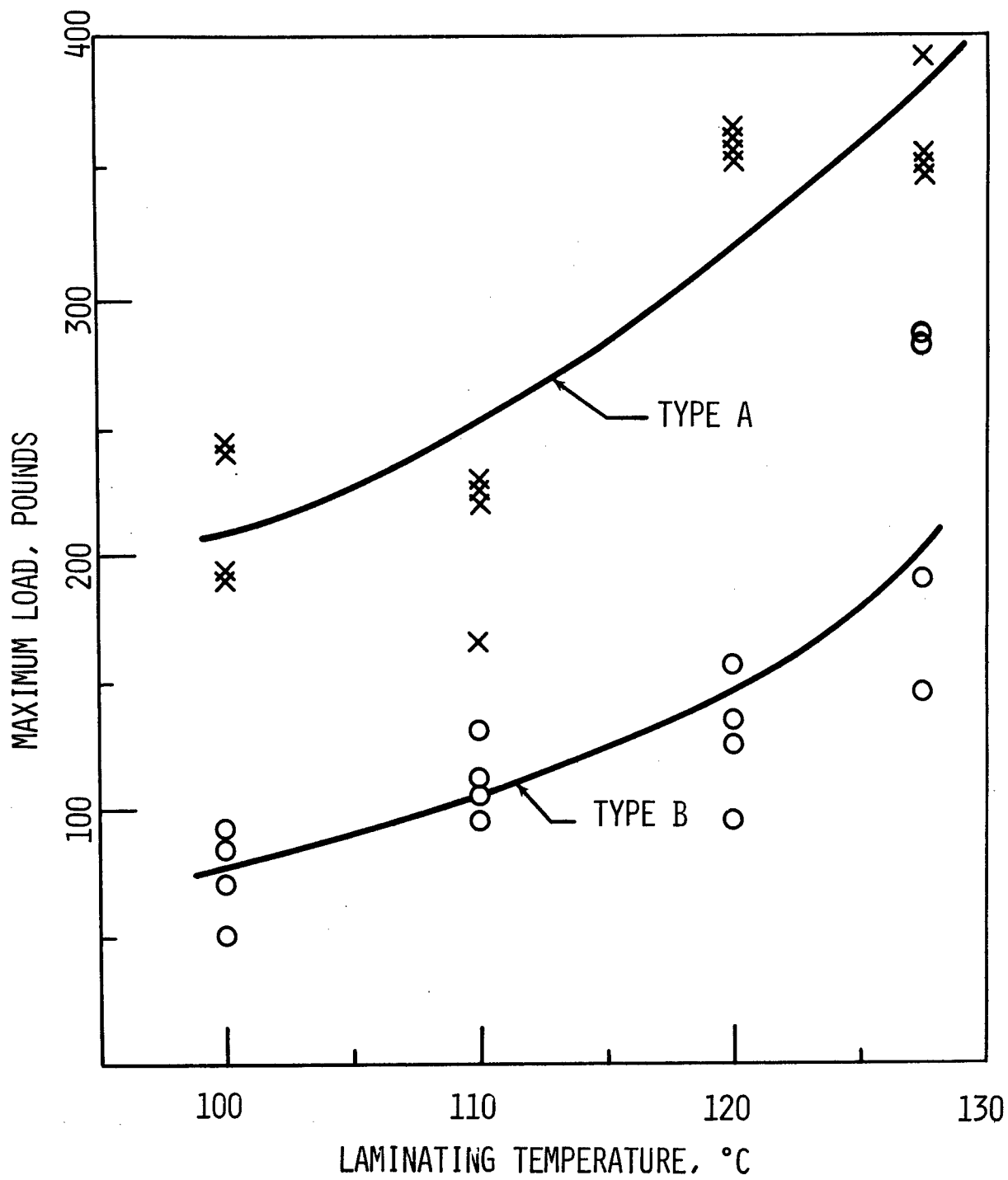
It can be seen that over the range of temperatures investigated there is a two fold increase in the maximum load, while the Type A adhesive has twice the tensile peak load as Type B, in qualitative agreement with peel tests using modified ASTM D903. The ballistic behavior is shown in Table IX.

TABLE IX  
BALLISTIC\* PERFORMANCE VS. LAMINATING TEMP

| Type of Adhesive | Laminating Temp.<br>°C | 4 shot V <sub>50</sub><br>fps |
|------------------|------------------------|-------------------------------|
| Type A 5 mil     | 100                    | 1625                          |
| Type A 5 mil     | 110                    | 1626                          |
| Type A 5 mil     | 120                    | 1645                          |
| Type A 5 mil     | 130                    | 1635                          |
| Type B 10 mil    | 100                    | 1605                          |
| Type B 10 mil    | 110                    | 1600                          |
| Type B 10 mil    | 120                    | 1613                          |
| Type B 10 mil    | 130                    | 1630                          |

\*Data obtained on 1/4" Plex 55 laminated to 1/8" Lexan, Type A adhesive = 275 psi, Type B adhesive = 500-600 psi pressure, 17 grain FSP, 0° obliquity.

Thus, it is evident that for the Plex/Lex system the strength of the adhesive bond does not affect the ballistic performance. Apparently, considering the marked effect of type of adhesive, it is the mechanical properties of the adhesive per se and not its adhesiveness, so long as delamination does not occur, that is the important parameter in determining the ballistic response.



References:

(1) Roylance, M. E., and Lewis, R. W., "Development of Transparent Polymers for Armor," AMMRC Technical Report, TR72-23 (1972).

(2) Parsons, G., and Lewis, R., "Ballistic Performance of Transparent Materials for Visor Applications," AMMRC Technical Report, TR72-36 (1972).

Acknowledgement:

The authors wish to thank Mr. Joseph M. Rogers for carrying out the ballistic tests and Mr. Richard W. Matton for preparing the urethane polymers.



PLEXIGLAS 70 - A NEW HIGH IMPACT PLASTIC

W. E. Feely  
Rohm and Haas Company  
Bristol, Pennsylvania

Paper not presented at Conference and unavailable  
for publication

## INTERLAYER NEEDS FOR SUBSONIC WINDSHIELDS

George Bickford  
The Boeing Commercial Airplane Company  
Seattle, Washington

## **INTERLAYER NEEDS FOR SUBSONIC WINDSHIELDS**

by George Bickford

The Boeing Commercial Airplane Company  
Seattle, Washington

### **ABSTRACT**

Windshield reliability is primarily related to interlayer characteristics. This is as true today as it was 25 years ago, and the predominant interlayer is PVB, as it was then. This paper reviews some interlayer history, the peculiar thermal behavior of PVB, probable failure mechanics, and design methods which reduce thermal stress damage. Desirable interlayer qualities are discussed, together with some comparative testing of other materials.

## INTRODUCTION

Interlayers have contributed directly or indirectly to most windshield service failures. This paper reviews interlayer functions, probable failure mechanisms, and the need for change. Discussion is limited to forward-facing, bird-resistant windshields, since these encompass the most severe requirements. It is also limited to subsonic airplanes, because these differ distinctly from supersonic airplanes, and also because they represent the major share of yearly flight hours of both military and nonmilitary airplanes.

### EARLY HISTORY OF PVB/GLASS WINDSHIELDS

In the 1930s PVB (polyvinyl butyral) became the standard interlayer for automobile safety windows because of its toughness, clarity, and excellent bond to glass. It also became the standard for aircraft, and remains so today. The 1940s saw two important advances which made aircraft windshield behavior more complex. These were:

- (1) A thick membrane for bird resistance and pressure fail-safe.
- (2) A conductive coating for heating.

In 1950, Kangas and Pigman of the CAA published their definitive work on bird impact (Reference 1), setting the practice for a generation of windshields. They established an optimum PVB plasticizer content of 20% and a useful impact resistance range of approximately 80° to 120°F.

There thus emerged a glass/PVB membrane type of windshield (so-called bird-bagging), examples of which are shown in Figures 1 and 2. These are representative of windshields used in airplanes of the 1950s and 1960s, including the vast production of the late 1960s. These airplanes have a long service life ahead.

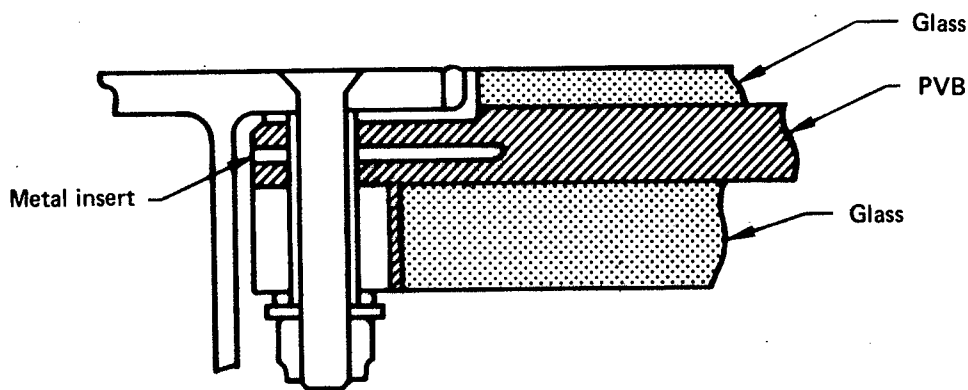


FIGURE 1.—707/727/737 WINDSHIELD

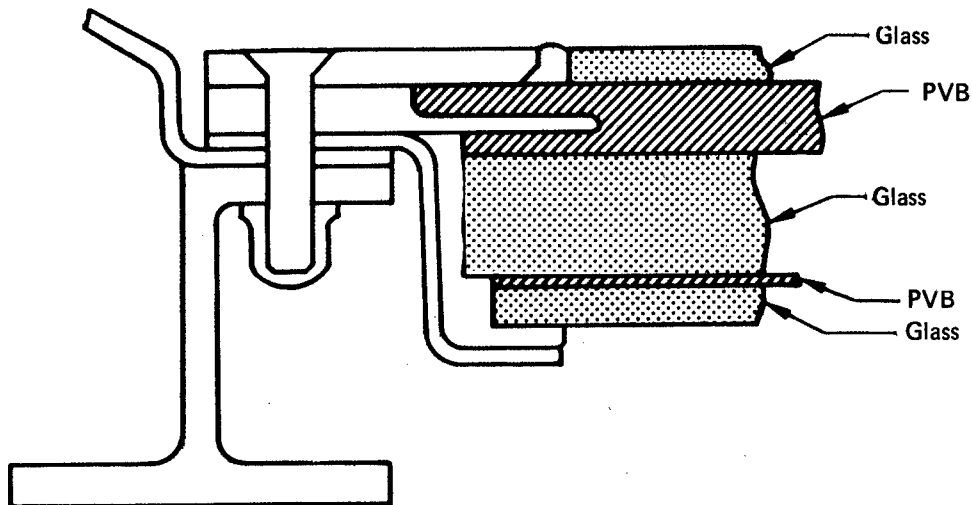


FIGURE 2.—DC-9 WINDSHIELD (ALSO ON STRETCHED DC-8)

### PVB SERVICE PERFORMANCE

Windshields of the B-52 and early Boeing commercial jets often required service replacement at less than 2,000 flight hours. Most common failures were delamination and cold chips, both associated with shrinkage of PVB. Addition of slip planes and other parting agents (Figure 3) reduced failures to a manageable level. In various forms, slip plane stress relief now appears in virtually all windshields using PVB and glass. These and other changes of heating components and controls greatly improved windshield life.

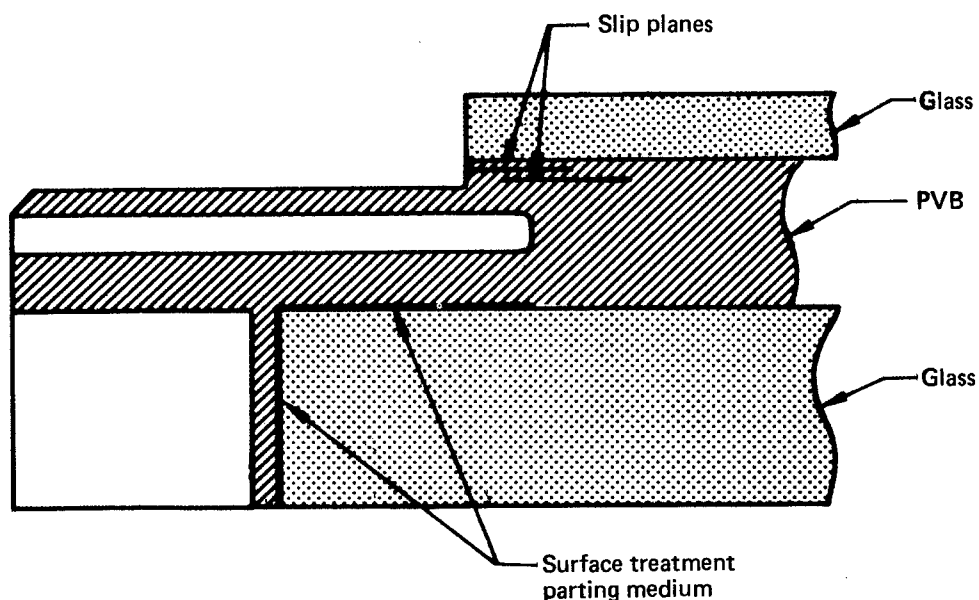


FIGURE 3.—PARTING AGENTS

The 707-727-737 windshield, representing a fleet of over 1900 airplanes, is now achieving an average life of 7,000 to 10,000 hours. It is instructive to note, however, that failures still relate mainly to PVB. In 1971, vinyl cracks, cold chips, and delamination accounted for 80% of warranty claims.

Two carriers have published significant studies of windshield replacements. A 1971 Eastern Airlines report (Reference 2) covers experience with 707, 727, DC-8, and DC-9 for a number of carriers in 1970 and part of 1971. 1971 SAS reports (Reference 3) cover SAS DC-8 and DC-9 removals in 1969 and 1970. These two independent studies each assign about 30% of failures to delamination and about 40% to arcs and arc cracks. Many carriers express unhappiness with windshield life. An interesting exception is the Convair 880, for which one carrier reports a 15,000- to 17,000-hour life. We will return to this later to see what can be learned.

Today, the principal failure modes are still related directly or indirectly to PVB. They are:

- Delamination
- Cold chips
- Vinyl cracks
- Arcing and cracks

## FAILURE MECHANICS

It is helpful to look once again at some properties of aircraft PVB, which is a remarkable material, but which has some disturbing tendencies when cold. At 110°F it is soft as a rubber band, but at -40°F it is like a piece of acrylic. This, coupled with the great difference in coefficient of thermal expansion ( $\alpha$ ) between PVB and glass, is largely the story of windshield service failures. Figure 4 shows some pertinent physical properties of PVB. Note the narrow range of effective pliability, the very rapid increase in tensile modulus (E) below room temperature, and the wide difference in  $\alpha$  between glass and PVB at all temperatures.

Figure 5 shows a plan view of the 707 windshield. Primary problem areas are along the short sides and at acute corners, which are the coldest. However, even when the pane is heated, the entire periphery is cold because of the rapid extraction of heat by the metal structure, metal PVB insert, and mounting bolts. The cold PVB areas, which are stiff and shrinking, induce a peak shear stress of approximately 500 psi, as shown in Figure 6.

Another thermal stress mode is the "cold soak," in which windshield and structure cool down to ambient temperature after heat is turned off. Here we may lock in interface stress until the next warmup, because PVB will not flow or relieve stress much below room temperature. This stress is approximately 1,000 psi, as shown in Figure 6.

Neither of these modes alone offers a completely satisfactory explanation of delamination, or, especially, face chip pulling, because they account for interface *shear* only. Delamination is encouraged by the slip plane. In ordinary structure this slip plane would be called an extremely sharp stress raiser if the stress were normal to it. So let us look for *transverse* membrane stresses.

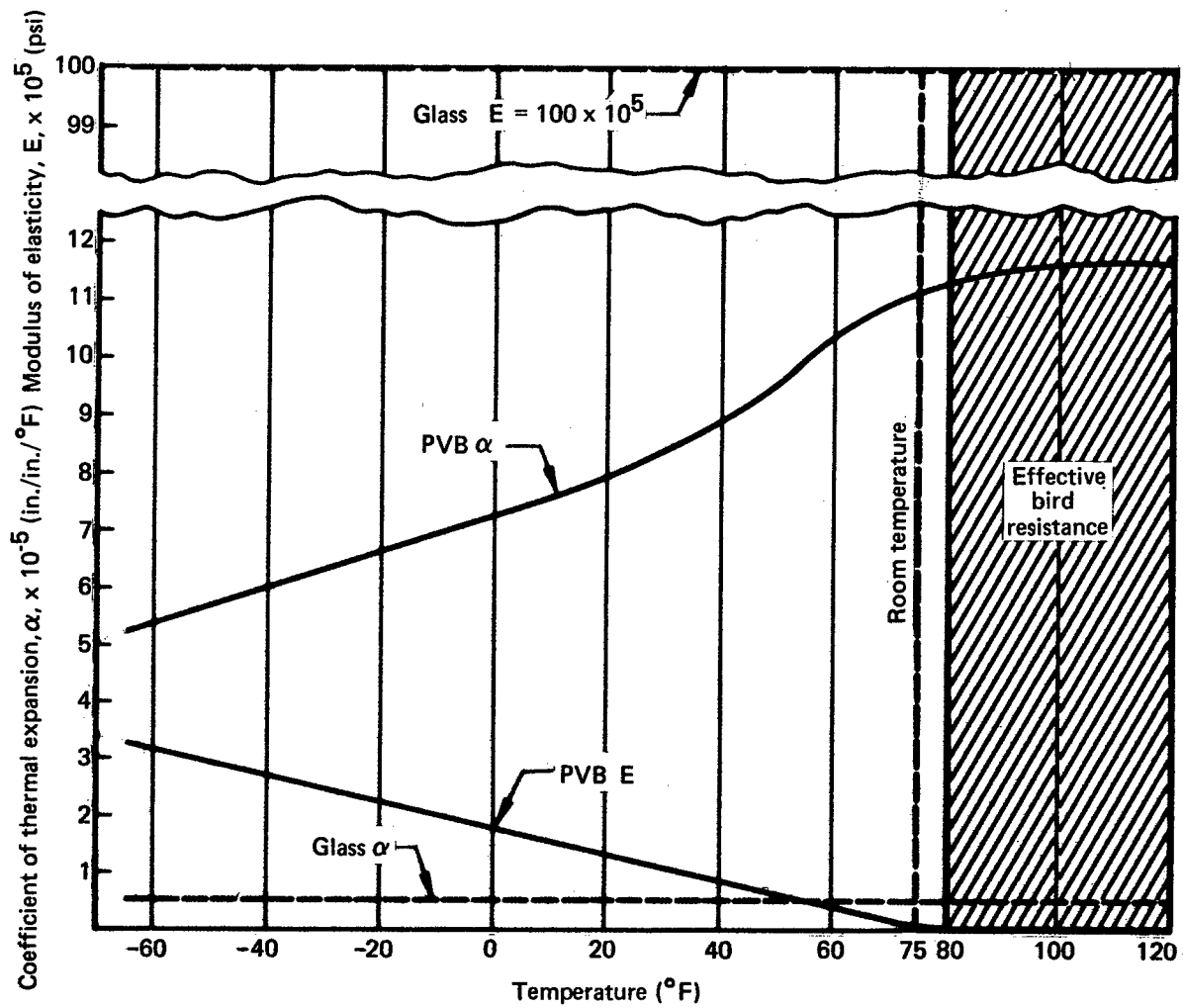


FIGURE 4.—GLASS/PVB THERMAL ELASTIC COMPARISON

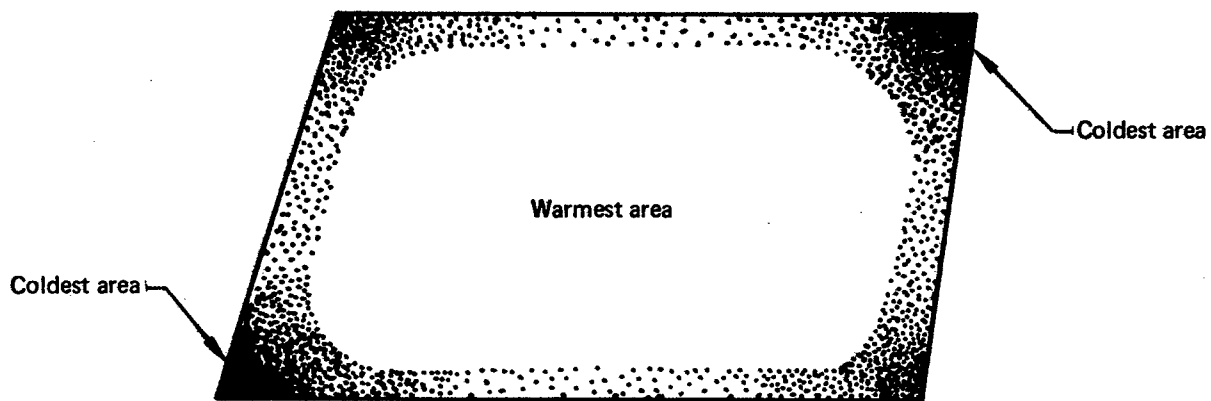


FIGURE 5.—WINDSHIELD PRIMARY AREAS OF DEFECT

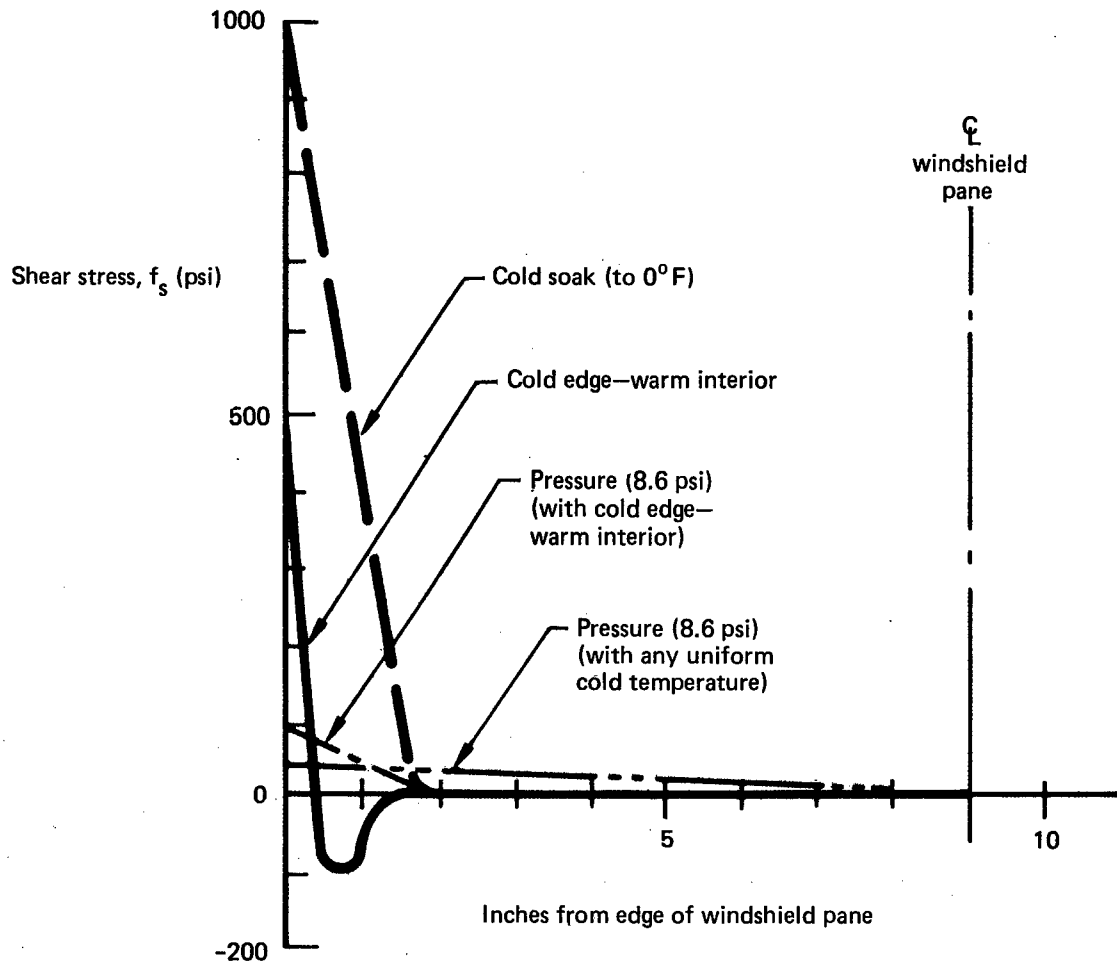


FIGURE 6.—PVB OUTER INTERFACE SHEAR STRESSES

A recent study of this problem was reported by Roberts of Triplex Safety Glass Company in a 1971 paper (Reference 4). Figure 7, adapted from that paper, shows isotherms plotted from sensors buried in the PVB of a Trident windshield. The temperature excursion of 90°F in 1.5 inches points up the stark nature of the thermal problem. This is seen as producing expansion of PVB in the hot area and shrinkage in the cold transversely to the PVB, producing the stress model shown in Figure 8.

We did not develop a stress method for this rather complicated model, which involves varying temperatures. However, delamination and pulling of face chips is made more understandable by this model than by the usual one of shear force alone. In a similar way we have found that chips are more readily pulled on flatwise tensile or offset cleavage bond tests than on similar specimens tested in shear, in which latter case internal shear failure of the PVB is more usual. This is also logical in the nature of heat-treated glass, in which strength may be said to have been added only in the X and Y direction on the surface, but not in the Z direction transversely.

Vinyl cracks, which start from the inside edge of a slip plane and progress toward the glass, appear to be another form of defect caused by forces similar to those producing delamination.



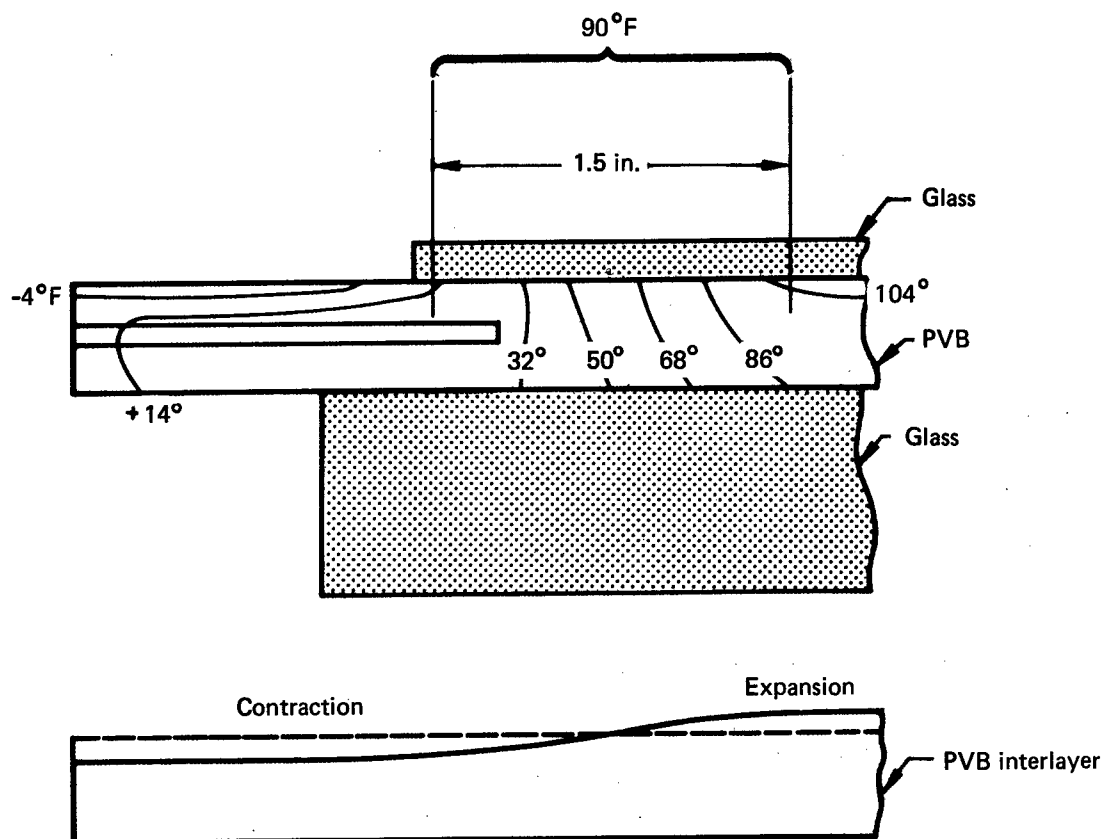


FIGURE 7.—COLD-EDGE INTERLAYER TEMPERATURE

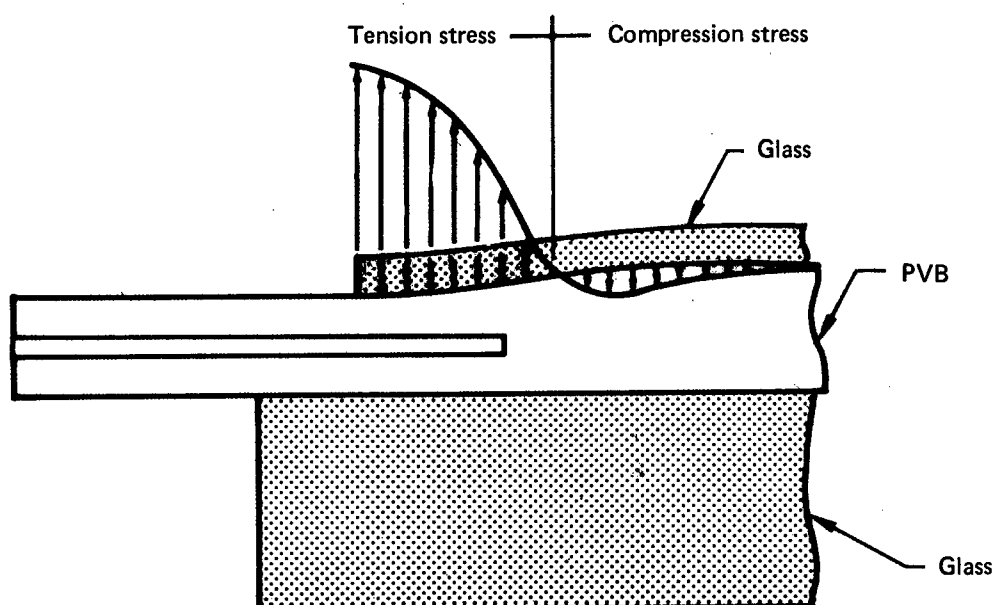


FIGURE 8.—COLD-EDGE TRANSVERSE STRESSES

We have recently examined the "cold-soak" condition, to find the nature of stresses transverse to the membrane when cooled to 0° F. This is a simpler case than that of the "cold edge," and we were able to use a finite-element computer solution, as in the previous shear stress calculations. Left to itself, the PVB would shrink in all dimensions, and its two faces would move together uniformly. However, the interface edge shear, previously noted, prevents in-plane shrinkage and puts the interior of the PVB into tension, which further reduces its thickness, except at the edge. The shape assumed by the PVB is represented in Figure 9. A peak tensile stress of 80 psi occurs a half inch from the edge. In this and previous shear calculations we have used a cool-down to 0° F as a fairly common occurrence. A cool-down to -65° F would produce approximately 50% more stress. These are not insignificant stresses, especially when repetitive. We have routinely seen chips pulled at a few hundred psi in flatwise tensile tests.

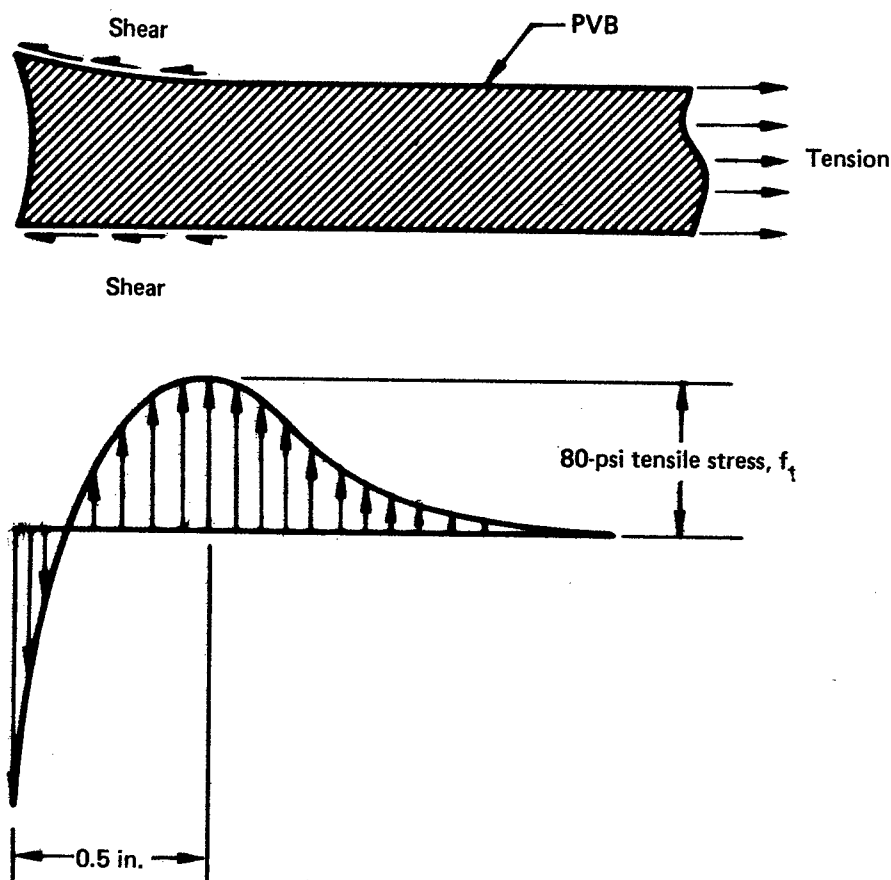


FIGURE 9.— COLD-SOAK TRANSVERSE STRESSES

In the 1961 B-52 Windshield Improvement Program, panes were cycled from hot to cold in an effort to produce failures. In *all* cases where there was chip pulling or glass breakage these were preceded by progressive delamination, often visible only with polarized light. This suggests the very pervasive nature of delamination in promoting other defects.

Weather seals have generated a great deal of discussion, and certainly they are a fertile area for improvement. Much has been said about penetration of the PVB by water at the interface or slip plane with resultant damage by hydrolysis of the coating or bus bar bond. This increases resistance, produces arcs, and eventually may cause a cracked pane. Again, what is more likely to promote water entry than a small, progressive delamination?

In a related way it is stated that water will damage PVB by replacing the plasticizer, but it is not apparent that such attack is very pronounced in the absence of delaminating forces. All operating stresses peak at or near the edge. As an example, we recently learned of an airplane pulled from the ocean off South America where it had lain since World War II. The windshield showed the milky evidence of water penetration for an inch or so around the periphery, but the interior was as clear as new.

It is fairly well established that ground-air-ground cycles are more directly damaging than total flight hours. Pressure cycle flexing of the pane has sometimes been advanced as the primary cause of damage. This deserves a closer look. Center pane deflection is perhaps 0.20 maximum, depending on temperature; angular deflection of the edge for such a case is negligible. As shown in Figure 6, the maximum pressure-induced interface shear is 100 psi for the cold-edge condition and only 50 psi for the cold-soak condition. Thus, for the case of flat panes, the evidence is not convincing that the *primary* delaminating force is pressure.

### LIVING WITH PVB

Several devices and practices have been used to moderate these stress effects. Slip planes which move peak stress to less vulnerable areas are mandatory. There are means for making heat more uniform over the pane, including coating gradation and edge heating. Separate defog and de-ice coatings are used to reduce total time at high heat on outer panes. Better sensor and control design have improved hot spot control. These are mainly methods for coping with the inherent limitations of PVB.

Concerning glass/PVB/glass lamination, note should be made of three structural details deserving of more use (see Figure 10);

- (1) *Thin interlayers:* There is evidence that thin interlayers deteriorate less. This is consistent with the previous discussion in that a thin interlayer shrinks less transversely. Also, considering in-plane shrinkage, thinner is weaker and less able to induce a bond shear failure. Careful design might reduce this to 0.06 or less; omission of a slip plane might then be possible.
- (2) *Location of structural membrane:* The structural membrane should be moved as far inboard as possible. This will produce a warmer edge.
- (3) *Nonmetallic insert:* A nonmetallic insert would reduce heat extraction from the PVB. This might even be a design improvement on some existing windshields.

In this connection, the Convair 880 windshield mentioned previously (Figure 11) has a 0.10-inch-thick outer PVB and the heavy membrane is inboard of the main pane.

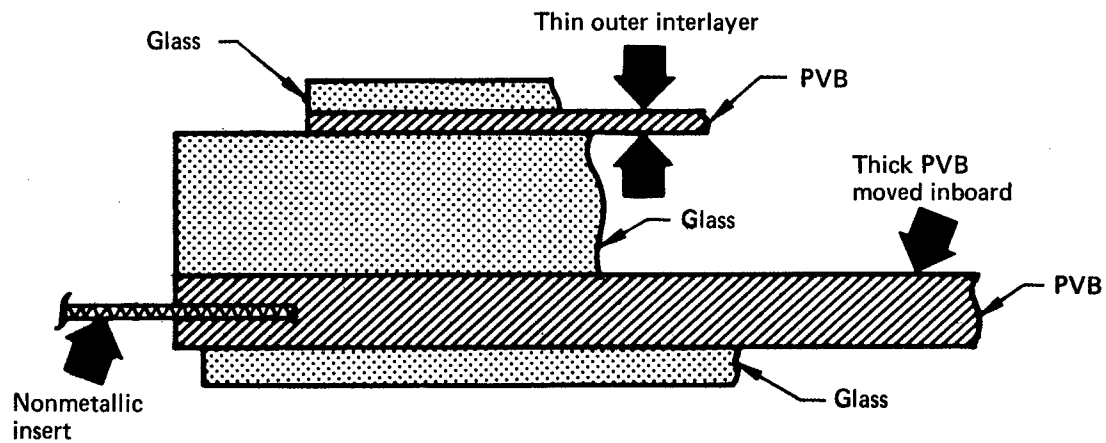


FIGURE 10.—IMPROVED PVB DESIGN

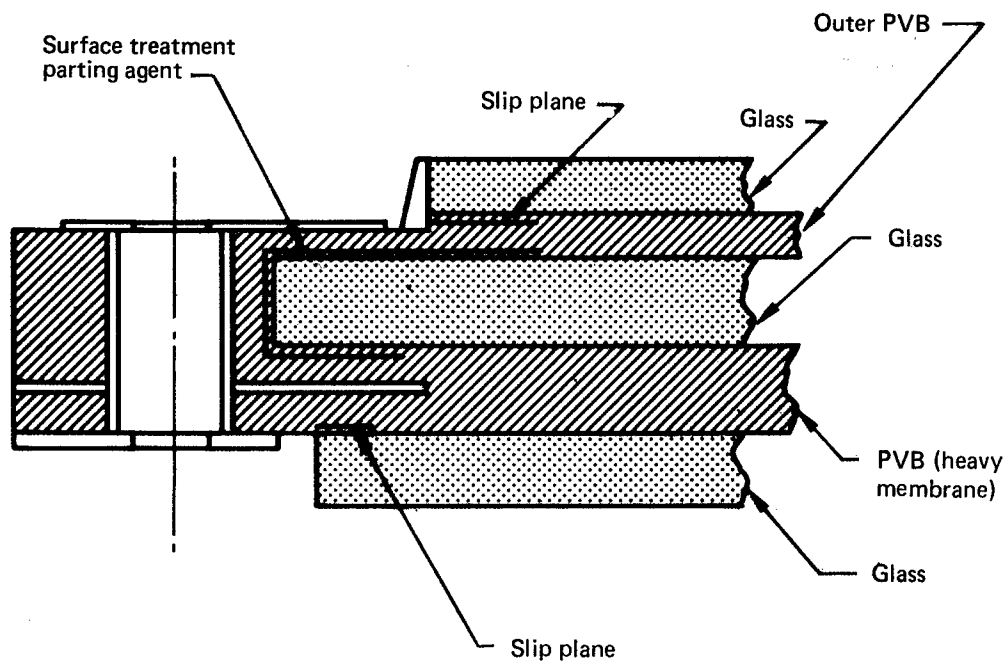


FIGURE 11.—CONVAIRE 880 WINDSHIELD

## ACRYLIC/GLASS WINDSHIELD

A very different use of PVB is in the acrylic/glass windshield used in the 747 (Figure 12). This has been well covered in the recent literature, and discussion here is limited to some thermal stress comments which have been the main theme of this paper.

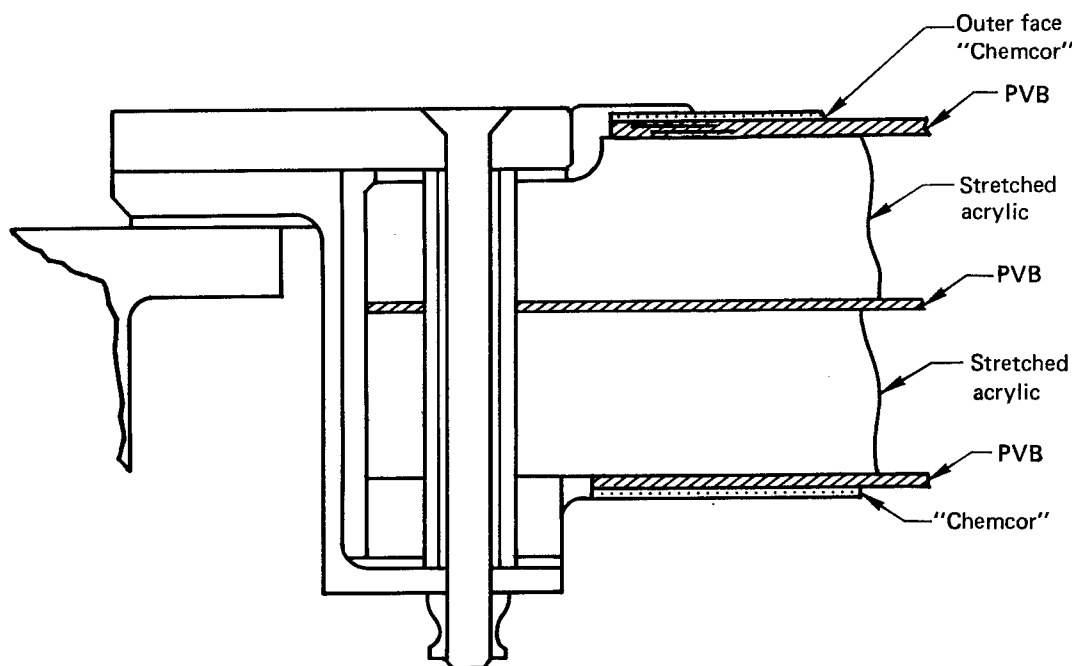


FIGURE 12.—747 WINDSHIELD

In simple terms, the 747 windshield is a thick acrylic curved shell with a thin Chemcor (Corning Glass Company chemically tempered glass) outer face. This pane, being curved, is much stiffer about one axis than the other, producing stress patterns more complex than in flat panes. Therefore, direct comparison of load effects with those from the preceding discussion is not possible. However, service defects are not totally new. Delamination and outer pane shattering have been the most common. The bond strength is lower than for normal glass/PVB/glass, because of limitations on process temperature, and this would be expected to contribute to delamination. Shattering is not so surprising, either, if we remember that what might be chip-pulling or cracking of a semi-tempered pane would be complete shattering of Chemcor, because of its inability to tolerate a local chip or crack.

Figure 13 is a sketch of the 747 pane with isotherms from the Triplex report overlaid and then extrapolated further into the acrylic. If the previous discussion of transverse shrinkage of PVB is valid, then it applies also here, because  $\alpha$  for acrylic, while lower than for PVB, is many times that of glass, and the cross-section thickness experiencing expansion and shrinkage is much greater. For this reason also the thin interlayer is not the saving feature that it is with glass/PVB/glass.

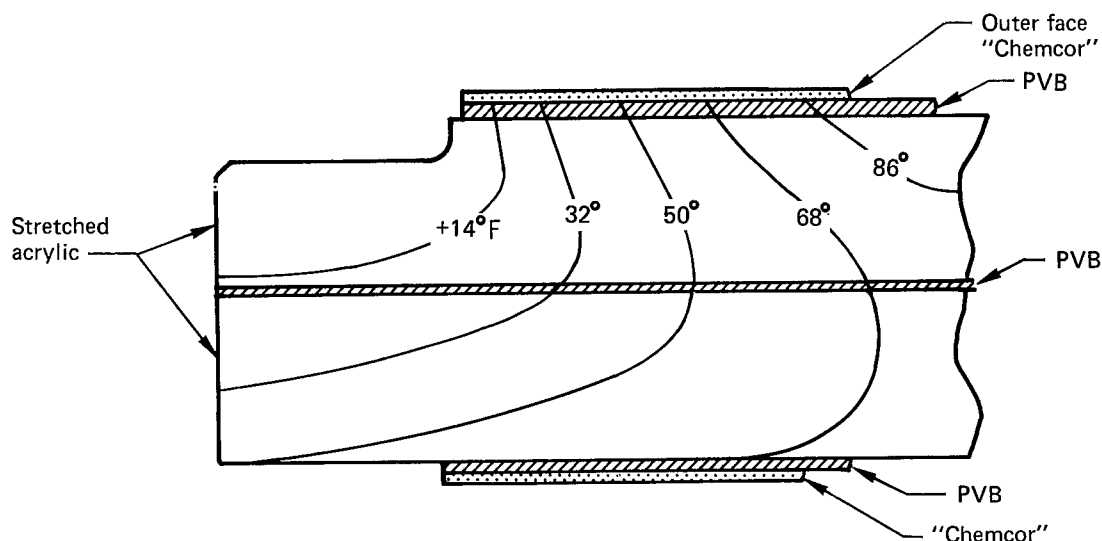


FIGURE 13.—TEMPERATURE GRADIENTS IN COLD ACRYLIC EDGE

If the earlier windshields represent a struggle between glass and thick PVB, the acrylic windshield is a struggle between glass and a thick piece of acrylic. What both types need most is an interlayer of low enough modulus at all operating temperatures to prevent a destructive build-up of large delaminating shear or tension stresses.

#### OTHER INTERLAYER MATERIALS

Interlayer research of the past generation has been directed at the very special problems of a hot, supersonic environment. New materials, mainly silicones and urethanes, have had very limited use in subsonic design. Recently we have compared seven interlayers submitted by producers, and work is continuing. So far, not all the ideal properties have appeared in one material. Combinations of two different interlayer/materials in one windshield may be entirely feasible.

In general, desirable interlayer properties are:

- (1) Clarity and color stability
- (2) Low or moderate tensile and shear modulus
- (3) Good adherence to glass and acrylic
- (4) Ability to be used without heat except for de-icing and defogging
- (5) Good tensile strength, notch toughness, and extensibility, especially if used for bird resistance, pressure fail-safe, or spall shield.

The demands upon an interlayer may be considered to increase with function in roughly the following order:

- (1) Glass to glass
- (2) Glass to acrylic
- (3) Pressure fail-safe diaphragm
- (4) Bird-resistant diaphragm

Our samples were of nominal 1/8-inch thickness. All were first subjected to a 12-inch-diameter diaphragm pressure test to 6-inch height (Figure 14). This represents a two-way tensile elongation of 57%. One sample failed this test. The hemispherical height bears a relation to the behavior of a fail-safe membrane. The radius of curvature of a flat membrane under increasing pressure decreases until it reaches hemispherical shape, at which point the radius starts increasing and growth proceeds with little or no increase in pressure, as in Figure 15. So, something less than hemispherical shape is the practical limit of fail-safe extension from a flat pane, perhaps 50% elongation or less.

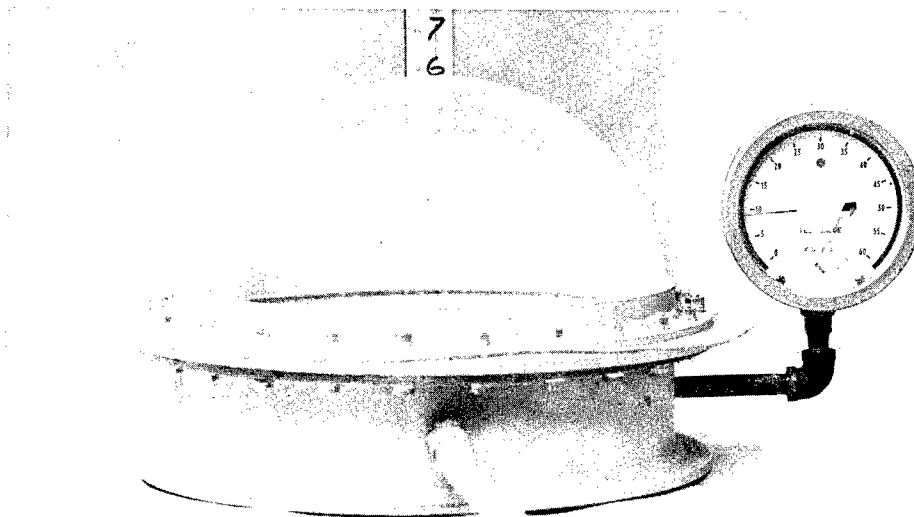


FIGURE 14.—MEMBRANE PRESSURE TEST TO HEMISPHERICAL SHAPE

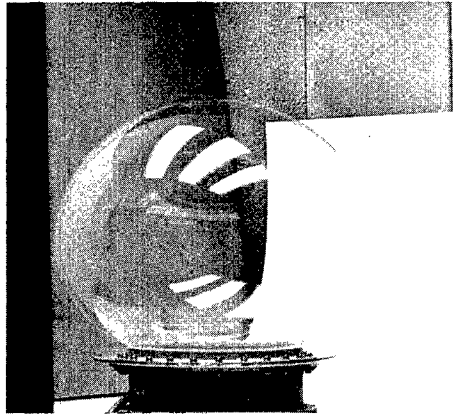


FIGURE 15.—MEMBRANE SHAPE BEYOND HEMISPHERICAL

It also appears that this test exceeds the material extension required for bird-bagging. Windshields which resist bird impact in this fashion seem to experience much less deflection than a hemispherical shape. Or, in the case of local pocketing, as occurs at the upper sill, we also see the shape of the pocket as being shallower than hemispherical.

Figure 16 shows membrane tests of two typical urethanes, a silicone, and aircraft PVB. All tests were at room temperature except for the PVB, which was at 105°F. It is perhaps of interest that the area under this curve—at least a rough approximation of energy—is similar for the PVB and the silicone.

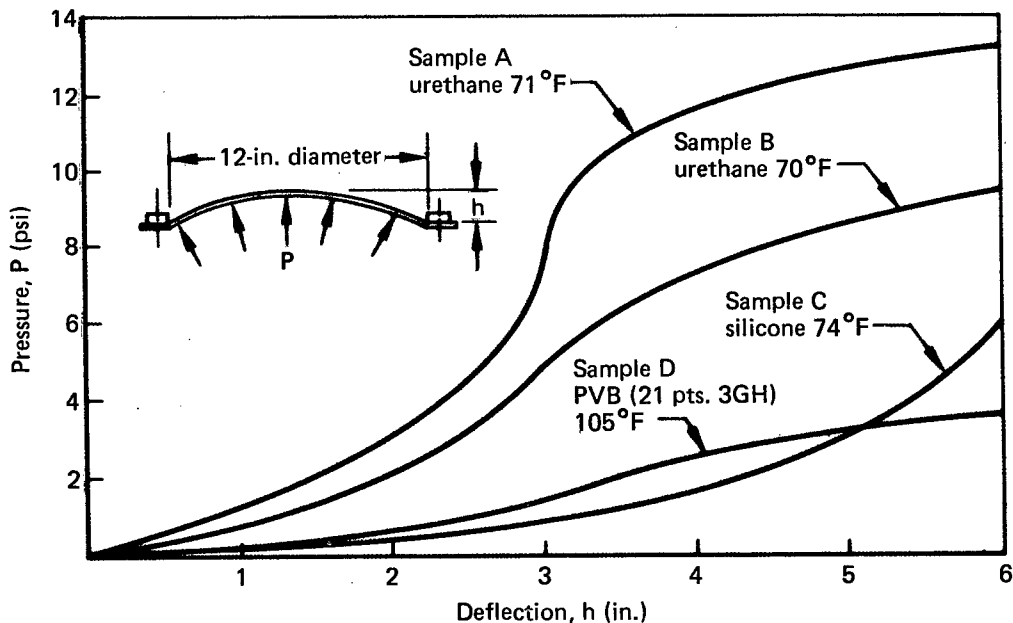


FIGURE 16.—MEMBRANE PRESSURE TESTS



Tensile tests of PVB at 105°F show only 72 psi required to produce 50% elongation. This low strength of warm PVB raises the question of how such weak material resists bird impact. At temperatures much below 75°F, the resistance of a PVB/glass windshield is dependent on the composite as a whole, because there is minimal membrane action and the PVB fails in shear. It is reasonable to assume that this resistance as a thick composite plate continues to operate at higher temperatures but that at some point shear resistance of the interlayer becomes so low and deflection so great that the glass panes fail individually as plates, and the PVB absorbs the remaining energy by membrane action. This raises a further question: Is this material, which is so low in strength at operating temperature, so unique that no other material can replace it for bird resistance or fail-safe?

Figure 17 shows E values for PVB and sample "C" silicone. Note that E differs at 0°F by an incredible factor of 770 and at -65°F by a factor of 340. If such a material as silicone were usable in other respects, it is clear that the previously discussed thermal stresses would be drastically lowered. Testing to date shows urethanes falling intermediately between these two curves, but cold tensile tests have not yet been completed. It is too early to say how well total needs are met by any of these materials.

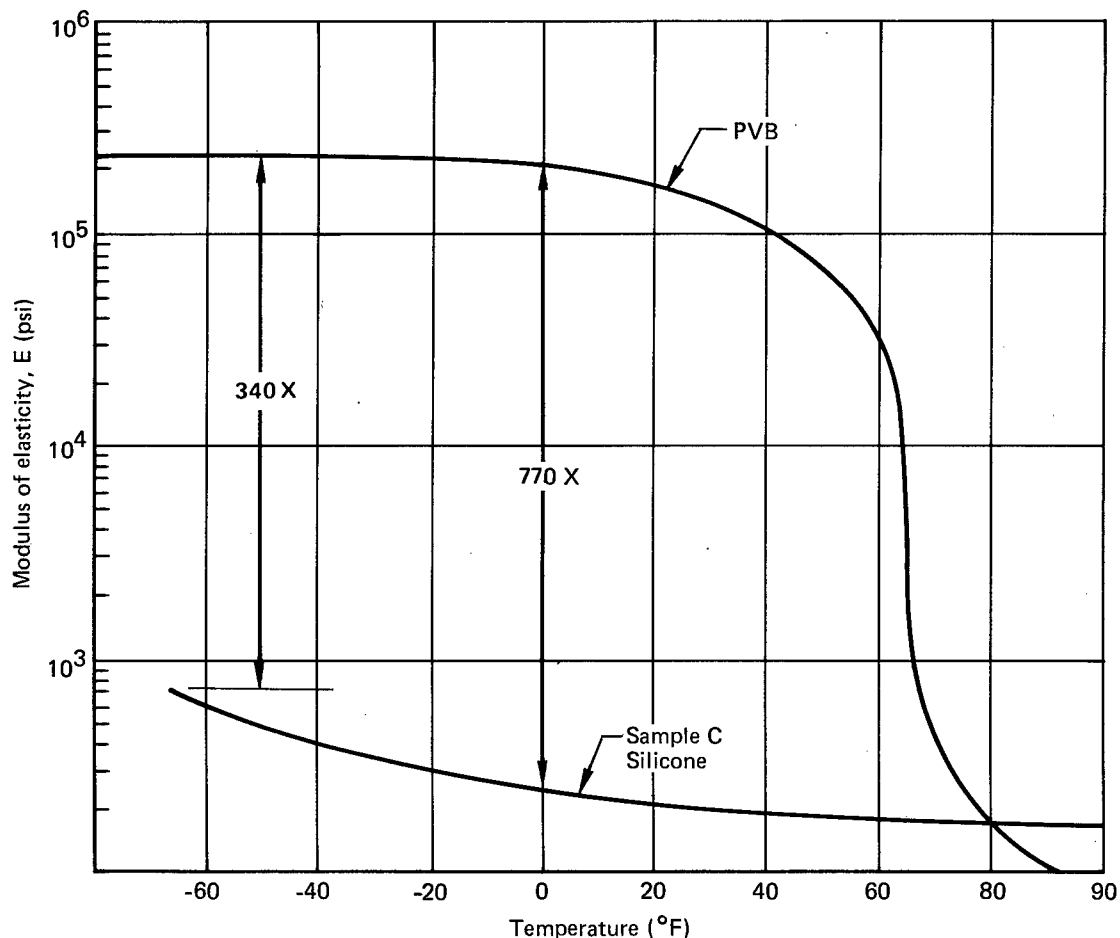
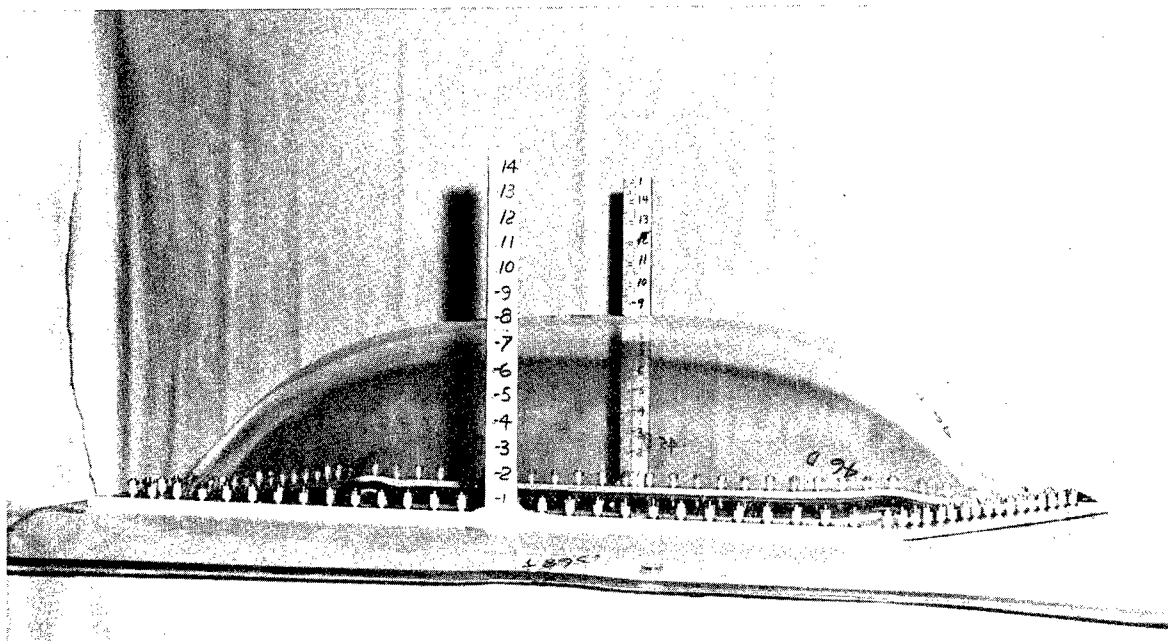


FIGURE 17.—EFFECT OF TEMPERATURE ON PVB VS SILICONE SAMPLE 'C'

Figure 18 shows silicone sample "C" in the form of a 3/8-inch-thick membrane the size and shape of a 707 windshield, pressurized to the operating pressure of 8.6 psi.



*FIGURE 18.—707 WINDSHIELD-SIZE MEMBRANE TEST*

### CONCLUSION

In this paper emphasis has been placed on thermal stress as the central problem of PVB. The need for more forgiving materials seems evident to us. Time has not permitted a rounded discussion of other materials, their physical properties, limitations of process, or cost, all of which are important. The usefulness of alternate materials is still an open question with us. We are continuing an active search in order to be aware of what is possible. We will welcome any candidate materials or data to support this effort.

## REFERENCES

- (1) Pel Kangas and George L. Pigman, *Development of Windshields to Resist Impact With Birds In Flight—Part III*, TDR No. 105, Aircraft Division, CAA, March 1950.
- (2) J. T. Timmons, *Windshield Failures*, Eastern Airlines Report No. 607, April 28, 1971.
- (3) *Technical Investigation Reports—Windshields*, SAS, CPHME-112, May 26, 1971; CPHME-116, July 20, 1971; STOTK-10427, June 16, 1971; STOTK-30, September 2, 1971.
- (4) W. G. Roberts, Triplex Safety Glass Co., Ltd., *The Development of Windscreen Reliability*, paper given at the 2nd S.B.A.C. Symposium on Optical Transparencies.

ENGINEERING DATA ON ETHYLENE TERPOLYMER  
AS AN ADHESIVE FOR POLYCARBONATE  
COMPOSITE AIRCRAFT TRANSPARENCIES

G. L. Ball and I. O. Salyer  
Monsanto Research Corporation  
Dayton, Ohio

ENGINEERING DATA ON ETHYLENE TERPOLYMER  
AS AN ADHESIVE FOR POLYCARBONATE  
COMPOSITE AIRCRAFT TRANSPARENCIES

G. L. Ball and I. O. Salyer  
Monsanto Research Corporation

Paper has been published as AFML-TR-72-109  
entitled "Engineering Data on Ethyleneterpolymer  
as an Adhesive for Polycarbonate Composite  
Aircraft Transparencies," July 1972.

INTERLAYER DESIGN FOR AIRCRAFT  
TRANSPARENCIES

Gene Nixon  
Swedlow, Inc.  
Garden Grove, California

INTERLAYER DESIGN FOR  
AIRCRAFT TRANSPARENCIES

Gene Nixon  
Manager of Engineering  
SWEDLOW, INC.

ABSTRACT

The majority of laminated transparencies fail either directly or indirectly due to interlayer delamination. Therefore, rather than discuss all the aspects of interlayer design, this paper concentrates on the design of interlayers to resist delamination.

Because laminated transparencies have, until recently, utilized polyvinylbutyral (P.V.B.) interlayer almost exclusively it is this construction which continues to delaminate. Therefore, to describe the design methodology a comparison is made between P.V.B. function and that of a silicone interlayer - Swedlow's SS-5272Y(HT).

Stresses as calculated by a finite difference approximation method are reported for a specific windshield interlayer design in both silicone and P.V.B. These stresses are supplemented by additional stresses resulting from isolated stress models which are used to more accurately describe worst case conditions.

Based on the stress - material property relationships, such items as windshield peripheral heating and slip planes are discussed.

## INTRODUCTION

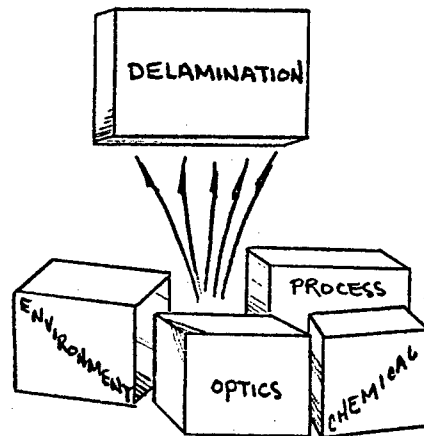
Swedlow, Inc. has, for the past eight years been developing the use of silicone as an interlayer material. The selection of silicone was not an arbitrary one but, was based on a theoretical examination of interlayer function and the families of plastics which might be used. From this search the silicone family of materials offered a near ideal solution to interlayer problems. Swedlow's SS-5272Y(HT) silicone interlayer is the result of this effort.

To illustrate the interlayer design method this experience is called on and is illustrated by way of a comparison between the function of the historical polyvinylbutyral interlayer and Swedlow's SS-5272Y(HT).

## TEXT

Out of the box of interlayer design considerations there is one key element which causes the bulk of windshield failures.

DELAMINATION!



For this reason this paper concentrates on the structural aspect of interlayer design.

Of course, this tunnel vision presupposes that optics, environmental resistance, chemical compatibility and processing features are inherent in the interlayer.

## DESIGN METHOD

- Generate math model
- Determine material properties
- Solve math model classically or by approximation
- Verify model by testing



The design method begins with the generation of a math model which will predict the effect of loads imposed on the interlayer. This math model requires a description of the interlayer and adherent material properties. These properties must be described over the anticipated material usage range. This is pointed out in order to make a distinction between the material's and the design engineer's reported properties.

The math model is, then, a description of the anticipated interlayer performance. It must be solved for response to the applied loads. This is done either classically or by approximation. Once the response is predicted, tests are made to check the theory.

It should be pointed out that deviation from this order of design events normally results in an unstable design foundation and leads to a lengthened time to product. It took Edison a lot of tries to get a light bulb!

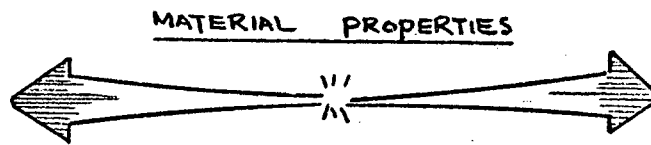
The method which Swedlow uses to execute this design method will add clarity and point out problems.

$$\begin{aligned}\frac{\partial \sigma_{xx}}{\partial x} + \frac{\partial \sigma_{xy}}{\partial y} &= 0 \\ \frac{\partial \sigma_{yx}}{\partial x} + \frac{\partial \sigma_{yy}}{\partial y} &= 0 \\ \nabla^2 (\sigma_{xx} + \sigma_{yy}) &= 0\end{aligned}$$

The math model is formed around generalized equilibrium and compatibility equations and several simplifying assumptions. These assumptions include,

- Plane stress
- Small deformations
- Hooke's Law applies
- Body stresses are negligible
- Steady state, unidirectional heat flow exists

It would appear that these assumptions have simplified the model right out of usefulness. But, the effect of these simplifications have been weighed in the light of analysis methods and are considered to be acceptable. It's possible that with more elaborate solution techniques some of these simplifications can be removed.



- TENSILE STRESS  $\sqrt$  STRAIN
- SHEAR STRESS  $\sqrt$  STRAIN
- BOND SHEAR STRENGTH

The material properties which are developed include the tensile and shear stress-strain curves and the bond shear strength. These properties must be statistically accumulated and should be evaluated for their time and temperature dependence. Also, as noted before, these properties should be determined over the anticipated deformation ranges. The typical materials engineers' reporting of modulus of elasticity based on an examination of 0.01 percent material strain is not sufficient. Full stress-strain curves are required.

Armed with the above method and properties we then solve the math model. A classical solution of the equations hasn't been accomplished yet and, therefore, a finite difference approximation to the solution has been made. This was done on a computer and the results seem to agree with other approximation methods.

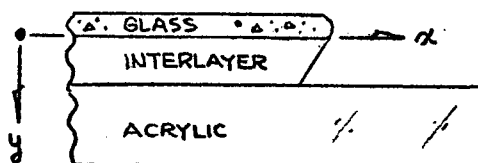
#### FULL SCALE TESTING

- Normally does not duplicate total environmental conditions
- Windows pass tests and fail in service
- Math models have not been verified

Tests are then conducted to verify these theoretical predictions. Normally full scale testing is required but, this has a few shortcomings. Testing does not incorporate all of the variables; windows still fail in an unpredicted fashion and, thus, the math model is not truly verified. In addition, no known instrumentation techniques are available which can be used with the interlayer materials to actually measure the stresses being developed.

To illustrate the results of this analysis, a comparison is presented of a silicone interlayer [Swedlow's SS-5272Y(HT)] and P.V.B. in a typical glass-acrylic windshield configuration. For this comparison, the interlayer is assumed to be .200 inches thick and the element length is 53 inches.

STRESS BASED  
ON  
FINITE DIFFERENCE  
APPROXIMATION



| STRESS      | SILICONE   | P.V.B.    |       | STRESS CONC. |
|-------------|------------|-----------|-------|--------------|
|             | 0° - 100°F | 0°F       | 100°F |              |
| $\sigma_x$  | 34 PSI     | 7,200 PSI | 4 PSI | 2.0          |
| $\sigma_y$  | 26         | 20,000    | 7     | 1.2          |
| $\tau_{xy}$ | 200        | 78,000    | 78    | 2.6          |

The pressure induced interlayer stresses have been examined for a thick windshield and found to be small by comparison to those which are thermally induced.

As can be seen, the shear stress is the predominate term and the stress concentration factor is high; approximately 2.6.

The stress in the "y" direction, or normal to the plane of the windshield, is based on no translation of the glass in this direction and, as such, is conservative.

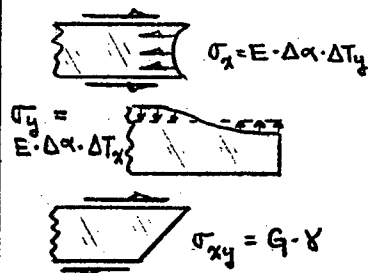
The P.V.B. when heated has very low induced stresses but if its temperature is allowed to fall the stresses rise sharply.

There are additional stresses which the finite difference, as modeled, does not account for.

One of these is the effect at the unheated boundaries of the interlayer. This condition has been examined by Triplex and reported on by Mr. Roberts in 1971. We have followed his lead and studied the limits of stresses which might occur in both the silicone and P.V.B.

#### ESTIMATED ADDITIONAL STRESSES

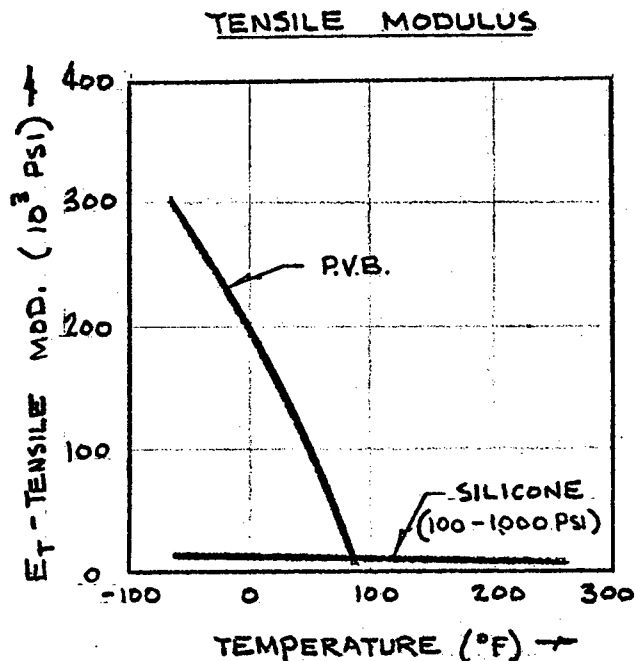
| STRESS               | SILICONE | P.V.B     |
|----------------------|----------|-----------|
|                      |          | 0°F       |
| $\sigma_x$           | 1 PSI    | 1,300 PSI |
| $\sigma_y$           | 4        | 800       |
| NOT ADDITIONAL       |          |           |
| $\sigma_{xy} (AVG.)$ | 80       | 18,000    |



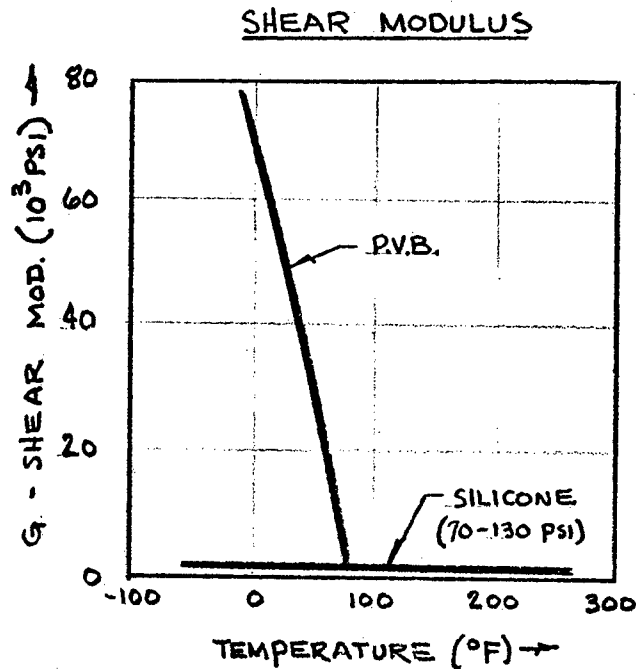
The relative magnitude of stresses for the two materials shown points out the material property/stress relationship.

From the math models for stresses, other material properties (such as urethanes) may be introduced and predicted effects noted.

To illustrate the material property importance to functionality it is necessary to examine a couple of those which are most important.



Shown is the tensile modulus vs temperature for both P.V.B. and silicone. Stresses are proportional to the modulus and because of the temperature dependence of E for P.V.B., the stresses will be some power of the temperature changes at the interlayer periphery. This is not the case for silicone.



Also shown is the shear modulus vs temperature and, again the shear stress is proportional to  $G$ ;  $G$  is a function of temperature and for P.V.B. at slightly depressed temperature the stresses rise quickly. Again this is not the case for silicone.

A few comments on some predominate interlayer design features should be made at this point:

- ° Slip planes, required in P.V.B. constructions, are necessary to minimize the cold edge effect and prevent glass chip pulling. Stress components in the "y" direction are the cause, and because they are very small for silicone, slip planes are not required.
- ° High shear stresses which develop in P.V.B. due to depressed temperatures require that the windshield be heated at all times. This is not necessary for silicone.
- ° P.V.B. becomes brittle at depressed temperatures (high modulus for low temperatures) and therefore, heat must be applied to make the windshield fail-safe. Heat is not required for a fail-safe silicone construction.
- ° And, silicone does not require the elaborate edge sealing necessary for P.V.B. interlayers.

Let's look at the conclusions based on this design method and analysis.

The estimation of stress levels is fundamental to design and new interlayer material developments. Also, engineering material properties, when viewed in the light of these stress estimates, brings function into focus. And, of the families of plastic materials, the silicones seem near ideal for interlayer application.

SESSION 4

BIRD AIRCRAFT STRIKE HAZARD (Part I)



FLIGHT SAFETY ASPECTS OF PRECISION  
RADAR NEAR AIR BASES

Warren L. Flock  
University of Colorado  
Boulder, Colorado

and

John L. Green and Ben B. Balsley  
National Oceanic and Atmospheric Administration  
Boulder, Colorado

## FLIGHT SAFETY ASPECTS OF PRECISION RADAR NEAR AIR BASES

Warren L. Flock, University of Colorado  
and

John L. Green and Ben B. Balsley  
National Oceanic and Atmospheric Administration  
Boulder, Colorado

### ABSTRACT

The ability of radar to detect birds is now well established. Long-range surveillance radars can detect birds to ranges of 50 nautical miles or more, depending on conditions, and can warn aircraft of bird concentrations. Such radars, however, can generally not detect targets in the near vicinity (within 2 or 3 nautical miles) of the radar. For this purpose, radars employing short pulses and having short receiver recovery times can be applied. The utility of either type of radar for providing warning of birds would be enhanced by the ability to identify targets quickly and unambiguously as birds and to provide information about numbers and types of birds. Identification can be accomplished by use of amplitude and/or doppler frequency signatures of bird echoes, which can be analyzed in real time with Fast Fourier Transform techniques. It appears that the doppler signatures may also be identifiable in some cases by ear, by use of headphones.

A fairly considerable amount of amplitude-signature data has been accumulated already in England. A limited number of doppler signatures have been obtained at Boulder, Colorado, and work is proceeding there on a pulse-doppler radar which will be used to obtain additional signatures. Pulsed noncoherent surveillance radars can be used to obtain amplitude signatures. Coherent pulsed radars (pulse-doppler radars) or cw radars are needed to obtain doppler signatures. Automatic tracking capability may be highly advantageous for signature purposes. For gathering signature data originally in a location where birds are plentiful, however, it may be satisfactory to simply point the antenna in a fixed direction and let birds fly through the beam.

## 1. Introduction

The ability of radar to detect birds is now well established (Refs. 1,2). Long-range L-band surveillance radars, such as FAA ARSR types and comparable Air Force radars can monitor bird movement to ranges of 50 nautical miles (NM) or more (93 km or more), depending on circumstances (Refs. 3,4). FAA ASR airport radars may record bird echoes to ranges of about 15 NM. Radars of these types can therefore provide useful warning of the presence of birds, but they are limited in their ability to detect birds in the very near vicinity of the radar and have little capability for identification of birds.

## 2. Close-in-seeing Radars

The greatest hazard of collisions between birds and aircraft tends to occur at low altitudes and in the vicinity of airports, and the ability of radar to detect birds within a few miles of the radar may thus be an important consideration. Long-range surveillance radars are not suitable for this purpose because of their long pulse lengths (usually 2  $\mu$ sec or more) and because of the lack of attention in the design process to "close-in-seeing" capability. Also such radars are expensive to install and operate. Airport surveillance radars can see closer in and are lower in cost than the long-range radars but are not entirely satisfactory in these respects either. For these reasons Schaefer (Ref.5) proposed the use of low-cost X-band marine radars for detection of birds in the near vicinity of air fields. One consideration of his proposal was that even a very small airport might be able to afford such a radar. Also the cost of supplying larger airfields with auxiliary radars of this type would not be excessive.

An X-band radar of the type suggested by Schaefer, a GEC-AEI 654 radar manufactured by what is now Marconi Radar Systems, Ltd., New Parks, Leicester, England, has been tested at Boulder, Colo. and found to be capable of detecting individual flying birds (radar cross sections of  $0.01 \text{ meter}^2$ ) out to ranges of about 2 nautical miles (NM) or 3700 meters, and groups of birds out to 6 NM or more, depending on the number and type of bird in a group. This radar has a peak power of 20 kw and normally uses pulses of 0.05  $\mu$ sec on  $3/4$  and  $1\frac{1}{2}$  NM ranges, 0.25  $\mu$ sec on 3 and 6 NM ranges, and 1  $\mu$ sec on 12, 24, and 48 NM ranges. When 0.05  $\mu$ sec pulses are used, birds can be detected as close as  $1/12$  NM. While the performance cited may be satisfactory for some purposes, certain improvements would increase the efficiency of this and similar marine radars for bird detection. These radars utilize slotted-waveguide antennas which have very broad vertical beamwidths, this feature being advantageous for a boat which is subject to roll. Using the same transmitted power but narrowing the vertical beamwidth, using a lower noise figure receiver, and matching the receiver bandwidth and pulse length more closely on long ranges, where 1  $\mu$ sec pulses can be used,

would increase the capability for detecting individual birds out to about 5 NM. The improvements would not be difficult to accomplish, and radar of this range capability would be more useful generally than one restricted to a range of 2 NM. Also the improved radar would be more efficient in the detection of birds on a runway, which may be an important consideration. The improved version might, for example, detect small birds on a runway to a range of 2000 m, according to calculations by Schaefer.

The 654 radar tested at Boulder was mounted in a 16-foot trailer, illustrated in Fig. 1, which shows the 12-foot slotted-waveguide antenna supplied with this model. A 4-foot parabolic antenna was used at other times. Figure 2 illustrates the high resolution obtained when the 12-foot antenna ( $0.7^\circ$  horizontal beamwidth) and 0.05  $\mu$ sec pulses are used on a  $3/4$  NM range. The radar is located, in the case of Fig. 2, at the edge of Valmont reservoir which is divided into three sections by dikes. The dark areas in the center are water which does not backscatter energy unless waves develop due to wind. The discrete echoes within  $1/4$  NM and the large echo at  $1/2$  NM, both in the upper right quadrant, are due to birds.

In attempting to detect birds on runways, it is necessary that the birds satisfy approximately the Rayleigh criterion for roughness (Ref. 6), the point being that birds on the runway must constitute "roughness" on an otherwise smooth runway which will not backscatter the incident radar pulses, just as the smooth water surface of Fig. 2 did not backscatter. The result of applying the Rayleigh criterion is that the radar antenna height must be equal to at least  $\lambda R/16 h$ , where  $\lambda$  is radar wavelength,  $R$  is distance to the birds, and  $h$  is the height of the birds, if birds of height  $h$  are to be detected at a distance of  $R$ . For the case that birds of a height of 0.2 meter (corresponding to a standing gull) are to be detected at a distance of 2000 meters, the height of the radar antenna should be about 20 meters.

### 3. Identification of Radar Echoes From Birds

An experienced observer can often quickly identify radar echoes as due to birds by noting how fast they move and their location of occurrence on the radar screen, etc. At other times, however, it may be difficult to determine quickly if a target is due to birds or a slow moving aircraft or if multiple targets are birds or ground echoes. Furthermore the appearance of the echoes on a PPI screen gives only a crude indication of whether the targets are caused by small or large birds or small or large flocks of birds. It would be highly desirable in certain circumstances to be able to tell quickly and positively if given targets were birds or not and if the birds were large or small and in large or small numbers.

Certain techniques are available for identification of echoes from birds in flight, but such identification procedures are still in research, rather than operational, stages. The procedures involve recording the amplitude and/or doppler frequency signatures of birds. Variations in the amplitude of the echo from a bird in flight are caused by variations in radar cross section as the bird flaps its wings. It has been proposed by Greenewalt (Ref. 7) that the rate at which a bird beats its wings is a function of the length of the wing. The particular relation that he proposed is

$$f\ell^{1.15} = 3540$$

where  $f$  is frequency of the wingbeat in cycles per second or Hz and  $\ell$  is the length of the wing in centimeters. Modulation at the wingbeat frequency can be expected to be a major feature of the amplitude signature of a bird in flight. It is of interest that such amplitude modulation was noticed on the first occasion when a radar echo from a bird was recorded in 1939, as described by Bonham and Blake (Ref. 8). Radar amplitude signatures of birds in flight have been recorded by several investigators, including Schaefer (Ref. 9), Konrad (Ref. 10), Bruderer (Ref. 11), Houghton (Ref. 12) and Emlen and co-workers. Such amplitude signatures tend to have characteristic features in addition to modulation at the wingbeat frequency. The frequency spectrum of the amplitude variations is of considerable interest and may be more readily interpretable or identifiable than the amplitude variations. Very interesting spectra of this type, showing the fundamental wingbeat frequency and harmonics of it, have been recorded by Houghton (Ref. 12).

Amplitude signatures can be obtained by using noncoherent pulsed radars, and the application of the 654 radar, mentioned earlier, to this purpose is being investigated. Coherent pulse radars (pulse doppler radars) or cw radars must be used to obtain doppler signatures. Considerably fewer doppler signatures than amplitude signatures have been recorded. Green and Flock (Ref. 13) reported doppler signatures obtained by using an improvised low-power cw radar. An example of a doppler signature, namely that of a Shoveler (*Spatula clypeata*) is shown in Fig. 3. This display was obtained by using a Sonograph to present the spectrum of the doppler record as a function of time. A complication in the case of a doppler signature is that the average doppler frequency is determined by the radial velocity of the bird; the signature appears as a variation about the average doppler frequency. In addition to the Shoveler signature, some doppler frequency data have been obtained concerning the Mallard (*Anas platyrhynchos*), Cinnamon Teal (*Anas cyanoptera*), Great Blue Heron (*Ardea herodias*), Ring-billed Gull (*Larus delawarensis*), Red-winged Blackbird (*Agelaius phoeniceus*), and Barn Swallow (*Hirundo rustica*). Some Fast Fourier Transform spectrum analyses have also been carried out, using a digital computer, but these initial analyses did not have sufficient detail to provide a signature. They did show the different radial velocities of

three Mallards flying close to each other, etc. Whereas the Sonograph displays intensity versus frequency over a given period of time, in terms of the relative darkness of the record, the computer analysis gives an actual plot of intensity versus frequency, averaged over one fixed time interval at a time.

Work is proceeding at Boulder on the development of an X-band pulse doppler radar for obtaining signatures of birds in flight. Such a radar can provide both amplitude and doppler signatures. A pulsed radar has the advantage, over a cw radar, of range discrimination which allows recording and distinguishing signals at different ranges. Also, the pulsed radar tends to have a better signal-to-noise ratio because the cw radar receives clutter signals, as from waves on a lake, from all ranges, whereas the pulsed radar uses range discrimination to eliminate clutter from all but the desired range interval. A block diagram of a coherent radar, utilizing separate transmitting and receiving antennas, is shown in Fig. 4. The radar being developed at Boulder will provide a peak power of 20 kw and will utilize solid-state Gunn diodes for the signal source, whose output is amplified by a pulsed klystron, and for the local oscillator.

To obtain a signature of a bird, it must be in the radar beam for a sufficient length of time to record at least several cycles of the wingbeat frequency. Thus it would be very difficult to obtain signatures with a continuous rotating surveillance radar, and one must normally be able to stop the rotation of a surveillance radar if it is to be used for signatures. Another alternative, of course, is to use a separate radar for signature purposes, either as an auxiliary unit in conjunction with a surveillance radar or by itself. Especially in operational applications, a radar having automatic tracking capability would be advantageous for obtaining signatures. In originally obtaining signatures, however, it may be sufficient in a suitable location to simply point an antenna in a favorable direction and let the birds fly through the beam. In this mode of operation, a rather broad beamwidth can be used. Ranges will be restricted when a broad beam is used, but such a beam will allow close targets to stay in the beam for a sufficient period of time and in obtaining signatures originally it would usually be desirable to only obtain signatures from birds at sufficiently close range that they can be identified visually.

Signatures can be recorded on magnetic tape for later analysis in a research application, as in the preparation of Fig. 3, but for operational purposes real-time analysis and identification would be needed. It is believed that a small computer, such as a Nova, can be readily adapted for this purpose, and a Nova will be tested as part of the research program at Boulder. The computer could prepare spectra (plots of amplitude versus frequency for given time intervals) using Fast Fourier Transform techniques and could also automatically indicate wingbeat

frequencies and perhaps even the species of birds. Preliminary indications are also that the simple procedure of listening to doppler signatures may be practicable and this approach will be tested further. The wingbeat frequencies of birds are too low to hear, of course, but the doppler frequencies recorded range up to 500 Hz, with a X-band radar, and can be heard.

The relative advantages of the different types of signature radars need to be investigated further. Noncoherent pulse radars and cw radars are considerably lower in cost than pulse doppler radars, but the latter type is more flexible in that it has range discrimination and can obtain both amplitude and doppler signatures. The transmitter power is a major factor in determining cost and performance also, especially in the case of the pulsed radars.

#### Conclusion

Small auxiliary radars designed for close-in-seeing and/or bird signature identification, by use of amplitude or doppler frequency variations, appear to have the potential for contributing to aircraft safety in the vicinity of air fields. Research is continuing on this application of radar to aircraft safety and environmental monitoring.

#### Acknowledgment

The research on close-in-seeing and bird-identification radar techniques at the University of Colorado and the National Oceanic and Atmospheric Administration is sponsored by the Air Force Weapons Laboratory, Kirtland Air Force Base, New Mexico.

### List of Illustrations

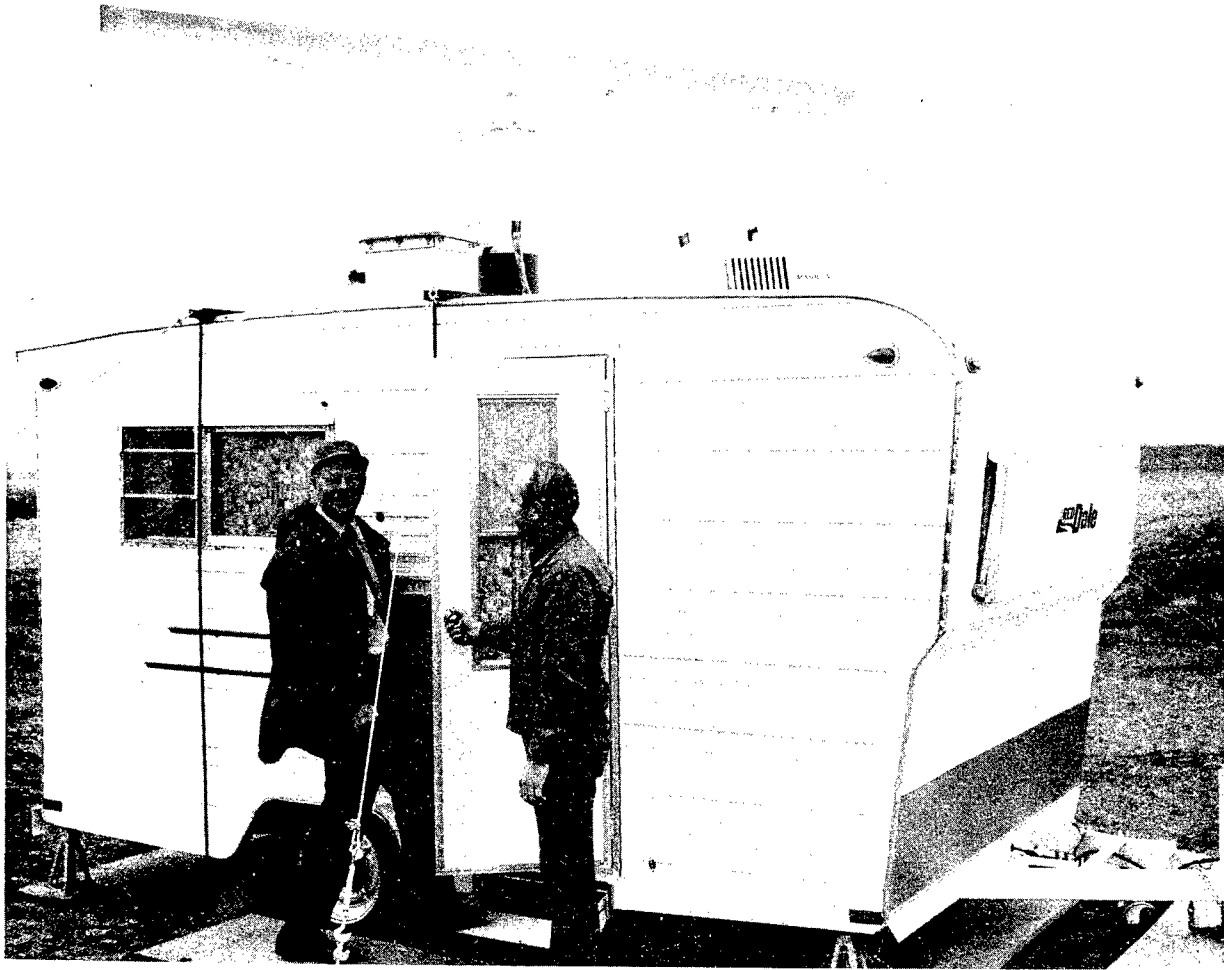
- Figure 1. Cargo Trailer, with the 12-foot Slotted-Waveguide Antenna of the 654 Radar Mounted on the Roof.
- Figure 2. 654 Radar Screen at Valmont Reservoir, Boulder, Colo., showing Bird Echoes. One Rotation Exposure, 0.05 Microsecond Pulses, Oct. 10, 1971.
- Figure 3. Doppler Frequency Record of Shoveler Duck at Baller Lake, near Boulder, Colorado, April 11, 1971. The Record is Calibrated to Display the Velocity Relative to the Radar in Meters per Second, as a Function of Time.
- Figure 4. Block Diagram of a Coherent Pulsed Radar.

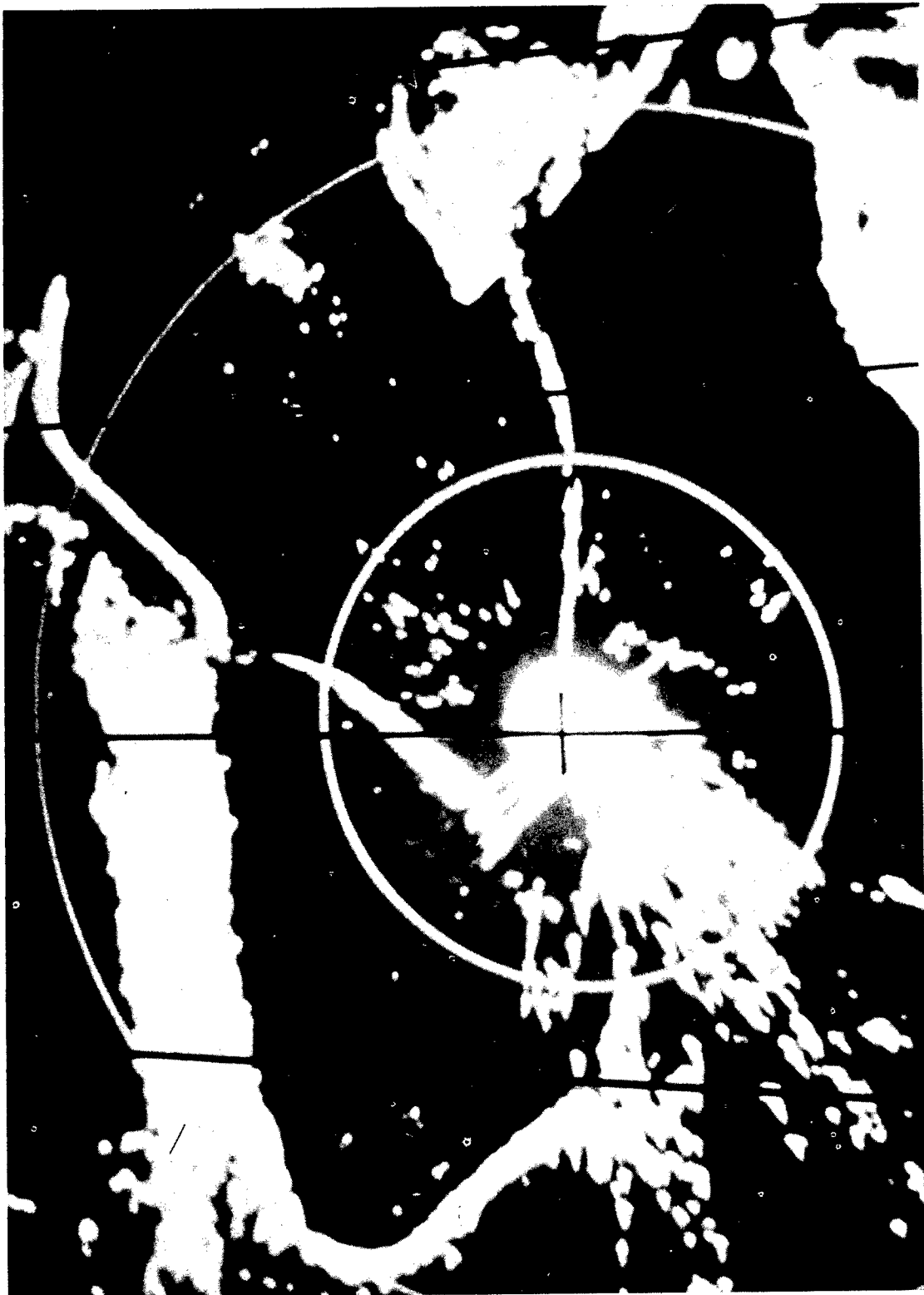


# REFERENCES

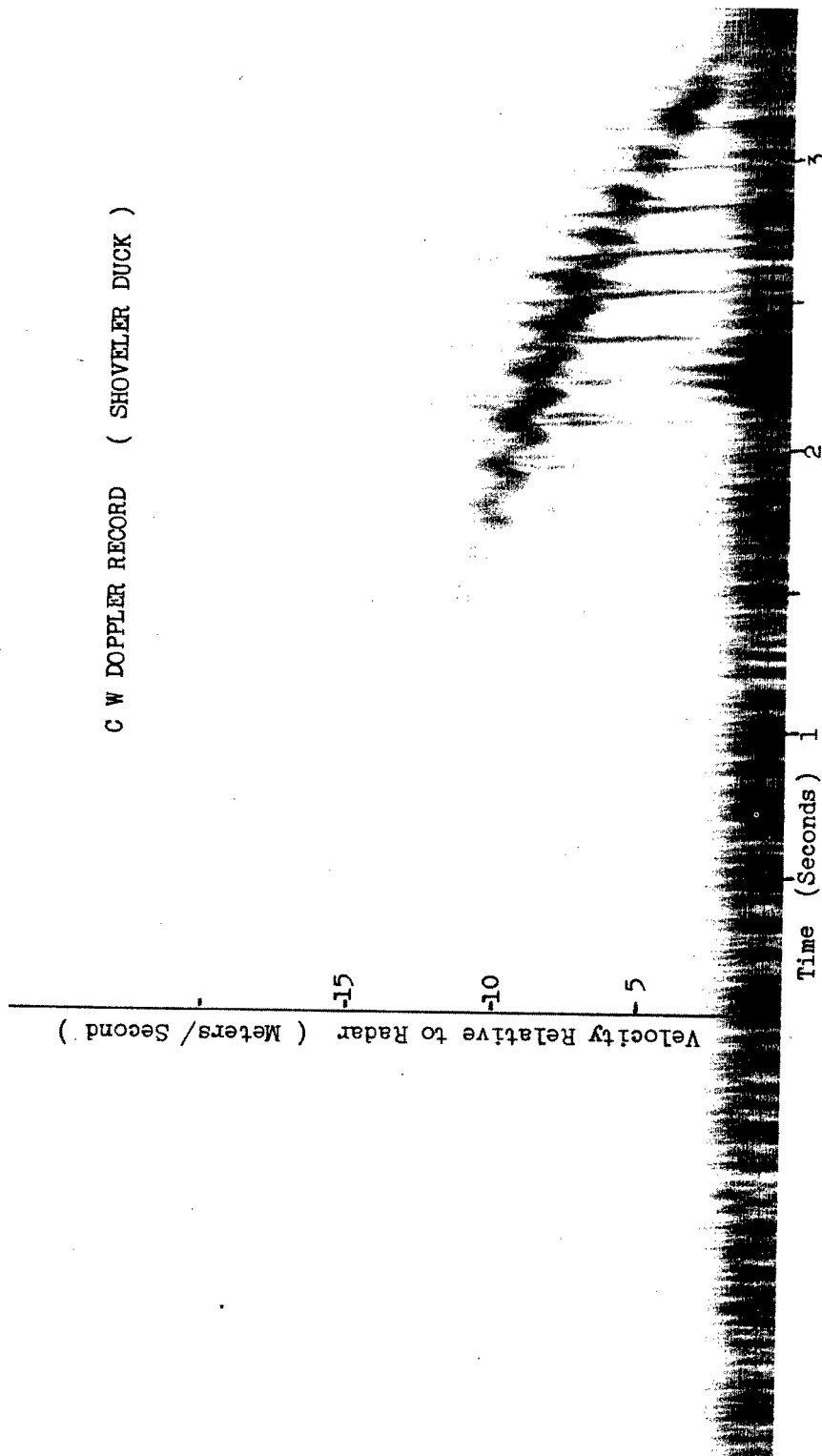
1. Eastwood, E., Radar Ornithology, Methuen & Co., London, 1967.
2. Myres, M.T., "The Detection of Birds and Insects, and the Study of Bird Movements, with Radar," Proceedings of the World Conference on Bird Hazards to Aircraft, 2-5 Sept. 1969, pp. 501-519, Associate Committee on Bird Hazards to Aircraft, National Research Council of Canada, Ottawa, 1970.
3. Flock, W.L., "Monitoring Bird Movements by Radar," IEEE Spectrum, 5, pp. 62-66, June, 1968.
4. Flock, W.L., Final Report, Flight Safety Aspects of Radar Techniques in Bird/Aircraft Collision Avoidance, Grant AF-AFOSR-1137-68, Air Force Office of Scientific Research, Sept., 1971 (unpublished).
5. Schaefer, G.W., An Airport Detection Radar for Reducing Bird Hazards to Aircraft, University of Technology, Loughborough, Leics., England, 32 pp., 1970 (Paper prepared for World Conference on Bird Hazards to Aircraft, 2-5 Sept., 1969, but not published in conference proceedings.)
6. Beckmann, P. and Spizzichino, A., The Scattering of Electromagnetic Waves from Rough Surfaces, Macmillan Co., New York, 1963.
7. Greenewalt, C.H., Hummingbirds, Doubleday and Co., Inc., Garden City, N.Y., 1960.
8. Bonham, L.L. and Blake, L.V., "Radar Echoes from Birds and Insects," Scientific Monthly, 82, pp. 204-209, 1956.
9. Schaefer, G.W., "Bird Recognition by Radar: A Study in Quantitative Radar Ornithology," in The Problems of Birds as Pests, pp. 53-56, Institute of Biology Symposia, No. 17, Academic Press, New York, 1968.
10. Konrad, T.G., "Radar as a Tool in Meteorology, Entomology, and Ornithology," Proceedings of the Fifth Symposium on Remote Sensing of the Environment, Willow Run Lab., University of Michigan, Ann Arbor, Michigan, 1968.
11. Bruderer, B., "Zur Registrierung und Interpretation von Echosignaturen an einem 3-cm-Zielverfolgungsradar." Orn. Beob., 66, pp. 70-88, 1969.

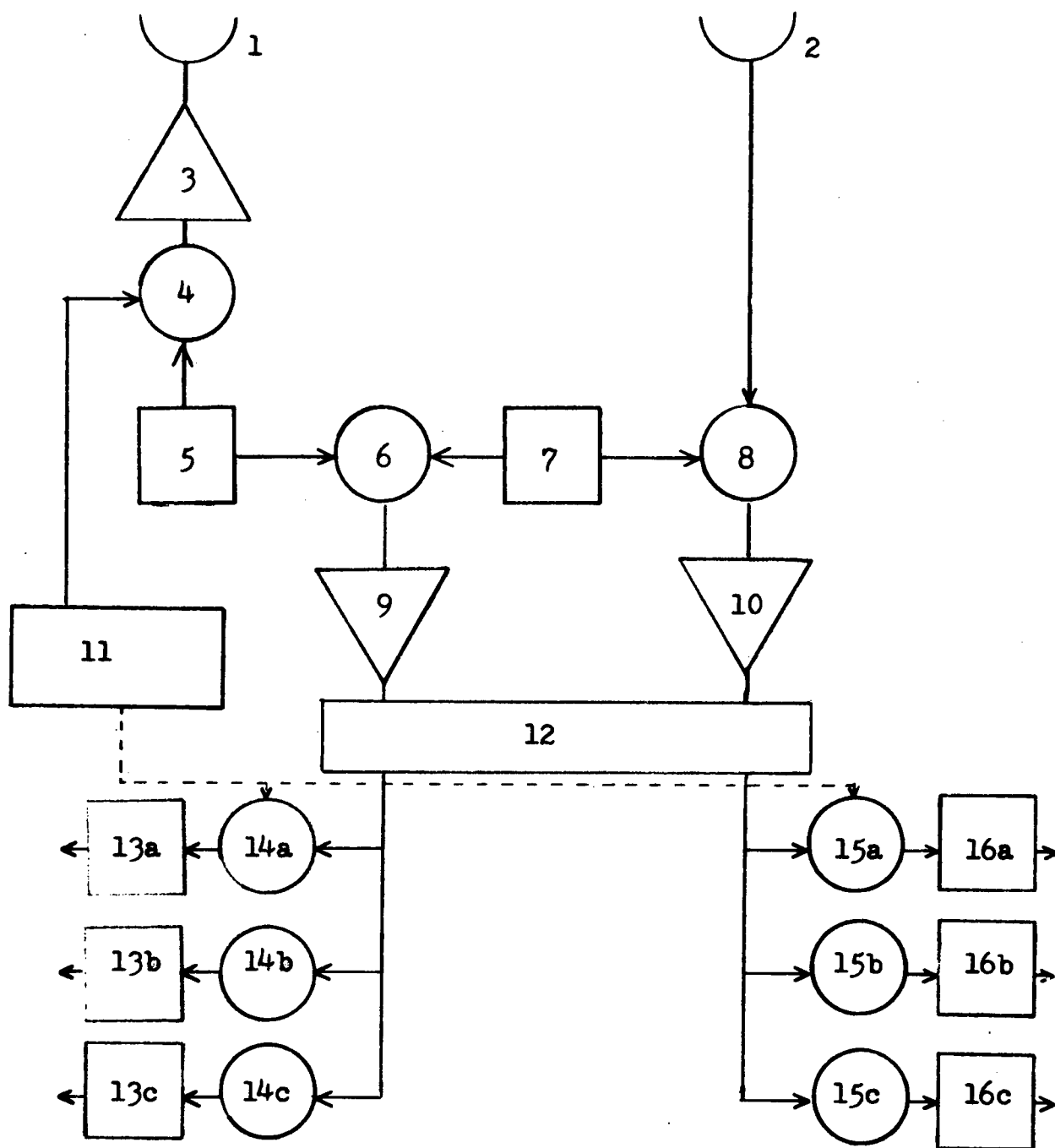
12. Houghton, E.W., "Use of Bird Activity Modulation Waveforms in Radar Identification," Royal Radar Establishment, Malvern, Worcs., England, 6 June 1972.
13. Green, J.L. and Flock, W.L., Characteristics of Radar Echoes from Birds in Flight, 1972 USNC-URSI Spring Meeting, April 13-15, 1972.





C W DOPPLER RECORD ( SHOVELER DUCK )





1. Transmitting Antenna
2. Receiving Antenna
3. Power Amplifier
4. Modulator
5. Oscillator, 9.600 GHz
6. Mixer
7. Oscillator, 9.630 GHz
8. Mixer
9. IF Amplifier (reference)
10. IF Amplifier (signal)

11. Radar Timing
12. Coherent Detector
- 14,15. Range Gates
- 13,16. Low Pass Filter
- a. First Range Interval
- b. Second Range Interval
- c. Third Range Interval



COMPOSITE BIRD-RESISTANT AIRCRAFT  
TRANSPARENCIES

H. Edward Littell, Jr.  
PPG Industries, Inc.  
Pittsburgh, Pennsylvania





## COMPOSITE BIRD-RESISTANT AIRCRAFT TRANSPARENCIES

H. Edward Littell, Jr.  
PPG INDUSTRIES, INC.  
Glass Research Center

### ABSTRACT

Since 1970, PPG Industries has engaged in an extensive test program to determine effective "bird-proof" aircraft transparency designs. In general, the results show that the best designs are composites which take advantage of the properties of components.

An extensive material evaluation has been part of the program to aid in selection of materials and combinations prior to actual bird impacting. Since impact resistance is critical, a laboratory impact simulator has been developed which fires a 150 gram missile at speeds up to 390 knots. This is not used to predict quantitative bird resistance, but rather to compare penetration resistances and measure the onset of go/no-go phenomena such as low temperature interlayer embrittlement where it has shown good correlation with bird impact results.

In the program, more than 100 constructions have been subjected to bird impacts over a range of speeds from 89 to 713 knots, angles from 22° to 65° and temperatures from -65°F to room temperature. Depending on the problem being investigated, both flat test panels and full-size transparency configurations have been used. Activity in two specific problem areas typifies the range of requirements and solutions encountered. The first concerns improved windshields for medium speed (e.g. STOL) aircraft. A laminate of thermally tempered glass and polycarbonate has exceeded the 4-lb bird/217 knot requirement over a wider temperature range with less weight than existing designs. It also eliminates the dangerous spall normally ejected from the inboard surface of the laminates of glass and polyvinyl butyral now used.

A different and particularly challenging problem is concerned with crew protection from bird impacts on low flying aircraft which operate at speeds of more than 500 knots. To obtain information in this regime, laminated glass-polycarbonate, clad polycarbonate and laminated acrylic-polycarbonate flat panels and full-size windshields have been tested with good agreement between the specimen types. The dynamic performance of the different constructions and the similarity between flat panels and actual windshields are indicated by a series of high speed motion picture scenes made during the testing at the National Research Council of Canada. These films show the superiority of one laminate of as-cast acrylic and polycarbonate, which has stopped 4-lb birds at speeds from 404 to 706 knots including different temperature and impact location conditions.

## COMPOSITE BIRD-RESISTANT AIRCRAFT TRANSPARENCIES

As a major aircraft transparency supplier, PPG Industries has been involved with bird-resistant windshields for commercial aircraft for a number of years. In 1970, a program was initiated to develop designs to "bird-proof" a wider range of aircraft from business or STOL types to high speed military aircraft. This effort has taken advantage of our experiences with the pertinent glass and plastic components and knowledge in glass-plastic composites gained with the development of bullet-resistant transparent armor. The bird impact phase has been design oriented rather than a study of material response, although considerable property evaluation has been conducted in selecting material and screening composite combinations.

In selecting materials, impact resistance is, of course, a critical criterion. To evaluate it, a laboratory impact simulator has been build (Figure 1A), which fires a 150 gram urethane-faced titanium missile against 12" x 12" targets at speeds up to 390 knots. Because of the number of variables involved in bird impact simulation, the cannon is not used to predict quantitative bird resistance but rather to compare material and combinations (Figure 1B), determine the effect of processing operations and exposure, and to evaluate the response and adhesion of interlayers from -80°F to +200°F. It has also been particularly useful for pinpointing the onset of go/no-go phenomena such as low temperature interlayer embrittlement where a constant velocity, slightly below the penetration limit, is employed, and temperature is the variable. As shown in Figures 2 and 3, this test has shown good correlation between air cannon impacts and bird impacts on full-size windshields incorporating the same interlayer.

The air cannon missile impacts are a useful screening device to indicate design direction but the designs themselves must finally be subjected to actual bird impact. In our program, over 100 constructions have been tested, usually with 4-lb birds, over a range of speeds from 89 to 713 knots, angles from 22° to 65° and temperatures from -65°F to room temperature. Depending on the problem, both flat 26" x 26" panels and full-size transparencies have been used. Rather than present an overview of this diverse program, this paper will concentrate on two specific problem areas which would be of interest to the Air Force while showing the range and diversity of the effort.

The first area concerns improved windshields for medium speed aircraft such as business or STOL types, many of which must meet Federal Aviation Regulation, Part 25. Windshields in this class have generally been laminates of thermally tempered glass with an edge attachment formed by an extended polyvinyl butyral interlayer, often containing a metal insert. These designs have been extensively tested and their drawbacks, verified by our test program, are well known. Table 1 illustrates these drawbacks in tests to meet our requirement of stopping a 4-lb bird at 217 knots (250 mph) with a panel at 45° from the line of flight. The first is decreased penetration resistance when impacted below room temperature. As shown

in the fourth line of Table 1, a change in interlayer can help. However, as has been demonstrated<sup>1</sup> for the 30% plasticized PVB shown here, for constructions with single interlayers, this leads to a shift rather than a broadening of the temperature range. In either case, even stopping the bird over a wider range of conditions still permits dangerous spall to be thrown off the rear face during impact.

For a complete solution, a new design was required which would be compatible with existing openings, stop the bird and contain the spall. This was accomplished by a laminate of glass and polycarbonate. As shown in the second portion of Table 1, by "scabbing on" a polycarbonate ply, it is possible to reduce glass thickness to yield a retrofit construction which is only .028" thicker yet .55 lbs per ft<sup>2</sup> lighter than the existing design. The new construction exceeds the impact requirement and has stopped the bird from +90°F to room temperature with no rear face spall. For retrofitting, glass outboard permits the same heating system to be used, but, as with any composite glass-plastic design, there are the problems associated with the 10:1 ratio of thermal expansion coefficients. Our experience has been, however, that these are not a problem if: (a) the plastic trailing section thickness is minimized; (b) there is good interfacial adhesion between the interlayer, glass and polycarbonate; and (c) laminating temperatures are minimized.

A different and particularly challenging problem has been to provide crew protection against bird impacts on high speed aircraft which operate in the 500 to 800 knot range. Adding to the difficulty in containing high energy impacts were limits imposed on weight (approximately 7.4 lbs per ft<sup>2</sup>), thickness (1.13") and the severe operating conditions of these aircraft. These limits, in effect, eliminated complete units of glass (for weight) and stretched acrylic (for its temperature limitations). Our effort was based on the bird "catch" philosophy and that, because of the limits imposed, only polycarbonate could meet the impact and structural requirements over the applicable temperature ranges. Design types tested (with advantages) included: acrylic-clad polycarbonate (ease of fabrication, optics and use in existing aircraft); laminated glass-polycarbonate (abrasion, and thermal resistance and coating adhesion); and acrylic-polycarbonate laminates (similar expansions, residual visibility and weight). These are compared in the motion picture scenes discussed in the appendix.

Constructions of the different transparency types were compared in both 26" x 26" flat panels and full-size windshields. The F-111 windshield configuration was selected for its size and availability of tooling since the current production part is manufactured by PPG Industries. In our

---

<sup>1</sup>Kangas and Pigman, "Development of Aircraft Windshields to Resist Impact With Birds in Flight," Part III, Civil Aeronautic Administration Technical Dev. Report No. 105, 1950.

tests at the National Research Council of Canada, there was good agreement between the flats mounted on a very rigid support and windshields supported by a more flexible frame. Examples of similar performance can be seen in the motion pictures and Figures 4 and 5. Figure 4 shows examples of one design after successful defeat of nominal 500 knot shots. Figure 5 shows another design in which the windshield sheared at the rear arch allowing slight tissue penetration. The flat sample was not penetrated, but the rearmost edge (the bottom in the photograph) also exhibited shearing. Windshields have also been tested recently in the airframe and again comparable results were obtained with a different support system. This correlation is important since it indicates the validity of using the simple flat panels for basic tests on these high performance designs.

Our tests since December 1971 indicate that a laminate of polycarbonate faced with an abrasion/thermal ply of glass, as-cast acrylic or others, will provide the best bird impact resistance. A .888" to .950" design (depending on facing ply thickness), shown in Figures 3, 4, 6 and 7, has shown a consistently high level of performance against 4-lb birds. This plastic composite has stopped 500 knot impacts in the center of the windshield from +20° soak temperature (Figure 3) to room temperature (Figure 4). It has also survived a room temperature impact (Figure 6) in the corner. At room temperature it has also stopped the bird at speeds up to 706 knots (Figure 7) where the kinetic energy is more than twice that at 500 knots. This protection level has been achieved with a windshield 21% thinner and 25% lighter than the allowed maximums.

In some ways, the thin design and relatively low modulus materials required to meet the weight limit can add new problems. One is deflection. As can be seen in the high speed films, center deflections of 6" or more are common with high speed impacts. Other problems are now being evaluated in this on-going program. Optics have been evaluated on bird impact samples and current production criteria have been met. Environmental and thermal cycling must also be made. However, a composite polycarbonate-based laminate of the type appearing in many of the following motion pictures has the best chance of providing the necessary trade-offs to be a viable "bird-proof" transparency system for high performance aircraft.

## APPENDIX

### HIGH SPEED MOTION PICTURES

#### Scene 1 (color)

PPG Industries' initial testing of bird-resistant high performance transparencies included designs based on modification of existing subassemblies and complete windshields now in production. This first scene shows a center impact by a 4-lb bird at 505 kt on a .610 inch laminate of glass and polycarbonate. The impact resulted in slight aft arch separation and penetration. Note the extent of glass fracture and spall from the impact surface. Temperature = 68°F.

#### Scene 2 (color)

The windshield in this scene is a laminate of acrylic-clad polycarbonate and polycarbonate. It prevented penetration upon center impact by a 4-lb bird at 500 kt. The outer ply sustained damage from cracks which originated in the acrylic and stopped at the interlayer. Temperature = 70°F.

#### Scene 3 (color)

This windshield consisted of monolithic .750 inch polycarbonate with as-cast acrylic cladding fused to the impact surface. A 500 kt center impact by a 4-lb bird resulted in brittle failure due to cracks which originated in the acrylic. Temperature = 73°F.

#### Scene 4 (color)

One acrylic-polycarbonate laminate construction exhibited slight rear arch shearing during center impact by a 4-lb bird moving at 494 kt with kinetic energy of 45,952 ft-lb. Temperature was 62°F. As can be seen by the flow of the bird, most of it was past the windshield when edge shearing allowed several ounces of tissue to extrude through.

#### Scene 5 (B/W)

The flat panel shown here is the same construction as the Scene 4 windshield. Although penetration of a 4-lb bird at 500 kt was prevented, the top edge did show some shearing in close agreement with the full-size windshield. Note, as in Scene 4, that some tissue is directed back toward the line-of-flight. Kinetic energy = 47,197 ft-lb and temperature = 63°F.

#### Scene 6 (color)

As will be seen in the next eight scenes, one nominal .92 inch acrylic-polycarbonate laminate has provided protection under a variety of conditions. Here, a center impact at 500 kt with kinetic energy = 46,807 ft-lb, caused no penetration or serious damage to the windshield. Temperature = 68°F.

#### Scene 7 (B/W)

This is the same test as the previous scene with the view from forward and below the panel looking past the forward arch along the inboard surface of the transparency. A grid with inch squares located at the rear arch indicates maximum deflection.

#### Scene 8 (B/W)

The same construction appearing in Scenes 6 and 7 was also tested in flat panels and showed good correlation with the windshield. In this test at 62°F, there was no penetration by a 4-lb bird at 509 kt with kinetic energy of 46,587 ft-lb.

#### Scene 9 (color)

In this scene, the design shown in Scenes 6 and 7 was impacted in a potentially dangerous location -- the beam-aft arch corner. There was no penetration and very little damage by a 4-lb bird traveling at 495 kt. Temperature was 70°F.

#### Scene 10 (B/W)

An inboard view of the corner impact shows that a deflection wave still results. The loose strip is a redundant fiber glass filler used in the corner between the windshield and a thin inboard Z-bar. The undamaged grid indicates no penetration by the bird.

#### Scene 11 (color)

As predicted by the laboratory studies, an impact at +20°F internal inter-layer temperature did not result in penetration. Resistance to the 4-lb bird at 511 kt was similar to that at room temperature.

#### Scene 12 (color)

The panel construction appearing in the previous seven scenes has also been successfully tested above a speed of Mach 1. The windshield in this scene prevented penetration by a 4-lb bird at 706 kt with kinetic energy of 95,460 ft-lb at 72°F. There was no serious structural damage to the windshield.

#### Scene 13 (B/W)

An inboard view of the events shown in the previous scene shows the large deflections encountered at the very high velocities. The undamaged grid confirms that no penetration occurred.



TABLE 1

FLEXSEAL® TRANSPARENCIES: 4-LB BIRD, 45°

|                                   | <u>Temp.<br/>(°F)</u> | <u>Speed<br/>(KT)</u> |                           |
|-----------------------------------|-----------------------|-----------------------|---------------------------|
| .150 TT* - .240" I/L - .375" TT   | 75                    | 223                   | OK W/Spall (20% 3GH PVB)  |
| (.765", 8.25 lb/ft <sup>2</sup> ) | 55                    | 222                   | Penetrated (20% 3GH)      |
|                                   | 54                    | 200                   | Just Penetrated (20% 3GH) |
|                                   | 53                    | 219                   | OK W/Spall (30% 3GH)      |
| .150" TT - .210" I/L - .250" TT - | 70                    | 217                   | OK W/Edge Spall           |
| .090" I/L - .093" PC              | 9                     | 228                   | OK No Damage              |
| (.793", 7.70 lb/ft <sup>2</sup> ) | 56                    | 252                   | OK No Spall               |

\*Thermally Tempered Glass

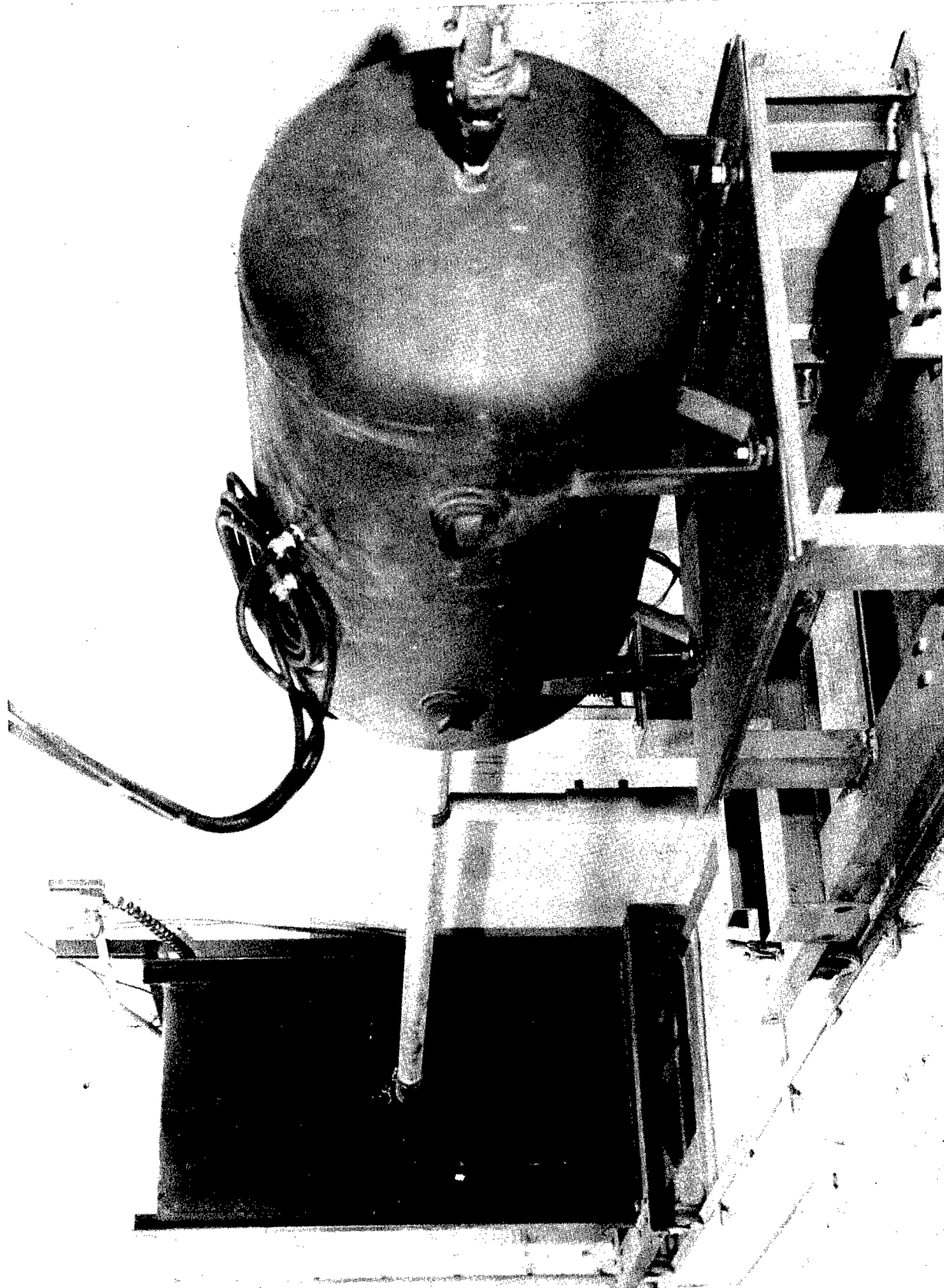


FIGURE 1A - LABORATORY AIR CANNON

# RESISTANCE TO 150 GM. MISSILE PENETRATION

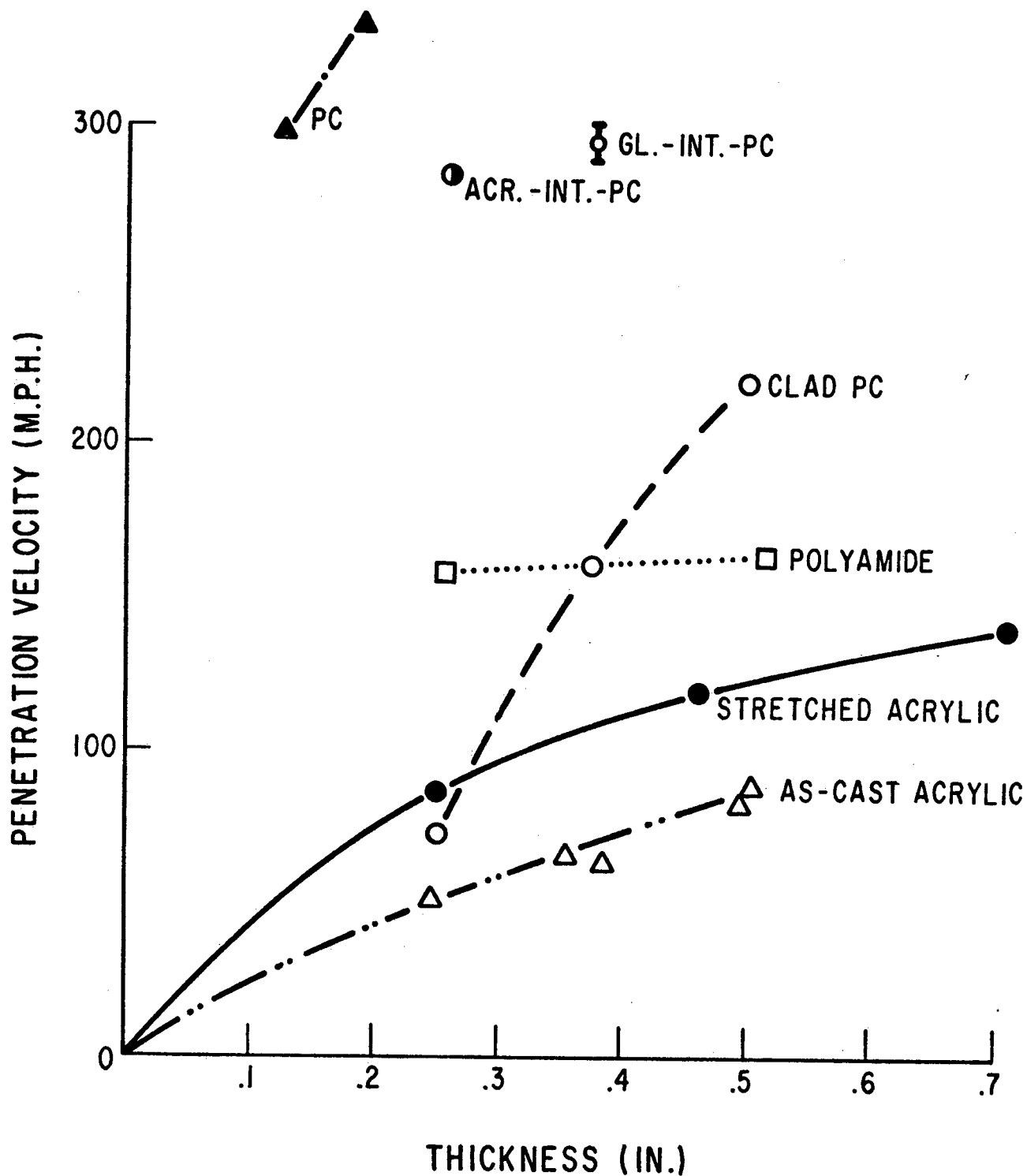
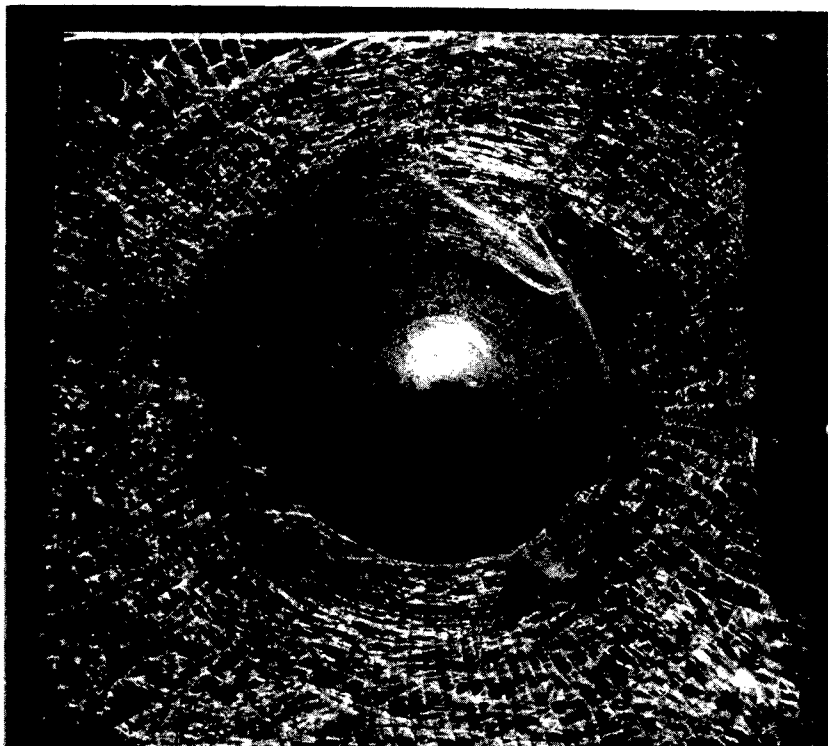
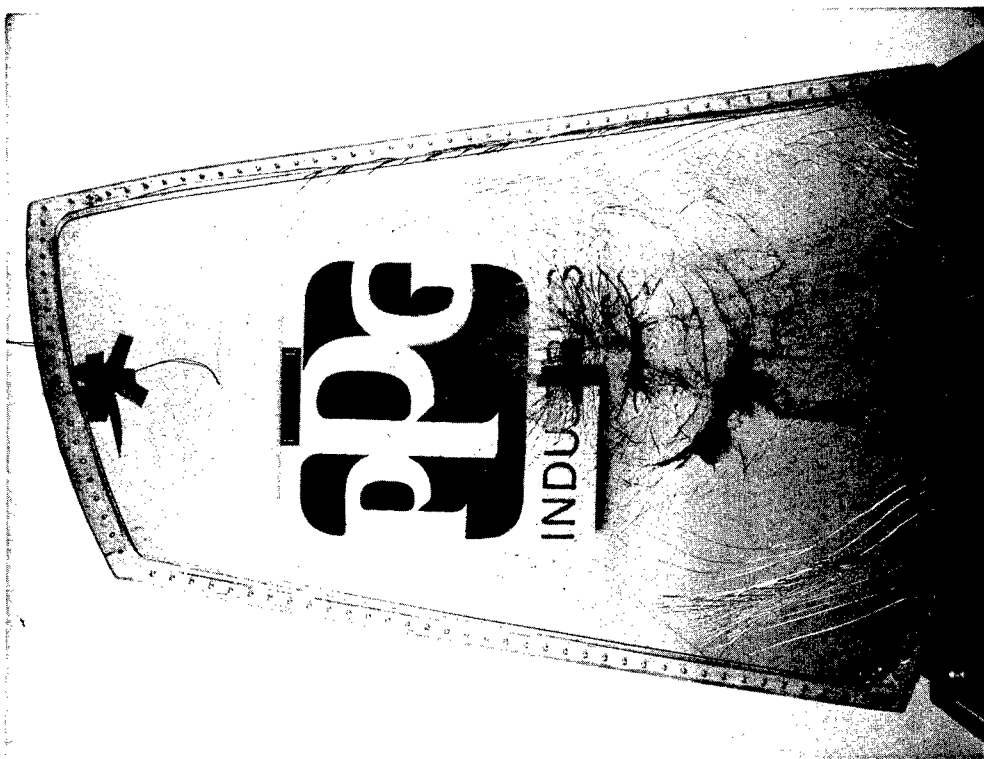


FIGURE 1B

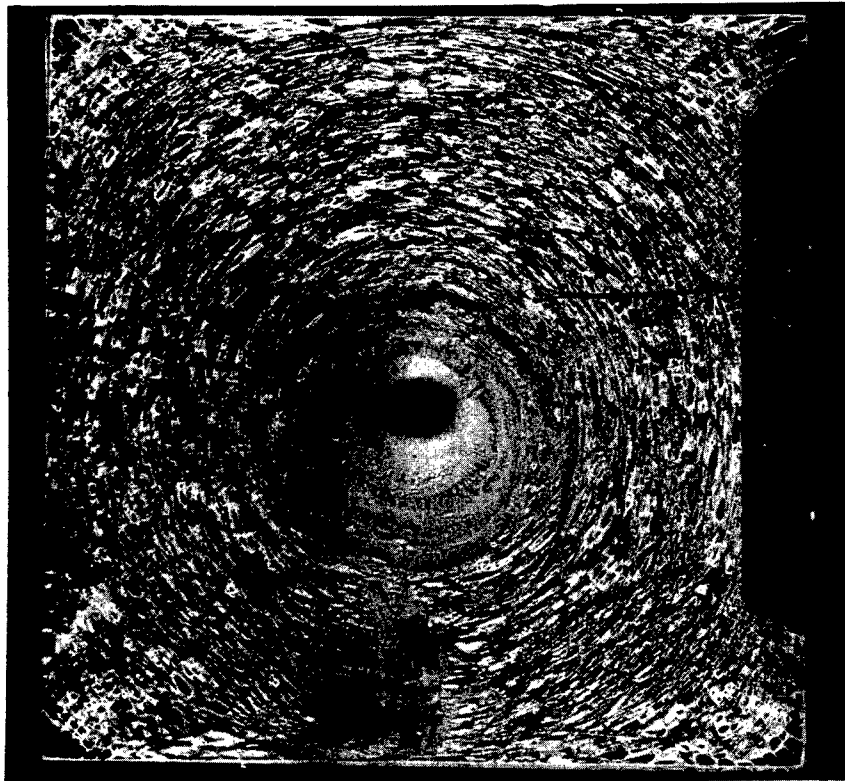


a) 12" x 12" Interlayer Test Specimen,  
287 mph Air Cannon Missile Impact (+11°F)



b) Test Windshield, Center Impact by  
4 lb Bird, 500 kt (+12°F)

FIGURE 2

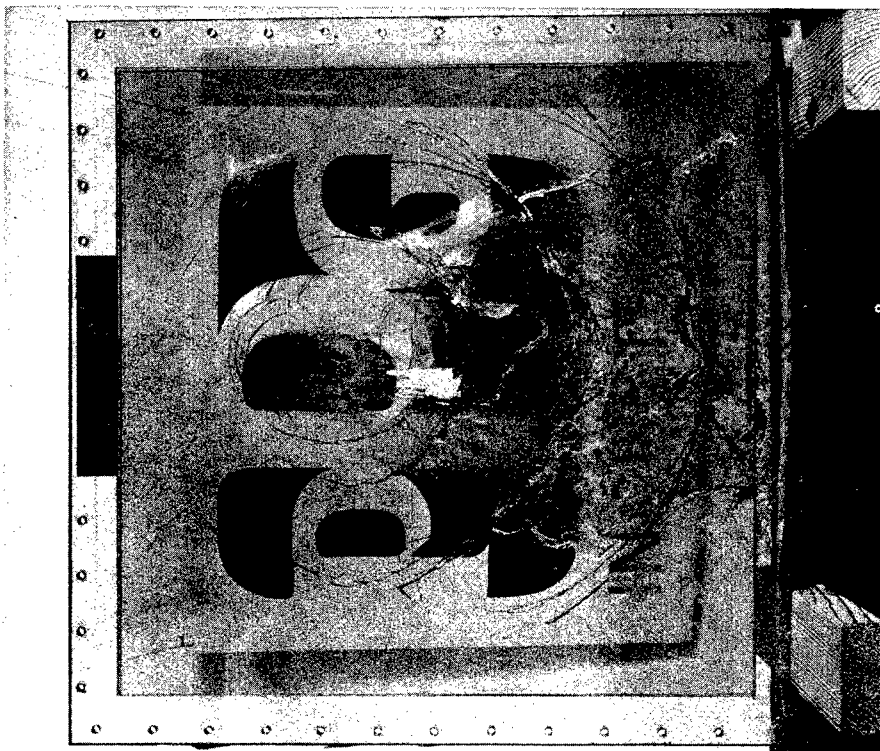


a) 12" x 12" Interlayer Test Specimen After  
290 mph Air Cannon Missile Impact (+18°F)

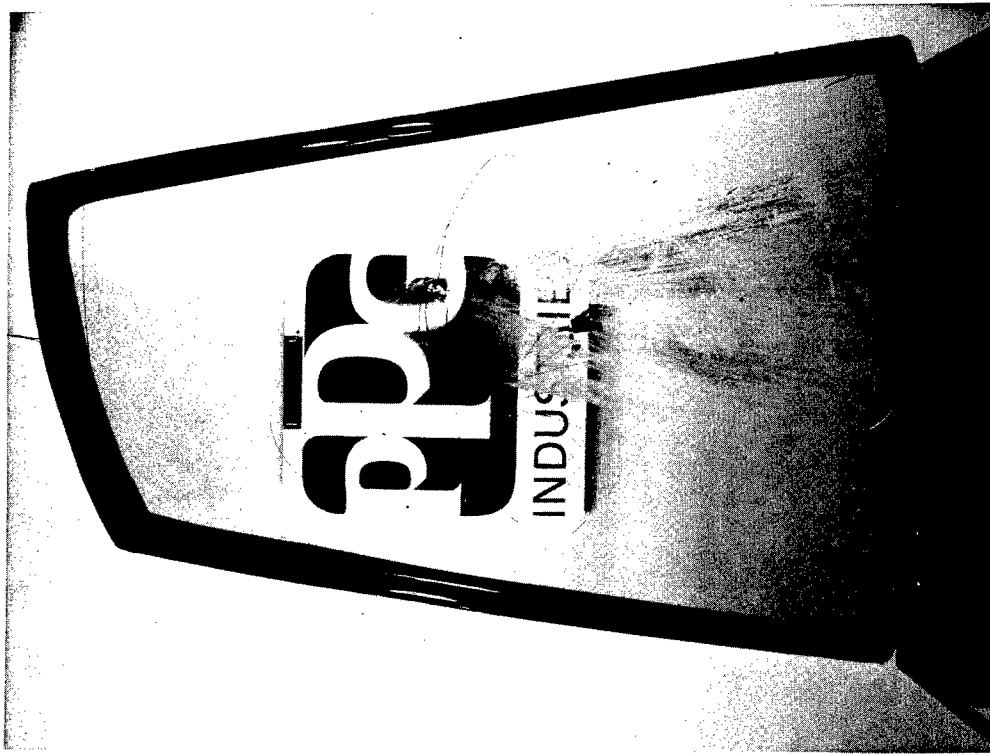


b) Test Windshield After Center Impact,  
4 lb Bird, 511 kt (+20°F)

FIGURE 3

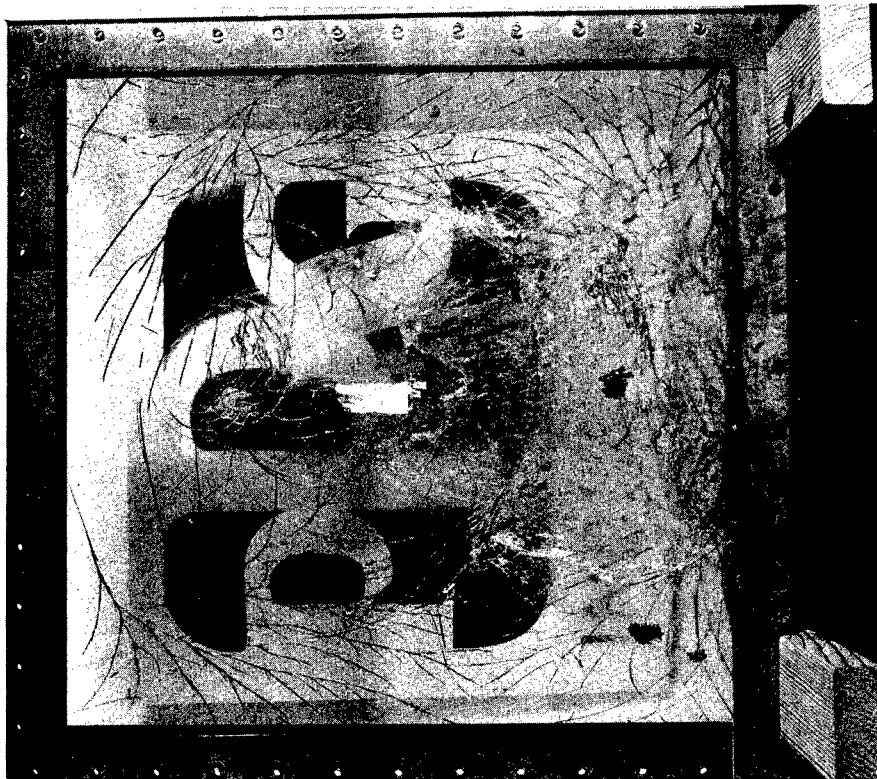


a) Flat 26" x 26" Panel After Center Impact  
by a 4 lb Bird, 509 kt, 62°F

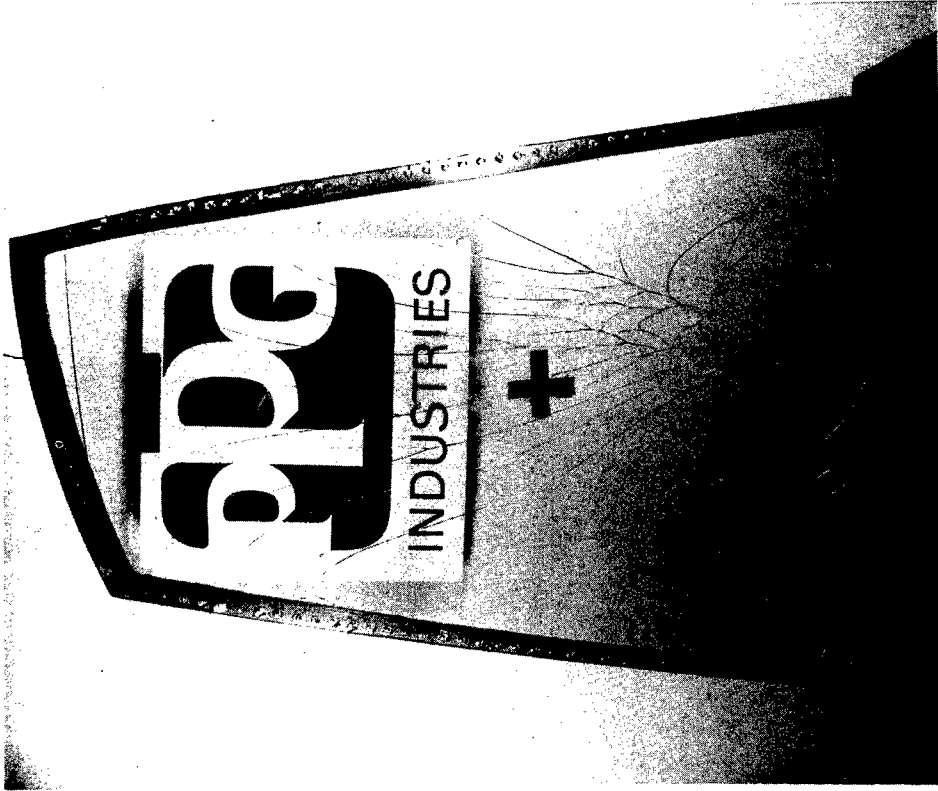


b) Windshield After Center Impact by a  
4 lb Bird, 500 kt, 68°F

FIGURE 4



a) Flat 26" x 26" ("B" Design) Panel After  
Center Impact by a 4 lb Bird, 500 kt, 63°F



b) ("B" Design) Windshield After Center  
Impact by a 4 lb Bird, 494 kt, 62°F

FIGURE 5



Figure 6 Beam-Aft Arch Impact by 4 lb Bird, 495 kt, 70°F



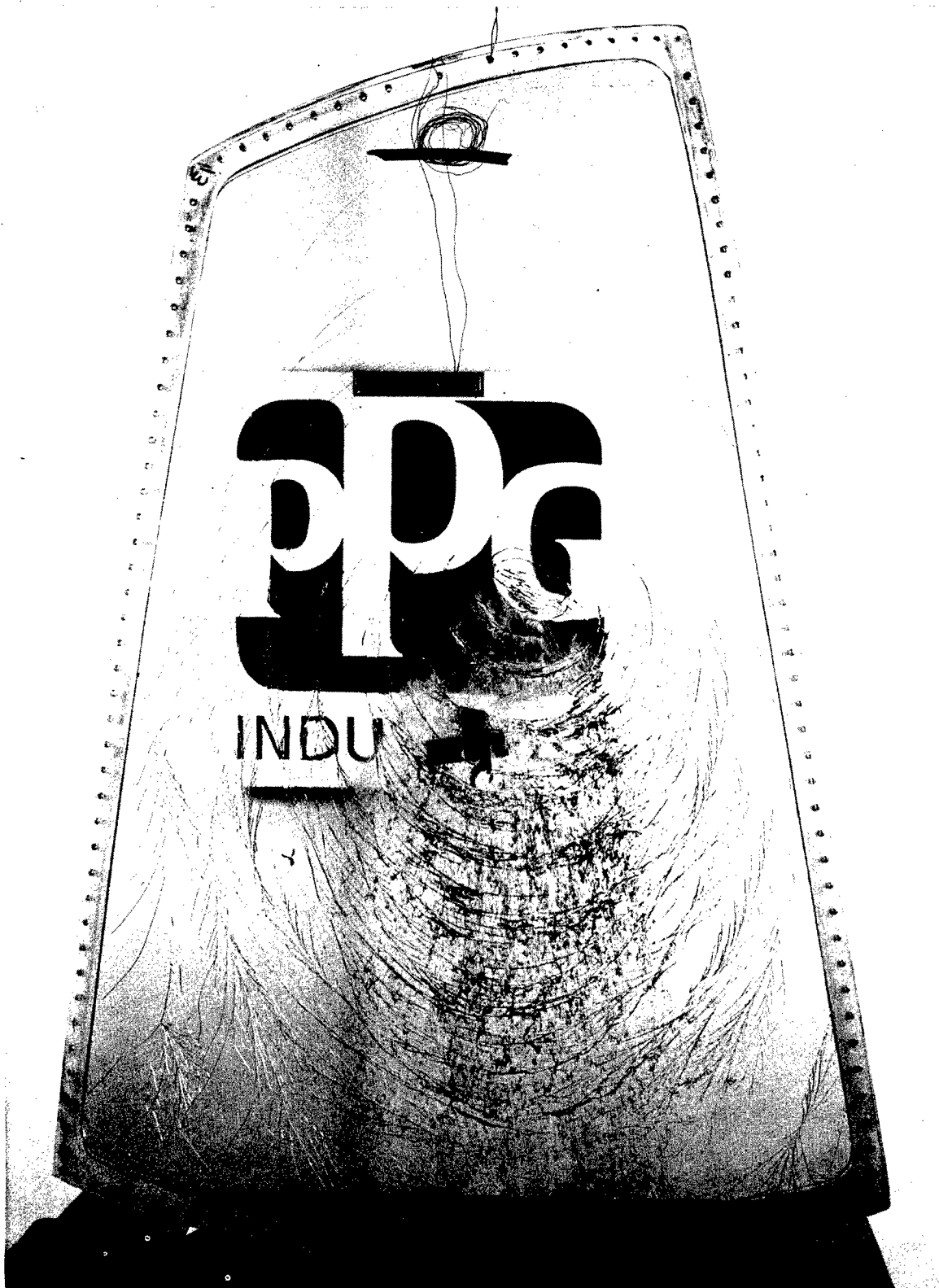


Figure 7      Center Impact by 4 lb Bird, 706 kt, 72°F

ALTITUDE AND PREDICTABILITY STUDIES OF  
WHISTLING SWAN MIGRATIONS

W. J. L. Sladen and J. G. Reese  
Johns Hopkins University  
Baltimore, Maryland  
and  
W. W. Cochran  
Illinois Natural History Survey  
Champaign, Illinois

Paper unavailable for publication.

EXPERIMENTAL INVESTIGATION INTO THE  
BIRD IMPACT RESISTANCE OF FLAT WINDSCREEN  
PANELS WITH CLAMPED EDGES

M. J. Mott  
Hawker Siddeley Aviation Ltd.  
Hatfield, Hertfordshire, England

Experimental Investigation into the Bird Impact Resistance  
of Flat Windscreen Panels with Clamped Edges.

M.J. Mott,  
Hawker Siddeley Aviation Ltd.,  
Hatfield.

SUMMARY

Bird impact tests conducted by the Royal Aircraft Establishment at Farnborough on clamped edge flat windscreen panels, in connection with the development of the Concorde windscreens, indicated that the penetration speeds achieved were considerably higher than those predicted using the design formula recommended in the R.A.E. Technical memorandum No. Mech. Eng. 106. <sup>1</sup> In view of the discrepancy a comprehensive test programme was prepared by Hawker Siddeley Aviation to assess the bird impact resistance of flat windscreens with the object of deriving new design formulae. These tests were carried out with the Company's compressed air bird gun at Hatfield. A brief description of the test facility will be given including details of the gun, the missile (bird and cup), timing, accuracy and speed range. The test programme set out to establish as much data as possible on the following design parameters which it was felt would have an influence on the bird resistance of flat windscreens:-

(a) clamping width, (b) main ply thickness, (c) main ply composition, (d) temperature, (e) impact angle, (f) bird weight, (g) impact position, and (h) frame stiffness. All these parameters were investigated for laminated thermally toughened glass windscreens, and a limited number for laminated stretched acrylic and Triplex Safety Glass Company's "Ten Twenty" high strength glass windscreens. Details will be included of the test specimens and the method of mounting.

The paper will conclude with an analysis of test results and recommended new design formulae.

## Experimental Investigation into the Bird Impact Resistance of Flat Windscreen Panels with Clamped Edges

### INTRODUCTION

In connection with the development of windscreens for the Concorde Project, the Royal Aircraft Establishment at Farnborough conducted tests on clamped edge flat windscreen panels. The results of these tests indicated that the penetration speeds achieved were considerably higher than those predicted using the empirical formula recommended in the R.A.E. Technical Note M.E.106<sup>1</sup> for the design of bird resistant windscreens. In view of the discrepancy, a comprehensive test programme was prepared by Hawker Siddeley Aviation to assess the bird impact resistance of flat windscreen panels, with the object of deriving new design formulae. These tests were conducted by Hawker Siddeley Aviation at Hatfield, under contract from the Ministry of Aviation Supply.

### TEST FACILITY

The principle of testing aircraft components by projecting a bird at a stationary test specimen is now accepted by the British aircraft industry and Government departments. All the tests discussed in this paper, unless otherwise stated, were conducted with the Hawker Siddeley Aviation compressed air gun. The gun comprises a stainless steel barrel, a compressed air reservoir, and a connecting breech mechanism. The volume of the air reservoir is 36 cubic feet. The barrel is 38 feet long with a honed bore of nominally 6 inches diameter. To permit the loading of the bird carcass, the gun barrel is disconnected from the breech mechanism and moved forward on rollers. The gun is fired by first pressurising the reservoir with air, which is retained by a Neoprene coated Terylene diaphragm clamped firmly within the breech mechanism, and then releasing the air by cutting the diaphragm with a circular knife. The knife is actuated remotely by an electro-pneumatic device.

### Fig.1. A general view of the test facility showing the gun and a windscreen under test

Pigeons or chickens, packed in nylon bags to prevent disintegration before impact, are used as missiles. The birds are stored in a deep freeze and then completely thawed out before firing. The missile is held centrally in the gun barrel by an expanded polyurethane plastic cup which is machined on its outside surface to be a standard fit in the gun barrel. For the majority of firings the foam plastic cup is split along its centre line, thus permitting the two halves to separate from the missile on leaving the gun. For projections at higher speeds the cup is not split but is retarded and broken up by a steel catcher ring mounted 12 inches beyond the muzzle of the gun barrel.

Fig.2. High speed film of Bird hitting a windscreen followed by the broken cup.

The speed of the bird is controlled by varying the air pressure in the reservoir. A considerable increase in the speed potential of the gun has been gained by sealing the muzzle of the barrel with a frangible 'Melanex' diaphragm and evacuating the air.

Fig.3. Performance curves for bird gun.

It has been standard practice at Hawker Siddeley Aviation to verify the speed of every firing of the gun. This is achieved by measuring, with a 'Chronotron' microsecond counter, the time interval between the breaking of two thin brittle wires stretched 5 feet apart. Experience has shown that normally the speed achieved is within 3% of that predicted from the calibration graphs.

#### TEST SPECIMEN AND MOUNTING DETAILS

The tests were conducted on windscreen panels with the main plies manufactured from three groups of materials.

- (a) Thermally toughened glass by Triplex Safety Glass Co. Ltd.,
- (b) Stretched acrylic to specification MIL-P-25690A by Lucas Aerospace Ltd.
- (c) "Ten Twenty" high strength glass by Triplex Safety Glass Co., Ltd.

All the test panels were rectangular, nominally 25 in x 19 in with rounded corners. This size was chosen in order to provide a direct comparison with previous R.A.E. results.

Fig.4. Typical sections of test panels.

One to four main load bearing plies of varying thicknesses were used, laminated to each other by .05 in. thick R.V.B. interlayers. The forward facing abrasion screen was reduced in size to form an edge rebate to permit clamping of the main load bearing plies only. For economy reasons no splinter shields nor heating systems were fitted and the panels were not to aircraft optical standards.

Fig.5. Typical section of installation of test panels in their mounting structure.

Each test windscreen was assembled into a relatively stiff light alloy cast mounting frame. Rubber gaskets were positioned above and below the edge of the windscreens to eliminate any panel to metal contact. Carefully selected thicknesses of packing rings were used to ensure an adequate but not over-tight clamping of the edges. The width of clamping was varied for the initial tests, but was then standardised at 0.6 in.

## SCOPE OF TEST PROGRAMME

The programme set out to establish as much data as possible on the following parameters which it was felt would have an influence on the bird impact resistance of flat windscreens.

- (a) Clamping width.
- (b) Main ply thickness.
- (c) Main ply composition.
- (d) Temperature.
- (e) Impact angle.
- (f) Bird weight.
- (g) Impact position.
- (h) Frame stiffness.

## Fig.6. Programme details.

All these parameters were investigated for the thermally toughened glass windscreens, but only a limited number for the stretched acrylic and "Ten Twenty" high strength glass windscreens.

## SUMMARY OF TEST RESULTS

A total of 125 panels have been tested during this series of tests and these were subjected to 280 shots.

## Fig.7. Effect of clamping width.

Windscreen material - Thermally toughened glass.

4 lb. bird, centre shot, 53° sweepback, ambient temperature.

This shows that for both thicknesses of panel under consideration the failing speeds, when tested with clamping widths of 0.6 in. and 0.84 in., did not vary significantly. Subsequent tests during the remainder of this work were all conducted at the smaller width of 0.6 in.

## Fig.8. Effect of variations in main ply thicknesses and composition

Windscreen material - A. Thermally toughened glass.

B. Stretched acrylic.

C. "Ten Twenty" high strength glass.

4 lb. bird, centre shot, 53° sweepback, ambient temperature.

A. Thermally toughened glass.

These results show that a linear relationship exists between the failing speed and the total glass thickness of the fully and semi-toughened glass plies independent of the main ply composition.



B. Stretched acrylic.

The failing speed  $V$  of multilaminated windscreen panels can be related to the total stretched acrylic thickness ' $t$ ' by the following empirical expression :-

$$V = k^3 \sqrt{t^2} \quad (1)$$

Monolithic panel results show failing speeds approximately 15% lower than multilaminated panels of the same total stretched acrylic thickness.

C. "Ten Twenty" high strength glass.

Compared with the results of the tests on thermally toughened glass the "Ten Twenty" high strength glass is approximately 30% more resistant to bird impact. The relationship between failing speed and total glass thickness is linear and independent of the main ply composition.

Fig.9. Effect of temperature.

Windscreen material - Thermally toughened glass and stretched acrylic.  
4 lb bird, centre shot, 53° sweepback.

The effect of temperature, over the range -40°C to +50°C, on the failing speeds of windscreens was in general small.

The stretched acrylic panels are more critical than glass at the lower temperatures whereas the reverse is true for the higher temperatures.

Fig.10. Effect of Impact angle.

Windscreen material - Thermally toughened glass.  
4 lb. bird, centre shot, ambient temperature.

The failing speed is proportional to the reciprocal of the cosine of the sweepback angle.

Fig.11. Effect of bird weight.

Windscreen material - Thermally toughened glass.  
Centre shot, 53° sweepback, ambient temperature.

The assumption that the energy of the bird on impact to produce similar damage is a constant value, gives a reasonable relationship for bird weights from 1 lb. to 4 lb.

Fig.12. Effect of impact position.

Windscreen material - Thermally toughened glass.

4 lb. bird, corner shot, 53° sweepback, ambient temperature.

From the very limited testing, it would appear that the failing strength of windscreens with four main ply laminations is less critical to corner shots than those with only two main ply laminations. Further testing is necessary to confirm or contradict this trend.

Fig.13. Effect of frame stiffness

Windscreen material - Thermally toughened glass and stretched acrylic.

4 lb. bird, centre shot, 53° sweepback, ambient temperature.

The effects of two different degrees of frame stiffness were explored :- Frame 'A' having equivalent stiffness to an aircraft mounting designed to withstand a working pressure of 5.25 lb/sq.in. with a stress in light alloy of 15,000 lb/sq.in. and Frame 'B' similarly designed to withstand a working pressure of 8.5 lb/sq.in.

Windscreens should be mounted in as rigid a frame as possible to obtain the highest bird impact resistance. This is relevant to thermally toughened glass windscreens which were shown to be particularly sensitive to reductions in frame stiffness.

DISCUSSION OF RESULTS

Fig.14. Comparison between M.E.106 empirical design formula curve and the curves produced from the test results.

These curves confirm that the M.E.106 formula gives predicted failure speeds below the speed achieved in these clamped edge windscreen tests particularly for the thicker windscreens.

If the failing speeds were plotted against panel weight and not thickness, the stretched acrylic windscreens would, very approximately, be twice as resistant as thermally toughened glass windscreens, and one and a half times as resistant as 'Ten Twenty' high strength glass windscreens.

The test evidence indicates that the following empirical formulae are realistic for the bird impact strength of flat windscreen panels with clamped edges. In determining the formulae it has been assumed that the relationships for sweepback angle and bird weight derived from the tests on the thermally toughened glass windscreens will also apply to windscreens manufactured in the other materials covered in this paper.

#### Thermally toughened glass

$$\text{Failing speed} = \frac{400 \times \text{total glass thickness (inches)}}{\sqrt{\text{bird weight (lb)} \times \cos.\text{sweepback angle}}} \quad (2)$$

#### Stretched acrylic

$$\text{Failing speed} = \frac{470 \sqrt[3]{\text{stretched acrylic thickness}^2 \text{ (inches)}}}{\sqrt{\text{bird weight (lb)} \times \cos.\text{sweepback angle}}} \quad (3)$$

#### "Ten Twenty" high strength glass

$$\text{Failing speed} = \frac{520 \times \text{total glass thickness (inches)}}{\sqrt{\text{bird weight (lb)} \times \cos.\text{sweepback angle}}} \quad (4)$$

Fig.15. Comparison of other test data with the empirical design formulae.

The correlation of these results is encouraging. The predicted failing speeds are in all cases below the test results. The largest discrepancies are shown in the results No.5 and 10. These may be accounted for, in result No.5, by the fact that the panel contains 3 layers of Chemoor glass (total thickness 0.25 in.) in addition to the stretched acrylic plies and in result No.10 the panel size was 32 in. x 20 in. compared to 25 in. x 19 in. for the standard test panel.

These formulae can only be a guide to the design of bird resistant windscreens as the test data from which they have been calculated has, for necessity, been simplified. The effect of some of the design variables such as clamping width, panel composition, temperature, impact position and frame stiffness has been demonstrated by test to be small when considering the overall bird impact resistance. So far little information is available on the effects of panel size and shape.

Final approval of any design for bird impact resistance can therefore only be obtained by tests on the actual windscreen installation under the required operational conditions. However, it is intended to extend the programme of tests to obtain further basic design data. Tests to investigate the effect of panel shape are already proceeding.

This paper has been prepared from the detail data published by Hawker Siddeley Aviation Ltd. 2.

### Figure Symbols

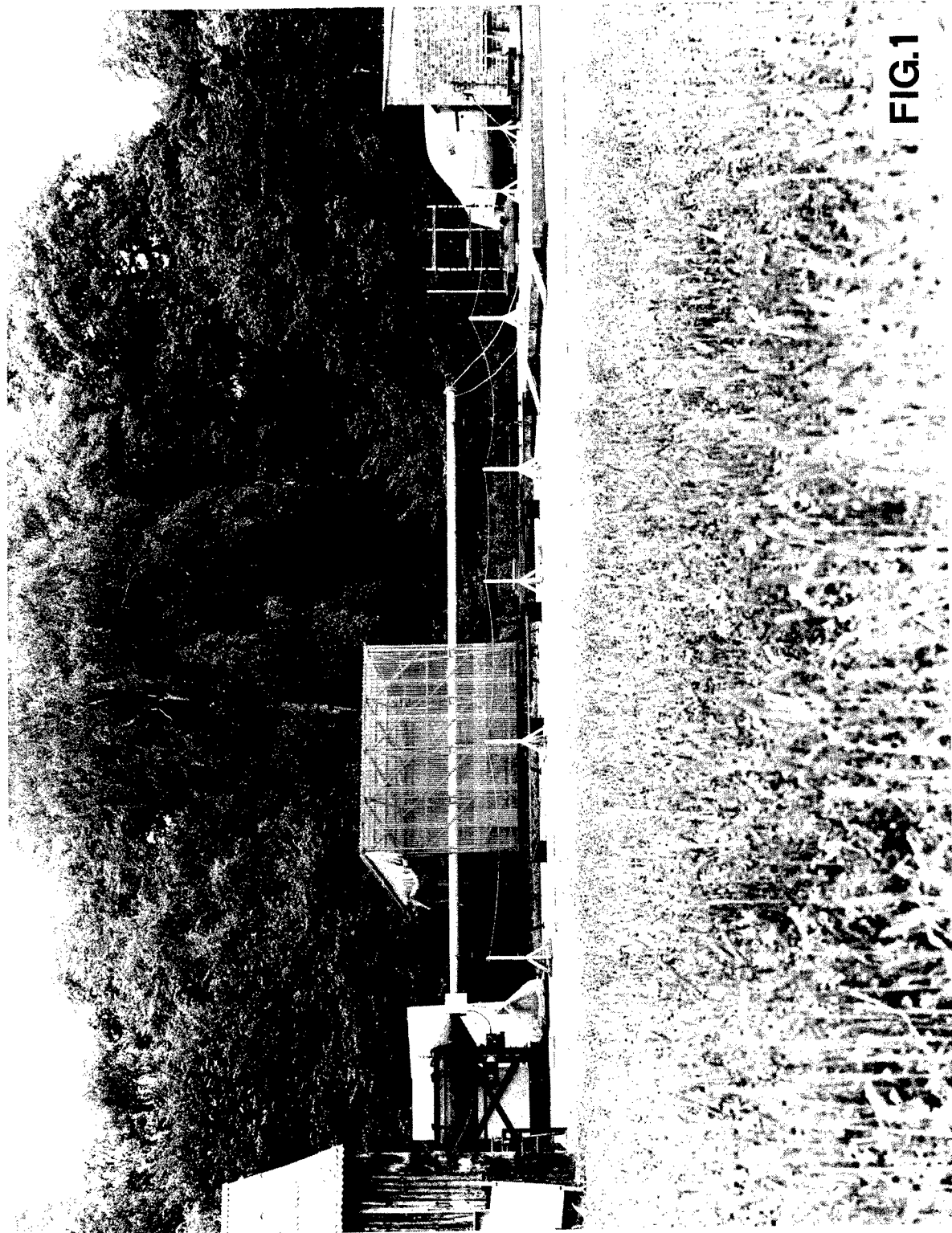
- △○▽□ No main plies failed.  
○▽■ At least one main plied failed.  
▲●▽□ All main plies failed.

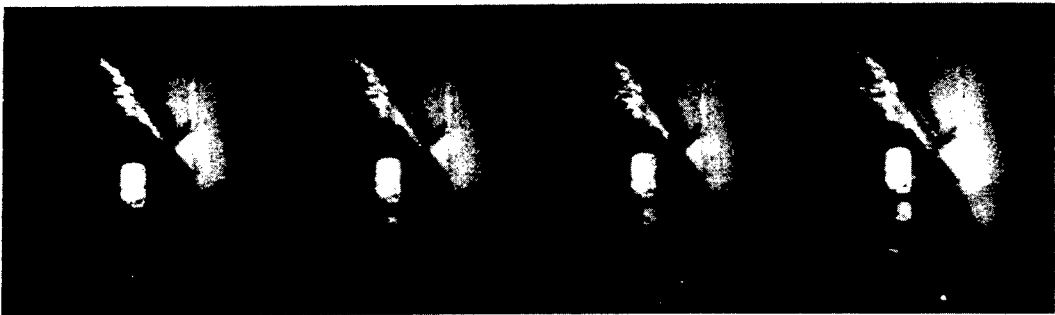
### References

| No. | Author                                   | Title   |
|-----|--|---|
| 1   | Staff of M.E. Dept.<br>R.A.E.            | The design of aircraft transparencies for resistance against impact by birds and hailstones R.A.E. Technical Note M.E.106 (1952).   |
| 2   | Staff of Structural<br>Test House.H.S.A. | Research programmes for the experimental investigation of the bird impact resistance of windscreen panels with clamped edges.<br>TRM 430 and Add 1 & 2.<br>TRM 431 and Add 1.<br>TRM 432 and Add 1.<br>TRM 460. |

### Acknowledgments

The author wishes to thank the Directors of Hawker Siddeley Aviation Ltd., for permission to give this paper but points out that the opinions and views expressed are his and not necessarily those of the Company. He would also like to thank the Ministry of Defence, the sponsors of this test programme, for permission to use the test data and Triplex Safety Glass Ltd., for the use of its test results.





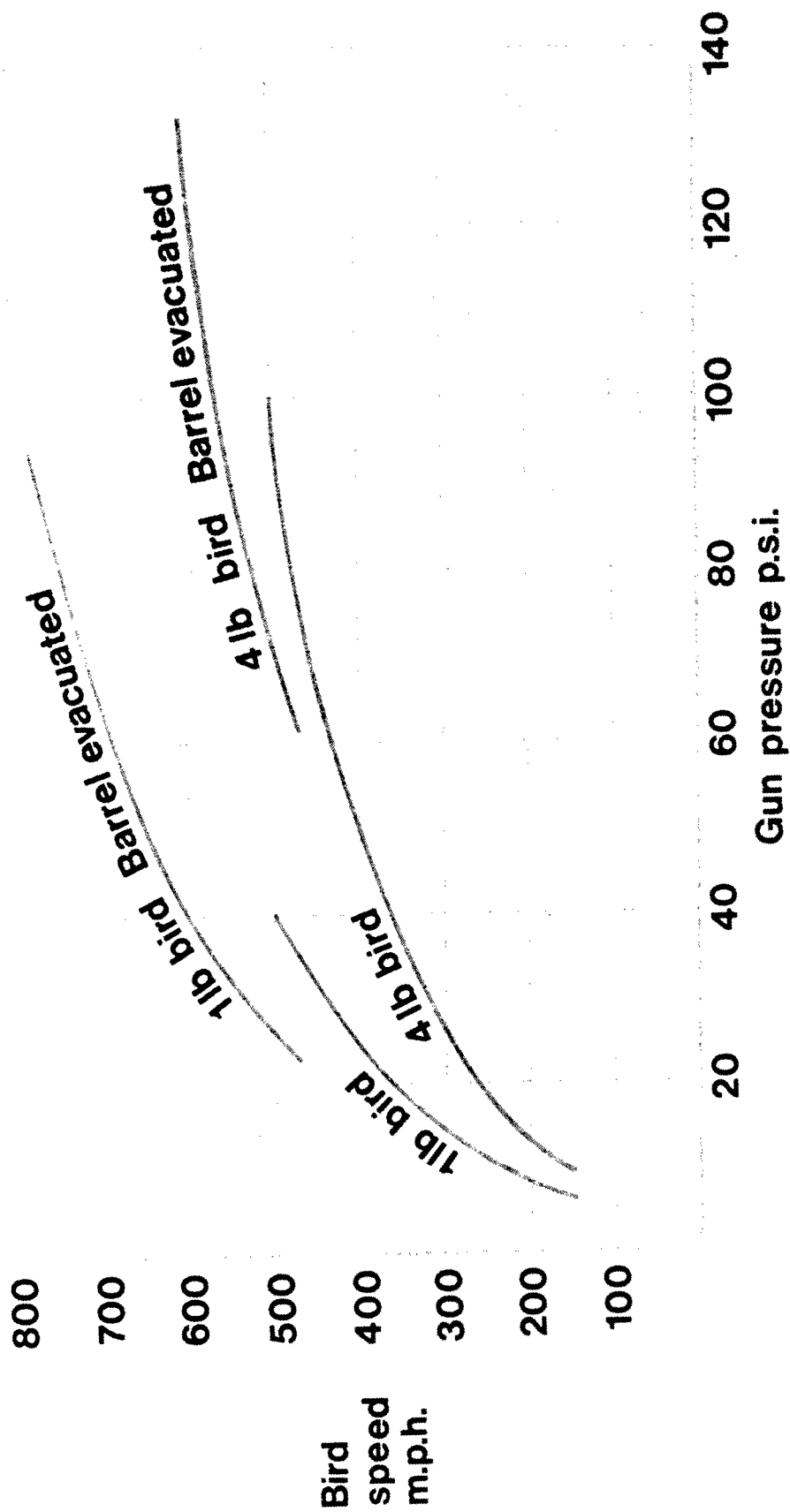
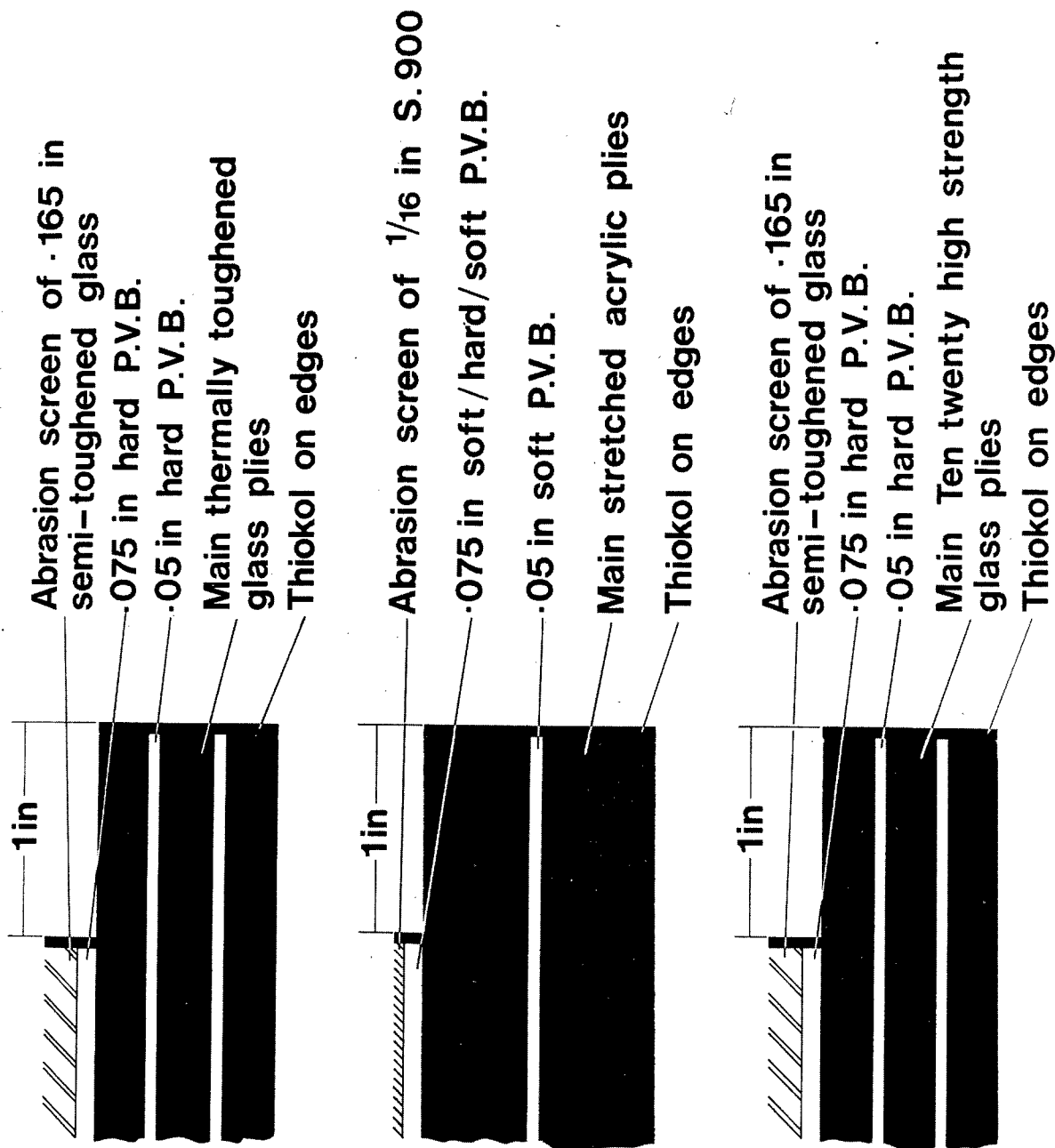


Fig.3



**Fig.4**



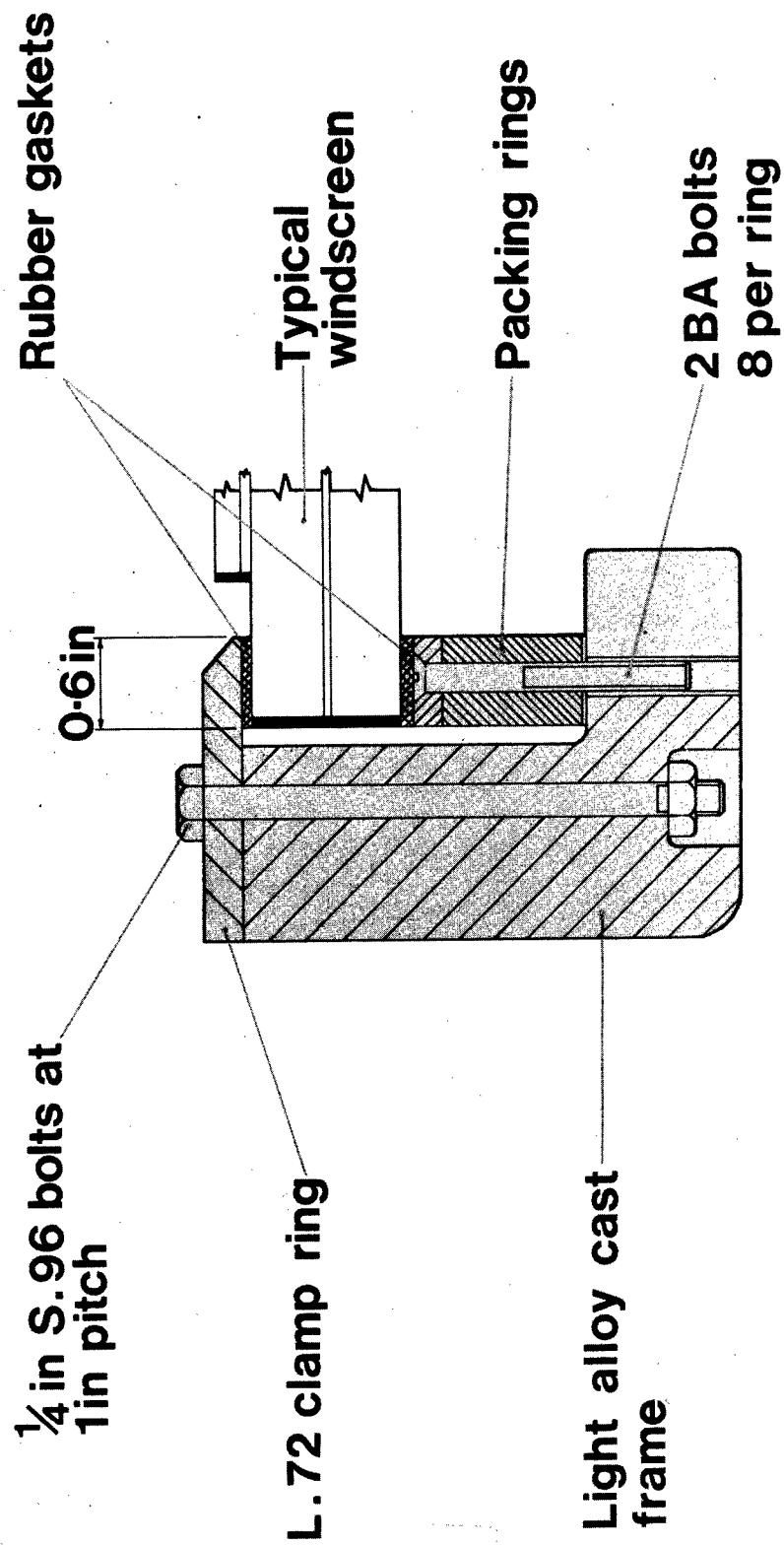
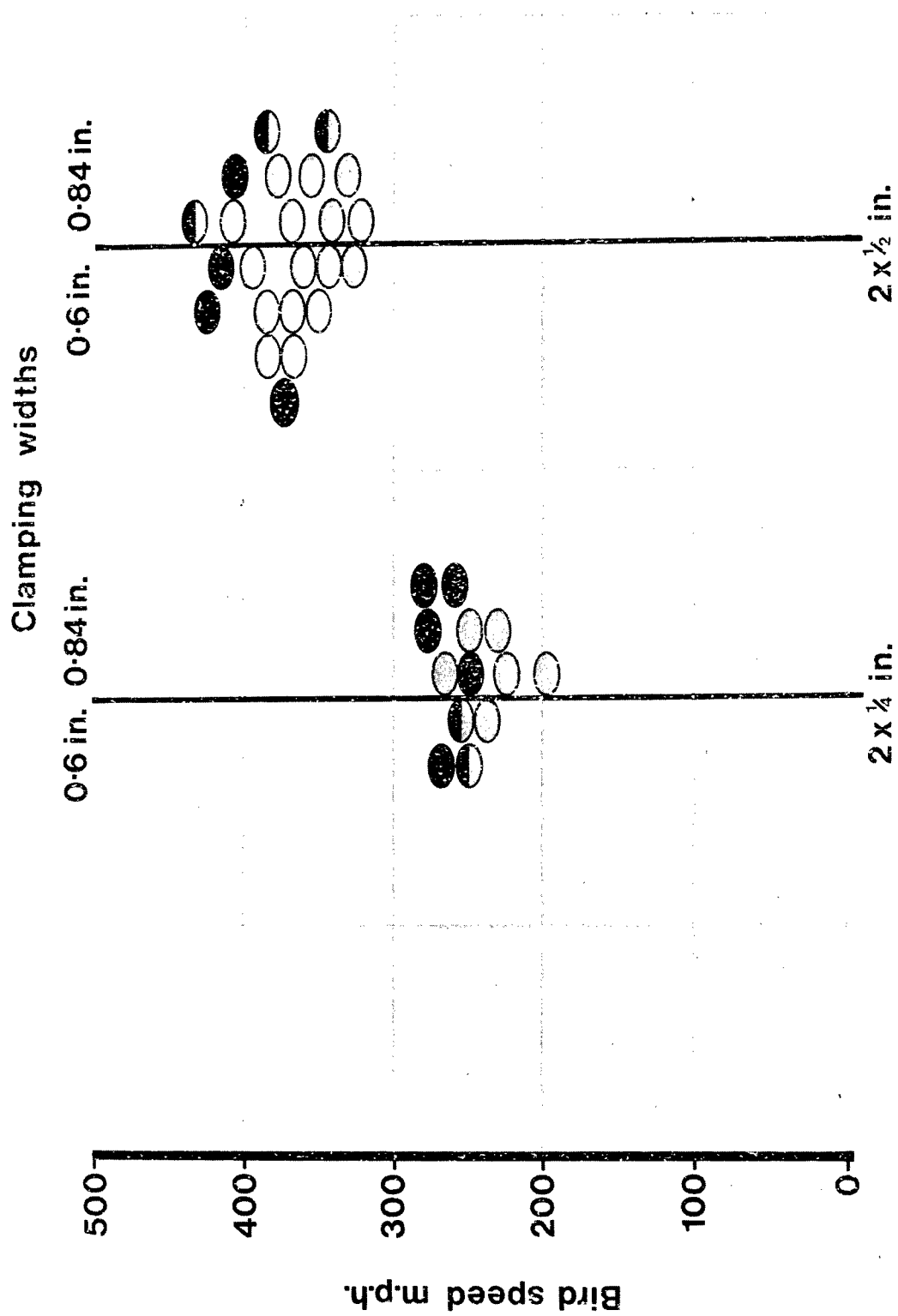


Fig.5

| Parameters           | Windscreen main ply material |                    |                                 |
|----------------------|------------------------------|--------------------|---------------------------------|
|                      | Thermally toughened glass    | Structural acrylic | Ten twenty' high strength glass |
| Clamping width       | ✓                            |                    |                                 |
| Main ply thickness   | ✓                            | ✓                  | ✓                               |
| Main ply composition | ✓                            | ✓                  | ✓                               |
| Temperature          | ✓                            | ✓                  |                                 |
| Impact angle         | ✓                            |                    |                                 |
| Bird weight          | ✓                            |                    |                                 |
| Impact position      | ✓                            |                    |                                 |
| Frame stiffness      | ✓                            | ✓                  |                                 |

Fig.6



Thickness of toughened glass main plies

Fig.7

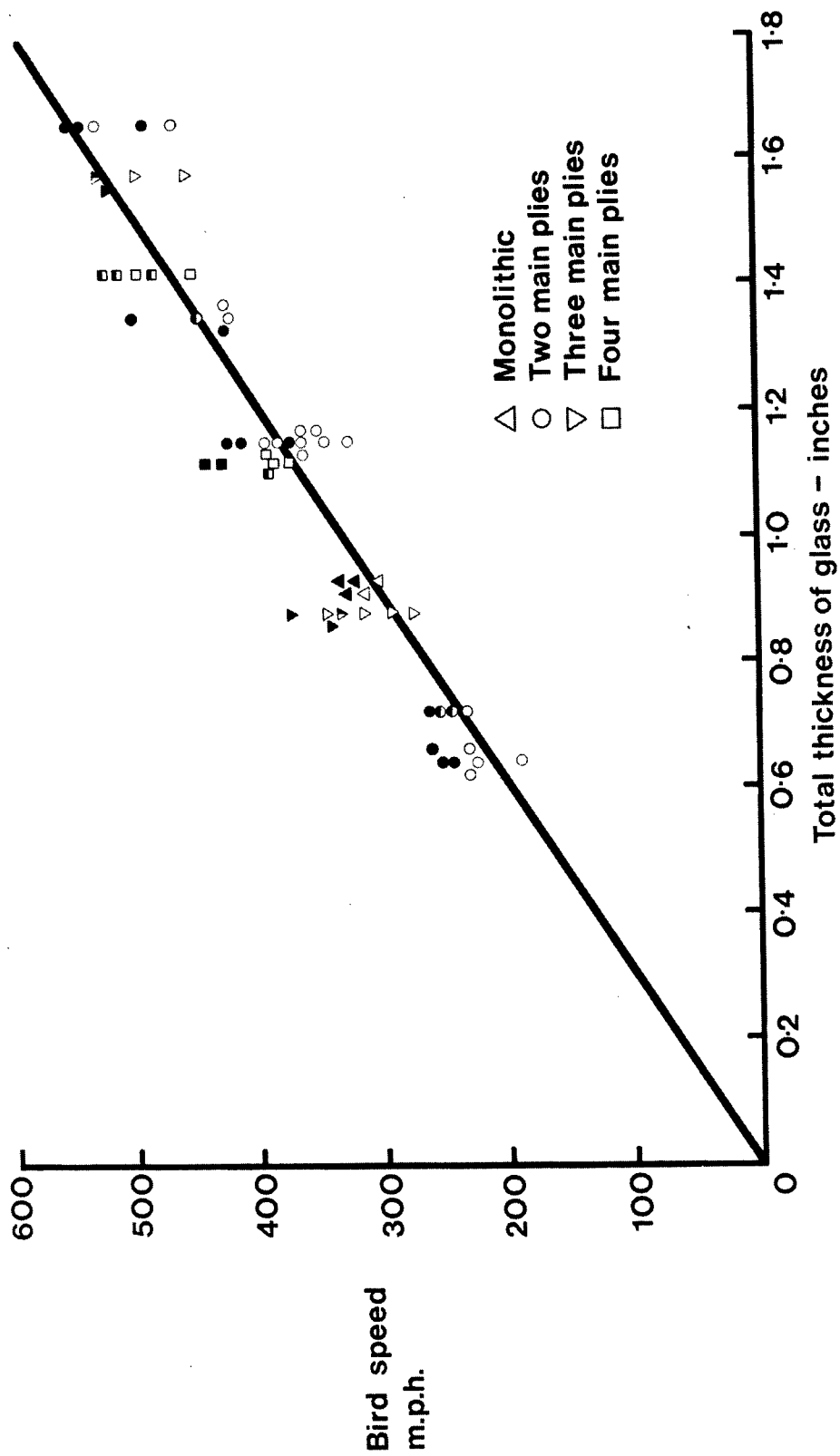


Fig. 8a

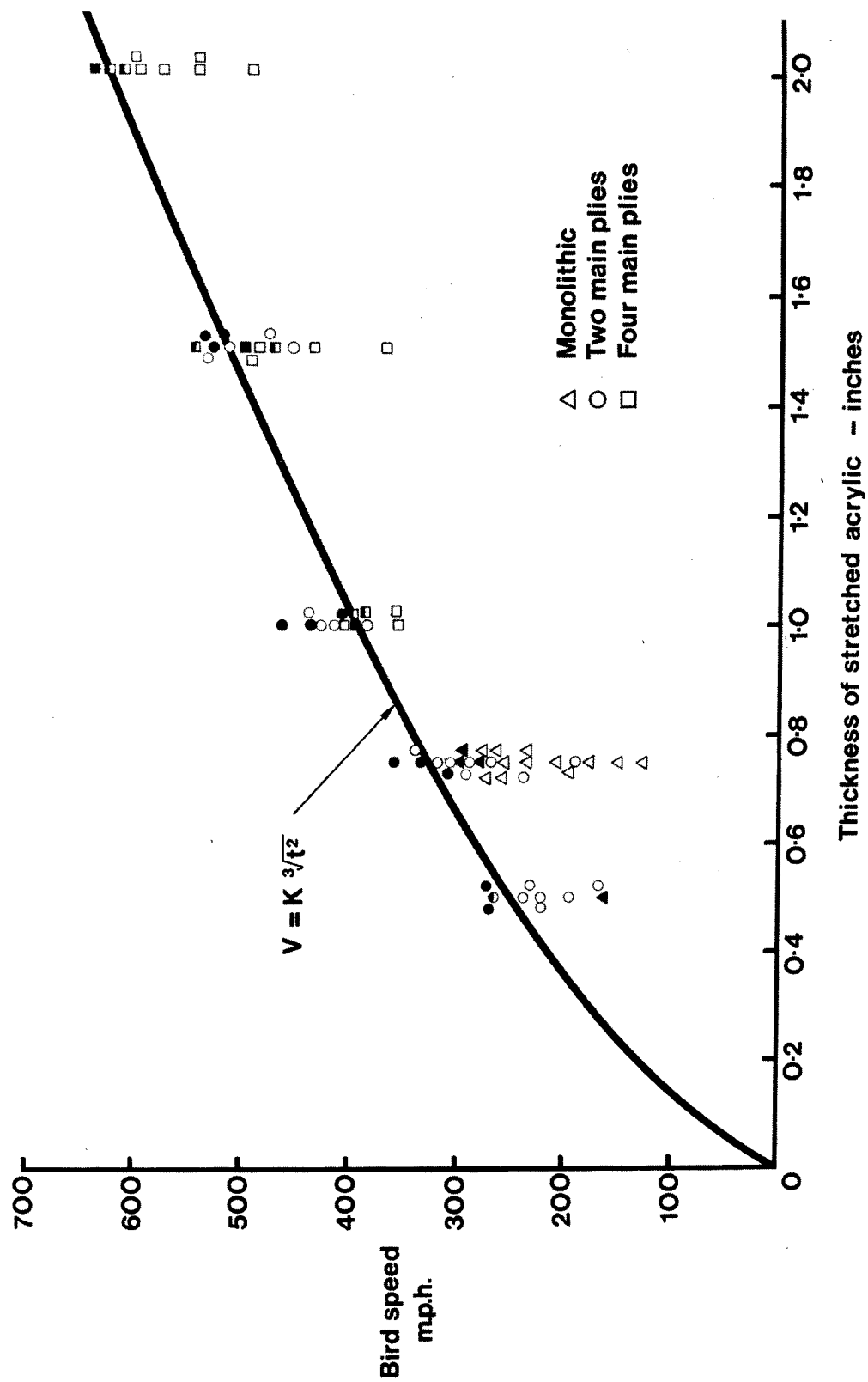


Fig.8b

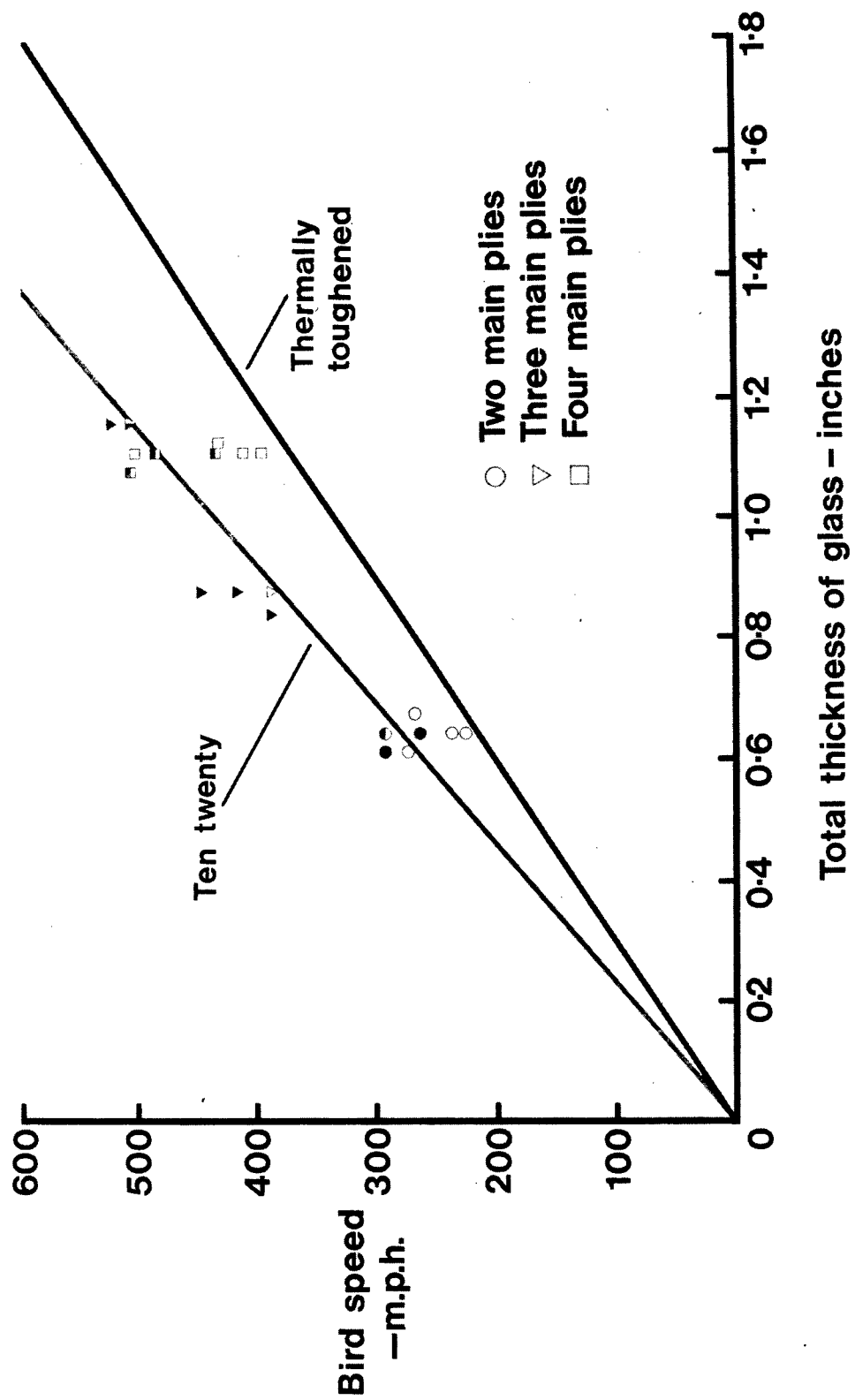


Fig. 8c



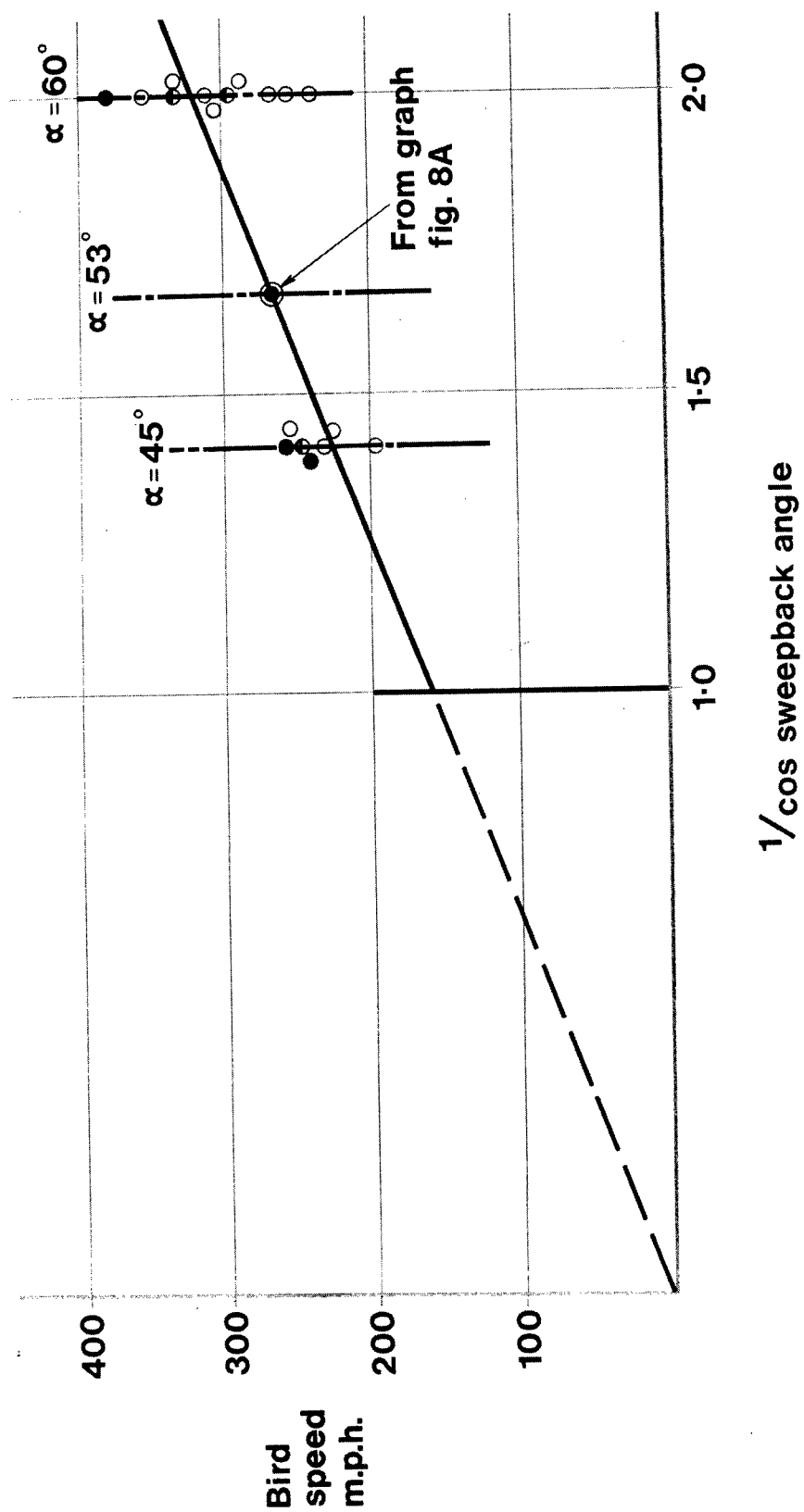


Fig.10



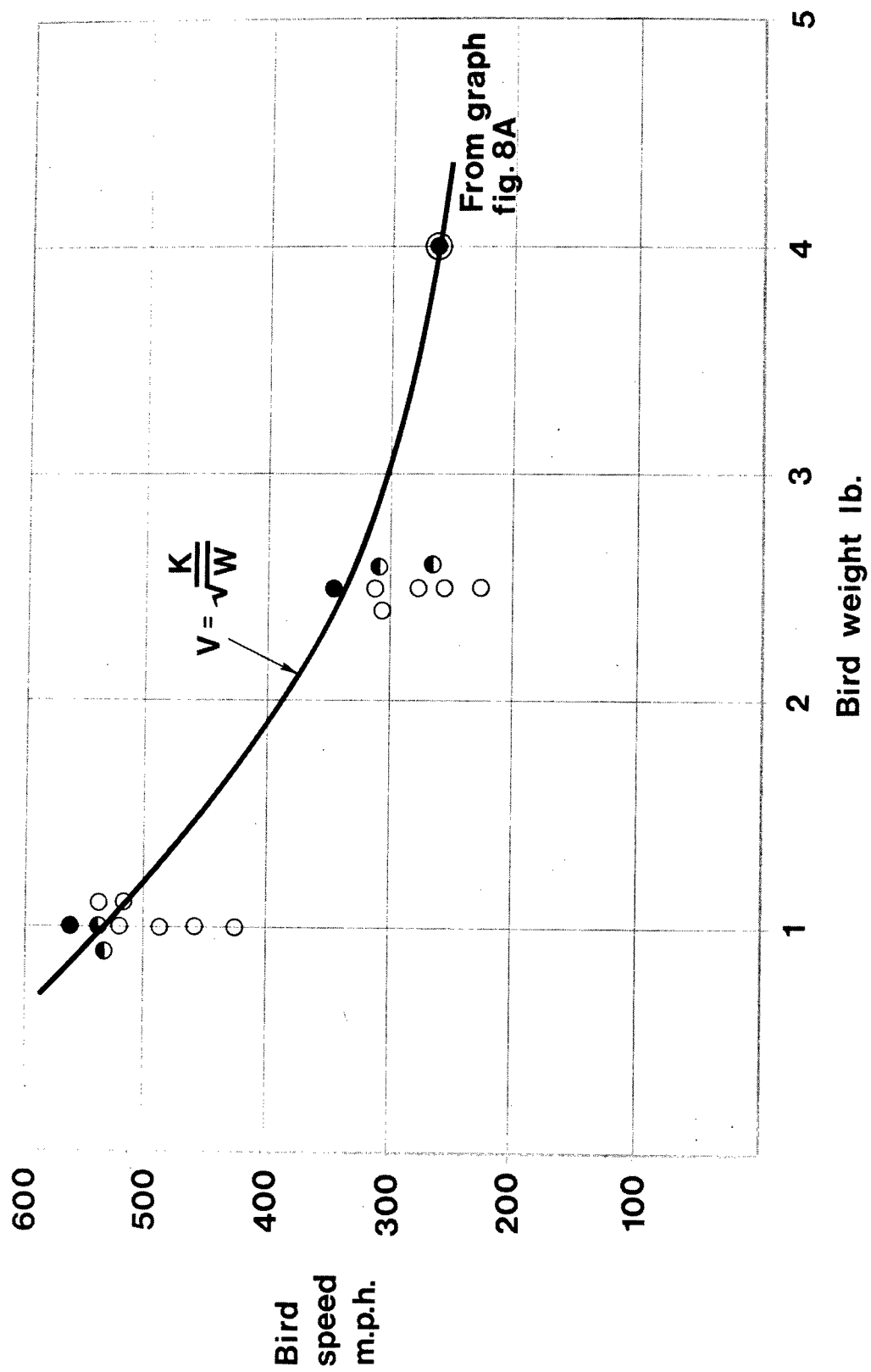


Fig.11

# Corner shots

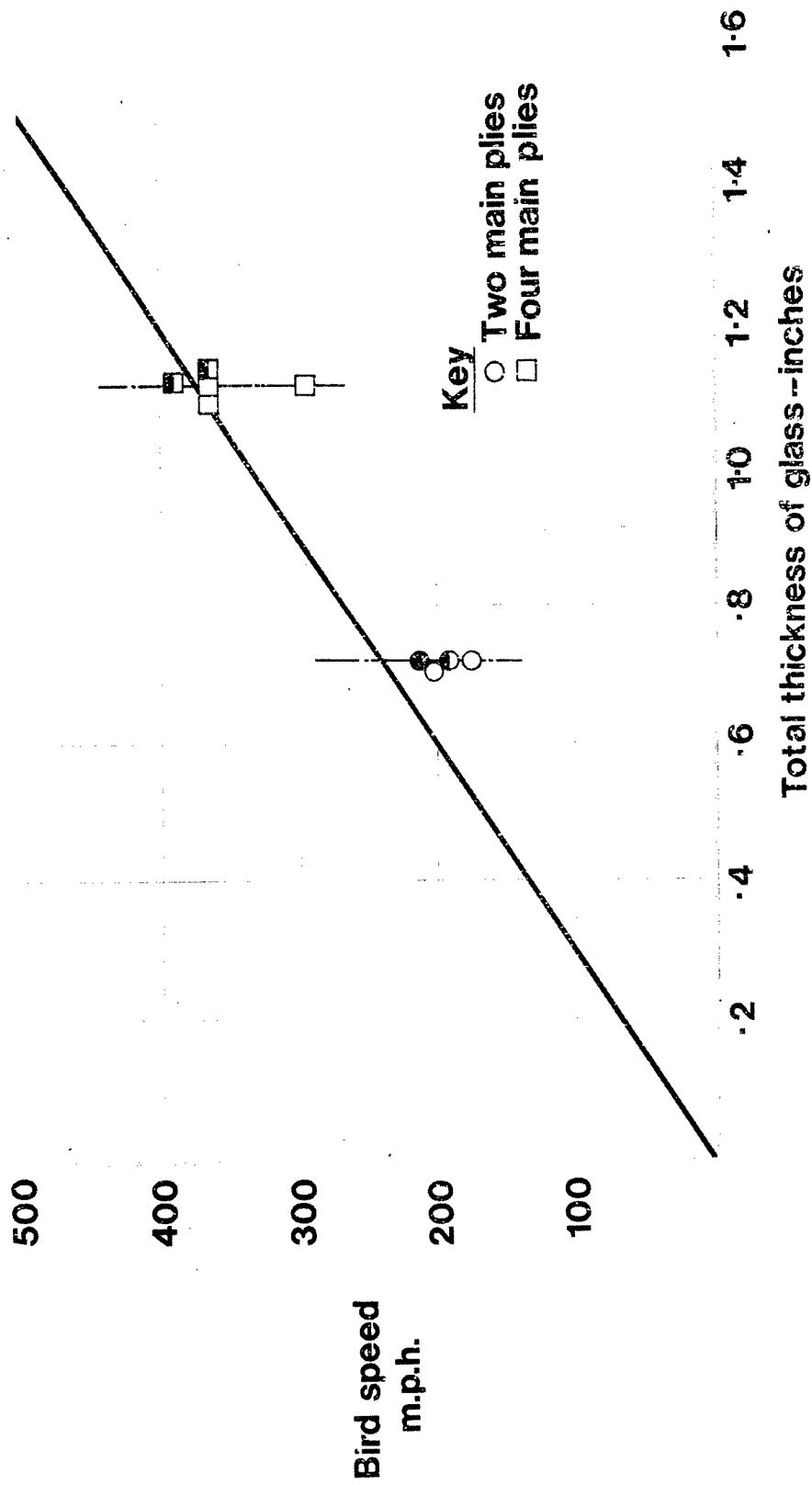


Fig.12

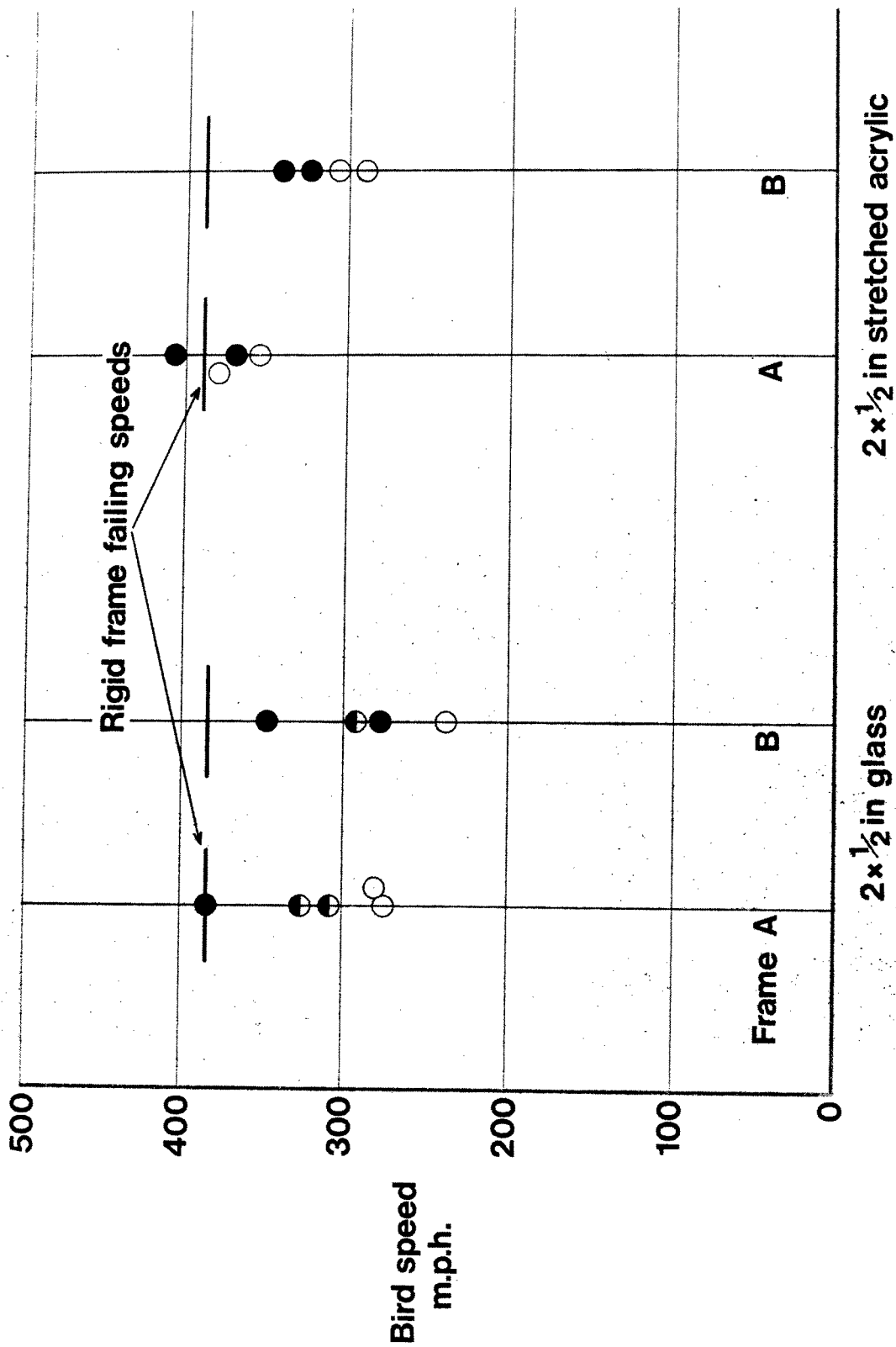


Fig.13

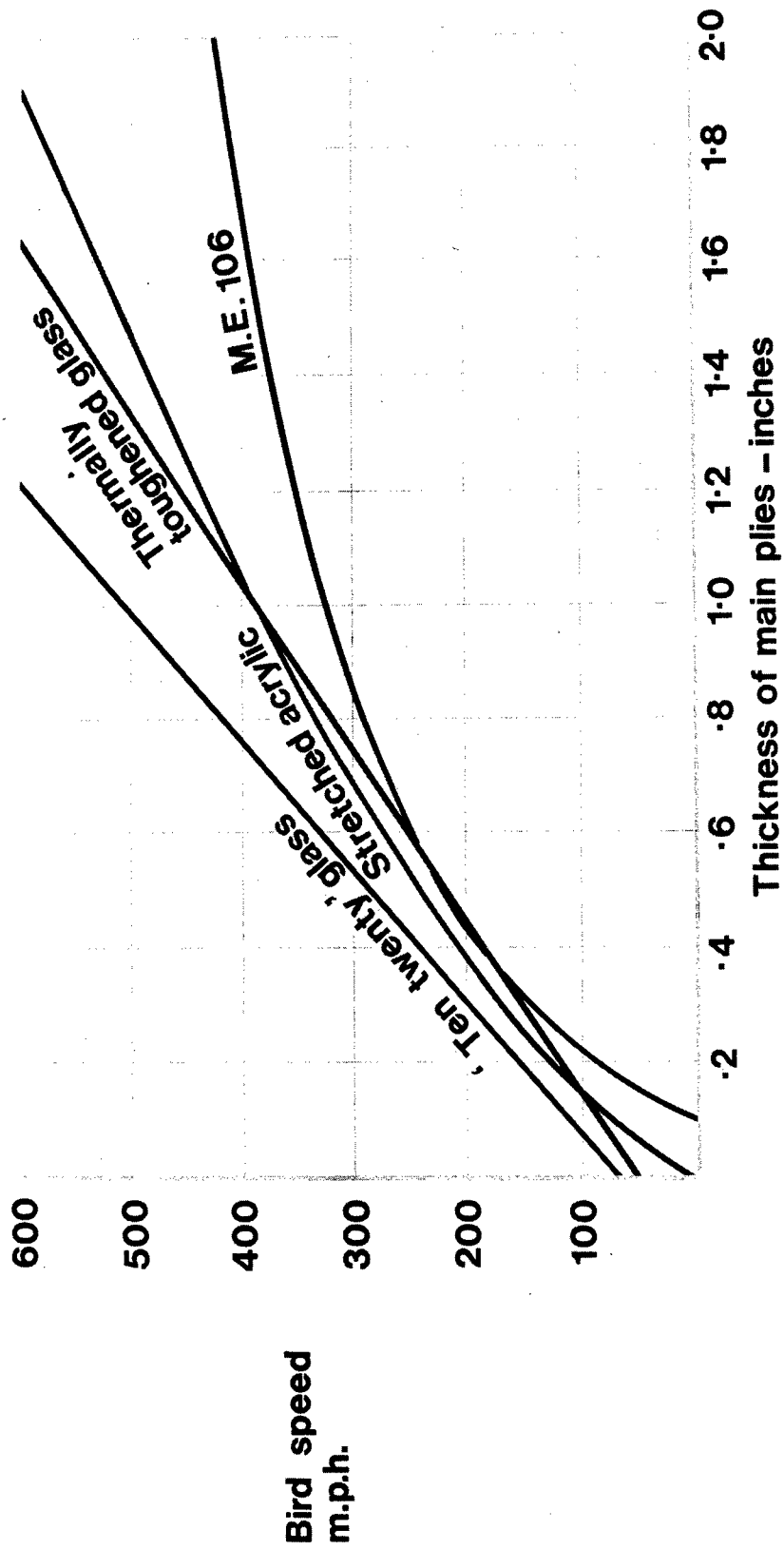
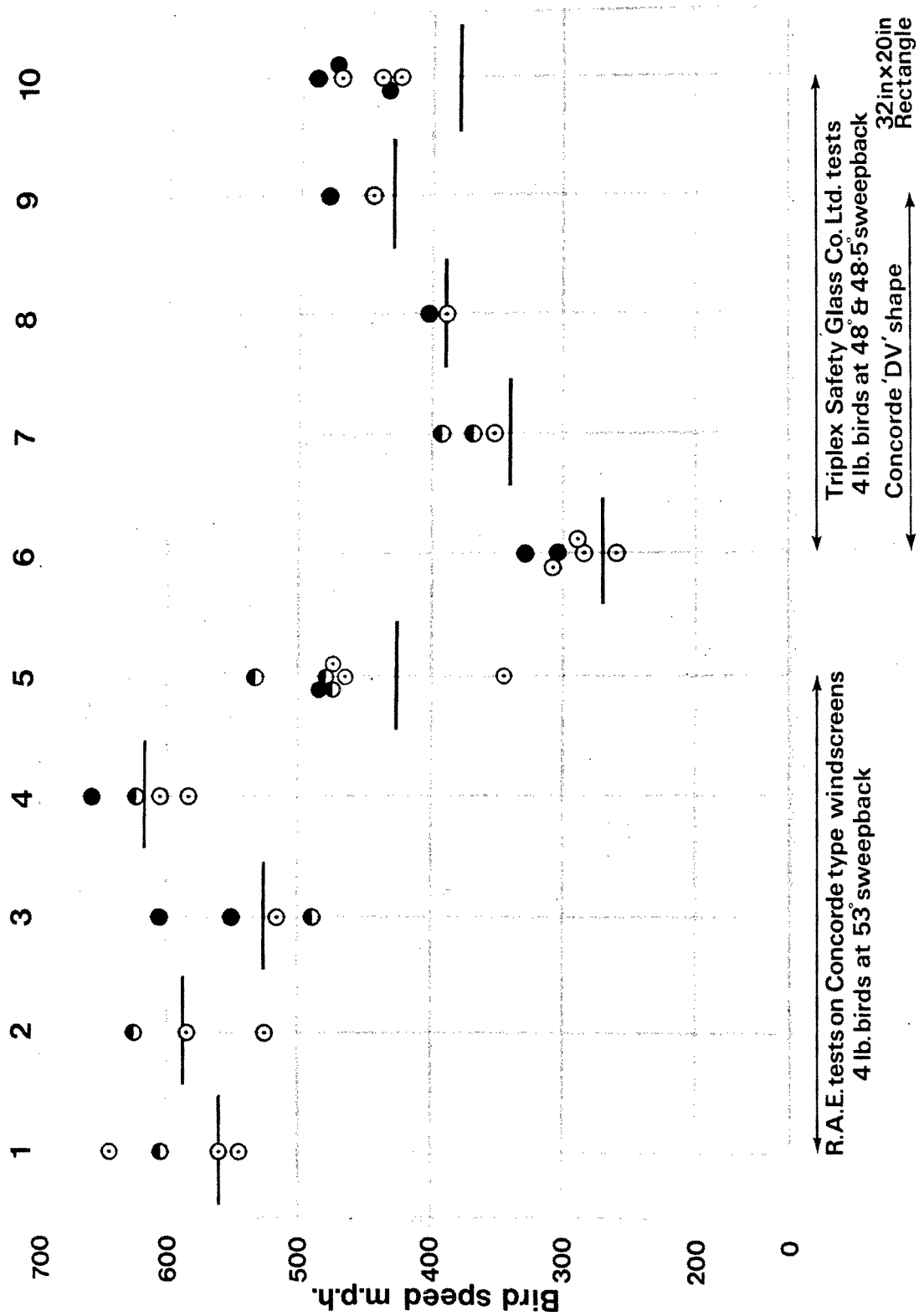


Fig.14



**Fig.15**

PHYSICAL TECHNIQUES FOR CONTROLLING  
BIRDS TO REDUCE AIRCRAFT STRIKE HAZARDS

Sheldon I. Lustick  
The Ohio State University  
Columbus, Ohio

PHYSICAL TECHNIQUES FOR CONTROLLING BIRDS  
TO REDUCE AIRCRAFT STRIKE HAZARDS

Sheldon I. Lustick

Ohio State University  
Zoology Department

ABSTRACT

Three species of birds (starling, Sturnus vulgaris; mallard duck, Anas platyrhynchos; and herring gulls, Larus argentatus) were used to determine if high-intensity laser light could decrease the bird-strike hazard to aircraft. The effects of both continuous and pulsing light on bird behavior and physiology were determined. The responses of the birds were monitored both visually and electronically. The birds were exposed to both a low-intensity strobe light pulsing at frequencies of from 100 to 1000 per minute and an argon laser capable of emitting either pulsed or continuous light of different wavelengths (454 to 515.5 nm) at intensities of 20 mW to 4 W. The intensity of laser light striking the bird could be varied further by changing the diameter of the laser beam.

It was found that a concentrated laser beam of 0.2 cm in diameter at a power above 0.5 W would cause an avoidance response in all the species tested and thus could be considered nonspecies specific. It is also the only light source to which the birds did not habituate. Though the initial response to pulsing laser light of lower intensity (beam expanded from 2 to 14 in.) was increased excitability (increased perch hopping and heart rate) the gulls and starlings soon habituated. The ducks were more sensitive than gull or starling to the expanded laser beam having an elevated heart rate and avoiding the laser beam expanded to six inches in diameter at least 50 percent of the time. All species tested showed a group avoidance response and could be denied a portion of the test enclosure when exposed to the concentrated laser beam. Also discussed are the feasibility of using a laser system, the problems of using a laser system, and further research needed before implementing a laser system for controlling birds.

## SECTION I

### INTRODUCTION

As man continues to develop the earth, he creates microhabitats which in turn create potential pest situations involving birds. In such new habitats as orchards, cities, and airfields, some species of birds congregate in large numbers, pest situations develop, and there is ultimately a need for some type of control. With the need for control established, one still must determine the control method that will give the best results. Therefore, the following study was conducted to determine if a laser system of bird control could be employed to decrease the bird-strike hazard without any adverse effect to the birds or the environment.

Regulatory methods are of two basic types: the direct methods of scaring, trapping, shooting, poisoning, and inhibiting reproduction, and the indirect methods of altering, shielding or removing a particular environment. In order to use the direct approach the operator must understand the organisms anatomy, physiology and behavior, and to use the indirect approach requires a knowledge of the organisms environment, including food, cover and competing and noncompeting organisms.

For a control program to be sound ecologically it should have specificity. That is, the control program affects only those individuals within the species that are in the pest situation (i.e., on the airfield). Besser<sup>1</sup> has stated that no one pest control technique can be considered a solution for all pest situations. In fact, many control techniques may be needed, with little assurance that they will be effective the following season. Bliese<sup>2</sup> found in four years of trying to control blackbirds that the efforts to control birds in one year had no effect on the blackbird response the following year.

The number of variables affecting a control method is large; for example, weather conditions and age of the birds. Siebe<sup>3</sup> indicated that in summer juvenile starlings were repelled by frightening devices and biosonics, whereas in the fall and winter these same devices were not effective at feed lots where large numbers of adult birds were concentrated indicating that either age or weather conditions affect the bird response to these controlling devices.

At first, control methods relied on fright techniques, followed by lethal techniques, and more recently on the preventive technique. Of course the perfect control would be one which would keep the birds out of the pest situation without destroying the birds or the environment. Up until now we have been considering bird control, in general. What about bird control in and around airports?



Both military and commercial equipment and personnel are endangered when aircraft strike birds. In 1965, 839 strikes were recorded by the Air Force; most were below 1000 feet. In 109 of these cases birds were drawn into the engine and 75 engine replacements were necessary, at a cost of four or five million dollars.<sup>4</sup>

Five basic methods for reducing the bird-aircraft strike hazards have been suggested:

1. Reduce the number of birds by killing
2. Rearrange bird habitat.
3. Make birds avoid planes.
4. Arrange for planes to avoid birds by use of a radar warning system.
5. Fortify the airplane.

Of these methods, the third would be the most desirable, and has been the subject of much research with various devices (acetylene exploders, biosonics, chemical agents, electronic shocking devices) being adapted for use.<sup>5,6,7</sup> Although these devices are helpful, none has been so successful that there has been a lessening in the need for further research into the means of combating the bird-strike hazard. The other methods mentioned, although they would work to some extent, are generally undesirable. With the general public working to preserve the ecology, the killing of birds and the manipulation of habitat create poor public relations and are essentially undesirable methods. To arrange for planes to avoid birds creates air traffic problems, especially with the present large amount of air-traffic near airdromes, while hardening the plane decreased its efficiency, especially a military plane.

What is needed then is a frightening device which is nonspecies specific that will cause the birds to either leave the airfield or avoid a flying aircraft.

Schaefer<sup>8</sup> suggested research into the use of lasers on aircraft, for confusing or burning birds in the direct line of flight. He stated that a medium-powered gas laser in the visible range could be pulsed so as to confuse birds into diving, escaping or performing stunned motions, when used at 1000 yards. He also suggested the use of a higher power infrared laser to burn birds in the immediate line of flight of climbing or level-flying craft.

To truly understand the psychophysiological effects of a control method on an organism, conditions should be constant, preferably in a laboratory without outside interference.

## SECTION II

### METHODS AND MATERIALS

#### 1. CAPTURE AND MAINTENANCE

##### a. Starlings

Thirty starlings (Sturnus vulgarus) were captured on The Ohio State University Farm by use of a large walk-in trap. They were then transported to the laboratory and maintained in individual cages (26 x 24 x 23 cm) in a windowless air-conditioned room. The starlings were maintained on a 12-hour photoperiod (0800-2000 hr), while the air temperature in the room varied between 20° and 24°C. The birds were fed ad libitum food (Purina turkey pellets) and water.

##### b. Mallard Ducks

Twenty mallard ducks (Anas platyrhynchos), 10 male and 10 female, were purchased from Whistling Wing in Chicago, Illinois, and shipped air mail to Ohio State University. These birds were placed in cages (43 x 30 x 39 cm) in an air-conditioned room and maintained on a 12-hour photoperiod (0800-2000 hr). The birds were fed ad libitum, a mixture of cracked corn and Purina laying mash. Ad libitum water was also supplied.

##### c. Sea Gulls

Nine juvenile sea gulls (Larus argentatus) were captured on Gull Island in Lake Erie in early June and transported to the laboratory at Ohio State University. The birds were maintained in cages (120 x 56 x 62 cm) in a windowless air-conditioned room on a 12-hour photoperiod (0800-2000 hr). The gulls were maintained on a diet of tuna fish and Alpo dog food (chicken) and given ad libitum water. The gulls were not used for experimentation until they reached adult size and obtained adult plumage. To minimize the effect of the laboratory on the birds they were allowed to adjust to laboratory conditions prior to testing.

#### 2. EXPERIMENTAL PROCEDURE

##### a. Starlings

Phase I consisted of testing the response of individual starlings of both sexes to low-intensity pulsing light. The light source used was a General Radio strobe light with a pulse range from 100 to 25,000 pulses per minute. The birds were tested in a darkened and lightened room, thus simulating night and day situations. The birds

were first tested in total darkness and then at pulse rates of 100, 200, 300, and 400 pulses per minute. Next they were tested in continuous room light (with the strobe off) and in continuous room light with the strobe pulsing at 200 pulses per minute. Each test period (light range) lasted from 30 to 45 minutes, thus giving some idea whether habituation took place. The responses of the birds were monitored visually and mechanically. The birds were placed in a cage (28 x 26 x 22 cm) equipped with four microswitch perchs which, in turn, were connected to a 10-channel variable-speed chart drive Esterline Angus event recorder. The recorder gave us a continuous recording of activity as the birds moved from perch to perch.

The next step was to test the effect of high-intensity laser light on the starlings. To do this we used a Spectro-physics Model 165-03 argon laser in conjunction with a Model 265 exciter. This laser was equipped with a prism, allowing us to vary the wavelength between 454.5 and 514.5 nm, and an all-wavelength mirror, allowing us to administer the entire spectrum between 454.5 and 514.5 nm at once. The maximum power capabilities at different wavelengths (with prism) are given in Table I. With the prism replaced by the all-wavelength mirror, the maximum obtainable power was approximately 4 W. The laser is water cooled and required a flow rate of 2.2 gallons per minute with a maximum water temperature of 35°C.

TABLE 1

Maximum output power (W) at different wavelengths for the Spectro-physics Model 165-03 argon laser

| Wavelength (nm) | Power (mW) |
|-----------------|------------|
| 514.5           | 1400       |
| 501.7           | 250        |
| 496.5           | 400        |
| 488             | 1300       |
| 476.5           | 500        |
| 472.7           | 150        |
| 465.8           | 100        |
| 457.9           | 250        |
| 454.5           | 100        |
| 454.5 - 514.5   | 4000       |

To either am or expand the laser beam, it was necessary to design a telescope and beam director to mount in front of the laser. The

telescope (19.1 power) was made by mounting an objective lens of 172-mm focal length and an adjustable eyepiece of 9-mm focal length on an optical bench. The beam director, which consisted of an aluminized first surface mirror (8 x 5.5 cm) mounted on a Coherent Optics Model 58 beam director was placed in front of the telescope so that any light passing through the telescope impinged on the mirror and thus could be accurately aimed by manipulating the micrometers of the beam director (Fig. 1). The laser was also connected to a pulse generator; therefore, we could administer either a continuous concentrated laser beam, a continuous expanded laser beam, a pulsing concentrated or pulsing expanded laser beam, all of varying intensities.

Table II lists the intensity in  $\text{W}/\text{cm}^2$  on the target (bird) as the diameter of the beam is increased from 0.2 cm to 35 cm.

The experimental procedure was similar to that previously described for the strobe light. The birds were first tested by using the concentrated laser beam (continuous and pulsing) at wavelengths of 514.5 and 488 nm and intensities varying between 50 and 1000 mW. The same birds were also tested using the expanded beam (4-5 in.) over the same range of intensities. The experiments were repeated at higher intensities using the all wavelength mirror in place of the prism.

After determining the response of individual birds to high-intensity laser light, we looked at the response of groups of starlings (3 per group) to these same light ranges (all-wavelengths mirror). These experiments were conducted in a much larger enclosure, 60 ft<sup>3</sup>. The cage was divided into two equal territories (though the birds could move freely from one territory to the other). We then attempted, through the use of different laser light ranges, to deny the birds one of these territories.

The synergistic effect of a combination starling distress call and high-intensity light on starling activity was tested. The procedure was to pulse the laser at a rate of 200 pulses per minute (4-in. diameter and 2-W intensity) while at the same time playing a taped starling distress call to the bird. The distress call (played on a Uher 4000 tape recorder) was played at approximately two-minute intervals for a duration of 30 seconds. The test period lasted 20 to 30 minutes; the distress call was played from 10 to 15 times during the test period.

#### b. Mallard Duck

The procedure for testing the effects of low- and high-intensity light on the mallard duck was similar to that described for the starling. In the mallard study the responses were monitored visually, (avoidance response) and electrically, using the heart rate (increased adrenalin) as an indication of excitement. The heart rate was continuously monitored by use of a Narco Bio-Systems telemetry system consisting of a Botelemetry receiver, Model FM-1100-6, and 18-gram transmitter, Model FM-1100-E2. The telemetry system was used in conjunction with a

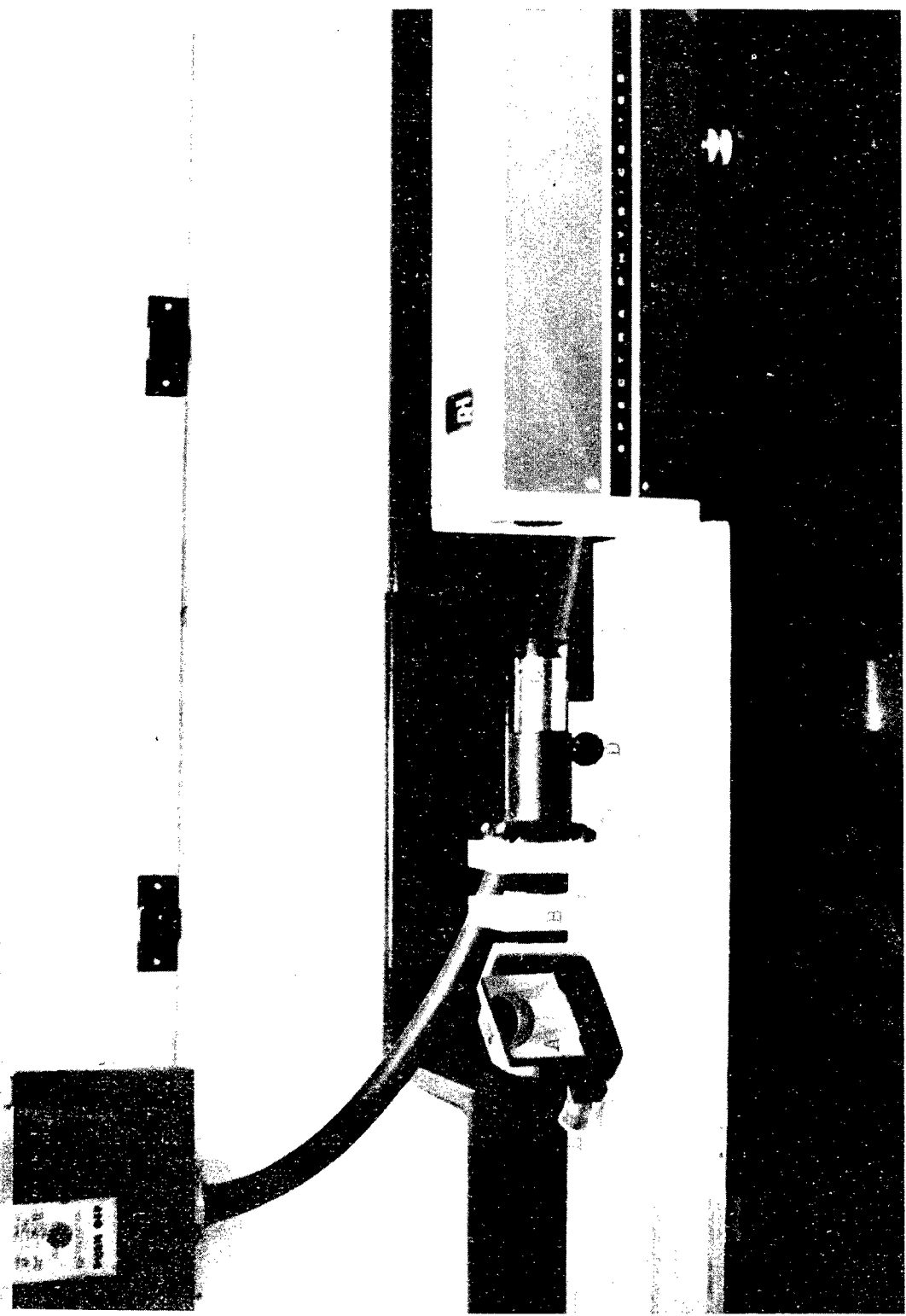
TABLE 2

Calculated and actual intensity of laser beam on target at different beam diameters ( $\text{W}/\text{cm}^2$ )

| Diameter of Beam<br>on Target (cm) | Surface<br>Area ( $\text{cm}^2$ ) | Intensity Setting on Laser (W) |                     |                    |                    |                    |        |
|------------------------------------|-----------------------------------|--------------------------------|---------------------|--------------------|--------------------|--------------------|--------|
|                                    |                                   | 1.6<br>(1.46)                  | 16.0<br>(14.6)      | 33.3<br>(28.0)     | 66.6<br>(52.5)     | 100<br>(87.0)      | 116.0  |
| 0.2                                | 0.031                             |                                |                     |                    |                    |                    |        |
| 0.5                                | 0.185                             | 0.267<br>(0.245)               | 2.67<br>(2.45)      | 5.3<br>(4.7)       | 10.8<br>(8.82)     | 16.8<br>(14.6)     | 18.9   |
| 1.0                                | 0.785                             | 0.063<br>(0.058)               | 0.637<br>(0.580)    | 1.27<br>(1.11)     | 2.55<br>(2.07)     | 3.81<br>(3.44)     | 4.45   |
| 2.0                                | 3.14                              | 0.016<br>(0.014)               | 0.159<br>(0.140)    | 0.318<br>(0.278)   | 0.638<br>(0.520)   | 0.955<br>(0.860)   | 1.11   |
| 2.5                                | 4.89                              | 0.010<br>(0.009)               | 0.101<br>(0.093)    | 0.204<br>(0.178)   | 0.410<br>(0.333)   | 0.615<br>(0.550)   | 0.718  |
| 5.0                                | 19.62                             | 0.0025<br>(0.0023)             | 0.025<br>(0.023)    | 0.051<br>(0.044)   | 0.102<br>(0.083)   | 0.155<br>(0.138)   | 0.179  |
| 10.0                               | 78.5                              | 0.0006<br>(0.00058)            | 0.0063<br>(0.0058)  | 0.0127<br>(0.0111) | 0.0255<br>(0.0207) | 0.0380<br>(0.0344) | 0.0445 |
| 15.0                               | 176.0                             | 0.0003<br>(0.00025)            | 0.0028<br>(0.0025)  | 0.0056<br>(0.0049) | 0.0113<br>(0.0092) | 0.0171<br>(0.0153) | 0.0199 |
| 35.0                               | 961.4                             | 0.000052<br>(0.000047)         | 0.0005<br>(0.00047) | 0.0010<br>(0.0009) | 0.0021<br>(0.0017) | 0.0031<br>(0.0028) | 0.0036 |

Numbers in parentheses equal laser power on target as determined with a Scientech laser power meter Model 3600.

Figure 1: Laser and telescope system  
 A = mirror of beam director  
 B = objective lens  
 C = eyepiece lens  
 D = focusing knob  
 E = micrometer for aiming beam



Packard-Hewlett Model 120-B oscilloscope and a Narco physiograph. This enabled us to continuously view and record the heart rates of the ducks under the various light ranges. An 18-gram transmitter was taped to the duck's back with masking tape. The electrodes which were gold-plated safety pins were pinned just under the skin below the humerus of the wing. The transmitter seemed to have no effect on the behavior of the bird. The enclosure used was the same as that used for groups of starlings. Individual ducks (fitted with transmitter) were placed in the test cage and allowed to adjust for 30 minutes in the dark. They were then exposed to various light ranges from the strobe light in both a darkened and lightened room. The light ranges consisted of total darkness, darkroom plus strobe pulsing at 100, 200, 300, 400, and 1000 pulses per minute. The experimental procedure in Table III was carried out under simulated day and night conditions with the all wavelength mirror. Under daylight conditions, the time it took the duck to avoid the laser beam was used in place of heart rate as an indication of excitement. The same laser light range was tested on groups of three mallards.

#### c. Gulls

The experimental procedure for determining the effects of low- and high-intensity light on gull behavior was similar to that used for the ducks except that the diameter of the laser beam was changed (concentrated, 1 cm, 2 cm, 2, 4, and 6 in.). All tests were conducted at an ambient temperature of between 22° and 25°C.

TABLE 3

Laser light ranges used to test the Mallard duck

| Beam Diameter<br>(on target) (cm) | Power Setting on the Laser (W) |     |     |     |     |                       |
|-----------------------------------|--------------------------------|-----|-----|-----|-----|-----------------------|
|                                   | 0.05                           | 0.5 | 1.0 | 2.0 | 3.0 | 2.0 Pulsing (144/min) |
| 0.2 - 0.5                         | x                              | x   | x   | x   | x   | x                     |
| 5                                 | x                              | x   | x   | x   | x   | x                     |
| 10                                | x                              | x   | x   | x   | x   | x                     |
| 15                                | x                              | x   | x   | x   | x   | x                     |
| 35                                | x                              | x   | x   | x   | x   | x                     |

x = light range tested



### SECTION III

#### RESULTS

##### 1. STARLINGS

###### a. Low-Intensity Strobe Light

The response (perch hops) of individual starlings to pulsating light from the strobe is shown in Fig. 2. As one would expect from a diurnal bird, there is very little movement by the bird kept in total darkness, (0.113 perch hops/min). There is also very little activity in birds kept in a dark room with the strobe light pulsing at either 100 or 200 pulses per minute (0.514 and 1.55 perch hops/min, respectively). In fact, there is no significant ( $P > .05$ ) difference between starlings in total darkness and at 100 to 200 pulses per minute. However, at these pulse rates (100-200 pulses/min) the starlings undergo displacement behavior (rotating of the head, pecking at cage, and staring at the light) which is an indication that they are nervous. At 300 pulses per minute there is a significant increase ( $P < .01$ ) in the amount of perch hopping over that of the lower pulse rates; birds now moving at a mean rate of 18.6 hops per minute. As the pulse rate was increased to 400 per minute, there was again a significant increase in activity.

We tried next the effect of continuous room light (strobe off). As can be seen from Fig. 2 there was a significant ( $P < 0.05$ ) increase in perch hop activity over that of birds in a dark room with the strobe pulsing at 400 per minute.

The next question to arise is, if the strobe at low pulse rates (100-200 pulse/min) can cause displacement behavior, indicating excitability in the bird, can the strobe (200 pulses/min) plus continuous room lights (simulating daytime conditions) elicit greater activity than continuous light? From Fig. 2 it can be seen that strobe light (200 pulses/min) plus continuous room light increased activity (perch hopping) significantly ( $P < 0.1$ ) over that of continuous light. There seemed to be little habituation to pulsing light after one test. For example, on the light range consisting of continuous light plus 200 pulses per minute, the mean activity at the start and 15 minutes later was 60 and 65 perch hops per minute, respectively.

###### b. Starling Exposed to Laser Light

The effect of the unexpanded continuous laser beam at wavelength of 514 and 488 nm at intensities ranging from 20 mW to 1 W was tested on starling behavior. At intensities between 0.5 and 1 W and wavelengths of 514 and 488 nm, the laser beam is capable of igniting the bird's body feathers (smoke rises from bird). Oddly enough this

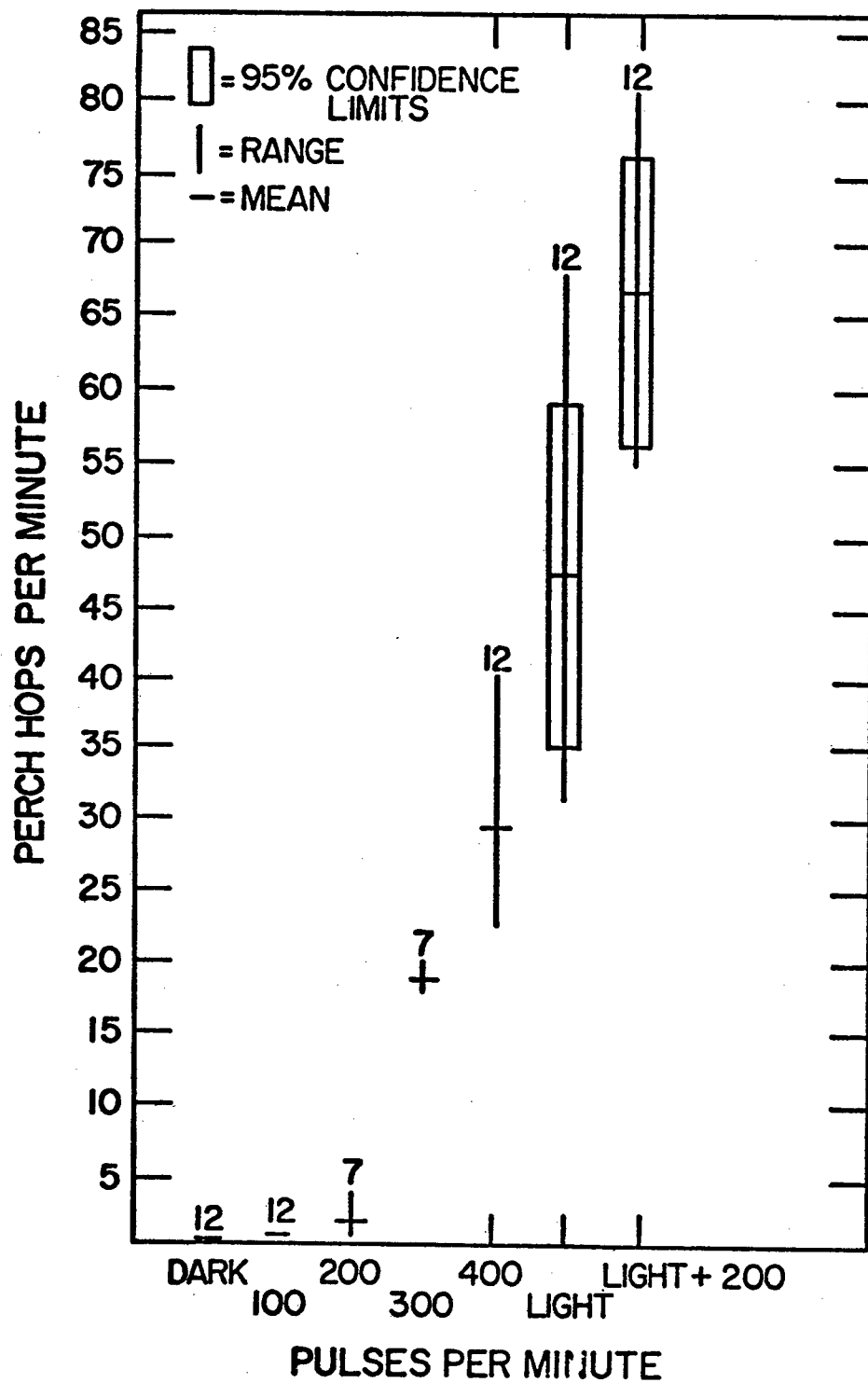


Figure 2. Response of starlings to low intensity light  
N = 7-12

does not elicit an avoidance response within 30 to 60 seconds. There is not significant movement in a room simulating night conditions and the bird does not make a distress call. If this same laser beam is aimed at the uninsulated portions of the starling's body (legs, beak and eye), intensities as low as 0.3 to 0.4 W on the birds beak and legs and 0.1 W in the eye will bring out an immediate avoidance response under both simulated day and night conditions.

Since one of the advantages of the laser light over that of the strobe light is greater intensity, we next expanded the laser beam (4-5 in. in diameter) and repeated the previous experiments conducted with the strobe light (on same birds) only this time using laser light of much greater intensity. The bird responded to the various wavelength tested (488-514 nm) in a similar fashion so all the data are pooled in the results. It can be seen from Table II, that the birds reacted to high-intensity laser light (not capable of burning 12 mW/cm<sup>2</sup>) in a manner similar to that of a low-intensity strobe light.

As with the strobe light, there was little difference in activity between birds in a darkroom and birds in a darkroom with the laser pulsing at 100 and 200 pulses per minute. Birds in a darkroom exposed to continuous laser light showed no greater activity than those exposed to pulsing light (100/min) in a darkroom (a mean of 1.7 hops/min versus 1.8 hops/min). There is no significant difference in activity between those starlings exposed to continuous room light (simulated day light) and those exposed to continuous room light plus the laser pulsing at 200 pulses per minute (Table IV).

Table IV also compares the mean responses from the first tests with pulsing light to the mean responses from later tests with pulsing light on the same birds. When one makes this comparison, it becomes obvious that there has been either no significant change or a great reduction in the response. For example, when we first tested the birds using pulsing light (200/min) plus continuous room light, the birds showed a mean activity of 66 perch hops per minute. Under similar conditions, but after repeated testing, the birds showed a mean activity of only 16.7 perch hops per minute, indicating habituation. Another indication of habituation is to determine at what point during the test period (20-30 min) the birds show the greatest response. Table IV indicates that although there is a reduction in the mean activity as computed over the entire test period, the greatest amount of activity occurs in the first few minutes of the test period, (76 perch hops in first 1.5 minutes) again indicating habituation.

As one would expect at higher intensities (2-3 W) the concentrated aimed laser beam, either pulsing (200/min) or continuous, elicited an immediate avoidance response. The high-intensity (2-3 W) expanded (2-3 in.) laser beam caused an initial increase in activity (Table V). Over a 20- to 30-minute test period the initial (first few minutes) rate of perch hopping was  $35.6 \pm 24$  hops per minute, again indicating

TABLE 4

Activity (perch hops/min) responses of starlings to various laser light ranges over a 20- 30-minute test period

| Continuous<br>Laser | Total<br>Darkness        | Laser<br>100/min        |                         | Laser<br>200/min +<br>Light | Laser<br>200/min<br>Dark Room | Cont. Room<br>Light |
|---------------------|--------------------------|-------------------------|-------------------------|-----------------------------|-------------------------------|---------------------|
|                     |                          | Pulse Rate<br>Dark Room | Pulse Rate<br>Light     |                             |                               |                     |
| 1.33 (33/2)         | 0.00                     | 3.0                     | 4.2 (76/1.5)            | 0.184                       | 13.7                          |                     |
| 3.6 (101/8)         | 0.62                     | 5.8 (34/3)              | 1.0 (24/0.5)            | 1.5 (47/4)                  | 13.4 (147/7)                  |                     |
| 1.0 (17/4)          | 0.33                     | 0.66                    | 2.5 (53/4)              | 1.2 (16/2)                  | 53                            |                     |
| 0.89                | 0.0050                   | 0.2 (4/1)               | 7.1 (34/0.5)            | 1.1                         | 41                            |                     |
|                     | 0.33                     | 0.1                     | 12.4                    | 2.3 (66/3)                  | 52                            |                     |
|                     | 0.35                     |                         | 37.0                    | 3.5 (78/9)                  | 21                            |                     |
|                     | 0.00                     |                         | 25.0                    | 2.6 (83/19)                 | 6.6 (74/1.5)                  |                     |
|                     | 1.00                     |                         | 45.0                    | 6.7                         | 29                            |                     |
|                     | 0.188                    |                         |                         |                             |                               |                     |
|                     | 0.90                     |                         |                         |                             |                               |                     |
|                     | 0.00                     |                         |                         |                             |                               |                     |
| $\bar{X} = 1.7$     | $\bar{X} = 0.37 \pm .33$ | $\bar{X} = 1.8 \pm 2.4$ | $\bar{X} = 16.7 \pm 16$ | $\bar{X} = 2.37 \pm 2$      | $\bar{X} = 25.8 \pm 18$       |                     |
|                     | $\bar{X} = 0.133^*$      | $\bar{X} = 0.514^*$     | $\bar{X} = 66.0^*$      | $\bar{X} = 1.5^*$           | $\bar{X} = 47.2^*$            |                     |

5.8 (34/3) = 5.8 perch hops per minute over the entire test period, 34 perch hops in the first 3 minutes

\*Mean value from previous test (before habituation)

TABLE 5

Response of starlings to high-intensity  
(2-3 W) laser light (expanded and pulsing,  
200 pulses/min)

| Perch hops in first<br>few minutes | Perch hops in last<br>few minutes |
|------------------------------------|-----------------------------------|
| 103/1.5                            | 13/2                              |
| 20/5                               | 10/5                              |
| 20/1.5                             | 0/2                               |
| 25/1                               | 0/2                               |
| 40/1                               | 20/1                              |
| 41/3                               | 0/2                               |
| 22/2                               | 0/2                               |
| 44/2                               | 0/2                               |
| 32/1                               | 3/2                               |
| 12/2                               | 0/2                               |
| 33/3                               | 0/2                               |
| $\bar{X} = 35.6 \pm 24.5$          | $\bar{X} = 4.1$                   |

22/2 = 22 hops in 2 minutes

habituation. The initial rate of activity at high light intensities is not significantly greater than the activity rate of birds on a similar light range of lower intensity. Of course, as the beam is concentrated below 2 inches in diameter at high intensities (3.5 W) there is increased activity.

A combination of high-intensity laser light (2 W, expanded beam) and the starling's distress call produced similar results to that of high-intensity laser light. The majority of the birds tested responded to this combination with increased activity only in the beginning of the 20- to 30-minute test period; again indicating that the birds habituate rapidly.

We were able to deny starlings a territory by using the concentrated aimed laser beam, either pulsing or continuous, at an intensity of from 1 to 3 W. The mean time it took to move the birds was  $11.6 \pm 11$  seconds; 73.4 percent of the time when one bird moved, the others followed. When exposed to the concentrated laser beam the birds moved out of the territory; they then returned a few times (during the first 2-5 minutes of the 20-minute test period) but left immediately when again exposed to the laser. After a few exposures to the concentrated beam (either pulsing or continuous) the birds did not return to the exposed territory in the cage. In fact, the birds would actually fly to the midline of the cage and turn around while with the laser off there was random movement between the two territories. The expanded laser beam (0.5 to 4 in dia.) at an intensity of 2 W had little effect on denying the birds a territory, although in some cases there was greater activity within the exposed territory.

#### c. Mallard Ducks

Whereas, low-intensity pulsing light brought about an increase in starling activity, it did not have any major effect on the mallard duck. Table VI illustrates the heart rates (beats/min) of mallard ducks after a 4-minute exposure to various light ranges. There was no significant difference in mean heart rate between any of the light ranges. There was a slight increase in the mean heart rate of ducks exposed to low-intensity pulsing light (400/min) and continuous room light. Whenever the light range was changed there was an initial increase in heart rate; this increase lasted in some cases for only a few seconds and seldom for over 4 minutes. The ducks habituated to the low-intensity light extremely fast.

Noise had more effect on the ducks than pulsing light. A combination of starling distress call and low-intensity pulsing light brought about a 37.5 percent increase in heart rate (from a mean of 150 to a mean of 240).

TABLE 6

The heart rate (beats/min) of Mallard ducks  
after a 4-minute exposure to various light  
ranges

| Bird No.                 | Total      |  | 100/min      | 200/min      | 300/min      | 400/min      | 1000/min     | Continuous<br>Light and<br>400/min |
|--------------------------|------------|--|--------------|--------------|--------------|--------------|--------------|------------------------------------|
|                          | Darkness   |  |              |              |              |              |              |                                    |
| 1                        | 240        |  | 240          | 240          | 240          | 240          | 240          | 300                                |
| 2                        | 180        |  | 144          | 144          | 144          | 156          | 132          | 300                                |
| 3                        | 156        |  | 140          | 140          | 120          | 120          | 120          | 140                                |
| 4                        | 170        |  | 144          | 130          | 144          | -            | -            | -                                  |
| 5                        | 156        |  | 160          | 160          | 160          | 156          | 144          | 160                                |
| 6                        | 130        |  | 170          | 130          | 130          | 120          | 130          | 130                                |
| Means                    | 172 ± 37.3 |  | 167.3 ± 37.8 | 157.3 ± 41.9 | 156.3 ± 43.2 | 158.4 ± 21.9 | 153.2 ± 49.0 | 206 ± 86.7                         |
| Mean ± one standard dev. |            |  |              |              |              |              |              |                                    |

The mallards were much more sensitive to high-intensity laser light than the starlings. It can be seen (Fig. 3) that there is not a significant ( $P = 0.05$ ) difference in heart rate in birds exposed to either pulsing laser light or continuous laser light at any of the intensities tested. Birds exposed to a concentrated laser beam showed the highest heart rates. Mallards exposed to laser beams (continuous and pulsing) varying in diameter from the concentrated beam (2-5 mm) to 4 inches had significantly ( $P < 0.05$ ) greater mean heart rates than mallards sitting quietly in total darkness and those exposed to laser beams of a diameter greater than 4 inches. It should also be pointed out that the heart rate of mallards exposed to laser beams greater in diameter than 4 inches were not significantly ( $P > 0.05$ ) different from mallards in total darkness.

In addition to heart rate as an indication of excitement, we recorded the percent of the birds avoiding the laser beam and the time it took the bird to avoid the beam. Tables VII and VIII show the percent avoidance and time to avoidance for mallard ducks exposed to various laser light ranges under daytime conditions. It is obvious from these tables that the greater the light intensity on the target the greater the avoidance response. For example, the concentrated laser beam elicited 100-percent avoidance at laser intensities above 0.5 W; whereas, the 2-inch diameter laser beam elicited 100 percent only at laser intensities of 2 W or better. The avoidance responses correlate well with the heart rate data; the best avoidance responses were obtained with laser beams no greater in diameter than 4 inches. Laser beams of 6 inches in diameter did elicit an avoidance response if the intensity was high enough (2 to 3 W).

Under nighttime conditions, our results are similar to those for daytime conditions (Table IX and X). The greatest amount of avoidance taking place was with laser beams no greater in diameter than 4 inches. The time to avoidance under day and night conditions was extremely fast (less than 60 sec.) for mallards exposed to laser beams of 4 inches in diameter or less (Tables VIII and X).

In many cases, although there was not 100-percent avoidance, the mallards did show a great deal of discomfort and eye irritation as evidenced by head-shaking. Headshaking occurred even with laser beams greater in diameter than 4 inches and occurred almost immediately in birds exposed to laser beams of 4 inches or less in diameter, especially if the intensity setting was above 1 or 2 W.

Unlike the starling, the duck knew the intense light was causing its irritation; in fact, the duck would attack the beam (biting at it). In approximately 25 percent of the tests (concentrated beam 0.5 W or better) the duck elicited a distress call.

The percent avoidance and time to avoidance for groups of three mallards are shown in Tables XI and XII, respectively. The avoidance



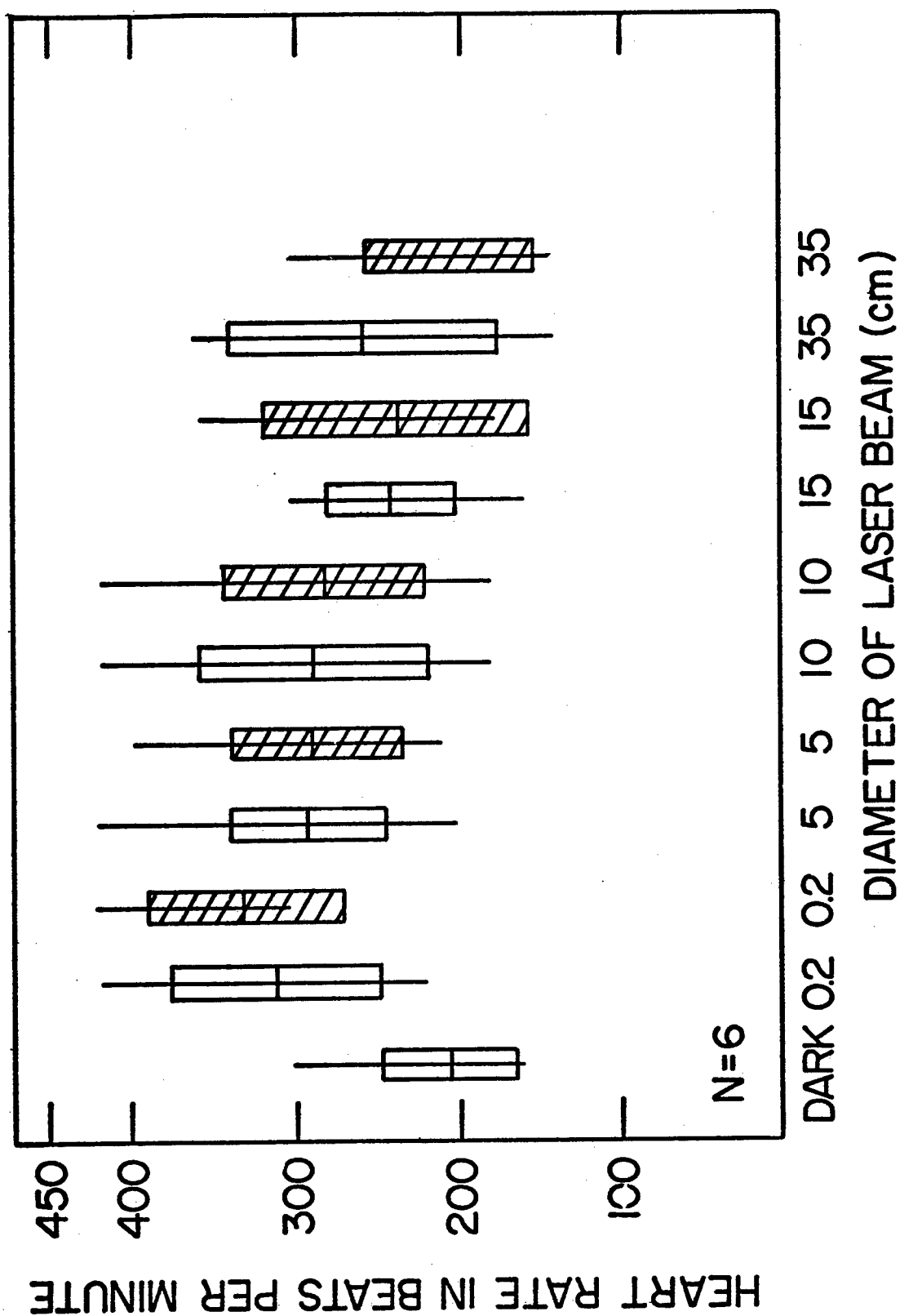


Figure 3. Heart rate of Mallard ducks exposed to 1 W continuous laser (unshaded boxes) and 2 W pulsing (shaded boxes) laser under night conditions. Symbols as in Fig. 2

TABLE 7

Percent of the Mallard ducks avoiding laser light of different intensities under simulated daylight

| Diameter of Beam<br>on Target (cm) | Power Setting on Laser in W |      |      |      |      |             |
|------------------------------------|-----------------------------|------|------|------|------|-------------|
|                                    | 0.05                        | 0.5  | 1.0  | 2.0  | 3.0  | 2.0 pulsing |
| 0.2-0.5                            | 14.3                        | 100  | 100  | 100  | 100  | 100         |
| 5.0                                | 33.3                        | 71.5 | 85.7 | 100  | 100  | 100         |
| 10.0                               | 0.0                         | 33.2 | 42.8 | 86.7 | 100  | 54.4        |
| 15.0                               | 0.0                         | 0.0  | 16.6 | 66.6 | 66.6 | 37.2        |
| 35.0                               | 00.0                        | 0.0  | 0.0  | 0.0  | 25   | 0.0         |

TABLE 8

Mean time to avoidance in Mallard ducks exposed to various laser light ranges under simulated daylight (sec.)

| Diameter of Beam<br>on Target (cm) | Power Setting on Laser (W) |            |           |            |            |             |
|------------------------------------|----------------------------|------------|-----------|------------|------------|-------------|
|                                    | 0.05                       | 0.5        | 1.0       | 2.0        | 3.0        | 2.0 pulsing |
| 0.2-0.5                            | 10.2                       | 6.7 ± 2.7  | 9.0 ± 4.6 | 2.8 ± 2.4  | 15         | 5.7 ± 2.1   |
| 5.0                                | 22                         | 33.3 ± 6.5 | 24.3 ± 6  | 16.6 ± 2.6 | 0.0        | 15.8 ± 2.0  |
| 10.0                               | ---                        | 9.3        | 9.6 ± 1.9 | 16.3 ± 4.6 | 18.8 ± 3.7 | 9.9 ± 2.1   |
| 15.0                               | ---                        | ---        | 28.4      | 23.7 ± 7   | 15.2       | 28.9 ± 6.3  |
| 35.0                               | ---                        | ---        | ---       | ---        | 16.5       | ---         |

Means are ± one standard error of the mean.

Only birds eliciting an avoidance response are included in the mean values.

TABLE 9

Percent of the Mallard ducks avoiding laser light of different intensities under simulated night conditions

| Diameter of Beam<br>on Target (cm) | Power Setting on Laser (W) |     |      |      |     |             |
|------------------------------------|----------------------------|-----|------|------|-----|-------------|
|                                    | 0.05                       | 0.5 | 1.0  | 2.0  | 3.0 | 2.0 pulsing |
| 0.2-0.5                            | 50                         | 100 | 100  | 100  | 100 | 100         |
| 5.0                                | 0.0                        | 40  | 83.3 | 83.3 | --- | 75          |
| 10.0                               | 0.0                        | 40  | 33.3 | 75   | --- | 83.3        |
| 15.0                               | 0.0                        | 0.0 | 14   | 75   | --- | 50          |
| 35.0                               | 0.0                        | 0.0 | 0.0  | 0.0  | 0.0 | 0.0         |

--- = birds not tested at this intensity.

TABLE 10

Mean time to avoidance in Mallard ducks exposed to various laser light ranges under simulated night conditions (sec.)

| Diameter of Beam<br>on Target (cm) | Power Setting on Laser (W) |           |            |            |     |             |
|------------------------------------|----------------------------|-----------|------------|------------|-----|-------------|
|                                    | 0.05                       | 0.5       | 1.0        | 2.0        | 3.0 | 2.0 pulsing |
| 0.2-0.5                            | 34                         | 3.7 ± 3.7 | 5.0 ± 5    | 0.0        | 0.0 | 0.0         |
| 5.0                                | ---                        | 18.7      | 21.8 ± 3.5 | 23.9 ± 5.7 | x-  | 15.7 ± 2.7  |
| 10.0                               | ---                        | 13.0      | 45.0       | 26.3 ± 2.8 | x-  | 17.0 ± 5.1  |
| 15.0                               | ---                        | ---       | 45.0       | 50.6 ± 5.2 | x-  | 33.5 ± 5.4  |
| 35.0                               | ---                        | ---       | ---        | ---        | --- | ---         |

Means are ± one standard error of the mean.

Only birds eliciting an avoidance response are included in the means.

--- = no response

x- = not tested

TABLE 11

Percent avoidance of groups (3/group) of Mallard  
ducks to various laser light ranges

| Diameter of Beam<br>(cm) | Power Setting on Laser (W) |      |     |      |      |             |
|--------------------------|----------------------------|------|-----|------|------|-------------|
|                          | 0.05                       | 0.5  | 1.0 | 2.0  | 3.0  | 2.0 pulsing |
| 0.2-0.5                  | 42.8                       | 87.5 | 100 | 100  | 100  | 93.8        |
| 5.0                      | 0                          | 16.6 | 57  | 71.5 | 75   | 55.5        |
| 10.0                     | 0                          | 0    | 50  | 50   | 75   | 50          |
| 15.0                     | 0                          | 0    | 0   | 0    | 33.3 | 0           |

TABLE 12

Mean time to avoidance in groups of Mallard ducks exposed  
to various laser light ranges (daytime conditions)

| Diameter of Beam<br>(cm) | Power Setting on Laser (W) |      |      |      |      |             |
|--------------------------|----------------------------|------|------|------|------|-------------|
|                          | 0.05                       | 0.5  | 1.0  | 2.0  | 3.0  | 2.0-pulsing |
| 0.2-0.5                  | 11.4                       | 13.0 | 6.8  | 5.4  | 3.5  | 8.0         |
| 5.0                      | ---                        | 8.6  | 4.1  | 10.3 | 9.3  | 9.3         |
| 10.0                     | ---                        | ---  | 33.7 | 21.5 | 27.0 | 20.4        |
| 15.0                     | ---                        | ---  | ---  | ---  | 43.7 | ---         |

responses in groups of ducks were similar to those of the individual ducks. Again the best avoidance response was elicited by a concentrated laser beam of 0.5 W or better intensity, while a laser beam greater than 4 inches in diameter (up to 3 W intensity) had little effect.

Though the avoidance responses were similar between the groups and individual ducks, there was an increase (up to 50%) in the amount of distress calling in groups. Even at intensities that did not elicit a definite avoidance response there was some distress calling plus a continuous nervous chatter among the ducks in the group.

#### d. Gulls

The response of individual gulls to intense laser light was similar to that of the starlings in that only the concentrated laser beam elicited a significant avoidance response (Tables XIII and XIV). At beam diameters above 1 cm, the gulls failed to elicit an avoidance response more than 37.2 percent of the time. Though the gull failed to avoid the expanded (2 cm - 15 cm) laser beam, they did show some irritation (head-shaking, eye-rubbing). Like the ducks, the gulls identified the source of irritation and would attack the laser beam on many occasions.

The response of groups of three gulls to intense laser light was similar to that of the individual gulls. The concentrated beam brought about severe head-shaking and eye-rubbing, with the birds attacking the beam. The beam elicited a distress call in 25 percent of the tests, there did not seem to be a group response. This lack of a group response can be explained because the birds established a peck order among themselves which seemed to elicit a greater avoidance response than the concentrated laser beam. Low-intensity pulsing light (100, 200, 300, 400, 600, 1000, 2000, 4000, and 25,000 pulses/min) from the strobe elicited only slight displacement behavior, as pecking at the cage and head-shaking. The pulse rates that elicited the greatest amount of displacement behavior were 400 and 600 pulses per minute.



TABLE 13

Percent of the gulls avoiding laser light of  
different intensities

| Diameter of Beam<br>on Target (cm) | Power Setting on Laser (w) |      |      |      |      |             |
|------------------------------------|----------------------------|------|------|------|------|-------------|
|                                    | 0.05                       | 0.5  | 1.0  | 2.0  | 3.0  | 2.0 pulsing |
| 0.2-0.5                            | 8.3                        | 69.3 | 91.5 | 85   | 71.3 | 89.5        |
| 1.0                                | 0                          | 12.5 | 25   | 55.6 | 37.5 | 16.7        |
| 2.0                                | 0.0                        | 10   | 37.2 | 33   | 17.7 | 0.0         |
| 5.0                                | 0.0                        | 0.0  | 14.3 | 8.3  | 0.0  | 6.2         |
| 10.0                               | 0.0                        | 0.0  | 0.0  | 0.0  | 0.0  | 0.0         |
| 15.0                               | 0.0                        | 0.0  | 0.0  | 0.0  | 0.0  | 0.0         |

TABLE 14

Mean time to avoidance in gulls exposed to various laser  
light ranges (sec.)

| Diameter of Beam<br>on Target (cm) | Power Setting on Laser (w) |     |      |      |     |             |
|------------------------------------|----------------------------|-----|------|------|-----|-------------|
|                                    | 0.05                       | 0.5 | 1.0  | 2.0  | 3.0 | 2.0 pulsing |
| 0.2-0.5                            | 41                         | 7.1 | 11.8 | 8.8  | 2.2 | 23.3        |
| 1.0                                | ---                        | 4   | 0.0  | 7.2  | 0.0 | 0.0         |
| 2.0                                | ---                        | 0.0 | 11   | 15   | 0.0 | ---         |
| 5.0                                | ---                        | --- | 9.2  | 38.4 | --- | 7           |
| 10.0                               | ---                        | --- | ---  | ---  | --- | ---         |
| 15.0                               | ---                        | --- | ---  | ---  | --- | ---         |

Only birds eliciting an avoidance response are included in the means.

## SECTION IV

### DISCUSSION

It has been known for centuries that light (photoperiod) is possibly the major environmental stimuli affecting bird behavior and physiology. The length of the light period stimulates the breeding cycle, migration, fat deposition, and molt in most species of birds. Therefore, it is only natural that one would think of using light as a means of bird control. In fact, light has already been used as a bird control; flood-light traps have been used to trap blackbirds;<sup>9</sup> Meanley states that 2000-W search lights have been used to alleviate depredation by ducks in rice fields.<sup>10</sup>

Pulsing light is already used on aircraft, aircraft hangers and high towers as a means of detouring birds.

With some positive results already obtained with light as a bird control, the next step is to see if a better light source (the laser) might not have a greater effect. The laser is basically an intense and coherent light with extreme directivity and, thus, might have greater influence on a bird's behavioral and physiological responses.

Practical lasers which cover a wide range of the spectrum are now available, any one of which could be tried in bird control experiments. Before selecting a laser it is necessary to understand something about bird vision. All the available evidence tends to support the belief that the visual acuity of birds is of the same order as that of man, but that the rate of assimilation of detail in the visual field is much higher in birds.<sup>11</sup> Also a bird with a single glance lasting perhaps a second takes in a picture which a man could accumulate only by laboriously scanning the whole field piece by piece with the most accurate portions of the retina. The fact that the visual information is taken in by birds at a high rate and simultaneously over a greater part of the visual field has been substantiated by studies of bird navigation,<sup>12</sup> for the only theory of navigation consistent with the evidence implies that birds can assess not only the elevation of the sun but also its rate of change of elevation and its azimuth with high accuracy.

Anyone who has ever watched birds doubts that their reception of color is as good as that of man. The studies of Watson,<sup>13</sup> Lashley,<sup>14</sup> and Hamilton and Coleman<sup>15</sup> have shown that the curve relating the least perceptible change of wavelength to wavelength has exactly the same form for the pigeon as for man, suggesting that the fundamental mechanisms for discriminating pure colors is the same for both. There is no satisfactory evidence that birds make use of extra-spectral frequencies at either end of the visible spectrum. Matthews and Matthews<sup>16</sup> showed that the dioptric system is quite opaque to infrared light.

Spectrophotometric analysis of visual pigment extracts prepared from various species of bird retinas have led to some valuable information. Crescitelli<sup>17,18</sup> found the great horned owl, screech owl, gull, and pelican to possess pigments with maximum absorption at wavelengths of 502, 503, 501, and 502 nm, respectively. Bridges,<sup>19</sup> found the maximum absorption at 502 nm for the duck. Recently, Sillman<sup>20</sup> extracted, analyzed, and characterized the visual pigments of 20 species of birds, representing 8 orders and 11 families. He found that each species examined yielded at least one visual pigment. In every case the major pigment (and the only pigment in 14 species) exhibited a maximum absorption within the spectral range of 500 to 506 nm. In five species of passerines, a second photopigment was detected which ranged in maximum absorbance from 480 to 490 nm, and which constituted from 5 to 10 percent of the total pigment content. It is highly probable that the major pigment isolated in these studies were scotopic or rhodopsin. In fact, in the work cited so far there has been no evidence for the presence of any cone pigments. Three species of birds have been reported to possess other pigments in addition to the rhodopsin.<sup>21,22,23</sup> This pigment (iodopsin) has a maximum absorbance ranging from 544 nm in the pigeon to 562 nm in the chicken and turkey. The important factor coming out of these studies is that the dominant photopigment displays a marked constancy in the spectral location of 500-506 nm. This being the spectral wavelength that birds are most sensitive to suggest that one would want to use a laser which includes this range. The argon laser emits light over a spectral range of from 454 to 514 nm and, thus would seem to be that to which birds are most sensitive. It should be pointed out that because few cone pigments have been found does not eliminate the possibility of their presence and it is possible that other wavelengths might be as effective or more effective in bird control.

## 1. STARLINGS

It is only natural that the starling, being a diurnal bird, will be more active during the daylight hours. This explains somewhat why there was an increase in activity with an increasing pulse rate (Fig. 2) under simulated night conditions--the shorter the dark period the greater the activity. Of greater interest is that there was significantly greater activity under simulated daytime conditions plus pulsing light than under simulated daylight alone. This indicates that pulsing light is annoying to the starling causing an increase in activity. That the starlings habituate to pulsing light was shown by the decrease in activity when exposed again to pulsing laser light; overall response was much less under daytime conditions plus the pulsing laser. Also the activity decreased during the test period (Table IV), again indicating habituation.

The response of the starling to high-intensity laser light of different wavelengths (488 and 514 nm) was similar. One would expect this response since the peak sensitivity of the bird was between 500-506 nm

(Fig. 6); thus, the starlings were equally sensitive to 488 and 514 nm. The remainder of the experiments were carried out using the all-wavelength mirror (454-514 nm).

As far as a bird strike with a flying airplane is concerned, it is more than likely that the initial response is important. This initial avoidance response would cause the bird to avoid the oncoming plane if the light source could be seen far enough in advance, thus giving the bird time to avoid a high-speed plane. In the case of the starling, pulsing light is much better than continuous light as a control, mainly because a continuous light source at night could act as an attractant for starlings,<sup>9</sup> where pulsing light is annoying. Remembering that the intense (1-3 W) expanded 4 inch laser beam gave results similar to the low-intensity strobe light, what then is the advantage of the laser? Of course the answer to this question is effective distance. The laser beam, having less divergence, has a greater range which, in turn, gives the bird more time to avoid the plane.

Although it was thought that the starlings would not habituate to intense laser light because it is irritating to the eye, the only laser beam that the starlings did not habituate to in the laboratory was the concentrated beam of at least 0.5-W intensity (irritating). This light range would deny starlings territory. Birds exposed to the beam a few times no longer returned to the area and the birds could be moved at will. Of course this is a highly focused light beam and must be accurately aimed since it can cause eye damage to man. The feasibility of using the concentrated laser beam as a bird control is discussed in a later section.

One can only speculate as to why the starlings and gulls (diurnal birds in general) are not sensitive to extremely intense laser light (expanded beam) capable of doing considerable damage to the mammalian eye. The birds should be extremely sensitive to the argon laser light since their rhodopsin has its peak sensitivity (Fig. 6) between 502-506 nm and the laser has its greatest power in this range also (Table I). Why then no headshaking or avoidance when exposed to continuous laser light (expanded beam)?

It is known that some birds "sun orient",<sup>24</sup> i.e., they look directly at the sun in order to get some idea of the azimuth. It is also known that birds fly at very high altitudes (23,000 ft.) where solar radiation is extremely intense. One need only look from an airplane window into the sun when flying it at 23,000 feet to determine just how intense it is. Yet these birds fly with their eyes open and possibly, looking right at the sun. Two hypotheses can be set forth to explain the ability of birds to withstand intense light. The first deals with the pecten, a pigmented conical, highly vascularized body. It arises near the attachment of the optic nerve and juts out in the vitreous humor toward the lens. It is an elaborate structure of thin folds richly supplied with small blood vessels (not capillaries). According

to Walls,<sup>25</sup> over 30 theories have been proposed to explain the function of the pecten, one of which is light absorption. The position of the pecten is such that it shades the fovea, thus decreasing the effect of intense light. Another feature of the pecten, its vascularity, would also explain how the heat of the laser beam is dispersed without burning the retina; for example, 4 watts for 30 seconds is equal to 120 joules or 28.5 calories. When concentrated by the lens of the eye this would be a tremendous heat load for the retina if it were not for some means of dispersing it.

The second hypothesis deals with the colored oil droplets found in the eyes of birds and reptiles. It is usually thought that these oil droplets enhance color vision by acting as filters. When one compares the absorption spectrum of the rhodopsin with the absorption spectrum of the oil droplets (Fig. 4) he will see that they overlap somewhat, especially between the wavelengths of 450 and 510 nm where birds have their greatest sensitivity.<sup>20</sup> As Sillman points out, the biological significance of the oil droplets still remains to be determined. Both reptiles and birds that are exposed to intense solar radiation (reptiles in deserts, birds at high altitudes) possess oil droplets. It has long been thought that the colored oil droplets enhance color vision; Ducker and Tiemann<sup>26</sup> have shown that oil droplets in reptiles have little to do with color vision. It is possible that these colored oil droplets act as filters for the intense light. The mechanism by which they could accomplish this is unknown, and further research into bird vision is necessary to determine if either the pecten or oil droplets are responsible for the diurnal birds' ability to look at intense light without any gross effects.

## 2. MALLARD DUCKS

As with the starlings, the mallards habituated to low-intensity pulsing light extremely fast, there being no significant difference in heart rate after four minutes in any of the low-intensity light ranges (Table VI). Although there was little response to low-intensity light, the mallards were much more sensitive to high-intensity laser light than the starlings. This is understandable if one knows something about the behavior of the mallard duck. According to Winner<sup>27</sup> the mallard duck moves to and from its feeding grounds during periods of very low light intensity (less than 0.1 ft-c). Also like many other waterfowl they are known to migrate at night. This would indicate that they have relatively good night vision. Indeed, they could see the investigator in a dimly illuminated room where the starlings could not see the investigator at all. In fact, the starlings would not move and could be picked up by hand in a dark room. The nocturnal feeding behavior of the mallard has already allowed rice farmers to use light as a control (illuminate rice fields and ducks do not feed). As Sillman<sup>20</sup> pointed out, nocturnal birds have a greater amount of rhodopsin (rod pigment) and, thus, would be expected to have greater sensitivity to

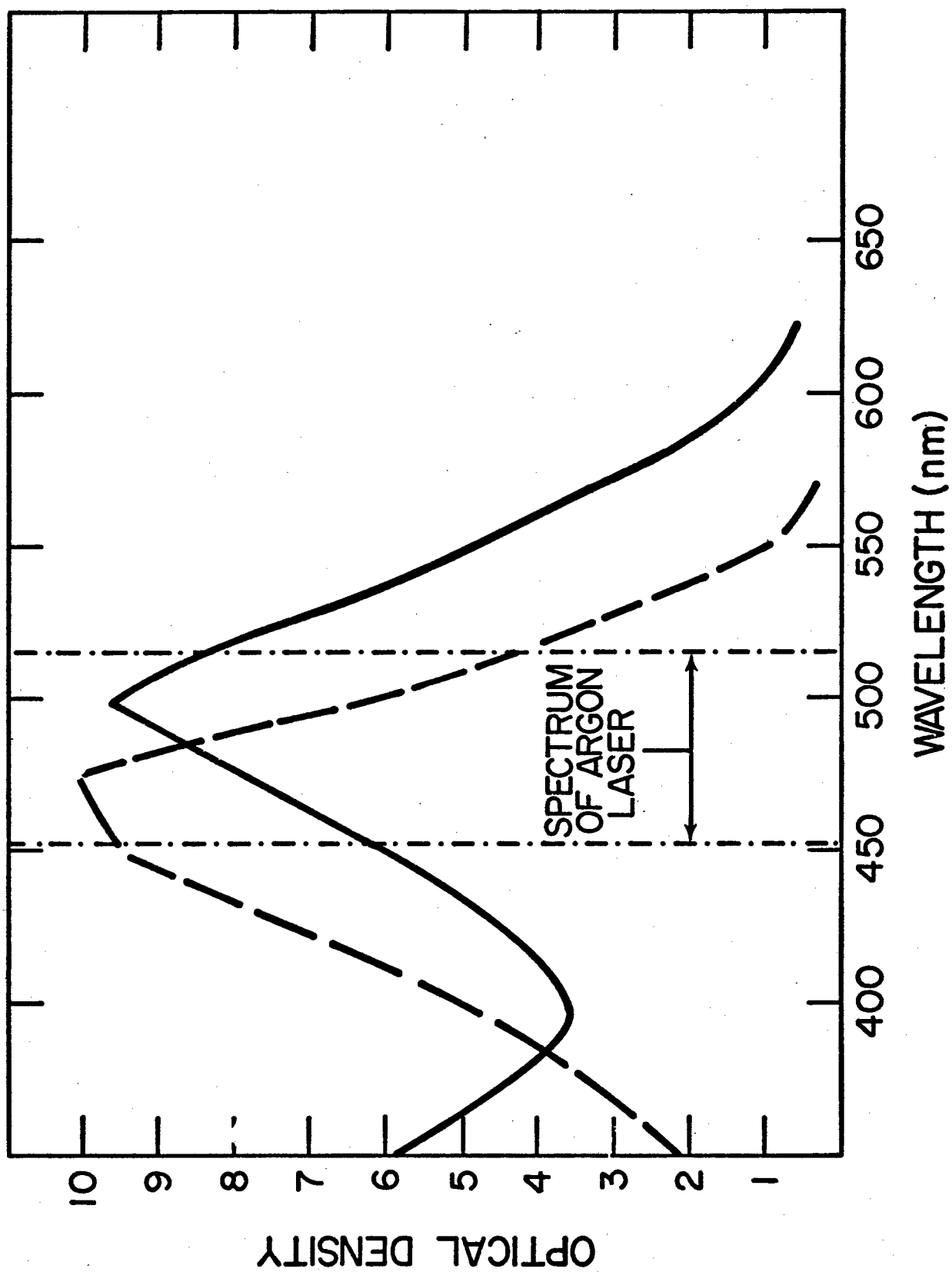


Figure 4. Absorbance spectra of oil droplets (---) and visual pigment extract (-), adapted from Sillman (1969)

light especially over the wavelengths emitted by the argon laser, since it is here that bird rhodopsin has its peak sensitivity.

To bring about an avoidance response in the mallard of at least 50 percent, the intensity of laser light hitting the bird had to be at least  $0.01\text{--}0.025\text{ W/cm}^2$ . Using the present laser system, the beam could only be expanded six inches and still give high enough intensities. Not only is it important that the bird avoid the laser beam but the time it takes the bird to avoid the light beam is equally important. In this study, for a response to be considered as avoidance response it had to occur within 60 seconds. As the flight speed of aircraft increases, response time will become even more important. For example, a plane flying at 600 miles per hour will travel 10 miles in 60 seconds indicating that if the bird is 10 miles away, it only has 60 seconds to avoid the plane. This points out another problem which we will discuss later, that is, the effective distance over which a laser beam can elicit an avoidance response. If the bird is only 1 mile away and the plane is travelling at 600 miles per hour, then the bird has to respond in six seconds or collide with the aircraft. Again, as with the starling, the concentrated laser beam elicited the greatest and fastest avoidance response; avoidance is almost immediate.

The duck identified the laser beam as the source of irritation and in some cases would bite at it, whereas the starling did not seem to recognize the source of irritation. This explains somewhat why the ducks elicited a distress call when exposed to high-intensity light and the starling did not. If the starling realized what the distress was (grabbing the bird) it too elicited a distress call. Equally important to an individual bird response is the response of a group of birds to the coherent laser light, since the beam cannot possibly hit every bird in the group. Although our groups were small (3 birds/group) there was a group avoidance response. The individuals not affected by the laser beam followed birds trying to avoid the beam.

### 3. GULLS

The gulls like the starlings, are diurnal birds, active during the daylight hours and quiet during the dark. Thus, one would expect them to have some mechanism for filtering out intense solar radiation. Although the expanded laser beam seemed to irritate the gulls (head-shaking, eye-rubbing) more than it did the starlings, the only laser beam that elicited an avoidance response was the concentrated beam of at least  $0.5\text{ W}$  intensity. The lack of a demonstratable group avoidance (found in starlings and ducks) response in the gulls might well depend on the size of the test cage ( $60\text{ ft}^3$ ). The gulls had established a pecking order and were afraid to get too close to each other; thus, if the dominant bird moved to another area, the subordinate bird did not follow. Since the gulls associated the distress with the intense light (bite at beam), they did utter a distress call and we know that under



natural conditions a gull distress call will cause the birds to leave the area at least temporarily.

#### 4. PROBLEMS FACED BY AIRCRAFT

The problem of air strikes is largely a function of airport location and construction. Runways built on or near ideal bird habitats bring birds and aircraft into conflict. The low, flat areas ideal for airports are frequently associated with water or marshland vegetation, which may be the breeding or roosting sites of large water birds or flocking, smaller, perching birds. The general construction of airports and large open spaces with extensive areas of short-cut grass provide a large amount of plant and invertebrate material to attract birds. Under conditions such as described, the majority of bird strikes would occur during landing and takeoff. Records show that about 95 percent of the bird strikes occur below 6000 feet and 60 percent below 2000 feet, at least for commercial airlines. For military aircraft, approximately 95 percent of the bird strikes happen below 2000 feet and about 70 percent below 500 feet. Thus, we are faced with two basic problems in controlling birds: (1) to keep the birds off the runway to minimize the probability that aircraft approaching and landing and taking off and climbing to altitude encounter birds and (2) to keep birds that are flying at low altitudes out of the path of low-flying planes, especially high-speed military aircraft. Seven F-104 jets were lost in Canada because of bird strikes at low-altitude, high-speed flight.

Several factors enter into the design of a bird control under these conditions:

1. species specificity,
2. pulsing or continuous light,
3. effective distance and effective power,
4. habituation, and
5. speed of the aircraft (avoidance time).

Now let's take each factor separately and apply it to the laser as a means of control. Many diverse ways (noise makers, distress call, falcons) of scaring birds have from time to time been tried to control birds around airports, but have generally been found wanting. They have been inadequate mainly because they are either species-specific or the birds habituate to them. The best control would be one that is nonspecies specific and that the birds would not habituate to. The laser system used in these tests fulfill both these requirements as long as the beam is irritating (concentrated). None of the species tested (repeatedly) failed to avoid a concentrated laser beam of at least 0.5 W, indicating it was nonspecies-specific and they did not habituate to it.

Once expanded (light intense but not capable of burning) the continuous laser beam was no longer species-specific under the laboratory

conditions, in fact starlings, and gulls to a lesser extent, could look directly into the beam without showing avoidance response. Pulsing laser light (expanded beam) did increase the initial activity of the starlings. Mallards were also sensitive to laser beams (pulsing or continuous) expanded up to 6 inches in diameter and showed little habituation to these beams at high intensities. It becomes clear that equally as important as laser intensity to species specificity is whether the laser is pulsing or continuous. Though a diurnal bird would not usually fly at night, if scared by a landing or leaving aircraft flying over their roost at night, they might fly toward a continuous light source, whereas a pulsing light (100-200 pulses/min) would seem to elicit an avoidance response. The nocturnal flying birds would most likely be repelled by either pulsing or continuous laser light.

The effective power of the laser at different beam diameters was calculated (Table II). It is obvious that the nonspecificity of the concentrated laser beam is due to the burning and not the light itself (especially since this highly aimed beam affects the bird even when aimed at the leg). For example, the time it took to move a mallard duck with the concentrated beam at 0.5 W was approximately 7 seconds. At this intensity the duck was hit with light at an intensity of 14.6 W/cm<sup>2</sup> (Table II); in 1 second this is equivalent to 14.6 J/cm<sup>2</sup>; in 7 seconds (mean avoidance time) it is equivalent to 102.2 J/cm<sup>2</sup> or 24.7 cal/cm<sup>2</sup>. This is enough heat to raise 1 gram of water to 24.7°C. This was the minimum tested power capable of eliciting an avoidance response in starlings and gulls. Schaefer<sup>9</sup> found that 6 J/cm<sup>2</sup> is required to ignite flight feathers. Powers as low as 0.3 W.cm<sup>2</sup> were capable of eliciting an avoidance response in duck. It should be pointed out that the concentrated laser beam would elicit an avoidance response no matter where it hit the bird, although the response was faster if the beam was aimed at the unfeathered portions (eye and bill).

The large size of airports (runways) and the high flight speeds of modern aircraft indicates that the effective distance of any control system will be extremely important in its use. Knowing the diameter of the laser beam needed to elicit a response at various power settings (W), one can calculate the effective distance of the laser.

The dispersion of the laser beam as it travels from the laser only, or from a laser/telescope combination where the focal point of one lens in the telescope exactly overlaps the focal point of the other lens is expressed by the equations

$$\theta = 1.22 \frac{\lambda}{D} \quad (1)$$

$$R(2 \times \theta) = d \quad (2)$$

$d + D$  = dispersion of beam at  
distance R

- $\lambda$  is the wavelength (cm),
- D is the diameter of the beam at the output of the laser or telescope,
- R is the distance to target,
- $\theta$  is the angle of dispersion, and
- d is the dispersion at distance R.

Table XV illustrates the diameter of the beam at various distances when the laser is used by itself and when the telescope used in this study (eye piece 9 mm focal length, objective lens 172 mm focal length) is in phase (telescope lenses are 181 mm apart). If we consider a diameter of from 0.2 to 0.5 cm (0.5 W or better) as the only laser beam which is not species-specific, it becomes obvious that the laser by itself will not be very efficient since its effective distance is extremely short (in 5 m the beam will be 0.55 cm in diameter). In 1 km the beam will be 80.15 cm in diameter (using only the laser). Using the in-phase telescope the beam can never be smaller in diameter than 3.5 cm (the diameter of the beam as it leaves the objectives lens). What is important is that now (using the telescope) at 1 km the beam is only 6.9 cm in diameter, whereas it was 80.15 cm in diameter using only the laser; thus, the telescope has increased the effective distance of the laser. Of course the telescope is adjustable, i.e., we can vary the distance between the lenses. As we increase the distance (above 181 mm) the beam will converge; as we decrease the distance (below 181 mm) the beam diverge much more than previously discussed. Thus, by choosing the proper telescope and by varying the distances between the lens one can obtain a concentrated laser beam at a much greater distance (Table XVI). It should be pointed out here that we have been discussing only those laser beams that were capable of bringing about 50 percent or better avoidance in the laboratory. This does not mean that a beam 1 m in diameter in the wild would not cause a flying bird to avoid the plane. Solomon<sup>28</sup> has reported that radar has shown night-flying geese to avoid a landing plane with its landing lights on. It is obvious that those birds were not irritated by intense light, they just saw the plane in time to avoid it. Under these conditions the laser with its greater effective distance would give the birds more time to avoid the aircraft, avoidance time being extremely important in high-speed, low-altitude flight.

We are concerned with a light source (laser beam) intense enough to bring about an avoidance response for control of birds on the runway, and we would thus need additional optics capable of delivering an intensely concentrated beam at a distance of at least 1000 meters.

TABLE 15

Beam expansion with distance in the argon laser, Model 165-03, and this same laser plus additional optics (telescope described in present experiments)

| Distance (m) | Diameter of beam, laser (cm) | Diameter of Beam, laser + telescope (cm) |
|--------------|------------------------------|--|
| 1            | 0.23                         | 3.503                                    |
| 5            | 0.55                         | 3.517                                    |
| 10           | 0.95                         | 3.53                                     |
| 100          | 8.15                         | 3.84                                     |
| 500          | 40.15                        | 5.20                                     |
| 1000         | 80.15                        | 6.90                                     |
| 2000         | 160.15                       | 10.3                                     |
| 3000         | 240.15                       | 13.7                                     |

In the telescope the focal point of the objective lens exactly overlaps the focal point of the eyepiece lens.

TABLE 16

Increased distance (greater than 181 mm) between objective and eyepiece lenses necessary to give a laser beam of 0.2-cm diameter on the target at various distances

| Distance (m) | Increased Distance<br>Between Lenses (mm) | Diameter of Beam<br>(cm) |
|--------------|---|--------------------------|
| 1.0          | 24.0*                                     | 0.2                      |
| 10.0         | 2.8                                       | 0.2                      |
| 100.0        | 0.3                                       | 0.2                      |
| 1000.0       | 0.03                                      | 0.2                      |
| 2000.0       | 0.014                                     | 0.2                      |
| 3000.0       | 0.010                                     | 0.2                      |

\*Not obtainable with the present system (limited adjustment in the telescope).

## 5. PROBLEMS IN USE OF LASER AS A CONTROL

When considering the problems (hazards) of using intense light as a bird control one must think in terms of the two control situations: (1) control of resident birds at the airport, and (2) control of birds encountered in flight. If the control in the airport situation is to be nonspecies specific, then either a concentrated laser beam will be used or an expanded beam of much greater power since it takes at least  $6 \text{ J/cm}^2$  to be irritating to the bird. This presents a human hazard since the acceptable safety limit to the human eye for irradiation from the argon laser is 20 mW for 1 ms.<sup>29</sup> In our experiments it took at least 500 mW to get an avoidance response from starlings and gulls; this is well above the safety limit. One possible way of alleviating the danger to the human eye would be to use a laser emitting in the infrared wavelengths, to which human eyes are not as sensitive. Another problem is that the more concentrated the beam, the more accurately it has to be aimed, indicating either that it has to be manned continually or radar aimed.

Though some birds might respond to a lower intensity beam (not eye irritating), it is possible that on cold days the heat energy contained in the laser beam would actually attract the birds instead of repelling them. Lustick<sup>30,31,32</sup> has shown that birds, when at ambient temperature below their lower critical temperature, will use incoming solar radiation between the wavelengths of 400 to 1400 nm to decrease the energy cost of maintaining a constant body temperature, and, thus, bask under artificial sunlight at low ambient temperatures.

With any light source, especially around airports, (usually built in low-lying marsh areas) fog is going to disrupt the light efficiency as a control method by cutting down on its intensity and effective distance.

These same problems will occur in flight, except that in flight the concentrated beam becomes more dangerous since it would be extremely difficult to aim. For example, a landing plane using a long-range laser beam might focus on another plane, or something or someone on the ground. Also the system described in this study is water-cooled, requiring 2.2 gallons of water per minute, thus, making it difficult to mount on an airplane. However, there are argon lasers that are air cooled also capable of putting out high-energy pulses. These would function as long as continuous laser energy is not needed.

## 6. SUGGESTED METHOD OF USE AND FEASIBILITY OF THE ARGON LASER AS A BIRD CONTROL

Again we have to consider the two control situations: (1) birds inhabiting (nesting, feeding) the runways and immediately adjacent areas, and (2) birds or bird flocks encountered in level flight. As

mentioned previously, the concentrated laser beam is nonspecies specific and would seem to be the best means of dispersing birds that are on the runways. In fact, resident birds exposed to an irritating laser beam a few times would soon learn to avoid the area. A system similar to that used with biosonics<sup>33</sup> might be set up with lasers. Lasers equipped with zoom telescopes positioned so that they could scan the entire field 4 inches above the ground could be controlled from a central point. Birds land on a particular part of the field and the observer turns on the laser scanning that portion of the field. To increase safety one would want a 6 inch high black metal shield around the perimeter of the field to trap the beam. An infrared laser would work equally as well as the argon device with less hazard to the human eye. The number of lasers required would depend on the type of telescope used (effective distance). An alternative to this method would be a mobile unit with the laser mounted in it. This method would be less expensive but would require a person to aim it accurately. This concentrated beam would be the only feasible way of denying all birds the airfield as a habitat.

Another method of keeping birds off the airfield that needs further research is a combination laser and distress call. Biosonics (amplifying the taped distress call to birds) has been somewhat successful but the birds soon habituate to it, or return to the area after the sound stops. The reason for this is that there is no actual distress. By combining the concentrated laser beam with the distress call it is possible that the bird after a few exposures will no longer habituate to the distress call. Here we are using the laser to reinforce the distress call.

In flight we are faced with a different problem. In this instance, I do not think a concentrated (irritation) laser beam could be used, though Shaefer<sup>8</sup> has suggested using lasers to burn the flight feathers off of the birds in the path of airplanes. What should be used is an expanded laser beam of low intensity with the advantage of laser light over regular landing lights being a greater effective distance, thus giving birds a longer time to avoid the plane. For example, a laser and telescope combination that emitted a beam 6 inches in diameter (2 W) would disperse to only 14 inches in diameter in 10 kilometers. The power 1 cm in front of the laser would be  $11 \text{ mW/cm}^2$ , and in 10 kilometers the power would be  $2 \text{ mW/cm}^2$ . Also it should be a laser pulsing approximately 100 to 200 per minute, thus diurnal birds at night would not be attracted toward the aircraft and at the powers just described the laser would not be irritating to the human eye. Here the use of radar to forewarn the pilot that he is apt to fly into a flock of birds would increase the efficiency of this method. If no other planes were in the area and the pilot were flying in level flight, a more intense, expanded beam could be used and the bird would have even greater time to avoid the plane.

Research required prior to using the methods described:

1. Determine the effects that weather (rain, ambient temperature, fog) might have on the efficiency of the laser as a bird control.
2. Determine the effects of the intense laser light on other diurnal and nocturnal species to ascertain if the responses described here are consistent; i.e., diurnal birds are not as sensitive to intense light as nocturnal birds.
3. Test synergistic effects of the concentrated laser plus the distress call (biosonics) on the birds response. Basically, the irritating laser would be used to reinforce the distress call, thus cutting down on habituation.
4. Try other wavelengths; the fact that birds have their greatest visual sensitivity at wavelengths between 500 and 506 nm does not rule out the possibility that there are cone pigments more sensitive to other wavelengths in the yellow or red.
5. Trial test under airport conditions.
6. A side light to bird control but an extremely interesting one would be further research into the filtering mechanism (pecten or oil droplets) within the eye of bird.



1. Besser, J. F., "Research on agricultural bird damage control problems in Western United States, "Unpublished ms. presented at 1st Bird Control Seminar, Bowling Green State Univ. 4 pp, 1962.
2. Bliese, J. C., "Four years of battle at "blackbird roosts: A discussion of methods and results at Ames, Iowa," Iowa Bird Life 29:30-33, 1959.
3. Siebe, C. C., "Starlings in California," In Proc. 2nd. Vert. Pest Control Conf., Univ. of California, Davis, pp. 40-42, 1964.
4. US Air Force, "Bird/aircraft collisions," Air Force Office of Scientific Research, Office of Aerospace Research, USAF, Arlington, Va., 1966.
5. Faulkner, C., "Urban bird problems," Unpublished ms. presented at 1st Bird Control Seminar, Bowling Green State Univ., 7 pp, 1962.
6. Frings, H., "Sound in vertebrate pest control," pp. 50-56, In Proc. 2nd Vert. Pest Control Conf., Univ. of California, Davis, 1964.
7. William, C. and J. Neff, "Scaring make a difference," In Birds in our lives. A. Stefferud (ed.) U.S. Dept. of Interior, Washington D.C., pp. 438-445, 1966.
8. Schaefer, G., "Recent developments in bird scaring on airfields," In The Problems of Birds as Pests. Symposia of the Institute of Biology No. 17., Murton, R. and E. Wright (ed.), Academic Press, pp. 50, 1968.
9. Meanley, R., "Blackbirds and the Southern Rice Crop," Resource Publication 100, United States Department of the Interior Fish and Wildlife Service, Washington, D.C., pp. 64, 1971
10. Wildlife Leaflet 409, United States Dept. of the Interior Fish and Wildlife Service, Bureau of Sport Fisheries and Wildlife, Washington, D.C., 1959.
11. Pumphrey, R., "Sensory Organs: Vision," In Biology and Comparative Physiology of Birds, A. J. Marshall (ed.), Academic Press. N. Y. pp. 55-68, 1961
12. Matthews, G., Bird Navigation, Cambridge Univ. Press, London and New York, 1955.
13. Watson, J., "Studies on the spectral sensitivity of birds," Pap. Dep. Marine Biol., Carnegie Inst., Wash. 7:87-104, 1915.
14. Lashley, K., "The colour vision of birds, 1. The spectrum of the domestic fowl," Animal Behaviour 6:1-126, 1916.

15. Hamilton, Wendt. Coleman, "Trichromatic vision in the pigeon as illustrated by the spectral line discrimination curve," J. Comp. Psychol. 15:183-191, 1933.
16. Matthews, L. and B. Matthews, "Owls and infrared radiation," Nature, 143:983, 1939,
17. Crescitelli, F., "The natural history of visual pigments," Ann. N. Y. Acad. Sci. 74:230-255, 1958a.
18. Crescitelli, F., "The natural history of visual pigments," Photobiology: Proc. of 19th Ann. Biol. Colloq, Oregon State C., pp. 30-51, 1958b.
19. Bridges, C., "Visual Pigments of the Pigeon (Columbia livia).", Vision Res. 2:125-137, 1962.
20. Sillman, A., "The visual pigments of several species of birds," Vision Res. 9:1063-1077, 1969.
21. Wald, G., "Photo-labile pigments of the chicken retina," Nature 140:545-546, 1937.
22. Wald, G., "Retinal chemistry and the physiology of vision," In Visual Problems of Colour., Symp. No. 8, Nat. Phys. Lab., H.M.S.O. London, pp. 7-61, 1958.
23. Crescitelli, F., B. Wilson, A. Lilyblade, "The visual pigments of birds. 1. The turkey," Vision Res. 4,275-280, 1964.
24. Kramer, G., "Long-distance orientation," In Biology and Comparative Physiology of Birds. A. J. Marshall (ed.), Academic Press, N.Y. pp. 341-369, 1961.
25. Walls, G., The Vertebrate Eye and Its Adaptive Radiation. Hafner, N. Y., 1942.
26. Ducker, G. and G. Tieman, "Die Entwicklung der Farbigen Olkugein in der Retina Von Anguis fregillis, Lacerta agilis, and Lucerta vivparce Farbsehvermogen (Reptilia, L. acertilial)," Z. Morph. Tiere 71:105-115, 1972.
27. Winner, R., "Field-Feeding Periodicity of Black and Mallard Ducks," J. Wildlife Management 23:197-202, 1959.
28. Soloman, V., "Bird hazards to aircraft,"In Proc. Fifth Bird Control Seminar, Bowling Green State University, Bowling Green, Ohio, pp. 39-45, 1970.
29. Handbook of Lasers, Robert Pressley (ed.), the Chemical Rubber Co. Cleveland, Ohio, pp. 631, 1971.

30. Lustick, S., "Bird Energetics: Effects of Artificial Radiation," Science 163:387-390, 1969.
31. Lustick, S., "Absorption of radiant energy in redwinged blackbirds (Agelaius Phoeniceces)," Condor 72:471-473, 1970.
32. Lustick, S. "Plumage color and energetics," Condor 73:121, 1971.
33. Busnel, R. and J. Givan "Prospective considerations concerning bio-acoustics in relation to bird scaring on airfields," In Symposia of the Institution of Biology, No. 17. The Problems of Birds as Pests, Ed. by Murton R. & F. Wright, Academic Press, pp. 17-28, 1968.

SESSION 5

BIRD AIRCRAFT STRIKE HAZARD (Part II)

## A REVIEW OF THE USAF BIRD STRIKE PROBLEM

Capt. J. P. Nemergut  
Air Force Weapons Laboratory  
Kirtland Air Force Base, New Mexico

## A REVIEW OF THE USAF BIRD STRIKE PROBLEM

John P. Nemergut  
CAPT            USAF

Bird/aircraft strike data have been collected by the Air Force Inspection and Safety Center, Directorate of Aerospace Safety. This paper reviews the bird strike problem as represented by those data from 1956 through 1972, which assess the biological, mission and structural factors bearing on the problem.

The thoughts expressed are those of the author and are not to be construed as the official opinion of the USAF.

## INTRODUCTION

As man increases his ability to travel farther and faster by air, he soon recognizes that he must share the airspace with birds and bats which, until recently, have had sole possession of this environment. Bird/aircraft strikes are a matter of record among many nations of the world, including the United States of America, Union of Soviet Socialist Republics, Canada, Great Britain and the Netherlands (Reference 1 and 2). Bird strikes result in much more than replacement of damaged parts and associated maintenance costs. For example, seventeen persons died in November, 1962 as a direct result of a Whistling Swan - Viscount strike over Ellicott City, Maryland. Environmental problems also surface in a discussion of bird strikes. For example, an aircraft, fully loaded with fuel, which strikes a bird on take-off, may require fuel venting prior to landing.

USAF directives (Reference 3) require accident reports for damaging bird strikes. The report should contain information on the Major Air Command (MAJCOM), type of aircraft, injury, damage, phase of flight, base of assignment, location, altitude, time of day and dollar cost. The narrative accompanying the incident report should include the aircraft velocity, type of bird, and a description of the incident and damage when known. The sources of the strike data presented in this paper are a paper by Victor Ferrari (Reference 4) and the Air Force Inspection and Safety Center, Directorate of Aerospace Safety, Norton AFB, California. Specific publications include annual "USAF Bird Strike Summaries," (Reference 5) and annual "USAF Accident Bulletins," (Reference 6). A substantial amount of data has been collected on the USAF bird/aircraft strike hazards. The purpose in presenting selected aspects of this data here is to assess the factors contributing to the problem both from the standpoint of bird strike data and field studies at Air Force Bases.

Bird strike data cannot be considered as sound scientifically as data from a controlled laboratory experiment or even a field research project. None-the-less, the data can be used to assess the problem of bird strikes. In some cases the bird strike is noted by maintenance personnel during postflight inspection. Consequently, information on when and where the strike occurred are unknown. In cases such as windscreen impact, the pilot is rightfully more concerned about his physical well-being than what kind of bird it is (Figure 1). When sufficient bird remains are available, feathers are forwarded to the "Feather File," Bureau of Sport Fisheries and Wildlife, Bird Division, U.S. National Museum, Washington, D.C. and blood remains are forwarded to the Coleman Physiology Branch, School of Aerospace Medicine, Task 3930-08, Brooks AFB, Texas in attempts to identify the species. However, the data to date reflect very little information down

to the species level. During calendar year 1965 and between 6 April 1971 and 22 November 1971, bird strike reports were required on non-damaging strikes, as well as damaging ones. During the latter period it was determined that for every USAF damaging strike there occurred approximately three non-damaging strikes.



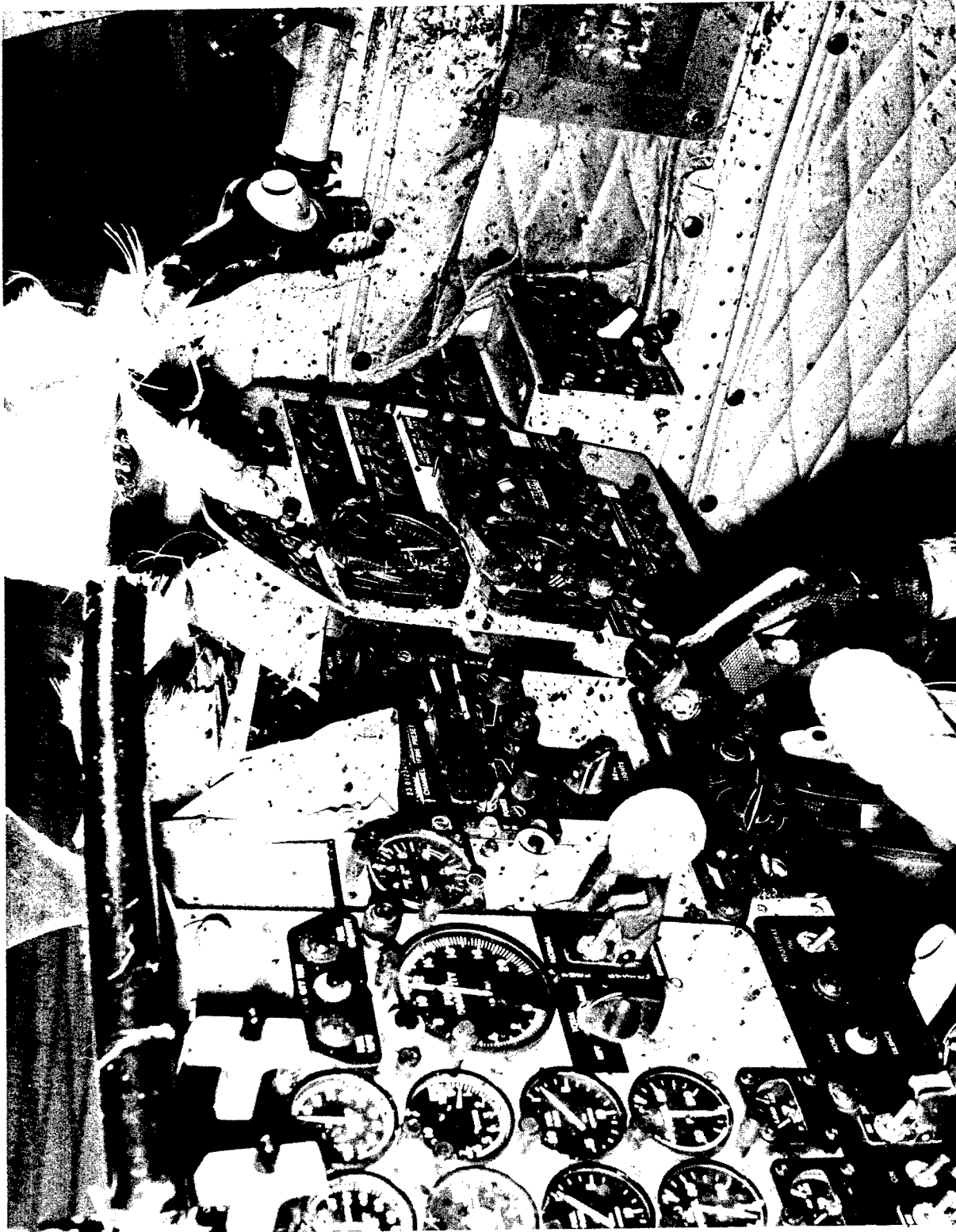


Figure 1. A Sandhill Crane Penetrated the Windscreen and Killed the Instructor Pilot

## FACTORS BEARING ON THE PROBLEM

The factors influencing the bird/aircraft strike hazard can be categorized into biological, mission and structural.

The biological factors consist of the geographical distribution of reported bird strikes, diurnal, monthly and annual fluctuations, and the types of birds hit. The largest number of bird strikes per installation occurred in the southwestern quarter of the United States, followed closely by the southeastern quarter (Table 1). This would be expected, considering that the southwestern US is most heavily used for undergraduate pilot training whereas the Southeast has greater species diversity and larger populations of birds (Reference 7) and many waterfowl overwinter in the southern United States (Reference 8). In 1972 more than three out of every five strikes occurred during daylight (Figure 2). However, there is no difference between the number of strikes occurring at dawn or dusk. The large number of daylight strikes can be attributed to the increased activity during daylight hours on part of both birds and pilots. One would expect the high percentage of night strikes to reflect the effect of migration. In some cases at least this is true. More than half of the bird-strikes at Beale AFB, California between 1966 and 1971 occurred at night and 65% occurred during migratory periods (Reference 9). Since the marked increase of damaging bird strikes in 1964, the number has levelled off averaging nearly 350 strikes per year (Figure 3). This increase can be attributed to three factors: more emphasis on the bird strike problem, more accurate reporting, and probably most significant: the transition from prop to jet aircraft. Using Duncan's New Multiple Range Test, at the 99% level, October is statistically different from all other months, September from all months except November, and November from all months except September, May and April (Table 2). These fluctuations appear to reflect the affect of migration on the number of bird strikes. Of the 1374 bird strikes reported from 1963 through 1966 less than half of the bird types were known (Table 3). In some cases the only description of the bird reported was "a large black bird" which describes the silhouette of any large bird. Probably the best identified types of birds are gulls which account for 7.4% of the total strikes. Better identification of gulls can be attributed to the fact that a majority of gull strikes occur in the immediate vicinity of the airdrome (Reference 10) and the general awareness of the gull hazard at bases where gulls are a problem. Only nine of 62 (15%) gull strikes from 1967 through 1971 occurred enroute. Probably the majority of the damaging small bird strikes are Starlings and blackbirds which pose a significant threat due to their behavioral pattern of flying in large, dense flocks. On the other hand raptors, which are generally single flyers, probably pose a greater threat to enroute aircraft (Reference 11). While soaring with their attention focused on the ground, raptors may be unaware of an oncoming, rapidly moving

TABLE 1  
GEOGRAPHICAL DISTRIBUTION OF USAF BIRD STRIKES  
1963-1972

| <u>Geographical<br/>Quadrant</u> | <u>No. of<br/>Strikes</u> | <u>No. of<br/>Installations</u> | <u>No. of<br/>Strikes per Installation</u> |
|----------------------------------|---------------------------|---------------------------------|--|
| Southwest                        | 1173                      | 34                              | 34.5                                       |
| Southeast                        | 912                       | 28                              | 32.6                                       |
| Northeast                        | 393                       | 27                              | 14.6                                       |
| Northwest                        | 285                       | 20                              | 14.3                                       |
| Total                            | 2763                      | 109                             | 25.4                                       |

# ANALYSIS OF BIRD STRIKES REPORTED BY TIME OF DAY-1972

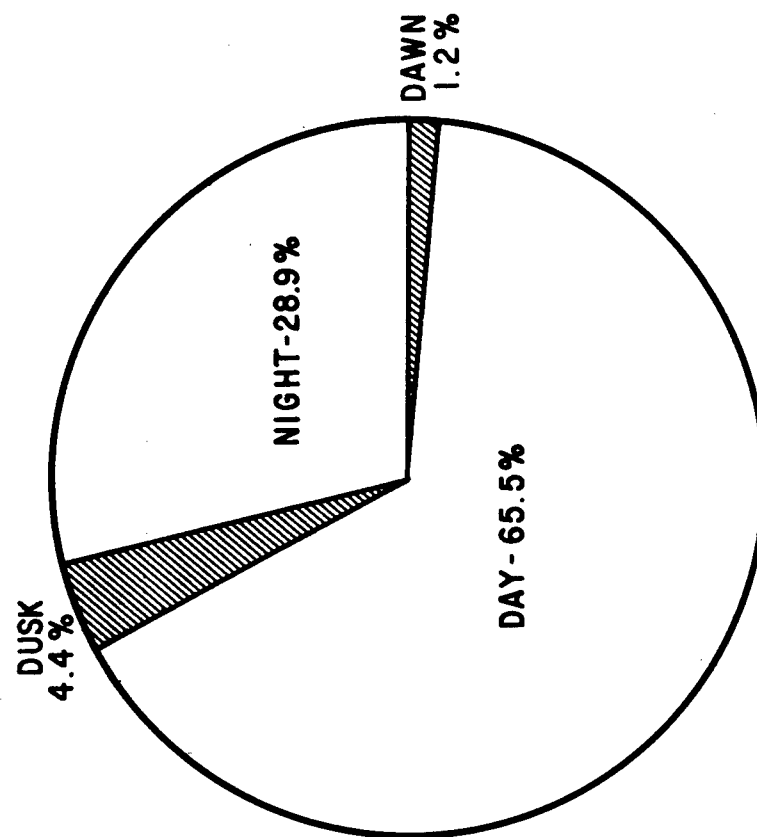


FIGURE 2

# ANNUAL VARIATIONS IN DAMAGING BIRD STRIKES 1956 - 1972



FIGURE 3

TABLE 2

## MONTHLY FLUCTUATIONS IN BIRD STRIKES

1966-1972

| Year      | Month      |            |            |            |            |            |            |            |            |            |            |            |       |
|-----------|------------|------------|------------|------------|------------|------------|------------|------------|------------|------------|------------|------------|-------|
|           | <u>Jan</u> | <u>Feb</u> | <u>Mar</u> | <u>Apr</u> | <u>May</u> | <u>Jun</u> | <u>Jul</u> | <u>Aug</u> | <u>Sep</u> | <u>Oct</u> | <u>Nov</u> | <u>Dec</u> | Total |
| 1966      | 14         | 19         | 22         | 23         | 22         | 10         | 15         | 39         | 35         | 63         | 38         | 24         | 324   |
| 1967      | 24         | 22         | 15         | 38         | 46         | 21         | 24         | 19         | 46         | 70         | 35         | 23         | 383   |
| 1968      | 20         | 14         | 35         | 38         | 31         | 23         | 17         | 24         | 47         | 53         | 40         | 20         | 362   |
| 1969      | 17         | 30         | 28         | 28         | 30         | 18         | 20         | 14         | 44         | 48         | 42         | 20         | 339   |
| 1970      | 24         | 24         | 21         | 35         | 31         | 18         | 25         | 23         | 49         | 55         | 27         | 18         | 350   |
| 1971      | 10         | 17         | 28         | 29         | 38         | 25         | 25         | 42         | 52         | 62         | 41         | 14         | 383   |
| 1972      | 30         | 26         | 30         | 26         | 36         | 16         | 20         | 26         | 31         | 44         | 36         | 30         | 351   |
| Total     | 139        | 152        | 179        | 217        | 234        | 131        | 146        | 187        | 304        | 395        | 259        | 149        | 2492  |
| Months    | <u>Oct</u> | <u>Sep</u> | <u>Nov</u> | <u>May</u> | <u>Apr</u> | <u>Aug</u> | <u>Mar</u> | <u>Feb</u> | <u>Dec</u> | <u>Jul</u> | <u>Jan</u> | <u>Jun</u> |       |
| $\bar{X}$ | 56.43      | 43.43      | 37.00      | 33.43      | 31.00      | 26.71      | 25.57      | 21.71      | 21.29      | 20.86      | 19.86      | 18.71      |       |

P&gt; .95

P&gt; .99

TABLE 3  
BIRD TYPES REPORTED IN BIRD/AIRCRAFT STRIKES  
1963-1966

| Year       | Large Birds<br>or Buzzards | Gulls | Ducks | Small<br>Birds | Unknown | Total |
|------------|----------------------------|-------|-------|----------------|---------|-------|
| 1963       | 10                         | 7     | 9     | 12             | 32      | 70    |
| 1964       | 27                         | 12    | 9     | 21             | 76      | 145   |
| 1965*      | 108                        | 68    | 30    | 217            | 416     | 839   |
| 1966       | 49                         | 15    | 15    | 20             | 221     | 320   |
| Total      | 194                        | 102   | 63    | 270            | 745     | 1374  |
| Percentage | 14.1                       | 7.4   | 4.6   | 19.6           | 54.2    |       |

\* Data includes non-damaging strikes

Adapted From Ref. 9.

aircraft. Migrating waterfowl probably account for a high percentage of the bird strikes at some bases. With increasing emphasis on the bird/aircraft strike hazard better identification of species is anticipated.

The use of a given air base will affect factors such as the type of aircraft, type of flying and aircraft velocities, which in turn influences the number of bird strikes. For example the Military Airlift Command (MAC) flying most closely approximates commercial flying. On the other hand, the trainer aircraft of Air Training Command (ATC), which trains undergraduate pilots, spend considerable time flying at low altitudes. As one might expect (Table 4) ATC averaged almost twice as many strikes per installation as MAC, even though MAC logged about 20% more flying hours per year than ATC from 1965 through 1970. Additionally, trainer and transport aircraft are involved in more bird strikes than fighter and bomber aircraft (Table 5). A comparison of enroute strikes and airdrome strikes (those strikes occurring during landing and takeoff) indicates no difference in numbers (Table 6). Although approximately 43% of the bird strikes do not mention the altitude (above ground level) where the bird strikes occurred, 52% of the strikes with known altitude, occurred below 3000 feet; the most hazardous altitudes appear to be below 2000 feet (Table 7). From the standpoint of altitude at which strikes occurred, one must keep in mind that the figures for enroute strikes include low level flying and ordnance delivery. Consequently, the altitude data better assess the bird strike problem. Table 8 establishes a working relationship between bird weights and aircraft velocities. The data used are from those bird strikes highlighted in the USAF Bird Strike Summaries (Reference 5), which include the more serious strikes. The birds in the strike reports weighing less than one pound (Reference 12) include Woodcocks, Starlings, blackbirds, swallows, pigeons, and Sparrow Hawks as well as bats; one to four pounds include ducks, hawks, gulls and cormorants; greater than 4 lbs include vultures, geese, eagles, frigatebirds, cranes, albatrosses and pelicans. The airspeed categories approximate takeoff and landing (<200 KIAS) approach (200-279 KIAS), and training mission (>280 KIAS), depending somewhat on the aircraft. Besides the large numbers for unknown bird types and unreported airspeeds it is important to draw attention to the greater than 4 lb birds at airspeeds in excess of 280 KIAS and the 1 to 4 pound birds at all airspeeds. As expected bird weights and airspeeds are directly related to the amount of damage. For example, a one pound bird, 3 inches in diameter striking an aircraft travelling at 50 MPH exerts a force of 332 lbs while at 600 MPH a force of 48000 lbs. Likewise a 16 pound bird, 8 inches in diameter striking an aircraft at 600 MPH exerts a force of 288,000 lbs under theoretical conditions. The fact of the matter is, too many assumptions have to be made to arrive at actual impact forces in bird strikes. For example, little is known "about the rate of deflection of the structure and the equivalent behavior of the bird carcass on impact... the approximate diameter of the bird, rather than its length... no consideration is given



TABLE 4

## DISTRIBUTION OF BIRD STRIKES BY MAJCOM INSTALLATIONS IN CONUS

1966-1972

| <u>MAJCOM</u> | <u>No. of<br/>Strikes</u> | <u>No. of<br/>Installations</u> | <u>No. of<br/>Strikes per Installation</u> |
|---------------|---------------------------|---------------------------------|--|
| ATC           | 713                       | 14                              | 50.9                                       |
| MAC           | 236                       | 8                               | 29.5                                       |
| SAC           | 626                       | 26                              | 24.1                                       |
| TAC           | 377                       | 22                              | 17.1                                       |
| ADC           | 50                        | 13                              | 3.9  |
| AFSC          | 22                        | 6                               | 3.7  |
| AFR           | 29                        | 10                              | 2.9  |
| AFLC          | 8                         | 6                               | 1.3  |
| Other         | 173                       | --                              | ---  |
| Total         | 2234                      | 105                             | ---  |

TABLE 5

## BIRD STRIKES ACCORDING TO TYPE OF AIRCRAFT

1963-1972

| <u>Aircraft Type</u> | <u>No. of Strikes</u> | <u>Percentage</u> |
|----------------------|-----------------------|-------------------|
| Trainer              | 1112                  | 31.3              |
| Transport            | 1083                  | 30.5              |
| Fighter              | 644                   | 18.2              |
| Bomber               | 611                   | 17.2              |
| Misc.                | 98                    | 2.8               |
| Total                | 3548                  |                   |

TABLE 6  
BIRD STRIKES BY PHASE OF FLIGHT  
1967-1972

| <u>Phase of Flight</u> | <u>No. of Strikes</u> | <u>Percentage</u> |
|------------------------|-----------------------|-------------------|
| Enroute                | 1074                  | 49.4              |
| Landing                | 581                   | 26.7              |
| Takeoff                | 519                   | 23.9              |
| Total                  | 2174                  |                   |

TABLE 7  
DISTRIBUTION OF BIRD STRIKES RELATIVE TO ALTITUDE  
1970-1972

| <u>Elevation (feet AGL)</u> | <u>No. of Strikes</u> | <u>Percentage</u> |
|-----------------------------|-----------------------|-------------------|
| 1-100                       | 96                    | 8.8               |
| 100-500                     | 131                   | 12.0              |
| 501-1000                    | 144                   | 13.2              |
| 1001-2000                   | 161                   | 14.7              |
| 2001-3000                   | 43                    | 3.9               |
| >3000                       | 44                    | 4.0               |
| Unknown                     | 475                   | 43.4              |
| Total                       | 1094                  |                   |

TABLE 8

Relationships between Bird Weights and Aircraft Velocities  
from Selected Bird Strike Incidents, 1964-1972

|  |            | Bird Weights (lbs) |            |              |                |              |
|--|------------|--------------------|------------|--------------|----------------|--------------|
|  |            | <u>&lt;1</u>       | <u>1-4</u> | <u>&gt;4</u> | <u>Unknown</u> | <u>Total</u> |
| V<br>e<br>l<br>o<br>c<br>i<br>t<br>i<br>e<br>s | Unreported | 2                  | 5          | 6            | 9*             | 22           |
|  | <200       | 7                  | 14         | 6            | 13             | 40           |
|  | 200-279    | 6                  | 12         | 8            | 8              | 34           |
|  | >280       | 2                  | 10         | 22           | 19             | 53           |
|  | Total      | 17                 | 41         | 42           | 49             | 149          |

\* One incident occurred during engine runup

here to the effect of spread wings etc..." (Reference 13). Many factors, few of which are well understood, affect the relationship between bird weights and aircraft velocities with respect to the actual forces generated. The 1 to 4 pound birds are involved in a large number of strikes at all airspeeds. This can best be explained by the large number of individuals and species of birds which fall into this category.

The assessment of the structural factors associated with the bird strikes consists of a review of the aircraft components struck in damaging strikes and those in the serious aircraft accidents (Tables 9 and 10). Engines and wings are the most frequently struck, primarily due to the area of each. The nature of jet engines to draw large volumes of air through them also greatly increases the number of strikes. The forward locations and large cross-sectional areas of the windscreen and nose increase the strike potential of these components. Serious bird strike accidents include those in which more than minor injury occurred to the aircrew and/or more than minor damage to the aircraft. In two of the serious bird strikes accidents, both windscreen damage and resultant engine ingestion occurred. Another accident was identified as a multiple strike and specifically mentioned engine ingestion. The windscreen strikes account for only 12% of the total strikes, yet they account for half of the serious aircraft accidents. A bird strike on the windscreen in addition to affecting the impacted area may injure the aircrew seriously and result in foreign object damage to the engines. All serious accidents involving engine ingestion occurred during takeoff when power requirements and reaction times are more critical. However the serious accidents involving the windscreen are evenly divided between enroute and airdrome strikes.

TABLE 9  
AIRCRAFT COMPONENT STRUCK IN BIRD/AIRCRAFT STRIKES  
1963-1972

| <u>Component</u>   | <u>Number</u> | <u>Percentage</u> |
|--------------------|---------------|-------------------|
| Engines            | 1112          | 31.3              |
| Wings              | 885           | 24.9              |
| Windscreen/canopy  | 415           | 11.7              |
| Nose/Radome        | 390           | 11.0              |
| Fuselage           | 217           | 6.1               |
| Flaps/Speed Brakes | 131           | 3.7               |
| Stabilizer         | 103           | 2.9               |
| Landing Gear       | 79            | 2.2               |
| Tanks              | 61            | 1.7               |
| Props/Rotor Blades | 22            | 0.6               |
| Other              | 133           | 3.8               |
| Total              | 3,548         |                   |

TABLE 10  
AIRCRAFT COMPONENT STRUCK IN MAJOR ACCIDENTS  
1963-1972

| <u>Component</u>  | <u>No. of Strikes</u> | <u>Percentage</u> |
|-------------------|-----------------------|-------------------|
| Windscreen/Canopy | 11                    | 50                |
| Engine            | 6                     | 27                |
| Other             | 5                     | 23                |
| Total             | 22                    |                   |

## SUMMARY

The bird hazard to aircraft is a significant problem which emphasizes the need to share, rather than compete for airspace. The conditions most conducive to a serious aircraft strike are either transport aircraft taking off during daylight hours at a coastal base, or trainer aircraft travelling in excess of 280 knots on a training mission below 2000 feet AGL during October in the southwestern United States.

The problem of birds and aircraft must be looked at as multidisciplinary, drawing on the necessary expertise in biology, environmental sciences, and engineering.

The problem can be divided into airdrome and enroute hazards. Biological control must be effected to reduce the bird concentrations around the airdrome. Habitat management offers the most promise by reducing those environmental features which attract birds. Birds may be found in the airdrome for any one or all of the following reasons: water, food, shelter, safety, movement routes and nesting. Through sound habitat management birds will no longer be attracted to the airdrome environment. Acoustical and other scare devices may effect short term avoidance responses. However, habituation to the stimulus becomes the problem if the environmental attractants are not concurrently eliminated. Close-in surveillance radar is a second palliative measure in that pilots can be warned of bird concentrations on the runway and delay take-off, for example. The least effective means of controlling birds is attempting to kill them. Again, this is so, because the environmental attractants will draw other birds into the area. Then one must ultimately kill all the birds to effect kill control, which is unacceptable. The strike potential to enroute aircraft can be effectively reduced by radar detection and subsequent avoidance of bird concentrations, i.e. bird forecasting, by scheduling aircraft operations to avoid peak periods of the hazard and through development of on-board aircraft devices (perhaps strobes) to alert birds of approaching aircraft. The extent of damage can be reduced through aircraft hardening. A re-evaluation of the materials criteria and standards is necessary, as is the development of materials capable of withstanding higher impact forces.

Some of the above methods are currently being investigated in Canada and Europe. The United States must address the problem in a manner similar to that set by the Canadians and Europeans. Their committees on bird hazards to aircraft are responsible for finding solutions to the problem and include their military and equivalents to our FAA, NASA, Bureau of Sport Fisheries and Wildlife, pilot associations, airlines, aircraft industries, and transportation safety organizations. One result of the coordinated efforts of the National Research Council of

of Canada/Associate Committee on Bird Hazards to Aircraft is the decrease in aircraft damage resulting from bird strikes. Air Canada's repair costs due to birds were reduced by 80% and there was an appreciable reduction in the number of strikes (Reference 14).

#### ACKNOWLEDGEMENTS

Appreciation is extended to Col Donald Johnson of the Air Force Inspection and Safety Center for providing the data, Ronald J. Sobieralski for assisting in tabulating the data and to Robert C. Beason for reviewing the manuscript.

## REFERENCES

1. Lewis, H. F., ed., Bulletin Number 5, Associate Committee on Bird Hazards to Aircraft, National Research Council of Canada, Ottawa, Canada, 1967.
2. Yakobi, V. E., Bird Behavior and Man-Made Objects, Field Note Number 57, Associate Committee on Bird Hazards to Aircraft, National Research Council of Canada, Ottawa, Canada, 1971.
3. Air Force Regulation 127-4, paragraphs 19, 20 and 21.
4. Ferrari, Victor J., An Epidemiologic Study of USAF Bird Strike Damage and Injury, 1960 to 1965, Air Force Safety and Inspection Center, Norton AFB, California.
5. USAF Bird Strike Summaries, 1963 through 1972, Directorate of Aerospace Safety, Air Force Inspection and Safety Center, Norton AFB, California, 1964-1973.
6. US Air Force Accident Bulletins, 1966 through 1970, Directorate of Aerospace Safety, Air Force Inspection and Safety Center, Norton AFB, California, 1967-1971.
7. Robbins, C. S. et al, eds. Birds of North America, New York, 1966.
8. Belrose, F. C., Migration Corridors of Waterfowl in the United States, Federal Aviation Agency, Systems Research and Development Service Report, FAA-RD-71-71, August 1971.
9. Nemergut, J. P., and R. C. Beason, Preliminary Evaluation of Bird Aircraft Strikes at Beale AFB, California, DE-TN-72-018, Air Force Weapons Laboratory, February 1972.
10. Wooten, R. C., G. E. Meyer, and R. J. Sobieralski, Gulls and USAF Aircraft Hazards, AFWL-TR-73-32, Air Force Weapons Laboratory, Kirtland AFB, New Mexico, 1973.
11. Beason, Robert C, Evaluation of the Bird Aircraft Strike Hazard in the Canal Zone, AFWL-TR-73-16, Air Force Weapons Laboratory, Kirtland AFB, New Mexico, 1973.
12. Kaiser, G., Weights of a Number of Birds, Field Note Number 51, Associate Committee on Bird Hazards to Aircraft, National Research Council of Canada, Ottawa, Canada, 1970.
13. Macaulay, G. A., Some Thoughts on the Forces Associated with a Bird Strike, Field Note Number 24, Associate Committee on Bird Hazards to Aircraft, National Research Council of Canada, Ottawa, Canada, 1965, pp 1-2.



14. Solman V. E. F., Bird Control and Airport Safety, Canadian Wildlife Service Report Series, Vol. 14, 1971, pp 7-14.

ECOLOGICAL ASPECTS OF GULL-AIRCRAFT  
HAZARDS

William H. Drury  
Massachusetts Audubon Society  
Lincoln, Massachusetts

## ECOLOGICAL ASPECTS OF GULL-AIRCRAFT HAZARDS \*

by

William H. Drury,  
Director, Scientific Staff  
Massachusetts Audubon Society

Bird hazards to aircraft exist primarily when birds are attracted to airspace around airports or aircraft enter airspace where birds habitually operate. Most of the earth's atmosphere and the vast majority of altitudes at which aircraft operate are essentially free of birds except under rare special circumstances. It appears obvious that in order to avoid bird strikes it is necessary to understand the reasons for the presence of both aircraft and birds in the narrow zones of competition. Studies of gulls have been useful in developing operating techniques which minimize airstrike hazards.

When gull strikes occur on or near airfields, birds have been attracted to the site by special circumstances. The attracting circumstances have been identified and corrective measures prescribed. Failure of corrective measures has apparently resulted not from biological limitations, but from failure of those responsible to give the hazard of bird strikes high enough administrative priority.

When gull strikes occur in airspace away from airfields the problem is more complex, but the movements of gulls in those places can also be understood. When the reasons for competition for airspace between birds and aircraft away from airfields are known it will in some cases be possible to change the forces affecting bird behavior, but often it will be advisable to make local or temporary alterations in the behavior of aircraft.

\* Contribution No. 106 from the Scientific Staff, Massachusetts Audubon Society, Lincoln, Massachusetts.

Gulls were among the first bird species involved in the increased hazards of bird strikes which accompanied the introduction of jet engines. Gulls were recognized as serious hazards at NATO military air bases in northwestern Europe by the middle 1950's where the first studies of dispersing gulls from airports were made. Subsequently a number of studies have been made of bird hazards on the immediate surroundings of airports. Recently data have been collected on where and under what circumstances in-flight collisions occur (Nemergut, this symposium). Except for strikes in the course of highspeed low level military exercises gulls appear to be the species most frequently involved.

The lessons learned from studies made of the circumstances under which gulls become hazards and the techniques for dispersing them can be applied to many other hazardous or pest species. One general point has become clear: that the time-hallowed strategy of attacking a technological problem intensively at the point where it is experienced has little chance of success in environmental situations.

Pest species are those which occur in large numbers in habitat modified by man and by their presence inconvenience man. Almost by definition they have demonstrated three kinds of adaptability: to occupy a changed environment, to modify their behavior in order to utilize it and to increase their numbers. Such species are likely to have come from habitats with a history of frequent environmental change and for them, an attempt by man to suppress their populations is merely another environmental change to which they already have the capacity to adjust. The strategy of management is then to seek the sensitive parts of the species adaptive system, and to use them to make the species adjust in ways that will benefit man.

This paper is primarily concerned with the New England population of the Herring Gull, Larus argentatus. General studies of gull biology have been made during the last decade along the New England coast. These studies were designed to clarify why the species is numerous enough to become a pest, and what population elements contribute to the problem at Logan Airport, Boston, Mass. In previous papers its history, numbers, breeding distribution, winter distribution, local movements, reproductive success, longevity, and population structure have been described (1,2,3). Suggestions for management of the population were made by Drury and Nisbet (4).

In 1972 about 100,000 pairs nested on about 300 islands in the eastern United States and about 35,000 pairs in contiguous parts of eastern Canada south of the Gulf of St. Lawrence. Including young, about 700,000 birds wintered along the Atlantic and Gulf coasts between 1965 and 1967. The population has doubled about every 15-20 years since about 1900 except for a period of rapid growth between 1920 and 1945 when it doubled every 12-15 years and a slow period between 1940 and 1955 when control measures were in operation (5).

#### The source of birds contributing to bird strikes.

During 1961 and 1962 studies of the movements of color-dyed gulls between their nesting colonies and food sources were made around metropolitan Boston. The results of these studies (1,2,4) indicated that the gulls visiting each stretch of shore line are local birds. Breeding birds seldom commute more than 25 miles between food sources and nesting site, and usually they find all their requirements for food, water, and loafing areas within 10 miles. Therefore the presence of gulls at any airport can be confidently

predicted to depend on the condition of its immediate environment.

The main foods of the Herring Gull are natural but in the breeding season garbage, sewage, fish wastes, and pig food may supply a critical 20-30% additional increment which has allowed them unusual breeding success. In winter a very large fraction of the population appears to depend heavily on foods of human origin, and for this reason gulls are concentrated around cities.

Most metropolitan areas support a shifting population of gulls whose composition changes with the seasons in addition to the gulls which breed on local islands and are essentially resident. In general the gulls use airports only for transit or loafing and not for feeding, nesting, or roosting. In this situation, attempts to condition individual birds to avoid the airports are likely to have only limited and temporary effects.

#### Movements of the population.

Detailed studies have shown (6) that when a dump is closed or fishing boats are idle the gulls which regularly feed in those places quickly go elsewhere. In successive weeks the number of gulls of a metropolitan area may vary 60-75% as the birds respond to local changes in food supply. Air surveys of the Atlantic shore showed more than half of the wintering population to be concentrated in the major metropolitan areas (where most large airports are sited). Another 25% were found around smaller towns where fish factory refuse, or dumps were available and less than 15% of the gulls "making an honest living" on the rocky and sandy shores. Thus the winter gull population is mobile and sensitively responsive to food sources.

Control measures in operation between 1940 and 1953 (5) showed that the breeding population is also mobile. The control program was designed to eliminate reproduction hence annual recruitment. Therefore after the existing young had grown up the population should have decreased at the average mortality rate of adults, 8-10% (3). But Gross's observations suggested decreases of 45% on single islands in Maine within three years of beginning treatment and the population of the treated islands for the whole of Maine dropped about 24% per year. At the same time the gull breeding population of islands in Massachusetts (where no control program was in effect) grew especially rapidly (1,7). It appears that elements of the breeding population of Maine emigrated to Massachusetts (8).

These studies show that large numbers of gulls will move from areas where the environment is less attractive into areas where they are not disturbed or where they find food. Nevertheless a certain segment of the population whether on wintering grounds or at breeding colonies remains "conservative." Although many gulls have moved away from the outer islands on the coast of Maine (the Herring Gull population center between 1900 and 1930) to islands close to larger cities in Maine and metropolitan areas from Massachusetts to New York, the outer islands still have small or moderate sized colonies (7,8).

Populations with variable dispersal behavior of this kind can change quickly to "take advantage of" changes in environmental selective forces. In this sense behavioral polymorphism constitutes "adaptability." From the viewpoint of management, the important point is that a change in the environment results in a rapid change in the proportion of individuals with different behaviors, and hence in the average behavior of the population. Measures taken against one segment of the population result in its replacement by

another which is affected less-- an ecological example of Le Chatelier's Principle. It is this pitfall of management which must be avoided in planning counter-measures.

#### Population dynamics.

The Herring Gull nests almost exclusively in dispersed colonies on small and medium-sized islands (usually 1-50 ha.). The choice of islands functions to avoid terrestrial predators; our experimental introduction of predators (foxes and raccoons) to some islands resulted in a rapid evacuation of the islands, followed by slow recolonization after the predators were removed (9).

Our studies in 53 colonies suggest that, on average, each breeding pair lays about three eggs and fledges about one young per season. In the course of its adult life of about 14 years, therefore, the average pair fledges 12-14 young, of which about four survive to the age of four or five years at which they enter the breeding population (3). There appear to be three main periods of chick losses: immediately before and after hatching, immediately after fledging, and perhaps again on the winter quarters (10,11,12). Each of these periods of loss coincides with a required change in behavior of either parent or chick, or both.

These average figures conceal substantial fluctuations. Reproductive success is reduced on all islands in years with long periods of fog or of hot sunny weather. More important, there are large differences between reproductive success on different islands, which remains consistent from year to year.

The results of a multivariate statistical analysis of data from 160 colony-years to determine the important environmental variables indicates that the factors which favor success is a set of characteristics typical of the colonies closest to metropolitan areas in southern New England. In fact more than half the breeding population of New England has assembled there (8).

These colonies include the majority of the highly successful breeding nuclei from which the large majority of young emigrate (30% of the colonies produce 85% of the young (8)); some colonies produce scarcely enough young to maintain themselves and into others there is net immigration. The differences in reproductive rates are so large (0.2-1.7 young per nest) as to represent strong selection in favor of the individuals in the "good" colonies. However for a variety of reasons the "bad" colonies have not been abandoned. The most important reasons are probably that on the average nearly all regional populations over-produce young and that young tend to settle near the colony where they hatched.

#### Significance of the present population structure for management purposes.

The magnitude of the problem becomes apparent when we realize that nearly 150,000 young Herring Gulls are produced annually on the eastern seaboard, of which only about 25,000 need to survive to the fourth year to maintain the present population. This indicates that attempts to alleviate the gull problem at airports and other specific sites by shooting will have as little success in the U. S. as they have elsewhere, because killing usually proves to be alternative to, not additional to, natural mortality (13). To the extent that numbers are limited by the available food supply, any artificial reduction in numbers permits a corresponding number of individuals to escape starvation (13). In fact, the Herring Gull population as a whole does not

seem to be food-limited, but there is indirect evidence that survival of young birds in the critical few months after fledging may be (11,12).

The over-production of young also suggest that attempting to reduce the population by inhibiting reproduction will not be effective. Data gathered on production and survival of young (4) suggest that production must be reduced by more than 50%, perhaps as much as 87%, to eliminate the surplus of young attempting to enter the breeding population. Furthermore there are many colonies of gulls in Canada apparently producing a surplus of young and if these were not included in the program, inhibition of reproduction would presumably only halt the growth of the local population as it did during the decade long experiment 1940-1953, not reverse the population trend.

Effective management must use techniques to which the pest population readily respond.

According to censuses taken in 1972 from New Jersey to New Brunswick the breeding gull population of New England has recently slowed its growth sharply although the whole east coast population does not show this effect (7). Furthermore recent measurements of the age structure following the 1972 breeding season indicate that on-colony or post-fledging survival has been significantly lowered in the last three years (14). This field evidence indicates that environmental changes have occurred which have had a measureable effect on the regional gull population. Although studies are not available to establish cause and effect relations, it seems reasonable to associate the changes with the recent rapid decline in the New England fishing industry and with recent environmental action to regulate solid waste disposal and water pollution.

Studies made around metropolitan waste disposal areas show how rapidly the gull population responds to changes in food supply (6) and how important are human sources of food to the survival of young immediately after hatching, immediately after fledging, and during their first winter (10,11,12). The environmental stimuli to which gulls are most responsive directly in terms of movements and indirectly in terms of survival, are changes in food, as has now been demonstrated in a number of studies. Therefore the most effective technique for habitat management on and around airports so as to minimize bird hazards from gull strikes is to remove sources of food. By removing such food a stimulus is removed which would attract gulls to the area and its absence amounts to a stimulus for local gulls to go elsewhere. The more widespread the clean-up, the more general will be the effect on the local or regional population.

Removal of food is the management technique which is most effective on a local scale without cooperation from neighboring areas and it is the one to which the birds are most responsive.

# REFERENCES

1. DRURY, W. H. 1963. Herring Gull populations and movements in southern New England. typescript unpublished report: U.S. Fish & Wildl. Service. 68pp.
2. DRURY, W. H. 1964. Results of a study of Herring Gull populations and movements in southeastern New England. Colloque: Le probleme des oiseaux sur les aerodromes (Nice, 1963). Paris: Inst. Nat. Rech. Agron.
3. KADLEC, J. A., and W. H. DRURY. 1968. Structure of the New England Herring Gull population. Ecology, 49: 644-676.
4. DRURY, W. H., and I. C. T. NISBET. 1969. Strategy of management of a natural population: the Herring Gull in New England. Proc. World Conf. Bird Hazards to Aircraft. Kingston, Ontario. Sept. 1969: 441-454.
5. GROSS, A. O. 1951. The Herring Gull - Cormorant Control Project. Proc. Xth Intl. Orn. Congr.: 533-536.
6. DRURY, W. H. 1967. Studies of Herring Gulls in New England. typescript final report: U.S. Fish & Wildl. Service. 48pp.
7. DRURY, W. H. in prep. Population changes in New England seabirds.
8. DRURY, W. H., and I. C. T. NISBET. in press. The importance of movements in the biology of Herring Gulls in New England. Proc. Conf. on Population Dynamics of Migratory Birds. Patuxent Wildl. Res. Ctr. Oct. 1969. AIBS
9. KADLEC, J. A. 1971. Effect of introducing foxes and raccoons on Herring Gull colonies. Journ. Wild. Mgt. 35: 625-636.
10. KADLEC, J. A., W. H. DRURY, and D. K. ONION. 1969. Growth and mortality of Herring Gull chicks. Bird-Banding, 40: 222-233.
11. DRURY, W. H., and W. J. SMITH. 1968. Defense of feeding areas by adult Herring Gulls and intrusion by young. Evolution, 22: 193-201.
12. NISBET, I. C. T., and W. H. DRURY. 1972. Post-fledging survival in Herring Gulls in relation to brood-size and date of hatching. Bird-Banding, 43: 161-172.
13. MURTON, R. K. 1968. Some predator-prey relationships in bird damage and population control. The Problems of Birds as Pests, eds. R. K. Murton and E. N. Wright: Academic Press, London and New York: pp. 157-169.
14. DRURY, W. H., and J. A. KADLEC. in prep. Is the Herring Gull of the northeastern United States still increasing?



## HAIL IMPACT ON AIRCRAFT TRANSPARENCIES

Ian I. McNaughtan  
Ministry of Defence  
Farnborough, Hants, England

## HAIL IMPACT ON AIRCRAFT TRANSPARENCIES

by

Ian I. McNaughtan, B.Sc., D.R.T.C.

Royal Aircraft Establishment, Farnborough

### ABSTRACT

The problems and frequency of in-flight encounters with hail are reviewed and the results are presented of hail impact tests on a variety of test panels and aircraft windcreens. The materials tested were poly(methyl) methacrylate, as-cast and biaxially stretched, polycarbonate and glass of various degrees of toughening. The tests were made with  $\frac{1}{2}$ in, 1in and 2in diameter hail impacting at speeds up to 2000 ft/s.

*British Crown Copyright reserved. Reproduced by permission of the Controller of Her Britannic Majesty's Stationery Office.*

## 1 INTRODUCTION

The restrictions in aircraft flight path imposed by the use of airways, and ground control together with the limitations of airborne weather radar and increases in aircraft operating speed caused concern that in-flight encounters with hail would become an increasing hazard. Because of the scarcity of data on the hail impact resistance of aircraft structure and components, a research programme was started at the RAE in 1968. In this paper the results are presented of our studies to date of the hail impact resistance of transparency materials.

## 2 OCCURRENCE OF HAIL

Hail is formed in cumulus clouds, most frequently in cumulonimbus cloud, which fulfil certain requirements in respect of wind shear, water content, altitude, growth rate etc. It is believed that the hail is formed in a narrow tilted core where it grows by the accretion of supercooled water droplets as it is raised in the updraught. When it is too large to be supported by the updraught it falls out of the tilted core and either falls to the ground or is entrained in the core in-flow at lower altitude to be recycled and increased in size. Hail can therefore be encountered in the cloud or in clear air below or to the side of the cloud.

The size of hail, based on samples collected on the ground, varies from pea size up to a maximum of 5½ in diameter. Fortunately the frequency of occurrence decreases with increase in size. The measurement of the variation in size distribution with altitude using aircraft mounted equipment has been attempted but is not a recommended pastime and less is known on this aspect than is desirable. Briggs developed an expression for the risk of encounter with hail, summarised in Appendix 1, from which the UK CAA developed a requirement for supersonic aircraft to resist impact by 2 in diameter hail at altitudes up to 30000 ft at the operating speed appropriate to the altitude. Above 30000 ft the size reduces to 1 in at 40000 ft, ½ in at 50000 ft and ¼ in at 60000 ft. For subsonic aircraft the UK CAA requirement is resistance to 2 in hail at the rough air speed of the aircraft. Resistance is defined as ability to complete the flight safely. The requirement for UK military aircraft is less well defined.

Information on in-flight encounters with hail is not as readily available as that on bird strike and a direct comparison of the hazards cannot be made. However, a comparison of the windscreen bird strike risk, based on 1966-71 strikes to British registered transport aircraft and hail strike rate based on Biggs<sup>1</sup> assessment, given in Appendix 1, shows that the risks are comparable (approximately one in a million). Equal emphasis should be given to hail resistance as is given to bird strike resistance in the design of aircraft forward facing transparencies.

### 3 EXPERIMENTAL APPARATUS

High pressure gas guns were used to fire ice projectiles against stationary targets. These 'hail' projectiles were formed by freezing measured quantities of distilled water in silicone rubber moulds at  $-15^{\circ}\text{C}$ . They had a hemispherical nose and cylindrical afterbody. Their weight was equal to that of a sphere of the same diameter as the hemispherical nose. The nominal  $\frac{1}{2}$  in,  $\frac{3}{4}$  in, 1 in and 2 in diameter hail weighed 1, 3.2, 7.4 and 59.2 grammes respectively.

Impact speed was obtained by timing the interruption by the projectile of two light beams immediately ahead of the target.

The test specimens were either aircraft windscreens or panel specimens mounted to a rigid frame by a simple rubber gasket/clamp edge attachment. The panel size was 1ft square for the tests with 1 in diameter and smaller hail and  $1\frac{1}{2}$ -2ft square for tests with 2 in hail. It was considered that these panel sizes were large enough to ensure that the test result was not adversely influenced by the mounting attachment.

### 4 RESULTS: AS-CAST POLY(METHYL) METHACRYLATE (PMMA)

The tests were made on monolithic panel specimens.

With increase in impact speed the first signs of damage were very faint surface marking at the point of impact, the marking increasing with increase in speed to an area approximately that of the impacting hail cross sectional area. Figure 1 shows this surface erosion marking and it can be seen to consist of a circular undamaged area surrounded by a shallow crater and circumferential cracking. The onset speed for this marking increased with impact angle and reduction in hail size. At impact angle  $\alpha = 45^{\circ}$  the onset speed with 1 in hail was about 700 ft/s.

The next sign of failure was the formation of a star shaped crack at the rear surface directly behind the impact point. Further increase in speed resulted in extension of the star cracks to the front surface and shatter failure of the panel by extension of the cracks to the panel edges.

Figure 2 shows the effect of hail diameter,  $D$ , on penetration speed,  $V_p$ , and indicates a relationship

$$V_p = KD^{-0.8} \quad (1)$$

to apply over the range of hail diameter  $\frac{3}{4}$  in to 2 in at normal impact and  $\frac{1}{2}$  in to 2 in at  $45^{\circ}$  impact.

The effect of panel thickness,  $t$ , on penetration speed is shown in Figure 3 and it can be seen that an approximately linear relationship exists.

$$V_p = Kt \quad (2)$$

The effect of impact angle  $\alpha$ , is shown in Fig.4 and the approximate relationship is

$$V_p \cos \alpha = K \quad (3)$$

for  $\frac{1}{4}$  in to 2 in diameter hail. The results with  $\frac{1}{4}$  in hail are not in agreement but the failure mode is different in that in most tests rear surface cracking only was obtained.

Combining equations (1) to (3) gives

$$V_p = Kt / \cos \alpha D^{0.8} \quad (4)$$

All the test results in Figures 2 to 4 were obtained with the specimens at laboratory temperature, approximately 20°C, but in the case of impact speeds in the range 1000-2000 ft/s this is unrepresentative of the in-flight case. Figure 5 shows that decreasing the specimen temperature to -15°C has little effect but increasing the temperature to 95°C causes a 10% reduction in penetration speed. At 120°C, well above the tolerable maximum, the reduction is 20% and considerable distortion of the panel occurred in the test giving a no-penetration result. Applying this 10% reduction factor, equation (4) becomes

$$V_p = 1800 t / \cos \alpha D^{0.8} \quad (5)$$

for  $t$  and  $D$  in inches and  $V_p$  in ft/s and this is suggested as a tentative empirical formula for the hail impact resistance of monolithic as-cast PMMA over an impact angle range up to 60° and for hail diameters from  $\frac{1}{4}$  in to 2 in.

## 5 RESULTS: BIAXIALLY STRETCHED PMMA

### 5.1 Monolithic panels

Tests were limited to room temperature tests on 0.39 in thick panels with 1 in hail at 45° impact angle and the results are given in Figure 6. The first signs of damage were observed at 755 ft/s, comparable with the onset speed for as-cast PMMA, but the form was completely different. There was no damage to the impacted surface but conical delamination occurred commencing some 0.008 in below the impacted surface. At 790 ft/s a large fragment spalled off the rear surface, the size was approximately 3 in diameter with very sharp edges. Penetration occurred at 997 ft/s, a speed comparable to the shatter speed for an equivalent as-cast panel.

However, it is considered that spalling of such fragments is an unacceptable hazard and the equivalent penetration speed should be based on that case. Assuming that equations (1) to (3) apply also to biaxially stretched PMMA, the equivalent tentative formula is, in the units of equation (5)

$$V_p = 1250t/D^{0.8} \cos \alpha \quad (6)$$

## 5.2 Laminated panels

Tests were made with  $\frac{1}{8}$ in, 1in and 2in hail on laminated panels of two  $\frac{3}{8}$ in thick stretched PMMA with a 0.050in PVB interlayer. Again the first visible signs of damage were small sub-surface marks at the point of impact. The onset speeds were 850 and 650 ft/s for  $\frac{1}{8}$ in and 1in hail at  $45^\circ$  impact angle and 920 and 850 ft/s at  $60^\circ$  impact angle. Increasing speed increased the size and depth of penetration of the sub-surface failure. Figure 7 shows the extent of damage for 1in hail impacting at approximately 1000 ft/s,  $\alpha = 45^\circ$ : the area of lost vision is about 2in diameter, allowing for windscreen slope. At 1100 ft/s the damage extended down to the vinyl interlayer and at 1250 ft/s onset of surface cracking was observed around the central clear zone.

All the above tests were made at  $20^\circ\text{C}$ . Tests at higher impact speeds, up to 2000 ft/s, were made with  $\frac{1}{8}$ in to 1in hail on panels at  $90/95^\circ\text{C}$  and damage was limited to the outer laminate only with the area of damage increasing with impact speed. The damage from  $\frac{1}{8}$ in hail was slight and confined to sub-surface failure over an area not exceeding  $\frac{1}{4}\text{in}^2$  area. With 1in hail, chipping and cracking of the impact face occurred around the central impact zone and at 2000 ft/s the area of damage was about 3in diameter. Figure 8 shows a cross section of the outer laminate damage caused by 1in hail impacting at 1400 ft/s on a panel at  $90/95^\circ\text{C}$ ,  $\alpha = 45^\circ$ . Although the conical cracks extend to inner surface the cone was still attached to the laminate at the impact face. Tests at  $-15^\circ\text{C}$  gave results similar to those at  $20^\circ\text{C}$  but were limited to impact speeds up to 1000 ft/s.

Tests with 2in hail were made at  $20^\circ\text{C}$  and  $\alpha = 45^\circ$ . At 800 ft/s damage, about 5 in. in diameter, was caused by sub-surface failure of the outer laminate. At 900 ft/s severe cracking and delamination of both laminates occurred over an area of 6in diameter and the specimen was nearly penetrated.

## 5.3 Glass faced PMMA laminates

Identical laminates to those described above but with an abrasion shield of 2mm Glaverbell VHR II laminated on with 0.050in PVB were tested at  $20^\circ\text{C}$  with 1in and 2in hail. In the tests with 1in hail, no damage resulted at impact speeds up to 1100 ft/s,  $\alpha = 45^\circ$  and 1300 ft/s,  $\alpha = 60^\circ$ , but failure of the glass ply occurred at 1200 and 1500 ft/s respectively.

A single specimen of 3 laminates of  $\frac{3}{8}$  stretched PMMA faced with a ply of 2mm Chemcor 0311 was tested at  $45^\circ$  with 1in hail and gave identical results to those from the 2 ply laminate, no damage at 1100 ft/s and glass ply failure at 1200 ft/s.

No damage to the PMMA layers was observed and in a test at 2000 ft/s with 1in hail at  $45^\circ$  impact angle damage was still confined to the glass ply only. Similarly with 2in hail,  $\alpha = 45^\circ$ , only glass ply damage occurred for impact at 1120 and 1310 ft/s, whereas severe damage to both plies of the unfaced specimen occurred at 900 ft/s.

## 6 RESULTS: THERMALLY TOUGHENED GLASS

In all our tests at representative aircraft impact angles of wind-screens and panel specimens incorporating one layer of  $\frac{1}{2}$  in or greater thermally toughened glass we have been unable to cause failure of the main ply at impact speeds up to 1500 ft/s with 1in hail and over 1000 ft/s with 2in hail. Failure of the facing ply occurs, the onset speed varying with the strength and thickness of the ply. The degree of loss of vision also varies from minimal for annealed glass to complete for high strength glass, Figures 9 to 11. Tables 1 and 2 indicate that the thicker the facing ply or the stronger the glass the higher the speed at which failure occurs.

Fig.12 gives the results of tests at  $20^\circ\text{C}$  with 2in hail on Trident windscreens over the impact angle range  $0^\circ$  to  $60^\circ$  and approximate agreement with  $V \cos \alpha = K$  is shown for the speed at which abrasion shield failure occurs. The abrasion shield was  $\frac{1}{4}$ in thermally toughened glass.

## 7 RESULTS: POLYCARBONATE

Figure 13 shows the variation in penetration speed with impact angle for  $\frac{1}{4}$ in polycarbonate sheet. Although the results are somewhat academic in that the sheet was not treated or faced to give craze protection, they do show the excellent impact resistance of this material. They show fair agreement with  $V \cos \alpha = K$  but the effect of hail size is  $VD^{-\frac{1}{2}} = K$  which differs from the relationship for as-cast PMMA. The failure mode is also different. An impact erosion mark similar to that for as-cast PMMA is formed but the polycarbonate is indented like a metal and was considerably drawn. Failure initiated from the deep circumferential cracks of the impact erosion mark.

## 8 CONCLUSIONS

Although the tests were of limited extent they indicate that, as far as penetration or failure is concerned, windscreens of subsonic aircraft which are bird proof will also be hail proof. For supersonic aircraft this will probably also apply but it will depend on the relationship between bird and hail encounter speeds.

Windscreens with glass abrasion shields will present a problem in connection with vision loss following hail encounter since all forward facing transparencies could be struck in a hail encounter. Wrap around screens present a problem in this respect.

Finally, it is considered that failure depends on a combination of stress due to the impact loading and the interaction of shock waves from the initial impact. All the materials tested behaved differently and a much more extensive programme would be required to obtain a complete understanding of the problem of hail impact on transparency materials. Until this is done all screens with strengthened or toughened glass erosion shields should be evaluated by hail impact tests with the correct size of hail at the correct impact speed.



## Appendix 1

### RELATIVE RISK OF BIRD AND HAIL STRIKES ON WINDSCREENS

#### A.1 Risk of hail encounter

In his article "The Probability of Aircraft Encounters with Hail" (Met. Mag. Vol.101, No.1195, February 1972) J. Briggs derived an expression for the risk of hail encounter on the assumption that no avoiding action was taken, that the diameter of a hail cell or shower was 1 nautical mile and that the duration of a hail shower at a point was 0.1 hour. His expression was that the number,  $N_0$ , of encounters per flight hour with hail  $x$  inches or greater in diameter was

$$N_0 = 7.26 \times 10^{-6} NVP_x$$

where  $N$  = number of thunderstorms per year on the ground at the geographical area considered

$V$  = aircraft speed in knots at the altitude considered

$P_x$  = probability of occurrence of hail of diameter  $x$  inches or greater during the storm at the altitude and geographical area considered.

$P_x$  is assumed constant up to mid-tropopause and decreases by one order of magnitude every 10000 ft above that level, and  $P_x = P_0 \times 10^{-x}$ . His suggested values for  $N$ , mid-tropopause height,  $H$  and  $P_1$ , the probability of occurrence of 1in diameter or greater hail are

|           | $N$ . | $H$ .    | $P_1$                 |
|-----------|-------|----------|-----------------------|
| UK        | 15    | 20000 ft | 1.25 $\times 10^{-3}$ |
| Europe    | 25    | 20000 ft |                       |
| Denver    | 80    | 25000 ft |                       |
| Singapore | 100   | 30000 ft | 2.5 $\times 10^{-4}$  |

#### A.2 Subsonic aircraft hail encounter rate

Consider an aircraft cruising in Europe at 30000 ft at 500 knots.

$$\begin{aligned}V &= 500 \\N &= 25 \\P_1 &= 1.25 \times 10^{-4}\end{aligned}$$

risk per hour of encountering 1in hail  $1.1 \times 10^{-5}$

risk per hour of encountering 2in hail  $1.1 \times 10^{-6}$

### A.3 Subsonic aircraft bird strike rate

From the analysis of 1966-71 bird strike data on UK registered transport aircraft exceeding 12500 lb AUW, a total of 1682 strikes, the following was derived:-

|  |      |
|--|------|
| strike rate per 10000 movements  | 3.33 |
| % of strikes on windscreens  | 13   |
| % of strikes in climb, cruise and descent,<br>i.e. at speed approaching the bird strike<br>requirement | 20.6 |

If an average movement is assumed to have a 1 hour duration, risk per hour of windscreen bird strike is  $8.9 \times 10^{-6}$ . Some of these will be with birds lighter than the requirement.

### A.4 Comparison of hail and bird strike rate

Since, in a hail encounter all forward facing areas of the aircraft will be struck, the chance of windscreen hail strike by 1 in or larger hail is 11 in a million. The chance of windscreen bird strike at speeds approaching the required speed is 8.9 in a million. The chance of 2in hail strike is 1.1 in a million which is about the same as the chance of being struck by the required 4lb bird at the required speed. The requirements for windscreen hail impact resistance and bird strike resistance both represent a one in a million risk.

Table 1

2in HAIL TESTS AT 20°C,  $\alpha = 50^\circ$ , ON 18in  $\times$  18in PANELS OF  $\frac{1}{2}$ in THERMALLY TOUGHENED GLASS WITH VARIOUS FACING PLIES. ONSET OF DAMAGE BRACKET, ft/s, FOR FACING PLY

| Facing ply thickness<br>mm | Tensile strength<br>$lb/in^2$ | 12000   | 18000     | 25/30000 | 45000   |
|----------------------------|-------------------------------|---------|-----------|----------|---------|
| 1.3                        |                               | -       | -         | -        | 680-780 |
| 2.2                        |                               | -       | 660-740   | 564-665  | -       |
| 2.8/3.2                    |                               | 660-750 | 920-935   | 895-945  | -       |
| 4.8/5.2                    |                               | -       | 1001-1042 | -        | -       |
| 12.7<br>monolith           |                               | -       | 1190-1460 | -        | -       |

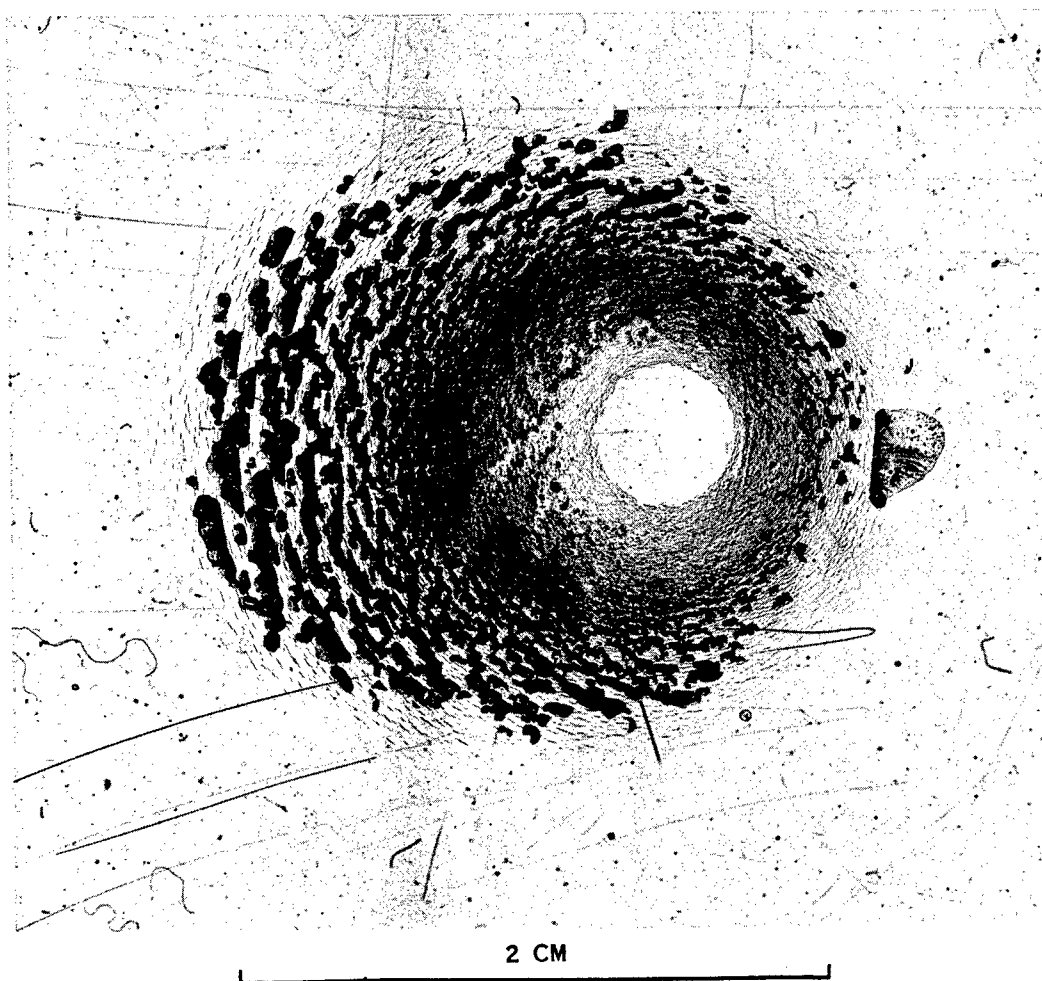
Table 2

1in HAIL TESTS AT 20°C,  $\alpha = 50^\circ$  AND  $60^\circ$ , ON 18in x18in PANELS OF  $\frac{1}{2}$ in THERMALLY TOUGHENED GLASS

WITH VARIOUS FACING PLIES. ONSET OF DAMAGE BRACKET, ft/s, FOR FACING PLY

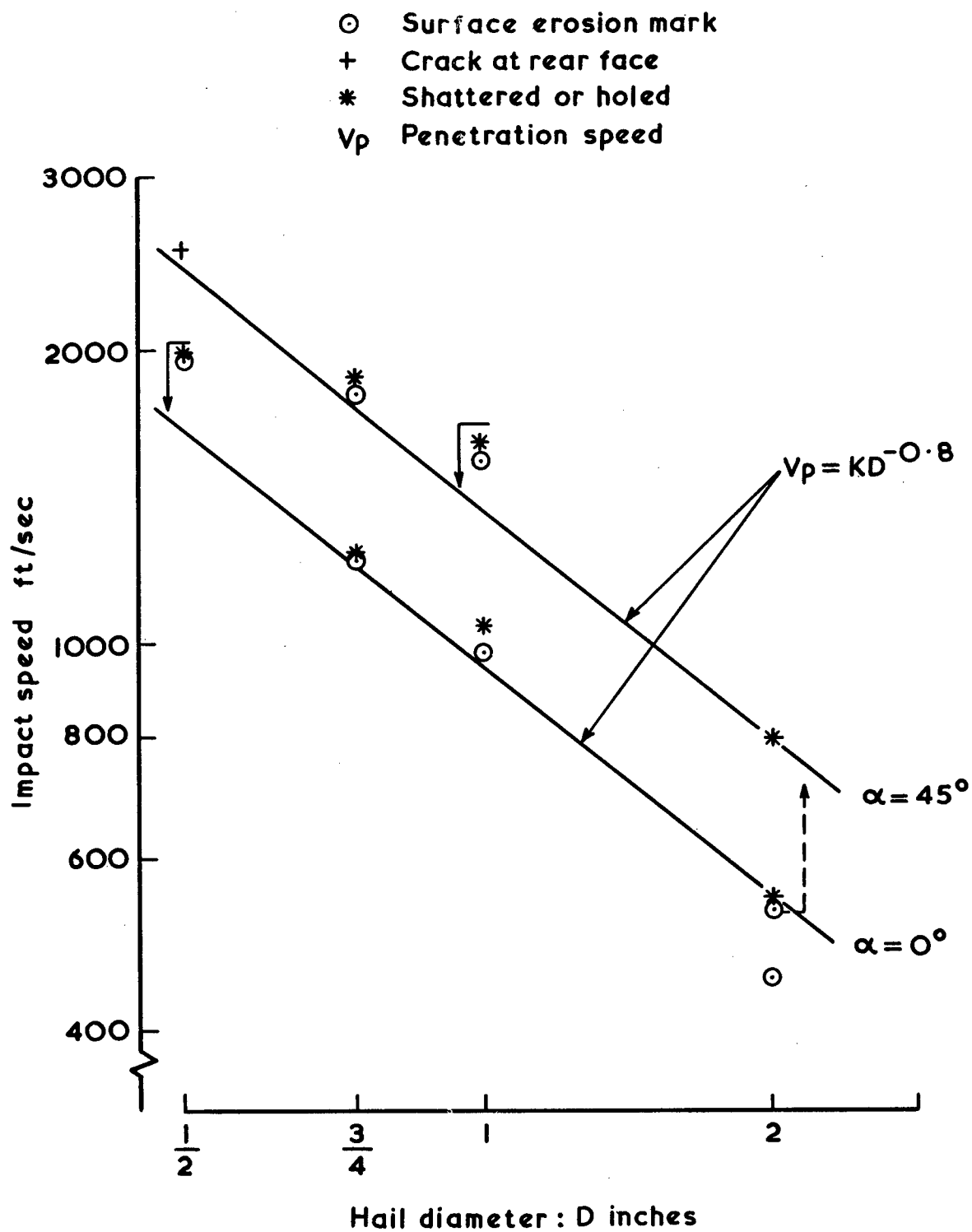
| Facing ply thickness<br>mm | Tensile strength<br>lb/in <sup>2</sup> | 12000              |                        | 18000                  |           | 25/30000           |           | 45000              |     |
|----------------------------|--|--------------------|------------------------|------------------------|-----------|--------------------|-----------|--------------------|-----|
|                            |  | 50°                | 60°                    | 50°                    | 60°       | 50°                | 60°       | 50°                | 60° |
| 1.3                        |  | -                  | -                      | -                      | -         | -                  | -         | 859-900<br>865-895 | -   |
| 2.2                        |  | -                  | -                      | 930-1015<br>- 905      | -         | 1292-1365<br>-1250 | 1440-1580 | -                  | -   |
| 2.8/3.2                    |  | 1120-1215<br>-1095 | 1300-1422<br>1092-1345 | 1230-1310<br>1280-1290 | -         | 1165-1200<br>-1115 | 1455-1522 | -                  | -   |
| 4.8/5.2                    |  | -                  | -                      | 1170-1210<br>1160-1172 | 1630-1715 | -                  | -         | -                  | -   |

**Fig.1**



**Fig.1** Surface damage to 1/2in PMMA plate by 1in hail impacting at 1180 ft/s,  $\alpha = 30^\circ$

Fig.2



Effect of hail size on penetration speed  
As-cast PMMA

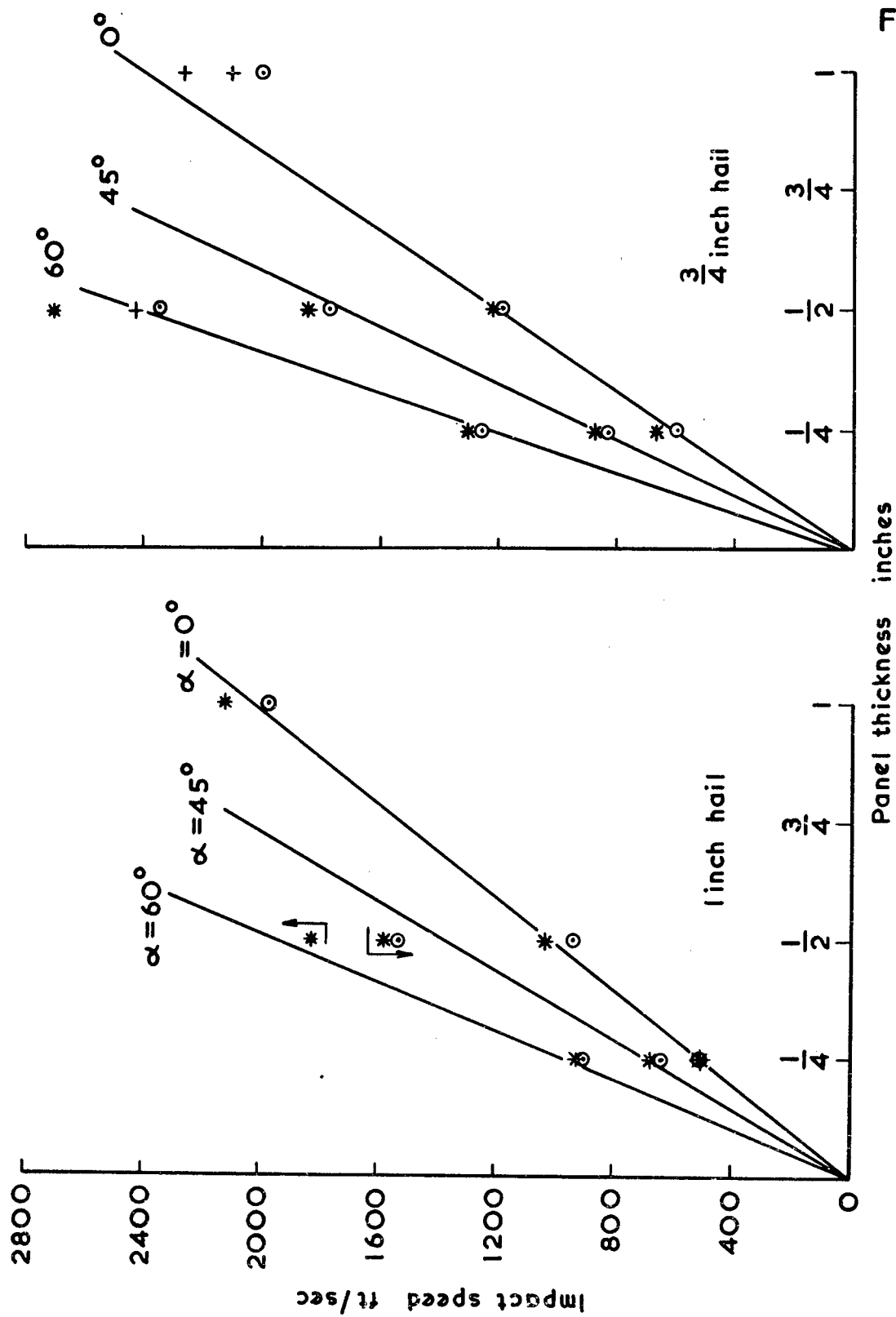
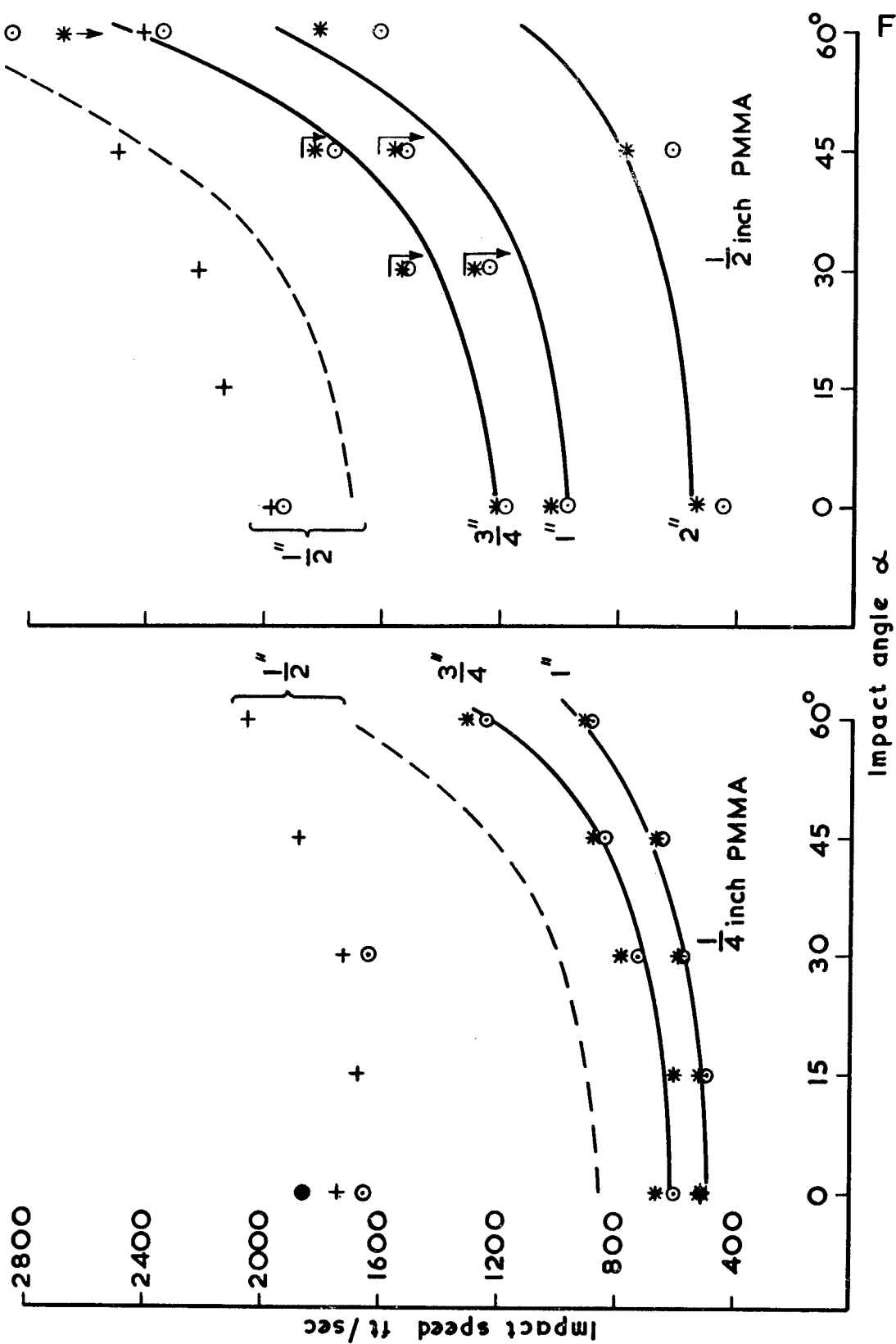


Fig.3

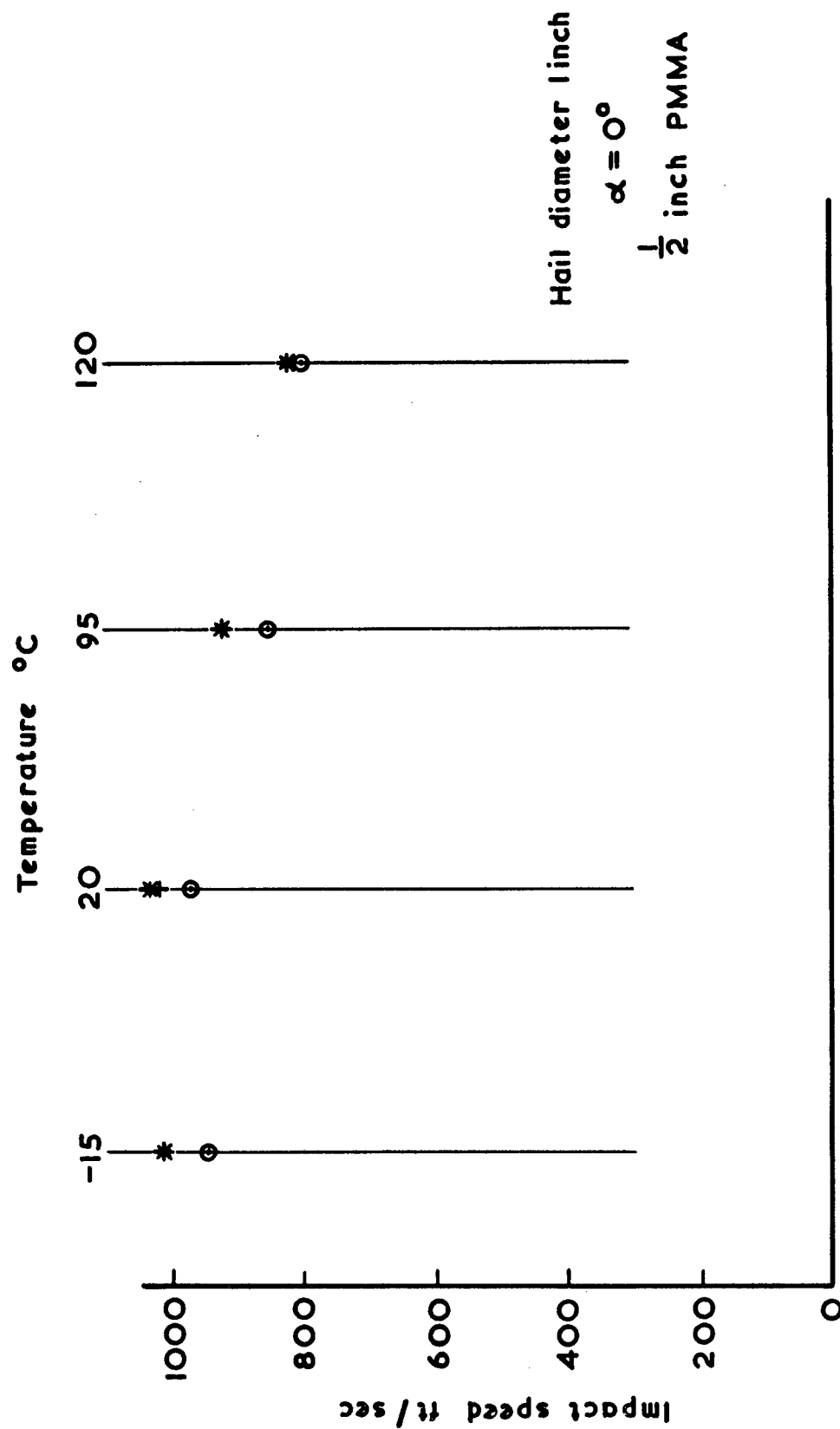
Effect of thickness on penetration speed. As-cast PMMA



Effect of impact angle on penetration speed. As-cast PMMA

Fig.4

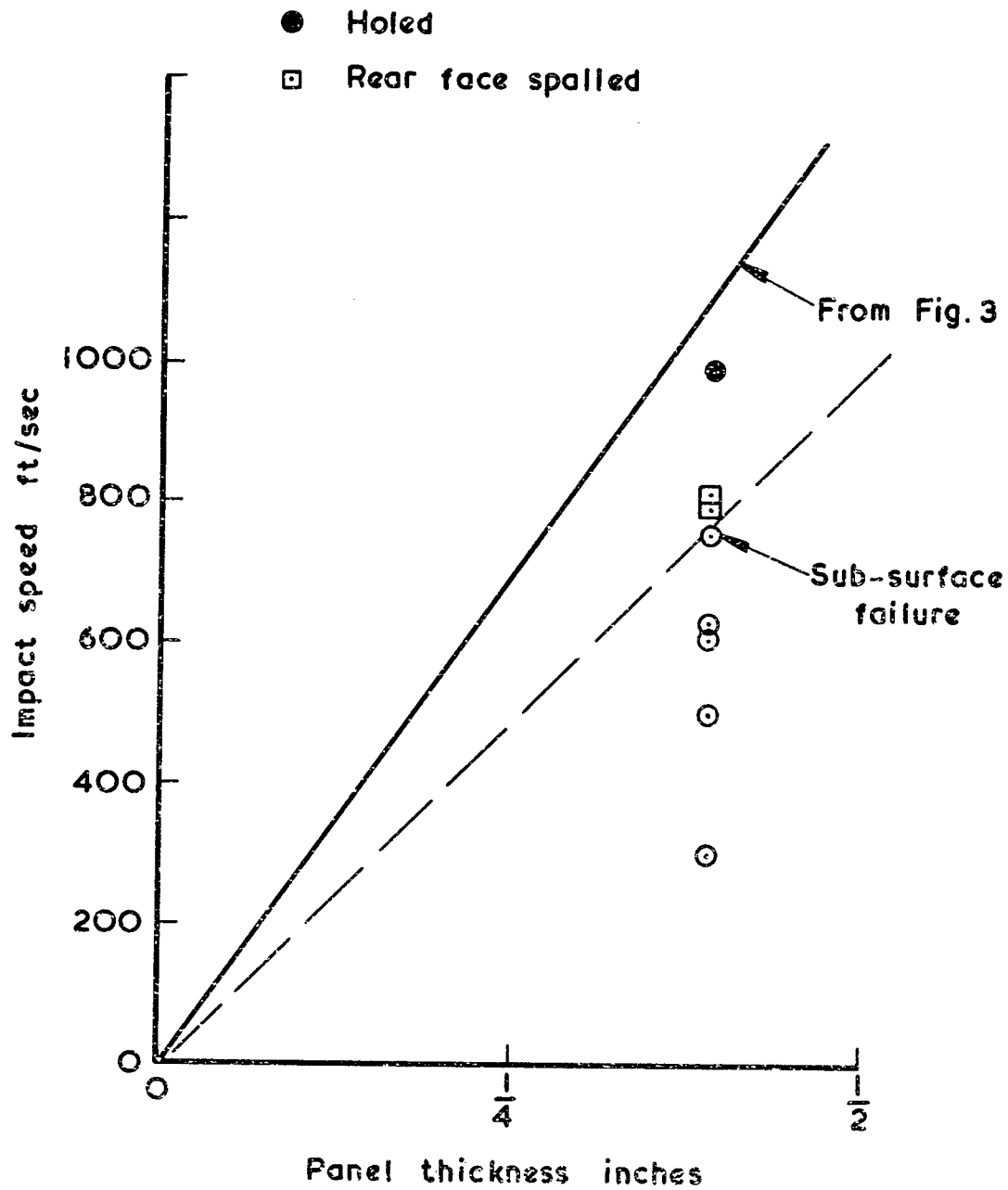




Effect of temperature on penetration speed.  
 As-cast PMMA

Fig.5

Fig.6



Hail diameter 1 inch . Temperature 20°C .  $\alpha = 45^\circ$

Test results - stretched PMMA

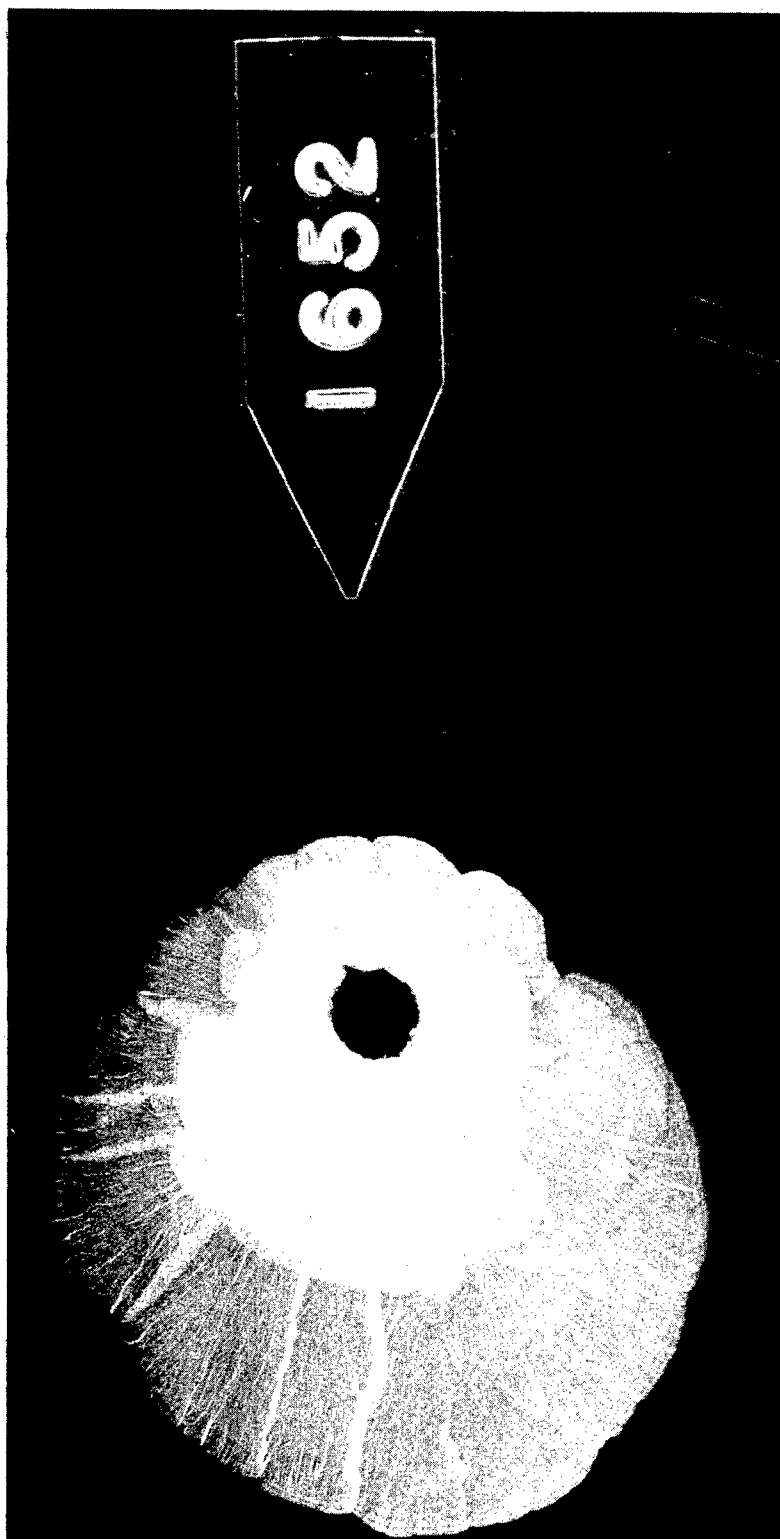


Fig.7 Sub-surface damage to stretched PMMA  
1in hail,  $\alpha = 45^\circ$ , 970 ft/s

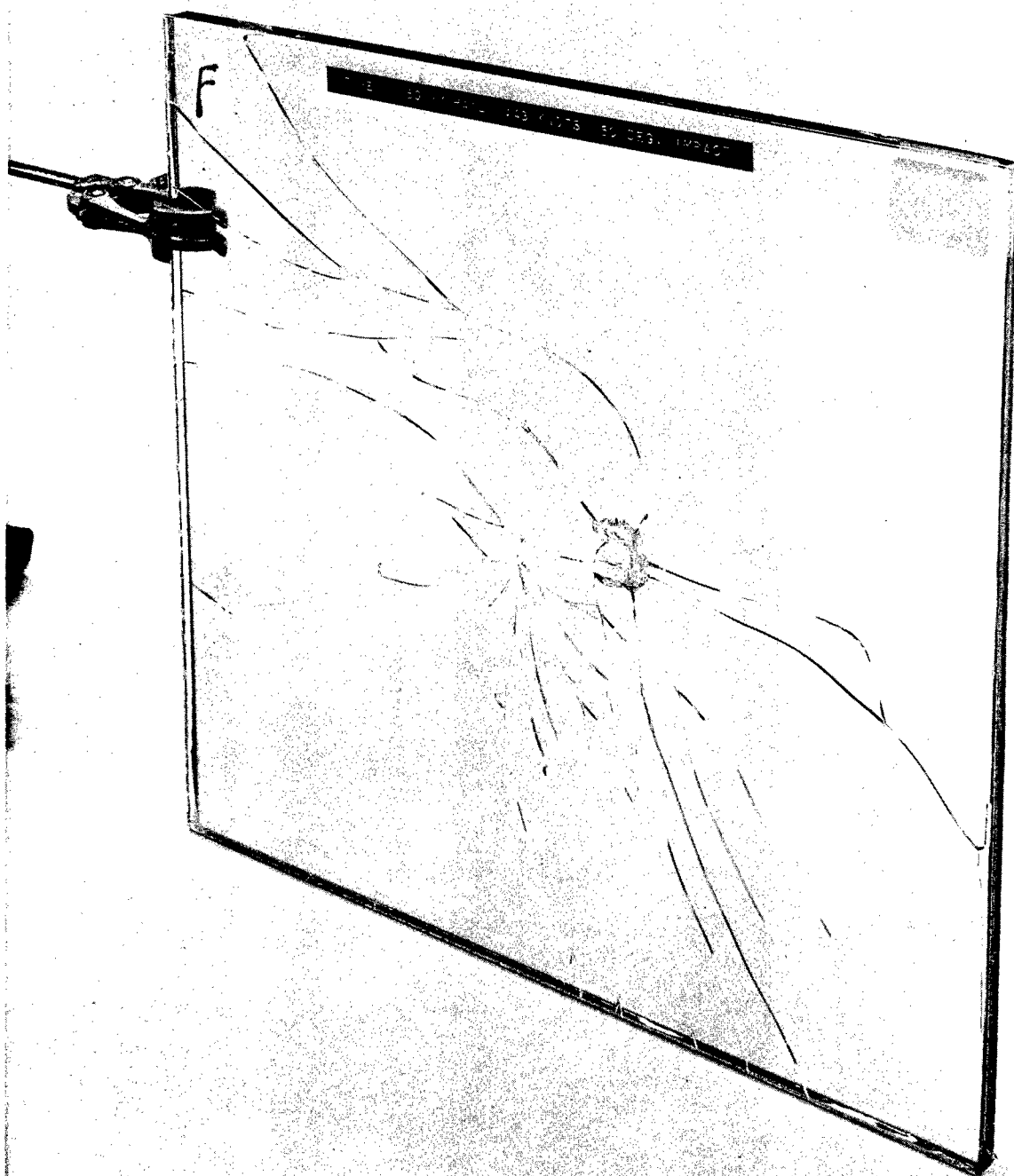
Fig.7



Fig.8 Sub-surface damage to stretched PMMA  
1in hail,  $\alpha = 45^\circ$ , 1400 ft/s

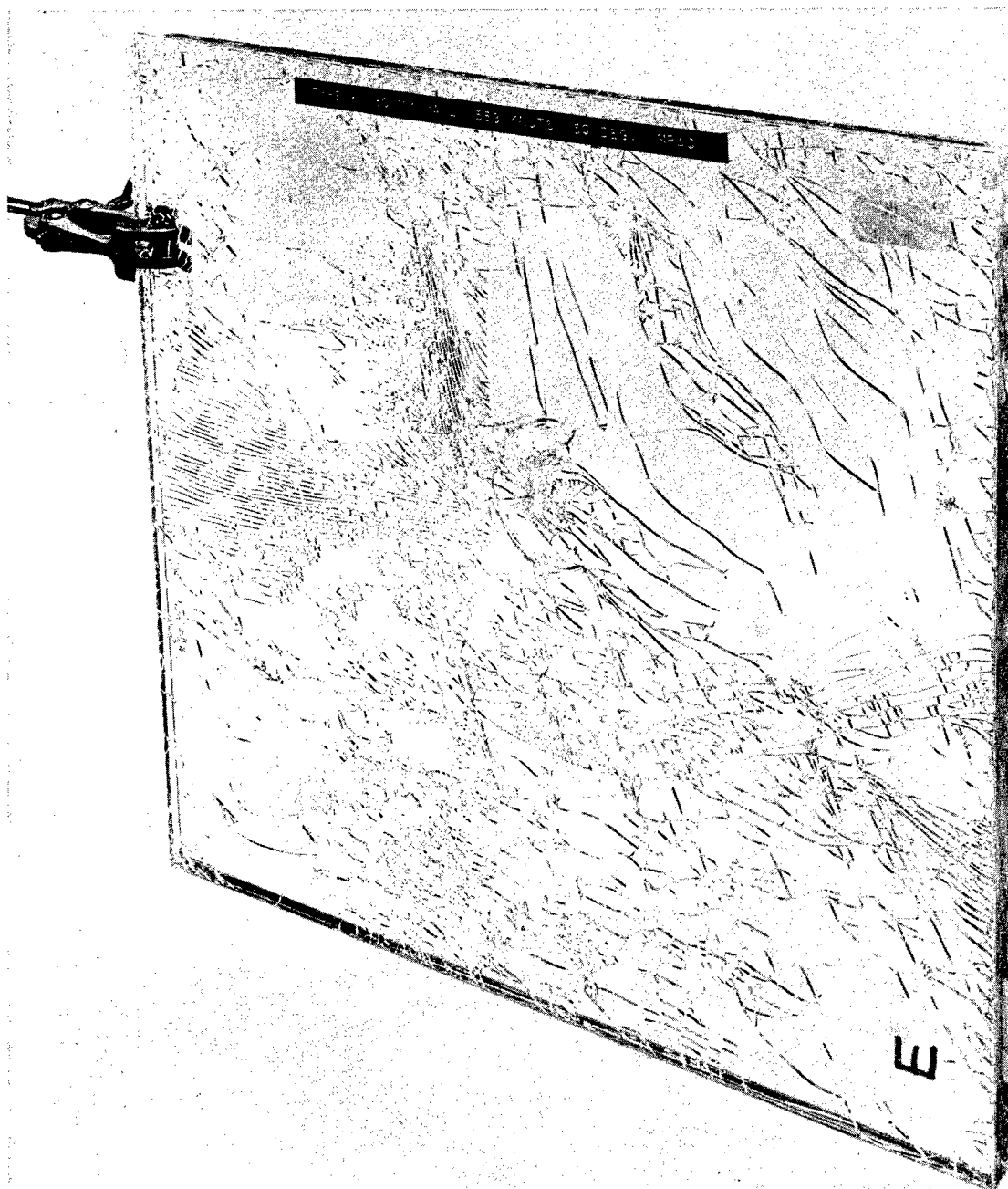
Fig.8

**Fig.9**



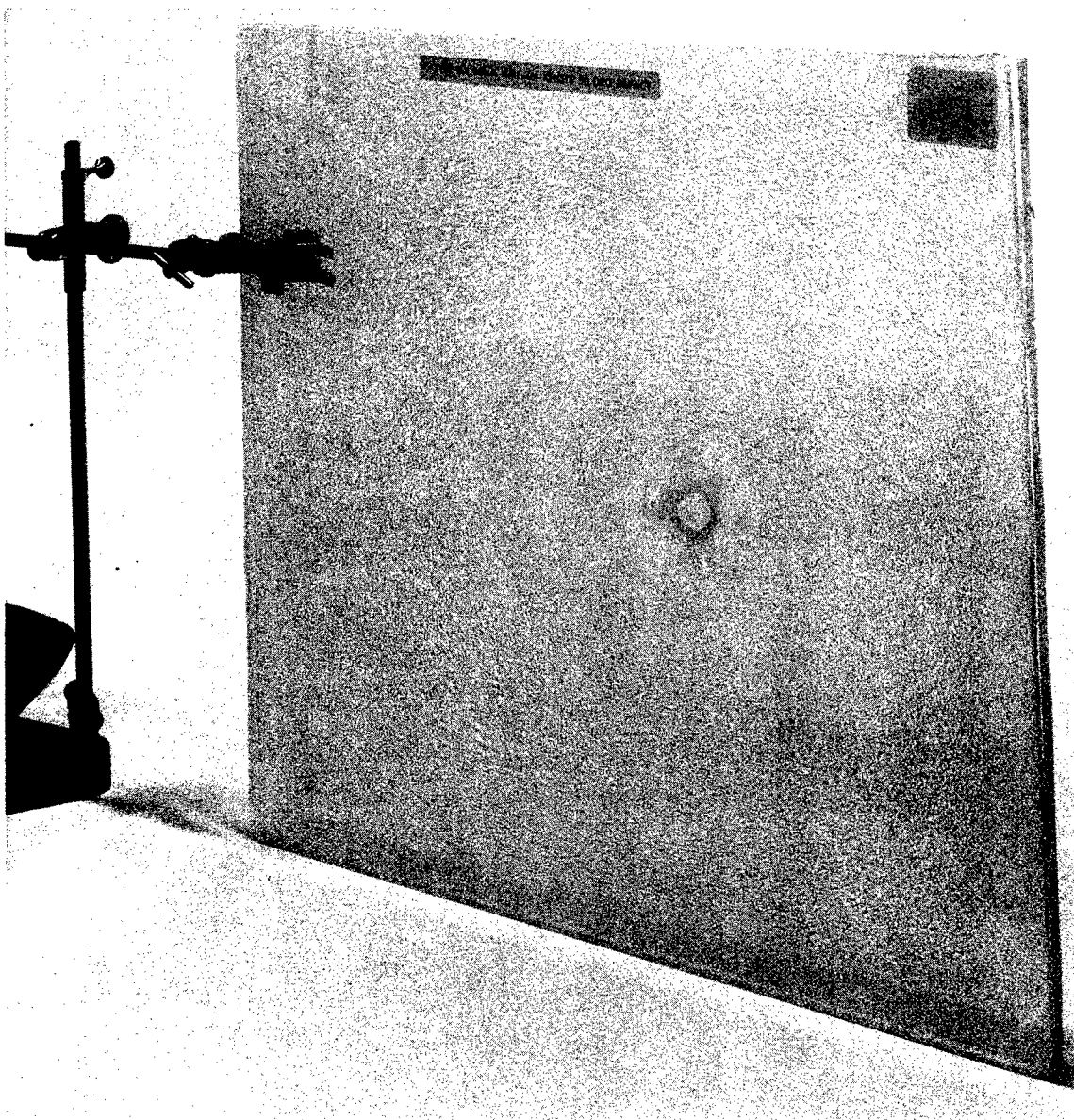
**Fig.9**    Damage to annealed glass abrasion screen

**Fig.10**



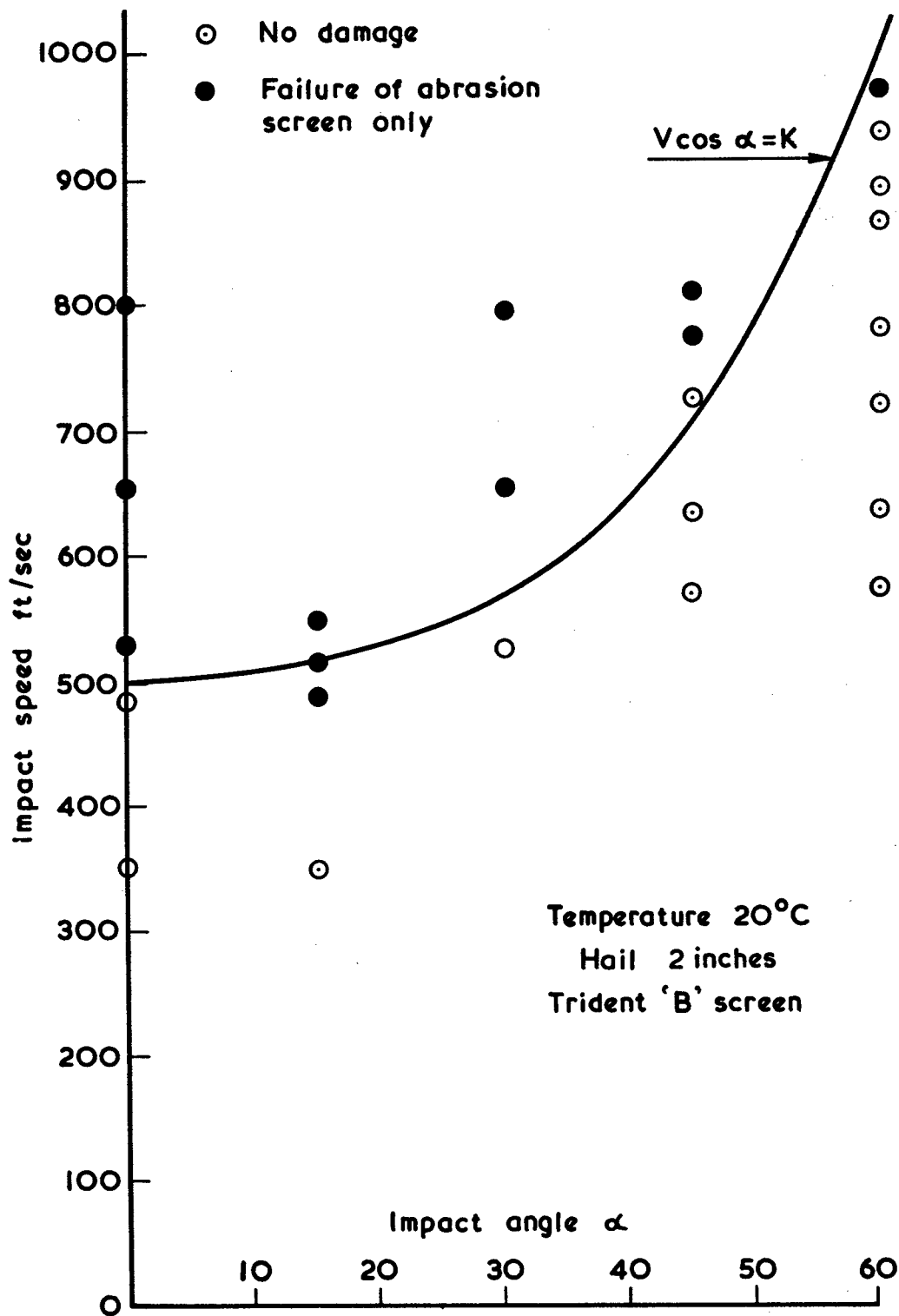
**Fig.10**    Damage to toughened glass abrasion screen

**Fig.11**



**Fig.11**    Damage to chemically toughened glass abrasion screen

Fig.12



Effect of impact angle on abrasion screen failure



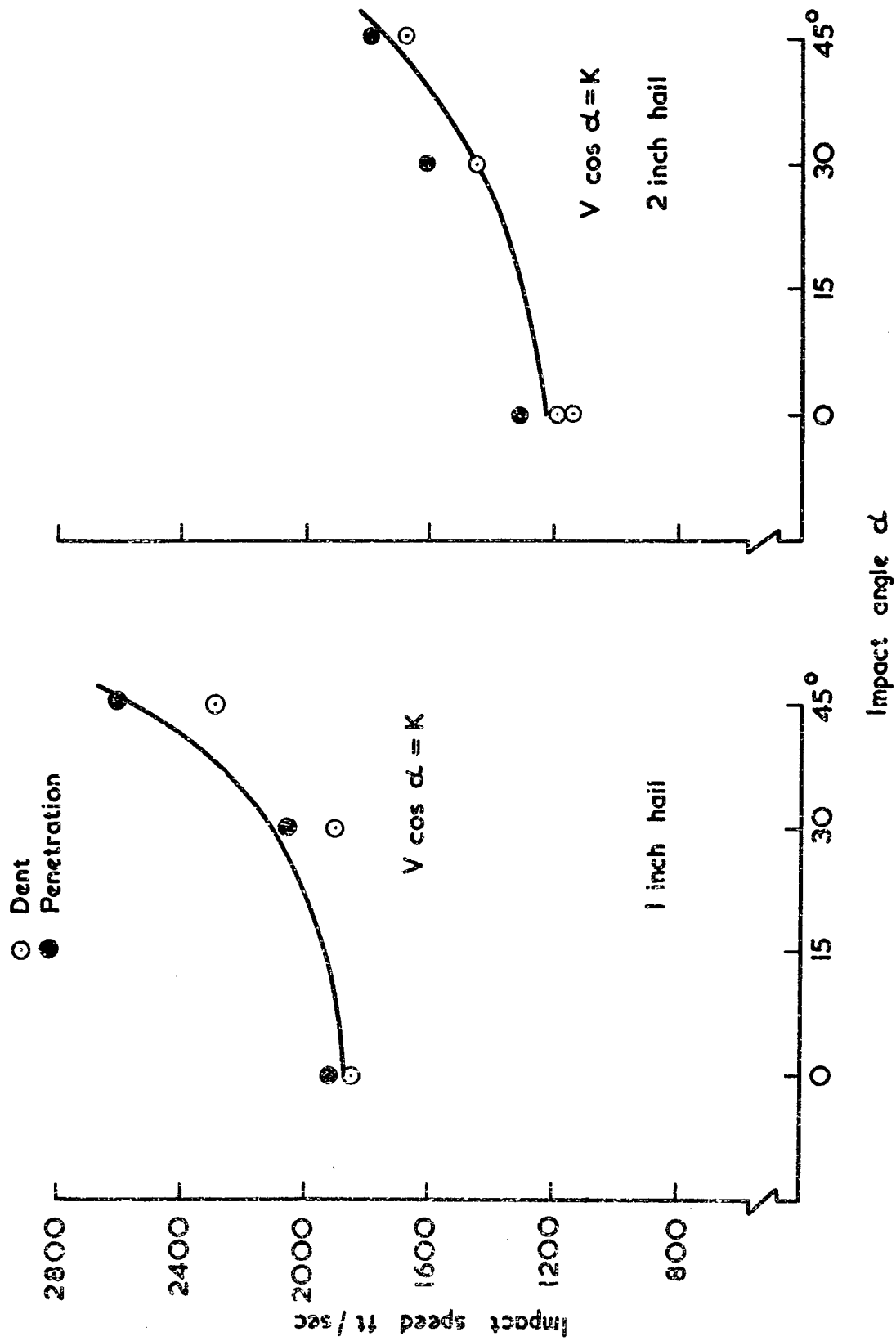


Fig.13

Effect of impact angle on penetration speed.  $\frac{1}{4}$  inch polycarbonate

ADEQUACY OF WINDSHIELD BIRD STRIKE  
STRUCTURE DESIGN CRITERIA

J. H. Lawrence  
Douglas Aircraft Company  
McDonnell Douglas Corporation  
Long Beach, California

**STATUS REPORT**

**ADEQUACY OF WINDSHIELD BIRD STRIKE STRUCTURE DESIGN CRITERIA**

**Contract No. F33615-73-C-3030**

**Air Force Flight Dynamics Laboratory**

**Air Force Systems Command**

**Wright-Patterson AFB, Ohio**

**Presented to:**

**Conference on Transparent Aircraft Enclosures**

**Las Vegas, Nevada**

**7 February 1973**

**Presented by:**

**J. H. Lawrence**

**Technical Manager**

**Douglas Aircraft Company**

**McDonnell Douglas Corporation**

**Long Beach, California**

The Douglas Aircraft Company was selected to perform a study contract for the Air Force Flight Dynamics Laboratory.

The purpose of the study is to evaluate existing windshield/structure bird impact design criteria and, if possible, to validate the criteria through extensive statistical studies of worldwide bird strike incident reports.

To develop meaningful criteria, three items are under scrutiny:

1. Finding a realistic bird weight
2. Flight altitude conditions
3. Aircraft speeds

To date we have received incident reports or compiled data that represents approximately 10,000 bird strikes.

Surprisingly, many bird strike incident studies were accomplished during the 1940's, and subsequently the F.A.A. issued design requirements for birdproofing the crew compartment windows for commercial aircraft.

During the 1950's commercial aircraft bird impact development testing programs were accomplished, but bird strike incident reports apparently were not compiled or reported.

After two catastrophes occurred in the early 1960's; one in which 62 persons were killed, and one incident in which 17 persons were killed; renewed interest was created in compiling and studying bird impact incidents.

As yet Douglas has not attempted to validate the existing criteria through statistical studies, but we have reviewed the data received and have done some arithmetic averaging.

#### 1. Bird Weights

We have found repeatedly that approximately 95% of the birds involved in mid-air collision that have been identified, weighed four pounds or less. The International Civil Aviation Organization located in Canada did an in-depth study of 3028 bird strike incidents on civil aircraft that occurred during the years 1967, 1968, and 1969. The I.C.A.O. study indicates that approximately 94.5% of the birds weighed less than 4 pounds, 4% of the birds weighed from 4 to 8 pounds, and 1.5%, or 45 incidents, indicated that the birds weighed 8 pounds or more, but none caused a catastrophe even though four hit the empennage.

The Royal Netherlands Air Force reported that in a given period 93% of their bird strikes weighed less than two pounds.

A study of the United States Air Force data indicates that the strikes frequently are with hawks, great horned owls, buzzards and vultures that may weigh more than 4 pounds. A review of 208 Air Force incidents that occurred during 1972 indicated that in 56 incidents the birds could be identified and 10 of the birds weighed between 4 and 10 pounds. Of the total incidents this represents 4.8%.

Since at least 4% of the bird strikes involve birds that weigh between 4 and 8 pounds, there may be a need to specify a bird weight of 8 pounds for aircraft that have extensive low level mission requirements. Particularly since an average of 21% of Air Force strikes occur during low level missions.

However, as a point of interest, doubling the weight of the bird only increases the impact force by a factor of 1.5.

## 2. Altitudes

Altitudes must be a key factor when considerations are made for the establishment of design criteria. At this time, this factor may be the most difficult to clearly define. The reason this may be difficult has to do with the mission profile of the aircraft and the final definition of speed requirements. To illustrate this difficulty, consideration must be given to bird migratory flight patterns. Most ornithologists indicate that birds migrate at altitudes at least 3000 feet above the terrain regardless of whether this terrain is sea level or over a mountain.

Based on the data from I.C.A.O., 75% of all confirmed bird strikes occur below 1000 feet AGL on the takeoff or landing approaches, 20% occur between 1000 and 5000 feet AGL, and 5% occur above 5000 feet AGL.

These altitudes then form a key part in the establishment of speed requirements.

## 3. Speeds

It is believed that the speed is the most critical item to define. Currently, there seems to be some lack of communication between designers; those who develop model criteria, aerodynamicists, and pilots in regard to the definition of speeds.

Each group of individuals uses different terminologies to define speeds, and each one relates a different speed. Such terminologies include  $V_C$ ,  $V_M$ , true air speeds, closing speeds, indicated air speeds, calibrated air speeds, stall speeds, mach numbers, and others.

Since there is considerable variance in the numbers represented by the speeds, it is readily apparent that for each aircraft design a complete mission profile study should be developed. The study should include an expected frequency of low level missions (including training), gunnery missions, the expected terrain heights, and the maximum obtainable true air speeds identified.

It may be necessary to consider the speed of the birds, since migratory birds travel as fast as 60 miles per hour.

Based on current knowledge, it appears that during the design and development phases of an aircraft design that a maximum obtainable true air speed should be established to some selected confidence level such as 95%. This selected speed should then be the design speed potentially additive to the bird speed for bird impact of the windshields and/or canopies.

The importance of selecting the correct speeds is evident when considering that as the speed doubles the force increases by a factor of 4. Therefore, only a minor variance in speed more than offsets the criteria of doubling the bird weight.

#### Adequacy of Existing Design Criteria

Next we may look at the adequacy of current design criteria. It is believed that commercial aircraft designed and tested to the F.A.A. requirement of a 4 pound bird at  $V_C$  = sea level, usually 350 knots is conservative if the users comply with the F.A.A. operational requirements, that speeds below 10,000 feet are restricted to 250 knots I.A.S.

In reality, however, a 4 pound bird at  $V_C$  or true air speed of 350 knots, imparts an impact force of approximately 50,000 pounds and at a true air speed at 250 knots would impart an impact force of less than 28,000 pounds; but a misnomer exists in this thinking since a 250 knot indicated air speed at 10,000 feet approaches 300 knots true air speed, thus, extensively reducing the greater margin of safety.

Probably the best existing criteria is the British Civil Aviation Authority that specifies a 4 pound bird at true air speeds at 8000 feet under expected operational temperature extremes.

To illustrate these two sets of criteria, the DC-10 was certified to both conditions hot, cold, and with cracked glass plies; to the F.A.A. where  $V_C$  = 350 knots and the British where true air speed = 387 knots at 8000 feet.

Since there are at least four U.S. military documents that relate to windshield bird strike criteria, at this time I am not confident that the criteria will meet all of the operational mission requirements for U.S. Air Force aircraft.

DESIGN DATA FOR BIRD IMPACT RESISTANT  
WINDSHIELDS - A STATUS REPORT

G. E. Wintermute  
Goodyear Aerospace Corporation  
Litchfield Park, Arizona

DESIGN DATA FOR BIRD IMPACT  
RESISTANT WINDSHIELDS - A STATUS REPORT

Since the advent of aviation, impacts between birds and aircraft in flight have occurred. As aircraft became more sophisticated and as flight performance increased, these bird impacts had more serious consequences. Traditionally, the design of "bird-proof" windshields has been performed on an individual problem basis.

Most of the testing has been conducted for specific program applications. As a result, such a wide range of variables has been experienced -- *i.e.*, speed, weight of bird package, impact angle, thickness and material, temperature, type of construction, edge attachment design, and supporting structural frame -- that direct correlation and extrapolation with new windshield design concepts are not accurate or feasible.

In recent years the need for developing a systemized approach to the design of bird-proof windshields has been recognized.

Presently the Goodyear Aerospace Corporation has a contract with the Air Force Systems Command, WPAFB, Ohio, to develop "Design Criteria on the Response of Transparent Aircraft Windshield Materials to Bird Impact". The contract number is F33615-72-C-1896, and the Air Force Project Engineer at WPAFB is R E Wittman.

Basically, the program is a systematic test and analytical evaluation of the resistance of various aircraft windshield glazing materials to bird impact at varying velocities, impact angles, and temperatures. These data will then be reduced and organized in design handbook form to aid in the design of future aircraft windshields. This type of information is not available to the aircraft designers at the present time. The test data are being developed for transparent panels typical of windshield panel size. However, the test facility is capable of accepting specimens as large as complete windshield/fuselage sub assemblies. The bird carcass accelerator or gun is capable of launching a 4 lb. bird at velocities of 70 knots to velocities in excess of 600 knots. (The contract requirement is 600 knots, but the air gun has approximately 15% excess capacity.) An environmental control system has been provided that will provide testing capabilities from -40°F to +200°F. The velocity is measured by electronic counters triggered by severing fine wires, and high speed camera coverage (up to 11,000 frames per second) is also available.

The actual program is quite extensive, covering an 18 months time span and involving approximately 250 individual panel tests. The testing has started using flat monolithic acrylic panels and flat monolithic polycarbonate panels, and will progress up the complexity scale using curved monolithic panels, curved CIP laminated polycarbonate and acrylic, flat Glass/Polycarbonate ethylene terpolymer laminate for a total of approximately 15 basic panel configurations. It should be noted that these panel configurations will also be tested in different thickness,



**Design Data for Bird Impact  
Resistant Windshields - A Status Report**

varying velocities, bird weights, varying temperatures ( $-40^{\circ}\text{F}$  to  $200^{\circ}\text{F}$ ) and varying impact angles. Official contract start date was June 15, 1972.

## THE AEDC BIRD IMPACT TEST FACILITY

E. J. Sanders  
Arnold Engineering Development Center  
Arnold Air Force Station, Tennessee

# THE AEDC BIRD IMPACT TEST FACILITY

E. J. Sanders

von Karman Gas Dynamics Facility  
ARO, Inc.  
Arnold Engineering Development Center  
Arnold Air Force Station, Tennessee

To be presented at the  
Transparent Aircraft Enclosures Conference  
Las Vegas, Nevada  
February 5-8, 1973

The research reported herein was sponsored by the Arnold Engineering Development Center (AEDC), Air Force Systems Command (AFSC) under Contract F40600-73-C-0004 with ARO, Inc. Reproduction to satisfy the needs of the U. S. Government is authorized.

## ABSTRACT

This paper describes the AEDC Bird Impact Test Unit (Range S-3) -- a new Air Force facility built primarily for evaluating the results of bird impacts on aircraft structural components. The results of shots made during the shakedown and calibration phase of testing are described, along with some of the problems encountered and the efforts made to solve them. Some of the operational and data gathering techniques that are probably unique to the AEDC facility are presented.

A description of the launcher, test area, and primary instrumentation systems is presented. Instrumentation systems described include those for (1) measuring velocity, (2) measuring target deflection during impact using high-speed motion picture cameras, and (3) measuring strain of plastic and metal aircraft components during impact.

Hygienic aspects of tests involving birds are discussed, including purchase, storage, and preparation of the birds for testing, and procedures used to clean and disinfect the test area after testing to make it ready for personnel entry.

## 1.0 INTRODUCTION

An increasing emphasis is being placed on protecting aircraft and their pilots from hazards over which they have little control, in particular, such environmental hazards as impacts with birds. One method used to provide this protection is the development of aircraft components to withstand bird impacts. The new AEDC Bird Impact Test Unit (Range S-3) was built to provide this development capability.

The test unit is located at the north end of the VKF S Building (Fig. 1). The facility consists of a launcher, which accelerates the bird to the desired launch velocity, and a test area, where the target and its associated instrumentation are housed.

Operation of the facility commenced with the firing of 35 calibration and shakedown shots to determine the operating characteristics of the launcher, evaluate the performance of the projectile sabot design and its stripper mechanism, verify the operational reliability of test instrumentation, and develop hygenic procedures for the use of organic projectile materials.

One of the goals of the calibration and shakedown phase of testing was to develop a capability of launching a 4-lb bird (chicken) in the velocity range of 400 to 1360 ft/sec. To date, the maximum velocity attained has been approximately 1100 ft/sec, which was sufficient to

meet the requirement of the first user test in the facility. It is thought that the goal of 1360 ft/sec can be reached with a modest development effort.

After the completion of the calibration and shakedown phase of testing, a short (7-shot) user test program involving actual aircraft components was successfully conducted in late 1972.

## 2.0 DESCRIPTION OF LAUNCHER AND TEST AREA

The launcher, the breech end of which is located inside the VKF S Building (Fig. 2), consists of a driver 31 ft long having an 8-in. -diam bore with a volume of 10.8 ft<sup>3</sup>, and a two-piece launch tube 60 ft long having a 7-in. -diam bore with a volume of 16 ft<sup>3</sup>. The bird and its sabot are loaded between the driver and the launch tube immediately forward of a double diaphragm section (Fig. 3). The bird is launched by charging the driver with air to the desired pressure, simultaneously charging the volume between the two diaphragms to some intermediate pressure, then venting the volume between the diaphragms, whereupon the diaphragms are over-pressured and rupture, propelling the sabot containing the bird down the launch tube. The diaphragms are made of Mylar<sup>®</sup> and vary in thickness from 0.005 to 0.014 in., depending upon the desired burst pressure.

The test area consists of a 22- by 32-ft covered concrete pad (Fig. 4) upon which are mounted steel H-beams used for mounting

target specimens. Two 0.5-in. -thick steel plates spaced approximately 3 in. apart serve as the backstop; single 0.25-in. -thick steel side plates can be rolled into place for personnel protection and to contain debris. Steel boilerplate of various thicknesses mounted at 45 deg to the flight path served as the target for the calibration shots (Fig. 5). The target was located 25 ft from the stripper muzzle. The accuracy of the launcher in striking the designated target point with the projectile was  $\pm 1$  in. for both the calibration shots and the test shots.

### 3.0 PROJECTILES AND SABOTS

Simulated birds were used as projectiles during the initial shots of the calibration phase. Polyethylene slugs and Duxseal<sup>®</sup>, a putty-like sealing compound, were used rather than real birds. As soon as some confidence was established in the use of the sabot and sabot stripper, chickens were used as projectiles for the remainder of the calibration phase.

Four-pound chickens were used because they had been stipulated for use as projectiles during the initial test entry. The chickens were purchased live from a local poultry producer, then asphyxiated, quick-frozen, and stored in a freezer. Twenty-four hours before they were to be launched, they were removed from the freezer and allowed to thaw. The chickens were packaged in a nylon bag (Fig. 6) before placing in the sabot in order to maintain them in a reasonably uniform shape during flight to the target.

Balsa wood was chosen as the sabot material because of its light weight, low cost, relatively high strength, ease of manufacture, and simplicity of removal from the stripper after a shot. The density of the balsa wood varied, the denser material being used for the higher speed shots because of its greater strength.

The sabot was prevented from traveling on and striking the target by a tapered stripper tube attached to the muzzle of the launch tube. The stripper tube (Fig. 7) consists of a 2-ft-long vent section to allow escape of the driving gas, then 10 ft of pipe with a taper machined in the bore from the 7-in. launch tube bore diameter down to approximately 5-1/4 in. diameter at the muzzle. The sabot was removed after the shot by driving it back into the vent section, then splitting it into pieces small enough to be removed between the vent section guide rails.

#### 4.0 TEST INSTRUMENTATION

Test instrumentation included the projectile velocity measuring systems, strain gage measurements of target strain during impact, measurement of transient target deflection during impact, and general motion picture coverage of the impact event.

The primary system for measuring projectile velocity consisted of two X-ray stations located a known distance apart along the flight path between the launcher muzzle and the target. X-ray pulsers and



various types of cameras were available for use, but the X-ray system was chosen rather than conventional camera systems because it is not sensitive to changing light conditions and it permits examination of the structural integrity of the bird after launch.

The X-ray pulsers were triggered by one of two available systems: the interruption of the path of light in a light/photodetector system, and the breaking of a 24-gauge copper wire in an electrical break-wire system. The time between firings of the pulsers was recorded with a digital chronograph, and, using this time together with the distance measured between images of the projectile on the X-ray film (after corrections for point source emission), velocity could be determined. A typical X-ray photograph is shown in Fig. 8. The uncertainty of the system was determined to be less than  $\pm 0.5$  percent. The velocity measuring system was mounted on an instrumentation dolly with the first station located approximately 3-1/2 ft from the muzzle of the stripper tube (Fig. 9).

A c-w homodyne (zero I-F) radar system operating at a frequency of approximately 8.6 GHz was also used as a "back-up" velocity measurement system in the event the X-ray system did not perform properly. The radar antenna was mounted in the center of the instrumentation dolly at an aspect angle of 45 deg. The projectile was in the radar beam during approximately 1 ft of its travel, and the resulting

radar signal was recorded on magnetic tape. The velocity was then derived by measuring the doppler frequency and converting to velocity by using the standard doppler equation.

Velocity was also determined from four electrical shorting probes located in the launch tube near the muzzle. The shorting probes protruded into the bore of the launch tube at known distance intervals. Physical contact with the bird/sabot package forced the shorting probe into momentary contact with the launch tube wall, thus completing an electrical circuit. The voltage change resulting from the circuit completion was electronically conditioned and used to start and/or stop digital chronographs. From the resulting time data and the known interval between probe stations, average velocity of the launch package in the launch tube could be computed.

Target strain during impact was also recorded by mounting BLH\* SR-4<sup>®</sup> strain gages at strategic locations on the test article. Ten channels were recorded by the magnetic tape system during each test shot.

Target deflection during impact was recorded photographically by comparing movement of the test article with fiducial lines located inside the camera lens. The cameras were mounted independently of the test article; thus, there was no movement of the fiducial lines

---

\*Baldwin-Lima-Hamilton Corporation, Waltham, Massachusetts.

during the impact event. Before the test shot was made, the cameras were located in their proper position, and a calibration film was run with scales placed on the test article in the plane for which deflection measurements were to be made. The scales were then removed and photographs made of the actual shot. Measurements were then made by first placing the calibration film on the film reader and determining a scale factor for points in the plane of the scale. The actual shot film was then placed on the film reader and measurements of movement made using the fiducial lines as references. The use of fiducial lines eliminated the need for placing grid boards on the test article which would have obscured the view of the impact event from other cameras.

## 5.0 DISCUSSION

### 5.1 CALIBRATION RESULTS

An available computer program for the expansion of gas from a reservoir was modified to simulate the launcher cycle. This program was used to select the driver pressures for the initial shots in the calibration series. The computer program was accurate in predicting launch velocities over the range 400-800 ft/sec, with some divergence at higher velocities. A plot of driver charge pressure vs. launch velocity is presented in Fig. 10. Total launch weight varied from 5 to 6.5 lbs, with the higher weights corresponding to points at higher velocities. There is a theoretical velocity loss of approximately

3.5 ft/sec for each additional 0.1 lb of in-gun weight in the 900-1000 ft/sec range. For driver charge pressures greater than 120 psia (velocities above 800 ft/sec), the launch tube was evacuated to a vacuum level of 100 mm Hg to gain an additional increase in velocity.

The launch velocity was repeatable to within  $\pm 4$  percent. The two main factors in determining repeatability were thought to be the fit of the sabot in the launch tube and friction between the bird and the sabot during their separation in the sabot stripper. Also, as can be seen from Fig. 10, launch velocity is very sensitive to driver charge pressure. The valving and readout system used to charge the driver with air was somewhat variable, making it difficult to hold precise values, therefore contributing to the problem of repeatability.

## 5.2 SABOT PERFORMANCE

The balsa wood sabots were successful in launching the projectile at velocities up to approximately 1000 ft/sec. At higher velocities, the balsa wood failed or was driven intact through the stripper by the propelling gas. Aluminum and fiberglass-reinforced epoxy liners were used to strengthen the sabots for shots at velocities above 1000 ft/sec, and although only one shot was made using the fiberglass liner, it performed satisfactorily and appeared to be the most promising method for achieving velocities above 1100 ft/sec.

### 5.3 RELIABILITY OF INSTRUMENTATION

For the initial shots of the calibration series, a photodetector velocity measurement system, which was built up of existing components which were not well suited for this particular application, proved to be unsatisfactory. A break-wire system was resorted to for the latter part of the calibration shots and all of the test shots. The break-wire system proved to be very reliable, with the only objection to its use being the possible detrimental effect on the chicken as a result of its impact with the wires. No damage could be observed in the X-ray shadowgraphs of shots made during the calibration phase; therefore, the system was used during the test entry with 100 percent coverage. The use of break-wires does not introduce any additional uncertainty into the measurement of velocity because the wires are used only to trigger the X-ray pulsers, with distance being measured from reference wires located on the X-ray cassettes.

An improved photodetector velocity measurement system may possibly be used in the future if its reliability can be proven with a sufficient number of development shots.

### 5.4 HYGENIC ASPECTS OF TEST

The planned methods of storing, preparing, and post-test cleanup of the test area proved to be satisfactory. A high-pressure, low flow rate water/detergent cleaning apparatus was used to clean the

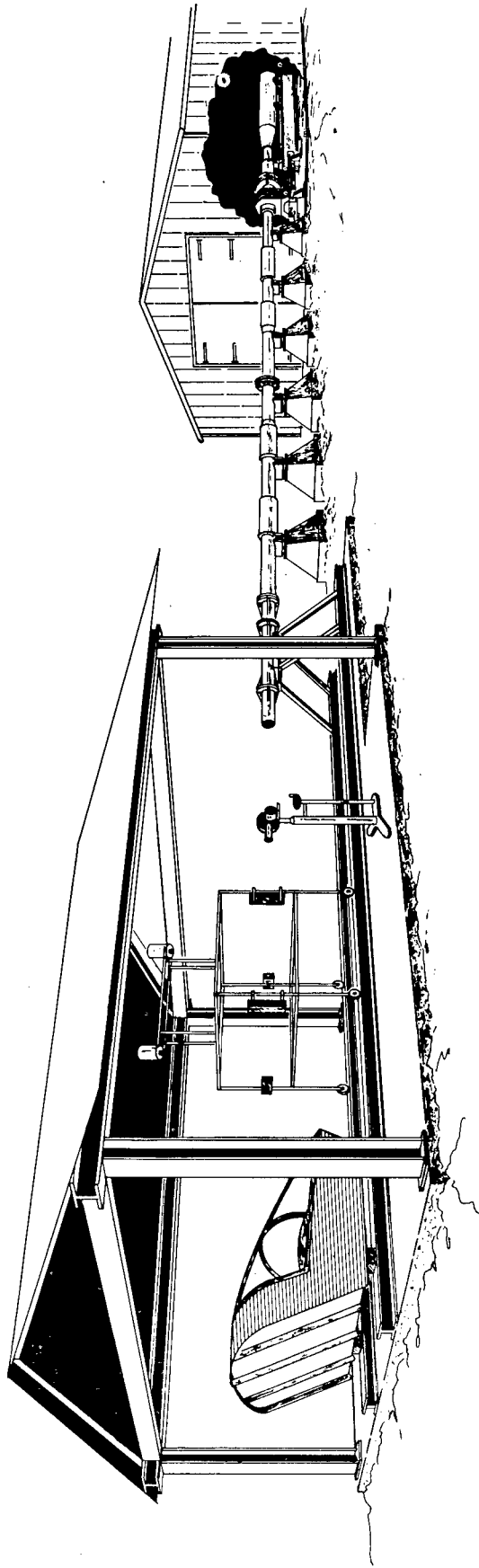
test area for the first few shots, but later it was found that the area could be cleaned more quickly using a fire hose with a high flow rate of water, if the operation could be accomplished before the bird debris had time to dry. The one percent (by weight) solution of chlorine in water used to disinfect the area after a shot was also successful in keeping the disagreeable odor associated with tests of this nature to a minimum.

## 6.0 CONCLUSIONS

A new low-speed impact facility, designed specifically for bird impact studies, has been installed at the AEDC and is now operational. Thirty-five calibration and shakedown shots have been made with the following results:

1. Four-lb birds (chickens) have been launched within the velocity range 400-1100 ft/sec.
2. Velocity repeatability has been  $\pm 4$  percent.
3. A velocity measuring system utilizing X-ray shadowgrams has proven reliable. Velocities have been measured with uncertainties of less than  $\pm 0.5$  percent.

The system provides an additional capability of assessing launch damage to the bird, if any.



A E D C  
72-1005

Note: Backstop and sideplates omitted for clarity.

Fig. 1 AEDC Bird Impact Test Facility

As with the glass panel, all panels employed an edge attachment which duplicates the type which would be used on the actual airplane. Fasteners were installed at approximately 1-1/2 inches apart through the metal outer retainer, the windshield panel edge member, the elastomeric sealing gasket, and the inner support structure. Figure 13 shows a typical edge detail used on the test.

The conditions for the tests were specified as follows:

1. Speed - 650 mph
2. Bird weight - 4 pounds
3. Temperature - 70° F
4. Angle of impact - 25°

Preliminary tests confirmed that the upper, inboard corner shot was the most critical. Consequently, most of the remaining shots impacted at this location on the panels.

#### CONCLUSIONS

A summary of the results of the tests is shown in figure 14. Of the five concepts tested, only the laminated polycarbonate panel and the all-glass panel prevented penetration. As shown in the figure, the weight of the polycarbonate panel, being nearly 300 pounds per airplane less than glass, makes it the logical choice for the B-1.

The final step in the development of the B-1 birdproof windshield will be the formal qualification tests to be conducted later this year. In these tests, full-scale production windshields, installed in the B-1 airframe structure, will be tested under bird impact. Because of the thorough material studies, and the extensive development testing described in this report, NR expects the final tests to demonstrate that the B-1 crew will be provided with the most complete protection from bird strikes that has ever been experienced in any aircraft.

#### FUTURE PROGRAMS

Other programs, in addition to the B-1, will also benefit from this windshield development program. Figure 15 shows an estimate of the new Government-sponsored aircraft programs anticipated during the next 15 years. The estimated date on which information will be required for the windshield design of these aircraft has been indicated with an arrow. An additional 20 new commercial airplanes can be conservatively estimated for this time period,



bringing the total to 35 new aircraft. Since the B-1 program described here has demonstrated the feasibility of birdproofing at transonic speeds, and the trend of these new airplanes is toward low-altitude operation at these speeds, the majority of these new programs will undoubtedly require birdproof transparencies. To support these programs, research and testing on the new materials such as polyolefin, polysulfone, polyarylsulfone, epoxy, and polycarbonate will be essential. Development of improved optics, lamination processes, and coatings will be required in addition to bird-impact-resistance. NR's development program for the B-1 forms a major step in the advancement of technology for these future programs.

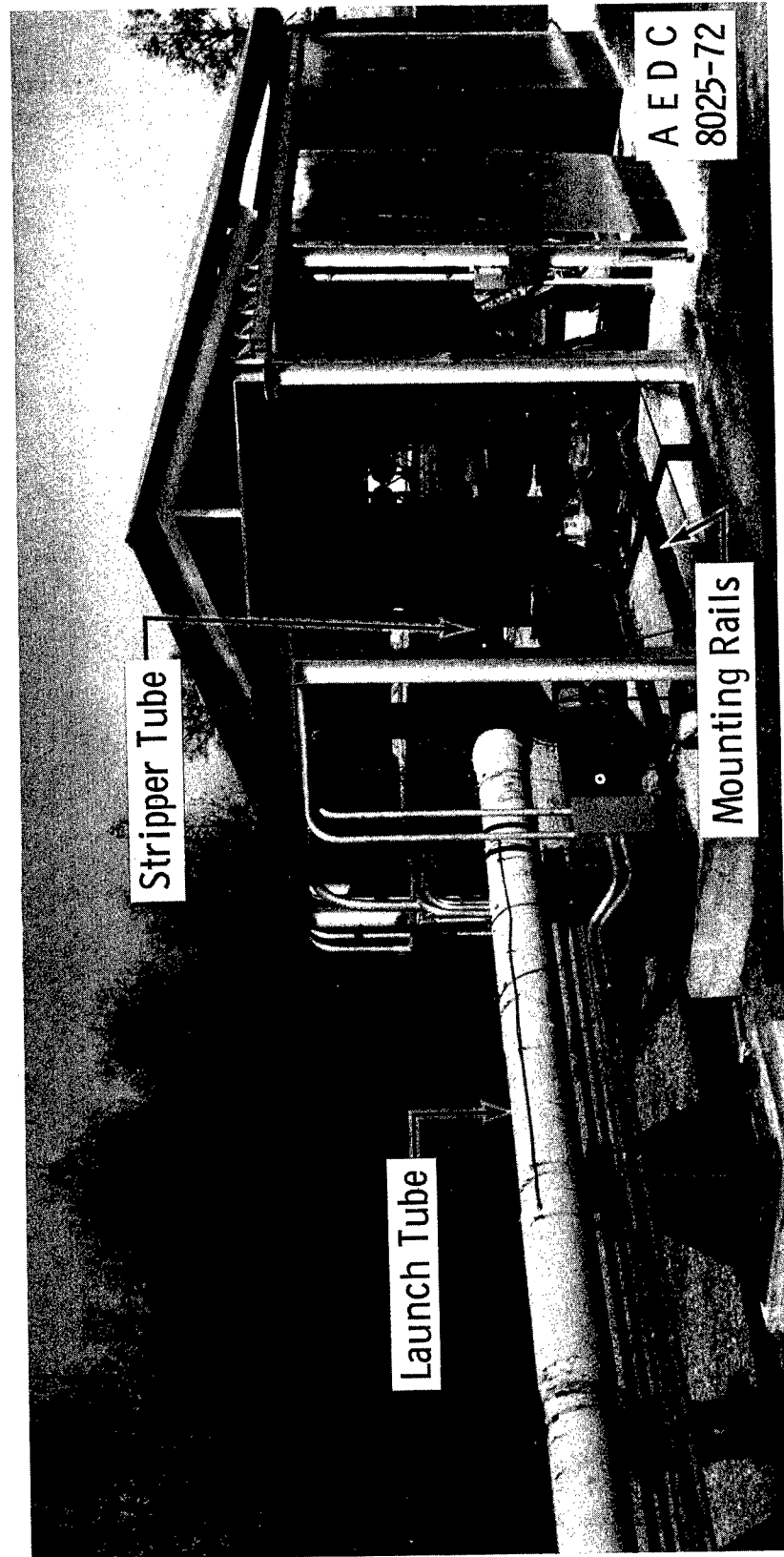


Fig. 4 Bird Impact Facility Test Area

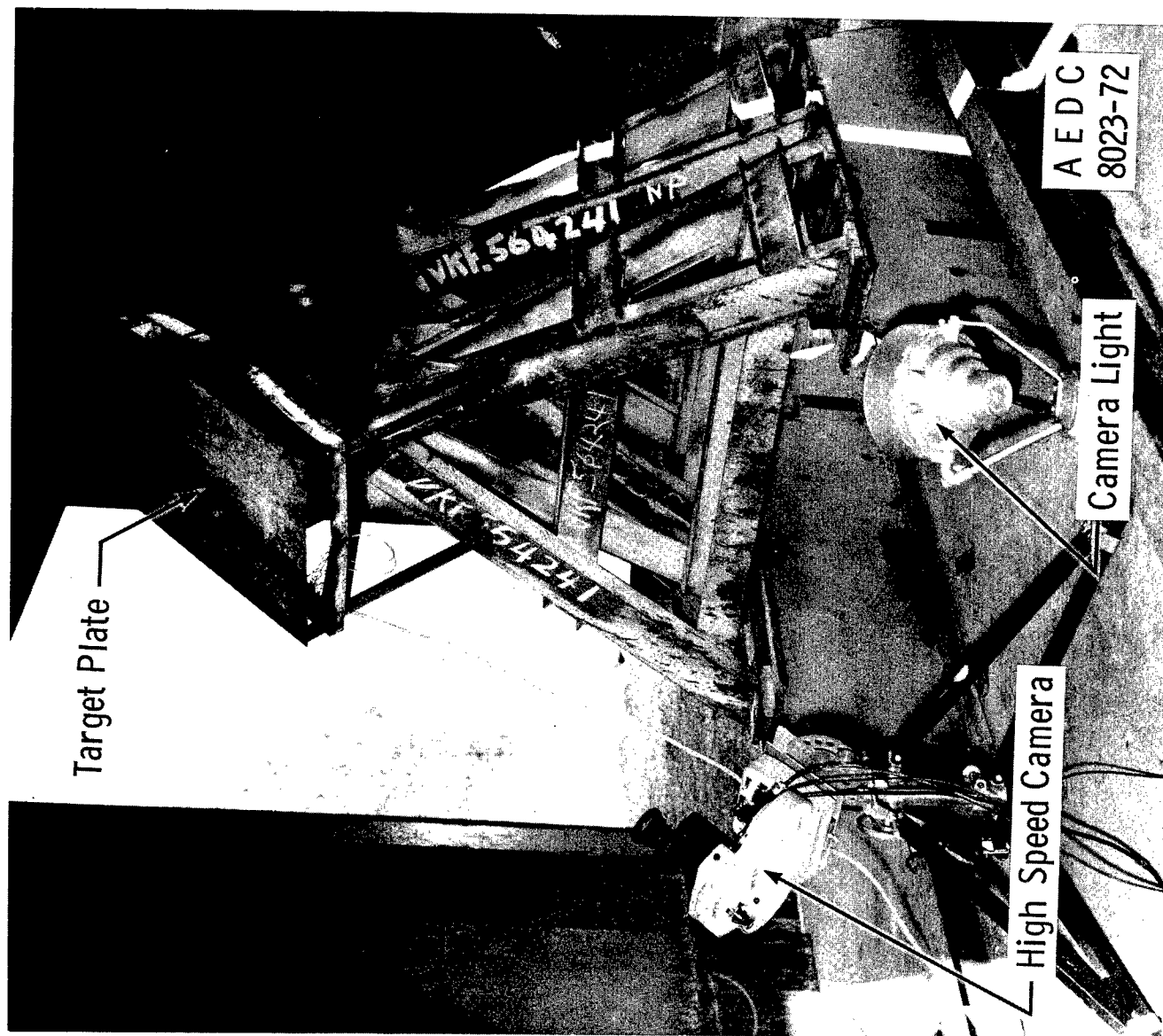


Fig. 5 Target Used for Calibration Shots

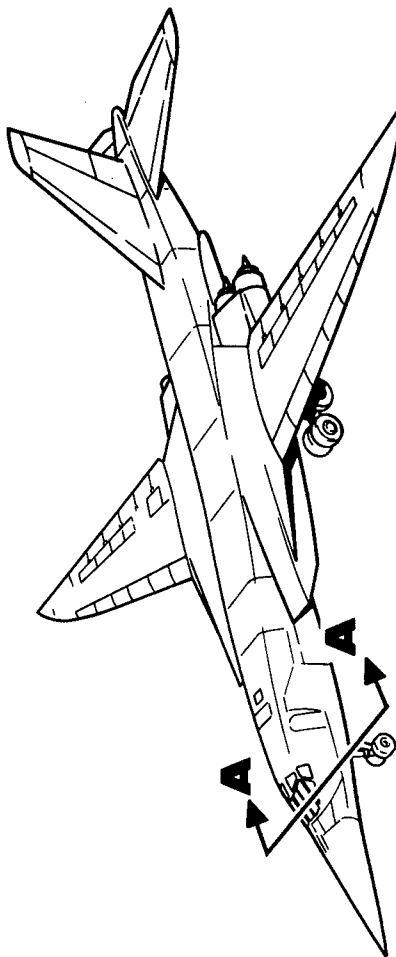
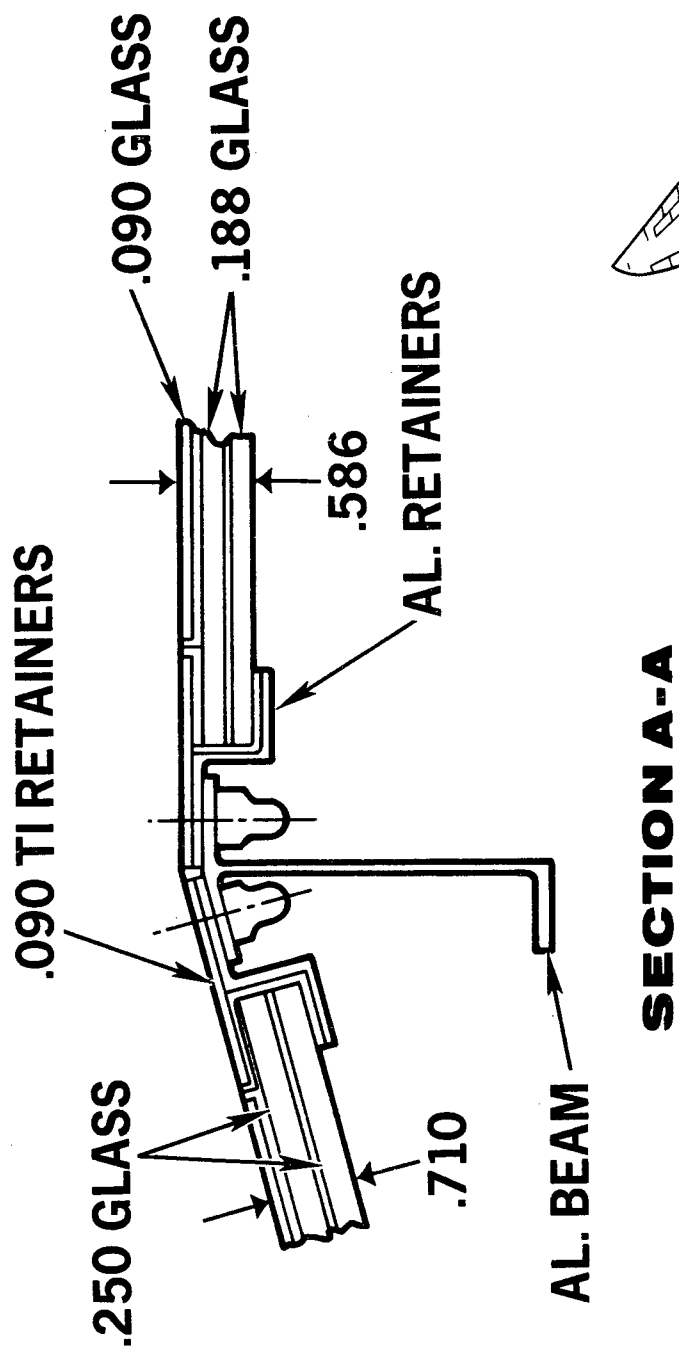


Figure 2. 1966 B-1 Configuration

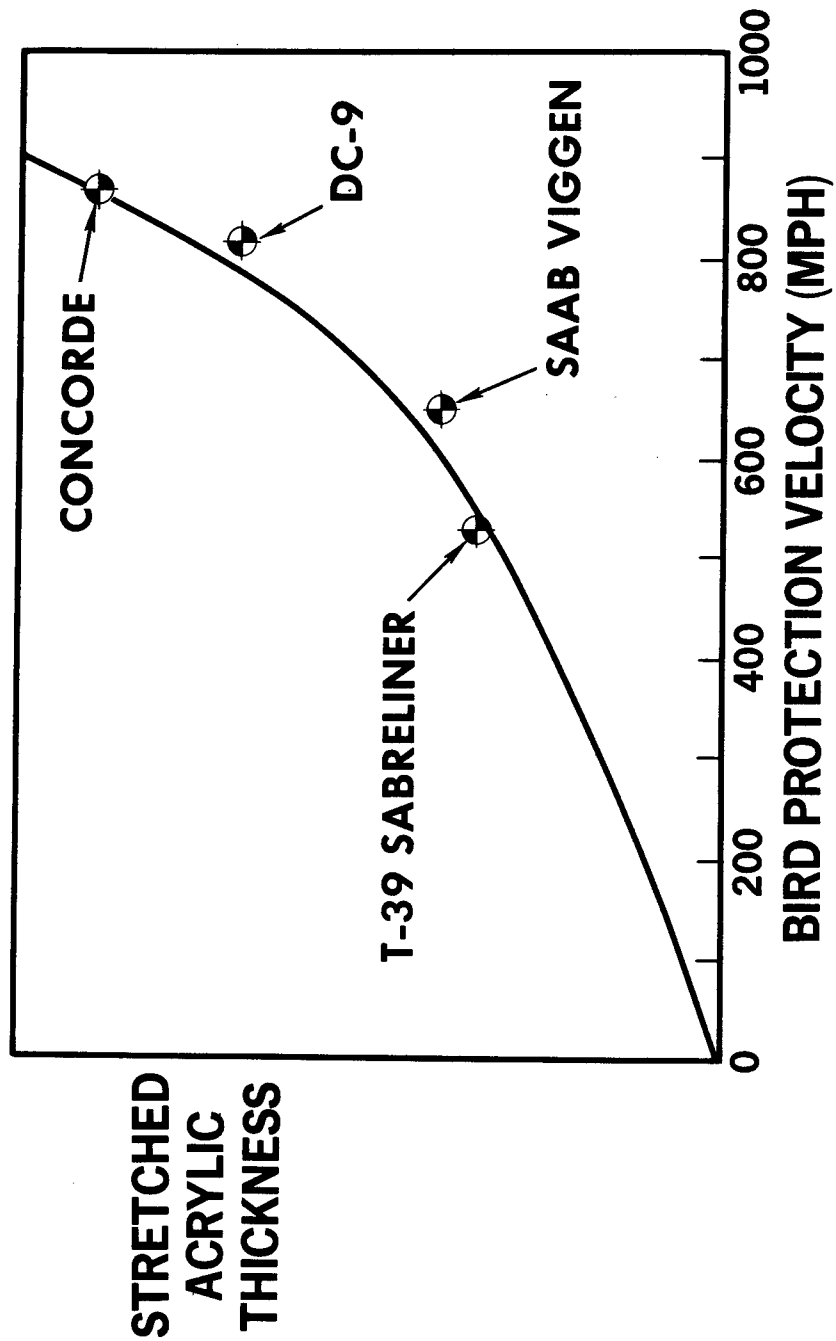


Figure 3. Material Thickness Required for Birdproofing

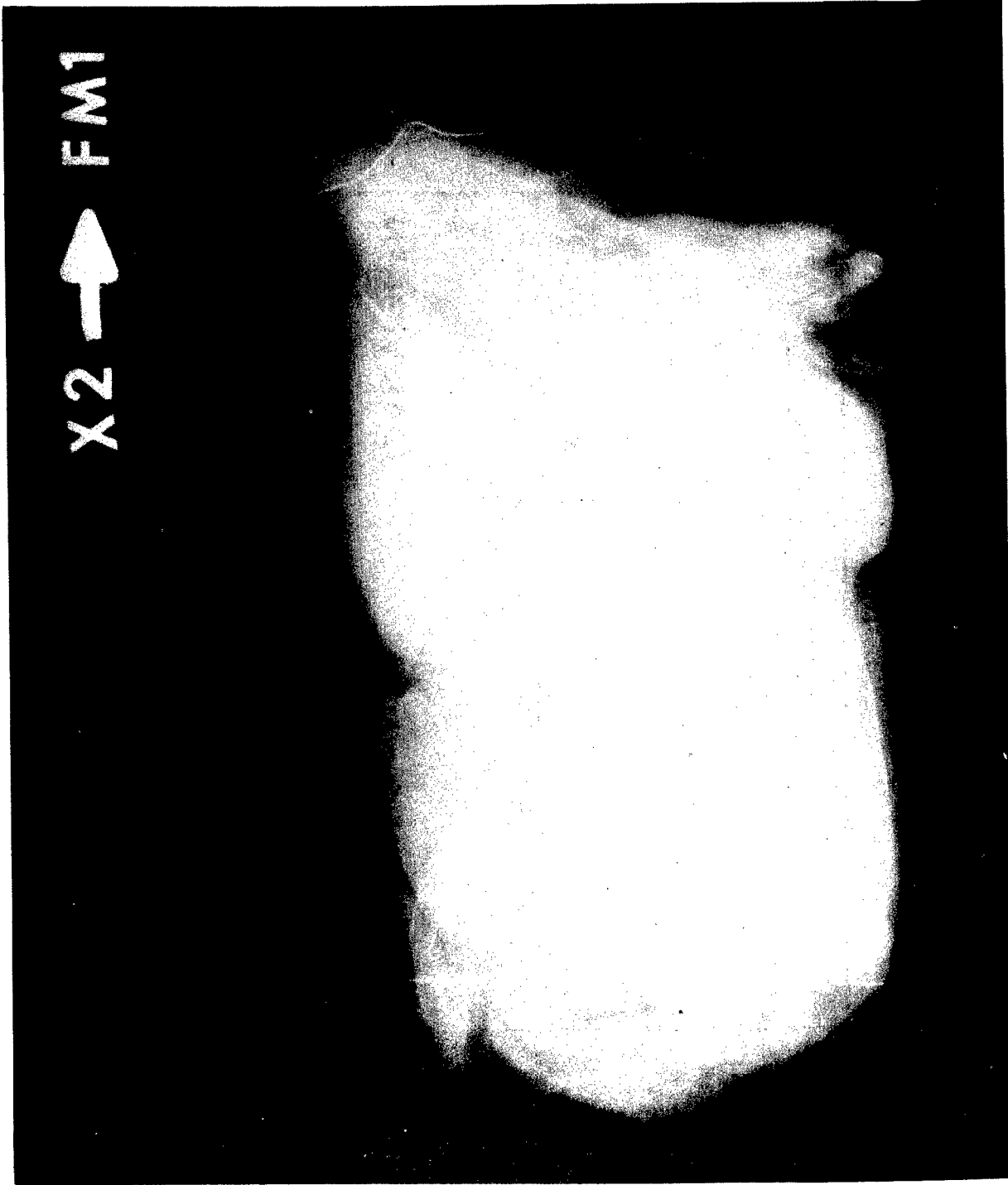


Fig. 8 X-Ray of Chicken in Flight

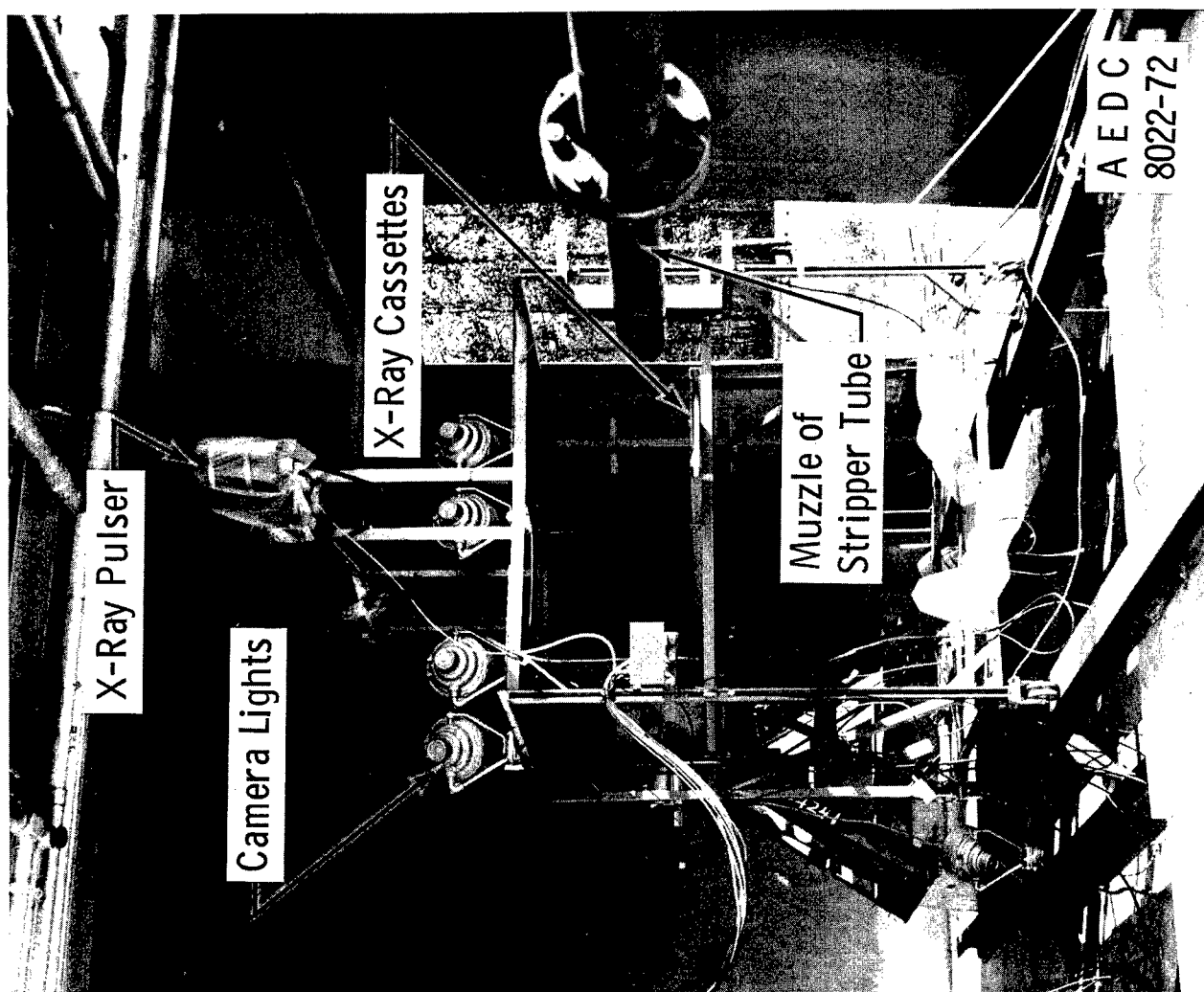


Fig. 9 Instrumentation Dolly

| MATERIAL  |                   | WEIGHT | COST     | TECHNICAL RISK | REMARKS                 |
|-----------|-------------------|--------|----------|----------------|-------------------------|
| OUTER PLY | STRUCTURAL PLIES  |        |          |                |                         |
| GLASS     | STRETCHED ACRYLIC | LOW    | MODERATE | MODERATE       | USED ON 747 & L1011     |
| ACRYLIC   | STRETCHED ACRYLIC | LOW    | LOW      | LOW            | USED ON F-111 PROTOTYPE |
| GLASS     | GLASS             | HIGH   | HIGH     | LOW            | USED ON DC10 & F-111    |
| GLASS     | POLY-CARBONATE    | LOW    | MODERATE | MODERATE       | DEVELOPMENT COST        |
| ACRYLIC   | POLY-CARBONATE    | LOWEST | LOW      | MODERATE       | DEVELOPMENT COST        |

Figure 6. Windshield Material Trade Study



# WINDSHIELD BIRD-TEST FIXTURE

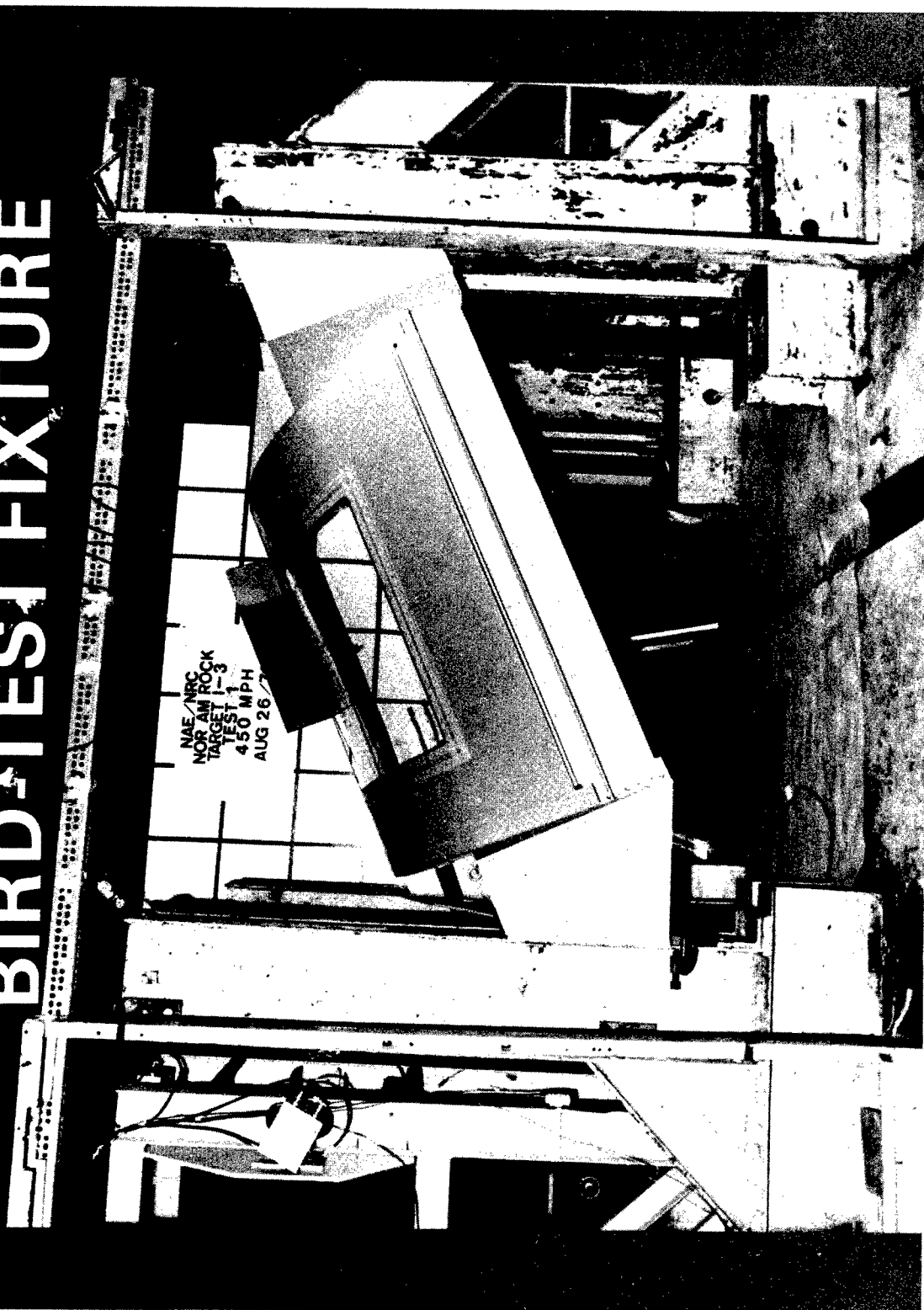


figure 7 Windshield Bird-Test Fixture

## QUANTIFICATION OF BIRD ECHOES ON AIRPORT SURVEILLANCE RADARS

S. A. GAUTHREAUX, JR., DEPARTMENT OF ZOOLOGY, CLEMSON UNIVERSITY

Radar has become an important tool for bird migration studies (Eastwood, Radar Ornithology, Methuen and Co., Ltd., London, 1967), but estimating bird densities from echo densities on the radar screen has often been difficult if not impossible. In this paper I report first on the use of the U. S. Weather Bureau's WSR-57 radar for quantitative studies of nocturnal bird migration. Emphasis is on (1) the direct visual quantification of bird densities aloft using a telescope directed to the moon on cloudless nights during full moon periods, or pointed up an intense light beam on nights when the moon was not available, and (2) the relationship between the density of birds aloft and the signal strengths of the echoes as measured by the radar's stepped attenuator. The results indicate that the WSR-57 can often be used successfully to estimate the number of birds aloft in much the same manner as rainfall intensity is measured by meteorologists using the radar. Because of the pulse volume (4.0  $\mu$ sec) and the recovery time of the WSR-57, it cannot provide detailed information on bird densities and distributions at ranges within six nautical miles.

During 1972, the ASR-4 radar operated by the Federal Aviation Agency was evaluated as a means of providing detailed information on bird movements in the immediate vicinity (within six nautical miles) of airports. Preliminary results of research on the quantification of bird movements displayed on the ASR-4 will be presented. The quantification procedure followed was similar to that used to quantify the bird densities displayed on the WSR-57 radar. (Research supported by grant 71-1974B from the Air Force Office of Scientific Research).

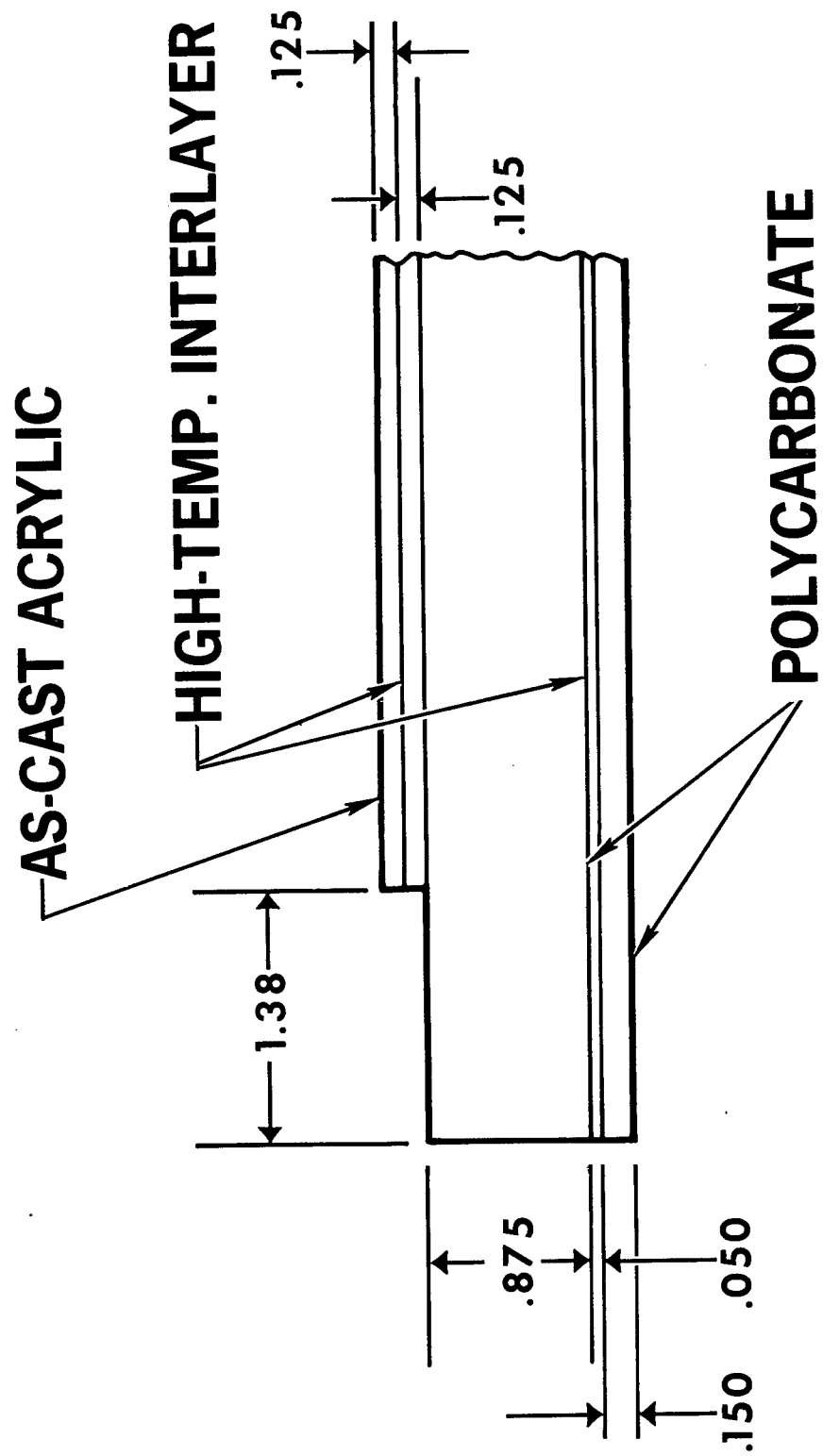


Figure 10. Laminated Polycarbonate Test Panel

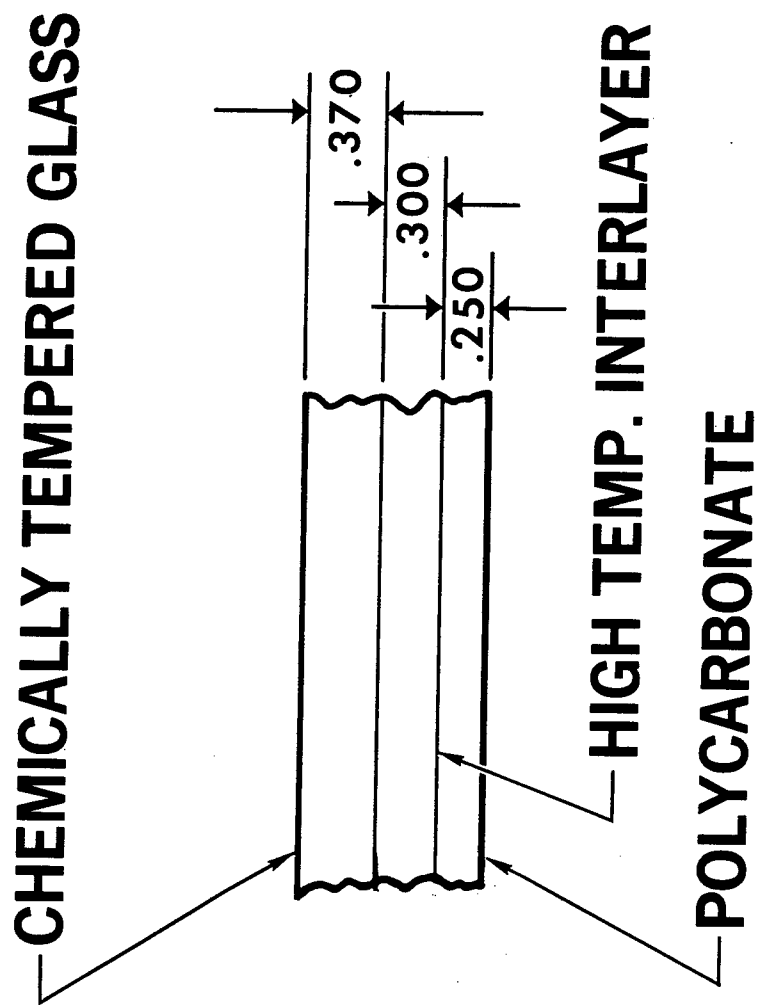


Figure 11. Glass-Polycarbonate Test Panel

that is normally used to measure the intensity of precipitation echoes. This circuit is the basis of the radar quantification technique.

Figure 1 shows the density scales I used to evaluate the density of bird echoes on the radar screen. The separate scales reflect the difference between the types of bird echoes that most frequently appeared on the radar screen. The fine dust-like echoes were characteristic of movements of passerine birds flying singly in the night sky. The fine echoes were usually so dense that they saturated the PPI within 20 nautical mile range. Once the radar screen was saturated with echoes, additional echoes could not be displayed even though migration traffic rates increased. To overcome this difficulty, I used the radar's stepped attenuator. By attenuating in increments of 3 db the solid or saturated area of echoes changed until it matched closely density pattern 4 in Figure 1. The amount of attenuation required to do this was recorded. Density pattern 4 was chosen as the base reference pattern for all attenuation readings because the pattern was easily identifiable on the radar screen, and the abundance of fine targets in the pattern precluded the possibility of attenuating until only echoes from isolated flocks and scattered large birds remained on the radar screen. Although I recorded the effect of attenuation on the entire echo pattern, the only attenuation information used in the quantification procedure was that gathered within a 2 x 5 nautical mile (3.7 x 9.3 km) area between the range limits of 10-12 nautical miles (18.5-22.2 km) and perpendicular to the direction of migratory movement. This area on the PPI covered an altitudinal stratum of approximately 2,500 feet (762 m). The antenna tilt was adjusted so that nearly all the migrants aloft were in this altitudinal zone.

To translate the attenuation information into numbers of migrating birds, simultaneous moon-watching traffic rates were compared with the amounts of attenuation required to reach pattern 4. The methods followed for these telescopic observations are essentially those described by Lowery and Newman (ref. 3). The telescope (either a 20X or 30X Bausch & Lomb BALscope, Sr., or a 40X Questar) was trained on the moon, and as the silhouettes of birds crossed the disc, their direction was recorded in terms of clock face numbers (e.g., three to nine). I analyzed all moon-watch data using the methods of Nisbet (ref. 4). The resulting figures express the estimated numbers of birds crossing a statute mile of front (1.6 km) per hour and are called migration traffic rates. When the moon was not available because of cloud cover or the phase of the lunar cycle, I pointed 20 x 60 or 10 x 50 binoculars up an intense, vertical beam of light (two 100 watt ceilometer bulbs) and watched the passage of migrating birds. This technique (ref. 5) yields information on the types of birds migrating and their numbers, but it has not yet been fully evaluated in terms of its contribution to the quantification of radar displays of migration.

In the spring of 1972, I began using the ASR-4 radar operated by the Federal Aviation Agency to study bird migration. These radars are located at approach control facilities throughout the United States and provide one with an excellent opportunity to study the movements of birds in the vicinity of airports (ref. 6). I have conducted my ASR-4 studies at three South Carolina installations: Greenville Municipal Airport, Shaw Air Force Base at Sumter, and Charleston Municipal Airport. The ASR-4 is called the FPN-47 at military bases.

The ASR-4 has a peak power output of 425 kw and a wavelength of 10.7 cm (S-band). The pulse repetition frequency is  $1200 \text{ sec}^{-1}$  with a pulse duration of 0.833 microseconds. The minimum detectable signal using the moving target indicator (MTI) is -107 dbm to -110 dbm, and without the MTI it is -109 dbm to -112 dbm. The beam width (1/2 power points) is  $1.5^\circ$  in the horizontal plane and  $6.5^\circ$  in the vertical plane. Above the 1/2 power point the beam is cosecant squared (fan shaped) up to  $30^\circ$ . The radar is equipped with a sensitivity time control (STC) circuit and two cross-sectional sensitivity circuits (CSS-1 and CSS-2). The latter two circuits bias the receivers 12 db and 9 db, respectively, to eliminate strong, close returns that are unwanted such as those from birds and insects. The range is variable from 6 to 60 nm (11.1 to 111.2 km). Richardson (ref. 7) gives additional details concerning the ASR-5 radar which also apply to the ASR-4. During most of my work the radar is on 6 nautical mile range, with MTI, vertical polarization, and high IF gain. The STC and CSS circuits are used only when the density of bird movements saturates the radar screen. The preliminary results of research on the quantification of bird movements displayed on the ASR-4 are based on the direct comparison of moon-watch traffic rates and the density of echoes on the radar screen at the same time. Once the display is saturated with bird echoes on 6 nautical mile range, the CSS-1 circuit is engaged and the resulting density on the PPI shows the effects of 12 db attenuation.

## RESULTS

Figure 2 shows the relationship between the amount of attenuation required to reach density pattern 4 of Figure 1 and the equivalent migration traffic rates as determined by moon-watching. The data were gathered on 19 nights during the spring and fall full moon periods from 1969 to 1972 at the WSR-57 radar stations at Athens, Georgia and Charleston, South Carolina. The correlation coefficient is +0.95 ( $P = 0.001$ ,  $N=37$ ), and the relationship is given by the formula:

$$\log_{10} (\text{traffic rate}) = 0.066 (\text{attenuation}) + 2.880.$$

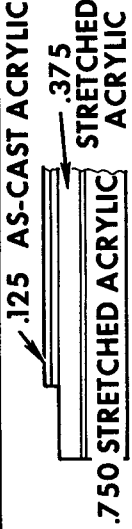
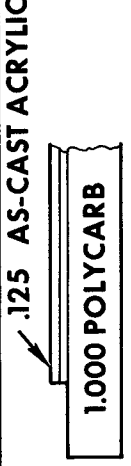
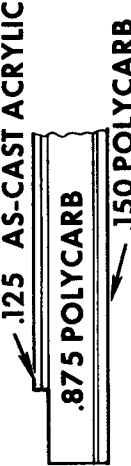
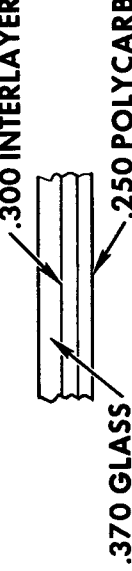
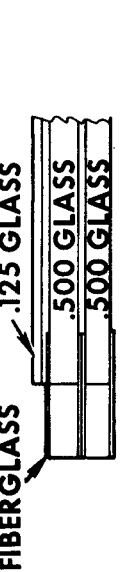
| CONFIGURATION   | LOCATION OF IMPACT | WEIGHT PER A/V (LBS) | RESULTS        |
|---|--------------------|----------------------|----------------|
|    | CENTER             | 255                  | PENETRATION    |
|    | CORNER             | 220                  | PENETRATION    |
|    | CORNER CENTER EDGE | 232                  | NO PENETRATION |
|   | CORNER             | 321                  | PENETRATION    |
|  | EDGE               | 513                  | NO PENETRATION |

Figure 14. Summary of Windshield Bird Tests

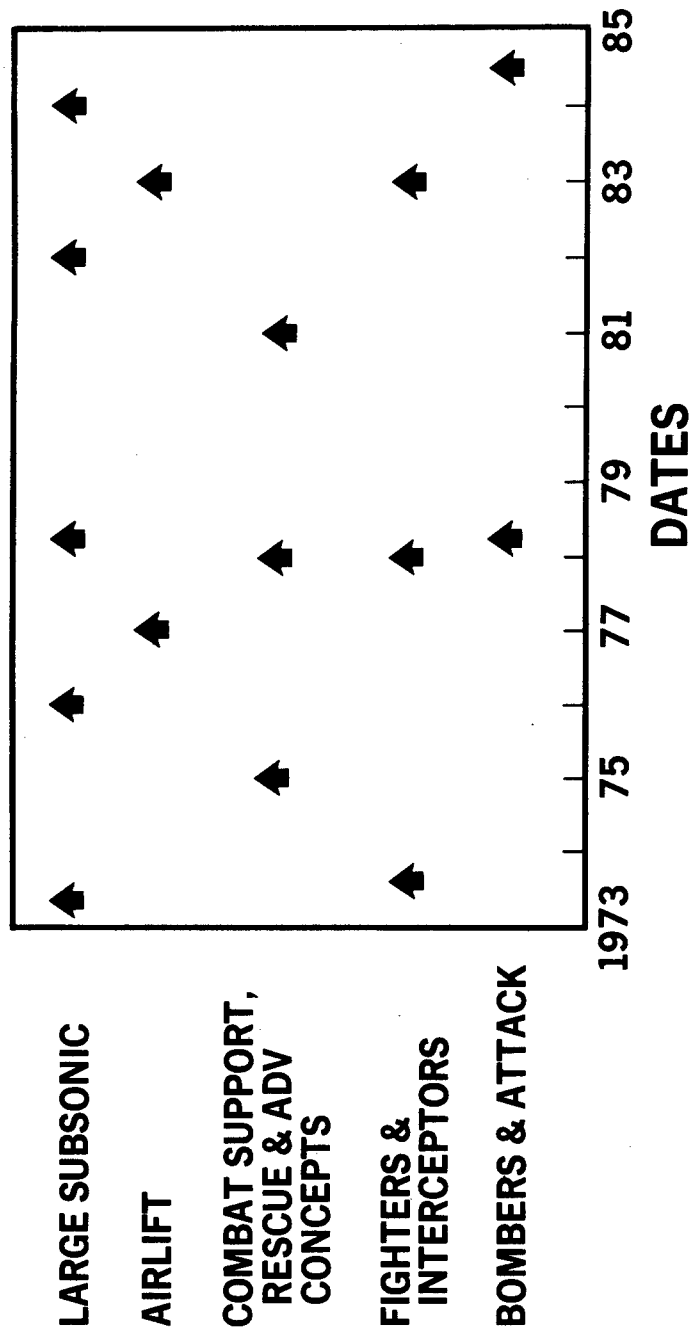


Figure 15. New Programs - U. S. Government Sponsored Aircraft



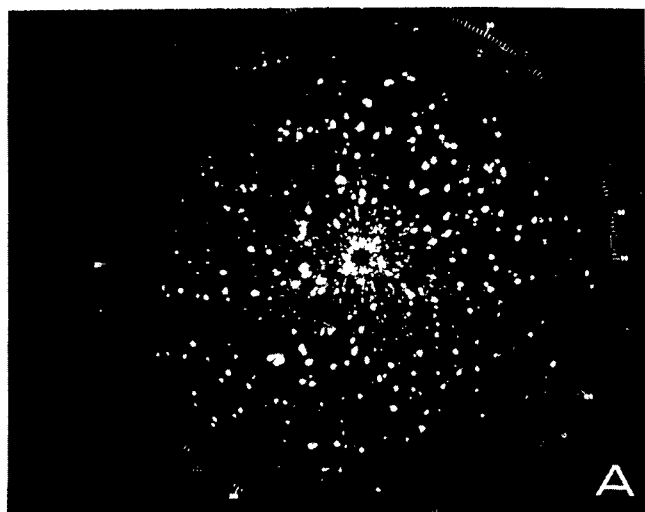
#### LITERATURE CITED

1. Eastwood, E. 1967. Radar Ornithology. Methuen & Co., Ltd., London. 278 pp.
2. Nisbet, I. C. T. 1963. Quantitative study of migration with 23-centimetre radar. *Ibis*, 105:435-460.
3. Lowery, G. H., Jr. and R. J. Newman. 1963. Studying bird migration with a telescope. Special Publ. Mus. Zool., Louisiana State University. 48 pp.
4. Nisbet, I. C. T. 1959. Calculation of flight directions of birds observed crossing the face of the moon. *Wilson Bull.*, 71:237-243.
5. Gauthreaux, S. A., Jr. 1969. A portable ceilometer technique for studying low-level nocturnal migration. *Bird-Banding*, 40:309-320.
6. Flock, W. L. 1968. Monitoring bird movements by radar. *IEEE Spectrum*, 5:62-66.
7. Richardson, W. John. 1972. Temporal variations in the ability of individual radars in detecting birds. Field Note Number 61, Associate Committee on Bird Hazards to Aircraft, National Research Council, Ottawa, Canada. 70 pp.
8. Gauthreaux, S. A., Jr. 1970. Weather radar quantification of bird migration. *BioScience*, 20:17-20.

- Figure 1. Radar density patterns for nocturnal and diurnal migration. Nocturnal density pattern 4 is the reference pattern for the quantification of migration displays on the WSR-57 radar.
- Figure 2. Graph of the attenuation-traffic rate relationship for nocturnal migration. Nocturnal density pattern 4 was used as the reference base.
- Figure 3. Radar photographs of bird displays on the ASR-4 at Greenville Municipal Airport. All photographs taken on 6 nautical mile range with MTI. Migration traffic rates are below each photograph. (A) 25 April 1972, 20:55 EST, (B) 26 April 1972, 20:54, (C) 24 April 1972, 20:19, (D) 26 April 1972, 21:17, (E) 28 March 1972, 22:15.
- Figure 4. Radar photographs of bird displays on the ASR-4. All photographs taken on 6 nautical mile range with MTI and CSS-1. Migration traffic rates are below each photograph. (A) 23 September 1972, Charleston, S.C., 23:07 EST, (B) 15 September 1972, Greenville, S.C., 21:08, (C) 27 April 1972, Greenville, S.C., 22:13.

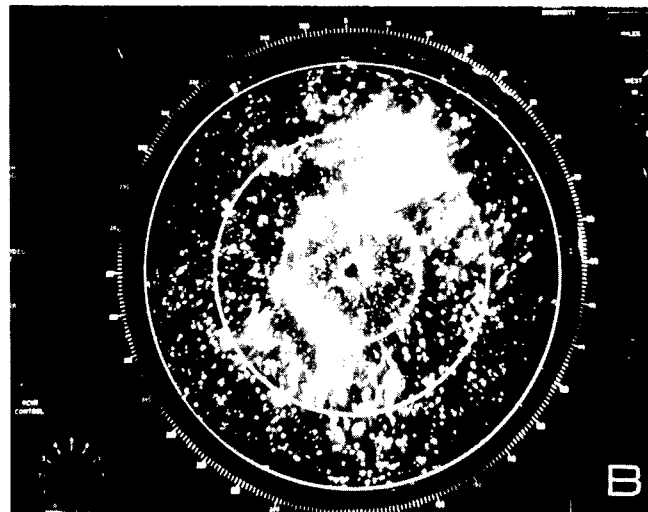
TRANSPARENCY DEVELOPMENT IN CIVIL  
AIRLINE OPERATION

B. D. Gibbs  
British European Airways  
Hounslow, Middlesex, England



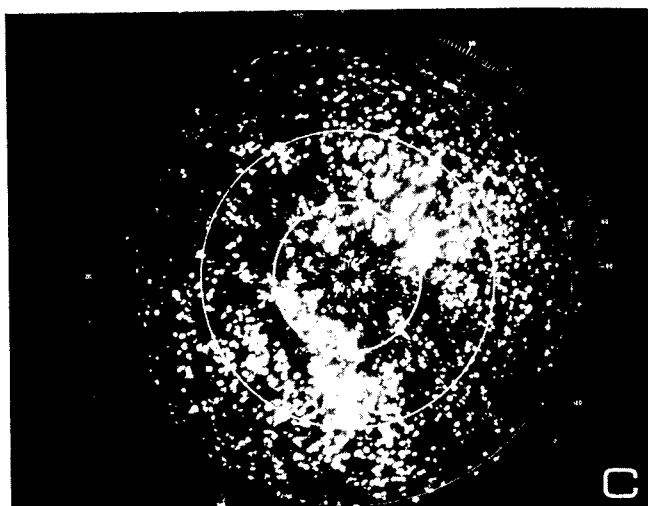
530

A



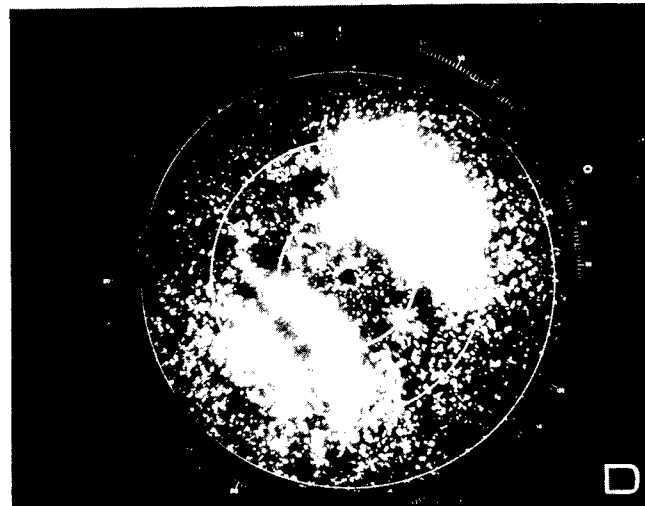
1049

B



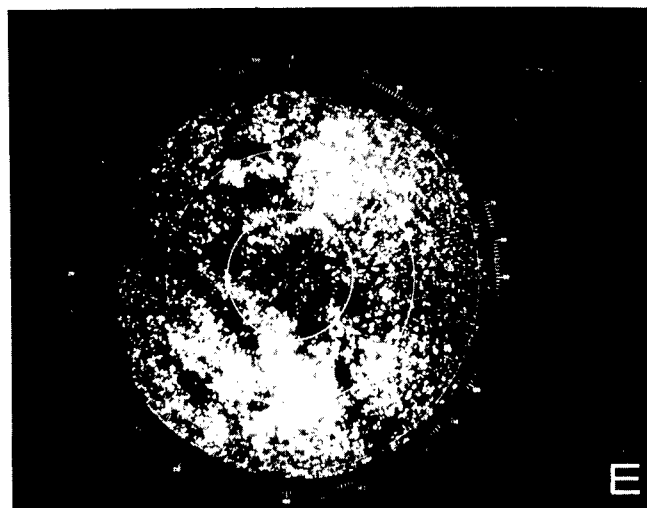
1672

C



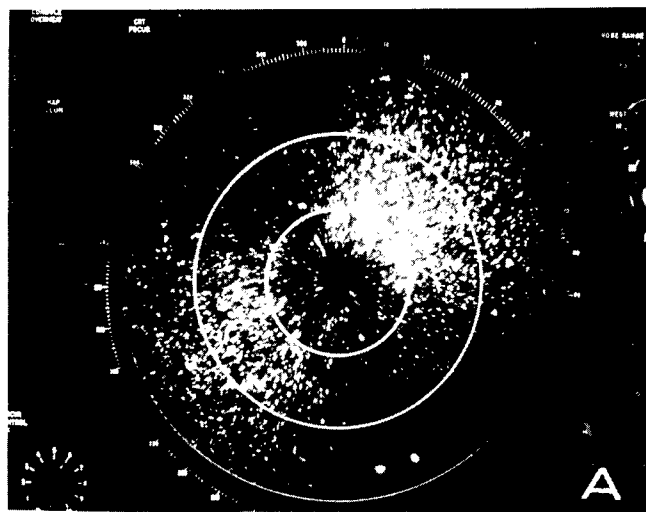
3027

D

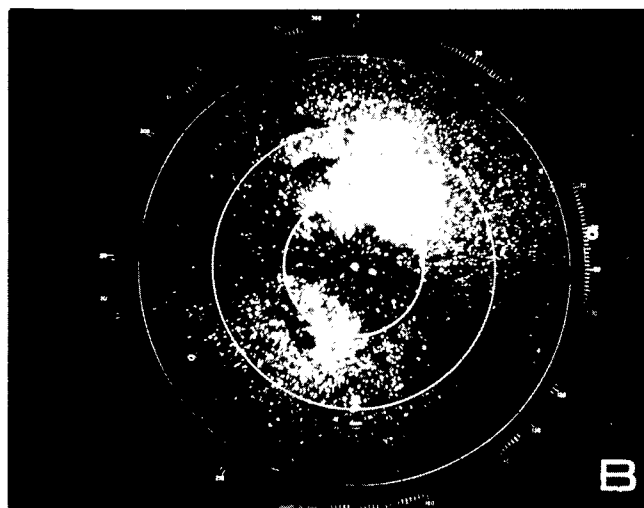


3822

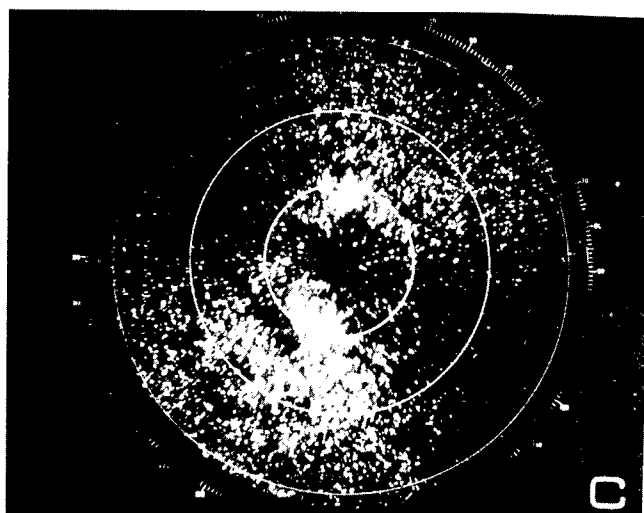
E



4308



7136



8160

## INTRODUCTION

The paper outlines our experience with the transparencies fitted to Trident, BAC. 1-11, Vanguard and Viscount aircraft and covers both operational and technical aspects. It also discusses some of the more important requirements we consider designers should endeavour to satisfy in order to minimise the operating cost of transparencies fitted to both future and current generation aircraft.

With few exceptions the flight deck transparencies fitted to our aircraft are of the extended vinyl interlayer type with glass used in the construction of the main and secondary plies.

The vast majority of our cabin windows, totaling some 7500, are manufactured in P.M.M. (Perspex). The remainder are constructed in Oroglass 55.

Since heated transparencies were first introduced to civil aircraft some 20 years ago, the operator has been confronted with a significant increase in the cost of maintaining his aircraft.

With some of the newer transparencies now costing upwards of 12,000 dollars the burden on the operator is likely to increase still further unless a significant improvement in reliability can be achieved. It is thus in the operator's own interest that the performance of the transparencies fitted to his aircraft should be carefully monitored in service.

Fig. 1 shows the annual variation in the cost of maintaining the transparencies fitted to our own aircraft.

## OPERATIONAL ASPECTS

### Bird Strikes

We have experienced very little trouble with respect to bird strikes on our transparencies. The most significant encounter occurred some 5 years ago when a seagull hit the centre windshield panel of one of our Viscounts just after take-off.

The panel was badly damaged, and although penetration did not occur the co-pilot was slightly injured by glass debris.

Fig. 2 shows the history of bird strikes that have occurred on our aircraft over the past five years.

### Hail Encounters

With weather avoidance radar now in general use on most civil aircraft it is possible to avoid the type of weather conditions where hail is likely to be present.

However, several years ago before weather radar became mandatory, one of our Viscounts encountered a particularly severe hail storm and suffered considerable damage as a result. The extent of this can be seen in Figs. 3 and 4.

It is interesting to note that although the airframe was substantially damaged by the hail, the flight deck transparencies escaped with just a single crack in the outer layer of the centre windshield panel.

More recently, however, one of our Tridents encountered a severe hail storm in the Mediterranean area which cracked the outer layers of the port and centre windshield panels. The vision loss was such that the subsequent landing had to be carried out from the co-pilot's position. The weather radar on the aircraft had apparently failed just prior to the encounter.

### Lightning Strikes and Static Discharges

Although some 40% of lightning strikes on our aircraft occur in the area of the nose, it has only ever been necessary to change one of our transparencies following a strike. The aircraft concerned was struck just forward of the flight deck area, causing spots of molten metal to precipitate onto the outer surface of the port windshield panel. The metal deposits were eventually polished out and the subject panel has since been refitted to another aircraft.

Build up of static electricity on the flight deck transparencies has caused some operators considerable trouble, and in extreme cases has even damaged electrical equipment used in the transparency heating system. The problem only appears to affect certain types of aircraft.

Although our pilots have reported that electro-static discharges take place on our transparencies, this phenomenon has never given rise to any problems.

### Rain Repellents

In flight applied rain repellent systems are fitted to all our jet aircraft. However, in some cases the performance of the system has been unsatisfactory mainly due to difficulties in getting the repellent onto the windscreen panels.

# THE DESIGN DEVELOPMENT OF A BIRDPROOF WINDSHIELD FOR THE B-1 STRATEGIC BOMBER

By

F. T. McQuilkin

Advanced Design

Aircraft Products Operations

North American Rockwell Corporation

## ABSTRACT

The North American Rockwell (NR) B-1 bomber is the first airplane to incorporate a windshield designed to resist the impact of a 4-pound bird at 650 mph. The birdproof requirement resulted from studies conducted by NR and Boeing on the cost-effectiveness of adding the requirement to the B-1 airplane specifications. These studies also produced new methods for predicting the performance of some of the newer transparent materials under bird impact.

After the initial screening of all available windshield materials, bird impact tests were conducted on the most promising candidates. The test fixture was a simplified version of the B-1 windshield and support structure. The test panels measured 3 feet by 3 feet and were curved to approximate the B-1 contour. Resilient backup structure was built into the fixture to duplicate the dynamic effects of the aircraft structure under bird impact. After being designed and built by NR's B-1 Division, it was shipped to Ottawa, Canada, where tests were conducted at the National Research Council's bird test facility.

Four material candidates were tested: stretched acrylic, polycarbonate, polycarbonate-glass composite, and glass. Of these, only the polycarbonate windshield and the glass windshield withstood the 650 mph bird impact. The polycarbonate windshield was selected for the air vehicle design, primarily because of its lower weight.



### Overhaul/Repair Considerations

Unlike the majority of flight deck transparencies a considerable proportion of cabin windows removed for crazing can be reclaimed by either polishing out the surface damage or by replacement of defective panels. In order to maintain close control of the work carried out all window recertification is cleared through our component overhaul facility.

This same facility is also capable of carrying out minor repairs to certain flight deck transparencies, although one of the most successful repair schemes developed over the years, namely relamination\*, is sub-contracted out to one of our transparency suppliers.

### SERVICE TRIALS

It has always been our policy to keep up to date with transparency development and to provide a means whereby new ideas in transparency design can be evaluated under service conditions.

### Wire Heated Transparencies

When our new jet aircraft entered service in 1964 the reliability initially achieved with the transparencies left a lot to be desired. (The M.T.B.F. for the main windshield panels being only 1500 unit hours). At that time, most of our competitors in Europe were operating aircraft fitted with wire heated transparencies achieving an M.T.B.F. in excess of 10,000 unit hours. A decision was thus taken in 1968 to fit a number of wire heated transparencies to our aircraft in order to establish whether a similar level of reliability could be achieved.

Special tests carried out on a test flight soon demonstrated that the new transparencies would not be suitable for use on our aircraft. Although the wire heater improved the light transmission in daylight, it produced adverse optical effects at night of sufficient magnitude to significantly affect the pilots judgement of the landing flare. This was particularly noticeable in conditions of marginal visibility. The effect was apparent even with the heating switched off.

\* This consists of re-autoclaving a transparency in order to remove areas of delamination.

### Edge Heating

In parallel with the trials on wire heating, ground tests were also being carried out to evaluate a development of the existing transparency featuring additional heating in the edge.

A number of these 'edge heated' transparencies were fitted to our aircraft for service evaluation and it quickly became evident that the reliability had been improved by a considerable margin. Edge heating now features in a large percentage of our transparencies and the M.T.B.F. currently being achieved is 12,000 unit hours, compared with the figure of 1,500 unit hours achieved with the original design.

### Acrylic Transparencies

Service trials have also been carried out with acrylic extended vinyl interlayer transparencies. A number of these fitted to our Vanguard aircraft have achieved lives in excess of 14,000 flying hours without failure. The results of these trials were instrumental in causing us to select transparencies of similar design for fitment to our twin jet transport aircraft.

### FUTURE REQUIREMENTS

#### Flight Deck

Flight deck panels constitute the major proportion of the civil operator's total expenditure on transparencies. It is therefore in this area that the maximum benefit can be derived from continued development and new thinking.

Even though the 'edge heated' transparency has proved to be reliable the manufacturers have now produced evidence to show that the multi-laminate transparency without a thick vinyl interlayer is more likely to achieve the order of reliability desired by the operator.

Early set backs with certain glass faced acrylic transparencies of this type, however, indicate that there are still a number of problems to be overcome. Although steps have been taken to improve the reliability it is too early to say whether it will achieve a level acceptable to the civil operator.

In the case of the glass multi-laminate transparency, the ever present problem of skyjacking involving the use of firearms has presented the transparency designer with a new set of problems. Whatever steps are taken to cope with these it is essential that the reliability potential of the transparency should not be compromised.

attrition, and growth factor resulting from increased windshield and structure weight, was used. The results, shown in figure 4, show that the greater amount of bird protection, the lower total flyaway cost. However, very little cost savings result if protection is provided above M 0.85. If only 2 percent of the penetrations caused loss of an aircraft, birdproofing would still be cost-effective.

Subsequently, the Air Force Request for Proposal included a requirement for a windshield resistant to penetration of a 4-pound bird at M 0.85.

#### AERODYNAMIC DRAG REDUCTION STUDY

As the development of the B-1 progressed, wind tunnel data revealed areas where aerodynamic drag could be reduced. Included in these refinement items was the flat panel windshield shown earlier. A new configuration resulted with revised lines incorporating the large, curved windshield shown in figure 5. It was this arrangement, with birdproof capability, which was presented in NR's B-1 proposal to the Air Force.

#### MATERIAL TRADE STUDIES

Although stretched acrylic was proposed for the windshield, additional material trade studies were conducted after contract award to insure that the latest technical development in transparencies were considered. New materials such as polyolefin, polyarylsulfone, polysulfone, and epoxy were reviewed. These were all rejected because of the high technical risk associated with developing new materials in time to meet a tight production schedule. Polycarbonate, however, appeared to be sufficiently developed to warrant further consideration. Five potential material candidates emerged from this study as shown in figure 6. Because of the anti-icing requirement, all panels are laminated. This allows the application of a conductive, anti-icing coating to a thin outer ply, which can efficiently transfer heat to the outer surface for ice removal. As shown in figure 6, both glass and as-cast acrylic were considered for this outer ply. Up to this point, the bird-impact-resistance of these concepts was purely analytical. As with the stretched acrylic, existing data on polycarbonate and glass were extrapolated to predict the thickness of material required for birdproofing.

#### DEVELOPMENT TESTS

To confirm these estimates and aid in selecting the final design, a series of tests were conducted on the candidate designs.

The tests were conducted on a special fixture designed and built by the B-1 Division of North American Rockwell. The fixture, shown in figure 7, was built of aluminum structure simulating the actual windshield support structure

of the B-1 airframe. Resilient backup structure was built into the fixture to duplicate the dynamic effects of the airframe during bird impact. A section of transparent material was installed on the right-hand side of the center post to provide the proper stiffness to this member. The test panels, installed on the left side of the center post, measured 3 feet by 3 feet, which approximates the unsupported span of the actual B-1 windshield. The panels and fixture were curved to duplicate the B-1 windshield contour.

The fixture and test panels were shipped to the National Research Council of Canada's bird test facility in Ottawa, where Jack Noonan and his staff conducted the tests. At the time of these tests, this was the only facility on the North American continent with the capability of meeting the B-1 speed requirements.

The panels selected for testing were all variations of the five candidates which emerged from the material trade studies. Figure 8 shows the stretched acrylic version. This was essentially the same arrangement presented in the B-1 proposal, with the exception of the outer ply. Since the thin outer ply does not contribute significantly to bird impact strength, as-cast acrylic, which could be procured in less time, was used for the tests. Because of the 0.91-inch thickness limitation for stretched acrylic sheet, two structural plies were used, one 3/4-inch and one 3/8-inch thick.

One version of the polycarbonate panel is shown in figure 9. A single 1-inch-thick polycarbonate ply forms the structural member.

A second polycarbonate panel concept is shown in figure 10. Here, the total polycarbonate thickness is approximately the same as in figure 9, but the material is divided into two plies, one of 0.875-inch thick and one of 0.150-inch thick. This arrangement was based on data furnished by GE, which showed that this material exhibits its maximum toughness up to approximately 0.150-inch thickness. This tough inner ply significantly improves the impact strength of the panel as well as serving as a spall shield.

A third polycarbonate panel concept is shown in figure 11. The outer glass panel, the proprietary interlayer, and the inner polycarbonate panel all contribute to the impact resistance of this panel.

A glass panel, shown in figure 12, was also tested. Although the weight of this panel makes it prohibitive for the current version of the B-1, it was felt that data on glass would be useful for growth versions of the B-1 where the higher speeds could obsolete the plastic windshields. On this design, the two structural plies of 0.5000-inch-thick glass were bonded to fiberglass edge members.

As with the glass panel, all panels employed an edge attachment which duplicates the type which would be used on the actual airplane. Fasteners were installed at approximately 1-1/2 inches apart through the metal outer retainer, the windshield panel edge member, the elastomeric sealing gasket, and the inner support structure. Figure 13 shows a typical edge detail used on the test.

The conditions for the tests were specified as follows:

1. Speed - 650 mph
2. Bird weight - 4 pounds
3. Temperature - 70° F
4. Angle of impact - 25°

Preliminary tests confirmed that the upper, inboard corner shot was the most critical. Consequently, most of the remaining shots impacted at this location on the panels.

#### CONCLUSIONS

A summary of the results of the tests is shown in figure 14. Of the five concepts tested, only the laminated polycarbonate panel and the all-glass panel prevented penetration. As shown in the figure, the weight of the polycarbonate panel, being nearly 300 pounds per airplane less than glass, makes it the logical choice for the B-1.

The final step in the development of the B-1 birdproof windshield will be the formal qualification tests to be conducted later this year. In these tests, full-scale production windshields, installed in the B-1 airframe structure, will be tested under bird impact. Because of the thorough material studies, and the extensive development testing described in this report, NR expects the final tests to demonstrate that the B-1 crew will be provided with the most complete protection from bird strikes that has ever been experienced in any aircraft.

#### FUTURE PROGRAMS

Other programs, in addition to the B-1, will also benefit from this windshield development program. Figure 15 shows an estimate of the new Government-sponsored aircraft programs anticipated during the next 15 years. The estimated date on which information will be required for the windshield design of these aircraft has been indicated with an arrow. An additional 20 new commercial airplanes can be conservatively estimated for this time period,

bringing the total to 35 new aircraft. Since the B-1 program described here has demonstrated the feasibility of birdproofing at transonic speeds, and the trend of these new airplanes is toward low-altitude operation at these speeds, the majority of these new programs will undoubtedly require birdproof transparencies. To support these programs, research and testing on the new materials such as polyolefin, polysulfone, polyarylsulfone, epoxy, and polycarbonate will be essential. Development of improved optics, lamination processes, and coatings will be required in addition to bird-impact-resistance. NR's development program for the B-1 forms a major step in the advancement of technology for these future programs.

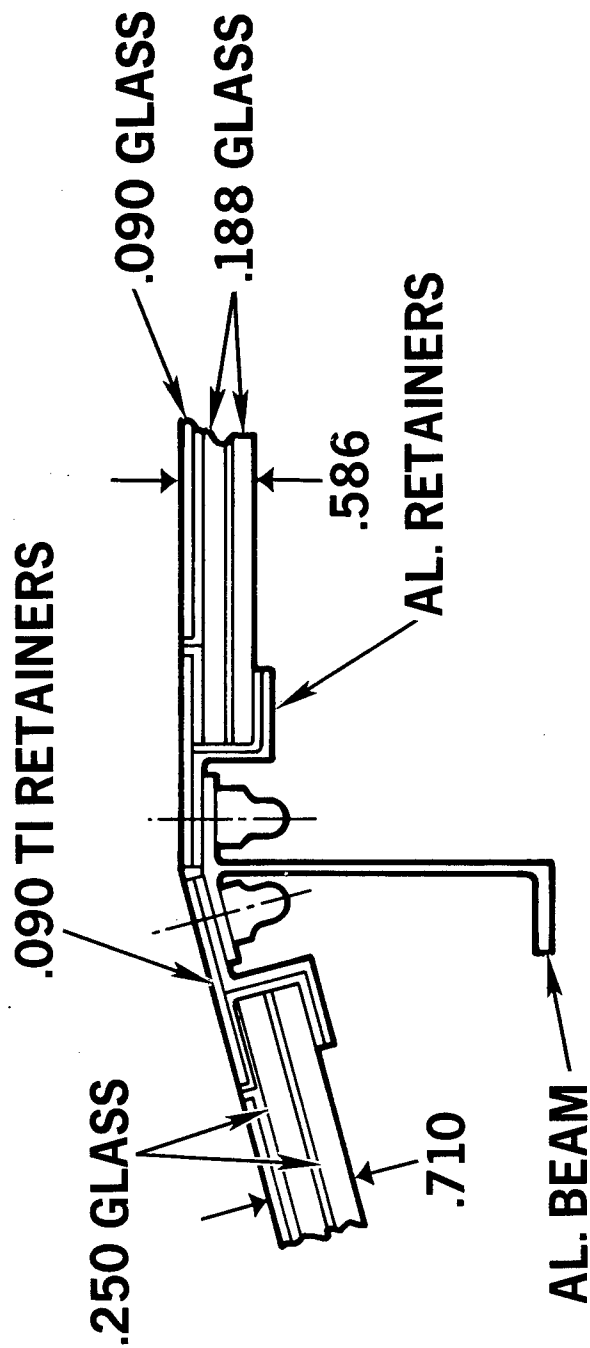
#### REFERENCES

1. McNaughtan, I. I., "The Resistance of Transparencies to Bird Impact at High Speed" Aircraft Engineering, December 1964
2. Mitchell, J., "More Thoughts on Forces Associated with a Bird Strike," Associate Committee on Bird Hazards to Aircraft of the National Research Council of Canada, Field Note No. 37, March 1966
3. "Development of Aircraft Windshields to Resist Impact With Birds in Flight," Kangas and Pigman Civil Aeronautics Administration, TDR No. 62, 74, and 105, February, March 1950
4. "The Probability of Bird Strikes by Aircraft Flying at Low Altitudes," Harry F. Kohl Systems Engineering Group, Research and Technology Division, AFSC, Wright-Patterson Air Force Base, SEG-TR-65-23, December 1965



Figure 1 North American Rockwell B-1





### SECTION A-A

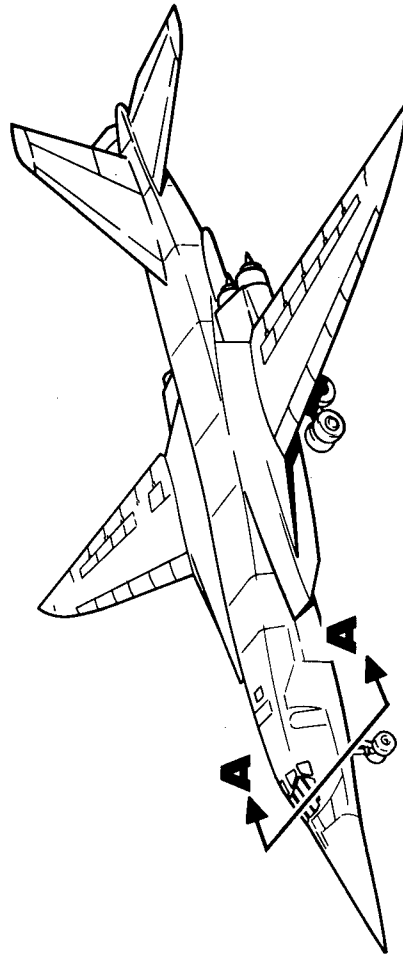


Figure 2. 1966 B-1 Configuration

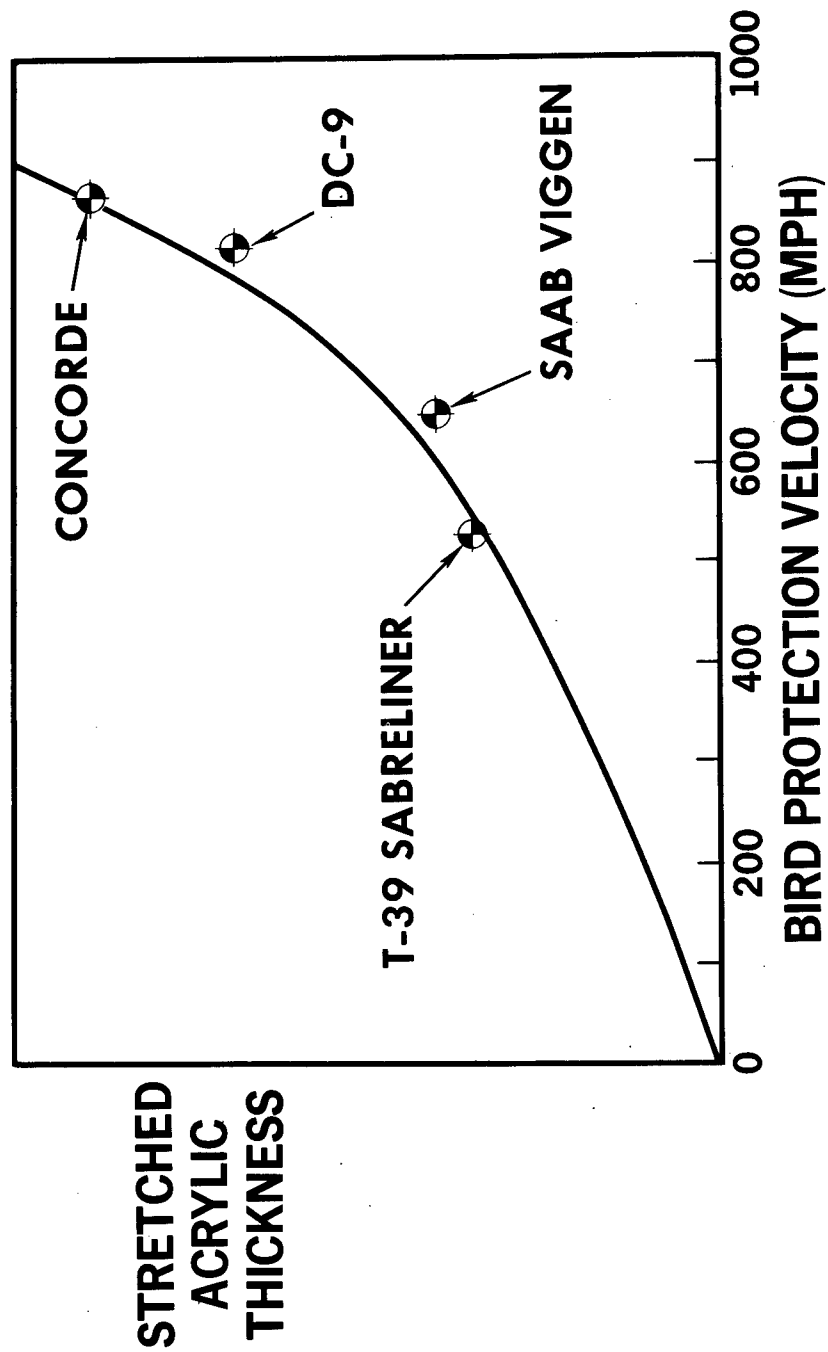


Figure 3. Material Thickness Required for Birdproofing

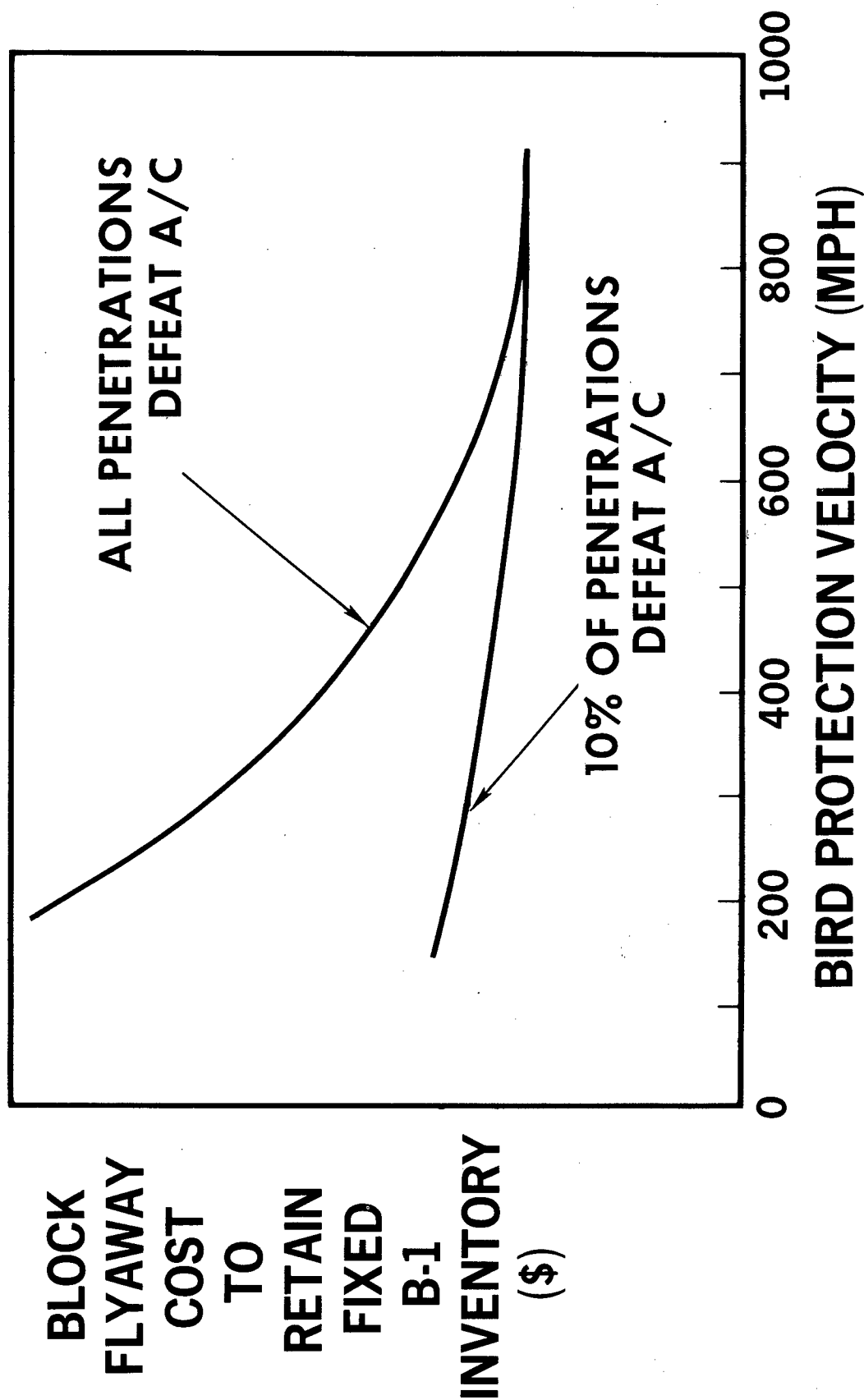


Figure 4. Cost-Effectiveness of Birdproofing the B-1



figure 5 B-1 Low-Drag Windshield

| MATERIAL  |                   | WEIGHT | COST     | TECHNICAL RISK | REMARKS                 |
|-----------|-------------------|--------|----------|----------------|-------------------------|
| OUTER PLY | STRUCTURAL PLIES  |        |          |                |                         |
| GLASS     | STRETCHED ACRYLIC | LOW    | MODERATE | MODERATE       | USED ON 747 & L1011     |
| ACRYLIC   | STRETCHED ACRYLIC | LOW    | LOW      | LOW            | USED ON F-111 PROTOTYPE |
| GLASS     | GLASS             | HIGH   | HIGH     | LOW            | USED ON DC10 & F-111    |
| GLASS     | POLY-CARBONATE    | LOW    | MODERATE | MODERATE       | DEVELOPMENT COST        |
| ACRYLIC   | POLY-CARBONATE    | LOWEST | LOW      | MODERATE       | DEVELOPMENT COST        |

Figure 6. Windshield Material Trade Study

# WINDSHIELD BIRD-TEST FIXTURE



Figure 7 Windshield Bird-Test Fixture

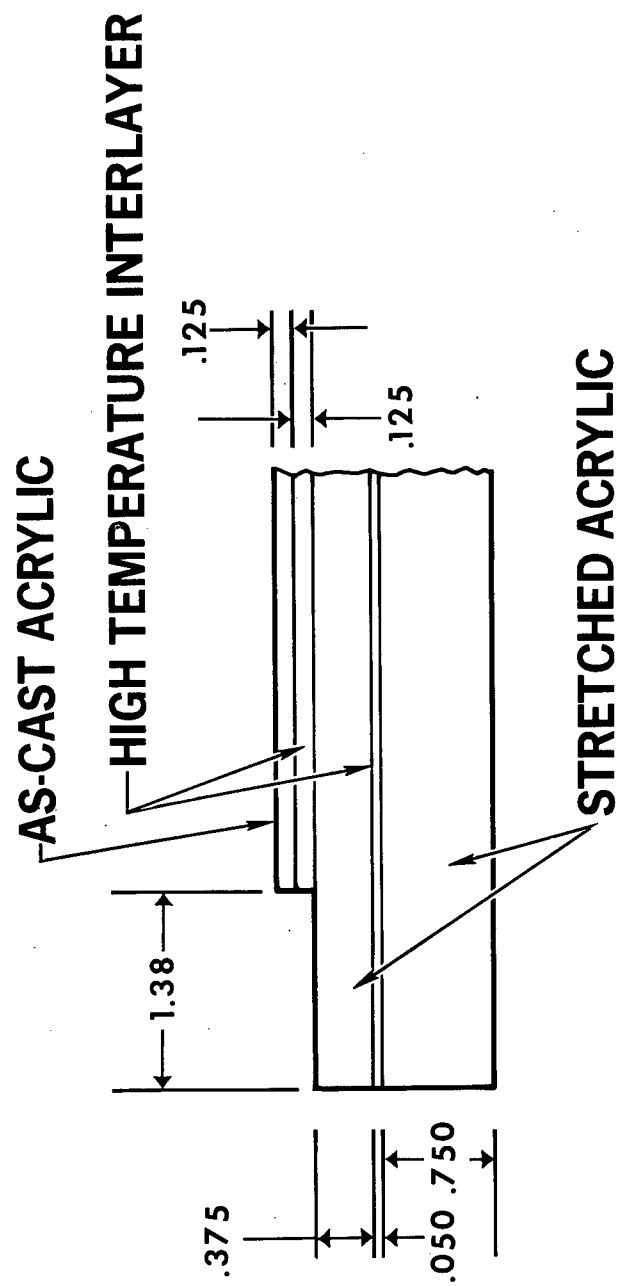


Figure 8. Stretched Acrylic Test Panel

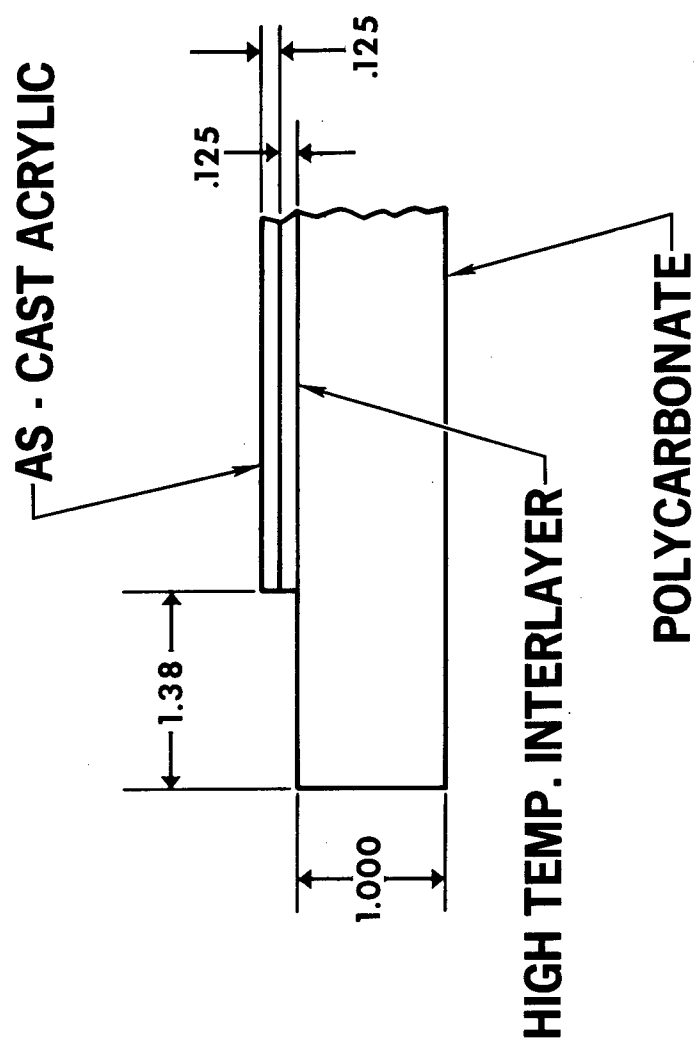


Figure 9. Monolithic Polycarbonate Test Panel



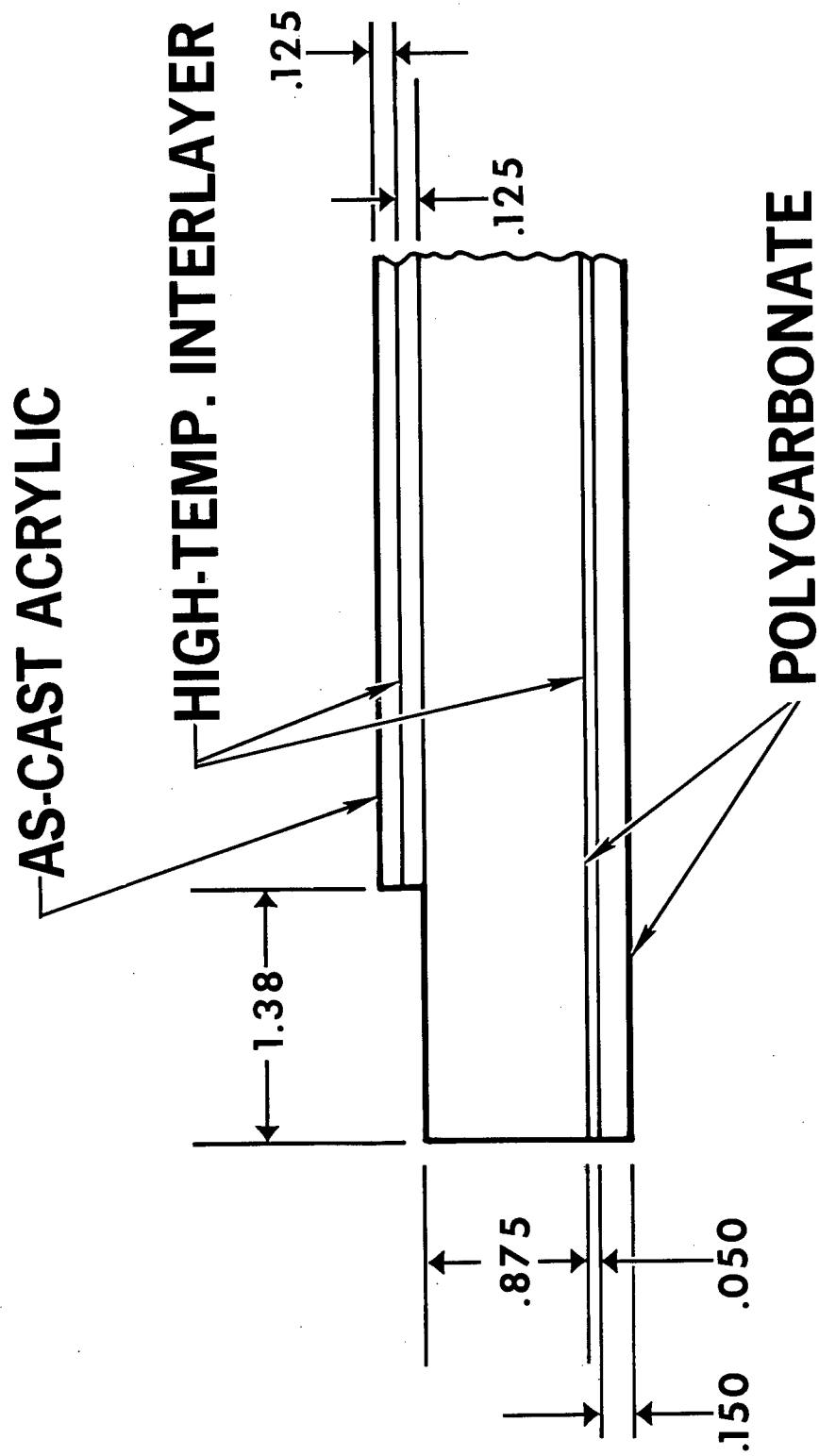


Figure 10. Laminated Polycarbonate Test Panel

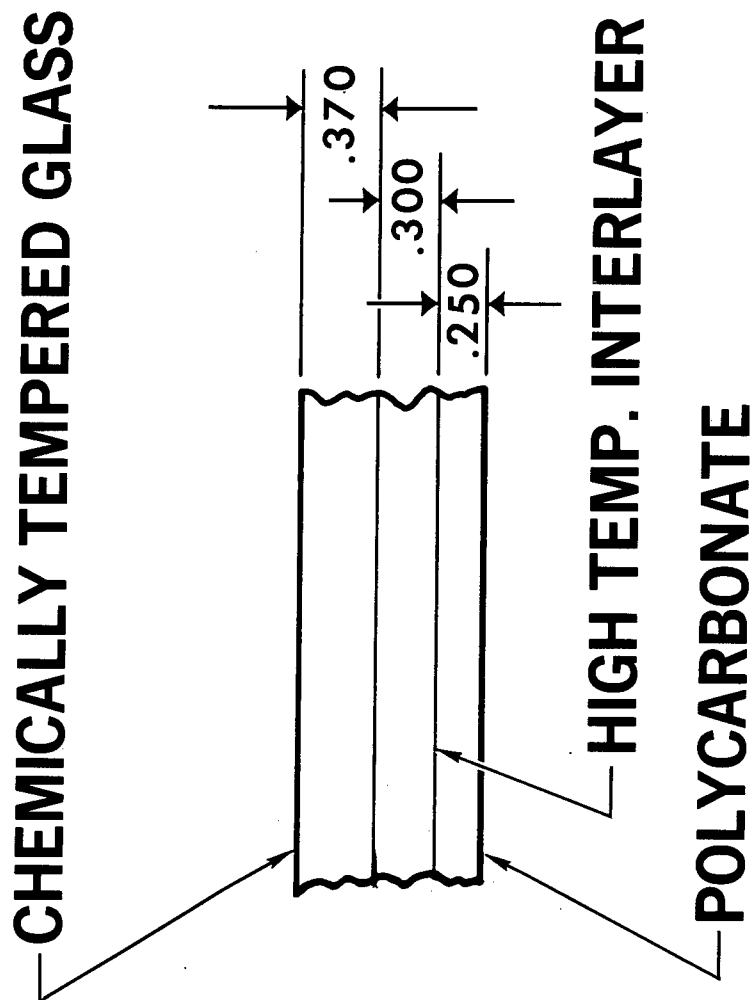


Figure 11. Glass-Polycarbonate Test Panel

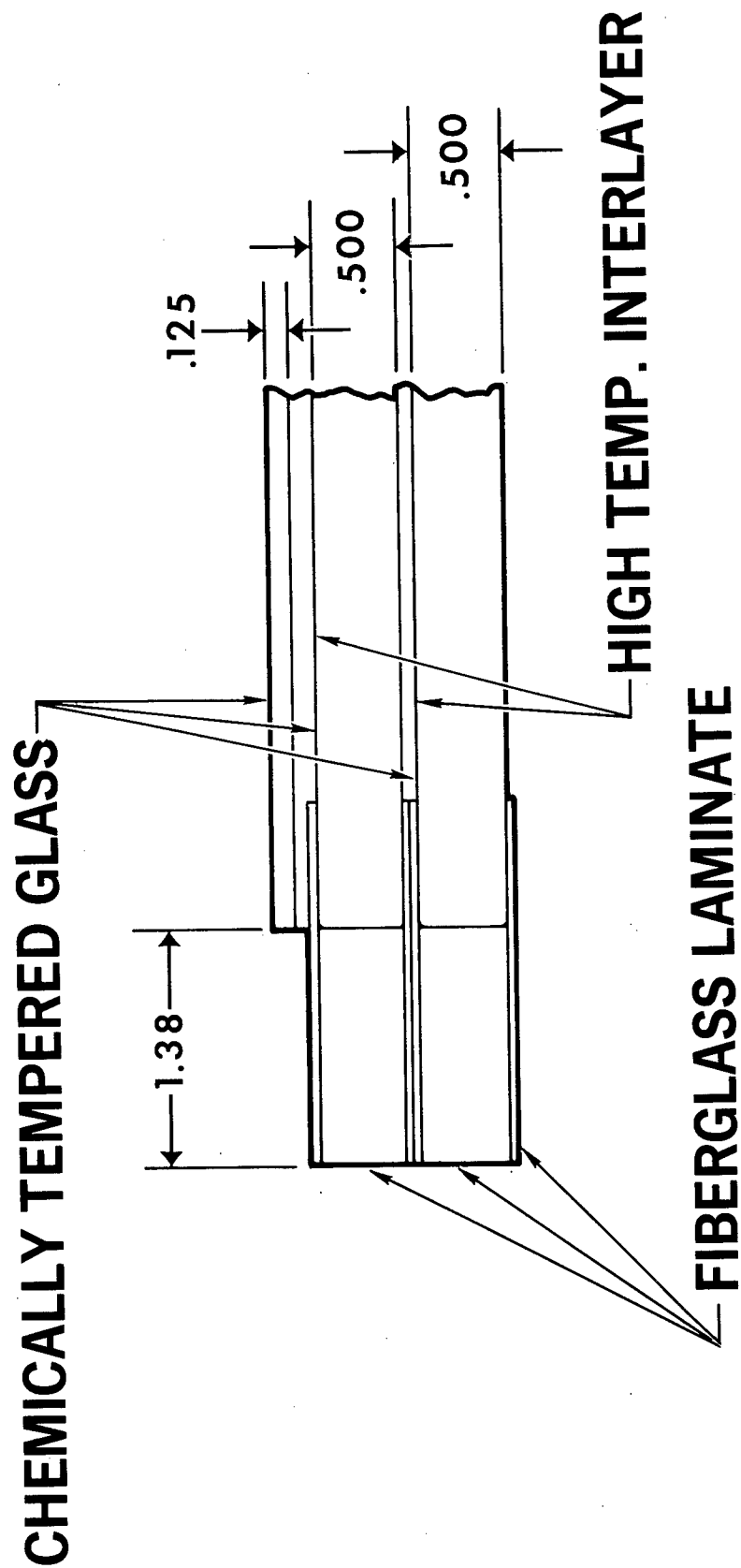


Figure 12. Laminated Glass Test Panel

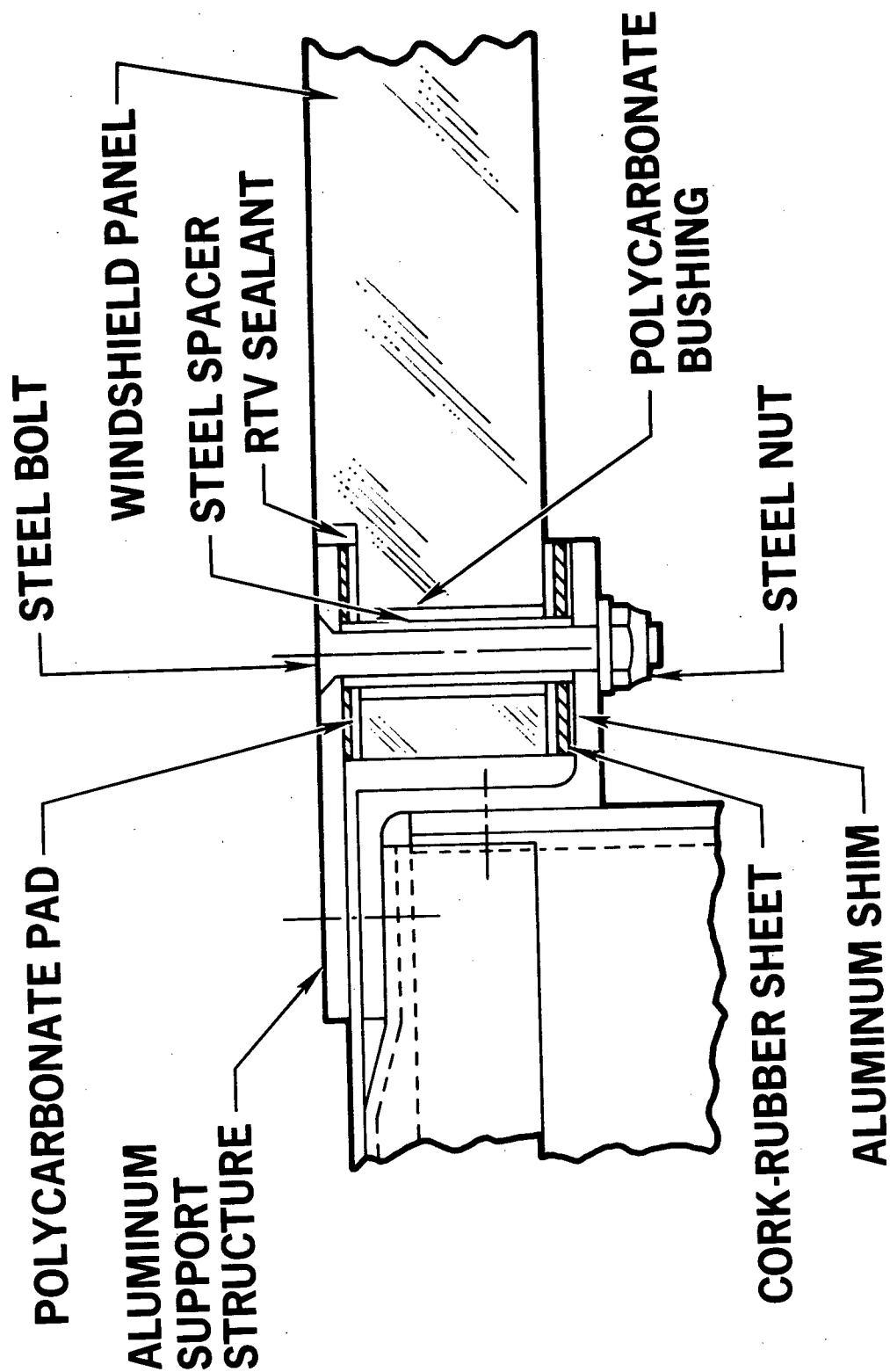


Figure 13. Typical Edge Attachment for Windshield Test

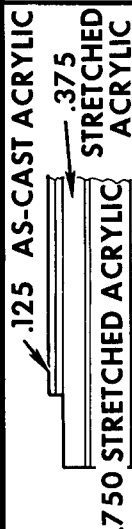


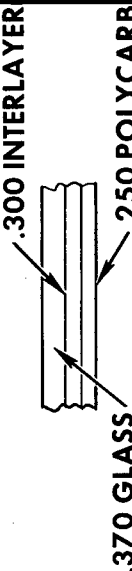
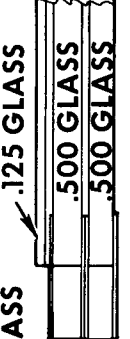
| CONFIGURATION   | LOCATION OF IMPACT       | WEIGHT PER A/V (LBS) | RESULTS           |
|---|--------------------------|----------------------|-------------------|
|    | CENTER                   | 255                  | PENETRATION       |
|    | CORNER                   | 220                  | PENETRATION       |
|    | CORNER<br>CENTER<br>EDGE | 232                  | NO<br>PENETRATION |
|   | CORNER                   | 321                  | PENETRATION       |
|  | EDGE                     | 513                  | NO<br>PENETRATION |

Figure 14. Summary of Windshield Bird Tests

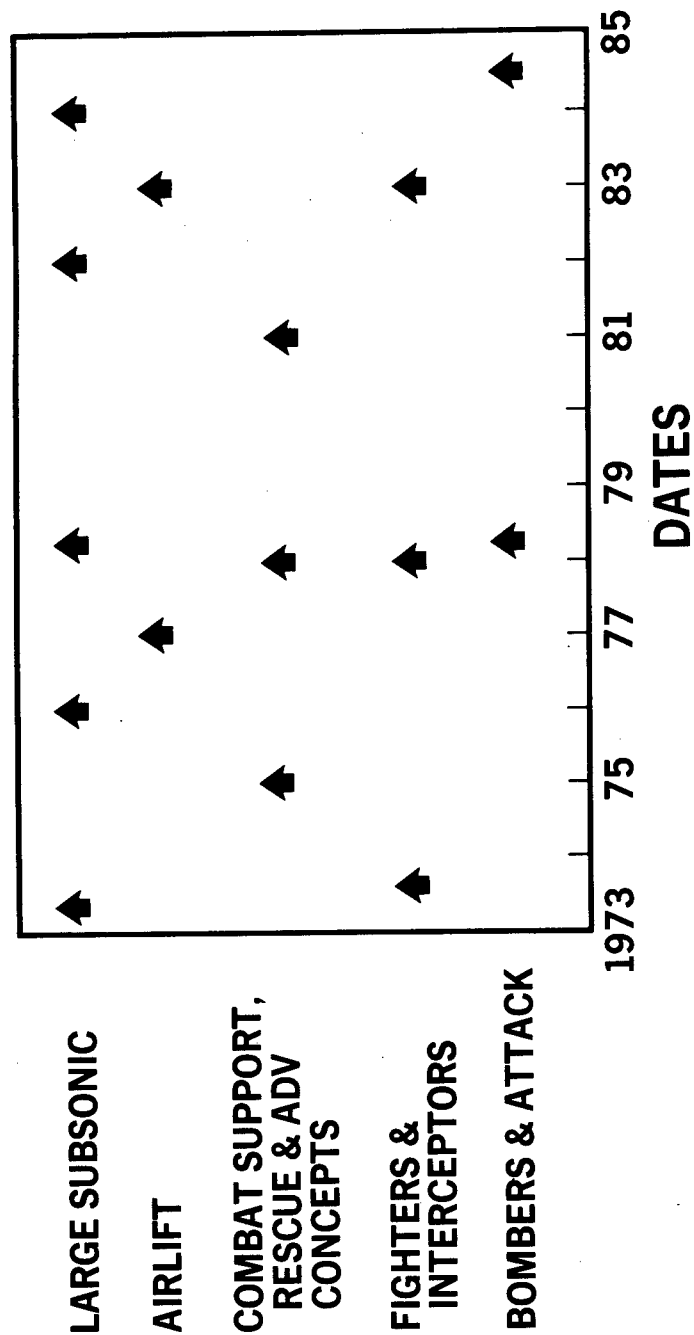


Figure 15. New Programs - U. S. Government Sponsored Aircraft

SESSION 6

DESIGN AND PERFORMANCE

TRANSPARENCY DEVELOPMENT IN CIVIL  
AIRLINE OPERATION

B. D. Gibbs  
British European Airways  
Hounslow, Middlesex, England



TRANSPARENCY DEVELOPMENT  
IN  
CIVIL AIRLINE OPERATION

B.D. Gibbs, C.Eng. A.F.R.Ae.S.

British European Airways

The introduction of more sophisticated transparencies has confronted the operator with a significant increase in the cost of maintaining his aircraft. To off-set this increase the reliability of transparencies must be improved. As current experience with new aircraft suggests that this will not be easily achieved, the civil operator is treating the matter with some concern and is taking an increasing interest in the service performance of the transparencies fitted to his aircraft.

The high initial cost and low overhaul capability of flight deck windows constitute a significant cost area for the operator. The situation, however, gives the designer ample opportunity to incorporate design improvements in the construction of replacement windows.

Delamination and electrical defects account for a large proportion of flight deck window removals, but innovations such as 'edge heating' have improved reliability by a very significant margin.

Most operators are aware of the limitations imposed by the use of stretched or as cast acrylic in the construction of cabin windows. With chemically or thermally toughened glass now available in thicknesses less than 4 mms. it is suggested that a significant advantage could be gained by considering such materials for cabin windows on sub-sonic as well as supersonic aircraft.

Provided the integrity of a multi-laminate design can be demonstrated there is considerable evidence to suggest that this particular type of construction offers the operator the optimum design for a flight deck window. However, it is felt that in the flight deck area particularly, there is still ample scope for further development and new thinking. In order to achieve further break-throughs it is necessary to take into account current experience and the civil operator is prepared to play his part in providing the transparency designer with the data he requires.

## INTRODUCTION

The paper outlines our experience with the transparencies fitted to Trident, BAC. 1-11, Vanguard and Viscount aircraft and covers both operational and technical aspects. It also discusses some of the more important requirements we consider designers should endeavour to satisfy in order to minimise the operating cost of transparencies fitted to both future and current generation aircraft.

With few exceptions the flight deck transparencies fitted to our aircraft are of the extended vinyl interlayer type with glass used in the construction of the main and secondary plies.

The vast majority of our cabin windows, totaling some 7500, are manufactured in P.M.M. (Perspex). The remainder are constructed in Oroglass 55.

Since heated transparencies were first introduced to civil aircraft some 20 years ago, the operator has been confronted with a significant increase in the cost of maintaining his aircraft.

With some of the newer transparencies now costing upwards of 12,000 dollars the burden on the operator is likely to increase still further unless a significant improvement in reliability can be achieved. It is thus in the operator's own interest that the performance of the transparencies fitted to his aircraft should be carefully monitored in service.

Fig. 1 shows the annual variation in the cost of maintaining the transparencies fitted to our own aircraft.

## OPERATIONAL ASPECTS

### Bird Strikes

We have experienced very little trouble with respect to bird strikes on our transparencies. The most significant encounter occurred some 5 years ago when a seagull hit the centre windshield panel of one of our Viscounts just after take-off.

The panel was badly damaged, and although penetration did not occur the co-pilot was slightly injured by glass debris.

Fig. 2 shows the history of bird strikes that have occurred on our aircraft over the past five years.

### Hail Encounters

With weather avoidance radar now in general use on most civil aircraft it is possible to avoid the type of weather conditions where hail is likely to be present.

However, several years ago before weather radar became mandatory, one of our Viscounts encountered a particularly severe hail storm and suffered considerable damage as a result. The extent of this can be seen in Figs. 3 and 4.

It is interesting to note that although the airframe was substantially damaged by the hail, the flight deck transparencies escaped with just a single crack in the outer layer of the centre windshield panel.

More recently, however, one of our Tridents encountered a severe hail storm in the Mediterranean area which cracked the outer layers of the port and centre windshield panels. The vision loss was such that the subsequent landing had to be carried out from the co-pilot's position. The weather radar on the aircraft had apparently failed just prior to the encounter.

### Lightning Strikes and Static Discharges

Although some 40% of lightning strikes on our aircraft occur in the area of the nose, it has only ever been necessary to change one of our transparencies following a strike. The aircraft concerned was struck just forward of the flight deck area, causing spots of molten metal to precipitate onto the outer surface of the port windshield panel. The metal deposits were eventually polished out and the subject panel has since been refitted to another aircraft.

Build up of static electricity on the flight deck transparencies has caused some operators considerable trouble, and in extreme cases has even damaged electrical equipment used in the transparency heating system. The problem only appears to affect certain types of aircraft.

Although our pilots have reported that electro-static discharges take place on our transparencies, this phenomenon has never given rise to any problems.

### Rain Repellents

In flight applied rain repellent systems are fitted to all our jet aircraft. However, in some cases the performance of the system has been unsatisfactory mainly due to difficulties in getting the repellent onto the windscreen panels.

Pre-flight applied repellents are used on some of our turbo-prop aircraft.

In general we have found that the effectiveness of a rain repellent only really becomes apparent when operating in very heavy rain. Such conditions are met rather infrequently on our European routes.

#### De-icing/Demisting

The heating intensities and control temperatures currently employed to de-ice/demist our transparencies appear to be adequate for the majority of conditions encountered on our routes.

In fact some years ago one of our Vanguard aircraft encountered some extremely severe icing conditions when operating over Spain. The water concentration level at the time was estimated to be some 6 times greater than the maximum continuous design case. Although some of the side (demisted) transparencies iced up, forward vision through the main windshield panels was maintained throughout the encounter without selecting HIGH heat. The heating intensity in use on the windshield panels at the time was 400 watts per sq.ft. with a control temperature of 35°C.

Slight misting of the internal surfaces occasionally takes place on some of our flight deck transparencies particularly when descending into conditions of high humidity.

A number of our older aircraft are not fitted with heated transparencies and employ a combination of fluid deicing and 'air blast' demisting for the purposes of maintaining forward vision.

#### In Flight Failures

There is little doubt that the sudden appearance of a crack in one of the flight deck transparencies can be rather disconcerting to a pilot if it occurs when the aircraft is pressurised. We have experienced several failures of this type but in each case the resultant damage was limited to one of the secondary plies.

However, to ensure that the correct action is taken by the pilot in the event of any trouble with the transparencies, data covering the more important transparency defects has now been included in the pilot's abnormal management drills.

A typical example of the information provided is shown in fig. 5.

Although our cabin windows are fitted with a standby pressure panel to comply with the fail safe philosophy, we instruct our pilots to descend and depressurise the aircraft whenever a panel cracks in flight.

Over the past 10 years we have experienced 8 such panel failures but in each case the standby pressure panel withstood the pressurisation load, and the subsequent action taken by the pilot resulted in the service being completed without further incident.

### ENGINEERING ASPECTS

It is generally accepted in civil aviation that there is little to be gained by lifing transparencies, consequently removals are only carried out in the event of unserviceability.

#### Types of Failure

With respect to the flight deck transparencies, delamination and electrical defects account for a large proportion of our total removals, the remainder being brought about by physical damage (e.g. cracking, glass shear, etc.), optical distortion, and other miscellaneous defects.

Virtually all our cabin window removals are caused by crazing, although this defect can be tolerated to a certain extent before a window change becomes necessary. It is interesting to note that with only a few exceptions our experience with crazing is limited to the outer panel even though on some of our older aircraft this particular panel is normally taking no pressure load.

This suggests that as contamination of the exposed surface is one of the factors giving rise to crazing, there is some advantage to be gained by installing the normal pressure carrying panel in the inner position.

Some five years ago a number of cabin windows were removed from our aircraft for suspected contamination of the interspace cavity between the two panels. Investigation revealed that the interspace surfaces were covered in a series of spider shaped deposits shown in fig. 6. Our immediate reaction was to assume that they were either a rare species of fungi or the results of a chemical change in the acrylic.

Sample windows were sent to the Commonwealth Mycological Institute in London for analysis.

In due course the Institute confirmed that the deposits were probably caused by the evaporation of water droplets (containing harmless impurities in solution) impinging on the interspace surfaces of the two pressure panels.

Provided vision is satisfactory we no longer remove windows affected in this manner.

### Overhaul/Repair Considerations

Unlike the majority of flight deck transparencies a considerable proportion of cabin windows removed for crazing can be reclaimed by either polishing out the surface damage or by replacement of defective panels. In order to maintain close control of the work carried out all window recertification is cleared through our component overhaul facility.

This same facility is also capable of carrying out minor repairs to certain flight deck transparencies, although one of the most successful repair schemes developed over the years, namely relamination\*, is sub-contracted out to one of our transparency suppliers.

### SERVICE TRIALS

It has always been our policy to keep up to date with transparency development and to provide a means whereby new ideas in transparency design can be evaluated under service conditions.

### Wire Heated Transparencies

When our new jet aircraft entered service in 1964 the reliability initially achieved with the transparencies left a lot to be desired. (The M.T.B.F. for the main windshield panels being only 1500 unit hours). At that time, most of our competitors in Europe were operating aircraft fitted with wire heated transparencies achieving an M.T.B.F. in excess of 10,000 unit hours. A decision was thus taken in 1968 to fit a number of wire heated transparencies to our aircraft in order to establish whether a similar level of reliability could be achieved.

Special tests carried out on a test flight soon demonstrated that the new transparencies would not be suitable for use on our aircraft. Although the wire heater improved the light transmission in daylight, it produced adverse optical effects at night of sufficient magnitude to significantly affect the pilots judgement of the landing flare. This was particularly noticeable in conditions of marginal visibility. The effect was apparent even with the heating switched off.

\* This consists of re-autoclaving a transparency in order to remove areas of delamination.

### Edge Heating

In parallel with the trials on wire heating, ground tests were also being carried out to evaluate a development of the existing transparency featuring additional heating in the edge.

A number of these 'edge heated' transparencies were fitted to our aircraft for service evaluation and it quickly became evident that the reliability had been improved by a considerable margin. Edge heating now features in a large percentage of our transparencies and the M.T.B.F. currently being achieved is 12,000 unit hours, compared with the figure of 1,500 unit hours achieved with the original design.

### Acrylic Transparencies

Service trials have also been carried out with acrylic extended vinyl interlayer transparencies. A number of these fitted to our Vanguard aircraft have achieved lives in excess of 14,000 flying hours without failure. The results of these trials were instrumental in causing us to select transparencies of similar design for fitment to our twin jet transport aircraft.

## FUTURE REQUIREMENTS

### Flight Deck

Flight deck panels constitute the major proportion of the civil operator's total expenditure on transparencies. It is therefore in this area that the maximum benefit can be derived from continued development and new thinking.

Even though the 'edge heated' transparency has proved to be reliable the manufacturers have now produced evidence to show that the multi-laminate transparency without a thick vinyl interlayer is more likely to achieve the order of reliability desired by the operator.

Early set backs with certain glass faced acrylic transparencies of this type, however, indicate that there are still a number of problems to be overcome. Although steps have been taken to improve the reliability it is too early to say whether it will achieve a level acceptable to the civil operator.

In the case of the glass multi-laminate transparency, the ever present problem of skyjacking involving the use of firearms has presented the transparency designer with a new set of problems. Whatever steps are taken to cope with these it is essential that the reliability potential of the transparency should not be compromised.

Although sufficient tests have been carried out in the past to demonstrate the advantages of stretched acrylic with respect to ballistic damage, these tests were concerned primarily with either fighter or helicopter canopies working at very low cabin pressure differentials.

Additional type testing should therefore be seriously considered for all new civil aircraft transparencies to verify that they are capable of withstanding damage caused by the use of firearms from within the pressure cabin.

The prospect of having to change an unserviceable flight deck transparency is an experience the civil operator would rather forgo, particularly as the transparencies on newer aircraft appear to be getting larger and heavier. In order to minimise the effect of such unserviceability it is suggested that both the aircraft and transparency designer should give serious consideration to the following requirements :-

- (1) The transparency shall be designed to tolerate minor damage likely to be incurred in service, at least until the next service check when a replacement can be fitted with minimum interruption to services. If necessary the operator is prepared to restrict the operating altitude or airspeed of the affected aircraft in order to achieve this aim.
- (2) The transparency shall also be designed to permit the operator to carry out certain in situ rectification.
- (3) Replacement of a transparency shall be carried out with the minimum amount of specialised ground equipment and without the need for special sealants.
- (4) The transparency shall also be designed to permit replacement of certain component parts in the operator's overhaul facility. This could extend to such components as the splinter shield or heater glass assembly.

#### Passenger Cabin

Most operators are aware of the limitation imposed by the employment of acrylic in the construction of cabin windows. Even stretched acrylic has to be treated with a reasonable amount of care.

With the advent of the SST aircraft the transparency designer has now been forced to consider new materials capable of withstanding the high temperature levels encountered at supersonic speed.

Although chemically toughened glass has been selected for this particular application certain types of thermally toughened glass have also been considered.



With the obvious advantages of these materials with respect to their excellent chemical and abrasion resistance and the fact that they can now be obtained in suitable thicknesses, it is considered that a strong economic case can be made for using these same materials in the construction of cabin windows on subsonic aircraft.

In conclusion it is hoped that continued research will ultimately come up with new transparent materials combining good chemical and heat resistance with satisfactory mechanical and optical properties.

In order to achieve further improvements in transparency design it is necessary to take into account current experience. By virtue of his high aircraft utilisation the civil operator is readily able to furnish the transparency designer with the data he requires on current transparency performance, and can also provide a 'platform' for evaluating the performance of new transparency designs under service conditions.

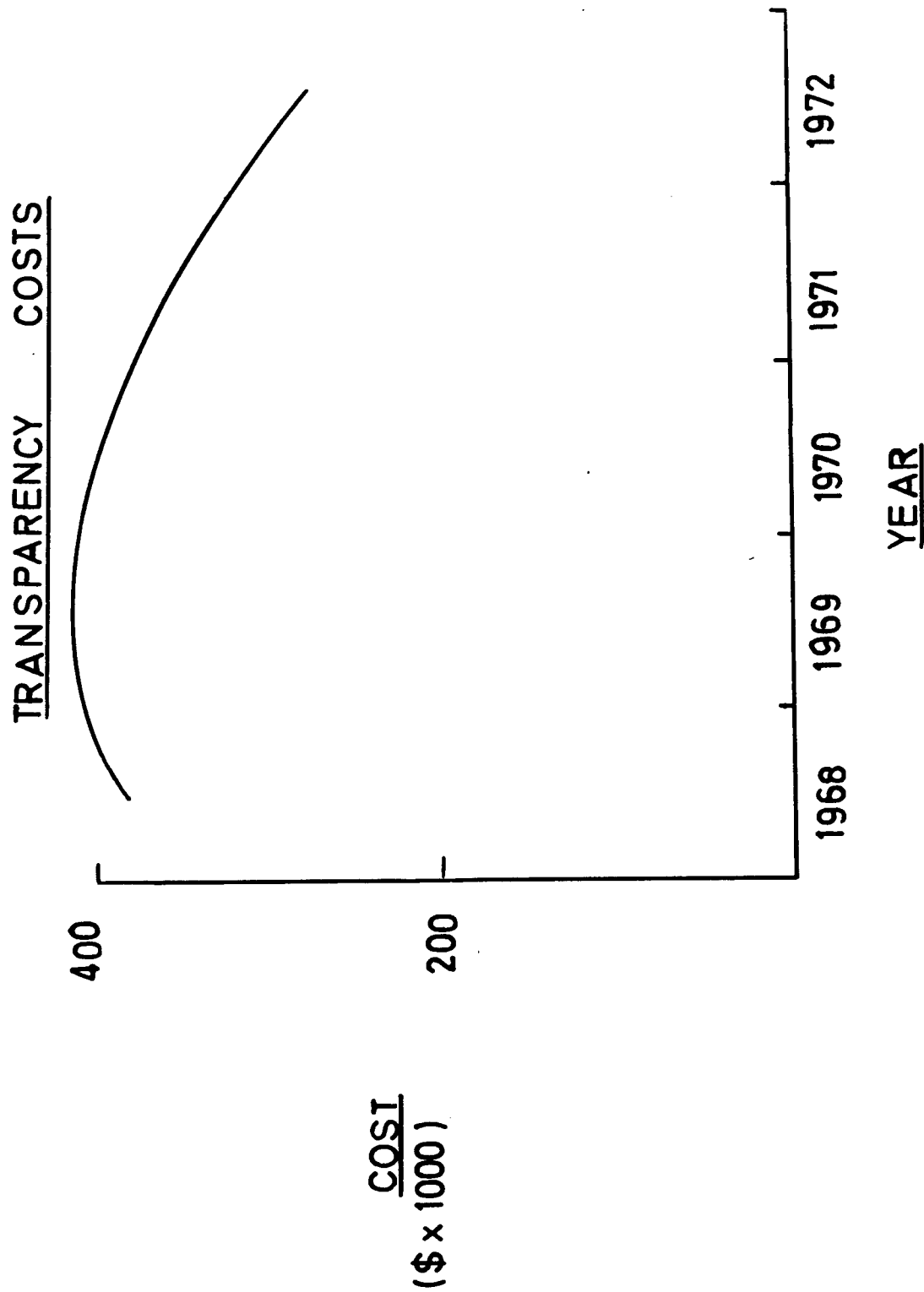


FIG.1

# RECORD OF BIRD STRIKES

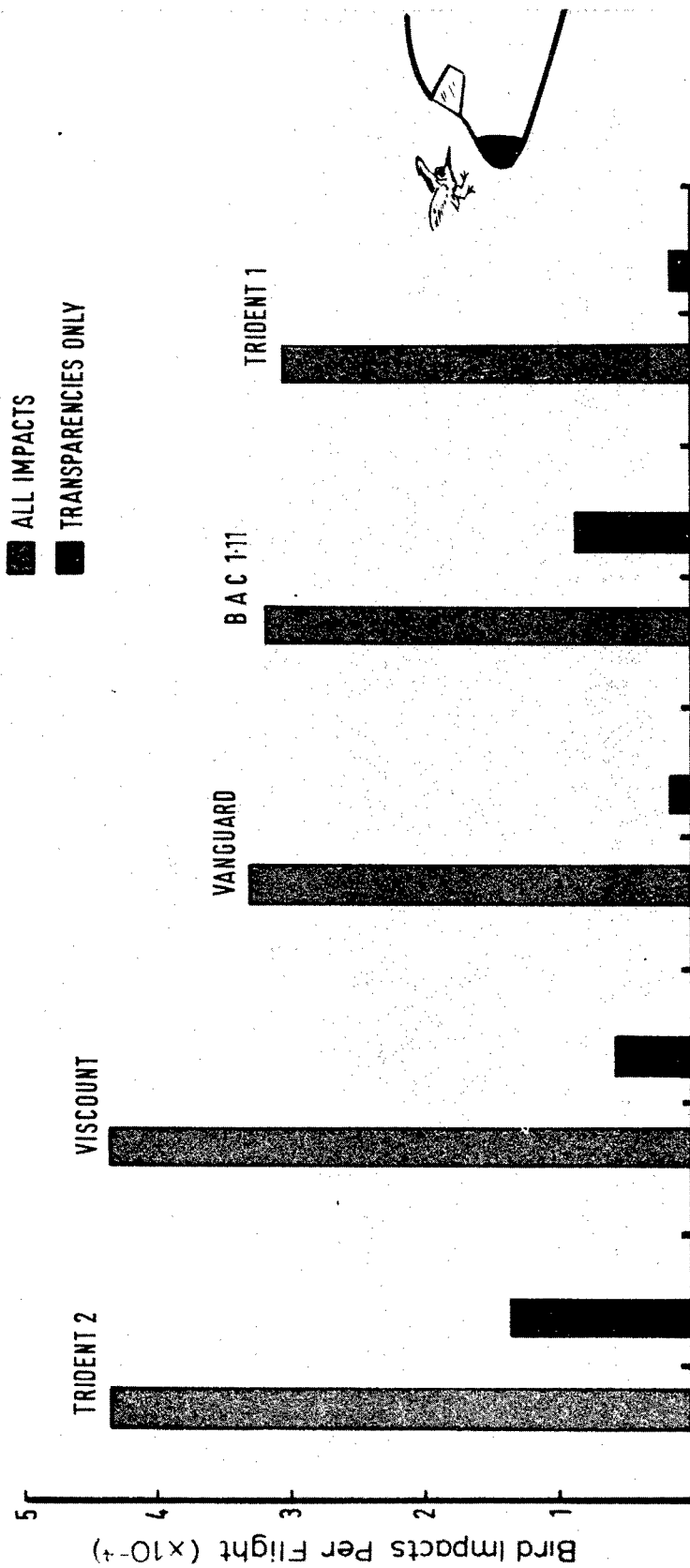


Fig 2



Figure 3 Hail Damage



Figure 4 Hail Damage

## WINDSCREEN/WINDOW FAILURE

| SYMPTOMS   | ACTION SEQUENCE |           |                |                        |                        |
|--|-----------------|-----------|----------------|------------------------|------------------------|
|  | Windscreen      | DV Window | Eyebrow Window | Rear (Teardrop) Window | Passenger Cabin Window |
| Shattering of intermediate glass laminate (complete loss of vision)          | 4:5             | 4:7       | -              | -                      | -                      |
| Cracking of outer glass laminate (partial loss of vision)                    | 5:8             | 6:8       | -              | -                      | -                      |
| Cracking of inner glass laminate (partial loss of vision)                    | 6:8             | 6:8       | -              | -                      | -                      |
| Delamination of the glass and vinyl in excess of one third of the panel area | 6:8             | 6:8       | 6:8            | -                      | -                      |
| Rapid increase in any delamination of the glass and vinyl                    | 4:7             | 4:7       | 4:7            | -                      | -                      |
| Shattering of inner glass laminate   | -               | -         | 4:7            | -                      | -                      |
| Shattering of outer glass laminate   | -               | -         | 6:8            | -                      | -                      |
| Cracking of outer panel  | -               | -         | -              | 1:4:9                  | 2:3:4:9                |

Action List (the items to be actioned in each particular case are indicated in the table).

1. Seat harness - On.
2. Cabin notices - On.
3. Evacuate area within 6 ft of window, if possible.
4. Descend and depressurise as soon as practicable.
5. Observe Unheated Windscreen Limiting Speeds.
6. No immediate action.
7. Further unpressurised flights are permissible provided any vision loss is accepted.
8. Further pressurised flights are permissible provided any vision loss is accepted.
9. Further unpressurised flights are permissible provided the outer panel is complete.

Fig. 5 Abnormal Management Drills

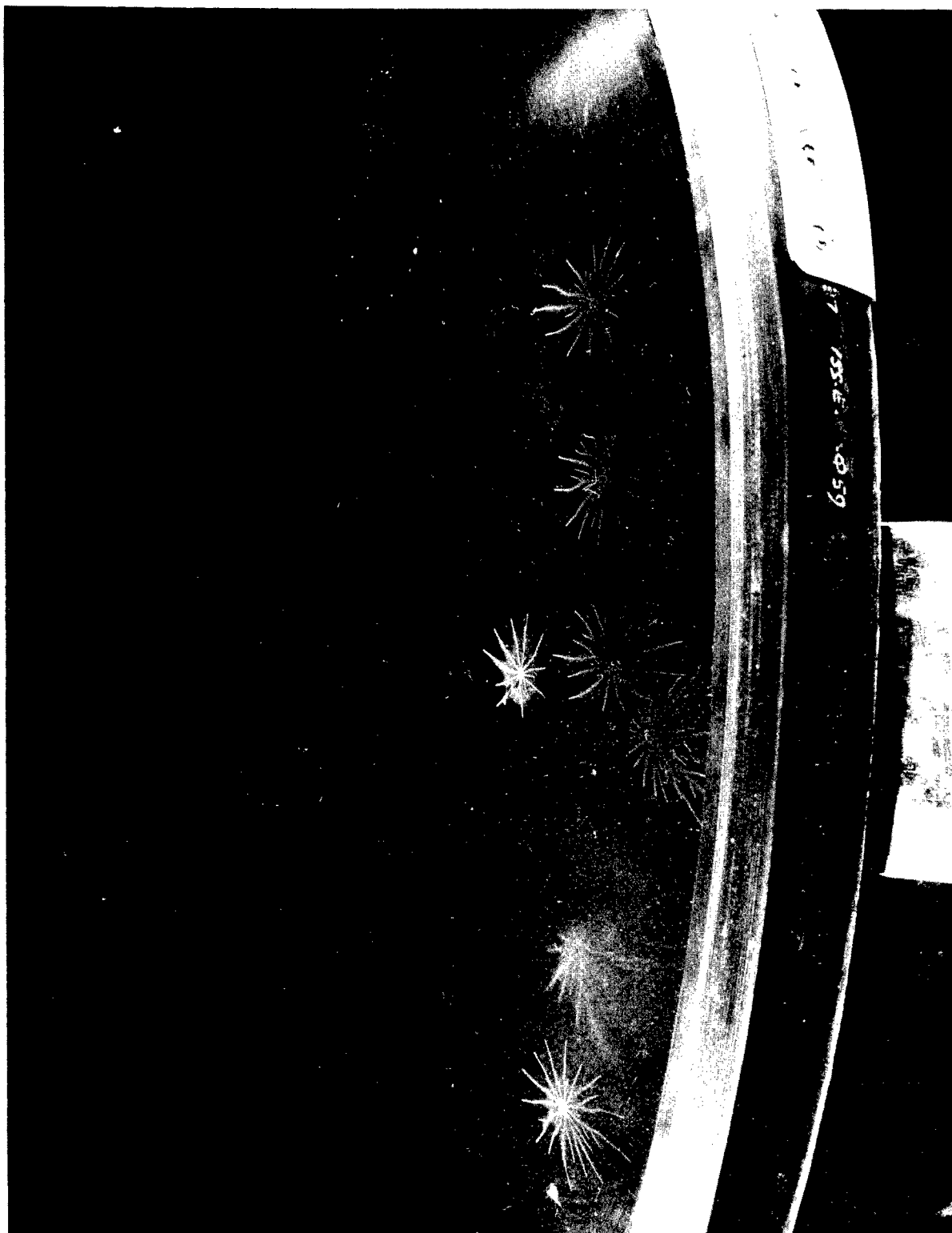


Figure 6. Interspace Contamination

DESIGN CONSIDERATIONS AFFECTING  
PERFORMANCE OF GLASS/PLASTIC  
WINDSHIELDS IN AIRLINE SERVICE

Jan B. Olson  
Sierracin Corporation  
Sylmar, California



DESIGN CONSIDERATIONS AFFECTING  
PERFORMANCE OF GLASS/PLASTIC WINDSHIELDS  
IN AIRLINE SERVICE

Jan B. Olson

Sierracin Corporation

ABSTRACT

The Boeing 747 was the first large airplane to use curved glass-faced plastic windshields. The numerous advantages of this type windshield have caused it to be used in other large commercial and military airplanes designed after the 747; these include the Lockheed L-1011 and AMD "Mercure" jet airliners, and the Lockheed S-3A reconnaissance jet.

The design, testing and early flight experience with the 747 glass-faced plastic windshield was reported in two papers presented at the 1969 "Air Force Conference on Transparent Materials for Aerospace Enclosures". Now, after three years of airline service, it is time to review its performance. This paper presents MTBR history of the 747 windshield, and compares it to that of conventional flat glass windshields of earlier jet airliners. Several early service problems with the 747 windshield are discussed and analyzed.

More important, various design improvements which were developed and introduced jointly by Sierracin and Boeing to correct these problems are described, and the resulting improvements in MTBR are assessed. Finally, it sets forth design philosophies for curved composite windshields and the surrounding airframe structure which will assure improved initial performance in new applications.

## INTRODUCTION

The Boeing 747 wide-bodied jet ushered in a new era in commercial airliner design and, with it, a new era in aircraft windshield design. All previous commercial airliners had used flat laminated glass windshields. Boeing adopted the curved windshield concept for the 747 at an early stage in the design based on two distinct advantages; namely, better visibility (FAA and flight crews continually press for improvement), and better aerodynamics including less drag and noise at the traditional trouble spot, the upper outboard corner. Contrast the smooth curvature of the 747 forward fuselage shape shown in Figure 1 and the similar L-1011 in Figure 2 with the conventional flat panel design represented by a 707 shown in Figure 3.

The composite construction, that is, a glass faced plastic design, was selected by Boeing for the 747 in spite of its novelty, as being the most practical, producible approach to the curved windshield, and it afforded the lightest weight, safest solution with the best prospects for achieving requisite optical and contour qualities. The fact that this construction is reworkable for almost any conceivable failure at a fraction of the cost of a new replacement has also been a factor in its selection. Lockheed followed suit and adopted the curved composite windshield design philosophy for the L-1011 for essentially the same reasons.

There were considerable teething troubles with the 747 windshield, most of which were corrected on the L-1011 on the drawing board, Lockheed having in part benefited by the service experience of Boeing's pioneering effort. From the experience gained on these programs, some design philosophies basic to the use of this construction have evolved, based both on theoretical considerations and, in most cases, in-service verification. The prime purpose of this paper is to acquaint both windshield and airframe designers with these philosophies, and to establish the importance of the interrelationship between these two separate structures.

## TECHNICAL DISCUSSION

### The Composite Cross-Section

The reasons for the selection of the composite cross-section have been thoroughly explored in previous papers (References a, b, c, d, e, f, g, and h) and therefore will be repeated here only briefly. This concept combines the excellent abrasion resistance and thermal conductivity of glass with the superior toughness of certain plastics. The result is a near optimum combination using a glass surface ply and a stretched acrylic load bearing ply. In this case, the plastic load bearing ply is comprised of two individual acrylic plies, each independently able to carry pressurization loads in accordance with the dual load path, or structural redundancy fail-safe requirements imposed on large commercial aircraft by FAR Part 25. In addition to its other attributes, this construction using polyvinyl butyral (PVB) interlayers is reworkable such that the only replacement, in the event of failure, is of the non-structural facing plies and their attaching interlayers.

### Two Divergent Mounting Philosophies

Using the best established design practices available to them at the time, and the wealth of experience with flat glass windshields on pre-747 models, Boeing employed on the 747 the traditional all-glass windshield mounting philosophy of totally isolating the windshield from aircraft structural loads. This is often referred to as a "clamped-in" design. The windshield installation and mounting design which evolved from this philosophy is shown in Figure 4. Note that the surrounding aircraft structure is stiff by virtue of its deep section so that it can carry fuselage loads around the windshield opening, and the windshield is structurally isolated within its sub-frame by thick walled silicone sponge bushings around the mounting bolts. Furthermore, the sub-frame can rotate to some degree on the pressure seal at its interface with aircraft structure. In the 747 design, the frame (which is supplied as part of the windshield assembly) constitutes only a rather loose clamping arrangement, and the inner row of bolts serves only to reinforce the clamp. In this mounting approach, it is necessary to design the surrounding structure to the airframe's fatigue life requirements without depending on the windshield for any support. This, of course, dictates a heavy structure.

Lockheed, who followed Boeing in the preliminary design activity and was therefore able to anticipate problem areas based on some of the early 747 service experience, took a fresh look at the mounting philosophy of a curved composite windshield. They conducted a comprehensive pre-design test and development program from which evolved a completely different edge design concept than that employed by Boeing. Instead of isolating the windshield from fuselage structural loads, the Lockheed design shown in Figure 5 purposely carries those loads through the windshield. In this manner, the windshield reinforces the surrounding structure, allowing a lighter weight structure to meet the fatigue life requirements than would otherwise be the case. In the L-1011 design, the aircraft structure surrounding the windshield is specifically designed to be "soft" at the corners and in effect expands on pressurization to place the windshield in membrane tension. The windshield-to-frame, and frame-to-aircraft junctures have been carefully designed and controlled to provide maximum direct structural coupling between airframe and windshield, both to reinforce the surrounding structure and to develop maximum hoop tension in the windshield. The relatively complex bushing design shown in Figure 5 evolved during this developmental test phase to allow the introduction of these high edge tensile loads into the acrylic without developing fatigue problems at the mounting holes.

#### Abrupt Local Deflection -- A Potential Culprit

A critical design aspect with respect to the service life of a curved composite windshield has been found to be the degree of localized bending at the curved upper and lower edges, or sills, due to pressurization. As this pressurization occurs, the glass faceply, which has been rigidized against bending in this direction by its curvature, attempts to resist this deviation from its normal simple, or "flat-wrap", contour. It is, however, forced to conform because of the retention provided by the adhesive interlayer.

This deflection and loading phenomenon has been thoroughly investigated in instrumented testing, both in the laboratory and in flight. Figure 6 shows a typical stress distribution as recorded from strain gages on the glass outer ply of a 747 windshield in flight due to the combined effects of pressurization deflection and thermal gradients. As can be seen, the glass is "stretched" in the central area and "compressed" peripherally. This is analogous to attempting to make something which is thin but two-dimensionally stable, such as a

sheet of paper, conform to a more rigid three-dimensional contour, such as a basketball. One would expect stretching, perhaps tearing, in the central area, and compressing, probably wrinkling, around the edges. The nature of glass and the function of windshields prevents us from designing to these dimensional extremes, but the same forces resisting conformation are at work, explaining the stress pattern in the glass faceply shown in Figure 6. The interlayer and bond stresses required to restrain the glass in this stressed condition can be inferred from these values by analysis.

In addition to this bending phenomenon, the outer surface of the windshield's structural ply has stretched due to the pressurization deflection. Because of the elastic attachment of the glass faceply, it does not elongate to the same degree, but instead slides on the surface causing some shear deflection of the interlayer.

The relative deflections between the glass outer ply and the plastic structural ply at the upper sill due to pressurization and thermal gradients have been closely examined in laboratory tests such as that shown in Figure 7, and typical values are shown in Figure 8. Note that for the typical readings shown, the "in-plane" (parallel-to-surface) shear deflection is considerably greater than the "prying" (perpendicular-to-surface) deflection (.019 vs. .003 inches), but the resolution of the deflection triangle which considers a single element or "strand" of interlayer shows that the normal deflection results in slightly more tensile elongation of the interlayer (.003 vs. .002 inches). Therefore, in terms of bond-line tensile stress, an excess of which is the root cause of delamination, the "prying" action is somewhat more significant than the "sliding" action in spite of the greater magnitude of the latter.

It should be noted at this point that the initial concern about the composite construction, that is, bond-line shear due to the differential expansion between glass and plastic, has never been a problem. There have been no indications of bond failures directly attributable to differential expansion, such as shear failures at the ends of the greatest gage length; i.e., the diagonally opposite corners. Two of these opposite corners, incidentally, are relatively "cold" by design as can be seen in Figure 9, thereby apparently discrediting the "cold-edge" delamination theory as applied to this construction. It can be concluded from this observation that the adhesive bonds involved are

quite tolerant of pure shear loading, but less tolerant of sustained tensile loads, including those created by shear offset and the resulting extension of elastic interlayer material.

Contrary to the commonly held opinion, a much softer interlayer might be disadvantageous because, while reducing the shear stress, it will increase the shear deflection, thereby increasing the tensile stress component which results from shear offset (Reference Figure 8). In addition, the decrease in shear coupling of the faceply will increase the overall windshield deflection (hence the local sill deflection) resulting in a greater "prying" action. These two factors increase the tensile elongation of the interlayer, which may result in a net increase in delamination-producing bond-line tensile stress in spite of the reduction in interlayer stiffness. The growth of a delamination is primarily a peel failure which is a special case of bond-line tension where interlayer "softness" permits localized load introduction at the edge of the delamination, and the softer the interlayer, the greater the effect.

#### Considering Alternate Basic Mounting Philosophies

A review of deflection profiles for a variety of aircraft windshield mounting methods is presented in Figure 10. These deflection profiles resulted from an analysis in which an idealized curved model windshield (square in flat pattern, cylindrical in contour with two acrylic plies, but no faceplies) is considered with a variety of means of reacting the uniformly applied pressure loading. The analysis clearly shows that the 747 "structural isolation" or "clamped-in" mounting philosophy, represented by the simply supported curved plate model, allows the largest and most abrupt windshield deflection of any of the practical mounting arrangements. Adding fixity, or rotational restraint, along the upper and lower sill has little beneficial effect, serving only to move the point of maximum deflection slightly inward toward the center of the windshield. A noticeable reduction in the magnitude and abruptness of the deflection is accomplished if the two structural plies are fully coupled (i. e., acting as a single monolithic ply), rather than independently like leaves of a spring. The actual 747 windshield mainply assembly, coupled to some degree by the vinyl interlayer between acrylic structural plies, falls somewhere between these two extremes. The benefits of increased coupling were taken advantage of in a design change which will be discussed later.

The lowest deflection is achieved when the windshield model is loaded in hoop tension, resulting in a reduction in deflection of over 80 percent compared to the simply supported, or "clamped-in" case. The ideal case is pure hoop tension with no restraint at the upper and lower sills, in which straight line elements are allowed to remain straight in spite of any radial deflection, and no local sill bending whatever can occur. Note that the effect of sill restraint does not extend inward far enough from the edge to overlap and reduce overall deflection on this model, rendering it a liability instead of a benefit from the standpoint of deflection and the related factor, service life.

Elimination of sill restraint can present some problems, such as maintenance of aerodynamic smoothness and sealing throughout the pressurization deflection excursion, but with hoop tension loading this deflection is slight and these problems can be readily overcome, particularly if the concept is established during the preliminary design phase. Elimination of the sill restraint on the 747 was seriously considered as a retroactive design change at one point, but lack of hoop tension allowed excessive deflection making this approach appear impractical.

The entire theoretical 80 percent deflection reduction is probably not available because it is not practical to design post structure and mountings sufficiently rigid to provide completely positive hoop tension restraint, and also some mainly coupling does exist in an actual windshield, so that neither of the idealized extremes shown in Figure 10 is totally accurate. It can be seen, however, that there is considerable latitude for improvement by encouraging hoop tension as opposed to simply clamping the windshield.

Comparison of pressurization deflection measurements of the original 747 design with those of the L-1011 windshield confirmed this analysis, as evidenced by the fact that the L-1011 deflected less than the 747 in spite of its larger size, thinner section and larger radius of curvature. Comparison of early service data also supports this conclusion as will be explained later. The geometry, size and cross-section of these two windshields are compared in Figure 11.

#### The Service Problem -- Upper Sill Delamination

Our extreme interest in these considerations was prompted by a chronic failure mode on the 747 which was not revealed by the

accelerated life test programs conducted in the laboratory, both at Boeing and Sierracin. This is often the case due to incomplete duplication of aircraft structure, service environment and time. It was, however, soon revealed in airline service. The nature and location of that characteristic failure (delamination in the center of the upper sill at the acrylic-to-front interlayer interface) is easily explained on the basis of the preceding discussions.

This delamination, an extreme example of which is shown in Figure 12, is non-structural, rarely caused an electrical failure and was therefore typically allowed to progress until it began encroaching on the prime vision area before replacement was required. The delamination was the result of high interlayer and adhesive stresses required to retain the glass faceply when subjected to localized pressurization deflections in the sill areas in flight.

These "hold down" stresses are most severe at the upper sill, largely due to the fact that the 747 windshield is a conical section, and the smaller radius at the upper sill both causes the glass to be stiffer in bending in that area, and also the stress required to retain the glass against a given hoopwise compressive load is inversely proportional to the radius (from the pressure vessel hoop tension equation, but in reverse). In addition, the flat pattern geometry (Reference Figure 13) shows this "indented" central portion of the upper sill to be "reinforced" by the adjacent protruding corners (shown shaded), and it is therefore stiffened because it is not able to deflect independently like a protruding "flap", such as exists at the lower sill (also shown shaded), would do. In support of these theories, note that over 93 percent of all localized delaminations on the 747 windshield have been at the upper sill in spite of the fact that greater overall deflection occurs in the lower sill area.

In the original design, this upper sill delamination failure mode was dominant, and occurred with regularity at low service times. Inasmuch as it was too late to revise the basic mounting philosophy (that would entail changes to the surrounding fuselage structure), it was necessary to solve the problem within the windshield itself. A very comprehensive design refinement program was undertaken jointly by Boeing and Sierracin, with the dual aims of reducing the localized deflection in the upper sill areas, and also minimizing the windshield's sensitivity to that deflection.



### Solution to the Service Problem -- Progressive Design Refinement

The 747 design evolution is shown in much simplified form in Figure 14. Using a test set up as shown in Figure 15, measurement of the deflection profile of a straight line element due to pressurization is used as a yardstick of the effectiveness of stiffness-enhancing design changes. These deflection profiles and corresponding service performances for the most significant design variations are shown in Figure 16.

The first structurally significant change to the 747 windshield was from a .085 inch thick pre-formed, chemically-strengthened glass (Corning's "Chemcor") outer ply to one of initially flat .050 inch thick glass, elastically formed during the lamination process. This change did nothing to enhance the stiffness of the windshield structure, but did reduce the resultant interlayer stresses by reducing the in-plane stiffness of the glass over 40 percent, and its bending stiffness nearly 80 percent. This change resulted in a significant increase in MTBR for upper sill delamination as can be seen in Figure 16. Both of these configurations are referred to as "unbalanced laminates" in Figure 14.

The next structurally important change was the substitution of a .050 inch thick glass abrasion shield for the original .12 inch polyester, making a "balanced laminate" sandwich structure of the windshield with high modulus glass "face sheets". This considerably reduced the deflection and also resulted in a very substantial improvement in service performance, again as shown in Figure 16.

A further increase in stiffness was accomplished by substituting a less plasticized, hence higher shear modulus version of the vinyl interlayer between the acrylic mainplies, thereby more closely approaching the fully coupled condition shown in Figure 10. Neither deflection measurements nor service data isolating this change are available yet, but initial service performance shows it to be superior to the preceding design.

This "stiff" vinyl was also used to attach the inner glass abrasion shield, thereby increasing the shear coupling at that juncture. Laboratory testing showed that the vinyl-to-acrylic interface where the delamination had been occurring is more resistant to creep tensile loading when "stiff" vinyl is used adjacent to the acrylic, but retention of the lower modulus "soft" vinyl was considered desirable, hence the "hybrid" (2/3 "soft", 1/3 "stiff") faceply interlayer.

The L-1011 windshield design has not yet adopted any of these stiffness-enhancing design changes and is therefore very similar in section to the original 747 design, differing only in acrylic thickness and substitution of a hard coat for the polyester abrasion shield/vinyl interlayer combination. As of this writing, the L-1011 windshield has not experienced a single sill delamination in service, with the high-time aircraft having over 2,000 hours and the total fleet time on 18 aircraft in excess of 17,500 hours. This clearly substantiates the conclusion of this paper that adoption of the structurally-loaded-windshield mounting philosophy used on the L-1011 will have a beneficial effect on service life, as the original 747 design had sustained several sill delamination failures at a comparable time in its introduction period.

Besides the major design improvements stated above, there have been a number of more subtle changes incorporated in both designs to improve delamination resistance; notably, improved laminating adhesives, more effective edge separators and refinement of laminating techniques. Some of these areas are not fully optimized yet, and work continues to refine them to maximum performance.

#### Other Windshield Problem Areas Exposed in Service

Two other significant design lessons were learned in the evolution of the current 747 windshield configuration, both of which coincided with the change from .085 inch thick to .050 inch thick glass. While the possibility of a precipitation static problem on the 747 was realized in the early stages of design, Boeing adopted a "wait-and-see" attitude knowing that a "fix" in the form of a stannous oxide static drain coating on the outside surface of the glass faceply could be easily incorporated if needed. Confirming this position, over 450 windshields flew in service without a static drain coating on the .085 inch thick faceply with no indication whatever of p-static problems. However, coincident with the change to the .050 inch thick glass, numerous glass faceply breakages occurred, some cases of which were known to have been the result of p-static penetration. The bulk of these breakages, however, resulted from using the same compressive layer thickness or "case depth" on the thin Chemcor (designated 0313) as was used on the thicker formed glass. Elastically forming the thinner glass has the effect of bringing the vulnerable central tension zone closer to the outside surface, or effectively reducing the depth of the protective compressive layer, making the .050 inch thick glass more prone to breakage due to surface damage, scratches, pits, etc.

The effect of bending and flight stresses on the "case depth" of the various types of faceply glass used is illustrated in Figure 17. Both the p-static and the case depth problems were corrected at Corning by adopting a revised Chemcor process with a thicker compressive layer (designated 0319), and adding a stannous oxide static drain coating to the outer surface. The incidence of glass breakage from all causes dropped abruptly with this change, and a valuable lesson had been learned.

Another chronic failure pattern, but less severe than the upper sill delamination, has been in the area of weather seals. There has been a series of changes to this design which ran the gamut from the original one which used three different silicones with a thin overlap onto the faceply, to an especially weather-resistant polysulfide with a very thick section over the glass edge. This last design has been performing very well and the incidence of failure due to moisture intrusion has dropped drastically.

Moisture ingress and resultant electrical failure is felt to represent the next service life limitation beyond delamination, and an overlapping metal Zee section to protect the seal has recently been adopted on the L-1011, largely due to some adverse service experience with the current seal design. The Zee section approach is also being considered on the 747, but not very actively as the most recent seal design is performing quite well without it. This Zee section has potential additional benefits in that it serves as a near ideal static drain path to ground, and can provide some degree of glass edge clamping, thereby reducing the edge load on the interlayer and bonds.

#### Peripheral Problems Affecting Windshield Performance

It is appropriate to mention some other problem areas that developed in service even though they are not attributable to the windshield or mounting design. Because these related problems caused windshield removals, thereby adversely affecting reported Mean-Time-Before-Removal (MTBR)/Mean-Time-Before-Failure (MTBF) values, they are therefore factors to be reckoned with by the windshield designer.

(For clarification, MTBR includes Removal for all causes, whether the fault of the windshield or not, and includes such things as accidental damage, bird strikes, hail and lightning encounters and unnecessary removals, while MTBF is intended to include only windshield Failures per se.)

About 5 percent of the total 747 failures have been reported as being due to overheat damage. Actually, there were probably many more, but the resulting delamination and burn-out often makes it impossible to positively identify overheat as the cause. These overheat failures are almost always the result of a system failure, usually the controller. They are, however, reported as windshield failures and therefore depress both windshield MTBR and MTBF figures, even though the windshield itself is not at fault.

Another similar case exists on the 747 with respect to outer ply glass breakage which, as a failure mode, accounts for about 13 percent of all removals. There was a windshield wiper alignment problem which occasionally permitted a metal button on the wiper arm to gouge and score the glass faceply at a specific point on the lower edge. It was subsequently overcome by adding a local thin stainless steel "ramp" over that area of the glass faceply, but until it was recognized as an "external" cause of windshield failure, it had had an undeserved adverse effect on windshield MTBF. It still appears in the MTBR figures. Undoubtedly other breakages resulted from external damage as well, but often the cause cannot be identified positively because the glass faceply, when it breaks in flight, tends to shed very cleanly, often leaving no trace of the origin of failure.

#### Structurally -- A Clean Bill of Health

A tribute to one of the basic attributes of the composite design approach, i. e., safety, is the fact that throughout all of this experience, there has never been a case of even the onset of any structural failure of either of the redundant acrylic plies. This experience includes some windshields which had been bird impacted and others which have been pummeled during radome- and fairing-destroying hail encounters.

#### Service Performance -- Reviewed and Projected

The cumulative results of all of the design changes as of November 30 was that the MTBR had been raised from a low of about 1,400 hours in early 1971 for the original design to a level of over 6,000 hours for the current "balanced" laminate design. Over 25 percent of the removals were for causes not attributable to windshield performance, per se. This data does not separately identify the stiff mainly inter-layer or the improved seal, and the MTBF of the latest configuration is undoubtedly much higher.

Figure 18 compares current 747 windshield MTBR's with those of other commercial aircraft during their early years. Note that the comparison is between the 747, currently three years after introduction, and others using the more conventional all-glass design philosophy after three years (in one case, after nine years) to present a valid basis for comparison. Some of those older models now show considerably better MTBR's owing to continuing refinement of the original windshield design. This typical pattern of low MTBR at the beginning of airline service, and steady improvement as problems are identified and solutions adopted, is already well established on the 747 composite windshield. With the aggressive continuing improvement program being conducted on it, an ultimate service potential exceeding a 10,000 hour MTBR is a realistic goal.

The continuing performance upgrading program consists of the comprehensive review and analysis of all failures, and the proposal and verification of all reasonable solutions. The verification testing of intended improvements varies with their nature, of course, but usually takes the form of deflection testing and measurements and/or laboratory life and environmental testing. If the improvement is unable to be adequately verified on these and analytical bases, the in-service evaluation is conducted before full-scale adoption. This program is being conducted on a continuing basis, with one or more intended design and/or process improvements under evaluation at any given time.

#### Fringe Benefits of Reworkability

Besides the obvious economic advantage, the reworkability of these windshields has another significant advantage. Virtually every removed windshield is returned to Sierracin for recycling. Upon receipt, each part is reviewed for cause of failure by experienced personnel, including full Engineering analysis where appropriate. Not only does this improve the reporting accuracy, but it significantly improves the response time and appropriateness of remedial measures, thereby compressing the time scale for the service life improvement which seems to be required by every new commercial airliner windshield as indicated in Figure 18.

## DESIGN CONCLUSIONS

A summary of the general design philosophies pertinent to curved composite windshields such as the 747 and L-1011 is as follows:

1. Unlike glass, modern transparent plastics are tough and ductile, with ultimate tensile elongations greater than those of most high strength aluminum alloys. Windshields of these materials should be designed to carry load as an integral part of the fuselage structure. This not only saves structural weight in both the windshield and surrounding aircraft structure, but it also improves the service performance of the windshield.
2. The edge mounting should be designated to minimize the deflection of straight-line elements, and this dictates maximum use of the hoop tension loading mode.
3. The windshield cross-section should be designed to maximize the bending stiffness consistent with considerations of weight optimization, bird resistance, fail-safe requirements, etc. Increased shear coupling of structural plies can be used to advantage to accomplish this.
4. The glass outer ply, interlayer and edge separator combination should be optimized to be tolerant to those local bending conditions that cannot be avoided.
5. At some point between .085 and .050 inches, glass faceplies reach a critical thickness for precipitation static on windshields with size, shape and aerodynamic considerations similar to those of the 747 windshield. A surface coating of stannous oxide has proved very effective in preventing p-static damage when the critical point is exceeded.
6. The weather seal design is important and deserves special design and test attention. In both the 747 and L-1011 windshields, seal failures showed up in service which had either escaped detection in the qualification test or had been masked by conditions peculiar to the test.
7. Careful attention must be paid to such peripheral equipment as windshield wipers and controllers lest they become important factors reducing the service life of the windshield.

## SUMMARY

This paper has described the lessons learned from early service experience on the Boeing 747 windshield, and how these lessons have been translated into design improvements on that windshield, and an improved initial design on the L-1011. In describing those lessons it has been necessary to dwell on the problem areas, and it is therefore important that we devote space and time to the positive aspects of the 747 windshield.

Actual service experience for the 747 windshield clearly demonstrates that the part has followed a typical windshield performance pattern. As service problems are identified and resolved, performance has improved resulting in 747 windshield MTBR after three years of service which compares very favorably with windshields in other airplanes at a similar point in their service history. An aggressive program of continuing refinement is expected to keep service life climbing steadily throughout the next several years. The L-1011 windshield has not accumulated enough service experience to date to yield meaningful MTBR data, but there is every indication that problems which plagued the early 747 windshield design have been avoided.

An interesting, cost effective and, we believe, unique aspect of this specific composite construction has proven out on the 747 windshield program; that is, the rework technology which allows complete rebuilding of a removed windshield to new-windshield standards. In this manner, the frame and mainplies are salvaged with a considerable resultant price reduction.

Windshields of the Boeing 747 initially, and subsequently the Lockheed L-1011, have pioneered a new concept for the aircraft designer. Their curved shape imparts the obvious aerodynamic, acoustic, and vision improvements, and additionally provides the designer further latitude in less obvious areas, such as providing more room for the installation of cockpit instrumentation. Beyond that, the use of plastic structural plies in these curved designs can result not only in the obvious weight savings in the windshield itself, but also allows the designer to save weight in the surrounding structure due to the plastic's toughness and ability to carry structural loads safely. The use of a glass outer ply provides the resistance to abrasion and

other environmental influences and the thermal conductivity necessary in windshields of this type. The increasing hijack threat may cause more emphasis to be placed on gunfire as a possible source of windshield failure, which would be yet another factor favoring the use of tough, ductile plastic materials.

Finally, the various "teething troubles" encountered in these programs, and their solutions, have been analyzed and condensed into a design philosophy in this paper to serve as a guide to the designers of future windshields of this general type.



## REFERENCES:

- a) Keith Gunnar, "Status of Program to Develop Composite Windshields Utilizing Plastics and Chemically Strengthened Glass". Paper presented at U. S. Air Force Conference on Transparent Materials for Aerospace Enclosures, Dayton, Ohio, December 1964. (The Sierracin Corporation)
- b) M. C. W. Davy, "The Design, Development and Testing of Glass/Plastic Composite Windshields". Paper published by The Sierracin Corporation, March 1967.
- c) Keith Haviland, "Improved Aircraft Windshield Glazing Techniques - Study". Report No. DAC 33494, Douglas Aircraft Corporation, February 1967.
- d) Frank Burnham, "L-1011's Cockpit Stresses Visibility, Comfort". American Aviation Magazine, March 3, 1969.
- e) George L. Wiser, "Sierracin Glass/Plastic Composite Windshields". Paper presented at U. S. Air Force Conference on Transparent Materials for Aerospace Enclosures, June 1969. (The Sierracin Corporation)
- f) Donald S. Eberhart, "Glass Plastic Composite Windshields, Boeing 747 Superjet". Presented at U. S. Air Force Conference on Transparent Materials for Aerospace Enclosures, Dayton, June 1969. (The Boeing Company)
- g) John A. Vaccari, "Safer Aircraft Glasses Up Visibility, Resist Impact". Materials Engineering Magazine, November 1969.
- h) George L. Wiser, "New Materials in Aircraft Windshields". Presented at Society of Automotive Engineers, National Aeronautics and Space Meeting, Los Angeles, California, October 1970. (The Sierracin Corporation)

FIGURE 1 -- BOEING 747 COCKPIT

Note smooth blending of windshield into side panel/fuselage contour and panoramic view afforded by rearward positioning of side posts.

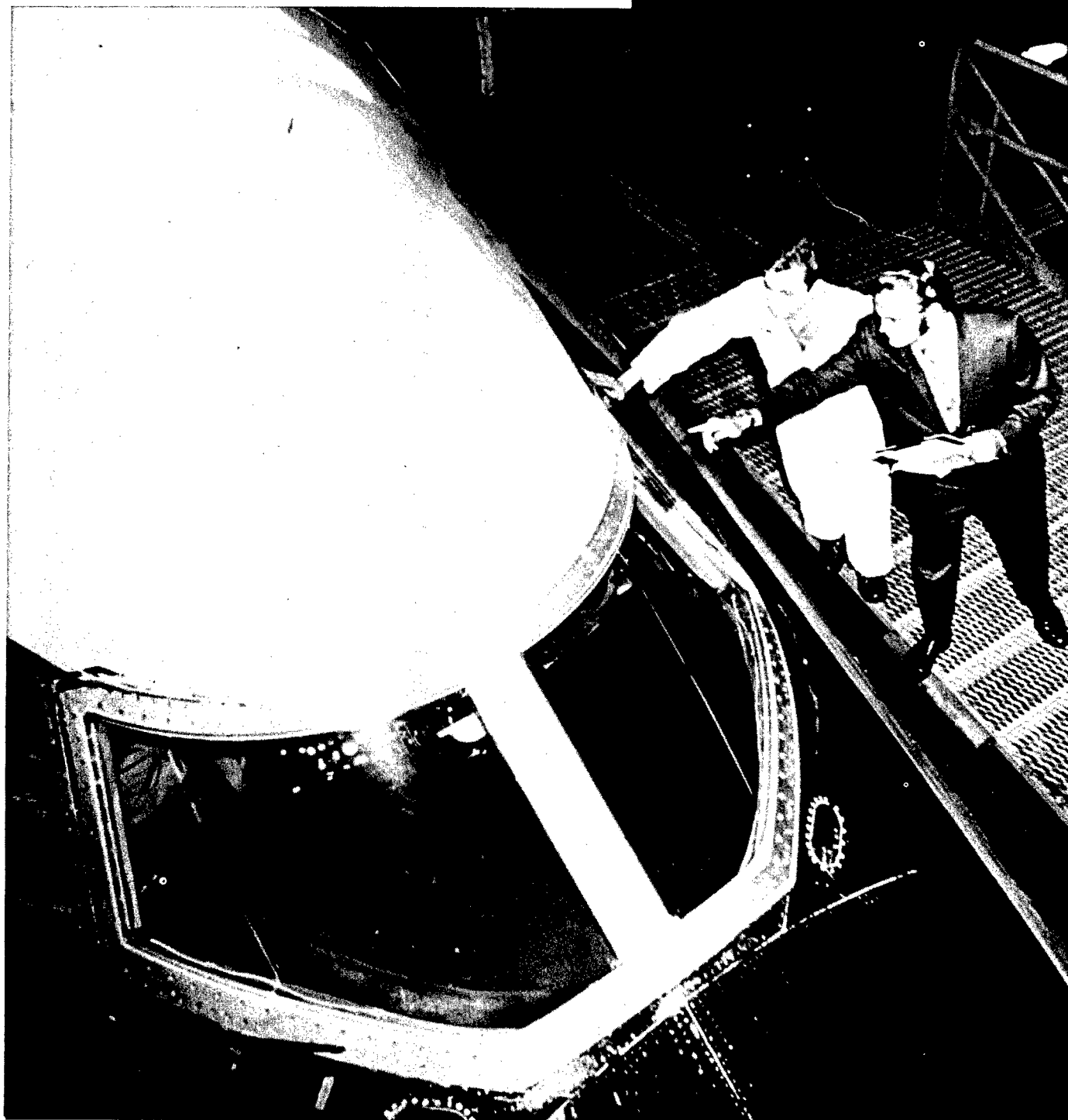


FIGURE 2 -- LOCKHEED L-1011 FORWARD FUSELAGE

Note how curved windshields and side panels blend smoothly into large diameter fuselage and how windshield side posts are positioned well aft (actually, in plane of control wheels) to provide panoramic view.

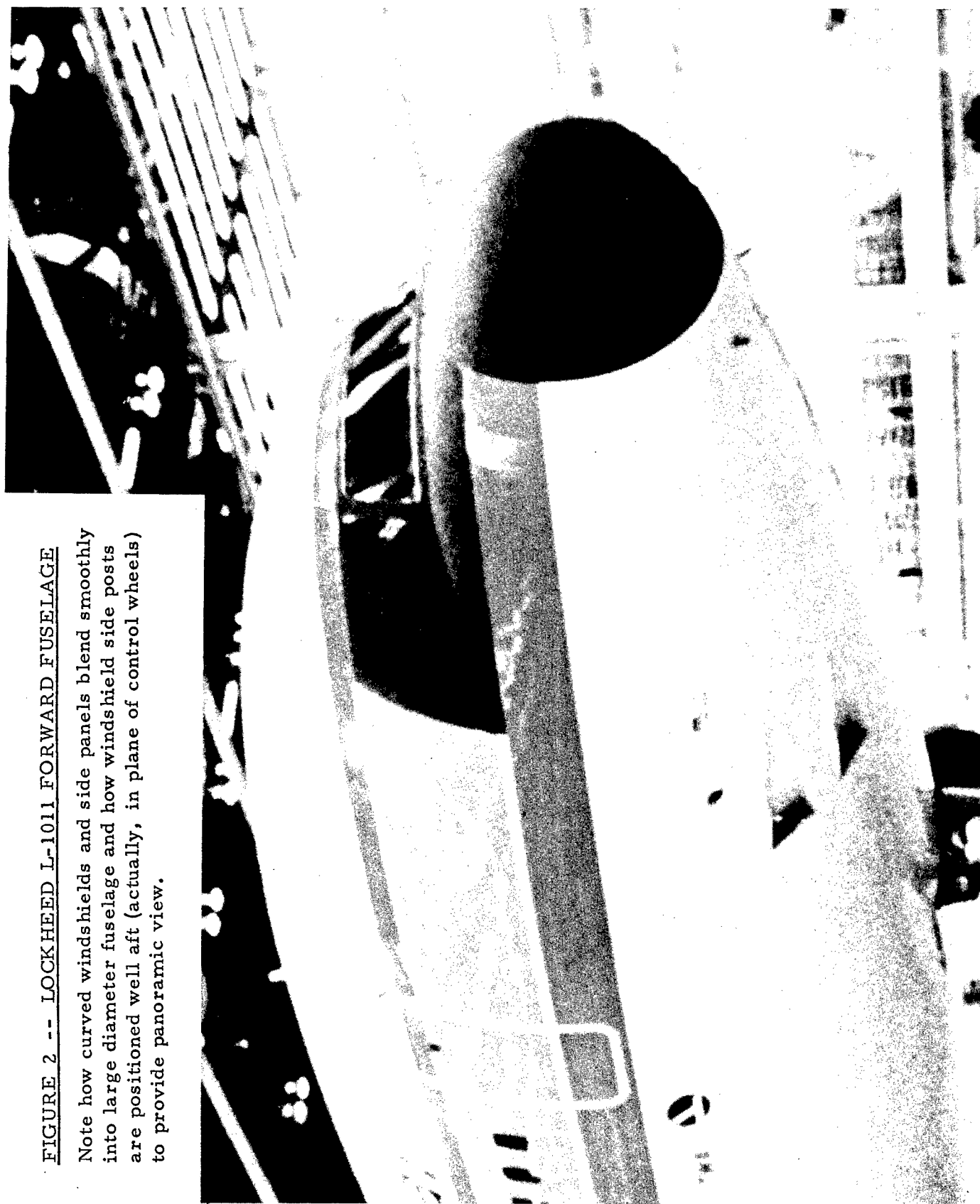
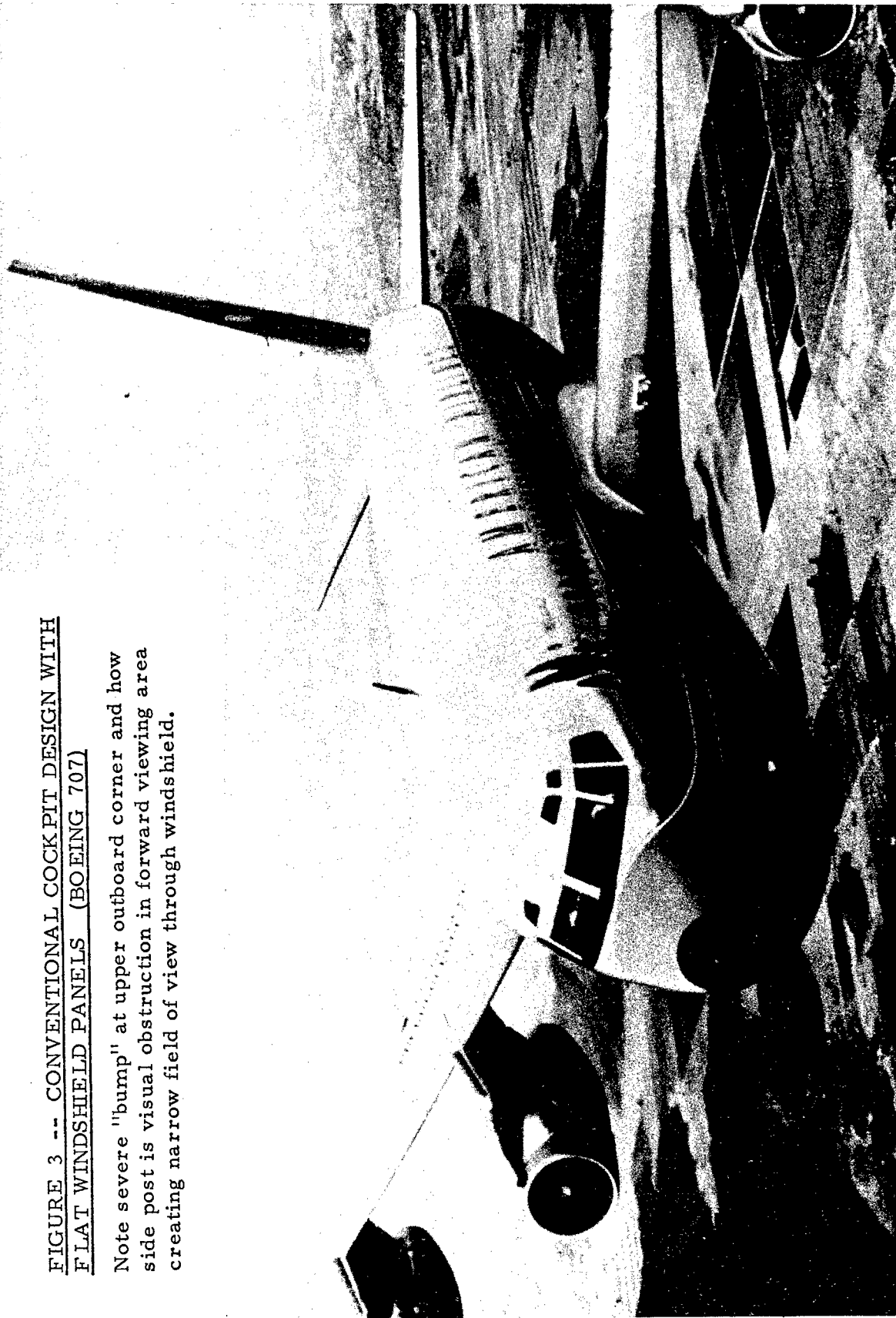
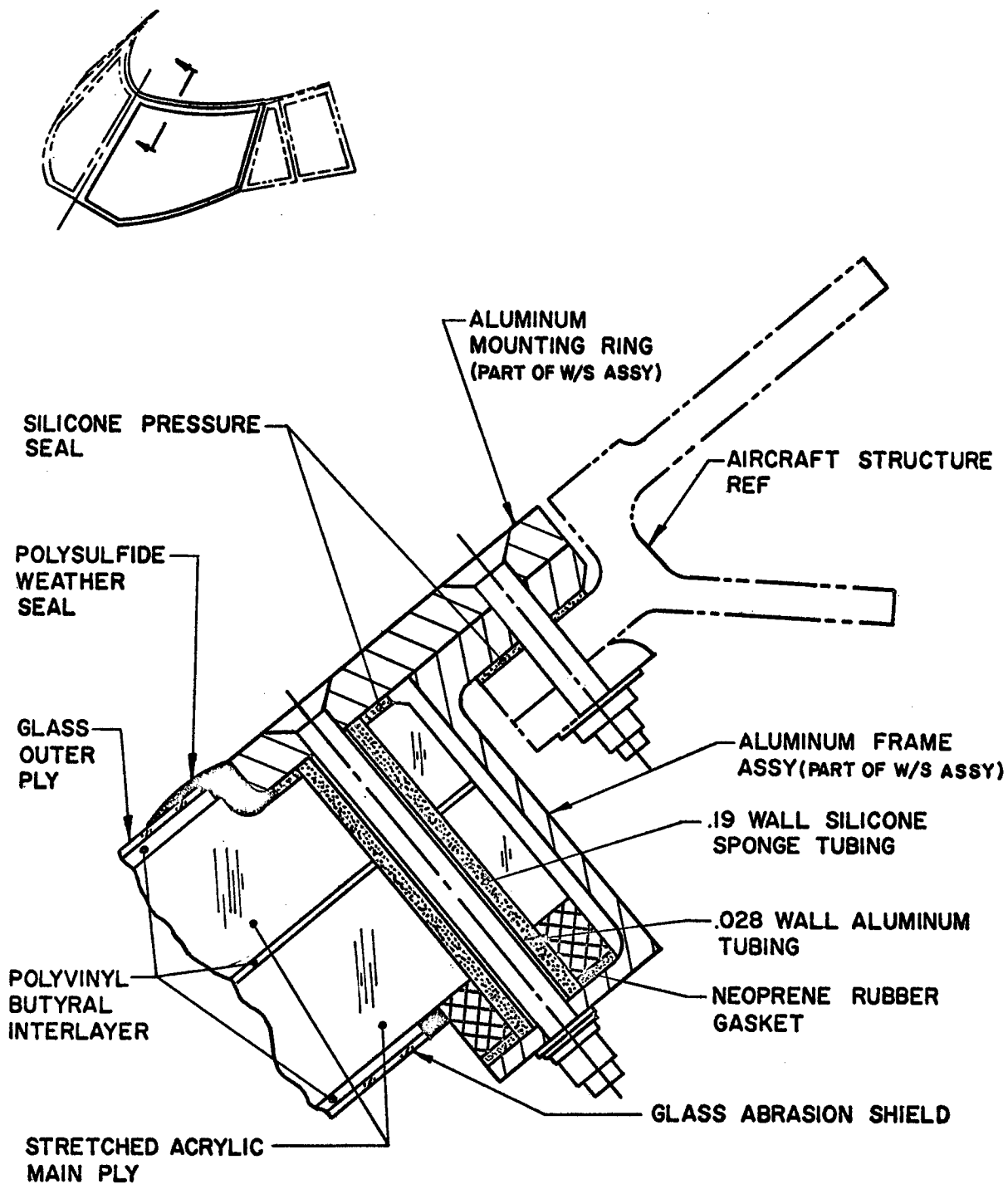


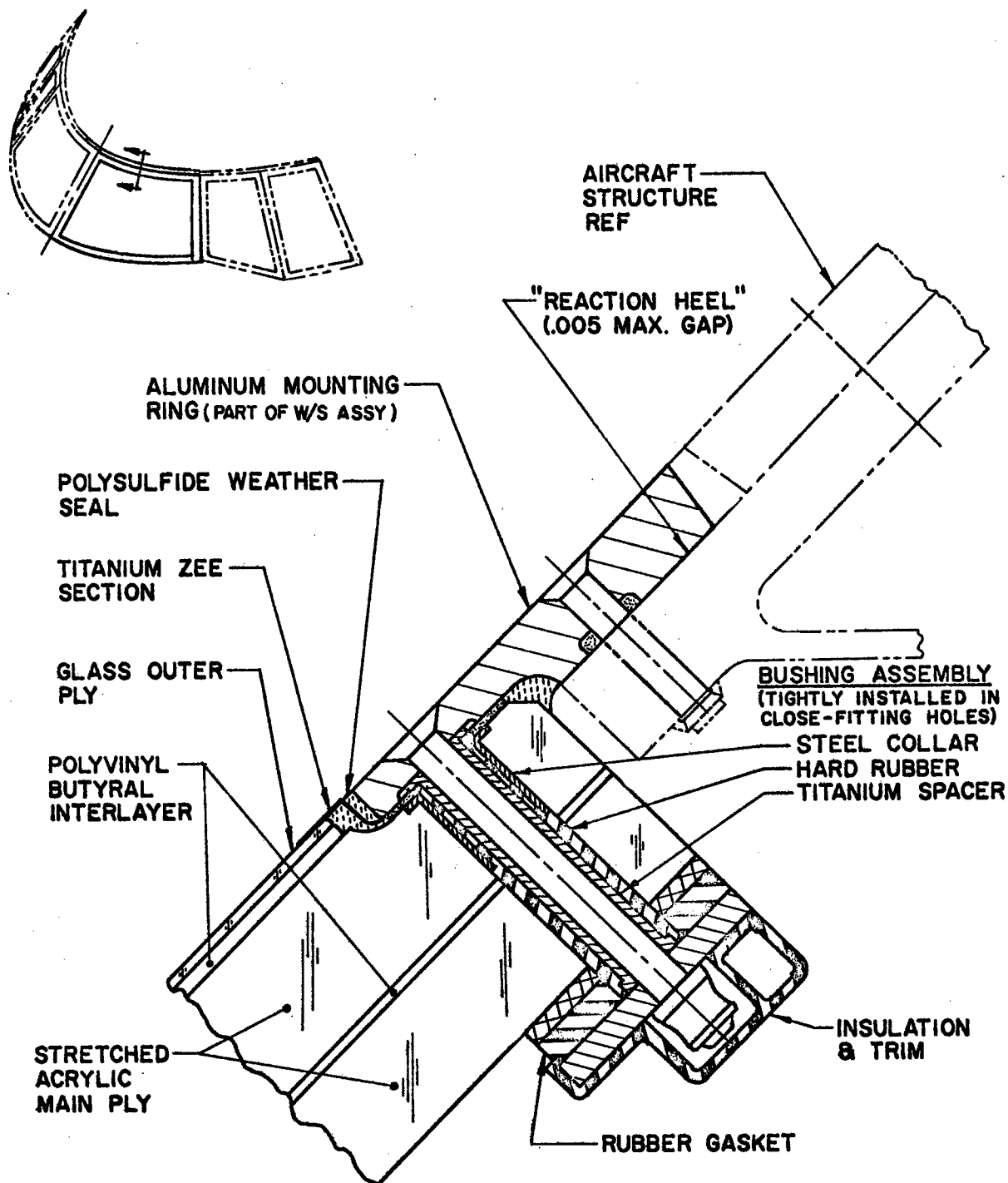
FIGURE 3 -- CONVENTIONAL COCKPIT DESIGN WITH  
FLAT WINDSHIELD PANELS (BOEING 707)

Note severe "bump" at upper outboard corner and how side post is visual obstruction in forward viewing area creating narrow field of view through windshield.

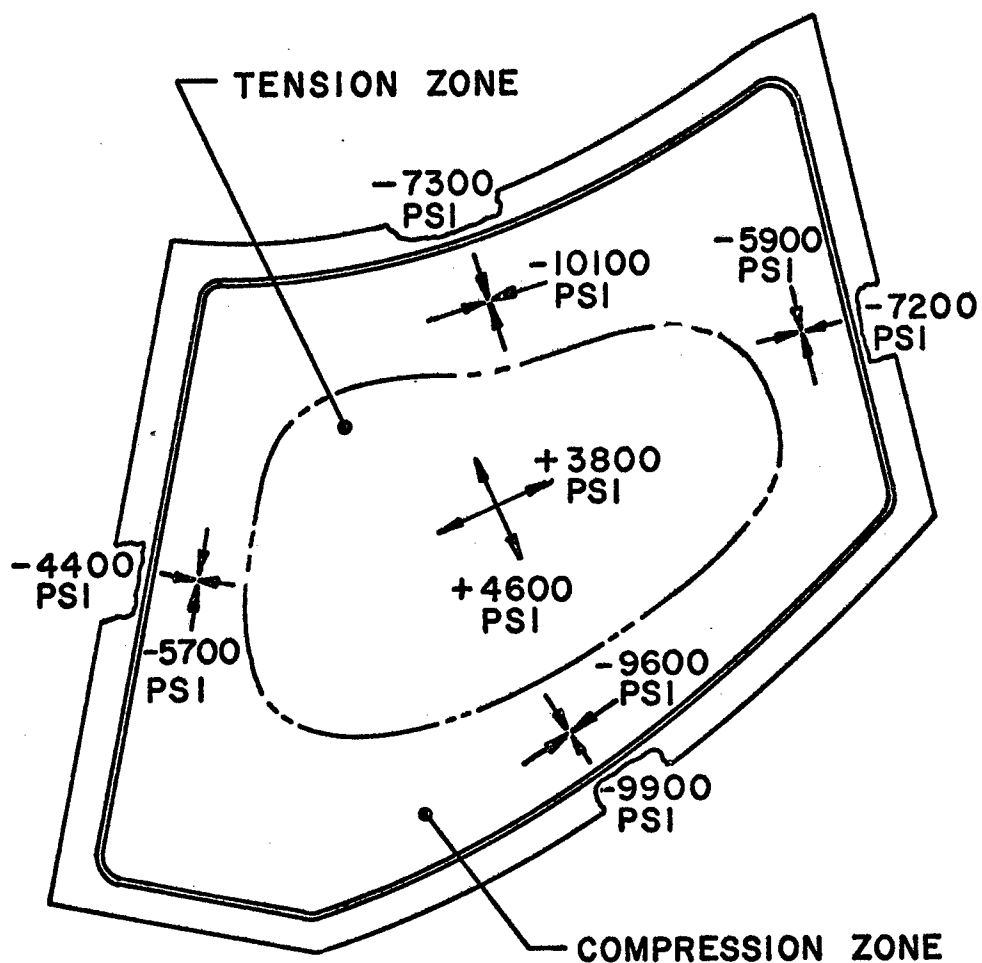




**FIGURE 4**  
**747 WINDSHIELD INSTALLATION**  
**(FULL SIZE)**



**FIGURE 5**  
**L-1011 WINDSHIELD INSTALLATION**  
**(FULL SIZE)**

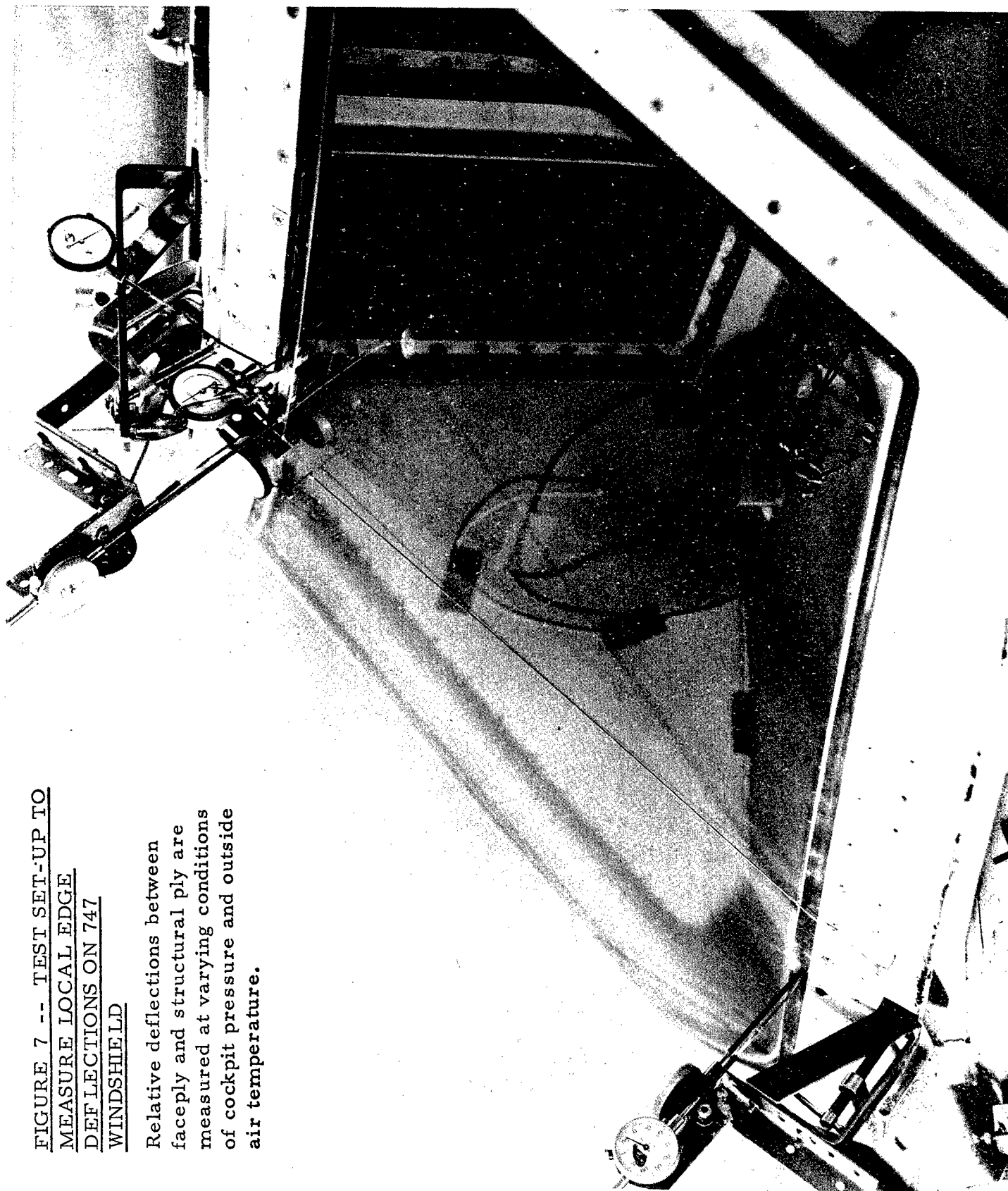


NOTE: READINGS SHOWN ARE TYPICAL OF DATA FROM 18 ROSETTE STRAIN GAGES ATTACHED TO GLASS OUTER PLIES OF TEST WINDSHIELDS AND FLOWN IN A VARIETY OF TEST CONDITIONS

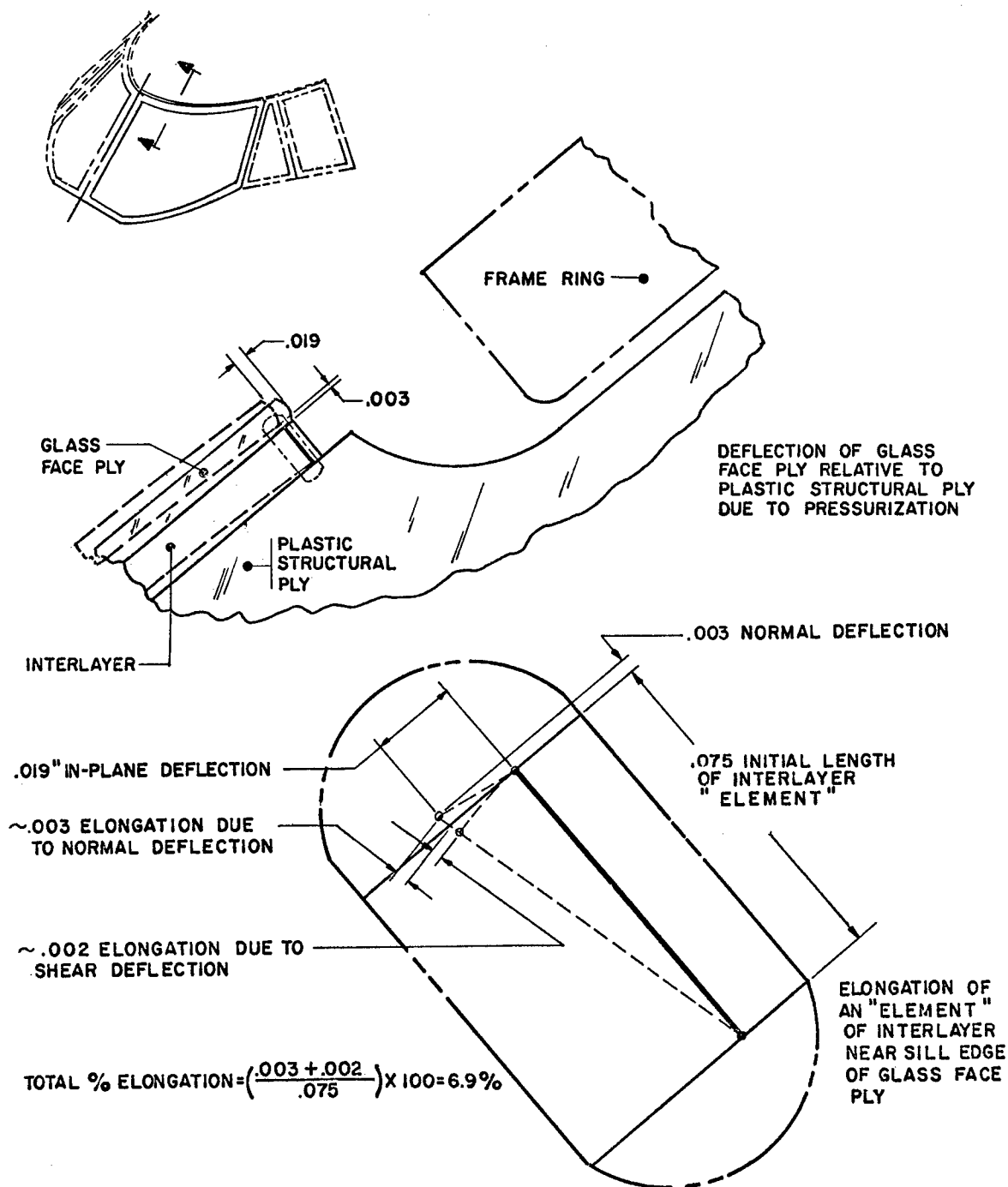
**FIGURE 6**  
**747 WINDSHIELD - GLASS**  
**STRESSES MEASURED IN FLIGHT**

FIGURE 7 -- TEST SET-UP TO  
MEASURE LOCAL EDGE  
DEFLECTIONS ON 747  
WINDSHIELD

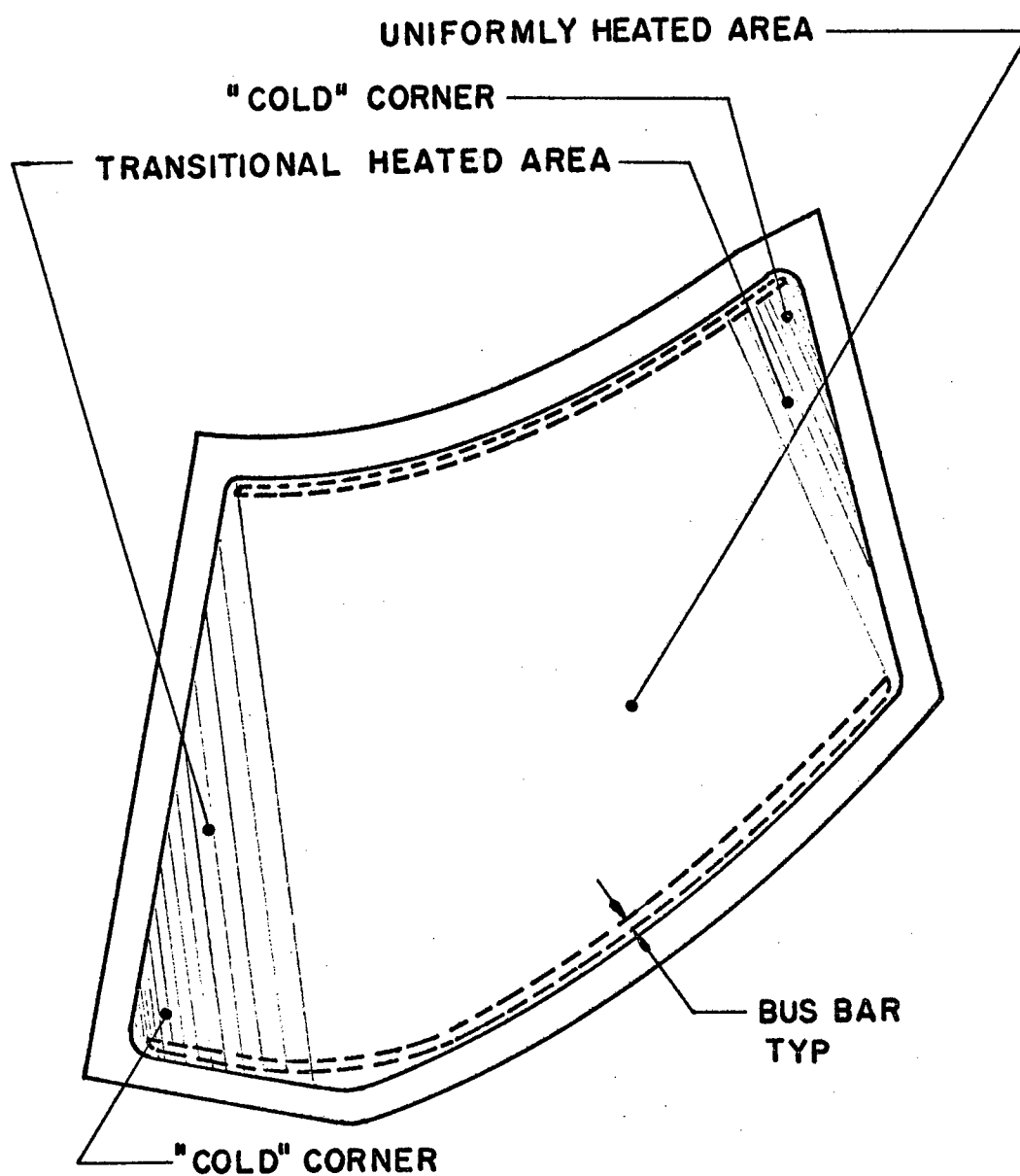
Relative deflections between  
faceply and structural ply are  
measured at varying conditions  
of cockpit pressure and outside  
air temperature.



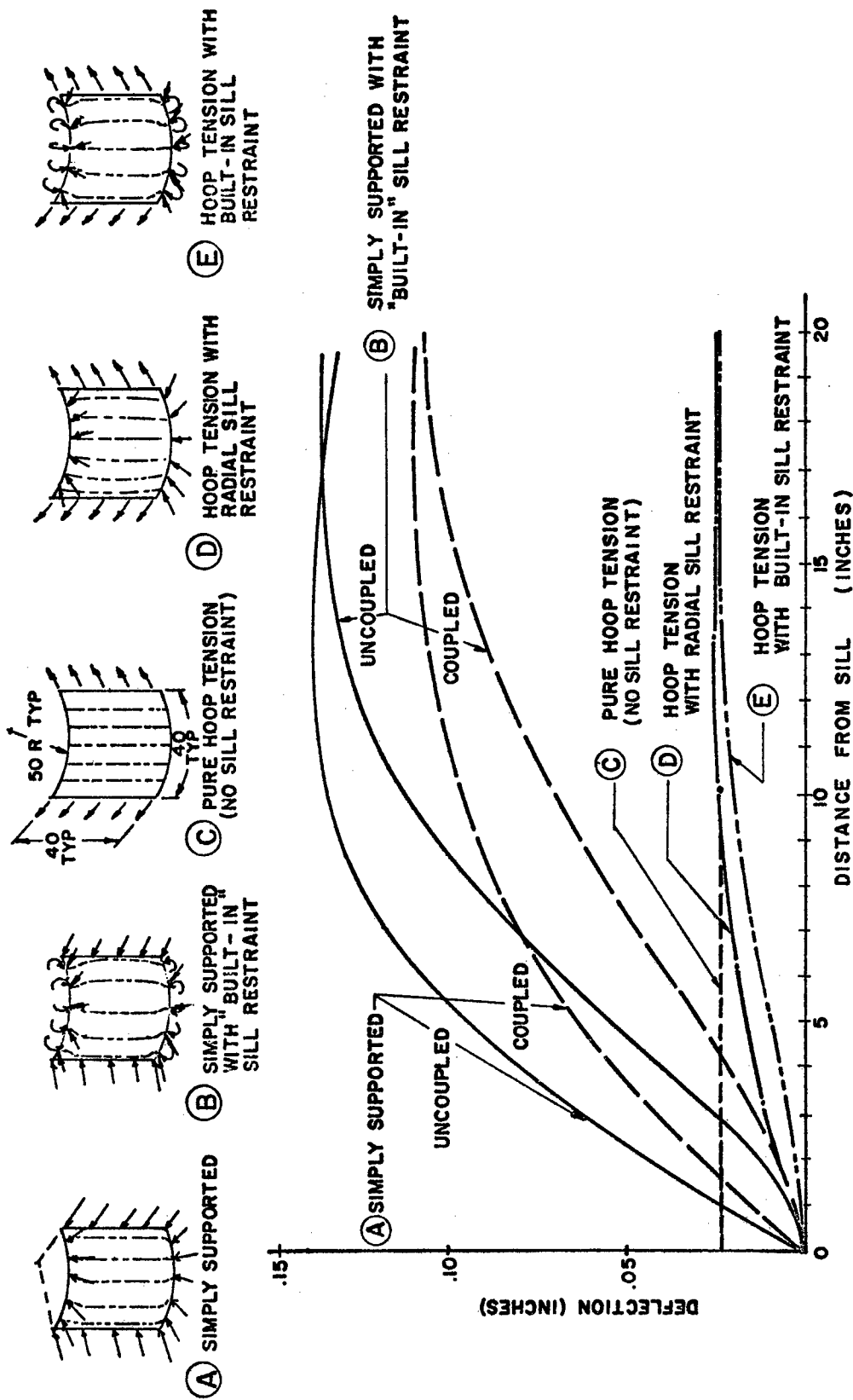




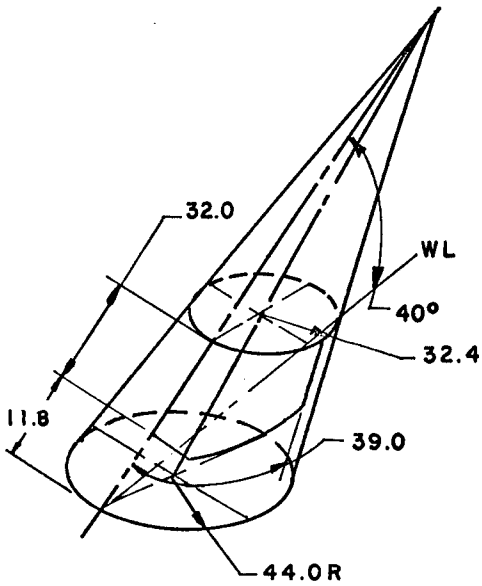
**FIGURE 8**  
**LOCAL RELATIVE COMPONENT DEFLECTIONS**  
**MEASURED DURING PRESSURIZATION**



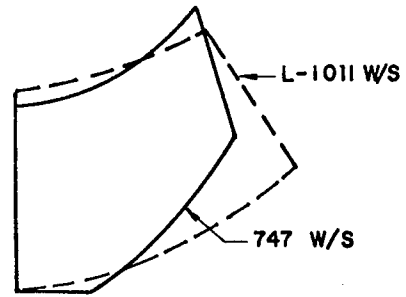
**FIGURE 9**  
**HEAT DISTRIBUTION ON 747 WINDSHIELD**



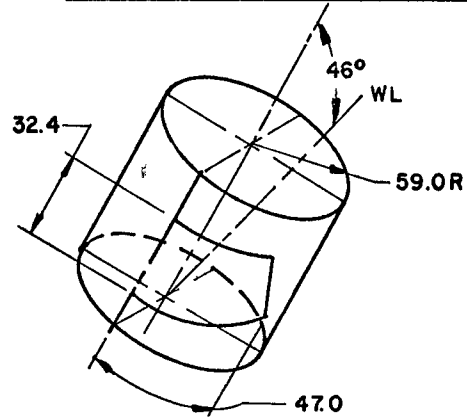
**FIGURE 10**  
**CALCULATED DEFLECTION PROFILES FOR A**  
**VARIETY OF WINDSHIELD MOUNTING CONCEPTS**



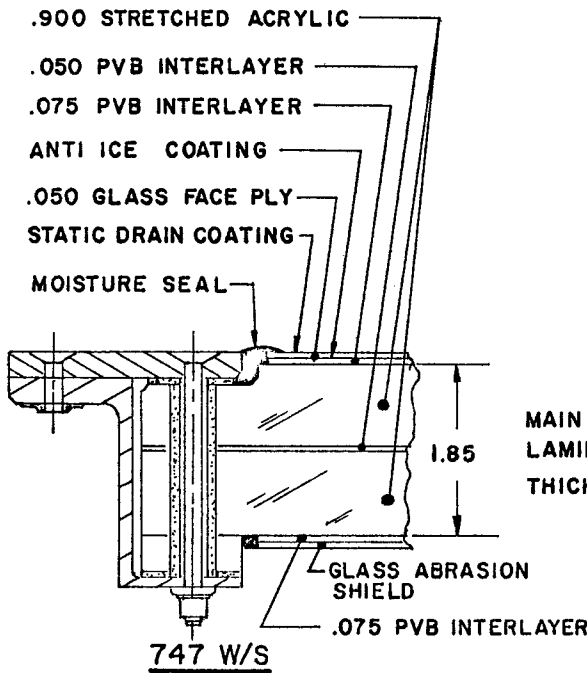
747 WINDSHIELD



FLAT PATTERN COMPARISON



L-1011 WINDSHIELD



MAIN PLY  
LAMINATE  
THICKNESS

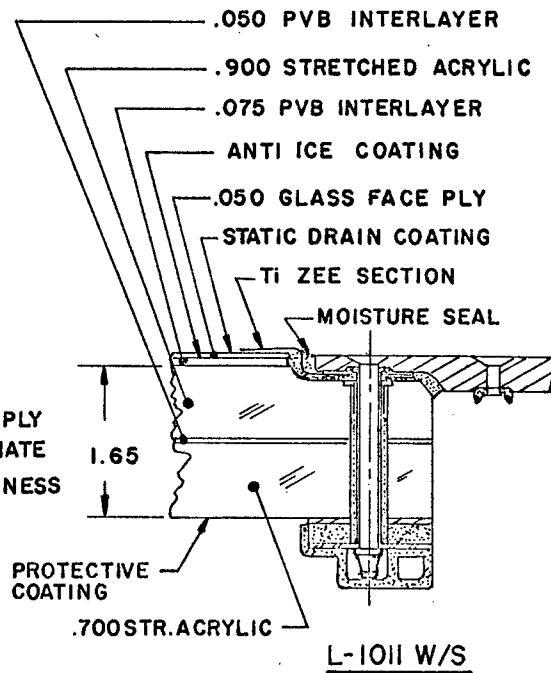


FIGURE 11

COMPARISON OF 747 & L-1011 WINDSHIELD DESIGNS

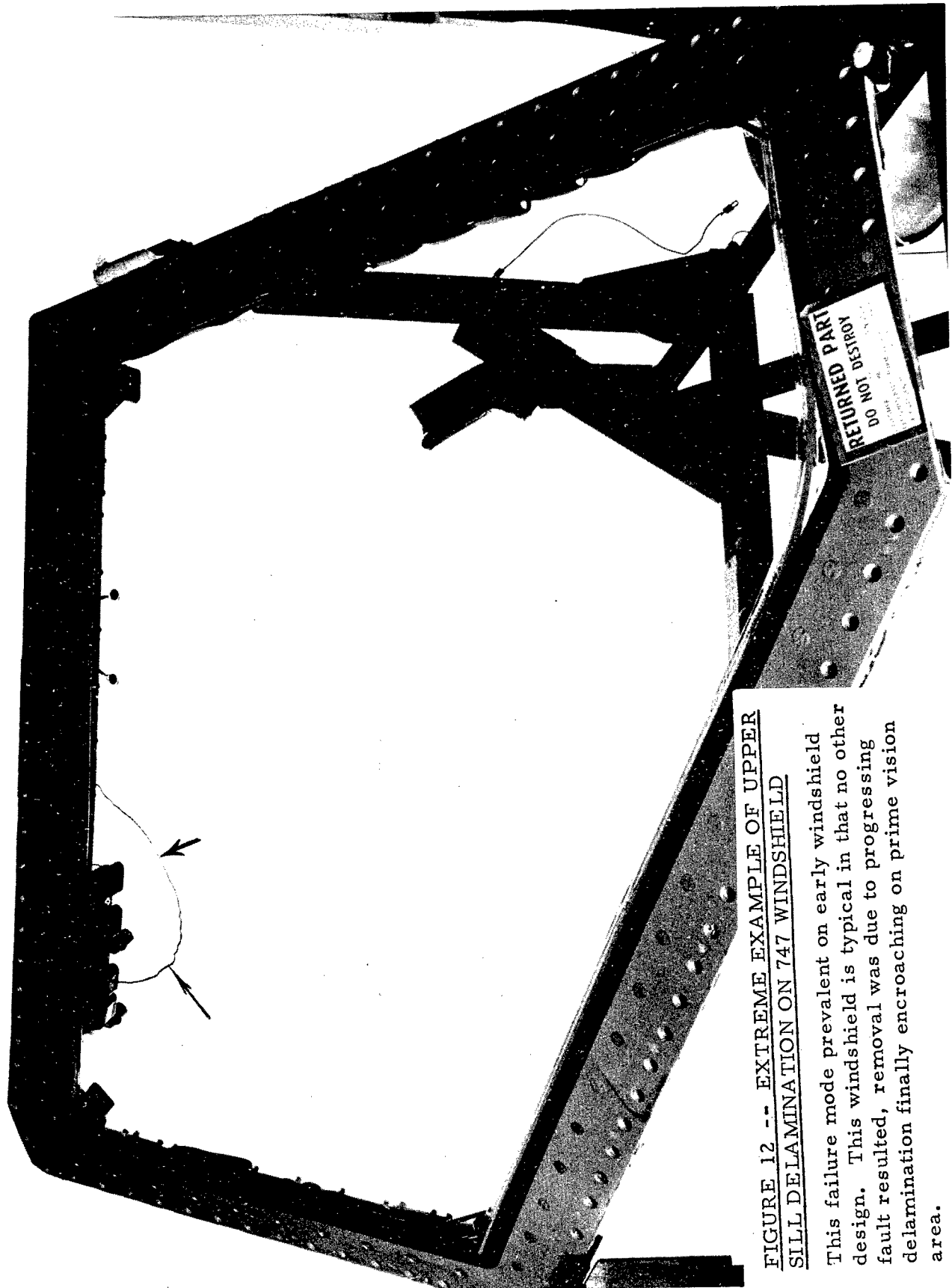
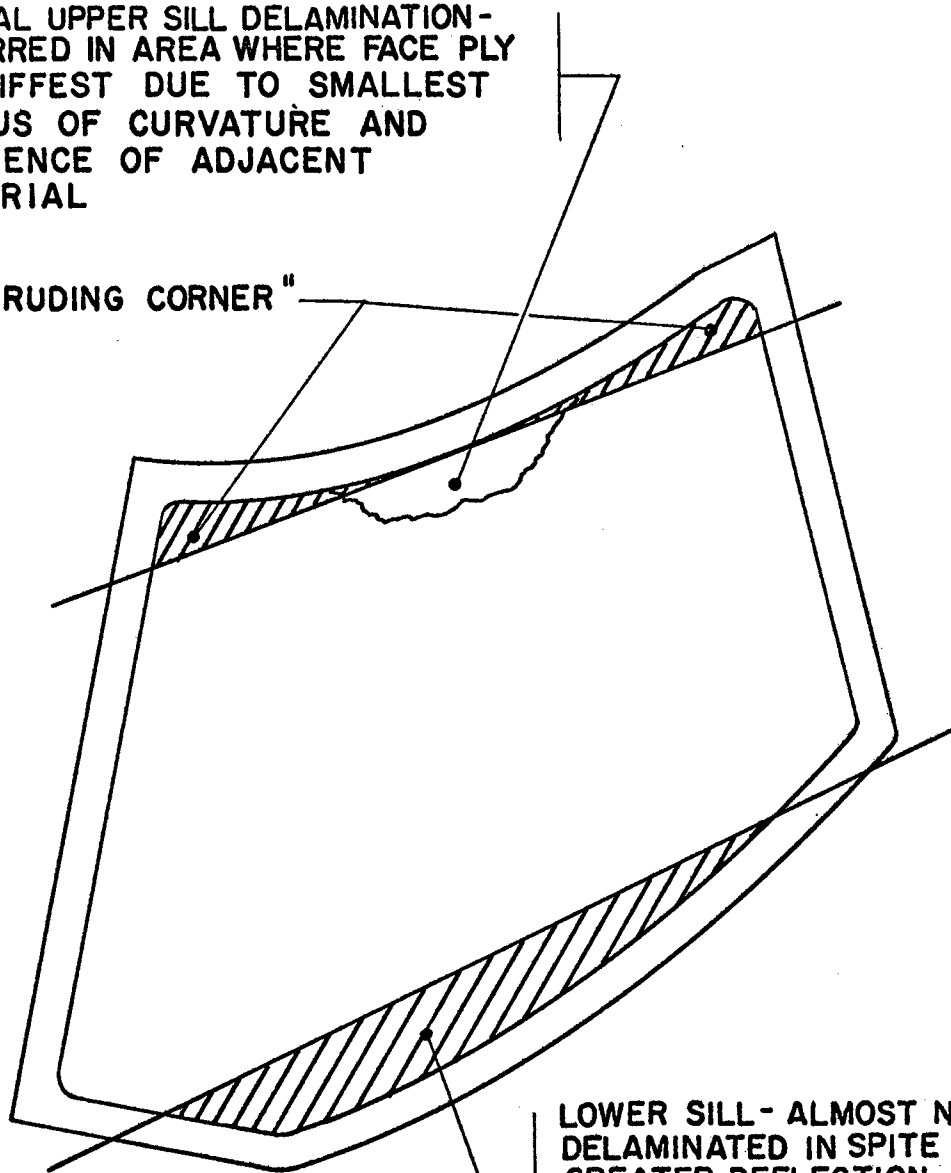


FIGURE 12 -- EXTREME EXAMPLE OF UPPER  
SILL DELAMINATION ON 747 WINDSHIELD

This failure mode prevalent on early windshield design. This windshield is typical in that no other fault resulted, removal was due to progressing delamination finally encroaching on prime vision area.

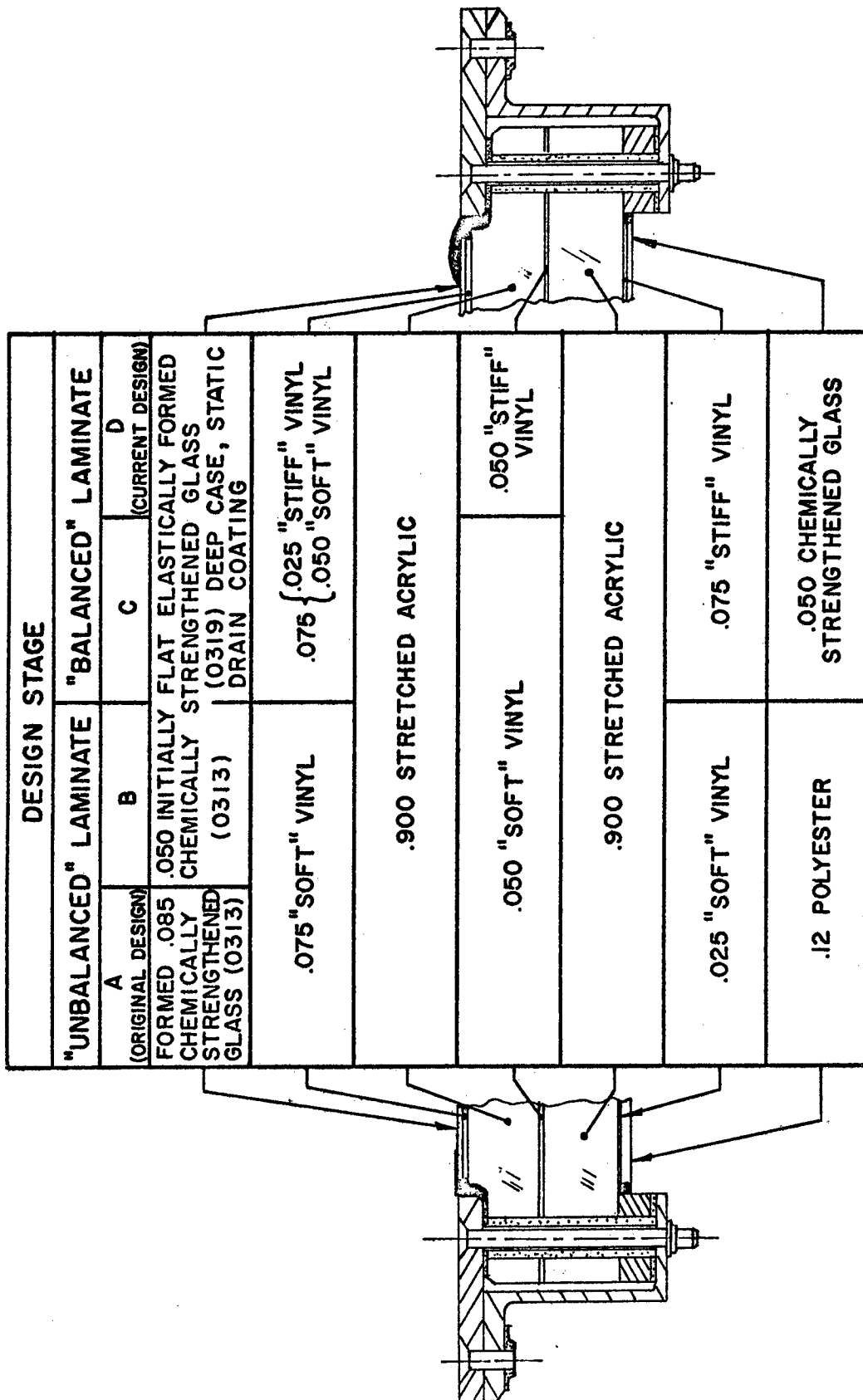
TYPICAL UPPER SILL DELAMINATION -  
OCCURRED IN AREA WHERE FACE PLY  
IS STIFFEST DUE TO SMALLEST  
RADIUS OF CURVATURE AND  
INFLUENCE OF ADJACENT  
MATERIAL

"PROTRUDING CORNER"



LOWER SILL - ALMOST NEVER  
DELAMINATED IN SPITE OF  
GREATER DEFLECTION -  
RADIUS OF CURVATURE  
IS LARGE AND PROTRUDING  
"FLAP" IS FREER TO BEND  
INDEPENDENT OF ADJACENT  
MATERIAL

**FIGURE 13**  
**INFLUENCE OF 747 WINDSHIELD**  
**GEOMETRY ON DELAMINATION**

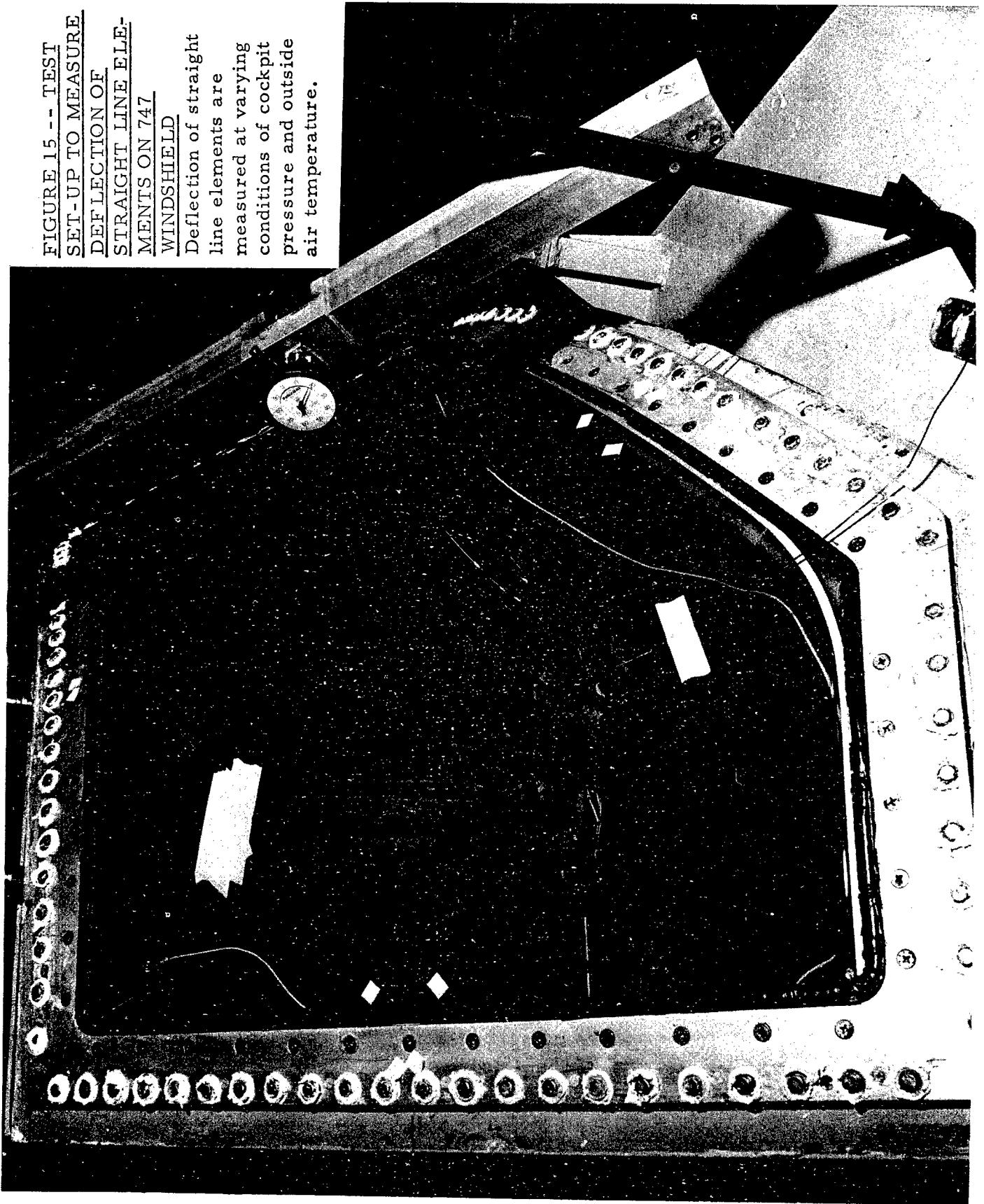


**FIGURE 14**

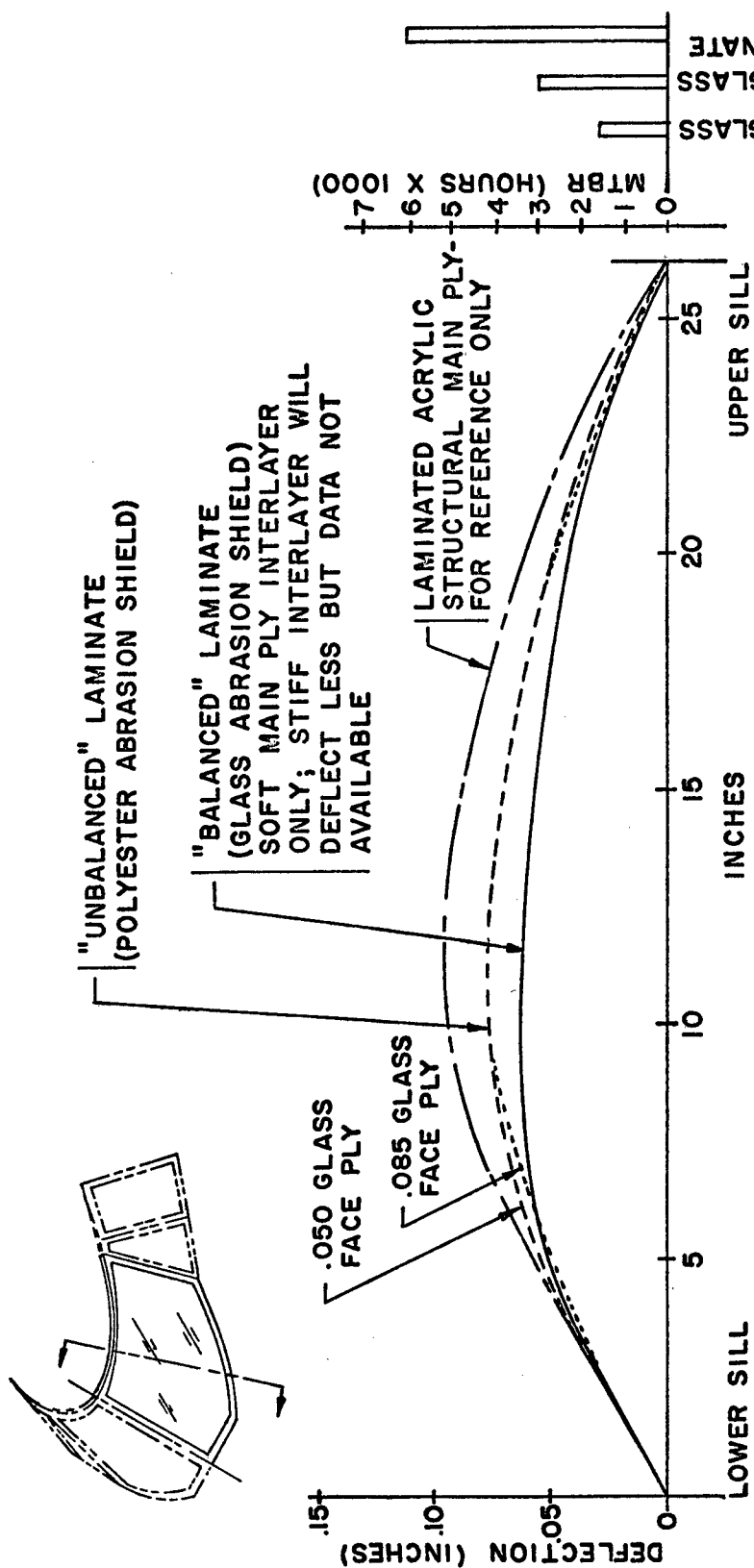
**SIGNIFICANT EVOLUTIONARY STAGES OF 747 WINDSHIELD DESIGN**

FIGURE 15 -- TEST  
SET-UP TO MEASURE  
DEFLECTION OF  
STRAIGHT LINE ELE-  
MENTS ON 747  
WINDSHIELD

Deflection of straight  
line elements are  
measured at varying  
conditions of cockpit  
pressure and outside  
air temperature.

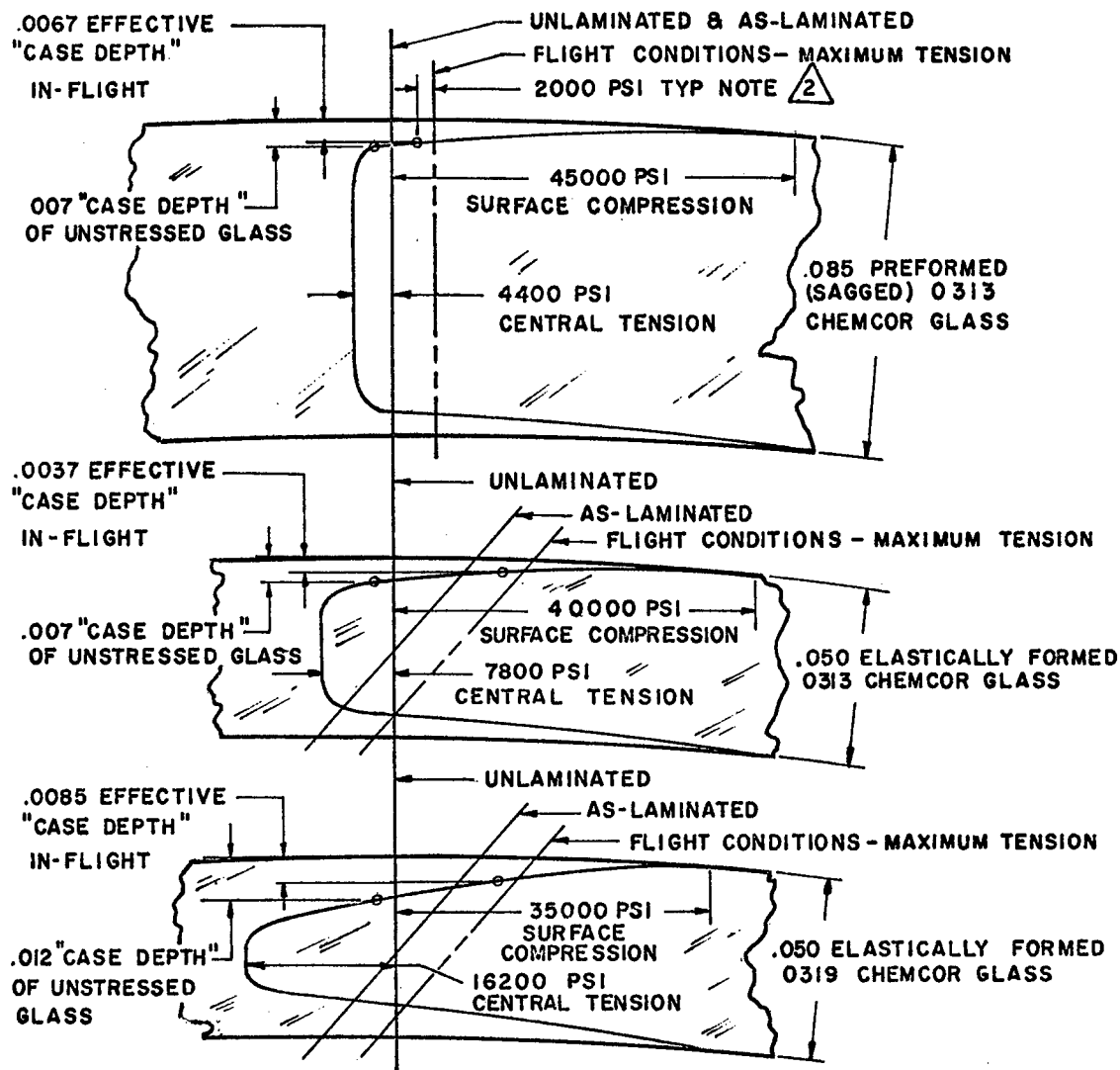






NOTE: DEFLECTION SHOWN MEASURED  
ON INITIALLY STRAIGHT LINE  
ELEMENT WHEN PRESSURIZED  
TO 9 PSI

**FIGURE 16**  
**747 WINDSHIELD DEFLECTION PROFILE AND**  
**RELATABLE SERVICE EXPERIENCE**



NOTES:

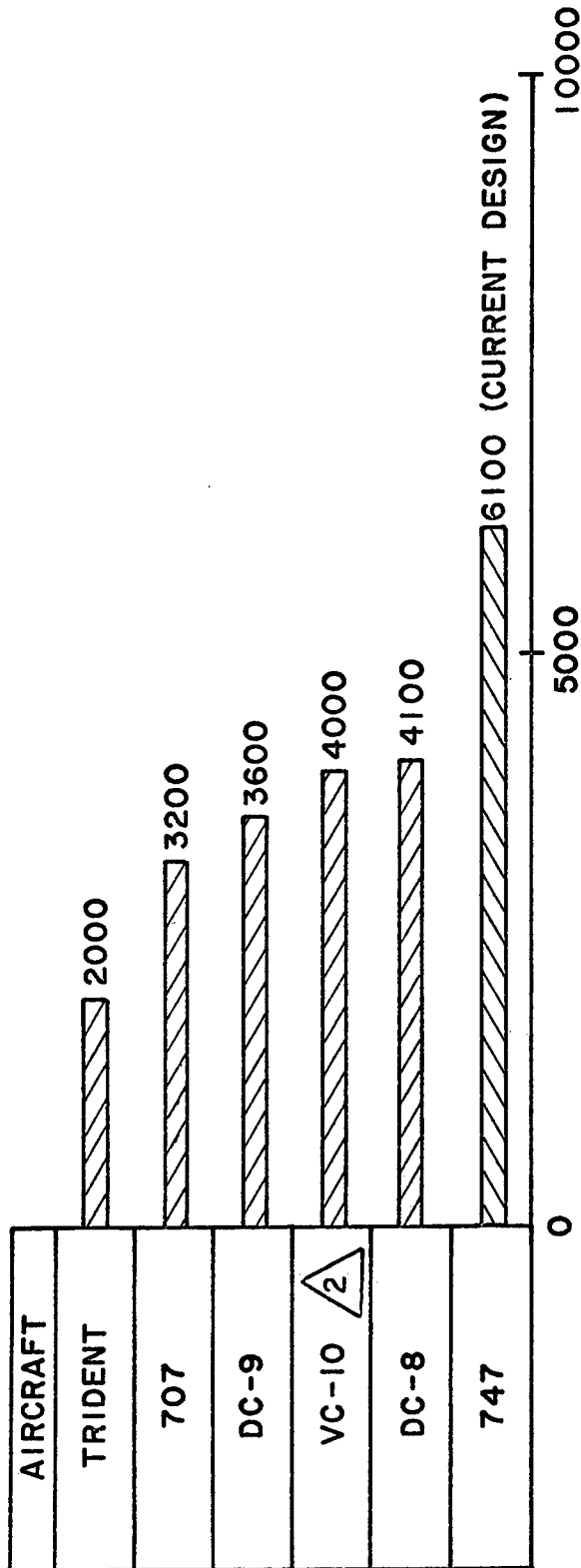
1 ALL LABELED STRAIGHT LINES ARE TYPICAL "ZERO STRESS" LINES FOR THE NOTED CONDITION

2 "CASE" CONSIDERED TO EXTEND TO DEPTH AT WHICH CENTRAL TENSION WILL PROPAGATE A CRACK - APPROX. 2000 PSI

3 CHEMCOR IS A TRADE NAME FOR CORNING GLASS WORKS CHEMICALLY STRENGTHENED GLASS

**FIGURE 17**

**GLASS FACE PLY "CASE DEPTH" CONSIDERATIONS**



# MTBR - FLIGHT HOURS

THREE YEARS AFTER INTRODUCTION INTO SERVICE

NOTE: 1 SUBSEQUENT IMPROVEMENTS AND REFINEMENTS CAUSED SUBSTANTIAL IMPROVEMENTS IN WINDSHIELD MTBR FOR MOST OF THE DESIGNATED AIRCRAFT AFTER THEY HAD BEEN IN SERVICE BEYOND THE FIRST 3 YEARS

2 EARLIER FIGURES NOT AVAILABLE - MTBR SHOWN FOR VC-10 W/S IS CURRENT FIGURE AFTER 9 YEARS OF AIRLINE SERVICE

**FIGURE 18**  
**COMPARISON OF EARLY SERVICE PERFORMANCE**  
**OF COMMERCIAL AIRLINER WINDSHIELDS**

## REFERENCES:

- a) Keith Gunnar, "Status of Program to Develop Composite Windshields Utilizing Plastics and Chemically Strengthened Glass". Paper presented at U. S. Air Force Conference on Transparent Materials for Aerospace Enclosures, Dayton, Ohio, December 1964. (The Sierracin Corporation)
- b) M. C. W. Davy, "The Design, Development and Testing of Glass/Plastic Composite Windshields". Paper published by The Sierracin Corporation, March 1967.
- c) Keith Haviland, "Improved Aircraft Windshield Glazing Techniques - Study". Report No. DAC 33494, Douglas Aircraft Corporation, February 1967.
- d) Frank Burnham, "L-1011's Cockpit Stresses Visibility, Comfort". American Aviation Magazine, March 3, 1969.
- e) George L. Wiser, "Sierracin Glass/Plastic Composite Windshields". Paper presented at U. S. Air Force Conference on Transparent Materials for Aerospace Enclosures, June 1969. (The Sierracin Corporation)
- f) Donald S. Eberhart, "Glass Plastic Composite Windshields, Boeing 747 Superjet". Presented at U. S. Air Force Conference on Transparent Materials for Aerospace Enclosures, Dayton, June 1969. (The Boeing Company)
- g) John A. Vaccari, "Safer Aircraft Glasses Up Visibility, Resist Impact". Materials Engineering Magazine, November 1969.
- h) George L. Wiser, "New Materials in Aircraft Windshields". Presented at Society of Automotive Engineers, National Aeronautics and Space Meeting, Los Angeles, California, October 1970. (The Sierracin Corporation)

Copyright 1973, Sierracin® Corporation

The information contained in this document is thought to be reliable, but the Sierracin Corporation expressly disclaims all responsibility for loss or damage caused by or resulting from the use of the information herein contained. The information is given on the express condition that the user assumes all risk.

## STUDY OF FAILED TA-4 AIRCRAFT CANOPIES

I. Wolock, D. R. Mulville, and R. J. Thomas  
Naval Research Laboratory  
Washington, D. C.

# STUDY OF FAILED TA-4 AIRCRAFT CANOPIES

by

I. Wolock, D. R. Mulville and R. J. Thomas

Naval Research Laboratory  
Washington, D. C. 20375

## Abstract

A number of in-flight failures have been encountered in TA-4 aircraft canopies after service periods of 3 to 5 years. The canopies were made of monolithic stretched acrylic with an acrylic-nylon edge attachment. An investigation was made of the properties of the stretched acrylic plastic taken from in-service TA-4 canopies and of the behavior of the edge attachment material. Tests of the acrylic plastic included fracture toughness, thermal relaxation, craze resistance, tensile strength, shear strength, and flexural strength. The only properties affected appreciably by the weathering were the fracture toughness and the crazing resistance. However, it is doubtful that the reductions observed in these properties could result in failure of the canopies.

Flexural tests conducted on the acrylic plastic at the junction with the edge attachment indicated that the strength of the aged material reduced approximately 20%, except that some specimens containing cracks were reduced 50% in strength. These cracks originated in the acrylic near the end of the edge attachment due to the sharp stress discontinuity. Microscopic examination indicated that they were fatigue cracks. It was possible to model the initiation of these cracks in laboratory fatigue tests. It was concluded that the failure of the canopies is due to fatigue cracks which originate in the acrylic near the end of the edge attachment due to the sharp stress discontinuity. The situation can be alleviated by tapering the edge attachment to reduce the stress concentration.

## Introduction

A number of in-flight failures of TA-4 aircraft canopies were encountered after the canopies had been in service for periods of approximately 3 to 5 years. These canopies were made of monolithic stretched acrylic with a nylon-acrylic edge attachment. Stretched acrylic has been used in a number of other planes with no reported in-flight failures. Nevertheless, it is possible that the stretched acrylic plastic may have undergone a degradation in mechanical properties that led to the failure of the canopies. Accordingly, an investigation was undertaken of the properties of stretched acrylic plastic taken from a TA-4 canopy after approximately 5 years of service. The scope of the study

was extended to conduct a limited failure analysis of the TA-4 canopies.

#### Evaluation of Stretched Acrylic Plastic Materials

Two intact TA-4 canopies that had been in service were received for study from the Naval Air Station, Lemoore, California. They were identified as a Fore Canopy, Part Number 5824254-1, Serial No. 017 3-66, and a Rear Canopy, Part Number 5824255-1, Serial No. 059 5-66. The stretched acrylic was approximately 1/4-inch thick. Tests were conducted on specimens obtained from the least curved areas of the canopy.

In addition, tests were conducted on specimens from flat sheets of stretched acrylic obtained from Swedlow, Inc. Tests were also conducted on control edge attachment material of the same configuration and materials as used in the canopies and also obtained from Swedlow, Inc.

#### Test Procedures

The tests performed are listed below and were conducted in accordance with Military Specification MIL-P-27390 (USAF); Plastic, Sheets and Parts, Modified Acrylic Base, Monolithic, Crack Propagation Resistant except as noted.

1. Fracture Toughness.

2. Thermal Relaxation.

3. Craze Resistance. The test method specifies that the load be applied to the specimen for 10 minutes, then the solvent applied to the specimen for 30 minutes over the fulcrum, after which the specimen is examined for crazing. Tests were conducted to determine if the time required for this test could be reduced by: (a) eliminating the 10-minute period after the load is applied before applying the solvent; (b) reducing the time the solvent is in contact with the specimen. In conducting these tests, the solvent was applied over the length of the specimen from the fulcrum to the point of load application, rather than merely at the fulcrum as stated in the specification. With this modified technique, one can measure the extent of crazing and calculate the corresponding stress which is the threshold stress for crazing for the given solvent and time period.

Tests indicated that the 10-minute period between load application and solvent application did not affect the threshold stress appreciably. However, examination of the specimens ten, twenty and thirty minutes after the application of solvent indicated that the extent of crazing was increasing appreciably during this period and the thirty-minute period was retained.

4. Tensile Properties. In addition to tensile strength, the modulus of elasticity was determined for some of the specimens by attaching micro-former extensometers to the specimens. A secant modulus was calculated

from 0-4000 psi over which range the deformation was fairly linear. Elongation was obtained by following the extension visually using a scale mounted on the specimen, since the extensometers would only operate up to 10% strain.

5. Shear Strength Parallel to the Surface. Values obtained for the shear strength were found to be extremely sensitive to the quality of machining in preparing the specimens. When the specimens were prepared in the specimen shop with no special treatment, the shear values obtained were low and quite variable. By using a new cutting tool and care in machining, the values obtained rose markedly and the variability decreased although sporadic low values were obtained. Apparently any chipping of the specimen surface during machining will lead to the low values and variability. Great care must be exercised in specimen preparation for this test.

It would appear to be desirable to modify the current test method by providing some type of controlled initial defect or crack in the test specimen. In the current method, uncontrolled flaws from the machining process are present, and these lead to scattered results.

6. Flexural Properties. Method 1031 of Federal Specification L-P-406 was used.

## Results and Discussion

### 1. Fracture Toughness

Since it was necessary to heat the canopy specimens to flatten them, tests were conducted to determine the effect of warm-forming on fracture toughness. The results indicated that heating the stretched acrylic for 1-1/2 hours at 205°F (96°C) resulted in a reduction in K from approximately 3200 lb/in.<sup>3/2</sup> to 3000 lb/in.<sup>3/2</sup>, with a shrinkage of approximately 0.1%. There was considerable variability observed in the test results, and the range observed for the canopy specimens was approximately twice that observed for the control specimens. In Table I, the control specimens for the aft canopy were unheated whereas those of the fore canopy were heated.

The results obtained on canopy specimens are presented in Table I. They indicate that the fracture toughness of the aged material decreases by approximately 25%, as measured by a reduction in K from 3000 down to approximately 2200 lbs/in.<sup>3/2</sup>. Under normal conditions, this is probably not serious, because many planes have been flying for years with stretched acrylic canopies without failing. If the reduction in toughness contributes to the failures observed, it must be in combination with other factors.

Douglas Aircraft Co. (Ref. 1,2) has reported the results of tests conducted on stretched acrylic from failed TA-4 canopies. K tests were conducted by Swedlow, Inc. for Douglas. The average results obtained on



material from one canopy was 2716 lb/in.<sup>3/2</sup> and from another with only five hours flying time was 2975 lb/in.<sup>3/2</sup>.

Specimens from the current investigation was also sent to Swedlow for comparative testing. Briefly, these tests resulted in slightly lower values for control specimens (approximately 2850 lb/in.<sup>3/2</sup>) as compared to those obtained at NRL, and slightly higher values for aged canopy specimens (approximately 2550 lb/in.<sup>3/2</sup>), so that the reduction in toughness on aging was approximately 10% from Swedlow's results.

## 2. Thermal Relaxation

The data are presented in Table II. The results were within the requirements of the specification and indicated that the degree of stretch of the aged canopies was 63%. There did not appear to be an appreciable change in the degree of stretching as a result of weathering, and this is in agreement with results reported by Rohm and Haas (Ref. 3).

## 3. Craze Resistance

The results are presented in Table III. The craze resistance of the aged stretched acrylic decreased appreciably and the exterior surface was more susceptible to crazing than the interior surface. The average results obtained were 4100 psi for the control material, 2900 psi for the interior surface of the canopy material and 2200 psi for the exterior surface. It was found that the aged material exhibited a distinct yellowing of the exterior surface, indicating degradation, and this is reflected in the increased sensitivity to crazing.

Rohm and Haas (Ref. 3) reported that MIL-P-8184 material multi-axially stretched 75% decreased in craze resistance from 4200 psi for control specimens to 3100 psi for material aged six months outdoors at Bristol, Pa. The results obtained in the current investigation indicated a similar decrease for the interior surface but a much larger decrease for the exterior surface.

## 4. Tensile Properties

Results of the tensile tests are presented in Table IV. There is no indication of any appreciable change in properties as a result of weathering. The average elongation for the control specimens in the aft canopy tests was higher than that of the canopy specimens. However the values obtained for the control specimens in the fore canopy tests, as well as those reported in Table VI in connection with the crazing tests, were appreciably lower than the values obtained for the control specimens in the aft canopy tests, and were very close to the results obtained for the canopy specimens. Thus there does not appear to be a significant change in elongation. This is somewhat surprising. The changes in fracture toughness and crazing threshold indicate a reduction in mechanical properties, brought about presumably by molecular changes. The tensile elongation is usually quite sensitive to such changes. Yet the value did not change in this case.

## 5. Shear Strength

The results are presented in Table V. The average shear strengths were considerably higher than the minimum values listed in the specification. However, any relaxation of the orientation of the stretched acrylic would result in higher shear values. Thus the values observed for the canopy material were higher than those for the controls. Even with careful machining, there was considerable variability in the results obtained.

## 6. Flexural Properties

The specimens did not break in the flexural tests. The average maximum stress was 17,440 psi for the control specimens and 18,485 psi for the canopy specimens. The respective elastic modulus values were  $5.0 \times 10^5$  psi and  $5.2 \times 10^5$  psi.

## 7. Tensile Properties of Craze Stretched Acrylic

Tests were also conducted to determine how surface crazing affects the tensile properties of stretched acrylic. Standard tensile specimens were crazed by subjecting them to a tensile stress of 5000 psi and then applying solvent to one surface using a blotter. Trichloroethylene was applied for four minutes to one group of specimens to produce significant crazing. Isopropyl alcohol was applied for twenty minutes to a second group of specimens. The extent of crazing can be observed in Figure 1.

The results obtained in the tensile tests of these specimen are presented in Table VI. For the extent of crazing produced in these specimens, there was no change in the tensile strength. However, the elongation decreased by approximately 1/3.

### Evaluation of Edge Attachment

While this study was in progress, it was reported that examination of failed TA-4 canopies indicated that failure did take place in the vicinity of the edge attachment and that cracks were observed in the stretched acrylic in this area. It appeared that the sharp discontinuity of the relatively thick nylon reinforcement on the interior surface of the assembly (Fig. 2) might introduce a stress concentration in the acrylic. In addition, microscopical examination of the aged edge attachment indicated some areas of poor bonding containing air bubbles, as well as areas in which the resin matrix had degraded due to weathering. The scope of the investigation was expanded to evaluate these effects.

### Static Tests

#### Test Procedures

Control samples of the edge attachment were obtained from the fabricator in the configuration used in the aircraft. Specimens 1/2-inch wide

and approximately 3-1/2 inches long were prepared from the control material, as well as from typical sections of the aged aft canopy and from pieces of the edge attachment from a failed canopy which were furnished by McDonnell-Douglas Co. Some of the latter specimens contained cracks in the acrylic as shown in Figure 3. Specimens were also prepared of the stretched acrylic with no edge attachment reinforcement. In some of the control specimens, the edge attachment was tapered by machining, as shown in Figure 4, to reduce the stress concentration. The specimens were loaded in flexure, as indicated in Figure 5, using a 2-inch span, to simulate service loading of the canopy or closely as possible in a uniaxial test. In actual use, the canopy is clamped at the edge attachment and internally pressurized, resulting in a similar type of loading.

## Results and Discussion

The results of these tests are presented in Table VII. The values shown for the stress are approximate because they do not take into account the stiffening of the acrylic beam due to the nylon laminate. The values are shown merely to indicate the approximate range of the stresses used. The results indicate the following:

- (1) The load and the deflection at failure are increased approximately 50% by tapering the edge attachment.
- (2) The properties of the edge attachment material in the aft canopy decreased an average of 20% compared to the control material. For some of the canopy specimens containing cracks, the strength reduction was as much as 50%.
- (3) The properties of the material from the failed canopy decreased to approximately one-half that of the control material. The highest values obtained in these specimens were approximately the same as the lowest values obtained in the control specimens.
- (4) Both the load and the deflection were much higher for the stretched acrylic without any edge attachment, raising the question once more as to the utility of the edge attachment when used with this material.

In conducting these tests, as the load was increased, a crack initiated in the stretched acrylic at the point at which the nylon reinforcement terminated, proceeding at an angle into the interior of the specimen in the same fashion as that observed in the canopy specimen of Figure 3. This similarity in behavior would tend to indicate that the loading used in the test was similar to that in actual service.

## Fatigue Tests

### Test Procedures

In analyzing the failed canopies, in view of the results indicating

no serious general degradation of mechanical properties of the acrylic due to aging, it was postulated that the canopy failures were caused by fatigue cracks that initiated in the edge attachment area. Limited studies were therefore undertaken of the fatigue behavior of the edge attachment material. The specimens and loading were the same as that used in the previously described static tests. A cycling rate of 4 cycles/minute was selected, corresponding to approximately 2000 cycles in eight hours. According to MIL-Handbook 17 (Ref. 4), this should result in failure of stretched acrylic when loaded at 50 to 60% of the static strength. These were considered reasonable conditions for these tests. A load of 60 pounds was used, corresponding to a stress of approximately 6000 to 8000 psi.

### Results and Discussion

The results are presented in Figure 6. They indicated that the aged material from the canopies fails in significantly fewer cycles than the control material, and that tapering the edge attachment results in somewhat improved fatigue life.

Photomicrographs of a crack observed in the edge attachment area of a failed canopy (Fig. 7) indicates that this is indeed a fatigue crack. The laboratory fatigue specimen (Figure 8) indicated similar markings.

### Summary and Conclusions

As a result of tests conducted on specimens obtained from TA-4 aircraft canopies that were in service for several years, from sections of failed TA-4 canopies, and from control material, the following conclusions may be drawn:

1. In-service aging of several years results in a reduction of fracture toughness and crazing resistance of stretched acrylic plastic but does not appreciably affect tensile, flexural, or shear properties.
2. Fairly heavy solvent crazing of the surface of stretched acrylic does not affect the tensile strength but does reduce the elongation approximately 30%.
3. There is a reduction in mechanical strength of the aged edge attachment material apparently due to degradation of the resin matrix, superposed on the stress concentration due to the reinforcement configuration.
4. In-service failure of TA-4 canopies are probably due to fatigue cracks induced at the end of the edge attachment by a stress concentration caused by the large change in stiffness of the assembly. The design can be improved by tapering the reinforcement to reduce the change in stiffness which should result in increased service life. The performance of the assembly can probably be improved further by using the stretched acrylic with no reinforcement whatsoever.

### Acknowledgement

This investigation was sponsored by the Naval Air Systems Command with Mr. Charles F. Bersch as project monitor. The authors wish to acknowledge this support as well as the many fruitful discussions held with Mr. Bersch. Specimens from failed canopies were kindly furnished by Douglas Aircraft Co. through Mr. J. W. Kozmata. The cooperation of Swedlow, Inc. is also acknowledged, from whom special edge attachment material was purchased.

### References

1. Kozmata, J. W. "TA-4F Canopy Service Failure Analysis". McDonnell-Douglas Laboratory Report LR-DAC-5363 (January 1971).
2. Kozmata, J. W. and Banton, A. L. "Canopy TA-4J; Failure Report". McDonnell-Douglas Laboratory Report LR-DAC-5561 (May 1971).
3. Gouza, J. J. and Hurst, D. A. "Investigation of Multiaxially Stretched Acrylic Plastic". WADC Technical Report 54-619 Part I (Dec. 1954).
4. Plastics for Flight Vehicles. Part II. Transparent Glazing Materials. MIL-Handbook 17 (Aug. 1961).

TABLE I. RESISTANCE TO CRACK PROPAGATION OF STRETCHED ACRYLIC

|                      | <u>AFT CANOPY</u>  | <u>FORE CANOPY</u>                |
|----------------------|--|-----------------------------------|
|                      | LB/IN <sup>3/2</sup>   | LB/IN <sup>3/2</sup>              |
| <u>CONTROL</u>       | Unheated 3215 (5) <sup>a</sup><br>(3030 - 3405) <sup>b</sup> | Heated 3005 (10)<br>(2755 - 3135) |
| <u>CANOPY</u>        |  |                                   |
| LEFT                 | 2380 (6)   |                                   |
| CENTER               | 2225 (6)   |                                   |
| RIGHT                | 2405 (6)   | 2140 (16)                         |
| AVERAGE              | Heated 2335 (18)<br>(1960 - 2770)                            | Heated 2140 (16)<br>(1695 - 2490) |
| <u>SPECIFICATION</u> | FLAT SHEETS  | 2700                              |
|                      | FORMED PARTS   | 2600                              |
|                      | AFTER WEATHERING (FORMED)                                    | 2100                              |

a. Number in parenthesis indicates number of specimens tested.

b. Numbers indicate range of test values.

TABLE II  
THERMAL RELAXATION OF STRETCHED ACRYLIC

|                           | AFT CANOPY           |          | FORE CANOPY |           | SPECIFICATION<br>LESS THAN 10.0% |
|---------------------------|----------------------|----------|-------------|-----------|----------------------------------|
|                           | CONTROLS             | CANOPY   | CONTROLS    | CANOPY    |                                  |
| 24 HR. AT 230° F (110° C) | 3.4%(2) <sup>a</sup> | 3.2%(2)  | 4.2%(10)    | 5.0%(10)  |                                  |
| 24 HR. AT 293° F (145° C) | 41.4%(2)             | 38.6%(2) | 41.0%(10)   | 38.5%(10) | MORE THAN 37.5%                  |

a. Number in parenthesis indicates number of specimens tested.

TABLE III. CRAZE RESISTANCE OF STRETCHED ACRYLIC<sup>a</sup>

|                      | <u>AFT CANOPY</u><br>PSI                            | <u>FORE CANOPY</u><br>PSI  |
|----------------------|---|----------------------------|
| <u>CONTROLS</u>      | 4155 (5) <sup>b</sup><br>(3905 - 4375) <sup>c</sup> | 4000 (10)<br>(3515 - 4375) |
| <u>CANOPY</u>        |   |                            |
| INSIDE SURFACE       | 2810 (5)<br>(2650 - 2970)                           | 2975 (10)<br>(2810 - 3200) |
| OUTSIDE SURFACE      | 2050 (5)<br>(1875 - 2185)                           | 2440 (10)<br>(2265 - 2575) |
| <u>SPECIFICATION</u> | 3000 PSI (MIN.)                                     |                            |

- a. Values reported are threshold stress for solvent crazing with isopropyl alcohol after application to surface for 30 minutes.
- b. Number in parenthesis indicates number of specimens tested.
- c. Numbers indicate range of test values.



TABLE IV.

## TENSILE PROPERTIES OF STRETCHED ACRYLIC

|                      | <u>AFT CANOPY</u>       |                        | <u>FORE CANOPY</u>     |                                       |
|----------------------|-------------------------|------------------------|------------------------|---------------------------------------|
|                      | <u>STRENGTH</u><br>PSI  | <u>ELONGATION</u><br>% | <u>STRENGTH</u><br>PSI | <u>ELONGATION</u><br>%                |
| <u>CONTROLS</u>      | 12,415 (5) <sup>a</sup> | 36.7 (5)               | 11,515 (10)            | 27.0 (10)                             |
|                      |                         |                        |                        | <u>MODULUS</u><br>10 <sup>5</sup> PSI |
| <u>CANOPY</u>        |                         |                        |                        | 4.5 (5)                               |
| <u>LEFT</u>          |                         |                        |                        |                                       |
| CENTER               | 12,850 (5)              | 28.3 (3)               | 12,035 (5)             | 29.7 (5)                              |
| RIGHT                | 12,900 (5)              | 32.2 (5)               | 12,020 (6)             | 29.1 (6)                              |
|                      | 12,915 (5)              | 27.3 (5)               |                        |                                       |
| AVERAGE              | 12,890 (15)             | 29.4 (13)              | 12,025 (11)            | 29.4 (11)                             |
|                      |                         |                        |                        | 4.6 (5)                               |
| <u>SPECIFICATION</u> | 9,000 (MIN)             |                        |                        |                                       |

a. Number in parenthesis indicates number of specimens tested.

TABLE V

## SHEAR STRENGTH OF STRETCHED ACRYLIC

| <u>CONTROLS</u>      | <u>AFT CANOPY</u> |  | <u>FORE CANOPY</u> |                        |
|----------------------|-------------------|--|--------------------|------------------------|
|                      | <u>psi</u>        |  | <u>psi</u>         |                        |
|                      | UNHEATED          | 5900 (4) <sup>a</sup><br>5840 (5) <sup>b</sup> | UNHEATED           | 6170 (10)<br>6070 (10) |
| <u>CANOPY</u>        |                   |  |                    |                        |
| LEFT                 |                   | 6425 (5)                                       |                    | 7200 (17)              |
| CENTER               |                   | 5885 (5)                                       |                    |                        |
| RIGHT                |                   | 6370 (5)                                       |                    |                        |
| AVERAGE              |                   | 6225 (15)                                      |                    | 7200 (17)              |
| <u>SPECIFICATION</u> |                   | 3000 (MIN)                                     |                    |                        |

a. Number in parenthesis indicates number of specimens tested.

b. Specimens were heated at 205°F (96°C) for 1 1/2 hrs. to flatten except where noted.

TABLE VI. TENSILE PROPERTIES OF CRAZED STRETCHED ACRYLIC <sup>a</sup>

|                           | <u>STRENGTH</u><br>PSI  | <u>ELONGATION</u><br>%                 |
|---------------------------|-------------------------|--|
| UNCRAZED                  | 11,460 (4) <sup>b</sup> | 28.7 (4)<br>(26.0 - 30.5) <sup>c</sup> |
| ISOPROPYL ALCOHOL/20 MIN. | 11,340 (5)              | 19.7 (5)<br>(10.0 - 25.0)              |
| TRICHLOROETHYLENE/4 MIN.  | 11,385 (5)              | 17.4 (5)<br>(14.0 - 19.5)              |

a. Specimens were crazed by applying tensile stress of 5000 psi and then applying solvent for times indicated.

b. Number in parenthesis indicates number of specimens tested.

c. Numbers indicate range of test values. Range of values for strength was small.

TABLE VII. FLEXURAL TESTS OF TA-4 EDGE ATTACHMENTS

|                    |                   | <u>LOAD</u><br>LB               | <u>STRESS</u> <sup>a</sup><br>KSI | <u>DEFLECTION</u><br>10 <sup>-3</sup> IN. |
|--------------------|-------------------|---------------------------------|-----------------------------------|---|
| CONTROL            | (20) <sup>b</sup> | 184<br>(118 - 255) <sup>c</sup> | 14.2<br>(9.7 - 18.7)              | 52<br>(34 - 81)                           |
| CONTROL (TAPERED)  | (5)               | 267<br>(245 - 288)              | 21.1<br>(19.1 - 22.4)             | 87<br>(71 - 105)                          |
| CANOPY I - AFT     | (13)              | 148<br>(97 - 252)               | 11.2<br>(7.9 - 17.6)              | 42<br>(26 - 75)                           |
| CANOPY II - FAILED | (9)               | 98<br>(72 - 125)                | 7.9<br>(5.9 - 9.2)                | 28<br>(22 - 38)                           |
| STRETCHED ACRYLIC  | (6)               | 321<br>(312 - 330)              | 23.8<br>(23.6 - 23.9)             | 189<br>(150 - 275)                        |

a. Values are approximate maximum stress in stretched acrylic.

b. Number in parenthesis indicates number of test specimens.

c. Numbers indicate range of test values.

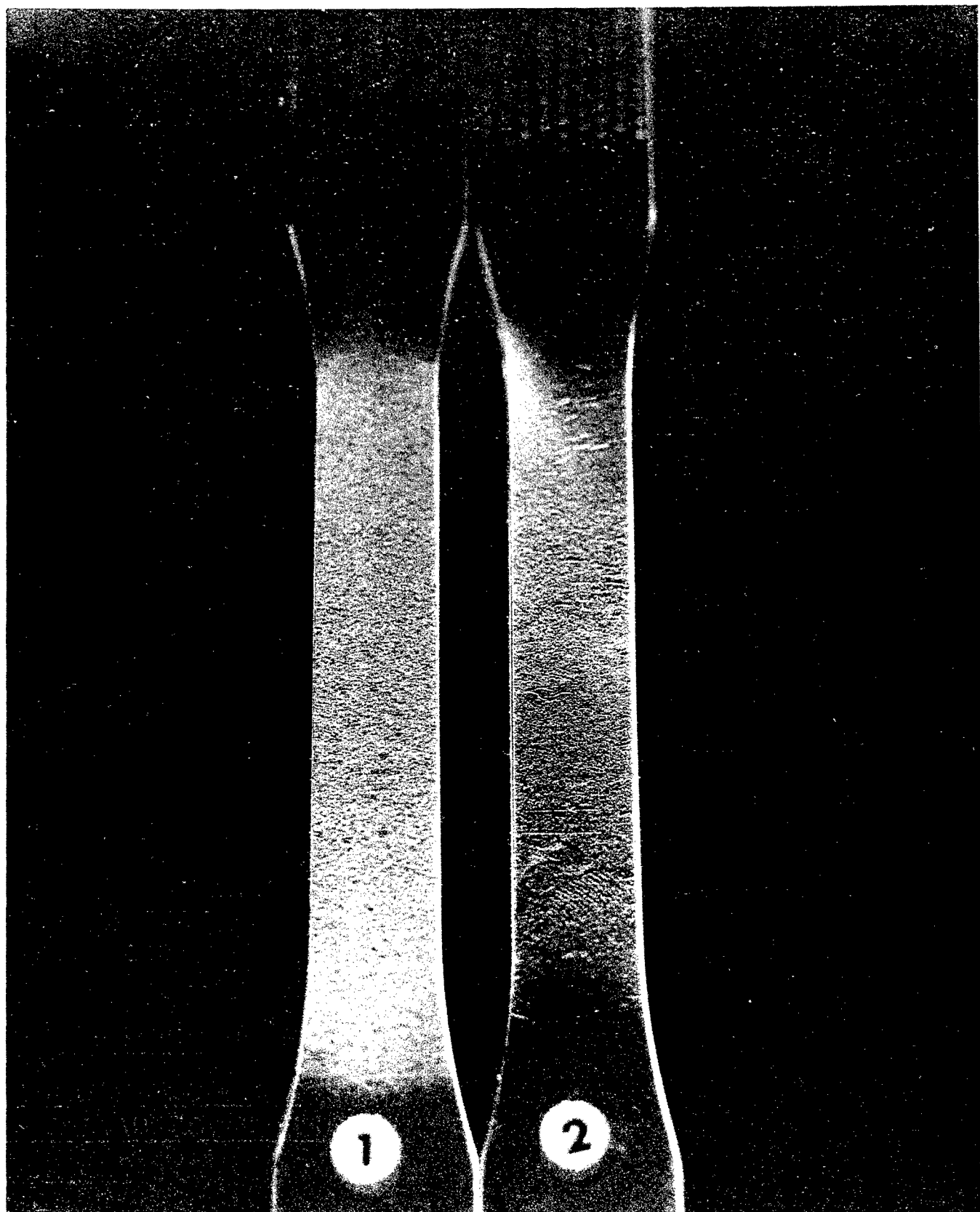


Figure 1: Solvent-crazed tensile specimens.  
No. 1: Trichloroethylene used.  
No. 2: Isopropyl alcohol used. 632

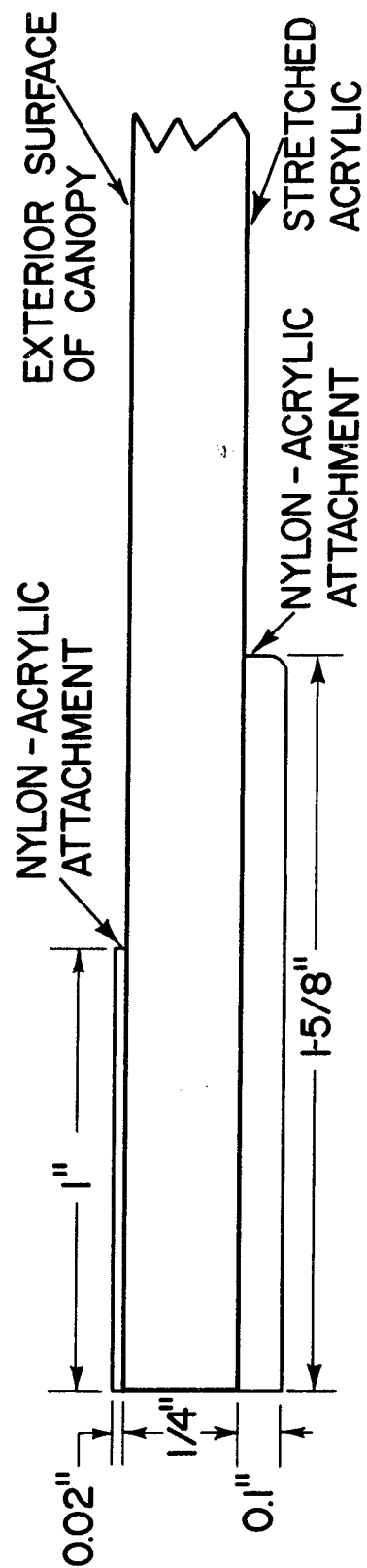


Figure 2: TA-4 Edge Attachment.

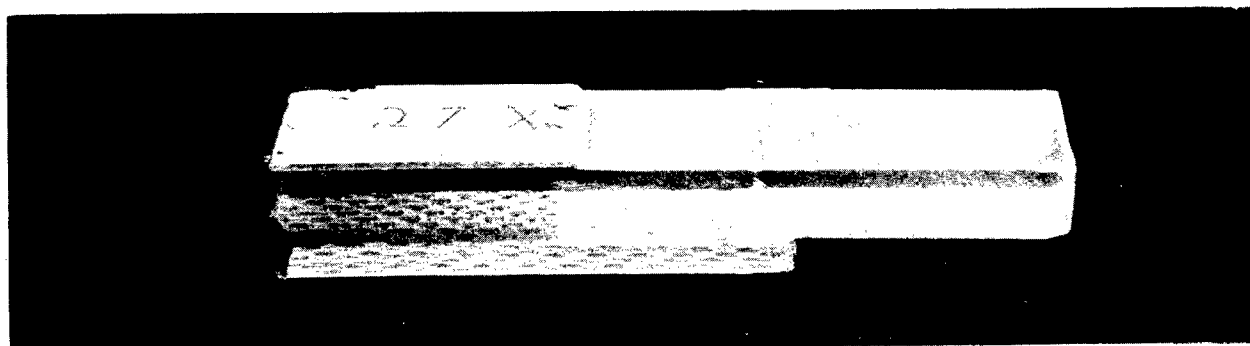


Figure 3: Specimen from edge attachment area of TA-4 canopy showing crack that developed in stretched acrylic plastic during service.

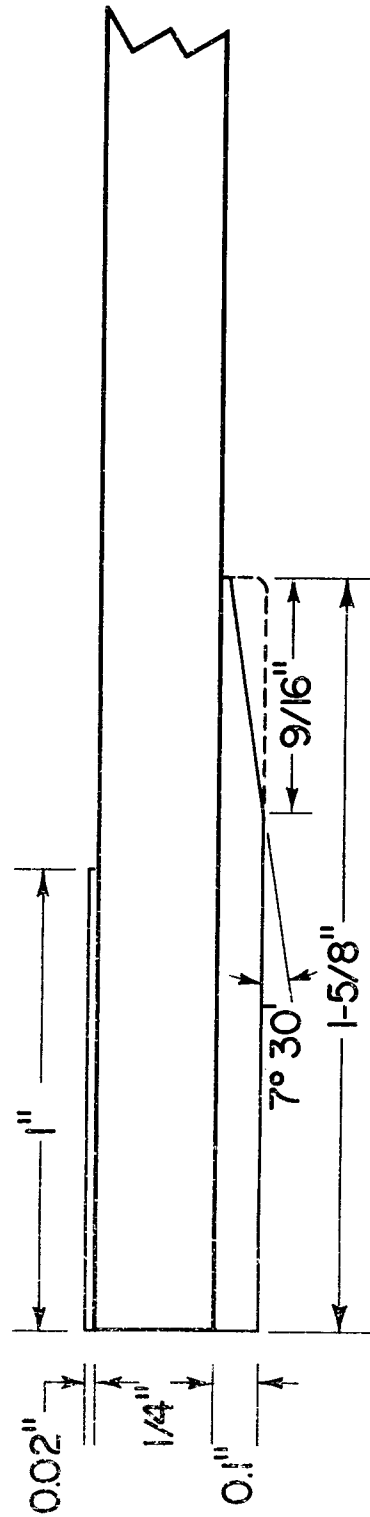


Figure 4: Details of taper machined in nylon-acrylic reinforcement in TA-4 edge attachment to reduce stress concentration.



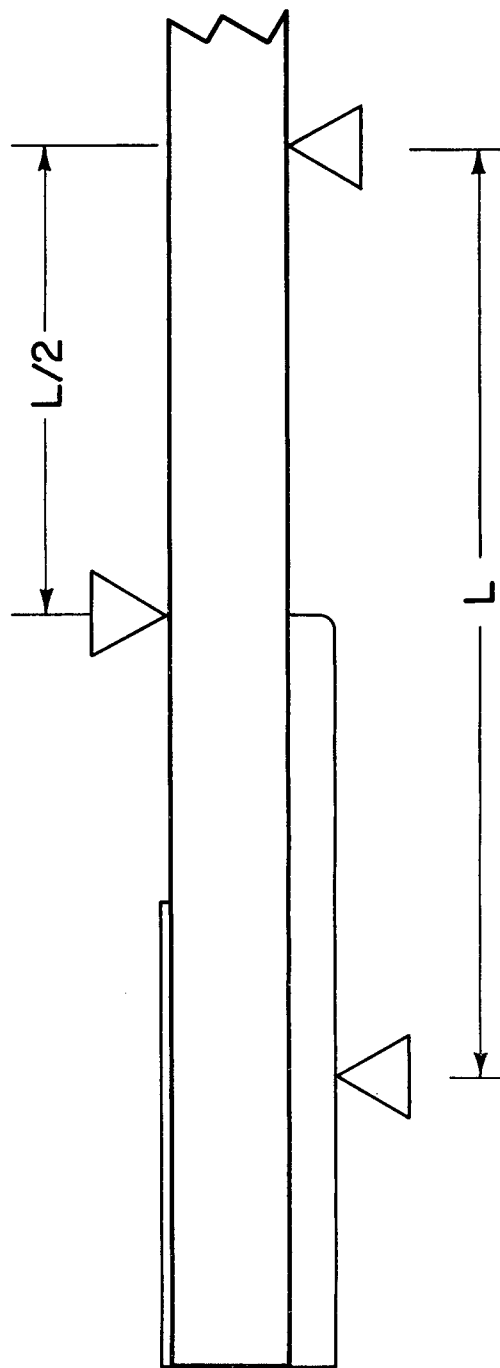


Figure 5: Loading arrangement used in flexural tests of TA-4 edge attachment.

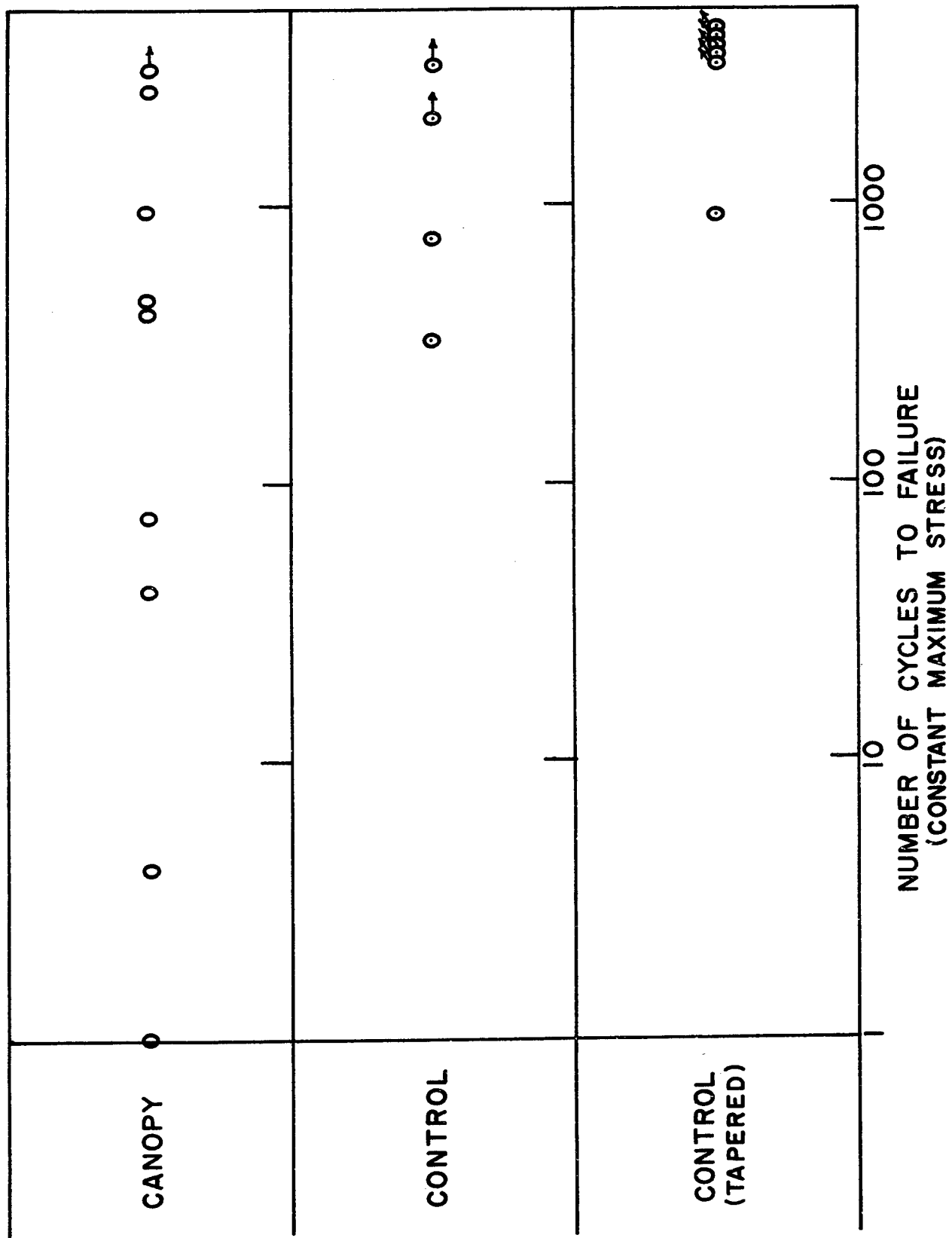


Figure 6: Data obtained in fatigue studies of TA-4 edge attachment material.

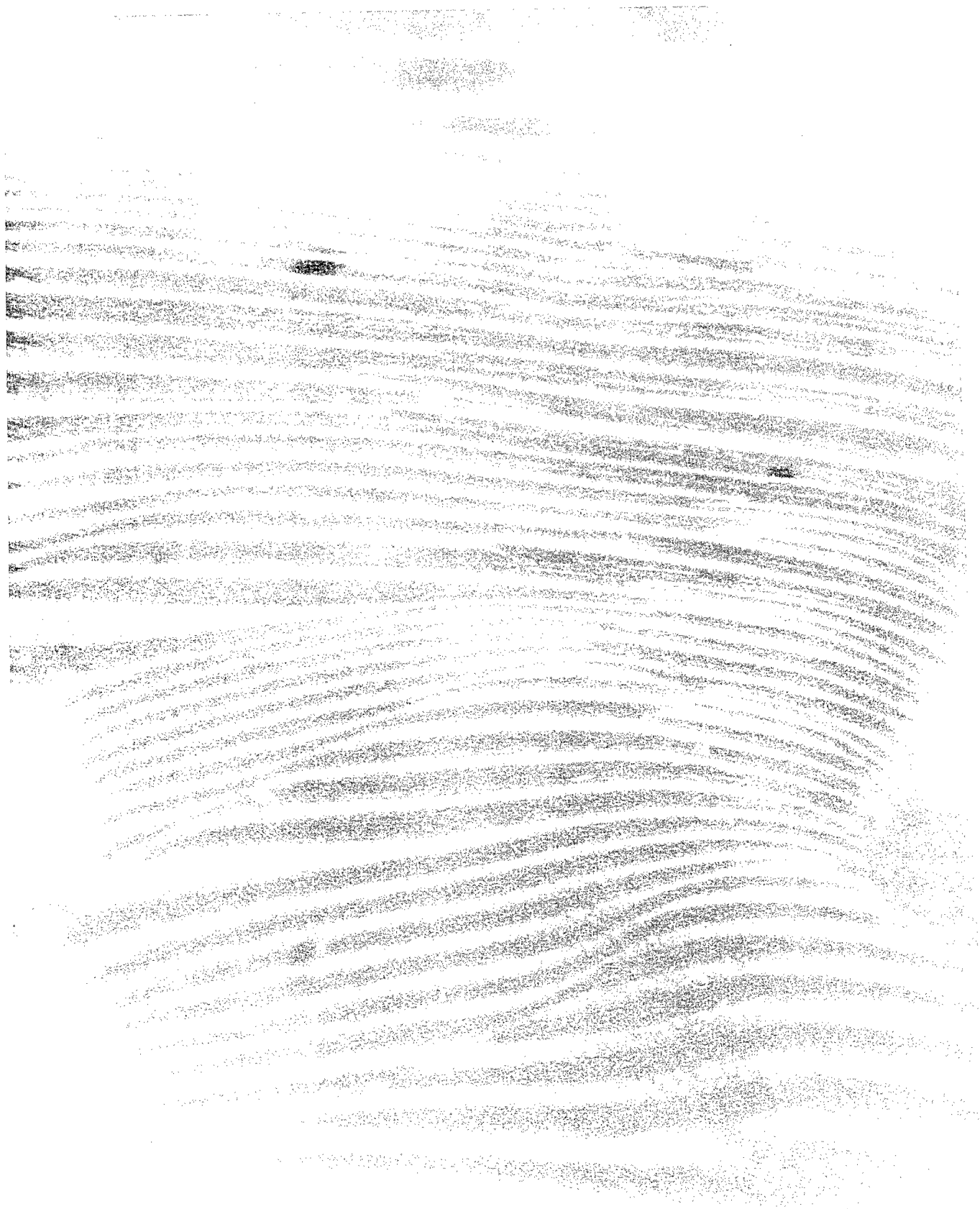


Figure 7: Photomicrograph of surface of crack observed in stretched acrylic from edge attachment area of failed TA-4 canopy.

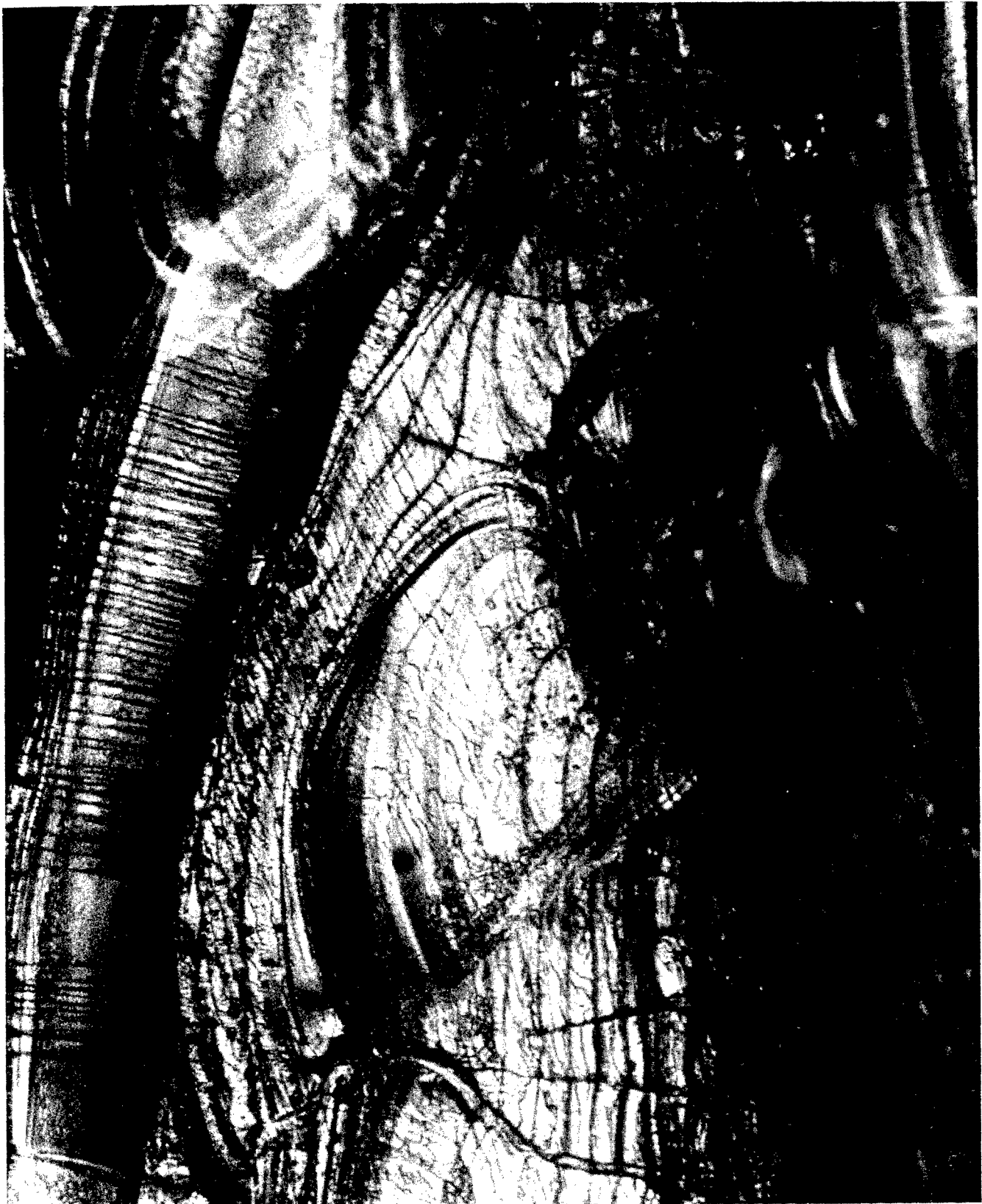


Figure 8: Photomicrograph of surface of specimen of control TA-4 edge attachment material loaded to failure under flexural fatigue in laboratory.

STATIC FATIGUE - ITS IMPLICATION TO  
RELIABILITY IN WINDOW DESIGN

Arthur F. Shoemaker  
Corning Glass Works  
Corning, New York

## Static Fatigue

### Its Implication to Reliability in Window Design

Arthur F. Shoemaker

Corning Glass Works

#### ABSTRACT

The Space Shuttle Program imposes reliability requirements not before encountered. Weight constraints, wide extremes in flight environment, many missions in combination with minimum refurbishment and quick turn-around time made it mandatory that a more sophisticated approach be taken in the manufacture, test and handling of window elements. Applying the science of fracture mechanics to glasses which are subject to static fatigue is a fundamental requirement. A considerable amount of work has been done in this area on ductile materials, especially for applications as pressure vessels, but little has been done on brittle materials. Mould & Southwick, Wiederhorn and others have studied various facets of the problem as related to glass, i.e. Crack Propagation Rates, Fracture Surface Energy, Influence of Water Vapor on Crack Propagation. However, this work has been scattered and limited in scope and types of glasses. From the practical standpoint, and adaption of appropriate techniques to the manufacture and test of full-scale windows, of different glasses, poses a large problem. The characterization and control of flaw size, shape, and depth for each stock removal operation must be determined. Based on theory and limited test data, glass will not fatigue, i.e. cracks will not propagate while under load in a moisture-free atmosphere. Therefore, if each stock removal operation is determined by tests, in a dry state, it should be possible to establish a pressure test level, in a moisture-free environment that would insure that there are no flaws remaining in the surface of the glass greater than a predetermined size. If this is true, then a high degree of reliability can be manufactured into each window panel.

Recently, concern has been expressed with the strength of glass under long-term and/or multi-cyclic loading. The reliability of a glass article traditionally has been based on designs using large safety factors on short-term loading test values. The material is further assumed to be capable of following Hooke's Law up to the point of failure. Fatigue has not been involved in most considerations. Reliability testing has been limited to a level of about 50% of the average breaking stress, basically as a recognition of the wide spread among individual failure points.

Generally, it is recognized that annealed glass has a wider spread of breaking stress than strengthened glass. This could be due to a slight flaw-healing effect created by the temperature or acid action of the particular strengthening operation. Probably more significant is the fact that the absolute spread is the same, but due to the much higher stress level, the percentage is smaller.

In any case, the point is that the reliability of a glass article currently is based on the average short-term breaking stress (usually the abraded value) and the testing of each article to a surface fibre stress of approximately 50% of this value. As long as the ultimate use load did not approach the test value, a reliable safety factor was assumed.

Due to the different mechanisms involved, this paper will cover only annealed glass as its subject matter. Further, the application of the science of fracture mechanics to the material glass is lacking in many aspects, and as such, my discussion is based more on theory than on fact supported by data.

The first indication that there may have been a problem with the conventional methods of designing glass articles was about three years ago. Face panels on pressurized instrument housings were breaking. Analysis of these failures indicated a discrepancy between the standard testing procedures and level of failures being encountered. The pretesting of the glass face panel was at a high enough level that all of the panels which failed in service should have been weeded out by the test.

As a result of this problem, the government agency involved assigned a man to study and survey the state-of-the-art of failure mechanisms in glass. After about a year the conclusion was reached that static fatigue was the mechanism involved. Based on studies of work done by Wiederhorn at NBS and Mould and Southwick at Preston Laboratories, it was determined that the science of fracture mechanics should be applied to control static fatigue. A new set of ground rules was considered which, while not identifying the mechanism, would oblige the producer to significantly revise manufacturing and test procedures.

An explanation of the concept is extremely difficult primarily due to the lack of specific data. However, the essence of the mechanisms can be summarized in order to present the general idea.

- (1) Every flaw in a glass surface has a characteristic related to depth, tip radius and width. In total, this is identified by the symbol "Q".
- (2) Water vapor in concentrations from 100% down to 0.1% has a significant contribution.
- (3) Under load and in the presence of water vapor each flaw will continue to grow with time.
- (4) With no load, but in the presence of water vapor, each flaw will become less severe.
- (5) Under load, but in a dry atmosphere, no flaw growth will occur regardless of time.
- (6) Each flaw "Q" has its own characteristic long-term and short-term wet breaking value.
- (7) At a point approximately 20% of the short-term wet breaking value no failure will occur, regardless of time.
- (8) For wet conditions, the strength under short-time loading is always greater than for long-time loading - (this is the static fatigue effect).



- (9) For dry conditions there is no difference between long-term and short-term loading strength values.

Figure I shows a typical static-fatigue curve. It must be pointed out, however, that this curve is only one of many, as each "Q" will have its own set of values. Further, and to give an indication of the complexity of the problem, a "Q" for one type of glass does not necessarily have the same value as the same "Q" in another glass type.

The introduction of this concept into the design criteria of structural glass articles requires that the manufacturer perform a number of tests to support his processes and identify selection rates. The primary goal is to achieve a known "Q" for each mechanical stock removal operation performed on the surfaces and edge of the glass blank. Each operation starting with the coarsest fixed abrasive grind through the finest loose abrasive lap must not only produce its own "Q" but also must completely remove all traces of the proceeding operation. To achieve this idealized condition data must be gathered using the following considerations.

- (1) The fixed abrasive must be controlled as to grit, concentration and, probably, manufacturer.
- (2) Feed rates and coolant must be monitored and locked into operational procedure.
- (3) Run-out time must be controlled.
- (4) Spindles must run true.
- (5) Both grinding head and work table must run flat and be parallel.
- (6) Loose abrasive is to be controlled by grit size and source.
- (7) Slurry, pressure and time must be fixed by procedure.

Figure II is an approximation of the values that could be expected through the range of normal stock removal operations.

The two curves are approximations of strength values over a normal range of expected flaw conditions. For the generalized conditions used in this paper, it can be assumed that the glass will always fail at stress levels above the upper curve and never fail below the lower curve. Space between the two curves is time-dependent as was shown by the curve of Figure I.

Figure III pulls the concept into focus. A dry surface does two things. First, stress values at failure are always higher than for a wet surface. Second, as previously stated, no fatigue, i.e. flaw growth, occurs up to the point of failure. With this in mind, one theoretically can select the maximum use stress off the bottom curve, then test under dry conditions, to the value of "Q" on the upper curve. The concept is now reduced to the condition whereby all flaw "Q" that are greater than a predetermined value, can be eliminated. This will then leave the manufactured surface in a predictable condition having a known design allowable with no unexpected or "wild" flaw, which is the usual cause for the severe skewing of the normal strength distribution of glass.

The surface conditions of "wet" or "dry" glass are related, in part, to the chemical attack rate of water on the composition of any given glass. On a microscopic scale, the etching performs a large work effort as it rounds off sharp reentrant angles or weakens the bond network in the matrix of the glass structure. As previously presented, "wet" relates to any water vapor in relative humidities from 100% down to approximately 0.1%.

Dry, on the other hand, relates either to the absence of any water vapor or the inactivation of the chemical attack mechanism. Conceptually, a surface exposed to a vacuum bake-out is dry. On the other hand, a surface exposed to say, liquid nitrogen has become inactivated as any liquid or gas has become frozen to a solid. For a pressure test environment, however, both of the above could be rather troublesome and/or costly. While both the vacuum and cryogenic approach have been used over the years in support of those studies on this subject that have been made, I believe there is a third option available. The article to be tested is installed in an appropriate pressure test fixture which in turn is located

in a furnace. Heating to a bakeout temperature in the 300°C range while continually pruging the surface with dry nitrogen during the heating and subsequent cooling to room temperature should present a dry surface for the test.

I will conclude this paper by again pointing out that there is a great lack of specific data that are necessary to make this concept viable. In theory it will support the need for a highly reliable manufacturing structural glass article. In practice, the question of how to perform a dry test that applies a uniform stress over the complete surface and edge area will have to be answered.

Lastly, assuming all of the preceeding has been accomplished, a further program would be required to identify the reliability factors arising from flaws occurring from handling and use environment.

It certainly will be necessary to insure that overzealous specifications are not involved which will result in excessive costs or underdesigned reliability.

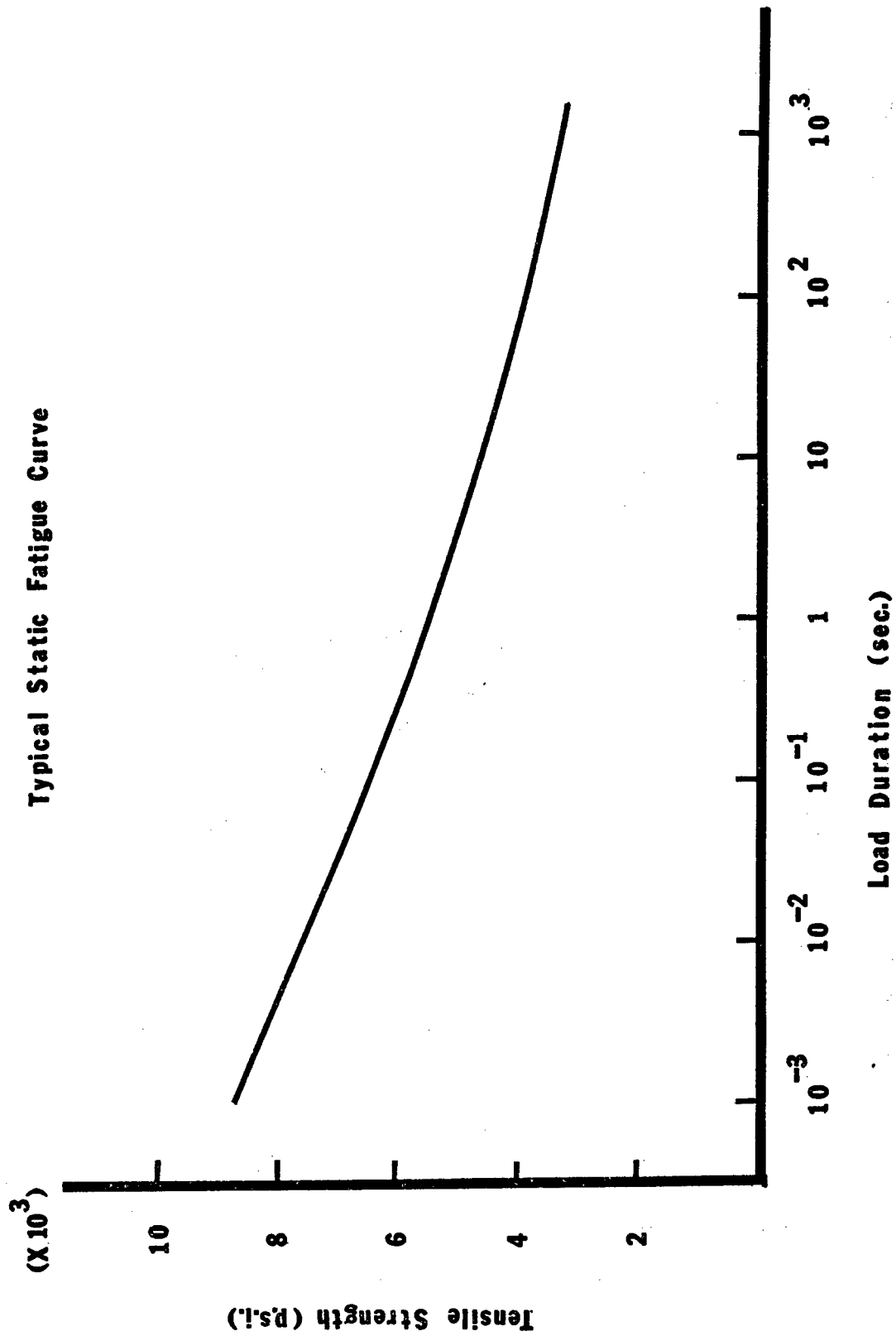


FIGURE I

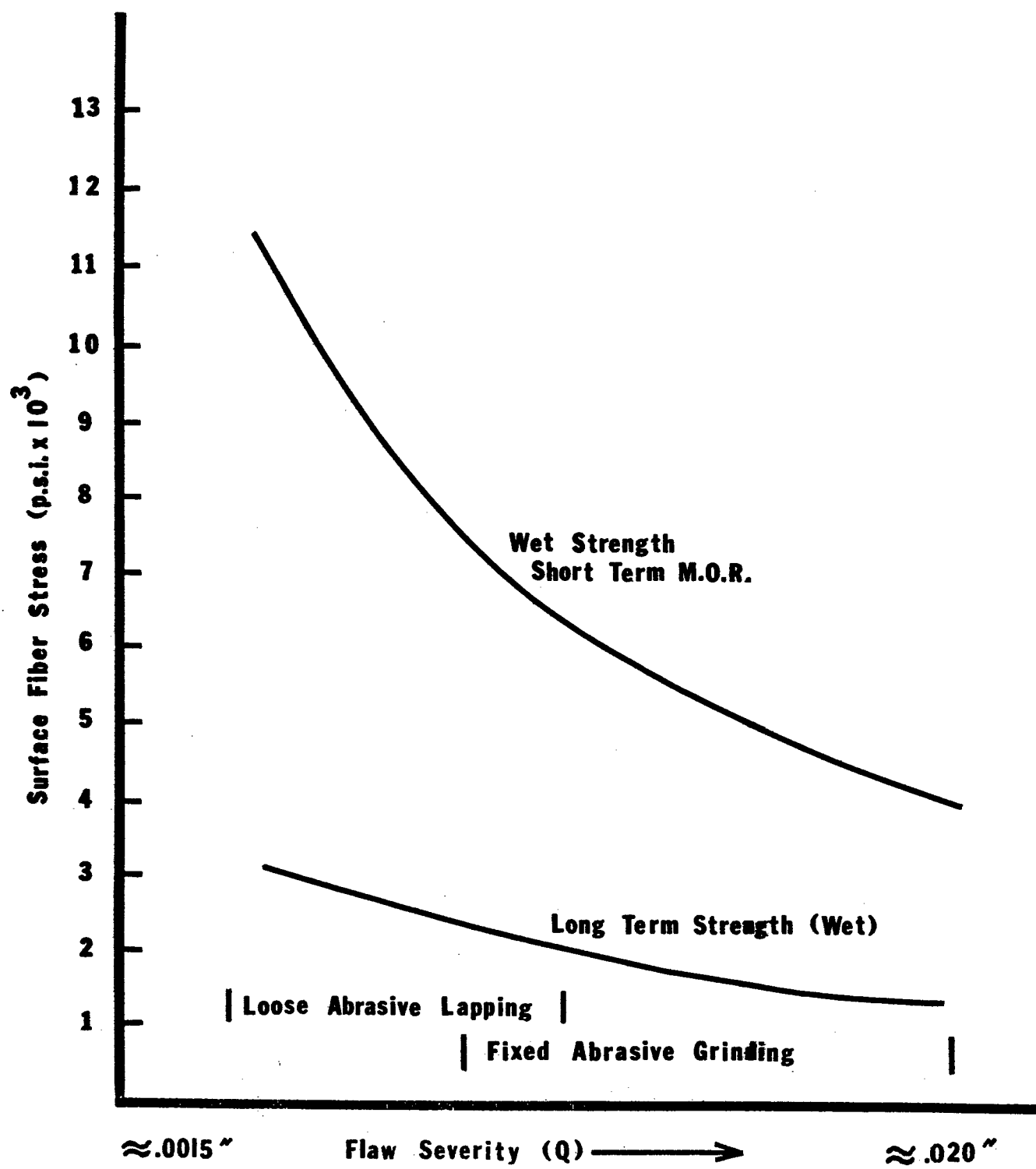


FIGURE II

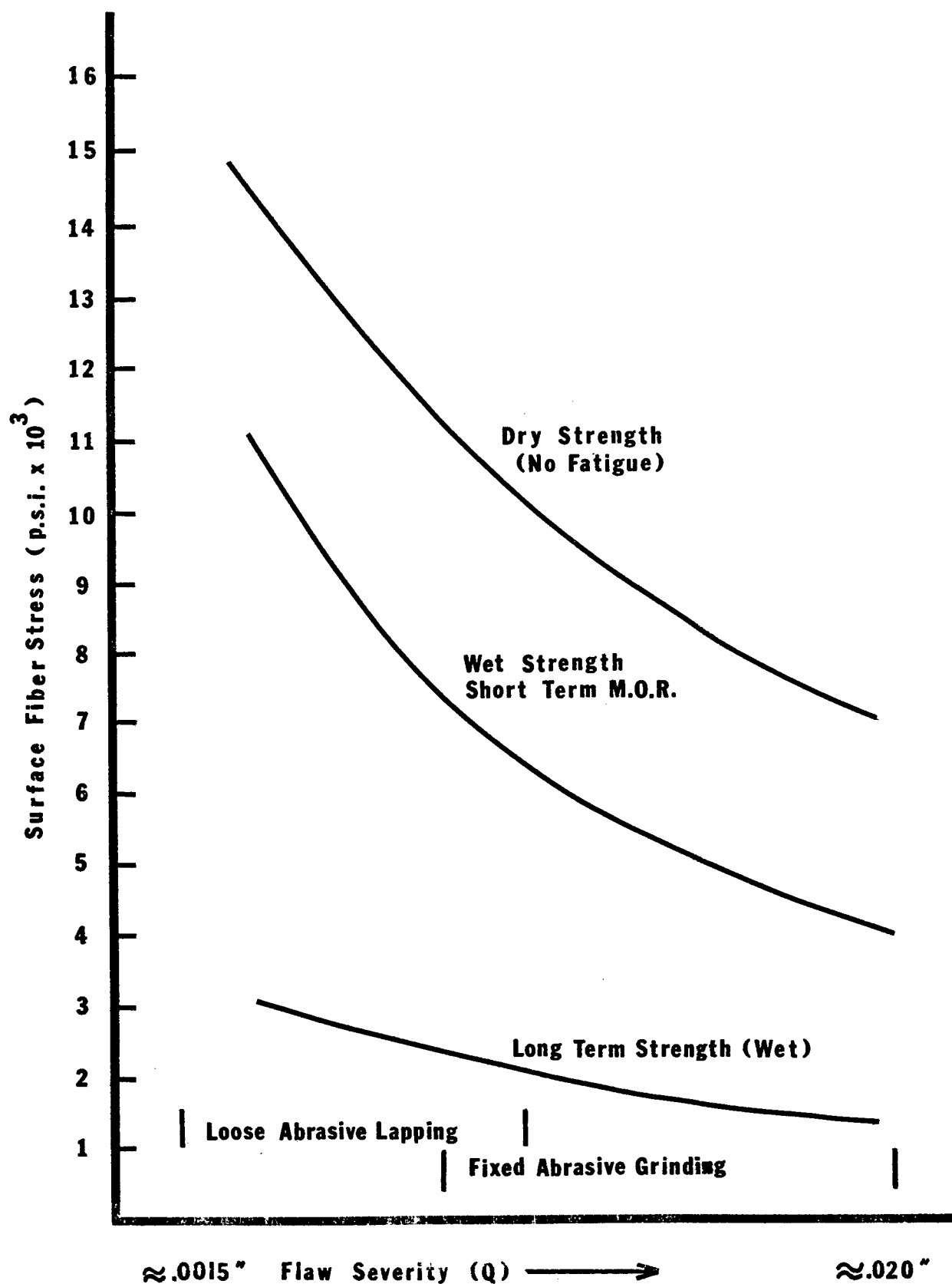


FIGURE III

HELICOPTER AND OTHER VTOL TRANSPARENCIES  
"AN UPDATING"

G. E. Freeman and J. B. Perkins  
PPG Industries, Inc.  
Huntsville, Alabama

## HELICOPTER AND OTHER VTOL TRANSPARENCIES

"AN UPDATING"

G. E. FREEMAN  
J. B. PERKINS

PPG INDUSTRIES, INC.

### ABSTRACT

At the previous transparency conference in 1969, PPG Industries presented a paper on this subject which addressed the problems presently being encountered with helicopter windows at that time, together with a series of projected possible solutions. Some of the problems identified were later verified and documented by a Helicopter Study Program sponsored by the U. S. Army Aviation Material Laboratories in Ft. Eustis, Virginia. PPG was one of two companies selected to conduct the study.

During the time period from 1969, the area of helicopter transparencies has been a very active one for PPG and one where much progress has been made. The principle technology that precipitated this progress was the ability to bend, temper and electrically heat thin lightweight glass.

Glass plates as thin as .075" were processed to complicated curvatures, tempered and treated with an electrically conductive film of NESA(R), PPG's tradename for tin oxide.

Resistivities as low as ten ohms per square have been obtained on the bent parts while maintaining light transmission requirements. This innovative processing has resulted in thin glass windshields being qualified for the CH-47, UH-1, CH-53 and AH-56A helicopters.

In addition to the thin glass solution, the composite approach has also been pursued from the standpoint of prototype fabrication and testing.

The success of this design approach depends to a large degree on interlayer selection which becomes a problem of material availability.



## INTRODUCTION

At the 1969 Conference on Transparent Materials, PPG presented a paper entitled "Helicopter & Other VTOL Transparencies." This paper will briefly review that discussion, tell of PPG's accomplishments during the period of 1969 to 1973, and look at the future requirements for helicopter transparencies.

## REVIEW

During the 1969 Transparency Conference, we examined the basic requirements for improved helicopter transparencies. These improvements were needed as the helicopter became increasingly sophisticated and a large proportion of our armed forces aircraft arsenal. Typical helicopter transparencies up to this time had been laminated or monolithic acrylic.

These basic requirements were:

1. Defogging and de-icing, thereby necessitating the use of a heating medium,
2. Rain removal, solved through the use of windshield wipers,
3. Good optics, a necessity especially for night time vision,
4. Reliability,
5. Minimum spall from gunfire,
6. Minimum weight.

Regardless of the magnitude of improvement in the six basic requirements, the major problem of resistance of the outboard surfaces to abrasion, particularly to wiper action, remained.

PPG's four part program to solve this problem centered around:

1. Thin glass laminate,
2. Composite laminate,
3. Hard coatings,
4. Lightweight glass.

The hard coatings approach was discarded because laboratory tests on these coatings were quickly disproved through flight tests. Because of the severe differences in the thermal expansion coefficients with the materials used in the composite approach, PPG's solution was the thin glass laminate.

In 1972, PPG was one of two companies awarded a helicopter transparency study contract by the Ft. Eustis Directorate of the United States Army. As a result of this study, the following data was compiled which supports our position on the primary problem area.<sup>(1)</sup>

Figure I shows the operational environment for helicopter transparencies. This environment and its effect was related to the eleven helicopters shown below:

| <u>Cargo</u>  | <u>Utility</u>     |
|---------------|--------------------|
| CH-47         | UH-1               |
| CH-46         | UH-2               |
| CH-54         |                    |
| CH-53         |                    |
| HH-3          |                    |
| <u>Attack</u> | <u>Observation</u> |
| AH-1G         | OH-6               |
| AH-56         | OH-58              |

The failure mode information shown in Figure II was obtained for these helicopters by visitations to various military installations, personal interviews, and questionnaires sent to over fifty personnel having a daily awareness of helicopter windshield problems. One can see that scratches were definitely the major problem area.

Since that beginning, most large classification helicopters, such as the Boeing Vertol CH-46, CH-47; Sikorsky CH-53; Kaman UH-2; and Bell UH-1, have had their forward vision transparencies redesigned and qualification tested. These aircraft have been retrofitted with a design that has as its basic requirement a glass outer surface.

The two types of glass faced windshields used currently are the thin glass laminate and a composite glass-acrylic laminate. Based on reports received from the air frame designers and military users, PPG's thin glass laminate helicopter transparencies have accrued many thousands of flight hours and are performing very well.

#### PPG'S INTERIM ACCOMPLISHMENTS

During the period of 1969 to 1973, PPG has been working in-house and has improved the design and process capabilities for production of the thin glass helicopter windshields.

Among the most important are:

##### I. Low Resistance Heating Films

PPG has continually worked on upgrading the deposition of our standard NES<sup>A</sup>(R) heating film to achieve lower resistivities. This film is stannus oxide fired on the glass at an elevated temperature resulting in a durable coating. We can now achieve resistivities as low as 12 ohms/square. In addition, our research facilities

continue to develop and evaluate various techniques for vacuum deposition and sputtering of various materials.

## II. Edge Attachment Development

PPG has always believed that the edge attachment design and adaptation for helicopter transparencies is a significant factor in prolonging the life cycle. This is due to the flight profile of these aircraft, which encounter more vibration, and shock loading than conventional aircraft. We have progressed in this area through the use of more flexible edge members such as fiberglass and resilient adhesive materials. One positive advantage of using these nonmetallic materials is the elimination of electrical faults previously encountered. This was accomplished without any sacrifice of strength. The use of proper installation techniques and cushion mediums have also resulted in greater service life.

## III. Three Phase Heating Films

As the requirements for three phase heating systems appeared, PPG developed methods for applying the NES<sup>A</sup>(R) films to glass in such a manner that the electrical load balance would be maintained. Also by selective grading, we have been able to guarantee that the windshield would de-ice in a uniform manner regardless of transparency shape.

## IV. Process Improvements

PPG has developed sophisticated equipment and tooling for forming, tempering, and coating thin glass that have made it possible to process large volume production runs of various curved and flat windshield shapes. Capability to repeatedly manufacture windshields to the required curvature and optical requirements has been achieved, while at the same time maintaining cost effectiveness.

In this interim period we have also been investigating alternate designs such as:

### I. Composite Design

PPG has fabricated composite helicopter transparencies using polycarbonate and glass. These designs indicate improved resistance to

ballistic and bird impacts which will be discussed in more detail later in this paper. The key to a successful composite glass/plastic windshield lies in the proper selection of the interlayer material. An interlayer material is needed that will adhere to both glass and plastic using relatively low bonding temperatures and also be resilient enough to withstand the thermal mismatch due to the different coefficients of expansion between glass and plastic materials. PPG is currently evaluating several new interlayer materials which have desirable characteristics for helicopter transparency applications.

## II. High-Strength Thin Glass

The investigation of this material shows that because of the unusually large areas associated with helicopter transparencies, a practical limit is reached on thickness of material used because of deflection. Also there has been a problem with the thickness of the compression strength layer on the extremely thin high strength glasses.

## THE FUTURE

We now come to the future of helicopter transparencies and the requirements that must be fulfilled.

There are many new helicopter programs underway throughout the world, especially in the United States. These so-called second generation aircraft, such as the UTTAS, HLH, AAH, and armored ships, are in the design stages at this time. Their purpose is to replace aging aircraft and at the same time implement operational improvements which have been found necessary.

The transparency requirements for these helicopters will require many new additional characteristics, some of which are as follows:

1. Ballistic protection,
2. Anti-reflective coatings,
3. Weight limitations,
4. Bird proofing,
5. Abrasion resistant coatings.

### I. Ballistic Protection

With the increasing use of rotary wing aircraft in combat roles and the susceptibility of any hovering type aircraft to ballistic threat, transparent armor has become an area of interest.

Transparent armor for crew protection can be considered for lower observation windows, main windshields, and internal partitions between crew members. Ballistic design properties of transparent materials are classified into two categories:

- (1) The projectile will penetrate the transparent material with a minimum spall being released, and
- (2) transparent armor that will defeat the projectile.

Existing windshield designs of both glass/stretched acrylic and all glass have been tested by the Army at Aberdeen Proving Grounds and found to have acceptable spall and residual vision characteristics when struck with 30 cal. projectiles. PPG has developed both all glass and glass-plastic armor capable of defeating A.P. projectiles up to .50 cal. The composite glass-plastic armor system is the most efficient, with merit ratings of 1.0 or less with no spall being released. Weight densities in the order of 10 to 20 pounds/sq. ft. are required for ballistic armor as compared to the nominal weight of 2.5 to 3.0 pounds/sq. ft. for conventional helicopter windshields.

## II. Anti-Reflective Coatings

Low-reflective coatings for internal and external application must be considered for new generation helicopters. Reflections from instrument lights when flying at night can be distracting to pilots. This is particularly true of the tandem seat attack type helicopter which typically has rather large windshield areas extending behind the instrument board with the windshield surface at relatively large angles of incidence to the instrument lights. The external application is considered when visual detection from reflected light is a design consideration. Existing low-reflective coatings are most efficient for angles of incidence up to 30° and are typically soft coatings. Areas such as evaluating the effectiveness of low-reflective coatings, application to various substrate materials and durability, require more investigation and testing.

### III. Weight Limitations

Existing glass faced windshield designs weigh approximately 2.5 to 3.0 pounds/sq. ft. It is conceivable that an areal density of 2.2 pounds/sq. ft. can be realized, but this should be used as a goal, and any efforts to reach this goal should be evaluated against flexural strength, rigidity, and other mechanical considerations. These considerations will be of primary interest as the trend advances to larger transparencies on higher speed helicopters.

### IV. Bird Proofing

Although resistance to bird impact has not been a primary design objective of helicopter transparencies in the past, it must be considered for future generation helicopters. Reports of bird strikes on helicopter transparent areas has been documented, and with the increased speed and mission profile of future helicopters, it could become a design requirement similar to conventional aircraft. Typical bird impact requirements for helicopter windshields will require defeating the bird in the range of 200 to 250 m.p.h. The superior impact properties of polycarbonate material have long been recognized by PPG and therefore is considered to be an optimum material for this application. Bird impact tests on 26" x 26" specimens of existing windshield constructions and advanced designs of composite glass/polycarbonate constructions have been conducted by PPG. The results of these tests are tabulated on Figure III and can be summarized as follows:

- (1) Existing windshields utilizing .250" stretched acrylic and the lightweight all glass configuration failed at speeds as low as 100 m.p.h. when impacted with a four-pound bird at room temperature.
- (2) Monolithic .250" polycarbonate is capable of defeating a four-pound bird at approximately 250 m.p.h.
- (3) Composite designs of glass and polycarbonate weighing 4.5 pounds/sq. ft. are capable of defeating a four-pound bird at 250 m.p.h.

## V. Abrasion Resistant Coatings

Abrasion resistant coatings for application to monolithic stretched acrylic windows to reduce wiper abrasion and generally extend the life of plastic transparencies is another area of interest. Existing windshield specifications do not require the use of hard coatings on acrylic plastic. The use of polycarbonate material will require protective hard coatings because of the low abrasion resistance of this material even to normal cleaning operations. Hard coatings have been developed for polycarbonate that appear to be suitable for interior surfaces but are still in the development and evaluation stages for external use.

The design of an optimum transparency that will meet all of these requirements is, indeed, an ambitious task. As has been discussed, it becomes apparent that a compromise design approaching this optimum will be necessary.

Let us all, the airframe designer, the military, and the transparency supplier work together to provide a functional, reliable end-use item that will serve its purpose regardless of the environment, either natural or man made.

- 
- (1) PPG Phase I Report  
"Develop Design, Test, and Acceptance Criteria for Army  
Helicopter Transparent Structures", Contract DAAJ02-72-C-0073.

FIGURE I

OPERATIONAL ENVIRONMENT

NATURAL ELEMENTS

TEMPERATURE  
HUMIDITY  
DUST/SAND  
SALT WATER  
RAIN  
ICE PARTICLE IMPINGEMENT  
HAIL  
ULTRA VIOLET RADIATION

MAN MADE ELEMENTS

BALLISTIC PROJECTILES & FRAGMENTS  
CHEMICAL ATTACKS BY:  
1. SOLVENTS  
2. CLEANING COMPOUNDS  
3. FUEL  
WINDSHIELD WIPER OPERATION  
AIRFRAME RACK & TWISTING  
CRASH WORTHINESS



FIGURE II

PREDOMINANT FAILURE MODES

|                     | <u>PERCENTAGE</u> |                |
|---------------------|-------------------|----------------|
|                     | <u>MODE #1</u>    | <u>MODE #2</u> |
| SCRATCHES           | 61                | 25             |
| CRACKING & BREAKING | 2                 | 4              |
| CLEANING PROBLEMS   | 4                 | 12             |
| SOLVENT ATTACK      | 0                 | 6              |
| DISTORTED VISION    | 10                | 20             |
| MISTREATMENT        | 8                 | 4              |

FIGURE III

BIRD SHOT RESULTS

| <u>MATERIAL</u>  | <u>SPEED</u> | <u>REMARKS</u>                                   |
|--|--------------|--|
| 1) 1/4" STRETCHED ACRYLIC  | 100 MPH      | BIRD PENETRATED,<br>COMPLETELY DESTROYED         |
| 2) 1/4" POLYCARBONATE -<br>(HARD COATED)                             | 245 MPH      | BIRD BOUNCED,<br>(BOLT HOLES DEFORMED)           |
| 3) .10" TEMPERED GLASS +<br>.10" INTERLAYER +<br>.10" TEMPERED GLASS | 100 MPH      | BIRD PENETRATED,<br>COMPLETELY DESTROYED         |
| 4) .10" GLASS +<br>.10" INTERLAYER +<br>1/8" POLYCARBONATE           | 250 MPH      | PENETRATED,<br>(BIRD CAUGHT IN<br>POLYCARBONATE) |

NOTE: ALL SHOTS MADE AT ROOM TEMPERATURE AND 65° ANGLE  
USING A 4-POUND BIRD.

|   |         |              |
|---|---------|--------------|
| 5) .10" TEMPERED GLASS +<br>.06" INTERLAYER +<br>.10 TEMPERED GLASS | 173 MPH | BIRD BOUNCED |
|---|---------|--------------|

NOTE: THIS SHOT MADE AT ROOM TEMPERATURE AND 45° ANGLE  
USING A 1-POUND BIRD.

CRACK FORMATION IN F-4 AIRCRAFT  
CANOPIES

D. R. Mulville, I. Wolock, and R. J. Thomas  
Naval Research Laboratory  
Washington, D. C.

## CRACK FORMATION IN F-4 AIRCRAFT CANOPIES

by

D. R. Mulville, I. Wolock and R. J. Thomas

Naval Research Laboratory  
Washington, D. C. 20375

### Abstract

The initiation of cracks in stretched acrylic plastic has been reported for F-4 canopies under storage conditions. The cracks started at the edge and propagated parallel to the plane of the sheet between the fiberglass-acrylic edge attachments. However, laboratory tests indicated that the presence of these cracks has negligible effect on the bearing strength of the edge attachment.

A limited investigation was undertaken to determine the conditions under which the crack formed in the canopy. There appears to be two separate processes: crack initiation and crack propagation.

The former is the more complex phenomenon. It was shown that cracks will initiate in stretched acrylic plastic when it contains over 1.6% moisture and is then exposed to low humidity. The exact conditions for crack initiation were not defined.

Cracks will propagate in stretched acrylic with a fiberglass edge attachment if cracks are present and the assembly is heated to 120°F or higher. They do not propagate with a nylon edge attachment. Using a fracture mechanics approach, in which the difference in thermal expansion produces an opening mode force, it is possible to predict the temperature at which an existing crack will propagate. This was calculated to be approximately 170°F. which was substantially verified in experimental tests. However, existing crack do not propagate at elevated temperatures when a nylon reinforced edge attachment is used because there is little difference in the coefficients of thermal expansion of the acrylic and the nylon-acrylic laminate.

### Introduction

The formation of cracks was observed in the stretched acrylic of F-4 aircraft canopies while in storage prior to service. The cracks initiated at the end of the edge attachment and propagated parallel to the plane of the sheet into the interior of the canopy as far as the end

of the edge attachment. These canopies are formed of 3/8-inch thick stretched acrylic and have a fiberglass-acrylic edge attachment. An investigation was undertaken of the origin of these cracks and of their effect on the performance of the canopy.

The investigation is divided into three parts: bearing tests, crack initiation studies and crack propagation studies. The effect of in-plane cracks on the performance of the edge attachment was evaluated by determining the bearing strength of specimens modeling an edge attachment assembly. In studying the problem of the origin of the in-plane cracks, attention was directed to the effects of variations in temperature and in humidity, since those are the two parameters that would vary during the storage of the canopies. This part of the study was subsequently divided into two separate problems; crack initiation and crack propagation, since it became apparent during the investigation that these processes occurred under different conditions.

#### Materials

Two F-4 aircraft canopies that had formed edge cracks during storage were furnished by Mr. R. E. Wittman of the Air Force Flight Dynamics Laboratory at Wright-Patterson Air Force Base. The stock number was 1560 788 6502. Uncracked specimens were obtained from samples of the typical edge attachment, purchased from Swedlow Inc. (Fig. 1). In addition, to provide a comparison, edge attachment material of the same configuration was obtained using nylon fabric as the reinforcement instead of fiberglass. In some cases, tests were also conducted on control stretched acrylic and on stretched acrylic taken from the canopy, both without an edge attachment.

#### Bearing Studies

A limited investigation was conducted of the effect of in-plane cracks in the acrylic on the bearing strength of the edge attachment at room temperature. Specimens were prepared using the geometry which approximated the configuration used in the aircraft. 1/4-inch diameter holes were drilled in specimens 1/2-inch from the end. The specimens were 1-inch wide, since the bolt holes on the canopy were that distance apart. The holes were drilled through the fiberglass edge attachment and the acrylic, and a metal face plate applied to each surface and the assembly bolted together using a typical service bolt tightened to the aircraft manufacturer's specified torque of 40 in.-lb. Tensile loading was applied to the acrylic plastic at one end of the specimen and to the edge attachment assembly at the other end through the bolt.

Tests were conducted on the control edge attachment material as well as on specimens taken from F-4 canopies and on specimens of stretched acrylic with no edge attachment. Some of the specimens were tested containing cracks parallel to the surface whereas others were uncracked.

Most of the specimens were tested with the bolts torqued to 40 inch-lbs., but several were tested with the bolts just finger tight.

The results are presented in Table I. They indicate the following:

1. Edge attachment specimens with cracks fail at approximately the same loads as those specimens without cracks. The presence of a crack parallel to the surface in the stretched acrylic does not reduce the bearing strength of the material.
2. Actually, stretched acrylic specimens with a fiberglass edge attachment do not fail in bearing. They fail in tension at the tapered junction of the edge attachment and the stretched acrylic due to the stress concentration caused by the difference in stiffness.
3. The canopy specimens with edge attachment failed at loads approximately 1/3 less than those for control edge attachment material. This reduction is probably caused by degradation of the resin matrix in the edge attachment composite, increasing the stress concentration at the tapered end of the edge attachment.
4. Stretched acrylic, tested in bearing, fails at the same or slightly higher load than control material with a fiberglass edge attachment. However, the acrylic does not decrease in bearing strength due to aging, and as a result its strength is almost double that of the aged canopy edge attachment material. The need for edge attachment reinforcement in combination with stretched acrylic glazing must again be questioned.
5. The data are not definitive with regard to the effect of bolt torque on the load at failure.

#### Crack Initiation Studies

In studying the initiation of cracks in the edge attachment assembly a series of tests were conducted to determine the effect of moisture and temperature on the behavior of the acrylic plastic with no initial cracks.

The results are summarized in Table II. It was found that heating the control fiberglass edge attachment assembly at 160°F for extended period of time did not result in crack initiation, nor did cycling from room temperature to 160°F for sixty-four cycles result in crack initiation. The possible role of moisture was introduced by conditioning the specimens at high humidity at various temperatures before heating to 160°F. Conditioning at 75°F and 95% RH followed by heating to 160°F did not result in crack formation. However preconditioning at 140°F and 95% RH did result in crack initiation in a number of specimens. Preconditioning at 160°F and 95% RH also resulted in some crack initiation, but when the preconditioning period was extended to 7 days, all of the specimens

cracked except for the stretched acrylic with no edge attachment, taken from the canopy. Making the exposed acrylic edge extremely smooth by polishing decreased the time for crack initiation, whereas roughening the surface with a coarse file increased the time required for a crack to form. Finally, preconditioning the specimen in water at 160°F for 7 days led to crack initiation in all of the specimens tested, including the stretched acrylic with no edge attachment exposed to 75°F and low RH.

To determine how the preconditioning affected the moisture content of the stretched acrylic, water absorption measurements were made on test specimens for various conditions for 7 days. The results are presented in Figure 2. It appears that if the moisture content of the stretched acrylic is 1.6%, which is achieved in water at 160°F in 7 days, then cracks will initiate in all specimens when exposed to low RH. From 1.4 to 1.6%, which is achieved at 160°F and 95% RH in 7 days, cracks will initiate in specimens with edge attachment when heated to 160°F. If the moisture content is approximately 1.1-1.3%, which is reached at 160°F and 95% RH in 4 days or 140°F and 95% RH in 7 days, then some specimens will crack. At lower moisture contents, stretched acrylic specimens will not form cracks when heated to 160°F.

The acrylic plastic edge of the as-received edge attachment assembly was fairly rough and tool marks were visible. However the limited tests conducted indicated that polishing would not retard the formation of cracks and instead might accelerate their initiation.

In several of the tests, acrylic plastic from the aged canopy did not crack whereas the remaining test specimens did. The reason for this behavior is not apparent.

There are a number of questions regarding crack initiation that were not answered by this limited investigation. Conditions under which cracks may initiate have been determined but it was not demonstrated that conditions of this type were encountered in the storage of the canopies that cracked. However, due to the limited scope of this investigation, further studies to clarify these questions were not pursued.

#### Crack Propagation Studies

The difference in coefficient of thermal expansion between acrylic plastic and fiberglass-acrylic laminate is well known and is presented in Figure 3 (Ref. 1). An analysis was conducted to determine under what conditions the stresses induced in the stretched acrylic plastic due to this thermal mismatch could produce crack propagation in the acrylic.

If the edge attachment segment is analyzed as a cantilever beam under uniform bending (Figure 4), a failure criterion can be developed to predict the temperature at which the initial crack will propagate.

At the acrylic-fiberglass interface the strain is

$$(\Delta\alpha \Delta T) = (\alpha_1 - \alpha_2) (T - T_0)$$

where  $\Delta\alpha$  is the difference in coefficients of thermal expansion,  $(\alpha_1 - \alpha_2)$ , of the acrylic and the fiberglass, respectively, and  $\Delta T$  is the difference in temperature  $(T - T_0)$ . Using this value of strain, the corresponding bending moment is,

$$M = \frac{2(\Delta\alpha\Delta T) EI}{h}$$

where  $h$  is one-half the thickness of the acrylic, and  $EI$  is the flexural rigidity of the beam.

For a cantilever beam under uniform bending, the strain energy release rate,  $\mathcal{G}$ , can be expressed as

$$\mathcal{G} = \frac{M^2}{bEI}$$

where  $b$  is the width of the acrylic specimen. Substituting the expression for the thermally induced moment,  $M$ , yields a relation between,  $\mathcal{G}$ , and temperature,

$$\mathcal{G} = \left[ \frac{2(\alpha_1 - \alpha_2) (T - T_0) EI}{h} \right]^2 \frac{1}{bEI}$$

This expression can then be solved for the temperature as follows,

$$T = \frac{(\mathcal{G}bEI)^{\frac{1}{2}} h}{2(\alpha_1 - \alpha_2)EI} + T_0$$

Since both  $\alpha$  and  $E$  are temperature dependent, these quantities must be represented as function of temperature in order to calculate the critical temperature at which crack propagation occurs,  $T$ .

In addition the strain energy release rate for this mode of crack propagation must be known. Broutman and McGarry (Ref. 2) have reported values of the surface work (or one-half the fracture energy) for crack propagation parallel to the plane of a multiaxially stretched (65%) acrylic sheet of  $1.65 \times 10^4$  ergs/cm<sup>2</sup> (0.094 in.-lb/in.<sup>2</sup>) at room temperature.

Using this value to compute the strain energy release rate, the critical temperature is estimated to be approximately 170°F. It should be noted that this is a two-dimensional analysis, and that the experimental value of fracture energy was reported for room temperature and not at the critical temperature. At corners of the canopy the bending moment acts in two directions, and hence initiation and propagation of cracks are more likely to occur here at lower temperatures.



Tests were conducted to determine experimentally under what conditions cracks would propagate in the stretched acrylic at the edge attachment. The results are summarized in Table III. In the first set of tests, it was found that when specimens with 60° grooves machined in the acrylic at the end of the edge attachment were heated to 160°F, cracks did not propagate from the tip of the groove. In the next set of tests, an actual crack was initiated in each specimen by machining a notch in the end and then driving a wedge into the notch until a uniform crack formed along the length of the specimen. When specimens of this type with a fiberglass-acrylic edge attachment were heated to 160°F, the crack propagated. However, with a nylon-acrylic edge attachment, the cracks did not propagate.

A third group of tests were conducted to determine the minimum temperature at which cracks will propagate. This was found to be between 110° and 120°F for stretched acrylic with a fiberglass-acrylic attachment.

Finally, tests were conducted to determine if there is a minimum length crack that will propagate when the assembly is heated. Cracks approximately 1/16-, 1/8-, and 1/4-inch long were initiated in specimens with a fiberglass edge attachment. Cracks propagated in all of the specimens when heated to 160°F.

Thus when a crack is initiated in stretched acrylic with a fiberglass edge attachment, the crack will propagate if the assembly is heated to 120°F or higher. Cracks do not propagate with a nylon edge attachment even at 160°F.

#### Summary and Conclusions

Studies were conducted to determine the effects of in-plane cracks in the stretched acrylic on the performance of a fiberglass edge attachment assembly and to determine the origin of cracks that form in storage in canopies using this material.

Bearing tests on the edge attachment assembly indicated that:

1. The presence of cracks parallel to the surface in the stretched acrylic does not reduce the bearing strength of the material.
2. This assembly does not fail in bearing but instead in tension at the tapered end of the fiberglass reinforcement due to the stress concentration caused by the change in stiffness.
3. The aged edge attachment material fails at loads approximately one-third less than that for unaged material.
4. When the stretched acrylic alone is tested in bearing, it fails in tension at the bolt hole at loads that are the same or slightly higher

than the control material with fiberglass reinforcement and approximately double that of the aged edge attachment. This again raises the question of the justification for fabric reinforcement when stretched acrylic is used in aircraft canopies.

Studies of the initiation of cracks in stretched acrylic indicate that if the moisture content is 1.6% or above, cracks will initiate when the material is exposed to low humidity. At lower moisture contents, crack initiation is not consistent. The exact conditions at which cracks will form after this preconditioning were not determined.

Once a crack has initiated in stretched acrylic with a fiberglass edge attachment, it will propagate if the assembly is heated to 120°F or higher. However, cracks will not propagate with a nylon edge attachment even at 160°F. Using a fracture mechanics approach, in which the difference in thermal expansion produces an opening mode force, it is possible to predict the temperature at which an existing crack will propagate. This analysis predicts the behavior of the fiberglass edge attachment as well as the nylon edge attachment.

This limited investigation has not established that F-4 canopies can attain a moisture content of approximately 1.6% in storage. However, it is not unreasonable that this condition is attained and that subsequent environmental conditions could lead to the formation and propagation of cracks that have been observed in the canopies. The use of a nylon edge attachment would eliminate the propagation of the cracks. However, it has not been demonstrated that these in-plane cracks pose a danger to the structural integrity of the canopy.

#### Acknowledgement

This investigation was sponsored by the Naval Air Systems Command with Mr. Charles F. Bersch as project monitor. The authors wish to acknowledge many fruitful discussions held with Mr. Bersch. Cracked F-4 canopies were kindly furnished by Mr. R. E. Wittman, Air Force Flight Dynamics Laboratory, Wright-Patterson Air Force Base. The cooperation of Swedlow, Inc. is also acknowledged, from whom special edge attachment material was purchased.

#### References

1. Plastics for Flight Vehicles. Part II. Transparent Glazing Materials. MIL-Handbook 17 (Aug. 1961).
2. Broutman, L. J. and McGarry, F. J. "Fracture Surface Work Measurements on Glassy Polymers by a Cleavage Technique. II. Effects of Crosslinking and Preorientation". J. Applied Polymer Science 9, 609 (1965).

TABLE 1. BEARING TESTS OF F-4 EDGE ATTACHMENTS

|                  | <u>CRACKED</u> <sup>a</sup> | <u>EDGE<br/>ATTACHMENT</u> <sup>b</sup> | <u>BOLT<br/>TORQUE</u> <sup>c</sup> | <u>FAILURE<br/>LOCATION</u> <sup>d</sup> | <u>FAILURE<br/>LOAD</u><br>lb. |
|------------------|-----------------------------|---|-------------------------------------|--|--------------------------------|
| CONTROL MATERIAL |                             | X                                       | 40                                  | EAB                                      | 1700                           |
|                  |                             | X                                       | F                                   | EAB                                      | 1750                           |
|                  | X                           | X                                       | 40                                  | EAB                                      | 1990                           |
|                  | X                           | X                                       | F                                   | EAB                                      | 1840                           |
|                  |                             |   | 40                                  | HOLE                                     | 2150                           |
|                  |                             |   | F                                   | HOLE                                     | 1710                           |
| CANOPY MATERIAL  |                             | X                                       | 40                                  | EAB                                      | 1180                           |
|                  |                             | X                                       | 40                                  | EAB                                      | 1245                           |
|                  |                             | X                                       | 40                                  | EAB                                      | 1210                           |
|                  | X                           | X                                       | 40                                  | EAB                                      | 1160                           |
|                  | X                           | X                                       | 40                                  | EAB                                      | 1070                           |
|                  | X                           | X                                       | 40                                  | EAB                                      | 1260                           |
|                  |                             |   | 40                                  | HOLE                                     | 2250                           |
|                  |                             |   | 40                                  | HOLE                                     | 2300                           |

- a. X indicates crack in stretched acrylic parallel to the plane of the sheet.  
b. Specimens without X were stretched acrylic with no reinforcement.  
c. 40 inch-pounds or finger tight.  
d. EAB indicates tensile failure in the acrylic at the end of the edge attachment.  
Hole indicates tensile failure initiating at the bolt hole.

TABLE II: CRACK INITIATION STUDIES OF F-4 EDGE ATTACHMENT

|   | CONTROL  |   |  | CANOPY                                |
|---|--|---|--|---------------------------------------|
|   | FIBERGLASS E/A <sup>a</sup>  | NYLON E/A                                     | NO E/A                                   |                                       |
| 1. 160°F  | (1/15) Cracked   |   |  |                                       |
| 2. Cycle 75°-160°F<br>64 3 Hr Cycles            | No Cracks  |   |  |                                       |
| 3. 75°F/95%RH/16 Days to 160°F                  | No Cracks  |   |  |                                       |
| 4. 140°F/95%RH/7 Days to 160°F                  | (1/3) Cracked in<br>1 Hr. b  | (3/3) Cracked<br>in 1½, 1½, 5 Hr. in 3, 5 Hr. | (2/3) Cracked<br>in 3, 5 Hr.             | (1/3) Cracked<br>in 3 Hr.             |
| 5. 160°F/95%RH/4 Days to 160°F                  | (1/3) Cracked  |   |  | (0/3 Cracked)                         |
| 6. 160°F/95%RH/7 Days to 160°F                  | (3/3) Cracked in<br>1/3, 3, 3 Hr.  | (3/3) Cracked<br>in 5 Hr.                     | (3/3) Cracked<br>in 2/3, 2/3,<br>3 Hr.   | (0/3 Cracked)                         |
| Varied Surface Roughness                        | Polished - 20 Min. <sup>c</sup><br>A/R - 40 Min.<br>Roughened - 120 Min. | A/R - 20 Min.                                 |  |                                       |
| 7. 160°F Water/7 Days to 160°F                  | (3/3) Cracked in<br>2/3, 1, 1½ Hr.                                       | (3/3) Cracked<br>in 1/3, 1½, 1½<br>Hr.        | (3/3) Cracked<br>in 2/3, 2/3,<br>2/3 Hr. | (3/3) Cracked<br>in 2/3, 1, 1½<br>Hr. |
| 8. 160°F Water/7 Days to 75°F<br>Low RH         |  |   | (4/4) Cracked                            |                                       |
| a. E/A = Edge Attachment                        |  |   |  |                                       |
| b. (1/3) = 1 specimen out of 3 specimens tested |  |   |  |                                       |
| c. A/R = As received                            |  |   |  |                                       |

TABLE III: CRACK PROPAGATION STUDIES OF F-4 EDGE ATTACHMENT

|   | <u>CONTROL</u>   |                               |
|---|--|-------------------------------|
|   | <u>FIBERGLASS E/A<sup>a</sup></u>  | <u>NYLON E/A</u>              |
| 1. HEAT AT 160°F<br>(60° GROOVES IN END) <sup>b</sup> | NO EFFECT  |                               |
| 2. HEAT AT 160°F<br>(CRACKS INITIATED IN END)         | PROPAGATE  | DO NOT PROPAGATE              |
| 3. HEAT AT VARIOUS TEMP.<br>(CRACKS INITIATED IN END) | PROPAGATES @ 130°F/1 HR.<br>PROPAGATES @ 120°F/3 HR.<br>NO PROPAGATION @ 110°F | NO PROPAGATION UP<br>TO 130°F |
| 4. HEAT AT 160°F<br>(CRACKS INITIATED IN END)         | 1/16 <sup>c</sup> , 1/8-, 1/4-INCH<br>CRACKS PROPAGATE                         |                               |

a. E/A = edge attachment.

b. End refers to stretched acrylic at free edge of canopy, in between fiberglass reinforcement. (See Fig. 1). Grooves or cracks were parallel to the plane of the sheet.

c. Length of cracks initiated in end.

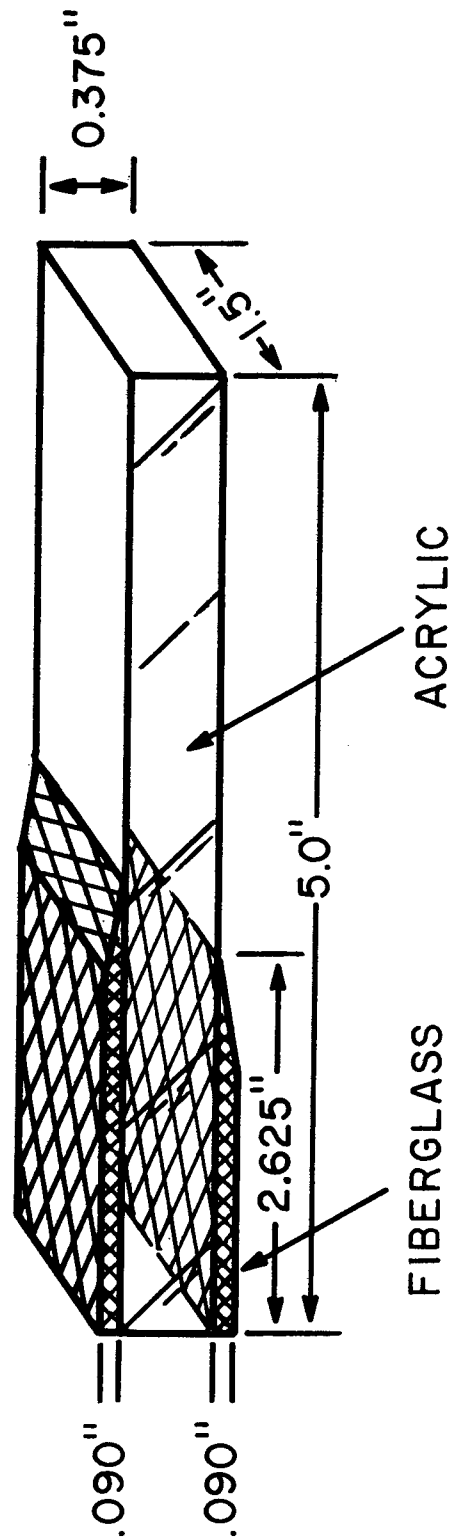


Figure 1: F-4 Canopy Edge Attachment

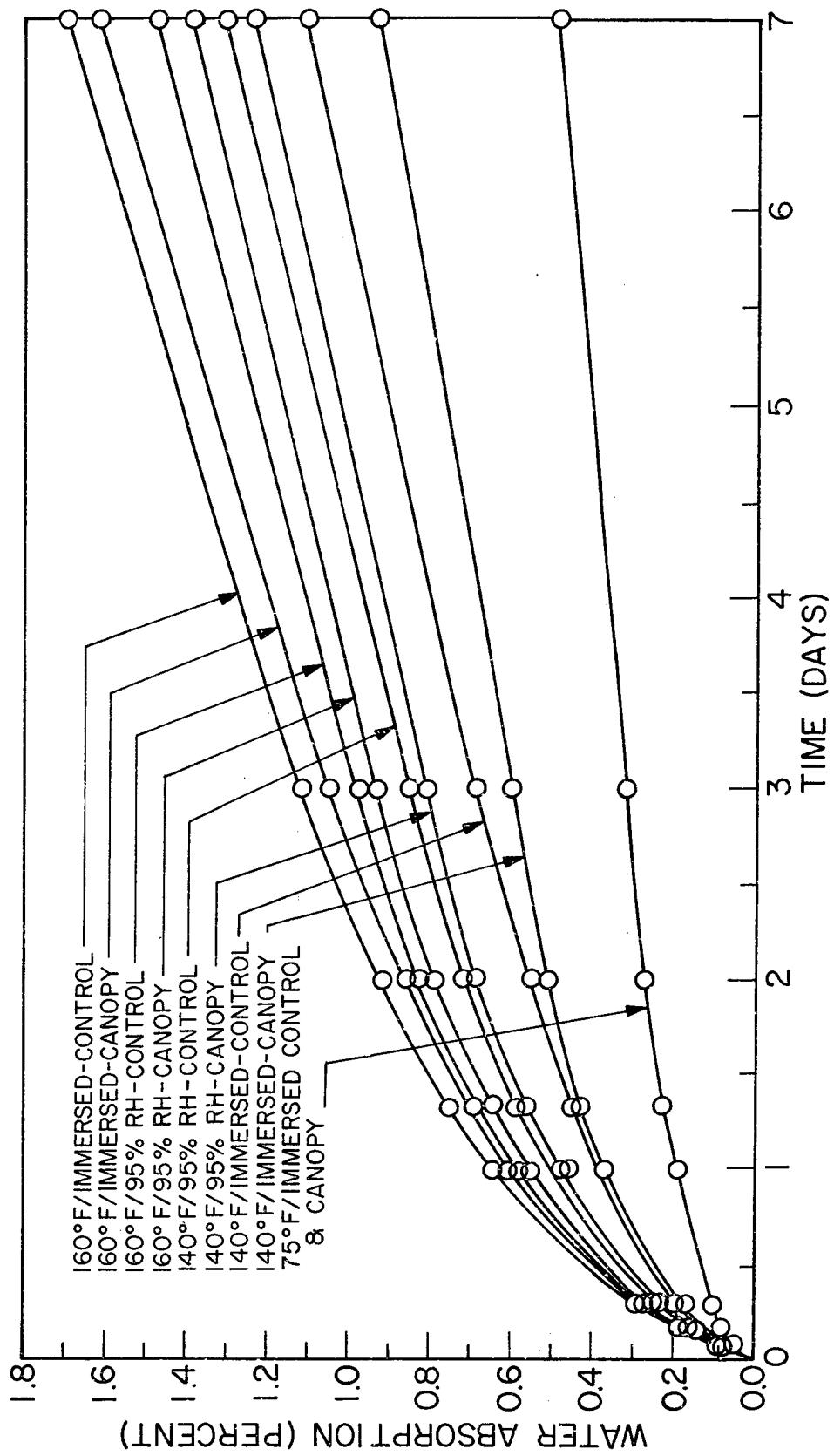


Figure 2 Water Absorption of Stretched Acrylic (65%)

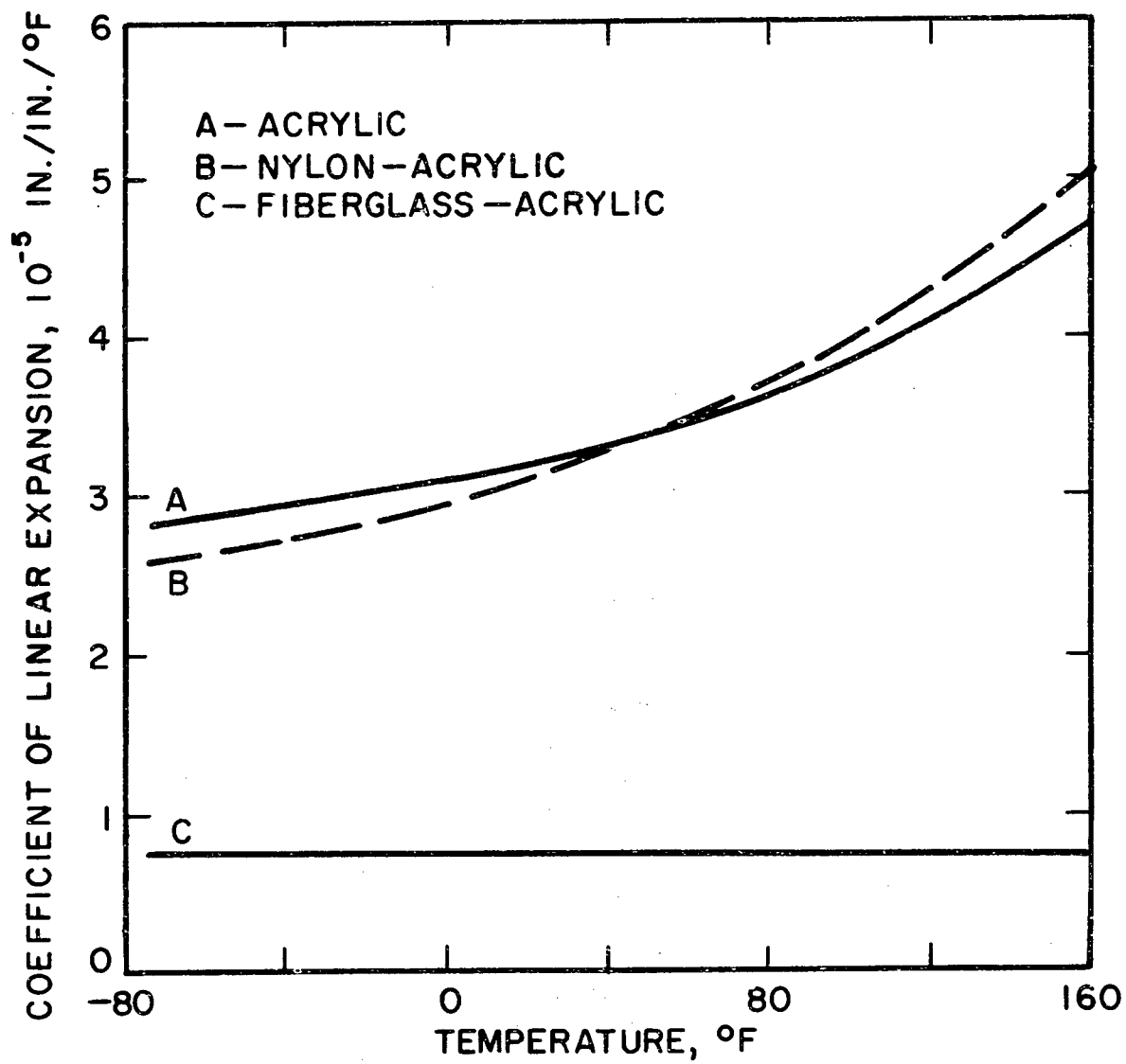


Figure 3 Effect of Temperature on Linear Coefficient of Thermal Expansion for Various Materials (Ref. 1)



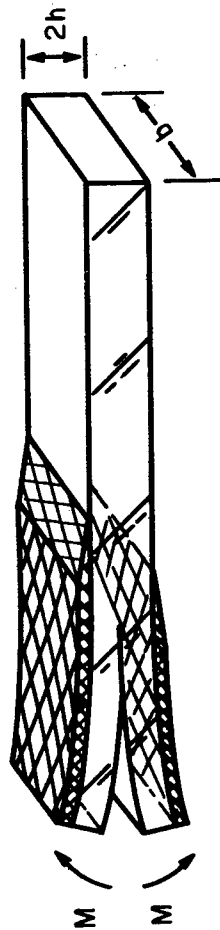


Figure 4: Effect of Thermal Loading on F-4 Edge Attachment

THE DESIGN, DEVELOPMENT AND TESTING OF  
FLAT AND CURVED ALL GLASS WINDSHIELDS FOR  
WIDE BODIED AIRCRAFT USING THE LATEST  
DEVELOPMENTS IN HIGH STRENGTH GLASS AND  
ELECTRO-CONDUCTIVE COATINGS

W. G. Roberts  
Triplex Safety Glass Co. Ltd.  
Kings Norton, Birmingham, England

THE DESIGN, DEVELOPMENT AND TESTING OF FLAT AND CURVED ALL GLASS WINDSHIELDS FOR WIDE BODIED AIRCRAFT USING THE LATEST DEVELOPMENTS IN HIGH STRENGTH GLASS AND ELECTRO-CONDUCTIVE COATINGS.

BY W. G. ROBERTS  
TRIPLEX SAFETY GLASS CO. LTD.

#### ABSTRACT

A light-weight flat windshield made of "TEN-TWENTY" high strength glass, designed from the outset for maximum reliability, is described. As bird impact was the critical case, the optimum design was initially established by test and later confirmed during Qualification Testing in representative aircraft structure.

The windshield's reliability has been subjected to intensive development involving the simulation of 10,000 hours flying in Triplex's Life Test facilities.

The design concepts developed for this flat windshield are now being extended for a curved windshield of similar construction. Although the use of two structural plies gives a fail-safe capability, a tertiary load path is provided by the polyvinyl butyral interlayer acting as a diaphragm, incorporating a newly developed system of edge attachment.

This windshield, which employs a sub-frame made up of extruded and forged sections, contains two curved 12 mm "TEN-TWENTY" plies, laminated with a thin glass facing ply. Again, a considerable amount of preliminary bird impact testing has been undertaken, which has yielded valuable design information on the difference between rigid test fixtures and actual aircraft structure.

The curved windshield is heated by Triplex "HYVIZ" electro-conductive film, "HYVIZ" being a newly developed high light transmission metal oxide coating, with a wide range of resistivity, capable of being graded in thickness to produce uniform heating over the complete area of the difficult shape involved.

#### INTRODUCTION

For many years most transport aircraft throughout the world have used a common form of windshield construction with a single ply of tempered glass for pressure resistance, combined with a thick polyvinyl butyral interlayer. This interlayer is usually reinforced at the edges with a metal insert and acts as a diaphragm to provide bird impact resistance, and also serves as a secondary load path to contain pressurization in the event of failure of the primary glass ply.

With material developments in both the glass and plastic fields we have seen in recent years the introduction of the glass-faced acrylic windshield, offering significant weight savings and, perhaps just as important, the ability to provide curved constructions of good optical quality.

This paper is concerned with a further alternative in design, consisting of a multi-laminate glass construction, where the resistance to both bird impact and pressurization is provided by two or more plies of tempered glass, with the interlayer holding the glasses together in an essentially non-structural role.

There is certainly nothing novel in this type of construction which has been in use for many years on military aircraft as a bullet resistant block. However, it has not been a serious contender in the transport field until recently, primarily on weight grounds.

There are several factors that have brought it back into consideration, primarily the availability of a high strength glass, tempered to a breaking strength of approximately twice the conventional product. This allows the multi-laminate windscreen to be designed at a weight which compares favourably with the other types of construction.

In addition, the clamped-in windshield has now been shown to have excellent reliability, as it can be insulated both mechanically and thermally from the surrounding aircraft structure.

## DISCUSSION

Figure 1 shows a modern example of this type of construction, i.e. the windshield of the European A300B Airbus. Figure 2 illustrates the construction showing in particular the two major structural elements which are Triplex "TEN-TWENTY" high strength glasses, each 10 mm (.394") thick with a conventional outer 5 mm (.197") facing ply which carries an electro-conductive gold coating for de-icing and de-misting. The windshield is finished off with an extremely precise silicone rubber edge moulding and is designed to be clamped in place into a rigid surround structure such that the windshield can be insulated as far as possible from structural deformation and the low soak temperatures achieved during high altitude cruise.

Triplex "TEN-TWENTY" high strength glass is a recently developed product with an extremely high Modulus of Rupture induced by thermal means. Figure 3 illustrates the induced stress profile through the thickness of a "TEN-TWENTY" glass, which is compared with the conventional tempered product. Strengths of up to 45,000 lb/square inch can be achieved in a range of glass thicknesses using conventional soda lime glass produced by the universal float process.

The European Airbus was the first application of "TEN-TWENTY" glass in a forward facing windshield and a considerable amount of experimental bird impact testing had to be carried out before the final design was established. A preliminary programme was first carried out on simple panels of rectangular construction to establish the performance of "TEN-TWENTY" glass, particularly in relation to the known performance of the conventional tempered product (see Figure 4). The testing was then extended to full size windshields (see Figure 5). In both cases, extremely rigid steel frames were used for mounting the test panels. The results have since been confirmed by the Certification Testing in full aircraft structure which has indicated that the initial use of the rigid test fixtures gave slightly pessimistic results, probably related to the energy absorption of the full aircraft surround structure.

It will be noted from Figures 4 and 5 that this type of windshield resists the energy of impact by "bird bouncing", in that the kinetic energy of impact is dissipated by the bending strength of the windshield. With suitable choice of facing ply, the bird-bouncing windshield can be left undamaged after impact up to the specified design level.

Reliability was considered paramount in the design of the Airbus windshield and was the major factor in the choice of this type of construction. To test for reliability, prior to Aircraft Certification, use was made of Triplex's Life Test facilities, in which windshields can be subjected to as close as possible a simulation of the environmental conditions of service, including differential pressurization, external heat transfer rates, low ambient temperatures and representative application of the de-icing/de-misting system. Two Airbus windshields have each recently completed the equivalent of 10,000 flying hours, both remaining in a fully serviceable condition.

Figure 6 shows the general arrangement of a typical Life Test facility which is basically a closed loop of ducting with a circulating air stream, cooled as required by the injection of liquid nitrogen into the system. Each windshield is coupled to a representative electrical supply and temperature control system and is mounted in the working section with the external face exposed to the high velocity air stream, typically about 80 m.p.h., to achieve the high heat transfer rates found during high altitude cruise conditions. Figure 7 shows an Airbus windshield mounted in representative edge structure which actually forms part of an integral pressure box. Differential pressurization is applied as required and the inside "Cabin" temperature is separately controlled to simulate the cabin environment.

Figure 8 illustrates a typical Life Test cycle for a subsonic transport windshield showing the variation throughout the cycle of duct air temperature and pressure differential. Seasonal changes in climate or variations in operational role, can easily be simulated by applying the cycles in programmed sequences with different conditions and the testing

can be made even more realistic by injecting water into the circulating air stream during certain parts of a cycle to simulate flying in high precipitation conditions.

The concept described above, of a clamped-in high strength glass construction has now been extended from flat to curved, in that a "TEN-TWENTY" glass windshield has recently been developed for the Boeing 747 as shown in Figure 9.

This design uses two pre-curved 12 mm (.394") plies of "TEN-TWENTY" glass in conjunction with a facing ply of flat .05" "CHEMCOR" which is elastically formed ("cold draped") to the contour of the "TEN-TWENTY" glass during lamination. The windshield is effectively clamped in although an integral surround frame is employed for installation into the aircraft structure, see Figure 10.

One interesting feature of this windshield is that the polyvinyl butyral interlayer between the two 12 mm "TEN-TWENTY" glasses also provides a tertiary load path for pressure resistance on the conventional diaphragm principle. This of course requires an edge restraint system to react the diaphragm loads back into the structure and this has been achieved using a flexible edge insert made of fabric material, which still allows the laminated glass block to 'float' inside the edge clamping structure.

A conventional aluminium alloy insert laminated into the periphery of the interlayer has two main drawbacks both associated with windshield reliability. It is difficult to isolate the windshield from movement of the surrounding structure and more important still, the metal insert is a very efficient way of forcing "cold" into the windshield edge, building up damaging thermal gradients which have a radical effect on reliability.

This new type of edge reinforcement has been proved by considerable detail and full scale testing, as shown in Figure 11, where the polyvinyl butyral diaphragm is shown holding 10 p.s.i. pressure differential two hours after all the glass plies were deliberately shattered.

In the past where interlayer has been used in this way to provide a reserve load path, it has also been used to provide bird impact resistance on a "bird catching" basis although to be effective it had to be heated to around 35°C (95°F). This has always caused difficulties, especially with cold despatch capability and particularly with impact resistance in unheated corners. The all-glass windshield for the Boeing 747, however, does not rely on the interlayer for bird impact resistance but behaves exactly like the Airbus windshield in that it has a "bird bouncing" capability, the strength being provided by the two "TEN-TWENTY" glasses which remained undamaged after impact.

In establishing the optimum thickness required for the "TEN-TWENTY" plies, bird impact was obviously the critical design case, and initially existing data for flat windshields was used, including the effects of extremes of temperature and corner impact. Experimental curved full size panels were then made up and mounted in solid fixtures as shown in Figure 12 and sufficient testing was carried out at this stage to verify the choice of glass thickness, and to establish the effects of curvature, impact position and the influence of the .05" "CHEMCOR" outer glass.

Further testing was then carried out to investigate the effect of mounting in the integral sub-frame and in particular the impact characteristics of the 'Z' Section which reacts the impact load into the aircraft structure. Early on in the programme it had been decided to forge the 'Z' ring members from an alloy which was specifically chosen for its high elongation characteristics, that is, its ability to absorb energy by deformation. These tests were for simplicity carried out on flat rectangular panels as shown in Figures 13 and were basically comparative, aimed solely at finding the effects of frame deformation.

The first step was to establish the penetration velocity under corner impact in a rigid mounting and in fact very close correlation was found with the previous curved test panel results. The rectangular panels were then mounted in dimensionally correct, 'Z' frames and an increase in performance of about 45 knots was found although the 'Z' frames suffered permanent deformation in each case as shown in Figure 14. As final proof of the effect, a panel which had withstood two identical impacts at 425 knots without damage when mounted in the 'Z' frame structure was re-mounted in a rigid frame and complete penetration occurred, at 390 knots.

The design data established during tests has now been confirmed during Certification Testing in full aircraft structure as shown in Figures 15 and 16 and in fact the critical corner impact under low temperature soak conditions was withstood without damage at 427 knots although some local deformation of the integral frame occurred. There was no damage to the actual aircraft structure. This test speed is well in excess of the FAR Part 25 requirement of 375 knots, and actually relates to the British CAA requirement which is more severe at 423 knots.

The deice/demist capability of the 747 windshield is provided by Triplex's recently developed "HYVIZ" electro-conductive coating, which is positioned on the laminated face of the outer "CHEMCOR" ply. To achieve maximum windshield reliability, the electrical heating should extend over the complete area of the outer ply, and the power density should be extremely uniform, particularly avoiding 'cold zones' and 'hot spots'.

This windshield presented an extremely difficult problem in achieving uniform heating over the entire area, due to the irregular shape, with curved, cranked bus bars of different lengths, and a constantly changing

path length of current flow. To attain the required uniformity a flow-lining technique is used, the coating being divided into thin strips which force the current flow in the required areas. These flowlines are less than .01" wide and are therefore virtually invisible.

"HYVIZ" coating is a vacuum deposited metal oxide of neutral colour, with a range of resistivity between 3 and 100 ohms/square, which spans the complete range of resistivity required to match available aircraft voltage systems. The coating has an extremely good light transmission (typically a 10 ohms/square coating is associated with a drop in light transmission of about 4%) and it has good durability, with excellent adhesion properties both to glass substrates and to polyvinyl butyral interlayer. This latter feature is of course of fundamental importance to windshield reliability.

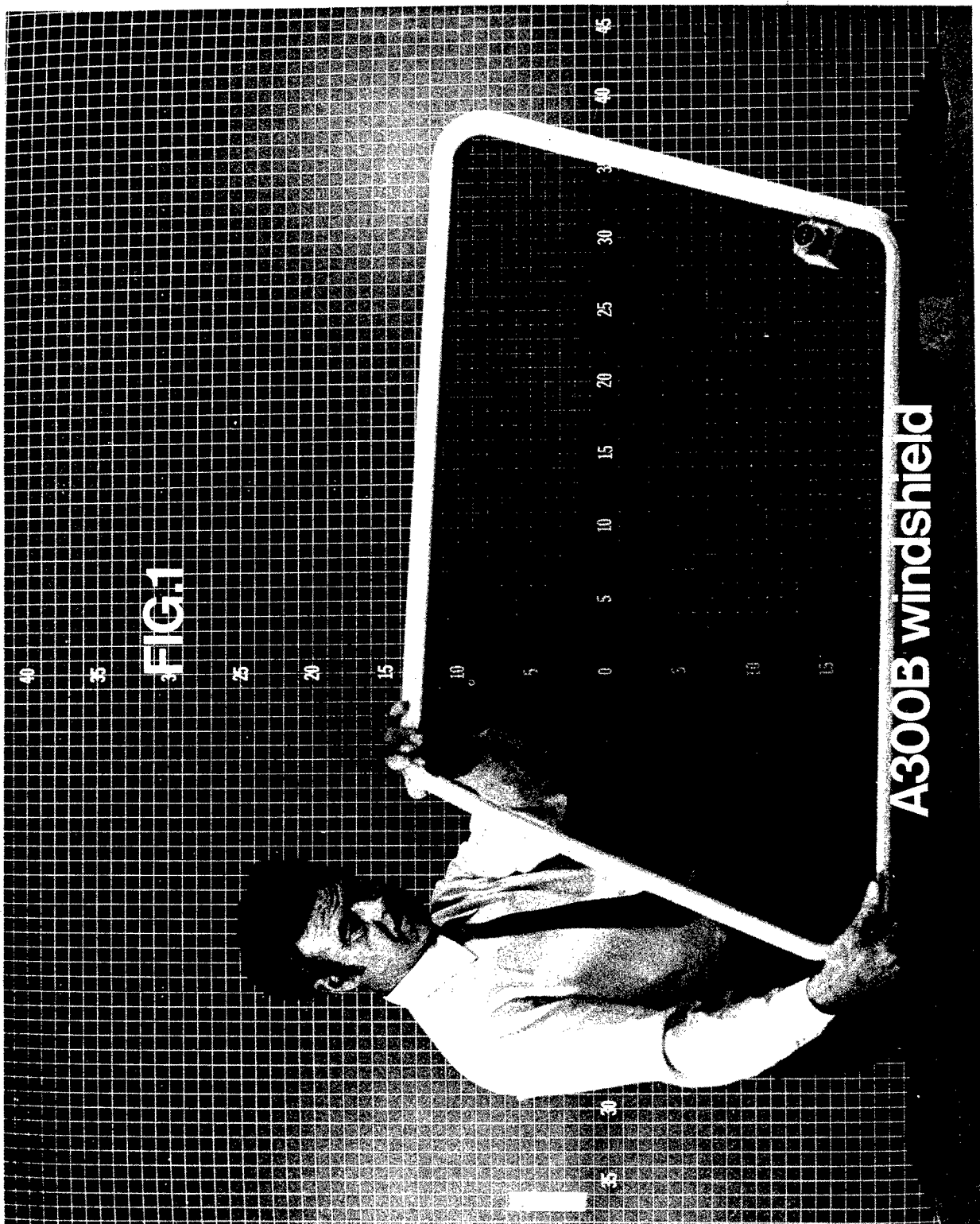
As reliability is considered of such importance, a new Life Test facility has been constructed specifically for the Boeing 747, which being a curved windshield requires a specially shaped working section as shown in Figure 17. For the first time, a novel feature is incorporated in the pressure box and mounting structure, which deflect under pressurization to simulate movement of the aircraft surround structure in the plane of the windshield.

Cyclic testing is now under way and will continue for many months.

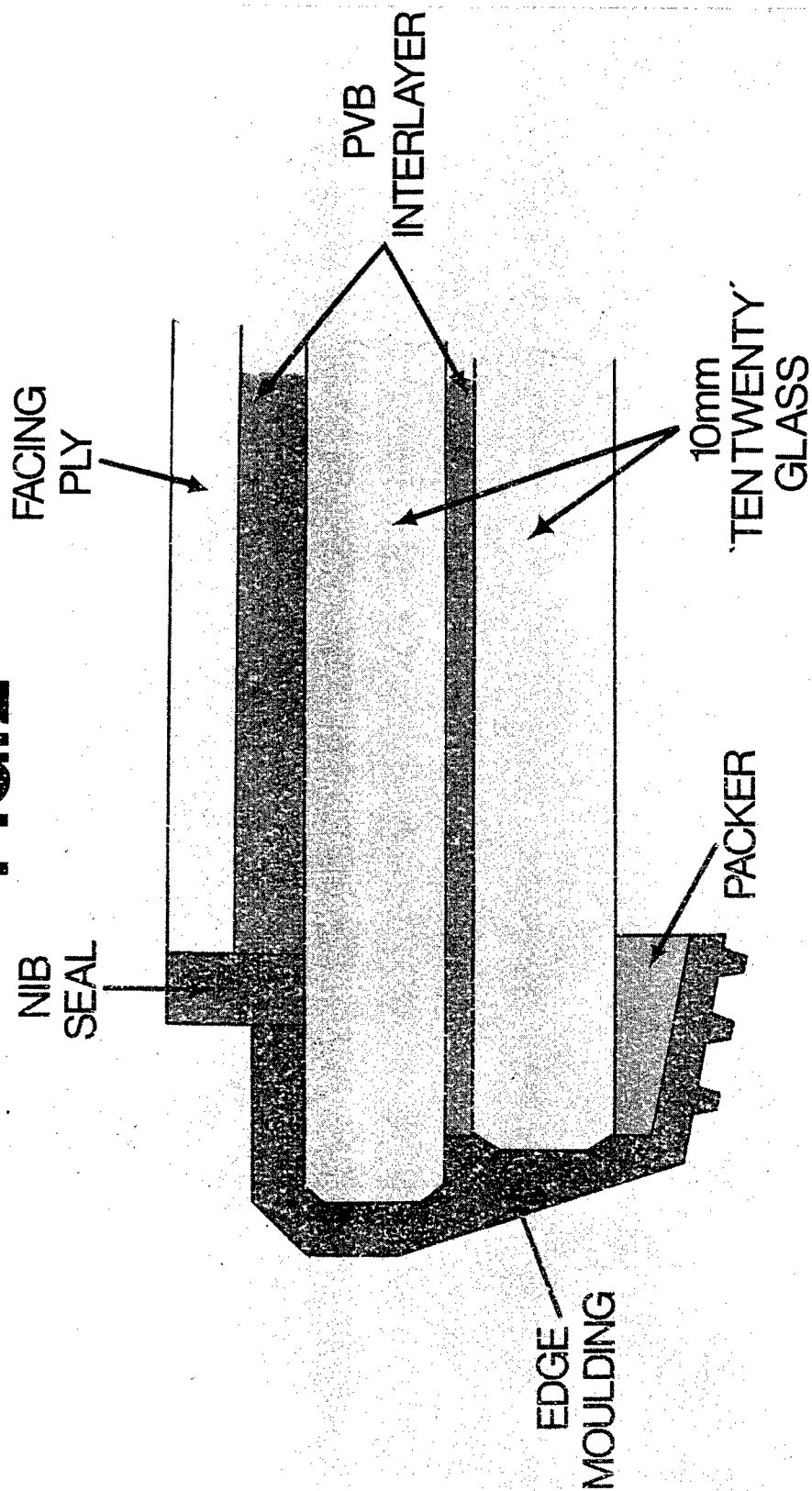
#### CONCLUSION

To sum up therefore, "TEN-TWENTY" high strength glass, and the "HYVIZ" high light transmission coating, have been used to provide light weight flat and curved windshields, with maximum reliability. Fully representative environmental testing to prove this reliability is considered an absolute necessity.



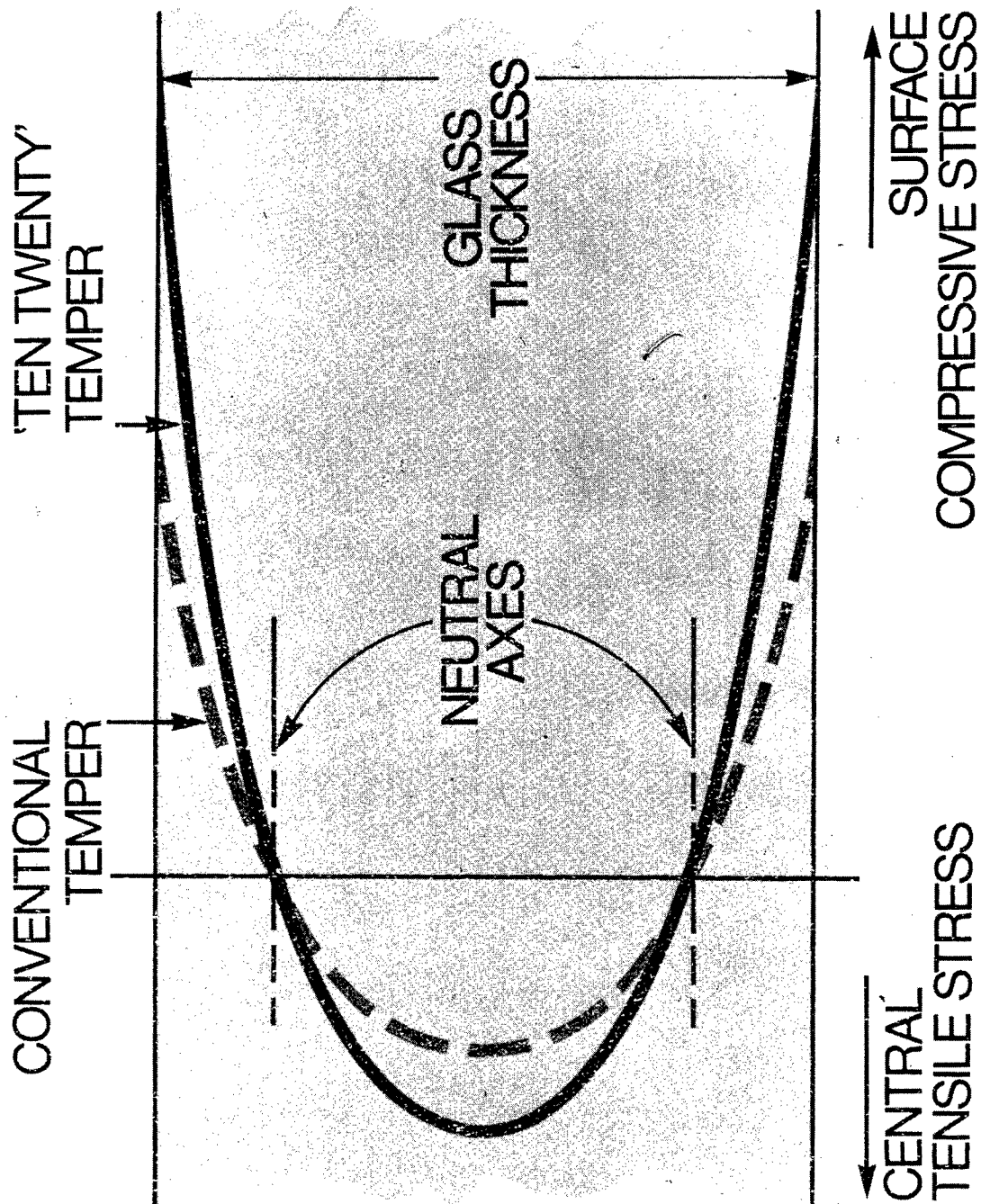


**FIG.2**



## Edge section of A300B windshield

**FIG.3**

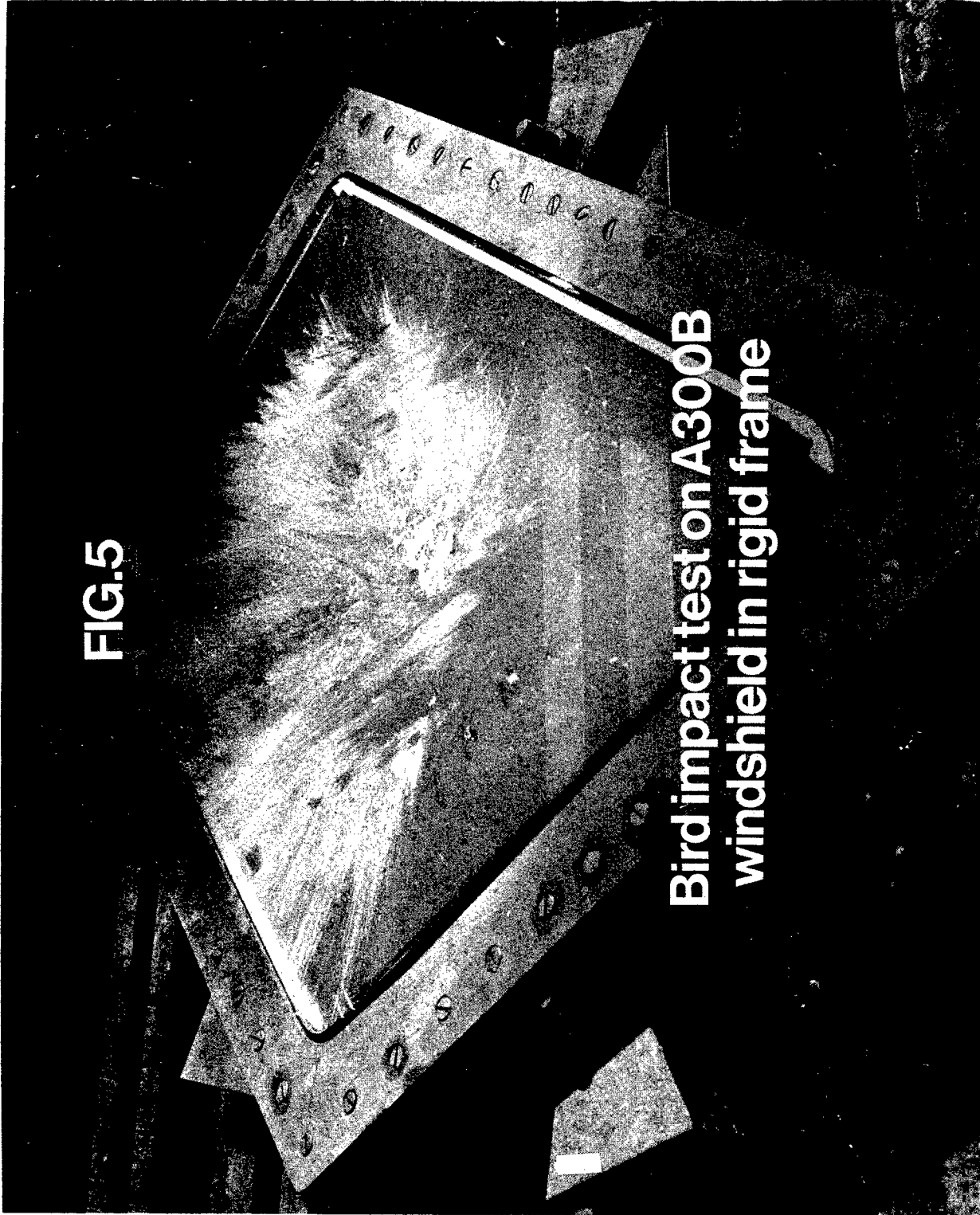


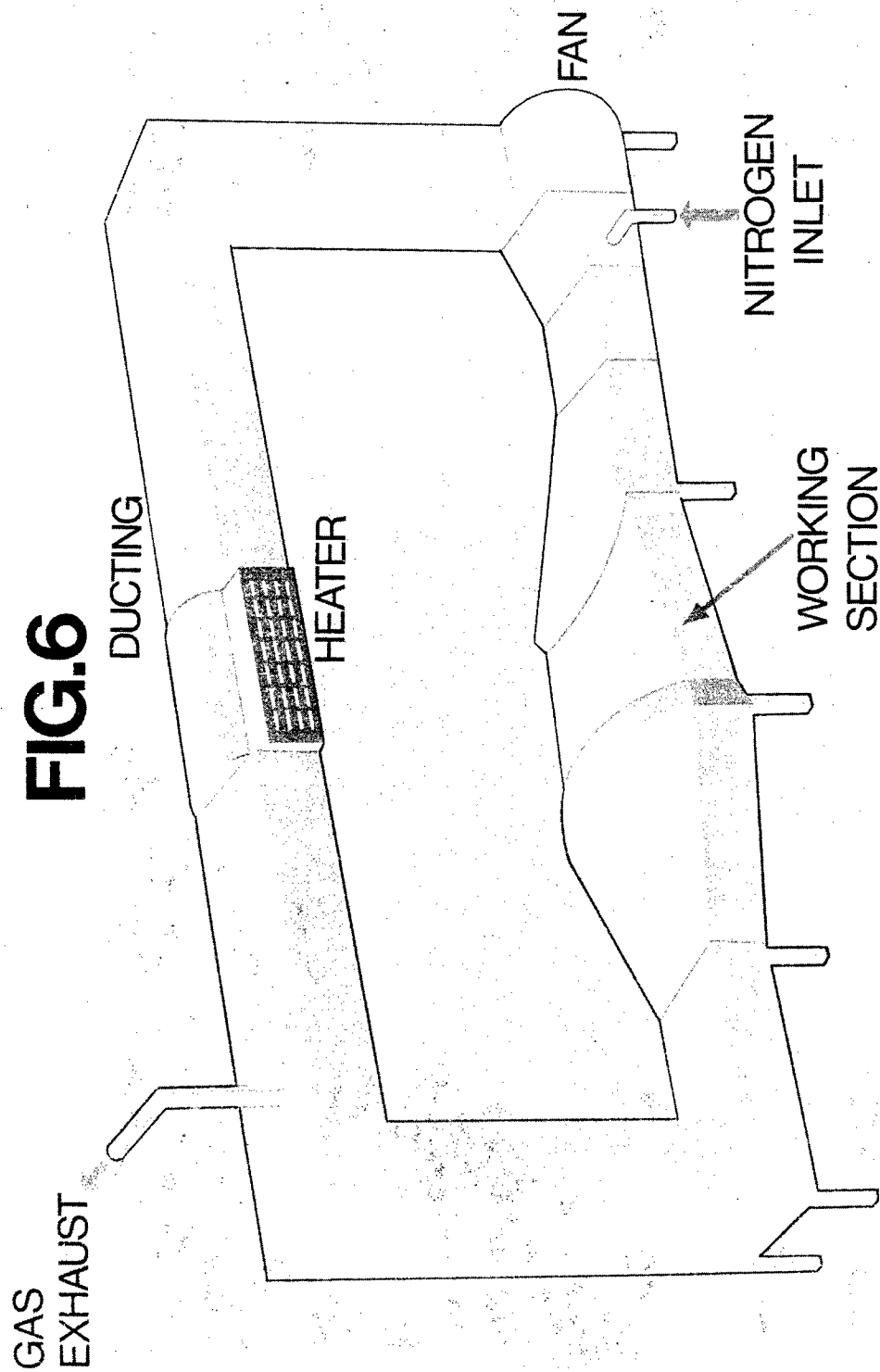
# **'Ten Twenty' Glass Stress Profile**



**FIG.5**

**Bird impact test on A300B  
windshield in rigid frame**

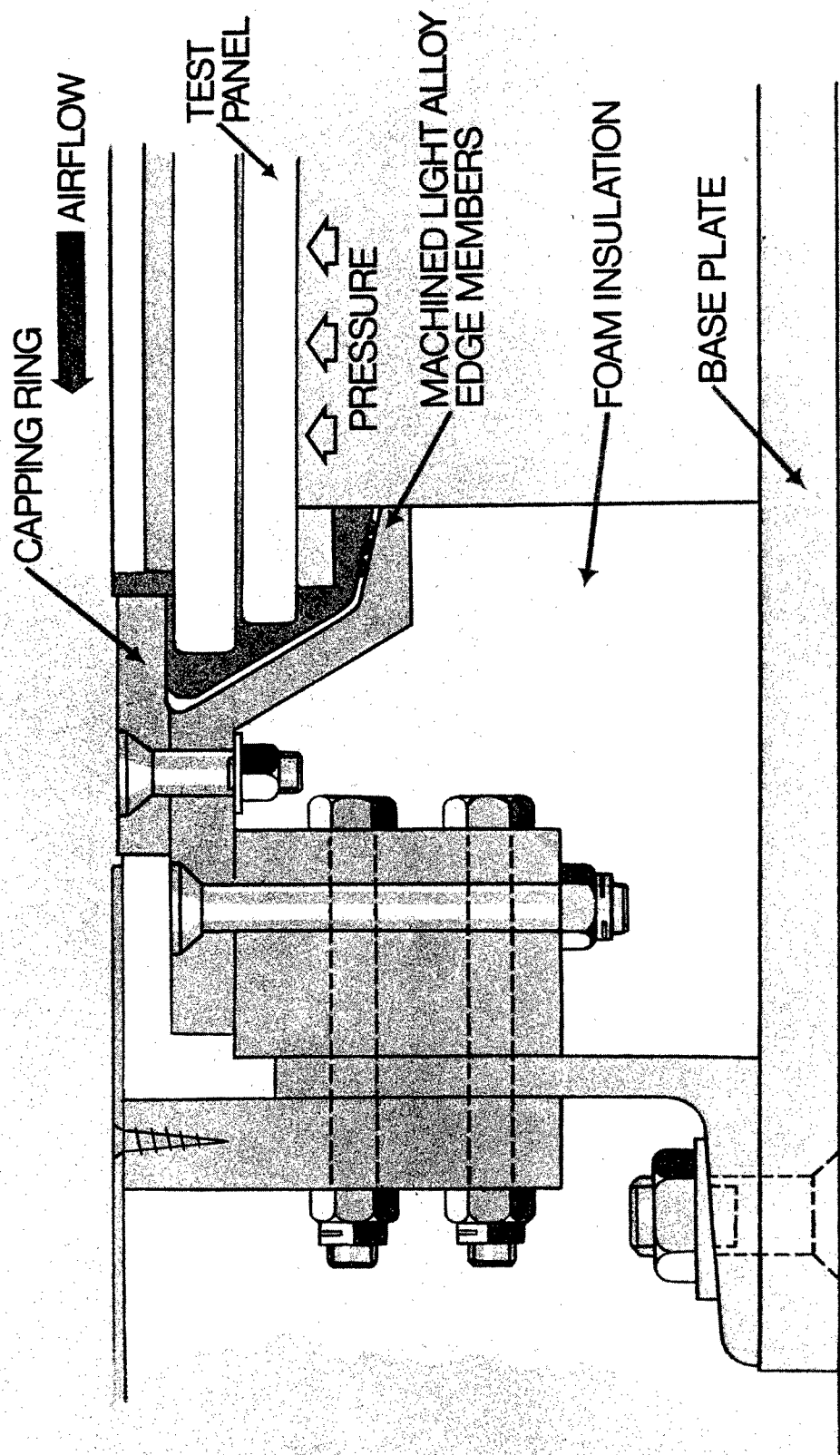




**FIG.6**

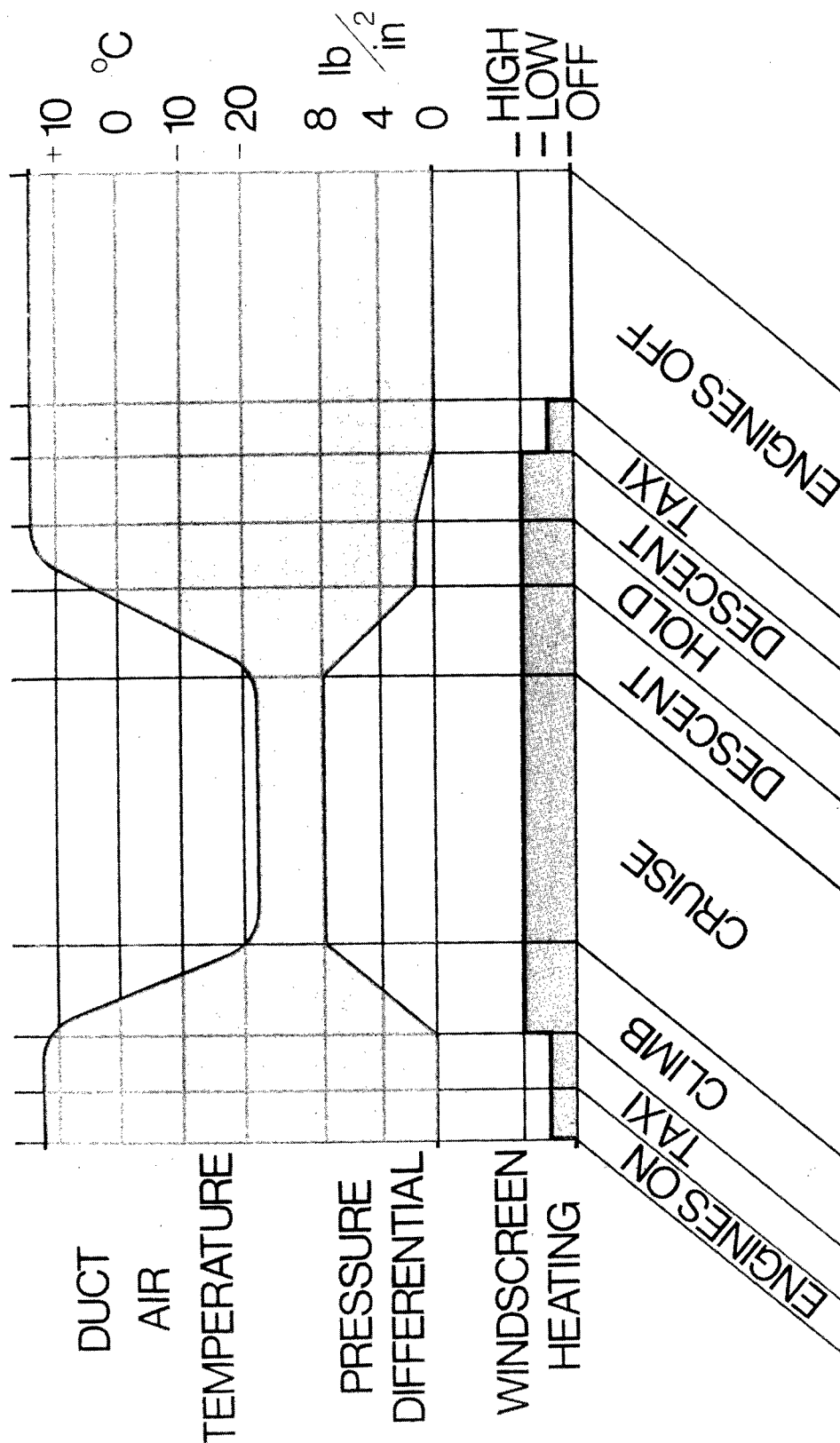
**Life test facility**

**FIG.7**



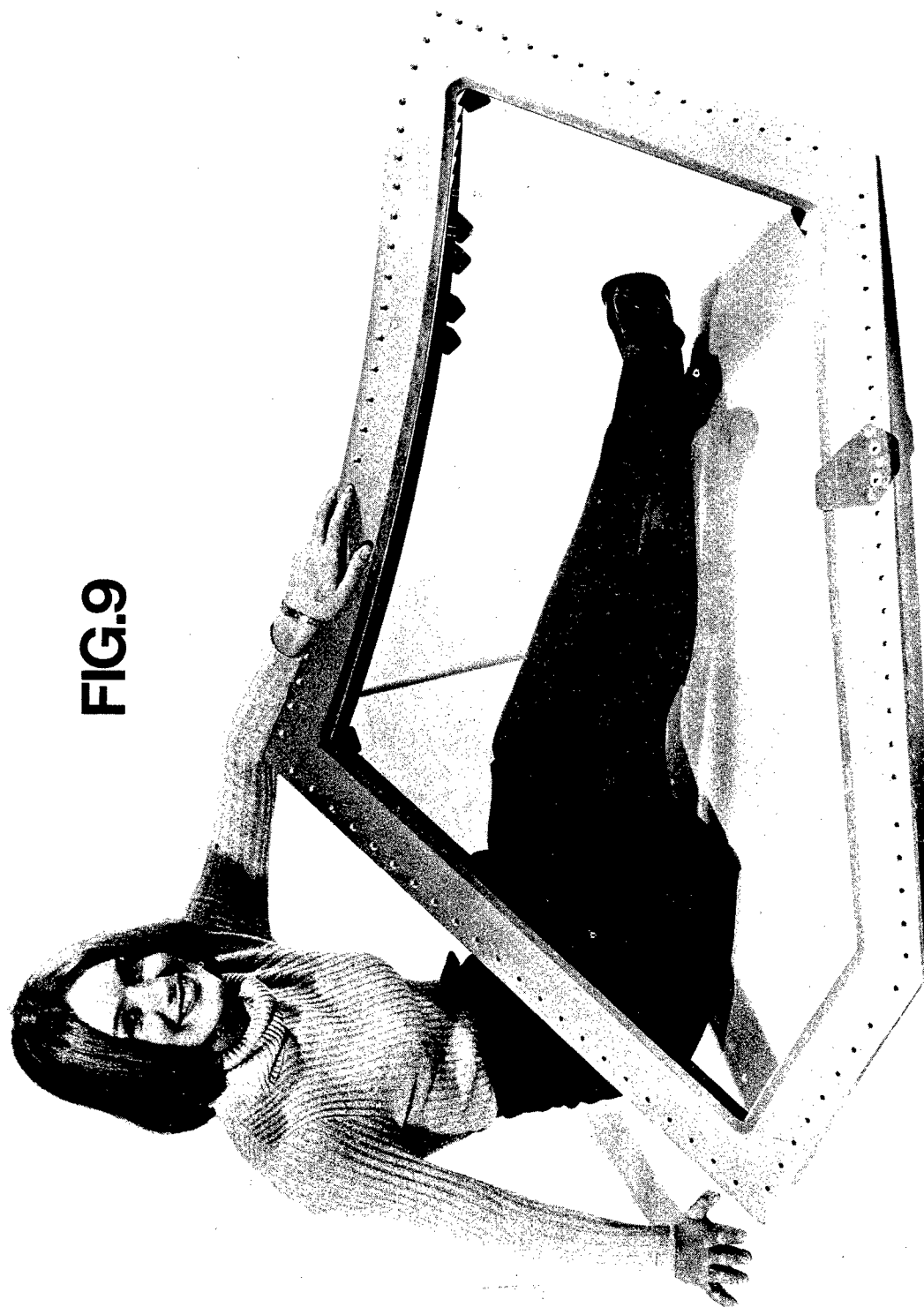
**Mounting of A300B windshield for life test**

# FIG.8



## Typical life test cycle

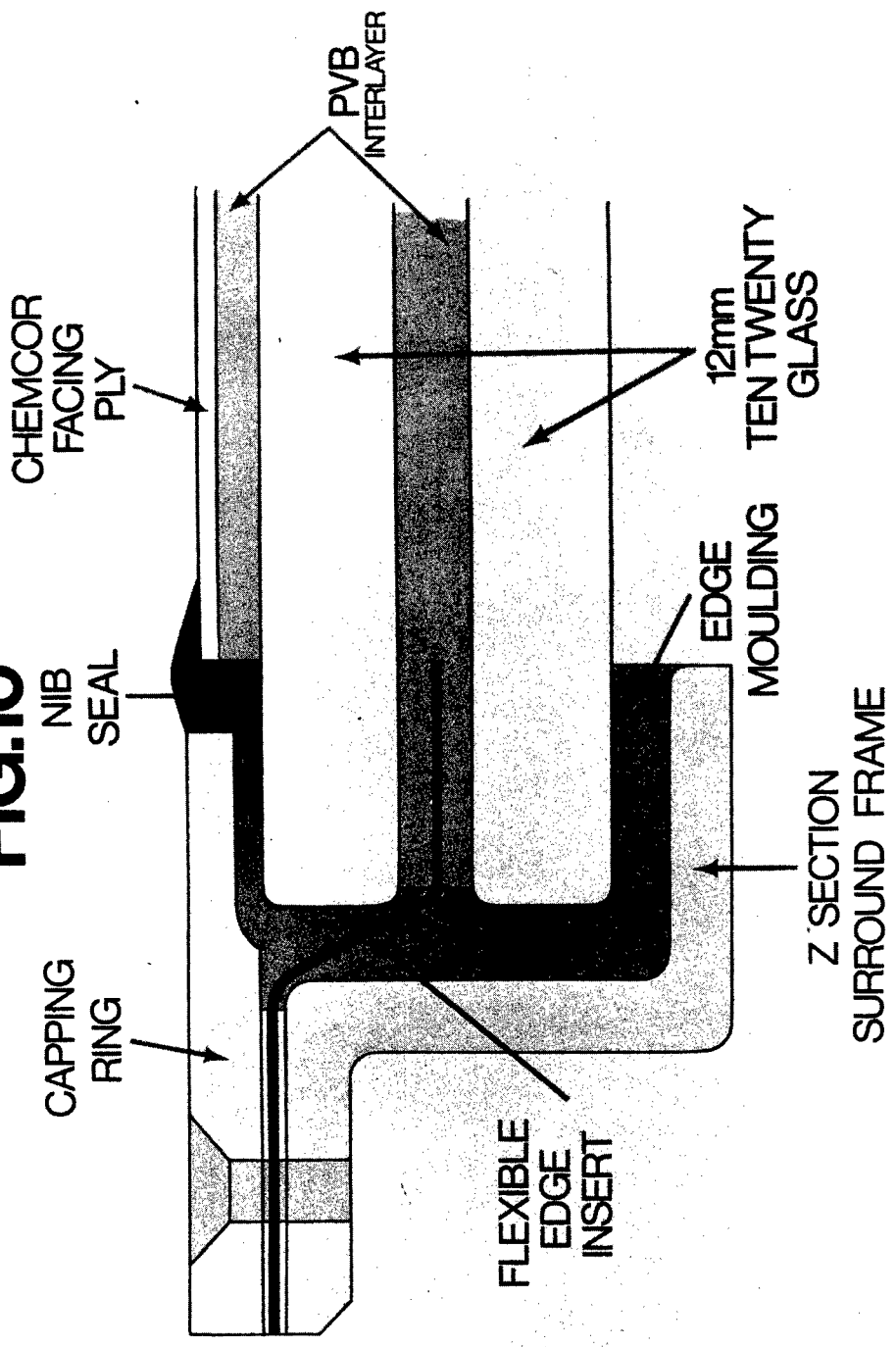




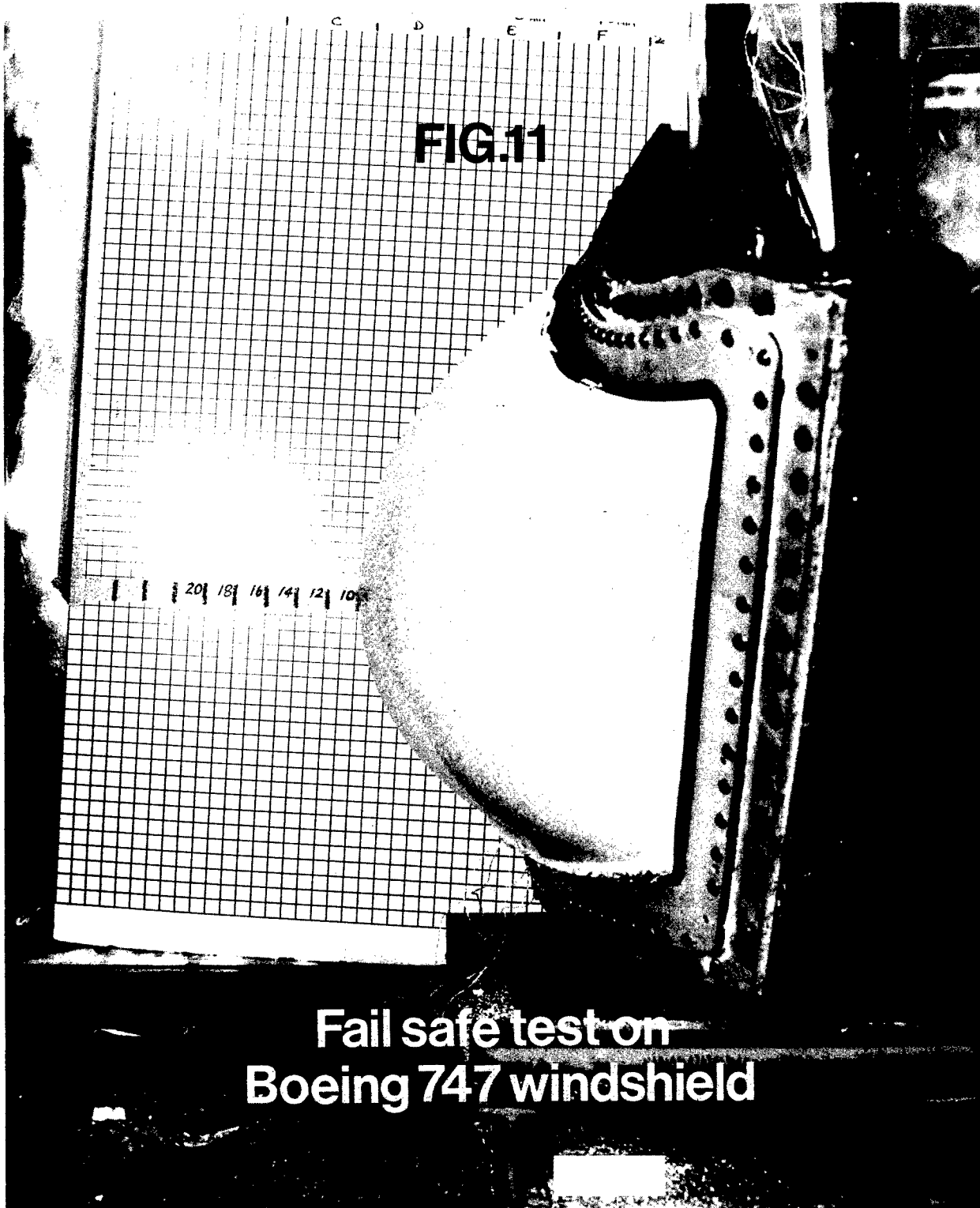
**FIG.9**

**Boeing 747 windshield**

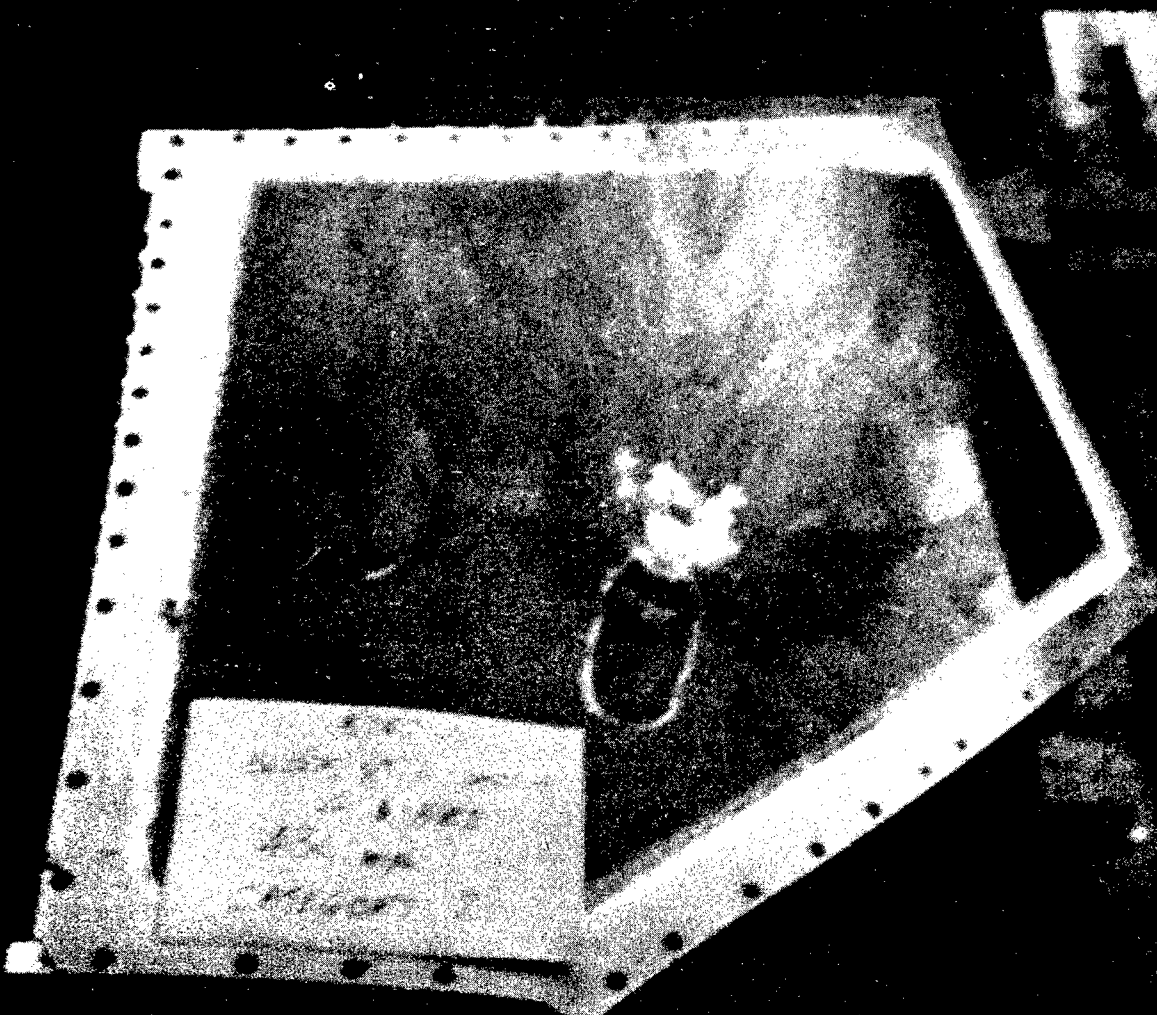
**FIG.10**



## Edge section of Boeing 747 windshield

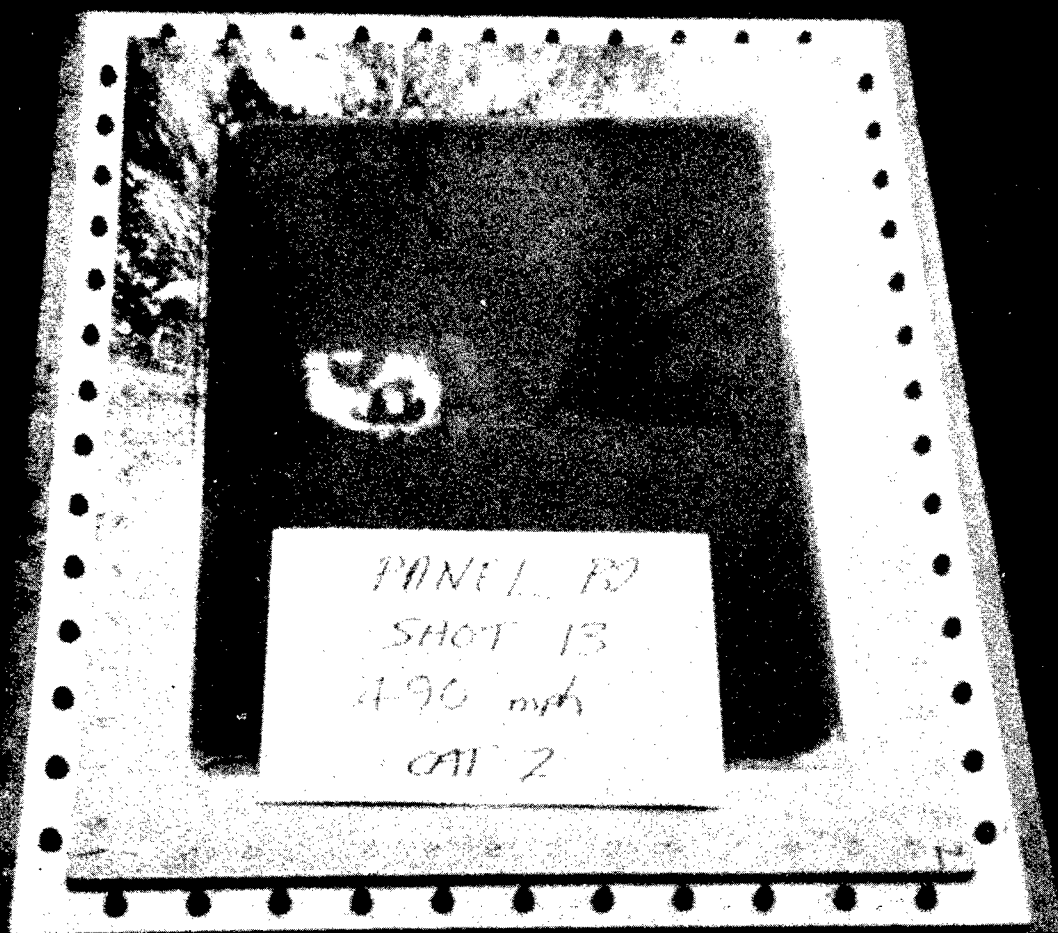


**FIG.12**



**Bird impact test on Boeing 747  
windshield in rigid frame**

**FIG.13**



**Rectangular test  
panel in rigid frame**

**FIG.14**

**Deformation of Z  
section under bird impact**

5-10-80  
1-600-0000  
C-17



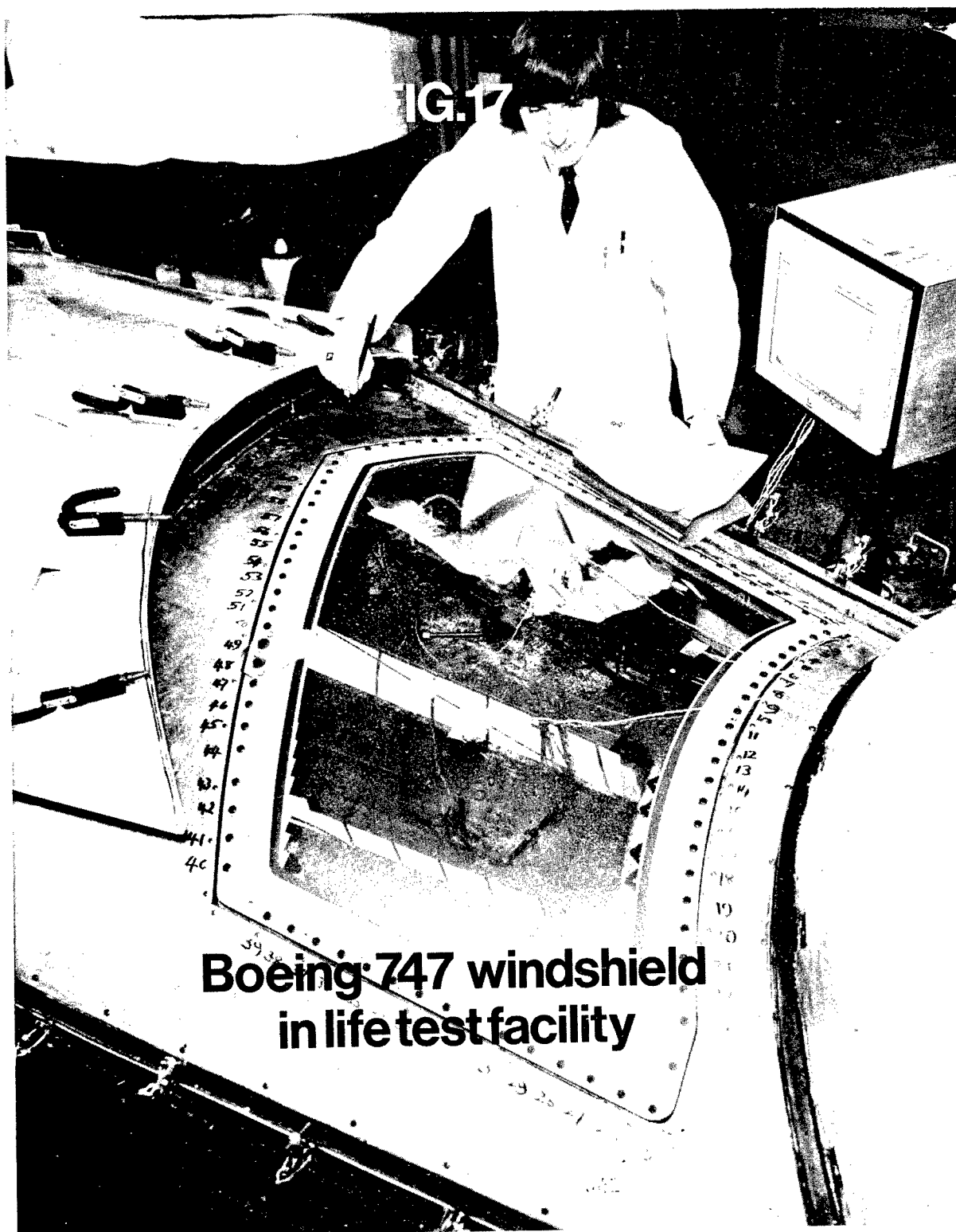
**FIG 15**

**Boeing 747 windshield—  
bird impact test at 380 knots**

**FIG. 16**

**Boeing 747 windshield -  
bird impact test at 427 knots**





**Boeing 747 windshield  
in life test facility**

SESSION 7

COATINGS FOR ENCLOSURES

DEVELOPMENT OF SCRATCH AND SPALL  
RESISTANT WINDSHIELDS

Capt. John R. Plumer  
Army Materials and Mechanics Research Center  
Watertown, Massachusetts

## DEVELOPMENT OF SCRATCH AND SPALL RESISTANT WINDSHIELDS

by

Captain John R. Plumer

Army Materials and Mechanics Research Center, Watertown, Mass. 02172

### ABSTRACT

Studies were performed to evaluate possible ways of improving the primary weaknesses in existing Army Helicopter windshields, namely, scratching and spalling. Three experimental windshield material configurations offering a potential solution were fabricated for test and evaluation. The spall problem was approached by using polycarbonate as a back-up material and was incorporated into each design. The scratch problem was approached by employing either, (1) a hard surface coating, (2) an acrylic cladding, or (3) a thin glass cladding to the polycarbonate back-up material. Commercially available materials and abrasion resistant coatings were evaluated utilizing a windshield wiper apparatus while spall performance was studied by ballistic testing and high-speed photography of each of three test configurations.

Results demonstrated that the most effective reduction of spallation was achieved with the hard surface coated polycarbonate design. Spallation from the system consisted of punched-out plugs of polycarbonate approximately the diameter of the ballistic projectile. The low spallation characteristics of polycarbonate were not found to be adversely affected by the addition of hard surface coatings when applied either to one or both sides of ballistic test samples. Stretched acrylic cladding on polycarbonate provided only limited improvement of abrasion resistance while the effectiveness of spall reduction decreased from that of plain polycarbonate. The glass clad polycarbonate configuration proved to be the most resistant to abrasion, but had the least spall resistance and the most weight of the designs evaluated. Spallation in this latter design was greater than coated polycarbonate by at least a factor 10, however, significant improvement is obtained over current windshield materials. Abcite, a hard surface coating, provided the best scratch protection for the plastic components. Resistance to abrasion over current windshield materials increased by a factor of several hundred.

### DISCLAIMERS

The findings in this report are not to be construed as an official Department of the Army position unless so designated by other authorized documents.

When Government drawings, specifications, or other data are used for any purpose other than in connection with a definitely related Government procurement operation, the United States Government thereby incurs no responsibility nor any obligation whatsoever; and the fact that the Government may have formulated, furnished, or in any way supplied the said drawings, specifications, or any other data is not to be regarded by implication or otherwise as in any manner licensing the holder or any other person or corporation, or conveying any rights or permission, to manufacture, use, or sell any patented invention that in any way be related thereto.

Trade names cited in this report do not constitute an official endorsement or approval of the use of such commercial hardware or software.

## I. INTRODUCTION

Current combat service has demonstrated that the most prevalent problems experienced with Army helicopter windshields are abrasion, loss of transparency, and spallation. Abrasion is a consequence of windshield wiper action and the impact of sand and gravel thrown up by the action of the rotor blades. The standard acrylic plastic does not have sufficient hardness to withstand the abrasive conditions encountered in field use. Acrylic windshields also are subject to severe cracking and spallation when impacted by small arms fire. Laminated glass windshields created an even greater problem. Glass spall can cause serious injuries to the pilot or co-pilot.

The objective of this effort is to develop a windshield fabrication concept which increases serviceability, provides increased crew safety, and is manufacturable in various configurations which allows adaption and retrofit to a number of different airship models. Fabrication is to be from commercially available materials.

This report will describe in some detail the methodology used to evaluate abrasion and spallation characteristics of plastic materials. Increasing serviceability was viewed as not only a materials problem, but also a design problem. The approach used was to consider abrasion and spallation individually, to offer potential design solutions for each problem area, and finally to merge the solutions with a number of workable windshield configurations. These configurations were fabricated from materials initially determined to offer the most advantageous characteristics, i.e., abrasion resistance and low spallation. Potentially acceptable configurations were similarly tested for these problem areas. Final approval and acceptance of a prototype windshield configuration is to be made on the basis of flight test performance and on evaluation of the in-service effects on its optical properties. The flight evaluation has not yet been completed.

## II. STRUCTURAL DESIGN AND MATERIALS

### Structural Design

From previous efforts, which demonstrated the superior impact properties of polycarbonate over acrylic plastic, the spall problem was approached by using polycarbonate as a back-up spall-resistant material. The polycarbonate, like acrylic, is sensitive to environmental abrasion and therefore requires a means of protecting it, consequently a scratch-resistant coating is necessary.

The scratch problem was approached by employing the following: (1) a hard surface coating, (2) an acrylic cladding, or (3) a thin glass cladding to a polycarbonate back-up material. The proposed solutions for the scratch and spall problems were combined to form three potential design solutions affording increased serviceability. The potential solu-

tions are:

- Type 1 - hard surface coating/polycarbonate/hard surface coating.
- Type 2 - acrylic cladding/adhesive/polycarbonate/hard surface coating.
- Type 3 - thin glass cladding/adhesive/polycarbonate/hard surface coating.

The UH-1 helicopter windshield was selected as the unit for test and development, and for the study of service conditions affecting windshield wear. The current UH-1 windshield is an uncoated monolithic, as cast acrylic structure, approximately one-quarter inch thick and weighing twelve pounds. The helicopter utilizes two windshield wipers for rain removal, these wipers are responsible for the severe abrasion and wear problem encountered with this system.

Three parameters were considered essential in the approach for the design of the improved windshield. They are the following: size and weight, which permit retrofit into existing helicopters, and the commercial availability of the materials. The project directed efforts toward improving the UH-1 windshields. To allow retrofit, current dimensions were maintained. Weight became a function of materials incorporated in the design. A unit of no more than 2-1/4 times greater weight than present was determined as desirable. The three types of potential configurations weigh as follows: type 1 - same as current windshield; type 2 - 1-1/2 times greater than current materials; and type 3 - 2 times greater weight. A materials analysis ensued to determine the optimum components for fabrication of the model.

### Materials

The initial material selection consisted of surveying available literature. These were primarily reports on the development and testing of materials and on transparent inclosure design and fabrication. Inquiries were also directed to industrial services and military agencies involved with aircraft glazings and related transparency work. Based on commercial availability and applicability to the problem, as determined by industrial specifications, samples of hard surface coatings, polycarbonates, acrylics, and glass cladding materials were obtained. The materials selected for evaluation are shown in Table I; this incorporates type 1.

Based on preliminary data, the most promising materials from (Table I) were chosen for incorporation into the fabrication of types 2 and 3 candidate windshield designs. Fabrication of these samples, in addition to materials, considered the effectiveness of the adhesive interlayer. Other efforts carried out at AMMRC provides essential guidance for this determination. Sample fabrications of design types 2 and 3 were performed as a contractual effort, and are listed in Table II.

TABLE I  
MATERIALS FOR EVALUATION

| <u>Coating</u>  | <u>Materials</u>    | <u>Description</u>                                | <u>Testing Code</u> |
|-----------------|---------------------|---|---------------------|
| Uncoated        | Polycarbonate       | Lexan, SL-2000-III                                | A                   |
| "               | Polycarbonate       | Lexan 9030-112                                    | B                   |
| "               | Acrylic, as cast    | Rohm Haas Mil-P-5425                              | E                   |
| "               | Acrylic, stretched  | Rohm Haas Mil-P-25690                             | F                   |
| "               | Polycarbonate       | Merlon M50U, Mobay Inc.                           | C                   |
| "               | Polycarbonate       | Rowland   | D                   |
| "               | Urethane            | 574, Goodyear Aerospace                           | G                   |
| "               | Acrylic, as cast    | Section UH-1 Windshield<br>(used, unserviceable)  | H                   |
| "               | Acrylic, as cast    | Section UH-1 Door Window<br>(used, unserviceable) | I                   |
| Abcite          | Acrylic, Mil-P-5425 | Dupont  | 1                   |
| Abcite          | Polycarbonate       | Dupont  | 2                   |
| Abcite GACA 701 | Urethane GAC 574    | Goodyear Aerospace                                | 3                   |
| Abcite GACA 701 | Polycarbonate       | Goodyear Aerospace                                | 4                   |
| Armor Clad      | Acrylic Mil-P-5425  | Symbolic Displays                                 | 5                   |
| #100-35 Astro   | Polycarbonate       | Astro Research Co.                                | 6                   |
| ESB             | Polycarbonate       | ESB Corp.   | 7                   |
| MR-4000         | Lexan 9030-112      | General Electric Corp.                            | 8                   |
| Mobay           | Merlon              | Mobay Inc.  | 9                   |
| Glass resin     |                     |   |                     |
| 650 type        | Acrylic, as cast    | Owens-Illinois                                    | 10                  |
| SS-6426 ARC     | Acrylic Mil-P-25690 | Swedlow Inc.                                      | 11                  |
| SS-6432         | Polycarbonate       | Swedlow Inc.                                      | 12                  |
| No 311          | Acrylic, as cast    | Sierracin Corp                                    | 13                  |
| Texstar Coating | Polycarbonate       | Sierracin Corp                                    | 14                  |
| 0401 type       | Glass               | Corning Glass Co.                                 | 15                  |



TABLE II

## COMPOSITE TYPE SAMPLES

| <u>Outer Layer</u>     | <u>Inter Layer</u>       | <u>Inner Layer</u>       | <u>Description</u>    | <u>Testing Code</u> |
|------------------------|--------------------------|--------------------------|-----------------------|---------------------|
| Corning 0401<br>0.085" | F- 5X-1<br>cast in place | Lexan<br>9030-112,0.187" | Goodyear<br>Aerospace | I                   |
| Corning 0317<br>0.050" | F- 5X-1<br>cast in place | Lexan<br>9030-112,0.187" | Goodyear<br>Aerospace | II                  |
| Corning 0319<br>0.050" | F- 5X-1<br>cast in place | Lexan<br>9030-112,0.187" | Goodyear<br>Aerospace | III                 |
| Corning 0401<br>0.085" | LR 3320<br>film, .030"   | Lexan<br>9034,0.125"     | General<br>Electric   | IV                  |
| Corning 0313<br>0.050" | LR 3320<br>film, 0.030"  | Lexan<br>9034,0.125"     | General<br>Electric   | V                   |
| Plex 55<br>0.250"      | LR 4330,0.010"           | Lexan<br>9034,0.125"     | General<br>Electric   | VI                  |

## III. INSTRUMENTATION AND GENERAL PROCEDURE

When tested for durability, hard surface coatings vary in performance, dependent on the test method used. The problem of evaluating plastics, coatings, and glass claddings for abrasion resistance was approached by designing and fabricating a windshield wiper test apparatus which approximated windshield environment while in service. The apparatus allowed control and monitoring of the test conditions.

Evaluation of abrasion effects was met by designing and fabricating a reciprocating arm felt pad abrader. This apparatus approximates the non-mechanical cleaning i.e., hand wiping by crew, of the windshield during operation of the helicopter. It also permits control and good reproducibility of data. This abrader was chosen over the Taber abrader as this device produces a significantly larger area of abrasion which provides a more quantitative evaluation of haze with the integration sphere type of haze meter. Unserviceable helicopter windshields were obtained from (ARADMAC)\* for evaluation and determination of type and levels of service produced abrasion. The data was used as a standard to evaluate laboratory abrasion equipment performance and evaluate improvements offered by new materials. The windshields were also used as a standard for evaluating spallation. Haze and light transmission in the plastic materials as a function of abrasion were the factors measured in the laboratory.

\*U. S. Army Aeronautical Depot Maintenance Center

### 1. Windshield Wiper Test Table

The apparatus, as shown in Figure 1, was designed, developed and built at AMMRC. It consists of sample holding table mounted at 45° with sample mounts to accomodate two 12" x 12" plastic or glass samples. Two O-ring seals and vacuum system in the mount area are used to hold the sample in place during testing. A Model 205 helicopter windshield wiper motor, arm, and blade are mounted on the table. Provisions were made to regulate the application of an abrasive slurry and to keep the slurry in suspension. This involved the use of a large separatory funnel and mechanical stirrer. A digital counter provided a record of the number of wiper blade sweeps. A Hewlett-Packard Model 6433B DC power supply provided the source of variable current to regulate wiper speeds to that of a UH-1 helicopter.

### 2. Reciprocating Arm Felt Pad Abrader

The apparatus was designed to provide (a) a wiping action which could be an approximation of conditions encountered by field cleaning of a helicopter windshield by aircraft personnel, and (b) a highly reproducible means of quantitatively evaluating various coatings and plastics for abrasion resistance. The unit consists of the following components: (1) Dayton gear motor, Model BM237, (2) a speed control rheostat, and (3) a three place digital cycle counter. The unit has a one-inch diameter abrading head for the mounting of a felt pad. The head can be weighted to produce 150, 400 and 1150 gram loads. The test unit in operation appears in Figure 2.

### 3. Haze Meter

Light transmission and transmitted haze were determined with a Hunter Lab color-color difference meter, Model 25 fitted with a Model D25P optical head, (integrating sphere).

### 4. Ballistic Range Equipment

(a) Ballistic testing for spallation with .22 cal. 17-grain fragment simulators was conducted utilizing a helium gun device in the range facilities of the Organic Materials Laboratories, AMMRC. The gun and operational procedures are described in reference (10). The test set-up is shown in Figure 3 and utilized the following equipment:

- (1) 2 chronograph stop grids
- (2) 2 pulzers
- (3) 1 Systron-Donner counter (10 megacycle time base)
- (4) 1 EG&G multiple microflash unit, model 502A
- (5) 1 8" x 10" Eastman Commercial View Camera
- (6) Film, Polaroid type 3000X, radiographic packet

(b) Spall evaluation from .30 caliber ball ammunition was conducted by the Ballistic Test Facility, Range #1, AMMRC. The test set-up

FIGURE 1

WINDSHIELD WIPER TEST TABLE

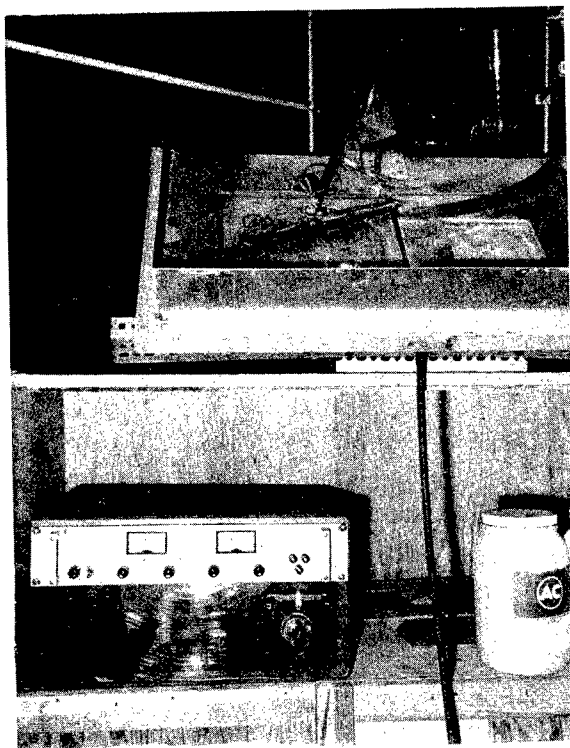


FIGURE 2

FELT PAD ABRADER

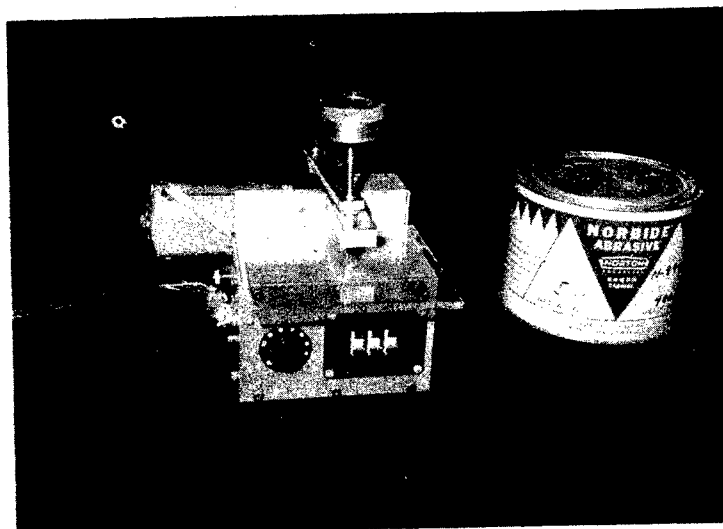
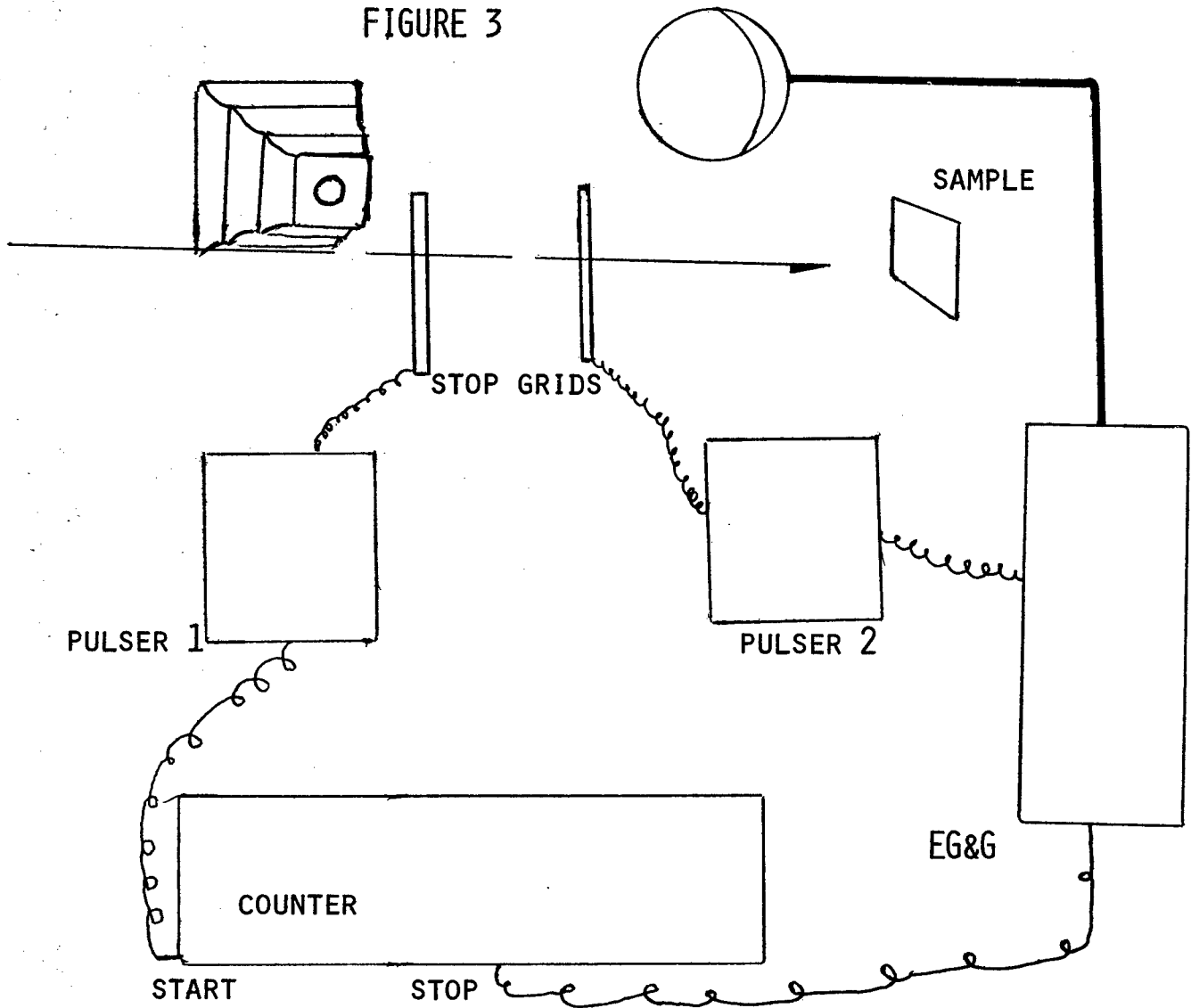


FIGURE 3



BALLISTIC TEST RANGE & CAMERA SET UP

consisted of the following equipment:

1. One 22" barrel Winchester, 30-06 caliber in a fixed mount.
2. Two chronograph stop grids, 10 ft. apart, 10 ft. from the gun muzzle and 10 ft. from the sample holder
3. Two pulsers.
4. Monsanto counter, model 101.
5. Area Evaluator

A light meter was used to determine the area of spall as measured by penetration produced in 2 mil aluminum foil witness plates. The equipment consisted of a light meter positioned one meter from a light box. Light intensities in foot candles were determined for known areas, and a graph plotted. After ballistic testing, damaged witness plates were placed on the light source box, recorded intensities were translated to area values from the graph.

#### IV. ABRASION AND SCRATCH RESISTANCE STUDY

##### A. Windshield Wiper Apparatus

###### (1) Methods

All materials in Table I were tested with the unit. Samples were cut to a 6" x 6" size and flush fitted into a mask for mounting. Test and control materials were mounted in left and right sides of the table. Hard surface coated plastic materials were tested using a similar but non-coated plastic as a control. Cycle speed was maintained at 100 cycles per minute, the approximate low speed for a UH-1 helicopter, while wiper arm load was fixed at six pounds. Wiper blade replacement was made after each 12,000 cycles. The abrasive slurry used for all testing consisted of AC air cleaner test dust, coarse (50% 30-80 micron) size continuously suspended in solution by a mechanical stirrer. The slurry contained 300 grams of grit per 3 liters of water; flow was regulated to approximately 300 milliliters per minute and discharged between test and control samples.

Samples and controls were removed, rinsed and dried, and evaluated for transmitted haze and light transmission at specific cycle counts. Table III tabulates this data. Evaluation of haze and light transmission was based on a worst spot technique, in which the area to be evaluated was determined by inspection to be the most abraded, and then evaluated with the pivotable sphere haze meter. Operation of this device was in accordance with ASTM D 1003-61.

###### (2) Results

Table III displays the data resulting from the windshield

wiper test.

This Table summarizes the performance of materials under simulated service conditions. It was found that chemically strengthened glass provides the most effective abrasion resistant surface. Unprotected polycarbonates performed poorest under the test conditions, while unprotected acrylic performed better (less haze development) than all but two of the coated polycarbonates. Abcite-coated acrylic provided the most resistant plastic surface, while Abcite on polycarbonate proved to be the second most resistant or durable plastic and about 130% more effective in retarding haze development than the next best performing coated polycarbonate.

This value is determined from data in Table III for % haze at 4000 cycles.

$$\frac{30-13 \text{ (Swedlow)}}{13 \text{ (Dupont Abcite)}} \times 100 = 130\% \text{ more effective}$$

The data represents average values obtained from three separate tests on each material. The values reported for haze vary up to  $\pm 5\%$ .

## B. Reciprocating Arm Abrader

### (1) Methods

All materials tested with the unit were cut to a 6" x 6" sample size permitting samples to be precisely refitted in the apparatus after each optical reading to allow the same area to be continually abraded. Reciprocating speed was maintained at 50 cycles per minute, while samples were run with 150, 400, and 1150 grams of load on the abrading head. A one-inch diameter disc of 100% wool felt 1/8" thick was cemented to the abrading head. The felt was impregnated with dry 400 grit Norbide boron carbide abrasive after each optical reading or after each 25 cycle period. Excess abrasive compound was brushed out of the abrading area by the action of head on the sample. The test was run until 10% transmitted haze developed or 1000 cycles were completed for each sample was run under various load conditions. Evaluation of the 1" x 2" abrasion area was made by the same procedure used for the windshield wiper test for values of transmitted haze and light transmission.

### (2) Results and Discussion

Felt pad abrasion results for potential windshield facing surfaces are given in Table IV.

TABLE III

## ABRASION RESISTANCE, WINDSHIELD, TEST TABLE

| Test*<br>Code | Uncoated<br>Material | Thick-<br>ness<br>(in.) | 0 Cycles          |        | 2000 Cycles       |        | 4000 Cycles       |        |
|---------------|----------------------|-------------------------|-------------------|--------|-------------------|--------|-------------------|--------|
|               |                      |                         | Light %<br>Trans. | Haze % | Light %<br>Trans. | Haze % | Light %<br>Trans. | Haze % |
| A             | (Lexan)              | 1/4                     | 84.0              | 4.0    | 82.9              | 26.0   | 81.0              | 42.0   |
| B             | (Lexan)              | "                       | 85.0              | 4.0    | 78.0              | 23.2   | 77.0              | 37.3   |
| C             | Merlon               | "                       | 81.5              | 5.6    | 79.1              | 32.6   | 78.9              | 45.0   |
| D             | Rowland              | "                       | 81.5              | 5.5    | 79.1              | 32.6   | 78.5              | 46.0   |
| E             | Acrylic              | "                       | 93.0              | 2.8    | 92.1              | 14.0   | 92.0              | 34.4   |
| F             | Acrylic              | "                       | 92.1              | 2.5    | 91.3              | 16.7   | 90.9              | 28.0   |
| G             | Urethane             | "                       | 81.7              | 2.7    | 81.0              | 25.1   | 80.5              | 34.0   |
| H             | Windshield           |                         |                   |        |                   |        |                   |        |
| I             | UH-1                 | 7/32                    | 91.6              | 4.7    | 89.5              | 28.0   | 86.0              | 41.5   |
|               | Door Window          |                         |                   |        |                   |        |                   |        |
|               | UH-1                 | 5/32                    | 92.0              | 3.9    | 89.0              | 26.0   | 87.5              | 39.1   |
|               | Coated<br>Material   |                         |                   |        |                   |        |                   |        |
| 1             | Abcite, A/C          | 1/4                     | 94.3              | 0.8    | 94.0              | 7.7    | 93.9              | 11.4   |
| 2             | Abcite, P/C          | "                       | 86.5              | 3.0    | 86.3              | 3.9    | 85.4              | 13.0   |
| 3             | Urethane, 574        | "                       | 81.7              | 2.6    | 81.0              | 9.0    | 80.5              | 21.6   |
| 4             | Abcite, P/C          | "                       | 85.5              | 6.1    | 84.3              | 12.0   | 83.3              | 19.9   |
| 5             | Symbolic Disp.       | "                       | 94.1              | 1.7    | 92.8              | 11.4   | 91.5              | 27.3   |
| 6             | Astro, P/C           | "                       | 85.6              | 4.0    | 84.0              | 32.0   | 81.0              | 40.0   |
| 7             | ESB, P/C             | 1/8                     | 89.1              | 1.5    | 89.0              | 20.9   | 87.0              | 40.8   |
| 8             | MR-4000, P/C         | "                       | 86.2              | 2.6    | 83.3              | 36.6   | 81.9              | 46.3   |
| 9             | Mobay, P/C           | "                       | 81.5              | 6.1    | 78.6              | 30.3   | 78.1              | 41.7   |
| 10            |                      |                         |                   |        |                   |        |                   |        |
| 11            | Swedlow, S/A         | "                       | 93.0              | 1.4    | 91.8              | 9.3    | 91.5              | 15.9   |
| 12            | Swedlow, P/C         | "                       | 81.6              | 6.6    | 81.2              | 20     | 79.5              | 30     |
| 13            | No 311, A/C          | "                       | 93.0              | 2.0    | 91.9              | 14     | 89.1              | 28     |
| 14            | Texstar, P/C         | "                       | 84.4              | 4.5    | 83.5              | 12.6   | 81.8              | 32.4   |



TABLE III (Cont'd)

|    |                  |       |      |     |      |     |      |     |
|----|------------------|-------|------|-----|------|-----|------|-----|
| 15 | Glass<br>Corning | 0.085 | 92.1 | 1.2 | 91.4 | 6.6 | 91.0 | 2.5 |
|----|------------------|-------|------|-----|------|-----|------|-----|

\* Complete material description in Table I.

Key S/A = Stretched Acrylic  
A/C = As-cast Acrylic  
P/C = Polycarbonate

TABLE IV

## FELT PAD ABRADER

| Test Code | Material           | Cycles to Produce 10% Haze<br>400 gram: 0.68 psi | Coating Efficiency*<br>Compared with<br>as Cast UH-1, Acrylic | Efficiency Compared<br>with Uncoated<br>Substrate |
|-----------|--------------------|--|---|---|
| A         | Lexan              | 3  | 1   | ---   |
| B         | Lexan              | 3  | 1   | ---   |
| C         | Merlon             | 2.5  | .8  | ---   |
| D         | Rowland            | 2.5  | .8  | ---   |
| E         | Mil-P-5425         | 3  | 1   | ---   |
| F         | Mil-P-25690        | 5  | 1.6   | ---   |
| G         | Urethane           | 6  | 2   | ---   |
| H         | Acrylic)Current    | 3  | -   | ---   |
| I         | Acrylic)Windshield | 3  | -   | ---   |
| 1         | Abcite, A/C        | 450  | 150   | 150   |
| 2         | Abcite, P/C        | 400  | 130   | 130   |
| 3         | Abcite, urethane   | 250  | 83  | 42  |
| 4         | Abcite, P/C        | 170  | 56  | 56  |
| 5         | Symbolic, S/A      | 220  | 73  | 44  |
| 6         | Astro, P/C         | 310  | 103   | 103   |
| 7         | ESB, P/C           | 150  | 50  | 50  |
| 8         | MR-4000, P/C       | 275  | 93  | 93  |
| 9         | Mobay, P/C         | 150  | 60  | 60  |

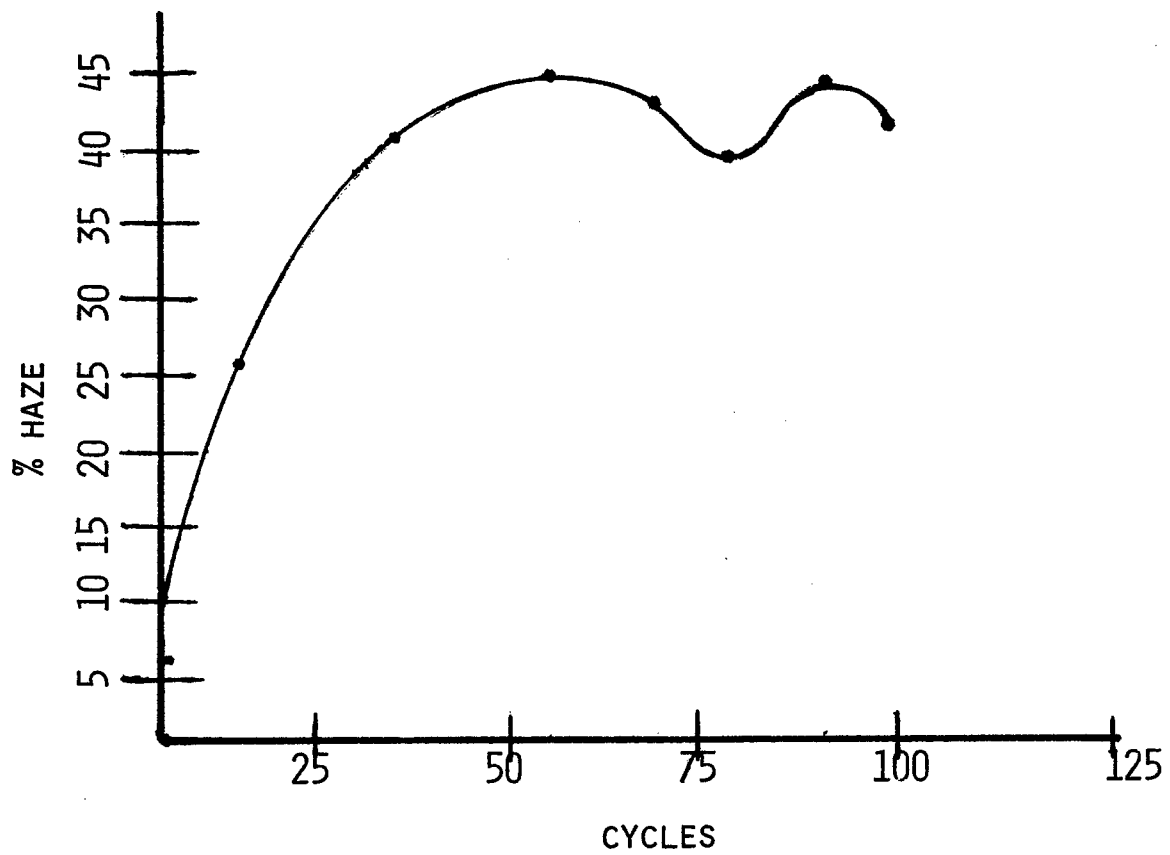
TABLE IV (Cont'd)

|    |                |       |      |     |
|----|----------------|-------|------|-----|
| 10 | OI, P/C        | 50    | 17   | 17  |
| 11 | Swedlow, S/A   | 10    | 3    | 2   |
| 12 | Swedlow, P/C   | 50    | 17   | 17  |
| 13 | Sierricin, P/C | 70    | 23   | 23  |
| 14 | Texstar, P/C   | 62    | 21   | 21  |
| 15 | Corning        | 3000+ | 1000 | --- |

\* efficiency

#Cycles, Coating or Substrate = efficiency, i.e., improvement over current material  
 #Cycles, Mil-P-5425  
 (UH-1, sample)

FIGURE 4  
ABRASION CURVE, LEXAN



Values in Table IV express the abrasion performance of glass, plastic, and coated plastic materials. The felt pad abrader test permitted an effective and reproducible means of evaluating material durability. Utilizing this test method on duplicate samples, the data were reproducible to a  $\pm 3.0\%$  for values of transmitted haze. It was found as in other studies, Reference 4, that some coatings may vary widely for values of abrasion resistance between sample lots, making a value of the durability very difficult to average.

Reference 4 also reported, haze increased rapidly with the development of surface abrasion up to a given point, above which haze developed at a more reduced rate. Results for polycarbonate, with this method and abrasive, shows this point to be approximately 40% transmitted haze. The abrasive action apparently polishes out previous scratches, as in Figure 4.

Data in Table IV demonstrated that glass provided an improvement (abrasion resistance) over present UH-1 windshield material by a factor in excess of 1000. Stretched acrylic provided little improvement (160%) over Mil-P-5425, compared to the coated materials. Abcite coated polycarbonate provided an improved durability over both UH-1 windshield material, and polycarbonate material by a factor of 130, i.e., coating efficiency is approximately 13,000%, while Abcite on Mil-P-5425 acrylic increased the abrasion resistance effectiveness of the substrate 15,000%. Abcite coated materials, acrylic or polycarbonate, exhibited 30% to 50% more effective abrasion protection than all other coatings tested. A precise correlation was difficult between performance of the two test methods, however, it was noted that relative levels of performance of various coatings tended to be similar in both methods.

## V. SPALLATION STUDY

### A. Spall Testing

#### (1) Methods

Ballistic testing was used to determine and evaluate spall characteristics for: (a) hard surface coated materials and, (2) composite windshield configurations.

The study was approached by considering spallation in terms of: (a) weight loss of plastic materials after penetration, (b) photographic appraisal of the particle characteristics, and (c) the amount of spall as determined by the area of the holes produced by spall in a 2 mil aluminum foil witness plate. The experiment was performed in two parts. In the first part, the helium gun apparatus was used in conjunction with the camera set-up. A witness plate 12" x 12", was positioned 12" behind the test sample. The test sample was held in rigid position by the sample holder during firing.

The controlled parameters were:

1. Sample obliquity, 0 degrees.
2. Camera orientation, 90 degrees to sample.
3. Sample thickness, 0.125", 0.22", 0.25", 0.38".
4. Projectile, .22 cal. 17-grain FSP (Fragment Simulating Projectile).
5. Projectile velocity, low range 1200 to 1600 fsp.  
Projectiles were fired at velocity just high enough to permit complete penetration.
6. Temperature and humidity, samples were conditioned 48 hours before weighing and testing, conditioning and testing factors (70°F, 40% RH).

In the second phase testing, the samples tested and evaluated in Part I, were subjected to ballistic penetration by .30 cal. ball ammunition. The parameter used was the average weight loss based on two complete projectile penetrations. A 20 mil aluminum foil witness plate was placed 6" from sample to verify complete penetration.

The controlled parameters were:

1. Sample obliquity, 0 degrees.
2. Sample thickness, 0.125", 0.22", 0.25", 0.38".
3. Projectile, caliber .30 ball.
4. Projectile velocity, 2,500 fps.
5. Temperature and humidity, samples were conditioned 48 hours before weighing and testing at 70°F and 40% RH.

## (2) Results and Discussion

Reduction of spallation is most effectively achieved by uncoated polycarbonate. There is little difference in the character of the spall among types and commercial brands of polycarbonate. Spallation from this material consisted of punched-out plugs of polycarbonate approximately the diameter of the 17-grain fragment simulator projectile. Low spallation characteristics with this projectile were found not to be significantly affected by the addition of hard surface coatings when applied either to one or both sides of the polycarbonate. Another study has shown that the ductile failure mode of polycarbonate changes to a brittle failure mode with a much thicker hard surface coating. (Ref. 14).

Figure 5 shows typical "plug" spallation in Abcite coated Lexan polycarbonate when penetrated by a 17-grain FSP. An average value for

1/4 inch material was 0.43 grams weight loss per complete penetration. (Table V).

Spallation by polycarbonate and urethane material when impacted by .30 cal. ball consisted of a "closed hole" with no punched plug, Figure 6. Weight loss in the latter was approximately 50% of that produced by 17-grain FSP testing in the same material.

Typical spallation from the current UH-1 windshield is shown in Figure 4. The 17-grain FSP has completely penetrated at 1175 fsp; spall, by weight loss, is approximately 1.5 times greater in the acrylic, sample H, Table V, than in polycarbonate approximately the same thickness, sample B. The weight of material lost by spallation of the acrylic windshield during .30 cal. ball testing increases to approximately 9.5 times greater than similarly tested polycarbonate. For partial penetration, however, polycarbonate shows no weight loss, while the acrylic plastic material undergoes weight loss. Ref. 15.

Residual optics for polycarbonates and urethanes were the best of the material evaluated after impact. Loss of visibility occurred in an area approximately the diameter of the projectile. Residual optics were similar for the .30 cal. testing, i.e., area of damage remained about the diameter of the projectile.

The acrylic clad polycarbonate design was less effective than plain polycarbonate for weight loss due to spallation, but still more effective than acrylic.

The residual optics, after projectile impact, for the stretched acrylic and the current UH-1 windshield are similar. Results show that .30 cal. testing produced a circle of damage one-inch in diameter on the stretch acrylic while polycarbonate resulted in a 0.40" dia. circle.

The glass clad polycarbonate configurations were initially evaluated for residual optics after projectile impact. Only configuration 1, Table II, demonstrated sufficient optics to warrant spallation testing at that time. That glass broke with a large pattern allowing visibility after impact. The diameter of the area of damage is approximately three times greater than that produced in acrylic. The weight loss due to spallation is approximately ten times greater than polycarbonate, however, still better than current materials. Figure 8 shows spallation in this design.

Evaluation of the witness plates, Table V, demonstrated that weight loss in this design, is to a great degree pulverized glass, the area of damage produced by the spall is 60% less than 0.25" Lexan and 650% less than acrylic materials. Figures 9, 10, and 11 depict the witness plate damage expressec above.

TABLE V

## SPALLATION RESULTS

2 Round Aver. at 75°F, 40% RH

| Test Code | Material*             | Thick-<br>ness (in.) | .22 FSP       |                  | .30 Ball      |                  | FSP<br>Spall<br>Descr. | Witness Plate<br>Area of<br>Penetration<br>(sq. in.) |
|-----------|-----------------------|----------------------|---------------|------------------|---------------|------------------|------------------------|--|
|           |                       |                      | Vel.<br>(fsp) | Wgt. Loss<br>(g) | Vel.<br>(fsp) | Wgt. Loss<br>(g) |                        |  |
| B         | Lexan, P/C            | 1/4                  | 1095          | 0.40             | 2524          | 0.22             | Punched<br>Plug        | 0.43   |
| B         | Lexan, P/C            | 3/8                  | -             | -                | 2538          | 0.35             | -                      |  |
| D         | Rowland, P/C          | 1/4                  | 1035          | 0.46             | -             | -                | Punched<br>Plug        |  |
| E         | Mil-P-5425            | 1/4                  | 1185          | 0.78             | 2552          | 3.49             | Conoidal<br>Fragment   | 1.53   |
| E         | Mil-P-5425<br>Plex 55 | 3/8                  | -             | -                | 2550          | 5.59             | -                      |  |
| F         | Mil-P-25690           | 1/4                  | 1180          | 0.51             | 2490          | 1.05             | Conoidal<br>Fragment   | 0.82   |
| F         | Mil-P-25690           | 3/8                  | -             | -                | 2464          | 2.15             | -                      |  |
| G         | Urethane, 579         | 1/4                  | 1112          | 0.29             | 2543          | 0.12             | Punched<br>Plug        |  |
| H         | UH-1 Wind-<br>shield  | 7/32                 | 1208          | 0.58             | 2498          | 2.90             | Conoidal<br>Fragment   | 1.30   |
| H         | UH-1 Wind-<br>shield  | 7/32                 | 1175          | 0.64             | 2520          | 1.89             | Conoidal<br>Fragment   | 1.25   |
| I         | UH-1 Door<br>Window   | 5/32                 | 1184          | 0.39             | 2526          | 0.87             | Conoidal<br>Fragment   | 0.87   |
| 2         | Lexan,<br>Abcite      | 1/8                  | 1193          | 0.17             | 2518          | 0.10             | Punched<br>Plug        | 0.25   |

TABLE V. (Cont'd)

|    |                        |     |      |      |      |      |   |
|----|------------------------|-----|------|------|------|------|---|
| 4  | Lexan,<br>Abcite       | 1/4 | 1036 | 0.46 | 2505 | 0.25 | Punched 0.38<br>Plug                            |
| 11 | Mil-P-25690<br>Swedlow | 1/4 | 1208 | 0.59 | 2515 | 1.14 | Conoidal 1.0<br>Fragment                        |
| 12 | P/C Swedlow            | 1/4 | 1208 | 0.41 | 2530 | 0.21 | Punched<br>Plug                                 |
| 14 | P/C Texstar            | 1/4 | 997  | 0.36 | 2476 | 0.25 | Punched 0.38<br>Plug                            |
| VI | Plex/Lexan             | 3/8 | 1573 | .49  | 2514 | 1.45 | Angular 0.21<br>Particles                       |
| I  | Glass/Lexan            | 3/8 | 1659 | .58  | 2528 | 2.0  | Powderized<br>glass<br>particles<br>of P/C 0.18 |



OML POL & COMP HS  
PHOTO IMPACT RES LAB JMR

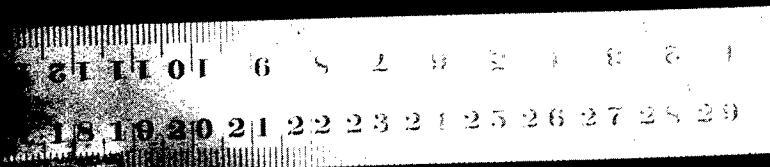


FIGURE 5

POLYCARBONATE SPALL, PUNCH-OUT PLUG

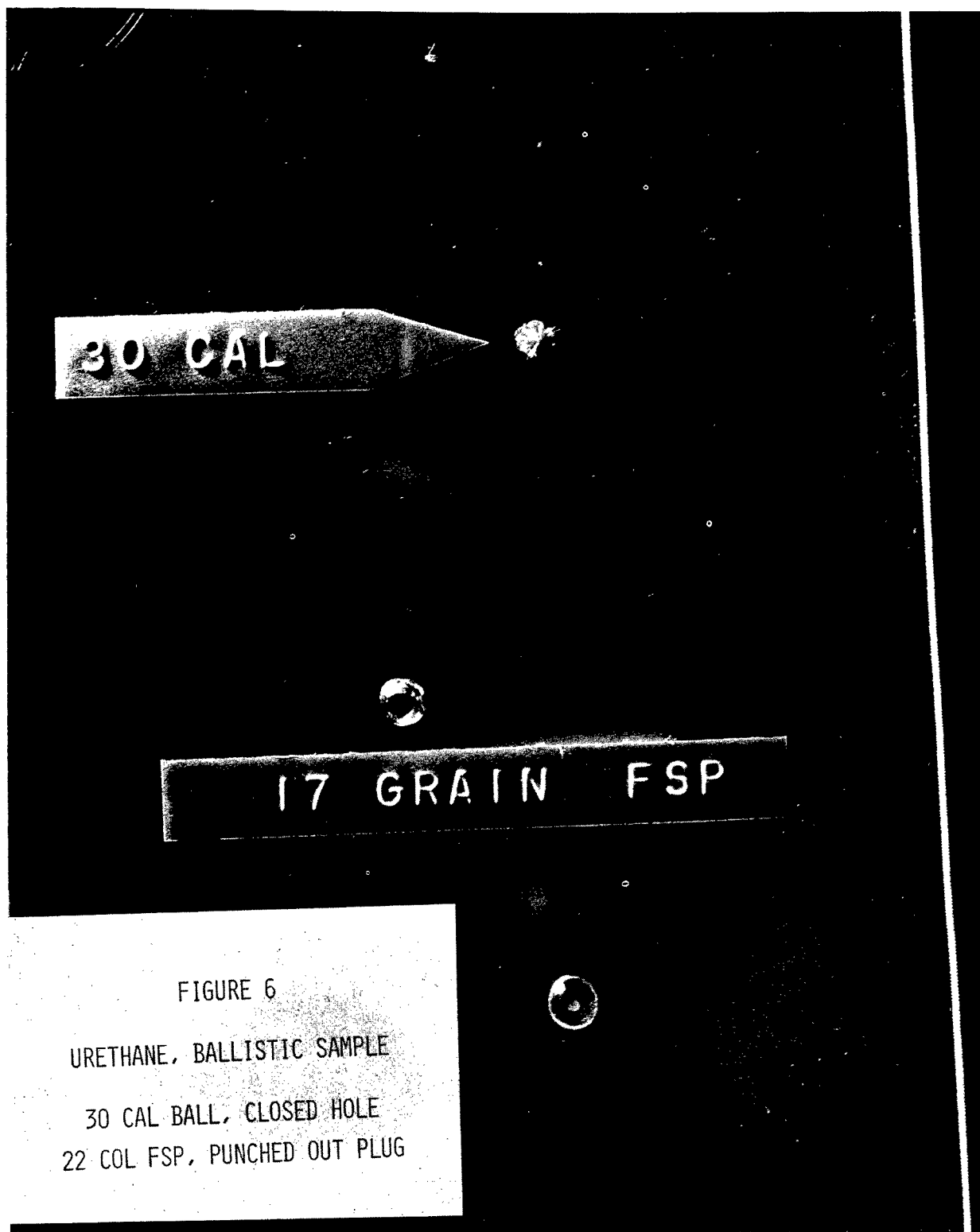
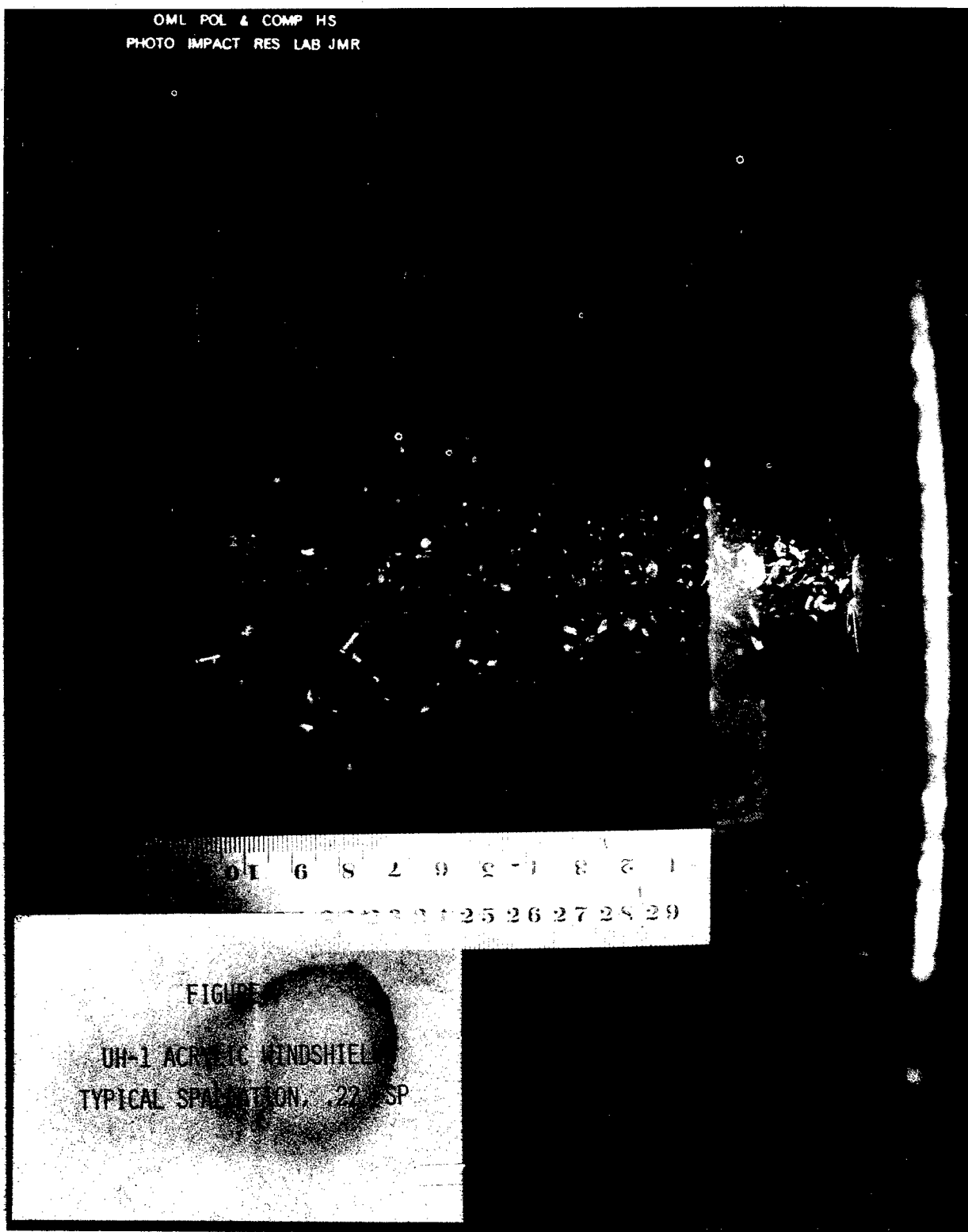


FIGURE 6

URETHANE, BALLISTIC SAMPLE

30 CAL BALL, CLOSED HOLE  
22 COL FSP, PUNCHED OUT PLUG

OML POL & COMP HS  
PHOTO IMPACT RES LAB JMR



OML POL & COMP HS  
PHOTO IMPACT RES LAB JMR

01 6 8 2 0 2 1 8 2 1  
21 22 23 24 25 26 27 28 29

FIGURE 8  
GLASS/POLYCARBONATE DESIGN  
TYPICAL SPALLATION, 17 GN FSP

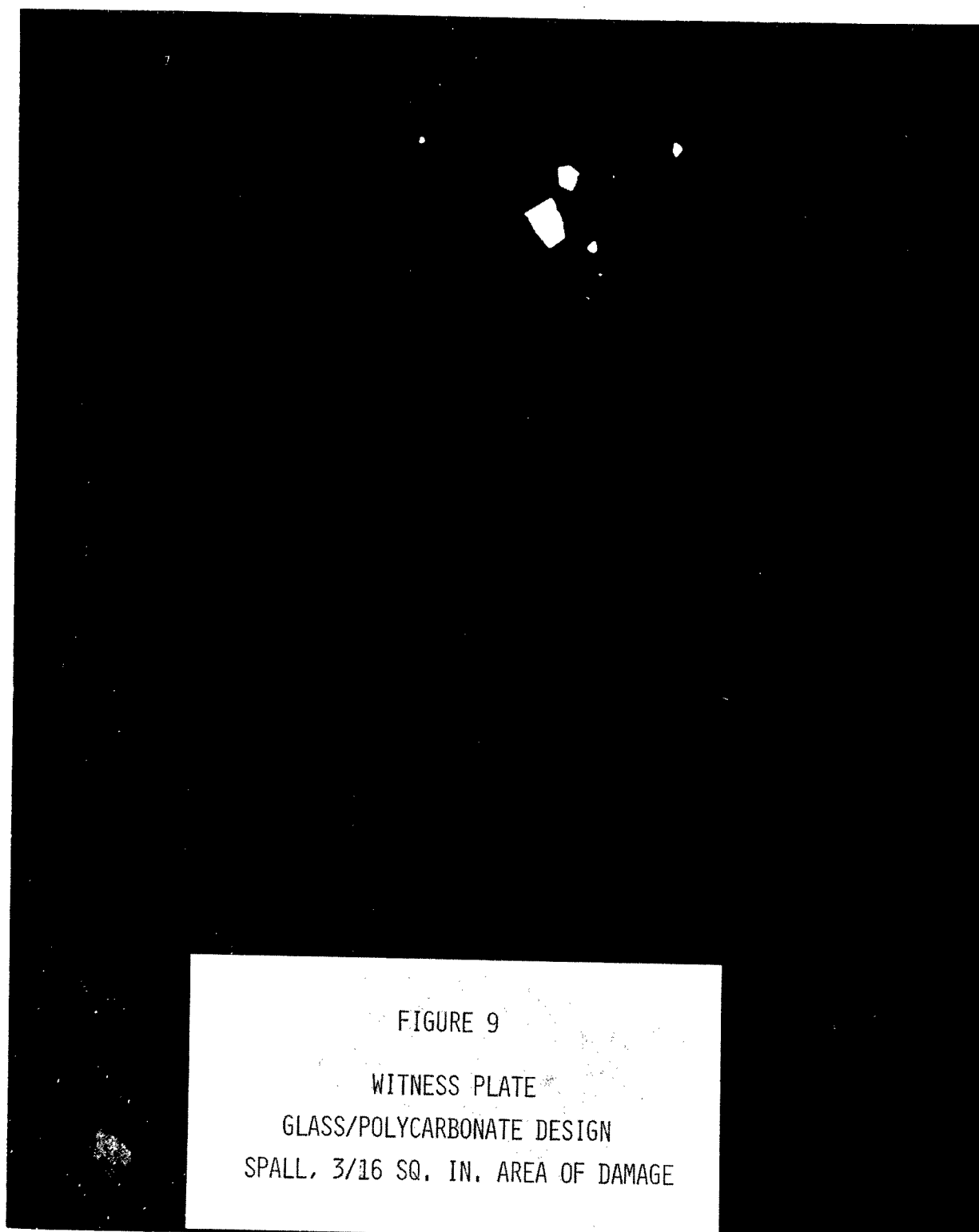


FIGURE 9  
WITNESS PLATE  
GLASS/POLYCARBONATE DESIGN  
SPALL, 3/16 SQ. IN. AREA OF DAMAGE

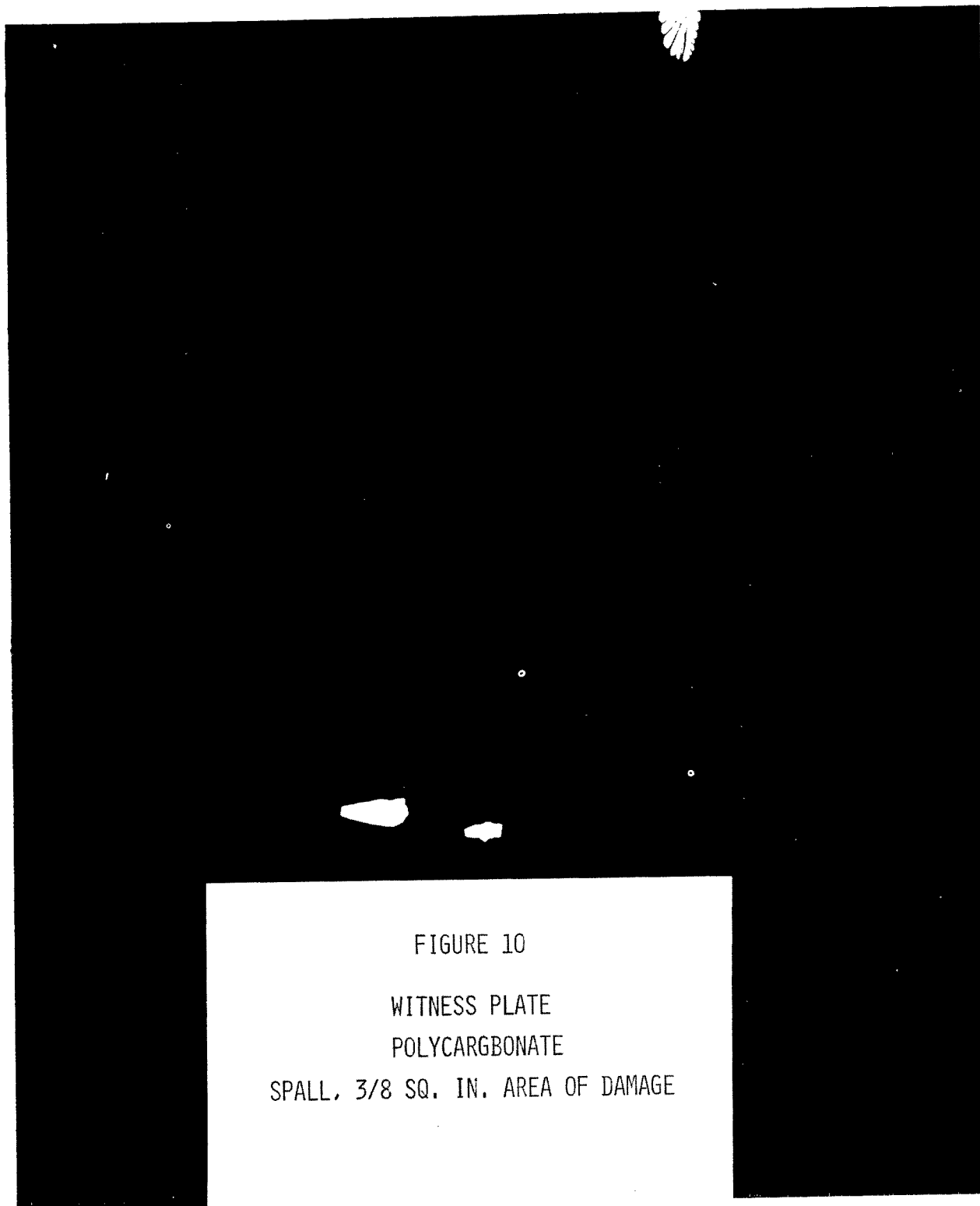


FIGURE 10  
WITNESS PLATE  
POLYCARBONATE  
SPALL, 3/8 SQ. IN. AREA OF DAMAGE

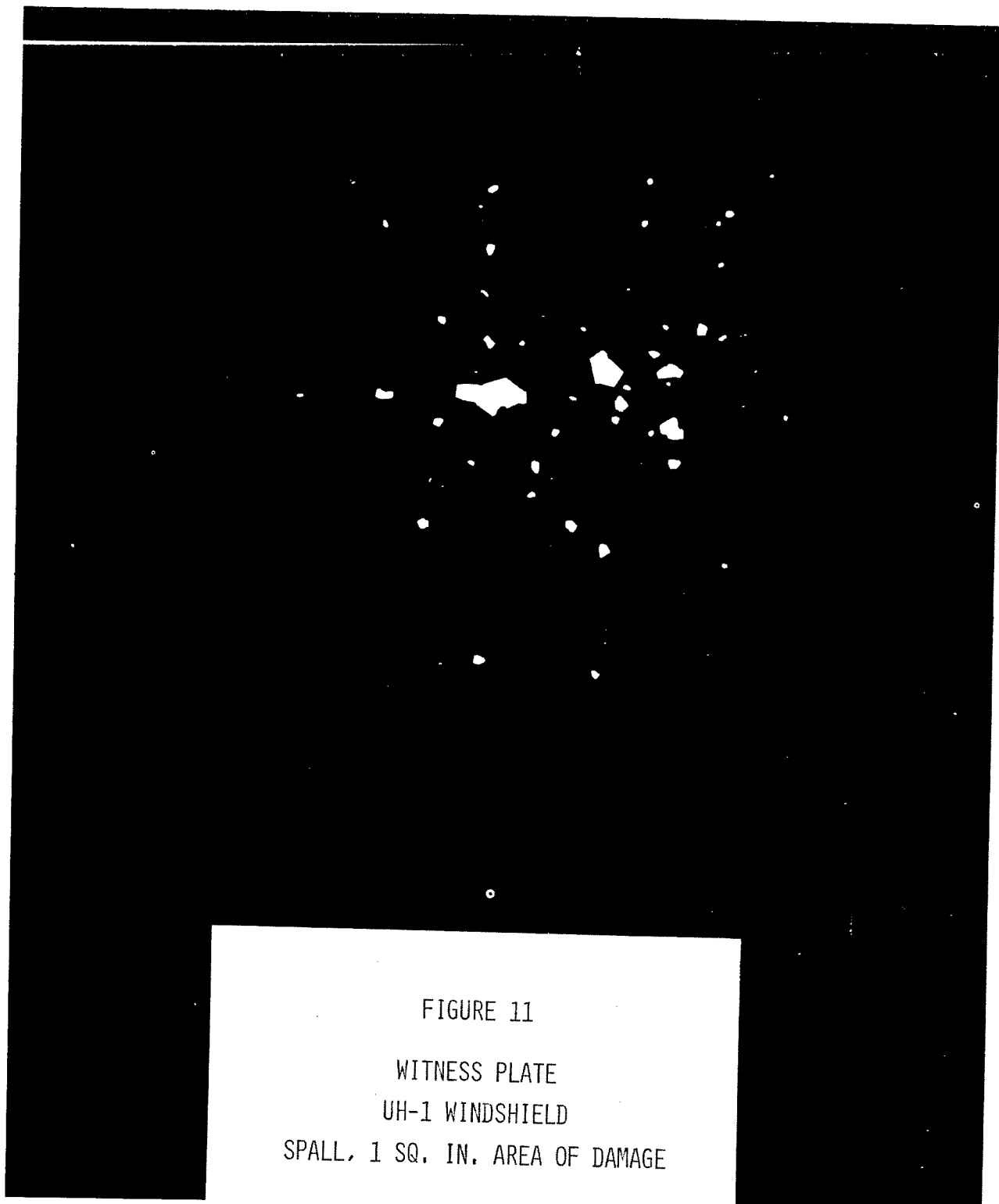


FIGURE 11  
WITNESS PLATE  
UH-1 WINDSHIELD  
SPALL, 1 SQ. IN. AREA OF DAMAGE

## CONCLUSIONS

The glass clad polycarbonate configuration provides the best abrasion protection. Abrasion resistance is the most important factor in service requirements. It also has the most weight, the least spall protection, and the poorest residual optics of the three improved configurations tested. Spallation in this design is greater than coated polycarbonate by approximately a factor of 10, but, it offers an improvement over the current acrylic material, of a least 150%, as measured by weight loss. The glass polycarbonate composite appears to offer the greatest increase in serviceability when utilized as pilot and co-pilot windshields, which are subjected to the severest durability requirements during the operation of the helicopter windshield wiper.

Stretched acrylic as a cladding on polycarbonate provides less potential abrasion protection than the best performing coated polycarbonate and only very limited improvement over current helicopter windshield material. Acrylic bonded to polycarbonate, provided less spall protection than plain or coated polycarbonate by a factor of 5; but it did offer an improvement over as-cast acrylic alone of 200% in weight loss due to spall. The effectiveness of the acrylic, in this system, to provide increased abrasion resistance was insufficient to warrant further development. Though coating the acrylic with Abcite could provide greatly improved protection, it would be less advantageous than coated polycarbonate, as the residual optics are poorer and the weight factor for a completed windshield is much greater than polycarbonate. Polycarbonate coated with Abcite provides improved abrasion protection than all coatings evaluated except Abcite on acrylic, however, the slightly better performance on acrylic does not justify use of this configuration in view of the weight and optical properties.

The windshield configuration affording the most effective reduction of spallation was achieved with the hard surface coated, Abcite, polycarbonate design. Spallation consisted of punched-out plugs of polycarbonate approximately the diameter of the projectile when low velocity fragment simulators were used. Low spallation characteristics of polycarbonate were not found to be adversely affected by the addition of very thin layers of Abcite or other hard surface coatings when applied either to one or both sides of the material. The spallation effectiveness of the material increased when high velocity .30 cal. ball ammunition was used. This configuration provides the greatest residual optics, i.e., the most undamaged area, due to the extremely small area of damage caused by impact of various projectiles, and has a weight factor essentially the same as current windshields.

Abcite coated polycarbonate provided improvement in abrasion resistant properties over acrylic UH-1 windshields by a factor of 130. Use of the coated polycarbonate should provide an effective increase in serviceability when incorporated as a windshield, although not as desirable as a glass surface. Coated polycarbonate is most applicable for glazing of the



remainder of the helicopter transparencies where complex configurations would make the use of a glass faced design impossible, and the absence of a wiper blade would reduce the severity of the abrasion. Coating performance in this role is under further evaluation, as the performance of coating is anticipated to vary greatly when mechanical action is reduced or not present in the abrasive environment.

Final evaluation of potential windshield design improvements will be made after flight testing of a glass clad polycarbonate and an Abcite coated polycarbonate prototype UH-1 windshield.

## BIBLIOGRAPHY

1. Aircraft Glass Replacement, Value Engineering Study 664999, ARADMAC, Corpus Christi, Texas, April 1969.
2. Ball, G. L. and Salyer, I. O., Development of a Transparent Adhesive Compatible with Polycarbonate for Use in Ballistic Shields, TR AFML-TR-70-144, Monsanto Research Corporation, June 1970.
3. Cully, D. C., Transparent Materials for Aircraft Canopies and Windows, Goodyear Aerospace Corp., AFML, Wright-Patterson AFB, Ohio, June 1969.
4. Hassard, R. S., Design Criteria Transparent Polycarbonate Plastic Sheet, TR AFML-TR-72-117, Air Force Materials Laboratory, Air Force Systems Command, Wright-Patterson AFB, Ohio, August 1972.
5. Maltenicks, O. J., Improved Rain-Repellent Coating for Aircraft Windshields, Canopies, and Other Nonmetallic Components, TR-AFML-TR-70-1099 Part II, Lockheed Georgia Co., August 1972.
6. Peters, J. R., Behavior Characteristics of Caliber .30 Armor Piercing Projectile After Penetrating Biaxially Stretched Acrylic, Army Materials Research Group Report No. 8339, U. S. Army Natick Laboratories, Natick, Mass. 01760, March 1967.
7. Plastics for Aerospace Vehicles, Mil-BBK 1FA, Part I, U. S. Department of Defense.
8. Plastics: Methods of Testing, Federal Test Method Standard No. 406, GSA Business Service Center, Washington 25, D.C.
9. Powell, J.H., Evaluation of Scratch/Abrasion-Resistant Coatings for Acrylic Windshields, Report No. 0068R-162, Bell Helicopter Company, 10/21/68.
10. Rogers, J. M., Development of a High Pressure Medium Velocity, Helium Gun for Firing 17-Grain Fragment Simulators, AMMRC TR 72-11, March 1972.
11. The Handbook for Aircraft Designers, Vol. 1, Unites States Air Force.
12. Transparent Glazing Materials for Flight Vehicles, Mil-HNDBK-17, Part II, U. S. Department of Commerce.
13. Wiser, G. L., New Materials in Aircraft Windshields, Sierrican Corp. October, 1940
14. Lewis, R., Roylance, M., Development of Transparent Polymers for Armor, AMMRC TR-72-34, July 1972.

15. Parsons, G., Lewis, R., Ballistic Performance of Transparent Materials for Visor Applications, AMMRC TR 72-37 (1972).

#### ACKNOWLEDGMENT

The Organic Materials Laboratory range facility is operated by Mr. Joseph M. Rogers whose efforts were responsible for the completion of the ballistic phase of this project. Acknowledgment is also made to Dr. Robert W. Lewis, Mr. Anthony L. Alesi, Mr. Gordon R. Parsons and Dr. Anthony F. Wilde for their technical review and helpful suggestions.

VACUUM DEPOSITED ELECTRICALLY  
CONDUCTIVE COATING DESIGN

Gene Nixon  
Swedlow, Inc.  
Garden Grove, California

VACUUM DEPOSITED ELECTRICALLY

CONDUCTIVE COATING DESIGN

Gene Nixon  
Manager of Engineering

SWEDLOW, INC.

ABSTRACT

This paper describes the process of designing vacuum deposited electrically conductive coatings by the transparency manufacturer when given the coating's functional requirements. An understanding of this process by the airframe manufacturer is necessary in order to establish coating geometry and electrical tolerance characteristics.

The coating's orthogonal current / voltage field and a graphic coating design technique is described. This first order graphic technique is verified and refined by electrolytic tank modeling, and translation from the theoretical resistivity profile (primary variable) to the actual vacuum process is set forth.

The methods of obtaining resistivity profiles and the tolerances on this process controlled factor are noted.

Variations in resistivity are manifest as variations in heat flow (generated power density) and this becomes the primary functional factor, not temperature uniformity.

A method for measuring heat flow directly is described along with known tolerances.

## INTRODUCTION

If you were building your own home would you design the water heater?

It's doubtful. Of course, you need one and it has to provide the correct amount of hot water and fit in the space provided, but you would probably have it designed by a water heater man.

By the same token it's suggested that the fellow who wants an aircraft built should have the windshield heater designed by the windshield heater man.

Transparency heating elements should be designed by the transparency manufacturer not the airframe manufacturer.

This paper builds the argument for your analysis so that you might determine whether or not it's the correct way to go.

In addition, the design process used at Swedlow for resolving vacuum deposited heater elements for transparencies is illustrated and some of the characteristics of these thin films are set forth.

The specifier needs to obtain information on the effect of power density grading and variations. What happens to optics when these variations occur? What happens at powered area boundaries and what are the manufacturing tolerances?

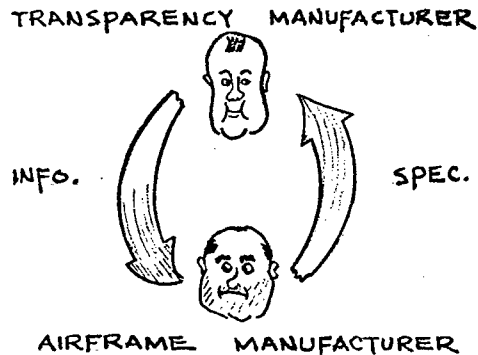
In addition, the sensors' compatibility with processing, proximity to the powered coating, quantity of sensors and their areal positioning needs to be ascertained.

The limits on resistivity and coating shape establish the voltage required and, the coating application tolerance and allowable current densities set the power limits.

Also, the coating affects optical light transmission and reflection and, due to power dissipation, may create distorted areas. So coating types must be selected and tailored to provide acceptable optical characteristics.

## TEXT

The beginning of the windshield heater element design process is the generation of the windshield specification. This specification is prepared by the airframe manufacturer and is based, in large part, on information obtained from the transparency manufacturer. It's rather easy to recognize the circular nature of this arrangement.



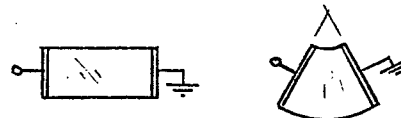
To get a feel for the quantity of information which the spec writer needs to obtain from the transparency manufacturer one must look at the content of the heated windshield specification.

### HEATING DESIGN SPEC. PRIMARY CONTENT

- Heated area
- Power density
- Control sensing
- Power characteristics
- Optical requirements

Heated area seems simple enough, but it actually creates the bulk of the problems. For uniform heating of a windshield area there are only two basic shapes possible and these shapes are further limited by coating resistivity grading possibilities. Also, the limits on power density variations which are acceptable to the coating are needed. Each of these must be obtained from the transparency manufacturer.

### SHAPES OF UNIFORM POWER DENSITY



As can be seen, there is quite an information merry-go-round in process and in most cases the information being transmitted - both ways - is based on half-truths. Each needs either a cushion or leverage. It's like a foot race in which a 100 yards gets the job done, but the finish line is placed at 120 yards and the runner wants to ride a bike.

With the specification in the manufacturer's hand the true heated transparency design beings.

#### GRAPHIC ELECTRIC FIELD GENERATION

- Orthognality of E & I
- Boundary conditions
- Equal area
- Relaxation

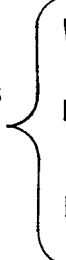
The first step is to generate a resistivity profile which will meet the power and area requirements of the specification. This is done, to a first approximation, graphically by constructing orthogonal voltage and current lines which create areas representing power density.

Second, the graphically generated resistivity profile is used to make a topographic model which is placed in an electrolytic tank and a plot is made of the actual current and voltage lines. Modification to the bottom geometry is made until the desired power density is reached. This yields the theoretically correct resistivity profile.

By the way, the electrolytic tank which is used is automatically driven and plots directly. This greatly reduces the testing effort.

From the resistivity profile coating machinery is selected which will be used in the vacuum chambers. This machinery may utilize point or extended sources for deposition; and, each of these source types has the possibility of incorporating masks for grading, may be moved in some manner, or have the deposition rate controlled.

#### SELECT & DESIGN COATING MACHINERY

- Point sources
  - Extended sources
- 
- Masks
  - Movements
  - Deposit rate



In addition to these coating sources there are other pieces of equipment which must be designed such as bus-bar and holding fixtures, deletion line apparatus, etc.

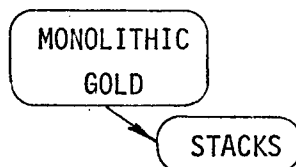
After this machinery is made, it is necessary to move into the vacuum chamber and begin to coat parts and refine the grading. Why must the grading be refined? Well, the resistivity is not directly controlled in the vacuum chamber and as such the translation of the theoretical design to vacuum processing is empirical.

VACUUM COAT AND  
REFINE GRADING

- Resistivity is not directly controlled -- cannot be independently monitored
- Translation of design to vacuum process is empirical

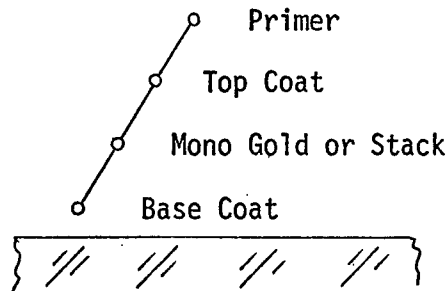
Of course, prior to this activity an electrically conductive film type must have been selected. Vacuum coatings which are used on transparencies for power dissipation are hinged around gold. Evolving from gold are coating stacks which incorporate metal oxide films on either side of the gold. These stacks act to modify the current conduction thus changing the resistivity limits. They also optically anti-reflect the gold.

VACUUM DEPOSITED  
CONDUCTIVE COATINGS



- Modify conduction due to Au orientation
- Anti-reflect Au

CONDUCTIVE COATING  
is a  
PORTION OF THIN FILM SYSTEM



These conductive coatings are in reality a portion of a thin film system. Base coats, top coats and primers are used in conjunction with the gold film. These additional film elements are required in order to enhance adhesion, to mask substrate surface scratches, and to offer processing protection to the conductive film. Also, these film elements vary with the types of substrate being used.

This completes the coating application design phase.

Now, to determine the coating functionability it is necessary to measure the coating's power dissipation - its ability to anti-ice or anti-fog.

Based on the impetus of Bob Paselk at North American Rockwell, Swedlow has been developing the use of the heat meter to measure the heat flow directly. As heat flow is the real measure of heater functionality, this method has many advantages over temperature uniformity measurements. The heat meter equipment required includes a commercially available low flux heat meter and a millivolt meter readout. The reverse side of the part is insulated, the sensor is thermally coupled to the windshield, and a convective guard is used. Heat flow is read out directly with the accuracy of the heat flow measurement being about 3 percent at 160 BTU/Hr/Ft<sup>2</sup>.

This concludes the design process as performed at Swedlow and perhaps key points should be reiterated:

- Consider having the transparency manufacturer design your next windshield heater element
- Remember that there are only a limited number of normally accepted coated area geometries available for uniform power dissipation
- It's possible to measure heat flow directly and heat flow is what's important.

OCULAR HAZARD FROM VIEWING THE SUN  
UNPROTECTED AND THROUGH VARIOUS  
WINDOWS AND FILTERS

W. T. Ham, Jr., H. A. Mueller, and R. C. Williams  
Virginia Commonwealth University  
Richmond, Virginia

OCULAR HAZARD FROM VIEWING THE SUN UNPROTECTED AND  
THROUGH VARIOUS WINDOWS AND FILTERS\*

---

W. T. Ham, Jr., H. A. Mueller, and R. C. Williams

Department of Biophysics

W. J. Geeraets

Department of Ophthalmology

Health Sciences Center

Virginia Commonwealth University

Richmond, Virginia

ABSTRACT

An optical source simulating the sun at the top of the atmosphere has been constructed and used to obtain retinal burn thresholds in the rhesus monkey for image diameters corresponding to that of the solar disc on the human retina. Powers incident on the cornea and retinal irradiances required to produce threshold lesions are given for exposure times ranging from one second to three minutes. It is predicted that gazing at the sun for one second with a pupillary diameter of 6.3 mm or three minutes with a diameter of 2.5 mm will produce a threshold lesion.

The ocular hazard associated with viewing the sun through an aircraft window system consisting of three acrylic units and a Polaroid VLT (Variable Light Transmitting) window in the uncrossed and crossed positions has been assessed in terms of these data. It is concluded that the Polaroid window which contains an IR absorbing component offers greater protection from retinal damage in either the open or closed positions, than conventional windows now in use on high flying aircraft and that radiation in the near infrared is less dangerous than visible light in producing thermal injury to the retina.

\*This research was supported primarily by the Polaroid Corporation, Cambridge, Massachusetts, and by contract DA 49-193-MD-2241, U.S. Army Medical Research and Development Command, Office of the Surgeon General, Washington, D. C.

## INTRODUCTION

The problem posed is the ocular hazard of viewing the sun from a high flying aircraft through various windows and filters. It was introduced by the concern of the Polaroid Corporation for the safety of a variable light transmitting (VLT) window under development for aircraft. The window consists of three acrylic sheets in conjunction with two Polaroid lamellae (polarizer and analyser). The polarizer also contains an infrared absorbing dye. The rotation of the analyser is under pushbutton control by the observer or passenger. In the crossed position, wavelengths below 800 nm are strongly attenuated while portions of the near infrared are transmitted in two broad bands centered at 1080 and 1300 nm. The problem of most concern is whether a passenger can sustain a retinal burn from prolonged exposure to the near infrared radiation transmitted in the crossed position, since these wavelengths are not visible and do not induce photophobia. Moreover, there is no sensation of pain on the human retina during photocoagulation of the retina.

A primary requirement for assessment of the safety of the VLT window relates to the ocular hazard involved in viewing the sun at zenith and at the top of the atmosphere without artificial attenuation, a worst case situation. Since reliable data on thresholds for solar retinitis at the top of the atmosphere are not available, it became necessary to simulate the solar spectrum in the laboratory so that it could be used as a source to determine thresholds for retinal burns in an experimental animal which could be related to man. The Rhesus monkey (*Macaca Mulatta*) was selected as the animal of choice for reasons which are given in this report.

Having established criteria for threshold solar retinitis in the monkey, the next procedure logically was to obtain threshold data with the simulated solar source after transmission through the VLT window. This proved to be experimentally unfeasible because the simulated solar source, while capable of introducing more power into the eye than unattenuated sunlight through an 8 mm pupil, was still not powerful enough to produce a burn on the monkey retina after passage through the VLT window, even in the uncrossed position. Next, an attempt to produce retinal lesions with the xenon lamp source after transmission through the VLT window in the crossed position was equally unsuccessful, despite the fact that this source produced three times more power than the simulated source and provided a spectral distribution on the retina similar to that of sunlight after transmission through the VLT window and the ocular media of the monkey. Under these circumstances it became necessary to resort to an infrared filter which would pass a major portion of the infrared radiation from the xenon lamp source. While the spectral distribution of this source on the retina did not correspond exactly to that of the solar spectrum after transmission through the crossed VLT window and monkey

ocular media, it did encompass those wavelength bands in the infrared passed by this combination. The power level of infrared radiation was sufficient to produce a burn after a 10 second exposure. Using this source it proved practicable to obtain infrared threshold burns for exposure times ranging from 10 seconds to 3 minutes.

#### SOLAR CHARACTERISTICS AND THE MAMMALIAN EYE

The sun subtends an angle of 32 minutes of arc (.00931 radians) at a distance of one astronomical unit, producing an image diameter of 158 micrometers ( $\mu\text{m}$ ) on the human retina. The solar spectra at the top of the atmosphere and at sea level are shown in Figure 1 (Ref. 1). Wavelengths less than 400 nm or greater than 1400 nm do not penetrate the ocular media of the mammalian eye and hence do not represent a hazard to the retina. Power densities or irradiances incident on the cornea within the spectral interval 400-1400 nm are  $102 \text{ mW-cm}^{-2}$  at the top of the atmosphere and  $64 \text{ mW-cm}^{-2}$  at sea level.

Transmittances through the ocular media of man, monkey and rabbit as a function of wavelength in nm are shown in Figure 2 (Ref. 2). For a solar spectrum at the top of the atmosphere incident on the cornea, the integrated transmittance through the ocular media in the spectral range 400-1400 nm is 0.735 for man and 0.737 for the Rhesus monkey. For the solar spectrum at sea level the corresponding integrated transmittances are 0.781 and 0.757 respectively.

These data can be used to calculate the retinal irradiance as a function of pupillary diameter for the human eye when viewing the sun at zenith and unattenuated by the atmosphere as well as at sea level. Retinal irradiances in  $\text{W-cm}^{-2}$  are given for pupillary diameters ranging from 1.5 to 8 mm in Table 1.

TABLE 1

Retinal irradiance in  $\text{W-cm}^{-2}$  vs pupillary diameter in mm. Solar constant at zenith, unattenuated by atmosphere taken as  $102 \text{ mW-cm}^{-2}$  for spectral range 400-1400 nm;  $64 \text{ mW-cm}^{-2}$  at sea level. Integrated transmittance of human ocular media for same spectral band is 0.735 and 0.781 respectively. Retinal diameter of sun's image is  $158 \mu\text{m}$ .

| Pupillary Diameter<br>mm | Retinal Irradiance in $\text{W-cm}^{-2}$ |           |
|--------------------------|--|-----------|
|                          | Top of Atmosphere                        | Sea Level |
| 1.5                      | 6.76                                     | 4.51      |
| 2.0                      | 12.0                                     | 8.01      |
| 3.0                      | 27.0                                     | 18.0      |
| 4.0                      | 48.0                                     | 32.0      |
| 5.0                      | 75.1                                     | 50.0      |
| 6.0                      | 108                                      | 72.1      |
| 7.0                      | 147                                      | 98.1      |
| 8.0                      | 192                                      | 128       |

#### COMPARATIVE DATA ON MAN, MONKEY AND RABBIT

Justification for selecting the Rhesus monkey as the test animal of choice is strengthened by the data shown in Table 2. These data have been collected in this laboratory over a period of years.

TABLE 2

Comparison of retinal burn thresholds in man, monkey and rabbit. Human volunteers and patients treated for diabetic retinopathy are compared to monkeys and rabbits under identical conditions of exposure, namely: retinal diameter 1 mm, exposure time 135 ms, filtered Osram lamp (XBO 2500) producing spectrum 400-800 nm. Energy density on retina given in J-cm<sup>-2</sup>.

| Species        | Area Exposed   |                | Comments                  |
|----------------|----------------|----------------|---------------------------|
|                | Paramacula     | Fovea          |                           |
| Man (A. E. G.) | 9.0 - 12.2     | 13.8           | only temporary afterimage |
| Man (M. Y.)    | 9.5 - 9.9      | 9.7            | absolute central scotoma  |
| Man (M. V.)    | 9.7            |                | foveal detachment         |
| Man (white)    | 9.3 $\pm$ 1.56 |                | 18 patients               |
| Man (black)    | 7.9 $\pm$ 1.86 |                | 10 patients               |
| Monkey         | 5.9 $\pm$ 1.5  | 5.7 $\pm$ 0.35 | 22 Rhesus monkey eyes     |
| Rabbit         | 4.1 $\pm$ 0.4  |                | 100 rabbit eyes           |

The threshold burn level in the monkey is slightly but not significantly lower than that for 10 black diabetic retinopathy patients. In the experience of this laboratory the variation in the burn threshold among humans is about a factor of 3, from 13.8 to 2.9 J-cm<sup>-2</sup>. The burn threshold in the Rhesus monkey may also vary by as much as a factor of 3. Research performed in collaboration with Dr. T. Kuwabara (3,4) has shown that 135 ms exposures to the same optical source at energy densities on the monkey retina 20 percent below the burn threshold as determined in the individual animal are not discernible by either electron microscopy or histological techniques. Morphological studies by Dr. Kuwabara using the electron microscope have demonstrated a remarkable similarity in retinal structure between man and Rhesus monkey (5).



## THRESHOLD BURNS WITH A SIMULATED SOLAR SOURCE

The source used to simulate the solar radiation was a xenon high pressure lamp (Osram XBO 2500) filtered by an Aerospace Control Corporation filter (ER 7187). A comparison of the simulated solar spectrum with that of the unattenuated solar radiation is shown in Figure 3. The laboratory source is somewhat deficient below 400 nm and lacks adequate irradiance in the near infrared, but it provides nonetheless a reasonable approximation to solar radiation throughout the visible spectrum. The power input into the eye exceeds that of the solar spectrum up to pupillary diameters of 8 mm. The integrated transmittance for the ocular media of the monkey is 0.77 as compared to 0.74 for the unattenuated solar spectrum.

The optical assembly of the laboratory source is illustrated schematically in Figure 4. Except for modifications and additions which are self-explanatory, it is basically equivalent to the Zeiss photocoagulator. The major differences reside in a special research lens ( $f/a < 0.9$ ) and the use of a Zeiss fundus camera with magnification of 8 to both view and photograph the retina, before, after and during an exposure. Irradiance at the cornea and image diameter on the retina can be varied at will by changing the diameter of the diaphragms designated one and two respectively in the diagram.

Animals to be irradiated are anesthetized with sodium pentobarbital, dilated with cyclopentolate hydrochloride and phenylephrine hydrochloride, and placed on a stereotaxic table device which secures the head and locates the eye coaxial to the beam. A lid speculum keeps the eye open; physiological saline is applied frequently to prevent drying of the cornea. Fundus photographs (2) of the unexposed eye are taken; one is used to mark and number exposure locations, the other is kept for future comparison with fundus photographs taken after exposure.

Preselected exposure times are made by means of an electronic timer controlling an air operated shutter. For any preselected exposure time the experimental procedure was as follows: beginning with the appearance, immediately after exposure, of a mild burn lesion, the irradiance was reduced progressively in finite steps (5-10 percent) until no lesion became visible during the first five minutes following exposure. A minimum of at least two further exposures were made at irradiance levels of 5 to 10 percent below previous levels. For a preselected exposure time, the number of actual exposures ranged from five to seven. The total number of exposures per monkey eye ranged between 25 and 30. All exposures were located within two disk diameters of the macula and were 158  $\mu$ m in diameter. A fundus photograph was then taken and the animal returned to his cage. Twenty-four hours later the monkey was anesthetized again and another fundus photograph taken. The burn lesion or lesions which appeared only 24 hours after exposure and were the smallest in diameter were used to define a minimal lesion

or so-called burn threshold. Each exposure entering the eye was monitored by means of a beam splitter reflecting into a photodiode which had been calibrated previously against a cone radiometer placed at the location of the exposed eye. Each reading of the photodiode was recorded on a strip chart recorder. The cone radiometer was calibrated in terms of a Bureau of Standards standard of irradiance. Calibrations of the photodiode were made before and after each animal experiment. The CW irradiance of the source varied by less than two percent over an 8 hour interval as determined by a calibrated Eppley cell.

The procedures outlined above were used to obtain threshold data on 5 monkeys (10 eyes) at preselected exposure times of 1, 10, 30, 60 and 180 seconds. A threshold for each exposure time was measured in each eye, requiring 5-6 exposures per threshold determination for a total of 25-30 exposures per eye. The results are tabulated in Table 3 where the power entering the eye and the retinal irradiance needed to produce a threshold lesion are given for each exposure time.

TABLE 3

Power in mW entering eye or corresponding retinal irradiance in  $\text{W-cm}^{-2}$  required to produce threshold burn lesion for exposure times of 1, 10, 30, 60 and 180 seconds. Image diameter,  $158 \mu\text{m}$ ; spectrum, simulated solar source shown in Figure 3; integrated transmittance through monkey ocular media, 0.77. Each data point represents the mean and standard deviation for 10 threshold determinations in 10 monkey eyes.

| Exposure Time<br>s | Power Entering Eye<br>mW | Retinal Irradiance<br>$\text{W-cm}^{-2}$ |
|--------------------|--------------------------|--|
| 1                  | $33.2 \pm 3.7$           | $131 \pm 14.5$                           |
| 10                 | $21.4 \pm 2.2$           | $84.1 \pm 8.60$                          |
| 30                 | $14.6 \pm 3.1$           | $57.4 \pm 12.2$                          |
| 60                 | $8.4 \pm 1.7$            | $33.0 \pm 6.70$                          |
| 180                | $4.8 \pm 0.8$            | $18.9 \pm 3.15$                          |

The relationship between the burn thresholds in Table 3 and pupillary diameter while viewing the sun unattenuated and at zenith is shown in Figure 5 where retinal irradiance in  $\text{W-cm}^{-2}$  vs pupillary diameter in mm is plotted from the data given in Table 1. The straight lines drawn parallel to the abscissa represent irradiances required to produce a threshold lesion in the monkey retina within a specified exposure time as taken from Table 3. For example, a 1 second exposure of the retina

to  $131 \pm 14.5 \text{ W-cm}^{-2}$  intersects the curve at a point corresponding to 6.3 mm pupillary diameter. Exposure of the human eye to the full power of the sun at zenith for 1 second with this pupillary diameter would produce a burn if the monkey eye is taken as a valid model for the human eye. Of course, photophobia and the blink reflex would normally prevent overexposure of the human eye to the sun. It must be emphasized, however, that there are numerous reports in the literature of solar retinitis and eclipse blindness. Some of the most recent are the papers by Geeraets (6) and Hatfield (7) on the solar eclipse of March 7, 1970, in which 145 cases of solar retinitis were reported.

### THE OPEN (UNCROSSED) VLT WINDOW

The spectral distributions of the unattenuated solar spectrum after transmission through the VLT window and through the human ocular media are illustrated in Figure 6. Relative irradiance in arbitrary units is plotted against wavelength in nanometers. A transmission band in the visible (430-800 nm) and two transmission bands in the infrared (950-1180 and 1180-1350 nm) penetrate the uncrossed VLT window. The dip at approximately 1180 nm is caused by the acrylic windows. In the uncrossed position, 11.4 percent of the solar power within the spectral range 400-1400 nm is transmitted; 60.5 percent of this power penetrates the ocular media to irradiate the retina. The ocular media practically eliminates the infrared bandwidth between 1180-1350 nm. For a pupillary diameter of 8 mm the irradiance on the human retina is  $18.0 \text{ W-cm}^{-2}$ . This is almost the irradiance required to produce a threshold burn in 3 minutes according to the data given in Table 3. However, the spectral distributions on the retina from the two sources are quite different. It was not possible to produce a burn lesion for image diameters of  $158 \mu\text{m}$  using this source after passage through the open VLT window for exposure times up to three minutes, even though the simulated solar spectrum was capable of producing greater power densities on the retina than the sun for pupillary diameters up to 8 mm.

Fortunately, the spectral distribution produced by the xenon lamp after transmission through the open VLT window proved to be remarkably similar to that of the sun after similar filtration. The same transmission band in the visible and the same two bands in the infrared are present but at a power density sufficient to produce retinal lesions for exposure times of one minute or more. Burn threshold data for exposure times of one minute and three minutes, representing the mean for 7 monkey eyes are  $31.5 \pm 10.7$  and  $24.4 \pm 6.4 \text{ W-cm}^{-2}$  respectively.

A comparison of the open VLT window with the commercial aircraft window is shown in Figure 7 where retinal irradiance in  $\text{W-cm}^{-2}$  when viewing the unattenuated sun at zenith through these windows is

plotted against pupillary diameter in mm. The threshold burn data of Table 3 are shown as lines horizontal to the abscissa for the appropriate retinal irradiances and exposure times. Where these lines intersect the commercial aircraft window a line has been drawn parallel to the ordinate to indicate the pupillary diameter required to produce a burn within a given exposure time. For example, a threshold burn would be produced by a one minute exposure to the sun at a pupil diameter of 4.3 mm and by a three minute exposure with a pupil diameter of 3.2 mm. The open VLT window provides protection out to pupil diameters of 8 mm where the standard deviation for a threshold burn in three minutes just overlaps the retinal irradiance of  $18.0 \text{ W-cm}^{-2}$ . The open VLT window provides approximately 7 times more protection than the commercial aircraft window now in use. The fact that passengers in high flying aircraft do not sustain retinal injury is a tribute to nature's protective devices, photophobia and the blink reflex. Also, of course, worst situation conditions have been assumed throughout this discussion (sun at zenith with no atmospheric attenuation, normal incidence to the window and relatively large pupil diameters).

#### THE CLOSED (CROSSED) VLT WINDOW

The most important aspect of this investigation was to assess the hazard of gazing at the sun without atmospheric attenuation through the VLT window in the crossed or closed position. Since all transmitted light with the exception of about 0.5 percent in the blue region of the spectrum is in the invisible infrared, the naturally protective and avoidance reactions including photophobia and the blink reflex would be absent, and one might gaze at the sun (perhaps hypnotically) with a false sense of security, not realizing that photocoagulation was materializing on the retina.

The spectral distributions of the sun on the cornea and on the retina of man after transmission through the closed or crossed VLT window are shown in Figure 8. Transmission begins at about 850 nm (the very small component of blue light does not show on the scale of this graph), reaches a peak at 1080 nm and then falls to a low value at 1180 nm because of the acrylic windows. There is a broad band of transmission between 1180 and 1350 nm but this is almost obliterated by the ocular media. Only 5.9 percent of the solar power penetrates the closed VLT window, and only 37 percent of this gets through the human ocular media. In consequence, irradiance on the retina is  $5.71 \text{ W-cm}^{-2}$  when viewing the sun at the top of the atmosphere with a pupil diameter of 8 mm.

Under these circumstances it became apparent that no available laboratory source using an image diameter of  $158 \mu\text{m}$  could produce a burn

lesion after transmission through the closed VLT window. The Osram xenon lamp produced more than three times the irradiance of the sun on the retina after transmission through the closed VLT window, but repeated attempts to produce a lesion on the monkey retina were unsuccessful. By increasing the image diameter from 158  $\mu\text{m}$  to 1000  $\mu\text{m}$ , it was possible to produce a threshold lesion in two monkey eyes out of ten using a three minute exposure. The irradiance on the retina was 18.9  $\text{W}\cdot\text{cm}^{-2}$ .

It was of paramount importance to determine the burn threshold for optical radiation after transmission through the closed VLT window so that a factor of safety could be estimated. Accordingly, the Osram xenon source was transmitted through a Jena glass RG-715 (RG-10) filter producing a broad band transmission in the infrared which is shown for radiation incident on the cornea and on the retina in Figure 9. The advantage of such a source is that approximately 200  $\text{W}\cdot\text{cm}^{-2}$  can be focussed on a retinal image diameter of 158  $\mu\text{m}$ , thus making it possible to determine threshold lesions for exposure times ranging from 10 seconds to three minutes. The spectral distribution on the retina is from 700-1200 nm as contrasted with 950-1150 nm for the sun after transmission through the closed VLT window and the ocular media. If anything, this discrepancy between the two infrared spectra is in the right direction insofar as ocular safety is concerned, since the shorter wavelengths are more efficient in producing thermal injury to the retina, primarily because the reflectance of the fundus increases with wavelength (Ref. 2).

Threshold burn data as determined with this source after transmission through the closed VLT window are given in Table 4 for seven monkey eyes. Each threshold represents the mean and standard deviation for seven monkey eyes.

TABLE 4

Power in mW at cornea or corresponding retinal irradiance in  $\text{W}\cdot\text{cm}^{-2}$  to produce threshold burn for exposure times ranging from 10 to 180 seconds. Image diameter on retina, 158  $\mu\text{m}$ ; spectral distribution on retina 700-1200 nm (see figure 9); each threshold and standard deviation represents mean for 7 monkey eyes; integrated transmittance through monkey ocular media, 0.707.

| Exposure time<br>seconds | Power entering cornea<br>mW | Retinal irradiance<br>$\text{W}\cdot\text{cm}^{-2}$ |
|--------------------------|-----------------------------|---|
| 10                       | 43.3 $\pm$ 5.8              | 156 $\pm$ 20.9                                      |
| 30                       | 37.0 $\pm$ 7.0              | 133 $\pm$ 25.2                                      |
| 60                       | 32.0 $\pm$ 7.7              | 115 $\pm$ 27.8                                      |
| 180                      | 27.0 $\pm$ 4.2              | 97.4 $\pm$ 15.1                                     |

In addition to the data tabulated in Table 4, which are restricted to image diameters of 158  $\mu\text{m}$ , thresholds at other image diameters have been investigated to provide empirical data on the effect of image size on burn threshold when other parameters are held constant. Thus, a three minute exposure on an image diameter of 158  $\mu\text{m}$  required 97.4  $\text{W}\cdot\text{cm}^{-2}$  to produce a threshold lesion; for the same exposure time and source it required only 23.4  $\text{W}\cdot\text{cm}^{-2}$  to produce a threshold lesion when the image diameter was 1000  $\mu\text{m}$ . The ratio 97.4/23.4 is 4.16 indicating that four times as much power density is required to produce a lesion when the smaller diameter is used.

According to Table 4, 97.4  $\text{W}\cdot\text{cm}^{-2}$  on the retina for three minutes will produce a threshold burn in the rhesus monkey. At the top of the atmosphere the sun at zenith produces an irradiance of 5.71  $\text{W}\cdot\text{cm}^{-2}$  on the human retina through the closed VLT window when the pupillary diameter is 8 mm. The ratio, 97.4/5.71 is 17, indicating that seventeen times the power density transmitted by the closed VLT window is needed to produce thermal injury to the retina.

If the burn thresholds tabulated in Table 3 are compared to those in Table 4 for comparable exposure times, the ratio of thresholds ranges from a factor of five for a three minute exposure to a factor of two for a ten second exposure. Since the only distinguishing feature between the two sets of data is the spectral distribution on the retina, it is concluded that a primarily white light spectrum produces thermal damage to the mammalian retina at much lower power densities than infrared radiation. This is in keeping with unpublished laser data from this laboratory which indicates that ruby radiation (694.3 nm) in the Q-switched mode is 7.5 times more effective in producing retinal damage in the rabbit than Nd - Glass (1060 nm); for the multiple spike, normal mode the ratio is 4.25.

## CONCLUSIONS

1. The VLT window in the open position is approximately seven times safer than the commercial aircraft window insofar as thermal injury to the retina from gazing at the sun under worst case conditions is concerned.
2. The VLT window in the closed position allows only one seventeenth of the irradiance needed on the mammalian retina to produce a thermal lesion. This is under worst case conditions, namely sun at zenith, no atmospheric attenuation, normal incidence to window, 8 mm pupil diameter, and a three minute exposure.
3. A primarily white light spectrum on the mammalian retina produces thermal injury at much lower power densities than a near infrared spectrum.

## REFERENCES

1. M. P. Thekaekara. Evaluating the light from the sun. *Optical Spectra*, 32-35 (March 1972).  
P. R. Gast. Solar Electromagnetic Radiation. Section 16.1. *Handbook of Geophysics and Space Environments*, Air Force Cambridge Research Laboratories, McGraw-Hill (1965).
2. W. J. Geeraets and E. R. Berry. Ocular spectral characteristics as related to hazards from lasers and other light sources. *Am. J. Ophthalm.* 66, 15-20 (July 1968).
3. W. T. Ham, Jr. et al. Low level radiation exposures to the monkey eye. A Report to the Xerox Corp. Dept. Biophysics, Health Sciences Division, Virginia Commonwealth University, Richmond, Va. (1970).
4. T. Kuwabara. Electron microscopic study of low level radiation exposures to the monkey eye. A Report to the Xerox Corp. Howe Laboratory of Ophthalmology, Harvard University Medical School, Boston, Mass. (July 1971).
5. T. Kuwabara. Structure of the Retina. Howe Laboratory of Ophthalmology, Harvard University Medical School, Boston, Mass. (1970).
6. W. J. Geeraets et al. Solar retinopathy following the eclipse of March 7, 1970. *Med. College Va. Quart.* 6, 3-7 (1970).
7. E. M. Hatfield. Eye injuries and the solar eclipse. *Sight-Saving Review*, 40, 79-86 (1970).

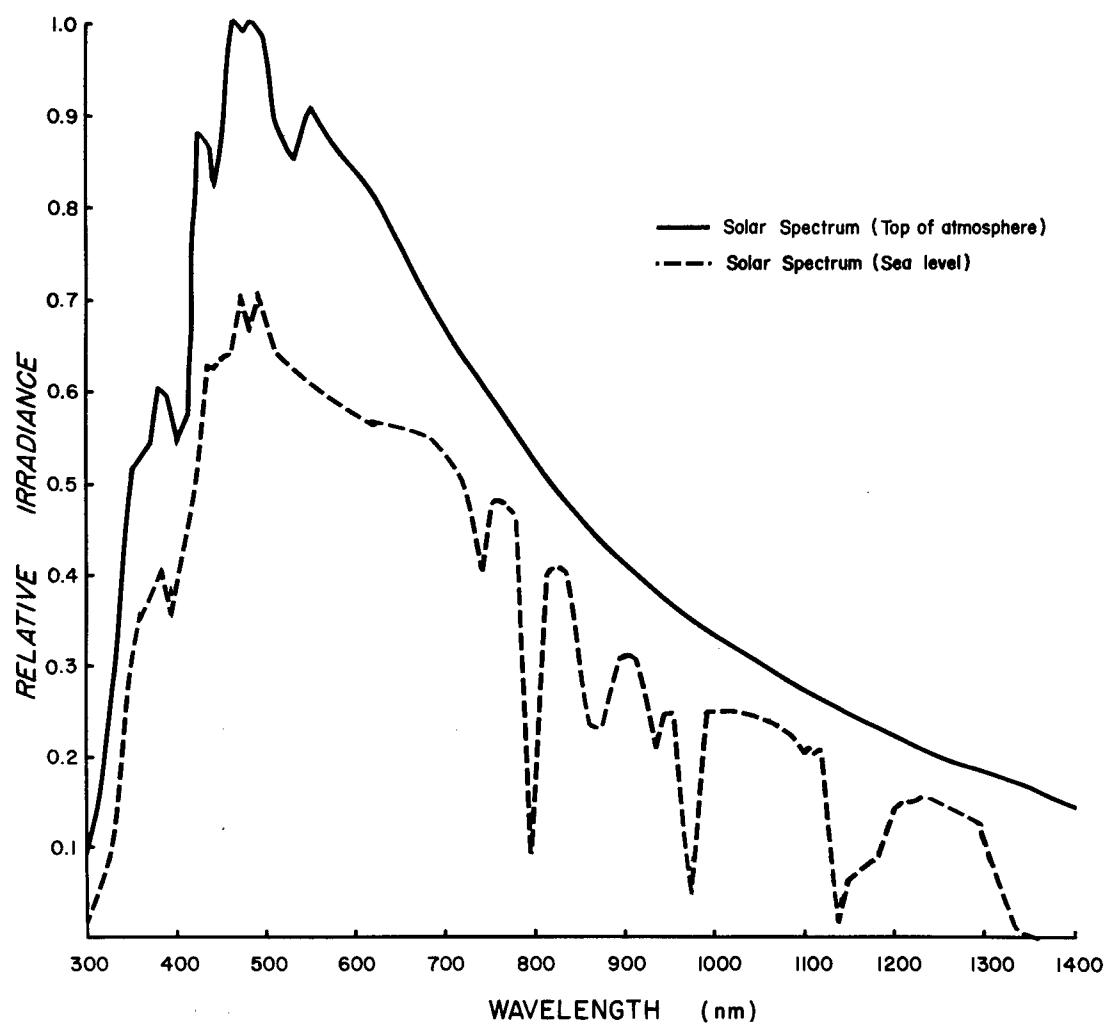


FIGURE 1

The spectral distribution of the solar spectrum at the top of the atmosphere and at sea level. Relative irradiance is plotted on the ordinate vs wavelength in nanometers (nm) on the abscissa.



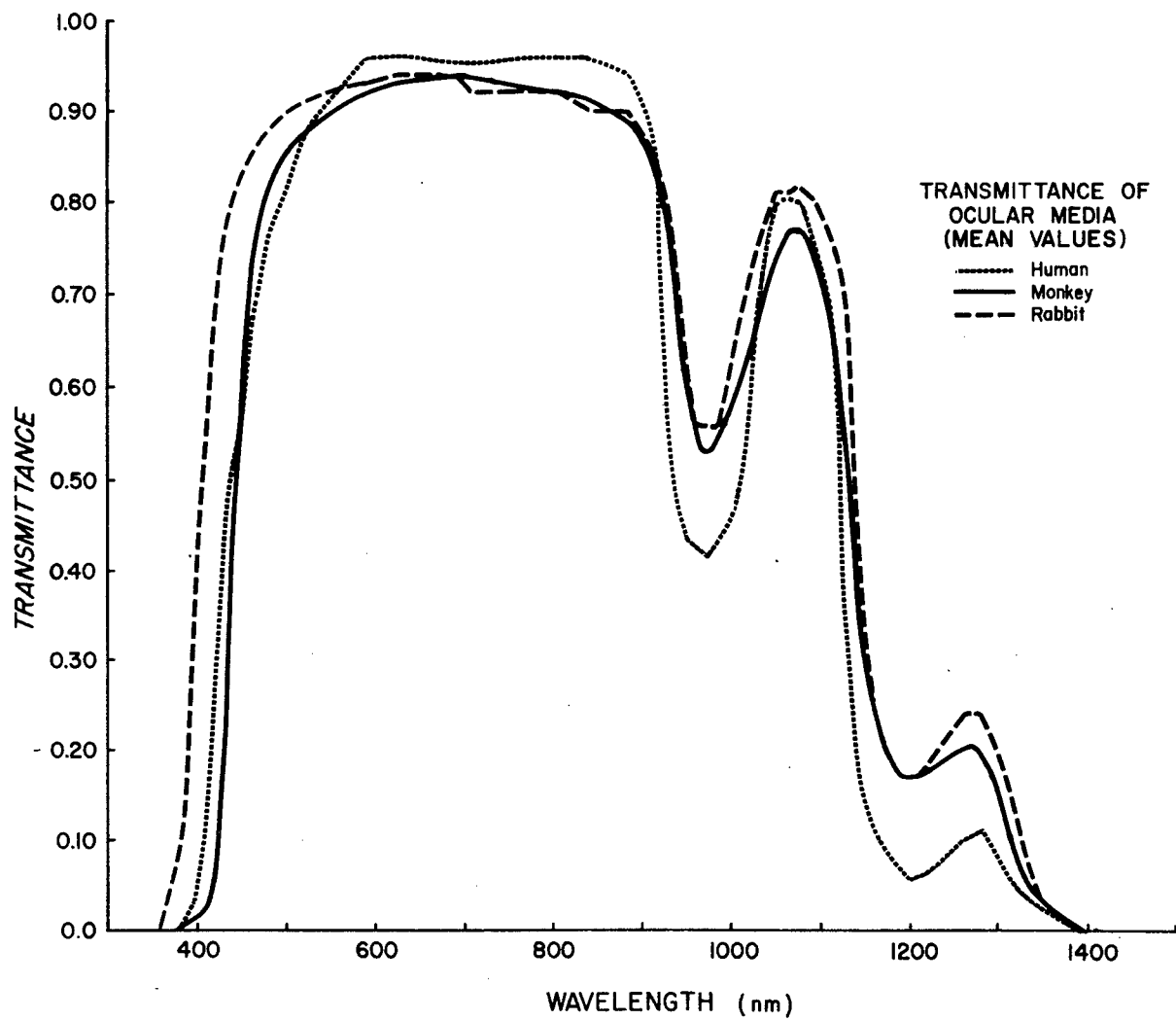


FIGURE 2

A comparison of transmittance through the ocular media of man, monkey and rabbit. Transmittance is plotted on the ordinate vs wavelength in nanometers (nm) on the abscissa.

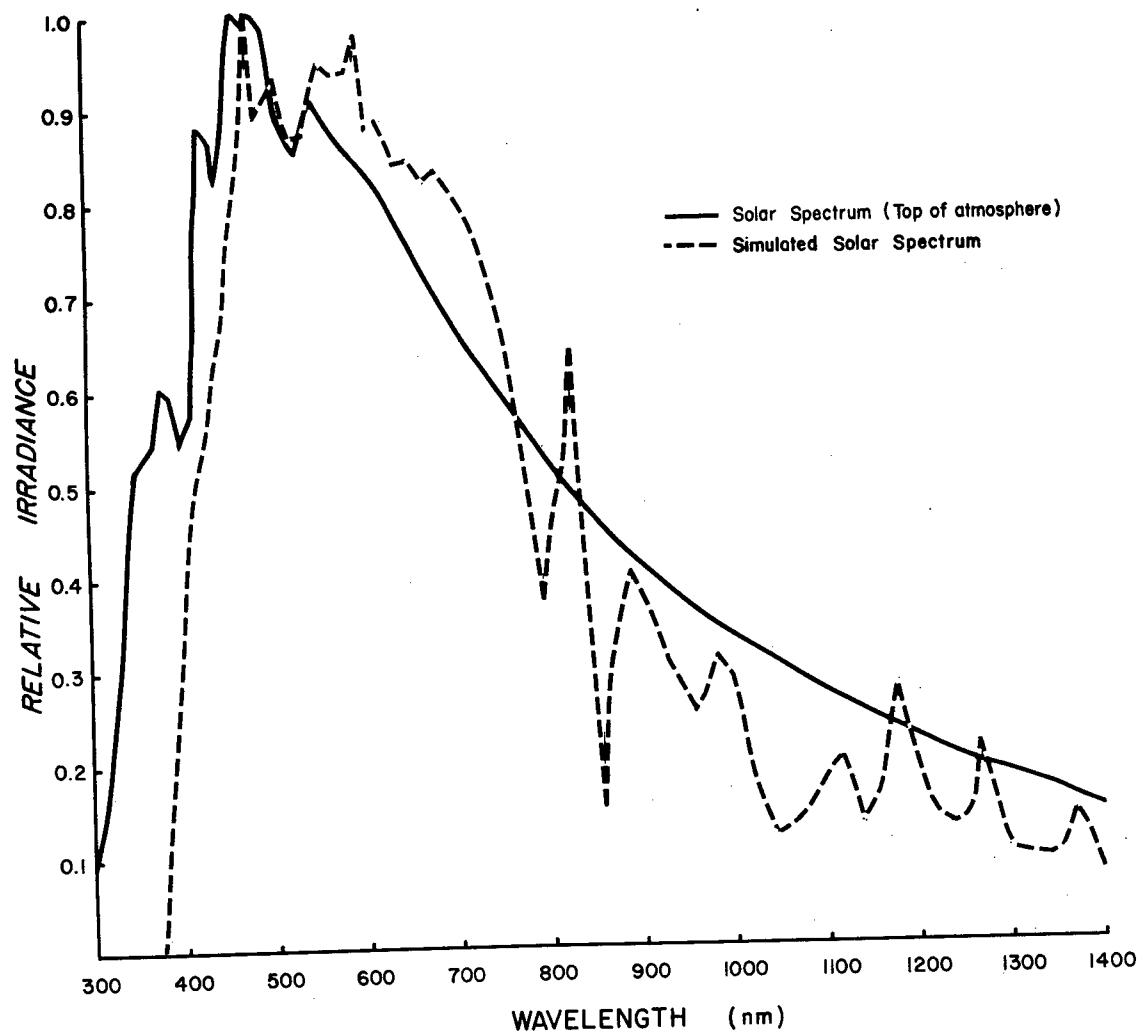
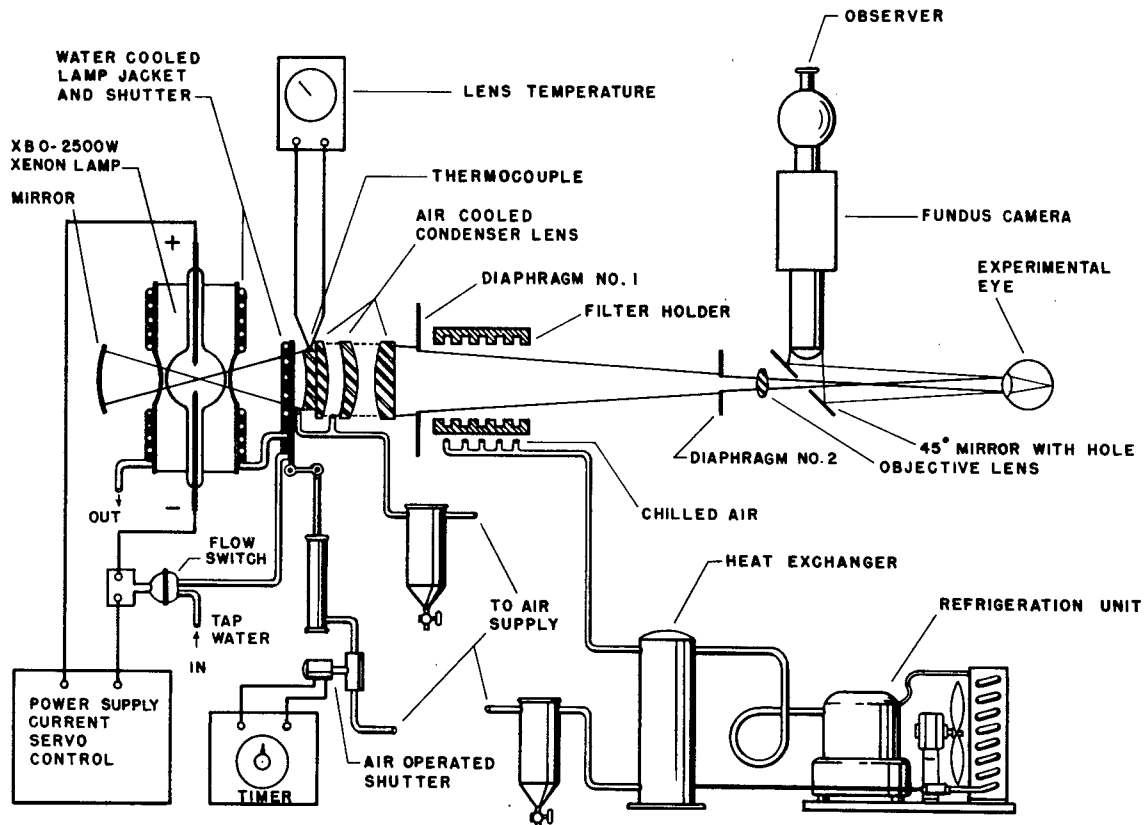


FIGURE 3

Comparison of the simulated solar spectrum with the natural solar spectrum at the top of the atmosphere. Relative irradiance is plotted on the ordinate vs wavelength in nanometers (nm) on the abscissa.

**SCHEMATIC DIAGRAM OF XENON LAMP AND OPTICAL SYSTEM  
USED TO PRODUCE EXPERIMENTAL BURNS IN THE MAMMALIAN RETINA**



**FIGURE 4**

Schematic diagram of the xenon lamp and associated optical system used to produce experimental burns in the mammalian retina.

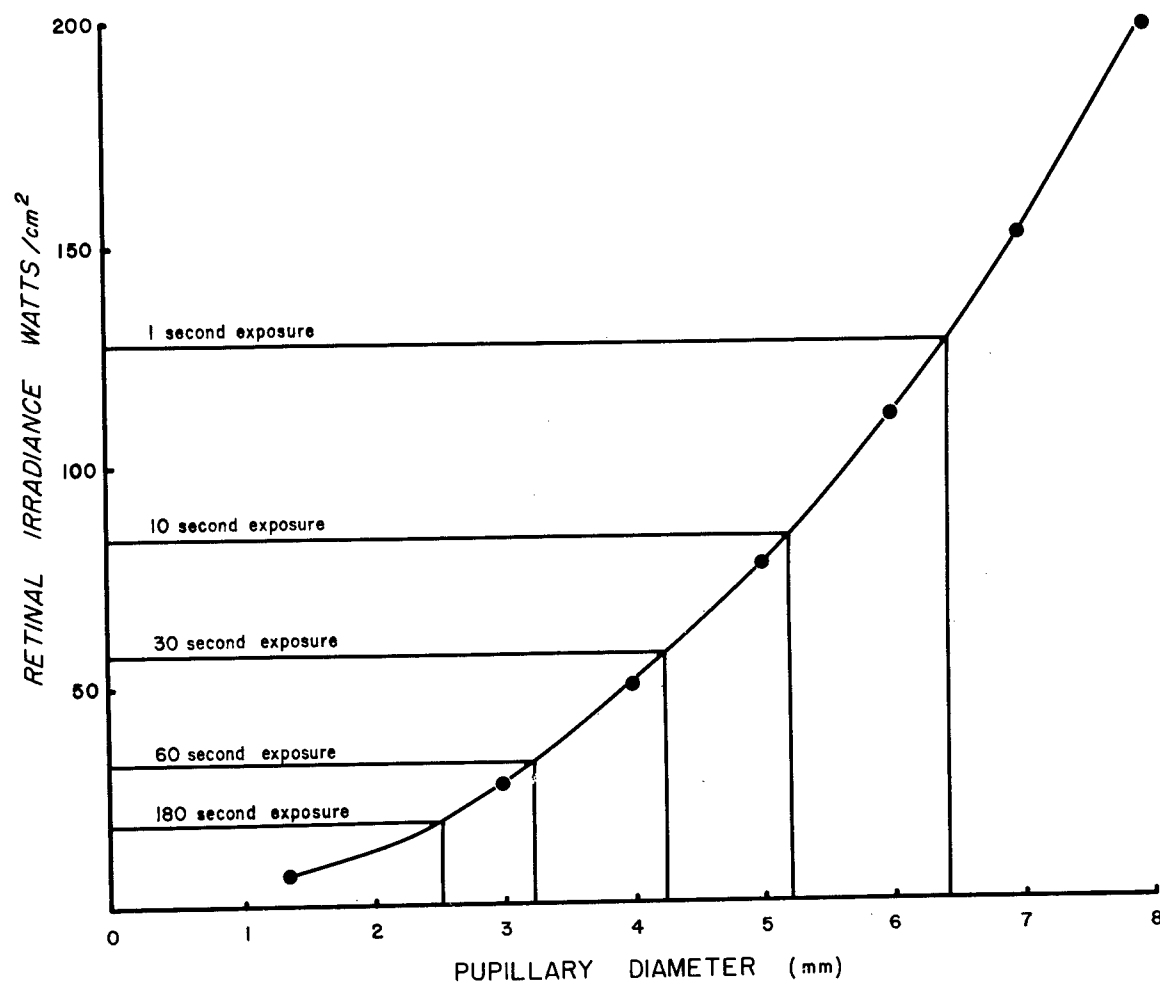


FIGURE 5

Retinal irradiance in  $\text{W-cm}^{-2}$  vs pupillary diameter in mm is plotted for exposure to the sun at the top of the atmosphere (taken from Table 1). The irradiance required to produce a minimal lesion for various exposure times is shown by the lines parallel to the x-axis as taken from Table 3. The intersection of these lines with the curve provides an estimate of the pupillary diameter needed to produce a threshold lesion for a given exposure time.

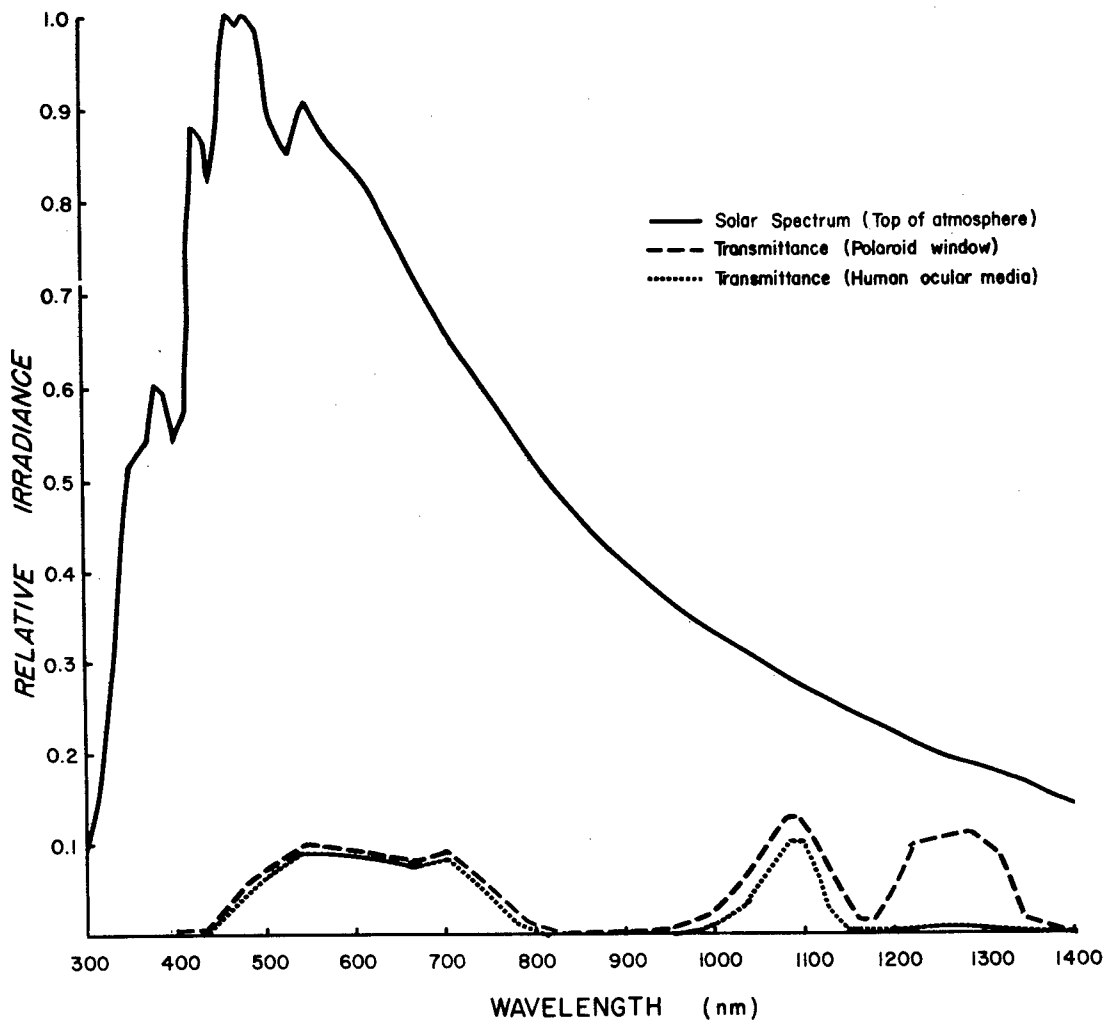


FIGURE 6

The spectral distribution of the sun at the top of the atmosphere and its spectral distributions after transmission through the open VLT window and after transmission through the ocular media of the human eye are shown. Relative irradiance is plotted along the ordinate vs wavelength in nanometers (nm) along the abscissa.

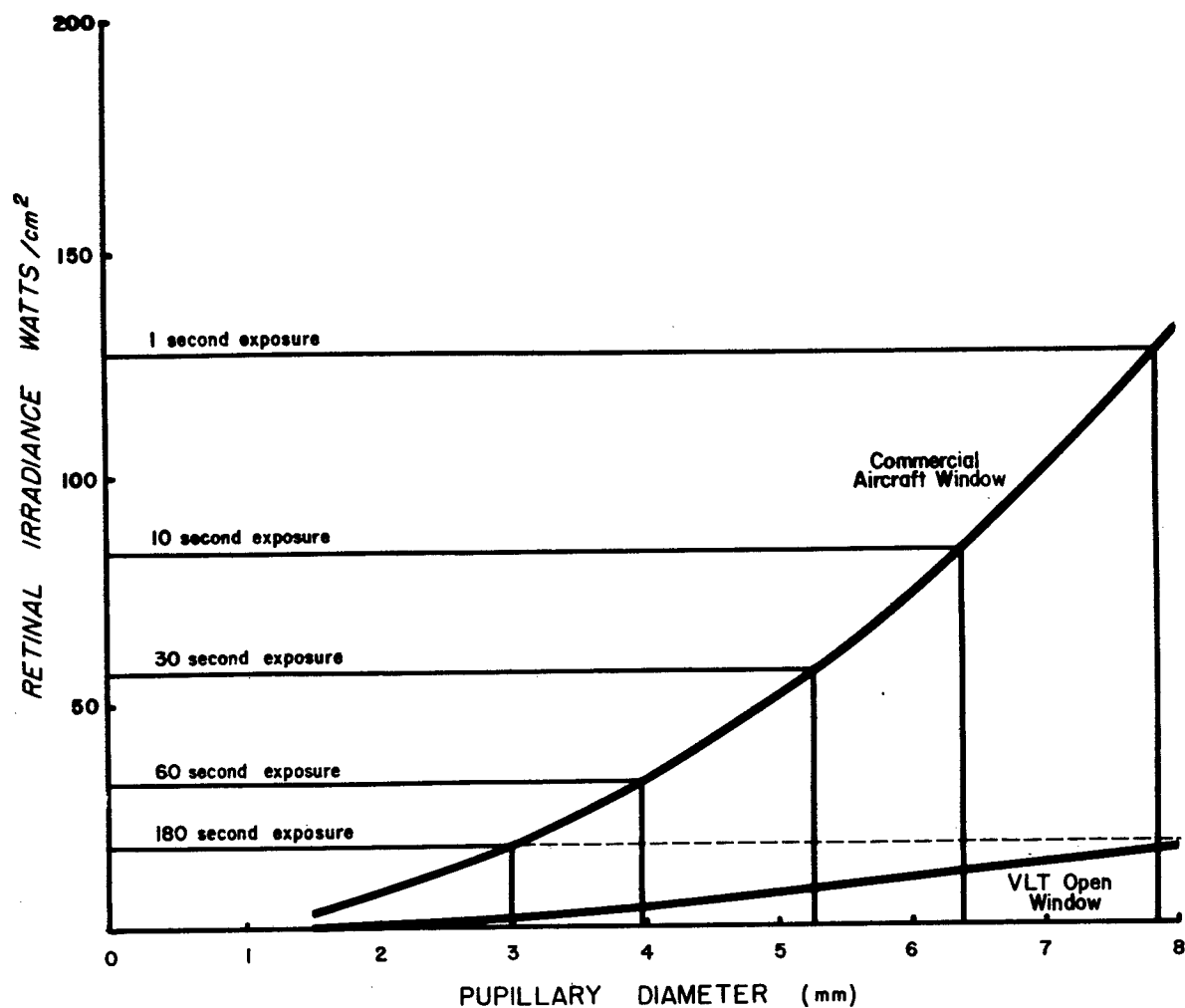


FIGURE 7

Retinal irradiance in  $\text{W-cm}^{-2}$  vs pupil diameter in mm when viewing the unattenuated sun at zenith through the open VLT window and through a commercial aircraft window. The threshold burn data taken from Table 3 are shown as lines horizontal to the abscissa for the appropriate retinal irradiances and exposure times.

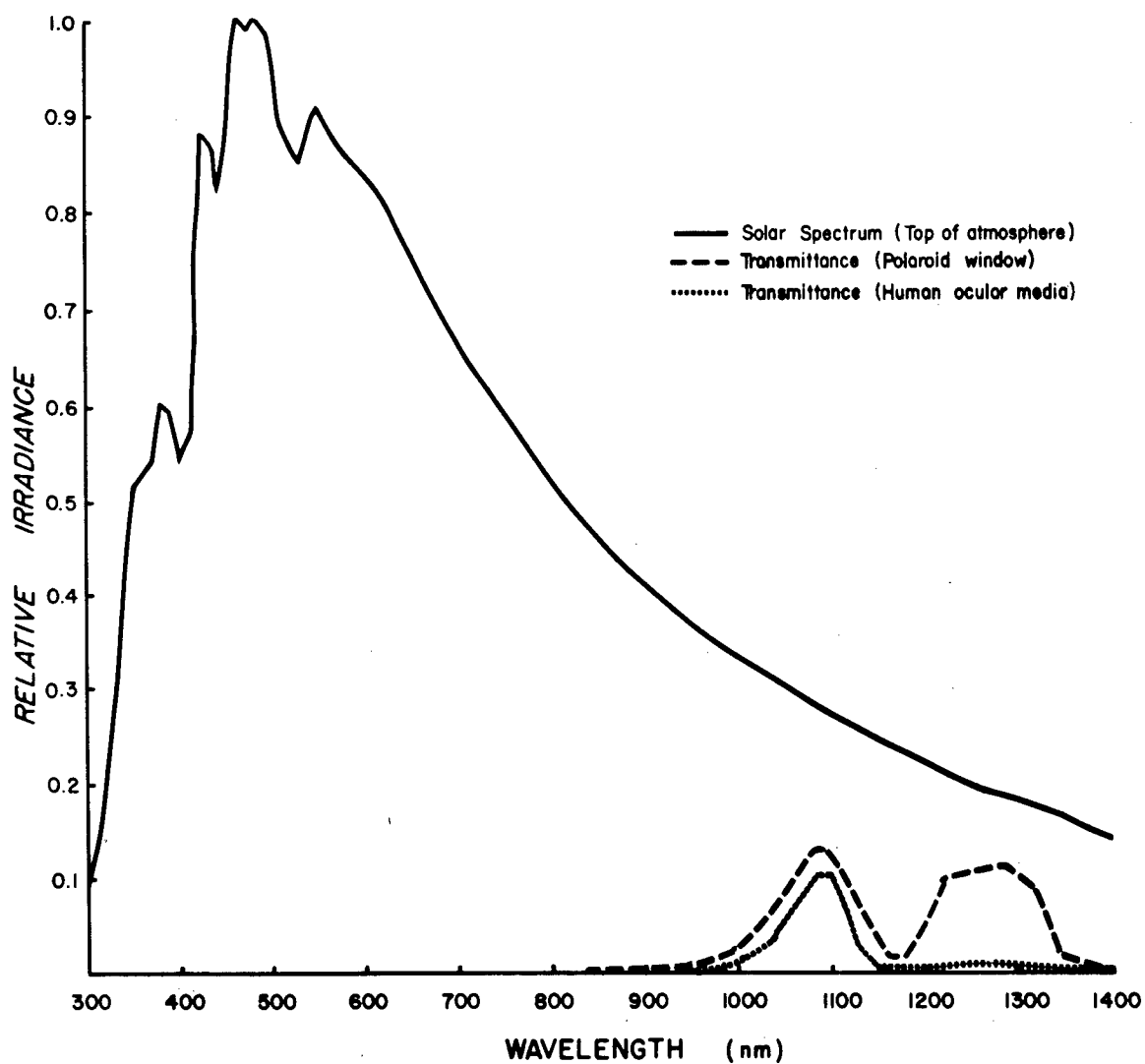


FIGURE 8

The spectral distributions of the unattenuated sun at zenith after transmission through the closed VLT window and after transmission through the human ocular media are shown. Relative irradiance is plotted along the ordinate vs wavelength in nanometers (nm) along the abscissa.

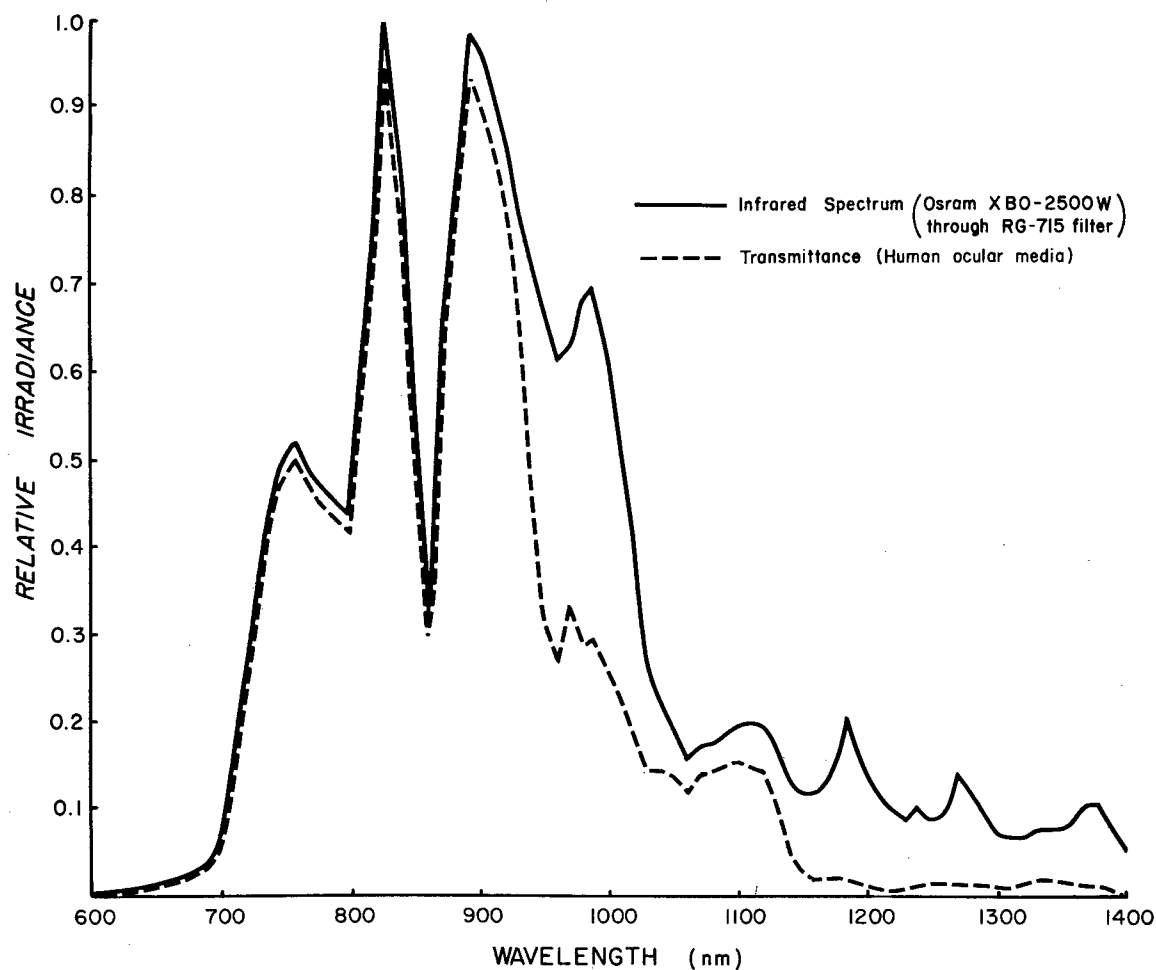


FIGURE 9

The infrared spectra of the Osram XBO-2500 W, xenon lamp after transmission through a Jena glass RG-715 (RG-10) filter and after transmission through the human ocular media are shown. Relative irradiance is plotted along the ordinate vs wavelength in nanometers (nm) along the abscissa.





## A COATING FOR HELICOPTER CANOPIES

George A. Lundgren  
Optical Coating Laboratory, Inc.  
Santa Rosa, California



## A COATING FOR HELICOPTER CANOPIES

George A. Lundgren

Optical Coating Laboratory, Inc.

January, 1973

### ABSTRACT

Sunlight reflected from helicopter canopies has been found to be a major cause of early visual acquisition of the aircraft.

Helicopter transparencies are currently manufactured from stretched methyl methacrylate (acrylic) which, due to its index of refraction of 1.5, reflects approximately four percent per surface (i.e., eight percent total).

Thin film optical coatings which are commonly used to reduce reflectance have, in the past, exhibited inadequate adherence and/or abrasion resistance when applied to stretched acrylic. Applying any optical coating to very large or highly curved pieces is, in itself, difficult.

Optical coating Laboratory, Inc., provided a low reflecting thin film coating on canopies for eight Bell AH-1G and two OH-58 helicopters for the Army's Land Warfare Laboratory. The coating was applied to both inside and outside surfaces of extremely curved sections as well as to sections up to eight feet in length.

To accommodate the apparent shifts in wavelength which all optical coatings exhibit at varying angles of incidence, a coating was used which reduces reflectance over a range of wavelengths significantly wider than the visual spectrum.

The coating typically reduced average visual reflectance by a factor of three. The spectral distributions of coating reflectance, solar energy, and human eye sensitivity are considered, from which the corresponding minimum detection distance is calculated to be reduced by one-half.

Additional advantages include higher visual transmittance, reduced extraneous reflections inside the cockpit during night flight, and improved abrasion resistance.

## INTRODUCTION

Sunlight reflected from helicopter canopies has been found to be a major cause of early visual acquisition of the aircraft.

The visual reflectance of commonly used stretched acrylic canopies can be substantially reduced with a thin film optical coating, thereby reducing the range at which the aircraft can be detected. Additionally, the optical coating can significantly improve the poor abrasion resistance of acrylic.

Obtaining satisfactory adherence is typically a problem when applying optical coatings to plastics. The problem is aggravated when large, highly curved parts are coated.

All optical coatings perform better in some portions of the wavelength spectrum than in others. They also have better spectral performance at some angles of incidence than at others. In any design it is necessary to use a compromise which is best for the specific use of the coating.

This paper discusses the results of such a coating applied both to the inside and outside surfaces of helicopter canopies for the Army's Land Warfare Laboratory by Optical Coating Laboratory, Incorporated.

## THEORETICAL CONSIDERATIONS

The reflectance of uncoated acrylic (methyl methacrylate) is approximately eight percent due to its refractive index of 1.5.<sup>1</sup> Since the prime purpose of the coating is to reduce visual reflected sunlight, it is necessary to look at the spectral distribution of the energy under question.

The spectral distribution of the visible portion of the sun's energy is shown in Figure 1.<sup>2</sup>

The wavelength sensitivity or spectral response of an average human eye under daylight conditions is shown in Figure 2. It is seen that the eye is most sensitive at wavelengths near .55 microns and is unable to detect energy at wavelengths below .4 microns or above .7 microns.

---

<sup>1</sup>approximately four percent per surface

<sup>2</sup>for air mass one

## THEORETICAL CONSIDERATIONS - Continued

The product of solar flux and eye response shown in Figure 3 is the combined response which is considered in the selection of an anti-reflecting coating.<sup>1</sup>

The characteristics of a simple anti-reflecting coating are such that a minimum reflectance exists at some center wavelength, with reflectance increasing at both longer and shorter wavelengths. The theoretical reflectance of such a coating is shown in Figure 4.

The coating may be designed to make the minimum reflectance occur at any desired wavelength, but the shape of the reflectance curve will remain similar to that of Figure 4. In other words, the curve may be shifted up or down in wavelength for a particular application.

Thus far we have considered the reflectance of the coating on acrylic when observed at an angle normal to the surface. When reflectances are observed at increased angles, the effect is such that the minimum reflectance will occur at decreased wavelengths. That is, the effect of increasing the angle of incidence is to shift the reflectance curve to a lower wavelength. Figure 5 shows the shift to shorter wavelengths for an angle of incidence of 45°.

Since the purpose of the coating is primarily to reflect the least visible solar energy, the coating should be designed so the reflectance minimum will occur at the same wavelength as the maximum in Figure 3. This, of course, should occur for the most predominant angle of incidence in a specific application.

The reflected solar energy which is detectable in such an application is shown in Figure 6.<sup>2</sup> It is simply a wavelength distribution of the product of solar flux, human eye response, and coating reflectance.

By integrating the area under the curve, the total detectable energy is found to be approximately one-fourth of that for uncoated acrylic. Since electromagnetic energy decreases as the inverse of the square of its distance from the source, the corresponding reduction in distance from the observer can be calculated as follows:

Assume detection distances are sufficient to create point

---

<sup>1</sup>in arbitrary units

<sup>2</sup>in the same arbitrary units as Figure 3

## THEORETICAL CONSIDERATIONS - Continued

sources, and let X and Y equal the maximum respective distances at which an observer can just detect aircraft with uncoated and coated canopies, as seen in Figure 7.

Let E = the energy reflected at the uncoated canopy.

Then E/4 = the energy reflected at the coated canopy.

So  $E/X^2$  = observed energy from uncoated canopy.

And  $E/4Y^2$  = observed energy from coated canopy.

Setting the observed energies equal:

$$\begin{aligned} E/X^2 &= E/4Y^2 \\ \text{or } Y &= X/2 \end{aligned}$$

In other words, compared to a helicopter with an uncoated canopy, a helicopter with a coated canopy should be able to get twice as close to an observer before being detected because of canopy glare.

## PRATICAL CONSIDERATIONS

The first helicopter transparencies coated were for the AH-1G Cobra Helicopter shown in Figure 8.

The overhead panels are some eight feet long; this necessitated modifying a coating machine to accommodate their large size.

The front and rear side panels, though smaller than the overhead section, have considerable curvature which increased the difficulty of obtaining uniformly thick coatings.

In order to design the coating it was first necessary to determine one angle of incidence which would best resemble the viewing angle of the canopy under most situations. Additionally, the optimum angle for minimizing extraneous reflectances inside the cockpit was also considered.

Since a detailed analysis of all parameters (including statistical probabilities) would have been a monumental task, the overall problem was approached subjectively using a small plastic model, and an angle of 45° was chosen. This solution is at best a broad compromise when the actual canopy geometry and all positions of the sun, aircraft, and observer are considered.

## PRACTICAL CONSIDERATIONS - Continued

However, picking a single angle of incidence to represent all reflectances is not as critical as it may appear, since the range of wavelengths over which the coating anti-reflects is significantly wider than the visible spectrum. This, in fact, is the reason a simple anti-reflecting coating was chosen. Other more sophisticated coatings offer lower reflectance, but are not useful over as wide a range of angles of incidence.

It should be reiterated that the purpose of picking an angle of incidence for the coating design is simply to produce a coating which will, when tilted to that angle, exhibit minimum reflectance over the range of wavelengths where visible solar energy is maximum.

Canopies were also coated for OH-58 helicopters, the configuration of which is shown in Figure 9. Because the panels are generally more vertically oriented than those of the AH-1G, a nominal design angle of incidence of 30 degrees was chosen.

## RESULTS

### Spectral

Measurements of reflectance as a function of wavelength are commonly measured on a spectrophotometer. The size of the helicopter panels precluded direct measurement, so all measurements were made from representative witness samples coated adjacent to each part.

In order to avoid errors due to polarization effects, measurements were made at normal incidence rather than at angle. For this reason, a maximum average single surface reflectance of two percent was specified for the AH-1G canopies over the wavelength range of .5 to .8 $\mu$ . This was chosen to be representative of the performance to be expected from .4 to .7 $\mu$  at an angle of incidence of 45°.

The specification for the OH-58 canopies was similarly chosen for the wavelength range from .45 to .75 $\mu$  in order to be representative of performance at a 30° angle of incidence.

Typically, single surface reflectance was less than 1.5% average, as shown in Figure 10. This compares to the four percent single surface reflectance of uncoated acrylic.



## RESULTS - Continued

It should be noted that an average reflectance does not best represent the solar reflectance that one would observe visually, due to the peaked shapes of the curves for coating reflectance, solar flux and eye sensitivity. As mentioned before, considering those curve shapes, actual detectable values would be lower than average values.

In addition to low reflection, low absorption is also desirable. For this reason, a transmittance measurement was made for each coating run in order to monitor absorptance.

Absorption is most predominant at shorter wavelengths as shown in Figure 11.<sup>1</sup> Increased transmittance, which is due to the lower reflectance of the coating, is partially offset at shorter wavelengths by absorption.

### Environmental

Witnesses from each coating run were subjected to the adherence test of MIL-M-13508B and the humidity and abrasion tests of MIL-C-675A.

The adherence test consists of pressing "scotch" tape tightly against the surface, slowly pulling it off, and visually inspecting for any coating removal.

Seventy-six percent of the AH-1G witnesses and 87% of the OH-58 witnesses showed no coating removal. The greater durability of the OH-58 witnesses was due to the experience gained from the AH-1G canopies, which were coated first. It should be noted that since the witnesses were of necessity placed at extreme positions and angles, they would be inherently less durable than the actual parts.

The humidity test involves storing a witness for 24 hours in a chamber having at least 95% relative humidity at 120°F, and then visually inspecting for coating stain, removal or similar deterioration.

No deterioration was observed on any witness in the humidity test.

The abrasion test is made by rubbing the coating 20 strokes with a .25" diameter rubber eraser, with a 2 to 2 1/2 pound normal force, and inspecting for any scratches or haze generated.

---

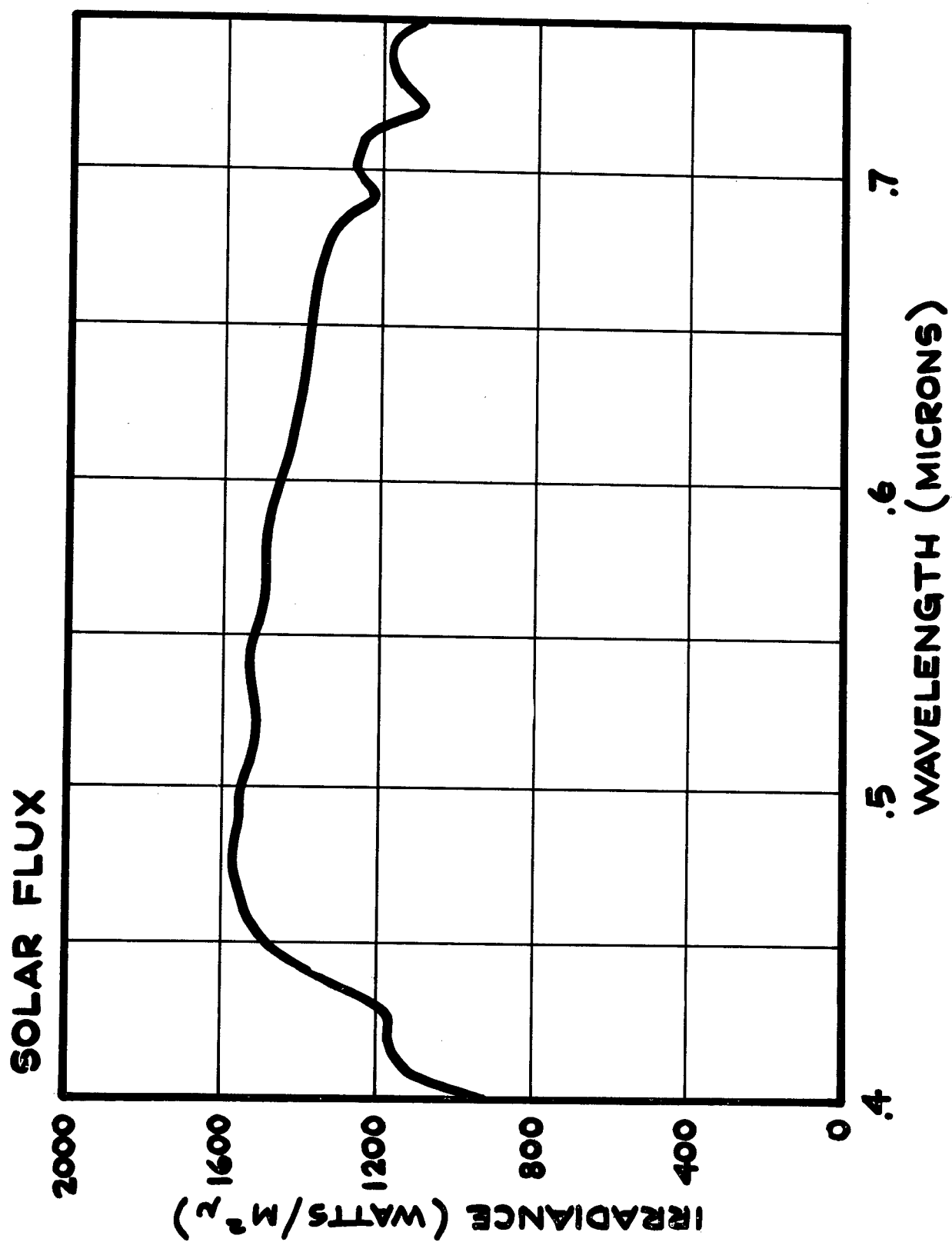
<sup>1</sup>both sides coated

## RESULTS - Continued

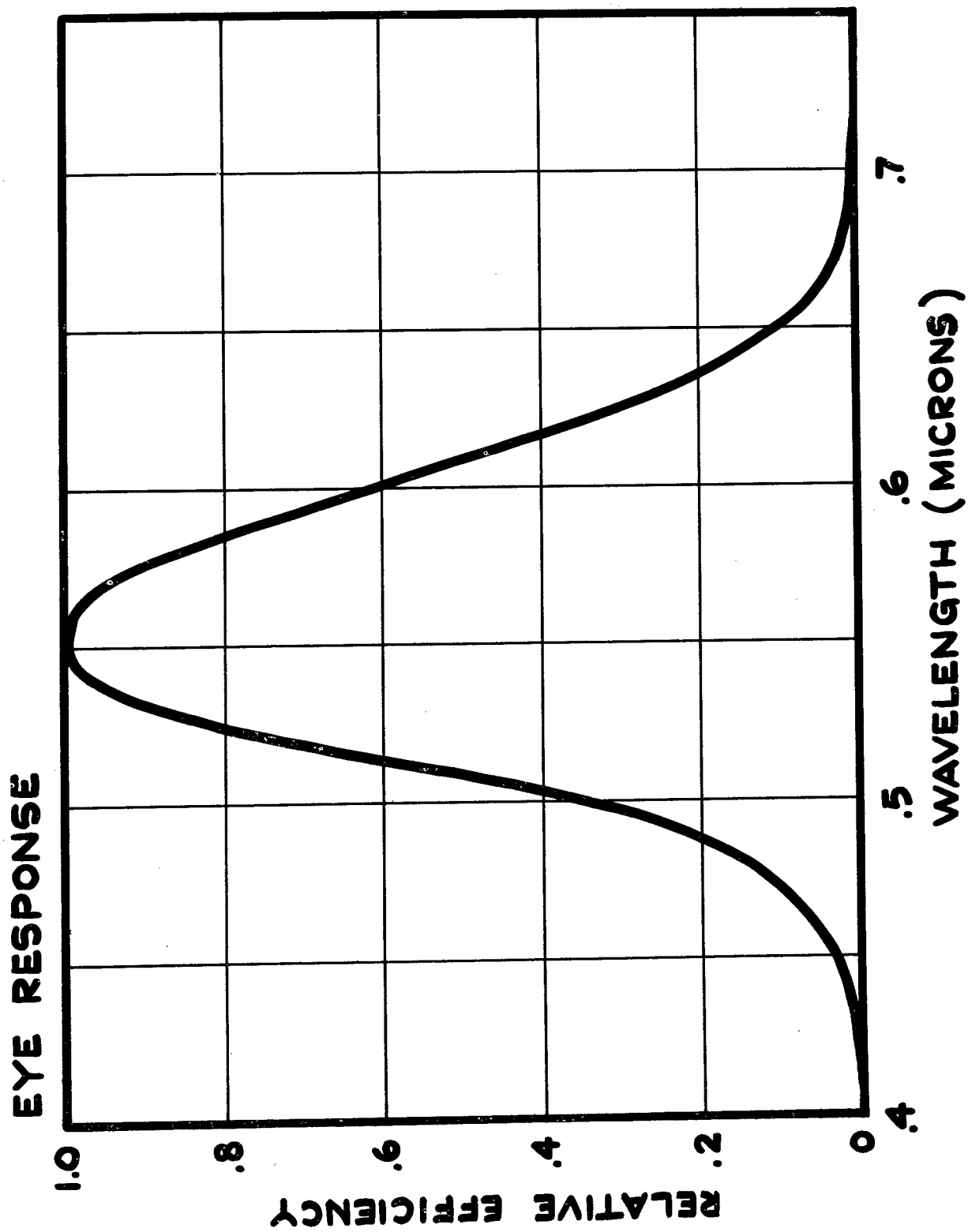
Fifty-five percent of the AH-1G witnesses and 71% of the OH-58 witnesses passed the 20 rub eraser tests. Again, because of the adverse placement of some of the witnesses, the actual canopies should have greater abrasion resistance than the witnesses. It should also be noted for comparison sake that uncoated acrylic is severely degraded from one eraser rub.

## SUMMARY AND CONCLUSIONS

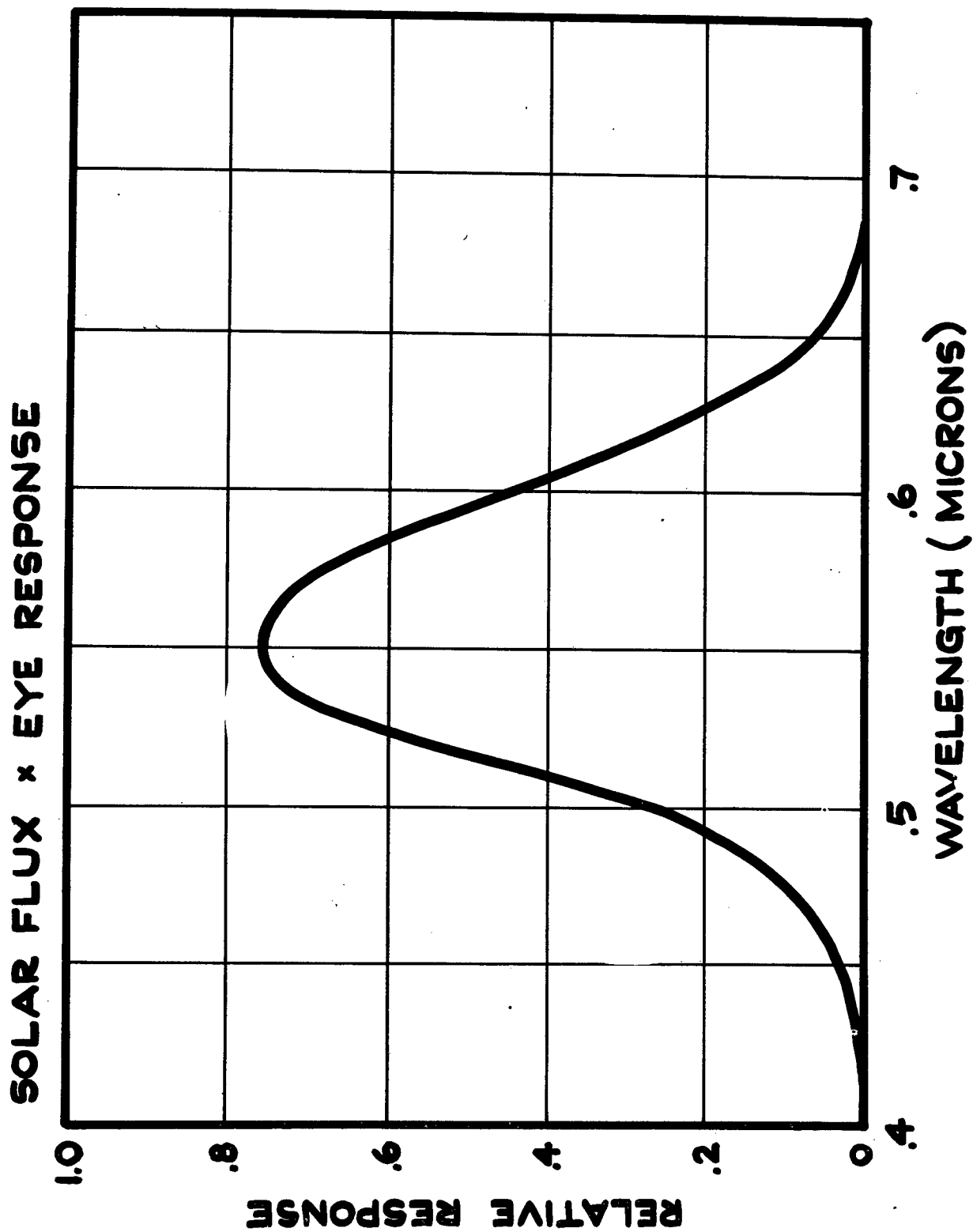
- 1) Large curved stretched acrylic canopies can be coated on both inside and outside surfaces to reduce reflectance and increase abrasion resistance.
- 2) Reducing reflectance over a range of different incidence angles necessitates compromise. A solution is to use a coating which has a wide range of effective wavelengths and is designed for a nominal angle of incidence which best approximates all the angles encountered. From a practical standpoint, the maximum design angle is about 60°.
- 3) Unwanted reflectances from red instrument lights during night flight will be substantially reduced at near normal (0°) angles of incidence. In other words, since red light is longer wavelength energy, minimum reflectance will occur at small angles of incidence than other visible light.
- 4) The same coating could be designed to reduce reflectance in the near ultra-violet or near infra-red with some sacrifice in visual performance.
- 5) Canopy sections with more than 90° curvature have to be flattened somewhat during coating to assure sufficient coating uniformity. Small, flat sections can be most easily coated for low reflectance.
- 6) Canopy segments with edge borders provide more convenient handling and fixturing during coating than those without borders.
- 7) Some staining problems were encountered, which were attributed to cleaning with hard water. Therefore, aqueous cleaning should be done only with soft water.



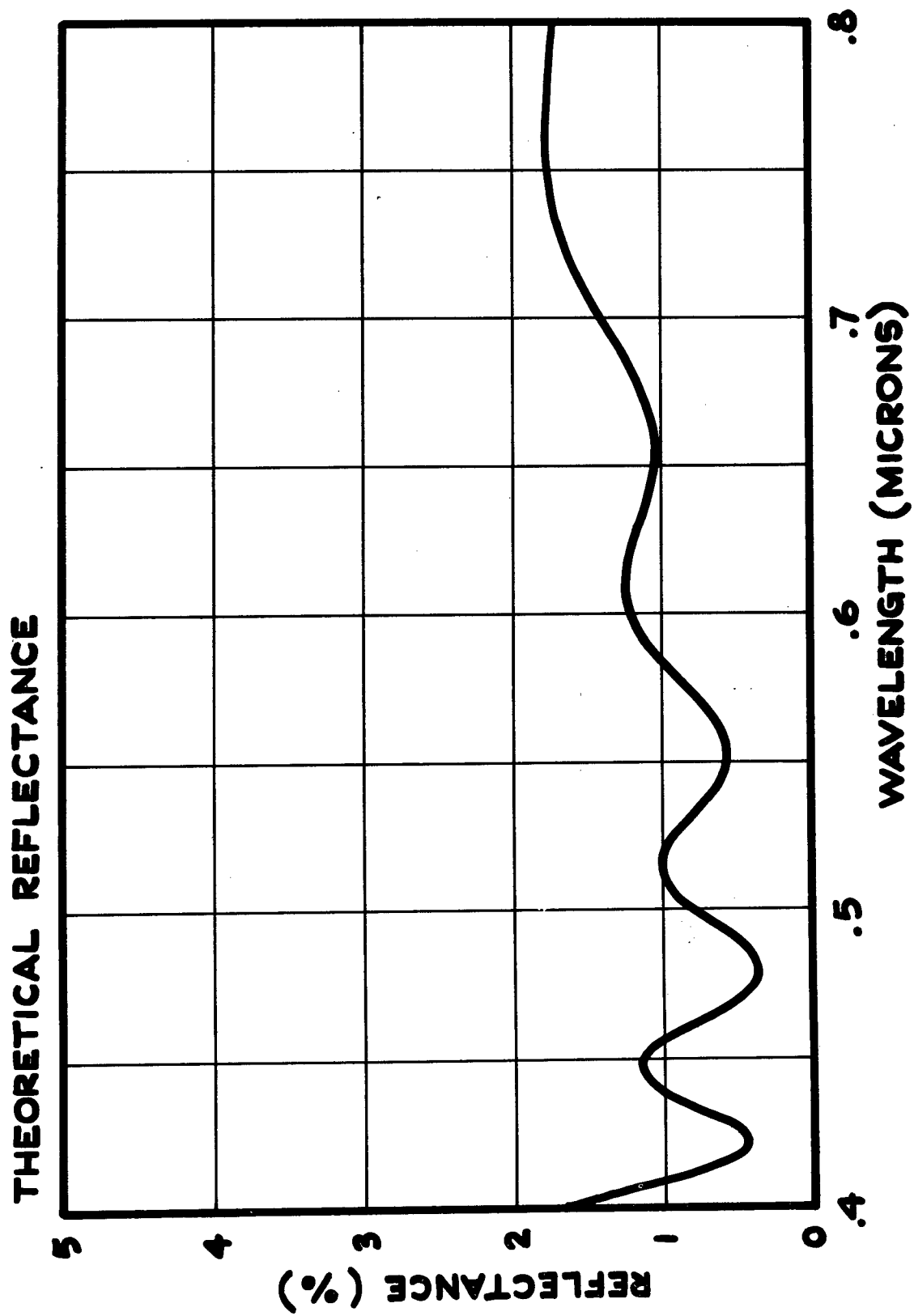
**FIG. 1**



**FIG.2**



**FIG. 3**



**FIG. 4**

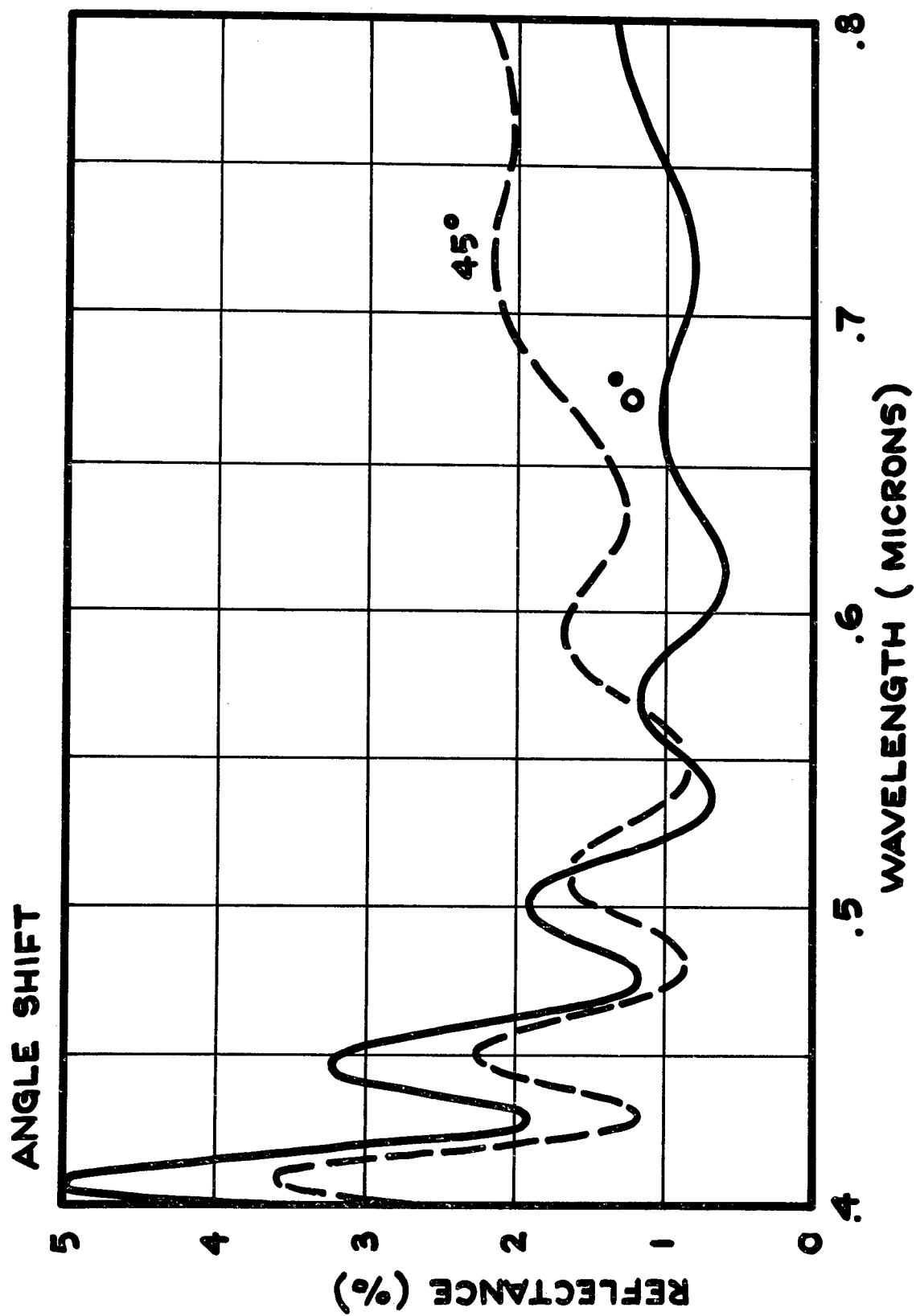
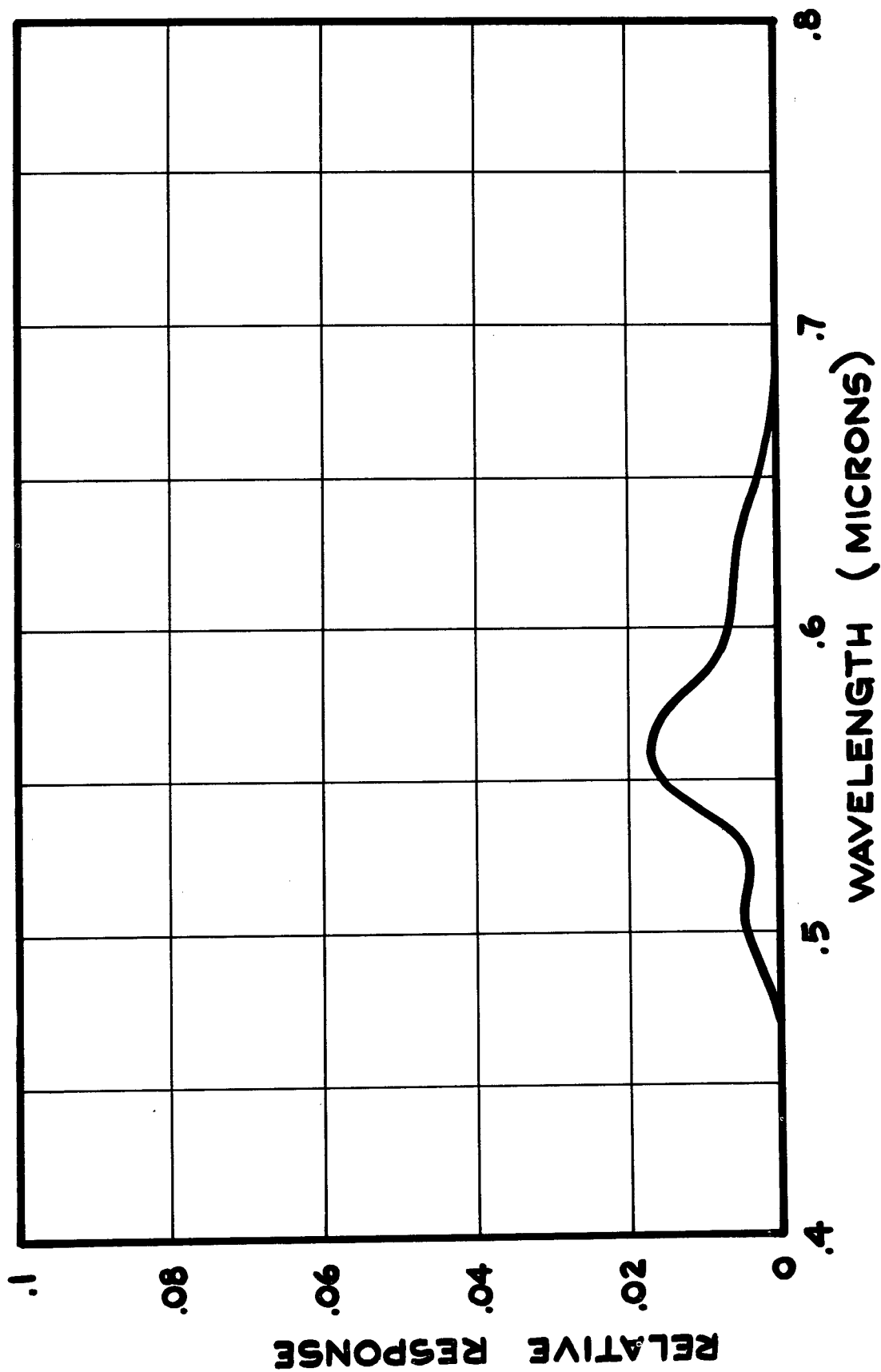


FIG. 5

**SOLAR FLUX  $\times$  EYE RESPONSE  $\times$  REFLECTANCE**



**FIG. 6**



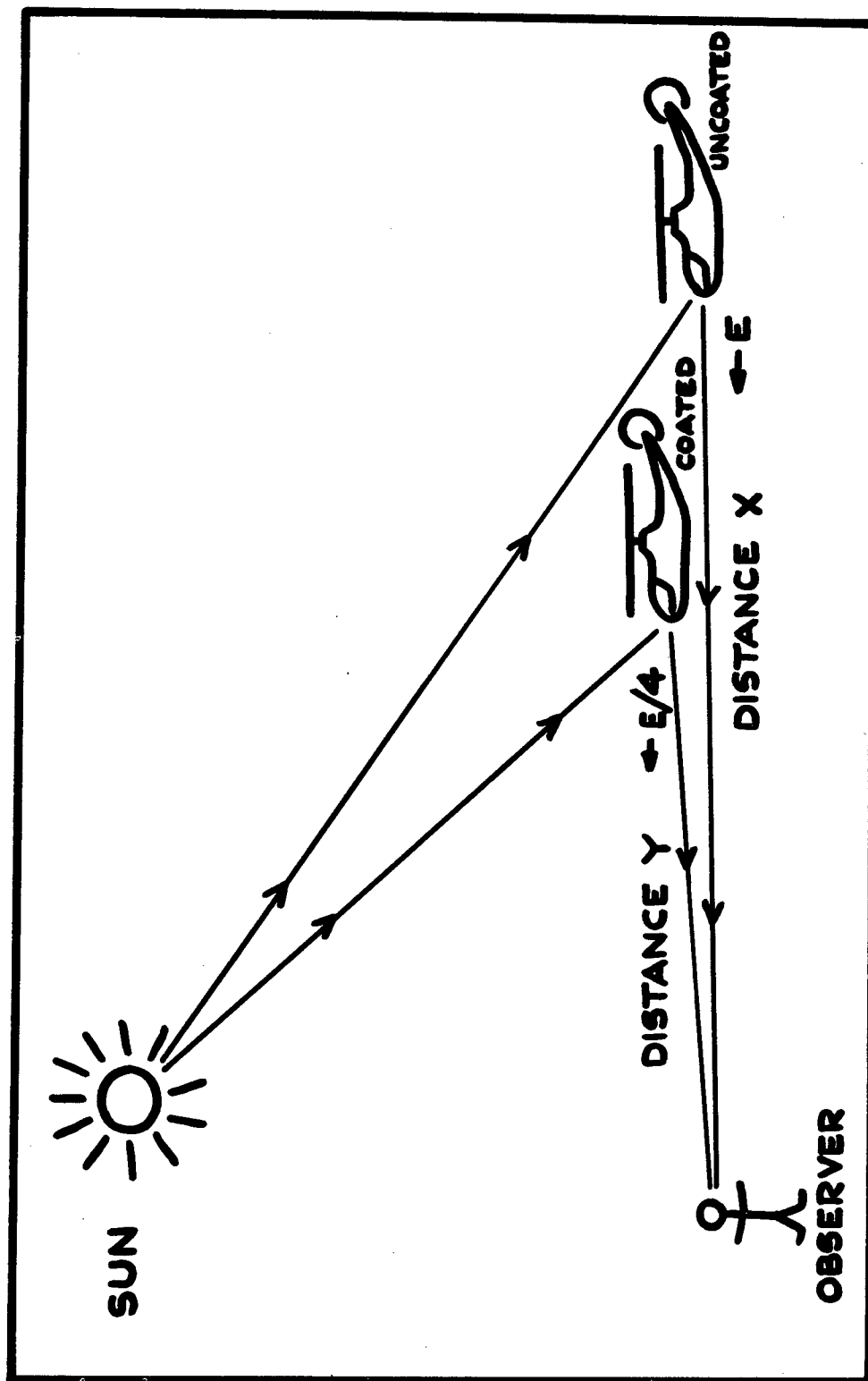


FIG.7

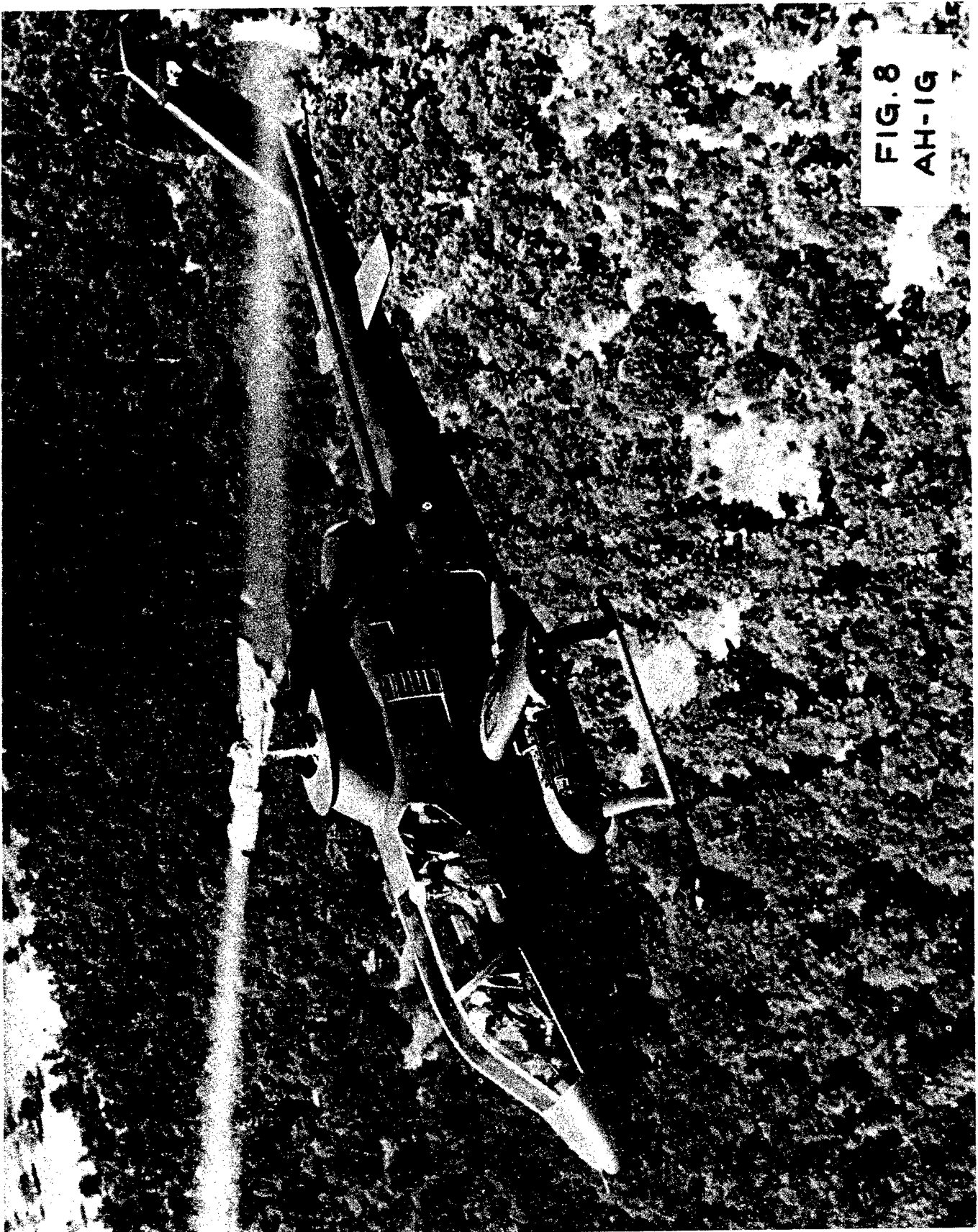
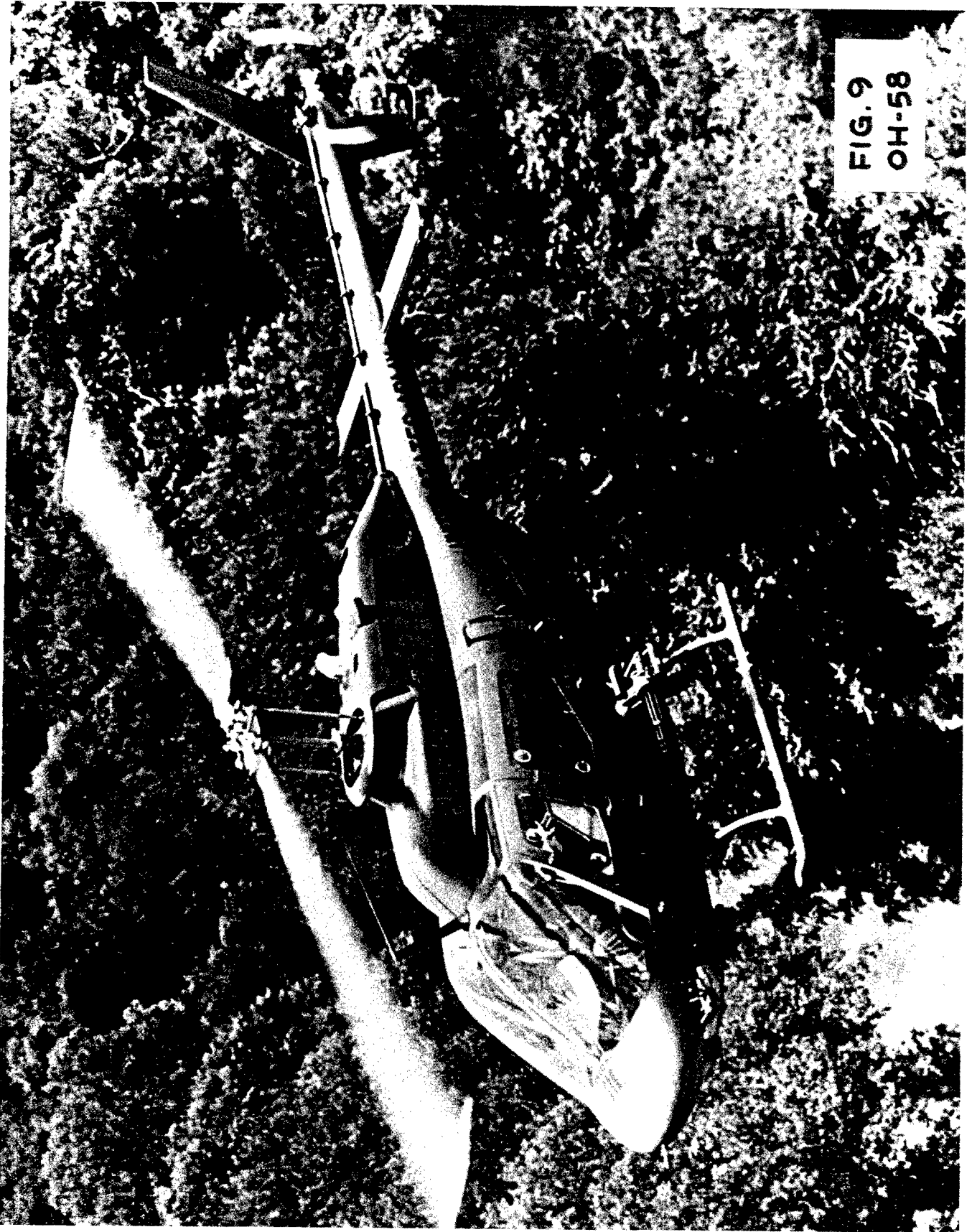


FIG. 8  
AH-1G



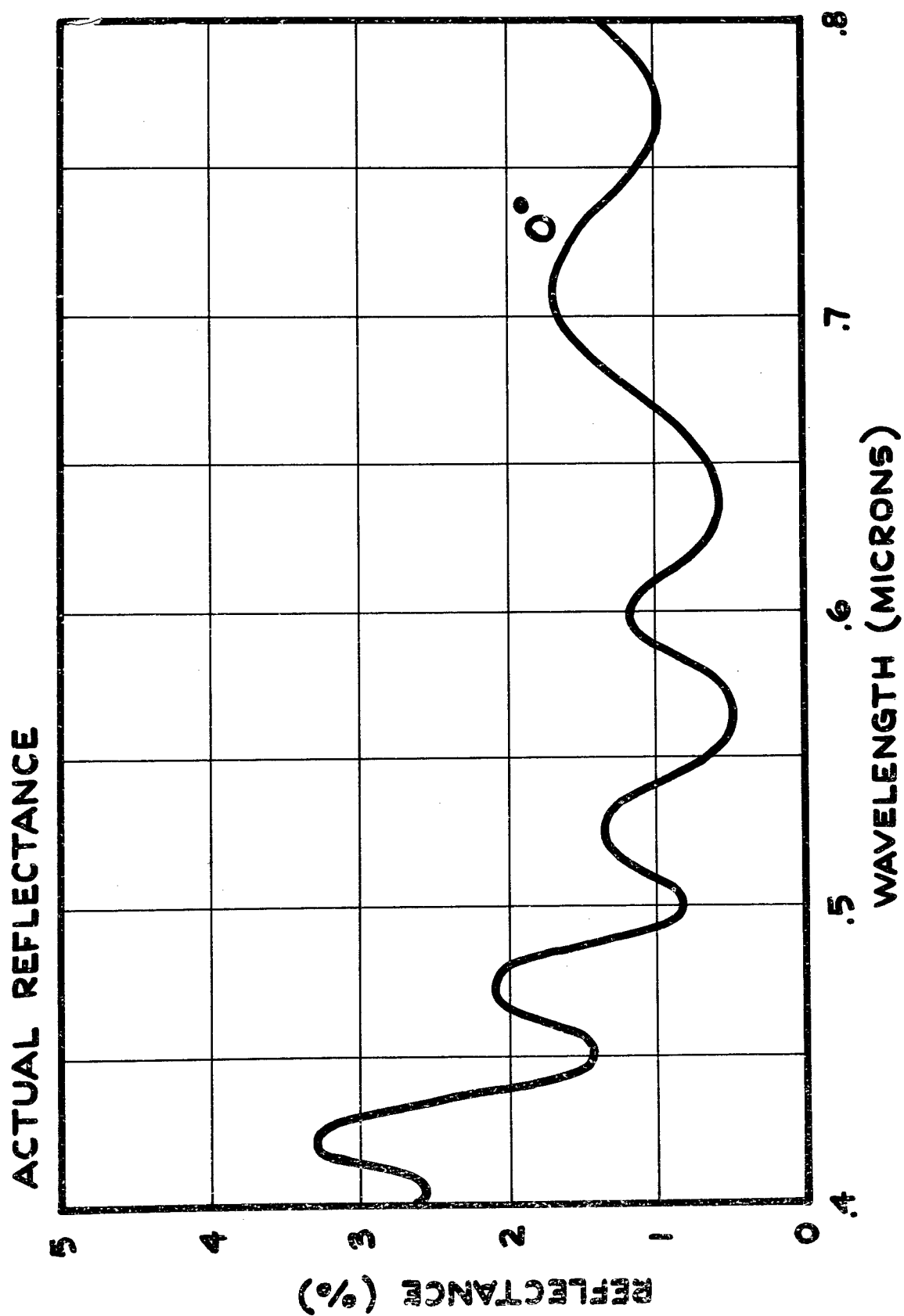
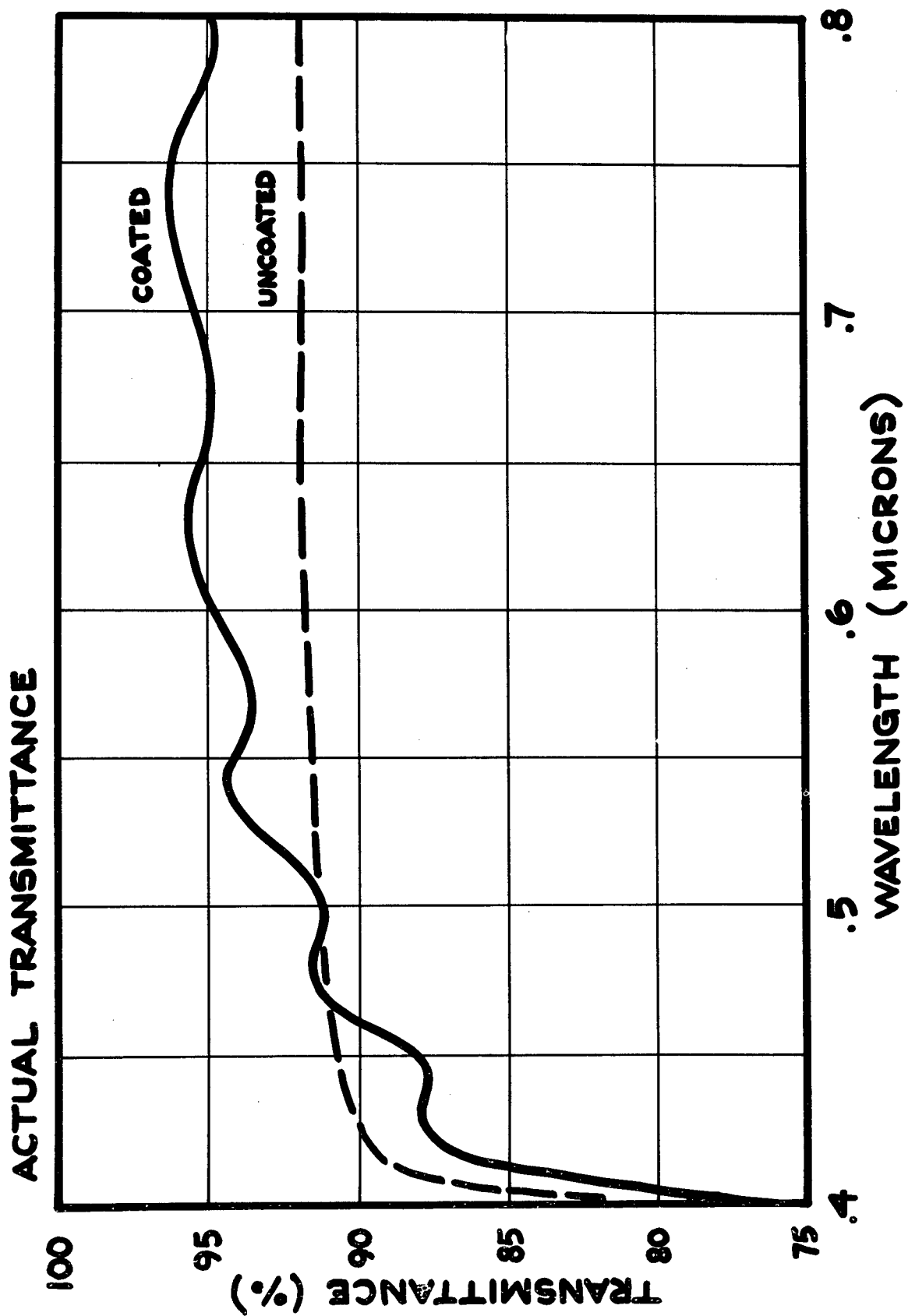


FIG. 10



**FIG. 11**

## PROTECTIVE COATINGS

D. L. Voss  
Sierracin Corporation  
Sylmar, California



## PROTECTIVE COATINGS

D. L. Voss

Sierracin Corporation

### ABSTRACT

Transparent plastics have several distinct advantages for aircraft applications, including their high strength/weight ratio, their toughness and non-shattering characteristics, and they can be formed into complex shapes.

To be fully effective in some applications, however, improved resistance to abrasion and solvents is desirable. This can be provided by laminating on a protective layer of thin glass or another plastic, or by cladding with a more resistant plastic, or by applying a thin protective coating directly to the plastic.

Sierracote<sup>®</sup> 311, a polymeric organosilicon compound, is applied as a thin protective coating on all exposed plastic surfaces of the Lockheed L-1011 windshields and cockpit windows to avoid hairline scratches from cleaning and normal handling. Sierracote 311 also provides excellent protection against harsh solvents. Actual service experience will be compared to data obtained from Sierracin accelerated laboratory testing.

Although Sierracote 311 has excellent environmental resistance and also excellent adhesion to acrylic, its adhesion to polycarbonate is unsatisfactory. Accordingly, a modified organosilicon compound, Sierracote 220 (formerly designated HC-2), with improved adhesion, was used on the inner and outer polycarbonate surfaces of early McDonnell-Douglas F-15 "Eagle" canopies. After more than one-hundred flights, these coatings appear to be unaffected. A ductile organic coating, Sierracote 230, was used on more recent F-15 canopies and windshields, and recently a further improved ductile coating, Sierracote 233, has been applied to F-15 and YF-16 polycarbonate canopies and windshields. Extensive laboratory evaluations of these coatings will be presented.

Thin protective coatings are the subject of this paper, although the laminating and cladding approaches will be discussed and described briefly.



## INTRODUCTION

The Sierracin Corporation has been fabricating aircraft transparencies for twenty years. During this period, the majority of the production has utilized plastic glazing materials, such as stretched acrylic, Sierracin 900, and, more recently, polycarbonate.

A number of different ways to protect the plastic surfaces from abrasion, solvent, and other aggressive environments will be described.

Perhaps the most effective way to protect the outer surface of plastic is by lamination of a protective layer of thin glass. For this reason, mention is briefly made of glass lamination, which is particularly applicable to the forward facing windshields of the Boeing 747 and Lockheed L-1011 aircraft.

Protective coatings, on the other hand, are readily applied to transparencies of compound curvature, do not increase weight, and are low in application cost compared to the laminated construction.

The basic structure of the Boeing 747 windshield is stretched acrylic, chosen because of the exceptional safety it provides.

The glass outer face provides maximum resistance to abrasion from the conventional windshield wipers which are teamed with a chemical rain-repellent system. Figure 1 shows the 747 windshield in cross-section.

The Lockheed L-1011 followed the Boeing 747 by about two years, and a significant difference between the 747 and L-1011 windshields is Lockheed's substitution of an abrasion-resistant coating, Sierracote 311, in place of the chemically strengthened glass used on the aft surface of the Boeing part. Figure 2 shows the L-1011 windshield in cross-section. Hardcoating offers two important advantages over the laminated glass shield; it saves weight (about 19 pounds per aircraft on the L-1011), and by eliminating one interlayer and one glass ply, it reduces the potential for optical distortion. Figure 3 shows a typical L-1011 windshield in airline service. L-1011 side windows incorporate hardcoating on both interior and exterior acrylic surfaces.

## PROTECTIVE COATINGS

Sierracote 311 was developed by Sierracin for the protection of acrylic surfaces. This coating contains "glass resins" produced by Owens-Illinois, Inc., Toledo, Ohio. Glass resins (so named because of their glass-like appearance) are based on an alternating silicon-oxygen system. Unlike conventional silicones, these glass resins can be cured to a hard, crystal-clear polymer without the use of hardeners.

A method of application of Sierracote 311 to stretched acrylic has been developed whereby the K-factor (a measure of "toughness") of the acrylic is not adversely affected. Methods for complete stripping of the coating have also been developed by Sierracin which allow the refurbishing of both monolithic and laminated parts after extended service.

Although the adhesion of Sierracote 311 to stretched acrylic is excellent and remains unaltered after extended flight service and also after laboratory accelerated environmental tests described in this paper, its adhesion to polycarbonate is poor. Attempts to improve the basic adhesion by modification of the 311 formulation and by investigation of a number of different polycarbonate surface preparations were unsuccessful.

Aircraft transparencies and protective coatings are exposed to a range of aggressive environments which include humidity, ultraviolet, temperature, chemical solvents, and abrasion. Resistance of coatings to these environments is, therefore, necessary for acceptable performance.

A number of coatings for polycarbonate were available, but no data on their performance in aggressive environments was available. It was believed that ultraviolet exposure would produce maximum degradation of a coating and, accordingly, accelerated weathering tests were performed by Sierracin.

Table 1 lists six coatings evaluated, and illustrates the fact that accelerated weathering caused degradation and adhesion loss in all of them. A comparison with the data in Table 8 shows the major improvement in resistance to weathering that we eventually achieved with Sierracote 233.

No doubt, improvements in some of the coating formulations listed in Table 1 have been and will continue to be made, as at Sierracin. It is our intention to use the best available protective coating for plastic surfaces, regardless of its source. At this time, our own coatings best meet our particular requirements.

After extensive research in polymer coatings, Sierracin synthesized an organosilicon material, originally designated HC-2 and now identified as Sierracote 220. This hardcoat was used in production on a number of McDonnell-Douglas F-15 monolithic polycarbonate canopies. After more than 100 flights since July 1972, no change in this coating has been observed. Figure 5 shows the first F-15 transparencies after 105 flight hours. However, canopy qualification tests performed by McDonnell-Douglas have shown that Sierracote 220, like other hard, brittle coatings, can be cracked by severe time-temperature profiles. At the same time, tests at Sierracin showed that long-term (18 months) natural weathering in Southern California resulted in some loss of adhesion. It was decided to replace Sierracote 220 with a more recently developed ductile coating, Sierracote 230, even though some degree of hardness would be sacrificed, as we now believe that only a ductile material can withstand the repeated rapid temperature changes that will be imposed on the F-15 canopies. The chemical structure of Sierracote 230 incorporates polymers with inherent flexibility. Extensive laboratory temperature cycling tests at Sierracin, which simulate the McDonnell-Douglas qualification tests have reproduced the cracking of Sierracote 220 and confirmed the ductile behavior of Sierracote 230 under conditions of severe thermal cycling.

Continued development in the field of transparent coatings recently resulted in an advanced ductile organic coating, Sierracote 233. Improved resistance to aggressive environments (solvents, temperature, humidity) has been achieved by reactions producing an extremely inert organic molecule.

The most recent polycarbonate canopies and windshields (shown in Figure 6) of the McDonnell-Douglas F-15, shown in Figure 7, and the General Dynamics Lightweight Fighter YF-16, shown in Figure 8, currently utilize Sierracote 233 on both inner and outer surfaces.

## TESTS AND TEST RESULTS

The protective coatings herein described for use with stretched acrylic and polycarbonate were subjected to a number of different tests to determine their effectiveness against a wide-range of aggressive environments. Details of each test method are given in the Appendix.

### Abrasion Resistance

Taber -- Four-inch discs of coated plastic were tested in a Taber Abraser. Abrasion of the coating by means of a grinding wheel is measured by a determination of light loss. Obviously, higher abrasion resistance is accompanied by lower loss of light transmission from scratches. Table 2 shows the results obtained.

Uncoated Sierracin 900, stretched acrylic, and polycarbonate are included for comparative purposes. Hard, glass-like coatings such as Sierracote 311 and Sierracote 220 make a dramatic improvement in the abrasion resistance of stretched acrylic and polycarbonate.

Sierracote 230 and Sierracote 233 are ductile materials previously described with lower but still very effective abrasion resistance.

Windshield Wiper Tests -- A wiper test which simulates the use of wipers on high-performance aircraft was performed on coated samples of stretched acrylic and polycarbonate. Table 3 shows the results of these tests.

The new ductile coatings on polycarbonate (Sierracote 230 and Sierracote 233) appear to be as effective in resisting wiper scratches as the harder, brittle coatings (Sierracote 311 and Sierracote 220). Figure 9 shows the effect of a wiper on uncoated and Sierracote 311 coated stretched acrylic. Severe scratching reduced the light transmission of the uncoated acrylic significantly, with a haze measurement of 22%. Coated acrylic is barely affected with a haze measurement of only 0.5%.

Surface Cleaning Tests -- A Surface Cleaning Simulator with wet and dry cycles was designed to simulate an average cycle for wet and dry cleaning. Isopropyl alcohol was selected as the cleaning fluid. Figure 10 shows the cleaning simulator. Table 4 shows the results of tests which simulated daily cleaning of plastic transparencies over a period of one year.

Scratching of uncoated polycarbonate was more severe than uncoated stretched acrylic, although vision was not significantly impaired for either material. Sierracote 311 and Sierracote 233 provide excellent protection for stretched acrylic and polycarbonate, respectively. Once again, the ductile coating (Sierracote 233) provides equal resistance to cleaning as the hard, brittle coating (Sierracote 311).

#### Chemical Resistance

Plastic materials are susceptible to varying degrees of solvent attack, and the coatings described in this paper do impart a high degree of chemical solvent protection. The ability of coatings to withstand solvents and to protect plastic surfaces has been investigated by using a one-inch diameter watchglass to contain the test solvent and dropwise addition of solvent around the edge. Test results presented in Table 5 show the extreme solvent resistance imparted by protective coatings, particularly Sierracote 233. A wide range of solvents that will contact aircraft transparencies was also examined (JP-4 fuel, hydraulic oil, paint stripper) and excellent resistance of the coatings was demonstrated in all cases.

#### Stress Craze

Windshield designs utilizing the high-impact strength of polycarbonate in a laminate with a polyvinyl butyral (PVB) interlayer require protection of the polycarbonate from the effect of plasticizer in PVB. Accordingly, tests conducted per MIL-P-8184 were performed using dibutyl sebacate (DBS), the plasticizer used in the PVB laminate construction. Data is presented in Table 6 and shows the significant improvement obtained by the use of coatings, particularly Sierracote 233. This type of construction has been used with success in the

acrylic facing of polycarbonate birdproof windshield for the Cessna T-37.

#### Light Transmission

The light transmission of 1/8 inch coated and uncoated MIL-P-25690 stretched acrylic and 1/8 inch coated and uncoated polycarbonate was measured per Specification LP-406, Method 3021. Results appear in Table 7. Sierracote 311 slightly improves the light transmission of acrylic, and Sierracote 233 significantly improves the light transmission of polycarbonate. This is due both to the favorable refractive index of the coatings, and the covering of minute scratches in the substrate.

#### Weathering Tests

A major West Coast airframe manufacturer has subjected Sierracote 311 coated stretched acrylic to accelerated weathering representing approximately three years of service. Testing consisted of temperature cycling with temperature excursions from -65°F to +180°F and also exposure in an Atlas Weatherometer. Only slight deterioration was noted with no loss of coating adhesion using the Scribe Tape Test described in the Appendix.

An F-15 polycarbonate canopy coated with Sierracote 220 has been exposed to Southern California weather for 18 months. After 12 months, little deterioration or loss of adhesion was noted, but after 18 months there was serious reduction in adhesion. The optical quality of the polycarbonate had also degraded with light surface crazing noticeable. Accelerated weathering tests combining UV, hot air and fog, were conducted on coated polycarbonate and acrylic. Data is presented in Table 8 and shows the effect on coated polycarbonate. The "230 series" of ductile protective coatings provided increased weathering resistance of polycarbonate compared to the hard Sierracote 220 coating. Sierracote 311 coated acrylic was relatively unaffected, and airline service (more than 1500 flight hours with no deterioration) on Lockheed L-1011's is evidence of excellent weatherability of the

coating, particularly on the exterior surface of the side windows.

Bare polycarbonate yellows severely after 10 days in the accelerated weathering test described above. This effect is noticeably reduced by the Sierracote protective coatings.

#### Temperature/Humidity Testing

Temperature -- Samples of stretched acrylic coated with Sierracote 311 including production size configurations, have been stored at room temperature for over a year with no evidence of deterioration of the coating. Samples of polycarbonate coated with Sierracote 220 have also been stored at room temperature for over one year with no deterioration of the coating. Samples similarly coated with Sierracote 230 and Sierracote 233 have been stored for 8 months and 4 months (to date), respectively, and show no deterioration of the coatings.

Samples of stretched acrylic coated with Sierracote 311 were subjected to elevated temperatures as shown in Table 9. No detectable change in the coating was observed even after 1000 hours at 200°F. Samples of Sierracote 220 and Sierracote 233 coated polycarbonate were unaffected after exposure to elevated temperatures up to 400°F.

To determine the ability of the Sierracote 311 coating to withstand thermal shock, samples of 311 coated stretched acrylic were soaked at -65°F for not less than 30 minutes, then immediately placed in a pre-heated oven at 140°F and held for 30 minutes. This cycle was repeated ten times. These same samples were then subjected to ten additional cycles with the oven temperature increased to 200°F. No deterioration or loss of adhesion could be detected.

Coated polycarbonate (Sierracote 220 and Sierracote 233) samples were cycled between room temperature and 330°F twenty times. Soak time at 330°F was one hour. Cracking of the hard Sierracote 220 was observed, but no change occurred in the ductile Sierracote 233. The Sierracote 233

samples were further temperature cycled between room temperature and 400°F. Again, no deterioration of the coating was observed.

Humidity -- The protective coatings discussed in this paper were subjected to elevated temperatures up to 160°F and relative humidity of 95-97%. The details of MIL-E-5272 specification are given in the Appendix.

130°F - 97% RH

Early Sierracote 311 coatings on stretched acrylic experienced early loss of adhesion and cracking when exposed to 130°F and 95% RH. Continuing refinements have resulted in the current production version of 311, which withstands these conditions for 60 days with no sign of degradation.

Sierracote 220 coated polycarbonate suffered no coating degradation after 5 days exposure, but some adhesion loss was observed. Sierracote 230 coated polycarbonate exhibited some adhesion failure, but no other change after 10 days exposure. Sierracote 233 showed no change in adhesion and no degradation after 45 days exposure.

Test data is presented in Table 10.

160°F - 97% RH

We consider this accelerated extreme humidity exposure test to be probably one of the most severe tests for any protective coating on a plastic surface. However, it serves as a useful guide in the selection of acceptable polymer systems for protective coating formulation.

Sierracote 311 coated stretched acrylic was unaffected after 25 days exposure. This readily demonstrates the inertness of this coating and the strength of the adhesive bond to acrylic.



Sierracote 220 coated polycarbonate exhibited some adhesion loss after 2 days exposure. Sierracote 230 coated polycarbonate exhibited some adhesion loss after 4 days exposure. Sierracote 233 coated polycarbonate remained unaffected after 25 days exposure. This readily shows the inertness of Sierracote 233 and the durable adhesive bond produced with polycarbonate. Data is presented in Table 10.

Water Immersion -- In addition to the humidity chamber testing noted above, water immersion tests have been performed. Results are presented in Table 11.

The humidity chamber and water immersion test results indicate the acceptability of Sierracote 311 coated acrylic and the improvements obtained by replacement of a brittle, hard organosilicon material with a ductile organic material, Sierracote 233, for protection of polycarbonate surfaces.

#### Impact Strength

Specimens of coated polycarbonate were impacted by dropping a 40-pound, one-inch diameter "dart" from a height of 7.5 feet. Tests at -65°F, 0°F, and room temperature showed that the impact strength of polycarbonate was not adversely affected by the application of thin protective coatings.

One other method for protection of polycarbonate is worthy of inclusion in this paper, namely:

#### Thin Glue Line

Extensive "dart" impact tests performed by Sierracin showed that the impact strength of polycarbonate is severely degraded by the fusion bonding of acrylic. Cracks in the acrylic propagate through the polycarbonate. Bonding the acrylic to the polycarbonate with a thin, flexible "glue line" acts as a "crack stopper" and avoids this problem. Figure 11 shows a windshield fabricated by Sierracin using this process. The flat laminate was thermoformed as a "monolithic" sheet.

In this case, the "glue line" was a .010-inch layer of Sierracin heat-resistant silicone interlayer. A glue line 0.010 to 0.050-inch thick is effective in bouncing a dart in the impact test previously described. An added advantage over fusion bonding is that the more durable cross-linked acrylic (MIL-P-8184) can be used, whereas fusion bonding works only with the older MIL-P-5425 material.

### CONCLUSIONS

1. Sierracote 311 is a highly satisfactory coating for stretched acrylic, and is currently used on Lockheed L-1011 cockpit transparencies.
2. Sierracote 233, currently used on both the F-15 and YF-16 windshields and canopies, is the most effective protective coating for polycarbonate that we have evaluated.
3. Sierracote 233 protects polycarbonate from PVB and may be laminated to PVB.
4. Laboratory accelerated testing is useful in predicting the service life of protective coatings. Humidity testing at elevated temperatures is particularly severe.
5. The impact strength of polycarbonate is unaffected by application of thin protective coatings.
6. The toughness of stretched acrylic is unaffected by application of a protective coating, provided that cure temperatures are carefully controlled.
7. As-cast acrylic can be fusion-bonded and bonded by means of a high-temperature adhesive to polycarbonate to produce a field-repairable surface.
8. Adhesive ("thin glue line") bonding of acrylic to polycarbonate maintains the high intrinsic impact strength of the polycarbonate.
9. Sierracote protective coatings improve the light transmission of polycarbonate.

## APPENDIX -- TEST METHODS

### Taber Tests

Four-inch discs of coated plastic were tested in a Taber Abraser, according to ASTM Method 1092-1. A load of 1,000 grams was used on a CS-10 Calibrase wheel for 50 revolutions. The results were evaluated by measuring the difference (loss) in visible light transmission before and after abrading. The greater the degree of abrasion damage, the greater the loss in light transmission.

### Windshield Wiper Tests

The Sierracin windshield wiper testing consists of a Marquette wiper motor and gearbox mounted on a wood frame which also supports the plastic panel to be tested. The wiper is a seven-inch aircraft-type with a special Hycar rubber blade. The motor operates at a rate of 55 complete sweeps per minute. The wiper arm is adjusted to exert a force of .57 pounds per inch of blade length, which represents the upper limit of wiper force used on high-performance aircraft. The wiper is run on the surface of the test part completely dry. Normal duration of this test is four hours.

### Surface Cleaning Simulator

The Surface Cleaning Simulator was designed to simulate an average cleaning cycle for wet and dry cleaning. This test closely simulates actual cleaning of plastic surfaces and details are, therefore, given. The unit has two wiper arms hinged to a carriage. The carriage, supported by nylon wheels, is cycled in a horizontal plane on a steel track by means of an arm attached to a concentric scribe. To eliminate skipping of the wipers over the surface, the arms are installed at a 15° angle to the specimen. Displacement solenoids raise and lower the arms from the test surface through a tandem timer. Each wiper arm contains a weight trough filled with leadshot, mounted across the wiper frame to maintain the proper cleaning pressure of the wiper. The wet or inner wiper contains two "soaker" tubes with adjusting valve assemblies, connected to a reservoir. When in operation, the wipers are cycled to produce a wet and dry cleaning function.

Actual determination showed that the average pressure applied during cleaning is 2.0 psi. An average of 20 rubbing strokes to apply the cleaner and 40 rubbing strokes to dry-polish the surface was determined by using a 12" x 12" test specimen. The dry wiper (10" x 1/2") required 10 pounds pressure to simulate the cleaning cycle. The wet wiper (8" x 1/2") required 8 pounds pressure. Due to the structural limitations of the test unit, the required cleaning pressures could not be used. The weight on the arms was, therefore, reduced to 1/5 actual, and the number of cleaning strokes was increased by a factor of 5. Thus, 200 strokes at 2 pounds simulated one dry cleaning, and 100 strokes at 1.6 pounds simulated one wet cleaning.

The drive motor was set at 120 strokes per minute and, using a tandem timer, the cleaning cycle was calculated:

$$\frac{200 \text{ dry strokes}}{120 \text{ strokes/min.}} = 1.7 \text{ minutes}$$

$$\frac{100 \text{ wet strokes}}{120 \text{ strokes/min.}} = .84 \text{ minutes}$$

$$\text{One cleaning period} = 2.54 \text{ minutes}$$

Tests were run on each sample for 365 cleaning periods (15 hours 27 minutes) to represent a total of one year cleaning performed daily. Isopropyl alcohol was used as the cleaning fluid as the flow to the wet wiper can be controlled to equal the evaporation rate. The evaporation rate is high and the dry wiper operates dry at least 80% of the dry wiper cycles. The fluid acts as a lubricant to remove particles from the surface. The cleaning cloth is artist's canvas, containing no starch or sealing compounds. It is flexible, absorbent, and coarse enough to initiate erosion of the test specimen in place of polishing.

#### Weathering Tests (FTMS 406, Method 6024)

One 24-hour cycle consists of:

- (1) 2 hours fog, followed by
- (2) 2 hours ultraviolet radiation (UV) and hot air (130°F), followed by

- (3) 2 hours fog, followed by
- (4) 18 hours UV and hot air.

#### Humidity Tests

MIL-E-5272, Procedure 1 consists of:

- (1) Over 2 hours raise temperature from 68-100°F.
- (2) Maintain 160°F for 6 hours.
- (3) Reduce the temperature to 68-100°F over 16 hours. The relative humidity throughout the 24-hour cycle shall be maintained at 97%. The cycle shall be repeated to extend the total time of test to 240 hours (10 cycles).

MIL-E-5272, Procedure 3 requires a constant temperature of 120°F at 97% relative humidity. Sierracin testing increased the temperature to 130°F.

#### Adhesion Scribe Tape Test

This test is based on a modification of methods described in Federal Test Method Standard #141, Method 6301; and Paint Cross-Cut Adhesion Test of Paint Testing Manual, 12th Edition, 1962. A length of one-inch wide #600 3M tape is manually pressed onto an X-scribed surface of a coated panel and then suddenly peeled off. The specimen is inspected for evidence of coating removal by being viewed in a good light against a dark background and by addition of methyl ethyl ketone.

#### Copyright 1973, Sierracin® Corporation

The information contained in this document is thought to be reliable, but the Sierracin Corporation expressly disclaims all responsibility for loss or damage caused by or resulting from the use of the information herein contained. The information is given on the express condition that the user assumes all risk.

**POLYCARBONATE COATINGS**  
**ACCELERATED WEATHERING-10 DAYS**

| <b>COATING<br/>SOURCE</b>             | <b>RESULTS</b>                                     |
|---------------------------------------|--|
| <b>BEE CHEMICAL<br/>R-99-16</b>       | <b>LOSS OF ADHESION</b>                            |
| <b>BALL CHEMICAL<br/>LEXCOTE 3399</b> | <b>CLOUDED<br/>LOSS OF ADHESION</b>                |
| <b>GENERAL ELECTRIC<br/>MR - 4000</b> | <b>LIGHT HAZE<br/>LOSS OF ADHESION</b>             |
| <b>DUPONT<br/>ABCITE</b>              | <b>OPTICALLY UNACCEPTABLE<br/>LOSS OF ADHESION</b> |
| <b>OWENS ILLINOIS</b>                 | <b>FAILED ADHESION</b>                             |
| <b>MOBAY CHEMICAL</b>                 | <b>FAILED ADHESION</b>                             |

**TABLE I**

## TABER ABRASION TESTS

| SUBSTRATE         | COATING        | LOSS OF LIGHT<br>TRANSMISSION<br>BY ABRASION |
|-------------------|----------------|--|
| SIERRACIN 900     | NONE           | 10.6 %                                       |
| STRETCHED ACRYLIC | NONE           | 50.0 %                                       |
| POLYCARBONATE     | NONE           | 51.0 %                                       |
| STRETCHED ACRYLIC | SIERRACOTE 311 | 7.0 %  |
| POLYCARBONATE     | SIERRACOTE 220 | 7.0 %  |
| POLYCARBONATE     | SIERRACOTE 230 | 25.0 %                                       |
| POLYCARBONATE     | SIERRACOTE 233 | 16.0 %                                       |

TABLE 2

## WINDSHIELD WIPER TESTS

| SUBSTRATE         | COATING        | OBSERVATIONS     | HAZE  |
|-------------------|----------------|------------------|-------|
| STRETCHED ACRYLIC | NONE           | SEVERELY ABRADED | 22.0% |
| STRETCHED ACRYLIC | SIERRACOTE 311 | FAINT SCRATCHES  | 0.5%  |
| POLYCARBONATE     | NONE           | SCRATCHES        | 4.0%  |
| POLYCARBONATE     | SIERRACOTE 220 | NO EFFECT        | 0.5%  |
| POLYCARBONATE     | SIERRACOTE 230 | SCRATCHES        | 0.5%  |
| POLYCARBONATE     | SIERRACOTE 233 | SCRATCHES        | 0.5%  |

TABLE 3



## CLEANING SIMULATOR TESTS

| SUBSTRATE         | COATING        | HAZE AFTER TEST |
|-------------------|----------------|-----------------|
| STRETCHED ACRYLIC | N O N E        | 1.5 %           |
| STRETCHED ACRYLIC | SIERRACOTE 311 | 0.5 %           |
| POLYCARBONATE     | N O N E        | 9.0 %           |
| POLYCARBONATE     | SIERRACOTE 230 | 3.5 %           |
| POLYCARBONATE     | SIERRACOTE 233 | 0.6 %           |

TABLE 4

## SOLVENT RESISTANCE TESTS

| SOLVENT                   | SUBSTRATE            | COATING        | AVE. TIME TO FAIL |
|---------------------------|----------------------|----------------|-------------------|
| METHYL<br>ETHYL<br>KETONE | STRETCHED<br>ACRYLIC | NONE           | 90 MINUTES        |
|                           |                      | SIERRACOTE 311 | 130 MINUTES       |
|                           | POLYCARBONATE        | NONE           | 0.1 MINUTE        |
|                           |                      | SIERRACOTE 220 | 33 MINUTES        |
|                           |                      | SIERRACOTE 230 | 45 MINUTES        |
|                           |                      | SIERRACOTE 233 | 480 MINUTES       |
| ACETONE                   | STRETCHED<br>ACRYLIC | NONE           | 115 MINUTES       |
|                           |                      | SIERRACOTE 311 | 145 MINUTES       |
|                           | POLYCARBONATE        | NONE           | 0.1 MINUTE        |
|                           |                      | SIERRACOTE 220 | 19 MINUTES        |
|                           |                      | SIERRACOTE 230 | 30 MINUTES        |
|                           |                      | SIERRACOTE 233 | 180 MINUTES       |

TABLE 5

# **STRESS CRAZE TESTS** **(DIBUTYL SEBACATE)**

| COATING SYSTEM ON<br>POLYCARBONATE | CRITICAL CRAZE LEVEL |
|------------------------------------|----------------------|
| NONE                               | 1000 PSI             |
| SIERRACOTE 230                     | 2700 PSI             |
| SIERRACOTE 233                     | 3800 PSI             |

**TABLE 6**



## LIGHT TRANSMISSION TESTS

| SUBSTRATE         | COATING        | LIGHT TRANSMISSION |
|-------------------|----------------|--------------------|
| STRETCHED ACRYLIC | NONE           | 92.0 %             |
|                   | SIERRACOTE 311 | 92.4 %             |
| POLYCARBONATE     | NONE           | 83.4 %             |
|                   | SIERRACOTE 233 | 87.1 %             |

TABLE 7

# ACCELERATED WEATHERING TESTS

## FTMS 406 METHOD 6024

| SUBSTRATE         | COATING        | DURATION<br>OF<br>EXPOSURE | RESULTS  |
|-------------------|----------------|----------------------------|--|
| STRETCHED ACRYLIC | SIERRACOTE 311 | 30 DAYS                    | NO EFFECT  |
| POLYCARBONATE     | SIERRACOTE 220 | 10 DAYS                    | LOSS OF ADHESION  |
|                   | SIERRACOTE 230 | 10 DAYS                    | NO EFFECT       |
|                   | SIERRACOTE 233 | 20 DAYS                    | NO EFFECT  |



COATING CRACKED



ADHESION UNACCEPTABLE

TABLE 8

## ELEVATED TEMPERATURE TESTS

| SUBSTRATE            | COATING        | TEMPERATURE | TIME OF EXPOSURE |
|----------------------|----------------|-------------|------------------|
| STRETCHED<br>ACRYLIC | SIERRACOTE 311 | 140 °F      | 332 HOURS        |
|                      |                | 200 °F      | 1000 HOURS       |
| POLYCARBONATE        | SIERRACOTE 220 | 250 °F      | 1000 HOURS       |
|                      |                | 300 °F      | 300 HOURS        |
|                      | SIERRACOTE 233 | 200 °F      | 1000 HOURS       |
|                      |                | 250 °F      | 1000 HOURS       |
|                      |                | 300 °F      | 1000 HOURS       |
|                      |                | 400 °F      | 168 HOURS        |

TABLE 9

## HUMIDITY TESTING

| SUBSTRATE            | COATING        | 130°F / 97% RH | 160°F / 97% RH |
|----------------------|----------------|----------------|----------------|
| STRETCHED<br>ACRYLIC | SIERRACOTE 311 | 60 DAYS        | 25 DAYS        |
| POLYCARBONATE        | SIERRACOTE 220 | 5 DAYS         | 2 DAYS         |
|                      | SIERRACOTE 230 | 10 DAYS        | 5 DAYS         |
|                      | SIERRACOTE 233 | 45 DAYS        | 25 DAYS        |

TABLE 10

## WATER IMMERSION TESTS

| SUBSTRATE         | COATING        | DURATION         | RESULTS          |
|-------------------|----------------|------------------|------------------|
| STRETCHED ACRYLIC | SIERRACOTE 311 | 60 DAYS AT 75°F  | NO CHANGE        |
|                   | SIERRACOTE 311 | 60 DAYS AT 150°F | NO CHANGE        |
| POLYCARBONATE     | SIERRACOTE 220 | 30 DAYS AT 75°F  | LOSS OF ADHESION |
|                   |                | 10 DAYS AT 150°F | LOSS OF ADHESION |
|                   | SIERRACOTE 230 | 30 DAYS AT 75°F  | LOSS OF ADHESION |
|                   |                | 10 DAYS AT 150°F | LOSS OF ADHESION |
|                   | SIERRACOTE 233 | 30 DAYS AT 75°F  | NO CHANGE        |
|                   |                | 10 DAYS AT 150°F | NO CHANGE        |

TABLE II



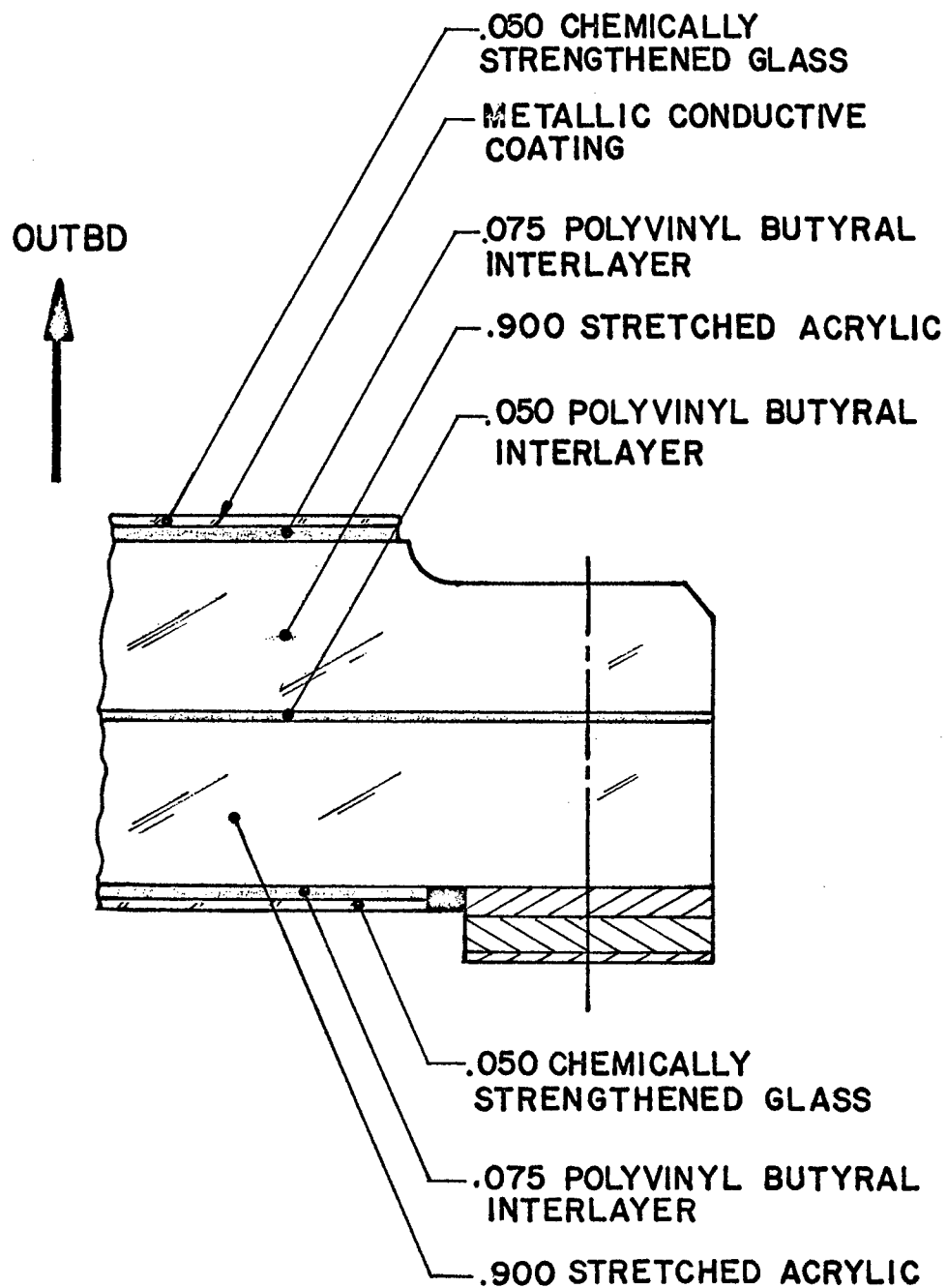


FIGURE 1

CROSS-SECTION OF BOEING 747 WINDSHIELD

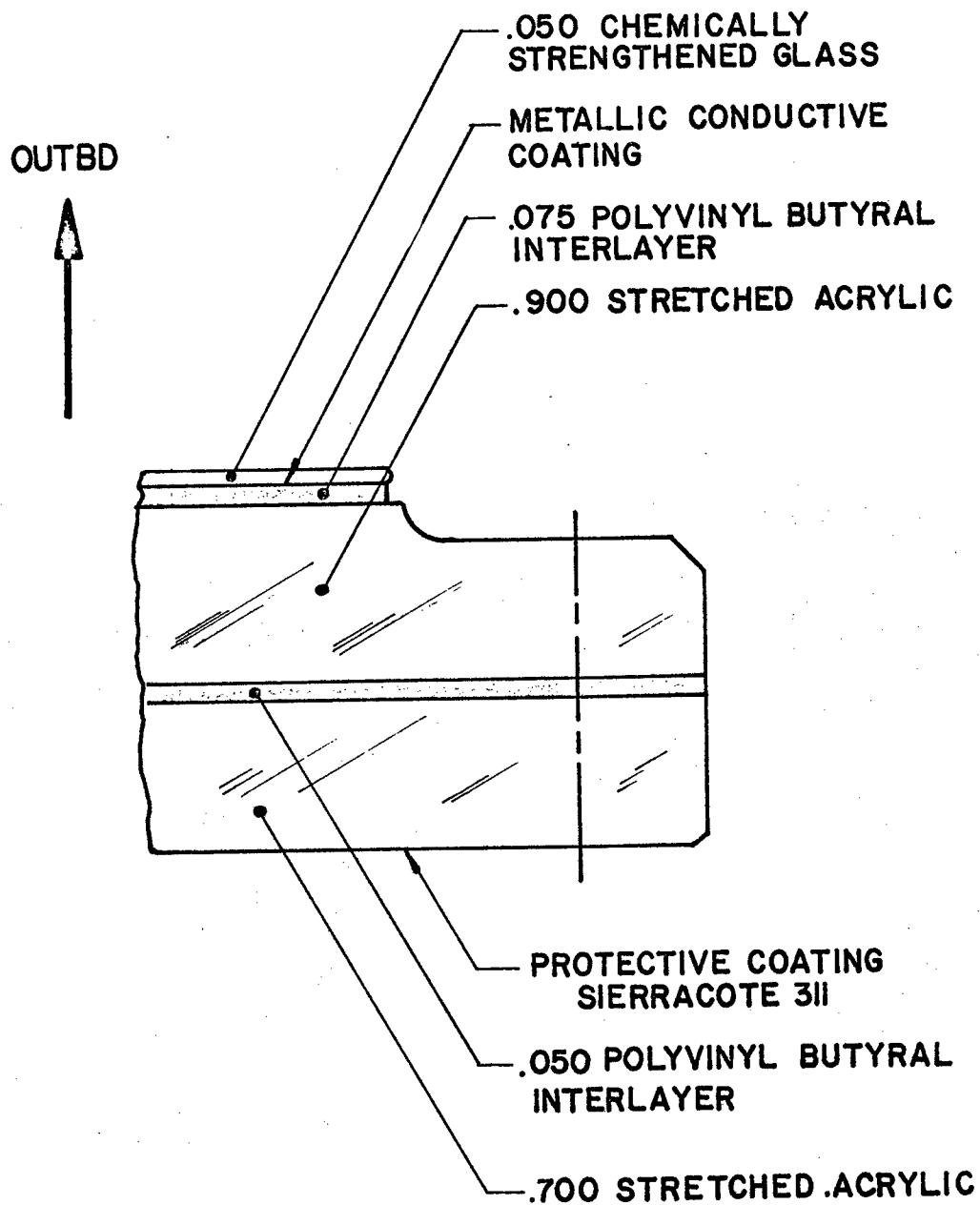


FIGURE 2

CROSS-SECTION OF LOCKHEED  
L-1011 WINDSHIELD

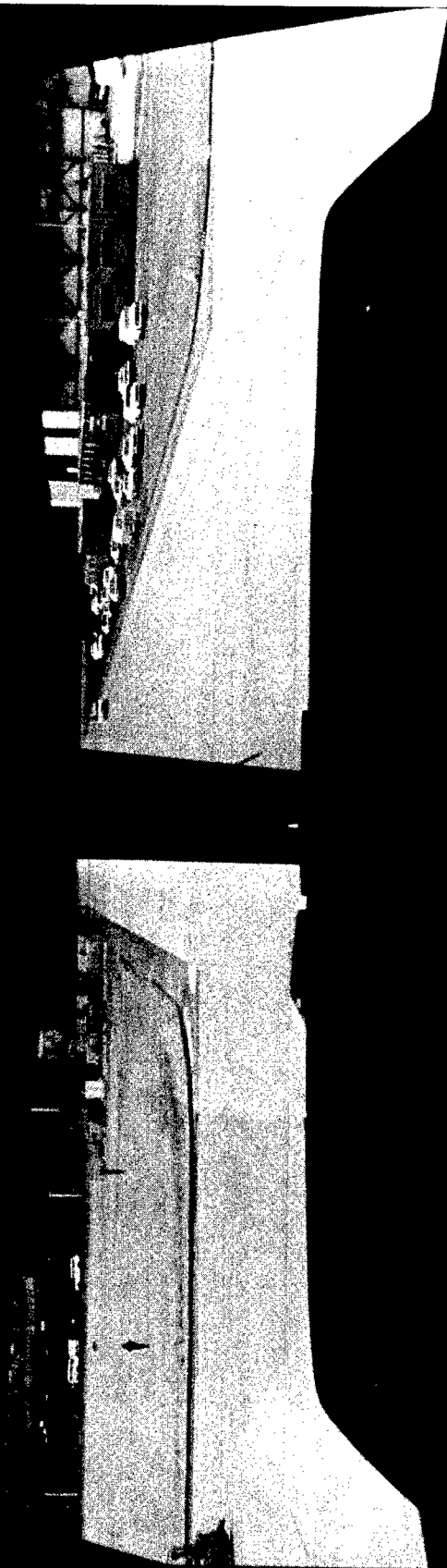


FIGURE 3

Lockheed L-1011 Windshield  
in Airline Service

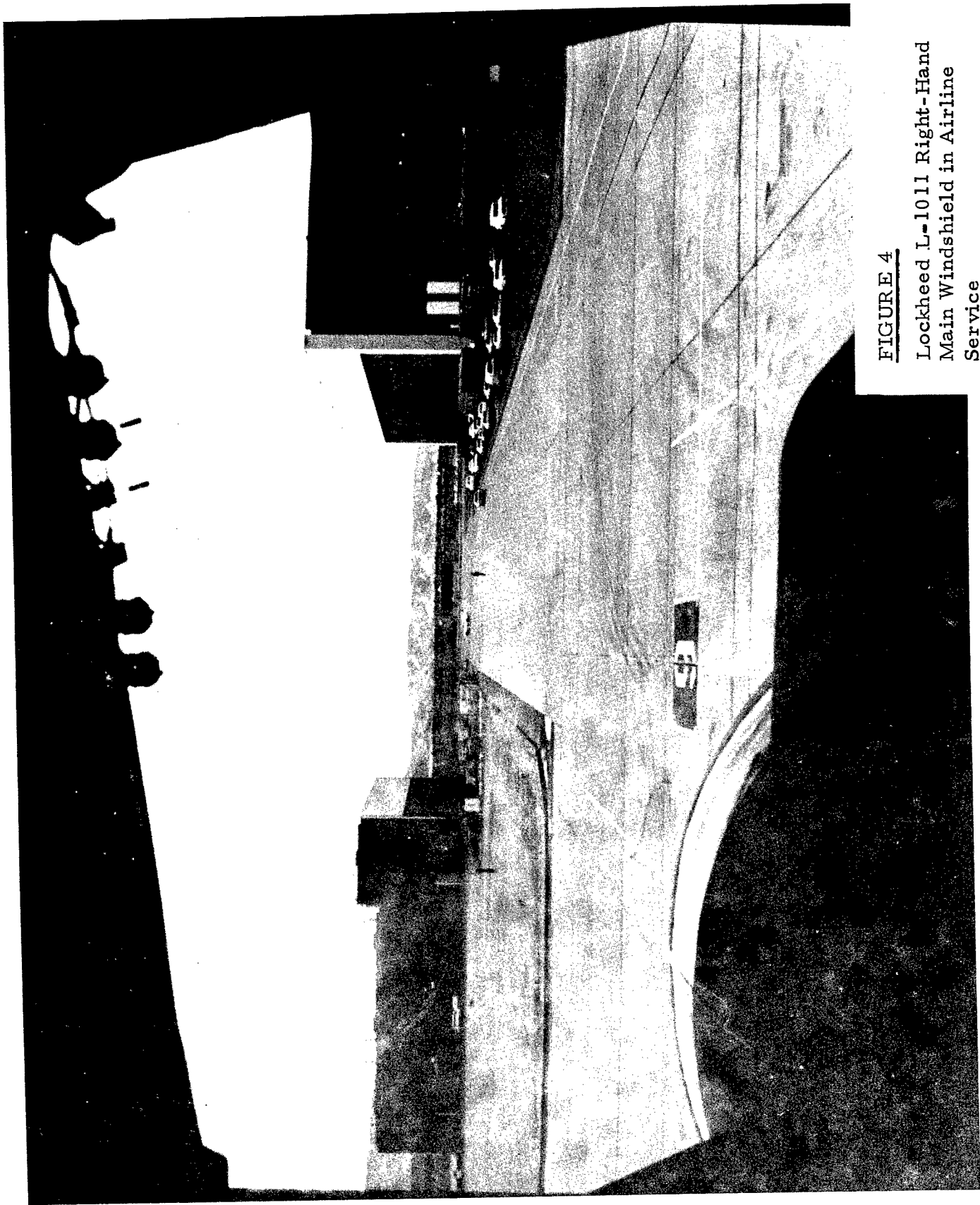


FIGURE 4

Lockheed L-1011 Right-Hand  
Main Windshield in Airline  
Service

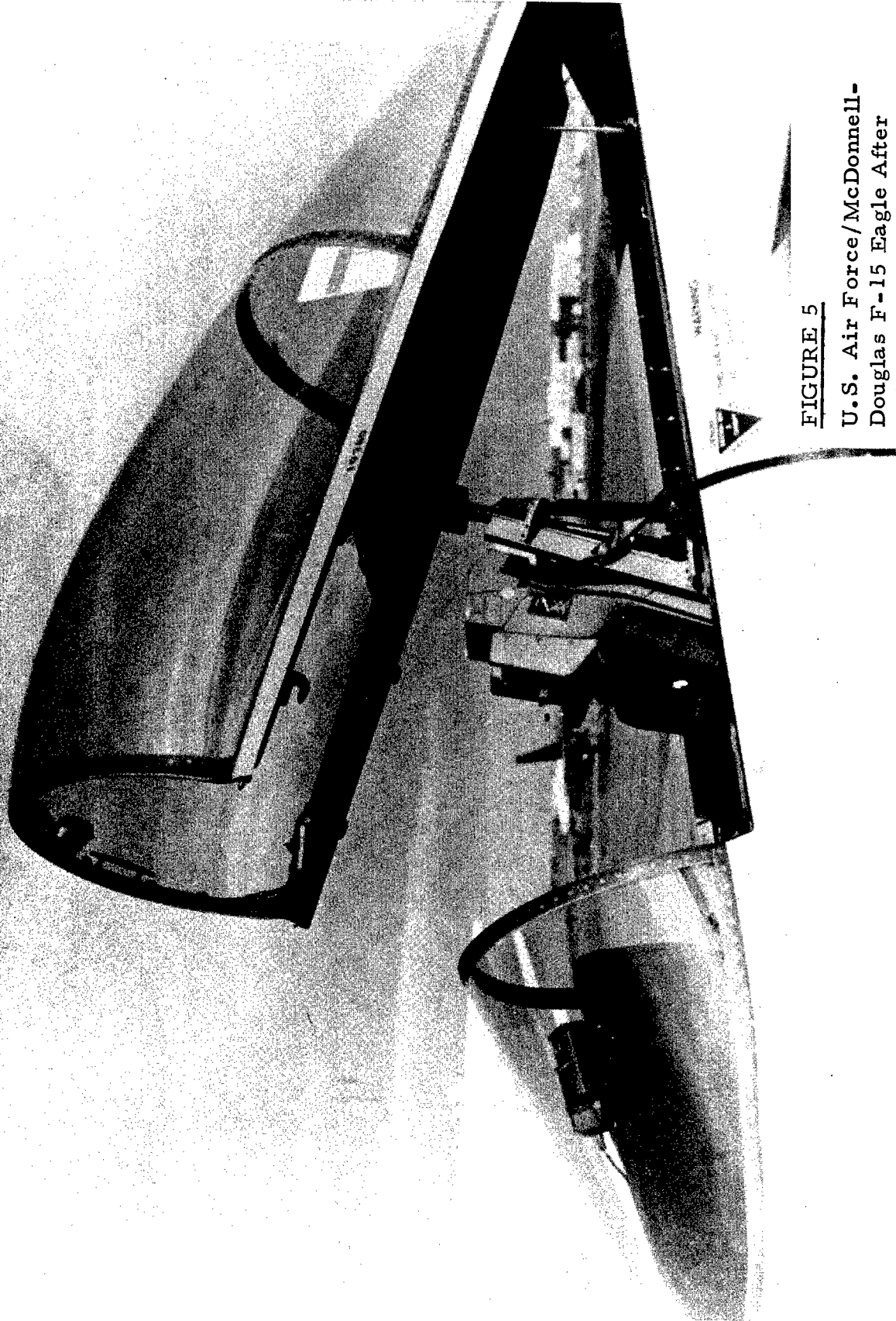


FIGURE 5

U.S. Air Force/McDonnell-  
Douglas F-15 Eagle After  
105 Flight Hours

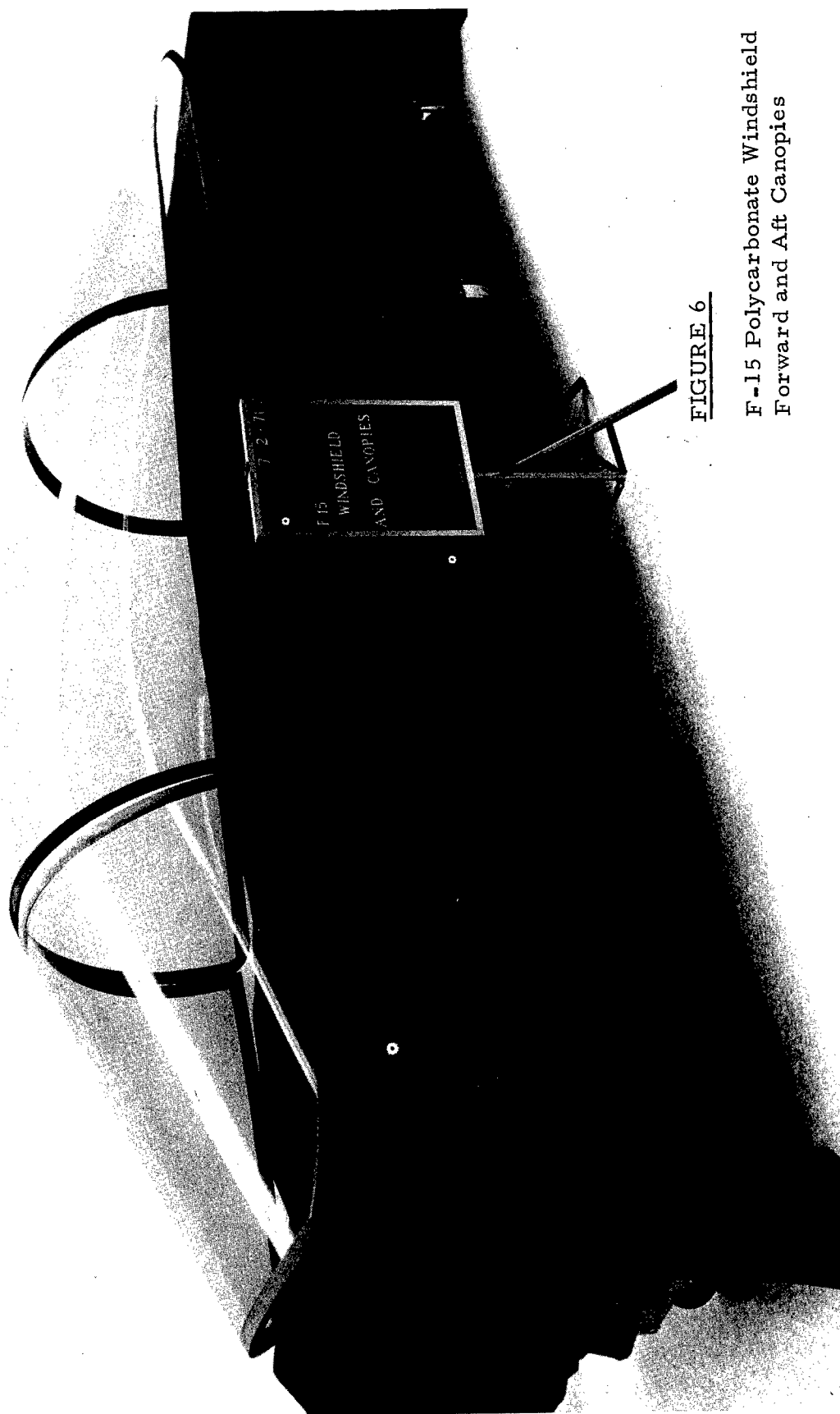


FIGURE 6

F-15 Polycarbonate Windshield  
Forward and Aft Canopies

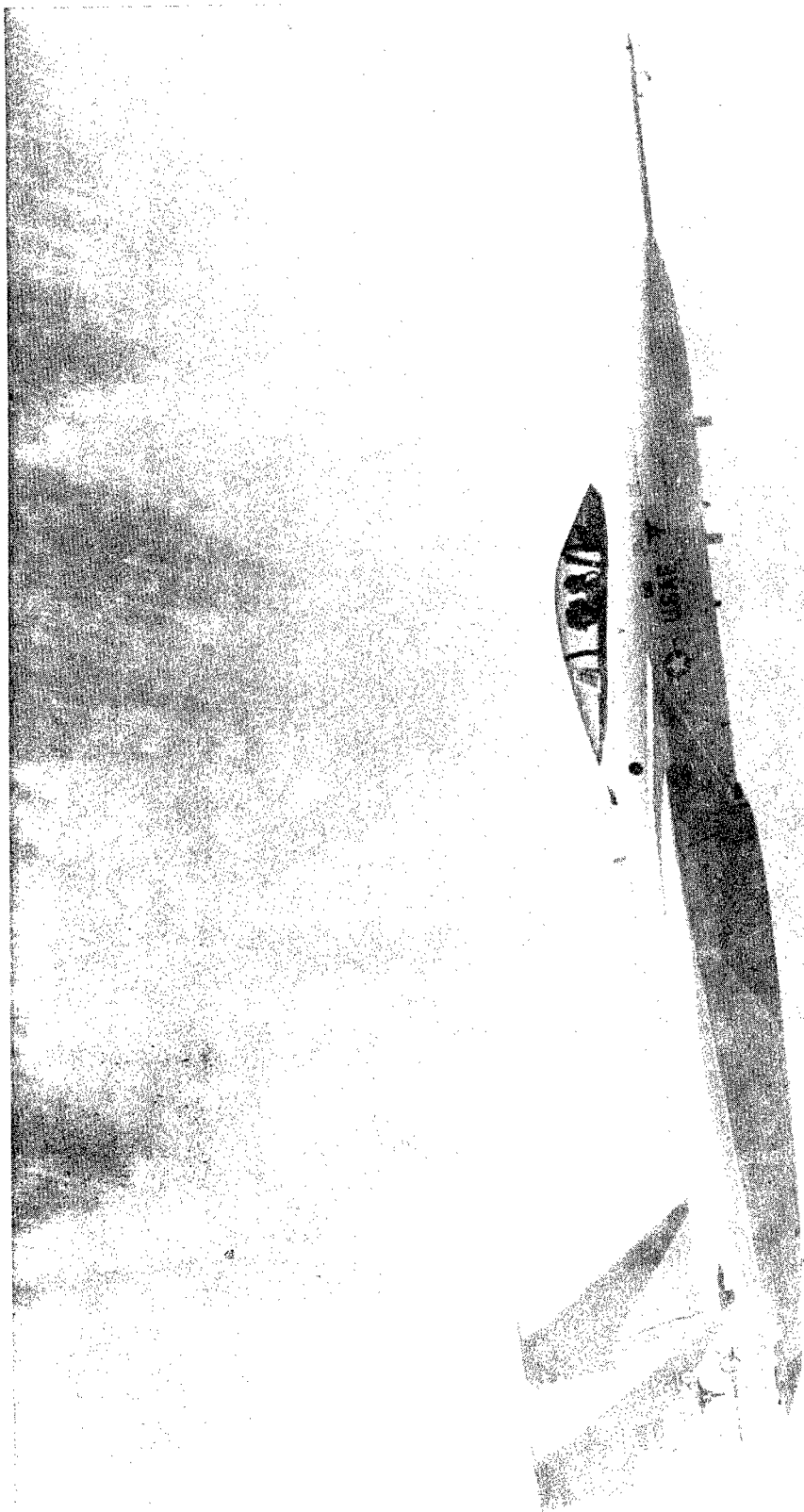


FIGURE 7

McDonnell-Douglas F-15  
Eagle

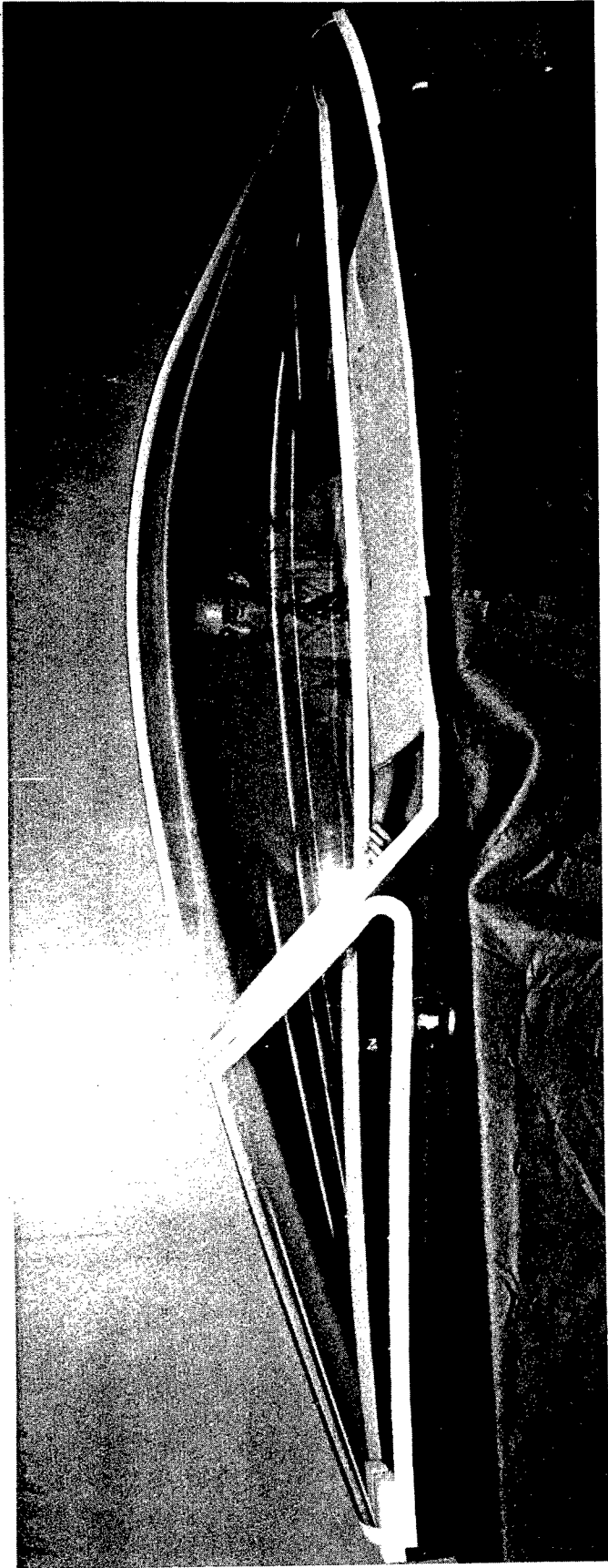


FIGURE 8

General Dynamics Lightweight Fighter  
YF-16 Polycarbonate Windshield (Right)  
Forward and Aft Canopies



STRETCHED ACRYLIC

WINDSHIELD WIPER TEST

OPTICAL EVALUATION

FIGURE 9

Stretched Acrylic After  
Wiper Test -- Uncoated (Right)  
Sierracote 311 Coated (Left)

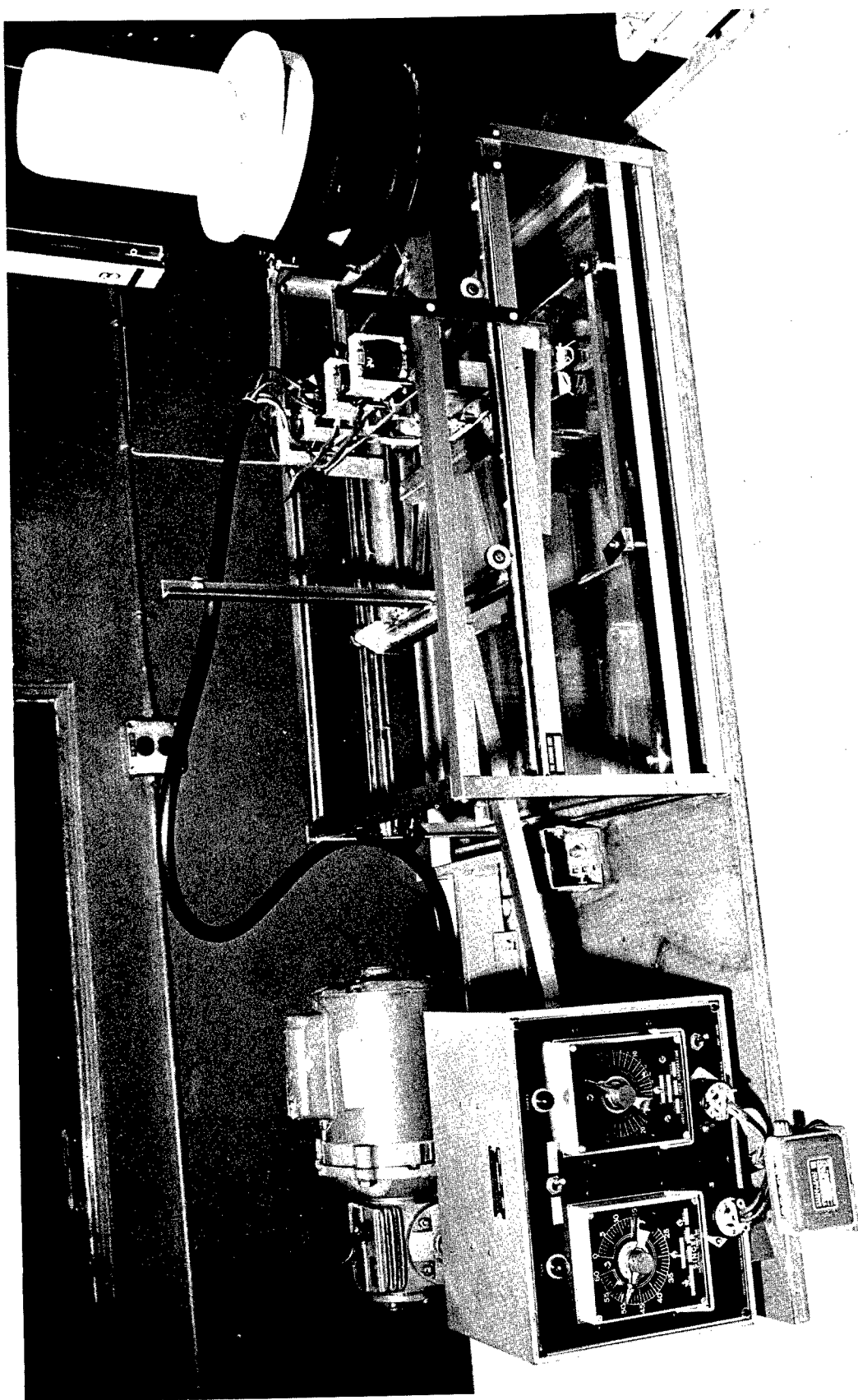


FIGURE 10  
Sierracin Surface  
Cleaning Simulator

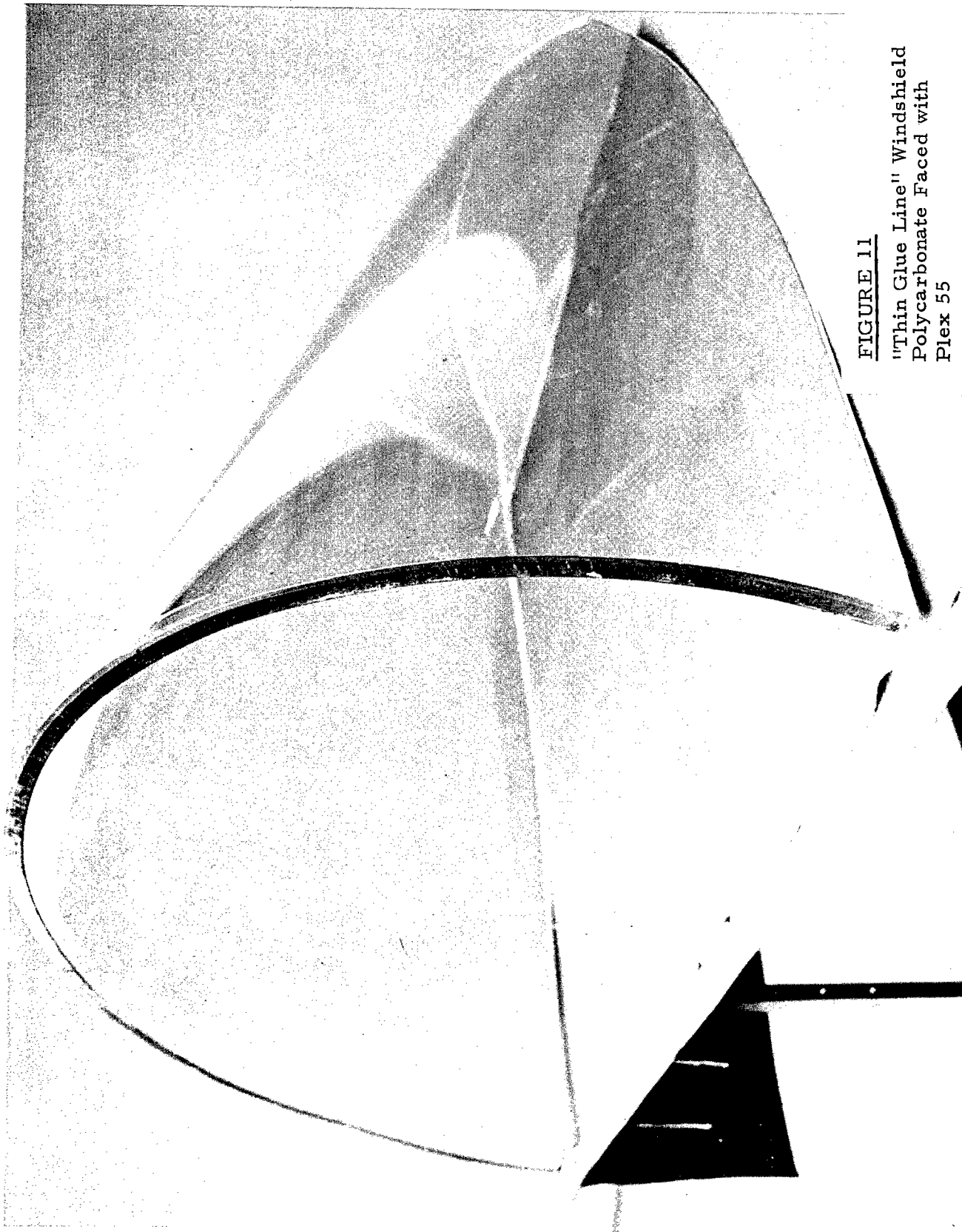


FIGURE 11  
"Thin Glue Line" Windshield  
Polycarbonate Faced with  
Plex 55

AN ANALYTICAL INVESTIGATION OF AIRCRAFT  
WINDSHIELD ANTI-ICING SYSTEMS

George C. Letton, Jr.  
Aeronautical Systems Division  
Wright-Patterson Air Force Base, Ohio



AN ANALYTICAL INVESTIGATION OF  
AIRCRAFT WINDSHIELD ANTI-ICING SYSTEMS

GEORGE C. LETTON, JR.  
ENVIRONMENTAL CONTROL & EQUIPMENT BRANCH  
DIRECTORATE OF PROPULSION & POWER ENGINEERING  
AERONAUTICAL SYSTEMS DIVISION  
WRIGHT-PATTERSON AFB, OHIO

ABSTRACT

The results of an in-depth study of the two windshield anti-icing methods used predominantly in today's aircraft are presented. The investigation was directed towards providing improved methods for determining the design requirements and performance of windshield anti-icing systems which use either an electrical conductive interlayer or an external hot-air jet as the heat source.

Available atmospheric icing data are discussed and recommended design ambient conditions (temperature, liquid water content, droplet diameter and altitude) are established for use in the design of future aircraft windshield anti-icing systems.

Analytical expressions are presented for calculating the heat required at the outer surface of an electrically heated aircraft windshield. Computer programs developed for rapidly calculating the required heat throughout the recommended design ambient icing conditions for any windshield configuration are cited. Graphs are presented which enable rapid estimation of the maximum required heat for any electrically heated windshield configuration. A graphical plotting technique is presented which enables one to have a complete picture of the maximum required heat at all points throughout the aircraft flight and icing envelopes.

Analytical expressions are presented for predicting the performance of a hot-air jet blast windshield anti-icing system. Discussion is included concerning the computer program developed to predict the windshield surface temperature at various distances downstream from the nozzle for any rectangular nozzle size, hot-air nozzle exit temperature and velocity, icing condition, and aircraft speed. Comparisons between analytical and experimental data for the windshield surface temperatures provided by hot-air jet blast windshield anti-icing systems are presented.

## INTRODUCTION

The capability to fly in adverse weather conditions is a design requirement for most military and commercial aircraft. Supercooled water droplets may exist in clouds at ambient temperatures far below the freezing point. These droplets are in an unstable thermodynamic state and would change to a solid if a nucleating substance or surface were present. When the supercooled water droplets are disturbed by an aircraft flying through them, the droplets will impinge and may freeze on wings, radomes, engine inlets, windshields and other areas. This results in weight and drag penalties, obstruction of vision through transparent surfaces, and the possibility of flight safety hazards. As a result, means are usually incorporated into the aircraft design to prevent ice buildup in critical areas.

Under adverse environmental conditions, maintenance of adequate visibility through aircraft windshields has been and remains a major concern to aircraft designers and users. Provisions are incorporated on most aircraft to provide an adequate field of vision for the crew during the adverse weather conditions of rain, snow and icing. It is essential that adequate visibility be maintained while landing the aircraft when operating under these adverse weather conditions. In addition, certain military aircraft have mission requirements which necessitate adequate visibility during numerous flight conditions other than just landing. The aircraft industry and government agencies within the United States are involved in a continuing effort to improve the methods of maintaining an adequate field of vision through aircraft windshields while flying in adverse weather conditions.

The investigation presented herein is directed mainly at providing improved analytical methods for determining the design requirements and performance of aircraft windshield anti-icing systems which use either an electrical conductive interlayer or an external hot-air jet as the heat source. These are the two types of windshield anti-icing systems used predominantly in today's aircraft.

## BACKGROUND

In the late 1930's, the NACA established the feasibility of three different windshield ice protection methods and the results of this work are presented in Reference 1. These methods were: (1) Internal electric heating by use of heating element wires between two panes of glass, (2) Internal hot-air heating by use of hot air passing through an air gap between two panes of glass, and (3) Alcohol dispensed on the external windshield surface in combination with a rotating wiper blade. Prior to 1941, most aircraft windshields were protected by alcohol spray systems which operated in conjunction with windshield wipers. United Air Lines pioneered the use of internally hot-air heated windshields. The double-paned windshields associated with the internal hot-air method introduce multiple reflections, particularly during night landings, and proved difficult to keep clean, but they were otherwise satisfactory. The NACA continued work on windshield ice protection in the 1940's as shown by References 2 and 3. These efforts were directed at establishing and outlining a procedure for calculating the heat required at the external windshield surface for ice prevention based on extensive flight tests. The results of this work are mainly applicable to internally heated windshields (electrical or hot-air); however, some data were obtained for a windshield ice prevention system in which heated air was discharged into the windshield boundary layer. The work presented in Reference 3 is the first known investigation of the external hot-air jet blast method of windshield ice prevention.

Probably the biggest development in the 1940's pertaining to windshield ice protection was the successful development of a very thin transparent electrical conductive coating which could be applied to an internal surface within a laminated windshield. The heat provided by the electrical conductive coating can be used to provide anti-icing for the external face of the windshield and defogging for the interior surface. The use of electrical heat also maintains the windshield interlayers of a glass/vinyl laminated windshield near the optimum temperature for resistance to bird impact. This method of windshield anti-icing was quickly adopted throughout the industry. It was first used on aircraft during World War II and is the most widely used method of aircraft windshield anti-icing today.

The advent of jet aircraft made possible the hot-air jet blast method of windshield anti-icing. This method was adopted on early military jet aircraft and it has been widely used on military aircraft, especially fighter type aircraft. The hot-air jet blast method is attractive for use on gas turbine powered aircraft because of the readily available engine compressor bleed air. An advantage of the hot-air jet blast method is that it can also be used for windshield rain removal. When the hot-air jet blast system is the only means of rain removal on the aircraft, the rain



removal requirements will dictate system design because it has been found that adequate rain removal demands a greater air flow rate than required for anti-icing.

With the development of effective in-flight applied liquid rain repellents in the early 1960's, the favored approach now for rain removal on high speed aircraft is to use a rain repellent in conjunction with a hot-air jet blast system. The repellent is effective by itself at all speeds above approximately 60 knots and the hot air is required only during ground static and taxi conditions. It has been found that this rain removal air flow requirement is less than that required for anti-icing. Therefore, the windshield anti-icing requirements dictate system design on aircraft which use a combination jet blast and rain repellent for windshield rain removal. When a rain repellent system is combined with a hot-air jet blast anti-icing system, it is possible to have both a good rain removal system and a good anti-icing system with minimum performance penalties to the aircraft.

The current trend in the design of commercial and military jet aircraft is to minimize the ice protection provisions. Ice protection is being eliminated for wing and tail surfaces on most new aircraft because it can be shown that the predicted ice buildup for all required missions does not adversely affect performance or create a flight safety hazard. Even though ice protection is being deleted on most new aircraft for the airfoils and in some cases the engine inlets, it is highly doubtful that the requirement for ice protection will ever be deleted for the windshields and certain air data sensors.

The current state-of-the-art of icing technology is about the same as it was in the late 1950's. The icing meteorological data used today is the same as generated from NACA work of the late 1940's and early 1950's. Icing technology progress since 1958 has been hampered because government research and development in this area was stopped in favor of work associated with hypersonic aircraft and space programs. The main contributions to icing technology since 1958 which are available to all of industry are References 4 and 5. Reference 4 is the result of a Federal Aviation Agency (FAA) sponsored study and it has become the "Bible" of the designers of ice protection systems and represents a very useful contribution to the art. Most of the significant fundamental principles and data about anti-icing technology developed prior to 1963 are to be found in Reference 4 or its comprehensive list of references. During April 1969, the FAA sponsored an Aircraft Ice Protection Symposium and the papers presented at this symposium are contained in Reference 5. They provide a general review of icing criteria, ice protection standards, methods of compliance and service experience. Most of the other contributions to icing technology since 1958 are the result of technology derived from actual aircraft development programs and the work financed by private corporations. Many of the reports developed through the efforts of these private corporations are of a proprietary nature and as a result are not available for industry-wide

usage. Most of the recent efforts in icing technology by industry have been directed towards improving the capability of accurately predicting ice accretion rates on airfoils and engine inlets.

Advances in windshield anti-icing since the 1950's have been limited mainly to the electrically heated windshield method. Advances in this area have been the development of new and improved conductive coatings, the use of new windshield materials, and various design changes in windshield construction to improve the life of heated windshields. There has been little improvement in the techniques used for predicting the quantity of heat required for electrically heated windshields. The methods most generally used in recent years for predicting the required heat are based on the procedures outlined in References 4, 6, 7, 8, and 9. All of these methods have the same shortcoming of requiring an extensive amount of repetitive hand calculating. The great quantity of hand calculations and the normal time shortage associated with the design of an aircraft make it impossible to look at all possible icing conditions. A recent publication concerning electrically heated windshields is Reference 9, which discusses the peculiarities of windshield anti-ice requirements in the helicopter environment.

There has been essentially no advancement in the state-of-the-art for the hot-air jet blast anti-icing method since the publishing of Reference 10 in 1958. The data presented in Reference 10 gives one a basis for making a "ballpark" estimate of the quantity of air flow required for windshield anti-icing. However, no analytical expressions were derived in Reference 10 for predicting the performance of a hot-air jet blast system as a function of the variables involved.

#### PURPOSE

For a number of years concern has existed within the Aeronautical Systems Division over several aspects of the design of aircraft windshield anti-icing. They are:

(1) The lack of available computerized methods for all of industry and government to use in calculating the required heat output to the exterior surface of an electrically heated windshield for all flight and icing conditions and all aircraft configurations.

(2) The lack of a generalized analytical approach and computer program for predicting the performance of a hot-air jet blast windshield anti-icing system. The lack of an acceptable analytical approach necessitates an extensive laboratory development test program for each new jet blast system.

(3) The possibility that currently established design meteorological conditions for icing are inadequate due to the fact that they were established approximately 20 years ago.

(4) The possibility that the current design requirements for heated windshields used on military aircraft cited in Reference 11 are inadequate. This specification defines the required heat as a function of speed only. The required heat quantity is known to be a function of a number of variables. Therefore, it was felt that the validity of the specification requirement should be investigated.

As a result of the above outlined areas of concern, the investigation presented herein was initiated. The goals of this investigation were as follows:

(1) Review all available atmospheric icing data and establish recommended design ambient conditions (temperature, liquid water content, droplet diameter and altitude) for use in the design of future aircraft windshield anti-icing systems.

(2) Develop analytical expressions for predicting the heat required at the outer surface of an electrically heated windshield for any aircraft configuration, speed and icing condition. Develop a computer program which rapidly calculates the required heat throughout the complete range of possible icing conditions for a particular aircraft configuration.

(3) Develop a generalized analytical expression for predicting the quantity of hot air required to maintain a particular height of windshield above freezing temperature for any rectangular nozzle size, hot-air nozzle exit temperature and velocity, icing condition and aircraft speed. Develop a computer program which rapidly calculates the performance of a hot-air jet blast windshield anti-icing system.

#### METEOROLOGICAL ICING CONDITIONS

Regardless of the method of windshield ice protection employed, the meteorological icing conditions stipulated as design requirements greatly influence system design. It is necessary to define requirements which will produce an effective windshield anti-icing system and at the same time not over design the system and possibly penalize the overall aircraft by requiring excessive electrical power or engine bleed air. The parameters which must be defined for a particular icing condition are liquid water content, effective droplet diameter, temperature, altitude and the horizontal and vertical extent of the condition.

The relationship between an optimum envelope of design meteorological icing conditions and the actual statistical distributions of the parameters as found in the atmosphere is complex. The actual atmospheric conditions are highly variable and the most extreme conditions are of brief time duration and small horizontal and vertical extent. The probability of encountering severe icing conditions is a function of the flight operating procedures and the climatological factors. The selection of design

meteorological icing conditions also requires consideration of the tolerance of the ice protection system to temporary overloading and its ability to recover after short periods in extreme icing conditions.

Icing clouds fall into the two general categories of stratus and cumulus. The characteristics of these two types of icing clouds as shown in Reference 4 are as follows:

(1) Stratus - These are layer type clouds that are characterized by moderate liquid water content ( $0.1$  to  $0.8 \text{ gm/m}^3$ ), maximum probable cloud depth of 6,500 feet, mean effective droplet diameters of 10 to 40 microns, temperature of  $+32^\circ\text{F}$  to  $-22^\circ\text{F}$ , altitude of sea level to 22,000 feet and horizontal extent of 20 to 200 miles.

(2) Cumulus - These clouds are characterized by high liquid water content ( $0.2$  to  $2.5 \text{ gm/m}^3$  or more), mean effective droplet diameters of 10 to 50 microns, temperatures of  $+32^\circ\text{F}$  to  $-22^\circ\text{F}$ , altitudes of 4,000 feet to 22,000 feet and horizontal extent of 2 to 6 miles.

The terminology "continuous maximum" has been applied to the atmospheric icing conditions associated with stratus clouds and the terminology "intermittent maximum" has been applied to the atmospheric icing conditions associated with cumulus clouds.

The NACA and cooperating groups conducted a rather extensive investigation of natural icing conditions over a number of years. These investigations began in 1944 and ended in 1959 and the results of these efforts are contained in Reference 4 and its comprehensive list of references. The data contained in these references form the major part of icing statistical data available today and are the basis for most U.S., Canadian, and British commercial and military design criteria. There have been no major efforts in the U.S. since 1959 to obtain additional natural icing data.

From the natural icing data gathered by NACA, envelopes for the various icing parameters associated with stratus and cumulus clouds were developed. The icing envelopes used for the design and certification requirements for commercial transport aircraft in the U.S. are contained in Reference 12. The same requirements with slight modifications are cited in Reference 13 as the design icing requirements for flight surfaces, ram air inlets, radomes, antennas and sensor windows of USAF aircraft. The icing design requirements for windshields of military aircraft are contained in Reference 11 as previously stated.

Although the currently used design icing envelopes of References 12 and 13 are based on data now approximately twenty years old, they are generally consistent with all the NACA gathered data and the data that have become available since their adoption. Since very little additional natural icing data have been gathered, the best tool for evaluating the adequacy of the currently used design icing envelopes is aircraft operational experience since their adoption. A high degree of flight safety has been demonstrated by aircraft certified to these icing envelopes and, therefore, it may be concluded that these design icing requirements are adequate. The relatively

few accidents attributed to icing encounters have generally involved older aircraft designed prior to use of these design icing envelopes.

Figures 1 and 2, which are based on a portion of the NACA natural icing data, show the number of icing encounters for particular temperature and altitude conditions for both stratus and cumulus icing clouds. An analysis of the data presented by Figures 1 and 2 and other data contained in Reference 4 and its list of references indicates a very low probability of icing encounters at altitudes above 22,000 feet or temperatures below  $-22^{\circ}\text{F}$ . Also, there is a very low probability of sea level icing encounters at temperatures below  $0^{\circ}\text{F}$ . It is not considered necessary to evaluate the intermittent maximum icing conditions for droplet diameters of less than 20 microns. The icing conditions for droplet diameters less than 20 microns are less critical because the reduction in catch efficiency with the smaller diameters outweighs the increase in liquid water content. Based on the reasons cited in this paragraph and the fact that windshield anti-icing systems are somewhat tolerant to off-design conditions, it is concluded that the design icing envelopes for windshield anti-icing should be reduced somewhat from those of References 12 and 13 in order to not over design the system. The recommended design meteorological icing conditions for aircraft windshield anti-icing systems are shown by Figures 3 and 4.

#### ELECTRICALLY HEATED WINDSHIELD ANALYSIS

The following analytical procedure defines the method of analysis, the assumptions made, and the derivation of the basic equations used in determining the heat required at the exterior surface of electrically heated windshields during flight in icing conditions. Figure 5 depicts the typical aircraft electrically heated windshield configuration used in the analysis presented herein. The analysis is based on maintaining the outer surface at  $35^{\circ}\text{F}$  in a "running wet" condition. The design value of  $35^{\circ}\text{F}$  for outer windshield surface temperature was selected because this is the value commonly used to assure that the surface temperature is maintained above the freezing point of water. The conservative value of  $35^{\circ}\text{F}$  has been used to allow for uncertainties due to variations in heat load gradients, heat transfer coefficients, water catch, etc.

##### Total Heat Loss at Outer Windshield Surface, $q_s$

The total unit heat flow,  $q_s$ , in  $\text{Btu/hr-ft}^2$  at the outer surface of an aircraft windshield during flight in icing conditions can be expressed by the sum of four individual heat losses as follows:

$$q_s = q_1 + q_2 + q_3 + q_4 \quad (1)$$

where

$q_1$  is the heat loss due to forced convection

$q_2$  is the heat loss due to the heating of the impinging water droplets (includes consideration of kinetic energy available from drops)

$q_3$  is the heat loss due to evaporation of some or all of the impinging water droplets

$q_4$  is the heat loss due to radiation

Each of these four individual heat losses are now analyzed in detail.

#### Convection Heat Loss, $q_1$

The basic equation for the unit convective heat loss is expressed by

$$q_1 = h_{avg} (t_s - t_{aw}) \quad (2)$$

where

$h_{avg}$  is the average convective heat transfer coefficient over the surface of the windshield in Btu/hr-ft<sup>2</sup> - °F

$t_s$  is the outside windshield surface temperature, which is 35°F for this analysis as previously stated

$t_{aw}$  is the adiabatic wall temperature in °F and is expressed by

$$t_{aw} = t_{\infty} + \frac{rU_L^2}{2g c_p J} \quad (3)$$

where

$t_{\infty}$  is the ambient temperature in °F

$r$  is recovery factor

$U_L$  is the local velocity over the windshield surface in ft/sec

$g$  is the acceleration of gravity in ft/sec<sup>2</sup>

$c_p$  is the specific heat of air in Btu/lb - °F

$J$  is the mechanical equivalent of heat, 778 ft-lb/Btu

The aircraft windshield case is assumed equivalent to flow over a flat plate and the analysis is based on the existence of a turbulent boundary layer. Therefore, an equation must be selected for calculating  $h_{avg}$  which is based on turbulent flow over a flat plate. Turbulent flow should usually exist over the aircraft windshield area for the flight conditions of interest in an icing analysis because of the velocities involved and the usual distances of the windshield from the stagnation point.

As a result of the assumption of turbulent flow, the recovery factor,  $r$ , may be expressed in terms of the Prandtl number,  $Pr$ , for air as follows:

$$r = Pr^{1/3} = \sqrt[3]{\frac{c_p \mu}{k}} \quad (4)$$

where

$\mu$  is dynamic viscosity of air in lb/ft-sec

$k$  is thermal conductivity of air in Btu/hr-ft-°F

The local velocity over the windshield,  $U_L$ , is assumed equal to the freestream or aircraft velocity,  $U_\infty$ , in ft/sec for the purposes of this analysis. The local velocities over certain parts of an aircraft may differ greatly from the freestream velocity. However, as indicated by Figure 4 of Reference 14, the local velocity over the windshield area of an aircraft does not vary greatly from the aircraft velocity for subsonic operation. This assumption is considered conservative because the local velocity over the windshield is expected to be less than the freestream velocity. As a result, the computed convective heat loss from this analysis may be somewhat greater than it would be if the actual local velocities were used. It would be necessary to use a complicated potential flow field digital computer program in order to use actual local velocities in this analysis. A flow field computer program requires an extensive amount of computer time and a great deal of time to learn how to use it properly. The incorporation and use of such a computer program in this analysis is considered unnecessary. It is considered unnecessary because the accuracy of the approach presented herein is considered adequate for aircraft design purposes as shown later by comparison of calculated values with flight test data.

Several equations for calculating the coefficient of convective heat transfer for turbulent flow over a flat plate have been developed over the years and are presented in published literature. The electrically heated aircraft windshield case in reality is a heated flat plate at essentially a constant surface temperature preceded by an unheated starting section. References 15 and 16 present equations for the coefficient of convective heat transfer which cover this particular type of case. The two equations presented in these two references were considered for use in this analysis along with equation 1C-107 of Reference 6 for the case of a constant

temperature flat plate without an unheated starting section. Each of these three equations were used in calculating windshield surface temperatures for the icing conditions evaluated during the flight testing of the Lockheed C-5 and Northrop F-5 aircraft. A comparison of the results obtained from the use of each of these three equations with flight test data indicates the equation from Reference 6 is the best for use in this analysis. The details of this comparison of the different heat transfer coefficients are presented later herein.

As a result of the above discussion and the fact that the heat transfer coefficient at the center of the windshield is approximately equal to the average coefficient over the windshield, the equation selected for  $h_{avg}$  in this analysis is expressed by

$$h_{avg} = 0.0296 \frac{k}{x} Re_x^{0.8} Pr^{0.333} \quad (5)$$

where

$x$  is the distance from the stagnation point to the center of the heated windshield area in feet

$Re_x$  is the dimensionless Reynolds number at the center of the heated windshield area

In selecting the proper value for  $x$ , a knowledge of the flow characteristics over the forward portion of the aircraft is required. The stagnation point is assumed to be at the aircraft nose for cases where the windshield blends quite smoothly with the fuselage nose contours. For applications where the windshield makes a sharp break with the contour of the nose, then the stagnation point may be at the windshield base or between the nose and the windshield base.

Since the analysis presented herein is valid for turbulent flow only, the value of  $Re_x$  should be greater than  $5 \times 10^5$ . The equation for the dimensionless  $Re_x$  is expressed as

$$Re_x = \frac{\rho U_L x}{\mu} \quad (6)$$

The value for air density,  $\rho$ , in  $lb/ft^3$  is calculated by the expression

$$\rho = \frac{P_B}{(53.35) (T_{aw})} \quad (7)$$



where

$P_B$  is the barometric pressure in  $\text{lb/ft}^2$

$T_{aw}$  is the adiabatic wall temperature in  $^{\circ}\text{R}$

A value of  $0.24 \text{ Btu/lb} - ^{\circ}\text{F}$  is used for the specific heat of air in this analysis. Air properties for  $\mu$  and  $k$  used in calculating  $q_1$  are based on  $t_{ref}$  which is defined by the following expression

$$t_{ref} = \frac{t_{\infty} + t_s}{2} \quad (8)$$

#### Heating of Impinging Water Droplets, $q_2$

The basic equation for the unit heat loss due to the heating of the water droplets impinging on the windshield heated area, which takes into consideration the kinetic energy available from the drops, is expressed by

$$q_2 = M_w c_{pw} (t_s - t_{\infty} - \Delta t_{kw}) \quad (9)$$

where

$M_w$  is the mass of water impinging on the heated area in  $\text{lb/hr-ft}^2$

$c_{pw}$  is the specific heat of water =  $1.0 \text{ Btu/lb} - ^{\circ}\text{F}$

$\Delta t_{kw}$  is the temperature rise due to the kinetic energy of the water droplets

The mass of water impinging on the windshield heated area is given by

$$M_w = 0.225 E (\text{Sine Angle } 1) (\text{Cosine Angle } 2) U_{\infty} (\text{LWC}) \quad (10)$$

where

$E$  is collection efficiency

$\text{LWC}$  is the liquid water content of the ambient air in  $\text{gm/m}^3$

The impingement of water droplets on an aircraft windshield is assumed equivalent to that of a rectangular half body (semi-infinite rectangle) having a half width the same as the projected height of the windshield heated area. Data for the collection efficiency and the procedure for calculating the collection efficiency of a rectangular half body are

contained in Reference 17. The procedure outlined in Reference 17 is used in this analysis for calculating the collection efficiency of an aircraft windshield. It is realized that this approach for predicting the collection efficiency for a windshield based on a rectangular half body perpendicular to the freestream is not likely to be highly accurate. However, this approach is considered conservative because the flow field around an aircraft windshield would not have to undergo as abrupt a change as around a rectangular half body; therefore, the collection efficiency for an equivalent windshield should probably be less than for an equivalent rectangular half body based on projected height of the windshield. To predict the collection efficiency accurately for all possible aircraft windshield and fuselage configurations would require the use of a complicated time consuming computer program for predicting droplet trajectories. The incorporation and use of such a computer program in this analysis is considered unnecessary for the reasons previously cited.

The collection efficiency of a windshield is a function of the free-stream Reynolds number,  $Re_o$ , and the dimensionless inertia parameter,  $K$ , which are defined as follows:

$$Re_o = \frac{2a\rho U_L}{\mu} \quad (11)$$

where

$a$  is droplet radius in feet

$$K = \frac{2\rho_w a^2 U_L}{9\mu(\text{Sine Angle } I)H} \quad (12)$$

where

$\rho_w$  is water density in  $\text{lb/ft}^3$

$H$  is length of heated windshield in vertical direction in feet

The collection efficiency,  $E$ , is then calculated by the following empirical equation taken from Reference 17.

$$E = \text{Antilog}_e \left[ \frac{\left( \frac{151}{K^2+150} + 0.267 + 0.225 Re_o^{0.28} \right) \left( 1.02 - \frac{180}{250+Re_o} \right)}{(K-0.15)^{0.74}} \right] \quad (13)$$

Figure 6 is a plot of the variation of E with  $Re_o$  and K as calculated by the above equation.

The temperature rise,  $\Delta t_k$ , due to the kinetic energy of the water droplets is expressed by

$$\Delta t_{k_w} = \frac{U_L^2}{2gJc_{p_w}} \quad (14)$$

### Heat Loss Due to Evaporation, $q_3$

The basic equation for the unit heat loss at the windshield surface due to evaporation of some or all of the impinging water droplets is expressed by

$$q_3 = M_{we} L_s F \quad (15)$$

where

$M_{we}$  is the maximum rate of evaporation which would occur in lb/hr-ft<sup>2</sup> if the total heated surface area is completely wet

$L_s$  is the latent heat of evaporation in Btu/lb of water at the windshield surface temperature,  $t_s$ . For this analysis  $L_s = 1073.46$  Btu/lb, since  $t_s = 35^\circ\text{F}$

$F$  is the surface wetness factor which varies between 0 and 1. It has a value of 1 for a completely wet surface and a value of 0 for a completely dry surface

From Reference 6, the maximum rate of evaporation,  $M_{we}$ , which could occur may be expressed by

$$M_{we} = k_m(W_s - W_\infty) \quad (16)$$

where

$k_m$  is the coefficient of mass transfer in lb dry gas/hr-ft<sup>2</sup>

$W_s$  is the absolute humidity at the liquid-air-interface in lb vapor/lb dry gas

$W_\infty$  is the absolute humidity of the surrounding ambient remote from the liquid-air interface in lb vapor/lb dry gas

From Dalton's law of partial pressures

$$W_s = \frac{0.622 P_s}{P_B - P_s} \quad (17)$$

where

$P_s$  is vapor pressure of saturated water at the windshield surface temperature,  $t_s$

$P_B$  is the barometric pressure

Since  $P_B \gg P_s$  for the application herein, then

$$W_s = \frac{0.622 P_s}{P_B} \quad (18)$$

By the same approach then

$$W_\infty = \frac{0.622 P_\infty}{P_B}$$

Therefore

$$W_s - W_\infty = \frac{0.622 (P_s - P_\infty)}{P_B} \quad (19)$$

where

$P_\infty$  is the vapor pressure of saturated water at the ambient temperature,  $t_\infty$

For a liquid evaporating into a gaseous atmosphere, it can be shown that there is a relationship between the mass transfer that takes place by evaporation and the heat transfer between the liquid and the gas. This relationship can be expressed by the Lewis relation,  $Le$ , which states

$$Le = \frac{h}{c_p k_m} \quad (20)$$

where

$h$  is the convective heat transfer coefficient

For air-water mixtures at low humidities  $Le = 0.89$  and use of this value is assumed valid for this analysis. Also, the previously calculated  $h_{avg}$  of Eq (5) is used for the value of  $h$  above.

Therefore

$$k_m = \frac{h_{avg}}{0.89 c_p} \quad (21)$$

Substituting Equations (19) and (21) and the value of 0.24 for the specific heat of air,  $c_p$ , into Equation (16)

gives

$$M_{we} = 2.91 h_{avg} \left( \frac{P_s - P_\infty}{P_B} \right) \quad (22)$$

The maximum rate of heat dissipation due to evaporation will occur when the wetness factor,  $F$ , is equal to 1. The value of  $F$  is 1 as long as the surface is completely wet. For this analysis, it is assumed that  $F = 1$  as long as the rate of water impingement on the windshield,  $M_w$  of Equation (10), is greater than the rate of evaporation  $M_{we}$  of Equation (22). For cases where the rate of impingement is less than the maximum rate of evaporation which could occur, then it is assumed that  $F = M_w/M_{we}$ . The rules used for calculating the wetness factor,  $F$ , may be summarized as shown below:

For  $M_w > M_{we}$ , then  $F = 1$

For  $M_w < M_{we}$ , then  $F = \frac{M_w}{M_{we}}$

The above assumptions are considered to be conservative. Inherent in the assumption of  $F = 1$  when  $M_w > M_{we}$  is the assumption that the water runs over the windshield heated area in a continuous sheet type of flow. However, in reality the flow over the windshield in many cases would be rivulet type flow with dry areas between the rivulets. Other investigators of this area have assumed rivulet flow for all conditions and as a result selected a constant value of  $F$  for all conditions.

In Reference 18, Northrop assumed a value of 0.6 for all conditions in analyzing the F-5 windshield heat requirements, and in Reference 19, Sierracin assumed a value of 0.2 for all conditions in analyzing the Cessna Citation windshield heat requirements. In reference 20, North American Aviation states that a value of 0.5 is considered to be the most realistic assumption. Other analyses, such as presented in Reference 21, have used a value of 1 for all conditions.

As can be seen by these cited references, there is no consistency on a recommended value for the wetness factor and none of the cited references have verified the validity of their wetness factor value for all icing conditions by test data. To date, there is no known theoretical or empirical correlation for calculating the value of the wetness factor for all icing conditions. It does not seem plausible that a constant value of F can be used for all icing conditions due to the wide range of water catch quantities that can be encountered.

The wetness factor is also influenced by the windshield surface material. Glass is very wettable or hydrophilic. Acrylic surfaces are naturally much less wettable than glass surfaces.

As shown by data presented later, the water catch rate during intermittent icing conditions can be much greater than the maximum evaporation rate. However, during continuous maximum icing conditions, the maximum water catch rate is close to the maximum evaporation rate. As a result, a value of F considerably less than 1 is probably realistic for continuous maximum icing while a value of 1 or near 1 is probably realistic during intermittent maximum icing conditions.

In conclusion, the approach presented for calculating the wetness factor is considered to be the best approach at present because, (1) It is conservative, (2) It accounts for a reduction in heat for the low water catch conditions, (3) Maximum heat is required for intermittent maximum icing conditions where F should have a value near or equal to 1, and (4) Accuracy using this approach is considered adequate for aircraft design purposes as shown later by comparison of the calculated values with flight test data.

#### Heat Loss Due to Radiation, $q_4$

The basic equation for the unit heat loss at the windshield outer surface due to radiation is expressed by

$$q_4 = \sigma \epsilon (T_s^4 - T_\infty^4) F_r \quad (23)$$

where

$\sigma$  is the Stefan-Boltzmann constant which equals  $0.173 \times 10^{-8}$  Btu/hr-ft<sup>2</sup>-°R<sup>4</sup>

$\epsilon$  is the emissivity of the windshield, which is assumed to be glass and have a value of 0.94 per Reference 6

$T_\infty$  is the absolute temperature of the ambient air in °R

$T_s$  is the absolute temperature of the windshield surface in  $^{\circ}\text{R}$ , which is  $495^{\circ}\text{R}$  for this analysis

$F_r$  is the radiation shape factor, which is assumed to have a value of 1 for this analysis

#### COMPUTER PROGRAMS AND CALCULATIONS FOR ELECTRICALLY HEATED WINDSHIELDS

Two computer programs have been developed which rapidly calculate the required heat at the outer surface for preventing ice on an electrically heated aircraft windshield during continuous maximum and intermittent maximum icing conditions for any aircraft configuration. These computer programs are based on the previously presented analysis and have been written to run on a Control Data Corporation 6600 computer system. One of the computer programs calculates the required heat for anti-icing throughout the complete range of meteorological conditions for continuous maximum icing defined by Figure 3. The other program calculates the required heat for anti-icing throughout the complete range of meteorological conditions for intermittent maximum icing defined by Figure 4.

The only input data required to run these two computer programs are data defining the particular aircraft configuration. These data are the windshield width and height, the distance from the stagnation point to the base of the windshield and angles 1 and 2 as defined by Figure 5.

The two programs are basically the same consisting of a main program, one subroutine subprogram and two function subprograms. The main program consists basically of numerous DO-loops which cause the program to calculate the windshield surface heat load for a range of aircraft velocities (100-500 knots) and the complete range of altitudes, temperatures, and median droplet diameters associated with the particular icing condition. The main purpose of the subroutine subprogram is to then calculate the total heat loss from the outer windshield surface for one particular set of environmental conditions and it includes all of the equations in the analysis previously presented. One of the function subprograms computes the partial pressure of water vapor in saturated air as a function of temperature. The other function subprogram calculates the liquid water content of the ambient air as a function of temperature and median droplet diameter for the particular icing condition. This function subprogram for each of the two icing conditions consists of polynomial equations for the ambient temperature curves of the upper graphs of Figures 3 and 4. The polynomial equations were obtained by use of available polynomial curve fitting computer programs.

The resulting output of these computer programs shows the values of  $q_1$ ,  $q_2$ ,  $q_3$ ,  $q_4$  and the total surface heat loss,  $q_s$ , for numerous possible combinations of aircraft velocity, ambient temperature, liquid water content, median droplet diameter and altitude. There are 570 combinations of these

conditions evaluated for continuous maximum icing and 560 combinations for intermittent maximum icing. Both programs include a sort routine to identify the five conditions requiring the maximum amount of heat.

For each combination of conditions evaluated by the computer programs, the water catch is computed on the basis of all droplets having the same size as the median diameter. In actual icing clouds, there will be a wide range of sizes present. Droplets considerably larger and smaller than the median may be present. For increased accuracy, a weighted sum corresponding to the specific droplet-size distribution pattern should be used in calculating water catch. However, this is difficult to do because the droplet size distribution pattern is variable, and use of a distribution pattern is not considered necessary for design purposes.

The two computer programs were used to evaluate the anti-icing heat requirements for 36 different aircraft configurations. The configurations evaluated and the calculated required maximum heat values for both continuous maximum and intermittent maximum icing conditions are shown in Table 1. Tables 2 and 3 present the calculated values for various important parameters for the configurations evaluated during the two icing conditions. The range of windshield heights, angles, and distances from the stagnation point were selected so as to cover the range of configurations most likely to be encountered when evaluating windshields located on the centerline of the aircraft with the base normal to the freestream. The results of the calculations show a wide difference in the required maximum heat values and the value is very much dependent on the configuration. The calculations show that the heat required for intermittent maximum icing conditions may be up to approximately 30% greater than for continuous maximum icing conditions. However, the percent of difference is not nearly this great for some configurations. The data of Table 1 show that in approximately one-half the cases the continuous maximum heat requirements are in excess of the current USAF design requirements for aircraft that can fly at speeds of 300 knots or greater. In almost all cases, the intermittent maximum heat requirements are greater than required by MIL-T-5842A.

Figures 7 through 9 show how the value for maximum required heat for continuous icing conditions varies with the distance from the stagnation point to the base of the windshield, windshield height, and the angle with the freestream (Angle 1). The same variations for intermittent maximum icing conditions are shown by Figures 10 through 12. An analysis of the data presented by Table 1 and Figures 7 through 12 shows that the value for maximum heat is decreased by increasing windshield height and increasing distance of the windshield base from the stagnation point. Increasing windshield height decreases the required heat because of a decrease in collection efficiency,  $E$ , with increasing height. Increasing the distance from the stagnation point decreases the required heat because of a reduction in the convective heat transfer coefficient with increasing distance from the stagnation point. This effect is much greater at short distances than at long distances from the stagnation point as shown by Figures 7 through 12.



In most cases, the result of increasing angle 1 while maintaining the same distance from the stagnation point is a reduction in the maximum heat due to a reduction in the collection efficiency. Increasing the angle has the same result of decreasing collection efficiency as increasing the windshield height. Increasing angle 1 decreased the required maximum heat for all configurations evaluated for continuous maximum icing conditions. The same result was obtained for configurations 13-36 during intermittent maximum icing conditions. This result was not obtained in all cases for configurations 1-12 because the resulting change in other variables which enter into the calculation of the total water catch,  $M_w$ , had a greater increase than the reduction in collection efficiency.

Verification of these conclusions concerning the effects of increasing distance from stagnation point, windshield height, and angle 1 can be determined by the parameter values presented in Tables 2 and 3 and the use of Figure 6.

Table 4 shows the combination of altitude, velocity, median droplet diameter and ambient temperature which results in the maximum heat requirement for both icing conditions and all the configurations evaluated. An analysis of the data presented in Table 4 shows that the same condition does not always define the maximum heat requirement. Table 4 shows that the maximum heat requirement for continuous maximum icing occurs in most cases at 7,000 feet altitude. Three of the configurations did have the maximum heat requirement for continuous maximum icing to occur at 22,000 feet and these were windshield configurations having a height of 4 feet, which was the maximum evaluated.

The altitude at which the maximum heat requirement for intermittent maximum icing occurs is split between 14,000 feet and 22,000 feet for the configurations evaluated. In general the shortest windshield configuration evaluated, 1.5 feet, required the maximum heat at 22,000 feet and the greater height configurations had the maximum heat requirement at 14,000 feet.

Figures 13 through 17 present a plot of the maximum heat required versus velocity for the ambient temperature conditions at each particular altitude evaluated for configuration 19 and continuous maximum icing conditions. Configuration 19 is equivalent to the Northrop F-5A/B aircraft configuration. The points on each curve of Figures 13 through 17 represent the maximum heat required for the range of median droplet sizes for that particular velocity, temperature and altitude condition.

The dashed line on each figure represents the locus of points requiring the maximum heat for a particular ambient temperature. Figure 18 is a consolidation of the locus lines of maximum heat from Figures 13 through 17 and presents a complete picture of the maximum heat required versus velocity for any altitude and ambient temperature of the complete continuous maximum icing envelope of Figure 3.

Figures 13 through 18 were plotted from data obtained by use of the computer programs previously mentioned. These figures show how the data obtained rapidly from the computer programs can be used to quickly analyze the heat requirements for a particular configuration over both of the icing envelopes. The approach of using both the computer program and the graphical plots shown is considered to be a very useful tool for getting a complete picture of the windshield anti-icing heat requirements.

For applications where a limit is placed on the heat output from the electrical interlayer which is less than that determined necessary for all of the possible icing conditions, graphical plots like Figure 18 will show the portions of each icing envelope which cannot be met with the heat provided. This approach can be used for determining the maximum required heat for aircraft which are incapable of flight throughout the complete altitude and speed range evaluated by the computer program, since once the graphs are obtained, then the altitudes and speeds not encountered can be easily eliminated from the plot. This technique can also be applied to aircraft applications where mission requirements are such that operation is infrequent are unlikely throughout portions of the altitude and speed range evaluated by the computer program. The maximum required heat can be determined by modifying the graphical plots to eliminate those portions where operation is infrequent or unlikely.

In addition to the two programs just discussed, a computer program was developed to calculate the outer surface temperature of an electrically heated aircraft windshield during a particular icing condition with a known heat input to the outer surface. The computer program was written to run on a Control Data Corporation 6600 computer system. The computer program consists of a main program, one subroutine subprogram and one function subprogram.

The approach used for computing the windshield exterior surface temperature is basically the same as that used for computing the exterior surface heat loss except the basic equations are rearranged to solve for surface temperature in lieu of heat loss. Using the previously defined equations for  $q_s$ ,  $q_1$ ,  $q_2$ ,  $q_3$ , and  $q_4$  and rearranging and combining results in the following equation for  $t_s$

$$t_s = \frac{q_s + h_{avg} t_{aw} + M_w c_{pw} (t_{\infty} + \Delta k_w) - M_{we} L_s F}{h_{avg} + M_w c_{pw}} \quad (24)$$

All values on the right hand side of the above equation, except  $q_s$  and  $L_s$ , are calculated as described in the previous electrically heated windshield analysis. The value for  $q_s$  in this case is the known value for heat input from the electrical interlayer to the outer surface. Since the latent heat of evaporation for water,  $L_s$ , varies with temperature and the surface temperature will not necessarily be 35°F, it is necessary to use an equation for calculating  $L_s$  as a function of temperature. For temperatures in the range of 32°F to 120°F, the latent heat of water is a linear

function of temperature and the following equation was developed for use in calculating  $L_s$

$$L_s = 1093.25 - 0.5653 t_s \quad (25)$$

The main reason for developing the computer program for predicting windshield surface temperature was to have a tool for verifying adequacy of the analytical approach presented previously for an electrically heated windshield.

Flight test data were obtained from Reference 22 for the Lockheed C-5 aircraft and Reference 23 for the Northrop F-5 aircraft which showed the measured windshield surface temperature for various flight and icing conditions with a known value of heat input to the exterior windshield surface.

Table 5 shows a comparison of the flight test data with temperatures calculated by the computer program for predicting windshield surface temperature using three different methods for calculating  $h_{avg}$ . A comparison by the sum of the squares of the deviations of the calculated surface temperatures with the flight test temperatures showed that Method 1 using Equation (5) for  $h_{avg}$  is overall the best for use in predicting the windshield surface temperature during icing conditions. The calculated temperature values using Equation (5) give reasonable agreement with the flight test data and as a result Equation (5) was selected for use in the analysis presented herein. Also, the fairly close agreement of flight test data and calculated temperatures, indicates that the analytical approach presented for an electrically heated windshield is adequate for design purposes.

Reference 24 contains a source deck listing for each of the three computer programs previously discussed. Card decks for these programs are available from the author upon request.

#### HOT-AIR JET BLAST ANALYSIS

A hot-air jet blast windshield anti-icing system operates on the principle of blasting a high temperature, high velocity air stream over the windshield exterior surface, thus deflecting, scrubbing, and evaporating moisture from the windshield surface. This type of system is most compatible with gas turbine powered aircraft because of the readily available engine compressor bleed air. The system is based on ducting hot engine compressor bleed air to a nozzle located at the base of the windshield.

The air from the jet blast system is sufficiently warm as it leaves the nozzle to maintain the temperature of the windshield above the freezing point of water, but its temperature decays very rapidly as it flows over the windshield. In order to be able to apply an analytical approach to the

design of a hot-air jet blast windshield anti-icing system for a new aircraft, it is necessary to have a generalized analytical expression which takes into account this temperature decay and predicts the resulting windshield surface temperature with distance from the nozzle for all operational conditions. Such a generalized analytical expression, which takes into account all of the variables involved, has not been available for use in the design of hot-air jet blast windshield anti-icing systems in the past.

The following analytical procedure defines the method of analysis, the assumptions made and the derivation of the basic equations used in developing a generalized analytical expression for predicting the performance of a hot-air jet blast aircraft windshield anti-icing system. Figure 19 depicts the typical hot-air jet blast system configuration used in the analysis presented. The nozzle design for this analysis is based on a thin continuous rectangular slot located at the base of the windshield and oriented so that the nozzle lower edge is flush with the windshield surface and discharges the air parallel to the windshield surface. This type of nozzle design has been shown to be the best in the past by Reference 10, and it is the design most predominantly used on aircraft to date.

#### Exterior Surface Heat Balance at Distance x from Nozzle

For steady state conditions, the total unit heat gain equals the total unit heat loss at any particular location, x, on the windshield exterior surface downstream from the jet blast nozzle and may be expressed by

$$q_{jb} + q_c = q_i + q_r + q_e \quad (26)$$

where

- $q_{jb}$  is the heat gain from the jet blast air in Btu/hr-ft<sup>2</sup>
- $q_c$  is the heat gain from the cockpit of the aircraft in Btu/hr-ft<sup>2</sup>
- $q_i$  is the heat loss due to the heating of the impinging water droplets (includes consideration of the kinetic energy available from the drops) in Btu/hr-ft<sup>2</sup>
- $q_e$  is the heat loss due to evaporation of some or all of the impinging water droplets in Btu/hr-ft<sup>2</sup>
- $q_r$  is the heat loss due to radiation in Btu/hr-ft<sup>2</sup>

Each of the above terms are now discussed in more detail.

### Jet Blast Heat Gain, $q_{jb}$

The basic equation for the unit convective heat gain by the exterior windshield surface at point x from the high velocity hot-air jet may be expressed by

$$q_{jb} = h_x (t_{aw_x} - t_{s_x}) \quad (27)$$

where

$h_x$  is the convective heat transfer coefficient at x in Btu/hr-ft<sup>2</sup>-°F

$t_{aw_x}$  is the adiabatic wall temperature at x in °F

$t_{s_x}$  is the windshield surface temperature at x in °F

### Cabin Heat Gain, $q_c$

The basic equation for the unit heat gain by the exterior windshield surface at point x from the cockpit air may be expressed by

$$q_c = U(t_c - t_{s_x}) \quad (28)$$

where

U is the overall heat transfer coefficient between the outer windshield surface and the interior cabin air in Btu/hr-ft<sup>2</sup>-°F

$t_c$  is the cockpit air temperature in °F, which is assumed to be 70°F for this analysis

### Impinging Water Droplet Heat Loss, $q_i$

The basic equation for the unit heat loss at point x due to the heating of the water droplets impinging on the windshield heated area, which takes into consideration the kinetic energy available from the drops, is expressed by

$$q_i = M_w c_{pw} (t_{s_x} - t_{\infty} - At_{kw}) \quad (29)$$

All terms of Equation (29) are as previously defined in the electrically heated windshield analysis except  $M_w$ . The analysis for the hot-air jet

blast system is limited to windshields with the base perpendicular to the aircraft centerline, and therefore,  $M_w$  is expressed by

$$M_w = 0.225 E (\text{Sine Angle } l) U_\infty (\text{LWC}) \quad (30)$$

For the jet blast case, it is assumed that the mass of water catch  $M_w$ , in lb/hr-ft<sup>2</sup> over the windshield area is the same as would exist for a windshield without a jet blast system. As a result, the collection efficiency is calculated in the same manner as used in the electrically heated windshield analysis previously presented.

#### Evaporative Heat Loss, $q_e$

The basic equation for the unit heat loss of the exterior windshield surface at point x due to evaporation of some or all of the impinging water droplets is expressed by

$$q_e = M_{we_x} L_{s_x} F_x \quad (31)$$

where

$M_{we_x}$  is the maximum rate of evaporation which would occur in lb/hr-ft<sup>2</sup> if the surface at point x was completely wet

$L_{s_x}$  is the latent heat of evaporation in Btu/lb of the water at the windshield surface temperature,  $t_{s_x}$

$F_x$  is the surface wetness factor at point x which varies between 0 and 1. It has a value of 1 for a completely wet condition at x and a value of 0 if the surface is dry

Since high windshield surface temperatures are likely to be encountered in the hot-air jet blast case, it is no longer valid to assume  $P_s < P_B$  as was done in the electrically heated windshield analysis. As a result, the maximum rate of evaporation per Reference 6 is expressed by

$$M_{we_x} = 2.91 h_x \left[ \frac{P_s - P_\infty}{P_B (1 - \frac{P_s}{P_B}) (1 - \frac{P_\infty}{P_B})} \right] \quad (32)$$

For the range of temperatures likely to be encountered, the latent heat of water is no longer a linear function of temperature. As a result, a polynomial curve fitting program was used to develop an equation for the latent heat of water as a function of temperature for temperatures in the

range of 32° to 500°F. The resulting equation is expressed by

$$L_{s_x} = 1092.971 + A(t_{s_x}) + B(t_{s_x})^2 + C(t_{s_x})^3 + D(t_{s_x})^4 \quad (33)$$

where

$$\begin{aligned} A &= -0.558414 \\ B &= -4.773113 \cdot 10^{-6} \\ C &= -1.929251 \cdot 10^{-7} \\ D &= -1.190444 \cdot 10^{-9} \end{aligned}$$

For the hot-air jet blast case, rivulet flow and dry surface areas are more likely to be encountered than for the electrically heated windshield due to the high velocity jet flowing over the exterior surface. As a result of this and good correlation of analytical results with test data, the following method was selected for calculating the wetness factor,  $F_x$ , in this analysis:

$$F_x = \frac{M_w}{3M_{wex}} \quad (34)$$

The factor 3 is introduced in the denominator to account for the rivulet flow reduction of the wetness factor. In addition, the factor 3 helps account for the fact that a portion of the droplets are evaporated within the jet before striking the windshield. A value of 3 was used because this resulted in the best correlation of analytical results with test data.

#### Radiation Heat Loss, $q_r$

The basic equation for the unit heat loss at point x on the windshield outer surface due to radiation is expressed by

$$q_r = \sigma \epsilon (T_{s_x}^4 - T_{\infty}^4) F_r \quad (35)$$

#### Equation for Windshield Surface Temperature - Jet Blast

In order to simplify the resulting equation for calculating the surface temperature of a hot-air jet blast heated windshield during icing conditions, the heat loss due to radiation, Equation (35), is neglected. The results of the electrical analysis show the heat loss due to radiation is small, and therefore, it can be neglected. Substituting Equations (27), (28), (29), and (31) into Equation (26) and rearranging and solving for  $t_{s_x}$  while neglecting radiation results in the following equation for the surface temperature at any point downstream from the nozzle for a hot-air jet blast heated windshield:

$$t_{sx} = \frac{h_x t_{awx} + U t_c + M_w(t_\infty + \Delta t_{kw}) - M_{we_x} L_{sx} F_x}{h_x + U + M_w} \quad (36)$$

All terms, except  $h_x$  and  $t_{awx}$ , in the above equation can be readily calculated or are known quantities as previously discussed. The values of the convective heat transfer coefficient,  $h_x$ , and the adiabatic wall temperature,  $t_{awx}$ , at any point  $x$  from the nozzle are dependent on the velocity and temperature of the hot-air jet at the particular point. The velocity and temperature of the air jet are decaying very rapidly with distance as the air mixes with the external freestream air and their decay is a function of a number of parameters. The complexity of the mechanism involved in the interaction of the hot-air jet and the cold external flowing freestream makes it very difficult to calculate the velocity and temperature of the jet with distance from the nozzle on a strictly theoretical basis. As a result, it is necessary to resort to empirical methods for predicting the jet temperature and velocity.

The configuration under consideration in this analysis is commonly referred to in published literature as a plane turbulent wall jet with a parallel freestream. A literature search was conducted to determine available published reports dealing with plane turbulent wall jets and a number of papers and reports pertaining to work in this area were uncovered. Most of the published literature for plane turbulent wall jets is directed towards the film-cooling application where the jet air is at a lower temperature than the total temperature of the external stream. All available reports were reviewed to determine if empirical correlations for  $h_x$  and  $t_{awx}$  were presented which covered all the variables involved in the hot-air jet blast windshield anti-icing system configuration under consideration in this analysis. Of all the reports reviewed, only three reports, References 25, 26, and 27, presented empirical correlations which were considered worthy of further consideration for use in this analysis. The work by Wieghardt presented in Reference 25 is the pioneer study of the effects of hot air injection from a discrete slot into a turbulent boundary layer. Wieghardt developed the following empirical correlation for predicting the surface temperature with distance from the nozzle:

$$\frac{t_{sx} - t_\infty}{t_n - t_\infty} = 21.8 \left(\frac{x}{s}\right)^{-0.8} \left(\frac{\rho_n U_n}{\rho_\infty U_\infty}\right)^{0.8} \quad (37)$$

where

$t_n$  is the temperature of the hot-air jet at the nozzle exit in °F

$s$  is the height of the nozzle slot as shown by Figure 19



$\rho_{\infty}$  is the density of the freestream air in lb/ft<sup>3</sup>

$\rho_n$  is the density of the hot-air jet at the nozzle exit in lb/ft<sup>3</sup>

$U_{\infty}$  is the freestream velocity in ft/sec

$U_n$  is the velocity of the hot-air jet at the nozzle exit in ft/sec

The work of Papell and Trout presented in Reference 26 resulted in the following empirical correlation for predicting the surface temperature with distance from the nozzle:

$$\frac{T_{s_x} - T_{\infty}}{T_n - T_{\infty}} = 12.6 \left( \frac{\rho_n U_n}{\rho_{\infty} U_{\infty}} \right) \left( \frac{s}{x} \right)^{0.72} \left( \frac{T_n}{T_{\infty}} \right)^{0.5} \quad (38)$$

where

$T_{s_x}$  is the surface temperature at x in °R

$T_n$  is the total temperature of the hot-air jet at the nozzle exit in °R

$T_{\infty}$  is the total temperature of the ambient free-stream air in °R

The work of Seban presented in Reference 27 resulted in the following empirical correlation for predicting the surface temperature with distance from the nozzle:

$$\frac{t_{aw_x} - t_{\infty}}{t_n - t_{\infty}} = 1.09 \left[ \left( \frac{\rho_{\infty}}{\rho_n} \right)^{1.5} \left( \frac{U_n - U_{\infty}}{U_n} \right)^{0.5} \left( \frac{U_n s}{12 \nu_n} \right)^{0.3} \left( \frac{x}{s} \right) \right]^{-0.5} \quad (39)$$

where

$\nu_n$  is the kinematic viscosity of the hot-air jet at the nozzle exit in ft<sup>2</sup>/sec

In addition, Seban also developed the following empirical correlation for the convective heat transfer coefficient,  $h_x$ , with distance from the nozzle:

$$\frac{h_x}{\rho_n U_n c_p} = 0.41 \left( \frac{U_n s}{12 \nu_n} \right)^{-0.3} \left( \frac{x}{s} \right)^{-0.6} \quad (40)$$

An analysis was conducted to determine if any of the above empirical correlations for temperature decay, Equations (37), (38) and (39), were acceptable for use in the windshield hot-air jet blast analysis.

Equation (37) was dropped from consideration because the nozzle design for the Wieghardt work was such that the hot-air jet was not discharged parallel to the windshield surface. North American, as shown by Reference 28, has been successful in using the Wieghardt correlation technique. Through test data, North American develops the appropriate constants for use in the empirical correlation for a specific nozzle design. As a result, the North American approach does not give a generalized equation. Since later analyses based on Reference 10 data showed the temperature decay to be dependent on considerably more parameters than contained in Equation (37), the Wieghardt correlation technique was not considered further for use in developing a generalized equation for temperature decay.

The acceptability of Equations (38) and (39) was investigated in great depth by comparing the temperatures predicted by these equations with experimental test data obtained from WADC TR 58-444, Reference 10.

Appendix IV of WADC TR 58-444 presents a large number of plots of windshield surface temperature versus distance downstream from the nozzle for a continuous rectangular slot nozzle located flush to the windshield surface and discharging the air parallel to the surface. A total of 46 of the test cases presented in WADC TR 58-444 for dry air conditions with the windshield located at an angle of 35° with the freestream were considered in this analysis. During the 46 test cases, various combinations of jet exit velocities (553 ft/sec, 829 ft/sec, and Mach 1), freestream velocities (50, 140 and 225 knots), jet exit total temperatures (250 and 450°F), nozzle flow rates (2, 4.5 and 7 lb/min/inch of nozzle length) and nozzle heights were used. A comparison of the predicted windshield surface temperatures using Equations (38) and (39) with the test data for the 46 cases of WADC TR 58-444 under consideration showed a wide difference between test values and predicted values of the two correlations for a number of the test conditions. Therefore, it was concluded that neither Equation (38) or (39) was acceptable for use in this analysis and the development of a new empirical correlation was required.

It was decided to develop a new empirical correlation for the adiabatic wall temperature,  $T_{awx}$  based on the data of the 46 test conditions of WADC TR 58-444 previously mentioned. The following generalized parametric relation for the dimensionless adiabatic wall temperature distribution was selected for determining if a satisfactory empirical correlation could be developed from the test data:

$$\frac{T_{awx} - T_{\infty}}{T_n - T_{\infty}} = a \left( \frac{\rho_{\infty}}{\rho_n} \right)^b \left( \frac{x}{s} \right)^c \left( \frac{U_n - U_{\infty}}{U_n} \right)^d (Re_n)^e (Re_{\infty x})^f \left( \frac{T_n}{T_{\infty}} \right)^g (Pr_n)^h (Pr_{\infty})^i \quad (41)$$

where

a,b,c,d,e, are constants to be determined  
f,g,h,i by correlation techniques

$T_{awx}$  is the adiabatic wall temperature  
at x in °R

$Re_n$  is the nozzle Reynolds number

$Re_{\infty x}$  is the freestream Reynolds number  
at point x

$Pr_n$  is the Prandtl number of the nozzle  
exit air

$Pr_{\infty}$  is the Prandtl number of the free-  
stream air

The equation for the nozzle Reynolds number is expressed by

$$Re_n = \frac{\rho_n U_n s}{12\mu_{\infty}} \quad (42)$$

The equation for the freestream Reynolds number is expressed by

$$Re_{\infty x} = \frac{\rho_{\infty} U_{\infty} x}{12\mu_{\infty}} \quad (43)$$

Two computer programs were used to arrive at the proper values for the constants contained in Equation (41). The values of the nine dimensionless expressions of Equation (41) were calculated with the computer program of Appendix D of Reference 24 for the 46 different test runs at three different values of x for each of the test runs giving a total of 138 test data cases used in developing an empirical correlation. The calculated values for the dimensionless parameters were then used as input data to an available computer program at the Computer Science Center, Wright-Patterson AFB, which computes the least-squares estimate of non-linear parameters. The program was set up in a manner to compute the values of the constants for Equation (41) on the basis of minimizing the absolute error between the test value and calculated value of  $(T_{awx} - T_{\infty}) / (T_n - T_{\infty})$  for the 138 test data cases. As a result of using the computer program in this manner, the following values were established for the constants of Equation (41):

|                             |                                 |
|-----------------------------|---------------------------------|
| $a = 0.10840800 \cdot 10^4$ | $f = -0.87089124 \cdot 10^{-2}$ |
| $b = 0.28518122 \cdot 10^2$ | $g = 0.46666781 \cdot 10^1$     |
| $c = -0.62386652$           | $h = 0.27404809 \cdot 10^3$     |

$$d = 0.23234195$$

$$i = -0.26457323 \cdot 10^3$$

$$e = -0.25074447$$

An analysis was conducted to determine the acceptability of the empirical correlation of Equation (41) using the above constants. This analysis was accomplished by comparing experimental test values for windshield surface temperatures under dry-air conditions from WADC TR 58-444 with calculated values using Equations (36), (40), (41) and the above constants for Equation (41). For dry-air conditions, Equation (36) simplifies to the following expression:

$$t_{s_x} = \frac{h_x t_{aw_x} + U t_c}{h_x + U} \quad (44)$$

For the experimental test results presented in WADC TR 58-444, it was assumed that the temperature on the interior side of the windshield,  $t_c$ , was equal to 70°F and the overall heat transfer coefficient,  $U$ , was equal to 1.28 Btu/hr-ft<sup>2</sup>-°F. The value of  $U$  was calculated on the basis of a windshield thickness of 0.75 inch, an assumed thermal conductivity for the glass of 0.54 Btu/hr-ft-°F, and an assumed value of 1.5 Btu/hr-ft<sup>2</sup>-°F for the free convection heat transfer coefficient on the internal surface of the windshield.

Figures 20 through 23 each contain four curves of windshield surface temperature versus distance downstream from the nozzle. Each figure is based on a particular test run of WADC TR 58-444 and curves are presented for the following:

- a. Experimental values for windshield surface temperature during dry air conditions.
- b. Calculated values for windshield surface temperature during dry air conditions based on the calculation method previously presented.
- c. Experimental values for windshield surface temperature during icing conditions.
- d. Calculated values for windshield surface temperature during icing conditions based on the approach recommended by this study.

A comparison of the experimental test values and the calculated values for windshield surface temperature during dry air conditions shows reasonable agreement, especially at the greater distances from the nozzle which are the most important. Therefore, it is concluded that the

empirical correlation of Equation (41) using the above constants in the equation is an acceptable approach for calculating the adiabatic wall temperature,  $t_{awx}$ . In addition, Equation (40) is considered an acceptable method for calculating the forced convective heat transfer coefficient,  $h_x$ .

#### COMPUTER PROGRAM FOR CALCULATING PERFORMANCE OF A WINDSHIELD HOT-AIR JET BLAST ANTI-ICING SYSTEM

A computer program was developed which rapidly predicts the performance of a hot-air jet blast aircraft windshield anti-icing system for any flight, icing and nozzle exit condition and any nozzle size when using the nozzle configuration previously described. The computer program is based on the previously presented analysis, and it was written to run on a Control Data Corporation 6600 computer system. The computer program listing is shown in Appendix E of Reference 24. A card deck for the program is available from the author upon request.

The input data required to run the computer program are data defining the aircraft and nozzle configuration, nozzle exit conditions, flight conditions and ambient icing conditions. These data are windshield height and angle with freestream, nozzle slot height, windshield overall heat transfer coefficient between outer surface and interior of aircraft, jet exit total temperature and velocity, aircraft velocity, altitude, ambient temperature, median droplet diameter, and liquid water content. Also, it is necessary to define the run number in the input data. This allows one to code each of the conditions being evaluated.

The computer program consists of a main program, a subroutine subprogram and a function subprogram. The main program reads the required input data and has a DO-loop which causes the program to compute the windshield surface temperature at various distances downstream from the nozzle. At present, the main program is written so as to result in calculating the surface temperature at points from 6 to 22 inches downstream from the nozzle in 2 inch increments. This range was established to coincide with the available data of WADC TR 58-444; however, the range is arbitrary and can be changed to suit the range of interest for the particular case being analyzed.

The subroutine subprogram computes the surface temperature,  $t_{sx}$ , of a hot-air jet blast heated windshield for a particular set of icing conditions and at one certain distance,  $x$ , from the nozzle. This subprogram is based on the use of all the equations in the analysis previously discussed. The function subprogram computes the partial pressure of water vapor in saturated air as a function of temperature, and it is the same as used in the computer program for electrically heated windshields.

The resulting output of the computer program shows the value for  $t_{s_x}$  at each value of  $x$  cited to be evaluated by the main program. The output shows the values of all input data, and also shown are the values of a number of the important parameters which were calculated by the subroutine subprogram in arriving at the value of  $t_{s_x}$ .

The computer program was used to calculate windshield surface temperature values for the eight test runs of WADC TR 58-444 which were done during icing conditions. Figures 20 through 23 show the resulting plots of the surface temperature calculated by the computer program for four of the test runs. As previously mentioned, figures 20 through 23 show the experimental values for the surface temperature during icing conditions. A comparison of the experimental test values and the calculated values for windshield temperature during icing conditions shows very good agreement in most cases. Therefore, it is concluded that the analytical approach presented and the resulting computer program is an adequate method for predicting the performance of a hot-air jet blast windshield anti-icing system.

The windshield surface temperatures predicted by this approach really apply to those downstream from the centerline of the nozzle. A somewhat lower temperature will exist to the right and left of the nozzle centerline. However, the temperature decay should not be appreciable for locations left and right of centerline which lie within the width of the nozzle. An analysis of the data presented in WADC TR 58-444 shows that in order to maintain adequate visibility during icing conditions, it is necessary to have a windshield surface temperature higher than the freezing point of water. Visibility is reduced downstream from the nozzle due to the runback of water towards the upper portion of the windshield. WADC TR 58-444 data shows that the surface temperature needs to be maintained above approximately 90°F in order to assure adequate visibility. Therefore, in order to include some factor of safety and to account for water runback and the temperature decay to left and right of nozzle centerline, it is concluded that the windshield hot-air jet blast anti-icing system should be designed to maintain the surface temperature at or above 90°F over the windshield height necessary for adequate pilot visibility.

## CONCLUSIONS

The following conclusions have been drawn as a result of this study:

1. Aircraft windshield anti-icing provisions should be designed to allow safe operation in the continuous maximum and intermittent maximum icing conditions defined by Figures 3 and 4.
2. It is possible to exceed the exterior surface heat requirements specified in MIL-T-5842A when operating in icing conditions defined by Figures 3 and 4.

3. The maximum heat required for an electrically heated windshield is very much dependent upon the configuration and there can be a wide difference in the maximum required heat between two different aircraft configurations.

4. There is no one particular flight and icing condition which always determines the maximum required heat for an electrically heated windshield. As a result, the complete range of possible icing conditions should be evaluated for a particular aircraft configuration.

5. Figures 7 through 12 can be used to get a quick estimate of the maximum required heat for any electrically heated center windshield configuration during continuous maximum and intermittent maximum icing conditions.

6. The analytical approach presented for determining the outer surface heat loss of an electrically heated windshield and the resulting computer programs are adequate for aircraft design purposes.

7. No previously published empirical correlations or theoretical expressions were found which could be used in developing a generalized analytical method for predicting the performance of an aircraft windshield hot-air jet blast anti-icing system. Therefore, it was necessary to develop an empirical correlation from available test data.

8. Based on WADC TR 58-444 test data, the analytical approach presented and the resulting computer program are an adequate means for predicting the performance of windshield hot-air jet blast anti-icing systems for windshield heights of up to two feet. The computer program can be used to predict windshield surface temperatures during both dry-air and icing conditions.

9. The electrical and hot-air jet blast analytical methods presented could be refined and improved by developing better approaches for calculating some of the parameters. Better accuracy could be achieved by use of more exact approaches for calculating the rate of water catch, convective heat transfer coefficients, local velocity over the windshield, wetness factor, and jet temperature decay.

## REFERENCES

1. Rodert, Lewis A.; An Investigation of the Prevention of Ice on the Airplane Windshield. NACA TN 754, 1940.
2. Kleinknecht, Kenneth S.; Flight Investigation of the Heat Requirements for Ice Prevention on Aircraft Windshields. NACA RM E7G28, 1947.
3. Jones, A. R.; Holdaway, G. H.; Steinmetz, C. P.; A Method for Calculating the Heat Required for Windshield Thermal Ice Prevention Based On Extensive Flight Tests in Natural Icing Conditions. NACA TN 1433, 1947.
4. Bowden, D. T.; Gensemer, A. E.; Skeen, C. A.; Engineering Summary of Airframe Icing Technical Data. Federal Aviation Agency Report ADS-4, 1964.
5. Aircraft Ice Protection. Report of Symposium Compiled and Published by Federal Aviation Administration, 1969.
6. SAE Aerospace Applied Thermodynamics Manual. Compiled and Published by the Society of Automotive Engineers, Inc., AC-9 Committee, Aircraft Environmental Systems, 1969.
7. Islinger, J. S.; Engineering Design Factors for Laminated Aircraft Windshields. WADC TR 53-99, Part I, 1954.
8. Gray, V. A.; Simple Graphical Solution of Heat Transfer and Evaporation from Surface Heated to Prevent Icing. NACA TN 2799, 1952.
9. Miller, P. A.; Anti-Icing Aspects of Helicopter Windshield Design. Sierracin Corporation, Presented at Ottawa International Helicopter Icing Conference, 1972.
10. Meline, H. R.; Smith, I. D.; Design Manual for Windshield Jet Air Blast Rain and Ice Removal. WADC TR 58-444, 1958.
11. Transparent Areas, Anti-Icing, Defrosting and Defogging Systems, General Specification for: Military Specification MIL-T-5842A, 1953.
12. Airworthiness Standards: Transport Category Airplanes. Federal Aviation Regulations, Part 25, 1966.
13. Environmental Control, Environmental Protection, and Engine Bleed Air Systems, Aircraft, General Specification for. Military Specification MIL-E-38453A, 1971.
14. Bore, C. L.; Some Practical Aspects of Kinetic Heating Calculations. Journal of the Royal Aeronautical Society, 1959.



# REFERENCES (Contd)

15. Rubesin, M. W.; The Effect of an Arbitrary Surface-Temperature Variation Along a Flat Plate on the Convective Heat Transfer in an Incompressible Turbulent Boundary Layer. NACA TN 2345, 1951.
16. Reynolds, W. C.; Kays, W. M.; Kline, S. J.; Heat Transfer in the Turbulent Incompressible Boundary Layer, II-Step Wall Temperature Distribution. NASA Memo 12-2-58W, 1958.
17. Lewis, W.; Brun, R. J.; Impingement of Water Droplets on a Rectangular Half Body in a Two-Dimensional Incompressible Flow Field. NACA TN 3658, 1956.
18. Qureshi, J.; Screen, T. R.; Sharpe, W. F.; Windshield Anti-Icing Analytical Studies F-5A/B (G). Northrop Corporation, Norair Division Report NOR 65-11, 1965.
19. Miller, P. A.; Cessna Citation Windshield Anti-Ice Capability. Sierracin Report ER-71-012, 1971.
20. Weiner, F. R.; Paselk, R. A.; Analysis of the Windshield Emergency Anti-Icing Capability for the Sabreliner Airplane. North American Aviation Report NA-67-373, 1967.
21. Islinger, J. S.; Engineering Design Factors for Laminated Aircraft Windshields. WADC TR 53-99, Part I, 1954.
22. Burr, W. L.; C-5A Category I Engineering Flight Test Anti-Icing Test Results. Lockheed Report No. LG1T19-1-3, 1970.
23. Kornblue, H. N.; Flight and Ground Test Evaluation of F-5A (Norway) Windshield and Engine Inlet Lip Anti-Icing Systems. Northrop Corporation, Norair Division Report NOR-67-200, 1967.
24. Letton, G. C.; An Analytical Investigation of Aircraft Windshield Anti-Icing Systems. Masters Thesis, Ohio State University, 1972.
25. Wieghardt, K.; Hot-Air Discharge for De-Icing. AAF Translation Report F-TS-919-RE, 1946.
26. Papell, S. S.; Trout, A. M.; Experimental Investigation of Air Film Cooling Applied to an Adiabatic Wall by Means of an Axially Discharging Slot. NASA TN D-9, 1959.
27. Seban, R. A.; Heat Transfer and Effectiveness for a Turbulent Boundary Layer with Tangential Fluid Injection. Journal of Heat Transfer, Transactions of ASME, Series C, Vol. 82, Pages 303-313, 1960.

REFERENCES (Contd)

28. Breeze, R. K.; Rudolph, J. D.; Windshield Enclosure Anti-Icing System Tests YF-100A Airplane. North American Aviation Report NA53-1054, 1954.

TABLE 1

Maximum Electrical Heat Required for Various  
Configurations Evaluated During Continuous  
Maximum and Intermittent Maximum Icing Conditions

| Config.<br>No. | H<br>Ft. | Dist. to Wind.<br>Base from<br>Stag. Point<br>Ft. | Angle 1<br>Deg. | Max. Heat Required for<br>Various Icing Conditions |                                       |
|----------------|----------|---|-----------------|--|---------------------------------------|
|                |          |   |                 | Cont. Max.<br>Btu/Hr-Ft <sup>2</sup>               | Inter. Max.<br>Btu/Hr-Ft <sup>2</sup> |
| 1              | 1.50     | 3.00  | 20.4            | 2793   | 3379                                  |
| 2              | 1.50     | 3.00  | 45.0            | 2787   | 3435                                  |
| 3              | 1.50     | 3.00  | 60.0            | 2784   | 3420                                  |
| 4              | 1.50     | 6.00  | 20.4            | 2497   | 3128                                  |
| 5              | 1.50     | 6.00  | 45.0            | 2491   | 3184                                  |
| 6              | 1.50     | 6.00  | 60.0            | 2488   | 3183                                  |
| 7              | 1.50     | 11.83   | 20.4            | 2219   | 2893                                  |
| 8              | 1.50     | 11.83   | 45.0            | 2213   | 2983                                  |
| 9              | 1.50     | 11.83   | 60.0            | 2210   | 2985                                  |
| 10             | 1.50     | 18.00   | 20.4            | 2057   | 2757                                  |
| 11             | 1.50     | 18.00   | 45.0            | 2051   | 2869                                  |
| 12             | 1.50     | 18.00   | 60.0            | 2048   | 2871                                  |
| 13             | 2.95     | 3.00  | 20.4            | 2533   | 2826                                  |
| 14             | 2.95     | 3.00  | 45.0            | 2484   | 2742                                  |
| 15             | 2.95     | 3.00  | 60.0            | 2326   | 2712                                  |
| 16             | 2.95     | 6.00  | 20.4            | 2296   | 2603                                  |
| 17             | 2.95     | 6.00  | 45.0            | 2274   | 2519                                  |
| 18             | 2.95     | 6.00  | 60.0            | 2216   | 2489                                  |
| 19             | 2.95     | 11.83   | 20.4            | 2134   | 2377                                  |
| 20             | 2.95     | 11.83   | 45.0            | 2046   | 2299                                  |
| 21             | 2.95     | 11.83   | 60.0            | 2044   | 2263                                  |
| 22             | 2.95     | 18.00   | 20.4            | 1999   | 2242                                  |
| 23             | 2.95     | 18.00   | 45.0            | 1902   | 2170                                  |
| 24             | 2.95     | 18.00   | 60.0            | 1900   | 2128                                  |
| 25             | 4.00     | 3.00  | 20.4            | 2134   | 2623                                  |
| 26             | 4.00     | 3.00  | 45.0            | 1977   | 2544                                  |
| 27             | 4.00     | 3.00  | 60.0            | 1892   | 2507                                  |
| 28             | 4.00     | 6.00  | 20.4            | 2034   | 2422                                  |
| 29             | 4.00     | 6.00  | 45.0            | 1862   | 2343                                  |
| 30             | 4.00     | 6.00  | 60.0            | 1761   | 2306                                  |
| 31             | 4.00     | 11.83   | 20.4            | 1930   | 2210                                  |
| 32             | 4.00     | 11.83   | 45.0            | 1758   | 2131                                  |
| 33             | 4.00     | 11.83   | 60.0            | 1674   | 2094                                  |
| 34             | 4.00     | 18.00   | 20.4            | 1865   | 2080                                  |
| 35             | 4.00     | 18.00   | 45.0            | 1699   | 2001                                  |
| 36             | 4.00     | 18.00   | 60.0            | 1634   | 1964                                  |

TABLE 2

Values of Various Calculated Parameters for the  
Configurations Evaluated During Continuous Maximum  
Icing for the Condition Requiring Maximum Heat

| Config.<br>No. | h <sub>avg</sub> | Re <sub>o</sub> | K    | M <sub>w</sub> | M <sub>wc</sub> | q <sub>1</sub> | q <sub>2</sub> | q <sub>3</sub> | q <sub>4</sub> |
|----------------|------------------|-----------------|------|----------------|-----------------|----------------|----------------|----------------|----------------|
| 1              | 41.5             | 209.3           | 1.38 | 1.64           | 1.03            | 1572           | 84             | 1100           | 37             |
| 2              | 41.5             | 261.6           | 1.06 | 1.51           | 1.03            | 1572           | 78             | 1100           | 37             |
| 3              | 41.5             | 314.0           | 1.25 | 1.45           | 1.03            | 1572           | 75             | 1100           | 37             |
| 4              | 36.9             | 209.3           | 1.38 | 1.64           | 0.91            | 1398           | 84             | 978            | 37             |
| 5              | 36.9             | 261.6           | 1.06 | 1.51           | 0.91            | 1398           | 78             | 978            | 37             |
| 6              | 36.9             | 314.0           | 1.25 | 1.45           | 0.91            | 1398           | 75             | 978            | 37             |
| 7              | 32.6             | 209.3           | 1.38 | 1.64           | 0.81            | 1234           | 84             | 864            | 37             |
| 8              | 32.6             | 261.6           | 1.06 | 1.51           | 0.81            | 1234           | 78             | 864            | 37             |
| 9              | 32.6             | 314.0           | 1.25 | 1.45           | 0.81            | 1234           | 75             | 864            | 37             |
| 10             | 30.1             | 209.3           | 1.38 | 1.64           | 0.74            | 1139           | 84             | 797            | 37             |
| 11             | 30.1             | 261.6           | 1.06 | 1.51           | 0.74            | 1139           | 78             | 797            | 37             |
| 12             | 30.1             | 314.0           | 1.25 | 1.45           | 0.74            | 1139           | 75             | 797            | 37             |
| 13             | 49.2             | 337.9           | 1.46 | 1.29           | 1.21            | 1131           | 62             | 1303           | 37             |
| 14             | 49.2             | 540.6           | 1.84 | 1.09           | 1.21            | 1131           | 51             | 1165           | 37             |
| 15             | 49.2             | 540.6           | 1.50 | 1.03           | 1.21            | 1131           | 49             | 1109           | 37             |
| 16             | 44.4             | 337.9           | 1.46 | 1.29           | 1.10            | 1021           | 62             | 1176           | 37             |
| 17             | 44.4             | 540.6           | 1.84 | 1.09           | 1.10            | 1021           | 51             | 1165           | 37             |
| 18             | 44.4             | 540.6           | 1.50 | 1.03           | 1.10            | 1021           | 49             | 1109           | 37             |
| 19             | 32.2             | 261.6           | 1.09 | 0.78           | 0.80            | 1220           | 40             | 837            | 37             |
| 20             | 39.5             | 540.6           | 1.84 | 1.09           | 0.98            | 910            | 51             | 1048           | 37             |
| 21             | 39.5             | 540.6           | 1.50 | 1.03           | 0.98            | 910            | 49             | 1048           | 37             |
| 22             | 29.9             | 261.6           | 1.09 | 0.78           | 0.74            | 1131           | 40             | 791            | 37             |
| 23             | 36.6             | 540.6           | 1.84 | 1.09           | 0.91            | 843            | 51             | 971            | 37             |
| 24             | 36.6             | 540.6           | 1.50 | 1.03           | 0.91            | 843            | 49             | 971            | 37             |
| 25             | 48.1             | 405.4           | 1.55 | 0.88           | 1.19            | 1107           | 42             | 948            | 37             |
| 26             | 39.2             | 418.6           | 1.02 | 0.41           | 0.97            | 1484           | 21             | 435            | 37             |
| 27             | 39.2             | 418.6           | 0.83 | 0.33           | 0.97            | 1484           | 17             | 354            | 37             |
| 28             | 43.8             | 405.4           | 1.55 | 0.88           | 1.08            | 1007           | 42             | 948            | 37             |
| 29             | 43.8             | 540.6           | 1.36 | 0.73           | 1.08            | 1007           | 34             | 784            | 37             |
| 30             | 43.8             | 540.6           | 1.11 | 0.64           | 1.08            | 1007           | 30             | 687            | 37             |
| 31             | 39.2             | 405.4           | 1.55 | 0.88           | 0.97            | 903            | 42             | 948            | 37             |
| 32             | 39.2             | 540.6           | 1.36 | 0.73           | 0.97            | 903            | 34             | 784            | 37             |
| 33             | 24.8             | 305.2           | 1.11 | 0.95           | 1.09            | 571            | 45             | 1021           | 37             |
| 34             | 36.4             | 405.4           | 1.55 | 0.88           | 0.90            | 838            | 42             | 948            | 37             |
| 35             | 23.1             | 305.2           | 1.36 | 1.02           | 1.01            | 531            | 48             | 1083           | 37             |
| 36             | 23.1             | 305.2           | 1.11 | 0.95           | 1.01            | 531            | 45             | 1021           | 37             |

TABLE 3

Values of Various Calculated Parameters for the  
Configurations Evaluated During Intermittent Maximum  
Icing for the Condition Requiring Maximum Heat

| Config.<br>No. | havg | Reo   | K    | M <sub>w</sub> | M <sub>we</sub> | q <sub>1</sub> | q <sub>2</sub> | q <sub>3</sub> | q <sub>4</sub> |
|----------------|------|-------|------|----------------|-----------------|----------------|----------------|----------------|----------------|
| 1              | 32.2 | 152.6 | 1.84 | 22.68          | 1.41            | 742            | 1086           | 1514           | 37             |
| 2              | 32.2 | 190.7 | 1.41 | 23.86          | 1.41            | 742            | 1142           | 1514           | 37             |
| 3              | 32.2 | 190.7 | 1.15 | 23.54          | 1.41            | 742            | 1127           | 1514           | 37             |
| 4              | 28.7 | 152.6 | 1.84 | 22.68          | 1.25            | 659            | 1086           | 1346           | 37             |
| 5              | 28.7 | 190.7 | 1.41 | 23.86          | 1.25            | 659            | 1142           | 1346           | 37             |
| 6              | 33.2 | 229.2 | 1.44 | 34.11          | 1.45            | 129            | 1458           | 1559           | 37             |
| 7              | 25.3 | 152.6 | 1.84 | 22.68          | 1.11            | 582            | 1086           | 1188           | 37             |
| 8              | 29.3 | 183.3 | 1.13 | 34.06          | 1.28            | 114            | 1456           | 1376           | 37             |
| 9              | 29.3 | 229.2 | 1.44 | 34.11          | 1.28            | 114            | 1458           | 1376           | 37             |
| 10             | 23.4 | 152.6 | 1.84 | 22.68          | 1.02            | 537            | 1086           | 1097           | 37             |
| 11             | 27.1 | 183.3 | 1.13 | 34.06          | 1.18            | 105            | 1456           | 1271           | 37             |
| 12             | 27.1 | 229.2 | 1.44 | 34.11          | 1.18            | 105            | 1458           | 1271           | 37             |
| 13             | 39.7 | 258.7 | 1.46 | 10.45          | 1.28            | 914            | 500            | 1375           | 37             |
| 14             | 39.7 | 362.2 | 1.41 | 8.70           | 1.28            | 914            | 416            | 1375           | 37             |
| 15             | 39.7 | 362.2 | 1.15 | 8.06           | 1.28            | 914            | 386            | 1375           | 37             |
| 16             | 35.8 | 258.7 | 1.46 | 10.45          | 1.16            | 825            | 500            | 1241           | 37             |
| 17             | 35.8 | 362.2 | 1.41 | 8.70           | 1.16            | 825            | 416            | 1241           | 37             |
| 18             | 35.8 | 362.2 | 1.15 | 8.06           | 1.16            | 825            | 386            | 1241           | 37             |
| 19             | 31.9 | 258.7 | 1.46 | 10.45          | 1.03            | 735            | 500            | 1105           | 37             |
| 20             | 25.0 | 228.9 | 1.04 | 10.68          | 1.10            | 576            | 511            | 1175           | 37             |
| 21             | 31.9 | 362.2 | 1.15 | 8.06           | 1.03            | 735            | 386            | 1105           | 37             |
| 22             | 29.6 | 258.7 | 1.46 | 10.45          | 0.95            | 681            | 500            | 1024           | 37             |
| 23             | 23.2 | 228.9 | 1.04 | 10.68          | 1.01            | 533            | 511            | 1089           | 37             |
| 24             | 29.6 | 362.2 | 1.15 | 8.06           | 0.95            | 681            | 386            | 1024           | 37             |
| 25             | 38.8 | 310.5 | 1.55 | 7.26           | 1.25            | 894            | 347            | 1345           | 37             |
| 26             | 38.8 | 362.2 | 1.04 | 5.60           | 1.25            | 894            | 268            | 1345           | 37             |
| 27             | 38.8 | 414.0 | 1.11 | 4.84           | 1.25            | 894            | 231            | 1345           | 37             |
| 28             | 35.4 | 310.5 | 1.55 | 7.26           | 1.14            | 814            | 347            | 1224           | 37             |
| 29             | 35.4 | 362.2 | 1.04 | 5.60           | 1.14            | 814            | 268            | 1224           | 37             |
| 30             | 35.4 | 414.0 | 1.11 | 4.84           | 1.14            | 814            | 231            | 1224           | 37             |
| 31             | 31.7 | 310.5 | 1.55 | 7.26           | 1.02            | 729            | 347            | 1097           | 37             |
| 32             | 31.7 | 362.2 | 1.04 | 5.60           | 1.02            | 729            | 268            | 1097           | 37             |
| 33             | 31.7 | 414.0 | 1.11 | 4.84           | 1.02            | 729            | 231            | 1097           | 37             |
| 34             | 29.4 | 310.5 | 1.55 | 7.26           | 0.95            | 677            | 347            | 1019           | 37             |
| 35             | 29.4 | 362.5 | 1.04 | 5.60           | 0.95            | 677            | 268            | 1019           | 37             |
| 36             | 29.4 | 414.0 | 1.11 | 4.84           | 0.95            | 677            | 231            | 1019           | 37             |

TABLE 4

Conditions Requiring Maximum Heat  
for Configurations Evaluated

Continuous Maximum Icing

| Altitude<br>Ft. | Velocity<br>Knots | Median<br>Droplet<br>Diameter<br>Microns | Ambient<br>Temp.<br>°R | Number<br>of<br>Configs. | Config. Numbers<br>Having this as<br>the Condition<br>Requiring<br>Max. Heat |
|-----------------|-------------------|--|------------------------|--------------------------|--|
| 7,000           | 300               | 20                                       | 438                    | 4                        | 1,4,7,10   |
| 7,000           | 300               | 25                                       | 438                    | 6                        | 2,5,8,11,19,22   |
| 7,000           | 300               | 30                                       | 438                    | 4                        | 3,6,9,12   |
| 7,000           | 300               | 40                                       | 438                    | 2                        | 26,27  |
| 7,000           | 400               | 25                                       | 438                    | 2                        | 13,16  |
| 7,000           | 400               | 30                                       | 438                    | 4                        | 25,28,31,34  |
| 7,000           | 400               | 40                                       | 438                    | 11                       | 14,15,17,18,20,<br>20,23,24,29,<br>30,32                                     |
| 22,000          | 400               | 40                                       | 438                    | 3                        | 33,35,36   |

Intermittent Maximum Icing

| Altitude<br>Ft. | Velocity<br>Knots | Median<br>Droplet<br>Diameter<br>Microns | Ambient<br>Temp.<br>°R | Number<br>of<br>Configs. | Config. Numbers<br>Having this as<br>the Condition<br>Requiring<br>Max. Heat |
|-----------------|-------------------|--|------------------------|--------------------------|--|
| 14,000          | 400               | 25                                       | 438                    | 4                        | 13,16,19,22  |
| 14,000          | 400               | 30                                       | 438                    | 4                        | 25,28,31,34  |
| 14,000          | 400               | 35                                       | 438                    | 10                       | 14,15,17,18,21<br>24,26,29,32,35   |
| 14,000          | 400               | 40                                       | 438                    | 4                        | 27,30,33,36  |
| 22,000          | 400               | 20                                       | 438                    | 4                        | 1,4,7,10   |
| 22,000          | 400               | 25                                       | 438                    | 3                        | 2,3,5  |
| 22,000          | 400               | 30                                       | 438                    | 2                        | 20,23  |
| 22,000          | 500               | 20                                       | 438                    | 2                        | 8,11   |
| 22,000          | 500               | 25                                       | 438                    | 3                        | 6,9,12   |

TABLE 5

Comparison of Flight Test and Computed Values  
for Windshield Exterior Surface Temperature

| Aircraft | Alt.<br>Ft. | Vel.<br>Kts. | MDD<br>Micron | $t_{\infty}$<br>°R | LWC<br>Gm/m <sup>3</sup> | $q_s$<br>Btu/Hr-Ft <sup>2</sup> | Windshield Surface Temperature |              |              |              |
|----------|-------------|--------------|---------------|--------------------|--------------------------|---------------------------------|--------------------------------|--------------|--------------|--------------|
|          |             |              |               |                    |                          |                                 | Flight Test                    |              |              | Meth 3<br>°F |
|          |             |              |               |                    |                          |                                 | Value<br>°F                    | Meth 1<br>°F | Meth 2<br>°F |              |
| C-5      | 23,200      | 244.5        | 30            | 442                | 0.10                     | 2100                            | 46.0                           | 46.57        | 40.27        | < 32.00      |
| C-5      | 23,275      | 246.0        | 30            | 437                | 0.75                     | 2100                            | 48.4                           | 37.36        | < 32.00      | < 32.00      |
| F-5      | 22,000      | 330.0        | 30            | 467                | 1.20                     | 2190                            | 40.0                           | 44.76        | 42.25        | 38.11        |
| F-5      | 22,000      | 250.0        | 30            | 474                | 1.20                     | 2220                            | 40.0                           | 53.00        | 49.29        | 44.71        |
| F-5      | 21,000      | 310.0        | 30            | 469                | 1.20                     | 2150                            | 42.0                           | 46.01        | 43.62        | 39.41        |
| F-5      | 21,000      | 310.0        | 30            | 470                | 1.50                     | 2090                            | 40.0                           | 44.70        | 42.22        | 38.75        |
| F-5      | 14,000      | 265.0        | 30            | 473                | 1.20                     | 2280                            | 40.0                           | 47.54        | 44.65        | 40.81        |
| F-5      | 16,000      | 264.0        | 30            | 465                | 1.20                     | 1875                            | 45.0                           | 42.67        | 39.55        | 35.02        |
| F-5      | 15,000      | 264.0        | 30            | 464                | 1.20                     | 1840                            | 45.0                           | 41.55        | 38.75        | 34.25        |
| F-5      | 15,000      | 352.0        | 30            | 464                | 0.40                     | 1825                            | 50.0                           | 43.99        | 41.26        | 36.62        |
| F-5      | 15,000      | 264.0        | 30            | 464                | 0.40                     | 1825                            | 50.0                           | 45.70        | 41.82        | 36.39        |
| F-5      | 15,000      | 212.0        | 30            | 463                | 0.40                     | 1820                            | 50.0                           | 48.33        | 43.99        | 37.59        |

- NOTES:
1. Method 1 uses  $h_{avg}$  calculated by equation (5).
  2. Method 2 uses  $h_{avg}$  based on NASA Memo 12-2-58W, reference 16.
  3. Method 3 uses  $h_{avg}$  based on NACA TN 2345, reference 15.
  4. The icing flight test data were obtained during flight in an icing cloud created by a KC-135 water spray tanker. The median droplet diameter for this icing cloud is assumed to be 30 microns.

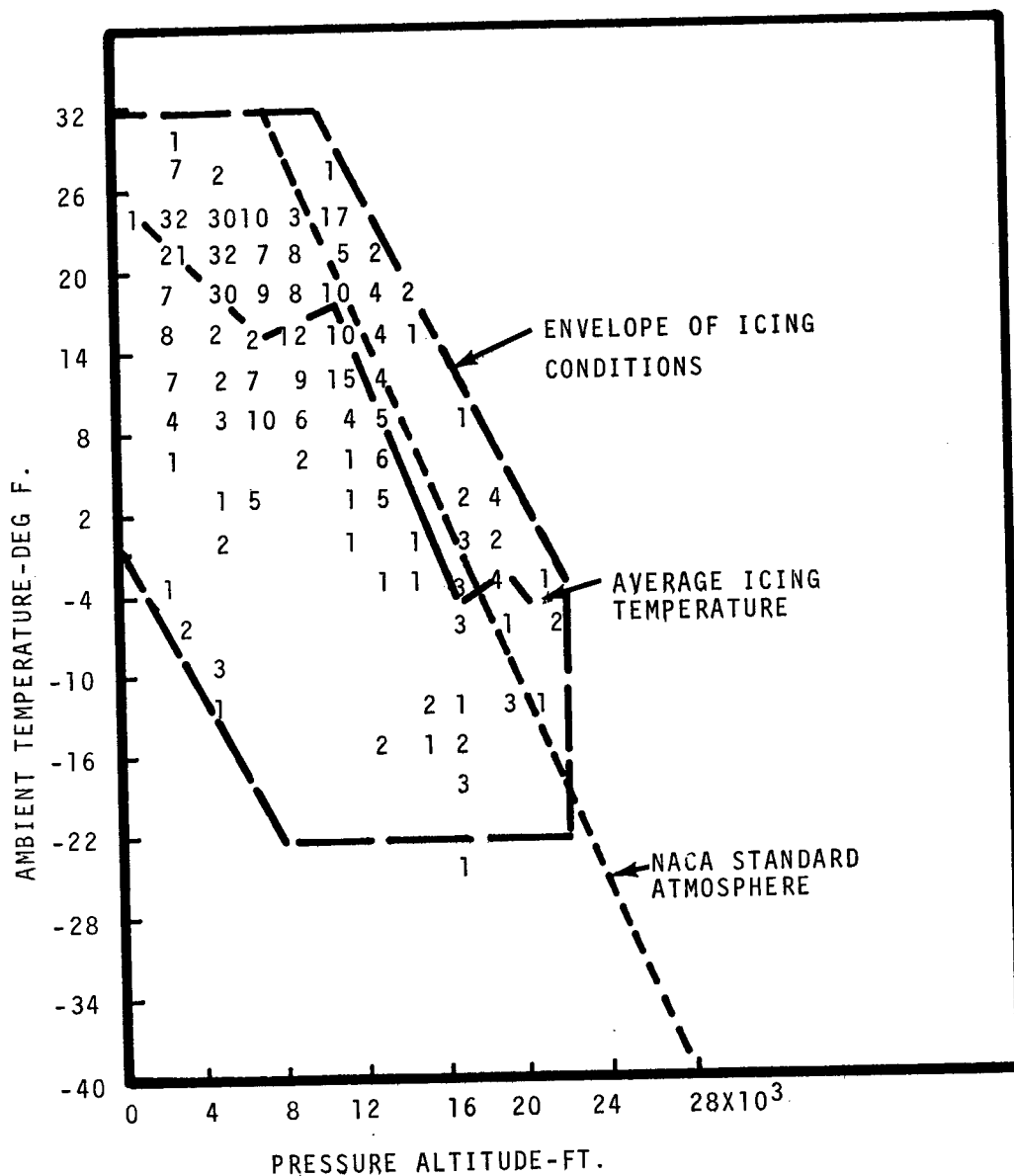


FIGURE 1 FREQUENCY DISTRIBUTION OF ICING ENCOUNTERS IN STRATIFORM CLOUDS FOR INCREMENTS OF TEMPERATURE AND ALTITUDE (FROM NACA TN 2569)



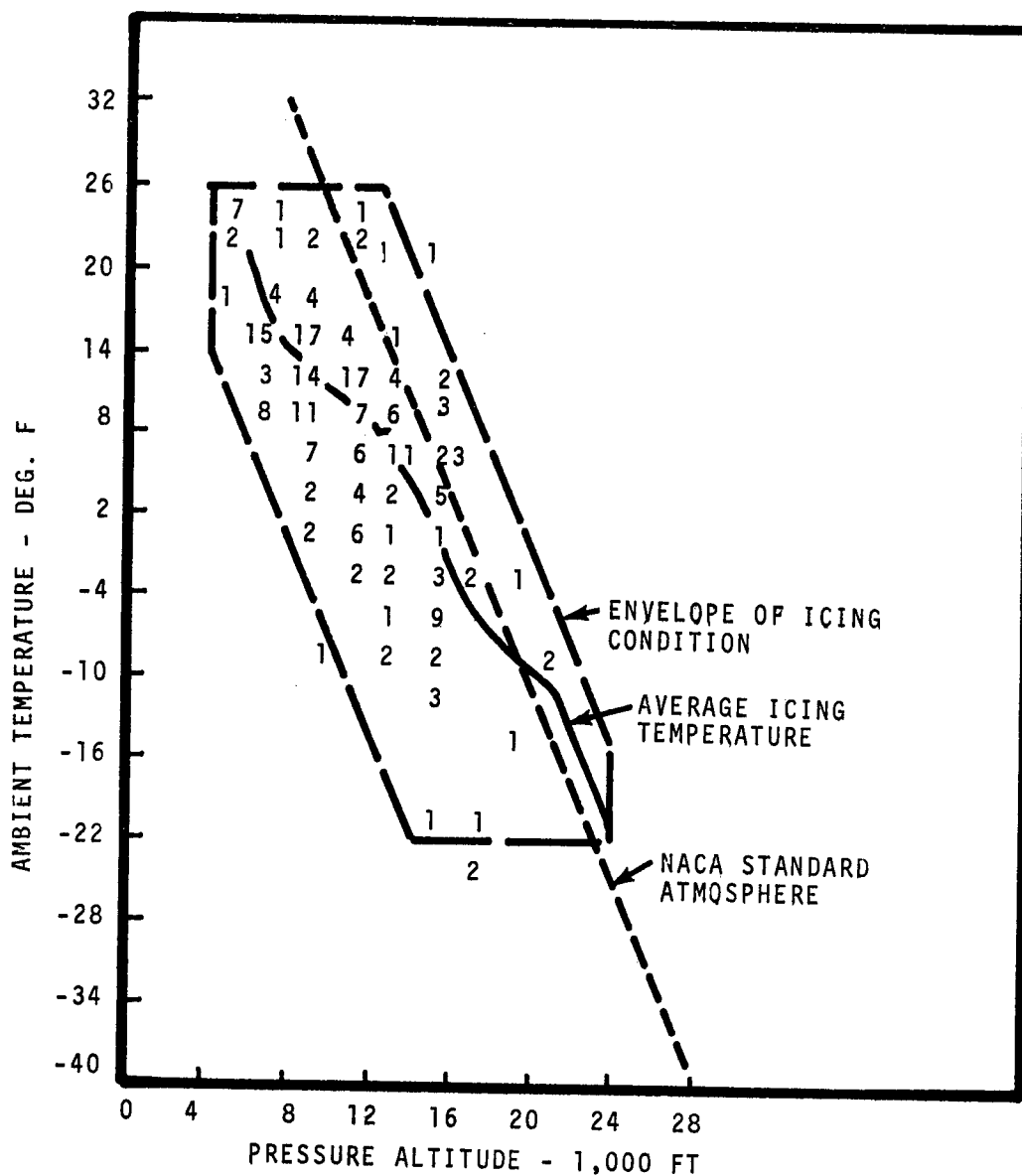


FIGURE 2 FREQUENCY DISTRIBUTION OF ICING ENCOUNTERS IN CUMULIFORM CLOUDS FOR INCREMENTS OF TEMPERATURE AND ALTITUDE (FROM NACA TN 2569)

- (1) ALTITUDE; SEA LEVEL TO 22,000 FEET
- (2) MAXIMUM VERTICAL EXTENT; 6,500 FEET
- (3) HORIZONTAL EXTENT; 20 STATUTE MILES

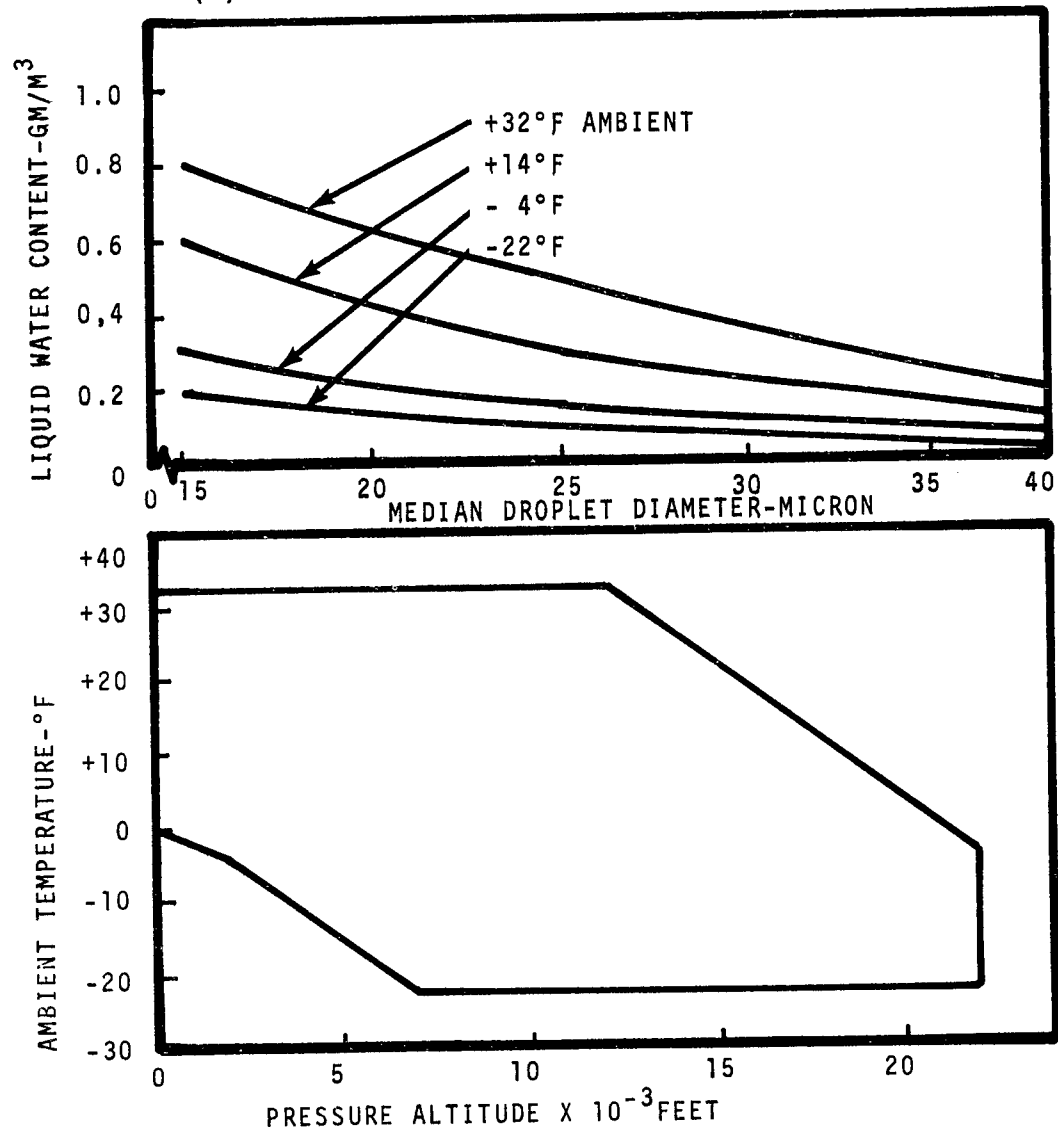


FIGURE 3 CONTINUOUS MAXIMUM ICING CONDITIONS

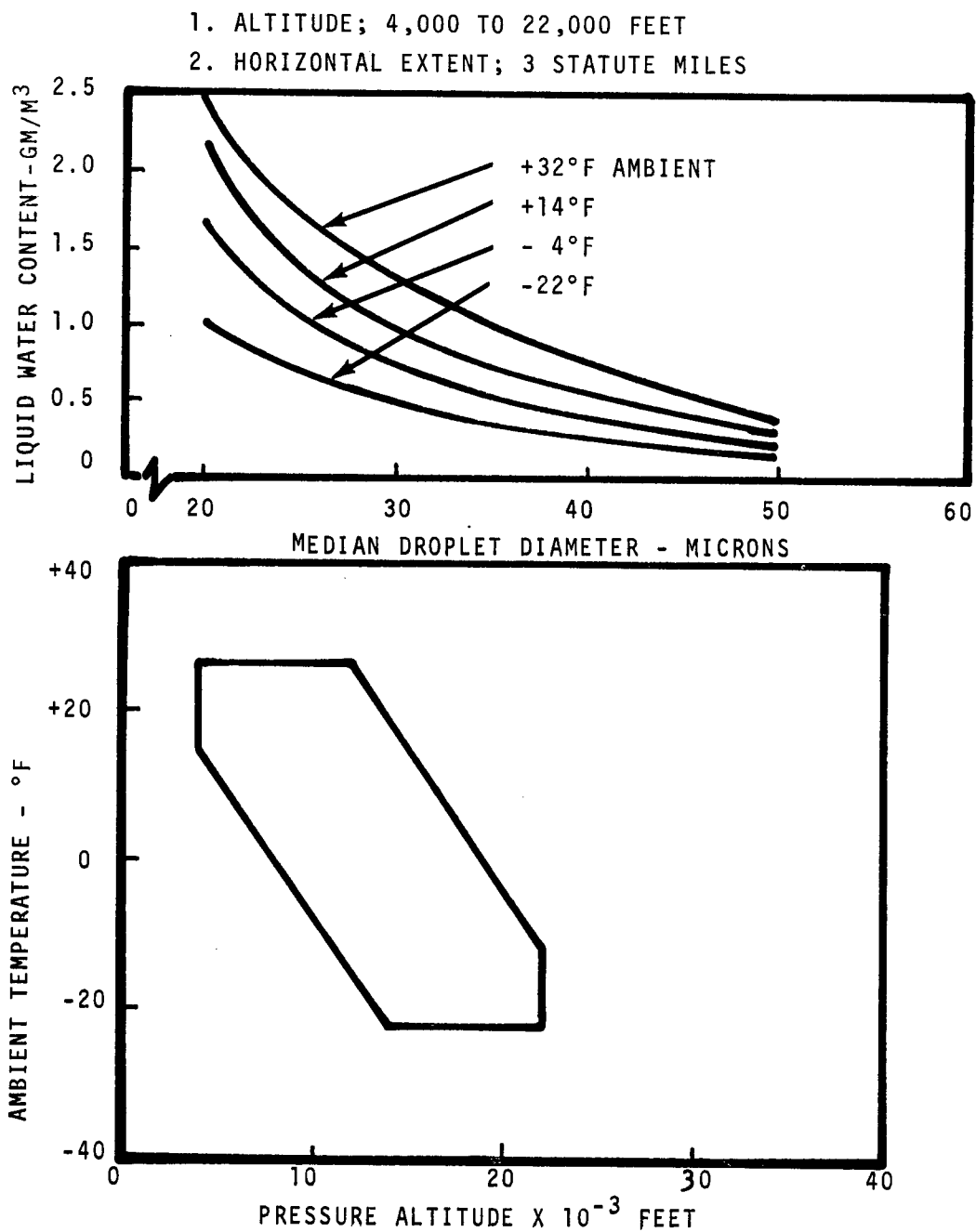
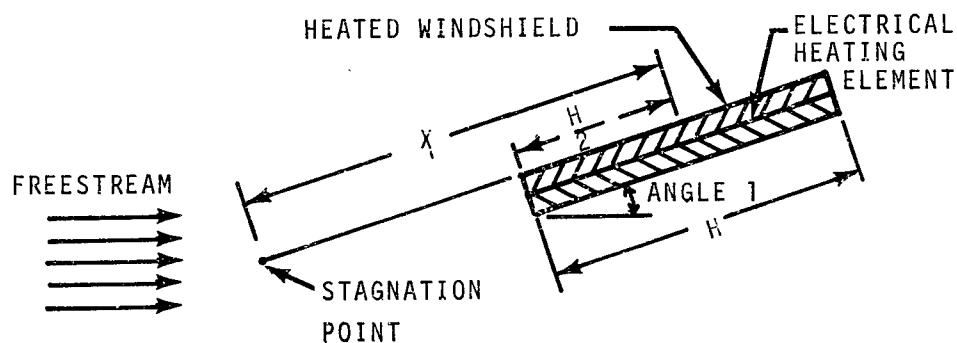
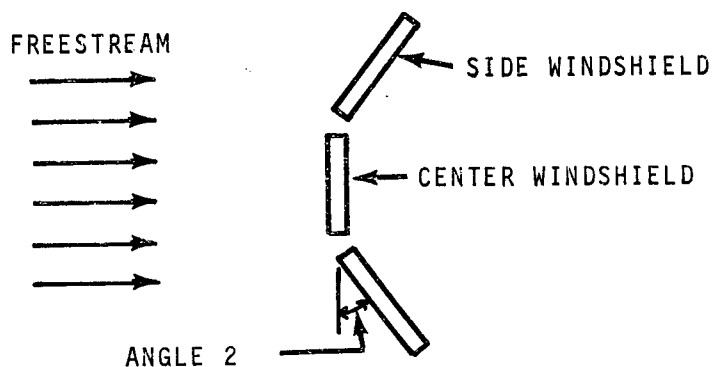


FIGURE 4 INTERMITTENT MAXIMUM ICING CONDITIONS



(a) WINDSHIELD SIDE VIEW



(b) WINDSHIELD PLAN VIEW

DEFINITION OF TERMS:

$X$ =DISTANCE FROM STAGNATION POINT TO CENTER OF HEATED WINDSHIELD AREA

$H$ =LENGTH OF HEATED WINDSHIELD IN VERTICAL DIRECTION

ANGLE 1=ANGLE OF WINDSHIELD WITH UNDISTURBED FREESTREAM AHEAD OF AIRCRAFT

ANGLE 2=ANGLE OF ROTATION OF BASE OF WINDSHIELD FROM LINE PERPENDICULAR TO UNDISTURBED FREESTREAM AHEAD OF AIRCRAFT

FIGURE 5 -TYPICAL ELECTRICALLY HEATED WINDSHIELD ANALYTICAL MODEL

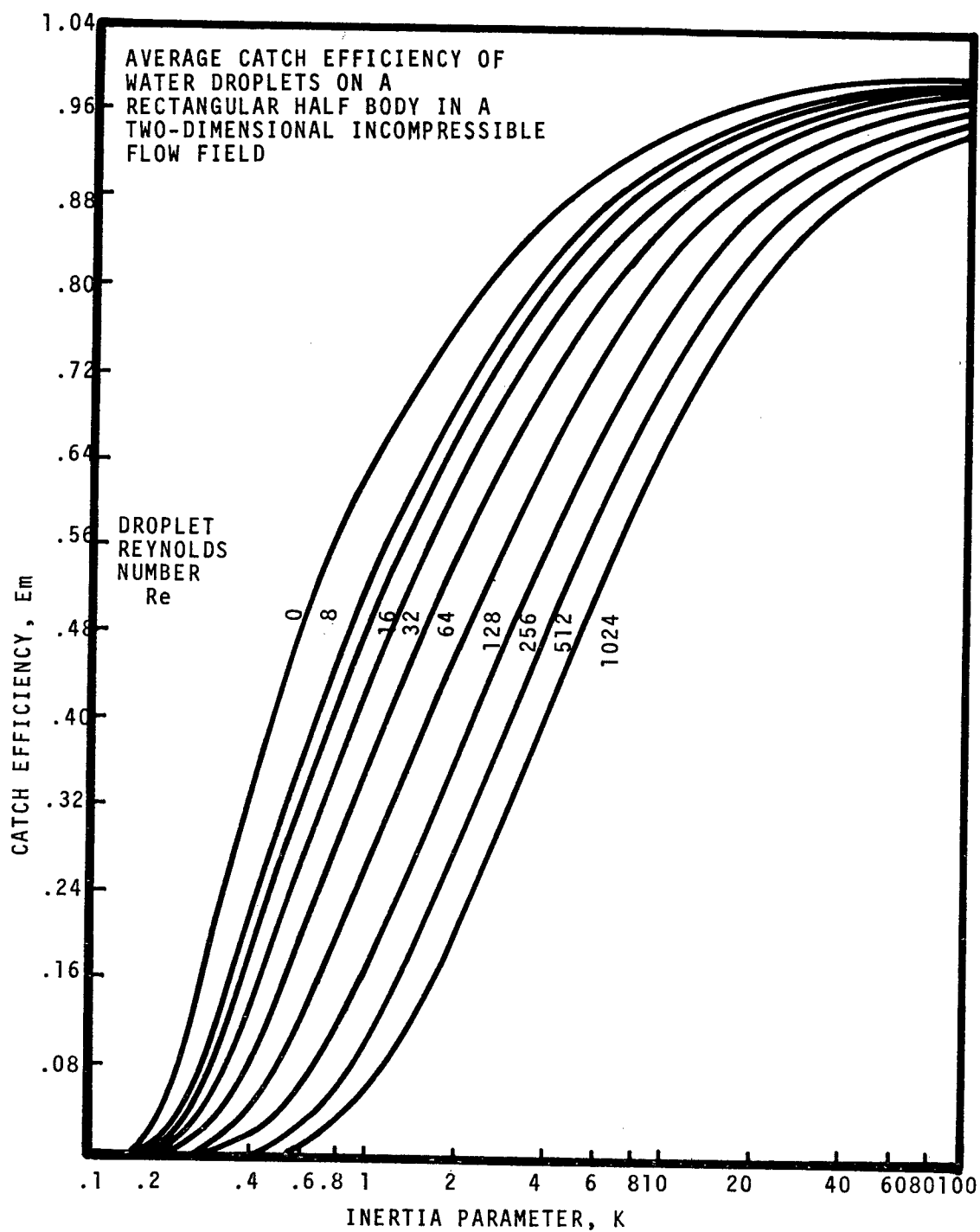


FIGURE 6 CURVE OF DROPLET CATCH EFFICIENCY

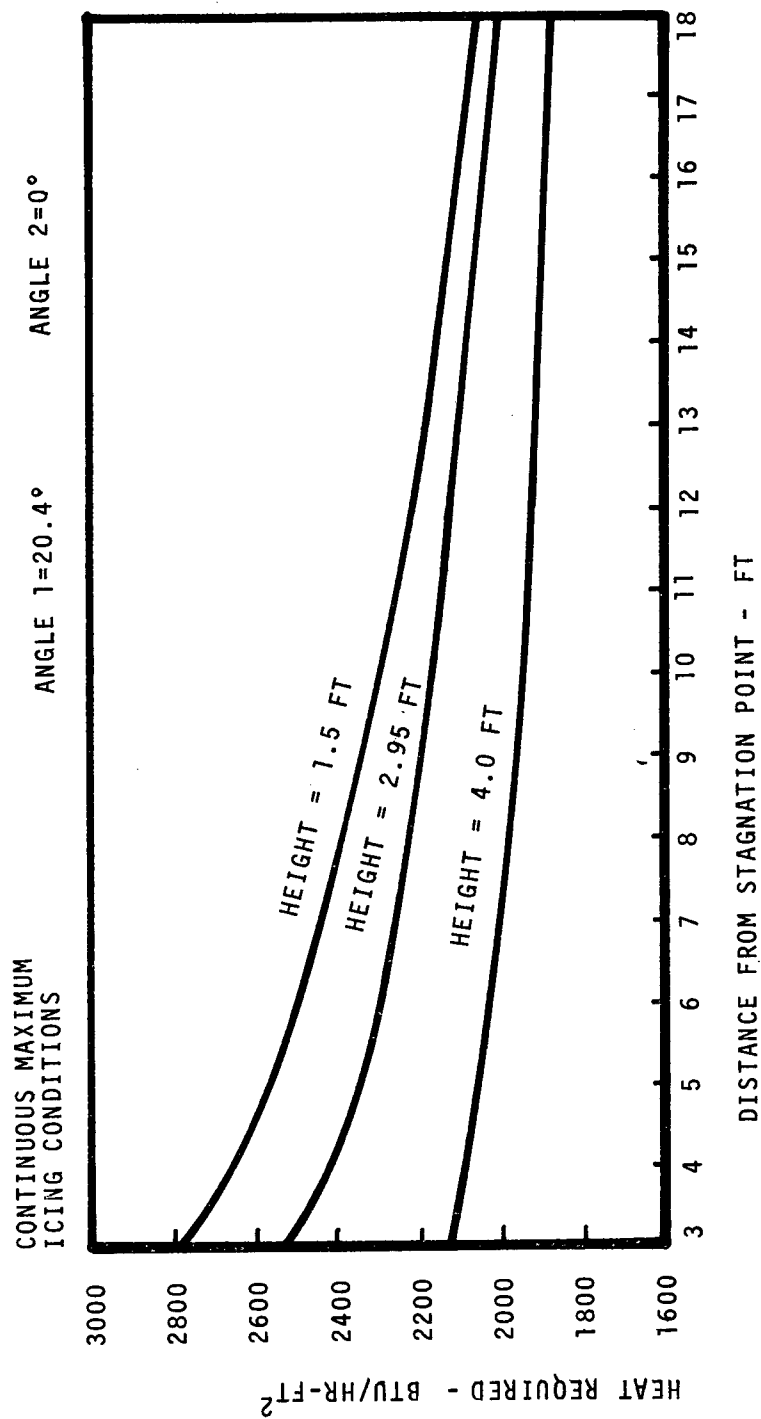


FIGURE 7 MAXIMUM HEAT REQUIRED VS DISTANCE FROM STAGNATION POINT CONTINUOUS MAXIMUM ICING CONDITIONS, ANGLE 1=20.4°, ANGLE 2=0°

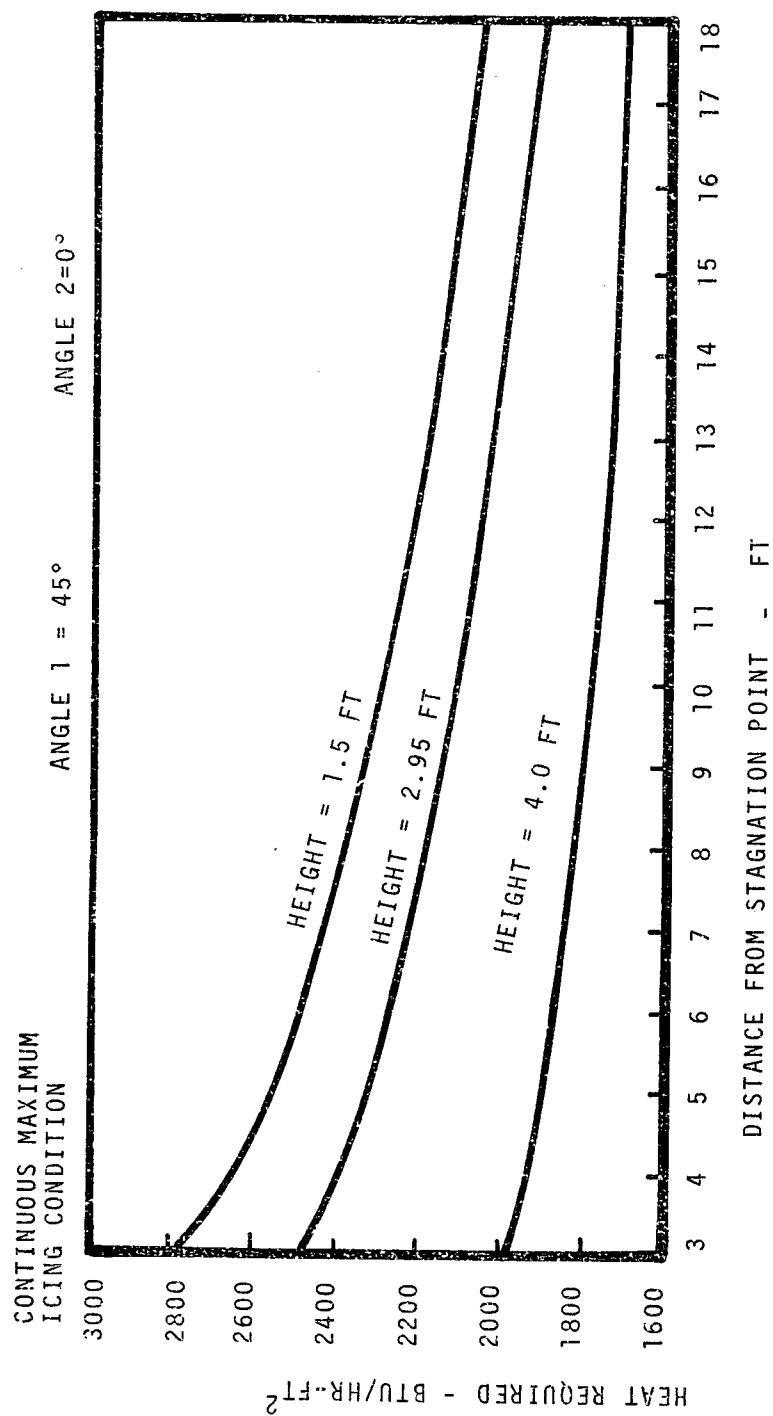


FIGURE 8 MAXIMUM HEAT REQUIRED VS. DISTANCE FROM STAGNATION POINT CONTINUOUS MAXIMUM ICING CONDITIONS, ANGLE 1=45°, ANGLE 2=0°

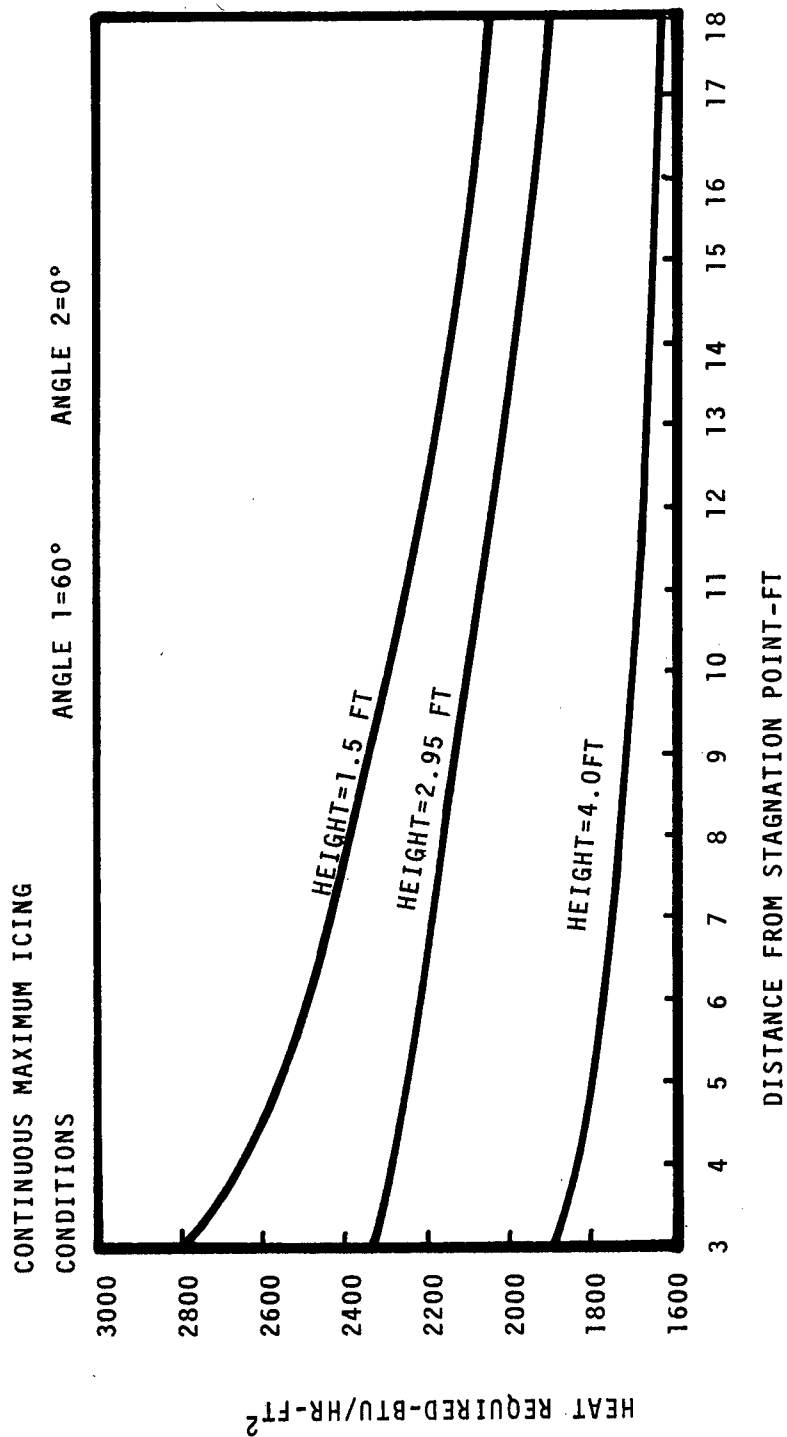


FIGURE 9 MAXIMUM HEAT REQUIRED VS DISTANCE FROM STAGNATION POINT CONTINUOUS MAXIMUM ICING CONDITIONS, ANGLE 1=60°, ANGLE 2=0°



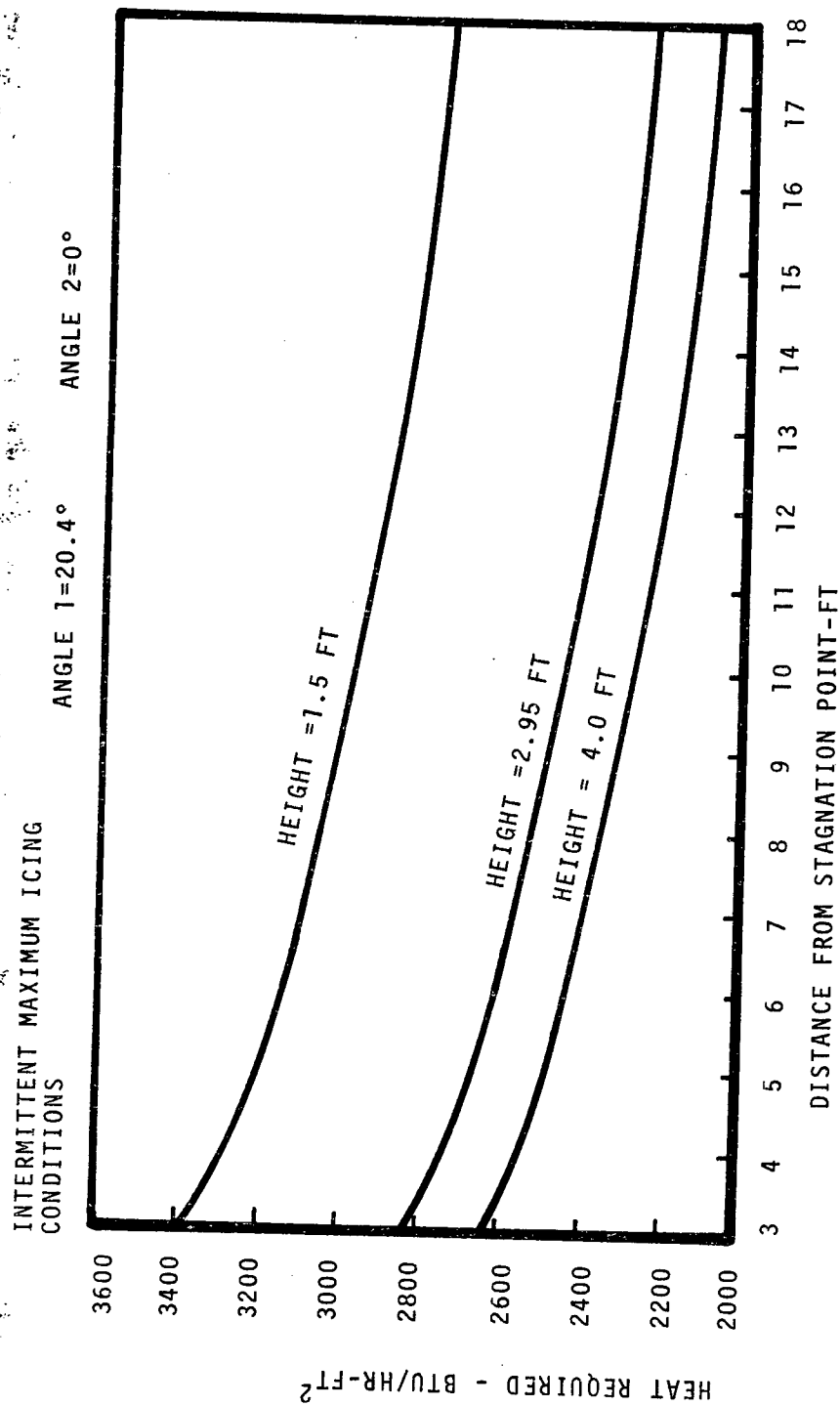


FIGURE 10 MAXIMUM HEAT REQUIRED VS DISTANCE FROM STAGNATION POINT INTERMITTENT  
MAXIMUM ICING CONDITIONS, ANGLE 1=20.4°, ANGLE 2=0°

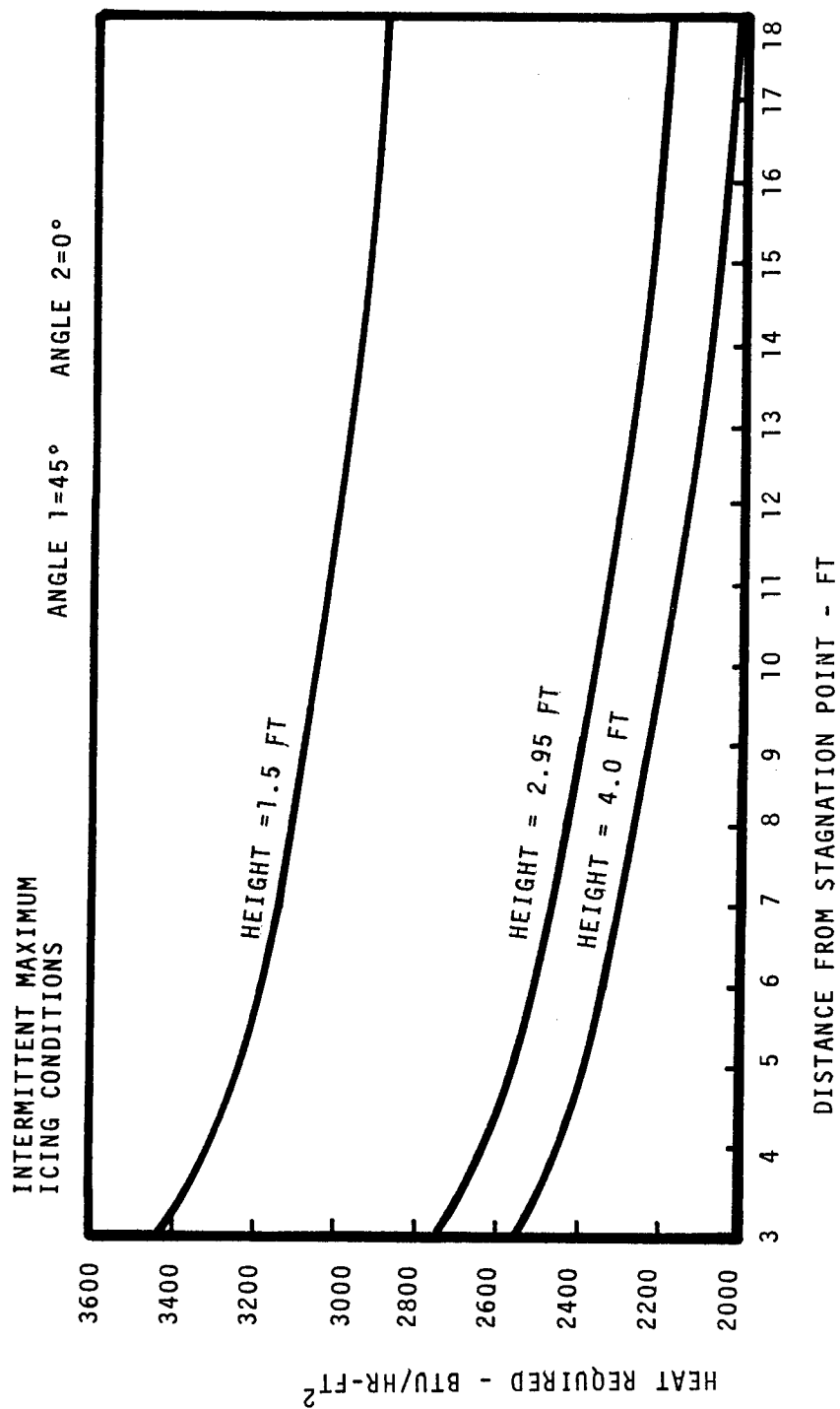


FIGURE 11 MAXIMUM HEAT REQUIRED VS DISTANCE FROM STAGNATION POINT INTERMITTENT  
MAXIMUM ICING CONDITIONS, ANGLE 1=45°, ANGLE 2=0°

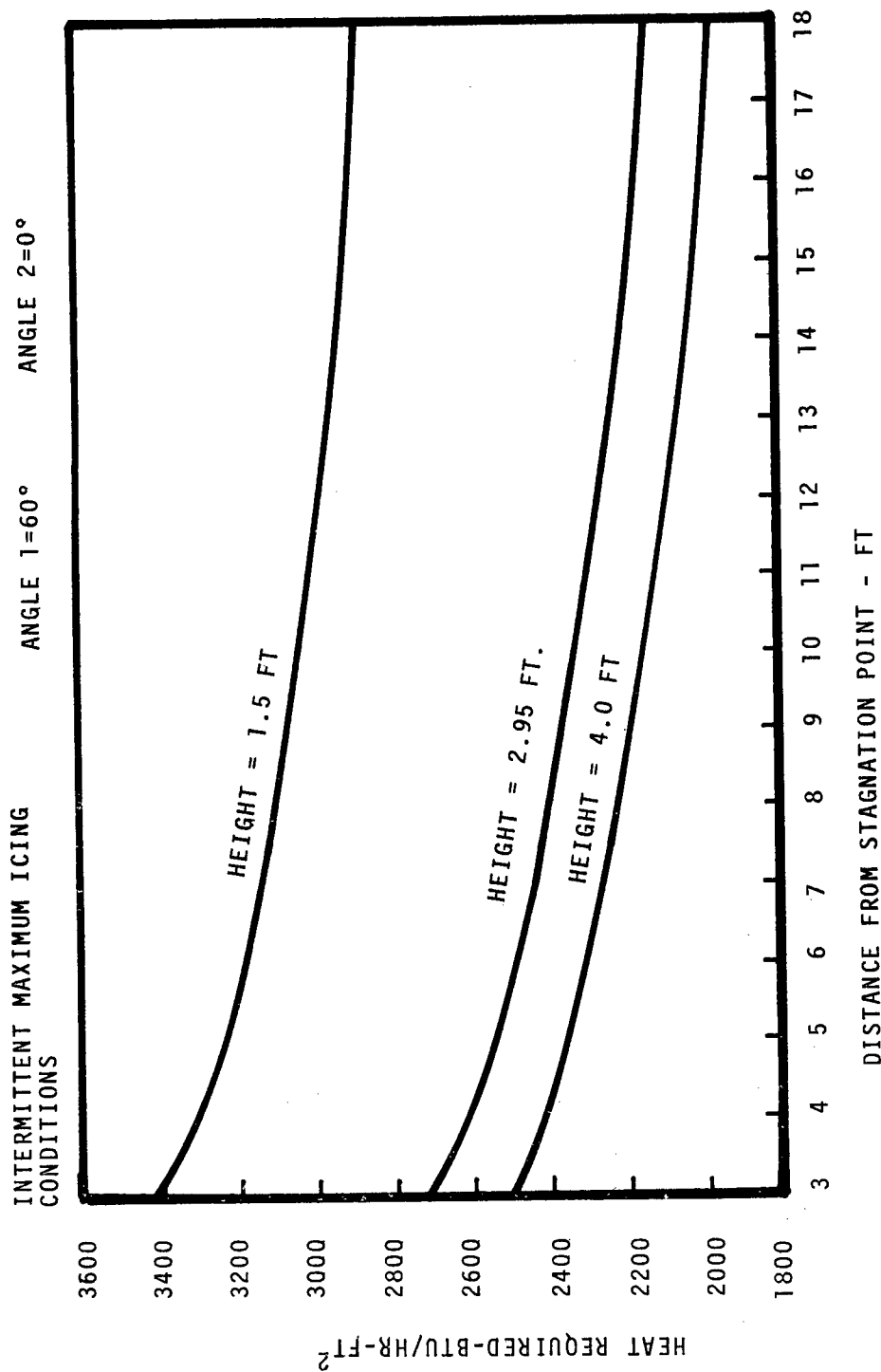


FIGURE 12 MAXIMUM HEAT REQUIRED VS DISTANCE FROM STAGNATION POINT INTERMITTENT MAXIMUM ICING CONDITIONS, ANGLE 1=60°, ANGLE 2=0°

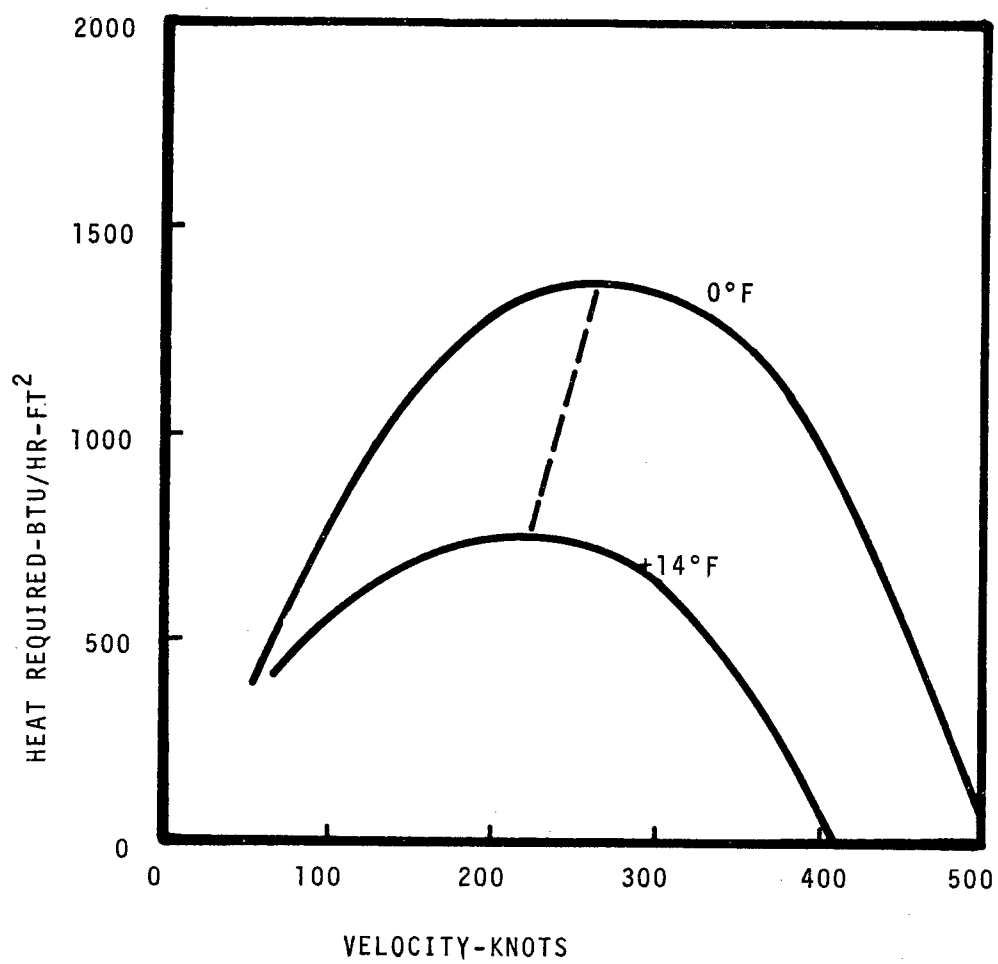


FIGURE 13 HEAT REQUIRED VS VELOCITY—SEA LEVEL CONTINUOUS  
MAXIMUM ICING CONDITIONS  
CONFIGURATION 19

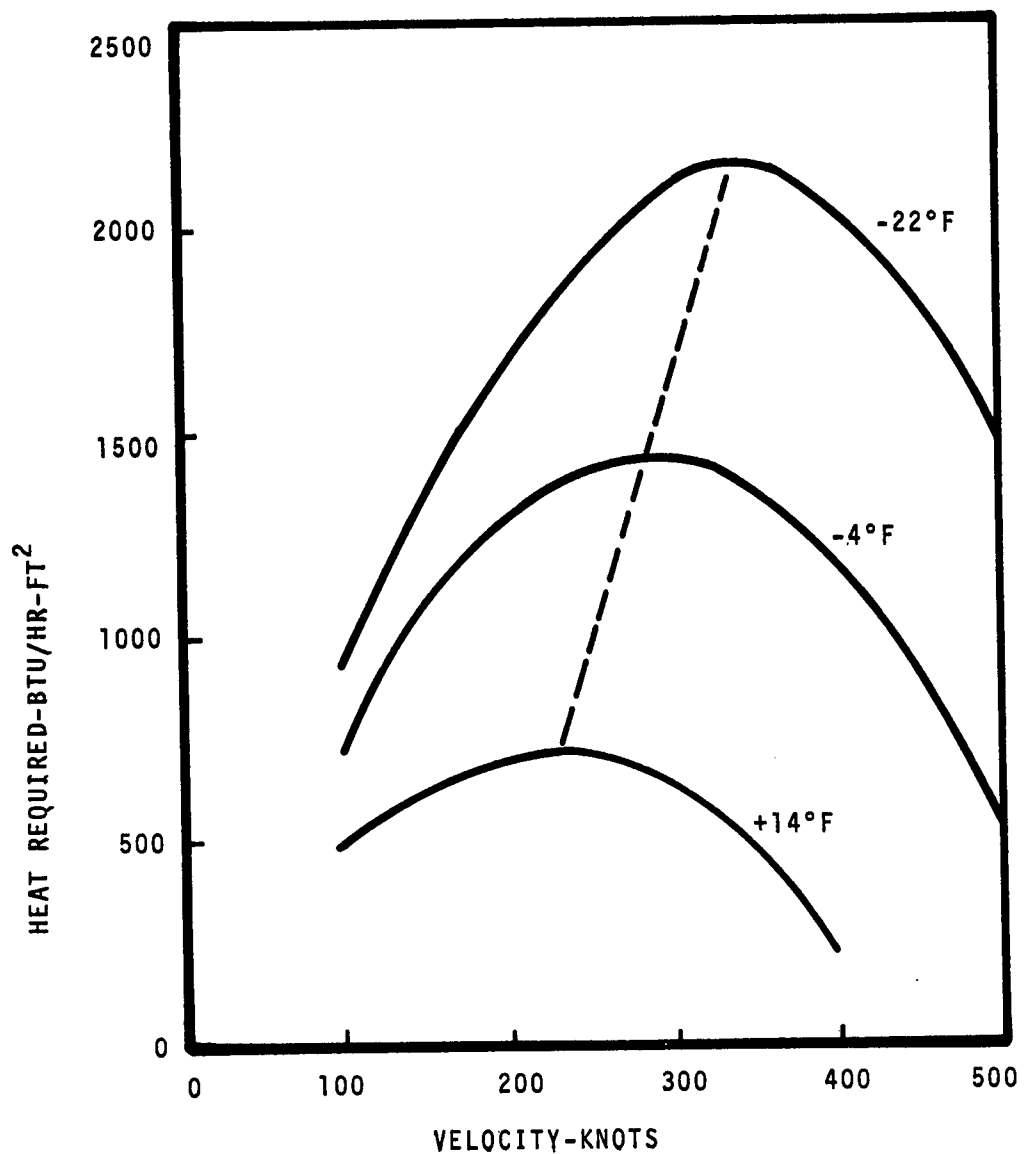


FIGURE 14 HEAT REQUIRED VS VELOCITY-7,000 FT  
CONTINUOUS MAXIMUM ICING CONDITIONS  
CONFIGURATION 19

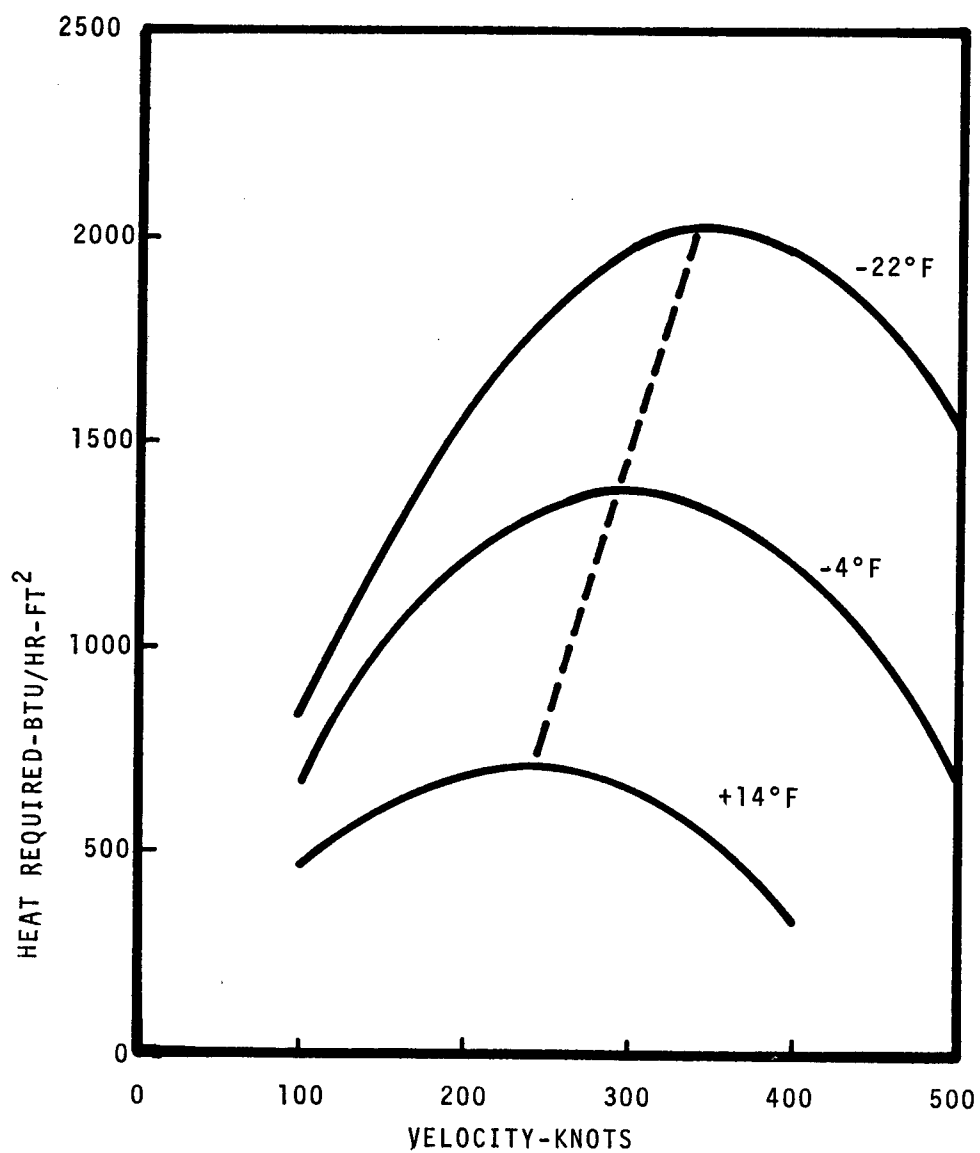


FIGURE 15 HEAT REQUIRED VS VELOCITY-12,000 FT.  
CONTINUOUS MAXIMUM ICING CONDITIONS  
CONFIGURATION 19

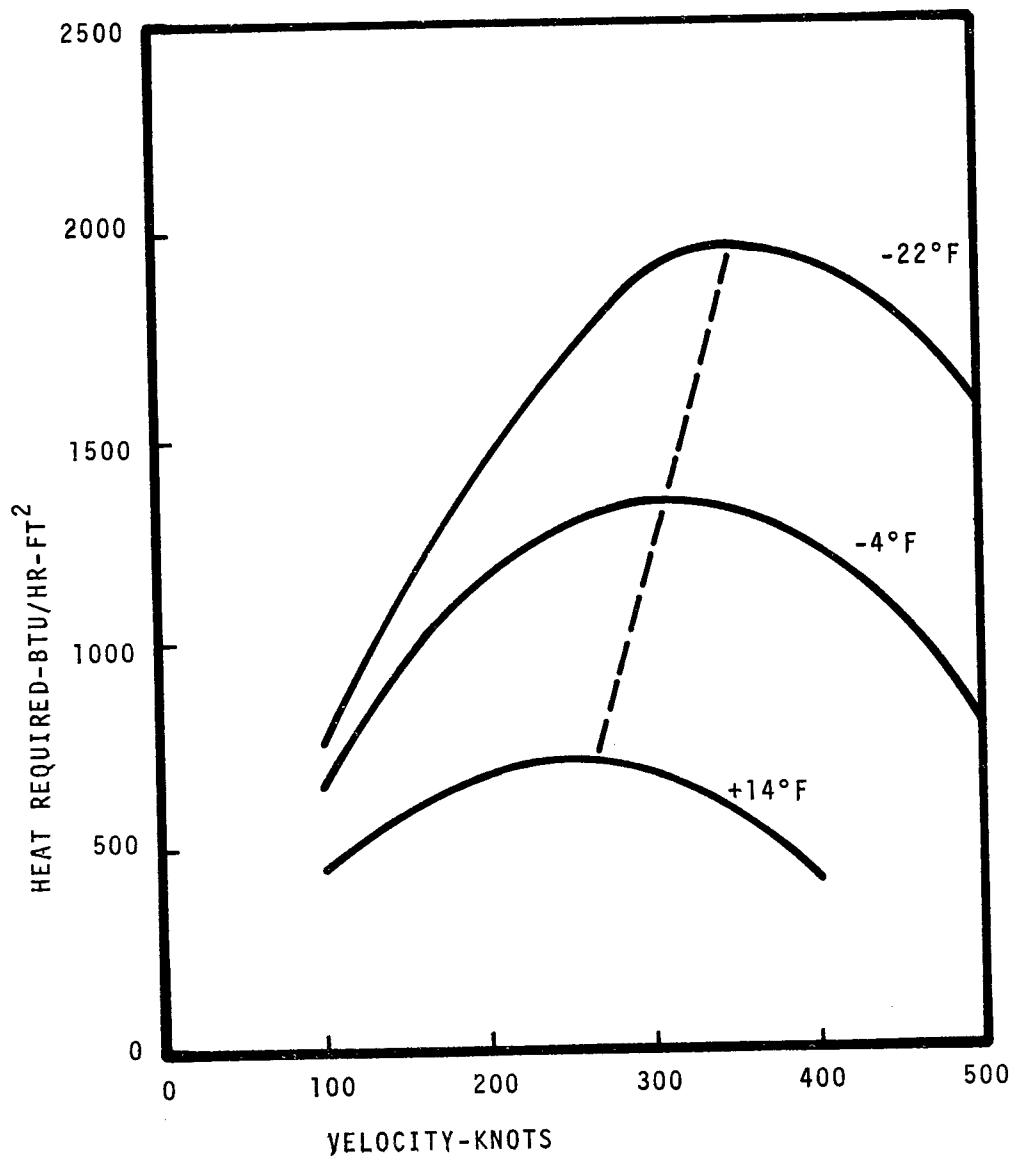


FIGURE 16 HEAT REQUIRED VS VELOCITY-17,000 FT  
CONTINUOUS MAXIMUM ICING CONDITIONS  
CONFIGURATION 19

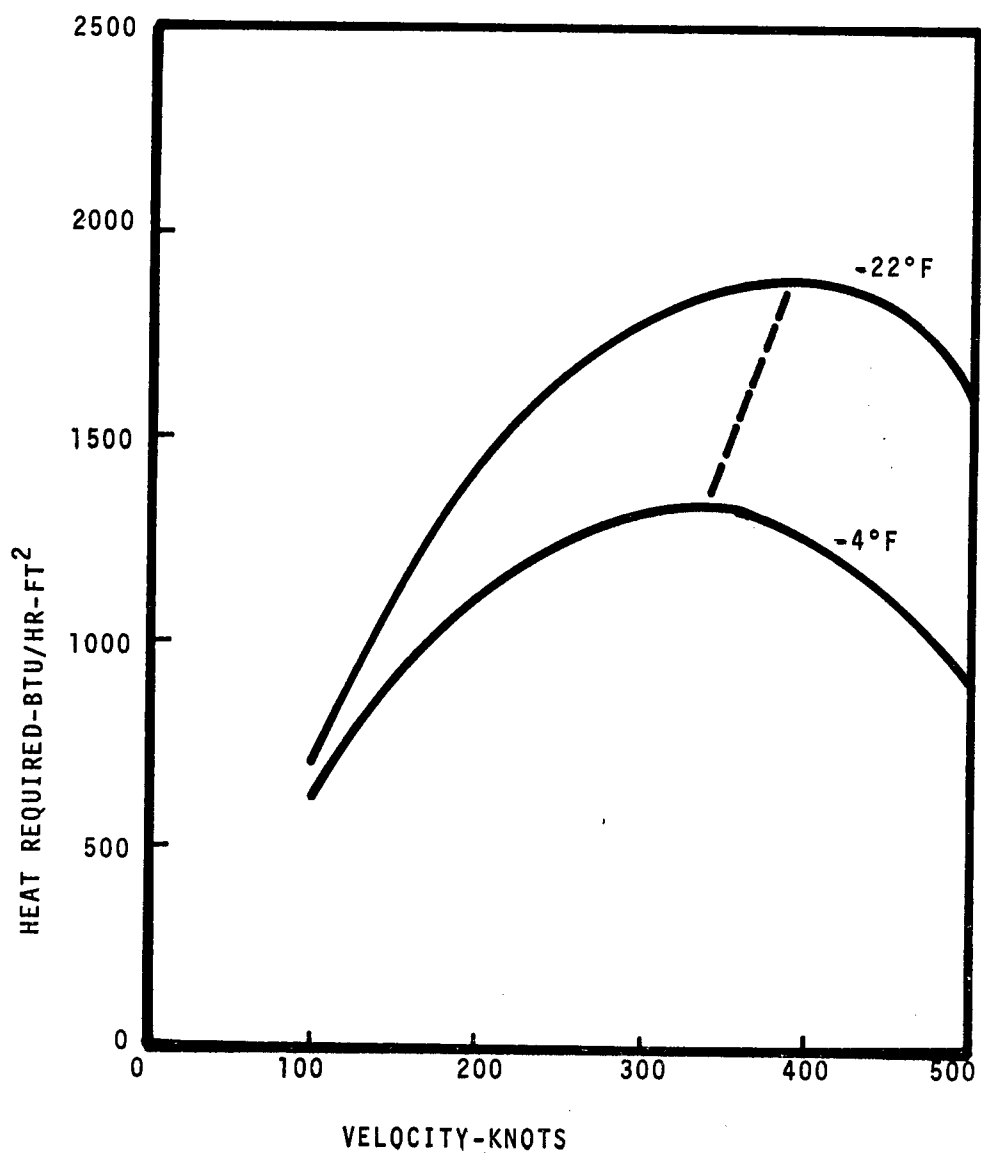


FIGURE 17 HEAT REQUIRED VS VELOCITY-22,000 FT  
CONTINUOUS MAXIMUM ICING CONDITIONS  
CONFIGURATION 19



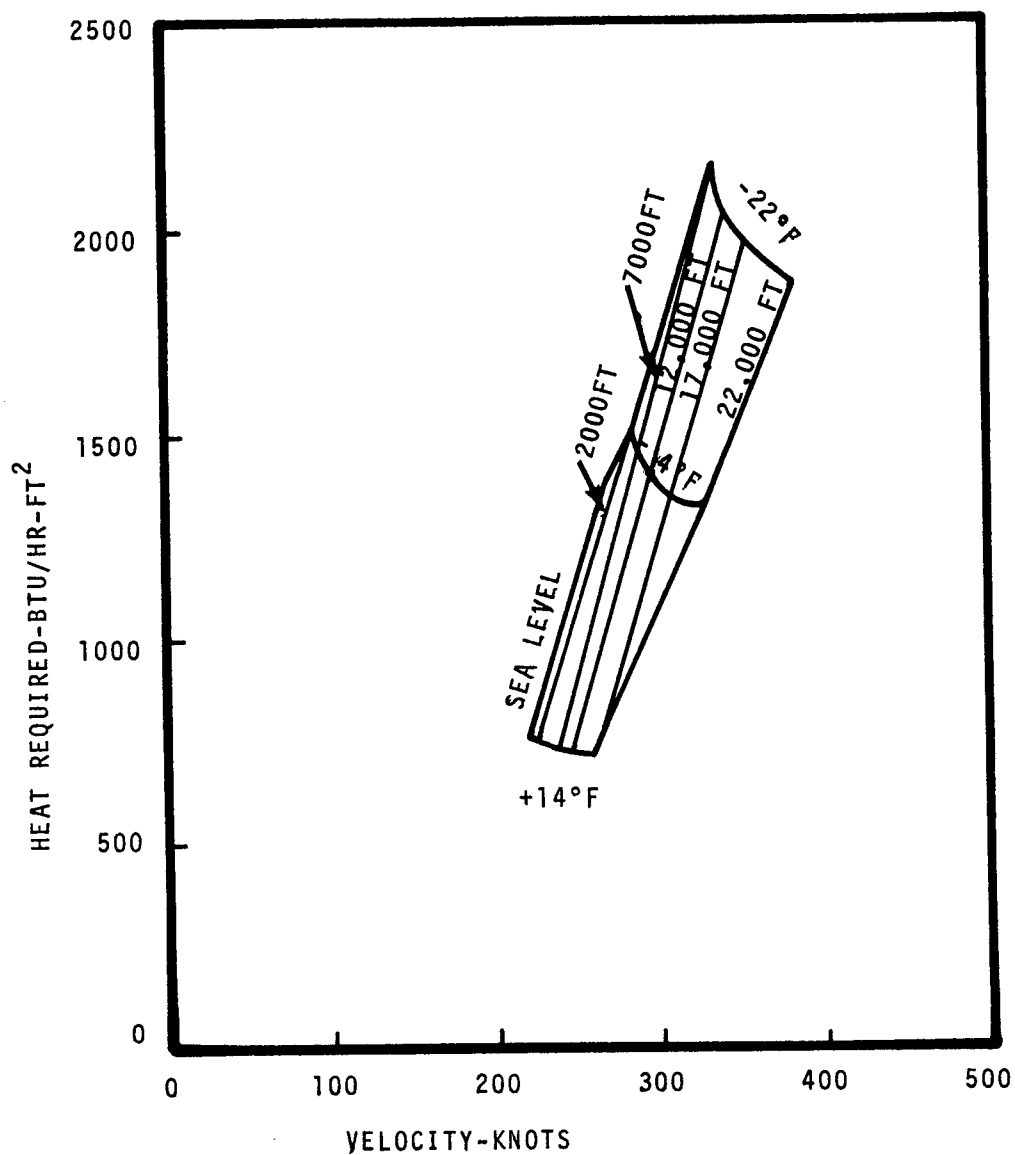
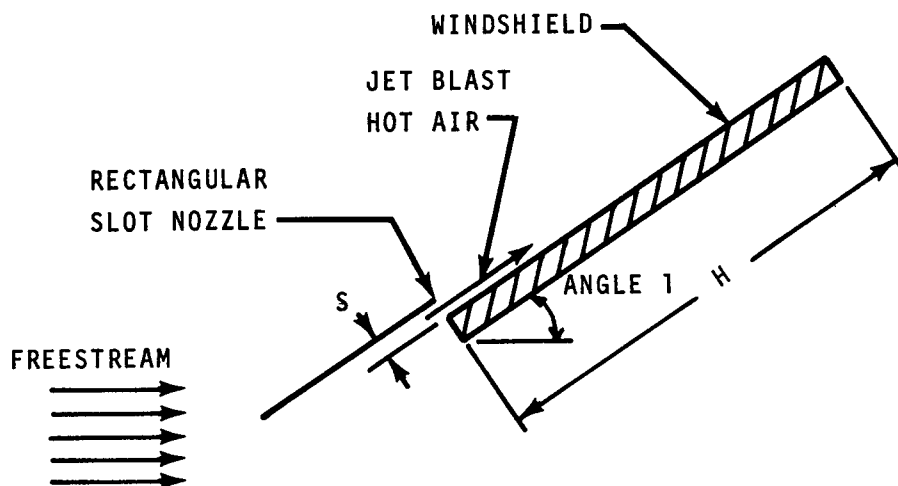


FIGURE 18 MAXIMUM HEAT REQUIRED VS VELOCITY  
CONTINUOUS MAXIMUM ICING ENVELOPE  
CONFIGURATION 19



DEFINITION OF TERMS:

H=LENGTH OF WINDSHIELD IN VERTICAL DIRECTION

S=HEIGHT OF THE RECTANGULAR SLOT JET BLAST NOZZLE

ANGLE 1 =ANGLE OF WINDSHIELD WITH UNDISTURBED FREESTREAM  
AHEAD OF AIRCRAFT

FIGURE 19-TYPICAL WINDSHIELD HOT AIR JET BLAST ANALYTICAL  
MODEL

FREESTREAM VELOCITY=225 KNOTS  
 JET EXIT VELOCITY=829 FT/SEC  
 JET EXIT TOTAL TEMPERATURE=250°F  
 NOZZLE FLOW RATE=4.5 LB/MIN/INCH  
 AMBIENT TEMPERATURE=35°F (DRY AIR) & 26°F (ICING)  
 LIQUID WATER CONTENT=1.0 GM/M<sup>3</sup> (FOR ICING CONDITIONS)  
 MEDIAN DROPLET DIAMETER=20 MICRONS

\*—\* DRY AIR-TEST                      —● ICING-TEST  
 \*--\* DRY AIR-ANALYTICAL            --● ICING-ANALYTICAL

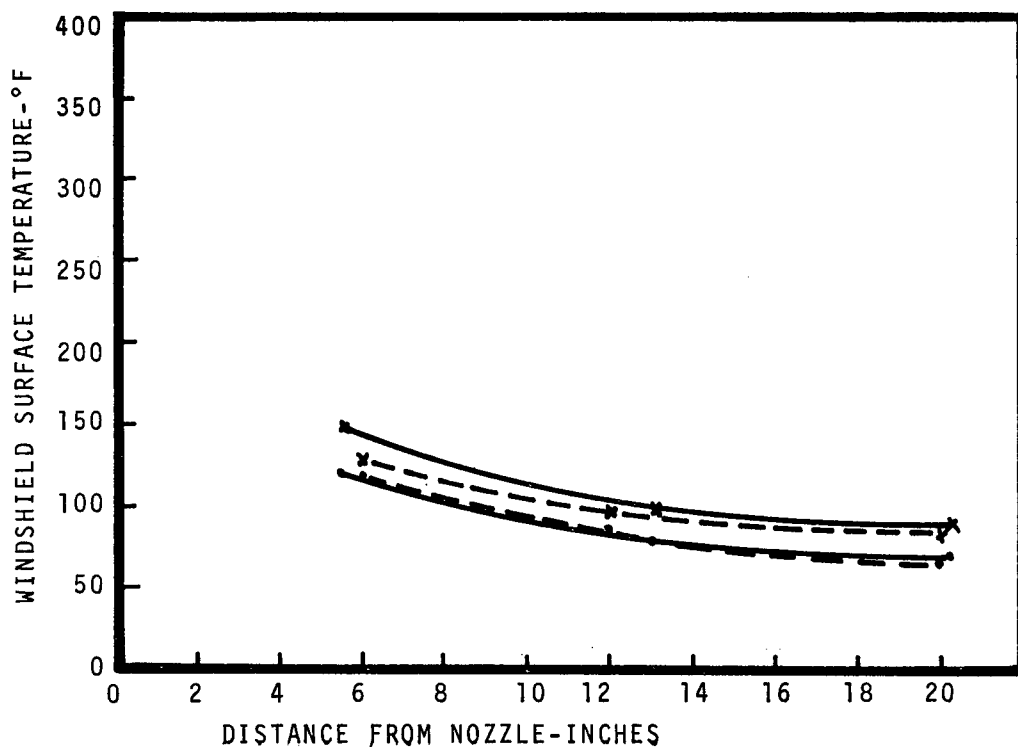


FIGURE 20-WINDSHIELD SURFACE TEMPERATURE vs DISTANCE  
 DOWNSTREAM FROM NOZZLE  
 RUN 37 WADC TR 58-444  
 HOT AIR JET BLAST SYSTEM

FREESTREAM VELOCITY=225 KNOTS  
 JET EXIT VELOCITY=829 FT/SEC  
 JET EXIT TOTAL TEMPERATURE=250°F  
 NOZZLE FLOW RATE=7.0 LB/MIN/INCH  
 AMBIENT TEMPERATURE=33°F (DRY AIR) = 24°F (ICING)  
 LIQUID WATER CONTENT=1.0 GM/M<sup>3</sup> (FOR ICING CONDITIONS)  
 MEDIAN DROPLET DIAMETER=20 MICRONS

x—x DRY AIR-TEST                      ●—● ICING-TEST  
 x---x DRY AIR-ANALYTICAL            ●---● ICING-ANALYTICAL

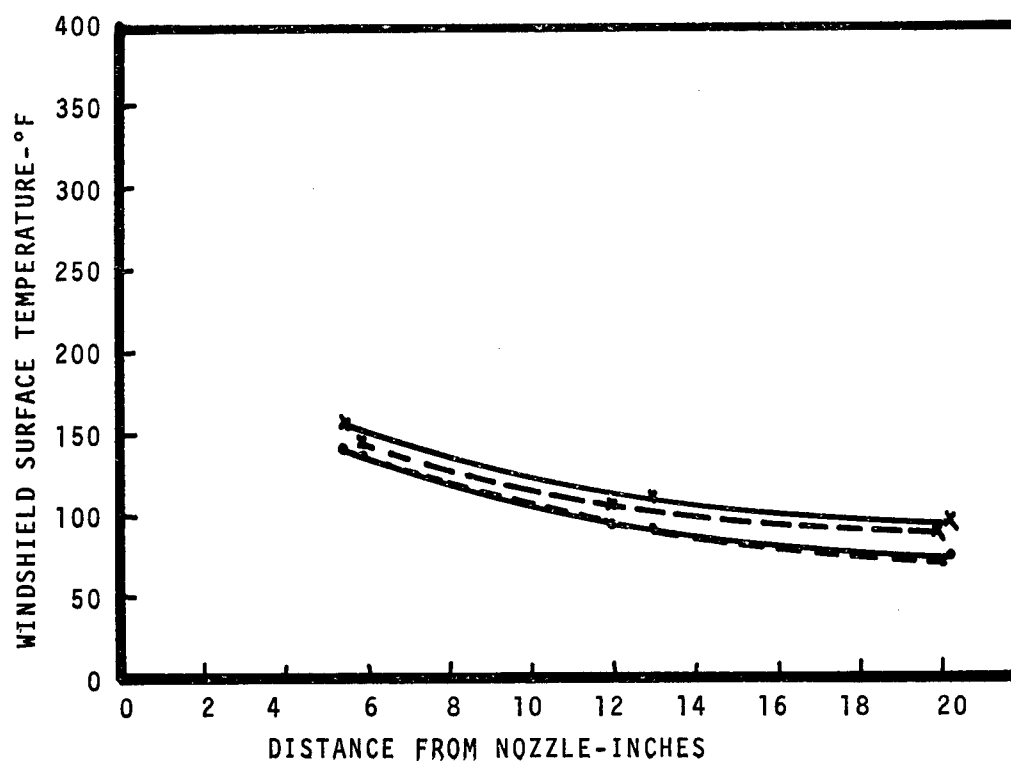


FIGURE 21-WINDSHIELD SURFACE TEMPERATURE vs DISTANCE  
 DOWNSTREAM FROM NOZZLE  
 RUN 65 WADC TR 58-444  
 HOT AIR JET BLAST SYSTEM

FREESTREAM VELOCITY=225 KNOTS  
 JET EXIT VELOCITY=829 FT/SEC  
 JET EXIT TOTAL TEMPERATURE=450°F  
 NOZZLE FLOW RATE=7.0 LB/MIN/INCH  
 AMBIENT TEMPERATURE=33°F (DRY AIR) & 29°F (ICING)  
 LIQUID WATER CONTENT=1.0 GM/M<sup>3</sup> (FOR ICING CONDITIONS)  
 MEDIAN DROPLET DIAMETER=20 MICRONS

—•— DRY AIR-TEST                      —•— ICING-TEST  
 - - - DRY AIR-ANALYTICAL              - - - ICING-ANALYTICAL

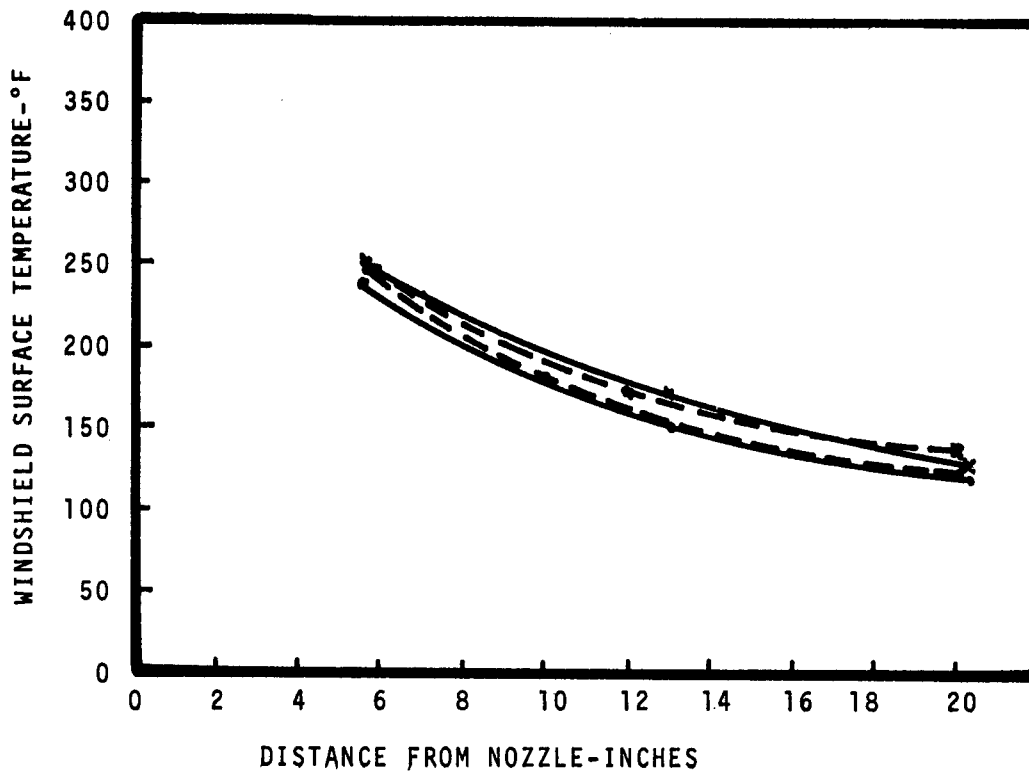


FIGURE 22-WINDSHIELD SURFACE TEMPERATURE vs DISTANCE  
 DOWNSTREAM FROM NOZZLE  
 RUN 66 WADC TR 58-444  
 HOT AIR JET BLAST SYSTEM

FREESTREAM VELOCITY=225 KNOTS  
 JET EXIT VELOCITY= MACH 1  
 JET EXIT TOTAL TEMPERATURE=450°F  
 NOZZLE FLOW RATE=4.5 LB/MIN/INCH  
 AMBIENT TEMPERATURE=37°F (DRY AIR) & 29°F (ICING)  
 LIQUID WATER CONTENT=1.0 GM/M<sup>3</sup> (FOR ICING CONDITIONS)  
 MEDIAN DROPLET DIAMETER=20 MICRONS

\*—\* DRY AIR-TEST                      —●— ICING-TEST  
 \*---\* DRY AIR-ANALYTICAL            —●--- ICING-ANALYTICAL

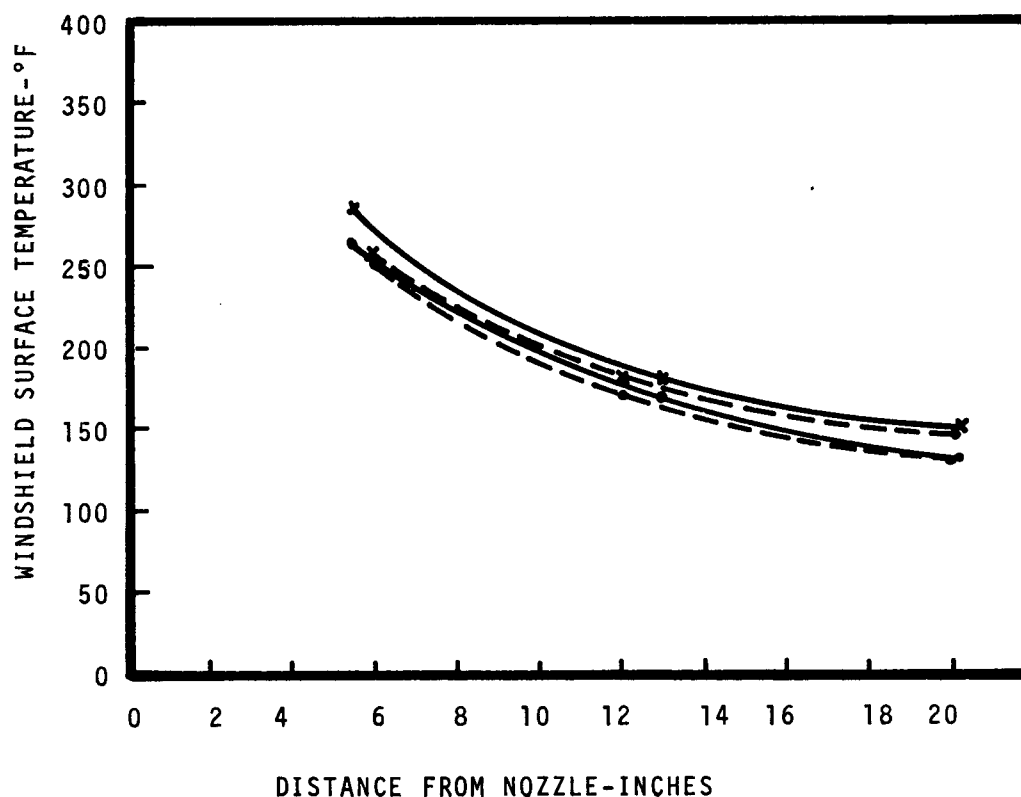


FIGURE 23-WINDSHIELD SURFACE TEMPERATURE vs DISTANCE  
 DOWNSTREAM FROM NOZZLE  
 RUN 69 WADC TR 58-444  
 HOT AIR JET BLAST SYSTEM

PPG SALT BLAST ABRADER TEST FOR  
AIRCRAFT PLASTIC WINDSHIELDS

M. S. Tarnopol  
PPG Industries, Inc.  
Pittsburgh, Pennsylvania

PPG SALT BLAST ABRADER TEST FOR

AIRCRAFT PLASTIC WINDSHIELDS

M. S. Tarnopol  
PPG INDUSTRIES, INC.  
Glass Research Center  
Pittsburgh, Pa. 15238

ABSTRACT

The need for "bird-proof" plastic windshields for aircraft has resulted in the replacement of acrylic with polycarbonate plastics. However, polycarbonates have poor abrasion resistance and are marred by the minute ice particles encountered in some clouds. It has, therefore, been necessary to apply "hard coatings" to these windshields in order to extend their service life.

In order to simulate the erosion produced by these ice crystals impacting the windshield, PPG has developed a machine which impacts a plastic sample with minute crystals of sodium chloride (MOH hardness 2.5 as compared to 1.5 for ice).

The impacts are in blasts of short duration, about 0.5 second, and the blasts are repeated for a specified number of cycles and the haze read with a Gardner haze meter.



## Introduction

The need for "bird-proof" plastic airplane windshields has resulted in the replacement of acrylics with polycarbonates. While polycarbonates have good impact resistance, they also have poor abrasion resistance. In flight, it was found that visibility was rapidly destroyed by the impact of minute ice crystals encountered in some clouds. In order to obtain a reasonable service life, a variety of "hard coatings" have been applied to these polycarbonate windshields.

At present these coatings are tested for adhesion and for resistance to humidity, solvents, and ultraviolet. The hardness of these coatings has been measured by various types of rubbing tests such as the Taber Abrader and the Goodyear Abrader. Both of these tests are based on resistance to wear by mechanical rubbing. In practice, these planes do not have windshield wipers and the major source of abrasion is "impact abrasion" encountered when a plane flies through a cloud containing ice crystals. In an attempt to simulate this service condition, PPG INDUSTRIES has developed the PPG Salt Blast Abrader Test.

It must be emphasized that this abrasion test is only one of a group of tests which are used to evaluate "hard coatings". Abrasion resistance must also accompany good adhesion under the various conditions of exposure to humidity, sunlight, solvents, etc. which are encountered in service.

## PPG Salt Blast Abrader

The PPG Salt Blast Abrader attempts to simulate flight conditions by impacting the plastic test sample with successive 1/2 second blasts of minute salt particles. The abraded area is a circle one-inch in diameter, and four test areas are produced on a three-inch square sample. The increase in haze is used as a measure of the abrasion resistance. A major advantage of this abrader is that the test piece need not be flat. Actual curved sections from windshields have been tested.

The PPG Salt Blast Abrader is based on a device used to sand blast trademarks, etc. on glass. After considerable trial and many errors, modifications were made which have enabled us to produce a uniformly abraded area by controlling the following variables:

1. Air pressure - 15 psi - 70 mph as sample
2. Salt delivery per 1/2 second blast - (1.9 grams/cycle)
3. No recycling of the salt
4. Accurate timing control of the 1/2 second on and 1-1/2 second off cycle
5. Automatic control of the number of cycles
6. Accurately sized free-flowing salt

Salt was chosen as the abrasive for the following reasons:

1. MOH hardness is 2.5 as compared with 1.5 for ice.
2. Non-toxic and water soluble.
3. Readily available in controlled particle size at a few cents per pound.

The particular grade of salt chosen after some experimentation is Morton's Extra Fine Flake. This is commercially available pan crystallized, non-pulverized salt which contains about 1/2% of tricalcium phosphate which prevents caking.

The following are two typical screen analyses of this salt:

TABLE 1

|             | <u>Screen Size</u> | <u>Mesh Size mm</u> | <u>%</u> | <u>%</u> |
|-------------|--------------------|---------------------|----------|----------|
| Retained on | #60                | .250                | 0.1      | 0.1      |
| on          | #120               | .125                | 52.3     | 43.1     |
| on          | #200               | .0029               | 35.3     | 41.1     |
| on          | #325               | .0017               | 9.5      | 10.7     |
| Through     | #325               |                     | 2.8      | 3.0      |

#### Test Procedures

The procedures for testing are as follows:

1. All samples are cut to 3-inch squares, code marked, and the initial haze read on a Gardner Hazemeter.
2. The salt blast abrader is run for at least 50 cycles to check its operation. Each cycle is 0.5 seconds on, and 1.5 seconds off.
3. Two acrylic samples are then run as standards. Each sample has four test areas: Two are run at four cycles, and two at eight cycles.
4. The remaining samples are then tested.
5. The samples after testing are washed with deionized water, dried, and recleaned with a 50-50 solution of isopropanol and water.
6. Haze measurements are made with a Gardner Hazemeter.

#### Reproducibility

Samples of 1/4-inch acrylic were run at daily intervals for four days. The averages of these eleven samples (22 readings at 4 cycles; 22 readings at 8 cycles) are 6.06% haze for 4 cycles and 10.78% haze at 8 cycles. The standard deviation was 0.47% at 4 cycles and 0.63% at 8 cycles. This is within the limits of the reproducibility of our hazemeter which is  $\pm 0.5\%$ .

A check on the number of cycles obtained from successive 25 lb. batches of salt was 6,064 cycles, and 6,059 cycles or 1.85 g/cycle.

## Test Data

Data on the following materials listed in Table 2 has been collected.

TABLE 2

### Materials Tested

|   | <u>Code</u> |
|---|-------------|
| Uncoated acrylic                          | A           |
| Uncoated polycarbonate                    | B           |
| Uncoated CR-39 (allyl diglycol carbonate) | C           |
| Coated polycarbonate                      | D           |
| Coated polycarbonate                      | E           |
| Coated polycarbonate                      | F           |
| Coated acrylic                            | G           |
| Coupons for two windshields               | H           |
| Coupons for four windshields              | I           |
| Windshield sections                       | J           |

The coated plastics and windshield sections are from various sources and identified by code letters only because these samples may not be representative.

The data is presented in Figures 4, 5, 6, 7, 8 and 9.

Figure 4 is a comparison of three uncoated transparent plastics; acrylic, polycarbonate, and CR-39 resin. The variation in abrasion resistance is quite large: ranging from 40% haze after 2 cycles for polycarbonate; 20% haze after 25 cycles for acrylic; 2% haze after 100 cycles for CR-39 resin.

Figure 5 compares uncoated and coated acrylic. The uncoated acrylic has 20% haze after 25 cycles; while the coated acrylic has only 3% haze after 50 cycles.

Figure 6 compares uncoated polycarbonate with coated polycarbonate flat sections from three different sources. The uncoated acrylic has 20% haze after 25 cycles. The coated polycarbonates showed for samples D, E, and F, at 50 cycles; 6%, 12%, and 6%, respectively.

Figures 7, 8, 9, compare uncoated acrylic with coupons and sections cut from airplane windshields from different sources. Again, with uncoated acrylic showing 20% haze after 25 cycles we find that Figure 7, Sample H, representing coupons for two windshields, varies between 7% and 10% haze at 50 cycles.

These variations in Figure 8 are due to real differences in the coating. Group I-1,2,3,4 represents coupons which were made with four windshields and are from a single manufacturer. The average haze and the standard deviation for each group of coupons at 50 cycles are:

TABLE 3

|     |       |   |               |
|-----|-------|---|---------------|
| I-1 | 24.3% | - | <u>+</u> 2.4% |
| I-2 | 38.6% | - | <u>+</u> 2.8% |
| I-3 | 65.3% | - | <u>+</u> 2.1% |
| I-4 | 78.6% | - | <u>+</u> 0.8% |

Group J represents the range for six samples cut from a single wind-shield. At 50 cycles, these ranged from 28 to 54%.

A reasonable question to raise is whether or not there is any real difference between resistance to rubbing abrasion and impact abrasion. The following table gives a comparison of the percent increase in haze produced by the Taber Abrader and the PPG Salt Blast Abrader.

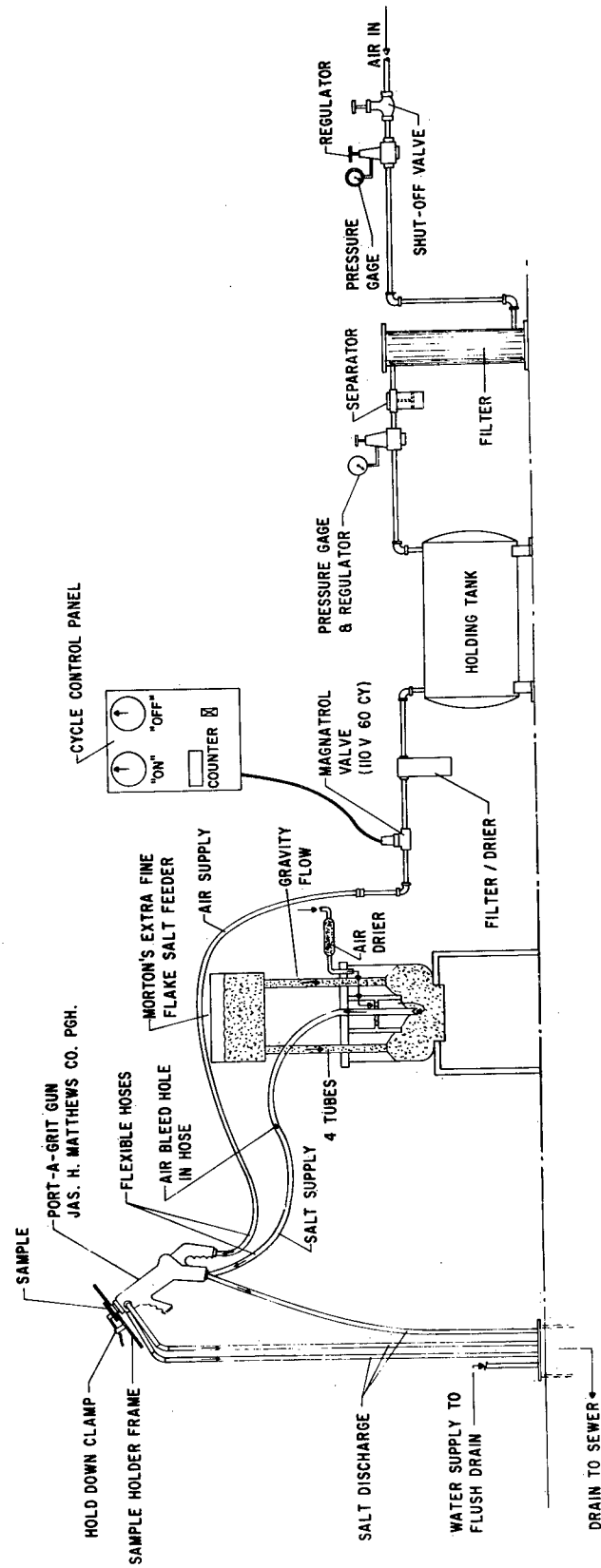
TABLE 4

Comparison of Haze Produced by the Taber Abrader and the PPG Salt Blast Abrader

| <u>Material</u>      | <u>Taber</u>        | <u>PPG</u>                           |
|----------------------|---------------------|--------------------------------------|
|                      | % Haze at 50 Cycles | Cycles to Produce Equivalent<br>Haze |
| Polycarbonate        | 50%                 | 3 Cycles                             |
| Acrylic              | 20%                 | 20 Cycles                            |
| Coated Polycarbonate | 3%                  | 20 Cycles                            |
| CR-39 Resin          | 3%                  | 160 Cycles                           |

It would therefore appear that the PPG Salt Blast Abrader is measuring a property not normally measured by the present abrasion tests.

FIGURE I. PPG SALT BLAST ABRASION TESTER



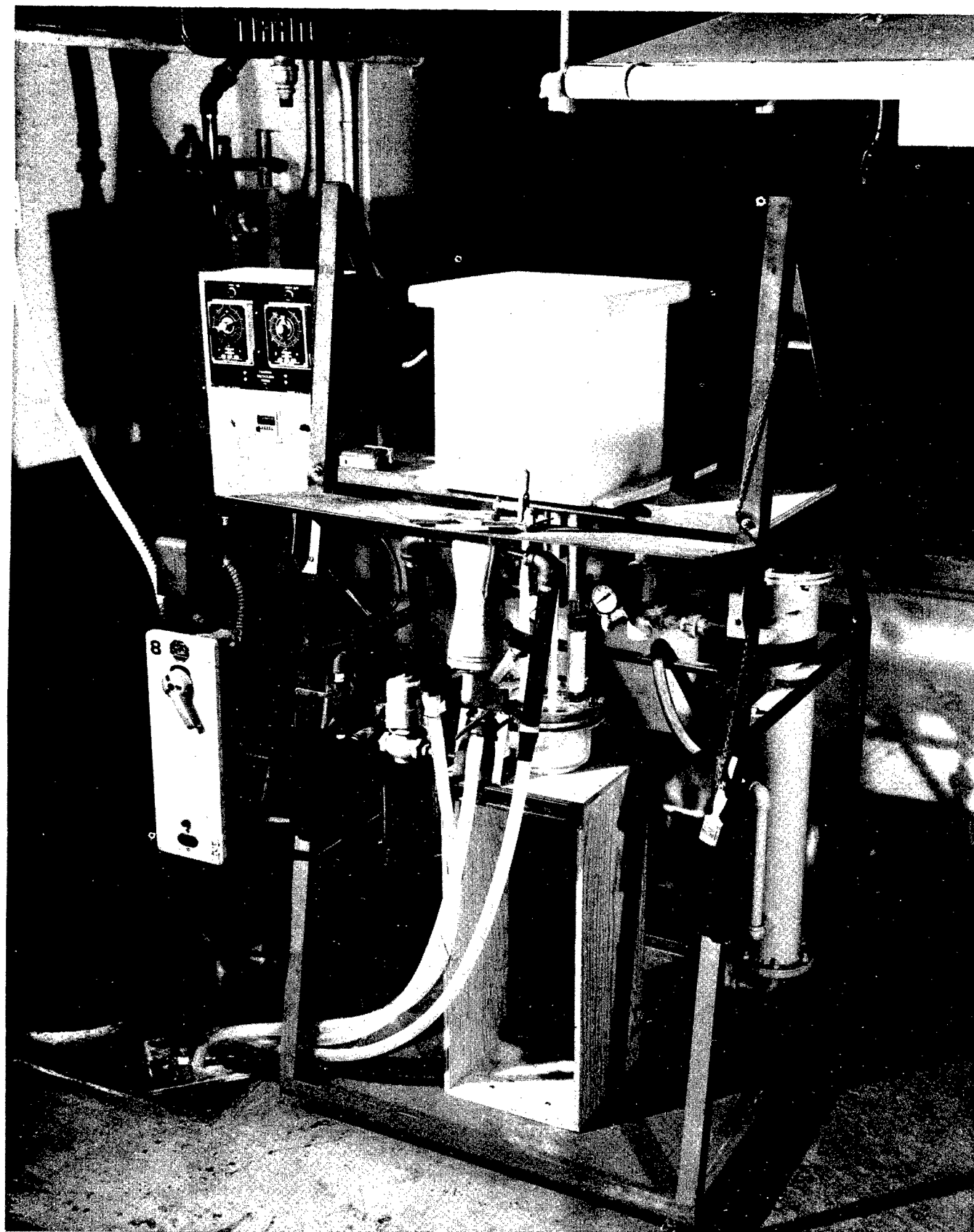


FIGURE 2 - PPG SALT BLAST ABRADER  
911

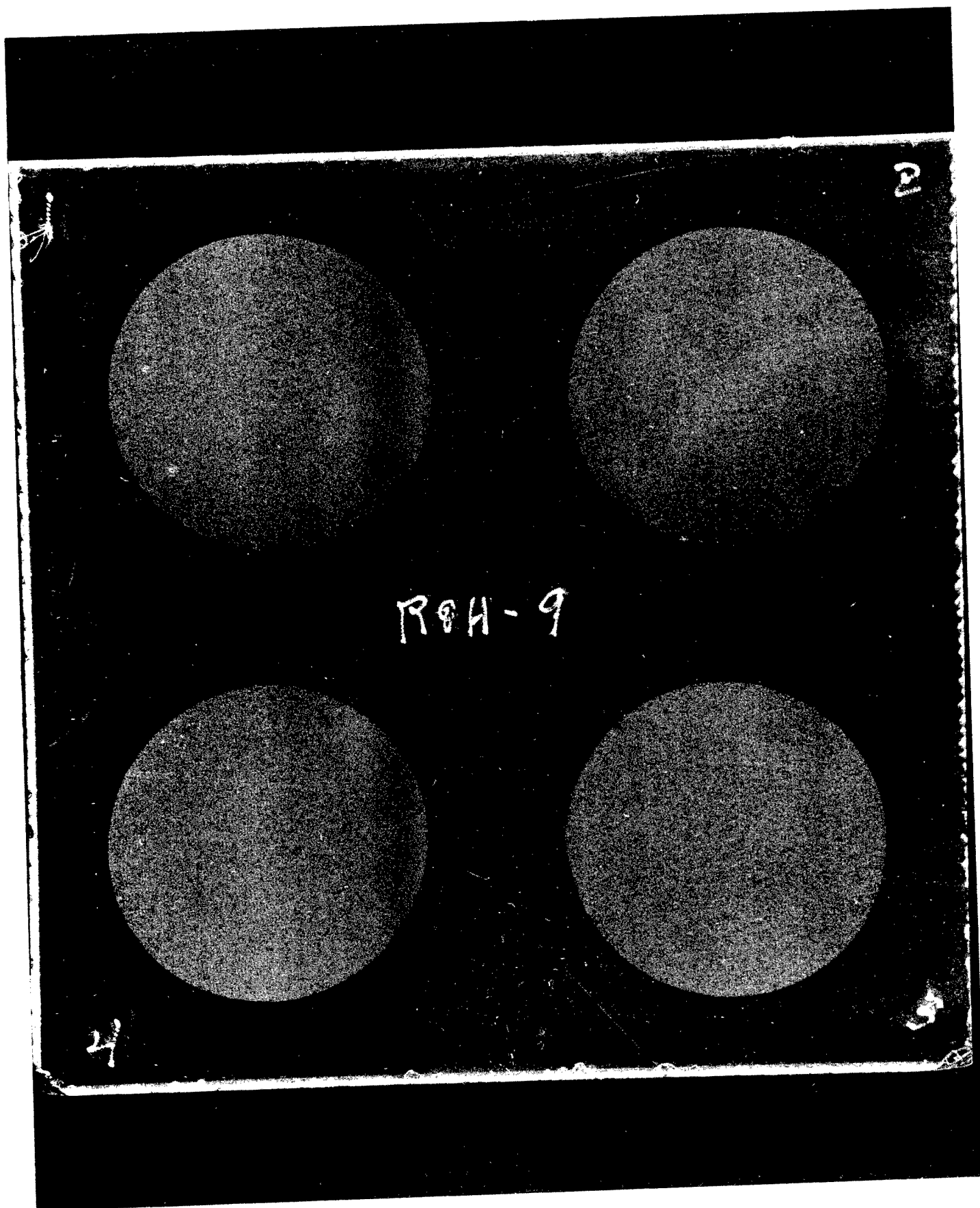


FIGURE 3 - SALT ABRADED AREAS ON PLASTIC SAMPLE

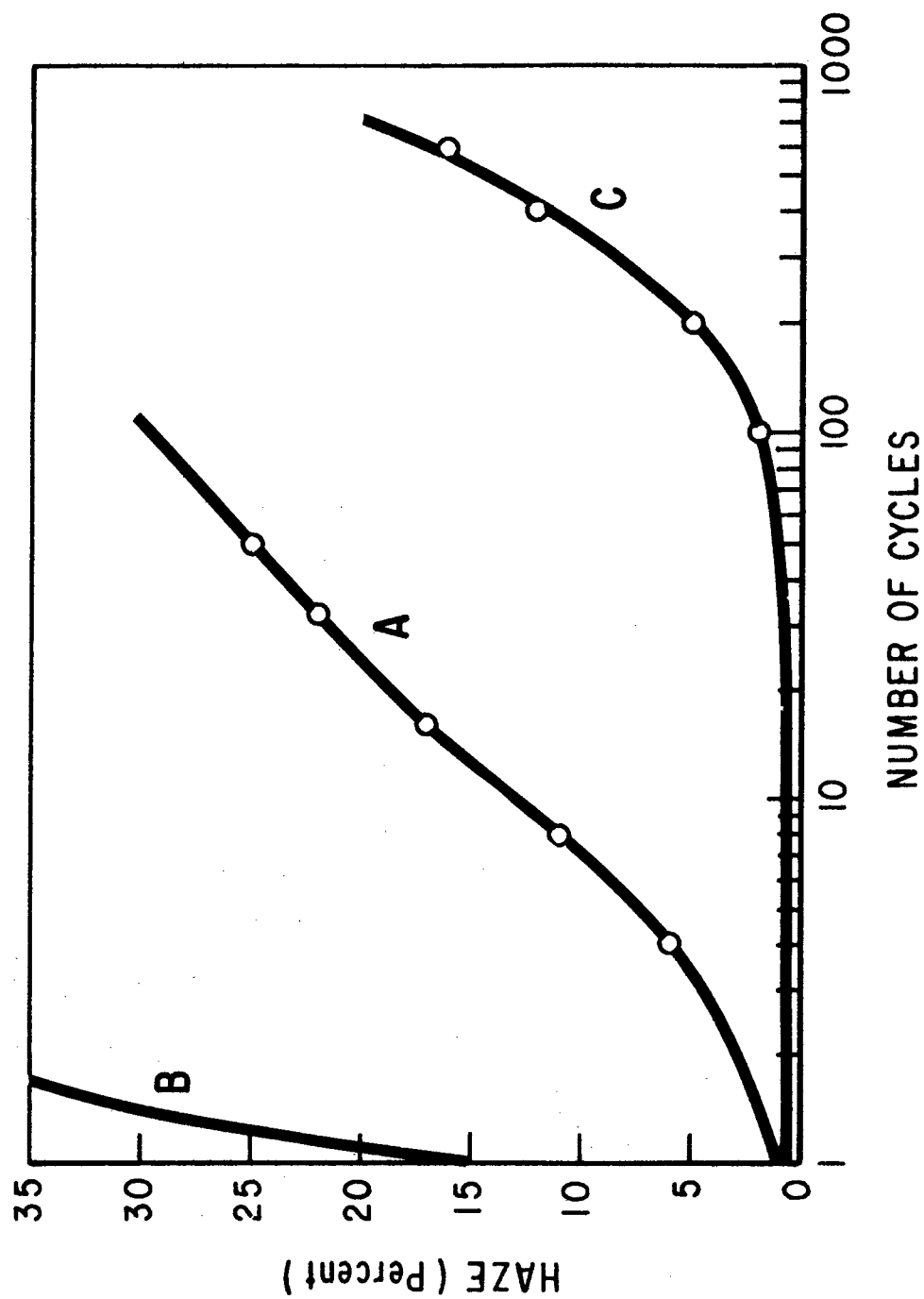


Figure 4. PPG Salt Blast Abrader Comparison of Uncoated Plastics  
Acrylic (A), Polycarbonate (B), CR-39<sup>®</sup>(C)



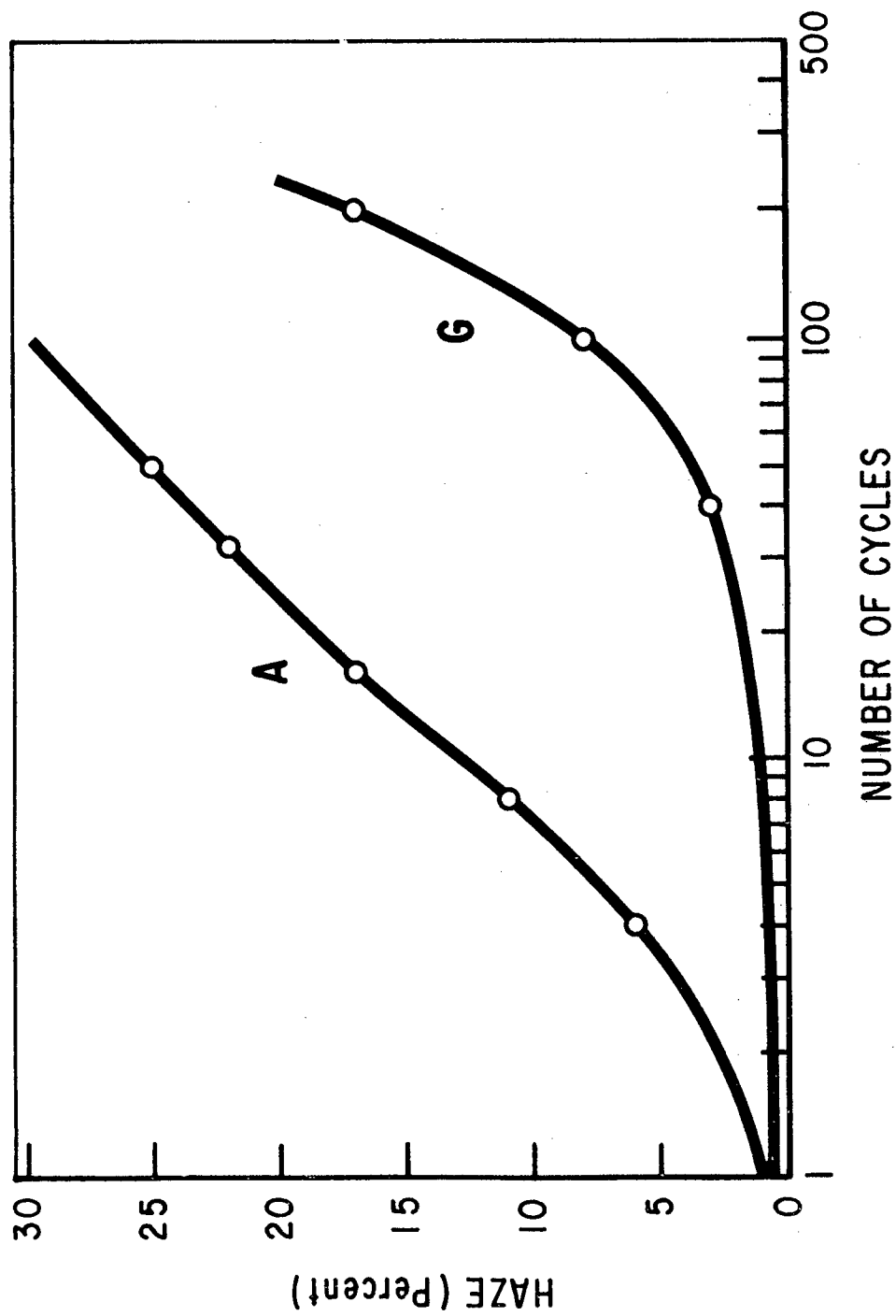


Figure 5. PPG Salt Blast Abrader Comparison of Uncoated Acrylic (A) and Coated Acrylic (G)

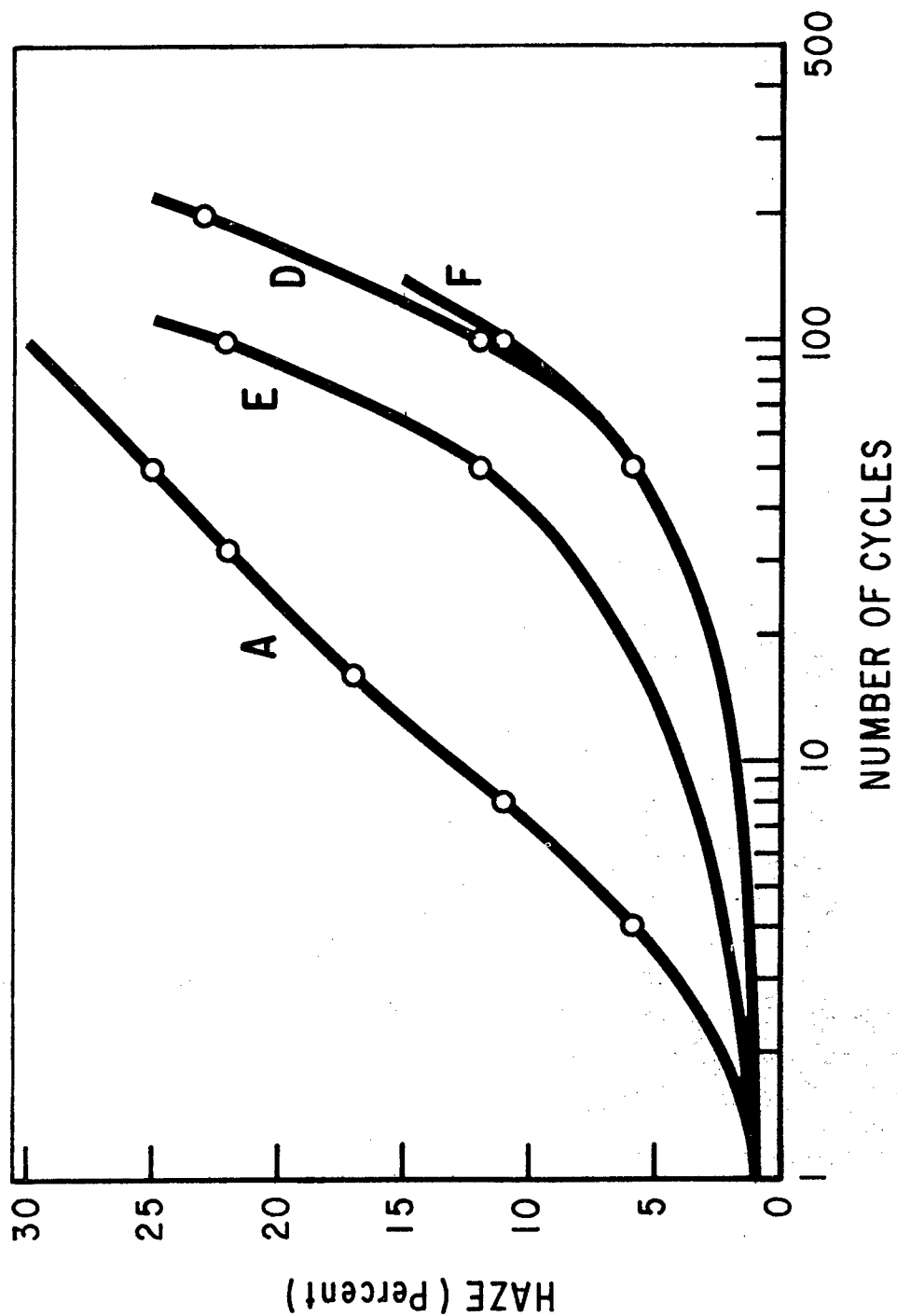


Figure 6. PPG Salt Blast Abrader Comparison of Uncoated Acrylic (A) and Coated Polycarbonates - (D), (E), (F)

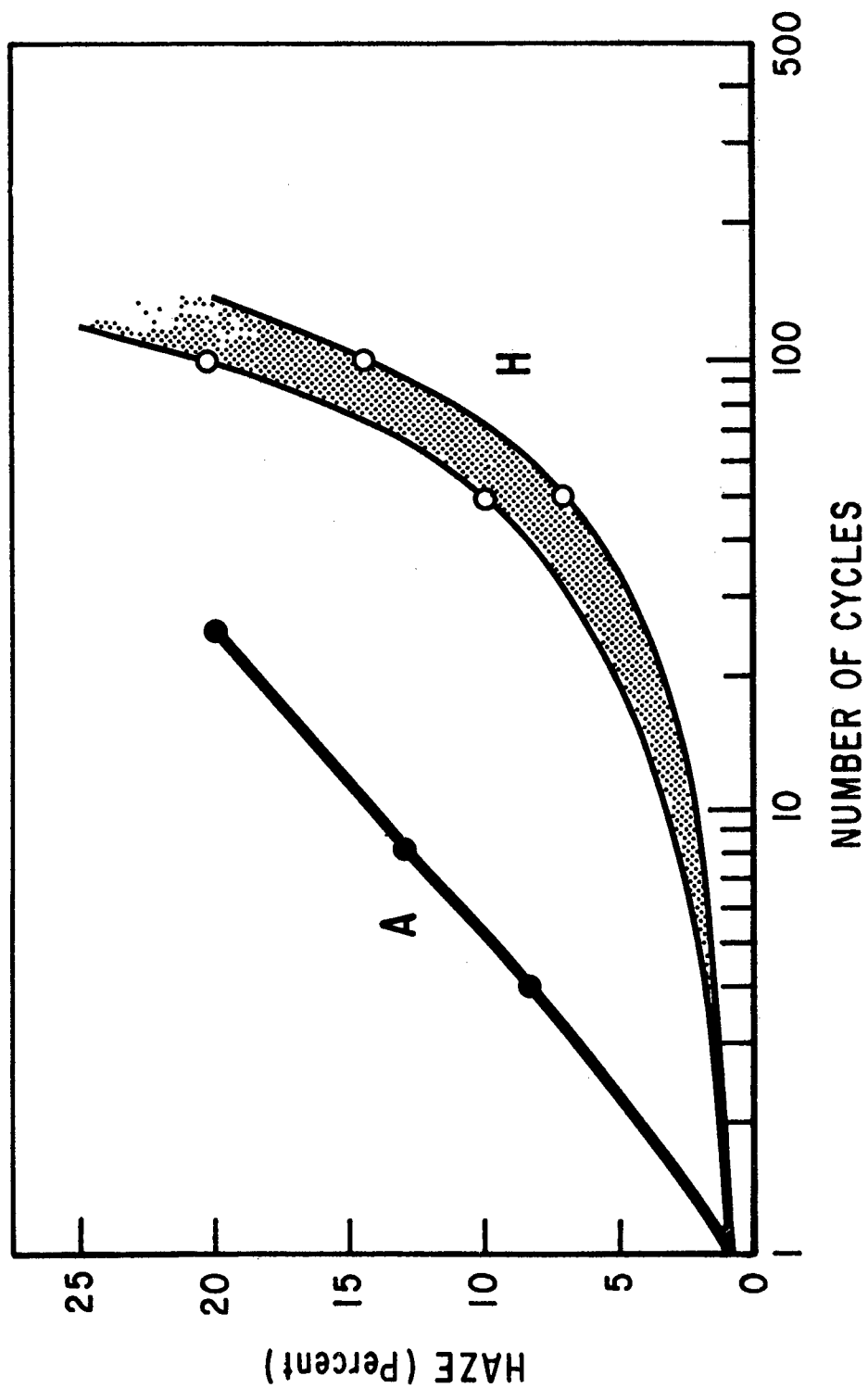


Figure 7. PPG Salt Blast Abrader Comparison of Uncoated Acrylic (A), and Coupons for 2 Windshields

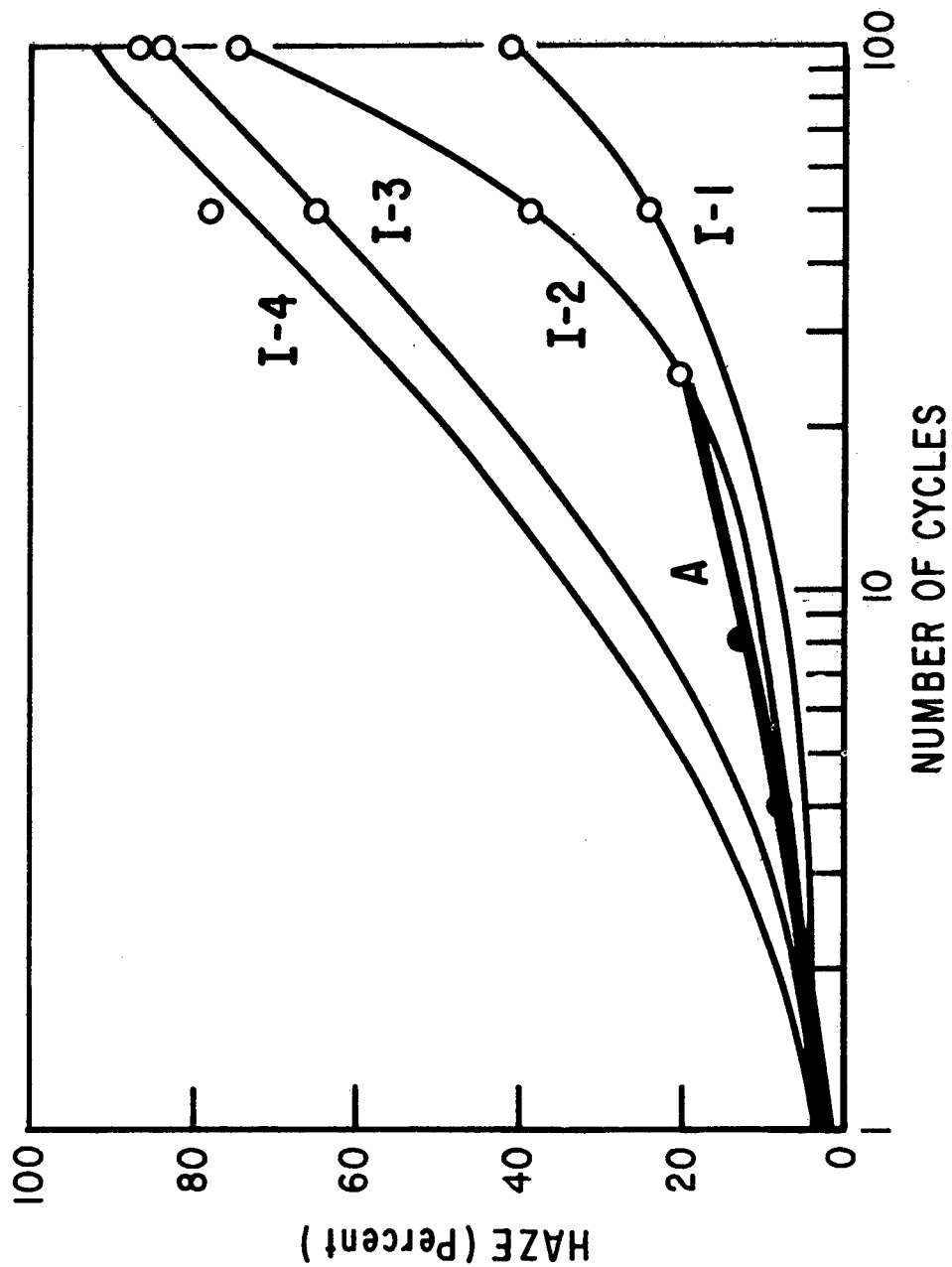


Figure 8. PPG Salt Blast Abrader Comparison of Uncoated Acrylic (A) and Coupons for 4 Windshields

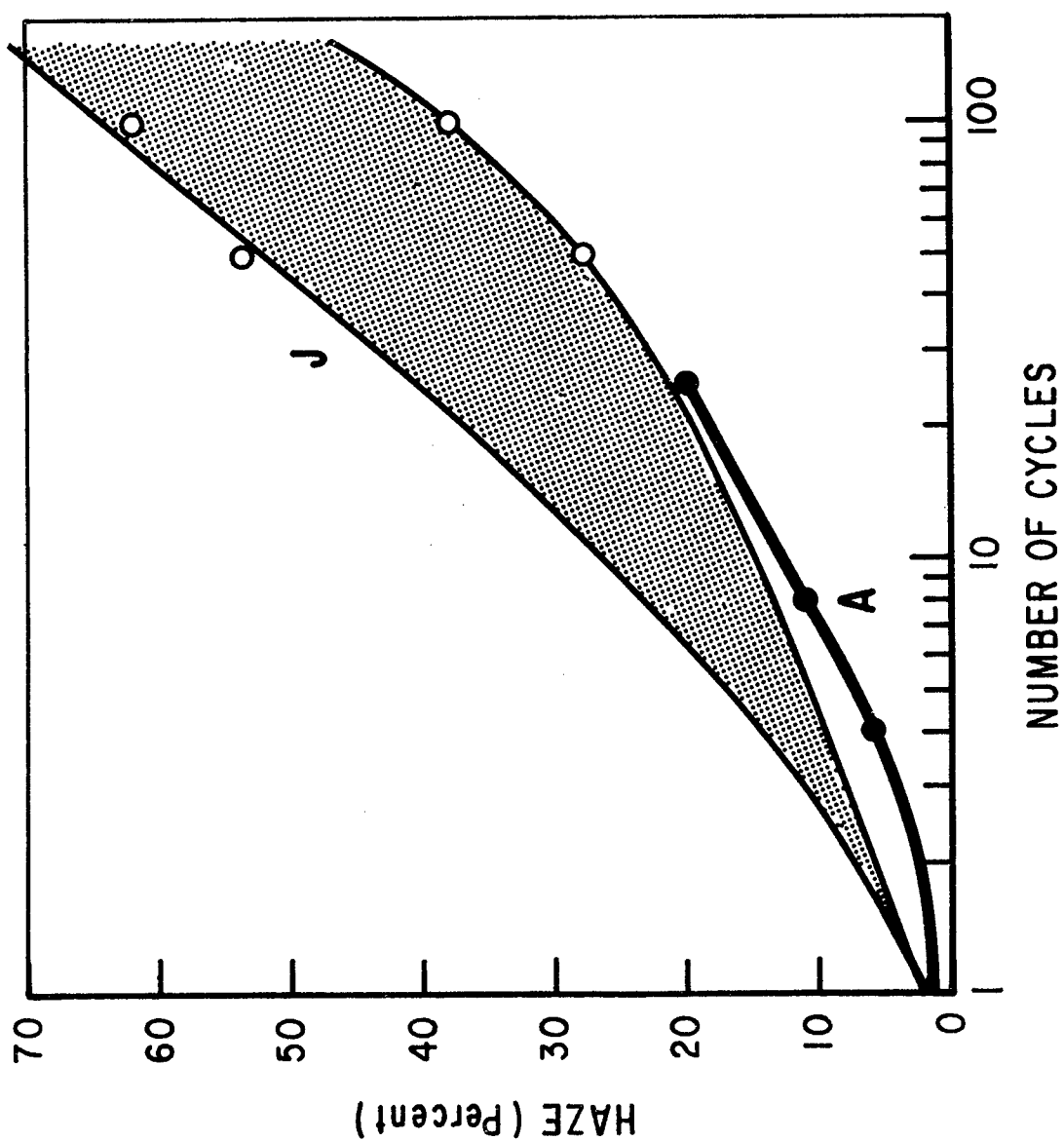


Figure 9. PPG Salt Blast Abrader Comparison of Uncoated Acrylic (A) and 6 Sections cut from Windshield (J)

UNCLASSIFIED

Security Classification

## DOCUMENT CONTROL DATA - R &amp; D

(Security classification of title, body of abstract and indexing annotation must be entered when the overall report is classified)

|   |  |   |                        |
|---|--|---|------------------------|
| 1. ORIGINATING ACTIVITY (Corporate author)<br>AFFDL/PTW<br>W-PAFB, Ohio 45433   |  | 2a. REPORT SECURITY CLASSIFICATION<br>UNCLASSIFIED                          |                        |
|   |  | 2b. GROUP<br>N/A  |                        |
| 3. REPORT TITLE<br>CONFERENCE ON TRANSPARENT AIRCRAFT ENCLOSURES  |  |   |                        |
| 4. DESCRIPTIVE NOTES (Type of report and inclusive dates)<br>Conference Report, Feb 5-8 1973  |  |   |                        |
| 5. AUTHOR(S) (First name, middle initial, last name)<br>Compiled by Robert E Wittman  |  |   |                        |
| 6. REPORT DATE<br>June 1, 1973  |  | 7a. TOTAL NO. OF PAGES<br>918   | 7b. NO. OF REFS<br>N/A |
| 8a. CONTRACT OR GRANT NO.<br>N/A  |  | 9a. ORIGINATOR'S REPORT NUMBER(S)<br>AFML-TR-73-126                         |                        |
| b. PROJECT NO.  |  | 9b. OTHER REPORT NO(S) (Any other numbers that may be assigned this report) |                        |
| c.  |  | N/A   |                        |
| d.  |  |   |                        |
| 10. DISTRIBUTION STATEMENT<br>Distribution Statement A<br>Approved for Public Release; distribution unlimited   |  |   |                        |
| 11. SUPPLEMENTARY NOTES   |  | 12. SPONSORING MILITARY ACTIVITY<br>AFFDL/AFML<br>W-PAFB, Ohio 45433        |                        |
| 13. ABSTRACT<br><p>The purpose of this report is to make available the technical papers presented at the recent Tenth Conference on "Transparent Aircraft Enclosures." This Conference was held for the exchange of knowledge on new developments and design concepts concerned with vision areas of crew enclosures. Also to make known the state-of-the-art with respect to transparent plastics, interlayer materials, and glass, of the type suitable for these applications.</p> <p>The papers contained herein have been reproduced directly from the original manuscripts.</p> |  |   |                        |

DD FORM 1473  
1 NOV 65

UNCLASSIFIED

Security Classification

Security Classification

| 14. KEY WORDS | LINK A |    | LINK B |    | LINK C |    |
|---------------|--------|----|--------|----|--------|----|
|               | ROLE   | WT | ROLE   | WT | ROLE   | WT |
|               |        |    |        |    |        |    |